QD
1
S923

ARKIV FÖR KEMI

UTGIVET AV

K. SVENSKA VETENSKAPSAKADEMIEN

Band 5

Med 54 avhandlingar

STOCKHOLM
ALMQVIST & WIKSELLS BOKTRYCKERI AB

LONDON
H. K. LEWIS & CO., LTD
136, GOWER STREET

1953

PARIS
LIBRAIRIE C. KLINCKSIECK
11 RUE DE LILLE

Häfte 1 innehållande Nr 1—11 utkom den 27 jan. 1953
» 2 » Nr 12—17 » » 4 febr. 1953
» 3 » Nr 18—27 » » 9 mars 1953
» 4 » Nr 28—37 » » 4 maj 1953
» 5 » Nr 38—44 » » 6 maj 1953
» 6 » Nr 45—54 » » 12 maj 1953

FEMTE BANDETS INNEHÅLL

Sid.

1. Lundberg, B., Methane fermentation of *Penicillium* mycelium . . . . 1— 9
2. Schotte, L., An investigation of S-alkyl-*iso*-thiuronium picrates and styphnates 11— 16
3. Matell, M., On the conditions for the formation of quasi-racemic compounds. II. Alkylsuccinic acids and S-alkylmercaptosuccinic acids . . . . 17— 37
4. Aurivillius, B., The structure of Bi_2NbO_5F and isomorphous compounds. . 39— 47
5. von Euler, H. & Hasselquist, H., Ascorbinsäure, Dehydro-Ascorbinsäure und Diketo-L-Gulonsäure . . . . 49— 55
6. Schotte, L., A study of possible methods for preparing α-ketomercaptans . 57— 60
7. Schlyter, K., On the coprecipitation of lanthanum ions and tri- or tetrapositive ions as fluorides . . . . 61— 72
8. ——, On the crystal structure of fluorides of the tysonite or LaF_3 type . . 73— 82
9. Hultin, E., Kriszat, G., Lindvall, S., Lundblad, G., Löw, H., Runnström, J., Vasseur, E. & Wicklund, E., On the interaction between the gametes of the sea urchin at fertilization . . . . 83— 87
10. di Bella, S., Free amino-acids in Jensen Sarcoma of rats studied by chromatography . . . . 89— 92
11. Forssberg, A. & Hevesy, G., Effect of irradiation with X-rays on phosphate incorporation in mice . . . . 93— 96
12. Lundegårdh, H., Properties of the cytochrome system of wheat roots . . . 97—146
13. Högfeldt, E., On ion exchange equilibria . . . . 147—171
14. Danielsson, C. E., A new type of preparative chromatographic paper column 173—176
15. Myrbäck, K. und Persson, B., Über die Inaktivierung der α-Malzamylase. II 177—185
16. Matell, M., Stereochemical studies on plant growth regulators. II . . . . . 187—192
17. von Euler, H. und Hasselquist, H., Zum Mechanismus der Decarboxylierung. II . . . . 193—201
18. Serck-Hansen, Klaus, Ställberg-Stenhagen, Stina and Stenhagen, Einar, Optically active higher aliphatic hydroxy-compounds. I . . . . 203—221
19. Fredga, Arne, Studies on synthetic growth substances. IV . . . . 223—227
20. Ehrensvärd, G. and Reio, L., The formation of tyrosine in *Escherichia coli* and *Neurospora crassa*, grown on isotope-labelled acetate as the sole source of carbon . . . . 229—234
21. Neumüller, Gunnar and Vasseur, Erik, The influence of pH on the periodate oxidation of carbohydrates . . . . 235—245
22. Lindqvist, Ingvar, The structure of the hexaniobate ion in $7\ Na_2O \cdot 6\ Nb_2O_5 \cdot 32\ H_2O$ . . . . 247—250
23. von Euler, Hans, Hasselquist, Hans und Eriksson, Erik, Zur Kenntnis des Buttergelb-Hepatoms und seiner Entstehung. III . . . . 251—259
24. von Euler, Hans und Bargoni, Nora, Einfluss des Histidins auf die Zahl der Vitalfärbbaren roten Rattenblut-Zellen . . . . 261—266
25. Hultin, Tore, Incorporation of N^{15}-labelled ammonium chloride into pyrimidines and purines during the early sea urchin development . . . . 267—275
26. Brune, Ursula und Lindner, Roland, Anwendung radioaktiver Indikatoren auf die Untersuchung von Pulverreaktionen in Silikatsystemen . . . . . . 277—282

Sid.

27. Williams, Trevor I. and Weil, Herbert, The phases of chromatography . 283—299

28. Reio, L. & Ehrensvärd, G., An improved method for degradation of tyrosine and phenols in general in connection with isotope studies . . . . 301—311

29. Garcia-Verduch, A. & Lindner, R., Selbstdiffusion in Bariummetatitanat 313—316

30. Myrbäck, K. & Svanborg, K., Starch degradation by salivary amylase. I 317—326

31. Ehrensvärd, G. & Reio, L., The formation of tyrosine in *Rhodospirillum rubrum* grown on acetate and carbon dioxide, isotope labelled, under anaerobic condition . . . . 327—332

32. Gatenbeck, S. & Ehrenberg, L., The influence of anesthetics on monomolecular films of cell lipids . . . . 333—340

33. Matell, M., Stereochemical studies on plant growth regulators. III . . . . 341—347

34. Lundgren, G., The crystal structure of $U_6O_4(OH)_4(SO_4)_6$ . . . . 349—363

35. Myrbäck, K. & Persson, B., Products of potato starch degradation by malt α-amylase . . . . 365—378

36. Matell, M. & Larsson, S., Stereochemical studies on plant growth regulators. IV 379—385

37. von Euler, H. & Heller, L., Studies in Experimental Rheumatism. II . . 387—392

38. Bánhidi, Z. G., Sjöström, A. G. M., Grömmer, S. & Lundin, H., On the behavior of various Lactobacilli, members of the vitamin B_{12} group and desoxyribosides in the cup plate assay of vitamin B_{12} . . . . 393—412

39. Rydberg, J., Studies on the extraction of metal complexes. X . . . . . . 413—423

40. Biedermann, G. & Sillén, L. G., Studies on the hydrolysis of metal ions. IV 425—440

41. Biedermann, G., Studies on the hydrolysis of metal ions. V . . . . 441—455

42. Hedström, B. O. A., Studies on the hydrolysis of metal ions. VI . . . . . 457—468

43. von Euler, H., Krebserregung durch chemisch definierte Noxen . . . . . 469—476

44. Myrbäck, K. & Persson, B., Action of heparin on barley β-amylase . . . 477—488

45. Forsling, W., Anion exchange and complex formation of hafnium in hydrochloric and hydrofluoric acid mixtures . . . . 489—502

46. Forsling, W., On the purification of zirconium from hafnium by anion exchange in hydrochloric and hydrofluoric acid mixtures . . . . 503—516

47. Rydberg, J., Studies on the extraction of metal complexes. XI . . . . . . 517—522

48. Weichert, R., Über Molekülverbindungen zwischen L-α-Aminosäuren und nichtreduzierenden Zuckern . . . . 523—532

49. Schotte, L., 1.3-Dimercaptoacetone and some derivatives . . . . 533—542

50. Hultin, T., The amino acid metabolism of sea urchin embryos studied by means of N^{15}-labeled ammonium chloride and alanine . . . . 543—552

51. Weichert, R., Über D,L-Desoxokynurenin [γ-(*o*-Aminophenyl)-α-aminobuttersäure] . . . . 553—557

52. Hultin, T., Incorporation of N^{15}-DL-alanine into protein fractions of sea urchin embryos . . . . 559—564

53. Klamerth, O., Nicotinsäureamid in Leber und Milz von Ratten nach Fütterung mit 4-Dimethylaminoazobenzol . . . . 565—568

54. Lagerkvist, U., The incorporation of ammonia into uric acid in pigeons and ribonucleic acid pyrimidines in rats . . . . 569—580

ARKIV FÖR KEMI Band 5 nr 1

Communicated 9 January 1952 by John Runnström and Karl Myrbäck

Methane fermentation of *Penicillium* mycelium

By Bengt Lundberg

During the production of penicillin a large quantity of moist mycelium—about 1 000 kg per kg of penicillin—is wasted in addition to the mash. Not much interest has been devoted to the utilization of the mycelium to date because research has been primarily concerned with biochemical and technical improvements so as to obtain the highest yield of penicillin. To test the possibility of producing saleable by-products efforts have, however, been made to extract vitamins (1–8) and enzymes (6, 9, 10) from the mycelium, but the yields have been small and, as a result, these processes are unprofitable compared with those employing other raw materials. The mycelium seems to be largely useless as a food for hens or pigs and reports that it is possible to grow mushrooms on mycelium beds have a curiosity value only. The waste products from the production of penicillin—mycelium or mash—do not present any problem if they can be disposed of via the communal sewers, i. e. treated together with other sewage at the sewage plants. However it is important that the community is big enough in relation to the penicillin factory. This is the case for instance in Stockholm, where the mash and the mycelium from AB Kabi are discharged into the sewers without causing trouble in sewers, pumping stations, sedimentation tanks or digestion chambers. But in small communities—no real limits between "big" and "small" have been fixed—trouble has occurred at the treatment plants (11, 12, 13), presumably due to solvents left in the mash. To deliver the separated mycelium direct to the recipient without purification will usually be impossible, as this would mean that the recipient would be loaded with large quantities of easily decomposed organic substances. Under such circumstances the self-purification capacity of the recipient must be exceptionally high, if serious nuisance is to be avoided. In Britain and the U. S. A., where streams are often heavily loaded with industrial and communal sewage, it has been necessary to dispose of the mycelium by burying or burning (11, 14, 15). The mycelium must be handled quickly and effectively destroyed as it putrifies rapidly and produces an unpleasant odour. Burying and burning are very expensive, and an alternative solution of the problem would be to ferment the mycelium anaerobically, so that the most labile substances would be digested, and the relatively stable residue can be composted with less trouble or may even directed to a good recipient. The gas evolved might serve as a source of energy. The following investigations indicate to what extent such an anaerobic fermentation can be carried under prescribed conditions, the minimum time required for the process, and the amount and composition of the gas evolved.

Table A. Loadings.

In all samples: 25.00 g digested sludge and 75 cc water.

Substance added	None	Fresh sludge g		Mycelium g				
Sample No.	1	2	3	4	5	6	7	8
Days								
0				1.00	1.00[1]	1.00[2]	0.50	0.50
10				1.00	1.00	0.50	0.50	1.00
20		1.00	0.50	1.00	0.50	0.50	1.00	1.00
30				0.50	0.50	1.00	1.00	1.00
40		1.00	1.00	1.00	1.00	1.00	1.00	1.00

[1] + 175 cc water
[2] + 75 cc water

25.00 g digested sludge contains 1.80 g dry substance and 0.87 g ash
1.00 g fresh sludge » 0.97 g » 0.23 g »
1.00 g mycelium » 0.98 g » 0.24 g »

The high ash content of the mycelium arises from the nutrients and precipitants added. The ash consists mainly of alumina and calcium oxide.

Anaerobic digestion takes place by a series of enzyme-catalyed reactions, the enzymes being provided in adequate amounts by the bacteria present during the fermentation. Sugars and other water-soluble substances are most easily attacked, followed by starch, proteins, celluloses and lignin (16, 17). The fermentation processes are very complicated, and little is known of their detailed mechanism. Four methane-producing bacteria have so far been detected and studied in enriched or pure cultures: *Methanosarcina methanica, Metahnococcus Mazéi, Methanobacterium Söhngenii* and *Methanobacterium Omelianskii* (18–22). Stephenson and Stickland have isolated a further organism (23). All are anaerobic and immotile and generally do not attack compounds of high molecular weight directly and must therefore normally live in symbiosis with other saphrophytes. They can utilize ammonia as a source of nitrogen. They are not spore producers in a strict sense, but spore-like formations have been found in which the bacteria is said to be able to survive under aerobic conditions for a considerable time (24).

Technical research has primarily been aimed at finding suitable conditions (appropriate water content, temperature, pH etc.) for the anaerobic fermentation of sludge, more or less loaded with industrial wastes (17, 25, 26). It is considered that the water content should be about 95 % but it may be less, in which case, however, the rate of decomposition will decrease. If the water content is below 70 % this decrease will be considerable (27, 28). The pH should be between 7.0 and 7.5 (29, 30) but normal digestion of sludge has been observed at a pH of 6.4. In peat mosses with a pH of 3.8 methane formation takes place, and in view of this it seems possible that the bacteria are able to adapt themselves to different hydrogen-ion concentrations (25). In the digestion chambers the pH is normally fixed by the bicarbonate equilibrium (17). Opinions are divided as to the most suitable temperature. Some workers have reported that they have

Table B. Yield of gas in cc at NTP per day.

Sample No.	1	2	3	4	5	6	7	8
Days								
1	14.1	16.3	10.4	33.9	32.6	31.2	23.9	21.5
2	28.1	28.3	21.1	50.3	56.4	46.1	54.0	29.1
3	16.6	16.9	12.8	58.7	56.3	59.5	53.8	67.6
4	11.3	9.1	20.3	49.4	44.8	59.2	47.9	52.4
5	7.5	7.4	7.7	43.5	44.7	55.6	28.2	35.4
6	6.3	5.7	6.9	35.0	33.5	28.8	19.0	21.3
7	6.3	6.4	7.0	28.4	32.8	9.1	14.2	12.1
8	3.7	5.5	5.5	17.0	15.5	17.6	11.3	10.2
9	3.8	4.2	3.5	8.9	5.8	10.0	3.9	3.7
10	3.0	2.7	3.1	4.1	2.4	6.4	3.6	3.7
11	1.6	1.6	2.7	83.4	61.1	46.8	44.4	74.7
12	4.8	4.4	5.6	39.0	56.2	27.6	26.2	48.1
13	4.0	3.7	5.2	38.5	18.9	28.6	17.0	36.2
14	3.7	3.7	4.4	49.0	37.0	39.9	20.5	39.4
15	2.9	2.7	2.2	63.5	49.7	12.2	30.4	40.3
16	2.5	2.7	3.0	21.1	21.9	10.2	10.5	21.1
17	2.7	2.1	3.9	17.6	17.5	9.0	8.8	18.9
18	3.0	3.7	3.6	13.0	13.6	9.0	7.4	6.0
19	2.1	1.2	2.0	9.5	12.4	5.8	4.4	9.7
20	2.2	3.0	3.6	14.4	9.1	6.1	6.6	11.3
21	1.8	31.7	18.4	60.0	70.1	23.3	89.0	101.6
22	2.1	28.6	23.3	22.9	43.6	23.5	75.8	114.8
23	2.0	30.3	20.1	46.7	50.1	40.7	93.5	77.2
24	1.6	24.3	13.3	59.6	20.3	34.0	33.1	47.0
25	1.7	27.7	14.7	45.3	14.4	15.3	16.1	26.8
26	1.6	31.3	17.1	26.2	11.7	13.5	12.1	18.1
27	1.8	28.6	14.9	17.6	8.9	8.4	10.2	12.6
28	0.9	23.9	13.1	16.3	7.5	7.9	7.8	9.8
29	1.8	20.1	11.0	9.3	3.6	3.0	4.7	6.9
30	1.7	22.5	11.6	9.5	4.5	4.3	4.3	6.0
31	1.8	22.5	9.8	69.2	59.3	77.6	112.0	99.4
32	1.5	16.5	5.8	25.0	23.3	27.3	35.3	44.0
33	1.6	13.1	5.4	26.2	26.4	30.8	27.5	19.2
34	0.7	12.1	5.2	37.1	15.8	47.3	29.9	14.3
35	0.8	11.6	4.7	17.2	14.9	64.4	73.6	25.9
36	0.5	6.5	4.6	8.0	5.3	17.5	27.4	65.8
37	0.9	9.4	4.5	7.8	8.7	15.6	20.2	25.3
38	1.0	4.4	1.1	5.6	4.5	9.9	11.3	14.9
39	0.8	7.4	3.9	6.5	6.0	9.5	4.5	13.4
40	0.6	3.8	0.3	7.5	4.1	9.7	5.8	8.0
41		39.9	40.3	90.5	106.8	113.3	98.4	111.8
42		32.8	33.9	41.1	93.5	87.9	95.8	53.3
43		32.0	33.8	102.3	73.5	87.8	98.6	39.9
44		30.6	33.2	48.1	23.5	34.7	35.0	58.9
45		28.8	28.6	30.1	18.3	27.4	21.1	76.0
46		21.5	22.2	16.1	14.3	16.4	13.3	25.7
47		20.2	23.6	13.0	11.1	12.0	11.2	16.4
48		19.2	26.4	10.1	8.0	9.7	8.9	13.5
49		17.6	24.9	8.7	6.8	8.8	9.3	11.5
50		15.2	22.3	6.3	6.3	6.1	4.9	7.2
51		13.3	15.6	4.5	5.4	5.4	6.6	6.4
52		12.3	10.0	4.2	4.4	4.9	5.5	6.9
53		12.3	4.4	4.2	4.2	3.7	4.1	6.3
54		12.6	3.0	4.1	3.7	3.6	3.6	5.3

Table B. Yield of gas in cc at NTP per day. (Cont.)

Sample No.	1	2	3	4	5	6	7	8
Days								
55		12.3	3.2	4.2	3.6	3.4	3.7	5.5
56		11.9	3.7	4.1	3.6	5.3	4.8	5.0
57		9.7	3.6	4.0	2.6	4.7	2.1	5.2
58		12.1	3.4	3.9	3.3	4.0	4.5	5.1
59		11.9	3.1	3.5	2.5	2.1	1.8	4.5
60		11.1	3.3	3.6	3.5	3.1	4.5	4.9

Table C. Total yield of gas in cc at NTP.

Sample No.	1	2	3	4	5	6	7	8
Days								
1	14.1	16.3	10.4	33.9	32.6	31.2	23.9	21.5
2	42.2	44.6	31.5	84.2	89.0	77.3	77.9	50.6
3	58.8	61.5	44.3	142.9	145.3	136.8	131.7	118.2
4	70.1	70.6	64.6	192.3	190.1	196.0	179.6	170.6
5	77.6	78.0	72.3	235.8	234.8	251.6	207.8	206.0
6	83.9	83.7	79.2	270.8	268.3	280.4	226.8	227.3
7	90.2	90.1	86.2	299.2	301.1	289.5	241.0	239.4
8	93.9	95.6	91.7	316.2	316.6	307.1	252.3	249.6
9	97.7	99.8	95.2	325.1	322.4	317.1	256.2	253.3
10	100.7	102.5	98.3	329.2	324.8	323.5	259.8	257.0
11	102.3	104.1	101.0	83.4	61.1	46.8	44.4	74.7
12	107.1	108.5	106.6	122.4	117.3	74.4	70.6	122.8
13	111.1	112.2	111.8	160.9	136.2	103.0	87.6	159.0
14	114.8	115.9	116.2	209.9	173.2	142.9	108.1	198.4
15	117.7	118.6	118.4	273.4	222.9	155.1	138.5	238.7
16	120.2	121.3	121.4	294.5	244.8	165.3	149.0	259.8
17	122.9	123.4	125.3	312.1	262.3	174.3	157.8	278.7
18	125.9	127.1	128.9	325.1	275.9	183.3	165.2	284.7
19	128.0	128.3	130.9	334.6	288.3	189.1	169.6	294.4
20	130.2	131.3	134.5	349.0	297.4	195.2	176.2	305.7
21	132.0	31.7	18.4	60.0	70.1	23.3	89.0	101.6
22	134.1	60.3	41.7	82.9	113.7	46.8	164.8	216.4
23	136.1	90.6	61.8	129.6	163.8	87.5	258.3	293.6
24	137.7	114.9	75.1	189.2	184.1	121.5	291.4	340.6
25	139.4	142.6	89.8	234.5	198.5	136.8	307.5	367.4
26	141.0	173.9	106.9	260.7	210.2	150.3	319.6	385.5
27	142.8	202.5	121.8	278.3	219.1	158.7	329.8	398.1
28	143.7	226.4	134.9	294.6	226.6	166.6	337.6	407.9
29	145.5	246.5	145.9	303.9	230.2	169.6	342.3	414.8
30	147.2	269.0	157.5	313.4	234.7	173.9	346.6	420.8
31	149.0	291.5	167.3	69.2	59.3	77.6	112.0	99.4
32	150.5	308.0	173.1	94.2	82.6	104.9	147.3	143.4
33	152.1	321.1	178.5	120.4	109.0	135.7	174.8	162.6
34	152.8	333.2	183.7	157.5	124.7	183.0	204.7	176.9
35	153.6	344.8	188.4	174.7	139.6	247.4	278.3	202.8
36	154.1	351.3	193.0	182.7	144.9	264.9	305.7	268.6
37	155.0	360.7	197.5	190.5	153.6	280.5	325.9	293.9

Table C. Total yield of gas in cc at NTP. (Cont.)

Sample No.	1	2	3	4	5	6	7	8
Days								
38	156.0	365.1	198.6	196.1	158.1	290.4	337.2	308.8
39	156.8	372.5	202.5	202.6	164.1	299.9	341.7	322.2
40	157.4	376.3	202.8	210.1	168.2	309.6	347.5	330.2
41		39.9	40.3	90.5	106.8	113.3	98.4	111.8
42		72.7	74.2	131.6	200.3	201.2	194.2	165.1
43		104.7	108.0	233.9	273.8	289.0	292.8	205.0
44		135.3	141.2	282.0	297.3	323.7	327.8	263.9
45		164.1	169.8	312.1	315.6	351.1	348.9	339.9
46		185.6	192.0	328.2	329.9	367.5	362.2	365.6
47		205.8	215.6	341.2	341.0	379.5	373.4	382.0
48		225.0	242.0	351.3	349.0	389.2	382.3	395.5
49		242.6	266.9	360.0	355.8	398.0	391.6	407.0
50	166.7	257.8	289.2	366.3	362.1	404.1	396.5	414.2
51		271.1	304.8	370.8	367.5	409.5	403.1	420.6
52		283.4	314.8	375.0	371.9	414.4	408.6	427.5
53		295.7	319.2	379.2	376.1	418.1	412.7	433.8
54		308.3	322.2	383.3	379.8	421.7	416.3	439.1
55		320.6	325.4	387.5	383.4	425.1	420.0	444.6
56		332.5	329.1	391.6	387.0	430.4	424.8	449.6
57		342.2	332.7	395.6	389.6	435.1	426.9	454.8
58		354.3	336.1	399.5	392.9	439.1	431.4	459.9
59		366.2	339.2	403.0	395.4	441.2	433.2	464.4
60	170.9	377.3	342.5	406.6	398.9	444.3	437.7	469.3

Table D. Yield of gas at each loading corrected for the effect of the inocculum (Sample 1) in cc at NTP.

Sample No.	2	3	4	5	6	7	8
Days							
1–10	(1.1)	(4.3)	228.5	224.1	222.8	159.1	156.3
11–20			319.5	267.9	165.7	146.7	276.2
21–30	349.1	175.6	296.4	217.7	156.9	329.6	403.8
31–40			199.9	158.0	299.4	377.3	320.0
41–50	363.8	329.0	357.0	352.8	394.8	387.2	404.9
51–60			36.1	32.6	36.0	36.7	50.9
Total	712.9	504.6	1 437.4	1 253.1	1 275.6	1 396.9	1 612.1

found evidence for two main types of methane producers, one mesophile type with a temperature range of about 10° to 45° C and one thermophile type with a range of about 40° to 70° C. Other investigators are of the opinion that the same bacteria can become adapted to different temperatures (25, 31). In modern separate sludge digestors the usual working temperature is between 25° and 35° C. Apart from the relative adaptability of the bacteria, it is common experience that rapid temperature drops (even of a few degrees) or sudden pH-

Table E. Yield of gas in cc at NTP per gram organic substance added.

Sample No.	2	3	4	5	6	7	8	Average
Days								
1–10			309	303	301	430	422	353
11–20			432	362	449	397	373	403
21–30	472	474	400	588	424	445	546	481
31–40			540	427	404	452	432	451
41–50	491	444	482	477	533	523	547	512
51–60			(49)	(44)	(49)	(50)	(69)	(52)
Average	482	459	432	431	422	449	464	440

Table F. The average percentage of CO_2 in the gas during each 10 day period, and during the total time of the investigation.

Sample No.	1	2	3	4	5	6	7	8
Days								
1–10	29.3	27.9	31.8	33.8	34.0	34.5	31.5	31.5
11–20		29.1	31.9	38.7	38.4	36.6	37.7	37.7
21–30		36.9	35.7	40.2	38.0	39.1	39.7	40.5
31–40		36.3	37.6	41.3	39.4	40.0	39.0	40.8
41–50		37.3	37.3	41.2	39.4	41.0	41.9	41.2
51–60		34.6	36.4	41.1	40.0	39.4	40.2	38.4
1–60	29.3	35.3	34.8	38.9	37.4	39.4	38.5	39.1
1–60[1]	—	36.3	37.3	40.0	39.5	39.7	39.5	40.1

[1] Corrected for the effect of the inocculum.

Table G. Variations in pH.

Sample No.	1	2	3	4	5	6	7	8
Days								
1–10	6.8–6.8	6.8–6.8	6.8–6.8	6.8–7.0	6.8–6.7	6.8–6.8	6.8–6.8	6.8–6.8
11–20				7.0–7.0	6.7–6.9	6.8–6.9	6.8–6.9	6.8–6.9
21–30		6.8–6.8	6.8–6.9	7.0–7.0	6.9–6.9	6.9–7.0	6.9–7.1	6.9–7.1
31–40				7.0–7.2	6.9–7.1	7.0–7.1	7.1–7.2	7.1–7.2
41–60		6.8–6.8	6.9–6.9	7.2–7.2	7.1–7.1	7.1–7.2	7.2–7.2	7.2–7.2

changes must be avoided if fermentation is to proceed satisfactorily. The gas evolved consists mainly of methane, carbon dioxide and some hydrogen. Nitrogen gas is formed only in the presence of nitrate or nitrite (32).

This investigation has been made with vacuum-dried mycelium from AB Kabi, Stockholm. The mycelium was mixed with sludge and more mycelium was added every 10th day. For comparison with common sludge under the same conditions, samples of dried fresh sludge were inocculated in the same way and more fresh sludge was added after 20 days. The loading of the digestion vessels is shown

Table H. Nitrogen balance in mg.

Sample No.	1	2	3	4	5	6	7	8
Added:								
Total N.....	54	120	104	177	164	164	164	177
Ammonia-N.	18	18	18	18	18	18	18	18
Remainder:								
Total N.....	53	112	107	168	164	159	167	170
Ammonia-N	19	33	38	117	113	112	119	122

Table 1. Organic substance balance in g.

Sample No.	1	2	3	4	5	6	7	8
Added	0.93	2.41	2.04	4.26	3.89	3.89	3.89	4.26
Remainder	0.62	1.18	1.00	1.90	1.61	1.62	1.49	1.77
Difference	0.31	1.23	1.04	2.36	2.28	2.27	2.40	2.49
Yield of gas ..	0.18	1.02	0.78	1 93	1.68	1.75	1.88	2.14
NH_4HCO_3	0.11	0.19	0.21	0.66	0.64	0.63	0.67	0.69
Total	0.29	1.21	0.99	2.59	2.32	2.38	2.55	2.83

in table A. A sludge digested for about 30 days was used as inocculum. The inocculum itself is tabulated as sample 1. Fermentation took place at a temperature of 32–33° C, the original temperature of the inocculum, and the samples were stirred intermittently for one hour each day. The gas evolved was measured continuously in an all-glass apparatus and was analyzed as soon as sufficient (about 100 cc) had been generated. The pH was checked at the beginning and end of the trial series, and at each new loading of the digestors. The percentage dry weight (at 105° C), the amount of "organic substance" (= loss of ignition) and the amounts of total nitrogen and ammonia nitrogen were determined for the mycelium, fresh sludge and inocculum, and for all samples at the end of the experiment. The results are shown in the following tables.

If the water contents of the samples are estimated from the figures in Table A, they are found to vary between 94 and 99 %. The true water content is, however, considerably lower in the sludge phase and correspondingly higher in the supernatant liquor except during stirring. Usually the sludge phase made up only about 40 % of the total volume, and thus the water content in samples 4, 7 and 8 has certainly been 85 % and probably lower. There does not seem to be any correlation between the water content and the yield of gas. This may be due to a lack of real variation in the water content, or to the fact that no significant correlation exists in the interval concerned.

The volume of gas (Table B–E) evolved during the anaerobic digestion of the mycelium is as large as that obtained from sewage sludge under the same conditions. The reaction proceeds however about twice as fast in the mycelium samples during the time when the major part of the fermentable substance is digested. Tables B and C prove that the speed of the decomposition decreases rapidly after the maximum has been reached. The mycelium samples almost always exhibit two rate maxima due to some lag in the production of available nutrient for the methane bacteria (16, 32, 33, 34). The speed decreases to about one tenth of the maximum after 20 days in the sludge samples, but after only 10 days in the mycelium samples. In the sanitary technique the normal detention time for sludge digestion on the large scale is usually fixed at some 30 days, so the corresponding time for the mycelium can consequently be fixed at about 15 days. During the second ten days of digestion, only about 10 % of the amount of gas evolved during the first ten days will be generated in the mycelium samples. A certain adaptation (specialization) by the bacterial flora to the new nutrient obviously takes place during the first ten days; later variations in the yield of gas may depend on the lags after former loadings. The average of this lag is about 10 % (Table E), and thus the mycelium evolves, on the average, 400 cc of gas per gram organic substance. The variation of the loading is reflected directly by the gas production. The addition of half a gram will give only a little more gas per unit of weight than the addition of one gram as the smaller loading will be used a little more effectively, but there is no reason to suspect that the addition of food has any deleterious effect. Calculated from the tables A and E the averages are 460 and 431 respectively.

The percentage of carbon dioxide (Table F) is somewhat higher in the gas from the mycelium samples than in that from the sludge samples, and this explains the small amount of carbon dioxide evolved initially when the effect of the sludge inocculum is more marked. No hydrogen or nitrogen was detected.

As shown in table G, the pH varied only slightly. The pH was on an average slightly higher in the mycelium samples than in those of the fresh sludge. The decrease in the first period of sample 5 is clearly reflected in the corresponding relatively small values for the gas production.

If the valuse for sample 1 in table H are subtracted from the corresponding values for the samples 2–8, the nitrogen values obtained show that, on the average, about 82 % of the nitrogen in the mycelium samples was converted into ammonia during fermentation, while the corresponding value for the fresh sludge samples is some 29 %. There were only negligible traces of nitrate and nitrite in some samples.

Table I shows the organic substance balance, on the supposition that all the ammonia is present as bicarbonate. The differences between added amounts and remainders are in relatively good agreement with the sums of gas and bicarbonate yielded. The evolved gas represents the real decrease in organic subtsance. This decrease is, on the average, 55 % in the mycelium samples, calculated from the values in table I corrected for the inocculum effect, and 56 % in the sludge samples.

It is evident that mycelium and fresh sludge digest very similarly, so the presence of mycelium will not raise any special problems in a sewage sludge digestor. Treated under suitable conditions 1 000 kg of wasted mycelium containing about 100 kg of organic substance will have some 55 kg of its most labile substance destroyed in 10–15 days and the yield of gas will be about 40 000 liters.

SUMMARY

Vacuum-dried waste mycelium from the production of penicillin was inocculated with sewage sludge on a laboratory scale, and digested anaerobically

at 32–33° C. The easily decomposed substances (about 55 % of the total organic substance) were destroyed in 10 days. The corresponding yiled of gas—methane containing 40 % CO_2—was about 400 cc per gram of organic substance added.

Institutet för organisk kemi och biokemi, Stockholms Högskola, Stockholm.

REFERENCES. 1. **Nilsson, R., Olsson, N.,** and **Nilsson, P. E.,** in *The Svedberg 1884 30/9 1944*, Uppsala 1944, p. 484. — 2. **Tanner, F. W., Pfeiffer, S. E.,** and **van Lanen, J. M.,** *Arch. Biochem.* **8** (1945) 29. — 3. **Savard, K.** and **Grant, G. A.,** *Science* **104** (1946) 459. — 4. **Angelotti, A.** and **Tappi, G.,** *Gazz. chim. ital.* **77** (1947) 112. — 5. **Peltier, G. L.** and **Borchers, R.,** *J. Bact.* **54** (1947) 519. — 6. **Povolotskaya, K. L.** and **Skarabogatova, E. P.,** *Biokhimiya* **12** (1947) 268; *Chem. Abstracts* **41** (1947) 6924 f. — 7. **Tappi, G.,** *Gazz. chim. ital.* **78** (1948) 311. — 8. **Tanner Jr., F. W.** and **van Lanen, J. M.,** *U. S. Patent* **2 449 340** (1948). — 9. **Mense, H. L., Corman, J., van Lanen, J. M.,** and **Langlykke, A. F.,** *J. Bact.* **54** (1947) 149. — 10. **Lynen, F.** and **Hoffmann–Walbeck, H. P.,** *Ann.* **559** (1948) 153. — 11. **Knoedler, E. L.** and **Babcock Jr., S. H.,** *Ind. Eng. Chem.* **39** (1947) 582. — 12. **Mohlman, F. W.,** *Water & Sewage Works* **96** (1949) 43. — 13. **Muss, D. L.,** *Water & Sewage Works* **97** (1950) 253. — 14. **Heukelekian, H.,** *Ind. Eng. Chem.* **41** (1949) 1412, 1535. — 15. **Hilgart, A. A.,** *Sewage and Industrial Wastes* **22** (1950) 207. — 16. **Waksman, S. A.,** *Principles of Soil Microbiology*, Williams & Wilkins, Baltimore 1932. — 17. **Johansson, H.** and **Westberg, N.,** *Tek. Tid. Uppl. E. Väg- och Vattenbyggnadskonst* **69** (1939) 57. — 18. **Söhngen, N. L.,** *Het Ontstaan en Verdwijnen van Waterstof en Methaan*, J. Vis Jr., Delft 1906. — 19. **Barker, H. A.,** *Arch. Mikrobiol.* **7** (1936) 404, 420; *Ibid.* **8** (1937) 415. — 20. —— *J. Biol. Chem.* **137** (1941) 153. — 21. **Buswell, A. M.** and **Sollo, F. W.,** *J. Am. Chem. Soc.* **70** (1948) 1778. — 22. **Stadtman, T. C.** and **Barker, H. A.,** *Arch. Biochem.* **21** (1949) 256. — 23. **Stephenson, M.** and **Stickland, L. N.,** *Biochem. J.* **27** (1933) 1517. — 24. **Giovanni, G. P.,** *Flüssige Abfallstoffe* **24** (1941) 261. — 25. **Wikén, T.,** *IVA* **13** (1942) 178; *Ib.* **19** (1948) 201. — 26. **Buswell, A. M.,** *Sewage Works J.* **19** (1947) 28. — 27. **Keefer, C. F.,** *Sewage Works J.* **19** (1947) 39. — 28. **Liebmann, H.,** *Gesundh.-Ing.* **71** (1950) 14, 56. — 29. **Griffin, G. E.,** *Sewage Works J.* **14** (1942) 170. — 30. **Walker, D.,** *Sewage Works J.* **20** (1948) 544. — 31. **Kluyver, A. J.** and **Baars, J. K.,** *Proc. Koninkl. Akad. Wetenschap. Amsterdam* **35** (1932) 370. — 32. **Viehl, K.,** *Gesundh.-Ing.* **64** (1941) 438. — 33. **Bach, H., Sierp, F.,** *Zentr. Bakt. Parasitenk. Abt. II* **62** (1924) 24. — 34. **Foster, J. W.,** *Chemical Activities of Fungi*, Academic Press Inc., New York 1949.

Tryckt den 25 oktober 1952

Uppsala 1952. Almqvist & Wiksells Boktryckeri AB

ARKIV FÖR KEMI Band 5 nr 2

Communicated 4 June 1952 by Arne Fredga

An investigation of S-alkyl-*iso*-thiuronium picrates and styphnates

By Lennart Schotte

With 1 figure in the text

It is already well known that S-alkyl-*iso*-thiuronium picrates are excellent derivatives for characterization of alkyl halides (1, 2 and 3), and a number of melting points of different salts of this type are to be found in the relevant literature (2, 4 and 5). However, the statements in sources (4) and (5) differ somewhat, and this investigation is thus of a completive and deciding character. Some new derivatives have also been prepared.

Table 1

Melting points of some S-alkyl- and two S-aryl-*iso*-thiuronium picrates and styphnates

Radical	Picrates according to			Styphnates according to the author
	(4)	(5)	the author	
Methyl	224°	224°	224°	226° d.
Ethyl	188°	188°	188°	179°
n-Propyl	181°	177°	177°	161°
iso-Propyl	148°	196°	196°	187°
n-Butyl	180°	177°	177°	164°
iso-Butyl	174°	167°	167°	150°
sec.-Butyl	190°	166°	166°	163°
tert.-Butyl	—	—	148° d.	151°
n-Amyl	154°	154°	155°	147°
Iso-Amyl	179°	173°	173°	159°
2-Amyl	—	—	155°	112°
3-Amyl	—	—	159°	114°
tert.-Amyl	—	—	127° d.	124° d.
n-Hexyl	157°	157°	157°	153°
iso-Hexyl	—	—	147°	144°
n-Heptyl	—	142°	143°	144°
n-Octyl	—	134°	134°	122°
Allyl	155°	155°	155°	154°
Benzyl	188°	—	187°	190°
p-Nitrobenzyl	—	—	205°	166°

It is evident from Table 1 that the results of this investigation agree completely with those of LEVY and CAMPBELL (4 and cf. also 2). A closer study of the different tabulated values shows that some alkyl halides have derivatives with nearly the same melting points. This is of course unsatisfactory for analytical purposes, and in order to obtain an alternative possibility for characterizing the halogen compound in such cases the S-alkyl-*iso*-thiuronium styphnates were prepared. Descriptions of these salts have not previously been published, and they are formed according to:

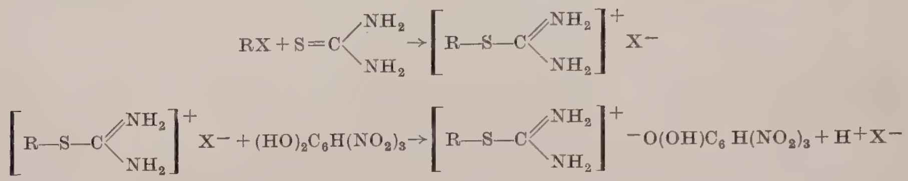

$$RX + S{=}C\begin{matrix}\diagup NH_2\\ \diagdown NH_2\end{matrix} \rightarrow \left[R{-}S{-}C\begin{matrix}\diagup\!\!\diagup NH_2\\ \diagdown NH_2\end{matrix}\right]^+ X^-$$

$$\left[R{-}S{-}C\begin{matrix}\diagup\!\!\diagup NH_2\\ \diagdown NH_2\end{matrix}\right]^+ X^- + (HO)_2C_6H(NO_2)_3 \rightarrow \left[R{-}S{-}C\begin{matrix}\diagup\!\!\diagup NH_2\\ \diagdown NH_2\end{matrix}\right]^+ {}^-O(OH)C_6\,H(NO_2)_3 + H^+X^-$$

where RX is the alkyl halide. Good yields of the styphnates are obtained, and they are highly crystalline solids possessing sharp melting points distributed over a wide range of temperature, and so they may be used with advantage in analysis as derivatives of alkyl halides. A list of the melting points is given in Table 1.

It is of particular interest to discuss more thoroughly the anomalous results of the reactions between a tertiary halide and thiourea. WILD has stated (2) that the attempts to obtain tertiary alkyl derivatives have failed because of reactions with the solvent, ethyl or methyl alcohol. The author has now prepared both the picrates

Table 2

Reaction time for the different halides in reaction with thiourea

Radical	Reaction time in minutes		
	Chloride	Bromide	Iodide
Methyl	15	15	5
Ethyl	15	15	5
n-Propyl	—	15	5
iso-Propyl	300	180	130
n-Butyl	180	20	5
iso-Butyl	—	120	20
sec.-Butyl	300	120	60
tert.-Butyl	—	270	—
n-Amyl	240	120	—
iso-Amyl	240	—	45
2-Amyl	—	200	—
3-Amyl	—	180	—
tert.-Amyl	—	270	—
n-Hexyl	—	—	20
iso-Hexyl	—	—	30
n-Heptyl	—	60	20
n-Octyl	—	—	20
Allyl	15	10	—
Benzyl	20	15	—
p-Nitrobenzyl	—	15	—

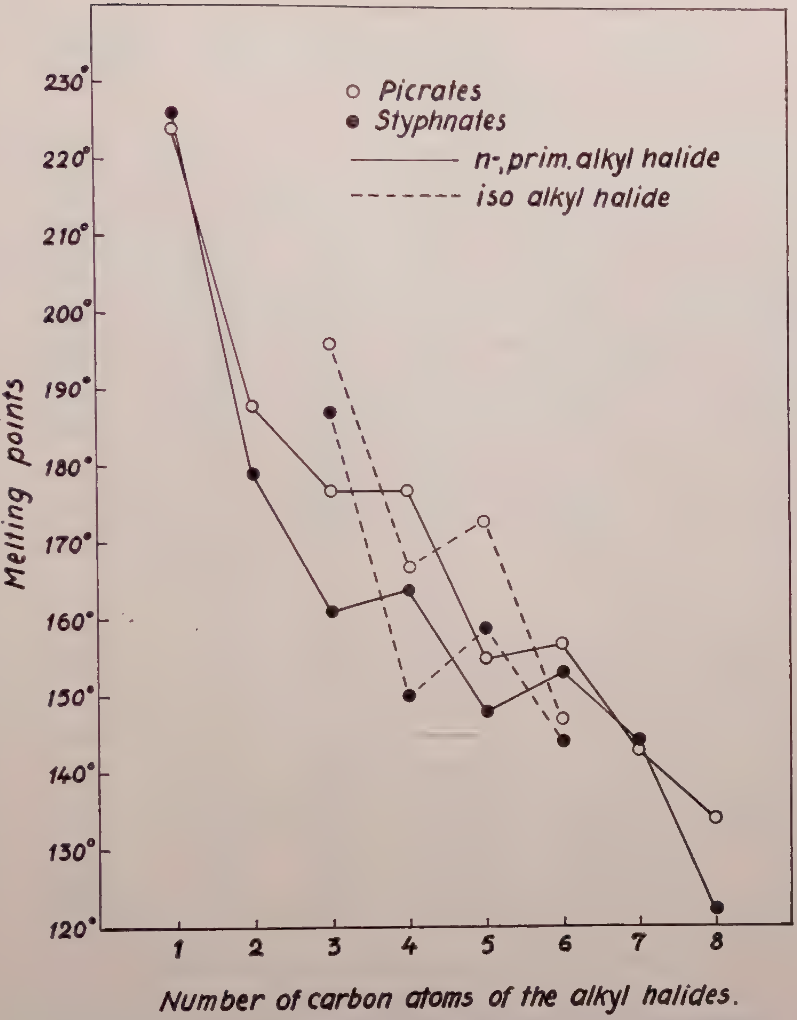

Fig. 1. Melting points of S-alkyl-*iso*-thiuronium picrates and styphnates.

and styphnates of *tert.*-butyl and *tert.*-amyl-*iso*-thiourea by using the corresponding tertiary alcohols as solvents, but the importance of this reaction from an analytical point of view is of course doubtful. However, the results is obviously of theoretical interest, as it may throw light upon the mechanism of the reaction in question.

Tertiary alkyl halides react according to a S_1-mechanism, *i.e.* a first order substitution reaction with the solvent, yielding *tert.*-butanol and the alkyl halogenide corresponding to the solvent alcohol. This reaction is very rapid. The alkyl compound formed then substitutes the thiourea, probably in a S_2-reaction, *i.e.* a second order substitution reaction. If the solvent is the corresponding tertiary alcohol, on the other hand, the S_1-reaction with the solvent is prevented or only leads to an exchange of radicals of the same kind, and the *tert.*-alkyl halide will react with thiourea ac-

Table 3

Nitrogen analysis of the salts by the DUMAS method

Radical	mg. subst.	ml N_2	t°	pcorr.	N (in %)	
					found	calc.
a) Styphnates						
Methyl	48.2	8.72	23.0	753.1	20.81	20.89
Ethyl	57.4	10.00	23.0	753.6	20.08	20.06
n-Propyl	50.4	8.45	23.2	752.5	19.28	19.28
iso-Propyl	63.7	10.76	24.2	744.3	19.15	19.28
n-Butyl	39.8	6.40	19.5	747.5	18.60	18.57
iso-Butyl	68.3	11.10	23.6	747.8	18.53	18.57
sec.-Butyl	61.2	10.02	23.0	738.8	18.50	18.57
tert.-Butyl	59.2	9.28	17.8	761.4	18.58	18.57
n-Amyl	61.3	9.58	23.6	750.6	17.90	17.90
iso-Amyl	65.1	10.15	23.3	748.8	17.84	17.90
2-Amyl	60.3	9.28	19.4	749.0	17.85	17.90
3-Amyl	64.4	9.81	20.3	759.0	17.85	17.90
tert.-Amyl	60.4	9.40	20.8	745.5	17.88	17.90
n-Hexyl	61.0	9.34	24.2	745.6	17.39	17.28
iso-Hexyl	65.4	9.67	19.2	748.4	17.15	17.28
n-Heptyl	63.0	9.34	24.0	743.6	16.81	16.71
n-Octyl	71.1	9.92	23.0	754.1	16.09	16.16
Allyl	58.9	10.76	24.1	742.7	19.49	19.39
Benzyl	65.6	9.55	19.6	749.9	16.89	17.03
p-Nitrobenzyl	64.0	10.30	23.0	748.2	18.42	18.42
b) Picrates						
tert.-Butyl	64.0	10.56	18.6	754.3	19.32	19.39
2-Amyl	60.2	9.82	20.9	745.2	18.72	18.67
3-Amyl	60.7	9.65	18.8	749.4	18.73	18.67
tert.-Amyl	60.5	9.72	19.0	744.2	18.54	18.67
iso-Hexyl	60.8	9.35	19.4	748.6	17.83	18.00
Benzyl	58.8	9.02	20.8	747.7	17.67	17.71
p-Nitrobenzyl	60.4	10.04	20.5	744.7	19.10	19.09

cording to a S_1-reaction. This reaction must of course be slower than the one mentioned above with a solvent such as ethyl alcohol, and also much slower than the assumed S_2-reaction of a primary halogenide with thiourea. Thus the resulting thiourea derivatives vary with the solvents in the tertiary cases because of the different velocities of the respective reactions.

A very approximate comparison between the different reaction velocities of the iodides, bromides and chlorides respectively is given in Table 2, and the combustion analyses (nitrogen determination by the DUMAS method) are collected in Table 3. — In Fig. 1 the variation of the melting points of S-alkyl-*iso*-thiuronium picrates and styphnates with the number of carbon atoms in the alkyl halides is given, and the alternate effect is rather obvious in the part between C_2H_5 and C_7H_{15}. It may also be observed that the melting points of the *iso*-compounds vary in a similar manner.

It is worth mentioning that experiments to obtain analogous salts from the alkyl-*iso*-thiourea compounds with 2.4-dinitrophenol and 2.4-dinitroresorcinol have failed in every solvent tried.

Experimental

S-Alkyl-*iso*-thiuronium styphnates

A mixture of 1 g of finely powdered thiourea, 1 ml of the alkyl halide and 15 ml of alcohol was placed in a small flask equipped with a reflux condenser. The mixture was refluxed for a period which depended upon the nature of the halide. (Cf. Table 2.) 1 g. of styphnic acid was then added, the solution was boiled until a clear solution was obtained and was allowed to stand over-night. If no precipitate appeared, some water was added. The resulting S-alkyl-*iso*-thiuronium styphnates were recrystallized from mixtures of water and alcohol and in some cases from pure alcohol. The melting points are well defined and decompositions have only been observed for tertiary alkyl derivatives. Unfortunately, the solubilities of the different homologues are usually too similar for an easily performed isolation by fractionated crystallization to be possible. — The yield is 70–80 %.

In addition to the alkyl derivatives listed in Table 1 the benzyl- and p-nitrobenzyl-*iso*-thiuronium picrates and styphnates have been prepared.

The reaction time for the alkyl chlorides is shortened by adding some potassium iodide to the reaction mixture.

The alkyl halides used

n-Hexyl-, *n-heptyl-* and *n-octyl iodide* were prepared from the corresponding alcohols (commercial products) and iodine and phosphorus.

iso-Hexyl iodide was prepared in the same way. The alcohol was obtained by reduction of ethyl *iso*-caproate with sodium and alcohol.

2-Bromo-pentane was obtained from pentanol-2 and PBr_3. The alcohol was synthesized by reduction of methyl *n*-propyl ketone with sodium and water.

3-Bromo-pentane was prepared according to the method mentioned above. Pentanol-3 was obtained by reduction of diethyl ketone with sodium and water.

tert.-Amyl bromide was prepared from *tert.*-butanol and hydrobromic acid in the prescence of sulfuric acid.

The other alkyl halides used were all commercial products.

The author is indebted to Fil. mag. BENGT NYGÅRD, Fil. mag. ÅKE SVENSSON, Fil. mag. MÄRTA TENOW, Fil. mag. LARS LINDQVIST, Fil. mag. GUNNAR JACOBSSON, Fil. mag. STIG HERBERTSON, Fil. mag. BO MAGNUSSON, Fil. kand. SALO GRONOWITZ, who have carried out a part of the experimental work of this investigation as student work under the supervision of the author and to Mr RAGNAR ÖBERG for most of the analyses.

SUMMARY

A number of S-alkyl-*iso*-thiuronium picrates and styphnates have been prepared. An explanation of the observed complications for tertiary alkyl halides is given.

Laboratory of Organic Chemistry, Chemical Institute, University of Uppsala, May 1952.

REFERENCES. 1. **R. L. Shriner** and **R. C. Fuson,** The Systematic Identifications of Organic Compounds, p. 159, New York (1945). — 2. **F. Wild,** Characterisation of Organic Compounds, p. 42 and 48, Cambridge (1947). — 3. **A. I. Vogel,** A Textbook of Practical Organic Chemistry, p. 290, London (1948). — 4. **E. L. Brown** and **N. Campbell,** J. Chem. Soc. (London) *1937,* 1699. — 5. **W. J. Levy** and **N. Campbell,** J. Chem. Soc. (London) *1939,* 1442.

Tryckt den 25 oktober 1952

Uppsala 1952. Almqvist & Wiksells Boktryckeri AB

ARKIV FÖR KEMI Band 5 nr 3

Communicated 27 February 1952 by Arne Fredga and Karl Myrbäck

---

On the conditions for the formation of quasi-racemic compounds.

II.[1] Alkylsuccinic acids and S-alkylmercaptosuccinic acids

By Magnus Matell

With 34 figures in the text

Introduction. Choice of methods

In an earlier paper (1) the present author pointed out that the experimental work, usually involved in establishing steric relationships using the method of quasi-racemates (2, 3) may be reduced if the conditions leading to the formation of such compounds are known. With this end in view the author in the years 1948–1950 studied these and related problems in two homologous series of substituted succinic acids which seemed suited to an investigation of this kind. The compounds were *n*-alkylsuccinic acids (I) and S–*n*–alkylmercaptosuccinic (alkylsulfidesuccinic) acids (II).

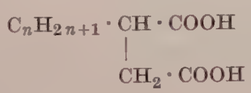

$$\begin{array}{ll} C_nH_{2n+1}\cdot & CH\cdot COOH \\ & | \\ & CH_2\cdot COOH \end{array}$$

I

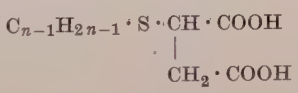

$$\begin{array}{ll} C_{n-1}H_{2n-1}\cdot S\cdot & CH\cdot COOH \\ & | \\ & CH_2\cdot COOH \end{array}$$

II

In these formulas $n = 1, 2, \ldots, 6$.

The results are given in tables 1–28 and fig. 5, 6, 8, 9, 11, 12, 14–18, 20–24, 26–33. In the tables and some of the figures -succinic acid is abbreviated -SA.

Some two-component systems made up of lower members of these series have already been described in the literature (1, 3, 4, 5). For the sake of completeness these systems (fig. 1–4, 7, 10, 13, 19, 25) are discussed together with the results of the present investigation.

Professor Arne Fredga, who suggested this investigation, was kind enough to provide the inactive, (+)- and (—)-forms of the alkylsuccinic acids and the inactive and (+)-forms of the sulfur compounds. (—)-S-propylmercaptosuccinic acid was prepared in connection with a similar work (1).

---

[1] First communication: Arkiv kemi *3* (nr 17), 129 (1951).

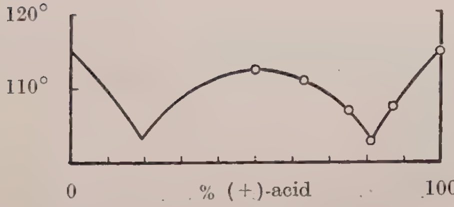

Fig. 1.

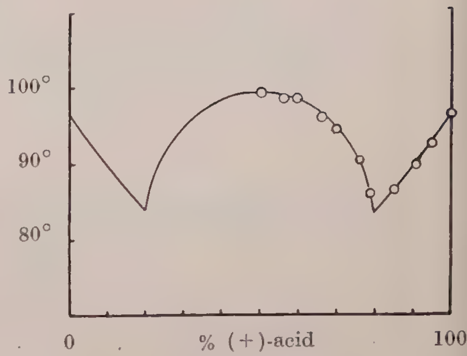

Fig. 2.

Fig. 1. (+)- and (−)-methylsuccinic acid. Berner *et al.* (5).
Fig. 2. (+)- and (−)-ethylsuccinic acid. Fredga (3).

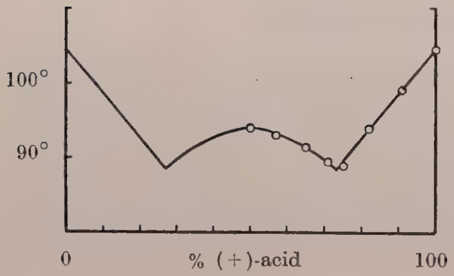

Fig. 3.

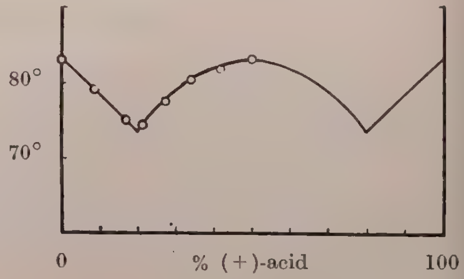

Fig. 4.

Fig. 3. (+)- and (−)-propylsuccinic acid. Fredga (3).
Fig. 4. (+)- and (−)-butylsuccinic acid. Fredga (3).

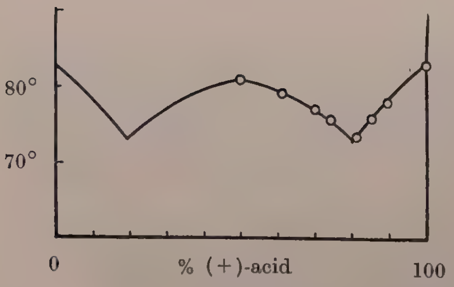

Fig. 5.

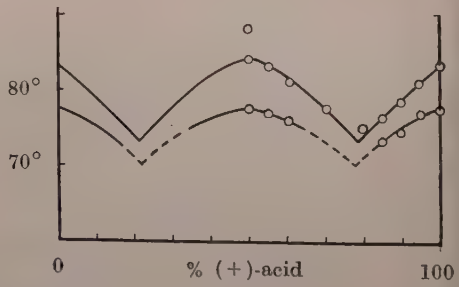

Fig. 6.

Fig. 5. (+)- and (−)-pentylsuccinic acid.
Fig. 6. (+)- and (−)-hexylsuccinic acid.

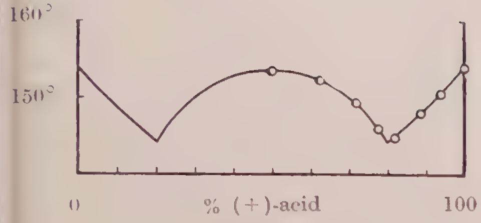

Fig. 7.

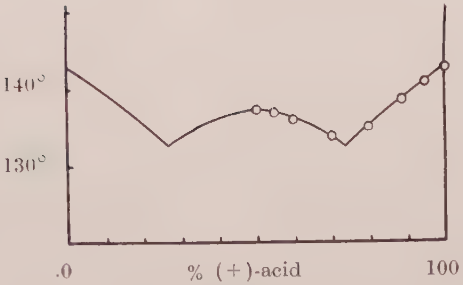

Fig. 8.

Fig. 7. (+)- and (−)-mercaptosuccinic acid. FREDGA (4).
Fig. 8. (+)- and (—)-methylsulfidesuccinic acid.

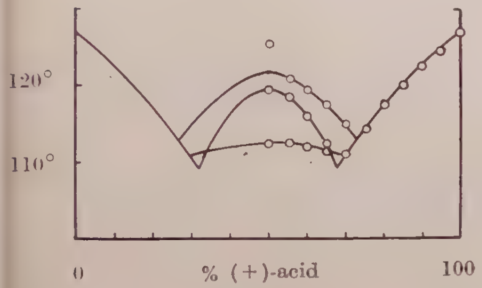

Fig. 9.

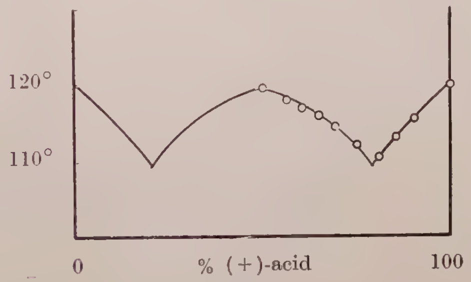

Fig. 10.

Fig. 9. (+)- and (−)-ethylsulfidesuccinic acid.
Fig. 10. (+)- and (−)-propylsulfidesuccinic acid. MATELL (1).

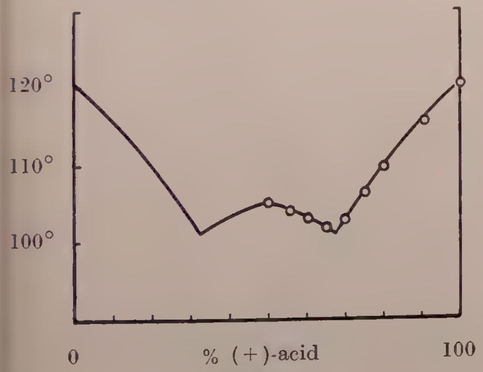

Fig. 11.

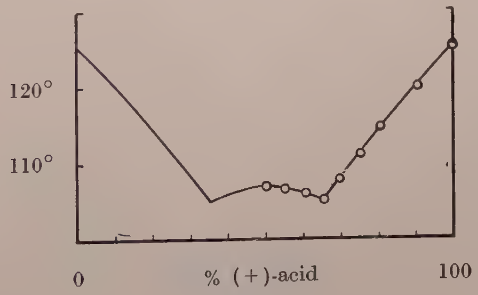

Fig. 12.

Fig. 11. (+)- and (−)-butylsulfidesuccinic acid.
Fig. 12. (+)- and (−)-pentylsulfidesuccinic acid.

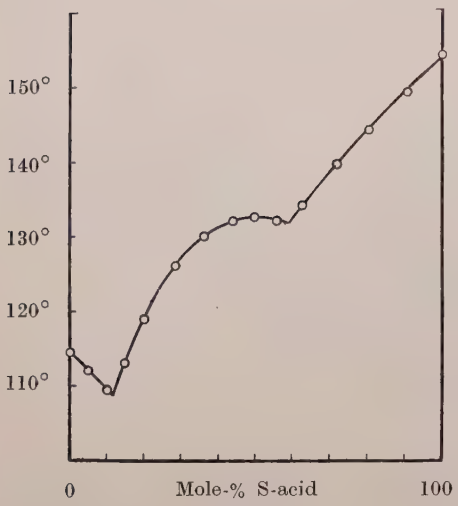

Fig. 13.

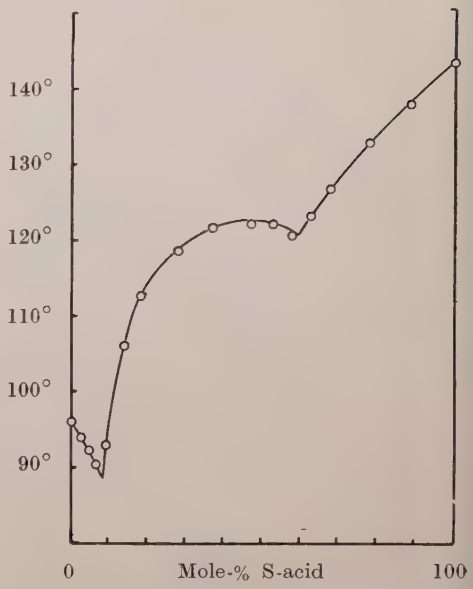

Fig. 14.

Fig 13. (−)-Methylsuccinic acid and (+)-mercaptosuccinic acid. FREDGA (4).
Fig. 14. (−)-Ethylsuccinic acid and (+)-methylsulfidesuccinic acid.

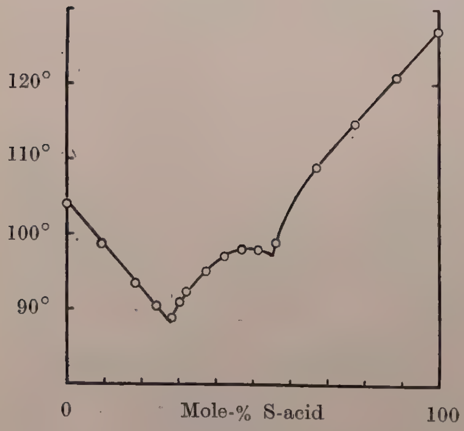

Fig. 15.

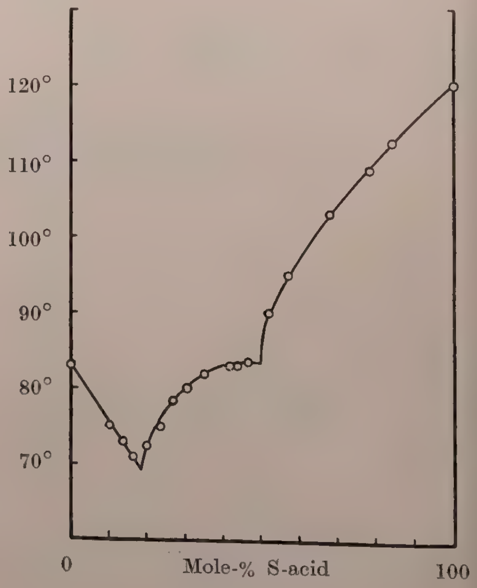

Fig. 16.

Fig. 15. (−)-Propylsuccinic acid and (+)-ethylsulfidesuccinic acid.
Fig. 16. (−)-Butylsuccinic acid and (+)-propylsulfidesuccinic acid.

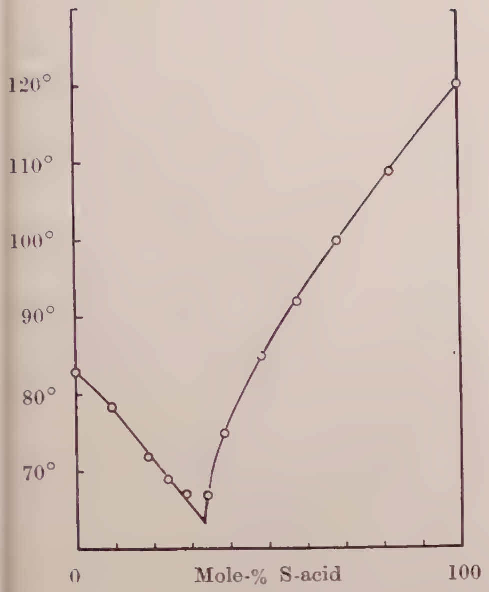

Fig. 17.

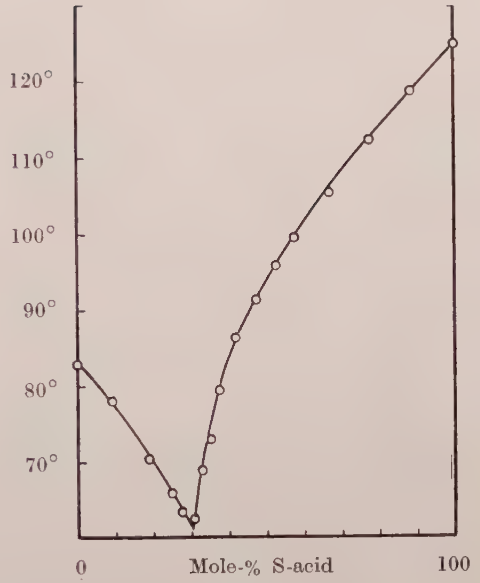

Fig. 18.

Fig. 17. (−)-Pentylsuccinic acid and (+)-butylsulfidesuccinic acid.
Fig. 18. (−)-Hexylsuccinic acid and (+)-pentylsulfidesuccinic acid.

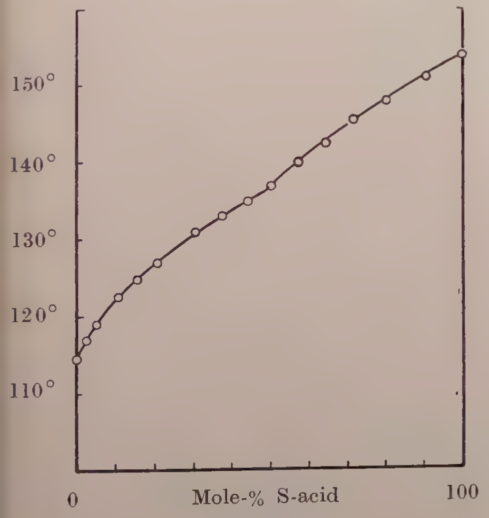

Fig. 19.

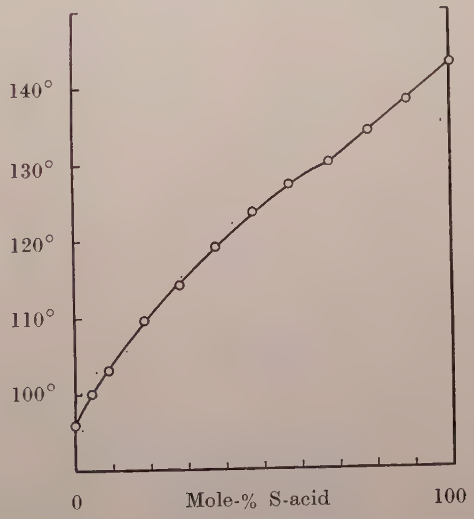

Fig. 20.

Fig. 19. (+)-Methylsuccinic acid and (+)-mercaptosuccinic acid. Fredga (4).
Fig. 20. (+)-Ethylsuccinic acid and (+)-methylsulfidesuccinic acid.

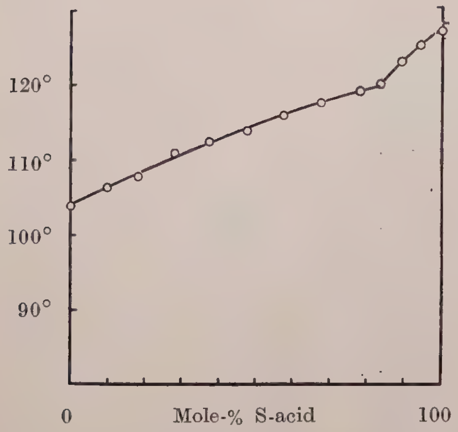

Fig. 21.

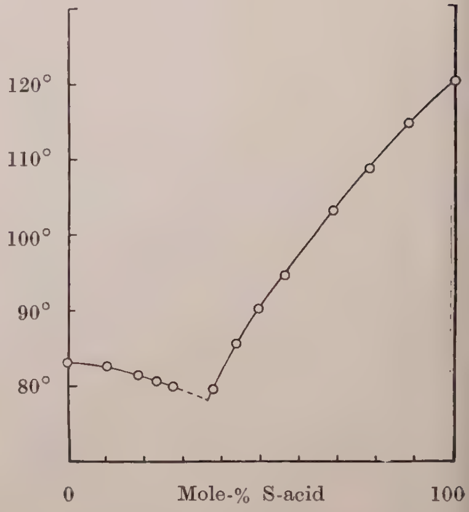

Fig. 22.

Fig. 21. (+)-Propylsuccinic acid and (+)-ethylsulfidesuccinic acid.
Fig. 22. (+)-Butylsuccinic acid and (+)-propylsulfidesuccinic acid.

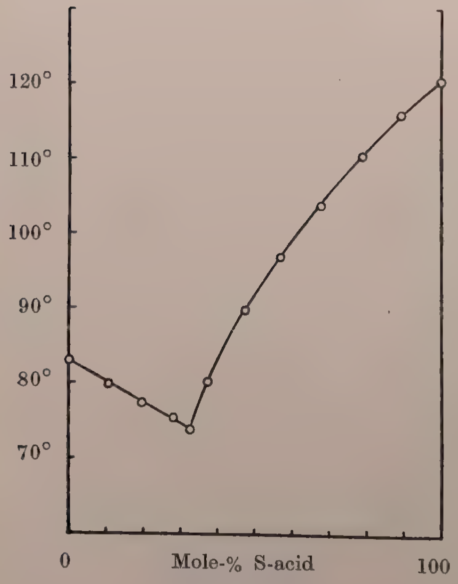

Fig. 23.

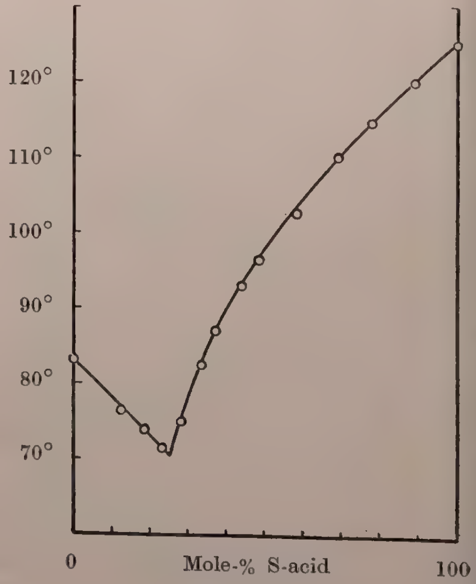

Fig. 24.

Fig. 23. (+)-Pentylsuccinic acid and (+)-butylsulfidesuccinic acid.
Fig. 24. (+)-Hexylsuccinic acid and (+)-pentylsulfidesuccinic acid.

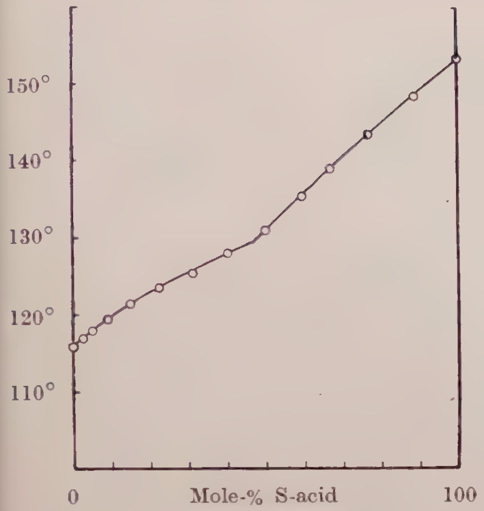

Fig. 25.

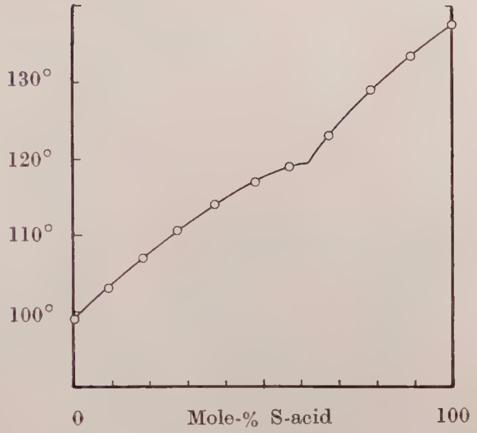

Fig. 26.

Fig. 25. *rac.*-Methylsuccinic acid and *rac.*-mercaptosuccinic acid. FREDGA (4).
Fig. 26. *rac.*-Ethylsuccinic acid and *rac.*-methylsulfidesuccinic acid.

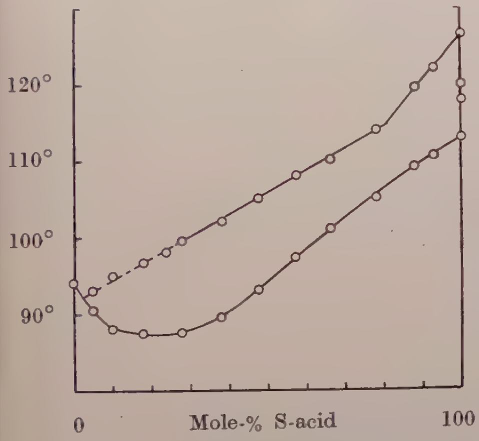

Fig. 27.

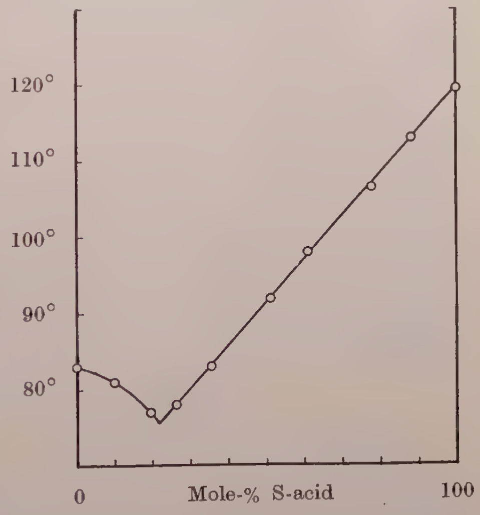

Fig. 28.

Fig. 27. *rac.*-Propylsuccinic acid and *rac.*-ethylsulfidesuccinic acid.
Fig. 28. *rac.*-Butylsuccinic acid and *rac.*-propylsulfidesuccinic acid.

The existence of a quasi-racemic compound is usually demonstrated by means of a melting point diagram. At this institute such diagrams were obtained earlier according to RHEINBOLDT (6). This method, however, is rather time-consuming and much work may be in vain if the components fail to form a quasi-racemate.

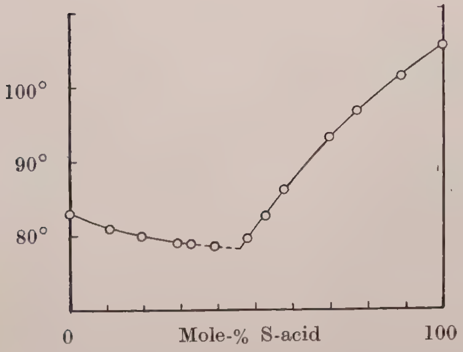

Fig. 29.

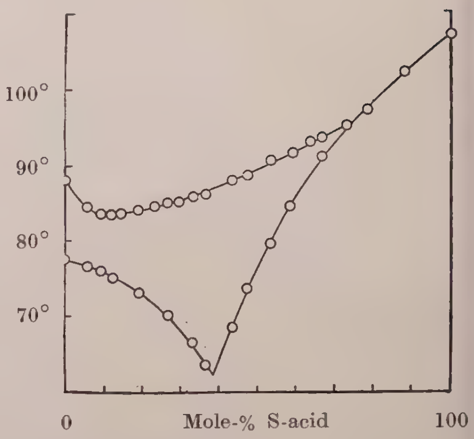

Fig. 30.

Fig. 29. *rac.*-Pentylsuccinic acid and *rac.*-butylsulfidesuccinic acid.
Fig. 30. *rac.*-Hexylsuccinic acid and *rac.*-pentylsulfidesuccinic acid.

In the present investigation part of the thermal analysis was performed in this manner but the microscopical methods of Kofler (7) were applied as well. By means of the contact method (8) a molecular compound can be detected in a few minutes with the consumption of about 0.5 mg of each component. After such a preliminary examination the more laborious method may be used to prove that the molecular compound is in the ratio 1 : 1.

A more comprehensive discussion of the usefulness of the microscopical methods for these problems is found elsewhere (9). In those cases where systems were studied with both methods good agreement was found. This appears from a comparison between fig. 13–30 and table 28.

In most cases the determination of the melting point curves did not involve any serious difficulties. For some of the mixtures, however, it was very difficult owing to the optical properties of the crystals or to poor tendency to crystallize. For this reason parts of the curves in fig. 22, 27 and 29 have been shown by a broken line.

Quasi-racemates and true racemates

According to Fredga one of the conditions leading to quasi-racemic compounds is that at least one of the components has a pronounced tendency to form a true racemate (10). This tendency may be roughly measured by the difference in melting points of the racemic compound and the enantiomorphs or by the extent of the branch of the melting point curve between the two eutectics. From fig. 1–12 it is evident that none of the compounds under investigation has such a very pronounced tendency. Still some conclusions on this question may be drawn from the experiments. If the curves in fig. 2 and 14 are compared with the corresponding diagrams of the other systems it is striking that in the case where one of the components (ethylsuccinic acid) has a more pronounced tendency to form a true racemic compound than any of the other components, the quasi-racemate is also manifested through a more pronounced maximum. On the other hand, in the two cases where no quasi-racemic compound could be detected (fig. 17, 18) one of the components has a rather small racemate formation tendency (fig. 11, 12). This result together with earlier observations supports the assumption that the formation of a quasi-racemate is more probable when one of the components or both have a great tendency to form a true racemate.

Isomorphism

A quasi-racemic compound may be regarded as a true racemic compound in which a small structural change has been introduced in one of the components. According to LETTRÉ the components fail to form a quasi-racemic compound if this structural difference exceeds the limits of isomorphous exchangeability (11, 12). This condition surely is too rigidly formulated as there are several cases known where the components with the same configuration are not isomorphous while those with opposite configurations form a quasi-racemic compound (3). It is probable, however, that the formation of a quasi-racemate is favoured if the components with the same configuration can form solid solutions. This can be seen in fig. 19–24. In the two higher pairs of homologues, where no quasi-racemic compounds have been found, the components with the same direction of optical rotation form simple eutectic systems while in the three lower pairs of homologues where quasi-racemates exist, the corresponding components show considerable mutual solubility in the solid state. The curve in fig. 22 is, as was mentioned in the introduction, a little uncertain but it probably represents a transition to the higher systems.

If the optically active compounds d and d′ are isomorphous their enantiomorphs of course are isomorphous too. According to LETTRÉ it is then reasonable to suppose that this applies to the racemates d,l and d,′l′ as well (11). In the systems investigated here the behaviour of the racemates generally resembles that of the optically active compounds with the same direction of rotation, which can be seen if fig. 19–24 are compared with fig. 25–30. This conformity to LETTRÉ's statement is disturbed by the system in fig. 30 which seems to be an exception, showing that this rule must be applied with care.

It should finally be pointed out that the compounds investigated here are anomalous in one respect. As a rule, isomorphism is less probable among the lower members of homologous series while here the contrary is valid.

Structural factors

It has been shown that the S-atom and the CH_2-group can replace each other isomorphously (4, 13). Consequently, two components with opposite configurations and structurally identical except for the replacement of a CH_2-group in the one by an S-atom in the other may be expected to give a quasi-racemic compound. The failure of the two higher pairs of homologues to give such compound is a little unexpected. It might be explained by a difference in the valency angles of the C-atom and the S-atom. The resulting difference in the space requirements of the molecules must increase with increasing length of the side chain. The angle at the S-atom in an open chain is, in contrast to the C-atom angle, not constant and no determination of this angle in compounds similar to the alkylsulfidesuccinic acids has been published. The theoretical value of the valency angle of the S-atom is 90° (14). This angle increases with the size of the substituents and is *e. g.* for the compound $CH_3{\cdot}S{\cdot}S{\cdot}CH_3$ 107° ± 3° and for $C_6H_5{\cdot}S{\cdot}S{\cdot}C_6H_5$ 113° ± 3° (15). If in the actual succinic acids the angle is intermediate between these values and the angle at the C-atom has its normal value, 109°.5, the difference will not exceed 6°.5. However, no definite conclusions can be drawn and this question must be unanswered for the present.

In order to study the influence of structural differences on the formation of quasi-racemates further, several systems were investigated by means of the contact method. In these systems both the components belonged to the same homologous series and the structural differences thus consisted of one or several CH_2-groups. It was found that (—)-propylsulfidesuccinic acid gave molecular compounds with all the other alkylsulfidesuccinic acids with opposite direction of rotation. As the corresponding acids with the same sign of optical rotation did not give molecular compounds it is most probable that these molecular compounds are quasi-racemic (table 1). It is remarkable that even as large differences between the components as two CH_2-groups do not prevent the formation of quasi-racemates. This experiment indicates that the S-atom in itself is not unfavourable for the quasi-racemate formation. It is thus probable that some difference between the S-atom and the CH_2-group is the main reason for the failure of quasi-racemates to appear in the systems in fig. 17 and 18.

A number of systems where both components were alkylsuccinic acids have been studied too. The results of this experiment are collected in table 2. These results together with some earlier results of FREDGA (3) are summarized in fig. 31. No molecular compound could be detected between (+)-ethylsuccinic acid and (—)-butylsuccinic acid by the contact method. PORATH, however, using the method of RHEINBOLDT, found a molecular compound in the ratio 1 : 1 in this system (16). This does not mean that either result must be wrong. The probable explanation is that the molecular compound has a poor tendency to

Table 1

Thermal data obtained by the contact method. Alkylsulfidesuccinic acids

(From fig. 34 the meaning of t_1—t_5 is clear)

Component 1	Component 2	t_1 (°C)	t_2 (°C)	t_3 (°C)	t_4 (°C)	t_5 (°C)
(−)-Propylsulfide-SA	(+)-Mercapto-SA	119.5	108	118	115	153
(−)- »	(+)-Methylsulfide-SA	119.5	108	119.5	117.5	145
(−)- »	(+)-Ethylsulfide-SA	119.5	101	105	100	126.5
(−)- »	(+)-Butylsulfide-SA	119.5	99	107	101	121
(−)- »	(+)-Pentylsulfide-SA	119.5	101	105	101	125
(+)- »	(+)-Mercapto-SA	121	Minimum 93°			145
(+)- »	(+)-Methylsulfide-SA	121	93			145
(+)- »	(+)-Ethylsulfide-SA	121	Minimum 98°			118
(+)- »	(+)-Butylsulfide-SA	121	Minimum 112°			121
(+)- »	(+)-Pentylsulfide-SA	121	Minimum 111°			125

Table 2

Thermal data obtained by the contact method. Alkylsuccinic acids

(From fig. 34 the meaning of t_1—t_5 is clear)

Component 1	Component 2	t_1 (°C)	t_2 (°C)	t_3 (°C)	t_4 (°C)	t_5 (°C)
(+)-Methyl-SA	(−)-Pentyl-SA	115	58			83
(+)- »	(−)-Hexyl-SA	115	69			83
(+)-Ethyl-SA	(−)-Propyl-SA	97	68.5	70.5	69.5	105
(+)- »	(−)-Butyl-SA	97	37			84
(+)- »	(−)-Pentyl-SA	97	40			83
(+)- »	(−)-Hexyl-SA	97	43			83
(+)-Propyl-SA.....	(−)-Butyl-SA	105	67	71	60	84
(+)- »	(−)-Pentyl-SA	105	49			83
(+)- »	(−)-Hexyl-SA	105	48.5			83
(+)-Butyl-SA	(−)-Pentyl-SA	84	57	63.5	60	83
(+)- »	(−)-Hexyl-SA	84	41			83
(+)-Pentyl-SA.....	(−)- »	83	65	67	65	83

crystallize. In the contact method the compound has to crystallize spontanously from the supercooled melt while in the RHEINBOLDT method crystallization can be initiated by scratching. For this reason a molecular compound has been ascribed to the system ethylsuccinic acid—butylsuccinic acid.

Also among this type of compounds very great structural differences, up to three CH_2-groups, can exist between the components of a quasiracemate. This, however, holds only for the lower homologues and the sudden decrease in quasiracemate formation when the substituent exceeds the C_4H_9-group is strikingly similar to the conditions of the system in fig. 13–18.

According to TIMMERMANS *et al.* (+)-propylsuccinic acid and (—)-hexylsuccinic acid can form a molecular compound 1 : 1 (17). As the contact method showed a simple eutectic system for these acids (table 2) the melting point curve was determined according to RHEINBOLDT. The diagram in fig. 32 is in good agreement with this result. Now the (—)-hexylsuccinic acid used by TIMMERMANS only contained 70 % of active acid while the other component

-SA	CH_3—	C_2H_5—	C_3H_7—	C_4H_9—	C_5H_{11}—	C_6H_{13}—
CH_3—	rac.	+	+	+	—	—
C_2H_5—	+	rac.	+	+	—	—
C_3H_7—	+	+	rac.	+	—	—
C_4H_9—	+	+	+	rac.	+	—
C_5H_{11}—	—	—	—	—	rac.	+
C_6H_{13}—	—	—	—	—	+	rac.

Fig. 31. Molecular compounds (+) between alkylsuccinic acids.

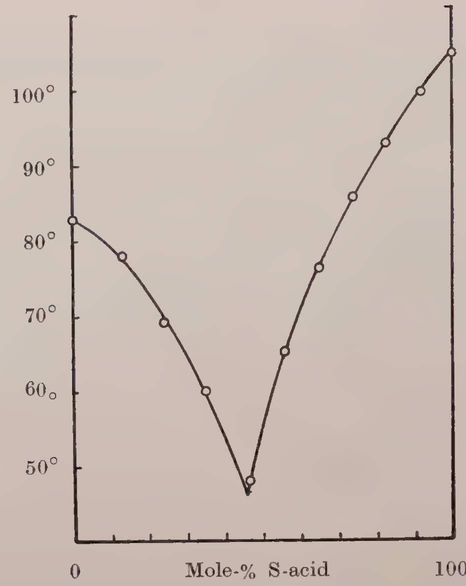

Fig. 32. (+)-Propylsuccinic acid and (−)-hexylsuccinic acid.

according to later investigators contained at most 50 % active propylsuccinic acid (18). From this it is evident that the result of TIMMERMANS is uncertain.

Finally a number of systems of the type:

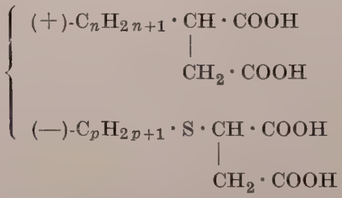

$$\left\{\begin{array}{l} (+)\text{-}C_nH_{2n+1}\cdot \underset{\displaystyle CH_2\cdot COOH}{\underset{|}{CH}}\cdot COOH \\[2ex] (-)\text{-}C_pH_{2p+1}\cdot S\cdot \underset{\displaystyle CH_2\cdot COOH}{\underset{|}{CH}}\cdot COOH \end{array}\right.$$

where $p \neq n - 1$

were studied. The results are collected in table 3 from which can be seen that in no case a molecular compound could be detected.

If all the facts from these experiments are summarized, it may be concluded that within the homologues series in question structural differences of a few CH_2-groups are of rather small importance for the formation of quasi-racemic compounds. If, on the other hand, a CH_2-group in one of the components corresponds to an S-atom in the other, the conditions are so less favourable that such a small change as the addition or the removal of a CH_2-group in one of the components is enough to destroy the ability to form a quasi-racemic compound completely.

Steric relationships

The conclusions as to the steric relationships which can be drawn from the existence of quasi-racemic compounds between the actual substances are sum-

Table 3

Thermal data obtained by the contact method. Structurally dissimilar alkyl- and alkylsulfidesuccinic acids

(From fig. 34 the meaning of t_1—t_5 is clear)

Component 1	Component 2	t_1 (°C)	t_2 (°C)	t_5 (°C)
(−)-Ethyl-SA	(+)-Mercapto-SA	97	87	153
(−)- »	(+)-Ethylsulfide-SA	97	73.5	126.5
(−)-Propyl-SA.......	(+)-Methylsulfide-SA	105	84	145
(−)- »	(+)-Propylsulfide-SA	105	69	121
(−)-Butyl-SA	(+)-Ethylsulfide-SA	84	65	126.5
(−)- »	(+)-Butylsulfide-SA	84	50	121
(−)-Pentyl-SA.......	(+)-Propylsulfide-SA	83	58	121
(−)- »	(+)-Pentylsulfide-SA	83	58	125
(−)-Hexyl-SA	(+)-Butylsulfide-SA	83	56	121

marized in fig. 33. Compounds that have been shown to form quasi-racemates have been connected by lines. As in all these experiments the components of the quasi-racemic compounds have opposite directions of optical rotation it can be concluded that the alkylsuccinic acids and S-alkylmercaptosuccinic acids with the same sign of optical rotation also have the same configuration. From fig. 33 it can be seen that for many of the compounds the steric relationships have been established in several ways. The fact that in no single case contradictory results have been obtained is a good argument in favour of the quasi-racemate method of establishing steric relations.

It has been shown by FREDGA that (+)-malic acid and (+)-mercaptosuccinic acid have the same configuration (4). Consequently the *dextro*rotatory forms of the compounds studied in this investigation all have the same configuration as D-glyceric aldehyde.

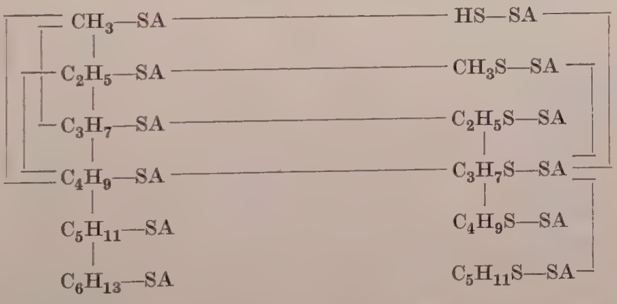

Fig. 33. Formation of quasi-racemic compounds between alkyl- and alkylsulfidesuccinic acids.

Polymorphism

The method of RHEINBOLDT which was first used for the thermal analysis, in some cases gave results that could not be interpreted. The introduction of the microscopical methods of Kofler, however, showed that these complications were caused by polymorphism. By combining these methods it was possible to analyse this phenomenon more closely. It was found that an unexpectedly large number of the succinic acids could exist in two or more modifications as 11 of the 24 compounds investigated were polymorphic (table 4). In some cases melting point curves of unstable systems could be determined (fig. 6, 9, 27 and 30). This of course involved considerable experimental difficulty and the curves of these unstable systems are perhaps not entirely accurate in details.

According to Deffet about 1 200 organic compounds possessing unstable modifications had been reported up to 1942 (20). This number of course would be much larger if organic compounds were more generally studied in the hot stage microscope as the microscopical methods are well suited for the detection

Table 4

Polymorphic modifications

Compound	Melting point (°C)	
	In capillary tube	Microscopical
Optically active acids:		
Butyl-SA	83	84
	73.5	74
Hexyl-SA	83	83
	77.5	80
Mercapto-SA	153	153
		145
Methylsulfide-SA	143	145
		140.5
		137.5
Ethylsulfide-SA	127	126.5
		120
		118
		114
Racemic acids:		
Ethyl-SA	99	100
		90
Butyl-SA	83	84
	69	69
Pentyl-SA	81	82
		72
Hexyl-SA	88	88.5
	84	84.5
	77.5	69
Methylsulfide-SA	137.5	138.5
		129
Ethylsulfide-SA	125.5	126
	(121.5)	
	119.5	119
	112.5	

Table 5

(+)-Pentyl-SA
(−)-Pentyl-SA

(+)-acid (%)	M.p. (°C)
50.0	81
60.8	79
70.2	77
74.6	76
81.2	73.5
85.4	76
89.7	78
100.0	83

Table 6

(+)-Hexyl-SA
(−)-Hexyl-SA

(+)-acid (%)	M.p. (°C)
50.0	88
	84
	77.5
55.3	83
	77
60.4	81
	76
70.3	77.5
79.8	75
84.9	76.5
	73.5
89.8	78.5
	74.5
94.6	81
	77
100.0	83
	77.5

Table 7

(+)-Methylsulfide-SA
(−)-Methylsulfide-SA

(+)-acid (%)	M.p. (°C)
50.0	137.5
54.8	137
59.8	136.5
69.9	134
79.7	135.5
88.8	139
94.8	141
100.0	143

Table 8

(+)-Ethylsulfide-SA
(−)-Ethylsulfide-SA

(+)-acid (%)	M.p. (°C)
50.0	125.5
	119.5
	112.5
55.4	121
	118.5
	112.5
59.9	119.5
	116.5
	112
65.0	117.5
	112
	111.5
70.0	115
	111
75.0	114.5
80.2	117.5
85.4	120
90.2	122.5
94.8	125
100.0	127

Table 9

(+)-Propylsulfide-SA
(−)-Propylsulfide-SA

(+)-acid (%)	M.p. (°C)
50.0	119.5
56.5	118
60.6	117
65.1	116
69.3	114.5
75.0	112
80.9	110.5
85.3	113
90.4	115.5
100.0	120

Table 10

(+)-Butylsulfide-SA
(−)-Butylsulfide-SA

(+)-acid (%)	M.p. (°C)
50.0	105
55.3	104
60.5	103
65.2	102
70.3	103
75.2	106.5
80.1	110
91.0	115.5
100.0	120.5

Table 11

(+)-Pentylsulfide-SA
(−)-Pentylsulfide-SA

(+)-acid (%)	M.p. (°C)
50.0	107
55.1	106.5
60.4	106
65.3	105
69.8	108
75.3	111.5
80.4	115
90.6	120
100.0	125

Table 12

(+)-Methylsulfide-SA
(−)-Ethyl-SA

S-acid (Mole-%)	M.p. (°C)
0.0	96
2.2	94
4.6	92.5
6.6	90.5
9.0	93
13.7	106
18.1	112.5
27.9	118.5
37.1	121.5
47.0	122
52.7	122
57.5	120.5
62.3	123
67.5	126.5
78.0	132.5
88.5	137.5
100.0	143

Table 13

(+)-Ethylsulfide-SA
(−)-Propyl-SA

S-acid (Mole-%)	M.p. (°C)
0.0	104
9.3	98.5
18.4	93.5
23.9	90.5
27.9	89
30.2	91
32.0	92.5
37.4	95
42.2	97
47.2	98
51.7	98
57.5	99
67.7	109
78.1	115
89.0	121
100.0	127

Table 14

(+)-Propylsulfide-SA
(−)-Butyl-SA

S-acid (Mole-%)	M.p. (°C)
0.0	83
9.7	75
14.1	73
16.6	71
19.7	72.5
23.3	75
26.8	78.5
30.9	80
35.2	82
41.7	83
43.4	83
46.4	83.5
52.0	90
57.0	95
67.9	103
78.6	109
84.0	112.5
100.0	120

Table 15

(+)-Butylsulfide-SA
(−)-Pentyl-SA

S-acid (Mole-%)	M.p. (°C)
0.0	83
9.1	78
18.4	72
23.2	69
28.3	67
33.9	67
38.3	75
48.2	85
57.7	92
67.8	100
82.0	109
100.0	120.5

Table 16

(+)-Pentylsulfide-SA
(−)-Hexyl-SA

S-acid (Mole-%)	M.p. (°C)
0.0	83
8.9	78
18.7	70.5
24.3	66
27.3	63.5
30.4	62.5
32.4	69
35.0	73
37.4	79.5
41.9	86.5
47.3	91.5
52.4	96
57.5	99.5
67.0	105.5
77.7	112.5
88.4	119
100.0	125

Table 17

(+)-Methylsulfide-SA
(+)-Ethyl-SA

S-acid (Mole-%)	M.p. (°C)
0.0	96
4.4	100
8.8	103
18.3	109.5
27.7	114
37.5	119
47.3	123.5
57.0	127
67.7	130
78.1	134
88.6	138
100.0	143

Table 18

(+)-Ethylsulfide-SA
(+)-Propyl-SA

S-acid (Mole-%)	M.p. (°C)
0.0	104
9.4	106.5
18.2	108
28.1	111
37.6	112.5
47.4	114
57.7	116
67.8	117.5
78.0	119
83.6	120
89.1	123
94.2	125
100.0	127

Table 19

(+)-Propylsulfide-SA
(+)-Butyl-SA

S-acid (Mole-%)	M.p. (°C)
0.0	83
10.4	82
18.2	81
22.9	80.5
27.4	80
37.7	79.5
43.6	85.5
49.4	80
56.3	94.5
68.6	103
78.0	108.5
88.0	114.5
100.0	120

Table 20

(+)-Butylsulfide-SA
(+)-Pentyl-SA

S-acid (Mole-%)	M.p. (°C)
0.0	83
10.4	80
19.4	77.5
27.9	75.5
32.6	74
37.3	80.5
47.7	90
57.0	97
67.9	104
79.2	110.5
89.4	116
100.0	120.5

Table 21

(+)-Pentylsulfide-SA
(+)-Hexyl-SA

S-acid (Mole-%)	M.p. (°C)
0.0	83
12.1	76.5
18.6	74
22.9	71.5
27.9	75
33.5	82.5
36.9	87
44.0	93
48.6	96.5
58.5	102.5
68.9	110
77.7	114.5
89.0	120
100.0	125

Table 22

rac.-Methylsulfide-SA
rac.-Ethyl-SA

S-acid (Mole-%)	M.p. (°C)
0.0	99
9,2	103
18.2	107
27.6	110.5
37.2	114
48.0	117
57.0	119
67.7	123
78.5	129
89.0	133.5
100.0	137.5

of polymorphism. Still it seems probable that the succinic acids described here are characterized by polymorphism to a larger extent than organic compounds in general.

Experimental

The melting point curves except fig. 22, 27, 29 and 30 were determined according to Rheinboldt (6) using Friedrichs' melting point apparatus (21)

Table 23

rac.-Ethylsulfide-SA
rac.-Propyl-SA

S-acid (Mole-%)	M.p. (°C)
0.0	94
5.1	93
	90.5
9.9	95
	88
18.1	96.5
	87.5
23.7	98
27.8	99.5
	87.5
38.0	102
	89.5
47.3	105
	93
57.1	108
	97
66.1	110
	101
78.0	114
	105
88.0	119.5
	109
92.8	122
	110.5
100.0	126.5
	120
	118
	114

Table 24

rac.-Propylsulfide SA
rac.-Butyl-SA

S-acid (Mole-%)	M.p. (°C)
0.0	83
10.1	81
19.8	87
26.1	78
35.5	83
51.1	92
60.9	98
77.8	106.5
88.3	113
100.0	119.5

Table 25

rac.-Butylsulfide-SA
rac.-Pentyl-SA

S-acid (Mole-%)	M.p. (°C)
0.0	82
10.4	81
19.3	80
28.9	79
32.4	79
39.0	78.5
47.6	79.5
52.5	82.5
57.7	86
69.7	93
77.2	96.5
89.1	101
100.0	105

Table 26

rac.-Pentylsulfide-SA
rac.-Hexyl-SA

S-acid (Mole-%)	M.p. (°C)
0.0	88
	77.5
5.5	84.5
	76.5
9.2	83.5
	76
11.9	83.5
	75
14.5	83
18.9	84
	73
23.1	84.5
26.6	85
	70
29.3	85
33.1	86
	66.5
36.6	86
	63.5
43.3	88
	68.5
47.2	88.5
	73.5
53.3	90.5
	79.5
58.5	84.5
59.2	91.5
63.7	93
66.7	93.5
	91
73.0	95
78.3	97
87.9	102
100.0	107

(tables 5–19, 21, 22, 24 and 27). The components were weighed into a small test tube, melted together at as low temperature as possible or dissolved in pure ether which was evaporated. The crystalline product was powdered and dried. The melting points for the curves in fig. 22, 27, 29 and 30 (tables 20, 23, 25 and 26) were determined in a hot stage microscope according to KOFLER (22). The same apparatus was used for the study of contact preparations (Tables 1—4, 28).

Table 27

(+)-Propyl-SA
(−)-Hexyl-SA

(+)-acid (Mole-%)	M.p. (°C)
0.0	83
12.9	78
23.8	69
35.0	60
46.5	48
55.9	65
64.8	76
74.1	85.5
82.8	92
92.2	99
100.0	104

Table 28

Thermal data obtained by the contact method. Structurally similar alkyl- and alkylsulfidesuccinic acids

(From fig. 34 the meaning of t_1—t_5 is clear)

Component 1	Component 2	t_1 (°C)	t_2 (°C)	t_3 (°C)	t_4 (°C)	t_5 (°C)	Type[1]
(+)-Mercapto-SA	(−)-Methyl-SA	153	125	130.5	108	115	
(+)- »	(+)- »	153	Peritecticum 134°			115	IV
		145				115	I
rac.- »	rac.- »	152	Peritecticum 126°			116	IV
(+)-Methylsulfide-SA..	(−)-Ethyl-SA	145	120	123	90	97	
(+)- » ..	(+)- »	145	Peritecticum 123°			97	IV
rac.- » ..	rac.- »	138.5	Peritecticum 116°			100	IV
		138.5				90	I
(+)-Ethylsulfide-SA ..	(−)-Propyl-SA	126.5	95	96.5	85	105	
(+)- » ..	(+)- »	126.5	Peritecticum 115°			105	IV
rac.- » ..	rac.- »	113	Minimum 88°			94.5	III
(+)-Propylsulfide-SA ..	(−)-Butyl-SA	121	80	81	62	84	
(+)- » ..	(+)- »	121	75			84	V
rac.- » ..	rac.- »	120	74			84	
(+)-Butylsulfide-SA...	(−)-Pentyl-SA	121	67.5			83	
(+)- » ..	(+)- »	121	73			83	V
rac.- » ..	rac.- »	105	<80			82	V
(+)-Pentylsulfide-SA ..	(−)-Hexyl-SA	125	62			83	
(+)- » ..	(+)- »	125	71			83	
rac.- » ..	rac.- »	108	Minimum 82°			88.5	III
		108	60			77.5	

---

[1] According to ROOZEBOOM (23).

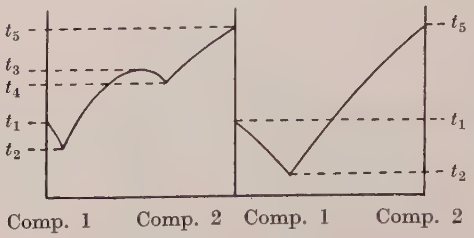

Fig. 34. Illustrative figure to tables 1—3 and 28.

SUMMARY

A number of two-component systems containing optically active alkylsuccinic acids (I) or S-alkylmercaptosuccinic acids (II) or both were studied by thermal analysis by the methods of RHEINBOLDT (6) and KOFLER (7). Some systems made up of optically inactive succinic acids were also studied.

The methods were found to give consistent results.

The conditions for the formation of quasi-racemic compounds are discussed and some conclusions concerning the influence of racemate formation, structural differences and isomorphism have been drawn.

A great number of polymorphic modifications of the actual substances could be detected.

The steric relationships between some alkylsuccinic acids and S-alkylmercaptosuccinic acids were established. The *dextro*rotatory acids most probably have the D-configuration.

The author is greatly indebted to Professor ARNE FREDGA for specimens of material as well as valuable advice and discussion.

Part of the micro thermal analysis was performed at the KOFLER private laboratory at Innsbruck. The author is extremely grateful to the late Professor L. KOFLER and to Dr. A. KOFLER for instruction in the use of the microscopical methods and many valuable discussions.

The investigation was finished at the Institute of Organic Chemistry of the Royal Agricultural College. The author is much indebted to the head of this institute, Professor NILS HELLSTRÖM, for his obligingness and kind interest in the work.

Part of the expenses involved in this investigation were defrayed by a grant from the Nobel Fund of the Royal Swedish Academy of Science (Kemiska prisgruppens särskilda fond).

Organic Department, Chemical Institute, University of Uppsala and Institute of Organic Chemistry, Royal Agricultural College, Uppsala, January 1952.

REFERENCES: 1. **M. Matell,** Ark. Kemi *3* (No 17), 129 (1951). — 2. **J. Timmermans,** Rec. Trav. chim. Pays-Bas [4] *48,* 890 (1929). — 3. **A. Fredga,** "The Svedberg 1884 $^{30}/_{8}$ 1944", p. 261. Uppsala 1944. — 4. ——, Ark. Kemi Min. Geol. *15 B,* No 23 (1942). — 5. **E. Berner** and **R. Leonardsen,** Liebigs Ann. *538,* 1 (1939). — 6. **H. Rheinboldt,** J. prakt. Chem. [2] *111,* 242 (1925). — 7. **L.** and **A. Kofler,** Mikro-Methoden, Innsbruck 1948. — 8. ——, Ibid. p. 115. — 9. **M. Matell,** Mikrochem.mikrochim. Acta, *38,* 532 (1951). — 10. **A. Fredga,** Ark. Kemi Min. Geol. *14 B,* No 15 (1940). — 11. **H. Lettré,** Z. angew. Chem. *50,* 581 (1937). —

12. ——, Ergebn. d. Enzymforschung *9*, p. 1. Leipzig 1943. — 13. **A. Lüttringhaus** and **K. Hauschild,** Ber. dtsch. chem. Ges. *73*, 145 (1940). — 14. **H. Stuart,** Z. phys. Chem. *B 36*, 155 (1937). — 15. **R. Kohlhaas** and **A. Lüttringhaus,** Ber. dtsch. chem. Ges. *72*, 897 (1939). — 16. **J. Porath,** private communication. — 17. **J. Timmermans** and **J. van der Haegen,** Bull. Soc. Chim. Belg. *42*, 448 (1933). — 18. **P. W. Clutterbuck, H. Raistrick** and **F. Reuter,** Biochem. J. *31*, 987 (1937). **A. Fredga** and **U. Sahlberg,** Ark. Kemi Min. Geol. *18 A*, No 16 (1944). — 19. **A. Fredga,** Ark. Kemi Min. Geol. *14 B*, No 27 (1941). — 20. **L. Deffet,** Répertoire des composés organiques polymorphes. Liège 1942. — 21. **F. Friedrichs,** Z. angew. Chem. *34*, 61 (1921). — 22. **L.** and **A. Kofler,** Mikro-Methoden. p. 3, Innsbruck 1948. — 23. **B. Roozeboom,** Z. phys. Chem. *30*, 385 (1899).

Tryckt den 24 november 1952

Uppsala 1952. Almqvist & Wiksells Boktryckeri AB

ARKIV FÖR KEMI Band 5 nr 4

Communicated 14 May 1952 by ARNE WESTGREN

The structure of Bi_2NbO_5F and isomorphous compounds

By BENGT AURIVILLIUS

With 1 figure in the text

X-ray studies made previously on the compounds $CaBi_2Nb_2O_9$, $Bi_4Ti_3O_{12}$ and $BaBi_4Ti_4O_{15}$ (1) showed that they have very similar structures. The symmetry is tetragonal or pseudotetragonal, and the structures are each built up of quadratic Bi_2O_2 layers alternating with perovskite layers, the latter having different heights in the three different cases. The generalized formula for the compounds might be written Me_2O_2 $(Me'_{m-1}\,R_mO_{3m-1})$ where Me' is the 12 coordinated metal atom in the perovskite layers and R the 6 coordinated atom. The formulae for the above compounds, $Bi_2O_2(CaNb_2O_7)$, $Bi_2O_2(Bi_2Ti_3O_{10})$ and $Bi_2O_2[(BaBi_2)\,Ti_4O_{13}]$ thus have m values of 2, 3 and 4. The simplest case, $m=1$, would correspond to the formula $Me_2O_2(RO_4)$ and to a structure built up of Me_2O_2 layers and layers of RO_6 octahedra each octahedron sharing four corners. Compounds of this type have, however, not been successfully synthesized as yet.

The present paper deals with the compounds Bi_2NbO_5F, Bi_2TaO_5F and $Bi_2TiO_4F_2$, which correspond to the simplest case, $m=1$ above, except that some of the O atoms are replaced by F atoms. The formulae of the compounds might thus be written: $Bi_2\,(O, F)_2Nb\,(O, F)_4$ etc.

Preparation, powder photographs and analyses

Bi_2NbO_5F: When a mixture of BiF_3 and Nb_2O_5 in the mol ratio 4:1 was heated in air at 800° C for a short time, a few single crystals (very thin plates) were obtained. Powder photographs of this sample indicated a tetragonal unit cell with the same cell dimensions as would be expected for the above general type when $m=1$. The best conditions for the formation of this phase were then studied by heating 2.5 g mixtures $(2BiF_3+{}^1/_2\,Nb_2O_5)$ in air at 640° C, this low temperature being chosen to reduce the volatility of the BiF_3. The reaction times were varied from 5–40 hours, and powder photographs were taken of each product. For reaction times of 7–15 hours the lines of the above tetragonal phase predominated in the powder photographs, the few extra lines were very weak (see Table 1).

The fluorine content was found to vary from 4.0 % (7 hours) to 2.4 % (15 hours), whereas the calculated value for Bi_2NbO_5F is 3.2 %. No variation in the size of the cell with the fluorine content was found, and it therefore seems probable that the composition of the phase is constant and that the observed variation in the F content is due to the presence of small impurities which are not visible in the powder photo-

Table 1

Powder photographs of Bi_2NbO_5F (sample with 2.8 % F)
Cr K radiation $\lambda_{Cr\,K_\alpha} = 2.2909$ Å

h k l	$10^4 \cdot \sin^2 \theta_{calc}$	$10^4 \cdot \sin^2 \theta_{obs}$	I_{obs}
1 0 3	1319	1332	st
0 0 6	1708	1711	m
1 1 0	1784	1795	m
1 1 2	1974	1969	vvw
1 0 5	2078	2083	vw
1 1 4	2543	2547	m
—	—	2785	vvw
0 0 8	3036	3033	w
—	—	3093	vw
1 1 6	3492	3490	st
2 0 0	3568	3567	st
2 0 2	3758	3754	vw
—	—	3808	vw
1 0 9 0 0 10	4734 4743	4737	st
1 1 8	4820	4827	w
2 1 3	4888	4891	st
2 0 6	5276	5292	m
2 1 5	5647	5658	w
1 1 10	6527	6529	vw
1 0 11	6631	6630	w
0 0 12	6830	6841	w
2 2 0	7137	7139	w
2 2 2	7327	7330	vw
3 0 1	8076	8080	vvw
2 1 9 2 0 10	8303 8311	8304	st
3 0 3	8456	8456	m
1 1 12	8614	8611	m
2 2 6	8845	8844	m
1 0 13 3 1 0	8908 8921	8919	m
3 1 2	9111	9119	vw
3 0 5	9215	9195	vw
0 0 14	9297	9292	vw

graphs. To check that the Bi/Nb ratio had not changed essentially during the heating, a complete analysis was made on one sample (9 hours heating). The following values were obtained as the mean of three analyses: Bi: 68.0±0.6 %, Nb: 14.2±0.6 %, F: 3.7±0.2 %.

The values calculated for Bi_2NbO_5F are:

Bi: 68.5, Nb: 15.2 %, F: 3.2 %.

From these figures it seems probable that the formula of the compound is Bi_2NbO_5F.

Bi_2TaO_5F was prepared in exactly the same way as Bi_2NbO_5F. No analysis was made since the powder photographs were similar to those of Bi_2NbO_5F and niobium and tantalum compounds are usually isomorphous.

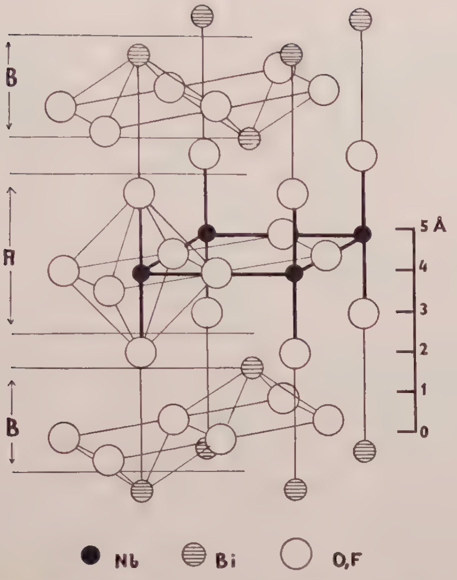

Fig. 1. One half of the unit cell of Bi_2NbO_5F. A denotes the region of $Nb(O,F)_4$ octahedra and B the $Bi_2(O,F)_2$ layers.

$Bi_2TiO_4F_2$: Mixtures of bismuth fluoride and titanium oxide in the mol ratio 2:1 (total 2.3 g) were heated in air at 640° for various lengths of thime. The powder photographs obtained from samples heated for 3 or 5 hours could be interpreted by assuming a mixture of BiOF (2) and a phase whose cell dimensions were nearly the same as those of Bi_2NbO_5F. (See Table 2, where the reflexions from the BiOF phase are designated by *b* and those from the other phase by *a*). The fluorine contents of the mixed samples were found to be 6.4 % (5 hours) and 8.4 % (3 hours) but no variation of the cell size with the fluorine content was found. The calculated values are 7.8 % for BiOF and 6.7 % for $Bi_2TiO_4F_2$. From the original Bi/Ti ratio, from the fluorine analysis and from the similarity of the powder photographs with those of Bi_2NbO_5F (Tables 1 and 2), it was concluded that the formula of the phase is $Bi_2TiO_4F_2$.

Methods of analysis: *Fluorine.* The samples were first decomposed by fusing with NaOH, and were then distilled with $HClO_4$ as described by WILLARD and WINTER (3). The distillate was titrated with $Th(NO_3)_4$ using Na-alizarinsulphonate as indicator.

Bismuth and Niobium. The samples were brought into solution, and niobium was determined as described in Scott's "Standard Methods" (4). Bismuth was first precipitated as Bi_2S_3, which was then redissolved, converted to Bi_2O_3 and weighed as such.

Unit cells and space group

The dimensions of the unit cells were determined from powder photographs taken with focusing cameras of the Phragmén type (Tables 1 and 2). The radiation used

Table 2

Powder photographs of $Bi_2TiO_4F_2$ (mixed with BiOF) *Cr K* radiation ($\lambda_{Cr K_\alpha} = 2.2909$ Å). *a* denotes the $Bi_2TiO_4F_2$ phase and *b* the BiOF phase

h k l	phase	$10^4 \sin^2 \theta_{calc}$	$10^4 \sin^2 \theta_{obs}$	I_{obs}
1 0 1	*a*	957	941	vvw
1 0 1	*b*	1270	1265	m
1 0 3	*a*	1351	1354	st
0 0 2	*b*	1352		
0 0 6	*a*	1771	1767	m
1 1 0	*a*	1816	1811	m
1 1 0	*b*	1864	1858	vvw
1 1 2	*a*	2013	1999	w
1 0 5	*a*	2138	2132	w+
1 0 2	*b*	2284	2288	vvw
1 1 4	*a*	2603	2601	m
—	—	—	3074	vw
1 1 2	*b*	3216	3231	w
1 0 7	*a*	3319	3320	vw
1 1 6	*a*	3587	3600	st
2 0 0	*a*	3631	3624	st
2 0 0	*b*	3728	3744	w
2 0 2	*a*	3828	3822	w
1 0 3	*b*	3974	3982	w
—	—	—	4352	vvw
2 0 4	*a*	4418	4426	vvw
2 1 1	*a*	4588	4590	w
—	—	—	4674	vvw
1 0 9	*a*	4893	4904	st
1 1 3	*b*	4906		
0 0 10	*a*	4919		
2 1 3	*a*	4982	4979	st
2 0 2	*b*	5080	5084	w
2 0 6	*a*	5402	5416	m+
0 0 4	*b*	5408		
2 1 5	*a*	5769	5768	m
2 1 2	*b*	6012	6025	m
1 0 4	*b*	6340	6353	w
2 0 3	*b*	6770	6786	m
2 0 8	*a*	6779		
1 0 11	*a*	6860	6869	m
2 1 7	*a*	6950	6950	vvw
0 0 12	*a*	7084	7075	m
2 2 0	*a*	7262	7262	m
1 1 4	*b*	7272		
2 2 0	*b*	7455	7456	w
2 2 2	*a*	7459		
2 1 3	*b*	7702	7709	m
—	—	—	8049	vw
3 0 1	*a*	8210	8210	vw
—	—	—	8352	vw
2 1 9	*a*	8524	8524	st
2 0 10	*a*	8550		
3 0 3	*a*	8613	8603	m
3 0 1	*b*	8736	8725	w
2 2 2	*b*	8814	8807	w
1 1 12	*a*	8900	8900	m

Table 2 (continued)

h k l	phase	$10^4 \sin^2 \theta_{calc}$	$10^4 \sin^2 \theta_{obs}$	I_{obs}
2 2 6	*a*	9033	9027	m
3 1 0	*a*	9078	9072	w
2 0 4	*b*	9136	9136	vw
3 1 2	*a*	9275	9272	m
3 1 0	*b*	9319	9319	w
1 0 5	*b*	9382	9384	m
3 0 5	*a*	9400		

was *Cr K* ($\lambda_{CrK_\alpha} = 2.2909$ Å). As mentioned above the powder photographs could be interpreted by assuming tetragonal unit cells; the cell dimensions are given below.

	a (Å)	*c* (Å)
Bi_2NbO_5F	3.835	16.63
Bi_2TaO_5F	3.829	16.64
$Bi_2TiO_4F_2$	3.802	16.33

The errors in these figures are estimated to be ±0.1 %.

The observed density was 8.0 for Bi_2NbO_5F (preparation with 2.8 % F), which agrees fairly well with the assumption of 2 formula units per unit cell, giving a calculated density of 8.26.

Zero and first order Weissenberg photographs around the *a* axis were taken. There was nothing in the Weissenberg photographs to indicate a Laue symmetry lower than D_{4h}—4 *mmm*. The only extinctions found were that *h*, *k*, *l* were absent for $h+k+l$ odd, which is characteristic of the space groups C_{4v}^9, D_{2d}^9 D_{2d}^{11} and D_{4h}^{17}.

Powder photographs only were taken of the compounds Bi_2TaO_5F and $Bi_2TiO_4F_2$, and from these it was concluded that these substances are isomorphous with Bi_2NbO_5F.

Positions of the metal atoms

Bi_2NbO_5F: With 2 formula units per unit cell there are 4 Bi and 2 Nb atoms per unit cell. The intensities of the spots in the Weissenberg photographs seemed in the main to depend only on the *l* values. Thus for *l* even $I_{00l} \approx I_{11l} \approx I_{20l}$ etc. and for *l* odd: $I_{10l} \approx I_{21l} \approx I_{30l}$ etc. With these intensity values a good approximation of the Patterson-Harker function along $00z$ could be obtained by using only the intensity values of $h0l$ and $h1l$. The Patterson-Harker function thus calculated (not given here) showed only one, big, maximum, at $z = 0.34$. This maximum, and the absence of others, could be explained only by assuming that 4 Bi atoms are situated at the positions $\pm 00z$ with $z = 0.17$ or $z = 0.33$, and the Nb atoms at the positions $00\frac{1}{2}$ or 000. Arbitrarily choosing 000 as the position for Nb, trial and error calculations gave the value 0.325 for the Bi parameter.

No determination of z_{Bi} was made for **Bi_2TaO_5F**.

For **$Bi_2TiO_4F_2$** the powder photograph data were used to determine the Bi parameter. Assuming the Ti atoms to be situated at 000 and the O and the F atoms to occupy the same positions as given below for Bi_2NbO_5F, the value $z_{Bi} = 0.327 \pm 0.006$ was obtained from trial and error calculations.

Table

Weissenberg photographs of

Zero layer

h k	0 0		2 0		4 0	
l	I_{calc}	I_{obs}	I_{calc}	I_{obs}	I_{calc}	I_{obs}
0	—	—	170	vst	37	w
2	—	—	10	w	3	vw
4	0.3	—	0.04	—	0.05	—
6	220	vst	67	w	34	vw
8	12	w	5	vw	6	vvw
10	3	vw	2	—	2	—
12	44	st	26	w	86	st
14	15	m	11	w		
16	10	w	10	w		
18	16	m	28	m		
20	22	m				

h k	1 0		3 0	
l	I_{calc}	I_{obs}	I_{calc}	I_{obs}
1	7	w	1	vw
3	270	vst	42	w
5	40	w	8	vw
7	1	—	0.2	—
9	75	m	30	vw
11	18	w	10	vw
13	3	vw	3	vw
15	20	m	19	m
17	12	w		
19	14	w		

Positions of the O and the F atoms

The positions of the O and the F atoms could not be distinguished either from the diffraction data, or from space considerations because of the similarity in the reflecting power and ionic radii of O^{2-} and F^-. The problem is therefore treated as though O and F were the same atomic species. In the following, the O and the F atoms are denoted by (O, F) and the discussion relates to Bi_2NbO_5F for which z_{Bi} could be accurately determined from the Weissenberg photographs.

It seemed reasonable to assume that the Nb atoms are surrounded by a regular or nearly regular octahedron of (O, F) atoms with distances Nb–(O, F) ≈ 2.0 Å. Neglecting the polar space group C^9_{4v}, these conditions are fulfilled only if 4 (O, F) atoms, here called $(O, F)_1$, are situated at the positions $\pm 0 0 z$ with $z \approx 0.12$, and 4 (O, F) atoms, $(O, F)_2$, at the positions $0\frac{1}{2}0$, $\frac{1}{2}00$. Assuming the distance (O, F)–(O, F) to be ≥ 2.5 Å and the distance Bi–(O, F) to be ≥ 2.2 Å there is only room for the remaining 4 (O, F) atoms, $(O, F)_3$, at the positions $0\frac{1}{2}\frac{1}{4}$, $\frac{1}{2}0\frac{1}{4}$.

3

Bi_2NbO_5F $Cu\,K\alpha$ radiation

First layer

	hk	11		31	
l		I_{calc}	I_{obs}	I_{calc}	I_{obs}
0		210	vst	36	w
2		17	w	4	vvw
4		11	w	2	—
6		110	m	33	w
8		27	vw	9	vw
		·······	·······	·······	·······
10		2	vvw	1	—
12		21	m	20	w
14		14	w	20	w
16		5	w	17	w
18		19	m		
20		58	st		

	hk	01		21		41	
l		I_{calc}	I_{obs}	I_{calc}	I_{obs}	I_{calc}	I_{obs}
1		7	—	2	vw	1	vvw
3		270	vst	74	m	33	w
5		40	m	13	w	7	—
7		1	—	0.3	—	0.2	—
						·······	·······
9		75	vst	40	w	53	w
11		18	m	12	vvw	51	w
				·······	·······		
13		3	vw	3	vw		
15		20	m	19	m		
17		12	w	19	m		
19		14	w				

The coordination and distances in Å will be:

$Bi-4\,(O, F)_3 = 2.29$

$Bi-4\,(O, F)_1 = 2.9$

$(O, F)_3-4\,(O, F)_3 = 2.71$

$(O, F)_1-4\,(O, F)_3 = 2.9$

$Nb-2\,(O, F)_1 = 2.0$

$Nb-4\,(O, F)_2 = 1.92$

$(O, F)_2-4\,(O, F)_2 = 2.71$

$(O, F)_1-4\,(O, F)_2 = 2.8$

The proposed structure is given in the summary. Calculated and observed intensities for the reflexions in the Weissenberg photographs are given in Table 3. I_{calc} is derived as follows:

$$I_{calc} = \frac{1+\cos^2 2\theta}{1\,600 \cdot \sin 2\theta} \cdot F^2 \quad \text{where} \quad F = \sum f \cos 2\pi (h\mathrm{x} + k\mathrm{y} + l\mathrm{z}).$$

The lines of maximum absorption in the Weissenberg photographs (see 5) are indicated by dotted lines in Table 3. If the absorption effects are taken into account, the agreement between calculated and observed intensities is quite good.

Discussion of the structure

Even if the $(O, F)_1$ atoms (see above) are assumed to occupy such a position that the distance Bi–4 $(O, F)_1$ is as small as possible [$z\,(O, F)_1 = 0.15$, $(O, F)_1$–4 $(O, F)_3 = 2.5$, Nb–2 $(O, F)_1 = 2.5$, Bi–4 $(O, F)_1 = 2.7$], the distance Bi–4 $(O, F)_1$ will still be much longer than the distance Bi–4 $(O, F)_3$. It therefore seems appropriate to describe the structure of Bi_2NbO_5F as being built up of $Bi_2\,(O, F)_2$ layers alternating with octahedral layers having the composition $Nb\,(O, F)_4$, both layers being perpendicular to the *c*-axis. It might be pointed out that the structure of $Bi_2(O,\ F)_2\,Nb\,(O,\ F)_4$ is basically of the same type as the "X_1 structures", Me_2O_2X, previously investigated by SILLÉN (6). Thus the octahedral sheets $Nb(O, F)_4$ correspond to single layers of halogen atoms, X, in Me_2O_2X.

Discussion of the distribution of the O and the F atoms

As seen above, the distance Bi–4$(O, F)_3$ is 2.29 Å for Bi_2NbO_5F. For $Bi_2TiO_4F_2$ the corresponding distance is calculated to be 2.26 ± 0.06 Å. These distances are very nearly the same as the corresponding distances, Bi–4 O, within the Bi_2O_2 layers of other bismuth oxicompounds (6). This need not, however, necessarily mean that the $Bi_2(O, F)_2$ layers (see the figure) are free from F atoms, since compounds with $Bi_2(O, F)_2$ layers which certainly contain F atoms have not been investigated hitherto, and thus the distances within such layers are unknown.

For the present it seems therefore best to make no special assumptions as to the distribution of the O and F atoms.

SUMMARY

The crystal structure of Bi_2NbO_5F has been investigated by means of Weissenberg and powder photographs. From powder photographs the compounds Bi_2TaO_5F and $Bi_2TiO_4F_2$ have been found to be isomorphous with Bi_2NbO_5F. The following structure is proposed for Bi_2NbO_5F:

D_{4h}^{17}–$I\,4/mmm$
$(0\,0\,0,\ \tfrac{1}{2}\tfrac{1}{2}\tfrac{1}{2})+$
2 Nb in 2 (a) : $0\,0\,0$
4 Bi in 4 (e) : $\pm 0\,0\,z$ $\quad z = 0.325 \pm 0.001$
4 $(O, F)_1$ in 4 (c) : $0\tfrac{1}{2}0,\ \tfrac{1}{2}0\,0$
4 $(O, F)_2$ in 4 (e) : $\pm 0\,0\,z$ $\quad z = 0.12 \pm 0.01$
4 $(O, F)_3$ in 4 (d) : $0\tfrac{1}{2}\tfrac{1}{4},\ \tfrac{1}{2}0\tfrac{1}{4}$

The cell dimensions are $a = 3.835$ Å, $c = 16.63$ Å for Bi_2NbO_5F. The positions of the metal atoms were determined from the diffraction data, those of the (O, F) atoms from space considerations. Although it does not seem improbable that O atoms alone occupy the positions $0\tfrac{1}{2}\tfrac{1}{4}$, $\tfrac{1}{2}0\tfrac{1}{4}$, Bi and O thus forming Bi_2O_2 layers as in other bismuth oxicompounds, nothing can be definitely stated as to the distribution of the O and F atoms.

The structure is built up of quadratic $Bi_2(O, F)_2$ layers alternating with octahedral sheets having the composition $Nb(O, F)_4$ (see figure) and the formula might thus be written: $Bi_2(O, F)_2Nb(O, F)_4$. The structure is formally related to a series of previously investigated structures of general formula Me_2O_2 ($Me'_{m-1}R_mO_{3m+1}$) and represents the simplest case of this series, i.e. $m=1$.

University of Stockholm, Institute of Inorganic and Physical Chemistry, May 1952.

REFERENCES. 1. **Aurivillius, B.,** Arkiv Kemi *2* (1950) 519. — 2. ——, Arkiv Kemi Mineral. Geol., *26 B* (1948) n:o 2. — 3. **Willard, H. H.** and **Winter, O. B.,** Ind. Eng. Chem. Anal. Ed. *5* (1933) 7. — 4. **Standard Methods** of Chemical Analysis by W. W. Scott, fifth edition, edited by N. H. Furman, New York 1925, p. 335 and p. 338. — 5. **Wells, A. F.,** Z. Krist. *96* (1937) 451. — 6. **Sillén, L. G.,** Dissert. Stockholm 1940.

Tryckt den 24 november 1952

Uppsala 1952. Almqvist & Wiksells Boktryckeri AB

ARKIV FÖR KEMI Band 5 nr 5

Vorgelegt am 9. Januar 1952

Ascorbinsäure, Dehydro-Ascorbinsäure und Diketo-L-Gulonsäure

Von Hans von Euler und Hans Hasselquist

Mit 2 Figuren im Text

Seitdem die Ascorbinsäure als Redukton und zwar als Endiol erkannt ist (Haworth, Hirst u. Mitarb.; Euler u. Martius; 1933) hat man in diesem biochemisch so wichtigen Stoff eine Laktonbindung, u. zw. die Existenz eines 5-Ringes angenommen.

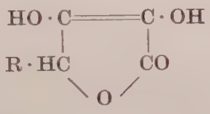
(I)

Schon vorher kannte man (Szent-Györgyi; Zilva) die leichte Oxydierbarkeit des C-Vitamins sowie dessen geringe Stabilität in alkalischer Lösung. Weniger eingehend war die weitere Umwandlung des ersten Oxydationsproduktes, der Dehydro-ascorbinsäure (DHAs) sowie die daraus entstehende Diketo-L-Gulonsäure (DKG) studiert worden. Unsere diesbezüglichen Kenntnisse gehen zurück auf die Arbeiten von Karrer[1], Hirst[2], Reichstein[3] sowie Micheel u. Kraft[4]; dieselben wurden ergänzt durch spätere Beiträge von Zilva (1943; 1945) und Roe et al. (1948).

Wie in der vorhergehenden Arbeit dieser Serie (dieses Arkiv 4 Nr 7, 1952) erwähnt wurde, verbraucht die Ascorbinsäure in alkalischer Lös. mehr als 1 Mol Tillmans Reagens (TR) (Dichlorphenol-indophenol), in saurer oder neutraler Lös. mehr als 1 Mol J_2 (Karrer).[5]

Die Reaktion verläuft ganz analog der von Micheel u. Jung (Chem. Ber. 67, 1660; 1934) an Oxytetronsäure festgestellten Oxydation zum Lakton der α, Diketobuttersäure. In alkalischer Lösung werden nach Karrer bei Überschuss von Jodlösung und dem 1,5fachen der ber. Menge NaOH in 15 Min. 4 Atome Jod auf 1 Mol Ascorbinsäure verbraucht.

Geht man von der als Öl isolierten, reinen DHAs aus[6] so findet man demgemäss in alkalischer (nicht aber in neutraler oder saurer) Lösung einen Verbrauch von rund *1 Mol TR per Mol DHAs.*

---

[1] P. Karrer, G. Schwarzenbach u. K. Schöpp, Helv. Chim. Acta 16, 302; 1933.
[2] E. L. Hirst u. Mitarb., Soc. 1933, 1270. — Soc. Chem. Ind. 52, 221; 1933.
[3] T. Reichstein u. R. Oppenauer, Helv. Chim. Acta 16, 988; 1933.
[4] F. Micheel u. K. Kraft, Z. physiol. Chem. 218, 280; 1933.
[5] P. Karrer, H. Salomon, R. Morf u. K. Schöpp, Biochem. Zs. 258, 4; 1933.
[6] Euler, H. Hasselquist u. I. Loeper, Dieses Arkiv 4; 1952.

Zur Beantwortung der Frage, worauf der gefundene Mehrverbrauch von TR beruht, können folgende Beobachtungen herangezogen werden:

1) Die alkalimetrische Titration der 60 Minuten in 1 n. NaOH auf 100° erhitzten DHAs ergibt einen Alkali-Verbrauch, welcher anzeigt, dass sich durch die alkalische Erhitzung saure Gruppen gebildet haben. a und b ist zu schliessen, dass eine Ketosäure entstanden ist, welche

Versuch 1

a) 160,4 mg DHAs (im Exsiccator getrocknetes Öl) wurden in 1 ml Wasser gelöst und mit 0,5 ml 2 n NaOH in 100 ml Wasser versetzt und *sofort* mit 0,1 n HCl zurücktitriert.

0,5 ml NaOH verbrauchten	10,2 ml 0,1 n HCl
Beim Zurücktitrieren verbraucht	2,7 ml 0,1 n HCl
Die Dehydro-Ascorbins. verbrauchte also	7,5 ml 0,1 n NaOH
160,4 mg DHAs sollen teor. verbrauchen (1 Mol = 160,4/0,1 × 174)	9,25 ml 0,1 n NaOH
Der gefundene Verbrauch von 7,5 ml entspr.	0,81 Mol NaOH

b) 140,5 mg DHAs wurden in 1 ml Wasser gelöst und unter N_2-Strom mit 1 ml 2 n NaOH versetzt und *60 Min. auf dem siedenden Wasserbad erhitzt*; hierauf mit 100 ml Wasser verdünnt und wie oben titriert.

1,0 ml NaOH verbrauchten	20,4 ml 0,1 n HCl
Beim Rücktitrieren verbraucht	3,9 ml 0,1 n HCl
Die DHAs verbrauchte also	16,5 ml 0,1 n NaOH
140,5 mg DHAs sollen theor. verbrauchen für 1 Mol NaOH (1 Mol = 140,5/0,1 × 174)	8,07 ml 0,1 n NaOH
Der gefundene Verbrauch von 16,5 ml entspricht also	2,04 Mol NaOH

Bei der oben beschriebenen Alkali-Behandlung wurde also auf 1 Mol DHAs rund 1 Mol Säure gebildet.

2) *Papier-Chromatographie.*

a) Erwärmt man die DHAs in 1 n. NaOH-Lösung 60 Minuten auf 90°, neutralisiert dann und unterwirft die neutrale Lösung der Papier-Chromatographie (80 Butanol, 20 Wasser, 20 Eisessig) und entwickelt mit Benzidin so tritt ein für das DHAs charakteristischer gelber Flecken mehr hervor.

b) Auch nach Entwicklung der nach a) alkalisch behandelten DHAs mit Tillmans Reagens (TR) in neutraler oder schwach saurer Lösung zeigen sich keine deutlichen Flecken.

c) Entwickelt man das gleiche Chromatogramm in alkalischer Lösung so treten mehrere charakteristische Flecken auf.

Hat man durch Erhitzen der DHAs mit 1 n. Natronlauge (Min. 100°) den Laktonring der DHAs geöffnet und säuert dann an, so wird durch Erhitzen aus der entstandenen Diketo-L-Gulonsäure CO_2 abgespalten, und zwar angenähert 1 Mol CO_2 aus 1 Mol DHAs bezw. 1 Mol DKG.[1]

Versuch. 1,5 ml wässrige Lösung von Dehydro-Ascorbinsäure, enthaltend 528 mg DHAs, wurde auf dem Wasserbad auf 100° erhitzt. Es entwickelt sich CO_2, welches in Barytwasser aufgenommen und als Baryumcarbonat gefällt und bestimmt wurde.

---

[1] Die aus DHAs entstehende DKG lässt sich nach ROE u. KUETHER (J. Biol. Chem. 147, 399; 1943) in gleicher Weise bestimmen wie DHAs. Nach PENNEY u. S. S. ZILVA (Biochem. J. 37, 403, 1943) liefern Ascorbinsäure, DHAs und DKG mit Dinitrophenylhydrazin das *gleiche* Hydrazon.

Gefunden: 0,5478 g $BaCO_3$ entsprechend 0,122 g CO_2.
Theor. möglich, wenn aus 1 Mol DHAs 1 Mol CO_2 abgespalten wird: 0,134 g CO_2.
Somit spaltet 1 Mol DHAs 0,91 Mol CO_2.

In diesem Zusammenhang sei auf Angaben von HERBERT, HIRST, PERCIVAL und SMITH (Soc. 1933 1281) hingewiesen, welche das erste Oxydationsprodukt der Ascorbinsäure (DHAs) durch die Drehung $[\alpha]_{5780} = +56^\circ$ charakterisieren. HIRST u. MITARB. beobachteten dass diese Drehung mit der Zeit abnimmt, u. zw. gleichzeitig mit der Zunahme der Acidität. „At the equilibrium position titration with alkali shows that about 85 % of the organic material exists as free acid and only about 15 % as lactone. For 0.10 g of ascorbic acid a total of 5.6 cc of N/10-alkali was required for the organic acid, and of this 4.8 cc were used immediately (free acid) and the remainder slowly (lactone)."

Für die Angabe von HERBERT, HIRST u. MITARB. (Soc. 1933, 1282), dass aus oxydierter Ascorbinsäure in Gegenwart von Sauerstoff Oxalsäure gebildet wird, liegen keine ausreichenden experimentellen Beweise vor.

Die Einwirkung von Alkali auf DHAs beginnt mit der Aufspaltung des Laktonringes zur Diketo-L-Gulonsäure. Die zu erwartende Analogie zwischen der Verseifung des Laktonringes der Ascorbinsäure und der DHAs mit der Verseifung anderer Laktone, die zuerst zusammenfassend von E. HJELT[1] beschrieben wurde, scheint insofern zuzutreffen, als z. B. β- und γ-Butyro- und Valero-Lakton sowie Phtalid wie normale Carbonsäure-Ester durch Alkali hydrolysiert (verseift) werden unter Bildung von Salzen der entsprechenden Oxysäuren. Da die Kinetik solcher Ester-Hydrolysen in diesem Institut eingehend studiert wird, soll hier weder auf die Behandlung dieser Reaktionen vom Standpunkt der chemischen Elektronentheorie noch auf die einschlägige Literatur eingegangen werden.

Dagegen sei über das Verhalten der DHAs bei und nach der Sprengung des Laktonringes, also über das Verhalten der Diketo-L-Gulonsäure[2] folgendes erwähnt:

Zunächst mag daran erinnert werden, dass die Oxydation der Ascorbinsäure zu DHAs reversibel ist.[3] Aus den Versuchen von PENNEY und ZILVA[4] geht hervor, dass *in vitro* der Laktonring der Ascorbinsäure und der DHAs ebenso wie andere Laktonringe aus den entsprechenden Oxysäuren bis zu einem Gleichgewicht zurückgebildet wird. DHAs und DKG scheinen nach BORSOOK[5] in Organen höherer Tiere in Spuren vorzukommen. Dies gilt auch bzgl. *canceröser* Organe.[6] In pflanzlichen Organen lässt sich hingegen DHAs in erheblichen Mengen nachweisen; über das Vorkommen von DKG in Pflanzen liegen noch keine endgültigen Ergebnisse vor.

---

[1] E. HJELT, Über die Laktone. Stuttgart, Verlag Enke, 1903, S. 40. — Siehe auch: HJ. JOHANSSON, Lunds Univ. årsskr. 12, No 8; 1016. — H. SIBELIUS, Diss. Lund 1928; E. OTT, Neuere Untersuchungen über Laktone 1920.

[2] Siehe hierzu J. R. PENNEY u. S. S. ZILVA, Biochem. J. 37, 39 u. 403; 1943, — 39, 1, 1945.

[3] Siehe hierzu auch die neueren Bestätigungen von J. H. ROE, M. B. MILLS, M. J. OESTERLING a. C. M. DAMRON, J. Biol. Chem. 174, 201; 1948. — J. H. ROE a. C. A. KUETHER, J. Biol. Chem. 147, 399; 1943.

[4] J. R. PENNEY a. S. S. ZILVA, Biochem. J. 37 u. 403; 1943. — 39, 1; 1945. Gegenteilige Ergebnisse von GOSH a. RAKSHIT, Biochem. Zs. 299, 394; 1938.

[5] H. BORSOOK, H. W. DAVENPORT, C. E. P. JEFFREYS a. R. C. WARNER, J. Biol. Chem. 117, 237; 1937.

[6] H. M. DYER a. H. E. ROSS, J. Nat. Cancer Inst. 11, 313; 1951.

Bei der im Tierkörper stattfindenden Rückbildung der Ascorbinsäure aus DHAs (BORSOOK, l. c.) tritt offenbar keine Veränderung am Laktonring ein. Jedoch liegen noch keine Entscheidungen darüber vor, *unter welchen Umständen* auch im lebenden Organismus (Abwesenheit von Hemmungsstoffen?) eine Öffnung und Schliessung des Laktonringes eintreten kann.

Gleichgewichte an einfachen Zuckerarten

Es liegt nahe, die an Ascorbinsäure und an DHAs studierte Laktonspaltung mit denjenigen Vorgängen zu vergleichen, welche an den *Halbacetal*-Formen der Zucker auftreten. In wiederholten Diskussionen hat man in der ersten Entwicklungsperiode der Zuckerchemie versucht, eine Entscheidung herbeizuführen zwischen den offenen Formeln von EMIL FISCHER und den Halbacetal-Formeln von TOLLENS.[1] Dagegen ist der Mechanismus der unter verschiedenen Bedingungen zweifellos eintretenden Übergänge zwischen diesen beiden Strukturformen nie eingehend bearbeitet worden, obwohl zahlreiche Reaktionen, z. B. die Umlagerungen und Gleichgewichte, welche LOBRY DE BRUYN und ALBERDA VAN EKENSTEIN[2] in alkalischen Lösungen von Glukose, Fruktose und Mannose gefunden haben, eine intermediäre Aufspaltung der Halbacetal-Ringe voraussetzen. In reaktionskinetischer Hinsicht erscheint es als eine wichtige Aufgabe, die Bedingungen der Gleichgewichte zwischen den offenen Formen und den Halbacetal-Formen der Zucker festzustellen.[3]

Vergleicht man die hydrolytischen Spaltungsreaktionen und Spaltungs-Gleichgewichte der einfachen Carbonsäure-Ester einerseits mit denjenigen der Laktone, besonders der Ascorbinsäure und Dehydro-Ascorbinsäure, andererseits mit den Spaltungsreaktionen und Gleichgewichten der Halbacetale der einfachen Zuckerarten, so sind zunächst die Unterschiede bezüglich des pH-Einflusses bemerkenswert.

Einfache Carbonsäure-Ester besitzen im allgemeinen ein Maximum der Stabilität im pH-Gebiet 3,5–5,5. Für die Stabilität der Laktone liegt noch kein genügend grosses Versuchsmaterial vor, um allgemeine Regelmässigkeiten daraus entnehmen zu können. Bis jetzt lässt sich nur sagen, dass im allgemeinen die Lakton-Spaltungen rascher und vollständiger in alkalischer als in saurer Lösung verlaufen, wobei aber zu berücksichtigen ist, dass durch die mit Alkali eintretende Salzbildung der entstehenden Oxysäuren eine Gleichgewichtsverschiebung herbeigeführt wird.

Papier-chromatographische Versuche mit Glucose und Triose-Redukton in alkalischer Lösung.

Für die weitere präparative Bearbeitung der aus Hexosen in alkalischer Lösung entstehenden Produkte haben wir orientierende chromatographische Versuche angestellt, deren Ergebnisse in folgender Figur 1 ersichtlich sind.

---

[1] Siehe hierzu E. FISCHER u. K. ZACH, Chem. Ber 44, 132 u. zu 141; 1911.

[2] LOBRY DE BRYUN u. AKBERDA VAN EKENSTEIN, Rec. Trav. Chim. Pays Bas; 1883.

[3] Vgl. DELAHAY a. STRASSNER, J. Am. Chem. Soc. 74, 893; 1952.

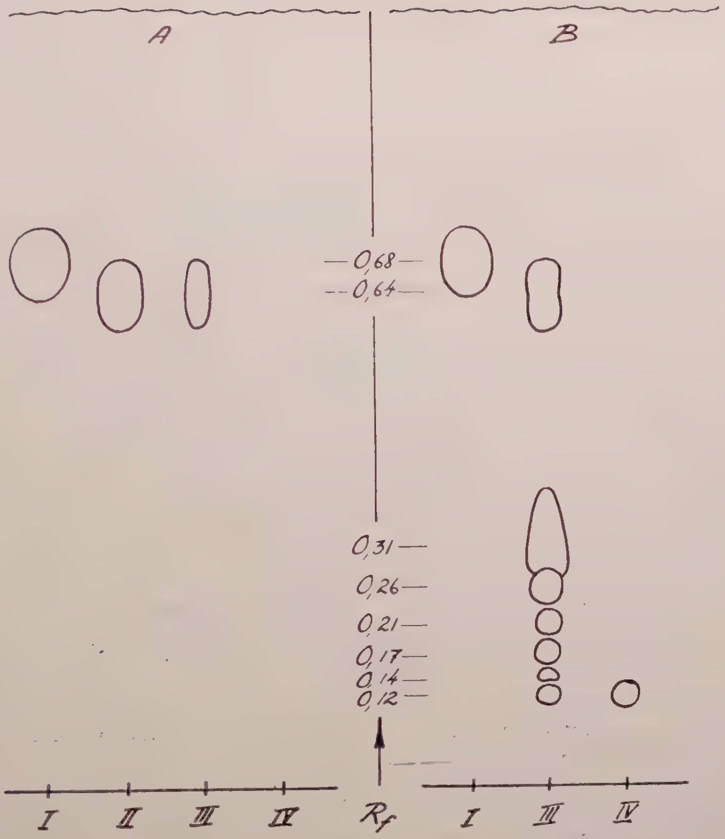

Fig. 1.

Lösung: 80 Tl. Butanol, 20 Tl. Eisessig, 20 Tl. Wasser.
In den chromatogrammen A und B waren die untersuchten Substanzen, Glucose und Triose-Redukton, folgendermaassen behandelt:

I. 20 mg Redukton in 1 ml Wasser + einige Tropfen Eisessig.

II. 20 mg Redukton in 1 ml 1 n NaOH in N_2-Atm. auf sied. Wasserbad 60 Minuten, hierauf angesäuert mit Essigsäure.

III. 20 mg Glucose in 1 ml 1 n NaOH in N_2-Atm. auf sied. Wasserbad 60 Minuten, hierauf angesäuert mit Essigsäure.

IV. 20 mg Glucose in 1 ml Wasser + einige Tropfen Eisessig.

Chromatogramm A bespritzt mit 0,005 n TR.
Chromatogramm B bespritzt mit 1 %-iger Ammoniak. $AgNO_3$-Lös.
Bei A erhält man auf rotem Grund, weisse Flecken blau-färbbar mit NH_3-Dampf.
Bei B erhält man braune Flecken (die Redukton-Flecken anfang schwarz).

Figur 1 zeigt folgendes:

Das mit NaOH behandelte Redukton liefert nur *einen* Flecken, dessen R_f-Wert 0,64 beträgt, während für Redukton 0,68 gefunden wird. Triose-Redukton wird

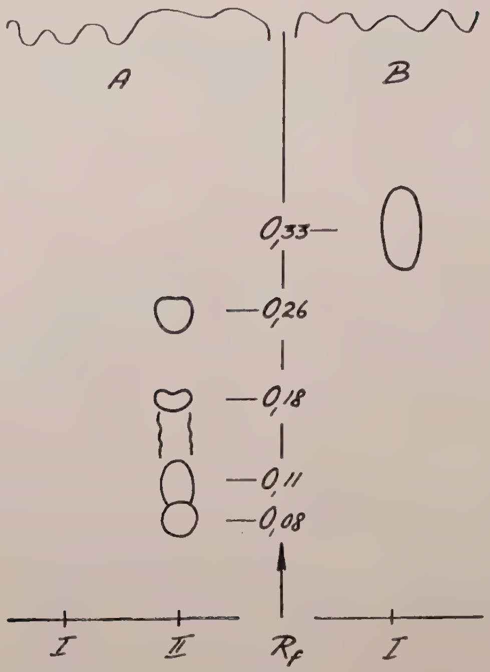

Fig. 2.

Die Nummern im Chromatogramm Fig. 2 zeigen folgende Behandlung des Glukurons an:

I. 80 mg Glukuron in 1 ml Wasser.

II. 80 mg Glukuron in 1 ml 2 n NaOH in N_2-Atm. 60 Minuten auf siedendem Wasserbad, dann neutralisiert.

Chromatogramm A bespritzt mit 0,005 n TR in NH_3-Atm. wobei farblose Flecken auf blauem Grund erhalten werden.

Chromatogramm B bespritzt mit 1 %-iger Lösung von p-Aminobenzoesäure; das Glukuron (bezw. die Glukuronsäure) tritt als rosaroter Flecken auf farblosem Grund hervor.

also in Alkali so umgewandelt, dass keine Ausgangs-Substanz übrig bleibt (andernfalls wären 2 Flecken erhalten worden).

Flecken III im Chromatogramm B (alkali-behandelte Glucose), $R_f = 0{,}64$, muss somit von dem zunächst (nach 2–3 Min. Erhitzen) entstandenen Redukton herrühren, das dann in Flecken III B–III A umgelagert wird.

Glukuron

Während aus der *Gluconsäure* durch Erhitzen mit Alkali keine mittels Tillmans Reagens nachweisbare Endiol-Gruppe entsteht[1], verhalten sich Glukuronsäure bezw. Glukuron in dieser Hinsicht insofern wie die einfachen Aldosen und Ketosen, als sie durch Alkali enolisiert werden und dann TR reduzieren. Dabei entsteht aus *1 Mol Glukuron 1 Endiol-Gruppe,* die *1 Mol TR reduziert.*[2]

---

[1] EULER u. KLUSSMANN, Dieses Arkiv, 11 B, Nr. 8 (1933).

[2] Der Firma F. HOFFMANN-LA ROCHE, Basel danken wir bestens für die freundliche Überlassung von Glukuron.

Versuch

2,4 mg D (+)-Glukuron wurden in 5 ml Wasser gelöst, mit 0,5 ml 2 n NaOH versetzt und unter Einleiten von N_2 mit 0,01 n TR bei 90° titriert.

Verbrauch	2,85 ml 0,01 n TR
Theor. für 1 Mol Endiol	2,73 ml 0,01 n TR

Also durch die alkal. Behandlung gebildet 1,05 Mol auf 1 Mol D (+)-Glukuron.

Bei der Titration grösserer Konzentrationen als der hier verwendeten stösst man auf Schwierigkeiten, da die dann entspr. grössere Menge TR verbraucht wird und eine Missfärbung auftritt, welche die Bestimmung des Umschlagspunktes für TR erschwert.

Ob bei der alkalischen Erhitzung von Glukuron Trioseredukton gebildet wird, haben wir nicht untersucht.

Aus Glukuronsäure entsteht, ebenso wie aus Galakturonsäure und vermutlich auch aus anderen Uronsäuren, durch Kochen mit starker Salzsäure neben Furfurol die REICHSTEIN'sche *Reduktinsäure* und zwar unter gleichzeitiger Abspaltung von CO_2.[1]

Die Empfindlichkeit der Glukuronsäure gegen Alkali geht ferner aus dem Chromatogramm hervor (Fig. 2).

Als Lösung wurde wieder die Mischung 80 Tle Butanol, 20 Tle Eisessig, 20 Tle Wasser verwendet.

Der Versuch zeigt, dass das Glukuron durch die Alkali-Behandlung ganz verschwindet. Ein eventuell unverändertes Glukuron hätte sich mit TR nachweisen lassen, da die alkalische Lösung des Glukurons TR entfärbt.

Frau Dr. INGRID LOEPER danken wir bestens für eifrige Hülfe bei der Ausführung der Versuche.

Stockholm, Universität, Vitamin-Inst. u. Inst. f. organ.-chem. Forschung.

---

[1] H. THIERFELDER, Zs. physiol. Chem. 11, 406; 1887. — T. REICHSTEIN u. R. OPPENAUER, Helv. Chim. Acta 16, 988; 1933. — Z. I. KERTESZ, The Pectic Substances, New York and London 1951.

Tryckt den 18 november 1952

Uppsala 1952. Almqvist & Wiksells Boktryckeri AB

ARKIV FÖR KEMI Band 5 nr 6

Communicated 4 June 1952 by Arne Fredga

A study of possible methods for preparing α-ketomercaptans

By Lennart Schotte

Mercaptoacetone was first synthesized by Groth (1) from monochloro-acetone and dithiocarboxy-glycolic acid by the decomposition of the thiocarb-acetonyl-mercapto-glycolic acid obtained from them. About twenty years later, 1948, Hromatka and Engel (2) prepared the same substance from sodium sulfhydrate and monochloro-acetone, a method which was also used by Ohta (3) in 1950.

Finally some supplementary investigations were carried out on the same substance by the author in 1951 (4). These confirmed the statement that mercaptoacetone could be obtained with a good yield from a simple reaction between sodium sulfhydrate and the corresponding halogen ketone. An analoguos result was obtained for 1.3-dimercaptoacetone (5 and 6).

It is of interest to discuss thoroughly the methods, by which the mercaptans mentioned are obtained.. In 1924 Groth (7) prepared phenacylmercaptan as the first known α-ketomercaptan, and he found that the reaction between phenacylbromide and sodium sulfhydrate, however the conditions were varied, always gave diphenacyl sulfide as the main product, and only a small yield of the intended mercaptan. Groth therefore examined other methods, and came to the conclusion that a suitable way of obtaining the ketomercaptan was from a decomposition in weakly acid solution of the acid

$$C_6H_5{-}CO{-}CH_2{-}S{-}CS{-}O{-}CH_2{-}COOH$$

according to

$$C_6H_5{-}CO{-}CH_2{-}S{-}CS{-}O{-}CH_2{-}COOH + 2\,H_2O \rightarrow C_6H_5{-}CO{-}CH_2{-}SH + H_2S + CO_2 + \\ + HO{-}CH_2{-}COOH.$$

This reaction was later found to be general (1), and decompositions of acids of the type $R{-}S{-}CS{-}O{-}CH_2{-}COOH$, where R contains the keto group, were used to prepare mercaptoacetone, methyl α-mercapto-ethyl ketone and mercapto-methyl ethyl ketone.

It may seem at this point that the different communications are contradictory, but an investigation of the sulfhydrate reactions gave an obvious explanation. It was early known that a reaction between a halogenated alkane and sodium or potassium sulfhydrate results in the corresponding mercaptan, with the exception of possible rearrangements in certain cases, *e.g.* if the halogen compound is tertiary. However, the author has now found that reactions between sodium sulfhydrate and methyl α-bromo-ethyl ketone, bromo-methyl ethyl ketone and phenacyl bromide respectively in water or alcohol as solvents always give a good yield of the corresponding sulfides. The last reaction is a complete confirmation of Groth's findings (7). On the other hand, the treatment of the alkali sulfhydrate with monochloro-acetone or 1.3-dichloroacetone in similar conditions resulted in the corresponding mercaptan. The explanation of this apparent discrepancy must be that mercaptoacetone and 1.3-dimercaptoacetone are dimeric (4 and 6), while the other mercaptans required are monomeric and therefore more soluble in the reaction medium. As the α-ketomercaptans are obviously acid in monomeric form, they can react faster than the sulfhydrate with the halogen ketone, added during the reaction, and produce a sulfide as end product according to, for instance,

$$\mathrm{R{-}CO{-}CH_2{-}S^- + Cl{-}CH_2{-}CO{-}R \rightarrow R{-}CO{-}CH_2{-}S{-}CH_2{-}CO{-}R + Cl^-}$$

where R is a phenyl or an alkyl group. The dimeric α-ketomercaptans, mercaptoacetone and 1.3-dimercaptoacetone, on the other hand, do not react according to this scheme, because the dimerisation tendency in these cases is such that the mercaptans are immediately precipitated from the solutions in the dimeric forms. Of course, any further reaction producing the corresponding sulfides cannot take place in such a case, and that seems to be the reason why only the first homologues of the aliphatic α-mercapto- and $\alpha.\alpha'$-dimercaptoketones can be prepared by alkali sulfhydrate reactions with the corresponding halogen ketones. It may be mentioned that even the dimeric form of 1.3-dimercaptoacetone has free mercapto-groups, but they do not react further, owing to the low solubility of the compound.

With a view to making a closer study of the homologous series of $\alpha.\alpha'$-dimercaptoketones, the possibilities of obtaining higher homologues of 1.3-dimercaptoacetone were investigated. It has already been mentioned by the author (6) that a method analogous to that used by Groth in his preparation of mercaptoacetone is not very successful in this case. Reactions between sodium sulfhydrate and $\alpha.\alpha'$-dibromomethyl-*iso*propyl ketone and $\alpha.\alpha'$-dibromo-di*iso*propyl ketone respectively have also been performed under various conditions, but without success. The mercapto-groups could certainly be detected by means of a qualitative test (8), but the yields of the mercaptans were too small for an isolation of the substance to be possible. However, the $\alpha.\alpha'$-dibromo-di*iso*propyl ketone reaction did give the corresponding sulfide, even though the yield was small, and the remarks above are therefore valid even for $\alpha.\alpha'$-dimercaptoketones. The sulfide mentioned is of a special interest, as it consists of an eight-membered ring:

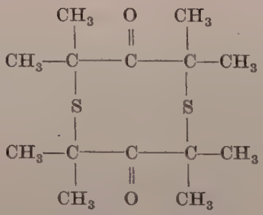

(I)

The compound gave no mercapto-group reaction and proved to have the right molecular weight. A model of the structure (I) could easily be constructed with Fisher-Hirschfelder-Taylor Atom Models. — But it was not possible to isolate any appreciable quantity of a unitary product from the $\alpha.\alpha'$-dibromo-methyl-*iso*propyl ketone reaction. This must be due to the different reaction velocities of the primary and the tertiary groups, as the reaction cannot then proceed at the same rate in different directions, which must of course diminish the possibility of a ring closure to form the corresponding sulfide. Thus the higher homologues of 1.3-dimercaptoacetone could unfortunately not be prepared by the methods investigated.

It may be asked, why the above mentioned *α.α'*-dibromoketones have been used in this investigation, as it is well known that tertiary alkyl halides often give anomalous results, owing to reactions of the so-called S_1 type. The answer is that the halogen compounds have been chosen so as to make impossible any suspicion of an unsymmetrical structure. It is actually rather difficult to produce symmetrically (*α.α'*) substituted dibromoketones (cf. 9). The author has made many attempts to get *α.α'*-dibromo-diethyl ketone by direct bromination or by treatment of 2.5-dimethylcyclopentatrione-1.3.4 (10 and 11) with sodium hypobromite, but they failed, in spite of varied conditions.

Experimental

Bis-(α-methyl-acetonyl)-sulfide

A solution of 30.2 g (0.20 mole) of methyl *α*-bromo-ethyl ketone (prepared by direct bromination of methyl ethyl ketone) in 35 ml of alcohol was dropped, with stirring, into a water solution (200 ml) of 12.5 g (0.22 mole) of sodium sulfhydrate. The reaction was performed at room temperature and was complete after two hours. The solution was extracted with ether, the ether layer was separated and dried with anhydrous sodium sulfate. The ether was then evaporated at reduced pressure, and the residue was fractionated *in vacuo*. The sulfide was obtained as a somewhat viscous liquid with boiling point 109–111°/8 mm. The yield was 15.2 g (87.5 %). — The semicarbazone decomposed at 213–215° (KOFLER) (cf. 1).

The reactions between bromo-methyl ethyl ketone and phenacyl bromide respectively and sodium sulfhydrate were performed in the way described above. The bromo-methyl ethyl ketone was obtained from butene-1 and HBrO (12). The corresponding sulfide boiled at 129–131°/8 mm and crystallized upon cooling to about 10° (cf. 1).

2.4.6.8-Dimethyl-1.5-dithiacyclooctadione-3.7 (I)

62 g (0.22 mole) of *α.α'*-dibromo-di*iso*propyl ketone, dissolved in 50 ml of alcohol, was dropped into a hot solution (about 70°) of 0.5 mole of potassium sulfhydrate in 100 ml of alcohol. The reaction was complete two hours after the halogen ketone had been added, and the mixture was then poured into four parts of water. The solution was extracted with ether, and the ether layer was dried with anhydrous sodium sulfate after separation. When the ether had been evaporated *in vacuo*, a substance sublimated from the residue. 4.0 g of a crude product was thus obtained. The remaining liquid boiled over an interval of 40° (60–100°/9 mm) without giving any unitary product of mentionable quantity. The crystalline substance obtained, which did not give any mercapto-group reaction, could be purified by sublimation or by recrystallization from a mixture of water and alcohol. The melting point was 104–106°. The sulfide was obtained as very long, colourless needles and had an obvious smell of camphor. The yield was 3.1 g (9.7 %).

The reaction has also been performed at room temperature, with different solvents and with different reaction time but always with the same result as above. However, the best yield was obtained with the described procedure.

Anal. Subst., 17.60 mg: CO_2, 37.44 mg; H_2O, 13.40 mg.
» 15.64 mg: 4.840 ml of 0.04532-N NaOH.
$C_{14}H_{24}O_2S_2$ (288.45) calc. C 58.29; H 8.39; S 22.23.
found C 58.05; H 8.52; S 22.48.

Molecular weight determination: (*by the ebullioscopic method*)

0.0498, 0.0960 g in 15.62 g benzene: E = 0°.030, 0°.056.
M.W. calc. 288, found 276, 286.

SUMMARY

Possible methods for preparing α-ketomercaptans have been discussed.

A general rule is given regarding the reactions of alkali sulfhydrate with halogen ketones, and apparent discrepancies in published reports thus explained.

A cyclic compound containing an eight-membered ring with two sulfide-functions has been prepared.

Laboratory of Organic Chemistry, Chemical Institute, University of Uppsala, May 1952.

REFERENCES. 1. **B. Groth,** Über α-Mercaptoketone und verwandte Stoffe. Diss. Uppsala (1926). — 2. **O. Hromatka** and **E. Engel,** Monatsh. *78,* 29 (1948). — 3. **M. Ohta,** J. Pharm. Soc. Japan *70,* 709 (1950). — 4. **L. Schotte,** Arkiv Kemi, *3* (1951) nr 43. — 5. **L. Schotte,** Acta Chem. Scand. *4,* 1304 (1950). — 6. **L. Schotte,** Arkiv Kemi, in press. — 7. **B. Groth,** Arkiv Kemi, Mineral. Geol. *A 9* (1924) nr 1. — 8. **H. Rheinboldt,** Ber. *60,* 184 (1927). — 9. **L. Schotte,** Acta Chem. Scand. *5,* 969 (1951). — 10. **O. Diels, J. Sielisch** and **E. Müller,** Ber. *39,* 1328 (1906). — 11. **L. Claisen** and **Th. Ewan,** Ann. *284,* 245 (1895). — 12. **M. de Montmollin** and **P. Matile,** Helv. Chim. Acta *7,* 106 (1924).

Tryckt den 10 december 1952

Uppsala 1952. Almqvist & Wiksells Boktryckeri AB

ARKIV FÖR KEMI Band 5 nr 7

Communicated 4 June 1952 by Arne Westgren and Gunnar Hägg

On the coprecipitation of lanthanum ions and tri- or tetrapositive ions as fluorides

By Kurt Schlyter

With 5 figures in the text

Introduction

The lanthanum ion La^{3+} has previously been shown to enter anomalous mixed crystals with the CaF_2 structure, where for instance 1 La^{3+} + 1 F^- replace 1 Sr^{2+} (1–5). However, anomalous mixed crystals with the LaF_3 (tysonite) structure had not been proved to exist at the time the present work was started. Part of the inspiration to this work came from a note on the behavior of plutonium which seemed to indicate the existence of such anomalous mixed crystals.

Cunningham and Werner (6) in their first isolation of plutonium made use of the fact, first discovered by Seaborg, Wahl, and Kennedy (7), that the lower oxidation states of Pu are coprecipitated with LaF_3 whereas the plutonyl ion PuO_2^{2+} is not. Pu could thus first be separated from the large amount of UO_2^{2+} originally present, using LaF_3 as a carrier; then the Pu of the precipitate could be oxidized to PuO_2^{2+} and the La removed by a new precipitation. — The coprecipitation of Pu with La is believed to have also been considered for the industrial production of Pu (8).

If Pu^{3+} coprecipitates with LaF_3 this is not too surprising. The ionic radii are very similar (La^{3+} 1.04 Å, Pu^{3+} 1.01 Å) (9). A partial or even a total replacement of the La^{3+} ions in LaF_3 by Pu^{3+} can thus be expected.

More remarkable, however, is that *tetrapositive* plutonium is also carried almost quantitatively by LaF_3 under circumstances where PuF_4 would not precipitate in the absence of La. This coprecipitation is generally ascribed to adsorption (10). On the other hand, Cefola and Smith (11) analyzed a number of LaF_3-PuF_4 precipitates, prepared with an excess of Pu in the solution, and found that the ratio La^{3+}/Pu^{4+} varied between 1.81 and 3.4 in the precipitate. Their conclusion was that a compound $La_2PuF_{10}(H_2O)_x$ is formed; they do not seem to have used X-ray photographs.

Evidence will now be given supporting a third explanation, namely that solid solutions are formed, which are in this case anomalous mixed crystals. For reasons easily understood I had no access to plutonium compounds. However, Ce^{4+} (radius about 0.87 Å) is likely to be a good stand-in for Pu^{4+} (0.86 Å).

The present work deals with the ability of La^{3+} to form mixed fluoride crystals of the tysonite type with tripositive lanthanide ions and certain tetrapositive ions. Quite apart from the special question touched on, it may have a general bearing on the mechanism of coprecipitation on carriers.

Preparative methods

An 0.1 C aqueous solution of lanthanum nitrate was mixed in a platinum crucible with an 0.1 C aqueous solution of a nitrate (in a few cases sulfate) of a tri- or tetrapositive ion, Me^{3+} or Me^{4+}. The mole ratio Me/(Me + La) will be denoted by x_{Me}; it was varied in a series of experiments so as to get x_{Me} values evenly distributed between 0 and 1.

The fluorides were then precipitated either by adding an aqueous solution of NaF or by adding dilute HF, both precipitants in excess. If the Me salt was a nitrate, HF-precipitated mixed fluorides were obtained as a residue on evaporation to dryness on a steam bath at 100° C. The small amounts of nitric and hydrofluoric acid remaining in the residue were of no importance in the subsequent X-ray work. — NaF-precipitated fluorides were heated on a steam bath at 100° C, filtered off, washed, and dried in air. Whenever it was possible without oxidation or reduction (as for U^{4+} or Ce^{4+}), the precipitate was first heated with the supernatant solution in an autoclave at 220° C.

After evaporation, x_{Me} of the HF-precipitated residue was necessarily equal to that of the original mixed solution. After filtering the NaF-precipitate, x_{Me} may on the other hand have changed, because of La or Me lost with the liquid; this change was, however, thought to be negligible.

The Me solutions were prepared from Me nitrates or oxides. The starting reagents were of varying purity. Most compounds were marked as "puriss". Because of anomalous results with Sm_2O_3, which had no purity label, it was analyzed spectrographically very carefully and found to be as pure as could be desired for the present purpose (see below). — It should be noted that even a contamination with as much as 5 % of the nearest neighbor in the lanthanide series would have a barely perceptible influence on the average ionic radius and the unit cell dimensions.

Many of the starting materials did not have a well-defined formula; the nitrates had absorbed moisture, and some oxides had been partially transformed into carbonates. Thus it was necessary to analyze the aqueous solutions. The following methods were used: a) A known volume of a nitrate solution was evaporated, the residue was ignited and weighed as oxide (Nd_2O_3, Sm_2O_3, Gd_2O_3, Er_2O_3, ZrO_2, CeO_2, and ThO_2). b) To a known volume of a praseodymium nitrate solution, excess of hydrofluoric acid was added. The supernatant solution was evaporated at 100° C, the residue was heated to 300° C and weighed as PrF_3. c) The concentration of U^{4+} was determined by permanganate titration in acid solution.

The preparations of $La(NO_3)_3(H_2O)_6$, and $Ce(NO_3)_3(H_2O)_6$ were found analytically to have the composition given by the formula. The "spectral pure" preparations of Eu_2O_3, Dy_2O_3, and Yb_2O_3 were available only in small amounts; since they were sealed in glass ampoules, their composition was taken to be correct. Solutions of known concentration could thus be prepared by dissolving a weighed amount of the nitrate in a known volume of water or by converting a weighed amount of the oxide into nitrate, which was then dissolved in a known volume of water.

Determination of cell dimensions

Powder photographs of the fluorides were made in two different types of PHRAGMÉN focusing cameras. The first, medium-angle, type gave an estimated maximum uncertainty of ±0.010 Å in a and ±0.015 Å in c. It was used for all HF precipitated fluorides, and moreover for the fluorides with U^{4+} and Ce^{4+} whether precipitated with HF or NaF. The second (large-angle), camera type was more accurate (uncertainty at most ±0.005 Å in a and ±0.007 Å in c), but required a better crystallized sample, giving sharp lines. It could be used for mixed fluorides of La^{3+} with Ce^{3+}, Pr^{3+} and Nd^{3+}.

Since the tysonite structure is hexagonal, we have for each reflexion

$$\sin^2\theta = (h^2+hk+k^2)\cdot\lambda^2/3a^2 + l^2\cdot\lambda^2/4c^2 \tag{1}$$

which may be written:

$$10^4\cdot\sin^2\theta = K_1(h^2+hk+k^2)+K_2\cdot l^2. \tag{2}$$

Through a parallel investigation (12), hkl for each reflexion was known. For each observed $\sin^2\theta$ value one could thus draw the corresponding straight line in a coordinate system with K_1 and K_2 as axes. The common point of intersection of all lines (2) in such a diagram should give the true values for K_1 and K_2, from which a and c can then be calculated with

$$a = 89.016/\sqrt{K_1}\ \text{Å};\quad c = 77.090/\sqrt{K_2}\ \text{Å}. \tag{3}$$

In (3) the weighed average wave length of $CuK\alpha_1$ and $CuK\alpha_2$ has been used

$$\lambda_a = 1.5418\ \text{Å}\ (13). \tag{4}$$

Actually, because of measuring errors, the points of intersection do not coincide but are scattered over a certain area, the greater, the more diffuse the powder reflexions. The determination of K_1 and K_2 was aided by the fact that the ratio c/a is practically constant = 1.772 for LaF_3, CeF_3, PrF_3, NdF_3, and SmF_3 (14). (Table 3 below). This ratio corresponds in the diagram to the auxiliary line

$$K_1 = K_2\cdot 4.187. \tag{5}$$

In all diagrams drawn, the points of intersection were reasonably centered around the auxiliary line (5), and so the values for K_1 and K_2 were assumed to be exactly on it.

Fig. 1 and Table 1 give an example of such a calculation for pure LaF_3 and for a mixed fluoride with $x_{Me} = 0.481$. The $\sin^2\theta_{calc}$ values have been computed from the values $K_1 = 460.5$ (467.4_0) and $K_2 = 109.0$ (111.6_5) obtained from Fig. 1. The corresponding cell dimensions are $a = 4.148$ Å (4.117 Å) and $c = 7.354$ Å (7.296 Å). Table 2 gives the experimental values for a and c at various x_{Me}, for a number of different Me^{3+} and Me^{4+}. The accuracy of a and c has been discussed above; that of x_{Me} should be better than ±0.005.

In Fig. 2, a is plotted as a function of x_{Me} for the various systems studied. A plot of c versus x_{Me} would give nothing new, since c has been assumed to be proportional to a. For each $a(x_{Me})$ plot, the best straight line has been drawn through the points.

Table 1

Powder photograph data used for constructing Fig. 1 a and Fig. 1 b. Cu*K* radiation

a) Pure LaF_3			b) LaF_3–PrF_3, $x_{Pr} = 0.481$		
h k l	$10^4 \sin^2 \theta_{obs}$	$10^4 \sin^2 \theta_{calc}$	*h k l*	$10^4 \sin^2 \theta_{obs}$	$10^4 \sin^2 \theta_{calc}$
1 1 6	5343	5338	1 1 6	5418	5422
2 2 0	5527	5526	2 2 0	5601	5609
1 0 7 (216 β)	5852	5846 (5854)	2 2 2	6062	6055
3 0 4	5911	5903	3 1 1	6189	6188
2 2 2 (215)	5965	5966 (5971)	3 1 3	7081	7081
3 1 1	6096	6096	2 1 7	8738	8743
4 0 1	7474	7478	3 1 5	8867	8867
3 0 6	8101	8101	3 2 1	8993	8992
4 0 3	8357	8357			
1 1 8	8417	8415			
2 1 7	8595	8609			
3 1 5	8731	8734			
3 2 1 (208)	8855	8859 (8876)			
1 0 9	9362	9362			
2 2 6 (501 β)	9481	9482 (9476)			
4 1 0	9666	9671			
3 2 3	9733	9739			

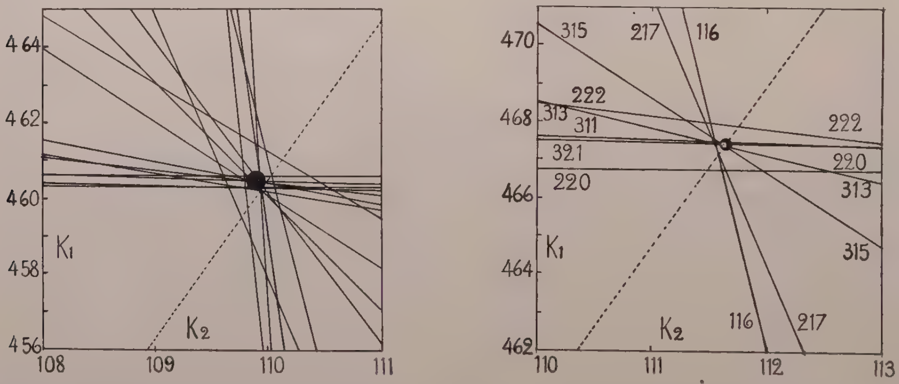

Fig. 1 a.

Fig. 1 b.

Fig. 1. Graphical determination of the cell constants for a) LaF_3, b) a mixed fluoride with $x_{Me} = 0.481$. Each line gives the relation between K_1 and K_2 following from (2) and the $\sin^2 \theta$ value measured for a certain *hkl* reflexion. The dashed line is the auxiliary line, and the solid circle is the estimated mean section point.

For the fluorides precipitated with NaF, the fit seems to be very good. For a few of the systems in Fig. 2, the experimental points are seen to spread considerably around the straight line. The deviations occur especially for HF-precipitated fluorides, with $Me^{3+} = Nd^{3+}$ or Pr^{3+}, and cannot be ascribed to measuring errors. A possible explanation is as follows. When hydrofluoric acid is added to a mixed solution of nitrates of La^{3+} and Me^{3+}, some fluoride precipitates, and the resulting

Table 2

Variation of cell dimensions (in ÅU) of mixed crystals LaF_3–MeF_3(MeF_4) with mole fraction x_{Me}

	Ce^{3+}	Pr^{3+}	Nd^{3+}	Sm^{3+}	Eu^{3+}	Gd^{3+}	Dy^{3+}	Er^{3+}	Yb^{3+}	Y^{3+}	Zr^{4+}	U^{4+}	Ce^{4+}
x_{Me}	0.110	0.236	0.494	0.107	0.116	0.100	0.105	0.091	0.104	0.134	0.121	0.147	0.110
a	4.144	4.133	4.104	4.121	4.137	4.132	4.128	4.101	4.145	4.094	4.14	4.113	4.121
c	7.343	7.324	7.272	7.302	7.331	7.322	7.315	7.267	7.345	7.255	7.34	7.288	7.302
x_{Me}	0.225	0.481	1.000	0.215	0.231	0.203	0.212	0.186	0.209	0.261	0.238	0.254	0.225
a	4.138	4.117	4.055	4.114	4.128	4.121	4.125	4.073	4.124	4.077	4.14	4.100	4.117
c	7.333	7.296	7.185	7.290	7.315	7.302	7.310	7.217	7.308	7.224	7.34	7.265	7.295
x_{Me}	0.333	0.735		0.324	0.345	0.311	0.320	0.288	0.316	0.385	0.356	0.355	0.330
a	4.134	4.101		4.101	4.102	4.088	4.114	4.083	4.075	4.084	4.12	4.087	4.094
c	7.325	7.267		7.267	7.269	7.244	7.290	7.235	7.221	7.237	7.30	7.242	7.255
x_{Me}	0.442	1.000		0.438	0.457	0.420	0.429	0.394	0.425	0.501		(0.449)	0.445
a	4.133	4.086		4.078	4.094	4.084	4.086	4.062	4.042	4.039		(4.087)	4.087
c	7.324	7.240		7.226	7.255	7.237	7.240	7.198	7.162	7.157		(7.242)	7.242
x_{Me}	0.557			0.547	0.578	0.643	0.541	0.502	(0.536)	0.609			
a	4.129			4.071	4.078	4.051	4.054	4.021	(4.047)	4.025			
c	7.317			7.214	7.226	7.178	7.184	7.125	(7.171)	7.132			
x_{Me}	0.668			0.663	0.678	0.762	0.653	(0.618)		0.714			
a	4.121			4.064	4.053	4.025	4.030	(4.035)		4.025			
c	7.302			7.201	7.182	7.132	7.141	(7.150)		7.132			
x_{Me}	0.775			0.775	0.786	(0.879)	(0.767)						
a	4.120			4.016	4.038	(4.004)	(4.030)						
c	7.301			7.116	7.155	(7.095)	(7.141)						
x_{Me}	0.890			(0.887)	(0.894)								
a	4.115			(4.016)	(4.031)								
c	7.292			(7.116)	(7.143)								
x_{Me}	1.000												
a	4.113												
c	7.285												
P	NaF	NaF	NaF	HF	HF	HF	HF	HF	HF	HF	HF	NaF	NaF
x_{max}	1.000	1.000	1.000	0.80	0.85	0.75	0.70	0.50	0.40	0.65	?	0.35	0.45

Data from photograms, where two phases were observed or believed to exist are surrounded by brackets.

P means precipitant used, and x_{max} a roughly estimated upper limit for x_{Me} for mixed crystals of LaF_3 structure.

pH becomes too low to allow a complete precipitation of the lanthanide ions. Only during the subsequent evaporation of the hydrofluoric acid, the remaining cations are converted into solid fluorides. Thus the distribution of Me atoms in the residue is likely to be uneven.

In Table 3 the cell dimensions of LaF_3, CeF_3, PrF_3 and NdF_3, obtained in the present work, are compared with those of OFTEDAL (14). It should be noted that in the present work only the values for LaF_3 and CeF_3 have been calculated without using the auxiliary line (5). The a values given by OFTEDAL have been transformed to Å units and divided by $\sqrt{3}$, so as to correspond to a cell containing 2 RF_3, which seems to be the real unit cell (12).

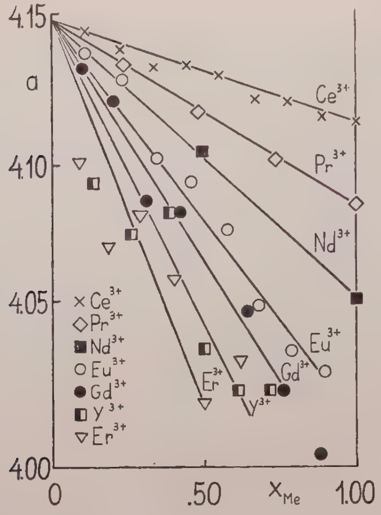

Fig. 2 a.

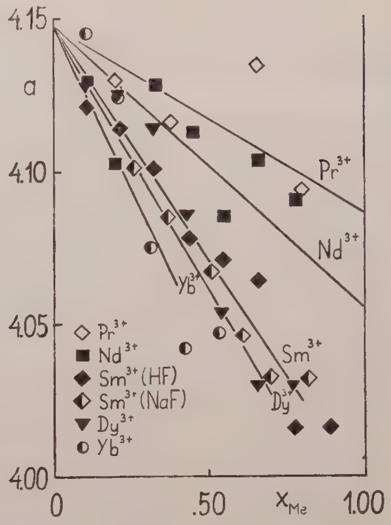

Fig. 2 b.

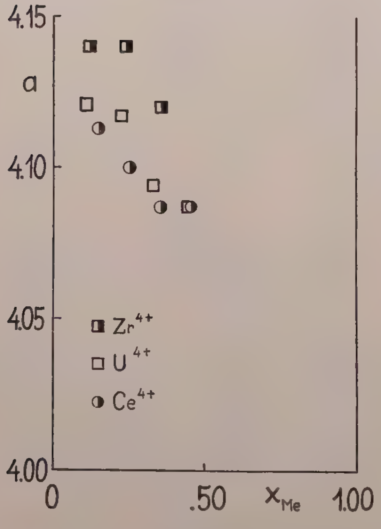

Fig. 2 c.

Fig. 2. Measured a values for mixed fluorides of tysonite type containing x_{Me} mole MF_3 or MF_4 per $(1-x_{Me})$ mole LaF_3, a) Ce^{3+}, Pr^{3+}, Nd^{3+}, Eu^{3+}, Gd^{3+}, Y^{3+}, Er^{3+} (all ions, excepting Eu^{3+}, NaF-precipitated), b) Pr^{3+}, Nd^{3+}, Sm^{3+}, Dy^{3+}, Yb^{3} (all ions, partly excepting Sm^{3+}, HF-precipitated), c) Zr^{4+}, U^{4+}, Ce^{4+} (NaF-precipitated). HF-precipitated Pr^{3+} and Nd^{3+} (b) are showing greater spread of the points than the corresponding NaF-precipitated samples in (a).

Table 3

Cell dimensions in Å obtained by OFTEDAL and the present author

Compound	a (IO)	c (IO)	$\frac{c}{a}$ (IO)	a (KS)	c (KS)	$\frac{c}{a}$ (KS)
LaF_3	4.144	7.344	1.772	4.148	7.354	1.773
CeF_3	4.115	7.288	1.771	4.113	7.285	1.771
PrF_3	4.085	7.233	1.771	4.086	7.240	(1.772)
NdF_3	4.062	7.211	1.775	4.055	7.185	(1.772)
			m. v. 1.772			m. v. 1.772

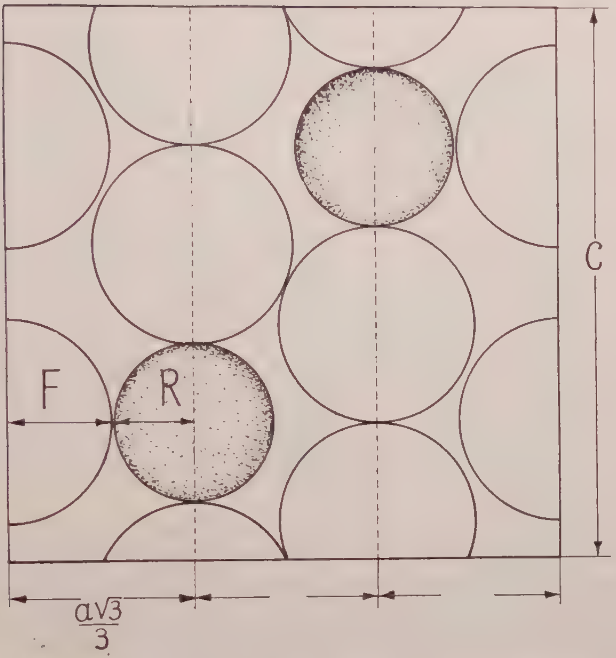

Fig. 3. Section $x+y=1$ through a unit cell with the tysonite structure. The shaded circles are heavy (R) atoms, open circles are fluoride atoms.

Tripositive ions

In the mixed fluorides LaF_3–MeF_3, it seems reasonable to assume that the La^{3+} and Me^{3+} ions are distributed randomly over the cation sites in the tysonite structure, acting like an average ion R^{3+} of radius

$$r(R^{3+}) = [1 - x_{Me}]\, r(La^{3+}) + x_{Me} \cdot r(Me^{3+}). \tag{6}$$

Fig. 3 gives a section through the hexagonal unit cell at $x+y=1$. Assuming the F^- and R^{3+} ions of the same z coordinate to be in contact, we obtain for a

$$a = \sqrt{3} \cdot [r(F^-) + r(R^{3+})]. \tag{7}$$

From (6) and (7) we obtain

$$a = \sqrt{3}\,[r(La^{3+}) + r(F^-)] - \sqrt{3}\,[r(La^{3+}) - r(Me^{3+})] \cdot x_{Me} = a_0 - k\, x_{Me}. \tag{8}$$

Equation (8) would give a linear relation between a and x_{Me}, as is also suggested by the data in Fig. 2. We shall compare the measured slopes k with those calculated from the ionic radii using (8).

From the cell constants of the Me_2O_3, GOLDSCHMIDT (15) calculated radii for all trivalent lanthanide ions (except for Pm^{3+}) and for Y^{3+}. Later on ZACHARIASEN has given radii for La^{3+}–Eu^{3+}, but not for Gd^{3+}–Lu^{3+} (9). From GOLDSCHMIDT's

Table 4

Ionic radii in Å according to GOLDSCHMIDT and ZACHARIASEN, and used in this work. Calculated slopes k of $a(x_{Me})$

Atomic number	Ion	r_G	r_Z	$r_G - 0.16$	r used	Δr	k_{calc}	k_{obs}
57	La^{3+}	1.22	1.04	1.06	1.04	0.00	0.000	0.000
58	Ce^{3+}	1.18	1.02	1.02	1.02	0.02	0.03_5	0.03_5
59	Pr^{3+}	1.16	1.00	1.00	1.00	0.04	0.06_9	0.06_2
60	Nd^{3+}	1.15	0.99	0.99	0.99	0.05	0.08_7	0.09_3
62	Sm^{3+}	1.13	0.97	0.97	0.97	0.07	0.12_1	0.15_4
63	Eu^{3+}	1.13	0.97	0.97	0.97	0.07	0.12_1	0.13_3
64	Gd^{3+}	1.11		0.95	0.95	0.09	0.15_6	0.16_1
66	Dy^{3+}	1.07		0.91	0.91	0.13	0.22_5	0.17_3
68	Er^{3+}	1.04		0.88	0.88	0.16	0.27_8	0.25_6
70	Yb^{3+}	1.00		0.84	0.84	0.20	0.34_6	0.21_3
39	Y^{3+}	1.06		0.90	0.90	0.14	0.24_2	0.20_2

radii r_G one may deduce ZACHARIASEN's values by first subtracting 0.08 Å (the difference between values of the ionic radius of O^{2-}, used by ZACHARIASEN and GOLDSCHMIDT), and then dividing with 1.07 – 1.08, to correct to the coordination number six. For the present purpose, the approximate formula

$$r = r_G - 0.16 \tag{9}$$

was used for computing radii for Gd^{3+}, Dy^{3+}, Er^{3+}, Yb^{3+}, and of Y^{3+}. The radii used are given in Table 4.

(With $r(La^{3+}) = 1.04$ Å and $r(F^-) = 1.33$ Å (9) (15) we obtain from (8) the cell constant for pure LaF_3, $a_0 = 4.12$ Å, which agrees fairly well with the experimental value 4.148 Å).

In Table 4, $\Delta r = r(La^{3+}) - r(Me^{3+})$; $k_{calc} = \Delta r \cdot \sqrt{3}$ according to equation (8); k_{obs} is the slope of the corresponding curve in Fig. 4.

Fig. 5 gives k_{calc} and k_{obs} as functions of the atomic number; Y^{3+} has been given at the atomic number 67 since the ionic radius seems to be close to that of Ho. Neither of the k values seems to form a very smooth curve. For k_{calc} the spread is explained by the fact that r is given only with an accuracy of 0.01 Å. The curve in Fig. 5 is an attempt to draw a smooth curve through the points; there may, however, well be an anomaly at 64, where the *4 f* shell is half-filled.

The values for k_{obs} in general agree as well as could be expected with k_{calc}. The two exceptions are Sm^{3+} and Yb^{3+}. Although the latter deviation seems to be very great, it may be due to experimental errors, since the x_{Me} range was small, and the powder photographs were blurred. The deviation for Sm^{3+} is more difficult to explain. In 1929 OFTEDAL gave $a = 4.03$ kX for a samarium flouride, said to have been prepared by GOLDSCHMIDT from samarium hydroxide and hydrofluoric acid (14). This would give $k_{obs} = 0.110$, which is less abnormal than the value now obtained. Whereas OFTEDAL reported his SmF_3 to be isomorphous with LaF_3, my preparations of pure SmF_3 had a different structure, and the tysonite structure was only found for LaF_3–SmF_3 mixed crystals in the range $x_{Sm} = 0$–0.80.

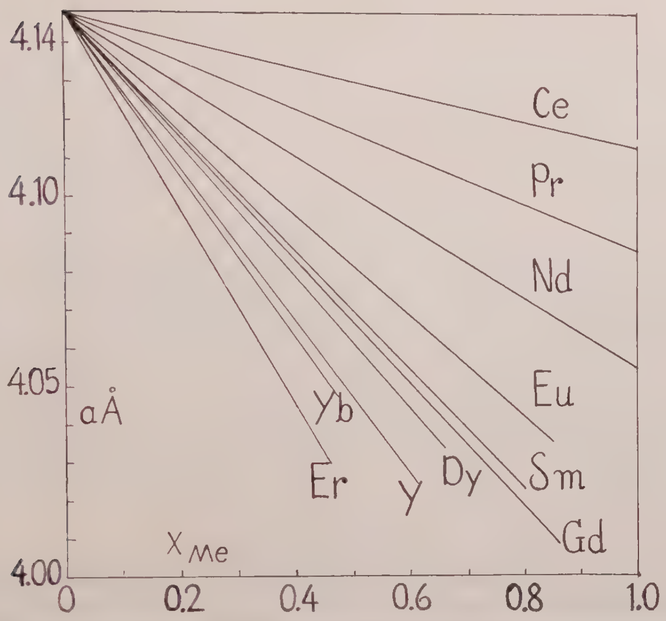

Fig. 4. Best straight lines $a - a_0 - k\,x_{\mathrm{Me}}$ for mixed crystals of LaF_3 and various MeF_3.

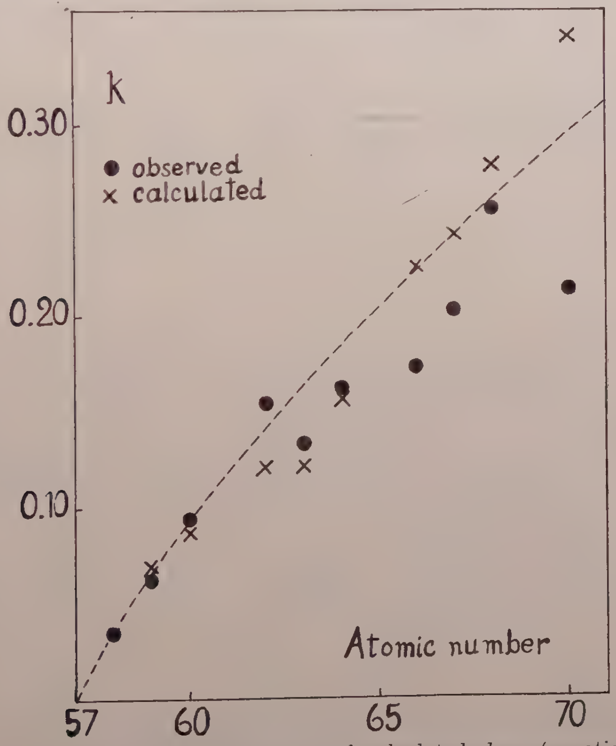

Fig. 5. Observed slope in Fig. 5 (circles) and calculated slope (equation 8), plotted versus atomic number (Y at 67).

The samarium oxide was analyzed spectrographically and found to be highly pure. (The only other lanthanide found was Eu (less than 0.1 %); a small impurity of thallium was also present.)

In order to rule out gross measuring or weighing errors, two experimental series were carried out, independent of each other. However, they showed excellent agreement.

Tetrapositive ions

Attempts were made to precipitate LaF_3 together with fluorides of Ce^{4+}, U^{4+}, Zr^{4+}, and Th^{4+}. With Th^{4+}, the cell dimensions of HF-precipitated LaF_3 did not change, indicating that only very small amounts of Th^{4+} enter the LaF_3 lattice. With Zr^{4+} a shrinkage was observed, though it was small and somewhat dubious.

With Ce^{4+} and U^{4+}, however, the cell dimensions of LaF_3 decreased much more than can be ascribed to experimental errors. Thus Ce and U must have entered the lattice in varying amounts. One might suggest that Ce^{4+} had been reduced to Ce^{3+} and entered the lattice as such; however, this cannot be the whole explanation since with Ce^{4+} an a value as low as 4.087 Å was observed, which is even less than a for pure CeF_3, 4.113 Å.

We thus conclude that the LaF_3 lattice really contains Ce^{4+} and U^{4+}. The same results were obtained when precipitating with HF or NaF; thus we need not assume a coupled substitution, say of $2\,Ce^{4+} + 1\,Na^{+}$ for $3\,La^{3+}$. One has to be somewhat cautious on this point; for instance, SILLÉN and SUNDVALL (16) have shown that the lanthanide wolframates, isomorphous with scheelite ($CaWO_4$), which had once been thought to be $Me_{2/3}\,(\text{hole})_{1/3}\,WO_4$, were really $Na_{1/2}\,Me_{1/2}\,WO_4$, without any empty sites.

A plausible reaction mechanism is the replacement of $4\,La^{3+}$ by $3\,Me^{4+} + 1$ "hole", leaving the fluoride framework unchanged. If La^{3+} were replaced by $Ce^{4+} + F^{-}$, the latter in lattice interstices, one would expect the cell dimensions to increase whereas they are actually found to decrease. Moreover, it is hard to see where extra fluoride ions could be squeezed in. — On the other hand, a coupled replacement of $La^{3+} + F^{-}$ by $Me^{4+} + O^{2-}$ cannot be completely excluded though it does not seem very likely.

For the tetrapositive ions, a numerical check analogous to that in Table 4 would be meaningless because of the low accuracy of the a and c values. Since on heating, Ce^{4+} was reduced to Ce^{3+}, and U^{4+} transformed to UO_2 or UO_2^{2+}, the preparations could only be recrystallized at 100° C and gave rather diffuse lines.

The plutonium(IV) ion, Pu^{4+}, can be expected to behave in the same way as Ce^{4+} and U^{4+}, since the radii are so similar. ZACHARIASEN (9) gave no value for the Ce^{4+} radius. However, from the cell dimensions of UO_2 ($a = 5.469$ Å) (17), CeO_2 ($a = 5.412$ Å) (17) and PuO_2 ($a = 5.386$ Å) (9), all of which have the CaF_2 structure, a radius of 0.87 Å for Ce^{4+} seems to be consistent with ZACHARIASEN's values (9) 0.89 Å for U^{4+} and 0.86 Å for Pu^{4+}.

Thus we may conclude that the coprecipitation of PuF_4 on LaF_3 is probably due to the formation of anomalous mixed crystals.

SUMMARY

Lanthanum fluoride has been coprecipitated with a number of tripositive lanthanide ions Me^{3+}, and some tetrapositive ions Me^{4+}. The precipitates were studied by means of powder photographs in PHRAGMÉN cameras; if a phase of the tysonite (LaF_3)

structure appeared, its cell dimensions were determined. The data are summarized in Tab. 2 and Fig. 2, where a is given as a function of the mole fraction $x_{Me} = Me/(Me + La)$.

Tripositive ions of radii close to that of La^{3+}, namely Ce^{3+}, Pr^{3+}, and Nd^{3+}, gave fluorides with the tysonite structure and gave a complete solid solution range with LaF_3. For lanthanides of shorter ionic radius, and Y^{3+}, the fluoride MeF_3 does not have the tysonite structure; however, a range of solid solutions was found, extending from pure LaF_3 to a certain x_{Me}, generally decreasing with increasing radius difference. The series seem to break off at about $a = 4.02$ Å. The slope of the curves $a(x_{Me})$ was approximately that calculated from the radius difference; with Sm, the slope was found to be much larger than expected, and contrary to previous work no SmF_3 with a tysonite structure could be prepared. This anomaly has not been explained.

With the tetrapositive ions Ce^{4+}, U^{4+}, and possibly Zr^{4+}, a range of solid solutions was also obtained. Probably we have mixed crystals where $4\,La^{3+}$ are replaced by $3\,Me^{4+}$ and 1 "hole". It seems likely that Pu^{4+} would behave similarly.

Acknowledgements

In June 1949 Professor LARS GUNNAR SILLÉN proposed to me the investigation, described above, as part of the research work for the degree of "teknologie licentiat". I am indebted to Professor SILLÉN for his eminently instructive advice and never-failing interest. I also wish to thank Dr. IDO LEDEN for many interesting discussions. Professor GUNNAR HÄGG was kind enough to let me have a sample of pure gadolinium oxide. Dr. JAN RYDBERG kindly carried out the spectrographic investigation of the samarium oxide. Mr ARNE BENGTSSON has been of valuable assistance both in the preparative work and in completing the X-ray apparatus. The text has been made linguistically more correct by the criticism of Professor RALPH G. PEARSON. At last I wish to thank the *Swedish Atomic Commission* for financial support.

Department of Inorganic Chemistry, Chalmers' Institute of Technology, Gothenburg.

Department of Inorganic Chemistry, Royal Institute of Technology, Stockholm.

REFERENCES. [1] **Ketelaar, J. A. A.**, and **Willems, P. J. H.**, Rec. trav. chim. *56* (1937) 29. — [2] **Zintl, E.**, and **Udgård, A.**, Z. anorg. allgem. Chem. *240* (1939) 150. — [3] **Croatto, U.**, Gazz. chim. ital. *73* (1943) 257. — [4] **Croatto, U.**, and **Bruno, M.**, Gazz. chim. ital. *78* (1948) 83. — [5] **Klemm, W.**, and **Klein, H. A.**, Z. anorg. u. allgem. Chem. *248* (1941) 167. — [6] **Cunningham, B. B.**, and **Werner, L. B.**, NNES *IV–14 B* (1943) 51. — [7] **Seaborg, G. T.**, **Wahl, A. C.**, and **Kennedy, J. W.**, NNES *IV–14 B* (1941) 3.— [8] **Irvine, J. W., Jr** in "The science and engineering of nuclear power". Cambridge, Mass. (1947) p. 375. — [9] **Zachariasen, W. H.**, Phys. Rev. *73* (1948) 1104. — [10] **Zachariasen, W. H.**, Private communication. — [11] **Cefola, M.**, and **Smith, C.**, NNES *IV–14 B* (1944) 822. — [12] **Schlyter, K.**, Arkiv Kemi *5* (1952), nr 23. — [13] **Bragg, W. L.**, J. Sci. Instrum. *24* (1947) 27. — [14] **Oftedal, I.**, Z. phys. Chem. *B 5* (1929) 272. — [15] **Goldschmidt, V. M.**, "Geochemische Verteilungsgesetze der Elemente, VII", Skrift. d. Norske Vid.-Akad. Oslo, Matem.-Naturvid. Klasse, No. 2, 1926, p. 35. — [16] **Sillén, L. G.**, and **Sundvall, H.**, Arkiv Kemi Mineral Geol. *17 A* (1943, no 10. — [17] **Magnéli, A.**, and **Kihlborg, L.**, Acta Chem. Scand. *5* (1951) 578.

Tryckt den 10 december 1952

Uppsala 1952. Almqvist & Wiksells Boktryckeri AB

Communicated 4 June 1952 by Arne Westgren and Gunnar Hägg

On the crystal structure of fluorides of the tysonite or LaF_3 type

By Kurt Schlyter

With 2 figures in the text

Previous work

Tysonite is a mineral of formula RF_3, where $R = La, Ce \ldots$ (1). In 1929 Oftedal (2) reported an investigation of the crystal structure of this mineral. By means of Laue and powder photographs Oftedal determined the cell constants and proposed positions of the atoms. For tysonite he found a hexagonal cell of dimensions $a = 7.124$ kX and $c = 7.280$ kX. However, all strong reflections corresponded to a smaller cell of dimensions $a = 7.124/\sqrt{3} = 4.112$ kX and $c = 7.280$ kX, which Oftedal regarded as a pseudocell.

As I was engaged in an investigation of the coprecipitation of LaF_3 with trivalent and tetravalent ions, I found it desirable to reinvestigate the tysonite structure by means of Weissenberg photographs.

Preparation of crystals with tysonite structure

Attempts were made to prepare single crystals by the following methods:

a) To an aqueous solution of lanthanum nitrate, hydrofluoric acid was added. The precipitate of lanthanum fluoride was filtered off at room temperature and dried in air. Also a precipitate of praseodymium fluoride was prepared in the same way. Popovici (3) claims to have obtained praseodymium fluoride crystals by this method.

b) A precipitate of lanthanum fluoride was prepared as in a) by adding hydrofluoric acid to an aqueous solution of lanthanum nitrate. The mixture was then heated to 100° C. The acids and the water evaporated and the residue (lanthanum fluoride and small amounts of nitric acid) was heated to about 500° C.

c) Lanthanum fluoride, prepared by mixing aqueous solutions of lanthanum nitrate and excess of sodium fluoride solution, was kept in an autoclave at 220° C together with the supernatant solution.

d) La_2O_3 and CaF_2 were fused together.

Methods a) and b) gave conglomerates of microscopic crystals of lanthanum (praseodymium) fluoride. Method b) gave in addition a few well-formed single

Table 1

Powder photograph of LaF_3. Cu *K* radiation. $\lambda_a = 1.5418$ Å, $\lambda_\beta = 1.3922$ Å. The line separates the angular ranges of the two powder cameras used

h k l	$10^4 \sin^2 \theta_{obs}$	$10^4 \sin^2 \theta_{calc}$	I_{calc}	I_{estd}
1 0 2	900	900	17	20
1 1 0	1382	1382	93	80
1 0 3	1450	1450	100	100
0 0 4	1753	1758	11	10
1 1 2	1830	1821	46	50
2 0 0		1842	6	
2 0 1	1950	1952	26	20
1 0 4	—	2219	4	not visible
2 0 2	2282	2282	3	5
2 0 3	2830	2831	15	20
1 1 4	3135	3140	12	20
1 0 5	3205	3208	5	10
2 1 0	—	3224	2	not visible
2 1 1	3340	3333	11	20
2 0 4	3600	3600	1	5
1 0 6 β		3601		
2 1 2	3670	3663	1	5
0 0 6	3950	3956	1	5
3 0 0	4150	4145	3	5
2 1 3	4213	4213	8	10
1 0 6	4420	4417	1	2
3 0 2	4590	4584	3	10
2 0 5		4590	1	
3 1 1 β	4970	4971		5
2 1 4		4982	1	
1 1 6	5330	5338	2	5
2 2 0	5530	5526	1	5
1 1 6	5343	5338	100	90
2 2 0	5527	5526	46	50
2 0 6	5793	5798	11	5
1 0 7	5852	5846	38	20
2 1 6 β		5854		
3 0 4	5911	5903	52	40
2 2 2	5965	5966	42	100
2 1 5		5971	47	
3 1 0		5987	11	
3 1 1	6096	6096	53	70
3 1 2	6424	6426	8	10
3 1 3	6972	6976	53	40
3 0 8	—	7034	3	not visible
2 1 6	7184	7180	11	10
3 2 1 β	7221	7223		10
2 0 7		7227	19	
2 2 4	7287	7284	26	20
4 0 0	—	7368	3	not visible
4 0 1	7474	7478	14	10
1 0 8	—	7494	2	not visible
3 1 4	7755	7745	7	10
4 0 2	7813	7808	3	5
3 0 6	8101	8101	26	40
4 0 3	8357	8357	17	20
2 1 8 β		8363		

Table 1 (continued)

$h\,k\,l$	$10^4 \sin^2 \theta_{obs}$	$10^4 \sin^2 \theta_{calc}$	I_{calc}	I_{estd}
1 1 8	8417	8415	14	20
2 1 7	8595	8609	26	30
3 1 5	8731	8734	18	30
3 2 0		8750	3	
3 2 1	8855	8859	20	40
2 0 8		8876	2	
4 0 4	—	9126	3	not visible
3 2 2	9185	9189	4	10
1 0 9	9362	9362	15	20
5 0 1 β	9481	9476		30
2 2 6		9482	25	
4 1 0	9666	9671	19	40
3 2 3	9733	9739	42	20

crystals of unknown composition. A preliminary X-ray investigation of one of the latter crystals was made. It seemed to be triclinic with axes ≈ 7 Å. The heat treatment in method c) made the crystal grains grow as shown by the sharpening of the lines in the powder photographs. However, no single crystals of sufficient size were obtained. Method d) gave single crystals, but they had not the tysonite structure. Since the attempts with methods a–d) were all in vain, I decided to use natural tysonite crystals in the structure investigation.

Unit cell dimensions. Possible space groups

A sample of tysonite from the quarry of Österby, parish of Skedevi, Dalecarlia, Sweden, was crushed in an agate mortar, and the best formed single crystal was picked out under a polarization microscope. This crystal was transparent, rod-like (height about 0.1 mm) and rather irregularly shaped, but for two reflecting surfaces. It was set on a WEISSENBERG camera (diameter 57.4 mm). Using CuK radiation I took photographs with three different rotation axes: 1)–2) around the a- and the c-axis of the "real cell" according to OFTEDAL and 3) around the a-axis of OFTEDAL's "pseudocell". In none of the rotation photographs were reflections found that would necessitate a larger cell than OFTEDAL's "pseudocell". However, extra reflections were observed, caused by impurities of bastnäsite (La, Ce)FCO$_3$ ($a \approx 7.1$ Å, $c \approx 9.7$ Å). From measurements on the WEISSENBERG photographs I arrived at the approximate unit cell dimensions for tysonite $a \approx 4.1$ Å and $c \approx 7.2$ Å.

For pure lanthanum fluoride more accurate cell dimensions were obtained from powder photographs of a sample that had been precipitated and heated to about 500° C. Two focusing cameras with different $\sin^2 \theta$ domains were used. (Table 1.)

The values in the third column have been calculated with the hexagonal cell dimensions

$$a = 4.148 \text{ Å}; \quad c = 7.354 \text{ Å}; \quad c/a = 1.773.$$

The WEISSENBERG photographs contained the reflexions $h\,k\,0$; $h\,k\,1$; $h\,0\,l$; $h\,1\,l$; $h\,h\,l$; $h, h+1, l$, and $h, h+2, l$. Reflexions with $h - k = 3\,n$ and l odd were systematically absent. With the symmetry $6/m\,m\,m$, indicated by the WEISSENBERG photographs, the possible space groups were $D_{6h}(1, 4)$, $D_6(1, 6)$, $C_{6v}(1, 4)$ and $D_{3h}(1, 3, 4)$.

Table 2 a. $F^2(h\,k\,0)_{\text{obs}}$

k \ h	0	1	2	3	4
0		4	8	58	7
1	4	46	8	11	6
2	8	8	49	4	
3	58	11	4		
4	7	6			

Table 2 b. $F_0^2(h\,k\,0)_{\text{calc}}$

0	1	2	3	4
	18	13	52	6
18	100	9	6	29
13	9	43	5	
52	6	5		
6	29			

The density of tysonite is 6.14 g/cm³ (1). Assuming the formula weight of tysonite to be 196.5 (average value of the formula weights of LaF_3 and CeF_3), the number of RF_3 units per cell was calculated to be $1.97 \approx 2$. Thus there are 2 heavy atoms per unit cell.

Positions of the heavy atoms

After visual estimation of the intensities of the reflections on the $h\,k\,0$ and $h\,0\,l$ photographs, the squares of the structure factors (F^2) were calculated with the simplified equation:

$$F^2\,(h\,k\,l) = I_{\text{obs}} \cdot \sin 2\,\theta / (1 + \cos^2 2\,\theta).$$

The results are listed in tables 2 a and 3 a.

Table 3 a. $F^2(h\,0\,l)_{\text{obs}}$

l \ h	0	1	2	3	4
0		19	41	96	12
1		25	55		33
2	19	4	7	80	9
3		34	34		23
4	27	6	5	56	6
5		17	15		
6	49	15	7	26	
7		19	14		
8	16	3	5		
9		9			

Table 3 b. $F_0^2(h\,0\,l)_{\text{calc}}$

0	1	2	3	4
	27	19	79	8
	59	42		22
100	7	6	42	4
	90	63		32
83	9	7	43	5
	28	24		
78	11	9	48	
	30	26		
30	4	4		
	27			

The data in table 2 a were used for calculating the two one-dimensional PATTERSON functions:

$$P_0(u\,0\,p) = \sum F^2(h\,k\,0)\cos 2\,\pi\,h\,u$$

$$P_0(u, 2\,u, p) = \sum F^2(h\,k\,0)\cos 2\,\pi\,(h + 2\,k)\,u.$$

These functions indicated peaks at $(0\;0\;p)$, $(\tfrac{1}{3}\;\tfrac{2}{3}\;p)$ and $(\tfrac{2}{3}\;\tfrac{1}{3}\;p)$. From the data in table 3 a the two-dimensional PATTERSON $h\,0\,l$-projection was calculated. The function

$$P_0\,(u\,p\,w) = \sum_h \sum_l F^2\,(h\,0\,l)\cos 2\,\pi\,h\,u\,\cos 2\,\pi\,l\,w$$

gave peaks at $(0\,p\,0)$, $(\frac{1}{3}\,p\,\frac{1}{2})$ and $(\frac{2}{3}\,p\,\frac{1}{2})$. Thus the three-dimensional PATTERSON function has maxima at $(0\,0\,0)$, $(\frac{1}{3}\,\frac{2}{3}\,\frac{1}{2})$ and $(\frac{2}{3}\,\frac{1}{3}\,\frac{1}{2})$. These maxima may be explained by either of the following sets of positions of the two heavy atoms: 1) 2R in $(\frac{1}{3}\,\frac{2}{3}\,\frac{1}{4})$, $(\frac{2}{3}\,\frac{1}{3}\,\frac{3}{4})$, 2) 2R in $(\frac{1}{3}\,\frac{2}{3}\,\frac{3}{4})$, $(\frac{2}{3}\,\frac{1}{3}\,\frac{1}{4})$, 3) 2R in $(\frac{1}{3}\,\frac{2}{3}\,0)$, $(\frac{2}{3}\,\frac{1}{3}\,\frac{1}{2})$, 4) 2R in $(\frac{1}{3}\,\frac{2}{3}\,\frac{1}{2})$, $(\frac{2}{3}\,\frac{1}{3}\,0)$. The sets 2), 3), and 4) are derived from 1) by displacement of the origin by $(0\,0\,\frac{1}{2})$ in (2), by $(0\,0\,\frac{3}{4})$ in 3), and by $(0\,0\,\frac{1}{4})$ in 4). The possible space groups are then reduced to

C_{6v}^4: 2R in 2(b), (set 1).
D_6^6 : 2R in 2(c), (set 1); or in 2(d), (set 2).
D_{6h}^4: 2R in 2(c), (set 1); or in 2(d), (set 2).
D_{3h}^1: 2R in 1(c+f) (set 3); in 1(d+e), (set 4); in 2(h) (set 1); or in 2(i) (set 2).
D_{3h}^4: 2R in 2(c), (set 1); or in 2(d) (set 2).

Positions of the fluorine atoms from interatomic distances

There are two heavy atoms present in the unit cell, and six fluorine atoms. The latter have little influence on the intensities, so it is hard to determine their positions by comparing the intensities of individual reflections. The coordinates of the fluorine atoms must thus be determined by other methods, namely by considerations of interatomic distances and, independently, by FOURIER synthesis of the electronic density.

The atoms were assumed to be spherical, and the radii of the R^{3+} and the F^- ions were set as $r(La^{3+}) = 1.04$ Å, $r(F^-) = 1.33$ Å (4, 5). To be on the safe side, the smallest literature value was chosen in each case. This would give minimum distances R–F = 2.37 Å and F–F = 2.66 Å.

In order to localize possible positions for the F atoms let us first imagine spheres drawn around the centers of the R atoms, with radii 2.37 Å. These spheres would enclose domains "forbidden" to the centers of the F atoms. The problem would be how to find positions for the F centers in such a way that the F–F distances are not much less than 2.7 Å.

The positions of the heavy atoms, R, were arbitrarily chosen to be $(\frac{1}{3}\,\frac{2}{3}\,\frac{1}{4})$ and $(\frac{2}{3}\,\frac{1}{3}\,\frac{3}{4})$. Fig. 1 shows the planar cuts at $x+y=1$, $z=\frac{1}{4}$, and $z=\frac{1}{2}$ through the unit cell; the first plane cuts two R atoms, the second one R atom and the last no R atom. If we consider the small unit cell (OFTEDAL's "pseudocell") and the LAUE symmetry $6/mmm$ as correct, the centers of the fluoride ions must be situated on the hexagonal axes $(0\,0\,z)$, $(\frac{1}{3}\,\frac{2}{3}\,z)$ or $(\frac{2}{3}\,\frac{1}{3}\,z)$. Then the only possible positions would be those indicated by crosses in Fig. 1.

If no use is made of the unit cell or symmetry supposed, small shifts of the atomic positions around those given in Fig. 1 become possible. Then some of the previously equivalent distances would be a little longer, whereas others would be shorter than usual. All such arrangements seem less likely than the symmetrical one. There seems to be no radically different way of arranging six fluorine atoms in a unit cell. It thus seems likely that the fluorine atoms are situated in the following positions, which can be described by space group D_{6h}^4.

2R in 2(c): $\frac{1}{3}\,\frac{2}{3}\,\frac{1}{4}$ and $\frac{2}{3}\,\frac{1}{3}\,\frac{3}{4}$
2F in 2(b): $0\,0\,\frac{1}{4}$ and $0\,0\,\frac{3}{4}$
4F in 4(f): $\frac{1}{3}\,\frac{2}{3}\,z$; $\frac{1}{3}\,\frac{2}{3}, \frac{1}{2}-z$; $\frac{2}{3}\,\frac{1}{3}\,\bar{z}$; $\frac{2}{3}\,\frac{1}{3}, \frac{1}{2}+z$.

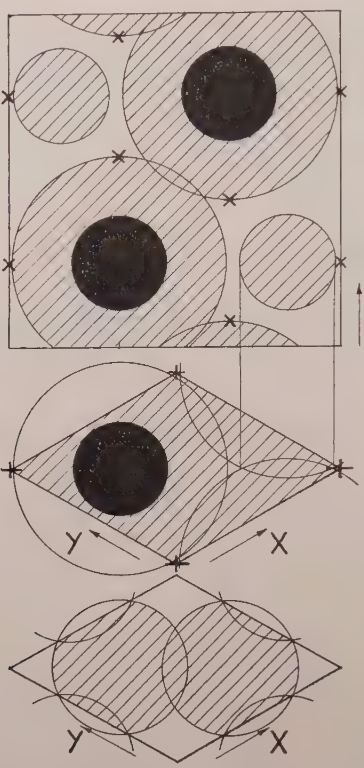

Fig. 1. Sections through unit cell of LaF_3 from the top: $x+y=1$, $z=\frac{1}{4}$ and $z=\frac{1}{2}$. The shaded areas in each section are forbidden to fluorine centers, and the black circles are the heavy (R) atoms. The crosses give the probable positions of the F centers.

These coordinates can also be described by the space groups D_6^6 and D_{3h}^4, but D_{6h}^4 was chosen because it has the highest symmetry.

From cut 1 (Fig. 1) the parameter $z_F \approx 0.57$ was found. To determine the possible z-range, the variation of the interatomic distances with z was studied for lanthanum fluoride, the cell constants of which had been accurately determined. The results

Table 4

Interatomic distances in LaF_3 with various values for the F parameter z_F

z_F	La–3 F_2 or F_2–3 La	La–2 F_4 or F_4–La	F_2–6 F_4 or F_4–3 F_2	F_4–F_4
0.550	2.39	2.20	2.81	2.94
0.560	2.39	2.28	2.77	2.79
0.570	2.39	2.35	2.73	2.64
0.580	2.39	2.42	2.70	2.50
0.590	2.39	2.50	2.66	2.35

are given in Table 4; F_2 means an F atom in a 2-fold position and F_4 an F atom in a 4-fold position. The most plausible interatomic distances (La–F ≈ 2.4 Å and F–F ≈ 2.7 Å) are obtained with $z = 0.57 \pm 0.01$.

c) Electronic density calculations

To check the structure obtained above, an attempt was made to find the fluorine positions also by means of FOURIER synthesis. For $F(h0l)_{\text{obs}}$, 10 times the square roots of the values in table 3a were used (Table 5). The sign was easily obtained, since the R atoms give the largest contributions to the structure factors.

Table 5.

$F(h0l)_{\text{obs}}$ used in the FOURIER synthesis

l \ h	0	1	2	3	4
0		−44	−64	98	−34
1		−50	74		−58
2	−44	20	26	−89	30
3		58	−58		48
4	52	−25	−22	75	−25
5		−41	39		
6	−70	39	26	−51	
7		44	−37		
8	40	−17	−22		
9		−30			

In this special case we have for l even $F(\bar{h}0l) = F(h0l)$; $F(h0\bar{l}) = F(h0l)$ and for l odd $F(\bar{h}0l) = -F(h0l)$, $F(h0\bar{l}) = -F(h0l)$. The electronic density function can be simplified as:

$$\varrho(x0z) = \sum_h \sum_{l_{\text{even}}} F(h0l) \cos 2\pi h x \cos 2\pi l z - \sum_h \sum_{l_{\text{odd}}} F(h0l) \sin 2\pi h x \sin 2\pi l z.$$

Because peaks corresponding to F and R atoms may be expected at $x = 0$ and $x = \frac{1}{3}$, I calculated the two one-dimensional functions:

$$\varrho(0pz) = \sum_{l_{\text{even}}} F(h0l) \cos 2\pi l z$$

$$\varrho(\tfrac{1}{3}pz) = \sum_{l_{\text{even}}} F(h0l) \cos \frac{2\pi h}{3} \cos 2\pi l z - \sum_{l_{\text{odd}}} F(h0l) \sin \frac{2\pi h}{3} \sin 2\pi l z.$$

The results of these calculations are plotted in Fig. 2 (solid curves). The problem was then how to recognize the F-peaks among the false peaks, caused by diffraction effects etc. Using THOMAS-FERMI scattering factors the structure amplitudes were calculated, that would be caused by lanthanum atoms alone. Then the corresponding functions $\varrho'(0pz)$ and $\varrho'(\frac{1}{3}pz)$ were calculated (dotted curves in Fig. 2). By comparing the curves for ϱ and ϱ', possible F-peaks were discovered at $z = 0.567$

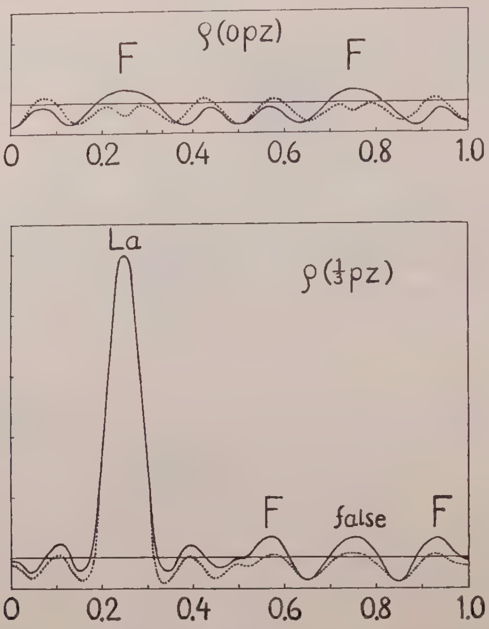

Fig. 2. Lines $\varrho\,(0\,p\,z)$ and $\varrho\,(\frac{1}{3}\,p\,z)$ in FOURIER projection $\varrho\,(x\,p\,z)$. Solid curves ϱ calculated from intensities; dotted curves ϱ' due to La atoms alone.

($z=0.933$) for $x=\frac{1}{3}$, and at $z=\frac{1}{4}$ ($z=\frac{3}{4}$) for $x=0$. (The peak at ($\frac{1}{3}\,p\,\frac{3}{4}$) must be false, since fluoride ions in this position would block the lattice so that 6 F per cell could certainly not be housed.)

The agreement of the F coordinates according to the two different methods is a good support to the atomic positions given.

Check of the structure factors

A set of $F_0(h\,0\,l)$-values was calculated for each of $z=0.55$, 0.56, 0.57, 0.58, and 0.59, using the equation $F_0=\frac{1}{2}f_{\mathrm{La}}\,A_{\mathrm{La}}+\frac{1}{2}\,f_{\mathrm{F}}\,A_{\mathrm{F}_2}+f_{\mathrm{F}}\,A_{\mathrm{F}_4}$ (F_0 denotes the structure factor for atoms at rest, A the structure amplitudes and f the scattering factors). The $F_0(h\,0\,l)$ values were compared with the observed values in the hope of eliminating some z values as improbable. Since the absorption effects were large and the contribution of the fluorine atoms to F_0 was small, it proved impossible to limit the z range in this way.

For $z=0.57$, $F_0(h\,0\,l)$ and $F_0(h\,k\,0)$ values were squared and in each case multiplied by a number, making the highest F_0^2 value equal to 100. These calculated structure factors are given in Tables 2 b and 3 b.

There are considerable deviations between the observed and calculated F^2 values. However, they are not random, as would be expected with an erroneous crystal structure. There is a tendency for enhancing the F^2_{obs} of spots in some areas in the diagram, which may be explained by the irregular shape of the crystal. Besides absorption effects, the spots in some fields were very sharp, in others broader, which made a visual estimation of the intensities difficult. Such differences seem to have been smoothed out in the PATTERSON and FOURIER diagrams, which thus give more reliable information than the comparison of individual pairs of spots.

Considering these effects, the figures in Tables 2 and 3 seem quite plausible.

An attempt was made to calculate an empirical temperature correction. Proceeding formally as usual, the equation $\log (F_0^2 / F_T^2) = 0.35 \sin^2 \theta$ was found; considering the discrepancies in tables 2 and 3, there would be no point in applying it.

Check with intensities in powder photographs

The relative intensities I for all observed powder reflections were calculated, using the equation $I = (1 + \cos^2 2\,\theta)\,(\cos \theta)^{-1}\,(\sin \theta)^{-2} F_0^2\, p\, T$. Here p denotes the number of equivalent reflections, and T an empirical temperature factor chosen to satisfy $I\,(103) : I\,(320) = 100 : 1$. For PHRAGMÉN focusing cameras, a number of factors come in, for instance the greater absorption in air for large values for θ, which together tend to make I decrease more rapidly than by this formula or the formula for DEBYE-SCHERRER cameras (HÄGG and REGNSTRÖM) (6). These effects were roughly corrected for by the empirical temperature factor. The agreement between calculated and estimated intensities is quite acceptable. (Table 1.)

The values in the I_{estd}-columns sometimes include the intensities of coinciding β lines, whereas the values in the I_{calcd}-columns do not.

SUMMARY

The hexagonal unit cell of tysonite has hitherto been given with $a \approx 7.1$ Å, $c \approx 7.3$ Å, space group D_6^6, and 6 RF_3 per cell. The structure has been reinvestigated, using well-exposed WEISSENBERG photographs of a good crystal of natural tysonite. The data give a unit cell, the volume of which is one-third of that previously assumed. Thus $a \approx 4.1$ Å, $c \approx 7.3$ Å, and there are 2 RF_3 per cell. No evidence has been found forcing one to assume a larger cell. The structure is then very simple: space group D_{6h}^4, 2 R in 2(c), 2F in 2(b) and 4F in 4(f) with $z = 0.57 \pm 0.01$.

Acknowledgements

In May 1950 Professor LARS GUNNAR SILLÉN, now at the Royal Institute of Technology, Stockholm, proposed to me the investigation reported above, as a second half of my licentiate work. I am indebted to Professor SILLÉN for his most inspiring aid. I also wish to thank Professor FRANS E. WICKMAN, Natural Historical Museum, Stockholm, and Professor SVEN O. GAVELIN, University of Stockholm, who gave me samples of natural tysonite. Professor J. ARVID HEDVALL, Silicate Research Institute, Gothenburg, allowed me to use the WEISSENBERG camera of his institute. With Dr. SVEN V. BERGER I have had many interesting discussions. In the practical X-ray work Mr. ARNE BENGTSSON has given me a valuable assistance. Finally I wish to thank the *Swedish Atomic Commission* for financial support.

March 1952.

Department of Inorganic Chemistry, Royal Institute of Technology, Stockholm.

Department of Inorganic Chemistry, Chalmers' Institute of Technology, Gothenburg.

REFERENCES. 1. **Gmelin,** *39* (1938) 55. — 2. **Oftedal, I.,** Z. phys. Chem. *B 5* (1929) 272. — 3. **Popovici, J.,** Ber. *41* (1908) 634. — 4. **Zachariasen, W. H.,** Phys. Rev. *73* (1948) 1104. — 5. **Goldschmidt, V. M.,** "Geochemische Verteilungsgesetze der Elemente VII", Skr. Norske Vid. Akad., Oslo, Mat. Naturvid. Klasse No 2, 1926. – 6. **Hägg, G.** and **Regnström, G.,** Arkiv Kemi 18 A, no 5, 1944.

Tryckt den 10 december 1952

Uppsala 1952. Almqvist & Wiksells Boktryckeri AB

ARKIV FÖR KEMI Band 5 Nr 9

Read 10 September 1952

On the interaction between the gametes of the sea urchin at fertilization[1]

By Eskil Hultin, Georg Kriszat, Sven Lindvall, Gunnar Lundblad, Hans Löw, John Runnström, Erik Vasseur, and Elsa Wicklund

Monroy and Runnström (7, 8) were able to isolate a certain fraction of the cytoplasm of *Arbacia punctulata* which contains the anti-fertilizin, a factor which precipitates the jelly coat and counteracts the agglutinating action of the egg water. The authors distinguished also a promoting action on the membrane elevation. The factor concerned seems to be localized in the pigment granules. The research carried out by Monroy and Runnström left unsettled whether the jelly precipitating and the membrane elevating action are due to one common or to two different factors. The present writers have separated one jelly precipitating (JePptF) and one membrane elevating factor (MbElF). We rather prefer to avoid the expressions fertilizin and antifertilizin (6, 14), and endeavor instead to make use of a merely descriptive provisional terminology pending the further chemical elucidation of the factors.

The eggs of *Arbacia lixula* were homogenized in isotonic NaCl and the granular components were spun down (8 000 × g, 30 minutes). The supernatant contains JePptF. The granules when broken up by distilled water proved to contain the MbElF. If the homogenization be carried out in sea water the granules break up due to the presence of Ca (4) and a separation of the factors in the way described is rendered impossible. The supernatant (S 1) was further fractionated. A fraction spun down at 30 000 × g for 30 minutes was inactive as JePptF. The supernatant (S 2) was centrifuged for three hours at 105 000 × g for 3 hours. Most of the sediment could be redispersed and proved to contain the main JePptF activity whereas the supernatant (S 3) was only slightly active. The centrifugal fractionation of S 1 was carried out with material from *Psammechinus miliaris*. The JePptF containing sediment consists of two main components viz. one which is broken down by cryst. trypsin, another which is resistent to trypsin. In this latter are included numerous granules which contain ribonucleic acid (microsomes). The JePptF corresponds to or is included in the first mentioned component.[2] Cryst. trypsin removes the JePptF-activity but cryst. ribonuclease does not.

---

[1] This work was carried out at the Stazione Zoologica, Naples, and the Zoological Station, Kristineberg, Sweden. The work was supported from The Swedish Natural Sciences Research Council.

[2] This component is fibrillar and exhibits when spun down a birefringence positive with respect to the longitudinal direction of the fibrils. In this regard the component resembles the constituents of the spindle and the astrospheres.

Strong suspensions of spermatozoa were prepared in sea water. The spermatozoa were spun down at 6 000–7 000 × g for 5 minutes and the supernatant was removed (S 1). The spermatozoa were resuspended in sea water and the centrifugation repeated. The supernatant (S 2) was removed. Usually five supernatants were prepared (S 1–S 5) in this way. In *Arbacia lixula* S 1 and S 2 had a pronounced dissolving action on the jelly coat. The active factor may be designated as JeDisF(Sp); Sp denoting that the factor is derived from the sperm. This activity decreased in the following supernatants whereas a jelly precipitating factor JePptF(Sp) augmented. This factor is probably not identical with JePptF(E), the jelly precipitating factor of the egg. In *Psammechinus miliaris* the jelly dissolving factor JeDisF(Sp) merely brought about a strong swelling of the jelly. At the same time a considerable improvement of the membrane elevation occurred. Thus the action of JeDisF(Sp) is rather similar to that of MbElF(E). Both these factors are thermolabile, being inactivated subsequent to a heating to 45° for 30 minutes. This inactivation seemed to be complete following heating to 60° for 30 minutes. This raises the question as to whether these factors have enzymic character. The supernatants obtained after the spermatozoa have been spun down in sea water contain several carbohydrases (amylase, cellulase, chitinase) but no measurable proteolytic activity. So far JeDisF(Sp) could not be identified with any special enzyme but this question is subject to further examination.

When the sperm supernatants have been heated to 45° or 60° the JePptF(Sp) becomes more active. In the non heated supernatant this factor is counteracted by the JeDisF(Sp); upon its heat inactivation the JePptF(Sp) becomes more prevalent.

Eggs with the jelly coat precipitated by addition of JePptF(Sp) can still be fertilized. Even if the control eggs gave low adherent membranes a perfectly smooth membrane was elevated in the eggs surrounded by the precipitated jelly. This is also the case if the precipitation of the jelly is brought about by JePptF(E). The eggs of *Arbacia lixula* were particularly suitable for this experiment as the membrane usually is of the low adherent type (12). Identical results were obtained when the same experiment was repeated with the eggs of *Echinus esculentus* and of *Psammechinus miliaris*.

Even preparations of JePptF too weak to effect a visible precipitation of the jelly still bring about an improvement of the membrane elevation.

The following tentative explanation of the membrane elevating effect of the JePptF is offered. A reaction of this factor with the jelly coat causes the release of a substance bound to the ground substance of the jelly. This substance has certain properties in common with the MbElF(E) and the JeDisF(Sp). It may be designated as MbElF(Je). It distinguishes itself, however, from the Sp and E-factors by being thermostable and dialysable through cellophane. MbElF(Je) seems also to activate the movements of the spermatozoa. It must be left open, however, if it really constitutes the sperm activating factor of the jelly (LILLIE (6), HARTMANN et al (2, 3); for further discussion cf. TYLER (15), RUNNSTRÖM (11) and VASSEUR (16)).

The MbElF(Je) can be demonstrated in the supernatant of eggs which have been subjected to the action of JePptF (E or S). Eggs (of *Arbacia lixula*) brought into this supernatant formed a well elevated smooth membrane. MbElF

(Je) has proved to exert a growth promoting action on *Lactobacillus casei* provided with a full supply of the necessary nutrients.

Certain results seem to demonstrate that periodate acts on eggs with jelly coat mainly by releasing the MbElF(Je). On the other hand it was shown that periodate ($\sim 10^{-4}$ N) is able also to activate eggs deprived of their jelly coat and a direct action of periodate on the cytoplasmic surface system must here be assumed (5).

It should be underlined that the supernatant of the eggs subjected to JePptF contains no active sperm agglutinating factor, SpAgglF (Je). At least in the presence of MbElF (Je) active SpAgglF is not necessary to bring about fertilization. On the contrary the membrane formation is more complete in absence than in presence of active SpAgglF under the conditions of the experiment described.

The addition of JePptF to the eggs deprived of their jelly coat is not followed by any improvement of the membrane formation. This indicates that the action of JePptF is an indirect one exerted by virtue of the release of MbElF(Je).

Conversely MbElF (E) acts directly on the egg which follows from the fact that it improves the membrane formation also in eggs deprived of their jelly coats.

The MbElF(E)-action has been further elucidated by observing its effect on the egg surface. *Psammechinus* eggs were exposed to a hypertonic medium in presence of MbElF(E). They exhibit a wrinkled surface only for a short time; thereafter the surface becomes smooth and the eggs assume a perfectly spherical shape. In untreated eggs the wrinkled state lasts for a considerably longer time. The MbElF(E)-treated eggs become also much more elongated (> 100 per cent) than the control when the eggs are centrifuged on the border between sea water and an isotonic sucrose solution. The JeDisF(Sp) brings about a similar change of the egg surface. Certain amino acids such as glycine, l-histidin, dl-leucine (0.05 M) and proteins (serum albumin, globin) act in the same way. They all cause a decrease in the rigidity of the cortex which is a prerequisite for the formation of a normal membrane. Addition of "fucoidin" (0.01–0.02 %) increases the rigidity of the cortical layer and inhibits the sperm attachment or the elevation of a membrane (1). The preparation of fucoidin was not highly purified but its action depends certainly on a polysaccharide component; addition of periodate in low concentrations quickly removes the activity of the preparation (1).

The fucoidin is counteracted by MbElF (E) and substances of similar action. If only fully mature eggs were available MbElF and similar substances were tested by their capacity of removing the fucoidin inhibition. Fucoidin although a powerful inhibitor of fertilization does not interfere with the sperm agglutinating power of the jelly substance in solution.

The question arises whether a factor has to be distinguished from the MbElF which toughens or solidifies the membrane; this appears very probable in view of Motomuras work (9). It was also shown for *Psammechinus miliaris* that even normal fertilization membranes can be made "tougher" for example by breaking up (fertilized) eggs in strongly hypotonic medium. In our experiments the change of the membrane was followed by a determination of the retardation in the polarization microscope. A 50 per cent increase of the retardation was observed. Motomura considered as a possibility the identity of his membrane toughening factor with "antifertilizin", i.e. JePptF(E). This seems very likely, see also (8). Motomura (10) has also shown that his membrane toughening factor activates the egg without introducing a membrane elevation. The same has been earlier demonstrated by Wicklund (17) for the JePptF(Sp). The physiological role of JePptF(E) is certainly not to precipitate the jelly but it may possibly serve as a link in the processes which bring about the differentiation of the fertilization membrane.

Echinocardium spermatozoa exhibit a non or only slowly reversible agglutination under the influence of the dissolved jelly substance which carries the SpAgglF (Je). Very sensitive methods are available for the estimation of fucose, the main carbohydrate unit of the jelly substance. It was thus possible to demonstrate that a part of the jelly substance was removed from solution when agglutinated spermatozoa were spun down. Spermatozoa of an other irregular sea urchin species, *Brissopsis lyrifera,* did not react with the jelly of *Echinocardium* which may be an expression of the species specificity of the reaction.

The above data may shed some light on the significance of the reaction between the jelly and the surface of the spermatozoon. This latter contains factors which act upon the jelly substance. By this action the MbElF(Je) may be released. This constitutes an important "cofactor" in the the processes of sperm fixation and membrane elevation. This cofactor is not absolutely necessary as the jelly free egg can be fertilized. Nevertheless the presence of the cofactor must have a great adaptive value under natural conditions. The reactions occurring between spermatozoon and jelly coat substance parallel probably similar but not necessarily identical reactions which take place between the surface of the spermatozoon and the cytoplasmic surface of the egg.

Finally a survey will be made of the different factors mentioned above and our terminology will be confronted with that of other authors.

Factors in the sperm:

Jelly Dissolving Factor, JeDisF(Sp) — Androgamon II (2, 3)?
Jelly Precipitating Factor, JePptF(Sp) — Antifertilizin (14).

Factors in the jelly coat:

Sperm Agglutinating Factor, SpAgglF(Je) — Fertilizin (6) Gynogamon II (2, 3)
Membrane Elevating Factor, MbElF(Je).

Factors in the egg:

Jelly Precipitating Factor, JePptF(E) — Antifertilizin (6, 13). Membrane toughening factor (9)?
Membrane Elevating Factor, MbElF(E).

This work is continued in several directions by members of our group. A more complete discussion will be postponed until after full presentation of the material.

SUMMARY

A preliminary attempt has been made to localize the different factors acting on sperm and egg surface at the fertilization of the sea urchin egg. Fractionation by ultracentrifuging has been applied to the homogenized egg contents

whereas the sperm has been subjected to repeated washings with sea water. Under this condition the sperm releases active factors to the sea water.

A factor promoting the membrane elevation (MbElF(Je)) has been demonstrated to be present in the jelly coat. This factor is released upon treatment with the extracts from egg or sperm containing the agents which precipitate the jelly (JePptF(E) and JePptF(Sp)).

From the Wenner-Gren Institute f. exp. Biology, University, Stockholm.

REFERENCES. 1. **Harding, C. V.**, and **Harding, D.**, Arkiv Zool., *3*, No. 24 (1952). — 2. **Hartmann, M.**, and **Schartau, O.**, Biol. Zentr., *59*, 571 (1939). — 3. **Hartmann, M.**, **Schartau, O.**, and **Wallenfels, K.**, Ibid., *60*, 398 (1940). — 4. **Hultin, T.**, Exptl. Cell Res., *1*, 272 (1950). — 5. **Kriszat, G.**, and **Runnström, J.**, Exptl. Cell Res., *3*, 597 (1952). — 6. **Lillie, F. R.**, Problems of Fertilization (1919). — 7. **Monroy, A.**, and **Runnström, J.**, Biol. Bull., *99*, 339 (1950). — 8. ——, Exptl. Cell Res., *3*, 10 (1952). — 9. **Motomura, I.**, Sci. Rep. Tohoku Univ. (4) *18*, 561 (1950). — 10. ——, Ibid., *19*, 203 (1952). — 11. **Runnström, J.**, Advances in Enzymology, *9*, 241 (1949). — 12. **Runnström, J.**, and **Wicklund, E.**, Arkiv Zool., *1*, 179 (1950). — 13. **Tyler, A.**, Proc. Natl. Acad. Sci., *26*, 249 (1940). — 14. **Tyler, A.**, and **O'Melveny, K.**, Biol. Bull., *81*, 364 (1941). — 15. ——, Physiol. Rev., *28*, 180 (1948). — 16. **Vasseur, E.**, The Chemistry and Physiology of the Jelly Coat of the Sea-Urchin Egg. Stockholm (1952). — 17. **Wicklund, E.**, Arkiv Zool., *40 A*, No. 5 (1947).

Tryckt den 10 december 1952

Uppsala 1952. Almqvist & Wiksells Boktryckeri AB

ARKIV FÖR KEMI Band 5 nr 10

Communicated 4 June 1952 by H. v. Euler

Free amino-acids in Jensen Sarcoma of rats studied by chromatography

By Salvatore di Bella

With 1 figure in the text

It was assumed that the processes of proteins synthesis in tumor run through abnormal ways (1, 2). Kögl and Erxleben affirm that in neoplastic proteins, d-aminoacids are present, particularly d-glutamic acid and aminoacids in the racemic form (oxiglutamic acid, leucine and lysine (3)). Investigations have been carried out to clear the question whether the malignancy of tumors is dependent on the presence of protein formed by aminoacids and peptides of the unnatural steric groups, which are attacked with difficulty from normal enzymes (4, 5, 6). A better knowledge of the composition and distribution of free amino-acids in normal and cancerous tissues could contribute to resolve this interesting question.

Schwaigert and Guthtreck observed that in liver tumor, produced by methylazobenzene, the proteins of nucleus contain more glutamic acid while the mitochondrial fractions show higher amounts of arginine, cystine and methionine (7). In autolysates of cancerous tissues Kocker (8) and Washizu (9) found a certain increase of diaminoacids. According to Schenk (10) the liver, kidneys and muscles of rats bearing Jensen sarcoma show increases of histidine and arginine, whilst lysine decreases. These results were not confirmed by Edlbacher (11). Roberts *et al.* (12) found that during the development and the hyperplasia of the skin of rats higher amounts of isoleucine, valine phenylvaline, methionine, threonine, glutamic acid, arginine, tryptophane and cystine are formed.

Recently Roberts and Tishkoff (13) stated in experimental carcinoma of the skin of rats a decrease of amino-acids amounts. On account of the uniform distribution of the set of free amino-acids, present in corresponding hydrolysates Roberts and Fraenkel (14, 15) were able to distinguish normal tissues from carcinomatous ones. The smaller percentage of the tumor amino-acids suggests an increase of the rate of synthesis of formative processes of cell proteins in tumors. This view is supported by Zamecnik and Frantz (16) who observed that the hepatoma cell embodies C^{14} labeled alanine quicklier than normal liver. Taking into account Roberts' statements and those of others, we analyzed the free amino-acids in protein hydrolysates of normal rats and of rats with Jensen Sarcoma, using paper-chromatography. This new procedure proved very useful in the identification and determination of amino-acids present in a mixture (18, 27), and was applied with good results in studying amino-acids from tumor hydrolysates (12, 15).

Experimental

White rats with a stem of Jensen Sarcoma St. 1 and normal rats as controls, body weight 300 350 g were used for research. Liver, kidney, spleen, lungs, heart and samples of sarcoma were taken directly after the death of the animals by bleeding. The tissues were placed in 90° alcohol, crushed in a mortar, transferred to acetone and then powdered. The hydrolysis took place in 6 n. HCl during 16 hours at 100° C.

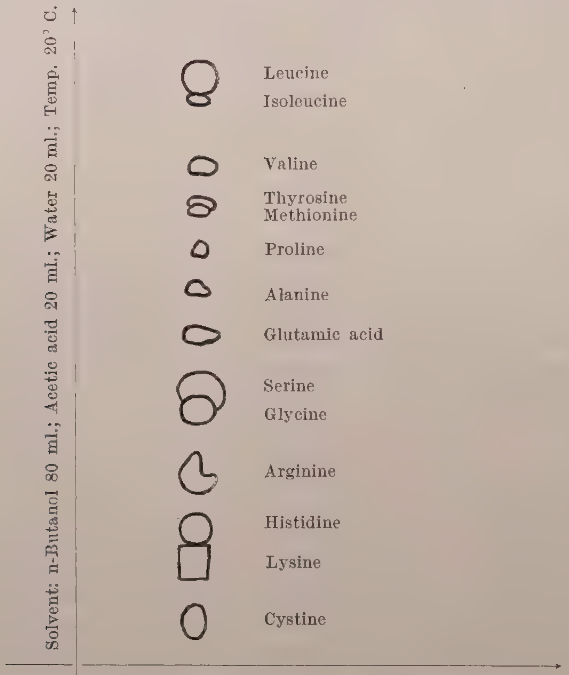
Solvent: n-Butanol 80 ml.; Acetic acid 20 ml.; Water 20 ml.; Temp. 20° C.
Leucine
Isoleucine
Valine
Thyrosine
Methionine
Proline
Alanine
Glutamic acid
Serine
Glycine
Arginine
Histidine
Lysine
Cystine

Chromatography of liver normal rat hydrolysate
(Whatman n° 1)
Reagent dye development 0.2 % Ninhydrin n-Butanol

The mixtures were neutralised with sodium hydroxyde and suitably concentrated to heat according to Craig *et al.*'s suggestions (28), so that the ultimate amount of hydrolysate submitted to chromatography corresponded to about 50 mg of fresh tissue. For unidimensional paper chromatography (Whatman I), the suggestions of Kirby-Berry *et al.* (29) were the following: the employed solvent was n-butanol 80 ml, acetic acid 20 ml, distilled water 20 ml. The reagent for dye development 0.2 % ninhidrine saturated with *n*-butanol; temperature 20° C. The spot identification was realised calculating the *Rf* value for each aminoacid. The estimation was according to Dent (30), Work (31), Polson (32) and controlled in a set of Standard solutions amino-acids[1] (µl 50, 200, 500 measured with a capillary pipette, contained 15–30 µg of pure substance).

---

[1] Amino-acids of the natural (L) set were produced by Merck-Darmstadt.

Results

The sets of tissues were submitted to chromatography: 1) liver, kidney, spleen, lung and heart of normal rats, 2) liver, kidney, spleen, lung and heart of rats bearing Jensen Sarcoma, 3) samples of Jensen Sarcoma. In all the chromatograms, leucine, isoleucine, valine, thyrosine, methionine, proline, alanine, glutamic acid, serine, glycine, arginin, histidine, lysine and cystine were present (the thin and slim appearance of tryptophane spot mostly hinders its identification). Appreciable quantitative differences were observed in the samples of sarcoma: an increase, generally constant for cystine and methionine; not so frequent for arginine, unstable for histidine. The lysine decrease was not always evident.

For want of data concerning other kinds of tumors, we cannot account for eventual differences between histologically different tumors. Between the tissues of normal rats and of rats with sarcoma we could not estimate differences appreciable with chromathographic method. On the whole, our results agree with Schenck's in many sarcomatous tissues (10), with Kocker's (8), Washizu's (9) in cancerous autolysates and with Roberts *et al.*'s (14, 15) in rat carcinoma.

The cystine and methionine increase in Jensen Sarcoma could be related to the observation of White *et. al.* that dietary restriction of sulphur-containing aminoacids retards the appearance of certain kinds of tumor.

I wish to express my best thanks to Prof. H. v. Euler, who welcomed me in the "Vitamin Institutet" in Stockholm and kindly put the material for this work at my disposal.

Stockholm University, Vitamininstitutet.

References. 1. **Rondoni, P.**, Schweiz. Med. Wochsh. Bale 18, 419–424, 1948. — 2. **Graffi**, Zeitschr. f. Krebsforsch. 50, 196, 1940. — 3. **Kögl** and **Erxleben**, H. S. Zeitschr. f. phys. Chem. 258, 57, 1939. — 4. **Arnow** and **Opsahl**, Science *90*, 257, 1939. — 5. **Chibnall et al.**, Nature 144, 71, 1939. — 6. **Dittmar**, Zeitschr. f. Krebsforsch. 50, 472, 1940. — 7. **Schwaigert, B. S.**, and **Guthtreck, B. T.**, Proc. Soc. Expt. Biol. Med. 72, 495–501, 1949. — 8. **Kocker, B. A.**, J. Biol. Chem. 22, 285, 1915. — 9. **Washizu, Y.**, Mitt. a. d. Med. Akad. zu Kioto 20, 1591, 1937. — 10. **Schenck, E. G.**, Arch. f. Exper. Path. u. Pharmakol. 175, 401, 1934. — 11. **Edlabacher, S.**, and **Bauman, W.**, Zeitschr. f. Krebsforsch. 44, 441, 1936. — 12. **Roberts, E., Caldwell L., Clowes, G. H.**, Cancer Research 9, 350–53, 1943. — 13. **Roberts, E.**, and **Tishkoff, G. H.**, Science 109, 14–15, 1949. — 14. **Roberts, E.**, and **Frankel, S.**, Cancer Research 9, 645–48, 1949. — 15. **Roberts, E.**, and **Frankel, S.**, Cancer Research (Scient. Proceed. 1950) 237, 1950. — 16. **Zamecnik, P. C., Frantz, C. et al.**, I. Biol. Chem. 175, 299–314, 1948. — 17. **Consden, R., Gordon, A. H.**, and **Martin A. J. P.**, Biochem J. 38, 225, 1944. — 18. **Woiwod, A.**, Nature 161, 169, 1948. — 19. **Gal, E. M.**, and **Greenberg, D. N.**, Proc. Expth. Biol. Med. 7, 88–89, 1949. — 20. **Block, R. J.**, Science 108, 608–9, 1948. — 21. **Block, R. J.**, Proc. Soc. Expt. Biol. Med 72, 337–41, 1949. — 22. **Awapara, J.**, J. Biol. Chem. 178, 113–16, 1949. — 23. **Hangaard, G.**, and **Kroner, T. D.**, J. Am. Chem. Soc. 70, 2135–7, 1948. — 24. **Fromageot, Cl., Sutisz, M.**, and **Lederer, E.**, Bioch. et Bioph. Acta 3, 487–98, 1948. — 25. **Schramm, G.**, and **Primosigh, J.**, Z. physiol. Chem. 282, 271–84, 1947. — 26. **Atkinson, R. D., Stuart, R. G.**, and **Stuckey, R. E.**, Analist 75, 447, 1950. — 27. **Govindarajan, V. S.**, and **Grenivasaya, M.**, (Indian Inst. Sci. Bangalore) Current Sci. 19, 39–42, 1950. — 28. **Graig, L. C., Gregory, J. D.**, and **Hausmann, W.**, Anual. Chem. 22, 1462, 1951. — 29. **Kirby–Berry, Sutton, Cain, Berry, S.**, Biochemical Inst. Studies IV. Univ. Texas Public. May I, 1951. — 30. **Dent, C. E.**, Biochem. J. 43, 169, 1948. — 31. **Work, E.**, Lancet 256, 652, 1949. — 32. **Polson, A.**, Bioch. et Biophysic. Acta 2, 575, 1948.

Tryckt den 9 december 1952

Uppsala 1952. Almqvist & Wiksells Boktryckeri AB

ARKIV FÖR KEMI Band 5 nr 11

Read 10 September 1952

Effect of irradiation with X-rays on phosphate incorporation in mice

By A. Forssberg and G. Hevesy

One would expect the effect of irradiation on phosphate incorporation into various organs of the body to manifest itself most markedly in experiments of very short duration. This induced us to compare the incorporation of administered ^{32}P into the organs of irradiated mice and in those of controls 15 minutes after administration of labelled sodium phosphate. Twelve to twentyfour mice weighing 17 to 25 g were used in each of the 11 experiments. Half of the group was irradiated with 2000 r, administered in the course of 15 minutes. The weight of the irradiated and of the control group did not differ more than 2% in each experiment. The animals were injected with 0.1 ml of 0.5 μ C or less of labelled phosphate immediately after irradiation. They were killed exactly 15 min. after injection.

As seen in Table 1 the liver of irradiated mice took up more ^{32}P than that of the controls in all experiments. The mean value of the excess ^{32}P uptake by liver of the

Table 1

Uptake of ^{32}P by 100 mg of dry liver tissue of irradiated and of control mice

Way of ^{32}P administration	Counts per min.		Percentage increase in the ^{32}P uptake by the liver of irradiated mice
	Irradiated	Control	
Intravenous	702	386	82
Intravenous	339	230	48
Intravenous	923	670	38
Intraperitoneal	850	624	36
Intraperitoneal	503	470	7
Intraperitoneal	344	318	8
Intraperitoneal[1]	1996	1196	71
Intravenous	15227	7035	117
Intravenous	3337	2795	19
Intravenous	4760	4410	8
Intravenous	3765	3745	1
			mean percentage increase in ^{32}P uptake due to irradiation = 39.5

[1] Injected immediately previous to irradiation.

irradiated mice amounted to about 40% of that taken up by the liver of the controls. A markedly increased (19 to 200%) ^{32}P content was also observed by the gall bladder (incl. content) of irradiated mice.

Similar investigations (1) have formerly proved that the specific activity of the liver inorganic P, including creatine P, differs less from the specific activity of plasma inorganic P in the irradiated than in the control rat. The dose varied in these experiments between 335 r and 1500 r, the time of the experiment between 30 and 660 minutes. Liver ^{32}P values were here found to be increased by 18–31 % in the irradiated rat.

The increased ^{32}P uptake by the liver of the irradiated animal is not only due to an increased rate of passage through the walls of the liver capillaries but through the liver cell membranes as well. The ^{32}P concentration of the extracellular space of the liver cannot be much larger than the corresponding plasma value. But in one of our experiments, for example, the activity of 1 g of plasma of the irradiated mice amounted to 800 counts per min. As the liver contains about 30% extracellular fluid the extracellular activity of 1 g of liver could be expected to remain below 250 counts per min. assuming an even distribution. We found however, in 1 g of liver a ^{32}P content corresponding to 4200 counts per min.

We isolated furthermore from acid soluble liver extracts propandiolphosphate and coenzyme according to Sachs (2). These compounds which are almost absent in the extracellular space (3) showed round 40% higher specific activity in irradiated mice. We may also note that Sherman and one of us (4) compared the specific activity of several acid soluble P fractions isolated from the liver of mice and found the creatine phosphate fraction of irradiated mice to contain more ^{32}P than that of the controls. These observations indicate an increased incorporation of ^{32}P into organic compounds of the liver cells of irradiated mice.

Irradiation has also been shown to increase the glycogen content of the liver (5). As glycogen formation involves phosphorylation processes the observed increase of phosphate may be a necessary step in the formation of additional glycogen.

The increase in the rate formation in the liver cells of other organic phosphorus compounds as these involved in glycogen formation may also result in a net increase of ^{32}P uptake by the liver of irradiated animals. Among other possible explanations of the enhanced ^{32}P uptake an increased rate of blood flow in the liver of irradiated mice should also be considered.

An increased uptake of ^{32}P by the liver of irradiated mice reflects itself in a marked depression of ^{32}P incorporation into the skeleton and a slightly reduced incorporation into the muscles as well as seen from Tab. 2.

Table 2

Percentage change in the ^{32}P content of bone and muscle of equal dry weight due to irradiation

Organ	Percentage change in ^{32}P content									
	No. of experiment									Mean value
	1	2	3	4	5	6	7	8	9	
Bone	−24	−23	−37	−13	−7	−17	+8	—	—	−16
Muscle	−2	−11	−29	−13	0	−15	−2	+11	+19	−5

8 groups of the irradiated mice had a lower, 3 groups a higher plasma ^{32}P content than the controls, the mean change being −11%.

The main competitors of the liver in the uptake of ^{32}P are the skeleton, muscles and digestive organ. As seen in Table 2 the uptake of ^{32}P by the bones of the irradiated animal is depressed by 16%, by the muscles by 5% only. We found 100 mg dry liver tissue in experiment in which the activity of 100 liver of controls were compared to have taken up 15 min. after intraperitoneal injection 3.0 times as much ^{32}P than 100 mg dry bone tissue. Assuming the total fresh skeleton of the mouse to make out 17% of its body weight and the corresponding figure for the dry skeleton to be 11, while for the total liver the figures are 7.0 and 2.1, the dry weight of the skeleton works out to be 5.2 times that of the dry weight of the liver. The total ^{32}P content of the skeleton is thus 1.7 times that of the liver. Should the enhanced uptake of ^{32}P by the liver be fully compensated by a corresponding decrease in the ^{32}P uptake by the bones, 100 mg dry bone of the irradiated mice should show a with 23% lower ^{32}P content than is shown by the controls. The decrease found by us makes out 16% only. To this figure has, however, to be added the difference in the ^{32}P uptake by the muscles of the controls and the irradiated mice. The activity of the total muscles is almost identical with that of the total liver. We arrive to this result from the activity ratio of 100 mg dry liver and the corresponding amount of dry muscle which we found to be 4.6 and from the fresh and dry muscle content of the mice which is assumed to be 42% and 9.2% resp., the dry weight of the muscles being thus $\frac{9.2}{2.1} = 4.4$ times that of the liver. A 5% increase in the ^{32}P content of 100 mg dry muscle of the irradiated animal corresponds thus to an about 5% decrease in the ^{32}P content of 100 mg dry liver. Thus decreased uptake of ^{32}P by the skeleton and muscles of the irradiated mouse accounts about for the increased ^{32}P content of the liver.

The decreased ^{32}P of the plasma of the irradiated mice has hardly any statistical significance as in our experiments taking 15 min. the ^{32}P content of the total plasma makes out about 1/5 only of the ^{32}P content of the liver. We arrive to this figure from the mean activity ratio of 100 mg dry liver and the same amount of dry plasma which we found to be 1.4 and by assuming the dry weight of the 6 ml of total plasma (6) of the mouse to have a dry weight of 0.6 gm thus 1/3.5 of that of the dry liver.

SUMMARY

With ^{32}P as a tracer it was shown that the liver of irradiated young mice (2000 r) took up about 40% more labelled phosphate than did the controls in the first 15 min. after injection. The increased ^{32}P-uptake in the liver was found to be about compensated by a corresponding decrease in the ^{32}P uptake of the skeleton and to a minor extent by that of the muscles. Possible explanations of these findings are discussed.

Institute of Radiophysics of Karolinska Sjukhuset and Laboratory for Organic and Biochemistry of the University of Stockholm.

REFERENCES. (1) **H. v. Euler** and **G. Hevesy**, Ark. f. Kemi (1944), *17 A*, No 30. — (2) **I. Sachs**, I. Biol. Chem. (1949), *181*, 655. — (3) **O. Lindberg,** Ark. f. Kemi (1946), 23 A, No 2. — (4) **F. G. Sherman** and **A. Forssberg,** Proc. Internat. Congress of Biochemistry 1952. — (5) **L. F. Nims,** Colloques Internat. du Centre National de la Recherche Scientifique (1951), p. 102. **M. H. Ross** and **I. O. Eley,** I. Cell. Comp. Physiol. (1951), *37*, 163. **M. Lourau**, personal communication. — (6) **N. Kaliss** and **D. Pressman,** Proc. Exp. Biol. Med. (1950), *75*, 16.

Tryckt den 9 december 1952

Uppsala 1952. Almqvist & Wiksells Boktryckeri AB

ARKIV FÖR KEMI Band 5 nr 12

Read 12 March 1952

Properties of the cytochrome system of wheat roots

By H. Lundegårdh

With 33 figures in the text

Introduction

The spectroscopic evidence of the existence of a complete cytochrome system in living roots of wheat and corn (17, 18) opens a new possibility of investigating the response of the oxidation-reduction balance of this system to varying conditions. The young roots are fairly transparent and the absorption spectrum is comparatively little confused by the simultaneous presence of other coloured substances. The direct spectroscopic observation of the living roots in their normal medium (aqueous solutions) is a guarantee against an undue influence of disorganized products. This is particularly important in the case of the cytochrome system. Owing to its intimate relations to the living structure of the protoplasm its activity is more or less hampered by mechanical homogenization. The interaction of the cytochrome system and electrolytes (salts), one of the fundamental physiological processes in plants, is thus severely changed after destruction of the cell structure. The coenzymatic effect of anions was, however, over looked by Chance (43) in his recent attempts to understand the reaction kinetics of the cytochrome system.

The previously demonstrated high permeability of the roots to various inhibitors (13) enables a detailed study of their effect upon the cytochrome system. Because the oxidation-reduction balance of the different cytochromes is not uniformly changed it was thus possible to satisfactorily compute the absorption spectrum of cytochrome *b*. The previously discovered causal relation between the cytochrome system and the active salt absorption (11) was further analyzed, also in respect of the time course of the proceedings. The presence of cytochrome oxidase in the surface of the living roots was biochemically demonstrated and utilized for a discussion as to the possible localization of the system in the cell.

Methods

The monochromator. The previously introduced recording spectrophotometer (18) has been completely rebuilt and perfectioned. The basic instrument is a large quartz monochromator with two quartz achromates (F 5). A micrometer screw moves synchronically the prism table and the focal position of the lenses. The wave-length of the outgoing light beam and the exact focussing on the exit slit are thus both controlled by the wave-length drum.

The drum has a diameter of 100 mm. A 1.5 mm wide furrow is milled at each 2.5 mμ interval on the scale. An electric contact device is placed on a carriage sliding parallel to the axis of the wavelength screw. The carriage is moved by means of a cam protruding into the milled screw line on the drum. The contact is operated by means of a spring the nose of which plungs into the above named milled furrows, thus disinterupting the electric current just when the drum is in the exact position of an interval, e.g. at 400, 402.5, 405, 407,5 mμ etc.

The current through the contact controls an electromagnetic clutch joining the wave-length screw with a grammophon motor. At closed contact the wave-length screw moves until the nose of the contact spring plungs into the next furrow on the drum. The start impulse is given by a main contact device attached to the Speedomax instrument (see below) and closing a shunt through the circuit once for a given multiple of 4 seconds (= the period of the Speedomax recorder). As two records are required for each wave-length interval, one for the reference beam (I_0) and one for the sample (I_1), the position of the wave-length drum has to be shifted in 8 seconds. The normal period of adjustment of the Speedomax is 3.6 seconds. As the change of position of the wave-length drum takes only 0.1–0.2 seconds single readings are fairly reliable, as was also shown statistically.

The multiplier photo tube. In this investigation an EMI tube 5060 was used. It has a multiplication factor of 10^7 and operates satisfactorily with eleven interstage potentials of 160–170 volts. The maximum spectral sensitivity lies at 520 mμ and the curve declines rapidly towards blues and red. Good results were obtained, however, from c. 380 to c. 650 mμ. As the monochromator gives a clean spectrum colour filters are not indispensable.

From a technical point of view the steep sensitivity curve of the photo cells is infavourable because it decreases the tolerable accuracy of the transparency records towards the ends of the spectral range unless special steps are taken in order to egalize the sensitivity. This intricate problem can be solved along two different lines: either by means of an automatic adjustment of the shunt resistance (because Speedomax works as a millivoltmeter the outgoing current from the photo tube is closed over an adjustable resistance of in maximum 10000 ohms; the potential difference between the ends of this resistance is measured by the Speedomax), or by means of an adjustable diaphragm between the illuminating lamp and the collimator tube. The first method has the serious disadvantage that the "dark current" from the photo tube varies synchronously with the magnitude of the shunt resistance, causing serious trouble in calculating the readings, because the dark current determines the zero position of the instrument (it amounts to 3–4% of the scale at a shunt resistance of 10000 ohms). With an adjustable diaphragm the zero position is constant. This method is therefore to be preferred. A detailed description of the adjustable diaphragm cannot be given here, but the leading idea is a cam working against a lever connected to the shutter mechanism. The cam is cut as the reversed image of the spectral curve of the photo cell and it is automatically moved one step for each recorded interval.

The object holder. The majority of the spectrograms were recorded from a 14 mm thick bundle of roots enclosed in a quartz tube (the recipient). By means of elastic clamps the tube is placed on a movable frame, sliding between the exit of the monochromator and the photo tube. The latter is enclosed in a metal cover, the horizontal top of which has a window coinciding with the photo cathode of the cell. The sliding frame carrying the object has two 5 mm wide slits, which can be alternatively brought in coincidence with the photocell window by means of a lever and an excenter disc. The shift of positions is controlled by an electromagnetical clutch similar to that one used for the movements of the wave-length screw. The recipient is placed over one of the two slits in the sliding frame. The second slit represents the reference beam. Because of the low general transparency of the thick root bundle the intensity of the reference beam must be highly reduced. A glass tube filled with cotton wool makes a suitable filter but a still better one is made by 6–7 layers of Munktell filtering paper Nr. 3 clamped under a ground glass plate and 2 mm Schott filter GG 17. This filter eliminates the disturbing influence of the violet end-absorption of the living tissue.

According to the electrical impulses from the main contact device (see above) the frame carrying the recipient shifts its position automatically every 4 seconds. In 8 seconds the Speedomax thus records the transparency values of I_0 and I_1. If the paper is logarithmically graduated the extinction values can be directly read from the difference between the two points. It is convenient to use different colours on the printing wheel of the Speedomax, e.g. blue for I_0 and red for I_1.

Preparation of the plant material. Seedlings of spring wheat (Diamant II) were grown in water cultures as previously described (11, 12). At a total length of 12–15 cm the lower 8–9 cm of the roots remain unbranched and show a uniform activity as to respiration, salt accumulation, and percentage of cytochrome (12, 18). A glass (or quartz) tube of 14 mm bore requires for tight filling roots from 150 plants. Mostly 75 plants were used for each experiment and the roots cut in two portions, viz. 0–25 and 25-50 mm. from the tip. Both portions were put together and the complete bundle introduced in the absorption tube. The recorded spectrograms thus give the medium spectral transparency of the total active zone.

The transparency of the root bundle is considerably increased if the air in the intercellulars of the cortex, and the air between the roots, is removed. The tube with its contents is evacuated under the water air pump for a few minutes. All cavities are then filled by water, a process not appreciably disturbing the normal functions of the roots. Removing of the air bubbles also facilitates the reduction of the cytochromes in O_2-free water.

Control of the physiological conditions. The tube with the roots is fitted with rubber stoppers provided with glass tubes for circulating water. The tubes are connected to an upper supply (some 30 cm above the level of the tube) and a lower ending exit. The connections are made by thin rubber tubes which do not empede the movements of the object frame when its position is shifted. The effectivity of the drainage may be measured by counting the drops per minute leaving the exit tube. The outflowing solution may be collected in small flasks for O_2-determination (WINKLER method) or analysis of the salt absorption, if such determinations are to be made simultaneously with the spectral records. Most experiments were made at a temperature of 19°C.

The spectral resolution and the slit width. The outgoing lighth beam from the monochromator was focussed on the object tube by means of a cylindrical quartz lens forming a narrow line of c. 10 mm length on the object. An aluminized mirror reflects the horizontal beam vertically down on the object. All parts are of course enclosed in a dark cover but are conveniently controlled from the outside.

The relation between slit width and band width is as follows:

	300	400	500	600 mμ
Band width at 0.05 mm. slit......	0.35 mμ	0.7 mμ	1.2 mμ	2 mμ
» » » 0.10 » ».......	0.70 »	1.4 »	2.4 »	4 »

In the previous experiments (17, 18) an instrument with two quartz prisms and the double resolving power was used, but its aperture was too low for 14 mm tubes. With the new instrument satisfactory results were obtained with a slit width of 0.05 mm for 10 mm bundles and 0.08–0.10 mm for 14 mm bundles. In the last named case the recorded intervals, however, were held at 2.5 mμ from 380–500 mμ and at 5 mμ from 500 to 650 mμ.

Analysis of the ox/red spectrum

As previously stated (17, 18) the ox/red spectrum, computed from ε reduced minus ε oxidized, proved very useful for the identification of the cytochromes in the living objects and the closer inspection of the changes in the oxidation-reduction balance at varying conditions. The ox/red spectrum was deduced from the record of the roots in streaming aerated water (or KCl) immediately followed by the record of the same roots in O_2-free water. CHANCE (43, p. 709) erroneously believes that only HCN was used as reducing agent.

It was previously shown that in respect of cytochrome *c* the height of the bands of the ox/red spectrum varied approximately linear with the percentage of reduced cytochrome in the object (18).

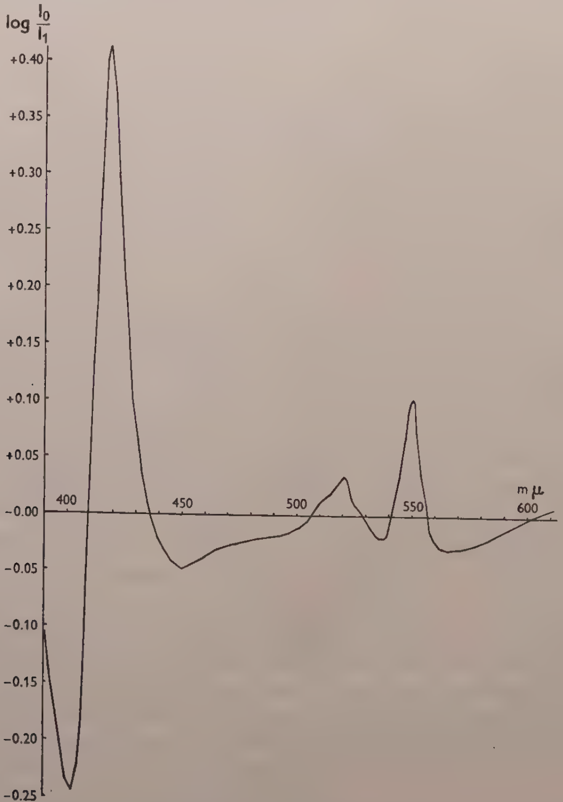

Fig. 1. The ox/red spectrum of a preparation of cytochrome *c*, calculated as ε reduced–ε oxidized. 3 μ mol/litre cytochrome completely oxidized and then completely reduced by dithionite. Cuvette 10 mm. Reference beam aqua dest. Slit width 0.03 mm.

Because the β- and α-bands of cytochrome *c* only appear in the reduced state the peaks in the ox/red spectrum are identical with the corresponding peaks in the red-spectrum. The γ-band, however, is present also in the oxidized state, but it moves at reduction c. 10 mμ towards red. The γ-peak of the ox/red spectrum is displaced c. 12 mμ from the position of the ox-band. In pure solutions of cytochrome *c* the ox/red spectrum cuts the zero line of extinction at several isosbestic points, 409, 435, 506, 529, 542, and 557 mμ, and the bands are lowered (fig. 1). In biochemical preparations or living objects it is unfortunately almost impossible to compute this optical zero line because of the inevitable variation of the opacity of the optical background induced by the added reducing agents. More satisfactory results are here obtained if the height of the bands is measured from certain intermediate points of minimum extinction, in the case of wheat roots e.g. 450 mμ (cf. fig. 1). For identification of cytochrome *c* the following quotients may be used:

$$\frac{550-450\ \text{m}\mu}{520-450\ \text{m}\mu}=1.8\ \text{and}\ \frac{418-450\ \text{m}\mu}{550-450\ \text{m}\mu}=3.$$

For approximate optical calculation of the concentration of cytochrome *c* in the roots the following figures may be used. The molar extinction coefficient, referred to readings at 420 mμ of the ox/red spectrum amounts to $13\cdot10^4$ $(\frac{1}{c}\cdot\frac{1}{d}\cdot\log\frac{I_0}{I_1};\ c=$ mols per litre, $d=$layer thickness in cm), if the extinction is calculated from zero ε. Calculated from the pure red-spectrum the molar extinction coefficient at 416 mμ amounts to $32\cdot10^4$ (22).

For conversion of the values measured in the ox/red spectrum to those of the red-spectrum of cytochrome *c* the following approximate quotients may be used:

$$\frac{(420-450\ \text{m}\mu)\ \text{ox/red}}{(415-450\ \text{m}\mu)\ \text{red}}=\frac{1}{2}\quad\frac{(550-450\ \text{m}\mu)\ \text{ox/red}}{(550-450\ \text{m}\mu)\ \text{red}}=1.$$

A more exact calculation of these quotients has no practical value because of the mentioned variations of the background of the spectrum in living organs. In all such calculations also the slit width in relation to the resolving power of the spectroscope has an influence.

The identification of the cytochromes *b* and *a* rests on less solid ground because none of these enzymes has been isolated. As to cytochrome *a* there is some confusion in the literature, owing to the fact that some authors, e.g. KEILIN and HARTREE (8), claim the existence of a cytochrome *a* besides of the cytochrome oxidase or cytochrome a_3, the latter assumed to be identical with the "Atmungsenzym" of WARBURG, whereas other authors have not been able to identify a cytochrome *a* but only the oxidase (39, 3). It will be shown below that also in the wheat roots the existence of a special cytochrome *a*, corresponding to KEILINS definition, is very doubtful, whereas the existence of the cytochrome oxidase is undisputed. For convenience's sake the cytochrome oxidase is mentioned under the name cytochrome *a* in the following. This nomenclature is justified also because of the fact that the spectral qualities of the oxidase are very similar to those of *b* and *c*, whereas the spectral behaviour of KEILIN's cytochrome *a* in several respects deviates from that of the others.

In a previous communication a tentative construction of the ox/red curve of the *a*-group according to STRAUB (34) proved useful for the optical analysis of the root spectrum. A recent publication of WAINIO *et al.* (39) conveys a more accurate picture of the spectrum (see also BALL *et al.* 3). According to our present knowledge the γ-bands of cytochrome *a* (or cytochrome oxidase) are located at 416–420 mμ oxidized and 442–443 mμ reduced and the α-band appears at 601–605 mμ. The ox-red spectrum has its γ-peak at c. 443 mμ. Isosbestic points appear at c. 425–430 and 460 mμ and there is a considerable minimum below the zero-line at 415–420 mμ, depending upon the fact that the γ-bands of the oxidized and reduced forms are much wider apart than in the case of cytochrome *c* (c. 25 mμ instead of c. 10 mμ).

The spectroscopical identification of the cytochrome oxidase is promoted by the well-known complex reaction with carbon monoxide. With CO the γ-band is partly moved to 430–435 mμ and new bands appear at 580–595 mμ (possibly also at 540–545 mμ), whereas the α-band is comparatively little changed. The spectrum of the cyanide compounds is less closely studied, but also here a marked change is seen. Cytochrome *c* forms no compound with CO or CN under physiological conditions, as was also shown in the present investigation. The values of the molar extinction of the cytochrome oxidase given in the literature are of course only approximative and somewhat varying. For the γ-band WARBURG calculated $38 \cdot 10^4$, whereas KIESE (41) recently found $23 \cdot 10^4$. Both values are not very different from the β-value of cytochrome *c*.

Cytochrome *b* was much less intensively studied than the two other cytochromes. No dates are available as to the position of the γ-band of its oxidized form and also the reports of the β-band are very incomplete. Very little is known, too, of the possible influence of CO and CN on the spectrum of cytochrome *b*. On the whole, however, the position of the bands of cytochrome *b* show a close analogy to those of cytochrome *c*. The cytochrome b_2 described by BACH et al. (1) has protohemin as prosthetic group and shows a molar extinction of similar magnitude as that of cytochrome *c*. The identity of this preparaton with other compounds described as cytochrome *b* is still doubtful, however. The present investigations supports the assumption that the cytochrome *b* in the roots is closely related to the corresponding cytochrome in animal tissues.

The general procedure of the optical analysis of the spectra was the following. From the measured extinction at 415 mμ the spectrum of cytochrome *c* is calculated (cf. 18). What remains of extinction after the subtraction of *c* from the observed spectrum represents *b* and *a*. The spectrum of cytochrome *a* can be calculated from the measured height of the reduced band at 600–605 mμ. For the relation between the γ- and α-bands the same value as concerning cytochrome *c*, viz. 5, was used, a figure not far from what may be calculated from the spectra of *a* published by STRAUB, WAINIO et al. (34, 39) and KIESE (41). The practical success of the calculation, viz. the found coincidence of the γ-values of *a* calculated from the α-band, and those obtained from the ox-red spectrum after subtraction of the cytochromes *c* and *b* shows that the real relation of the two named bands of the oxidase amounts to approximately 5.

The optical analysis yields an ox-red spectrum of cytochrome *b* with bands at 425–428, 535, and 560–565 mμ. The positions and dimensions of the bands arise the suggestion that the γ-bands of oxidized and reduced cytochrome *b* are only a few mμ apart and that *b* γ red has its position at c. 427.5 mμ.

Because the instruments allow the accurate measurement of extinction differences of only 0.003–0.005 ε ($\log \frac{I_0}{I_1}$) also small elevations or peaks of the observed curves may be significant and this fact calls for some discussion as to the diagnostic value

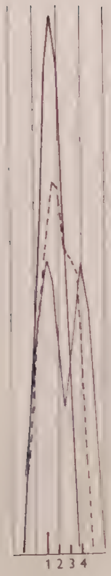

Fig. 2.

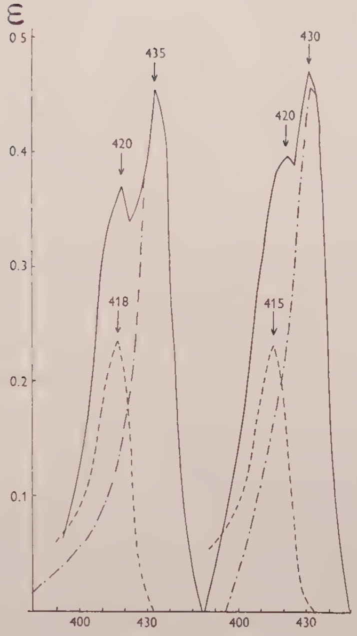

Fig. 3.

Fig. 2. Construction of joined bands from two similar γ-bands (A, B) of cytochrome *c* placed at increasing distances from one another. 1 is the fixed position of A. 2 (———) B 5 mμ from A; the joined peak is moved 2.5 mμ from A (intermediate position). 3. (------) B 10 mμ from A; the joined band is asymmetrical, with one high peak 2.5 mμ from A and a hump 2.5 mμ to the right of B. 4. (———) B 15 mμ from A; twin peaks coincident with the peaks of the components.

Fig. 3. Construction of joined bands from two γ-bands of different intensity (1/2). Distance between the bands (------) 15 mμ. The lower peak of the joined band is moved 2.5–5 mμ to the right.

of peaks in spectrograms of mixtures. The limitations implied by the instruments and the mode of recording, value of the intervals etc., were emphasized already in a previous communication (18). As to the accuracy of the wave-length determination it ought to be mentioned that 2.5 mμ intervals of observation raise the limit to c. ± 1 mμ. Because intervals of 5 mμ were used above 500 mμ the single wave-length determinations of the β- and α-bands of *b* and *a* are accurate only within ± 2 mμ. Because the observations were repeated several times the accuracy may rise considerably, however.

A second point of importance is the joined effect of bands lying close together. A few examples are given in the figs. 2 a 3. They refer to actual recording conditions prevailing in this investigation (slit 0.08–0.10 mm., intervals 2.5 mμ). Two γ-bands combine to one single, higher band if they lie in a distance from one another of only 5 mμ. If the distance is 10 mμ the lower band appears as a hump on one side of the joined band. If the distance rises to 15 mμ the two bands appear as peaks from a joined basis. It is furthermore important to notify that the peak of a combined band may be moved in one direction or the other according to the relative intensity of the components (fig. 3). These facts are frequently neglected in the literature when spectrograms of mixtures of two or more enzymes are discussed.

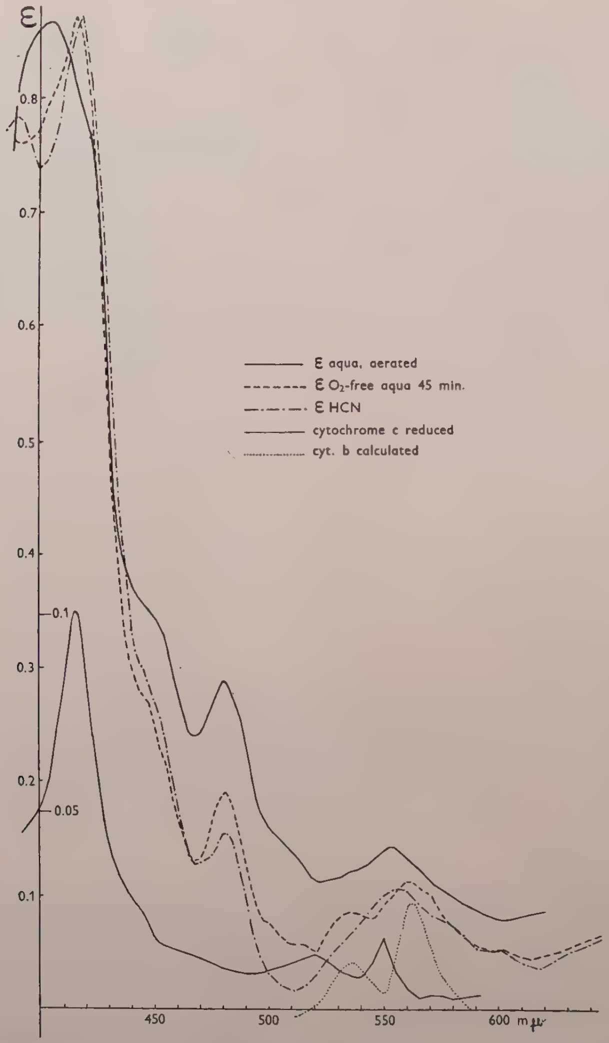

Fig. 4. Crude spectrum of a 14 mm thick bundle of wheat roots. For comparison is the reduced spectrum of a preparation of cytochrome *c* of the same concentration as in the roots (20 mg/1 litre) plotted in accordance with the height of the observed β- and α-bands of the crude spectrum. A subtraction of the spectrum of cytochrome *c* from the crude spectrum yields the spectrum of cytochrome *b*.

Analysis of the crude spectrum

The crude spectrum is calculated as ε roots–ε reference filter (filter paper + Schott filter; see p.99), viz. is plotted from values read directly from the record (see figs. 4, 5, 22). The crude spectrum shows the single bands of all cytochromes but owing to the fact that the enzymes are only partially oxidized in aerated water both oxidized and reduced γ-bands are simultaneously present.

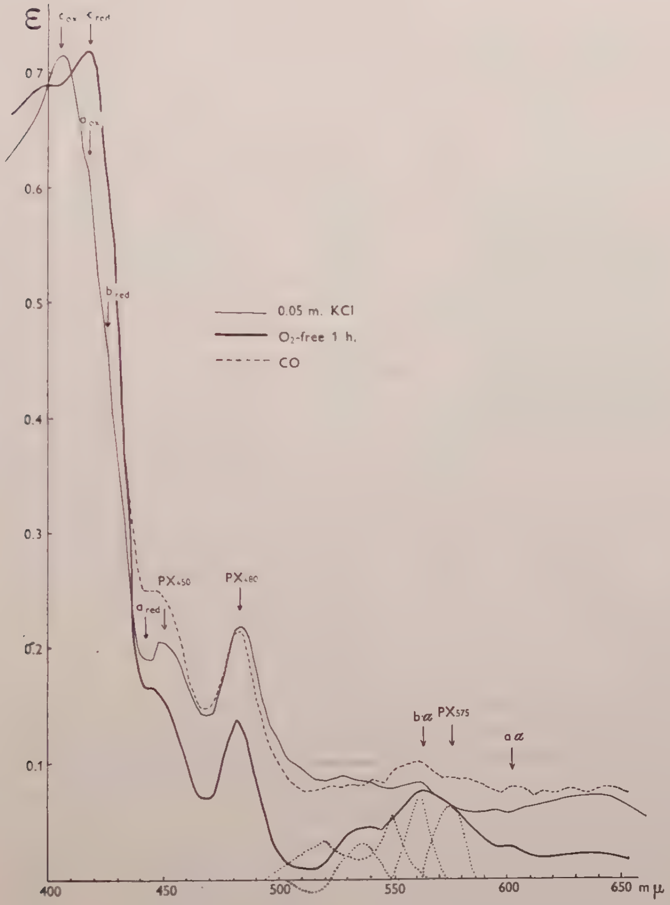

Fig. 5. Crude spectrum of a 14 mm thick bundle of wheat roots. The increased oxidation in 0.05 m. KCl produces a deep pit at the place of the reduced γ-band of the cytochrome oxidase (442.5 mμ). ...... constructed curves of cytochromes *c*, and *b*, and PX 575, participating in the anaerobic crude spectrum.

Fig. 6 illustrates the reduced bands of the three cytochromes. The spectrum of *c* is measured from pure preparations, that of *b* and of *a* is calculated from the observed curves of the roots according to the scheme discussed in the foregoing section. The heights of the bands are chosen in accord with the relative quantities of the cytochromes in the roots (see below).

The crude spectrum obtained with the standard reference beam shows the following characteristics (see figs. 4, 5, 22): 1. a high broad peak in violet, comprising the combined γ-bands of *c*, *b*, and *a*; 2. an elevation or a pit at 440–445 mμ; 3. a band of varying height at 450 mμ, sometimes completely absent; 4. a strong distinct band at 480–483 mμ, present in all roots (also of corn) and strikingly constant; 5. an elevation at 560–570 mμ. Of these bands nr. 4 does certainly not belong to the cytochrome system. Also nr. 3 probably refers to another system, possibly a flavo-protein (see

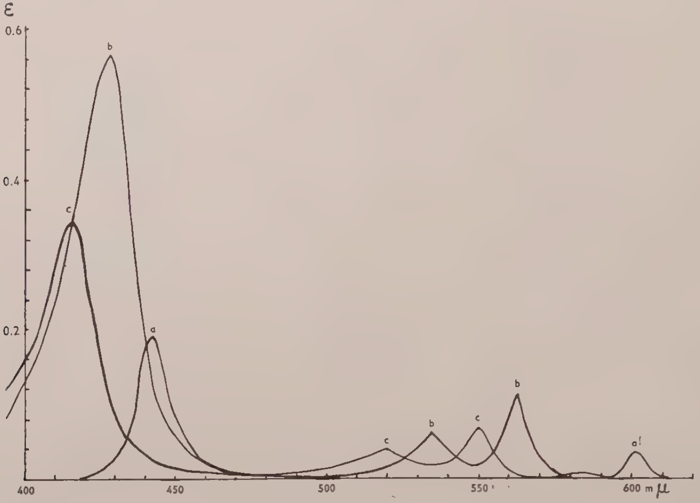

Fig. 6. Calculated reduced spectra of the cytochromes *a* (oxidase), *c* and *b* in the roots. The height of the bands reflects the relative quantities of the components.

below); because its intensity varies considerably without any measurable variation in the physiological behaviour of the roots its enzymatic character is questionable, however.

The large band in violet and blue as a rule shows smaller peaks or elevations, appearing at a "safe" distance from one another (cf. above p. 103), viz. 406–407 mμ, 415–420 mμ (sometimes 417.5 mμ), and 425–428 mμ. Of these 406–407 mμ obviously corresponds to the γ ox-band of cytochrome *c*; it always disappears at reduction. 415 mμ is probably the γ ox-band of cytochrome *a* (the oxidase), more or less mixed, however, with a weak γ red-band of cytochrome *c* and the γ ox-band of cytochrome *b*. The latter has obviously no "safe" distance from the γ ox-band of *a*, and has very probably the value 418–420 mμ. The elevation at 425–427.5 mμ is obviously the γ red-band of cytochrome *b*, because also the α-band at 562 mμ is recognized under aerobic conditions (water or salt solutions). The position of the γ-band of *b* in the ox-red spectrum is practically the same, whereas the corresponding band of cytochrome *c* is displaced c. 2 mμ towards red (see above).

The γ red-band of the cytochrome oxidase is only occasionally recognized as separate peak or hump in the crude spectrum. It is to a large extent covered by the broad foot of the γ-band of cytochrome *b*, the concentration of which is three or four times that of *a* (cf. fig. 6). Also the back-ground of this part of the spectrum changes under conditions of reduction, influences which are not quite eliminated in the ox/red spectrum. Measurements of the extinction differences 442.5–460 mμ, however, satisfactorily reflect the response of the γ-band of the cytochrome oxidase. Under conditions of extreme oxidation, e.g. in strong salt solutions, the disappearing of the reduced γ-band of *a* is observed as a growing pit at 442.5 *m*μ (fig. 5). Occasionally the γ ox-band at 415 mμ also appears under these conditions (fig. 22).

The uniformly increasing end-absorption of the living roots towards violet is probably caused by flavanons (cf. 20) and brownish substances in the lignified walls of the vessels. The rapid increase of the end-absorption if pH rises above 7 (cf. 18) is probably due to the colour change of the flavanons. Owing to these complications the medium must always be held at a pH below 7. It is interesting to notify that a pH of 6.2-6.5 represents a point of conversion also from the view-point of the physiological process of sap movement in the roots (13). The normal pH of the wheat roots is c. 6.2. The flavanons possibly participate in the ground respiration of the roots (20). The cytochrome system is on the other hand fairly insensitive to variations in the pH, a circumstance which is reflected not only in the spectral behaviour but also in the undisturbed proceeding of the anion respiration.

After complete reduction in O_2-free water the large band in violet and blue moves to 420–422.5 mμ (figs. 4, 5). It now represents the joined γ-bands of the cytochromes *c* and *b*. A similar band appears after treatment with HCN (fig. 4). After reduction strong bands appear at 530-535 and 560–565 mμ, the latter frequently moved towards 570–575 mμ, and weaker bands at 595 and 600–605 mμ. These bands belong to the reduced cytochromes *b* and *a*, the α-band of *b* being reinforced by the development of a new band at 575 mμ.

The β- and α-bands of *b* were measured in a large number of spectrograms. The extinction of *b*β is 0.023 and of *b*α 0.042 and the quotient $\frac{\alpha}{\beta}$ is 1.84 or almost exactly the same as in the case of cytochrome *c* (1.83; zero line = 450 mμ).

The spectrum of cytochrome b

Assuming a value of $\frac{b\gamma}{b\alpha} = 3$ (see p. 101) the calculation of the γ-band of *b* from the observed value of *b*α fairly well agrees with an independent calculation of the γ-band from the ox/red spectrum, as mentioned in the foregoing. This agreement

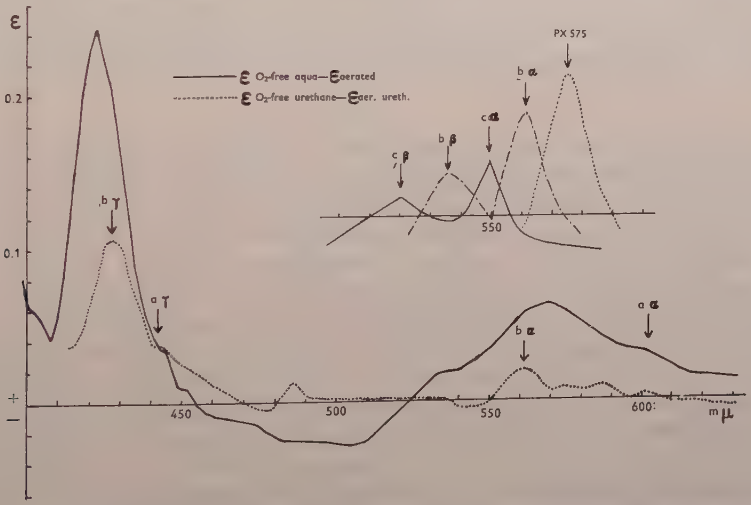

Fig. 7. Ox/red spectrum illustrating the optical isolation of cytochrome *b* by urethane. Fixed in to the right is an analysis of the components of the β- and α-region showing the dominant position of PX 575 at anaerobiosis.

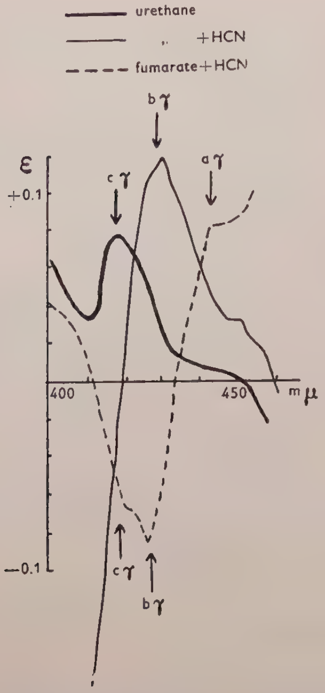

Fig. 8.

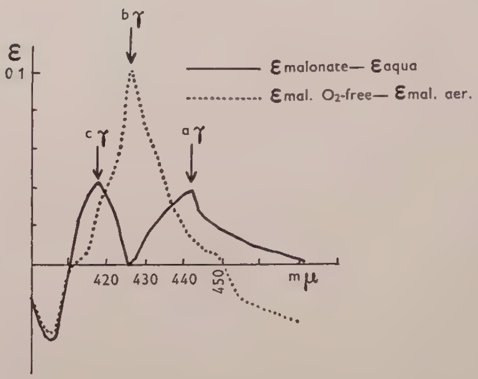

Fig. 9.

Fig. 8. Ox/red spectrum. Partial reduction of cytochrome *c* in 10% urethane, and absence of a further reduction after adding HCN. Failing reduction of cytochrome *b* in 10% urethane and strong reduction after addition of HCN. Strong anaerobic oxidation of cytochromes *c* and *b* in 0.1 m. fumarate, pH 3.2. — Fig. 9. Ox/red spectrum showing the partial reduction of cytochrome *c* in 0.1 m. malonate, pH 3.3, the reduction of the cytochrome oxidase but the failing reduction of cytochrome *b*. Anaerobiosis in malonate lets the reduction of cytochrome *b* appear, whereas only little further reduction of *c* and *a* is observed.

between calculations obtained from different starting-points enables a comparatively accurate construction of the pure spectrum of cytochrome *b* (see fig. 6). From this spectrum the participation of *b* in the joined γ-band of the ox/red-spectrum can be calculated for any values of the ordinate at 430 (or 425), after previous subtraction of the calculated spectrum of *c* (see above).

The results of these analytical calculations of the spectrum of cytochrome *b* are corroborated by experiments with urethane, malonate and fluoride.

Urethane in 10% solution inhibits under anaerobical conditions the reduction of cytochrome *c*, whereas *b* and to some extent *a* are reduced (cf. 8). After changing to an aerated solution of urethane cytochrome *b* remains reduced to a considerable extent. The γ-band of *b* at 425–427.5 mμ and the α-band at 560–565 mμ are now clearly distinguished (fig. 7). Urethane alone partly reduces *c* (fig. 8). With HCN accordingly only a small further reduction of cytochrome *c* was observed, whereas *b* and *a* were even stronger reduced than in O_2-free aqua (fig. 8).

In a solution of 0.1 to 0.05 m. *malonate* (pH 3.3; see 12 on the more rapid penetration of the undissociated acid) cytochrome *c* is partially reduced, whereas the re-

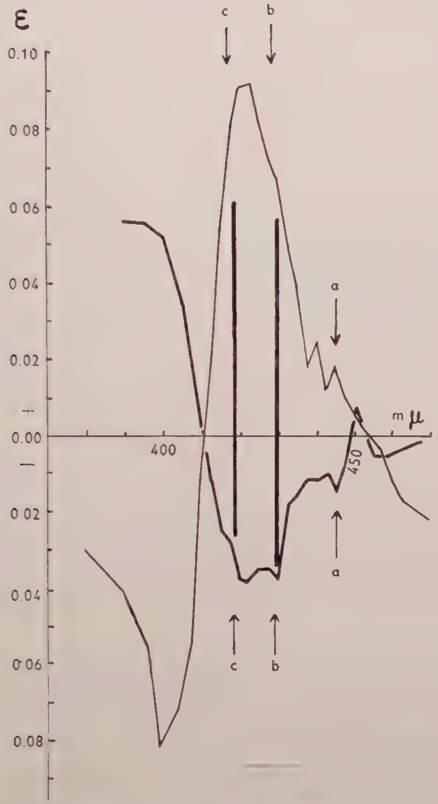

Fig. 10. Upper curve: ε malonate + HCN–ε malonate aerated. Lower curve: ε fumarate + HCN–ε malonate + HCN. The anaerobic oxidation in fumarate is more pronounced in respect of cytochrome *b*, but also *c* is oxidized, whereas the cytochrome oxidase remains reduced in the presence of CN.

duction of *b* decreases (fig. 9). If the malonate is given anaerobically or combined with 0.001 m. HCN *b* is only partially reduced (70–75%), and the further reduction of *c* is rather small. In a spectrum calculated from ε mal. O_2-free–ε mal. aer. (fig. 9) or ε (malonate + HCN)–ε malonate the γ-band of *b* is thus clearly visible at 425–427.5 mμ. If the malonate + HCN is exchanged for fumarate + HCN (pH 3.3) cytochrome *b* is almost completely oxidized as can be seen from the sharp drop of extinction at 425 mμ (see figs. 9, 10). Also cytochrome *c* is oxidized in fumarate, but the effect on *b* is more prominent.

Sodium *fluoride* inhibits the reduction of cytochrome *b* (and of *a*). A strong negative band, with its peak at 427.5 mμ appears under the influence of 0.02 m. NaF at pH 3.3–4.0 (figs. 11, 12). This band completely coincides with the calculated γ-band of *b*. Cytochrome *c* is very little influenced by fluoride.

A differentiation of the absorption spectrum in favour of cytochrome *b* is also obtained if the aerated aqua destillata is exchanged for a *salt solution*. As previously stated (17, 18; see also below) the presence of movable anions in the surroundings of the cytochrome system accelerates the transference of electrons. The oxidation-

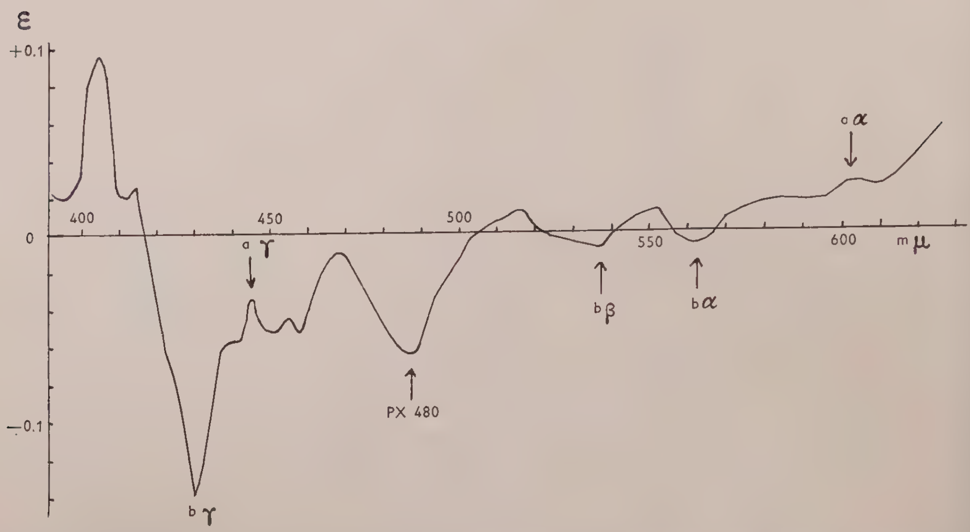

Fig. 11. Ox/red spectrum showing the strong oxidation of cytochrome *b* in 0.02 m. fluoride pH 3.2 (ε fluoride–ε 0.05 m. KCl). The cytochromes *a* and *c* remain partly reduced. The band at 402.5 mμ is possibly peroxidase·F⁻. PX 480 disappears completely.

reduction balance is concomittantly displaced and the percentage of reduced cytochrome *a* and *b* decreases, whereas cytochrome *c* is much less influenced. Hence a negative band appears at 425 mμ.

The wave-length position of the γ-band of cytochrome *b* is somewhat lower than the values given by earlier investigators (e.g. KEILIN and HARTREE, 8). In the ox/red records the γ-band of cytochrome *c* has its peak at 417.5–420 mμ, with preference to the latter value. The γ-band of cytochrome *b* appears at 425–427.5 mμ with preference to the latter value. As was mentioned above the position of the peak of the *b*γ-red-band in the crude spectrum is very probably almost exacly the same as in the ox/red spectrum.

The α-band of cytochrome *b* has its peak between 560 and 565 mμ with preference to 560. The value 562 mμ proposed in the literature thus coincides with the results of this investigation. The right position of the β-band is 535 mμ, not 530 as was occasionally proposed in the literature.

In the earlier stages of the present investigation there was much hesitation as to the possible existence of a second cytochrome *b* with bands very close to the common *b*. The occasionally observed twin peaks in the region 420–430 mμ caused this trouble. The analysis of possible twin peaks (see p. 103) conveyed the conviction, however, that the observed small peaks and humps are satisfactorily explained from a combination of cytochrome *c* and a single cytochrome *b*. In 80% of all spectrogrammes (ox/red spectrum) a single peak appears at 422.5 mμ, representing the summation of the γ-bands of the cytochromes *c* and *b*. It is sometimes extended to the left (420 mμ), sometimes to the right (425 mμ), dependent on the individual quantitative relation between the two cytochromes. In some cases the right slope of the band shows a hump or elevation at 427.5 mμ. The combined γ-bands of two cytochromes tend to result in an asymmetric peak, because of a slight asymmetry

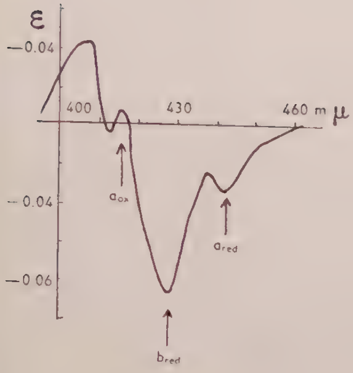

Fig. 12.

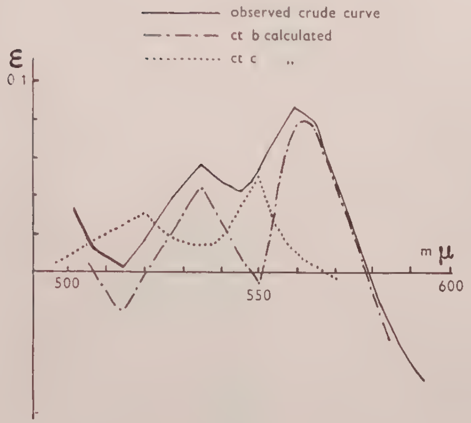

Fig. 13.

Fig. 12. Ox/red spectrum showing the strong oxidation of cytochrome *b* by fluoride. The cytochrome oxidase is comparatively strongly oxidized, showing a small *a* γ ox-band at 415 mμ and a depression of *a* γ red at 442.5 mμ, illustrating the continued activity of the cyanide sensitive respiration in fluoride. — Fig. 13. Diagram illustrating the optical resolution of the crude spectrum in the components cytochromes *c* and *b*.

of the single bands. The slope on the left side is namely steeper and more linear than that of the right side. The highest portion of the joined band is to the left, if the two components are of about the same concentration, but the peak appears on the right side of cytochrome *c*, viz. at 422.5 mμ instead of 420 mμ. In single cases a separate peak appears near the position of the *b* γ-band (427.5–430 mμ). A careful analysis of the ox/red spectrum leaves no room for the assumption of more than one cytochrome *b*.

Also the reproduction of the region 550–570 mμ at small intervals (2.5 mμ) reveals no trace of a duplication of the *b* α-band. The occasional duplication of the top of the joined γ-bands is satisfactorily explained by the mentioned interference of the *b* γ-band with a *c* γ-band of very similar shape but c. 30% lower intensity. Of deciding value is also the fact that all treatments which suppress the appearance of the *c* γ-band, e.g. urethane, malonate or fluoride, result in the development of single *b*-bands.

As to the effect of *cyanide* on the reduced spectrum of cytochrome *b* earlier investigators assume that there is no visible influence. No quantitative measurements were previously made, however. The results of a large number of experiments, in which roots were treated with 0.00001 to 0.001 m. solutions of HCN (pH 6.5), may be summarized as follows.

The position of the reduced bands of cytochrome *b* remains the same but their intensity is changed. Most important is the decrease of the intensity of α- and β-bands, primarily the former. The quantitatively dominating bands of cytochrome *b* usually quite cover the α- and β-bands of cytochrome *c*, if reduction is brought about by removal of the oxygen only (see figs. 4, 5, 13). After the addition of HCN (anaerobically of aerobically) the *c* α-band regularily appears, however (see figs. 14, 15). The resolvation of the spectrum shows that the α- and β-bands of *b* now are c. 50% lower than without CN.

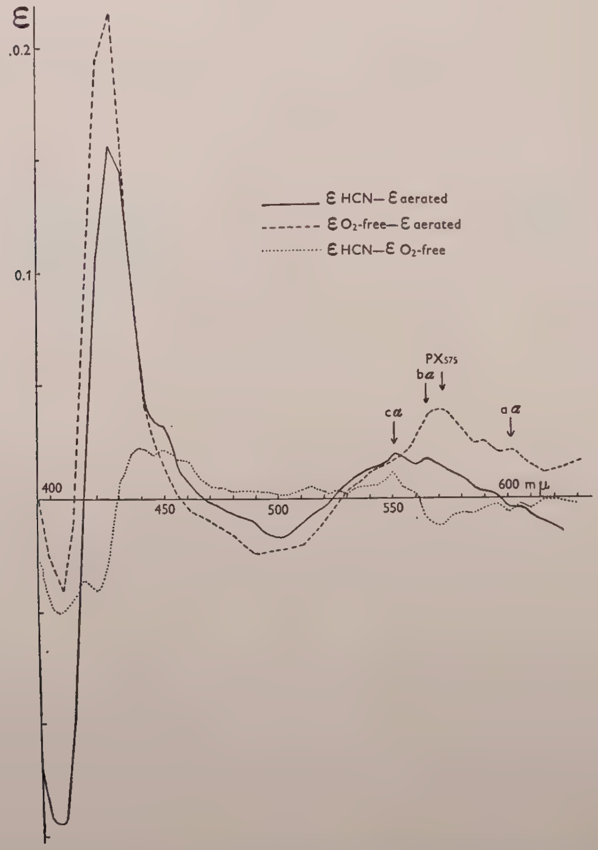

Fig. 14. Ox/red spectrum of a 10 mm thick bundle of roots, showing the appearance of PX 575 under complete anaerobiosis, its diasppearance in HCN, and the simultaneous appearance of *c*α and *b*α in HCN. The difference spectrum between HCN and O_2-free illustrates the appearance of the cyanide modification of the *a* γ band, the movement of *a*α to 595 mμ and the weakening and displacement of PX 575 to c. 580 mμ.

The cleaning effect of HCN on the reduced spectrum is enhanced by its influence on the non-identified band at 575 mμ (cf. 18). This band appears in O_2-free aqua or salt solution and may be called PX 575. It is optically isolated after subtraction of the calculated bands of cytochromes *c* and *b* from the observed spectrum (see figs. 5, 7). PX 575 is weakened and moved to 580–585 mμ under the influence of HCN (fig. 15), a circumstance contributing to the mentioned cleaning of the spectrum.

As to the possible nature of PX 575 it is obviously no hemochromogen comparable to the ones present in the cytochromes, because there is no trace of a band in violet. As the band at 575 appears only after removal of the oxygen it belongs to a substance, however, which changes its molecular constitution at reduction. From the order of reduction it can be concluded that the unknown substance has a comparatively low oxidation-reduction potential. As previously stated (18) the time order of reduction is $a>c>b$. PX 575 is reduced later than cytochrome *b*. Because *a* has the highest potential it oxidizes *c* and *b* and is then itself reduced. If *c* or *b* oxi-

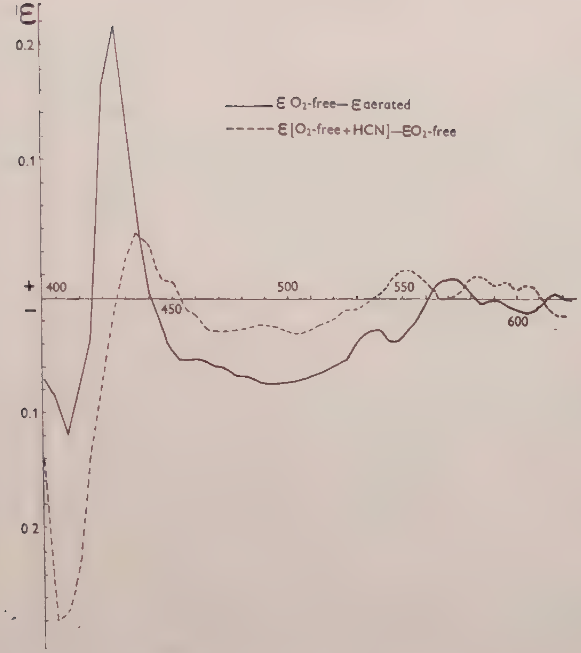

Fig. 15. Ox/red spectrum showing the weakening and displacement of the band PX 575 to 580–585 mμ, the consecutive appearance of $c\alpha$, and the appearance of the CN-modification of $a\gamma$.

dizes PX 575 this substance will remain oxidized longer than the former ones. PX 575 is thus probably linked after *b*, a conclusion of some interest in the later discussion as to the biochemical object of the different enzymes co-operating with the cytochrome system.

The spectrum of cytochrome *a* (cytochrome oxidase)

As already mentioned the identification of the $a\gamma$-band in the crude spectrum is hampered by the fact that the endabsorption of the roots in violet increases at reduction. The covering effect on $a\gamma$ of the three to four times stronger $b\gamma$-band was also mentioned. In the ox/red-spectrum, however, $a\gamma$ appears as an elevation or a hump (figs. 7–11). After subtraction of the calculated γ-bands of *c* and *b* from the observed ox/red spectrum a band remains the peak of which lies just on this hump. The height of the band approximately coincides with the value calculated from the $a\alpha$-band. The quotient $\frac{a\gamma}{a\alpha}$ approximately attains the value 5. The calculated $a\gamma$-band has its peak at 442.5 mμ, a value in accordance with several earlier observations (34, 39, 3). Measured from the extinction value in aqua dest. the ox/red $a\alpha$-band attains an average height of 0.091 against 0.341 for *b* 427.5 mμ and 0.214 for *c* 420 mμ.

Because of the considerable distance between the γ-bands of oxidized and reduced cytochrome *a* the ox/red band has exactly the same position as the reduced band in

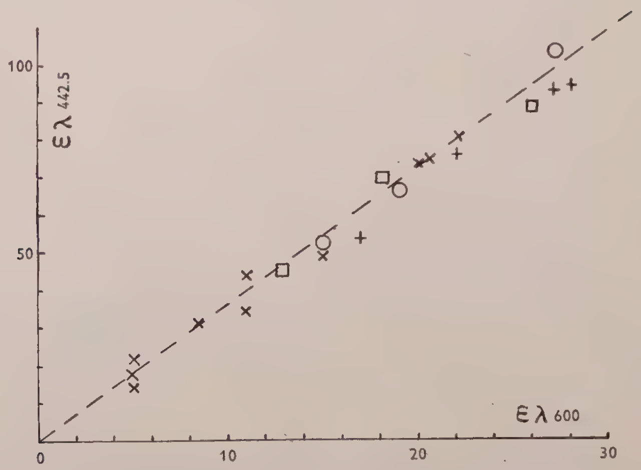

Fig. 16. Diagram showing the linear relation betweeen the α- and γ-bands of the cytochrome oxidase. Roots in: × aqua (aerated), + aqua or KCl (O_2-free), □ HCN, ○ CO.

the crude spectrum and its height is less influenced than in the case of cytochrome *c*. The relation $\frac{\gamma \text{ red crude}}{\gamma \text{ ox/red}}$ amounts to 1.5, against 2 regarding the other cytochromes. This figure is probably correct because it tallies with other calculations. The relation $\frac{\gamma}{\alpha}$ amounts to approximately 5 in the case of the cytochromes *c* and *b* (p. 102). The spectral curves of cytochrome *a* published by STRAUB (34) and WAINIO et al. (39) allow no accurate calculations. According to WARBURG, WAINIO et al. (39) and BALL et al. (3) the said quotient for cytochrome *a* is claimed to attain even higher values (towards 10). A calculation of seventy crude spectrograms of wheat roots obtained under varying conditions yielded, however, the value $\frac{442.5\text{–}460\,\text{m}\mu}{605\text{–}620\,\text{m}\mu} = 5.0$. It ought to be mentioned that this value cannot be directly compared with earlier ones because the zero line of extinction obtained in biochemical preparations has no fixed value. It coincides, however, with the recent results of KIESE (41).

According to the choice of experimental conditions (aerated and non-aerated aqua, salt solutions, HCN, CO) the height of the ox-red bands are raised or lowered but the γ- and α-bands maintain a strict linear relation as is shown by the diagram in fig. 16.

There is still some discussion as to the true position of the *a*α-band. Measurements of the ordinates at 600 and 605 mμ show a linear relation at varying heights. The quotient $\frac{\varepsilon\ 600}{\varepsilon\ 605} = \text{c. } 1.33$ supporting a propenderance of 600 mμ as the tentative extinction maximum of the *a*α-band.

No definite conclusions can be drawn from the crude spectrum as to the existence and position of an *a*β-band. In the ox/red spectrum calculated from ε anaerobical–ε aerobical no bands appear between 570 mμ and 590 mμ, the former representing the joined band of *b*α and PX 575. In about 50% of the analyzed 20 spectrograms a slight hump appeared at 590 595 mμ. The $a\,\alpha$-band at 600 605 mμ was clearly recognizable in 70% of the cases.

A real duplication of the $a\,\alpha$-band develops under the influence of cyanide. 82% of the spectrograms, calculated from ε HCN ε aqua aer., show a low peak at 585–590 mμ. It appears irrespective of the presence or the absence of oxygen. The peak at 600 mμ still persists in HCN and the new band thus represents no simple displacement. This duplication of the $a\,\alpha$-band does not appear in CO. Carbon monoxide, on the other hand, slightly broadens the band from 600 mμ towards 595 mμ. Neither in CN, nor in CO, however, is the extinction at 600–605 mμ appreciably changed as compared with the effect of simple anaerobiosis. The quotient $\frac{a\,\gamma}{a\,\alpha}$ remains approximately the same irrespectively of the mode of reduction (fig. 16).

It is commonly assumed that cyanide inactivates the cytochrome oxidase by combining with oxidized iron. The spectral behaviour is more in accord with the idea that CN competes with oxygen at the contact surface of the enzyme and thus acts similar to an aerobic anaerobiosis. This idea is supported by earlier observations in this laboratory as to the competitive effect of the oxygen pressure on the cyanide inhibition of the anion respiration (11a, p. 39).

A further effect of CN and CO is the appearance of new bands between $a\,\alpha$ and $b\,\alpha$, viz. in CN at 570-575 mμ and in CO at 575–580 mμ. As mentioned above these bands are probably related to PX 575, and not to the cytochrome oxidase. An increase of the extinction at 540 mμ is sometimes observed and some authors have ascribed it to the oxidase.

Similar to the behaviour of the $a\,\alpha$-band also the γ-band 442.5 mμ is comparatively little changed by CN and CO. The quotient $\frac{\gamma}{\alpha}$ is slightly lowered, however, from 5 to c. 4 in the case of CO. In twelve experiments with 14 mm thick root bundles spectrograms were recorded in 1. aerated aqua dest., 2. O_2-free aqua (during 1–2 hours), and 3. 0.001 m. HCN. The height of the γ-band, measured as 442.5–460 mμ in the crude spectrum, remained approximately the same under anaerobic reductions and under the influence of CN (aerobically or anaerobically), whereas the height of the α-band was slightly increased (c. 18 %) with CN resulting in a lowering of the quotient $\frac{\gamma}{\alpha}$. Unfortunately a direct comparison of CO and simple anaerobiosis suffers from the inability of CO to produce a complete reduction. It frequently attains only 50 % of the total value. On an average the quotient $\frac{\gamma}{\alpha}$ attained the value 4.7, but a few experiments yielded considerably lower values, indicating a distinct decrease of the band at 442.5 mμ.

Several authors claim a complete displacement of the $a\,\gamma$-band to c. 430 mμ under the influence of CO. A new band at 430–435 mμ was indeed observed also in the spectrum of the wheat roots, and it belongs undoubtedly to the oxidase (figs. 17, 18). The partial persistance of the main band at 442.5 mμ corroborates the conclusion as to the competitive effect of CO on oxygen, similar to what was said about CN. The results are in agreement with recent observations on purified oxidase (41).

It is worth mentioning that an extra band at 435 mμ appears also in HCN under anaerobical, sometimes also under aerobical conditions (figs. 21, 22).

Keilin and Hartree (8) claimed the existence, besides of the cytochrome oxidase, of a cytochrome *a* of deviating spectral behaviour. They build their conclusions primarily on the observation of a differentiation after the addition of CO or CN resulting in a doubling of the bands and a change in their apparent density. According to these authors *a* does not combine with the inhibitors and its bands maintain their position, whereas those of the oxidase move towards violet.

A broadening or doubling of a band under the influence of an inhibitor is no conclusive argument supporting the assumption of two separate enzymes. Such cases are frequently noticed in the literature, e.g. in the case of the peroxidase (10).

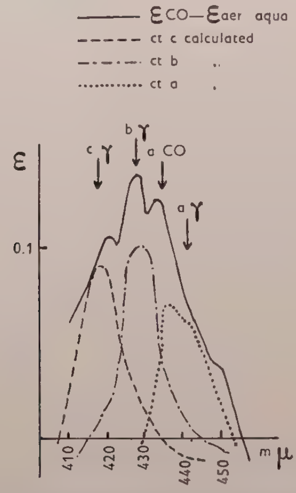

Fig. 17. Ox/red spectrum of ε CO–ε aerated aqua and its resolution in the individual bands of the cytochromes *c*, *b* and *a*.

As to the region around 450 mμ, thus close to the hypothetical second cytochrome *a*, measurements of the extinction in the spectrograms from wheat roots show that this region varies in linear relation with 442.5 mμ. The quotient $\frac{450\ \text{m}\mu}{442.5\ \text{m}\mu}$ calculated from 100 single spectrograms had the mean value 0.56, if the oxidase was reduced anaerobically, and a slightly lower value, if CO was added. Similar measurements of the γ-band of cytochrome *c* yielded the value 0.57 $\left(\frac{425\ \text{m}\mu}{417.5\ \text{m}\mu}\right)$. This is almost exactly the same value, a fact decidedly supporting the conclusion that the region 450 mμ belongs to the slope of the γ-band of the cytochrome oxidase. The appearance of an extra band at 430–435 mμ in CN and CO must be interpreted either as a doubling of the reduced γ-band of a single enzyme, or as a mixed effect of a competitive exclusion of the oxygen and of a chemical combination with the inhibitor.

The mentioned measurements of the extinction at 450 mμ show a complete covariation of this region with 442.5 mμ under conditions of complete reduction. If the crude spectrum is observed under varying conditions it must be concluded, however, that a band may appear at 450 mμ which is not directly related to the cytochrome system, but possibly corresponds to a flavoprotein. The intensity of the band varies

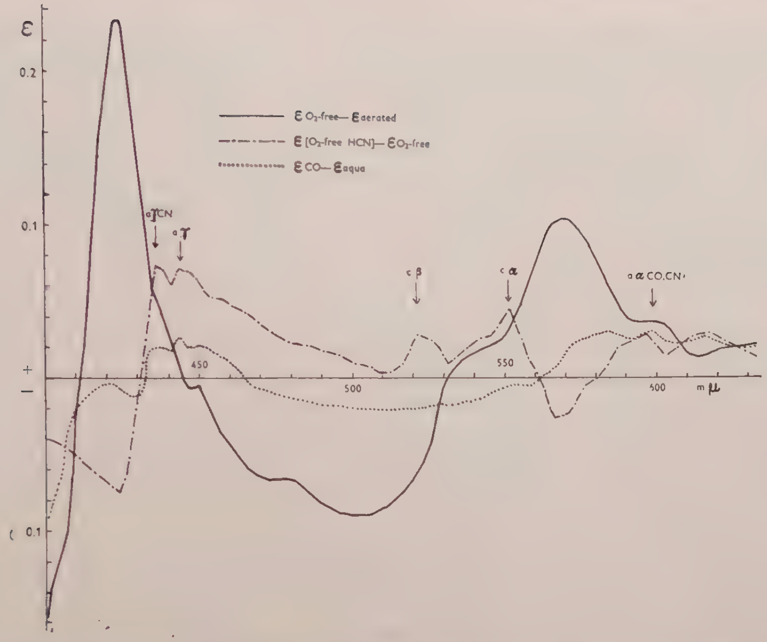

Fig. 18. Ox/red spectrum showing the complete anaerobiosis and the consecutive changes induced by HCN under anaerobical conditions. The record of ε CO–ε aqua aerated illustrates the similarity between the CN- and CO-modifications of the *a* γ-band and the displacement of *a* α towards 595 mμ.

considerably with the season, is frequently very low, but can occasionally rise to the same intensity as the PX 480 band, the intensity of which on the contrary is fairly constant. The extinction of the band PX 450 does not vary much in the course of single experiments but it runs more or less in opposite direction to that of the cytochrome bands. It is high in aqua dest. and low in CN or under anaerobical conditions. If the roots are treated with salt solutions (0.05 m. KCl) the peak of the band moves from 450 to 447.5 mμ.

Because the intensity of the *a* γ-band has c. 50 % of its maximum density at 450 mμ (see above) the separate study of PX 450 encounters special difficulties, but it seems appropriate to assume that PX 450 behaves much in the same way as a flavoprotein would do if reduced, viz. going over to a leuco-substance. PX 450 is intensified and broadened under the influence of fluoride (see below).

The response of the cytochrome system to urethane, malonate, fumarate and fluoride

Urethane. According to KEILIN and HARTREE (8) urethane inhibits the reduction of cytochromes *c* and *a* and the oxidation of *b*. As already mentioned this substance is thus a useful tool for the optical isolation of cytochrome *b*. Urethane inhibits the transference of electrons from cytochrome *b* to oxygen, viz. probably the oxidation of *b* by cytochrome *c*. The linkage to the dehydrogenase system is on the other hand not inhibited. Urethane thus isolates cytochrome *b* from the rest of the cytochrome system. Urethane alone acts slightly reducing on cytochrome *c*, but not on *b*. After addition of HCN therefore the reduction of cytochrome *b* dominates, whereas the additional reduction of *c* is comparatively small (figs. 7, 8). Because cytochrome *a* is reduced in the presence of urethane this substance does obviously not inhibit the linkage between *a* and *c*.

After an exchange of urethane + HCN with fumarate + HCN cytochromes *b* and *c* are both oxidized "the reversed way", viz. an anaerobical oxidation at still reduced cytochrome *a* (fig. 8).

Malonate. Previous studies of the effect of this inhibitor of the succinate dehydrogenase system were not successful (13) and it was concluded that this system may probably be absent from the roots. This negative result was primarily based on the observation that malonate did not appreciably inhibit the respiration. The active salt absorption was retarded with malonate, but the effect was interpreted as a competitive one, similar to the effects of malate, succinate etc. A study of the literature on the succinate dehydrogenase system, however, has later shown that its presence in plant tissues is not so easy to demonstrate (cf. 24). The discovery of a complete cytochrome system in the roots now opens the possibility of taking the question under renewed consideration.

Recently SLATER (31) called attention to a probable participation of two separate dehydrogenase systems, alternatingly supplying the cytochrome system with electrons, viz. the succinate dehydrogenase system (in the following called DH I), and a system operating by means of cozymase and a flavoprotein (diaphorase), in the following called DH II. According to SLATER both systems are figured to co-operate with a hypothetical factor serving as a collector of cytochrome *c*, the electrons from here passing over to cytochrome *a* (30).

In the experiments with malonate it is important to secure a rapid absorption of undissociated molecules of the acid. The malonate is thus held as near to the lowest tolerable pH, viz. 3, as possible. Mostly a 0.1 m. solution of pH 3.3 was used. The effect of malonate on the absorption spectrum resembles the effect of salts. These promote the oxidation of the cytochromes, primarily *b* and *a* (see below). Malonate alone induces a deep depression of the oxidation-reduction level held in aerated aqua destillata (figs. 10, 19) but the depression is primarily restricted to cytochrome *b*. On spectrograms recorded with an interval of a few minutes one can see the decrease of the reduction (increase of the oxidation) begin more at the side of cytochrome *c* and then rapidly turn over to cytochrome *b* (fig. 19). The final stage is attained in about 15 minutes or the average time it takes for a substance to penetrate the bulk of the root tissue (see 13). Simultaneously with the oxidation of cytochrome *b* cytochrome *c* is partly reduced. The general result of a treatment with malonate is thus an inhibition of the reduction of cytochrome *b* and a partial acceleration of the reduction of cytochrome *c*. The reduction of cytochrome *b* is however not completely inhibited if the pH is held above 3. After removal of the oxygen the reduced band of cytochrome *b* appears at *c*. 425 mμ (fig. 9), whereas the increase of the reduced band of *c* is less marked because this cytochrome was already partly reduced in aerated malonate. At intensive malonate inhibition (pH below 3; see fig. 19) the DH I system is almost completely paralyzed.

The considerable retardation of the DH I system in malonate is reflected in the decrease of the height of the reduced band at 425 mμ as compared with ist normal height. It amounts only to 50–75% of the normal. At prolonged treatment with malonate + HCN the reduced band of cytochrome *b* decreases still more.

The results with malonate strongly support the assumption of succinate dehydrogenase as the main reducing system linked to cytochrome *b*. Also pyrophosphate acts similarily (cf. 9). The previously observed maintenance of a nearly full intensity of the aerobic respiration in malonate demonstrates the presence of still another dehydrogenase system. The returning reduction of *c* in malonate indicates the connection of this DH II system with cytochrome *c*. The oxidation may then proceed over cytochrome *a* which remains intact in malonate. It may be tentatively assumed that the DH II system is identical with a cozymase system of similar pattern as that proposed by SLATER. The presence of a system composed by cozymase and flavoproteins and additional compounds in wheat roots was recently assumed by WAYGOOD (40). The presence in the roots of a band PX 450, coinciding with the main absorption band of flavoproteins (36) was already emphasized. The presence of two alternating path-ways of reduction of the cytochrome system opens a possibility to explain a number of earlier observations, as will be more fully discussed on later pages.

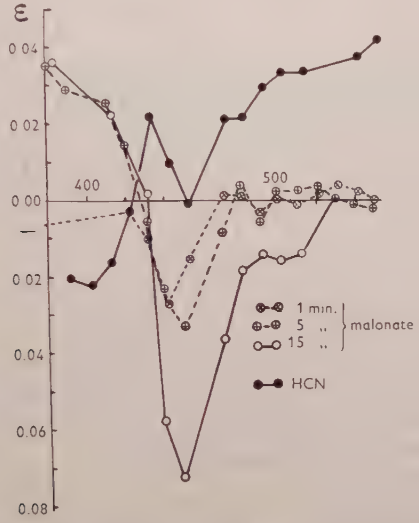

Fig. 19. Ox/red spectrum of a 10 mm thick root bundle showing the increasing oxidation of predominately cytochrome *b* in 0.1 m. malonic acid (pH 2.8). In this case the inhibition of DH I is so intensive that the following addition of HCN produces only a very incomplete reduction of cytochrome *b* whereas *c* is visibly reduced. The pH is unphysiologically low.

Fumarate. The retarding or inhibiting effect of malonate on cytochrome *b* is reversed by fumarate (0.1–0.05 m. at pH 3.3). It can easily be studied if malonate + HCN is exchanged for fumarate + HCN and the reversion proceeds both aerobically and anaerobically. As the cytochrome oxidase is blocked in the presence of HCN the oxidation comes from behind, viz. electrons are moving from cytochrome *b* to the fumarate. The equilibrium between cytochrome *b* and the DH I system is thus reversible, as also shown by SLATER (31). In the roots, however, also cytochrome *c* is oxidized by fumarate, a fact demonstrating a reversible oxidation-reduction balance between the cytochromes *b* and *c*. The predominating oxidation of *b* by fumarate is also shown without preceding treatment with malonate (see fig. 20).

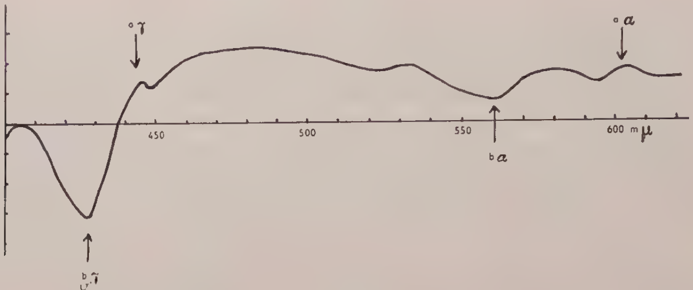

Fig. 20. Ox/red spectrum illustrating the strong oxidation (negative bands at 427.5 and 562 mμ) of primarily cytochrome *b* in fumarate at completely inhibited oxidase (reduction bands of *a* are visible at 445 and 600 mμ). The conditions are aerobical and the spectrum is calculated from ε 0.1 m. fumarate (pH 3.2) + HCN–ε HCN (aerobic solution).

Because the cytochrome oxidase remains blocked by HCN no respiratory oxidation *via* DH I occurs, however.

Table 1

Behaviour of the cytochrome system and the respiration in 0.1 m. fumarate + 0.0001 m. HCN, pH 3.2

Consumed O_2 (μmol/1 h 10 mg)		Inhibited anion respiration	Height of bands in the ox/red spectrum		
			c γ	*b* γ	*a* γ
In aqua dest. (aerated) . .	3.17	—	—	—	—
In 10^{-4} HCN	2.38	0.79	+0.140	+0.320	+0.132
In 10^{-4} m. HCN + fumarate	2.20	0.97	−0.120	±0.0	+0.130

This is shown from the experiment quoted in table 1. Fumarate turns over the cytochromes *c* and *b* in a strongly oxidized state but the DH I (or anion) respiration remains blocked by the completely reduced cytochrome oxidase.

That part of the total respiration which is not inhibited by cyanide, CO, or azide, viz. the ground respiration, amounted to 70% in the experiment quoted in table 1. This respiration is not conducted by the cytochrome oxidase but may be identical with the ascorbic acid system described by Waygood (see below). As cozymase and flavoprotein are figured as links in this non-cyanide sensitive respiration (40) and, according to the previous discussion, a similar system (DH II) is probably also linked to the cytochrome system, one here discerns a possible way of combination between the two systems.

Fluoride. A still more intensive retardation of the reduction of cytochrome *b* is executed by a solution of 0.02 m. NaF at pH 3.3 (figs. 11, 12). As c. 50% of cytochrome *b* is reduced in aerated distilled water and the oxidizing effect of *a* is not diminished by fluoride the far reaching oxidation, probably very near to the bottom level, points to a very effective inhibition of the DH I system. The inhibition is probably quite different from that caused by malonate. Fluoride is known as an inhibitor of certain links of the chain of glycolysis leading over to pyruvic acid.

Fluoride thus probably retards the formation of succinic acid and puts the DH I system out of action but an additional direct inhibition of a factor between *b* and DH I cannot be excluded.

Previous experimental observations revealed no appreciable retardation of the aerobic respiration with fluoride, but a clear inhibiting effect on the salt absorption and on the growth (13). If now, according to the spectroscopic observations, fluoride switches off cytochrome *b* it is to be supposed that the DH II system takes over the delivery of electrons and protons to the cytochrome oxidase. The criterion of the appropriateness of this supposition is the cyanide sensitivity of one fraction of the aerobic respiration in fluoride (see table 2).

Table 2

The response on fluoride (0.01 m. NaF at pH 3.3 + 0.004 m. KCl during 15 minutes)

Medium (aerated)	O_2-consumption in µmol/ 1 h 10 mg	O_2-consumption in cyanide	Cl-absorption	Extinction		
				c γ	*b* γ	*a* γ
aqua dest.	2.7	—	—	0	0	0
fluoride + chloride	3.4	2.5	trace	−0.028	−0.110	−0.042

The fraction of the aerobic respiration inhibited by cyanide amounts to 3.4–2.5 = 0.9 µmol O_2 or about the same as in the normal anion respiration (12). No chloride anions were absorbed in this experiment. Unpublished experiments show that at weaker fluoride inhibition (0.01 m. NaF at pH 7) chloride may be actively absorbed.

Because the anion respiration is not increased above the normal level the violent increase of the oxidation of cytochrome *b* cannot be interpreted as a stimulated activity, similar to the rising anion respiration in salt solutions, but only as a retarded reduction. The oxidation of *b* in fluoride considerably exceeds the oxidation in KCl (maximum anion respiration). This excessive oxidation reflects the decreasing reduction from DH I. The cyanide fraction of the respiration now runs over DH II, cytochromes *c* and *a*, but it is not capable of transporting salts, because this process requires the co-operation of cytochromes *b* and *a* (see below). At lower concentrations of fluoride, absorbed by the roots, e.g. at higher pH-values (cf. 13), the retardation of DH I is not gone so far that the salt transport is severely affected (cf. fig. 21). The growth processes are even more sensitive (13). A remarkable thing regarding fluoride is its insignificant effect on the structure and streaming of the protoplasm and on the surface potential of the roots, whereas an abnormal exudation of organic products begins already at low concentrations of the inhibitor. This indulgent effect on the protoplasm is certainly due to the inhibition of the production of organic acids, the abnormal accumulation of which, as in malonate, is strongly poisonous.

Still another side of the fluoride problem is its unparalleled effect on the pigments PX 450 and 480. The former shows a broadening of the band and an extension towards 460 mµ. The latter disappeared in one experiment completely after the treatment with 0.02 m. fluoride at pH 3.3. It remains to be investigated if the response of PX 450 is causally related to the acceleration of the DH II system. A similar effect appears after treatment with pyruvate.

Owing to the switching off of cytochrome *b* in fluoride solutions a following anaerobiosis or the addition of HCN has very little effect on this part of the spectrum, the cytochrome *b* remaining largely oxidized whereas *c* and *a* are visibly reduced (fig. 11). At lower fluoride concentrations the inhibition of *b* is incomplete and a following anaerobiosis consequently reduces also this enzyme.

Fluoride gives a characteristic spectrum with *peroxidase*. Strong bands appear at 403–404 mμ and 612 mμ (Keilin and Hartree, 10). The roots show a prominent band at 402.5 in fluoride and in a few cases also a band at 612–620 mμ was observed.

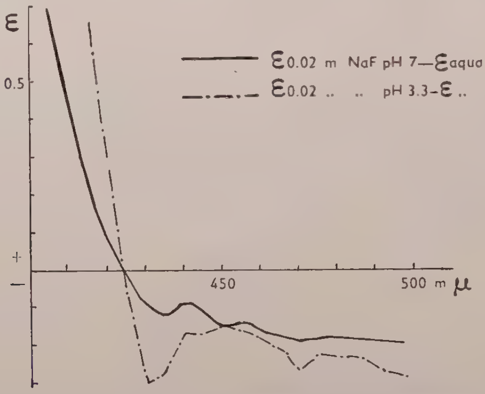

Fig. 21. The increasing effect of fluoride at lowering of pH. Increasing oxidation of primarily cytochrome *b*.

The presence of peroxidase in the roots was supposed in previous investigations, too (20). Very little is known about the biochemical tasks of peroxidase. It is most probably not co-operating with the cytochrome system, but it may possibly in some way participate in the ground respiration (20, 40).

The response of the cytochrome system to salts.

It was previously shown that the presence of neutral salts (electrolytes) in the medium induces sinking extinction values of the cytochromes *b* and *a*, whereas cytochrome *c* is less influenced (18). The oxidation-reduction balance of the cytochromes *a* and *b* is thus displaced to the side of oxidation. Solutions of low molecular organic salts (malate, succinate) have a similar effect. It was shown that the effect of salts is non-specific but confined to the anions (11, 11a). The effect is exerted by anions present in the immediate surroundings of the cytochrome system. The anions must be freely movable.

In order to secure a maximal availability of salt ions the experiments were conducted with 0.05 to 0.1 m. solutions. Effects were however obtained also in very dilute solutions, 0.002 to 0.004 m.

Previous experiments illustrated the rapid primary adsorption of the salt ions to the surface of the root (11, 11a). Already in dilute solutions the adsorbed salt ions form an approximately saturated film in the boundary between the medium and the living protoplasm. For the undisturbed continuous supply of salts to the active mechanism an intensive stirring of the medium is frequently as effective as a rise of the concentration (14). Some roots may, however, be coated by wall mucilage or the salts may otherwise be hindered to get a rapid access to the roots and it is therefore not surprising that in certain experiments the effect of a rise of the concentration is almost nil whereas in other experiments positive effects are shown (14).

The experiments were carried out in the following way. After evacuation of the root bundle (see p. 99) it was exposed to a rapidly flowing aerated aqua dest. of

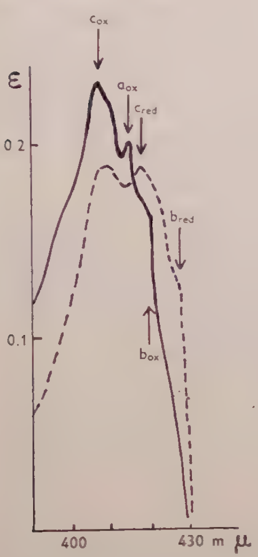

Fig. 22.

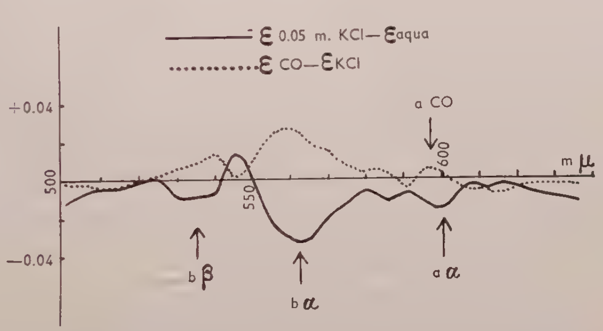

Fig. 23.

Fig. 22. The crude spectrum of roots in aerated aqua dest. (------) and in aerated 0.05 m. KCl (———). Owing to the c. 50 % reduction of cytochromes *c* and *b* in aerated aqua (see table 3) the reduced bands are conceivable at 417.5 and 427.5 mμ respectively. In KCl appear the bands of oxidized *c* and *b* at 407.5 and 420 mμ respectively, as well as the oxidized band of the cytochrome oxidase at 415 mμ. — Fig. 23. Ox/red spectrum showing the strong oxidation of cytochrome *b* and the cytochrome oxidase in 0.05 m. KCl (↑ – negative bands) and the reduction in CO. The *a*α-band is slightly moved to the left under the influence of CO.

constant temperature (mostly 19°C.). After some time (15–30 minutes) a spectrogram was recorded, showing the "normal" oxidation-reduction level of the cytochromes. The distilled water is then exchanged for an aerated salt solution, equally streaming. After the end of the start period (c. 15 minutes; see below) a second spectrogram is recorded, showing the increasing oxidation of the cytochromes. The flow of the salt solution is then stopped. The remaining oxygen is soon consumed and a completely reduced spectrum may be recorded in 1/2 to 1 hour. Finally aerated or O_2-free HCN or CO is conducted through the tube and a fourth record taken.

After calculation of the extinction values crude curves are plotted and ox/red curves are constructed, e.g. ε KCl–ε aqua, ε O_2-free–ε KCl, etc. (see figs. 22–24). The participation of the single cytochromes is calculated according to the scheme on p. 102. The height of the bands, positive or negative, reveals the decrease or increase of the oxidation/reduction balance.

Table 3 gives the average values, calculated from six experimental series.

Table 3

The effect of salts on the oxidation-reduction balance of the cytochromes. Root bundle 14 mm

Height of the bands in ε	*c* γ	% ox.	*b* γ	% ox.	*a* γ	% ox.
1. Completely reduced (O_2-free)	+0.241	0	+0.341	0	+0.091	0
2. Aerated aqua (desalted roots)	±0.0	60	±0.0	61	±0.0	48
3. 0.05 m. KCl (19° C.).............	−0·013	64	−0.130	84	−0.038	69
4. Calculated zero reduction (from NaF and malonate series)	−0.140	100	−0.217	100	−0.097	100
Total ε...........................	0.354		0.558		0.188	

The values of zero reduction were calculated from series with fluoride (see p. 120). Similar values were obtained with 10^{-4} ascorbic acid, a substance obviously isolating cytochrome *a* from cytochrome *c*. With malonate only c. 50 % of the maximal decrease below the level of distilled (aerated) water was obtained (p. 118).

The experiments quoted in table 3 corroborate the previous results (17, 18) as to the indifference of cytochrome *c* to the presence or absence of salts. The close cooperation of *b* and *a* in the response to salts is illustrated by the approximately constant relation $\frac{b}{a}$. After the addition of KCl ox/red is increased with the factor c. 3 in respect of both enzymes.

The response of the cytochromes *a* and *b* on salts is shown not only by the oxidized γ-bands in the crude spectrum (fig. 22) and the negative bands at 442.5 (see also fig. 5) and 427.5 mμ in the ox/red spectrum but also by the appearance of negative bands at 560–565 (*b*α) and 600–605 (*a*α) in the ox/red spectrum (fig. 23).

Regarding the question of cyt. *a* as the "enzyme of anion respiration" (18) the new results underline the key position of *a*, because no real anion respiration, viz. a respiration accompanied by an active anion transport, occurs if cytochrome *a* is put out of action. The experiments with fumarate are here elucidating. If fumarate is given together with HCN *b* (and *c*) is oxidized; cytochrome *b* thus remains active. But the anion respiration and the transport of salts is completely inhibited because cytochrome *a* is blocked by the cyanide.

Other experiments now show that no real anion respiration occurs if *b* is out of action but cytochrome oxidase still active. This case is realized after treatment with fluoride, a substance intercepting cytochrome *b* from the preceding stages of intermediate metabolism. The cytochrome oxidase exerts its influence on *b* (*via c*) and holds it completely oxidized, but the transport of electrons is slowed down near to the zero level between *b* and *c*. Between *c* and *a*, however, an intensive transference of electrons goes on. But this transference of electrons between *a* and *c* is unable to accomplish a real salt accumulation. The electronic interrelations between *c* and *b* are obviously a necessary condition for this task. In fluoride a cyanide sensitive respiration continues, but it is not accompanied by salt accumulation.

Similar effects were observed with 2,4-dinitrophenol (DNP).

DNP is a strong inhibitor of all kinds of phosphorylation (7, 35). This substance severely disturbs the normal course of respiration (see fig. 25). At concentrations

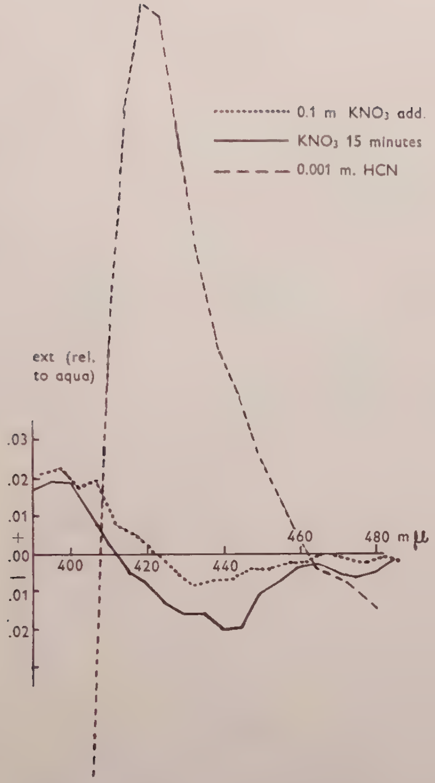

Fig. 24. The increasing oxidation of the cytochromes in 0.1 m. KNO_3 as compared with aerated aqua dest. The first spectrogram was recorded c. 30–60 seconds after the change to salt solution.

rising from 10^{-6} m. DNP (pH c. 5) the respiration first rises above the normal value, then slowly sinks below this value. A considerable fraction of this respiration is inhibited by cyanide (33, 27). The active absorption of salts, however, declines more rapidly than the decrease of this fraction (see fig. 25).

The results indicate that the cytochrome system is still operating but has partially or completely lost its power of salt accumulation. An explanation near at hand is a disorder of the system under the influence of DNP (33). Robertson et al. offer a more complicated explanation (27). They venture the hypothesis that phosphorylation processes, including the high energy phosphate metabolism, directly participate in the active transport of salts. The idea of high energy phosphates participating in the transportation of ions was originally adopted in purpose of explaining the high values of Q an/O_2 $\left(\frac{\text{absorbed anions}}{\text{consumed } O_2}\right)$ in special animal tissues. Regarding plants values above the theoretical limit 4 (see 26) are not known (26, 12). There is consequently yet no need to search for complimentary processes besides of the main electronic mechanism (11a, 15; see below). An analysis of the spectral response to DNP corroborates the previous explanation implying a partial disorganization of the cytochrome system.

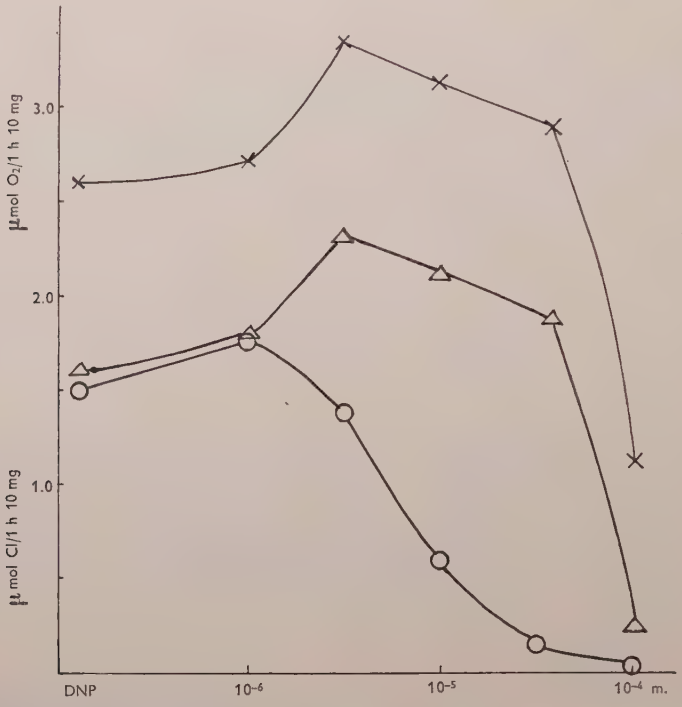

Fig. 25. Diagrammatic representation of an experimental series with 2,4-dinitrophenol. × —— × the total respiration (as O_2-consumption), △——△ the cytochrome respiration (total minus ground respiration), ○——○ the absorption of chloride from 0.0005 m. KCl. Experiments with intact plants in circulation vessels (12).

The effect of DNP on the anion respiration was studied by means of the combined electro-chemical and chemical technique elaborated for the investigation of the time course of salt absorption (14). The absorption of Cl from 0.0005 m. KCl was determined electrometrically and was also continuously recorded from the decrease in electric conductivity of the medium.

DNP was added as neutral solution but the pH sinks to c. 5 in the course of the experiments (14; on the effect of pH on the absorption of DNP see STENLID 33). The respiration was determined by means of the WINKLER method. The cyanide sensitive fraction was determined after the addition of 0.001 m. HCN.

The results of three series are plotted in fig. 25. The normal anion respiration is slightly stimulated in 10^{-6} DNP but at higher concentrations the curves for cytochrome respiration and Cl-absorption separate, the former rising to a maximum at $3 \cdot 10^{-6}$, the latter rapidly sinking. An inhibition of the cytochrome respiration begins at concentrations above $3 \cdot 10^{-5}$ m.

Observations of the cytochrome spectrum now show that the reduction of cytochrome *b* during anaerobiosis or in HCN is markedly inhibited if the roots are pretreated with 10^{-5} m. DNP during 1–2 hours, whereas *c* and *a* are normally reduced. Another characteristic feature of the spectrum after DNP treatment is a rise of the band PX 450. The spectral behaviour of the cytochrome system thus corroborates the assumption that the normal co-operation of *a*, *c*, and *b* is disturbed and the latter partially or completely isolated from the dehydrogenase systems. The picture reminds of that obtained with fluoride inasmuch as *a* and *c* apparently continue their work and now maintain a cytochrome respiration fed by DH II alone. This respiration is incapable of accomplishing a real salt accumulation.

The crude spectrum of roots treated with DNP reveals a pit at 442.5 mμ because the cytochrome oxidase is largely oxidised and the band thus moved to c. 415 mμ ($a\gamma$ ox). PX 450 now alone dominates the region 440–460 mμ. After reduction the pit at 442.5 disappears and $a\gamma$ red + PX 450 together form a more or less straight line rising towards $b\gamma$. PX 450 thus grows inversely to $a\gamma$ red, viz. parallel with the oxidation of the cytochrome oxidase. At intensive activation of the cytochrome system, e.g. in KCl solutions, PX 450 decreases and its peak moves 2.5 mμ towards violet. The oxidized bands of cytochromes *a* and *b* are observed in the crude spectrum at 412.5–415 mμ and 420 mμ respectively. The presence of a certain amount of reduced cytochrome *b* is shown by the presence of bands at 535 and 560 mμ.

The *non-specific effect of salt ions* on the anion respiration was demonstrated in experiments with different salts, e.g. KCl, KNO_3, $Ca(NO_3)_2$, sodium or potassium malate and succinate. An experiment with KNO_3 is shown in fig. 24.

According to the *theory of anion respiration* freely movable anions counterbalance the electric tensions arising from the movement of electrons through the cytochrome system (11a, 15). The absence of movable anions acts as a brake on the activity of the system, comparable with the effect of a competitive inhibitor. The situation is in principle the same as in the case of an electric battery, if the outer circuit is regulated by the conductivity of an electrolyte.

The spectrograms show that 20–22 % of that quantity of reduced cytochrome *a* and *b* which is present if the medium is aerated water is carried over in the oxidized state if the medium is changed to a salt solution. Previous investigations and unpublished determinations have shown that desalted roots hold organic acids, primarily malate, the anions of which may participate in an idling anion respiration (12). It was calculated that these "native anions" share the activity of the cytochrome system with the salt anions coming from the medium. The native anions dispose of c. 50 % of the total activity of the cytochrome system.

These findings are in good agreement with the results computed in table 3. Desalted roots show an oxidation of 48–52 % of the cytochromes *a* and *b* respectively. After the addition of salts the oxidation rises to 69–84 % respectively. The oxidation-reduction balance now corresponds to a maximum power of the system. The relation $\frac{\text{oxidized}}{\text{reduced}}$ amounts to c. 2 for cytochrome *a* and c. 5 for *b*, whereas the balance of *c*, which remains only little influenced by salt ions, amounts to c. 2.

At complete absence of movable anions the cytochromes *a* and *b* would presumably be fully reduced. Because it is practically impossible to remove all organic acids from the roots, even if most of the salts can be removed, this situation will never be realized as far as roots are concerned, but a considerable reduction of the quantity is attained at prolonged treatment with slightly acid water (cf. 12 and unpublished experiments).

The co-variation of 1. the oxidation-reduction balance of the cytochromes (measured as the height of the reduced bands), 2. the respiration (O_2-consumption) and 3. the Cl-absorption from KCl was more closely followed in two experimental series plotted in figs. 26, 27. Fig. 26 shows the relation between the oxidation-reduction balance of the three cytochromes and the quantity absorbed chloride anions. In fig. 27 the O_2-consumption on the abscissa refers to the anion respiration, viz. that fraction of the total respiration which is inhibited by cyanide. The ground respiration amounted to c. 1.25 µmol O_2/1h 10 mg (dry weight). If no salt ions are absorbed from the outside, only native ions transported (see above), the anion respiration amounts to 0.90 µmol. O_2. A rising absorption of chloride from the medium is accompanied by a rise of the anion respiration. Simultaneously also the extinction value of *a*α decreases. The relation between the quantity oxidized cytochrome and the quantity consumed oxygen is approximately linear.

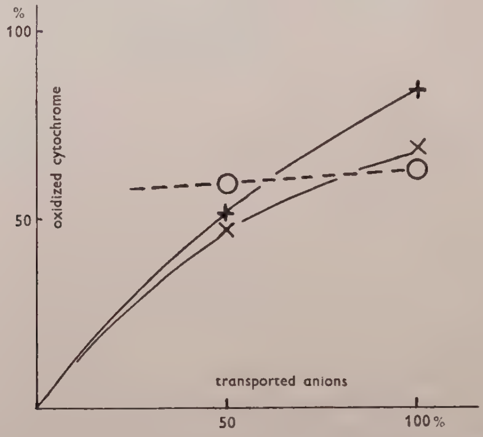

Fig. 26. Diagram of one experiment with simultaneous determination of the quantity absorbed chloride and the oxidation-reduction balance of the cytochromes. The spectrum was recorded during the passage of the salt solution (0.004 m.) through the recipient with the roots. ×——× cytochrome *a*, +——+ cytochrome *b*, ○---○ cytochrome *c*. The percentage oxidized refers to the total quantity present.

The causal relation between the transport of salts and the anion respiration is further illustrated by spectral records of the time course of the increasing oxidation of the cytochromes. One of these series is plotted in fig. 28. Records were taken of the region 410–450 mμ in intervals of 2.5 mμ The recording lasted 2½ minutes and the spectrogram was immediately repeated. After the first spectrogram a 0.05 m. KCl solution was introduced. The extinction was measured at 417.5 (*c*), 425 (*b*), and 442.5 (*a*) mμ. The curves show, as expected, that the oxidation-reduction balance of *c* only varies unspecifically around the start value (see also fig. 26). The extinction of the reduced bands of *a* and *b* falls uniformly along a concave curve ending asymptotically after 6½–12 minutes. The half-time of the process amounts to c. 4 minutes.

Owing to experimental difficulties a continuous control of the chloride absorption could not be effected in this experiment. The author's extensive experience of the behaviour of wheat roots, however, has shown that they behave very constantly if cultivated under constant conditions. It may therefore seem appropriate to compare these results with the time curves from earlier experiments on the Cl-absorption (12). The absorption of anions starts almost immediately after the contact of the roots with a salt solution, if desalted roots are used. If isolated roots are used the intensity of the absorption per unit time attains its maximum in 10–20 minutes (20° C.). In experiments with very diluted solutions the full speed of absorption was attained after 30–35 minutes (14). In this case intact seedlings were investigated, a circumstance which probably delays the attainment of an equilibrium. The start period of 10–20 minutes is quite adequate for comparison with the present results. Other experiments have shown (16) that also the non-metabolical exchange of salt ions between the medium and the roots is completed in c. 12 minutes. The previous results as to the time course of the active salt absorption and the present results as to the adjustment of the oxidation-reduction balance to the presence of salts are thus in fairly good agreement.

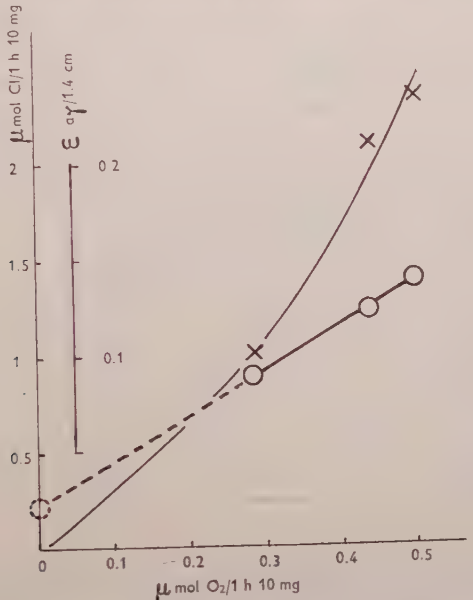

Fig. 27. Diagrammatic representation of one experiment with simultaneous determination of 1. the respiration (O_2-consumption), 2. the chloride absorption (from 0.004 m. KCl) and 3. the height of the negative a γ-band, determined simultaneously with the flowing of the sample through the recipient. ×—× chloride absorption, ○—○ height of $-a\gamma$ (the height below the zero line in aerated aqua dest.).

Because the roots have a diameter of only 0.5 mm a time course of 4–10 minutes is a very strong argument in favour of the conclusion that the cytochrome system is not concentrated in the surface of the roots only but is uniformly distributed over the bulk of the tissue, at least comprising the total cortex or c. 90 % of the root volume. Previous experiments dealing with the effect of various inhibitors on the bleeding (13) yielded similar time values. It is known that these inhibitors exert their full influence only after they have penetrated the whole root tissue. The salt absorption starts with an ion exchange process (= the primary non-metabolic phase of absorption) comprising not only the surface layer but also the inner surfaces, viz. primarily the individual cell membranes. From here the anions are caught by the exchange mechanism anions ⇌ electrons operating at the cytochrome system of

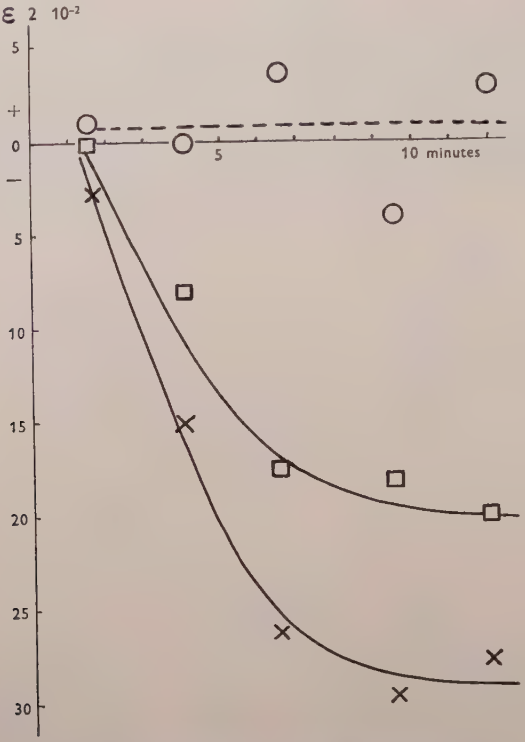

Fig. 28. The time-course of the changing oxidation-reduction balance of the cytochromes after the switching from aqua dest. to 0.05 m. KCl. The height of the γ-bands is given on the ordinate. □——□ cytochrome *a*, ×——× cytochrome *b*, ○——○ cytochrome *c*.

each cell (15, 18) and exert their accelerating influence on the oxidation power of the system resulting in rising anion respiration. The time course of the total process thus includes 1. the non-metabolical adsorptive forwarding of the salt ions to the living surfaces of the cells of the whole tissue, and 2. the biochemical activation of the cytochrome system. The latter on its side is also dependent on a number of elementary processes, e.g. the supply of sugar as raw material and the whole chain of desmolysis to be run through before the material is handed over to the cytochrome system.

The localization of the cytochrome system in the cell.

Several authors have recently advanced the opinion that the cytochrome oxidase is localized in the mitochondria (22, 32). The experimental back-ground of these assumptions is the assumed identity of certain fractions of tissue homogenates with mitochondria in living cells. With regard to plant tissues mitochondria are cytologically identified only in special cells, and it is still very questionable if such structures play a rôle as individual carriers of enzyme systems in all plant cells. After mechanical disintegration of a plant tissue many things may happen, e.g. the coating

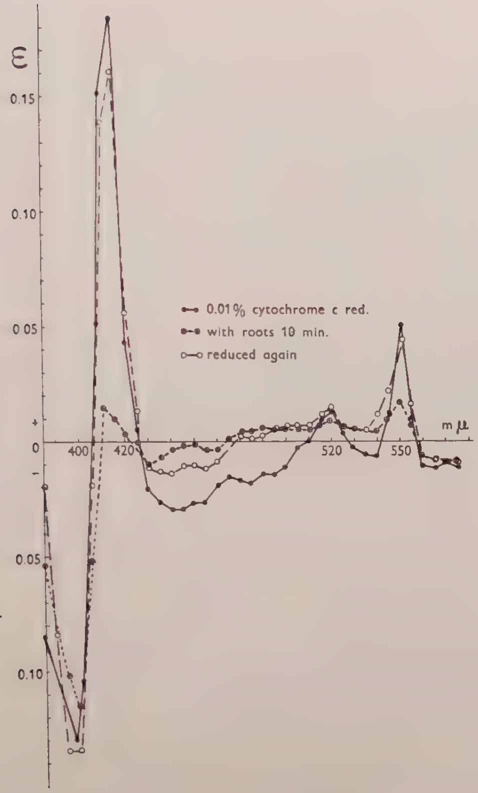

Fig. 29. Spectrographic control of one experiment as to the presence of cytochrome oxidase in the surface of roots. See the text.

of small droplets of protoplasm with a film of material characteristic for the normal surface layer. It is to be supposed that several enzyme systems are attached to the outer and inner surface of the protoplasm. After disintegration these systems will be recovered on droplets originally derived from the internal protoplasm, and so on. The protoplasm of most young tissues, e.g. the active parts of the roots, is continuously streaming and no mitochondrial structure is visible. The only solid place in such cells is actually the surface layer. This living wall is probably organized as a complex multimolecular layer provided with certain metabolic qualities (11, 15, 16). It is likely to assume that the cytochrome system known to stick very closely to the living structure is attached to this surface layer (or/and to the vacuole membrane). Its close linkage to the process of salt transport supports this idea. One of the fundamental results with regard to the movements of salts is the fact that these are only to a very small extent passively transported through the cell surface. The passive leakage of once accumulated salts from the cell proceeds very slowly (11, 15, 26). An adsorption layer of salts is on the other hand coating the cell surface. From this layer the cytochrome system fetches its anions. The localization of the cytochrome system close to the surface would thus appear as a feasible assumption. The localization of the cytochromes in the cell cannot yet be spectroscopically investigated. But cytochromes in the cell surface would undoubtedly coat the epidermis layer of the roots with enough of oxidase to react with added reduced cytochrome *c*. The following experiments try to answer this question.

0.6 mg cytochrome *c* was dissolved in 10 cc phosphate buffer (pH 6.5). The cytochrome was reduced with 0.001 m. dithionite and afterwards aerated. The spectrum of the completely reduced cytochrome was recorded in a 10 mm cuvette (fig. 29). 137 mg roots (fresh weight) were then slowly stirred in the solution during 15 minutes at 19°C. After removal of the roots the spectrum was again recorded. It shows a marked reduction of the height of the reduced bands (see fig. 29), indicating that cytochrome oxidase is present in the physical surface of the roots. As some cytochrome may have been absorbed by the roots, however, fresh dithionite was added to the solution after removal of the roots. As shown from this third spectrum (see fig. 29) only a few percent of the original cytochrome *c* has disappeared. The experiment may now be continued after convenience. It was observed that the power of cytochrome oxidation slowly declines, probably according to the adsorption of disorganization products of cytochrome *c* on the root surface. That such products are developed is seen from the spectrum.

137 mg fresh roots show an anion respiration of 1.2 μmol O_2/1h at 19° C. Because the reduction of one mol O_2 to 2 H_2O requires 4 electrons and 4 protons this respiration corresponds to the oxidation of 4.8 μmol cytochrome. In the given example only 0.038 μmol cytochrome *c* were oxidized, corresponding to c. $\frac{1}{125}$ of the anion respiration. Repeated experiments yielded similar values.

A solution containing 0.6 mg cytochrome per 10 cc is about 10 times more concentrated than roots in respect of cytochrome *c* and it may consequently be expected that the observed oxidation reflects the activity of the cytochrome oxidase present in the living surface. A rough calculation of the total internal surface of the cortex cells results in a value about 100–125 times larger than the surface of the epidermis. The biochemical experiment thus corroborates the assumption of a localization of the cytochrome system in or close to the surface of the root cells.

The time course of cyanide inhibition

The sensitivity of the cytochrome oxidase to cyanide is extremely high. A beginning reduction is observed in 10^{-7} m. HCN. The time course is considerably more rapid than in the case of salts or at the absorption of such inhibitors as fluoride, iodine acetate and malonate (cf. 13). The half-time only amounts to c. 30 sec. (see fig. 30). The rapid penetration of HCN exceeds that of any other known substance with the exception of low molecular alcohols. It may possibly depend on small dimensions of the molecule and interrelations with lipoids but another explanation is an accelerated surface activity induced by the specific adsorption of HCN to a cytochrome oxidase layer in the surface of the cells. In this case it would not be necessary for the HCN molecules to traverse the cells, only to slide along the interfaces between the single cells, thus a sort of surface gliding at the boundary between the cell walls and the living protoplasm. Unpublished new experiments, however, show an approximately equally rapid penetration of O_2.

Owing to our previous discussion (p. 115) CN probably combines with the cytochrome oxidase in two ways: 1. in a competitive adsorption, thus preventing the oxy-

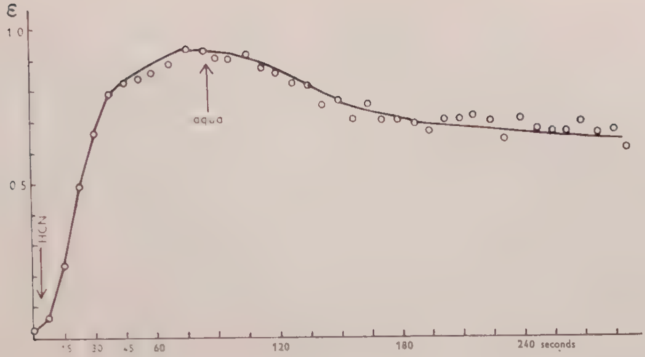

Fig. 30. The time course of the reduction of the cytochrome oxidase in the roots after the addition of 0.001 m. HCN. The line 445 mμ was continuously recorded. The washing out of the cyanide proceeds much slower.

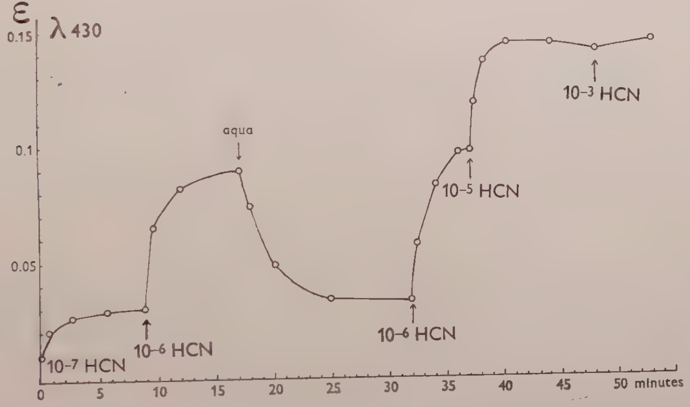

Fig. 31. The time course of the reduction of cytochrome *b* in cyanide and the influence of the concentration. The line 430 mμ was continuously recorded.

gen molecules to come in contact with the active iron atoms, and 2. in chemical combination with iron. An apparent dissociation constant can of course be calculated from the relation between the concentration of HCN and the reducing effect (see fig. 30), but an adsorptive linkage would as well as a chemical linkage satisfy the observed effects. The inhibition with cyanide is completely reversible, a frequently observed fact. The washing out of HCN proceeds much slower than the absorption (see figs. 34, 35), a fact illustrating the strong displacement of the equilibrium in favour of an adsorptive or chemical combination between the inhibitor and the oxidase. The reduction of cytochrome *b* proceeds much slower than that of *a* (see fig. 31), a fact also observed in new unpublished experiments and illustrating the less rapid transferance of electrons between DH I and *b* than between *a* and *b*.

Further discussion of the results

General features of the cytochrome system in the roots. Only three individual cytochromes can be optically distinguished. They are apparently identical with the main cytochromes in animal tissues, viz. *a* (= cytochrome oxidase), *b* and *c*. Cytochrome *b* could be more closely studied than in any previous publication. The fact that the position of the γ-band slightly deviates from what is known from animal tissues is insufficient as an argument for the existence of a cytochrome *b* in plants different from the cytochrome *b* in animals. The properties of the cytochrome oxidase and of cytochrome *c* in the roots are identical with those observed in animal preparations. The deviating observations as to the response of the cytochrome oxidase on CO and CN are certainly not caused by some modification of the enzyme, but reveal new sides of the interaction between these inhibitors and oxygen (cf. p. 102).

It may be of some interest to know the quantity of cytochrome per unit weight of the roots. Calculated in terms of the γ-bands under the assumption of approximately identical molar extinction coefficients (see p. 101 a. 102) the relative quantities are 1 mol. *a*, 2 mol. *c* and 3–4 mol. *b* (see table 4).

Table 4

The content of cytochrome in the wheat roots

Cytochrome	*a*	*c*	*b*
Per 1 kg fresh weight	0.84 µmol.	1.56 µmol.	2.46 µmol.
» 1 kg dry »	9.2 »	17.2 »	27.1 »

Assuming a molecular weight of 13.000 for cytochrome *c* the absolute quantities are 21.6 mg per 1 kg fresh weight and 237 mg per kg dry weight. These quantities are much higher than those observed by GODDARD (5) in wheat embryos (4.6–10 mg per kg dry weight) but are comparable with those reported for animal tissues (from c. 50 to c. 2000 mg per kg; see 22). The quantitative relation between the components is considerably varying in different tissues, however. Cytochrome *c* is commonly more dominating in animals, but there are examples of extremely low contents of this enzyme in special tissues (38). The dominance of cytochrome *b* in the roots may have something to do with the other functions of this enzyme discussed below.

The interaction of the cytochrome components. It was shown that a reversible electron transference links *c* and *b* together and that this linkage may be still active at complete inactivation of the oxidase. It is commonly assumed that the cytochrome oxidase acts directly on cytochrome *c*, eventually *via* a fourth substance (KEILIN's cytochrome *a*). Nothing in the present investigation contradicts this opinion. As to cytochrome *b* the results corroborate the common view that it is linked to the succinic dehydrogenase system (DH I).

It has sometimes been believed that cytochrome *b* were identical with the succinic acid dehydrogenase (DH I), but recent investigations do not support this hypothesis (6, 37). SLATER has brought some evidence pointing to the existence of a factor between cytochrome *b* and DH I (31). Whereas the intimate relation between cytochrome *b* and DH I has been demonstrated in the foregoing no definite results have been obtained concerning the existence of a "Zwischenenzym" but due attention was paid to the band PX 575 and its probable belonging to a substance of lower oxidation potential than cytochrome *b*. Further investigations will have to show if PX 575 represents the succinic dehydrogenase or not.

Of the known physiological-biochemical properties of the cytochrome system no one is more apted to support the idea of its organization as a structural unit than the active transport of anions. The idea was previously advanced (15, 18) that the single cytochromes together compose a "potential ladder". If the normal electron transference through the cytochrome system proceeds along the chain DH I→b→c→a→O_2 the order of the oxidation-reduction potentials will be the reversed, beginning on the negative side and rising to the maximum value of oxygen, $E_0 = +0.78$.

The oxidation-reduction potential of cytochrome *c* is of course the best known. Under physiological pH-values it amounts to $E_0 = 0.254$. Single observations have been made concerning cytochrome b ($E_0 = 0.04$ according to BALL, 2), whereas the potential of the cytochrome oxidase is not yet known (for "*a*" a value of 0.29 has been proposed, 2). As a true equilibrium is never attained in living cells no accurate calculations can be made from the observations of the height of the absorption bands, but an approximate equilibrium prevails between two enzymes if the electron transference between them and the surroundings is slowed down near to zero. For approximative calculations the following formula may be used.

If E_{01} is the oxidation-reduction state (at $\frac{\text{ox}}{\text{red}} = 1$) of one cytochrome, E_{02} that of another the relation between the states and the heights of the bands in the ox/red spectrum $\left(= \log \frac{\text{red}}{\text{ox}}\right)$ is expressed by the following equation:

$$E_{01} - 0.06 \log \frac{\text{red}_1}{\text{ox}_1} = E_{02} - 0.06 \log \frac{\text{red}_2}{\text{ox}_2}.$$

If the absolute value of E_0 is unknown for both components the difference in the two states can be calculated from the following expression:

$$E_0 = \left(\log \frac{\text{red}_1}{\text{ox}_1} - \log \frac{\text{red}_2}{\text{ox}_2}\right) \cdot 0.06 \text{ volts.}$$

If the cytochrome oxidase is screened off from its electron acceptor O_2, e.g. by anaerobiosis or the competitive effect of CN, CO, an approximate equilibrium will be attained between *a* and *c*. All experiments showed a complete reduction of the oxidase under these circumstances even if *c* (and *b*) may be partially oxidized, e.g. after the addition of fumarate. The E_0-value of *a* is consequently considerably higher than that of *c*. At a presumed relation $\frac{a_{\text{ox}}}{a_{\text{red}}} = 100$ and 50 % oxidation of *c* the E_0-value of *a* is $0.06 \cdot 2 = 0.12$ volts higher than that of *c*. At a relation $\frac{a_{\text{ox}}}{a_{\text{red}}} = 1000$ the difference will be 0.18 volts, corresponding to $E_0 = 0.33$. The values are of course only tentative, because it is impossible to accurately measure a balance near to the limit. A large gap between the oxidation-reduction potential of *a* and that of oxygen ($E_0 = 0.78$) ensures the observed complete oxidation of the oxidase if the electron transport from the rest of the system is retarded.

An indispensable condition for the occurrence of an electron transference from cytochrome oxidase to oxygen is the compensation of the involved electrical charges by a reciprocal translocation of freely movable anions. The absence of free anions acts as a specific inhibitor of the cytochrome oxidase, quite as effective as CN or CO.

No calculations as to the approximate E_0-value of the cytochrome oxidase can be made from the normally prevailing balance between the three cytochromes. In aqua dest. *a* is less oxidized than *c* and *b* (see table 3) and if the ox/red balance is changed, e.g. at activated anion respiration, the balance is moved fairly uniformly, especially with regard to *a* and *b*. The observed differences only correspond to a few millivolts.

50 % oxidation in aqua dest. as medium represents of course only a steady state, no real equilibrium, and it is determined largely by the turnover numbers of the single enzymes. The cytochrome oxidase has a strong tendency to oxidize *c* but this tendency is counterbalanced by a strong tendency of the oxygen to oxidize the oxidase. In respect of the interaction of *a* and *c* the controlling agents are the turnover numbers, the intra- and intermolecular resistance to electron movements and the mobility of the compensating anions, viz. a more or less constant group of factors, maintaining a fairly constant steady state if the temperature is not changed.

The main controlling factor of the cytochrome oxidase, viz. the "anion factor", varies with the concentration of salts. The result of an increasing supply of salts is an increased oxidation of the oxidase, and a consequential change of the internal balance. The remarkable fact that the apparent oxidation-reduction balance of *c* hereby is less changed than that of *b* will be discussed below. Also the time-course of the activation of the single enzymes (see 18 and p. 133) reflects the primacy of the cytochrome oxidase at all changes which attack the electron transference to oxygen and illustrates the path of electron transference: $O_2 \leftarrow a \leftarrow c \leftarrow b$.

A change in the ox/red balance of the cytochrome system may also occur if the "anion factor" is held constant but the total resistance is changed, e.g. by variations in the temperature. A rise of the temperature from 19° to 46° C. causes a rapid decrease of the extinction of *all* cytochromes. The figure illustrates the difference between this uniform oxidation and the oxidation of primarily *a* and *b* caused by the "anion factor" (fig. 32).

The tendency of cytochrome *b* to be comparatively more oxidized than *c* reflects its low oxidation-reduction potential as compared with *c* and *a*. The mutual heights of the states are also reflected in the molar concentrations of the enzymes. At equal ox/red balance, e.g. 50–60 % (tab. 3) one may approximately calculate with a reversed relation between molar quantity and oxidation-reduction balance, because the latter must be proportional to the tendency of the enzyme to attract electrons from a second system. If cytochrome *a* holds the double quantity of molecules of *c* at the same ox/red balance the E_0-value of *a* will be about twice as high as that of *c*, or c. 0.50, whereas the E_0-value of cytochrome *b* will be $\frac{2}{3}$. 0.254 = c. 0.17.

The approximate E_0-value of *b* may also be calculated from the observed ox/red balance at inhibited dehydrogenation, viz. from the experiments with malonate and fluoride. The experiments with malonate rendered the value $E_0 = 0.18$ and the experiments with fluoride the value $E_0 = 0.14$, thus not very far from that one calculated from the molar concentrations.

An E_0-value of 0.14–0.17 for cytochrome *b* is considerably higher than the value —0.04 proposed by BALL (2), and does not support the idea of a special enzymatic factor between *b* and *c*, advanced by SLATER (31). The DH I system is on the other hand probably composed by more than one enzyme. The hypothetical cooperation

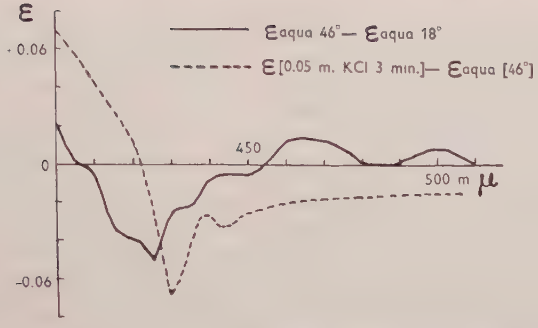

Fig. 32. The increase of the oxidation level of the cytochromes after a rise in the temperature from 18° to 46° C. For comparison is also the effect of a 3 min. exposure to 0.05 m. KCl recorded. The salt affects primarily the cytochromes *b* and *a*, whereas the rise in temperature uniformly accelerates the oxidation of the total system.

of PX 575 was already mentioned. As to the gap between cytochrome *a* and *c* a "Zwischenenzym" similar to the hypothetical "*a*" would be useful, no doubt, but it was not identified in the roots and this question must therefore be left open for the present.

From the approximate molar concentration of the cytochromes in the roots and the known intensity of the anion respiration the turnover number (T.N.) may be calculated. The anion respiration amounts to 2 μmol O_2/1 h 10 mg dr.w. Four electrons are required for the reduction of one molecule O_2. It is assumed that each molecule of the enzyme holds one atom Fe and that the molar extinction values of *a*, *b* and *c* are approximately the same (see p. 102).

The cytochrome oxidase (*a*) of the wheat root has a T.N. (number of electrons emitted per minute per molecule) of 1700 at 19° C. Owing to the higher quantities of the cytochromes *c* and *b* their turnover numbers are only c. 800 and 500 respectively, presuming a direct electron transference.

For comparison it may be mentioned that according to BALL et al. (3) the cytochrome oxidase of the heartmuscle has a T.N. of 4500 at 37° C. Assuming a Q_{10}-value of 2 this corresponds to 1610 T.N. at 19° C. or almost exactly the same as in the wheat roots. For yeast KEILIN and HARTREE calculated the value 3800 at 37°. BACH et al. (1) claim the value 2900 with regard to cytochrome b_2. Systems *in vitro* commonly yield lower values, e.g. 1400 against 3800 in the case of the system succinate dehydrogenase-cytochrome *c*.

Survey of the effect of inhibitors. Malonate (and pyrophosphate) attacks primarily the DH I system in its linkage to cytochrome *b*. Electrons and protons are delivered from DH I and succinate in its oxidation to fumarate. The latter equilibrium is reversible. The electronic equilibrium between cytochromes *b* and *c* is also reversible. At an excess of fumarate its reduction to succinate consumes electrons from *b* and *c*. The partial anaerobic oxidation of cytochrome *c* by fumarate supports the conclusions as to the comparativley small difference in oxidation-reduction potential between *b* and *c*.

The response of the cytochrome system to malonate resembles in its beginning the effect of neutral salts or indifferent organic acids, but is slowly turned over to a more marked oxidation of cytochrome *b*. Because a complete inhibition of the succinate system requires unphysiologically high concentrations of malonate (see above and 9) a reduced anion respiration still continues even if a 0.1 m. malonate solution is supplied at pH 3.3. The reducing power of the partly inhibited DH I system is also sufficient to develop a comparatively strong reduction of cytochrome *b* if the cytochrome oxidase is put out of action.

The switching over from DH I to DH II — probably a cozymase flavoprotein system — is reflected in the increasing reduction of cytochrome *c* in malonate. DH II is obviously linked to cytochrome *c* and its activity is increased simultaneously with the retarding of DH I. Both systems share the supply from the main chain of desmolysis from sugar. But also other interactions between the two systems may be touched upon. POTTER (23) has called attention to an inhibition of the succinate dehydrogenase by cozymase via oxaloacetate, one of the products of the DH II line. The increased reduction of *c* in malonate is counterbalanced by the unchanged oxidation from the side of the cytochrome oxidase, and also by the decreasing reducing demands from the side of *b*. Even a partially reduced *c* is capable of oxidizing a cytochrome *b*, the reduction of which is retarded by the malonate. A strongly oxidized *b*, e.g. in the presence of an excess of fumarate, is able to partially oxidize cytochrome *c*, owing to the mentioned limited difference in potentials. The inability of fumarate to move the balance of reduced cytochrome oxidase, however, depends upon the large gap in oxidation-reduction potential between *c* and *a*.

With regard to *fluoride* the foregoing pages have shown that it leaves DH II intact, too, but inhibits the DH I system on a way quite different from malonate. The difference between malonate and fluoride is notified in several respects of which some were already mentioned. Fluoride probably inhibits the supply of C_4-acids to the DH I system and hereby not only inactivates cytochrome *b* but also stops a number of synthetic processes which are supplied from the organic acid cycle. The decreasing synthetic power is reflected in the tremendously decreasing exudation of water to the ascending sap stream (15), in the rapid inhibition of the growth (13) etc.

If the intensity of the ascending sap stream, measured as bleeding (13, 15), is taken as an indicator of the intensity of the synthetic processes in the root it is interesting to notify the different effects of malonate and fluoride. Malonate exerts a much weaker effect on the bleeding than fluoride. This observation tallies with the fact that malonate only inhibits the linkage of DH I to cytochrome *b* and thus leaves the supply to the organic acid cycle untouched, whereas fluoride inhibits processes supplying the cycle with raw material. Another consequence of these fundamental differences is an abnormal accumulation of organic acids during malonate inhibition. This abnormal acidification has severe effects on the protoplasm as is shown by the tremendously increased vacuolization of the protoplasm in malonate. Such effects are not observed with fluoride because the mere production of organic acids is inhibited.

Because the cytochrome system is located near the cell surface it is more protected against the partial destruction of the protoplasm and it is also surprising how little the optical picture of the cytochrome system is affected by malonate. Only after the definite death of the cells the system is slowly disintegrated. A spectral disconfiguration of the cytochrome system is on the other hand observed after treatment with DNP, a substance probably controlling many structural qualities of the protoplasm.

Regarding the real nature of the DH II system which is obviously attached to cytochrome *c* it was already mentioned that WAYGOOD (40) claims the existence of a system composed of cozymase, a flavoprotein and a hypothetical pigment. It cooperates with a malate dehydrogenase oxidizing malate to oxaloacetate. The dehydrogenase reduces cozymase which is then oxidized by a flavoprotein. WAYGOOD belives that the further oxidation runs over a hypothetical pigment and ascorbic acid oxidase to oxygen, but he also touches upon the possibility that the cytochrome system may be responsible for the end-oxidation under certain circumstances.

It is doubtful if WAYGOODS system has anything to do with our hypothetical DH II system. If malate were the source of electrons and protons the system would be inhibited by fluoride because malate is an oxidation product of succinate. The DH II system is however not affected by fluoride. It is more likely to assume that the cozymase, if it participates in DH II, is reduced at an earlier stage of the desmolysis, e.g. at the oxidative conversion of 1,3-diphosphoglyceraldehyde to 1,3,-diphosphoglycerate, a process which runs independently of the inhibition of the enolase by fluoride. Cozymase may of course participate in various processes of intramolecular oxidation.

A cozymase-flavoprotein system is no doubt able to combine with a second oxidase system, too, e.g. a copper oxidase, eventually ascorbic acid oxidase. These enzymes have been frequently observed in plant tissues (4) and the existence of the ground respiration definitely proves that a second oxidase system operates in the roots besides of the cytochrome system. The copper oxidases are not quite insensitive to cyanide but the sensitivity is far below that of the cytochrome oxidase and leaves the ground respiration practically intact at c. 1 hour treatment with 0.001 HCN. Prolonged treatment with cyanide affects also other systems, e.g. succinoxidase. Under physiological conditions cyanide may, however, be used as a fairly significant inhibitor of the cytochrome system.

The ground respiration is incapable of promoting effective growth (13), of accumulating salts and of the maintenance of an effective ascending sap stream (13, 15). The ground respiration is nevertheless a guarantee for the existence minimum of the roots, viz. life devoid of development. The constructive processes leading to synthesis of protein, cellulose, organic acids, etc. and maintaining progressive growth are more or less dependent on the C_4-acid cycle and the undisturbed proceeding of the succinic dehydrogenase system.

If cozymase is one of the fundamental enzymes of the ground respiration it may possibly serve as the connecting link between the two oxidase systems, under normal conditions with active anion respiration furnishing the ground respiration system over oxidase II and at inhibited DH I supplying also the cytochrome system over *c* and *a* (see fig. 33).

If cytochrome *c* serves as a link between the ground respiration and the anion respiration, viz. between the chains ending in oxidase II or cytochrome oxidase, these two fractions of the total aerobic respiration must be in some way inversely variable. There will be competition as to the raw material and competition as to oxygen, also more specific competitive interrelations (cf. 23). It is to be supposed that an anion respiration running at maximal speed will partly suppress the ground respiration. The ground respiration will on the other hand not be able to take over the products of the DH I system, if the anion respiration is inhibited, because it is linked to cytochrome *c* with its high oxidation-reduction potential. And the only specific oxidase of cytochrome *c* is the cytochrome oxidase.

Provided there exists an interrelation between the two main aerobic systems as pictured in the scheme in fig. 33 the experimentally determined ground respiration

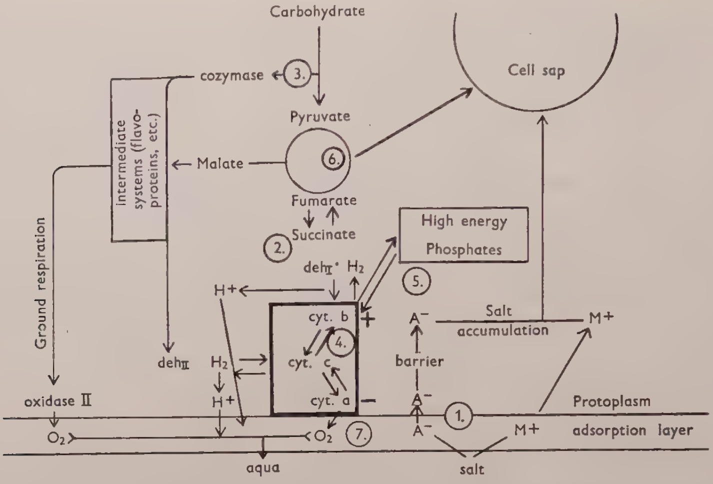
Carbohydrate
Cell sap
cozymase
3.
Pyruvate
intermediate systems (flavo-proteins, etc.)
Malate
6.
Fumarate
Succinate
2.
High energy Phosphates
Ground respiration
dehII· H2
H+
cyt. b
+
5.
A−
Salt accumulation
M+
4.
cyt. c
barrier
dehII
H2
H+
cyt. a
−
oxidase II
A−
1.
Protoplasm
O2
O2
7.
A−
M+
adsorption layer
aqua
salt

Fig. 33. Scheme of the cytochrome system of wheat roots and its linkage to the carbohydrate metabolism and the salt accumulation. The circles indicate specific inhibitors: 1. the salt factor controlling the activity of the total system, 2. malonate inhibiting the succinate dehydrogenase, 4. urethane isolating cytochrome *b* from cytochrome *c*, 5. 2,4-dinitrophenol inhibiting phosphorylation and disorganizing the structural salt barrier, 6. fluoride inhibiting the production of succinate, 7. cyanide, carbon monoxide and azide inhibiting the oxidation of the cytochrome oxidase by molecular oxygen.

(= the difference between the total respiration and the fraction inhibited by 0.001 m. cyanide) will give a too high value because at working anion respiration a part of the raw material of the ground respiration is carried over to the cytochrome system. From the view-point of the quantitative relations between the anion respiration and the accumulated salt (Q an/O_2), however, the difference between the salt respiration and the HCN-respiration accurately reflects that fraction of the total respiration which is responsible for the salt accumulation, because the DH II system does not participate in this work.

Suggestions have been put forward as to the possible participation of the cytochrome system in the synthesis of high energy phosphates. SLATER (29) claims a linkage of phosphorylation to the reduction of cytochrome *c* and the oxidation of α-ketoglutarate. On the other hand succinate dehydrogenase is assumed to be one of the steps responsible for the formation of energy rich phosphates (28). The present investigation has shown that 2,4-dinitrophenol (DNP), known as an inhibitor of phosphorylation, partly inactivates cytochrome *b*. DNP is also claimed to attack the linkage between cozymase and the cytochrome system (35). Because phosphorylation occurs at several points of the chain of glycolysis and respiration and both of these continue under the influence of DNP it must be concluded that this substance attacks certain processes of phosphorylation more intensively than others. It may be tentatively assumed that one of the more important points of building up high energy phosphates is linked to cytochrome *b* (and *c*) and that the normal proceeding of this side-chain is an important condition for the appropriate function of the total cytochrome system (cf. 33).

It was experimentally shown that DNP partially or completely inactivates cytochrome *b*. The raised oxidation level together with the partly stimulated respiration (fig. 25) indicates a continued oxidative metabolism, also including cytochrome *b*. This stimulation is probably caused by the switching off of the side-chain from the cytochrome system to the phosphorylation processes, as a consequence of which the whole capacity can be devoted to the complete oxidation through *c* and *a*.

There are certain indications, however, e.g. the severe disturbance of the salt accumulation, that the processes inhibited by DNP play an important rôle for the maintenance of the normal protoplasmic structure, including the cytochrome system and its anchoring to the living organs of the cell. As far as we know the phosphate metabolism is intimately linked to ADP–ATP and nucleotides which besides of the proteins build up the structural skeleton of the protoplasm and which also appear in the surface layer of the cells (20, 16). A few more points regarding the relations with the phosphate metabolism are mentioned in the following section.

The anion respiration. The theory of anion respiration is based on the fact that free valencies or free electrons do not exist in an aqueous medium, because the former attract ions of opposite charge and the latter are attached to anions. In an active cytochrome enzyme the iron atoms are undergoing rapid changes of free valency, $Fe^{++} \underset{\varepsilon}{\overset{\varepsilon}{\rightleftharpoons}} Fe^{+++}$. The changes are consequently accompanied by the attraction or the releasement of freely movable anions in the surroundings of the system. Freely movable anions certainly facilitate a very rapid turnover in comparison e.g. to internal salt couplings in the enzyme molecule itself. The experimentally shown fact that the T.N. of the cytochrome oxidase is nearly proportional to the concentration (activity) of movable ions in the surroundings clearly shows that such internal salt couplings play a very subordinate rôle in the case of the cytochrome oxidase. Cytochrome *b* is probably in a similar situation, whereas less firm conclusions can be drawn regarding cytochrome *c*.

The cytochrome system may be figured as a "potential ladder" along which electrons move from dehydrogenase systems to oxygen (15 p. 109, 17 p. 70). The molecular skeleton of the system hereby functions as a metallic conductor. The contact area between the cytochrome oxidase and the oxygen molecules is the negative pole of the system (= production of electrons), the contact area of the dehydrogenase is the positive pole (= consumption of electrons). Similar to the conditions in an electric battery electrons will flow through the system only if an external circuit is closed between the poles. Electrolytes in the immediate surroundings of the cytochrome system constitute the outer circuit. Anions are thus transported from the negative pole to the positive and an equivalent quantity of cations is moved in the opposite direction. Because anions are not produced near the negative pole of the system anionic components of the medium are caught by the current produced from the cytochrome system. As to cations such are produced by the dehydrogenase system. For each electron entering the cytochrome system one proton is released according to the formula $2DH \cdot H_2 = 2DH + 4\varepsilon + 4H^+$. As the equivalent quantity of protons is consumed at the negative pole, forming water, according to the formula $O_2 + 4\varepsilon + 4H^+ = 2H_2O$, no external cations are caught by the current.

The picture of the cytochrome system, acting as a sub-micro electric battery, is convenient and elucidating, but the process can also be figured as a pulsating stream of electrons between the iron atoms, balanced by a stream of anions in the opposite direction (11a, 15). The mutual relationship between the movement of electrons through the cytochrome system and the active transportation, in the opposite direction, of salt anions may be pictured in one way or the other, the final result will be the same.

The experimental results of this investigation show that an activation of cytochromes *a* and *b* is required for salt accumulation, whereas an electron transference only between *a* and *c* is not accompanied by active salt absorption. Because the electron transference between *a* and *b* runs over *c* it must accordingly be concluded that the activity of the total cytochrome system is required for salt accumulation. This conclusion tallies with the idea of the complete cytochrome system functioning as a motor for electrophoretic transport of anions. As pointed out in a previous publication (18 p. 492) the flow of anions along the axis of the cytochrome system will, however, accomplish a real accumulation only if the anions are moved across a barrier preventing the passive back-flow. The existence of such a barrier is shown from the very restricted leakage of salts once accumulated. Already the normally prevailing electronegative charge of the protoplasmic membrane (11) creates an effective barrier against passive diffusion of anions through the cell wall. If the cytochrome oxidase is located near the cell surface its electrical pulsations during the electron transference to oxygen will provide the energy for the overcoming of the membrane barrier. But the fact that the activity of the cytochrome oxidase alone is not sufficient for a real accumulation clearly shows that still another barrier has to be surmounted before the salts are safely accumulated. This definite barrier is probably in some way related to cytochrome *b*.

It would be premature to discuss the possible location of this diffusion barrier serving as a sluice of salts because we know too little about the molecular configuration of the cytochromes and the mode on which the cytochrome system is attached to the protoplasmic structure. As far as we know are the salts first accumulated in the protoplasm and from here exuded into the cell sap. The possibility is still lurking that this internal exudation may have some barrier function. Some information is discerned from the effects of DNP and similar inhibitors obviously affecting the structural basis of the protoplasm.

ROBERTSON (27) advanced the idea that the phosphate metabolism is in some way linked to the process of salt accumulation and may serve as a complemental effect to the electron transference through the cytochrome system and thus raise the Q an/O_2 above the theoretical limit 4. The existence of such complementary processes is of course by no means excluded, because electron transferences occur on many points of the oxydative metabolism, but it must be emphasized that as far as plant cells concerns the combination of the electron transference with a salt barrier is indispensable for real accumulation. At the present state of knowledge we limit ourselves to the cytochrome system as the main mechanism of salt accumulation. From this point of view the deleterious effects of an inhibitor attacking phosphorylation mechanisms may be explained as the destruction of the salt barrier located somewhere between the cytochromes *a* and *b* (see fig. 33) or between *b* and DH I. The linkage between cytochrome *b* or/and *c* and the phosphate metabolism can be figured as the guardian of the internal salt barrier. If this barrier is disorganized the salts will be able to circulate around the cytochrome system but not to be accumulated. The circulating salts[1] will however serve as the balancing factor for the activity of the system cytochrome *a*–cytochrome *c* after an inhibition of the DH I system by malonate, fluoride, or DNP.

---

[1] Such irregularily circulating salts probably maintain the activity of cytochrome systems *in vitro*, a fact explaining a number of varying influences of salts described in the biochemical literature (cf. 25). Under physiological conditions the organic acids may play this rôle as "anionic coenzymes" (cf. 13).

The single reactions conducting anions through the cytochrome system of the wheat roots may be summarized as follows (see also fig. 33):

1. Oxidase (Fe^{++}) $+ \frac{1}{2}O +$ anion $\rightarrow$ Oxidase ($Fe^{++})^{+} \cdot$ anion $+ \frac{1}{2}O^{--}$.

2. Oxidase ($Fe^{++})^{+} \cdot$ anion $+$ Cytochrome *c* (Fe^{++}) $\rightarrow$ Oxidase (Fe^{++}) $+$ Cytochrome *c* ($Fe^{++})^{+} \cdot$ anion.

3. Cytochrome *c* ($Fe^{++})^{+} \cdot$ anion $+$ Cytochrome *b* (Fe^{++}) $\rightleftharpoons$ Cytochrome *c* (Fe^{++}) $+$ $+$ Cytochrome *b* ($Fe^{++})^{+} \cdot$ anion.

4. Cytochrome *b* ($Fe^{++})^{+} \cdot$ anion $+ \frac{1}{2}$DH I$\cdot H_2 \rightleftharpoons$ Cytochrome *b* (Fe^{++}) $+ \frac{1}{2}$DH $+$ $+$ anion $+ H^{+}$.

5. $H^{+} + \frac{1}{2}O^{--} = \frac{1}{2}H_2O$.

The protons consumed in the final reaction nr. 5 are produced from nr. 4. These protons are equivalent with the quantity of anions absorbed in nr. 1. The released anions (nr. 4) are combined with metallic cations present everywhere in the protoplasm according to its predominating acid dissociation (11, 11a). The cations are exchanged against protons in the surroundings and immediately replaced by cations from the adsorption layer at the cell surface (11, 15, 16), thereby restituted from the medium. No net loss of protons occurs during this process. These adjacent processes are summarizied as follows (R^{-} = acidoid components of the protoplasm, $M^{+} \cdot A^{-}$ = neutral salt).

6. $R^{-} \cdot H^{+} + M^{+} \cdot A^{-} \rightleftharpoons R^{-} \cdot M^{+} + H^{+} \cdot A^{-}$.

$R^{-} \cdot M^{+}$ may be movable (e.g. in streaming protoplasm) or a transportation of metallic cations may occur as gliding along internal adsorption surfaces (“adsorption tracks”).

As pointed out by ROBERTSON (26; cf. 13) the theoretical maximum value of Q an/O_2 is 4 provided that equivalent quantities of electrons and anions are exchanged according to the reaction nr. 1. This rule will hold as long as the cytochrome oxidase controls the entrance of anions into the protoplasm. The results hitherto obtained with plant material support this idea inasmuch as higher quotients than c. 4 were not observed. In other cases and especially regarding animal tissue and animal cells — some of which contrary to the plant cells are impermeable to cations but permeable to anions (e.g. erythrocytes) — no surface barrier against anions may exist. In such cases the cytochrome system will conquer its balancing partners without the need of extra energy and is here probably even not endowed with the property of conducting osmotic work. This circumstance may be held in mind if the localization of the cytochrome system in the cells is discussed (cf. p. 130). But even if a cytochrome system anchored at the surface of mitochondria will scarcely be able to accomplish a salt accumulation comparable to that one in plant cells a certain circulation of salts will always occur as long as the system is active and such an intracellular stirring mechanism may not be without some importance for the metabolism of the animal cell.

The polar transportion of salts, eventually a high grade accumulation opposite to the osmotic gradient, is one of the physiological fundamentals of plants and most plant cells. In the animal body and in most animal cells the problem of salt transportation is solved in other ways and salt accumulation in the cells is by no means a fundamentally constructive process as it is in the plants. But certain animal tissues nevertheless are endowed with a power of ion or salt transportation comparable to that one in the plant cells, viz. the exuding tissues of the kidney and the gastric mucosa and the resorbing tissues of the intestines. It remains to be investigated if these cells are provided with a different localization of the cytochrome system than the majority of the somatic cells. A more pronounced anion permeability of these specialized animal cells of course opens the possibility of the attainment of Q an/O_2-values higher than 4, because a number of other electronic mechanisms than the cytochrome system will then have the possibility to act as carriers of anions entering the cells by passive diffusion or "adsorption gliding".

The production of electricity in the cytochrome system makes it sensitive to the electrical conditions of the surroundings, a circumstance previously demonstrated in a series of experiments (11 p. 340). Because the root tips normally have a surface potential of. c. —60 mV, measured against the basis as zero, an electrical current continuously flows through the root from the basis to the tip. This current is opposite to the movement of the absorbed salt anions and thus visualizes the circuit through the cytochrome system: an inner stream of electrons through the body of the enzyme system and an outer stream of free anions. The intensity of the production of electricity reflects the intensity of the anion respiration. If this current was enhanced by means of an extra current ($5 \cdot 10^{-5}$ amperes) sent from the outside through the roots the anion respiration increased from 100 (= the controls) to 124. The same current sent in the opposite direction lowered the respiration from 100 to 64.

The last named experiments emphasize the close connection between the cytochrome system and the structural organization of the cells and tissues in the roots, properties imperative for the system's production of osmotical work. In cells and tissues with a more diffuse distribution of the system such influences will probably be less striking. Cases may even occur in which the components of the cytochrome system are not structurally linked together. This may at least be a hypothetical possibility concerning cytochrome *c*, because this enzyme is apparently not so closely attached to the living structure as the other cytochromes. It is even conceivable that cytochrome *c* may have an ambulatory function in the cell, distributing oxidation power to other systems. This cytochrome would *ceteris paribus* also be able to transport anions to places distant from the structurally anchored *a* and *b*. In a hypothetical scheme of salt respiration ROBERTSON (26) ascribes a carrier function to cytochrome *c*. It is however difficult to understand how such a function could be associated with the key position of cytochrome *b* in the anion respiration.

SUMMARY

A very sensitive and rapidly working automatic spectrophotometer was constructed by means of which absorption spectrograms were accurately recorded of bundles of living roots simultaneously with their exposure to experimentally controlled physiological and biochemical conditions.

The wheat roots are provided with a complete cytochrome system, including cytochrome oxidase and the cytochromes *c* and *b*. The molar (Fe) quantities are approximately 1 oxidase, 2 cytochrome *c* and 3–4 cytochrome *b*.

The cytochromes are arranged in a potential ladder maintaining an internal stream of electrons from the dehydrogenase systems to the oxygen. This internal current is balanced by an external transport of salt anions in the opposite direction and a transport of protons, produced by the dehydrogenases, from these to the oxygen activated by the electron transference from the cytochrome oxidase (= the anion respiration).

The turnover number of the cytochrome oxidase is of similar magnitude as in the heart muscle. The cytochrome oxidase is completely reduced in the absence of oxygen and in 0.001 m. HCN. CN and CO act competitively against oxygen, causing an aerobic anaerobiosis, but these inhibitors are probably also to some extent chemically combined with oxydase iron. An inhibited cytochrome oxidase remains reduced at subsequent anaerobic oxidation of the cytochromes *c* and *b* by fumarate.

Two alternating dehydrogenase systems furnish the cytochrome system with electrons and protons, viz. the succinate dehydrogenase system (DH I) attached to cytochrome *b* and a second system (DH II) probably identical with a cozymase-flavoprotein system, attached to cytochrome *c*. At inhibition of DH I by malonate or fluoride DH II is accelerated and maintains an end-oxidation over *c* and *a*. Fluoride is probably not inhibiting the DH I system itself but systems in the chain of glycolysis supplying succinate to the DH I system. The annihilating effect of fumarate on the malonate inhibition has a competitive character and fumarate in excess reverses the electronic equilibrium between DH I and cytochrome *b* and between cytochromes *b* and *c*, an effect also observed after urethane inhibition. Urethane inhibits the electron transference between cytochromes *b* and *c*.

A normal anion respiration, viz. a causal relation between the cytochrome respiration and the active transport of salts from the medium into the cells, postulates the activity of the complete cytochrome system, including the activity of the DH I-cytochrome *b* system. The system DH II–cytochrom *c*–cytochrome oxidase is incapable of accumulating salts. The activity of cytochrome *b* probably implies the surmounting of a diffusion barrier impeding a passive back-flow of the accumulated salts. This barrier function is probably controlled by a phosphate metabolism in some way connected to the cytochrome system over *b* and/or *c* and sensitive to 2,4-dinitrophenol.

REFERENCES. 1. **Bach, S. J.** *et al.*, Bioch. J., *40*, 1946, 229. — 2. **Ball, E. J.**, Ann. N.Y. Acad. Sc., *45*, 1944, 363. — 3. —— *et al.* J. Biol. Chem., *193*, 1951, 635. — 4. **Dawson, C. R. & W. B. Tarpley**, The Enzymes (Sumner, Myrbäck), II, P. 1, 1951, 454. — 5. **Goddard, D. R.**, Amer. J. Bot., *31*, 1944, 270. — 6. **Johns, A. T.**, Biochem. J., *49*, 1951, 559. — 7. **Judah, J. D.**, Biochem. J., *49*, 1951, 271. — 8. **Keilin, D. & Hartree, E. F.**, Proc. Roy. Soc., B, *127*, 1939, 167. — 9. ——, Biochem, J., *44*, 1949, 305. — 10. ——, Biochem. J., *49*, 1951, 205. — 11. **Lundegårdh, H.**, Ann. Roy. Agr. Coll. Sweden, *8*, 1940, 233. — 11a. ——, Ark. f. Bot., Stockholm, *32 A*, 1945, Nr. 12. — 12. ——, Ann. Roy. Agr. Coll. Sweden, *16*, 1949, 339. — 13. ——, Ann. Roy. Agr. Coll. Sweden, *16*, 1949, 372. — 14. ——, Physiologia Plant., *2*, 1949, 388. — ——, 15. Physiologia Plant., *3*, 1950, 103. — 16. ——, Lärobok i växtfysiologi med växtanatomi. Stockholm 1950. — 17. ——, Ark. f. kemi, Stockholm, *3*, 1951, 69. — 18. ——, Ark. f. kemi, Stockholm, *3*, 1951, 469. — 19. —— & **H. Burström**, Ann. Agr. Coll. Sweden, *12*, 1944, 51. — 20. —— & **G. Stenlid**, Ark. f. Bot. Stockholm, *31 A*, 1944, Nr. 10. — 21. **Mapson, L. W. & D. R. Goddard**, Biochem. J., *49*, 1951, 592. — 22. **Paul, K. G.**, The Enzymes (Sumner, Myrbäck), II, P. 1, 1951, 357. — 23. **Potter, V. R.**, Ark. f. kemi, etc., Stockholm, *13 B*, 1939, Nr. 7. — 24. **Price, C. A. & K. V. Thimann**, Arch. Biochem. Biophys., *33*, 1951, 170. — 25. **Riley, V.**, Proc. Soc. Exp. Biol. Med., *75*, 1950, 644. — 26. **Robertson, R. N. & Marjorie J. Wilkins**, Austr. J. Sci. Res., *B 1*, 1948, 17. — 27. —— *et al.*, Austr. J. Sci. Res., *B 4*, 1951, 248. — 28. **Schlenk, F.**, The Enzymes (Sumner, Myrbäck), II, P. 1, 1951, 316. — 29. **Slater, E. C.**, Nature, *166*, 1950, 982, — 30. ——, Biochem.

J., *45*, 1949, 14. — 31. ——, Biochem. J., *46*, 1950, 484. — 32. **Stafford, Helen A.,** Physiologia Plant., *4*, 1951, 696. — 33. **Stenlid, G.,** Physiologia Plant., *2*, 1949, 350. — 34. **Straub, F. B.,** Hoppe-Seyler's Zeitschr. f. physiol. Chem., *268*, 1941, 227. — 35. **Terner, C.,** Biochem. J., *49*, 1951, 11. — 36. **Theorell, H.,** The Enzymes (Sumner, Myrbäck), II, P. 1, 1951, 335. — 37. **Tsou, C. L.,** Biochem. J., *49*, 1951, 512. — 38. ——, Biochem. J., *49*, 1951, 658. — 39. **Wainio** *et al.*, J. Biol. Chem., *192*, 1951, 349. — 40. **Waygood, E. R.,** Canad. J. Res., *C 28*, 1950, 7. — 41. **Dannenberg, H.** and **M. Kiese,** Bioch. Zeitschr., *322*, 1952, 395. — 42. **Chance, B.,** Nature, *169*, 1952, 215. — 43. ——, Ann. Rev. Biochem., *21*, 1952, 687.

Tryckt den 12 januari 1953

Uppsala 1953. Almqvist & Wiksells Boktryckeri AB

ARKIV FÖR KEMI Band 5 nr 13

Communicated 27 February 1952 by ARNE WESTGREN and GUNNAR HÄGG

On ion exchange equilibria

II. Activities of the components in ion exchangers

By ERIK HÖGFELDT

With 15 figures in the text

Introduction

Most literature on ion exchange equilibria refers to a number of different methods of representing experimental data e.g. by giving an empirical equation, by plotting the sorption isotherm or by plotting the mass action constant against some function of the ionic concentrations.

There are also a number of different theoretical approaches. For instance: the law of mass action especially in the form of Donnan equilibrium, and statistical equations have been applied. For further details on these subjects the reader is referred to the books by NACHOD [1] and by KUNIN and MYERS [2].

The mass action law has proved to be a useful approach. The equilibrium quotient λ_{21} defined by equation (20) below, has been found to be approximately constant in limited concentration ranges but in general the equilibrium quotient is a variable [3].

HÖGFELDT, EKEDAHL and SILLÉN [3] studied the $Ag^+ - H^+$ exchange on two sulfonic acid exchangers. Their measurements were summarized in $\varkappa(\beta)$ curves, where $\varkappa$ is the equilibrium quotient (see equation (3) in Part I [3]) and β the mole fraction of silver in the exchanger. Within the concentration range studied $\varkappa$ was found to vary considerably with β as is seen from Figs. 1 and 2. Analogous results have been obtained in the meantime by a number of other investigators [3].

If the equilibrium quotient were a constant this would mean that the components in the exchanger could be treated as if they formed ideal solid solutions. This not being the case it seemed tempting to treat the ion exchanger in analogy with non-ideal liquid mixtures by applying Gibbs-Duhem's equation and obtaining the activity factors of its components by graphical integration. Some of the formulas and results below have been given in preliminary communications [4–6].

The assumption of equivalent exchange

Suppose we have a certain amount of a cation exchanger (R^-) in equilibrium with a solution containing two ions $A_1^{z_1+}$ and $A_2^{z_2+}$. The ions are considered to be exchanged in equivalent amounts. As the exchanger is electrically neutral this means that it contains no other negative ions than the R^- of the resin framework. This assumption has been found to hold by a number of investigators, such as MARINSKY [7] and KRESSMAN and KITCHENER [8]. In Part I of this series [3] Table 6 may be said to be a test on the assumption of equivalent exchange; if this assumption were not correct, the different ways of calculating $\varkappa$ would have given different values, whereas they were found to agree within the limits of experimental error.

Choice of components and concentration units

The "molecular weights" of the components can be chosen in two ways giving two different formal treatments. The components can either be written as $A_{1/z}R$ or AR_z. These two choices of molecular weights are referred to below as (E) and (M). For $z_1 = z_2 = 1$ (E) and (M) are of course equal. One can conveniently express the concentrations of $(A_1)_{1/z_1}R$ and $(A_2)_{1/z_2}R$ by equivalent fractions β_1, β_2 and of $A_1R_{z_1}$ and $A_2R_{z_2}$ by mole fractions X_1, X_2.

Let us consider a certain amount of an ion exchanger containing $n_1\,A_1^{z_1+}$, $n_2\,A_2^{z_2+}$ and $(n_1z_1 + n_2z_2)\,R^-$. We have thus $n_1z_1\,(A_1)_{1/z_1}R$, $n_2z_2\,(A_2)_{1/z_2}R$ or $n_1\,A_1R_{z_1}$, $n_2\,A_2R_{z_2}$. The equations defining β_1, β_2 and X_1, X_2 are:

$$\beta_1 = \frac{n_1z_1}{n_1z_1 + n_2z_2};\quad \beta_2 = \frac{n_2z_2}{n_1z_1 + n_2z_2};\quad \beta_1 + \beta_2 = 1 \tag{1}$$

$$X_1 = \frac{n_1}{n_1 + n_2};\quad X_2 = \frac{n_2}{n_1 + n_2};\quad X_1 + X_2 = 1. \tag{2}$$

From (1) and (2) we find:

$$\frac{\beta_1}{\beta_2} = \frac{X_1z_1}{X_2z_2}. \tag{3}$$

The relations between the equivalent and mole fractions follow from (1), (2), and (3):

$$\beta_1 = \frac{X_1z_1}{X_1z_1 + X_2z_2};\quad \beta_2 = \frac{X_2z_2}{X_1z_1 + X_2z_2} \tag{4}$$

$$X_1 = \frac{\beta_1z_2}{\beta_1z_2 + \beta_2z_1};\quad X_2 = \frac{\beta_2z_1}{\beta_1z_2 + \beta_2z_1}. \tag{5}$$

Choice (E) ("equivalents")

The components in the exchanger are $(A_1)_{1/z_1}R$ and $(A_2)_{1/z_2}R$. The exchange reaction can be written:

$$z_1A_2^{z_2+} + z_1z_2\,(A_1)_{1/z_1}R \rightleftarrows z_2A_1^{z_1+} + z_1z_2\,(A_2)_{1/z_2}R. \tag{6}$$

We introduce the activities a_{E1}, a_{E2} and activity factors γ_1, γ_2 of $(A_1)_{1/z_1}R$ and $(A_2)_{1/z_2}R$. The pure components are chosen as standard states. The capacity of the sorbent is s_0 (in arbitrary units). For the concentrations and activities of the components we obtain:

$$[(A_1)_{1/z_1} R] = \beta_1 s_0; \qquad [(A_2)_{1/z_2} R] = \beta_2 s_0$$
$$\{(A_1)_{1/z_1} R\} = a_{E1} = \gamma_1 \beta_1; \ \{(A_2)_{1/z_2} R\} = a_{E2} = \gamma_2 \beta_2. \tag{7}$$

The equilibrium quotient $\varkappa_{21}$ of (6) and its inverse value $\varkappa_{12}^{1}$ are defined by:

$$\varkappa_{21} = \varkappa_{12}^{-1} = \frac{\{A_1^{z_1+}\}^{z_2}}{\{A_2^{z_2+}\}^{z_1}} \cdot \left(\frac{\beta_2}{\beta_1}\right)^{z_1 z_2}. \tag{8}$$

It may be noted that GAPON [9] has introduced an ion exchange constant which is equal to $[\varkappa_{12}]^{\frac{1}{2}}$.

The quotient of the ionic activities in the liquid solution may generally be determined with good accuracy. β_1, β_2 are obtained by analysis of the sorbent at equilibrium. $\varkappa$ is thus a quantity obtained directly from the experiments.

For the thermodynamic constant K_{21}^E of reaction (6) we obtain from (7) the following expression:

$$K_{21}^E = \frac{\{A_1^{z_1+}\}^{z_2}}{\{A_2^{z_2+}\}^{z_1}} \cdot \left(\frac{\gamma_2 \beta_2}{\gamma_1 \beta_1}\right)^{z_1 z_2}. \tag{9}$$

From (8) and (9):

$$\varkappa_{21} = K_{21}^E \left(\frac{\gamma_1}{\gamma_2}\right)^{z_1 z}. \tag{10}$$

From (10) it is seen that K_{21}^E can be determined if we can evaluate the quotient between the activity factors. In order to obtain expressions for evaluation of the activity factors we apply Gibbs-Duhem's equation to the binary mixture $(A_1)_{1/z_1} R$ and $(A_2)_{1/z_2} R$:

$$\beta_1 \, d \ln (\beta_1 \gamma_1) + \beta_2 \, d \ln (\beta_2 \gamma_2) = 0. \tag{11}$$

From (1) and (11):

$$\beta_1 \, d \ln \gamma_1 + \beta_2 \, d \ln \gamma_2 = 0. \tag{12}$$

By logarithmic differentiation of (10), remembering that K_{21}^E is a constant:

$$d \ln \gamma_2 = d \ln \gamma_1 - \frac{1}{z_1 z_2} d \ln \varkappa_{21}. \tag{13}$$

From (12) and (13):

$$d \ln \gamma_1 = \frac{1}{z_1 z_2} \beta_2 \, d \ln \varkappa_{21}$$
$$d \ln \gamma_2 = -\frac{1}{z_1 z_2} \beta_1 \, d \ln \varkappa_{21} = \frac{1}{z_1 z_2} \beta_1 \, d \ln \varkappa_{12}. \tag{14}$$

In order to integrate (14) we introduce the values of γ_1, γ_2 and $\varkappa_{21}$ at the limits $\beta_2 = 0$ and $\beta_2 = 1$. The limiting values are denoted by $'$ and $''$ which refer to $\beta_2 = 0$ and $\beta_2 = 1$ respectively. As the pure components are chosen as standard states γ_1' and $\gamma_2'' = 1$ we obtain:

$$\begin{aligned} &\beta_2 = 0 \text{ (pure } (A_1)_{1/z_1} R); \quad \gamma_1 = 1; \quad \gamma_2 = \gamma_2'; \quad \varkappa_{21} = \varkappa_{21}'. \\ &\beta_2 = 1 \text{ (pure } (A_2)_{1/z_2} R); \quad \gamma_1 = \gamma_1''; \quad \gamma_2 = 1; \quad \varkappa_{21} = \varkappa_{21}''. \end{aligned} \tag{15}$$

(14) is transferred to decadic logarithms and with the limiting values defined by (15) we obtain:

$$\begin{aligned} &\int_1^{\gamma_1} d \log \gamma_1 = \log \gamma_1 = \frac{1}{z_1 z_2} \int_{\varkappa_{21}'}^{\varkappa_{21}} \beta_2 \, d \log \varkappa_{21} \\ &\int_1^{\gamma_2} d \log \gamma_2 = \log \gamma_2 = -\frac{1}{z_1 z_2} \int_{\varkappa_{21}''}^{\varkappa_{21}} \beta_1 \, d \log \varkappa_{21} \,. \end{aligned} \tag{16 a, b}$$

From (16) it is seen that $\log \gamma_1$ and $\log \gamma_2$ may be obtained by integration of the curve $\log \varkappa(\beta)$.

One need not make two integrations to obtain both γ_1 and γ_2. From (10) and (15):

$$\left.\begin{aligned} &\log K_{21}^E = \log \varkappa_{21}' + z_1 z_2 \log \gamma_2' \\ \text{and} \quad &\log K_{21}^E = \log \varkappa_{21}'' - z_1 z_2 \log \gamma_1''. \end{aligned}\right\} \tag{17}$$

Thus K_{21}^E may be calculated from (17) and then $\log \gamma_1$ is easily obtained from (10) if $\log \gamma_2$ is obtained by integration and vice versa.

In the application of Gibbs-Duhem's equation mentioned above, the term for the variation of the water activity has been omitted. In the Appendix it will be shown that no serious error has been introduced in this way.

Choice (*M*) ("moles")

The components in the exchanger are chosen as $A_1 R_{z_1}$ and $A_2 R_{z_2}$. This case may be treated in a manner analogous to (*E*). The exchange reaction may be written:

$$z_1 A_2^{z_2+} + z_2 A_1 R_{z_1} \rightleftarrows z_2 A_1^{z_1+} + z_1 A_2 R_{z_2}\,. \tag{18}$$

We introduce the activities a_{M1}, a_{M2} and activity factors g_1, g_2. As above, the pure components are chosen as standard states. The concentrations and activities of the components in the exchanger are:

$$\begin{aligned} &[A_1 R_{z_1}] = X_1; \qquad &&[A_2 R_{z_2}] = X_2 \\ &\{A_1 R_{z_1}\} = a_{M1} = g_1 X_1; \quad &&\{A_2 R_{z_2}\} = a_{M2} = g_2 X_2\,. \end{aligned} \tag{19}$$

The equilibrium quotient λ_{21} is defined by:

$$\lambda_{21} = \lambda_{12}^{-1} = \frac{\{A_1^{z_1+}\}^{z_2}}{\{A_2^{z_2+}\}^{z_1}} \cdot \frac{X_2^{z_1}}{X_1^{z_2}}. \tag{20}$$

For $z_1 = z_2 = 1$ λ_{21} in (20) and $\varkappa_{21}$ in (8) are of course identical. For the thermodynamic equilibrium constant K_{21}^M of (18) we obtain from (19):

$$K_{21}^M = \frac{\{A_1^{z_1+}\}^{z_2}}{\{A_2^{z_2+}\}^{z_1}} \cdot \frac{(g_2 X_2)^{z_1}}{(g_1 X_1)^{z_2}}. \tag{21}$$

From (20) and (21):

$$\lambda_{21} = K_{21}^M \frac{g_1^{z_2}}{g_2^{z_1}}. \tag{22}$$

Gibbs-Duhem's equation gives:

$$X_1\, d \ln g_1 X_1 + X_2\, d \ln g_2 X_2 = 0. \tag{23}$$

From (2), (4), (22) and (23) we get in the same way as above:

$$\begin{aligned} d \ln g_1 &= \frac{\beta_2}{z_2}\, d \ln \lambda_{21} \\ d \ln g_2 &= -\frac{\beta_1}{z_1}\, d \ln \lambda_{21} = \frac{\beta_1}{z_1}\, d \ln \lambda_{12}. \end{aligned} \tag{24}$$

We introduce the values of g_1, g_2 and λ_{21}, at the limits $\beta_2 = 0$ and $\beta_2 = 1$. Since the pure components are chosen as standard states, g_1' and $g_2'' = 1$, we obtain:

$$\begin{aligned} &\beta_2 = X_2 = 0 \text{ (pure } A_1 R_{z_1}\text{)},\ g_1 = 1,\ \ g_2 = g_2';\ \ \lambda_{21} = \lambda_{21}' \\ &\beta_2 = X_2 = 1 \text{ (pure } A_2 R_{z_2}\text{)},\ g_1 = g_1'',\ g_2 = 1;\ \ \lambda_{21} = \lambda_{21}'' \end{aligned} \tag{25}$$

(24) is transferred to decadic logarithms and with the limiting values defined by (25) we obtain:

$$\begin{aligned} \int_1^{g_1} d \log g_1 &= \log g_1 = \frac{1}{z_2} \int_{\lambda_{21}'}^{\lambda_{21}} \beta_2\, d \log \lambda_{21} \\ \int_1^{g_2} d \log g_2 &= \log g_2 = -\frac{1}{z_1} \int_{\lambda_{21}''}^{\lambda_{21}} \beta_1\, d \log \lambda_{21}. \end{aligned} \tag{26 a, b}$$

Just as for choice (E) one need not make two separate integrations for getting g_1 and g_2. From (22) and (25):

$$\log K_{21}^{M} = \log \lambda_{21}' + z_1 \log g_2'$$

or

$$\log K_{21}^{M} = \log \lambda_{21}'' - z_2 \log g_1''. \tag{27}$$

$\log K_{21}^{M}$ is then obtained from (27) and $\log g_1$ from (22) if $\log g_2$ has been obtained by integration and vice versa.

Even in this case the variation of the water activity should have been taken into consideration, but the error is of the same magnitude, as for choice (*E*).

The connections between choices (*E*) and (*M*)

In order to obtain the relations between the quantities obtained with choices (*E*) and (*M*) we make use of the simple relation that holds between the "molecular weights" of $A_{1/z}R$ and AR_z.

The chemical potentials of the components are:

$$\begin{aligned} &\text{I.}\quad \mu_{1E} = \mu_{1E}^{0} + RT \ln \gamma_1 \beta_1; \quad \mu_{2E} = \mu_{2E}^{0} + RT \ln \gamma_2 \beta_2 \\ &\text{II.}\quad \mu_{1M} = \mu_{1M}^{0} + RT \ln g_1 X_1; \quad \mu_{2M} = \mu_{2M}^{0} + RT \ln g_2 X_2. \end{aligned} \tag{28}$$

Since the molecular weight of $A_1 R_{z_1}$ is z_1 times that of $(A_1)_{1/z_1} R$ and the molecular weight of $A_2 R_{z_2}$ is z_2 times that of $(A_2)_{1/z_2} R$ we obtain:

$$\mu_{1M} = z_1 \mu_{1E}; \quad \mu_{2M} = z_2 \mu_{2E}. \tag{29}$$

Since the standard states are the same for choices (*E*) and (*M*), namely the pure components, we get from (29),

$$\mu_{1M}^{0} = z_1 \mu_{1E}^{0}; \quad \mu_{2M}^{0} = z_2 \mu_{2E}^{0}. \tag{30}$$

From (28), (29) and (30) we derive the following relations between the activities of (*E*) and (*M*):

$$\begin{aligned} g_1 X_1 &= (\gamma_1 \beta_1)^{z_1} \\ g_2 X_2 &= (\gamma_2 \beta_2)^{z_2}. \end{aligned} \tag{31}$$

This equation makes it possible, either to calculate γ_1, γ_2 from (16), (17) and (10) and g_1, g_2 from (31) or to find g_1, g_2 from (26), (27) and (22) and γ_1, γ_2 from (31). All the quantities $\gamma_1, \gamma_2, g_1, g_2$ can thus be obtained by only *one* integration. From (9), (21) and (31) we find

$$K_{21}^{E} = K_{21}^{M} = K_{21}. \tag{32}$$

The thermodynamic equilibrium constants of reactions (6) and (18) are thus equal as one might have seen directly.

ΔG° for the reaction:

$$z_1 A_2^{z_2+} + z_2 A_1 R_{z_1} \rightleftarrows z_2 A_1^{z_1+} + z_1 A_2 R_{z_2} \tag{18}$$

can be calculated from (32) according to the equation:

$$\Delta G^{\circ} = -RT \ln K_{21}. \tag{33}$$

From (3), (10), (22), (31), and (32) we obtain the following relation between λ_{21} and $\varkappa_{21}$:

$$\lambda_{21} = \left(\frac{z_1}{z_2}\right)^{z_1 z_2} \cdot \frac{X_1^{z_2(z_1-1)}}{X_2^{z_1(z_2-1)}} \cdot \varkappa_{21}. \tag{34}$$

The limiting values of activity factors and equilibrium quotients

The evaluation of the activity factors depends upon the existence of finite limits for the values in (15) and (25). Table 1 shows the possible cases. $\varkappa_{21}$ respectively λ_{21} can be zero, finite or infinite. The corresponding λ_{21} respectively $\varkappa_{21}$ values are obtained from (34). From (10) and (22) g' and γ_2' are obtained considering that $\gamma_1 = g_1 = 1$. An analogous discussion is made for $\varkappa_{21}''$ and λ_{21}''. It may be mentioned that the two halves of Table 1 are independent of each other.

From Table 1 for example, it is seen that λ_{21}' and g_2' cannot have finite limits simultaneously with $\varkappa_{21}'$ and γ' when $z_1 = 1$, $z_2 = 2$. In order to decide whether to choose (*E*) or (*M*) for calculating the activity factors, log $\varkappa(\beta)$ and log $\lambda(\beta)$ may be plotted. It is convenient to choose that function, if any which seems to have finite limits.

Table 1

The connections between the limiting values in (15) and (25)

Charge	Pure A_1R				Pure A_2R			
	$\varkappa_{21}' = \lambda_{21}'$		$\gamma_2' = g_2'$		$\varkappa_{21}'' = \lambda_{21}''$		$\gamma_1'' = g_1''$	
$z_1 = 1$ $z_2 = 1$	0 Finite ∞		∞ Finite 0		0 Finite ∞		0 Finite ∞	
	$\varkappa_{21}'$	λ_{21}'	γ_2'	g_2'	$\varkappa_{21}''$	λ_{21}''	γ_1''	g_1''
$z_1 = 1$ $z_2 \neq 1$	0 0 Finite ∞	0 Finite ∞ ∞	∞ ∞ Finite 0	∞ Finite 0 0	0 Finite ∞	0 Finite ∞	0 Finite ∞	0 Finite ∞
$z_1 \neq 1$ $z_2 = 1$	0 Finite ∞	0 Finite ∞	∞ Finite 0	∞ Finite 0	0 Finite ∞ ∞	0 0 Finite ∞	0 Finite ∞ ∞	0 0 Finite ∞
$z_1 \neq 1$ $z_2 \neq 1$	0 Finite ∞ 0	0 ∞ ∞ Finite	∞ Finite 0 ∞	∞ 0 0 Finite	0 Finite ∞ ∞	0 0 Finite ∞	0 Finite ∞ ∞	0 0 Finite ∞

Applications

I have applied the equations developed above to calculate the activity factors of the components in ion exchangers to a number of equilibrium data in the literature. The systems chosen were the $Ag^+ - H^+$ exchange on Wofatit KS and Dowex 50 in Part I [3] and the $Ba^{2+} - H^+$ exchange on Dowex 50 studied by MARINSKY [7] and by DUNCAN and LISTER [10].

Uni-univalent exchange: First let us write down the equations for evaluating the activity factors. As $z_1 = z_2 = 1$ the exchange reaction is:

$$A_2^+ + A_1 R \rightleftarrows A_1^+ + A_2 R. \tag{35}$$

From (1) and (2) $X_1 = \beta_1$, $X_2 = \beta_2$ and from (31) and (34) $g_1 = \gamma_1$, $g_2 = \gamma_2$, $\lambda_{21} = \varkappa_{21}$. For brevity we set $K_{21} = K$, $\varkappa_{21} = \varkappa$, $\beta_2 = \beta$, $\beta_1 = 1 - \beta$, and $a_{E1} = a_{M1} = a_1$, $a_{E2} = a_{M2} = a_2$.

From (16)

$$\begin{aligned} \int_1^{\gamma_1} d \log \gamma_1 &= \log \gamma_1 = -\int_{\varkappa'}^{\varkappa} \beta \, d \log \varkappa \\ \int_1^{\gamma_2} d \log \gamma_2 &= \log \gamma_2 = -\int_{\varkappa''}^{\varkappa} (1-\beta) \, d \log \varkappa . \end{aligned} \tag{36 a, b}$$

From (10):

$$K = \varkappa \frac{\gamma_2}{\gamma_1}. \tag{37}$$

From (17):

$$\begin{aligned} &\log K = \log \varkappa' + \log \gamma' \\ \text{and} \quad &\log K = \log \varkappa'' - \log \gamma_1''. \end{aligned} \tag{38}$$

Equations (36)–(38) have been applied to the exchange between $H^+ = A_1^+$ and $Ag^+ = A_2^+$ on Wofatit KS and Dowex 50. In Table 2 the values of γ_1'', γ_2', $\varkappa'$, $\varkappa''$, K and ΔG° are given for the two exchangers. For detailed information on the calculations see the Appendix.

In Figs. 1 and 2 $\log \varkappa$ is plotted against β for Wofatit KS and Dowex 50. In Figs. 3, 4, 5 and 6 the activity factors and activities are plotted against β for the two exchangers.

Table 2

Some limiting values and constants for the exchange $Ag^+ - H^+$ on Wofatit KS and Dowex 50 [3]

Ion exchanger	γ_1''	γ_2'	$\varkappa'$	$\varkappa''$	K	ΔG° from (33) kcal/mole
Wofatit KS............	0.547	0.187	27.5	2.82	5.16	−0.97
Dowex 50	1.44	0.624	15.9	14.2	9.90	−1.36

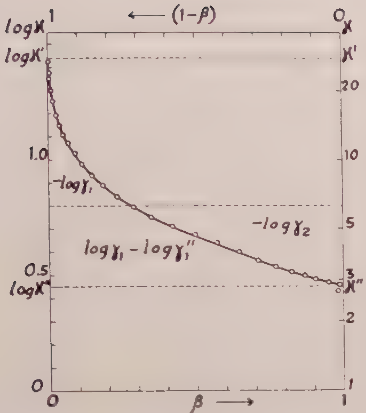

Fig. 1.

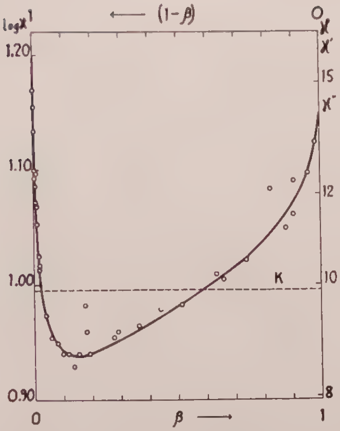

Fig. 2.

Figs. 1–2. log $\varkappa$ is plotted against β for the Ag^+–H^+ exchange. Fig. 1 gives $\varkappa$ for Wofatit KS. For $\beta \geq 0.04$ the points were calculated from an elution curve, for lower β from static measurements. The areas — log γ_1, log γ_1 — log γ_1'' and — log γ_2 are marked out. Fig. 2 gives $\varkappa$ for Dowex 50. The dotted line gives the value of log K, which is the average value of log $\varkappa$.

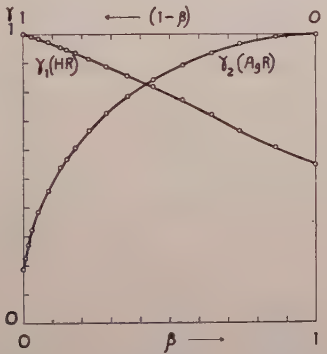

Fig. 3.

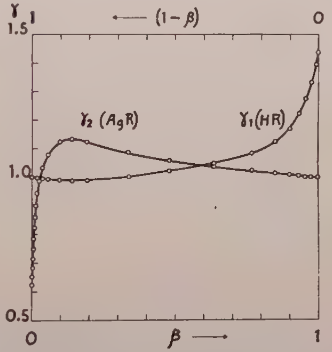

Fig. 4.

Figs. 3–4. The activity factors γ_1 and γ_2 are plotted against β for the Ag^+–H^+ exchange. Fig. 3 gives γ for Wofatit KS. Fig. 4 gives γ for Dowex 50.

Uni-divalent exchange. Let $H^+ = A_1^{z_1+}$ and $Ba^{2+} = A_2^{z_2+}$; then the functions $\varkappa_{21}$ and λ_{21} are according to (8) and (20):

$$\varkappa_{21} = \varkappa_{12}^{-1} = \frac{\{H^+\}^2}{\{Ba^{2+}\}} \cdot \frac{[Ba_{1/2}R]^2}{[HR]^2} = \frac{f_1^2 c_1^2}{f_2 c_2} \cdot \left(\frac{\beta_2}{\beta_1}\right)^2 \tag{39}$$

and

$$\lambda_{21} = \lambda_{12}^{-1} = \frac{\{H^+\}^2}{\{Ba^{2+}\}} \cdot \frac{[Ba\ R_2]}{[HR]^2} = \frac{f_1^2 c_1^2}{f_2 c_2} \cdot \frac{X_2}{X_1^2}. \tag{40}$$

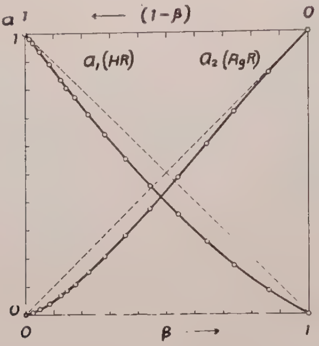

Fig. 5.

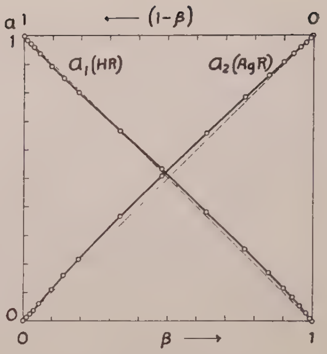

Fig. 6.

Figs. 5–6. The activities a_1 and a_2 are plotted against β for the Ag^+–H^+ exchange. Fig. 5 gives a for Wofatit KS. Fig. 6 gives a for Dowex 50. The dotted lines give a_1 and a_2 if Rauolt's law were valid.

f_1, f_2 and c_1, c_2 are the activity factors and concentrations of H^+ and Ba^{2+} in the liquid solution.

The functions $\varkappa_{21}$ and λ_{21} defined above have been calculated from the primary values in the papers by MARINSKY [7], and DUNCAN and LISTER [10]. The equations of both choices (E) and (M) have been applied to the two sets of measurements. It may be mentioned that MARINSKY treated his resin with NaOH in order to obtain a more homogeneous product whereas DUNCAN and LISTER mention no pretreatment of their resin. In Table 3 the values of γ_1'', γ_2', g_1'', g_2', $\varkappa_{21}'$, $\varkappa_{21}''$, λ_{21}', λ_{21}'', K and ΔG° are given for the two investigations. For detailed information on the calculations see the Appendix.

In Figs. 7 and 8 log $\varkappa_{21}$ and log λ_{21} are plotted against β_2, in Figs. 9 and 10, γ_1 and γ_2 against β_2, in Figs. 11 a, b g_1 and g_2 against X_2, in Figs. 12 and 13 a_{E1}, a_{E2} against β_2 and in Figs. 14 and 15 a_{M1}, a_{M2} against X_2 for the two sets of measurements.

Discussion: By comparing for instance Figs. 5, 12 and 15 it is seen that the systems studied can be divided into three main types: 1) those with only negative deviations from Raoult's law (Fig. 5), 2) those with only positive deviations (Fig. 12), and 3) those with both positive and negative deviations (Fig. 15). It is also seen from the equilibrium quotient curves (see for instance

Table 3

Some limiting values and constants for the exchange Ba^{2+}—H^+ on Dowex 50 from the measurements by MARINSKY [7] and DUNCAN and LISTER [10]

Investigator	γ_1''	γ_2'	g_1''	g_2'	$\varkappa_{21}'$	$\varkappa_{21}''$	λ_{21}'	λ_{21}''	K	ΔG° from (33) kcal/mole
Marinsky	2.06	∞	0.998	0.573	(0)	589	245	141	140	−2.92
Duncan and Lister	1.61	∞	0.809	(8.41)	(0)	229	(10)	55.0	84.1	−2.62

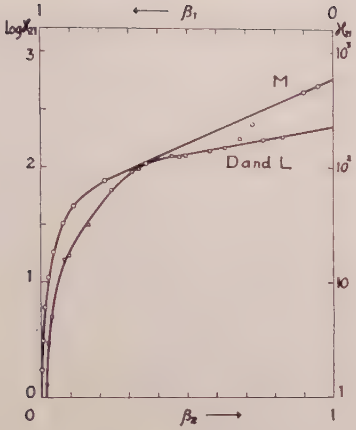

Fig. 7.

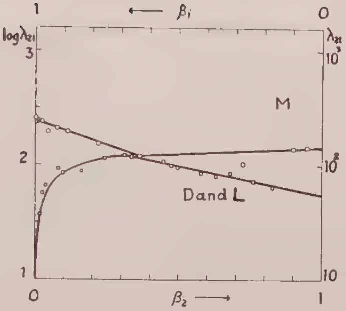

Fig. 8.

Fig. 7. log $\varkappa_{21}$ is plotted against β_2 for the Ba^{2+}–H^+ exchange on Dowex 50. ○: MARINSKY. □: DUNCAN and LISTER.

Fig. 8. log λ_{21} is plotted against β_2 for the Ba^{2+}–H^+ exchange on Dowex 50. ○: MARINSKY. □: DUNCAN and LISTER.

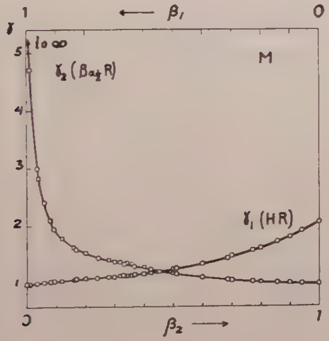

Fig. 9.

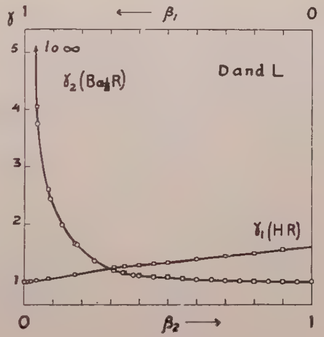

Fig. 10.

Figs. 9–10. The activity factors γ_1 and γ_2 are plotted against β_2 for the Ba^{2+}–H^+ exchange on Dowex 50. Fig. 9 gives γ from MARINSKY's measurements. ○: Values calculated from choice (*E*). □: Values calculated from choice (*M*). Fig. 10 gives γ from DUNCAN's and LISTER's measurements. ○: Values calculated from choice (*E*). □: Values calculated from choice (*M*).

Figs. 1, 7 and 8) that negative deviations seem to be connected with equilibrium quotients decreasing with β_2 and positive deviations with increasing equilibrium quotients. Those with both positive and negative deviations seem to be connected with the equilibrium quotient curves having a maximum or minimum.

These observations can be made into a general law. The following argument uses (*E*), but an analogous proof can be made with (*M*).

To find the conditions for positive or negative deviations let us transform (14):

$$\frac{d\ln\varkappa_{21}}{d\beta_2} = \frac{1}{\varkappa_{21}}\frac{d\varkappa_{21}}{d\beta_2} = +\frac{z_1 z_2}{\gamma_1\beta_2}\frac{d\gamma_1}{d\beta_2} = -\frac{z_1 z_2}{\gamma_2\beta_1}\frac{d\gamma_2}{d\beta_2}. \qquad (41)$$

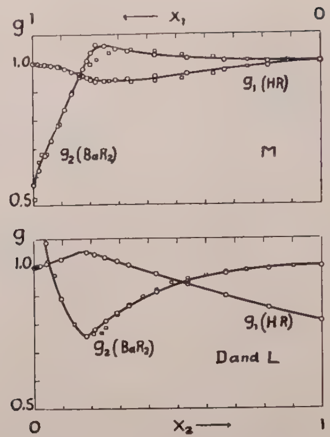

Fig. 11. The activity factors g_1 and g_2 are plotted against X_2 for the Ba^{2+}–H^+ exchange on Dowex 50. Fig. 11 a gives g from MARINSKY's measurements. ○: Values calculated from choice (M). □: Values calculated from choice (E). Fig. 11 b gives g from DUNCAN's and LISTER's measurements. ○: Values calculated from choice (M). □: Values calculated from choice (E).

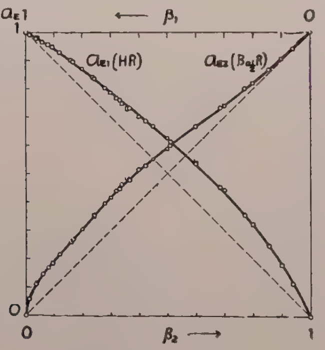

Fig. 12.

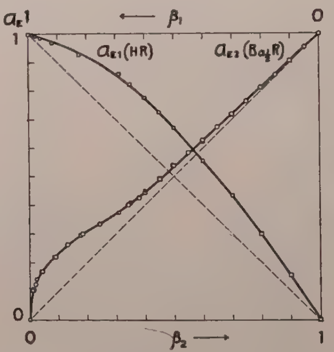

Fig. 13.

Figs. 12–13. The activities a_{E1} and a_{E2} are plotted against β_2 for the Ba^{2+}–H^+ exchange on Dowex 50. Fig. 12 gives a_E from MARINSKY's measurements. ○: Values calculated from choice (E). □: Values calculated from choice (M). Fig. 13 gives a_E from DUNCAN's and LISTER's measurements. ○: Values calculated from choice (E). □: Values calculated from choice (M). The dotted lines give a_{E1} and a_{E2} if Raoult's law were valid.

From definition $\gamma_1 = 1$ for $\beta_1 = 1$ and $\gamma_2 = 1$ for $\beta_2 = 1$.

If for instance $\frac{d\varkappa_{21}}{d\beta_2} < 0$ in the interval $0 \leq \beta_2 \leq 1$, we obtain from (41) $\frac{d\gamma_1}{d\beta_2} < 0$ and $\frac{d\gamma_2}{d\beta_2} > 0$. Thus when we go from $\beta_2 = 0$ to $\beta_2 = 1$ γ_1 must decrease from 1 to γ_1'' and γ_2 must increase from γ_2' to 1. Thus $\gamma_1 \leq 1$, $\gamma_2 \leq 1$ in the interval $0 \leq \beta_2 \leq 1$ which means that we have negative deviation from Raoult's law. This shows that a decreasing $\varkappa_{21}(\beta_2)$ curve gives negative deviations from

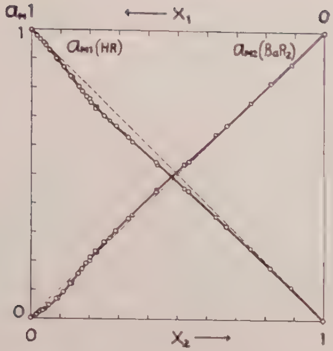

Fig. 14.

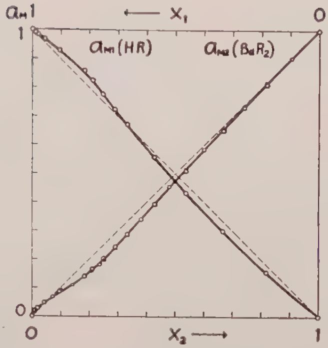

Fig. 15.

Figs. 14 – 15. The activities a_{M1} and a_{M2} are plotted against X_2 for the B_a^{2+}–H^+ exchange on Dowex 50. Fig. 14 gives a_M from MARINSKY's measurements. ○: Values calculated from choice (M). □: Values calculated from choice (E). Fig. 15 gives a_M from DUNCAN's and LISTER's measurements. ○: Values calculated from choice (M). □: Values calculated from choice (E). The dotted lines give a_{M1} and a_{M2} if Raoult's law were valid.

Raoult's law. In the same manner $\frac{d\varkappa_{21}}{d\beta_2} > 0$ gives rise to positive deviations. A curve with a maximum or minimum must cause both positive and negative deviations. Consider a curve with a maximum in the point $\beta_2 = \bar{\beta}_2$. Thus $\frac{d\varkappa_{21}}{d\beta_2} > 0$ for $0 \leq \beta_2 < \bar{\beta}_2$ and $\frac{d\varkappa_{21}}{d\beta_2} < 0$ for $\bar{\beta}_2 < \beta_2 \leq 1$. From (41) γ_1 rises from 1 to a maximum $\bar{\gamma}_1$ at $\beta_2 = \bar{\beta}_2$ and then it must decrease from $\bar{\gamma}_1$ to γ_1'' when β_2 approaches 1. Analogously γ_2 must decrease from γ_2' to $\bar{\gamma}_2$ at $\beta_2 = \bar{\beta}_2$ and then it must increase to 1 when β_2 approaches 1.

If $\gamma_1'' \geq 1$ $a_1 \geq X_1$ in the whole interval. If $\gamma_1'' < 1$ $a_1 \lesseqgtr X_1$.

If $\gamma_2' > 1$ $a_2 \gtreqless X_2$ and if $\gamma_2' < 1$ $a_2 \leq X_2$ in the whole interval. For a curve with a minimum an analogous discussion can be made.

From Figs. 1, 2, 7 and 8 it is seen that the Ag^+—H^+ exchange on Wofatit KS is of type 1, choice (E) for Ba^{2+}—H^+ on Dowex 50 according to both MARINSKY and DUNCAN and LISTER give curves of type 2 while the remaining exchanges studied in this paper belong to type 3.

When comparing the two choices (E) and (M), the latter in this special case seems to be the most useful one. To begin with it gives more sensitive functions than choice (E). For instance with (M) the measurements of MARINSKY and those of DUNCAN and LISTER give very different curves as is seen from Figs. 8, 11, 14, and 15. With choice (E) they give curves of essentially the same form as is seen from Figs. 7, 9, 10, 12, and 13. This way of representation does not bear out the difference between the two sets of measurements. Secondly, the activity factor curves obtained with (M) resemble more those for univalent ions, cf. Figs. 3, 4 and 11. Last but not least (M) seems to give finite values of log λ_{21}', a fact which permits integration of (26), while log $\varkappa_{21}'$ seems to tend towards $-\infty$.

From Figs. 9, 10 and 11 it is seen that the deviations in γ_1, γ_2 and g_1, g_2 calculated from (31) compared with those obtained directly by integration are small. They are of course due to the fact that the smoothed curves log $\varkappa_{21}(\beta_2)$ and log $\lambda_{21}(\beta_2)$ are not exactly equivalent.

The considerable difference between the measurements of MARINSKY and DUNCAN and LISTER may be due to the pretreatment of MARINSKY's resin. In addition samples from different batches may not always have the same properties.

As is seen from Figs. 3, 5, 9, and 12 the activity factors and activities of types 1 and 2 resemble those of non-ideal liquid mixtures, cf. for instance those of the chloroform-acetone and the carbondisulfide-acetone systems, calculated from the measurements by ZAWIDSKY [11] and reproduced in HILDEBRAND-SCOTT [12].

DOLEZALEK [13] has shown that for liquid mixtures activity factors and activity curves of type 1 could be explained in certain cases, by assuming compound formation and those of type 2 by assuming association of one of the components. In a following paper an attempt will be made to account for the deviations from ideality in a way analogous to that made for liquid mixtures by assuming association, dissociation, compound formation and perhaps some other mechanisms too.

SUMMARY

By formally regarding an ion exchanger containing two ionic species as a binary non-ideal mixture the activity factors of the components and the thermodynamic equilibrium constant can be evaluated by means of graphical integration of the functions log $\varkappa_{21}(\beta_2)$ or log $\lambda_{21}(\beta_2)$. $\varkappa_{21}$ and λ_{21} are the equilibrium quotients defined by equations (8) and (20) and β_2 the equivalent fraction defined by (1).

In the evaluation of the equations for the graphical integration the variation of the water activity has not been taken into consideration. In the Appendix it is shown that no serious error has been introduced in this way.

The problem can be treated formally in two ways by assuming the components to be either $(A_1)_{1/z_1}R$, $(A_2)_{1/z_2}R$, ["choice (E)"] or AR_{z_1}, AR_{z_2}, ["choice (M)"]. For $z_1 = z_2 = 1$ the choices (E) and (M) are of course equal. The equations (16) and (26) derived from the above mentioned assumptions have been applied to the data of 4 different ion exchange equilibrium studies: the $Ag^+—H^+$ exchange on Wofatit KS and Dowex 50 by HÖGFELDT, EKEDAHL and SILLÉN [3] where $(E) = (M)$ and the $Ba^{2+}—H^+$ exchange on Dowex 50 by MARINSKY [7] and by DUNCAN and LISTER [10], where both (E) and (M) have been applied. (M) seems in these cases to be the most fruitful approach, as it gives more sensitive functions than (E), cf. Figs 7, 8, 9, 10, and 11. Moreover the equilibrium quotient λ_{21} seems to have finite limiting values in contrast to $\varkappa_{21}$, which is necessary for the integration.

The systems studied contain examples of all three possible kinds of deviation from Raoult's law, cf. Figs. 5, 12, and 15. It is shown that a decreasing $\varkappa_{21}(\beta_2)$, $(\lambda_{21}(\beta_2))$ curve will give negative deviations from Raoult's law, an increasing curve gives positive deviations and a curve with a maximum or minimum will give both positive and negative deviations.

Acknowledgements: I wish to thank Professor GUSTAF LJUNGGREN and Professor ARNE ÖLANDER for their interest in my work. I wish also to thank Professor L. G. SILLÉN, who gave me the idea to carry out this work and since then has helped me in many ways. I have also had many valuable discussions with Mr. ERIK EKEDAHL.

Note: When the preliminary communications on this work [4 6] were published and this paper was written for publication my attention was called to a paper by W. J. ARGERSINGER et. al. [14], which seems to have been published at about the same time as the preliminary communications. Their paper contains essentially the same approach as above, although only (M) was considered. The equations analogous to (24) were integrated by parts and the graphical integration was thus made with elements analogous to $\log \lambda \, d\beta$ instead of $\beta \, d \log \lambda$ as is done here. The equations arrived at were applied to an investigation of the $Na^+ - H^+$ exchange on Dowex 50.

Appendix

Calculations

The water activity:

In the derivation of the equations for the graphical integration, the variation of the water activity has not been taken into consideration. In order to get an idea of the magnitude of the error so introduced we shall apply Gibbs—Duhem's equation to the tertiary system of $(A_1)_{1/z_1}R$, $(A_2)_{1/z_2}R$ and H_2O, choice (E). The application to choice (M) is quite analogous.

$$\beta_1 \, d \ln (\beta_1 \gamma_1) + \beta_2 \, d \ln (\beta_2 \gamma_2) + q \, d \ln a_{H_2O} = 0 \tag{11'}$$

where q = moles water/mole R^- and a_{H_2O} = the water activity.

From (1) and (11′):

$$\beta_1 \, d \ln \gamma_1 + \beta_2 \, d \ln \gamma_2 + q \, d \ln a_{H_2O} = 0 . \tag{12'}$$

From (12′) and (13):

$$\left.\begin{aligned} d \ln \gamma_1 &= \frac{\beta_2}{z_1 z_2} d \ln \varkappa_{21} - q \, d \ln a_{H_2O} \\ d \ln \gamma_2 &= -\frac{\beta_1}{z_1 z_2} d \ln \varkappa_{21} - q \, d \ln a_{H_2O} . \end{aligned}\right\} \tag{14'}$$

By integrating (14′) we obtain:

$$\left.\begin{aligned} \log \gamma_1 &= \frac{1}{z_1 z_2} \int_{\varkappa'_{21}}^{\varkappa_{21}} \beta_2 \, d \log \varkappa_{21} - \int_{a'_{H_2O}}^{a_{H_2O}} q \, d \log a_{H_2O} \\ \log \gamma_2 &= -\frac{1}{z_1 z_2} \int_{\varkappa''_{21}}^{\varkappa_{21}} \beta_1 \, d \log \varkappa_{21} - \int_{a''_{H_2O}}^{a_{H_2O}} q \, d \log a_{H_2O} \end{aligned}\right\} \tag{16 a, b'}$$

where a'_{H_2O} and a''_{H_2O} are the water activities for pure $(A_1)_{1/z_1}R$ and $(A_2)_{1/z_2}R$. Both

$$\int_{a'_{H_2O}}^{a_{H_2O}} q\, d \log a_{H_2O} \text{ and } \int_{a''_{H_2O}}^{a_{H_2O}} q\, d \log a_{H_2O} < \Delta = q_{\max} \cdot \log a''_{H_2O}/a'_{H_2O}.$$

As we have equilibrium the water activity must be the same in the solution and in the exchanger. The water activity in dilute aqueous solutions can be calculated from freezing-point depressions according to the formula [15]

$$-\ln a_{H_2O} = 9.696\ 10^{-3}\,\vartheta + 5{,}1 \cdot 10^{-6}\,\vartheta^2 \qquad (A_1)$$

where ϑ = the freezing point depression. Rough values of ϑ may be interpolated from Landolt-Börnstein. As an example we may calculate Δ for the $Ag^+—H^+$ exchange on Wofatit KS.

In 100.0 mC HNO_3 $\vartheta = 0.35$ [16]
From (A_1) we obtain $\log a'_{H_2O} = -0.0078$
In 100.0 mC $AgNO_3$ $\vartheta = 0.33$ [17] (interpolated)
From (A_1) $\log a''_{H_2O} = -0.0074$.

Wofatit KS has approximately the sorption capacity of $2 \cdot 10^{-3}$ moles/g air dried resin [3]. According to SAMUELSON [18] 1 g Wofatit KS dried over P_2O_5 takes up 0.50 g H_2O over 2.5 C H_2SO_4. We use these values in order to get a rough value of $q_{\max}$ and Δ.

$$\Delta = \frac{0.50}{18 \cdot 2 \cdot 10^{-3}}(-0.0074 + 0.0078) = 0.005.$$

The total integrated area can be obtained from Table 5. It is found to be 0.9900 and $\Delta = 0.5\,\%$ of 0.9900. The value of Δ is thus small and may be neglected. For the other exchanges studied analogous discussions give similar results.

It may be pointed out that for multivalent ions the error caused by the neglection of Δ is larger than for univalent ions. However, the uncertainty of the activity factors in the solution is also larger, so that values for exchanges concerning multivalent ions are always more uncertain than values for exchanges between monovalent ions.

The accuracy:

The activity factors and activities are given with 4 or 5 digits to avoid errors in the calculations, but these quantities are probably only reproducible within 2 or 3 figures as the spread in the equilibrium quotient is about ± 5 % [3].

1. The $Ag^+—H^+$ exchange on Wofatit KS

Table 4 contains $\varkappa$ and β values obtained from an elution curve measured by EKEDAHL [19]. The rate of flow was so low that the $\varkappa(\beta)$ curve obtained from the elution data agreed with that obtained from static measurements within the experimental limits. For further information on this subject, see the theoretical papers by SILLÉN [20—21] and the short communication on the experimental work in Nature [22]. For $\beta < 0.04$ the values are taken from Table 7 a in Part I [3] and in Fig. 1 $\log \varkappa$ is plotted against β.

Table 4

$\varkappa$ and β values obtained from an elution curve [19]. The ionic strength I = 0.1000 C. The $Ag^+ - H^+$ exchange on Wofatit KS

β	$\varkappa$	log $\varkappa$	β	$\varkappa$	log $\varkappa$
0.0399	14.27	1.154	0.7128	3.66	0.563
0.0532	13.06	1.116	0.7744	3.43	0.535
0.0700	11.83	1.073	0.8276	3.26	0.513
0.0910	10.67	1.028	0.8724	3.14	0.497
0.1169	9.59	0.982	0.9077	3.03	0.481
0.1493	8.60	0.934	0.9340	2.97	0.473
0.1883	7.72	0.888	0.9539	2.93	0.467
0.2355	6.93	0.841	0.9673	2.90	0.462
0.2906	6.24	0.795	0.9776	2.81	0.449
0.3531	5.65	0.752	0.9840	2.69	0.430
0.4242	5.15	0.712	0.9891	2.86	0.456
0.4993	4.73	0.675	0.9930	2.79	0.446
0.5745	4.35	0.638	0.9974	2.15	0.332
0.6474	4.00	0.602			

From Fig. 1 one finds by extrapolation:

$$\log \varkappa' = 1.440 \qquad \log \varkappa'' = 0.450$$
$$\varkappa' = 27.5 \qquad \varkappa'' = 2.82\,. \tag{42}$$

The integration was performed by means of Simpson's formula. First $\log \gamma_1$ was calculated for round $\log \varkappa$ values by means of (36 a). The corresponding area is marked out in Fig. 1. Then the thermodynamic equilibrium constant was obtained from (38). Now, for each β, $\log \gamma_2$ was obtained from (37):

$$\log \gamma_2 = \log K + \log \gamma_1 - \log \varkappa\,. \tag{43}$$

From the integration

$$\log \gamma_1'' = -0.2623_7\,. \tag{44}$$

By inserting the value of $\log \varkappa''$ and $\log \gamma_1''$ from (42) and (44) in (38) we obtain:

$$\log K = 0.7123_7\ ;\quad K = 5.16\,. \tag{45}$$

From (33) and (45) with T = 298

$$\Delta G^\circ = -0.971 \text{ kcal/mole}\,. \tag{46}$$

In Table 5 about every third point from the integration is listed. The activities calculated from equation (7) are also given.

In Figs. 3 and 5 γ_1, γ_2 and a_1, a_2 are plotted as functions of β.

Table 5

Activity factors and activities of HR ($=1$) and AgR ($=2$). The $Ag^+ - H^+$ exchange on Wofatit KS. I = 0.1000 C

β	$\log \varkappa$	$\log \gamma_1$	γ_1	$\log \gamma_2$	γ_2	a_1 from (7)	a_2 from (7)
0.000	1.440_0	0.000	1.000	-0.7276_3	0.187_2	1.000	0.000
0.0278	1.200_0	-0.0028_7	0.993_4	-0.4905_0	0.323_2	0.965_8	0.009_0
0.127_4	0.960_0	-0.0198_2	0.955_4	-0.2674_5	0.540_2	0.833_7	0.068_8
0.225_2	0.850_0	-0.0382_6	0.915_7	-0.1758_9	0.667_0	0.709_5	0.150_2
0.443_8	0.700_0	-0.0868_9	0.818_7	-0.0745_2	0.842_3	0.455_4	0.373_8
0.740_0	0.550_0	-0.1759_4	0.666_9	-0.0135_7	0.969_2	0.173_4	0.717_2
1.000	0.450_0	-0.2623_7	0.546_6	0.000	1.000	0.000	1.000

As an example we shall calculate γ_1 and γ_2 for $\beta = 0.225_2$. By graphical integration $\log \gamma_1 = -0.0382_6$ and thus $\gamma_1 = 0.915_7$. From (45) and (43): $\log \gamma_2 = 0.71237 - 0.03826 - 0.8500 = -0.1758_9$, and thus $\gamma_2 = 0.667_0$, from (7)

$$a_1 = 0.7748 \cdot 0.9157 = 0.709_5$$

$$a_2 = 0.2252 \cdot 0.6670 = 0.150_2 \,.$$

2. The $Ag^+ - H^+$ exchange on Dowex 50

Fig. 2 gives $\log \varkappa$ as function of β. The values are taken from Table 8 in Part I [3]. There is a minimum $\varkappa$-value, $\varkappa_{\min}$ at $\beta = 0.140$. From Fig. 2 one finds:

$$\begin{array}{lll} \log \varkappa' = 1.200 & \log \varkappa_{\min} = 0.936 & \log \varkappa'' = 1.153 \\ \varkappa' = 15.8_5 & \varkappa_{\min} = 8.63 & \varkappa'' = 14.2_2 \end{array} \tag{47}$$

The graphical integration was performed principally in the same manner as for Wofatit KS. First a set of $\log \gamma_1$ values were obtained by integrating (36 a) from $\beta = 0$ to $\beta = 0.140$ and another set of $\log \gamma_2$ values by integrating (36 b) from $\beta = 1$ to $\beta = 0.140$. Then $\log K$ was obtained from (37):

$$\log K = \log \varkappa_{\min} + \log \gamma_{2\,\min} - \log \gamma_{1\,\min} \,. \tag{48}$$

The corresponding $\log \gamma_2$ values in the interval $\beta = 0 - 0.140$ and $\log \gamma_1$ values in the interval $\beta = 0.140 - 1$ were then obtained from (37).

From the integration:

$$\begin{array}{ll} \log \gamma_{1\,\min} = -0.0048_{70} & \log \gamma_{2\,\min} = 0.0545_{77} \\ \gamma_{1\,\min} = 0.989 & \gamma_{2\,\min} = 1.13 \,. \end{array} \tag{49}$$

By inserting the values from (47) and (49) in (48) we obtain:

$$\log K = 0.9954_{47}\,; \quad K = 9.90 \,. \tag{50}$$

Table 6

Activity factors and activities of HR (= 1) and AgR (= 2). The Ag^+-H^+ exchange on Dowex 50. I = 0.1000 C

β	$\log \varkappa$	$\log \gamma_1$	γ_1	$\log \gamma_2$	γ_2	a_1 from (7)	a_2 from (7)
0.000	1.200	0.000	1.000	-0.2045_{53}	0.624_{38}	1.000	0.000
0.003_5	1.120	0.0001_{15}	0.999_{67}	0.1246_{98}	0.750_{42}	0.996_2	0.002_6
0.013_0	1.040	-0.0007_{57}	0.998_{26}	-0.0453_{10}	0.900_{93}	0.985_3	0.011_7
0.055_4	0.960	-0.0029_{28}	0.993_{28}	0.0325_{19}	1.07_{77}	0.938_3	0.059_7
0.336_3	0.960	0.0011_{63}	1.00_{26}	0.0366_{13}	1.08_{80}	0.665_4	0.365_9
0.848_6	1.040	0.0507_{79}	1.12_{40}	0.0062_{26}	1.01_{44}	0.170_2	0.860_8
0.956_8	1.100	0.1055_{37}	1.27_{51}	0.0009_{84}	1.00_{23}	0.055_1	0.959_0
1.000	1.153	0.1575_{53}	1.43_{73}	0.000	1.000	0.000	1.000

From (33) and (50) with $T = 298$

$$\Delta G^\circ = -1.35_7 \quad \text{kcal/mole}. \tag{51}$$

In table 6 about every fourth point from the integration is listed. The activities calculated from (7) are also given.

In Figs. 4 and 6 γ_1, γ_2 and a_1, a_2 are plotted as functions of β.

3. The $Ba^{2+}-H^+$ exchange on Dowex 50 according to MARINSKY [7]

J. A. MARINSKY [7] has studied the exchange reaction between Ba^{2+} and H^+ on Dowex 50. In order to get a more homogeneous product than the commercial one he treated the resin for 48 hours with 6 C NaOH at 95° C. By means of ordinary analytical and radiochemical methods a large concentration range could be covered, the experimental points were, however, rather few and unevenly distributed.

Table 7 gives $\varkappa_{21}$ and λ_{21} calculated with (39) and (40) from the data in Table 6 in MARINSKY's paper [7] with the notation H^+ (= 1) and Ba^{2+} (= 2).

Table 7

Equilibrium quotients $\varkappa_{21}$ and λ_{21} for the exchange $Ba^{2+}-H^+$ on Dowex 50. The data taken from MARINSKY [7]. I varies from 0.104—0.228

c_1	c_2	f_1^2/f_2	β_1 from (1)	β_2 from (1)	$\varkappa_{21}$ from (39)	$\log \varkappa_{21}$	X_1 from (2)	X_2 from (5)	λ_{21} from (40)	$\log \lambda_{21}$
0.1036	$1.27 \cdot 10^{-7}$	1.78	0.996_6	0.003_{40}	1.75	0.243	0.998_3	0.001_{70}	257	2.410
0.1036	$2.62 \cdot 10^{-7}$	1.78	0.993_6	0.006_{44}	3.06	0.486	0.996_8	0.003_{23}	237	2.375
0.1037	$5.12 \cdot 10^{-7}$	1.78	0.987_5	0.012_5	5.99	0.777	0.993_7	0.006_{29}	238	2.377
0.1037	$9.39 \cdot 10^{-7}$	1.78	0.977_4	0.022_6	10.9	1.037	0.988_6	0.011_4	238	2.377
0.1039	$2.39 \cdot 10^{-6}$	1.78	0.954_6	0.045_4	18.2	1.260	0.976_8	0.023_2	195	2.290
0.1043	$3.92 \cdot 10^{-6}$	1.78	0.924_9	0.075_1	32.6	1.513	0.961_0	0.039_0	209	2.320
0.1048	$6.81 \cdot 10^{-6}$	1.79	0.888_3	0.111_7	45.6	1.659	0.940_8	0.059_2	193	2.286
0.1069	$2.16 \cdot 10^{-5}$	1.79	0.779_8	0.220_2	75.5	1.878	0.876_3	0.123_7	153	2.185
0.1102	$6.65 \cdot 10^{-5}$	1.81	0.638_7	0.361_3	106	2.025	0.779_5	0.220_5	120	2.079
0.1190	$7.70 \cdot 10^{-4}$	1.84	0.275_3	0.724_7	234	2.369	0.431_7	0.568_3	103	2.013
0.1271	$5.25 \cdot 10^{-3}$	1.92	0.103_1	0.896_9	447	2.650	0.186_9	0.813_1	138	2.140
0.1313	$2.855 \cdot 10^{-2}$	2.19	0.048_1	0.951_9	518	2.714	0.091_8	0.908_2	143	2.155

The functions $\log \varkappa_{21}(\beta_2)$ and $\log \lambda_{21}(\beta_2)$ are plotted in Figs. 7 and 8. From these Figs. one finds by extrapolation:

$$\text{From Fig. 7.} \quad \log \varkappa'_{21} = (0) \quad \log \varkappa''_{21} = 2.770_0$$
$$\varkappa'_{21} = (1) \qquad \varkappa''_{21} = 589\,. \tag{52}$$

$$\text{From Fig. 8.} \quad \log \lambda'_{21} = 2.390_0 \quad \log \lambda''_{21} = 2.150_0$$
$$\lambda'_{21} = 245 \qquad \lambda''_{21} = 141\,. \tag{53}$$

According to Table 1 $\lambda'_{21} = \infty$ if $\varkappa'_{21}$ is finite and $\varkappa'_{21} = 0$ if λ'_{21} is finite. From Fig. 8 it is seen that λ'_{21} is very probably finite whith means that $\varkappa'_{21} = 0$ and $\log \varkappa'_{21} = -\infty$. The value of $\varkappa'_{21} = 0$ will be adopted as more reliable than $\varkappa'_{21} = 1$.

The area between the $\log \varkappa$-axis and the curve $\log \varkappa_{21}(\beta_2)$ gives the activity factor, as is easily seen from equation (16). It is seen from Fig. 7 that the area between the $\log \varkappa$-axis and the curve for $0 \geq \log \varkappa_{21} \geq -\infty$ may be negligible in comparison with the area for $0 \leq \log \varkappa_{21} \leq \log \varkappa''_{21}$.

Choice (*E*). The calculations of the activity factors were performed so that $2 \log \gamma_1$ was obtained by graphical integration of (16 a) and $\log K_{21}$ was then obtained from (17):

$$\log K_{21} = \log \varkappa''_{21} - 2 \log \gamma''_1\,. \tag{54}$$

$\log \gamma_2$ could then be obtained from (10):

$$2 \log \gamma_2 = \log K_{21} - \log \varkappa_{21} + 2 \log \gamma_1\,. \tag{55}$$

From the integration:

$$2 \log \gamma''_1 = 0.629_{10}$$
$$\gamma''_1 = 2.06. \tag{56}$$

By inserting the values of $\log \varkappa''_{21}$ and $2 \log \gamma''_1$ from (52) and (56) in (54) we obtain:

$$\log K_{21} = 2.140_{90} \quad \text{and} \quad K_{21} = 138. \tag{57}$$

From (33) and (57) with T = 298

$$\Delta G^\circ = -2.91_8 \text{ kcal/mole}. \tag{58}$$

Table 8

Activity factors γ_1, γ_2 and activities a_{E1}, a_{E2} of *HR* (= 1) and $Ba_{1/2}R$ (= 2) calculated from (*E*). The Ba^+-H^+ exchange on Dowex 50. MARINSKY [7]. I = 0.104 — 0.228

β_2	$\log \varkappa_{21}$	$2 \log \gamma_1$	γ_1	$2 \log \gamma_2$	γ_2	a_{E1} from (7)	a_{E2} from (7)
0.000	$-\infty$	0.000	1.000	2.1409_0	∞	1.000	0.000
0.037	1.200	0.0136_2	1.01_6	0.9545_2	3.00_1	0.978	0.111
0.168	1.800	0.0634_7	1.07_6	0.4043_7	1.59_3	0.895	0.268
0.368	2.040	0.1265_1	1.15_7	0.2274_1	1.29_9	0.731	0.478
0.600	2.300	0.2526_3	1.33_8	0.0935_3	1.11_4	0.535	0.668
0.856	2.600	0.4713_3	1.72_1	0.0122_3	1.01_4	0.248	0.868
1.000	2.770	0.6291_0	2.06_3	0.000	1.000	0.000	1.000

In Table 8 about every third point from the integration is listed. The activities calculated from equation (7) are also given.

The functions γ_1, γ_2 and a_{E1}, a_{E2} are plotted against β_2 in Figs. 9 and 12.

The functions g_1, g_2 and a_{M1}, a_{M2} have been calculated from the data obtained by graphical integration of log $\varkappa_{21}$ (β_2) by the aid of (31). The corresponding X_1, X_2 values have been calculated from (5) and (2). The results are given in Figs. 11 a and 14 where g_1, g_2 and a_{M1}, a_{M2} are plotted against X_2.

Choice (*M*). From Fig. 8 it is seen that log λ_{21} (β_2) has a minimum in the point $\beta_2 = 0.362$ with log $\lambda_{21\min} = 2.060_0$. It is also seen that the function can be approximated with two straight lines intersecting in the minimum point.

For $\beta_2 \leq 0.362$ one finds from Fig. 8:

$$\log \lambda_{21} = -0.911_6\, \beta_2 + 2.390_0 \tag{59}$$

and

$$d \log \lambda_{21} = -0.911_6\, d\beta_2 . \tag{60}$$

From (26 a) and (60):

$$2 \log g_1 = -\int_0^{\beta_2} 0.911_6\, \beta_2\, d\beta_2 = -0.455_8\, \beta_2^2$$

and

$$\log g_1 = -0.227_9\, \beta_2^2 . \tag{61}$$

For $\beta_2 \geq 0.362$ one finds:

$$\log \lambda_{21} = -0.141_0\, \beta_1 + 2.150_0 \tag{62}$$

and

$$d \log \lambda_{21} = -0.141_0\, d\beta_1 . \tag{63}$$

By inserting the value of d log λ_{21} from (63) in (26 b) and integrating from $0 \rightarrow \beta_1$ we get:

$$\log g_2 = 0.070_5\, \beta_1^2 . \tag{64}$$

In the minimum point from (59), (61) and (64):

$$\begin{array}{lll} \log \lambda_{21\min} = 2.060_0; & 2 \log g_{1\min} = -0.059_{73}; & \log g_{2\min} = 0.028_{70} \\ \lambda_{21\min} = 115 & g_{1\min} = 0.934 & g_{2\min} = 1.06_8 . \end{array} \tag{65}$$

From (22):

$$\log K_{21} = \log \lambda_{21} + \log g_2 - 2 \log g_1 . \tag{66}$$

By inserting the values of λ_{21}, g_1 and g_2 from (65) in (66) we get:

$$\log K_{21} = 2.148_{43} \quad K_{21} = 141 . \tag{67}$$

From (33) and (67) with $T = 298^\circ K$:

$$\Delta G^\circ = -2.92_9 \text{ kcal/mole.} \tag{68 a}$$

The value of $K_{21} = 141$ is in good agreement with that in (57). As a mean we can take:

$$K_{21} = 140: \ \Delta G^\circ = -2.92 \text{ kcal/mole.} \tag{68}$$

Table 9

Activity factors g_1, g_2 and activities a_{M1}, a_{M2} of HR (= 1) and BaR_2 (= 2) calculated from choice (M). The Ba^{2+}—H^+ exchange on Dowex 50. MARINSKY. I = 0.104 — 0.228

β_2	$\log \lambda_{21}$	X_1	$2 \log g_1$	g_1	a_{M1} from (19)	X_2	$\log g_2$	g_2	a_{M2} from (19)
0.000	2.390_{00}	1.000	0.000	1.000	1.000	0.000	-0.2415_7	0.573	0.000
0.120	2.280_{61}	0.936	-0.0065_6	0.992	0.929	0.063_8	-0.1387_4	0.727	0.046
0.240	2.171_{22}	0.864	-0.0262_5	0.970	0.838	0.136	-0.0490_4	0.893	0.121
0.320	2.098_{29}	0.810	-0.0466_7	0.948	0.768	0.190	0.0034_7	1.00_8	0.192
0.362	2.060_{00}	0.779	-0.0597_3	0.934	0.728	0.221	0.0287_0	1.06_8	0.236
0.500	2.079_{50}	0.667	-0.0513_0	0.943	0.629	0.333	0.0176_3	1.04_1	0.347
0.800	2.121_{80}	0.333	-0.0238_1	0.973	0.324	0.667	0.0028_2	1.00_7	0.672
1.000	2.150_{09}	0.000	-0.0015_7	0.998	0.000	1.000	0.000	1.000	1.000

It may be noted that K_{21} seems to be equal to λ_{21}'' in (53). For $\beta_2 \leq 0.362$ $\log \lambda_{21}$ and $\log g_1$ were obtained from (59) and (61). By inserting these values and the value of $\log K_{21}$ from (67) in (66) $\log g_2$ was obtained. For $\beta_2 \geq 0.362$ $\log \lambda_{21}$ was obtained from (62), $\log g_2$ from (64) and $\log g_1$ from (66) and (67). In Table 9 about every third point is listed. The activities a_{M1}, a_{M2} calculated from (19) are also given.

In Figs. 11 a and 14 g_1, g_2 and a_{M1}, a_{M2} are plotted against X_2. The functions γ_1, γ_2 and a_{E1}, a_{E2} have been calculated from the data obtained by integration of $\log \lambda_{21}$ (β_2) by means of (31). The results are given in Figs. 9 and 12 where γ_1, γ_2 and a_{E1}, a_{E2} are plotted against β_2.

4. The Ba^{2+}—H^+ exchange on Dowex 50 according to DUNCAN and LISTER [10]

J. F. DUNCAN and B. A. J. LISTER [10] have studied the exchange equilibrium Ba^{2+}—H^+ on Dowex 50 by means of static and break through methods. The Ba^{2-} was analysed by the aid of radiochemical methods.

The notation H$^+$ (= 1) and Ba^{2+} (= 2) is the same as in the treatment of MARINSKY's data. Table 10 gives $\varkappa_{21}$ and λ_{21} calculated by (39) and (40) from the data in Table 1 in their paper.

The functions $\log \varkappa_{21}$ (β_2) and $\log \lambda_{21}$ (β_2) are plotted in Figs. 7 and 8.

From Fig. 7 one finds by extrapolation:

$$\begin{aligned} \log \varkappa_{21}' &= ? & \log \varkappa_{21}'' &= 2.360 \\ \varkappa_{21}' &= ? & \varkappa_{21}'' &= 229. \end{aligned} \tag{69}$$

From Fig. 8 one finds:

$$\begin{aligned} \log \lambda_{21}' &= (1): & \log \lambda_{21}'' &= 1.740 \\ \lambda_{21}' &= (10) & \lambda_{21}'' &= 55.0. \end{aligned} \tag{70}$$

Log λ_{21}' seems to have a finite value but the strong curvature of $\log \lambda_{21}$ (β_2) near $\beta_2 = 0$ makes the value of λ_{21}' very uncertain. The area between the curve and the $\log \lambda_{21}'$ axis seems to be negligible between $\log \lambda_{21} = 1$ and 1.5. The uncertainty of λ_{21}' thus does not influence the integration in any significant manner. As $\log \lambda_{21}'$ seems to be finite $\log \varkappa_{21}' = -\infty$ accord-

Table 10

The equilibrium quotients $\varkappa_{21}$ and λ_{21} for the exchange $Ba^{2+}-H^{+}$ on Dowex 50. DUNCAN and LISTER [10]. Total equivalent concentration $C_s = 0.2$

c_1	c_2	f_1^2/f_2	β_1	β_2	$\varkappa_{21}$ from (39)	log $\varkappa_{21}$	X_1 from (2)	X_2 from (2)	λ_{21} from (40)	log λ_{21}
0.207_5	$6.27 \cdot 10^{-3}$	1.15	0.172	0.828	183	2.262	0.294	0.706	64.5	1.810
0.204_5	$2.75 \cdot 10^{-3}$	1.15	0.240	0.760	175	2.243	0.387	0.613	71.6	1.855
0.207_5	$1.27 \cdot 10^{-3}$	1.15	0.320	0.680	176	2.246	0.485	0.515	85.4	1.931
0.205_1	$9.55 \cdot 10^{-4}$	1.15	0.370	0.630	147	2.167	0.540	0.460	79.9	1.903
0.207_7	$6.75 \cdot 10^{-4}$	1.15	0.422	0.578	138	2.140	0.594	0.406	84.6	1.927
0.208_2	$3.83_5 \cdot 10^{-4}$	1.15	0.504	0.496	126	2.100	0.670	0.330	95.6	1.980
0.207_3	$3.29 \cdot 10^{-4}$	1.15	0.526	0.474	122	2.086	0.689	0.311	98.4	1.993
0.210_5	$2.71 \cdot 10^{-4}$	1.15	0.552	0.448	124	2.093	0.711	0.289	107	2.029
0.209_7	$1.36 \cdot 10^{-4}$	1.15	0.664	0.336	95.2	1.979	0.798	0.202	118	2.072
0.209_8	$1.15_5 \cdot 10^{-4}$	1.15	0.688	0.312	90.1	1.955	0.815	0.185	122	2.086
0.209_8	$8.15 \cdot 10^{-5}$	1.15	0.758	0.242	63.3	1.801	0.862	0.138	115	2.061
0.194_9	$5.12_5 \cdot 10^{-5}$	1.14	0.838	0.162	31.6	1.500	0.912	0.088_1	89.5	1.952
0.203_9	$3.15 \cdot 10^{-5}$	1.14	0.904	0.096_2	17.0	1.230	0.949	0.050_5	84.4	1.926
0.195	$2.18 \cdot 10^{-5}$	1.14	0.918	0.081_5	15.7	1.196	0.957	0.042_5	92.3	1.965
0.200	$1.31_5 \cdot 10^{-5}$	1.14	0.963	0.036_6	5.01	0.700	0.981	0.018_6	67.0	1.826
0.200	$1.12_5 \cdot 10^{-5}$	1.14	0.982	0.017_6	1.30	0.114	0.991	0.008_{88}	36.7	1.565
0.200	$1.05_5 \cdot 10^{-5}$	1.14	0.975	0.025_4	2.93	0.467	0.987	0.012_9	57.2	1.757

ing to Table 1. From Fig. 7 it does not seem permissible to neglect the area between the curve and the log $\varkappa_{21}$ axis for log $\varkappa_{21} < 0$.

Choice (*E*). I have determined γ_2 by (16 b) but not γ_1 as the total area between the curve and the log $\varkappa_{21}$ axis is unknown as mentioned above.

For $\beta_2 \geq 0.380$ log γ_2 was approximated by:

$$\log \gamma_2 = 0.125_0 \, \beta_1^2. \tag{71}$$

Table 11

Activity factors γ_2 and g_2, activities a_{E2} and a_{M2} of $Ba_{1/2}R$ and BaR_2 calculated from choice (*E*). The $Ba^{2+}-H^{+}$ exchange on Dowex 50. DUNCAN and LISTER $C_S = 0.2$

β_2	X_2	log γ_2	γ_2	a_{E2} from (7)	a_{M2} from (31)	g_2 from (31)
0.000	0.000	∞ (From Table 1)	∞	—	—	—
0.021	0.010_6	0.7679	5.86_0	0.123_1	0.015_{15}	1.42_9
0.132	0.070_7	0.2981	1.98_7	0.262_3	0.068_{80}	0.973
0.344	0.208	0.0641	1.15_9	0.398_7	0.159_0	0.764
0.450	0.290	0.0378	1.09_1	0.491_0	0.241_1	0.831
0.600	0.429	0.0200	1.04_7	0.628_2	0.394_6	0.920
0.750	0.600	0.0078	1.01_8	0.763_5	0.582_9	0.972
0.850	0.739	0.0028	1.00_6	0.855_1	0.731_2	0.989
1.000	1.000	0.000	1.000	1.000	1.000	1.000

For lower β_2 the integration was performed by means of the Simpson formula.

The functions a_{E2}, g_2 and a_{M2} were also calculated by means of (7) and (31). The results are given in Table 11 where about every third point is listed. γ_2 and g_2 are plotted against β_2 respectively X_2 in Figs. 10 and 11 b. a_{E2} and a_{M2} are plotted in Figs. 13 and 15 against β_2 respectively X_2.

Choice (*M*). The integration of the log λ_{21} (β_2) curve was performed as follows. For $\beta_2 \leq 0.312$ log g_1 was obtained by integrating (26 a) by means of Simpson's formula.

For $\beta_2 \geq 0.312$ log λ_{21} was calculated from:

$$\log \lambda_{21} = 0.508_7\, \beta_1 + 1.740_0 \tag{72}$$

and log g_2 from

$$\log g_2 = -0.254_{35}\, \beta_1^2. \tag{73}$$

In the maximum point at $\beta_2 = 0.312$, $\beta_1 = 0.688$

$$\begin{array}{lll} \log \lambda_{21\max} = 2.090_0; & 2 \log g_{1\max} = 0.045_0; & \log g_{2\max} = -0.120_4 \\ \lambda_{21\max} = 123 & g_{1\max} = 1.05 & g_{2\max} = 0.758 \\ & \text{(from Simpson's formula)} & \text{(from (73))}. \end{array} \tag{74}$$

By inserting the values of $\lambda_{21\max}$, $g_{1\max}$ and $g_{2\max}$ from (74) in (66) we obtain:

$$\log K_{21} = 1.924_6 \text{ and } K_{21} = 84.1. \tag{75}$$

From (33) and (74) with T = 298:

$$\Delta G^{\circ} = -2.62_3 \text{ kcal/mole}. \tag{76}$$

For $\beta_2 \leq 0.312$, log g_2 was obtained from (66) and for $\beta_2 \geq 0.312$ log g_1. In Table 12 every third point is listed.

Table 12

Activity factors g_1, g_2 and activities a_{M1}, a_{M2} of *HR* (= 1) and BaR_2 (= 2) calculated from (*M*). The Ba^{2+}—H^+ exchange on Dowex 50. DUNCAN and LISTER. $C_S = 0.2$

β_2	log λ_{21}	X_1 from (2)	2 log g_1	g_1	a_{M1} from (19)	X_2 from (5)	log g_2	g_2	a_{M2} from (19)
0.000	(1.000)	1.000	0.000	1.000	1.000	0.000	(0.9246)	(8.40_6)	0.000
0.042	1.800	0.979	0.0056	1.00_6	0.985	0.021_5	0.1302	1.35_0	0.029
0.312	2.090	0.815	0.0450	1.05_3	0.858	0.185	−0.1204	0.757_9	0.140
0.450	2.019_8	0.710	0.0183	1.02_1	0.725	0.290	−0.0769	0.837_7	0.243
0.700	1.892_6	0.462	−0.0549	0.938_8	0.434	0.538	−0.0229	0.948_6	0.510
1.000	1.740_0	0.000	−0.1846	0.808_5	0.000	1.000	0.000	1.000	1.000

The value of g_2' is very difficult to ascertain depending upon the uncertainty in λ_{21}'.

In Figs. 11 b and 15 g_1, g_2 and a_{M1}, a_{M2} are plotted against X_2.

γ_1, γ_2 and a_{E1}, a_{E2} have been calculated by means of (31). The results are given in Figs. 10 and 13. From Fig. 10 one finds by extrapolation $\gamma_1'' = 1.61$.

Department of Inorganic Chemistry, Royal Institute of Technology, Stockholm.
Institute of Inorganic and Physical Chemistry, University of Stockholm and FOA 1, Sundbyberg, Sweden.

LITERATURE: [1] **Nachod, F. C.**, Ion Exchange, Academic Press, N. Y. 1949. — [2] **Kunin, R.** and **Myers, R. J.**, Ion Exchange Resins, John Wiley and Sons, N. Y. 1950. — [3] **Högfeldt, E.**, **Ekedahl, E.** and **Sillén, L. G.**, Acta Chem. Scand. *4* (1950) 1471. — [4] **Ekedahl, E.**, **Högfeldt, E.** and **Sillén, L. G.**, Ibid. 556. — [5] **Högfeldt, E.**, **Ekedahl, E.** and **Sillén, L. G.**, Ibid. 828. — [6] **Högfeldt, E.**, **Ekedahl, E.** and **Sillén, L. G.**, Ibid 829. — [7] **Marinsky, J. A.**, Diss. Report to the Office of Naval Research NR–026–001 (1949). — [8] **Kressman, T. R. E.** and **Kitchener, J. A.**, J. Chem. Soc. (1949) 1201. — [9] **Gapon, E. N.**, J. Gen. Chem. (U. S. S. R.) 3 (2) (1933) 144, cf. KRISHMAMOORTHY, C. and OVERSTREET, R., Soil Science *68*. 4 (1949) 307. — [10] **Duncan, J. F.** and **Lister, B. A. J.**, Faraday Discussion 7 (1949) 104. — [11] **von Zawidski, J.**, Z. phys. Chem. *35* (1900) 129. — [12] **Hildebrand, J. H.** and **Scott, R. L.**, The Solubility of Nonelectrolytes, 3rd ed. Reinhold Publishing Corp. (1950) 30—32. — [13] **Dolezalek, F.**, Z. phys. Chem. *64* (1908) 727. — [14] **Argersinger, W. J.**, **Davidson, A. W.** and **Bonner, O. D.**, Trans. Kansas Acad. *53* (3) (1950) 404. — [15] **Harned, H. S.** and **Owen, B. B.**, The Physical Chemistry of Electrolytic Solutions, 2nd Ed. (1950) 285. — [16] **Landolt-Börnstein, H. W.**, II, 1442. — [17] — **Landolt-Börnstein, Eg.**, II b. 1470. — [18] **Samuelson, O.**, Diss. (1944) 23. — [19] **Ekedahl, E.**, Arkiv Kemi, to be published. — [20] **Sillén, L. G.**, Arkiv Kemi *2* (1950) 477. — [21] **Sillén, L. G.**, Ibid. 499. — [22] **Ekedahl, E.**, **Högfeldt, E.** and **Sillén, L. G.**, Nature *166* (1950) 723.

Tryckt den 12 januari 1953

Uppsala 1953. Almqvist & Wiksells Boktryckeri AB

ARKIV FÖR KEMI Band 5 nr 14

Communicated 8 October 1952 by Arne Tiselius

A new type of preparative chromatographic paper column

By Carl Erik Danielsson

With 3 figures in the text

Many attempts have been made to adapt the paper chromatography method to a macro scale, e.g. the "chromatopile" (1), a column of filter paper disks, placed on top of each other, further the "chromatopack" (2), consisting of filter paper sheets, pressed between two glass plates. Finally several types of columns containing cellulose powder have been applied (3). However, the separation in all these cases is far from ideal because broad and unsharp zones are obtained. Good results have sometimes been obtained with cellulose powder, but in most cases these results do not agree with those obtained in "paper trip" experiments.

In the paper chromatography method the separation is not only a result of partition since the chemical composition of the paper, the orientation of the fibers and the capillarity are also factors involved. All possible surface effects, which cause a broadening of the zones must also be eliminated. In order to get experimental conditions as similar as possible to those in "paper strip" experiments, the author has tried the following method by which the paper chromatography method is used on a macro scale.

A cylinder, 30 cm high and with 10 cm outside diameter was rolled on a cylindrical rod with 1 cm diameter from a machine-made filter paper, Munktell 20 R. This procedure was carried out in a special machine at Grycksbo Pappersbruk, Grycksbo, Sweden. At one end of the cylinder a thin, 10 cm high brass ring was attached in order to form a container for the solution to be passed through the column. The column was then saturated with water. The 10 mm hole in the centre of the column was filled with paraffin. The substance under investigation was dissolved in about 10 ml of water and placed at the top of the column, and then eluted with water during the time desired. The column was then cut into halves along its vertical axis. The result is shown in Fig. 1. This figure shows that the whole cross-section of the column cannot be used, because the velocity of the front is higher near the outer and inner column surfaces. If only that part of the cross-section is used where the front is approximately horizontal, the above-mentioned surface effect is eliminated. Experiments have shown that the horizontal diffusion is not very fast. It is very probable, that no diffusion at all occurs from one paper to another.

The method described above has been modified in later experiments in the following way (Fig. 2).

The commercial paper column (bought from Grycksbo Pappersbruk, Grycksbo, Sweden) is saturated with solvent. Seven concentric rings, with inner radius = 1.5 cm and outer radius = 4 cm, are cut from Muntkell filter papers, No. 3.

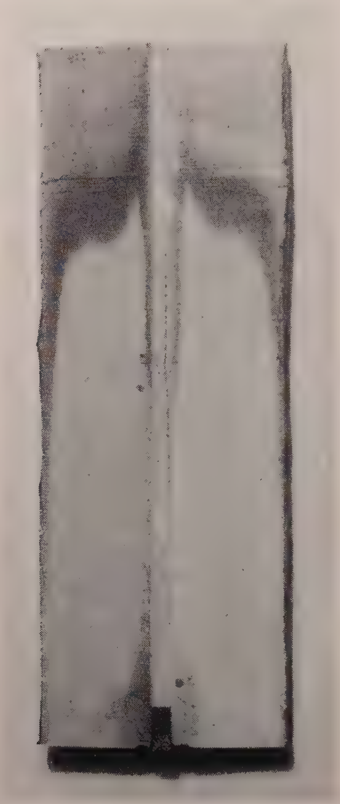

Fig. 1. The shape of the front when the whole cross-section of the column is used. Naphthol green, eluted with water.

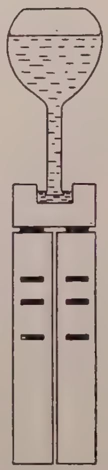

Fig. 2. Schematic view of the experimental arrangement.

These rings are placed on a watch glass with a known amount of the solution under investigation. The solvent evaporates in 24 hours at + 20° C, and the substance is in this way uniformally taken up by the filter paper rings, which are then placed on the top of the column. Then a new, 10 cm high cylinder of exactly the same type as the one used as the column, but with its centre hole (10 mm) filled with paraffin is placed in the filter paper rings on the top of the large column (Fig. 2). This cylinder is also saturated with solvent. It has a cylindrical hole in the top, filled with solvent. The level of the liquid is kept constant by an inverted volumetric flask (volume 3 liters).

By this method absolutely straight fronts are obtained, i.e. the substance moves with the same velocity at different distances from the centre of the column (Fig. 3 and Table 1). After the experiment is finished, the column is cut along its vertical axis with a knife, and by using the ninhydrin reaction on some papers at different distances from the centre of the column, the position of the separated substances can be determined. The substances can then be obtained by cutting out the different zones and eluting with water.

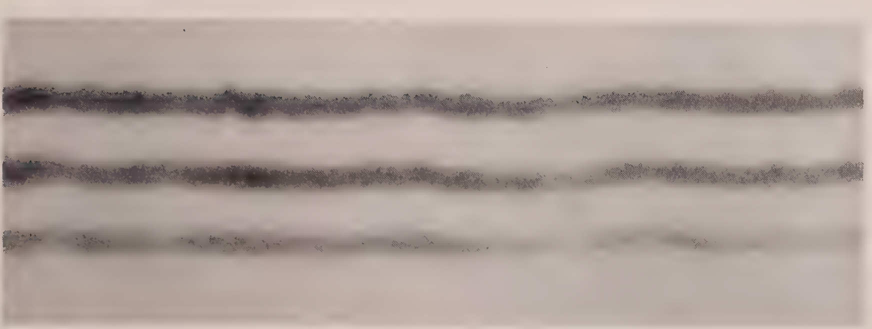

Fig. 3. Separation of glycine (top), alanine (centre) and valine (bottom) in 70 % ethanol — 5 % acetic acid. The figure represents one turn of the unrolled filter paper from the column.

Fig. 3 shows a separation of three amino acids, valine, alanine and glycine in 70 % ethanol — 5 % acetic acid on a piece of unrolled filter paper from the column. 25 mg of each acid were used. In this case a larger diameter column was used. The separation is satisfactory, and each amino acid moves across the column as a clear-cut zone with the same R_F-value as in a "paper strip" experiment (Table 1).

Table 1

The constancy of migration at different distances from the centre of the column. The zones were in all cases 10–12 mm wide

Distance from the centre (mm)	Distance of migration (mm)		
	Valine	Alanine	Glycine
35	129	103	73
45	129	104	74
57	130	103	74

These columns can easily be coupled to a fraction collector, and one and the same column can then be used for many experiments. Glycine, alanine and valine were separated in a very satisfactory way by this method in the preliminary experiments, carried out together with L. Hagdahl. It has not yet been determined if the separation is quantitative, because too high blank values were obtained, probably depending on ammonia absorption in the cellulose and in the open tubes in the fraction collector (4). Thus the method can at the moment only be used as a preparative one. A similar type of paper column for separating still larger amounts has been constructed and will be described in a later communication. Work to improve these methods are in progress at this Institute.

The author wishes to thank Professor A. Tiselius for his great interest in this work and for valuable discussions. This investigation was supported by a grant from the Nobel Foundation.

Institute of Biochemistry, University of Uppsala, Uppsala, Sweden.

REFERENCES

1. MITCHELL, H. K. and HASKINS, F. A., Science *110* (1949) 278.
2. PORTER, W. L., Analyt. Chemistry *23* (1951) 412.
3. HOUGH, L., JONES, J. K. N. and WACHMAN, W. H., Nature *162* (1948) 448.
4. FOWDEN, L., Biochem. J. *48* (1951) 327.

Tryckt den 12 januari 1953

Uppsala 1953. Almqvist & Wiksells Boktryckeri AB

ARKIV FÖR KEMI Band 5 nr 15

Vorgelegt am 10. September 1952

Über die Inaktivierung der α-Malzamylase II

Inaktivierung durch Heparin

By Karl Myrbäck und Barbro Persson

Mit 2 Figuren im Text

Durch Versuche über die Inaktivierung von Enzymen durch gewisse Reagenzien ist es in günstigen Fällen möglich, die Anwesenheit für die enzymatische Aktivität essentieller Gruppen in den Enzymmolekülen festzustellen. So konnte z. B. im Fälle der Saccharase (1) durch Inaktivierungsversuche mit Schwermetallionen bzw. gewissen Anionen die Annahme von Michaelis (2) sehr stark gestützt werden, dass das Enzym ein Ampholyt mit dem isoelektrischen Punkt bei pH = etwa 5 ist. Später ist ja durch Isolierung vieler Enzyme in einheitlicher Form die Eiweissnatur derselben bewiesen worden; dass sie Ampholyte sind, ist also jetzt als selbstverständlich zu betrachten. Die durch die erwähnten Inaktivierungsversuche nachgewiesenen, sauren bzw. basischen Gruppen sind also aller Wahrscheinlichkeit nach mit den gewöhnlichen sauren bzw. basischen Gruppen der Proteine zu identifizieren.

Dass die Aktivitäts-pH-Kurven der Enzyme, wie zuerst von Michaelis angenommen wurde, im Grossen und Ganzen durch die elektrochemischen Eigenschaften der Enzyme bestimmt werden, ist jetzt ausser allem Zweifel gestellt, wobei selbstverständlich anzunehmen ist, dass auch die Eigenschaften von Substrat und etwaigen Aktivatoren mitbestimmend sind. Ebenfalls ist sicher, dass in einigen Fällen irreversible Vorgänge wie z. B. Zerstörung bei nichtoptimaler Azidität, mitspielen können. Es ist zuzugeben, dass in einigen Fällen der Zusammenhang zwischen Aktivitäts-pH-Kurve einerseits und andererseits den Säure- und Basenkonstanten des Enzyms ein ziehmlich verwickelter zu sein scheint. Erstens ist in mehreren Fällen gezeigt worden, dass sich die pH-Kurve eines Enzyms mit der Substratkonzentration verschiebt, wobei geschlossen werden kann, dass unter den substratbindenen Gruppen auch solche vorhanden sind, die den elektrochemischen Charakter des Enzyms beeinflussen. So konnte gezeigt werden, dass im Falle der Saccharase bei der Bindung der Substrate eine basische Gruppe beteiligt ist, die anscheinend die basische Dissoziationskonstante des Enzyms im Wesentlichen bestimmt (1, 3). Auch auf die pH-Kurven anderer Enzyme lässt sich diese Betrachtungsweise übertragen (4—7). Die Verhältnisse können z. B. dadurch kompliziert werden, dass mehrere basische Gruppen mit gleicher oder verschiedener Basenstärke bei der Substratbindung beteiligt sind (7). Da ja anzunehmen ist, dass in einem Enzymmolekül die Zahl sowohl der sauren wie die der basischen Gruppen meistens verhältnismässig hoch ist, so ist es ja auch möglich, dass z. B. eine schwach basische Gruppe Substrat bindet, während andere, stärker basische Gruppen die Dissoziationskonstante bestimmen. Dass der isoelektrische Punkt eines Enzymproteins immer mit dem Aziditätsoptimum zusammenfallen sollte, kann deshalb gar nicht erwartet werden, auch wenn die Michaelissche Theorie in ihren Grundzügen richtig ist.

Wormall, Wills und Mitarbeiter (8—10) haben die Inaktivierung einiger Enzyme durch Suramin und ähnliche Stoffe untersucht. Der Schluss wurde gezogen, dass bei mehreren Enzymen das Suramin nur an kationisch geladenen Gruppen der Enzyme gebunden wird, und zwar weil es nur auf der sauren Seite des Aziditätsoptimums eine Wirkung hat. Nach den zitierten Verfassern ermöglicht die Festlegung einer „Inaktivierungs-pH-Kurve“ mit Suramin die Bestimmung des isoelektrischen Punktes des Enzymproteins, wobei also angenommen wird, dass die suraminbindenden, basischen Gruppen dieselben sind, die die Aktivitäts-pH-Kurve des Enzyms bestimmen, eine Annahme die wohl nicht immer ohne weiteres zutreffen muss. Immerhin wurde in mehreren Fällen durch die Suraminmethode Werte des isolektrischen Punktes erhalten, die gut mit den nach anderen Methoden gewonnenen übereinstimmen. In anderen Fällen traten unerklärte Abweichungen auf (10): Im Fall der α-Malzamylase gab die Suraminmethode den Wert pH = 5,0, während andere Verfasser (11—14) 5,7—5,9 angeben.

Ohne auf den Mechanismus der Inaktivierung hier näher einzugehen, wollen wir folgendes bemerken: Es ist zweifelsohne anzunehmen, dass Suramin und ähnliche Stoffe nur mit kationisch geladenen Gruppen der betreffenden Enzyme reagieren. Beim Aziditätsoptimum und auf der alkalischen Seite desselben findet man oft keine Wirkung. Geht man aber ins saure Gebiet über, so tritt von einem bestimmten pH-Wert ab starke Inaktivierung des Enzyms ein. Es dürfte angenommen werden können, dass bei diesem pH-Wert die Ionisierung der suraminbindenden basischen Gruppen (praktisch) anfängt. Wenn auch der Zusammenhang nicht klar ist, so muss die Inaktivierungs-pH-Kurven mit Suramin und ähnlichen Stoffen von der Basenkonstante K_b des Enzyms irgendwie abhängen, dagegen nicht von der Säurekonstante K_a. Der isoelektrische Punkt dagegen hängt ja von beiden Konstanten ab:

$$[\mathrm{H}_i^+]^2 = K_a \cdot K_w / K_b$$

wo K_w das Ionenprodukt des Wassers ist. Es scheint uns deshalb als könnte man wohl einen nahen Zusammenhang zwischen den Inaktivierungskurven und den sauren Ästen der Aktivitäts-pH-Kurven vermuten, dagegen nicht oder nicht immer einen ähnlichen Zusammenhang zwischen einer Inaktivierungskurve und dem isoelektrischen Punkt des Enzyms.

Die Inaktivierung der α-Malzamylase durch Silberionen und durch Pikrinsäure wurde von Myrbäck und Frostell (15) untersucht. Es wurde gefunden, dass die Inaktivierung durch Ag-Ionen mit steigendem pH stark zunahm, während für die Inaktivierung des Enzyms durch Pikrinsäure das Umgekehrte beobachtet wurde. Es konnte geschlossen werden, dass die Inaktivierungen prinzipiell in derselben Weise gedeutet werden konnten, wie dies früher für die Saccharase geschehen war.

Die Untersuchung der α-Malzamylase wird dadurch erschwert, dass das Enzym in saurer Lösung ($pH<4$) so instabil ist, dass die wahre pH-Kurve nicht einmal festgelegt werden kann. Mit Heparin kann aber, wie unten gezeigt werden soll, in pH-Gebieten gearbeitet werden, in welchen keine Spontaninaktivierung des Enzyms eintritt.

Über die Einwirkung des Heparins auf die β-Amylase der Gerste haben Myrbäck und Persson eine Arbeit veröffentlicht (16), in der auch ältere Arbeiten über die Wirkung des Heparins auf Enzyme angeführt worden sind. Qualitativ sind die mit verschiedenen Enzymen gewonnenen Ergebnisse übereinstimmend. Unten wird gezeigt, dass auch bei der α-Malzamylase prinzipiell dieselben Verhältnisse beobachtet werden.

Experimenteller Teil

Enzym war ein teilweise gereinigtes Präparat aus sechszeiligem Gerstenmalz. Das Malzextrakt wurde nach Ohlsson (17) durch Erhitzung auf 70° bei $pH = 6$ von β-Amylase befreit. Um alle β-Amylase sicher zu beseitigen wurde die Erhitzung so lange fortgesetzt, dass etwa die Hälfte der α-Amylase inaktiviert wurde. Die in den Versuchen angewendeten Enzymlösungen wurden zwecks Stabilisierung mit 40 mg $CaCl_2$ pro Liter versetzt.

Heparin, hochgereinigtes Präparat mit etwa 100 Einheiten pro mg. Herr Professor Dr E. Jorpes sei auch hier für die Überlassung des Heparins bestens gedankt.

Puffer. Mischungen von 2 *N* Essigsäure und 2 *N* Natriumacetat. In jeder Versuchsmischung wurde das pH elektrometrisch bestimmt.

Aktivitätsbestimmung. Zu 50 ml 2 % Stärkelösung und 5 ml Puffer wurde Enzym und so viel wasser gesetzt, dass das Volumen 100 ml wurde. Versuchstemperatur 30 °. Zu verschiedenen Zeiten wurden Proben von 5 ml herausgenommen und in 25 ml etwa 0,02 *N* Jodlösung pipettiert. Zuckerbestimmung nach Willstätter und Schudel. Sämtliche Werte der folgenden Tabellen bedeuten prozentische Spaltung, d.h. gefundene Menge „Glucose“ in % der Stärkemenge. Die Spaltungswerte wurden dann in ein Diagramm eingetragen (Fig. 1). Die Zeit-Umsatzkurve ist anfangs geradlinig oder auf alle Fälle so schwach gekrümmt, dass eine Tangente durch O unschwer gezogen werden kann. Aus der Kurve bzw. der Tangente erhält man die Anfangsgeschwindigkeit: % Umsatz pro Minute. Im folgenden wird die relative Aktivität angegeben, wobei die optimale Aktivität bei $pH = 5$—6 ohne Hemmstoff mit 100 bezeichnet wird.

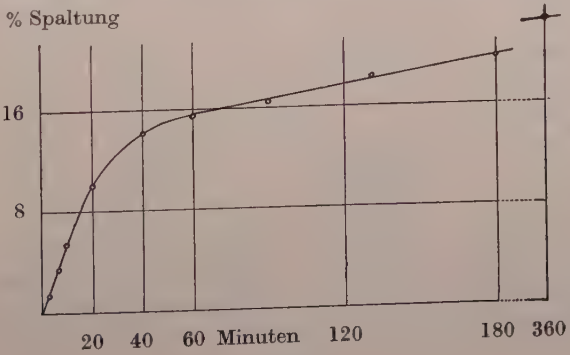

Fig. 1.

Es sei hervorgehoben, dass die in dieser Untersuchung gefundenen Zeit-Umsatzkurven immer die Form hatten, die wir früher gefunden haben und als für die α-Malzamylase charakteristisch betrachten (17): Die Spaltungsreaktion zerfällt ziehmlich scharf in eine schnelle Dextrinierung, die eine Hydrolyse etwa 16 % der Bindungen des Substrats umfasst, und eine nachherige, verhältnismässig langsame Verzuckerung. Es sei hervorgehoben, dass diese Form der Kurve von der physikalischen Beschaffenheit der Substratlösung unabhängig ist. Sie ist also z. B. nicht durch „Retrogradation" der Substratlösung bedingt, wie von MEYER und Mitarbeiter (17) angenommen worden ist. Dass die Spaltung in zwei Phasen mit sehr verschiedenen Geschwindigkeiten zerfällt, hängt damit zusammen, dass das Enzym zu langkettigen Substraten eine hohe Affinität, zu kurzen Ketten ($n <$ etwa 8) dagegen eine sehr niedrige hat (18). Die Lage des Knickpunktes der Kurve wird vom Verzweigungsgrad des angewendeten Substrates bestimmt (17).

Orientierende Versuche

A. *Enzym ohne Vorbehandlung.* 2 ml Enzymlösung (Tabelle 1).

B. *Enzym mit Puffer vorbehandelt.* Vorbehandlung 30 Minuten bei 20°; pH wie bei der Aktivitätsmessung (Tabelle 1).

C. *Enzym + Heparin ohne Incubation.* Wie in der Versuchsreihe A aber 0,05 mg Heparin in jeder Versuchsmischung (Tabelle 1).

D. *Vorbehandlung mit Heparin.* 2 ml Enzymlösung + 1 ml Heparinlösung + 0,5 ml Puffer + 0,5 ml Wasser. Nach 30 Minuten bei 20° wird eine auf 30° vorgewärmte Mischung von 5 ml des betreffenden Puffers, 41 ml Wasser und 50 ml 2 % Stärkelösung zugesetzt (Tabelle 2).

E. *Incubation mit verschiedenen Heparinmengen.* pH = 4,11. 2 ml Enzymlösung + 1 ml Heparinlösung verschiedener Konzentration + 0,5 ml Puffer + 0,5 ml Wasser. Nach 30 Minuten bei 20° wird die Aktivität wie unter D bestimmt (Tabelle 2).

Tabelle 1

Versuchsreihe	pH	% Spaltung nach							Relative Aktivität
		7	10	20	40	60	90 Min.	24 St.	
A	5,00	2,3	3,9	8,4	13,2	—	22,8	26,9	100
	3,50	2,2	3,6	7,3	11,9	15,8	20,2	27,3	87
	3,27	2,2	3,4	5,9	10,3	14,2	18,0	25,5	78
B	5,01	1,8	3,6	—	12,0	15,4	18,6	26,2	95
	4,51	3,0	4,5	7,3	12,7	16.6	20,0	27,6	97
	4,11	3,2	4,2	7,3	13,5	17,0	18,9	27,7	102
	3,33	2,0	3,8	5,0	9,1	14,2	18,0	—	74
	3,29	2,7	3,4	6,6	9,9	12,9	15,3	26,2	75
C	6,11	2,5	4,1	7,8	14,4	18,2	20,6	—	102
	5,38	3,5	4,1	7,8	14,4	18,0	20,8	27,5	102
	5,06	3,2	4,4	—	14,5	18,4	21,2	28,2	102
	4,63	2,3	3,8	7,0	12,8	17,4	20,8	27,2	100
	3,50	1,8	3,2	7,3	12,4	16,5	20,2	27,1	90
	3,27	1,6	2,7	5,1	8,9	12,4	15,3	24,6	69

Tabelle 2

Versuchs-reihe	pH	Heparin mg	% Spaltung nach 7	10	20	40	60	90 Min.	24 St.	Relative Aktivität
D	6,11	0,05	3,0	4,0	7,0	14,5	18,5	20,7	27,2	100
	4,11	0,05	0,8	1,1	2,4	4,9	6,5	8,1	26,0	36
	3,25	0,05	0,3	0,9	1,8	3,5	4,8	5,6	19,0	22
E	4,11	—	3,2	4,2	7,3	13,5	17,0	18,9	27,7	100
	4,11	0,01	3,0	3,4	6,4	10,5	13,8	17,1	26,5	75
	4,11	0,03	1,9	2,5	4,7	8,8	12,2	16,8	27,3	63
	4,11	0,05	0,9	2,0	2,7	4,9	6,6	7,9	26,6	36

In der Figur 2 sind die Werte der Versuchsreihen A und B mit punktierten Kreisen, die der Reihe C mit Dreiecken markiert.

Es geht aus den obigen Versuchen hervor, dass mit dem angewendeten Enzympräparat und unter den gewählten Versuchsbedingungen keine Spontaninaktivierung des Enzyms eintritt. Ohne Incubation mit dem Enzym hat das Heparin bei keinem untersuchten pH eine Wirkung, was einer Schutzwirkung durch Substrat und Reaktionsprodukten der Stärkehydrolyse zugeschrieben werden muss. Incubation vom Enzym mit Heparin bei pH = 3—4 bedingt starke Inaktivierung, während Incubation bei pH = 6 wirkungslos ist.

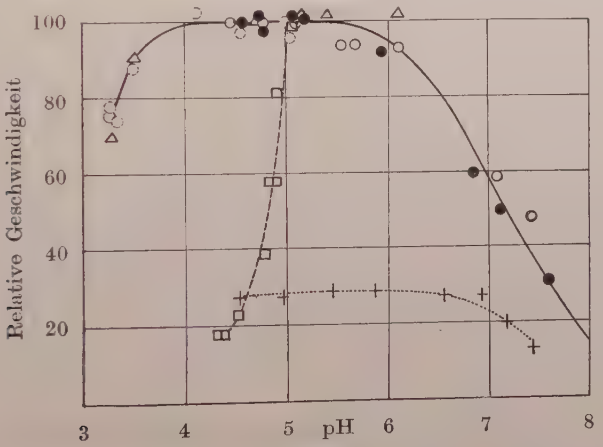

Fig. 2.

pH-Kurve und Stabilität

Zu den folgenden Versuchen wurde ein anderes, ähnliches Enzympräparat angewendet. Es wurde als Acetondauerpräparat aufbewahrt und bei Bedarf aufgelöst. Die Aktivitäts-pH-Kurve vor und nach Incubation des Enzyms mit Pufferlösungen von variierendem pH wurde in dem infragekommenden Gebiet festgelegt:

Tabelle 3

Versuchsreihe	pH	% Spaltung nach						Relative Aktivität
		7	10	20	40	60 Min.	24 St.	
A	7,41	2,1	2,2	3,3	5,9	8,1	18,4	47
	7,10	1,9	2,7	3,9	6,9	8,6	19,0	59
	6,11	3,2	5,7	9,4	12,4	13,9	23,3	92
	5,69	3,5	5,3	9,6	13,3	15,2	26,2	93
	5,51	3,6	5,3	9,7	13,1	15,0	26,5	93
	5,09	5,0	6,6	10,9	13,4	15,3	—	100
	4,74	4,9	6,4	10,5	14,8	15,7	26,0	100
	4,42	5,0	6,9	10,7	14,1	15,5	22,5	100
B	7,57	1,3	1,6	3,4	5,6	6,4	—	30
	7,10	2,1	2,4	5,0	7,7	8,1	16,3	50
	6,83	2,8	3,6	5,3	10,3	11,0	19,5	60
	5,94	3,6	5,0	8,8	13,2	14,9	24,5	91
	5,14	3,9	5,6	9,9	15,5	15,6	28,0	101
	5,08	—	5,9	10,3	14,5	15,4	27,3	103
	4,75	4,0	5,3	10,3	15,0	16,4	—	97
	4,73	4,1	5,7	11,0	13,8	16,0	27,2	102
	4,54	4,2	5,3	9,9	14,1	15,4	22,5	100

A. *Ohne Vorbehandlung.* 2 ml Enzymlösung; Versuchsmischung wie oben beschrieben (Tabelle 3).

B. *Vorbehandlung mit Puffer.* 4 ml Enzymlösung + 0,5 ml Puffer + 85,5 ml Wasser wurden während 60 Minuten bei 20° gehalten. Das pH der Mischungen war $4{,}50 \pm 0{,}03$. Nach der Incubation wurden die Mischungen schnell auf 30° gebracht und 45 ml davon mit 50 ml 2 % Stärkelösung + 5 ml Puffer (vorgewärmt) gemischt. Das pH der Versuchsmischungen wurde in jedem Fall elektrometrisch bestimmt (Tabelle 3).

In der Figur 2 sind die Werte der Versuchsreihe A mit weissen, die der Reihe B mit schwarzten Kreisen veranschaulicht. Die Vorbehandlung bei pH = 4,5 hat offenbar das Enzym in keiner Weise beeinflusst. Der in der Figur gezogene, absteigende Ast der pH-Kurve ist die theoretische Dissoziationskurve einer Säure mit $K_a = 10^{-7,1}$. MYRBÄCK und FROSTELL (15) fanden früher den Wert $10^{-6,8}$. Es mag sein, dass sich die Kurve mit dem Reinheitsgrad des Enzympräparats verändert oder dass die Ca-Ionen auf die Lage derselben einen Einfluss haben.

Vorbehandlung mit verschiedenen Heparinmengen

Je 4 ml Enzymlösung wurden mit 0,5 ml Puffer, pH = 4,60, Heparinlösung und Wasser gemischt, so dass das Volumen 90 ml betrug. Nach 60 Minuten bei 20° wurde schnell auf 30° erwärmt und 45 ml davon zu einer vorgewärmten Mischung von 50 ml 2 % Stärkelösung und 5 ml desselben Puffers gegeben (Tabelle 4).

Die Wirkung einer gewissen Heparinmenge ist hier viel kleiner als in den orientierenden Versuchen. Dies hängt vor allem mit dem höheren pH, teilweise wohl auch mit dem viel grösseren Volumen während der Vorbehandlung zusammen.

Tabelle 4

Heparin mg/90 ml	% Spaltung nach							Relative Aktivität
	3	7	10	20	40	60 Min.	24 St.	
—	1,6	3,5	5,4	10,0	14,2	15,4	29,5	100
—	1,3	3,8	5,1	9,5	14,1	16.2	—	
—	2,1	4,5	6,2	10,3	15,0	16,4	29,5	
2,4	1,9	3,9	5,4	10,3	15,2	16,1	28,0	100
3	1,6	3,8	4,8	9,1	14,0	16,6	27,2	98
5	1,8	3,7	5,3	9,2	13,6	16,3	27,2	97
10	1,1	2,7	3,7	7,4	11,2	14,1	25,8	65
20	0,5	0,6	1,4	2,1	3,2	5,5	21,8	19

Tabelle 5

pH während der Bestimmung	% Spaltung nach							Relative Aktivität
	3	7	10	20	40	60 Min.	24 St.	
4,52	1,3	1,6	2,3	3,2	5,8	8,7	19,9	27
4,96	1,1	1,4	1,5	3,1	6,0	7,8	23,8	27
5,47	1,0	1,8	2,2	3,7	6,1	8,4	22,2	28
5,88	0,5	0,9	1,3	2,7	6,6	9,3	24,3	28
6,58	0,3	1,0	1,8	3,4	6,2	8,1	22,5	27
6,93	0,3	1,4	1,8	3,4	—	7,0	20,0	27
7,16	0,3	0,8	1,1	2,3	4,7	6,2	22,2	20
7,46	0,3	0,5	0,7	1,5	3,7	4,8	—	14

In einer zweiten Versuchsreihe wurde die Vorbehandlung von 4 ml Enzymlösung mit 10 mg Heparin genau so vorgenommen wie in der vorangehenden Versuchsreihe. Das pH während der Vorbehandlung war 4,48 ± 0,02. Das pH während der Aktivitätsbestimmung wurde dagegen durch Zugabe zweckmässiger Puffer variiert (Tabelle 5).

Die Versuchswerte sind in der Figur 2 mit Kreuzen veranschaulicht. Es geht hervor, dass durch pH-Verschiebungen nach der während der Vorbehandlung eingetretenen Inaktivierung keine nennenswerte Reaktivierung erziehlt werden kann.

Vorbehandlung bei verschiedenen Aziditäten

Da die Vorversuche gezeigt hatten, dass die Inaktivierung durch Heparin nur in deutlich saurer Lösung eintritt, wurden Versuche ausgeführt, in welchen die Vorbehandlung mit 10 mg Heparin auf 4 ml Enzym in 90 ml Totalvolumen genau so ausgeführt wurde wie in der vorangehenden Versuchsreihe; die Puffermenge war überall dieselbe, aber das pH während der Vorbehandlung wurde variiert. 60 Minuten bei 20° (Tabelle 6).

Die Inaktivierungs-pH-Kurve ist in der Figur 2 gestrichelt (Vierecke). Die Kurve zeigt, dass jedenfalls unter den hier gewählten Versuchsbedingungen, eine Inaktivierung nur unterhalb von pH = 5,1 eintritt.

Tabelle 6

pH während der Vorbehandlung	% Spaltung nach							Relative Aktivität
	3	7	10	20	40	60 Min.	24 St.	
4,31	—	0,6	1,6	2,4	4,4	—	—	18
4,36	—	0,6	1,5	2,4	4,4	7,6	20,8	18
4,50	0,5	1,0	2,0	3,1	6,0	9,1	20,8	23
4,78	0,6	1,9	2,7	5,6	7,8	10,3	—	39
4,80	1,1	2,7	3,8	6,1	10,4	13,0	—	58
4,82	1,1	2,7	3,4	6,4	10,3	15,3	23,7	58
4,91	1,8	3,8	5,4	9,2	14,4	16,0	29,3	82
5,07	2,0	4,7	6,2	10,3	14,8	16,4	—	99
Ohne Heparin pH = 5,1	2,4	4,8	6,4	10,5	14,5	—	—	100

Versuche zur Reaktivierung

Bei der Untersuchung der Heparininaktivierung der β-Amylase (16) wurde gefunden, dass bei gleichbleibendem pH die durch eine gewisse Heparinmenge hervorgerufene Inaktivierung stark vom Gehalt der Incubationsmischung an Puffersubstanzen und Neutralsalzen wie NaCl abhängt. War genügend NaCl während der Incubation anwesend, so trat durch eine gewisse Heparinmenge keine Inaktivierung ein, die im Parallellversuch ohne NaCl das Enzym total hemmte. Es wurde nun untersucht, wie sich die α-Amylase in dieser Beziehung verhält, und ob durch nachträglichen Zusatz von NaCl eine Reaktivierung des inaktivierten Enzyms erziehlt werden kann.

A. 4 ml Enzym + 0,5 ml Puffer, pH = 4,31 + 10 mg Heparin + Wasser zu 90 ml. 60 Minuten bei 20° (Tabelle 7).

B. Versuch wie in A aber 2 g NaCl von Anfang an anwesend.

C. Versuch wie in A. Nach 60 Minuten wurde das pH auf 5,3 gebracht und die Vorbehandlung während 60 Minuten fortgesetzt.

D. Versuch wie in A. Nach 60 Minuten wurden 2 g NaCl zugesetzt und weiter 60 Minuten bei demselben pH behandelt.

E. Versuch wie in A. Nach 60 Minuten wurden 2 g NaCl zugesetzt und das pH auf 5,2 gebracht. Nach weiter 60 Minuten wurde die Aktivität wie oben bestimmt (Tabelle 7).

Man findet also, dass grössere Mengen von NaCl, während der Vorbehandlung des Enzyms mit Heparin anwesend, dasselbe vor der Inaktivierung schützt. Das einmal durch Heparin inaktivierte Enzym wird aber durch Kochsalz nicht reaktiviert, und zwar weder bei pH 4,3 noch bei 5,2. Wenn nach der Inaktivierung das pH (ohne oder mit Kochsalzzusatz) auf 5,3 gebarcht wird, so scheint allmählich eine zwar kleine aber deutliche Reaktivierung einzutreten.

Die hier gefundenen Ergebnisse sind durchgehend denen entsprechender Versuche mit β-Amylase sehr ähnlich: Die Inaktivierung tritt nur auf der sauren Seite von pH = 5,1 ein. Ob dies dahin gedeutet werden kann, dass der isoelektrische Punkt des Enzymproteins bei pH = 5,1 liegt, wollen wir unter Hinweis auf das eingangs gesagte dahinstellen. Die Inaktivierungs-pH-Kurven verlaufen wie bei der Suramininaktivierung verschiedener Enzyme äusserst steil.

Tabelle 7

Versuch	% Spaltung nach							Relative Aktivität
	3	7	10	20	40	60 Min.	24 St.	
A	0,2	0,6	1,6	2,4	4,4	7,2	—	18
B	0,7	2,8	—	6,6	13,3	14,8	—	52
C	0,5	0,9	2,0	4,1	5,7	8,8	27,5	24
D	0,5	0,8	1,2	2,1	3,9	5,7	20,0	15
E	0,4	1,4	2,0	2,6	5,3	8,3	27,5	23

Zusammenfassung

Die Einwirkung von Heparin auf α-Malzamylase wurde untersucht. Ohne Incubation mit dem Enzym in Abwesenheit von Substrat ist das Heparin Wirkungslos. Wird das Enzym bei pH-Werten unterhalb von 5,1 mit Heparin vorbehandelt, so tritt starke Inaktivierung ein. Sind grössere Mengen von Salzen (NaCl) während der Incubation mit Heparin anwesend, so üben sie eine beträchtliche Schutzwirkung aus, können aber wenn sie nach der Incubation zugesetzt werden, das schon inaktivierte Enzym nicht reaktivieren. Wird das unterhalb von pH = 5,1 inaktivierte Enzym längere Zeit bei pH = 5,3 aufbewahrt, so tritt eine deutliche aber weit von vollständige Reaktivierung ein. Die α-Malzamylase verhält sich gegenüber dem Heparin wie die früher untersuchte β-Amylase. Es ist anzunehmen, dass die Heparinwirkung primär eine Salzbildung mit kationischen Gruppen des Enzymproteins ist, dass aber nachträglich schnell irreversible Umwandlungen eintreten.

Institut für organische Chemie und Biochemie der Universität Stockholm.

LITERATUR: 1. **Myrbäck, K.**, Z. physiol. Chem. *158*, 160 (1926). — 2. **Michaelis, L.** und Mitarbeiter, Biochem. Z. *35*, 386 (1911); *49*, 333 (1913); *110*, 217 (1920). — 3. **Myrbäck, K.** und **Björklund, U.**, Arkiv Kemi *4*, 567 (1952). — 4. **Myrbäck, K.**, Acta Chem. Scand. *1*, 142 (1947). — 5. **Myrbäck, K.**, Arkiv Kemi *3*, 437 (1951). — 6. **Myrbäck, K.** und **Willstaedt, E.**, Arkiv Kemi *3*, 443 (1951). — 7. **Myrbäck, K.** und **Persson, B.**, Arkiv Kemi *4*, 495 (1952). — 8. **Town, B. W., Wills, E. D., Wilson, E. J.** und **Wormall, A.**, Biochem. J. *47*, 149 (1950). — 9. **Wills, E. D.** und **Wormall, A.**, Biochem. J. *47*, 158 (1950). — 10. **Wills, E. D.**, Biochem. J. *50*, 421 (1952). — 11. **Danielsson, K. E.** und **Sandegren, E.**, Acta Chem. Scand. *1*, 917 (1947). — 12. **Hultin, E.** und **Kristiansson, I.**, Svensk Kem. Tid. *61*, 219 (1949). — 13. **Schwimmer, S.** und **Balls, A. K.**, J. Biol. Chem. *179*, 1063 (1949). — 14. **Fischer, E. H.** und **Haselbach, C. H.**, Helv. Chim. Acta *34*, 325 (1951). — 15. **Myrbäck, K.** und **Frostell, K.**, Arkiv Kemi, Mineral. Geol. *24 A*, No. 11 (1947). — 16. **Myrbäck, K.** und **Persson, B.**, Arkiv Kemi, *in press* — 17. Siehe **Myrbäck, K.** Inc., **Myrbäck, K.** und **Neumüller, G.** in **Sumner, J. B.** und **Myrbäck, K.**, The Enzymes, Acad. Press. New York 1950, Vol. I, p. 653. — 18. **Myrbäck, K.** und **Johansson, N. O.**, Arkiv Kemi, Mineral. Geol. *20 A*, No. 6 (1945).

Tryckt den 12 januari 1953

Uppsala 1953. Almqvist & Wiksells Boktryckeri AB

ARKIV FÖR KEMI Band 5 nr 16

Communicated 10 September 1952 by ARNE FREDGA

Stereochemical studies on plant growth regulators. II. The enantiomorphs of α-(2-naphthylsulphide)-propionic acid and α-(2-naphthylmethyl)-propionic acid

By MAGNUS MATELL

Recent reports by FREDGA and MATELL (1, 2) and ÅBERG (3, 4) suggest that optically active α-aryloxy-alkylcarboxylic acids, which have greater auxin-activity than their respective antipodes, have the D-configuration. Work now in progress at this institute supports this view but further evidence is necessary before this theory may be used for the deduction of configuration from the biological effects of similar compounds.

One of the questions raised by these investigations is in what degree the growth-regulating properties are changed or modified if the oxygen atom linking the side chain to the ring system is replaced by other atoms or groups. This problem has been dealt with by ERDTMAN and NILSSON, who prepared some sulphur analogues of herbicidic phenoxyacetic acids which were found to possess auxin activity (5).

The replacement of an oxygen atom in α-(2-naphthoxy)-propionic acid (I) by a sulphur atom or a methylene group leads to α-(2-naphthylsulphide)-propionic acid (II) and α-(2-naphthylmethyl)-propionic acid (III) respectively. As a comparison of this series of compounds may give an answer to the above-mentioned question the acids II and III have been synthesised and resolved into the optical antipodes. As far as the author knows no descriptions of these resolutions have yet been published.

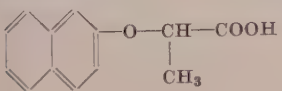

I

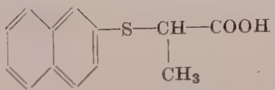

II

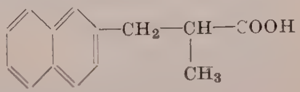

III

The racemic form of the acid II has been prepared by FREDGA (6) and the racemic acid III by VARGHA and GYÖRFFY (7). The latter authors, starting with 2-bromomethylnaphthalene and the sodium compound of ethyl methylmalonate, obtained a product with melting point 73°. The present author on the other hand, using ethyl α-cyanopropionate instead of methylmalonate and proceeding over the intermediates IV and V, obtained an acid which melted at 89.5–90.5°. This divergence could arise from polymorphism and the compound therefore was carefully examined in the hot stage microscope but only one modification could be obtained *viz.* that with melting point 90.5°. The fact that the compound with the higher melting point could be resolved into optical isomers makes it highly probable that the acid prepared by the present author is α-(2-naphthylmethyl)-propionic acid. This problem will be more closely investigated in connection with similar work on the isomeric 1-naphthalene derivative.

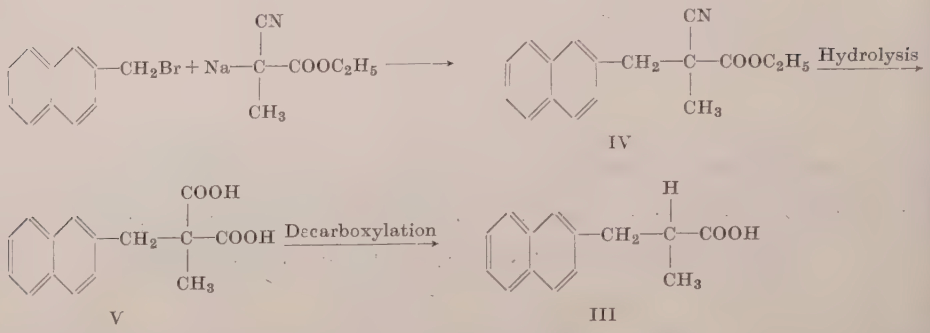

The biological investigation of these compounds will be undertaken by Dr. BÖRJE ÅBERG, who has been kind enough to provide the author with some preliminary results. Thus the (+)-form of α-(2-naphthylsulphide)-propionic acid (II) has a strong auxin activity while the (−)-form is about 300 times less active. (+)-α-(2-Naphthylmethyl)-propionic acid (III) is a weak auxin. The (−)-form is about 20 times less active than the (+)-form.

The work on the steric relations of the acids I–III is in progress and will be published elsewhere. Some results already available indicate that the (+)-forms of II and III, which have higher plant physiological activities than their antipodes, have the same configuration.

Experimental

***rac.*-α-(2-Naphthylsulphide)-propionic acid (II).** This acid was prepared according to FREDGA (6) from β-thionaphthol and α-bromopropionic acid. The yield was almost theoretical. The crude acid was recrystallised 6 times alternately from formic acid and cyclohexane. M.p. 85–87°.

Preliminary experiments on resolution. Crystalline salts containing excess of the (+)-acid were obtained with quinine and (+)-α-phenylethylamine, the latter base being about twice as effective as the former. Cinchonine and (−)-α-phenylethylamine yielded salts from which a levorotatory acid was obtained. The latter base gave the best result.

(+)-α-(2-Naphthylsulphide)-propionic acid. 11.6 g (0.05 mole) inactive acid and 6.1 g (0.05 mole) (+)-α-phenylethylamine were dissolved in 500 ml of hot 50 % alcohol. On cooling, the salt separated and after standing overnight in a refrigerator the crystalline solid was collected, dried in the air and weighed. A small sample was treated with dilute hydrochloric acid and the organic acid extracted with ether which was evaporated. The optical rotation of the acid was measured in abs. alcohol. The salt was recrystallised several times and treated as above giving the following series of crystallisations:

Crystallisation nr	1	2	3	4	5	6
ml alcohol	250	100	60	30	25	25
ml water	250	100	60	30	25	25
Weight of salt (g)	9.6	7.8	7.2	6.9	6.6	6.3
$[\alpha]_D$ of the acid	+79.6°	+114.8°	—	+130.9°	+131.1°	+132.6°

The salt from crystallisation 6 above yielded 4.2 g crude acid, which was recrystallised alternately from formic acid and cyclohexane. 3.0 g pure (+)-acid were collected as small, white needles with m.p. 53-54°.

89.06 mg acid: 8.01 ml 0.04792-*N* NaOH

$C_{13}H_{12}O_2S$ calc. equiv. wt. 232.3
found " " 232.0

0.1069 g dissolved in abs. *alcohol* to 10.00 ml: $\alpha_D^{25} = +1.499°$. $[\alpha]_D^{25} = +140.2°$; $[M]_D^{25} = +325.7°$. — 0.1065 g dissolved in *acetone* to 10.00 ml: $\alpha_D^{25} = +1.654°$. $[\alpha]_D^{25} = +155.3°$; $[M]_D^{25} = +360.8°$. — 0.1004 g dissolved in *benzene* to 10.00 ml: $\alpha_D^{25} = +1.748°$. $[\alpha]_D^{25} = +174.1°$; $[M]_D^{25} = +404.4°$. — 0.1048 g dissolved in *chloroform* to 10.00 ml: $\alpha_D^{25} = +1.438°$. $[\alpha]_D^{25} = +137.2°$; $[M]_D^{25} = +318.7°$. — 0.1027 g neutralised with *aqueous sodium hydroxide* and made up to 10.00 ml: $\alpha_D^{25} = +0.983°$. $[\alpha]_D^{25} = +95.7°$; $[M]_D^{25} = +222.3°$.

(−)-α-(2-Naphthylsulphide)-propionic acid. From the mother liquor from crystallisation 1 above 5.1 g (0.022 mole) acid with $[\alpha]_D = -101°$ (c = 1 in abs. alcohol) were obtained. This acid was dissolved with 2.7 g (0.022 mole) (−)-α-phenylethylamine in 100 ml of hot 50 % alcohol. The crystallisations were carried out as described above. The following series of crystallisations was obtained:

Crystallisation nr	1	2	3	4	5
ml alcohol	50	50	30	25	25
ml water	50	50	30	25	25
Weight of salt (g)	6.2	5.6	5.4	5.1	4.9
$[\alpha]_D$ of the acid	−111.6°	−124.8°	−133.1°	−138.9°	−137.0°

The pure salt on decomposition yielded 3.3 g crude (−)-acid. After recrystallisation 3 times from cyclohexane 2.1 g (−)-acid were collected. It closely resembled the (+)-form and melted at 52–53.5°.

87.62 mg acid: 7.84 ml 0.04792-*N* NaOH

$C_{13}H_{12}O_2S$ calc. equiv. wt. 232.3
found " " 233.2

0.0952 g dissolved in abs. *alcohol* to 10.00 ml: $\alpha_D^{25} = -1.323°$. $[\alpha]_D^{25} = -139.0°$; $[M]_D^{25} = -322.8°$. —

Ethyl α-cyano-β-(2-naphthyl)-*iso*-butyrate (IV). 4.6 g (0.2 g atom) sodium were dissolved in 80 ml abs. alcohol. To the solution were added 25.4 g (0.2 mole) ethyl α-cyanopropionate [prepared according to HOFFMAN and BARBIER (8) and WIDEQVIST (9)] and finally 48.6 g (0.22 mole) 2-bromomethylnaphthalene [prepared according to OLIVIER and WIT (10)] were added in portions while stirring. The reaction which started spontaneously was completed by boiling with reflux for 4 hours. The liquid was cooled down, water added and the alcohol distilled off. The oil which separated was washed with water, dilute sodium carbonate solution and water and was finally dried with anhydrous sodium sulphate. The product (45 g) was distilled *in vacuo* yielding 38.6 g (72 %) ethyl-α-cyano-β-(2-naphthyl)-*iso*-butyrate boiling at 218–224°/9 mm.

1-(2-Naphthyl)-propane-2,2-dicarboxylic acid (V). The ester was refluxed with 14.5 g sodium hydroxide in 50 ml water and enough alcohol to give a single phase system. After 55 hours no more ammonia was evolved. After the alcohol had been distilled off the alkaline residue was extracted with ether and acidified with dilute hydrochloric acid when an oil separated. This was taken up in ether, the water layer extracted with another portion of ether and the ether driven off from the combined extracts by a current of air. The remaining oil soon crystallised. The yield of 1-(2-naphthyl)-propane-2,2-dicarboxylic acid was 31.6 g (85 %). It melted under decarboxylation at 164° and was not further purified.

***rac.*-α-(2-Naphthylmethyl)-propionic acid (III).** The dicarboxylic acid was heated at 170° for 30 minutes when no more carbon dioxide was given off. The remaining oil crystallised in about one day. Yield 25.6 g (98 %). The acid was dissolved in dilute sodium hydroxide and the solution extracted with ether and benzene. The aqueous layer was again acidified with dilute hydrochloric acid when the organic acid was obtained in a crystalline state. The product was recrystallised once from 50 % alcohol, twice from formic acid and finally twice from petrol (b.p. 60–80°). 11.5 g pure acid were collected as irregular scales with m.p. 89.5–90.5°.

23.44 mg acid: 10.92 ml 0.1001-*N* NaOH.
43.52 mg acid: 124.42 mg CO_2 and 25.36 mg H_2O

$C_{14}H_{14}O_2$	calc.	equiv. wt. 214.3,	C 78.48,	H 6.59
	found	" " 214.4,	" 78.02,	" 6.52

Preliminary experiments on resolution. From the salts of cinchonidine and (−)-α-phenylethylamine an acid containing excess of the (+)-form was obtained. Brucine, quinine and (+)-α-phenylethylamine yielded the (−)-form. Cinchonidine and α-phenylethylamine gave the best resolution.

(+)-α-(2-Naphthylmethyl)-propionic acid. 8.6 g (0.04 mole) racemic acid and 11.8 g (0.04 mole) cinchonidine were dissolved in 200 ml hot alcohol. 200 ml cold water were added and the solution set aside in a cool place after seeding with crystals from a preliminary run. The salt which separated was recrystallised according to the scheme below:

Crystallisation nr	1	2	3	4	5	6	7	8	9	10	
ml alcohol	200	250	250	250	150	100	75	75	80	100	1
ml water	200	250	250	250	150	100	75	75	80	100	1
Weight of salt (g) .	18.7	15.8	13.1	8.7	7.4	6.9	6.6	6.3	5.8	5.3	
[α]D of the acid ...	—	+3.9°	+5.9°	+16.8°	+20.6°	+21.6°	+21.6°	+22.7°	+23.4°	+23.7°	+2

The pure salt from the last crystallisation yielded 1.9 g (+)-acid which was recrystallised from petrol (b.p. 60–80°). 1.4 g pure (+)-acid were collected as colourless, glistening plates with m.p. 84–85°. The compound is dimorphic and has a lower melting modification which can often be obtained when the melt is supercooled to room temperature. This unstable form crystallises in rectangular plates melting at 69°.

78.67 mg acid: 7.63 ml 0.04792-*N* NaOH

$C_{14}H_{14}O_2$ calc. equiv. wt. 214.3
found " " 215.2

0.0966 g dissolved in abs. *alcohol* to 10.00 ml: $\alpha_D^{25} = +0.233^\circ$. $[\alpha]_D^{25} = +24.1^\circ$; $[M]_D^{25} = +51.7^\circ$. — 0.0990 g dissolved in *acetone* to 10.00 ml: $\alpha_D^{25} = +0.317^\circ$. $[\alpha]_D^{25} = +32.0^\circ$; $[M]_D^{25} = +68.6^\circ$. —0.0971 g dissolved in *benzene* to 10.00 ml: $\alpha_D^{25} = +0.237^\circ$. $[\alpha]_D^{25} = +24.4^\circ$; $[M]_D^{25} = +52.3^\circ$. — 0.1042 g dissolved in *chloroform* to 10.00 ml: $\alpha_D^{25} = +0.253^\circ$. $[\alpha]_D^{25} = +24.3^\circ$; $[M]_D^{25} = -52.0^\circ$. — 0.0908 g neutralised with *aqueous sodium hydroxide* and made up to 10.00 ml. $\alpha_D^{25} = +0.322^\circ$. $[\alpha]_D^{25} = +35.5^\circ$; $[M]_D^{25} = +76.0^\circ$.

(−)-α-(2-Naphthylmethyl)-propionic acid. From the mother liquors from crystallisations 1–5 above, 5.1 g partially active (−)-acid were obtained. $[\alpha]_D = -11.2^\circ$ (c = 1 in abs alcohol.) This acid (0.024 mole) and 2.9 g (0.024 mole) (+)-α-phenylethylamine were dissolved in a hot mixture of 95 ml alcohol and 190 ml water. The salt which had separated after standing over night in a refrigerator was recrystallised according to the following scheme:

Crystallisation nr	1	2	3	4	5	6
ml alcohol	95	90	75	65	60	50
ml water	190	180	150	130	120	100
Weight of salt (g)	6.1	5.1	4.4	4.8	3.2	2.7
$[\alpha]_D$ of the acid	−15.6°	−19.0°	−20.2°	−22.0°	−20.7°	−22.4°

From the last fraction 1.65 g crude (−)-acid could be isolated. After recrystallisation from petrol (b.p. 60–80°) 0.9 g pure (−)-acid was collected. It closely resembled the (+)-form and melted at 83–84.5°. The unstable modification melted at 69°.

66.82 mg acid: 6.50 ml 0.04792-*N* NaOH

$C_{14}H_{14}O_2$ calc. equiv. wt. 214.3
found " " 214.5

0.0980 g dissolved in abs. *alcohol* to 10.00 ml: $\alpha_D^{25} = -0.226^\circ$. $[\alpha]_D^{25} = -23.1^\circ$; $[M]_D^{25} = -49.4^\circ$. —

The author is much indebted to Prof. A. FREDGA for valuable discussion and advice. Thanks are due to Prof. N. HELLSTRÖM, the head of this institute, for his kind interest in this work and all the facilities put at the author's disposal. Part of the expenses involved have been defrayed by a grant from *Statens Naturvetenskapliga Forskningsråd* which is gratefully acknowledged.

SUMMARY

In order to obtain more material for the study of stereochemical specificity and the relations between chemical structure and growth regulating properties, α-(2-naphthylsulphide)-propionic acid and α-(2-napthylmethyl)-propionic acid have been synthesised and resolved into optical antipodes. The rotatory power has been determined in different solvents.

Department of Organic Chemistry, Royal Agricultural College, Uppsala, August 1952.

REFERENCES: 1. **A. Fredga** and **M. Matell,** Ark. Kemi *3,* 429 (1951). — 2. ——, Ibid. *4,* 325 (1952). — 3. **B. Åberg,** Ark. Kemi *3,* 549 (1951). — 4. ——, Physiol. Plant. *5,* 305 (1952). — 5. **H. Erdtman** and **G. Nilsson,** Acta Chem. Scand. *3,* 901 (1949). — 6. **A. Fredga,** Private communication. — 7. **L. Vargha** and **Z. Györffy,** Mag. Chem. Fol. *50,* 6 (1944). — 8. **C. de Hoffmann** and **E. Barbier,** Bull. Soc. Chim. Belg. *45,* 565 (1936). — 9. **S. Wideqvist,** Ark. Kemi Min. Geol. *19 B,* No 9 (1945). — 10. **S. Olivier** and **J. Wit,** Rec. Trav. chim. Pays-Bas, *57,* 90 (1938).

Tryckt den 12 januari 1953

Uppsala 1953. Almqvist & Wiksells Boktryckeri AB

ARKIV FÖR KEMI Band 5 nr 17

Vorgelegt am 28. Mai 1952

Zum Mechanismus der Decarboxylierung. II

Von Hans von Euler und Hans Hasselquist

In der vorhergehenden Mitteilung dieser Serie[1] wurden teils die Phenylhydrazone der Dehydro-Ascorbinsäure und der Diketogulonsäure (HH 143 und HH 144) beschrieben, teils Angaben über den zeitlichen Verlauf der CO_2-Abspaltung aus Dehydro-Ascorbinsäure und aus Brenztraubensäure gemacht, der unter Verwendung von Ammoniak und Aminoderivaten (Aminosäuren) gemessen worden war.

Eistert und Hasselquist[2] sowie Hasselquist[3] haben vor kurzer Zeit Anilin- bezw. o-Phenylendiamin-Derivate des Triose-Reduktons und der Diketogulonsäure dargestellt, und die Konstitutionsformeln ihrer Produkte besprochen.

Wir behandeln hier zunächst die Umlagerung des in der vorhergehenden Mitteilung beschriebenen Monohydrazons der Dehydro-Ascorbinsäure, sowie die Reaktionsprodukte der Brenztraubensäure mit p-Aminobenzoesäure und mit Anthranilsäure und einige Derivate dieser Substanzen. Das p-Phenylendiamin, welches ebenfalls die Decarboxylierung beeinflusst, wurde auch deshalb in den Kreis dieser Studien gezogen, weil es als Spaltprodukt des Dimethyl-aminoazobenzols (Buttergelbs)[4] im Organismus der mit diesem Farbstoff behandelten Tiere mit Aldehyd- und Ketogruppen reagiert. Nur die Reaktionsprodukte von p-Phenylendiamin mit Brenztraubensäure, nicht die mit Dehydro-Ascorbinsäure sind in krystallisierter Form erhalten worden.

Umlagerung des Dehydro-Ascorbinsäure-Phenylhydrazons durch Alkali

520 mg des Phenylhydrazons wurden mit 5,2 ml 2-n. Natronlauge vorsichtig erwärmt, wobei die anfänglich entstandene rote Farbe der Lösung innerhalb c:a 1 Minute in gelbrot umschlug. Die hierauf abgekühlte Lösung wurde mit dem gleichen Volumen Wasser verdünnt und mit Essigsäure angesäuert, wodurch das Reaktionsprodukt sich als gelbrot gefärbte flockige Fällung ausschied, die abfiltriert und mit wenig Wasser gewaschen wurde. Das Rohprodukt (120 mg) wurde, zweimal aus wenig Methanol umkrystallisiert, in Form gelber prismatischer Nadeln vom Schmpt 170°–171° erhalten. (Sbst. HH 149.) Da der Schmpt des Ausgangsmateriales wenig verschieden war (169°–169,5°), wurde der Mischschmelzpunkt der beiden Substanzen bestimmt; er ergab sich zu 159°–165°, und zeigte also deutlich die Verschiedenheit der beiden Substanzen.

---

[1] Euler u. H. Hasselquist, Dieses Arkiv 4, No. 38; 1952.

[2] B. Eistert u. H. Hasselquist, Dieses Arkiv 4, No. 12; 1952.

[3] H. Hasselquist, Dieses Arkiv 4, No. 24; 1952.

[4] Siehe B. v. Euler, H. v. Euler u. H. Hasselquist, Dieses Arkiv 4, No. 33; 1952.

Das Produkt 149 ist leichtlöslich in Alkali, ziemlich leicht löslich in Methanol und in siedendem Wasser.

Analyse.

$C_{12}H_{12}O_5N_2$	ber.	C 54,54 %	H 5,58 %	N 10,60 %
	gef.	54,77	4,81	10,69

Die Analyse zeigt, dass sich durch die Alkali-Behandlung die Zusammensetzung des Dehydro-Ascorbinsäure-Phenylhydrazons nicht geändert hat. Wir nehmen also eine Änderung der Laktonbindung von 1,4 in 1,5 an.

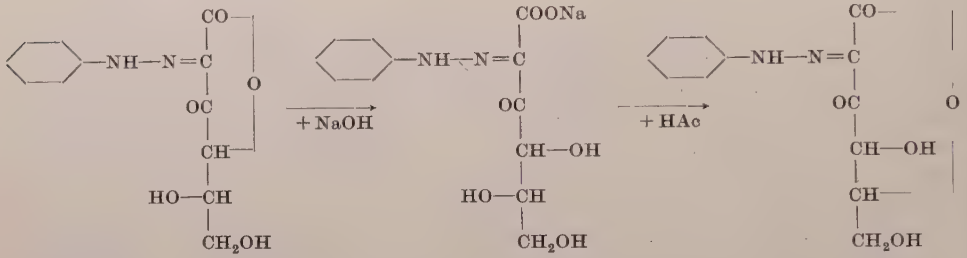

Reaction der Brenztraubensäure mit o-Amino-Benzoesäure. HH 150

1,2-Dihydro-chinaldin-tricarbonsäure-(2,4,8). — $C_{13}H_{11}O_6N$.

4,5 ml frisch destillierte Brenztraubensäure (77 %ig) in 15 ml Wasser wurden mit 6,85 g o-Aminobenzoesäure auf dem siedenden Wasserbad erwärmt, wobei schnell vollständige Lösung eintrat. Nach etwa 1 Minute begann eine kräftige CO_2-Entwicklung, wobei sich ein Reaktionsprodukt in krystallisierter Form ausschied. Nach Aufhören der CO_2-Entwicklung wurden keine weiteren Mengen Reaktionsprodukt erhalten; die Krystalle wurden aus der abgekühlten Lösung abfiltriert und mit Wasser gewaschen.

Dieses Rohprodukt (8,95 g) wurde in wenig Methanol aufgekocht um o-Aminobenzoesäure zu entfernen, abfiltriert und mit Methanol gewaschen. Die mikroskopischen hellgelben Prismen A schmolzen bei 215°–225° unter Zersetzung. Die Mutterlauge wird mit B bezeichnet.

Nach Aufschlämmen in Aceton stieg der Schmpt. auf 223°–228°. Da die Sbst. sich in den üblichen organischen Lösungsmitteln schwer löste, wurde ein analysenreines Produkt in folgender Weise dargestellt:

Die Prismen A wurden in Wasser aufgeschlämmt und mit tropfenweise zugesetzter 2-n. Natronlauge in Lösung gebracht. Nach Reinigen durch Filtration wurde die Lösung zum Sieden erhitzt. Beim Ansäuern der heissen Lösung mit 4-n. HCl krystallisierte die Sbst. in Form schwach citronengelber grösserer Prismen aus. Nach Waschen mit Wasser schmolzen sie bei 232° (Zers).

Analyse.

$C_{13}H_{11}O_6N$	ber.	C 56,32 %	H 4,00 %	N 5,05 %
	gef.	56,31	4,18	5,04

Sbst. HH 150 ist in der Wärme schwer löslich in Wasser, Benzol, Chloroform und Äthylacetat, ziemlich löslich in der Wärme in Eisessig, Aceton und Methanol, leicht löslich in warmem Alkohol und in verdünntem Alkali.

Im sichtbaren Licht färbt sich die Sbst. 150 an der Oberfläche innerhalb 1 Minute grün, und zwar am schnellsten in blauem Licht, langsamer in rotem, sehr wenig in ultraviolettem Licht. Lässt man die bestrahlte Sbst. 2 Tage im Dunkeln stehen, so nimmt sie ziemlich vollständig ihre ursprüngliche gelbe Farbe wieder an; beim Stehen in der Kälte (0°) dauert diese Rückkehr zu gelb viel länger. Ohne Belichtung erleidet die gelbe Sbst. während 5 Tagen bei Luftzutritt ihren Farbenumschlag in grün nicht.

Decarboxylierung. Einen wesentlichen Einfluss auf die CO_2-Abspaltung aus Brenztraubensäure scheint die o-Aminobenzoesäure nicht auszuüben (vgl. Tab. 2).

Tierversuche. Weisse, Jensensarkome tragende Ratten unseres norwegischen Stammes erhalten seit 4 Wochen zur gewöhnlichen Diät tägliche Injektionen

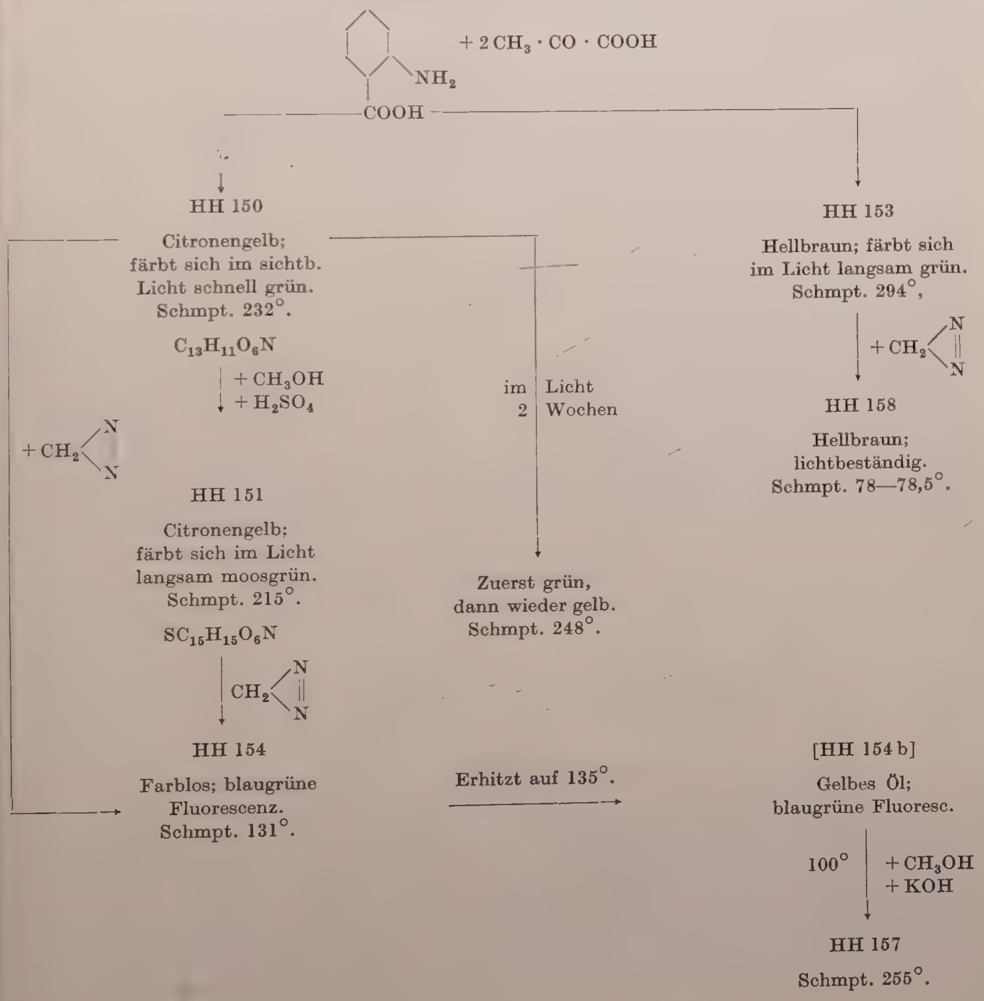
+ 2 CH₃ · CO · COOH
NH₂
COOH
HH 150
Citronengelb; färbt sich im sichtb. Licht schnell grün. Schmpt. 232°.
C₁₃H₁₁O₆N
+ CH₃OH
+ H₂SO₄
+ CH₂ N N
HH 151
Citronengelb; färbt sich im Licht langsam moosgrün. Schmpt. 215°.
SC₁₅H₁₅O₆N
CH₂ N N
HH 154
Farblos; blaugrüne Fluorescenz. Schmpt. 131°.
im 2
Licht Wochen
Zuerst grün, dann wieder gelb. Schmpt. 248°.
Erhitzt auf 135°.
HH 153
Hellbraun; färbt sich im Licht langsam grün. Schmpt. 294°,
+ CH₂ N N
HH 158
Hellbraun; lichtbeständig. Schmpt. 78—78,5°.
[HH 154 b]
Gelbes Öl; blaugrüne Fluoresc.
100°
+ CH₃OH
+ KOH
HH 157
Schmpt. 255°.

von 1 mg der Sbst. 150 in schwach alkalisierter Lösung (pH = 7). Über eine Hemmung des Sarcomwachstums können noch keine endgültigen Aussagen gemacht werden.

Veresterung der Sbst. 150 mit Methanol. Sbst. 151

1 g Sbst. 150 in 20 ml Methanol aufgeschlämmt wird mit 0,5 ml konc. Schwefelsäure 30 Min. auf dem siedenden Wasserbad erhitzt, bis alles in Lösung geht, und vorsichtig mit Wasser bis zur beginnenden Krystallisation verdünnt. Durch die Veresterung erhält man grosse citronengelbe Prismen vom Schmpt 205°–206° (Zersetzung). Krystallisiert man das Rohprodukt (0,7 g) aus Methanol um, so erhält man die reine Sbst. als grosse, citronengelbe halb durchsichtige Prismen vom Schmpt. 215°–215,5°.

Auch dieser Ester 151 färbt sich im Licht moosgrün, aber wesentlich langsamer als Sbst. 150.

Analyse.

		C	H	N
$C_{15}H_{15}O_6N$	ber.	C 59,01 %	H 4,95 %	N 4,59 %
	gef.	58,86	5,02	4,55

Die Zusammensetzung entspricht einem Dimethylester der Sbst. 150.

Bearbeitung der Mutterlauge B der Sbst. 150

Chinaldin-dicarbonsäure-(4,8).

Aus der zur Hälfte eingeengten Mutterlauge B krystallisierte nach 2-tägigem Stehen bei Zimmertemperatur ein Reaktionsprodukt in Form grosser brauner Prismen aus, die abfiltriert und mit ein wenig Methanol gewaschen wurden. Das Rohprodukt schmolz bei 280°–290°.

Durch zweimaliges Umkrystallisieren wurden die nunmehr schwach braunen Stäbchen analysenrein erhalten und schmolzen bei 295–297,5° unter Zersetzung.

Die Sbst. 153 ist schwer löslich in allen üblichen organischen Lösungsmitteln, etwas löslich in warmem Methanol u. Äthanol. Färbt sich am Licht langsam grün.

Alkali-Titration. 32,2 mg Sbst. wurden in Alkohol aufgeschlämmt und mit 0,0926-n. NaOH und Phenolphtalein titriert. Verbrauch: 2,80 ml.

$$E_{\text{gef.}} = \frac{32{,}2}{2{,}80 \cdot 0{,}0926} = 124 \qquad E_{\text{ber.}} = 116$$

Analyse.

		C	H	N
$C_{12}H_9O_4N$	ber.	C 62,33 %	H 3,92 %	N 6,06 %
	gef.	62,73	4,17	6,09

Substanz HH 154

500 mg der Substanz 151 wurden fein pulverisiert und mit einem Überschuss von in Äther gelöstem Diazomethan (ohne Methanolzusatz) versetzt, wobei die Substanz unter kräftiger Stickstoff-Entwicklung in Lösung ging. Nach Ablauf der nur 2 Minuten dauernden Reaktion wurde die Lösung von den kleinen Mengen des entstandenen Polymethylens durch Filtration befreit; dann wurde die ätherische Lösung im Vacuum bei 10° eingeengt, wobei das Reaktionsprodukt

nach Reiben in Form kleiner, schwach gelber Prismen auskrystallisierte. Nach Eindunsten zur Trockne wurde die Masse mit wenig Äther versetzt; die Krystalle wurden abfiltriert und vorsichtig mit 1 ml Äther gewaschen.

Das Rohprodukt, 400 mg, schmolz unter Gasentwicklung bei 125° ohne dass eine Missfärbung auftrat. Nach Abschluss der Gasentwicklung kann aus dem geschmolzenen Material ein neues Produkt isoliert werden.

Umkrystallisiert aus Chloroform-Petroleumäther bildet Sbst. 154 grosse farblose Prismen, die im durchscheinenden Licht blau fluorescieren. Sie schmelzen unter starker Gasentwicklung bei 131°. Sie sind leicht löslich in den gewöhnlichen organischen Lösungsmitteln, schwer löslich in Petroleumäther und in Wasser.

Umsetzung der Sbst. HH 153 mit Diazomethan. Sbst. HH 158

Chinaldin-dicarbonsäure-(4,8)-dimethylester.

Da an der Sbst. 150 eine Veresterung mit Methanol + H_2SO_4 durchgeführt werden kann, wurde versucht, Sbst. 153 in analoger Weise zu methylieren. Es zeigte sich aber, dass mit diesem Verfahren kein Methylester gebildet wurde. Es wurde nun ein Versuch mit Diazomethan angestellt:

500 mg Sbst. wurde mit Überschuss von Diazomethan-Äther-Lösung (ohne Methanolzusatz) bei Zimmertemperatur 24 Stunden stehen gelassen; dabei ging das Ausgangsmaterial unter langsamer aber gleichmässiger N_2-Entwicklung in Lösung. Die ätherische Lösung wurde hierauf im Vacuum bei 20° zur Trockene eingedunstet, wobei ein braunes Öl zurückblieb, das beim Reiben allmählich krystallisierte.

Das Rohprodukt, das noch ein wenig Öl enthielt wurde in möglichst wenig Benzol aufgelöst und mit grossen Überschuss von Petroleumäther versetzt. Es bildeten sich nun kleine, schwach hellbraun gefärbte Prismen, die immer noch ein wenig Öl enthielten und bei 75°–78° ohne Zersetzung schmolzen. (Vgl. Sbst. HH 154.)

Die Krystalle wurden nun wieder in wenig Benzol gelöst und mit Petroleumäther versetzt; die Lösung, durch eine kleine Menge von ausgefälltem Öl opalescent, wurde abfiltriert und in Eiswasser abgekühlt wobei die Substanz nunmehr ölfrei auskrystallisierte. Der Schmpt. 78°–78,5° verblieb nunmehr konstant. Ausbeute an reiner Sbst. 80 mg.

Die Sbst. 158 ist leichtlöslich in allen üblichen organischen Lösungsmitteln, ein wenig löslich in Petroleumäther, schwerlöslich in Wasser.

Analyse.

$C_{14}H_{13}O_4N$	ber.	C 64,86 %	H 5,06 %	N 5,40 %
	gef.	65,11	5,18	5,43

Erhitzung der Sbst. HH 154 auf 135°. Sbst. 157

500 mg der Sbst. 154 wurden im Paraffinbad auf 135° erhitzt. Als der Schmelzpunkt erreicht wurde setzte eine kräftige Gasentwicklung ein: sie hörte nach etwa 3 Minuten auf, worauf das Reaktionsgefäss auf 20° abgekühlt wurde. Es entstand ein grüngelbes kräftig fluorescierendes, in allen üblichen organischen Lösungsmitteln äusserst leichtlösliches Öl, das weder sublimiert noch durch Abkühlen auf —21° zur Krystallisation gebracht werden konnte.

Da anzunehmen war, dass dieses Öl noch eine Methylestergruppe enthielt, (das Ausgangsmaterial war ja ein Methylester-Derivat) wurde versucht das Produkt zu verseifen.

Das grüngelb fluorescierende Öl wurde in 5 ml abs. Alkohol gelöst und mit 5 ml alkoholischen Kalilauge 60 Min. auf dem Wasserbad erwärmt. Die Lösung wurde hierauf mit dem doppelten Volumen Wasser verdünnt, und mit HCl angesäuert wodurch eine Substanz in Form kleiner farbloser Stäbchen langsam auskrystallisierte, wozu 3 Tage erforderlich waren. Ausbeute an Rohprodukt 200 mg vom Schmpt. 255° (Zersetzung). Aus Äthylacetat umkrystallisiert wurde die Sbst. in Form farbloser Nadeln vom Schmpt 255° erhalten.

Die Sbst. 157 ist schwerlöslich in Benzol, Chloroform und Wasser, wenig löslich in Methanol, Äthanol, Aceton und Äthylacetat.

Die Lösungen der Sbst. 157 fluorescieren stark blauviolett im sichtbaren Licht.

Reaktion der Brenztraubensäure mit Sulfanilamid. Sbst. 155

1 Mol (5 g) Sulfanilamid wurden mit 2 Mol (5 ml frischdestilliert) Brenztraubensäure in 100 ml Wasser auf 50°–60° 20 Minuten erwärmt ohne dass in dieser Zeit CO_2-Entwicklung eintrat. Ein Reaktionsprodukt fiel in Form kleiner farbloser Stäbchen aus, die mit Wasser gewaschen wurden.

Die Mutterlauge wurde nochmals auf dem Wasserbad, diesmal bis 85° erwärmt, wobei eine schwache CO_2-Entwicklung eintrat, während etwas mehr von der gleichen Substanz, wie oben erwähnt ausfiel. Die Fällung A wurde aus der warmen Lösung abfiltriert (Rohprodukt 640 mg, Schmpt. 272–274° (unter Zersetzung).

Aus der Mutterlauge fiel bei Abkühlung ein gelbes Öl aus (Sbst. B), das durch Dekantieren abgeschieden werden konnte. Durch Zusatz von Methanol konnte es zur Krystallisation gebracht werden.

Subst. A wurde durch Auskochen mit Methanol gereinigt, in welchem sie sehr schwer löslich ist. Schmpt. 280°–281°. Nach zweimaligem Umkrystallisieren aus Aceton wurde der konstante Schmpt. 281° erreicht (Zersetzung).

Die Subst. A (155) ist schwer löslich in fast allen organischen Lösungsmitteln, ziemlich löslich in Aceton und in starkem Alkali.

Analyse.

Ber. für $C_9H_{10}O_3N_2S$	C = 47,80 %	H = 4,43 %	N = 12,42 %	S = 14,20 %
Gefunden	48,08	4,50	12,59	14,81

B. Einfluss verschiedener NH_2-Derivate auf die Decarboxylierung

Die *Methodik,* die zur Messung der CO_2-Abspaltung verwendet wurde (Wägung des abgespaltenen CO_2 als $BaCO_3$) haben wir in der 1. Mitteilung dieser Serie beschrieben. Später wurden die Messungen volumetrisch ausgeführt.

In der gleichen Mitt. haben wir auf die früheren Arbeiten von Böttinger, Döbner, besonders von Langenbeck und Boklund hingewiesen. Langenbeck hat in seiner Monographie[1] eine Reihe von „Carboxylase-Modellen" erwähnt; er hat ihre an Phenylglyoxylsäure gemessenen Aktivitätswerte für die Temperaturen 37°, 100° und 137° angegeben und fand 3-Amino-oxindole, und zwar besonders 3-Amino-6-oxy-naphtoxindol am wirksamsten. Es mag schon hier darauf hingewiesen werden, dass die 3-Amino-oxindole in ihrer mesomeren Form als *Amino-reduktone* vorliegen können, analog z. B. der Amino-tetronsäure und der Scorbaminsäure von MICHEEL.[2]

---

[1] W. Langenbeck, Die organischen Katalysatoren und ihre Beziehungen zu den Fermenten. Berlin, Springer, 1935.

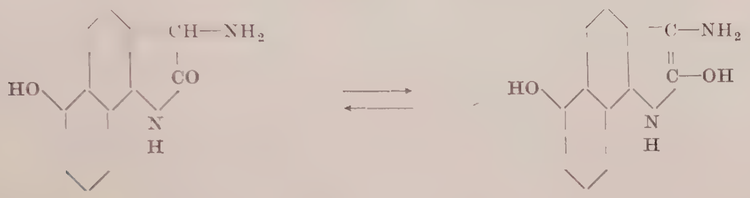

Im Anschluss an unsere früheren Versuche[3] haben wir zunächst einige Messungen an Dehydro-Ascorbinsäure bezw. Diketogulonsäure angestellt, und geben die für die Temperatur 40° erhaltenen Werte in der folgenden Tabelle an.

Tab. 1

Diketogulonsäure (DKG) resp. Dehydro-Ascorbinsäure (DHAs)

Nr.	Konzentr. Mol	Katalysator, Mol	Temp.	pH	Min.	ccm CO_2 in % d. theor. Menge
1 a	0,005 DHAs	Ohne Katalysator	40°	7,0	60	7,0
1 b	0,005 »	» »	»	11,5	»	3,21
2	0,005 »	p-Phenylendiamin 0,015	»	7,0	»	7,0
3	0,005 »	» » 0,005	»	6,0	»	8,7
4	0,005 »	» » 0,0025	»	7,0–6,0	»	7,1
5	0,010 »	» » 0,030	»	7,5	»	9,5
6	0,010 »	Anilin 0,030	»	7,5	»	7,3
7	0,005 »	o-Aminobenzoesäure 0,005	»	7,0–5,5	»	7,6
8	0,010 »	Rattenblutserum	»	5,0–3,5	»	0,8
9	0,010 »	»	»	7,0–3,5	»	2,2
10	0,010 »	»	»	7,0–3,5	»	1,7
11	0,0033 DKG	Ohne Katalysator	85°	1,7	70	30
12	0,0033 »	Anilin 0,0033	»	4,0	»	35
13	0,005 DHAs	Ohne Katalysator 5 mg KCN	40°	7,5	60	7,4
14	0,005 »	» » —	»	7,0	»	10

Bei den in Tab. 1 angegebenen Versuchen wurde frisch dargestellte Dehydro-Ascorbinsäure eingewogen. In neutraler und alkalischer Lösung geht DHAs in DKG über, von welcher die CO_2 in den Versuchen 1–10 stammt.

Durch Versuch 13 (Zusatz von KCN) sollte in Bezugnahme auf die von EULER, MYRBÄCK und LARSSON (Z. physiol. Chem. 217, 1933; siehe auch die Ergebnisse von MAURER (1936) und DIEMAIR (1950) nachgewiesene Cu-Katalyse der Sauerstoffaufnahme festgestellt werden, ob an der Decarboxylierung der DHAs bezw. DKG ein oxydativ wirkender Metallkatalysator beteiligt ist, was nicht der Fall zu sein scheint. (Vgl. auch Vers. 6 b in Tab. 2.)

---

[2] F. MICHEEL u. Mitarb. Z. physiol. Chem. 247, 34; 1937.

[3] Siehe auch EULER u. HASSELQUIST, Dieses Arkiv 4, No 7; 1952.

Tab. 2

Brenztraubensäure. — CO_2 entwickelt bei 83–85°

Nr.	Mol Brenztraubensäure	Katalysator	Konc.	Min.	pH	ccm CO_2 in % der theor. Menge
1 a	0,022	Ohne Katalysator	0,022	80	7	1,16
1 b	0,022	Anilin	0,022	80	11,5	~0
2	0,06	»	0,06	64	3	10,1
3	0,06	»	0,06	66	8,3	1,2
4	0,06	»	0,06	66	8,0	0,5
5	0,02	»	0,02	66	8,2	5,6
6 a	0,015	»	0,015	66	3,1	18,0
6 b	0,006	» 5 mg $CuSO_4$[1]	0,006 mol	60	3,5	18,1
7	0,003	»	0,003 »	80	2,5	6,9
8	0,003	»	0,003 »	80	7	2,4
9	0,003	»	0,003 »	80	3,2	11,8
10	0,06	p-Phenylendiamin	0,06 »	66		12,9
11	0,023	» »	0,023 »	30	4,0	20
12	0,06	o-Aminobenzoesäure	0,05 »	60	2	16,5
13	0,05	» »	0,05	60	7	6,3
14	0,06	m- »	0,06 »	66		20,6
15	0,05	Isatin[2]	0,05 »	60	2	20
17	0,06	Guanidin	0,06	66	2,6	7,0
20	0,02	L-Tyrosin[3]	0,02 »	60		7,6
	Na-Salz des Oxalessigsäure-methylesters 0,02	Anilin	0,02 »	60	7,5	10,2
21	0,01	Anilin	0,01 »	60	5,8	14,0
22	0,02	»	0,02 »	60	7,5–6	10,2

[1] Versuch 6 b zeigt, dass die Decarboxylierung nicht durch Cu-Spuren oxydativ beeinflusst wird.

[2] Isatin (GRASSMANN u. ARNIM, Lieb. Ann. 510, 1934) und Ninhydrin (S. RUHEMANN, J. Chem. Soc. 99, 1911) entwickeln beim Erhitzen mit Eisessig CO_2.

[3] Histidin und Dopa wurden in anderen Konzentrationen untersucht und werden später besprochen.

Übereinstimmend mit früheren Autoren ist anzunehmen, dass die untersuchten Amine ihre decarboxylierende Wirkung ausüben, indem sie mit den Ketogruppen des Substrates Schiff'sche Reaktionen eingehen. Inwieweit der Laktonring der Dehydro-Ascorbinsäure die Bildung dieser Schiff'schen Basen beeinflusst ist noch unbekannt. Man kann aber wohl nicht umhin annehmen, dass die Aufspaltung des Laktonringes *vor* der Decarboxylierung eingetreten sein muss.[4] Vermutlich machen sich dabei Einflüsse sterischer Art geltend. Jedenfalls handelt es sich bei den Versuchen der Tab. 1 um die Decarboxylierung der *Diketogulonsäure*.

---

[4] In diesem Zusammenhang mag erwähnt werden, dass die *Ringform* der Zucker in mancher Fällen reaktionsbereiter sind als die freien Aldehydformen.

Was den Einfluss verschiedener Amine auf die Decarboxylierung der Brenztraubensäure betrifft, so wurde schon S. 198 auf die Versuche von LANGENBECK hingewiesen. An den in die Tabelle 2 aufgenommenen decarboxylierenden Stoffen (gegen die nach LANGENBECK verwendete Bezeichnung „Katalysator" können Einwände gemacht werden) haben wir die Reaktion mit Brenztraubensäure präparativ untersucht, um dadurch Anhaltspunkte darüber zu erhalten, aus welchen Atomgruppen die CO_2-Abspaltung erfolgt. Mehrere der dabei isolierten Produkte sind S. 194 beschrieben. In saurer Lösung werden Schiff'sche Basen zum grossen Teil zerlegt. Unsere Fragestellung betrifft die Elektronen-Verschiebung[1], welche der CO_2-Abspaltung vorangeht oder sie bedingt. Man wird annehmen, dass das die Carboxylgruppe bindende Elektronenpaar

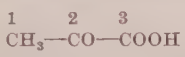

$$\overset{1}{CH_3}—\overset{2}{CO}—\overset{3}{COOH}$$

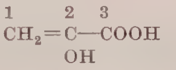

$$\overset{1}{CH_2}{=}\underset{OH}{\overset{2}{C}}—\overset{3}{COOH}$$

an die C-Atome 2 und 1 hin wandert, wenn die verschiedenen aromatischen, heterocyklischen und aliphatischen Amine, je nach ihrer Konstitution an die Brenztraubensäure gebunden werden.[2]

Abgespalten wird also CO_2 *aus der freien Carboxylgruppe.* Dagegen ist das *Ion* $CH_3·CO·COO^-$ bezw. das *Ion* $CH_2{=}\underset{OH}{C}—COO^-$ *stabil.*

Man könnte in Betracht ziehen, dass die Cocarboxylase (Aneurinpyrophosphat) auch ohne Mitwirkung ihres Apoenzyms die Fähigkeit hat, Brenztraubensäure zu decarboxylieren. Vermutlich bildet aber die freie Cocarboxylase mit der Brenztraubensäure keine Verbindung. Ihre besondere Wirkung beruht darauf, dass sie durch ihr specifisches Apoenzym mit der Brenztraubensäure zu einem Komplex zusammentritt, wodurch sie sich stets in Reaktionsnähe zur Brenztraubensäure befindet und eine Elektronen-Verschiebung veranlasst, wie wenn sie an die Brenztraubensäure direkt gebunden wäre.[3]

Herrn Ingenieur ERIK ERIKSSON danken wir bestens für eifrige experimentelle Mitarbeit.

Stockholm, Universität, Inst. f. organ.-chemische Forschung.

---

[1] Bekanntlich liegen über die in analogen Fällen eintretenden Elektronen-Verschiebungen mehrere spezielle Hypothesen vor, die aber inhaltlich noch nicht so gefestigt sind, dass sie quantitativ verwertet werden können.

[2] Probleme ähnlicher Art treten auf bezgl. des Mechanismus der Decarboxylierung der α-Aminosäuren, sowie in gewissem Grad, bezgl. der (oxydativen) CO_2-Abspaltung beim sog. Isocitronensäure-Zyklus nach SZENT-GYÖRGYI-MARTIUS.

[3] Eine Wanderung des die Carboxylgruppe bindenden Elektronenpaares, wie in der freien Säure findet beim Anion also anscheinend nicht statt. Bezgl. des Verhaltens der Schiff'schen Basen vom Typus

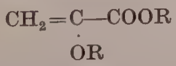

$$CH_2{=}\underset{OR}{C}—COOR$$

(R = Anilin u. dergl.) haben wir noch keine sicheren Anhaltspunkte.

Tryckt den 9 januari 1953

Uppsala 1953. Almqvist & Wiksells Boktryckeri AB

ARKIV FÖR KEMI Band 5 nr 18

Communicated 9 January 1952 by ARNE FREDGA and KARL MYRBÄCK

Optically active higher aliphatic hydroxy-compounds

I. The resolution of 3-acetoxybutanoic acid and the synthesis of (+)- and (−)-eicosanol-2

By KLAUS SERCK-HANSSEN, STINA STÄLLBERG-STENHAGEN and EINAR STENHAGEN

With 2 figures in the text

A large number of optically active, aliphatic, long-chain compounds which owe their optical activity to the presence of secondary hydroxyl groups have been isolated from natural sources. To this class of compounds belong the wax alcohols, (+)-octadecanol-2 and (+)-eicosanol-2, from the avian tubercle bacillus (1) and the timothy grass bacillus (2), and several hydroxy-acids, such as ricinoleic acid, (—)-3-hydroxydecanoic acid from *Pseudomonas aeruginosa* (3), and the cerebronic and oxynervonic acids from brain lipids. Secondary hydroxyl groups are also present in optically active compounds of more complicated structure, such as the alcohol phthiocerol from the human (4) and the bovine (5) types of the tubercle bacillus, and in the mycolic acids also isolated from bacterial lipids (6, 7, 8).

In a long series of papers published from 1911 onwards, PICKARD and KENYON (9, 10, 11) have described the resolution of a large number of secondary alcohols, and studied the rotatory dispersion of the alcohols and derived compounds, such as esters and ethers. The alcohols were esterified with one carboxyl group of a dibasic acid, and the acid ester resolved via an alkaloid salt. In the case of the homologous series of 2-hydroxyalkanes, the highest member resolved by PICKARD and KENYON was tridecanol-2 (methyl-*n*-hendecylcarbinol (9, 12). Although it seems possible that the method of resolution used by PICKARD and KENYON could be employed for the preparation of the enantiomorphs of still higher homologues such as octadecanol-2 and eicosanol-2 mentioned above, it is likely that direct resolution would become more difficult with increasing molecular weight. Furthermore, direct-resolution methods are usually not applicable in the preparation of the optically active forms of more complicated molecules with more than one active centre. In such cases it may be possible and convenient firstly to resolve suitable smaller molecules containing only one active centre, and then to synthesize the desired optically active form of the large or complex molecule from an appropriate combination of small resolved parts. For example, the optically active forms of 2-hydroxyalkanes, should, for instance, result from lengthening of the chain of the enantiomorphs of 3-hydroxybutanoic acid, and, similarly, optically active hydroxyacids from the enantiomorphs of a monoester of β-hydroxyglutaric acid. In the present communication the synthesis of the enantiomorphs of eicosanol-2 along the lines indicated above will be described.

The most convenient chain-lengthening method appeared to be the Kolbe synthesis. The operation is carried out in one step and does not involve the use of high temperatures or other conditions which might cause racemization of the active centre. However, in a preliminary attempt to prepare DL-eicosanol-2 by mixed electrolysis of racemic 3-hydroxybutanoic acid and stearic acid, difficulties due to side-reactions, indicated by skin-formation at the electrodes were encountered. This, together with the hygroscopic nature and the high water-solubility of 3-hydroxybutanoic acid, and the slowness with which it is extracted from aqueous solutions with ether, making the preparation of anhydrous acid for checking the optical activity laborious, led us to try the acetyl derivative instead of the hydroxyacid in the Kolbe synthesis.

The mixed electrolysis in ethanol-methanol solution of racemic 3-acetoxybutanoic acid and stearic acid in equimolar proportions gave racemic 2-acetoxyeicosane in a yield of 18% of the theoretical. The acetate has two crystalline modifications, melting at 32.8–33.3°, and 25.0–25.2°, respectively. Hydrolysis of the acetate gave racemic eicosanol-2, which, on crystallization from ethyl acetate, was obtained in the form of well-developed plates melting at 60.1–60.4°. On solidification of the melt another crystalline form melting at 49.9–50.1° was obtained. A specimen of the racemic alcohol has previously (13) been prepared by two of the present authors by the Grignard reaction, from octadecylmagnesium bromide and acetaldehyde. After several recrystallizations, the m.p. of the specimen was 52.0–52.7° (after previous melting, 50.9–51.1°). More recently the racemic alcohol has been prepared by the Grignard procedure by Churchward, Gibson, Meakins, and Mulley (14). After purification by chromatographic absorption on alumina, followed by crystallization from light petroleum, distillation, and crystallization from alcohol or benzene, the racemic eicosanol-2 had a (uncorrected) melting-point of 58.5–59.0°. In spite of the rigorous purification thus attempted, the melting-point reported is more than one degree lower than that shown by the specimen prepared by the Kolbe reaction. It is evident that the earlier specimen prepared in this laboratory must have contained some impurity (probably octadecanol-1), and that the Grignard reaction as applied above gives by-products that are very difficult to remove.

The acetylation of 3-hydroxybutanoic acid by means of acetyl chloride has been reported in the literature (15), but in our experience this method, and also that using acetic anhydride alone, is less satisfactory than that employing acetic anhydride + pyridine. Even so, the yield of the pure acetyl derivative was only 50% of the theoretical. This made it desirable to resolve the racemic acetoxy-compound instead of preparing the enantiomorphs by acetylation of the previously-known enantiomorphs (16, 17) of the free 3-hydroxybutanoic acid.

In a paper which appeared after our work had been completed, Mills (18) has shown that good results in the esterification of unstable alcohols are obtained if the reaction is carried out in benzene with only a moderate excess of pyridine, thus avoiding decomposition catalysed by the pyridinium ion. It seems possible that a better yield of 3-acetoxybutanoic acid can be obtained if the acetylation is carried out under these conditions.

(+)-3-Acetoxybutanoic acid, α_D^{23} +2.78° (homogeneous; *l*, 1), was prepared via the quinine salt, as described in the experimental part. The laevorotatory enantiomorph, α_D^{24}–2.86° (homogeneous; *l*, 1), was obtained via the morphine salt. There is a very marked difference in the solubility of the diastereoisomeric salts in this case, and

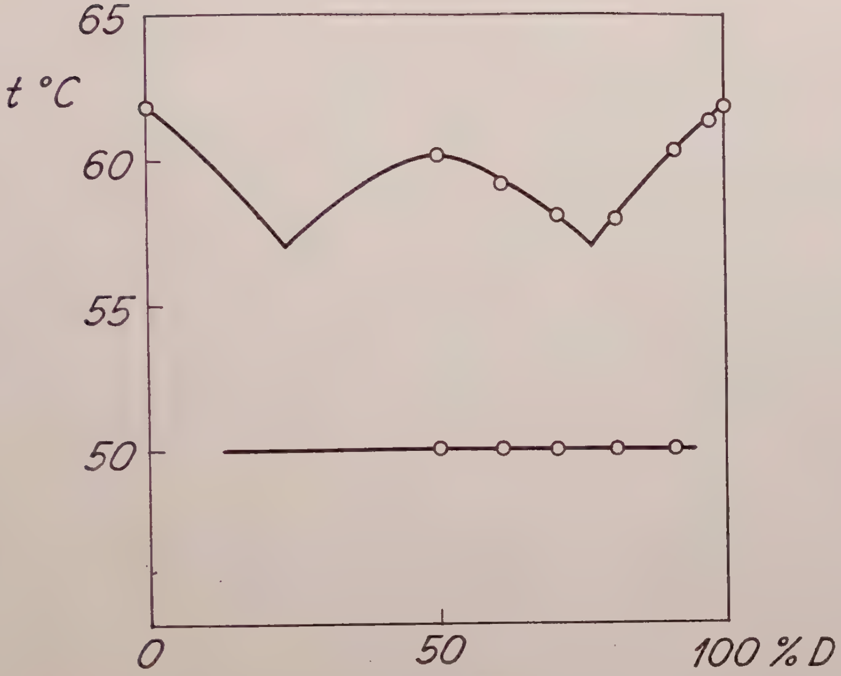

Fig. 1.

only two or three crystallizations were needed to give the pure salt of (—)-3-acetoxybutanoic acid.

The rotations of the enantiomorphs recorded above refer to dried, but not distilled, material. Different samples of the enantiomorphs showed the same rotation within very narrow limits, and the difference in magnitude between the dextro- and the laevo-rotation is almost certainly caused by traces of alkaloids whose presence lowers the rotation of the dextro- but increases that of the laevo-rotatory enantiomorph.

The free acids could not be distilled even at 0.1 mm pressure without some decomposition. The rotations were also found to have changed after keeping the acids for about a week at room-temperature. In order to prepare an alkaloid-free derivative they were converted into the methyl esters by means of diazomethane.

(+)-Methyl 3-acetoxybutanoate, b.p. 75–76°, 9 mm, showed a molecular rotation of $[M]_D^{21}$ +0.86° (homogeneous), and that of the antipode was $[M]_D^{21}$–0.82°. The esters show anomalous rotatory dispersion (see Table I) and the rotation changes sign when going from the green to the violet mercury line. The low rotations of the methyl esters do not allow definite conclusions about the optical purity of the resolved acids. The best check of the optical purity of these is provided by the behaviour of the stereoisomeric 2,5-dihydroxyhexanes, to be dealt with below.

The synthesis of the enantiomorphs of eicosanol-2 was carried out analogously to that of the racemic alcohol. Mixed electrolysis of (+)-3-acetoxybutanoic (I) and stearic acid (cf. Chart I) gives (+)-2-acetoxyeicosane (IV). The acetate (IV) has three crystalline modifications, with melting points at 35.3–35.5°, 31.6–31.9°, and 25.2–25.3°, respectively. Hydrolysis of the acetate gave (+)-eicosanol-2 (V), m.p. 61.8–61.9°, $[\alpha]_D^{23}+3.9°$ (chloroform; *c.* 10.0), $[M]_D^{23}+11.6°$.

For (+)-eicosanol-2 derived from timothy bacillus wax, PANGBORN and ANDERSON (2) give m.p. 62.5–63°, $[\alpha]_D$ in chloroform $+4.2°$ (actual polarimeter reading not given). For the acetate, PANGBORN and ANDERSON give m.p. 35–37°, and for the acid phthalate they give m.p. 60–61°, $[\alpha]_D^{18}+27.5°$ (chloroform; concentration not given). For comparison with the data for the last-mentioned derivative, and in order to check the optical purity, our synthetic specimen was converted into the acid phthalate. The optical rotation was found to be $[\alpha]_D^{20}+26.4°$ (chloroform; *c*, 5.0). As described in detail in the experimental part, the acid phthalate has three different crystalline modifications, melting at 59.2–59.7°, 55.3–55.5°, and 25.7–26.3°, respectively. The synthetic acid phthalate was converted into the brucine salt, and the latter crystallized twice from acetone. The recovered acid phthalate had $[\alpha]_D^{22}+26.4°$ (chloroform; *c*, 5.0), and the melting-points were 59.3–59.8°, 55.0–55.4°, and 25.0–25.8°, respectively. The original synthetic specimen therefore seems to have been of satisfactory optical purity.

The melting-point of the lowest-melting form of the acid phthalates is raised by the presence of higher-melting impurities. The long crystal-spacing of 36.6 Å, and the strong diffuse side-spacing of 4.12 Å, indicate that within each layer the molecules are vertical but orientated at random in relation to each other.

(—)-Eicosanol-2 was prepared in the same manner as its antipode. It had m.p. 61.7–61.8°, $[\alpha]_D^{23}—3.8°$ (chloroform; *c*, 10.0), $[M]_D^{23}—11.3°$. The acetate showed the same thermal behaviour as the antipode, the melting-points being 35.3–35.5°, 31.5–31.8°, and 25.3–25.6°, respectively. The acid phthalate had melting-points at 59.2–60.0°, 55.1–55.4°, and 25.6–25.8°, and the optical rotation was $[\alpha]_D^{22}—26.0°$ (chloroform; *c*, 5.0).

The melting-point diagram (liquidus curves) for the binary system of the enantiomorphs of eicosanol-2 is shown in Fig. 1. The higher-melting form gives a racemic compound, whereas the lower-melting form gives a continuous series of solid solutions. The lower-melting modification of the pure enantiomorph is very unstable and the melting-point of this form has not been observed in mixtures containing less than about 10% of one antipode.

The melting-point of the lowest-melting modification of the optically active acetates is the same as that of the low-melting form of the DL-acetate, and in this case we also have a continuous series of solid solutions. The X-ray investigation shows that in this form the molecules are vertical but distributed at random within the layers (single diffuse side-spacing of 4.12 Å). Higher-melting, long-chain impurities, *e.g.* free alcohol, evidently form solid solutions with this form, as the m.p. is raised by their presence. Purification of the acetates therefore raises the highest but lowers the lowest melting-point.

The long crystal-spacing of the intermediate melting form of the active acetates indicates an arrangement with tilted double molecules. For the higher-melting form the X-ray spacing suggests an arrangement with tilted single molecules.

There is thus a satisfactory agreement between the physical constants of the synthetic enantiomorphs and their derivatives and those of natural (+)-eicosanol-2 and its derivatives. The slightly higher melting-points recorded by PANGBORN and ANDERSON are most likely caused by differences in technique; these authors have probably employed a higher rate of heating than we have.

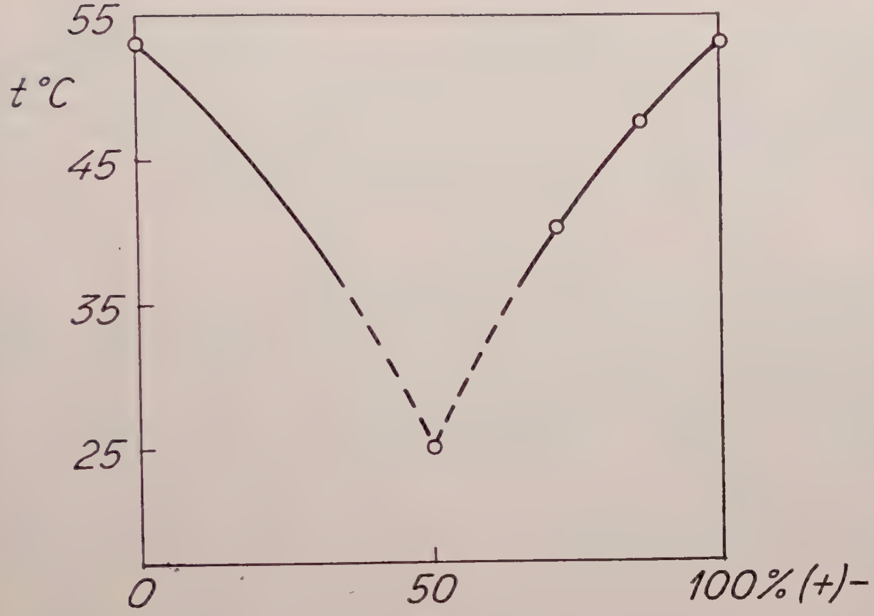

Fig. 2.

The main by-products in the Kolbe synthesis in the present case are *n*-tetratriacontane (III), and 2,5-diacetoxyhexane. The dextrorotatory stereoisomer (VI), $[M]_D^{22}+9.8°$, is obtained from dextrorotatory acetoxybutanoic acid (I). The diacetate from the electrolysis is difficult to separate from small amounts of de-acetyled derivatives and hydrocarbon by-products (*n*-heptadecane and *n*-heptadecene-1); pure (VI) is therefore best prepared by acetylation of the glycol (VII). (+)-Dihydroxyhexane (VII), $[M]_D^{25}+41.5°$ (chloroform, *c*, 9.49), a beautifully-crystalline compound of m.p. 53.0–53.3°, is obtained by hydrolysis of the crude diacetate. The corresponding laevorotatory stereoisomer had $[M]_D^{25}-41.3°$ and m.p. 53.0–53.4°.

DL-2,5-Dihydroxyhexane obtained by crystallization of equal amounts of the antipodes from ether melted at 24.5–25.5°. Part of the curve representing the binary system of the active 2,5-dihydroxyhexanes has been determined, and is shown in Fig. 2. Mixtures containing between 45 and 30% of one antipode either did not crystallize or showed a melting-range starting from the melting-point of the DL-mixture and extending over a wide range. However, the form of the upper part of the branches suggests a simple eutectic.

meso-2,5-Dihydroxyhexane of m.p. 40–41° was prepared by repeated crystallization of the mixture of inactive glycols obtained from the electrolysis of DL-3-acetoxybutanoic acid. The two inactive glycols have previously been prepared by Dupont (19) from the inactive stereoisomeric 2,5-dihydroxy-$\Delta^{3:4}$-hexynes. The higher-melting form of these gave a 2,5-dihydroxyhexane of m.p. 43–44°, and the low-melting form gave a "liquid" saturated glycol. It can now be concluded that the higher-melting of the acetylenic glycols is the *meso*-form.

If the active 3-acetoxybutanoic acid used for the synthesis of an active 2,5-dihydroxyhexane contains antipodal impurity, the glycol will be contaminated mainly by *meso*-glycol. It was found that 5% of *meso*-form lowered the melting-point of the active glycol by two degrees. The fact that active glycol obtained by evaporating off the solvent from the mother liquor showed only a very small depression (less than 0.5°) compared with the crystals filtered off, is an indication that the active 3-acetoxybutanoic acids used as initial material have been of satisfactory optical purity.

Configurational relationships

Note on nomenclature. In the absence of any established rules for indicating the configuration of the different asymmetrical carbon atoms in long-chain compounds with more than one active centre, one of the present authors some time ago (20) suggested a notation in which the configuration of each centre is indicated by a small capital letter D or L placed within brackets immediately after the number indicating the position of the centre in question. A substituent is labelled D or L according to whether it falls on the right or left side in the FISCHER projection, when carbon atom no. 1 is placed at the top. Placing carbon atom no. 1 at the top, regardless of the nature and position of the functional groups present, makes priority-rules for the latter unnecessary.

Capital letters D and L[1] are only used when describing compounds whose steric relations to the standard of reference, glyceraldehyde, have been derived in a dependable manner. The sign of the rotation for sodium light is indicated by a (+)- or (—)-sign.

A nomenclature essentially similar to that outlined above has recently been suggested by W. KLYNE[2], who has also dealt with its application to various types of ring compounds. It seems evident to us that this nomenclature is much to be preferred for practical purposes to that recently proposed by CAHN and INGOLD (21), whose scheme suffers from the great disadvantage that there is no strict correspondence between the name of the compound and its FISCHER projection, *i.e.* an L in the name does not always mean that the corresponding substituent falls to the left in the projection. We believe that this feature of the CAHN-INGOLD proposals would give rise to great confusion if they were adopted in practice.

Hydrolysis of (--)-3-acetoxybutanoic acid gave (—)-3D-hydroxybutanoic acid. The acid was isolated as zinc-calcium salt, the rotation of which was found to be $[\alpha]_D^{20}$—16.0°, in close agreement with the figure $[\alpha]_D^{20}$—16.26° given by SHAFFER and MCKIM MARRIOTT (22).

The steric relations between glyceraldehyde and 3-hydroxybutanoic acid are already known. The various steps connecting D(—)-3-hydroxybutanoic acid with D(+)-glyceraldehyde are summarized in Chart II. It might be pointed out that the formal inversion of the configuration in the synthesis of (—)-2L-acetoxyeicosane from (—)-3D-acetoxybutanoic acid is due to the turning of the acid residue through 180° in the projection.

The configurational relations between the three lowest optically active 2-hydroxyalkanes (*i.e.* methylethyl-, methyl-*n*-propyl-, and methyl-*n*-butylcarbinol) and lactic acid have been determined by LEVENE and co-workers (23, 24, 25). The chemical transformations were equivalent to a conversion of the carboxyl group of lactic acid to the longer-chain alkyl group in the secondary alcohols. In each case dextrorotatory lactic acid was found to correspond to the dextrorotatory enantiomorph of the latter. According to the nomenclature used in this paper, dextrorotatory lactic acid is (+)-2L-hydroxypropanoic acid (cf. Chart II). However, when the carboxyl group is converted into an ethyl or longer alkyl group and the carbon atom of the methyl group is labelled 1 the corresponding projection-formula has to be turned through 180°. The dextro-rotatory methyl-*n*-alkylcarbinols thus become (+)-2D-hydroxyalkanes.

---

[1] These letters vill no longer be placed within brackets.

[2] Personal communication.

LEVENE and HALLER (26) have shown that laevorotatory methylallylcarbinol gives laevorotatory methyl-*n*-propylcarbinol on catalytic hydrogenation, whereas ozonization gives laevorotatory 3-hydroxybutanoic acid.

The molecular rotations of the higher 2-hydroxyalkanes, and the corresponding acetates and acid phthalates, vary in a regular manner with chain-length, and the conclusion has therefore been drawn (11) that 2-hydroxyalkanes rotating in the same direction possess the same configuration, a conclusion confirmed by the work reported in this communication.

Rotatory-dispersion-data are given in Table I. The long-chain secondary alcohols show simple dispersion, whereas all acetyl derivatives show anomalous dispersion. These results are in general agreement with the earlier results of PICKARD and KENYON (for a summary see LOWRY (27)).

Table I[1]

Molecular rotations of hydroxy-compounds and acetyl derivatives

Compound	Wavelength Å					
	3131	3650	4046	4358	5461	5893
Methyl 3L-acetoxybutanoate (homogeneous; *l*, 1 (micro-tube); temperature 21° C)	—	− 7.5	− 3.02	− 1.21	+ 0.74	+ 0.86
Methyl 3D-acetoxybutanoate(homogeneous; *l*, 0.5 (micro-tube); *t*, 21° C)	—	+ 7.3	+ 2.9	+ 1.18	− 0.63	− 0.82
2L-Acetoxyeicosane (chloroform; *l*, 1 (micro-tube); *c*, 5.91; *t*, 21° C)	—	− 0.3	− 2.9	− 3.1	− 2.6	− 2.3
2D-Hydroxyeicosane (D(+)-eicosanol-2) (chloroform; *l*, 1 (micro-tube); *c*, 6,65; *t*, 22° C)	—	+ 34.2	+ 28,0	+ 23.0	+ 14.0	+ 12.1
2L-Hydroxyeicosane (L(−)-eicosanol-2) (chloroform; *l*, 1 (micro-tube); *c*, 7.82; *t*, 22° C)	—	− 34.3	− 27.1	− 22.1	− 13.5	− 12.1
2D,5L-Diacetoxyhexane (homogeneous; *l*, 0.5; *t*, 22° C)	− 7.5	+ 12.4	+ 14.6	+ 14.5	+ 11.2	+ 10.2
2D,5L-Dihydroxyhexane (chloroform, *l*, 1; *c*, 9.49; *t*, 25° C)	+ 195.0	+ 127.4	+ 98.6	+ 82.4	+ 49.1	+ 41.5
2L,5D-Dihydroxyhexane (chloroform; *l*, 1 (micro-tube); *c*, 8.29; *t*, 21° C)	− 193.3	− 127.2	− 98.1	− 82.1	− 48.8	− 41.3

---

[1] The optical rotations recorded in this table were obtained with the use of an ultraviolet polarimeter of the BRUHAT-GUINIER type (cf. BRUHAT, G., article in "La polarimétrie en lumière ultra-violette", Paris 1934, p. 27).

Chart I

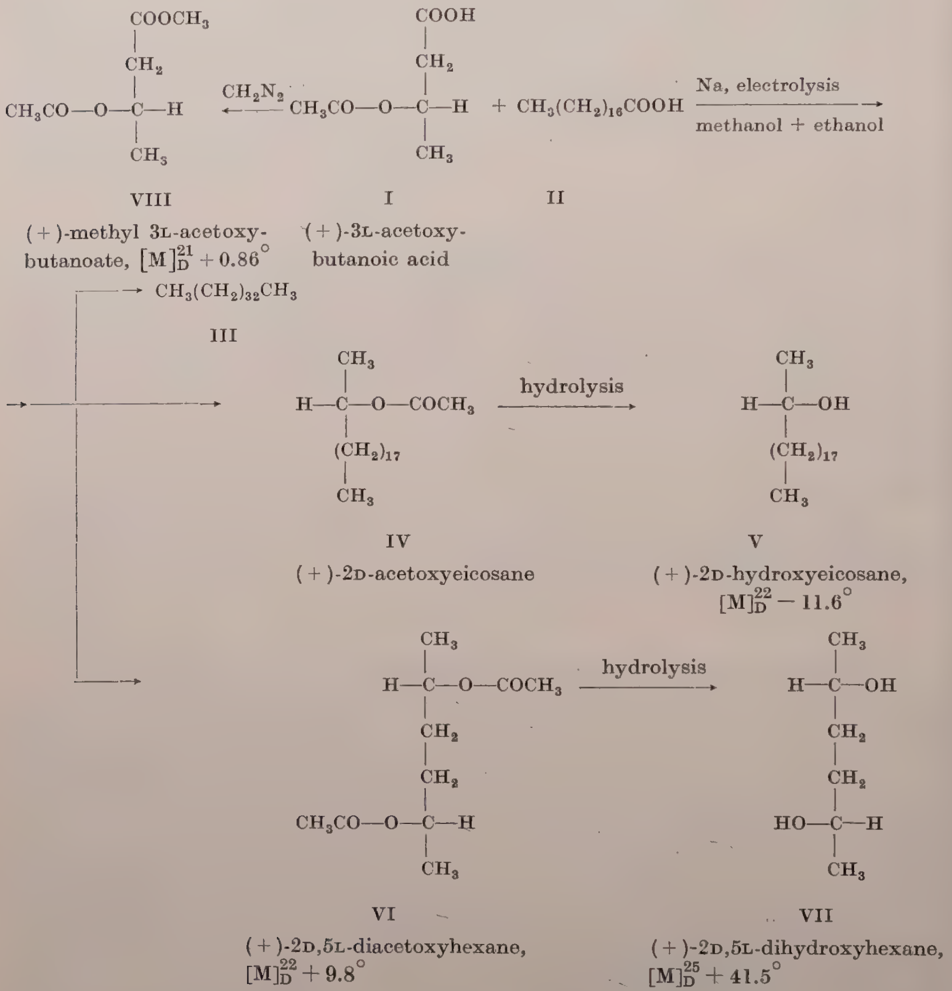
COOCH₃
CH₂
CH₃CO—O—C—H
CH₃
CH₂N₂
COOH
CH₂
CH₃CO—O—C—H
CH₃
+ CH₃(CH₂)₁₆COOH
Na, electrolysis
methanol + ethanol
VIII
I
II
(+)-methyl 3L-acetoxy-butanoate, [M]D21 +0.86°
(+)-3L-acetoxy-butanoic acid
CH₃(CH₂)₃₂CH₃
III
CH₃
H—C—O—COCH₃
(CH₂)₁₇
CH₃
hydrolysis
CH₃
H—C—OH
(CH₂)₁₇
CH₃
IV
V
(+)-2D-acetoxyeicosane
(+)-2D-hydroxyeicosane, [M]D22 − 11.6°
CH₃
H—C—O—COCH₃
CH₂
CH₂
CH₃CO—O—C—H
CH₃
hydrolysis
CH₃
H—C—OH
CH₂
CH₂
HO—C—H
CH₃
VI
VII
(+)-2D,5L-diacetoxyhexane, [M]D22 + 9.8°
(+)-2D,5L-dihydroxyhexane, [M]D25 + 41.5°

Experimental[1, 2, 3]

DL-3-Acetoxybutanoic acid

DL-Ethyl 3-hydroxybutanoate was prepared by high-pressure hydrogenation of ethyl acetoacetate over RANEY nickel (28). When carried out in the presence of 25 ml

---

[1] The melting-points recorded in this paper were taken in capillary tubes (carefully cleaned and dried before use) using calibrated ANSCHÜTZ thermometers completely immersed in a well-stirred bath of liquid paraffin. A very low rate of heating was used near the melting-point.

[2] Crystal spacings were measured using nickel-filtered Cu K_α radiation, the specimens being deposited by slight pressing, or melting, on to small glass slides. The slides were mounted on a simple goniometer and the diffraction patterns were recorded on a flat film at a distance of 10 cm.

[3] The optical rotations recorded in the experimental part were measured in a SCHMIDT & HAENSCH polarimeter of the triple-field LIPPICH type.

Chart II[1]

Steric relations between glyceraldehyde and eicosanol–2

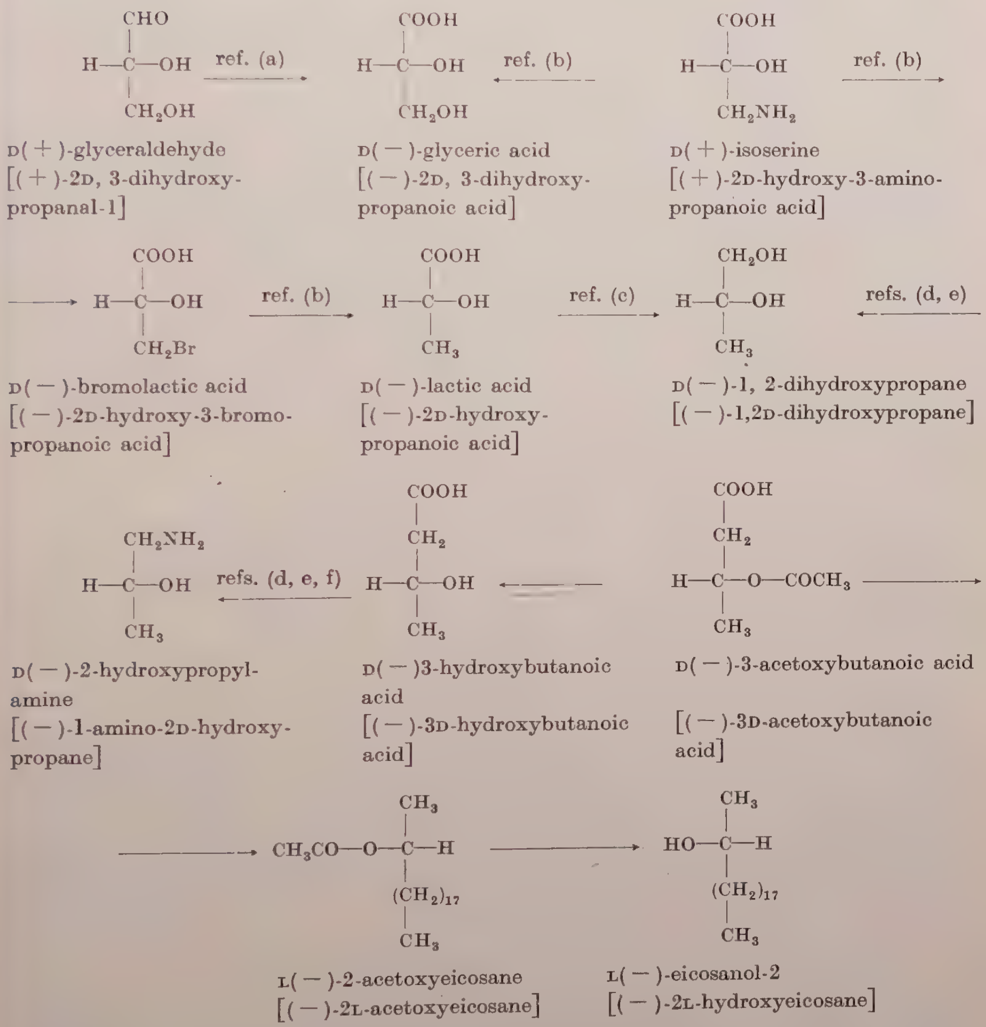
CHO
H—C—OH
CH$_2$OH
ref. (a)
D(+)-glyceraldehyde
[(+)-2D, 3-dihydroxy-propanal-1]
COOH
H—C—OH
CH$_2$OH
ref. (b)
D(−)-glyceric acid
[(−)-2D, 3-dihydroxy-propanoic acid]
COOH
H—C—OH
CH$_2$NH$_2$
ref. (b)
D(+)-isoserine
[(+)-2D-hydroxy-3-amino-propanoic acid]
COOH
H—C—OH
CH$_2$Br
ref. (b)
D(−)-bromolactic acid
[(−)-2D-hydroxy-3-bromo-propanoic acid]
COOH
H—C—OH
CH$_3$
ref. (c)
D(−)-lactic acid
[(−)-2D-hydroxy-propanoic acid]
CH$_2$OH
H—C—OH
CH$_3$
refs. (d, e)
D(−)-1, 2-dihydroxypropane
[(−)-1,2D-dihydroxypropane]
CH$_2$NH$_2$
H—C—OH
CH$_3$
refs. (d, e, f)
D(−)-2-hydroxypropyl-amine
[(−)-1-amino-2D-hydroxy-propane]
COOH
CH$_2$
H—C—OH
CH$_3$
D(−)3-hydroxybutanoic acid
[(−)-3D-hydroxybutanoic acid]
COOH
CH$_2$
H—C—O—COCH$_3$
CH$_3$
D(−)-3-acetoxybutanoic acid
[(−)-3D-acetoxybutanoic acid]
CH$_3$
CH$_3$CO—O—C—H
(CH$_2$)$_{17}$
CH$_3$
L(−)-2-acetoxyeicosane
[(−)-2L-acetoxyeicosane]
CH$_3$
HO—C—H
(CH$_2$)$_{17}$
CH$_3$
L(−)-eicosanol-2
[(−)-2L-hydroxyeicosane]

of ethanol at a temperature of 150° C and an initial pressure of 145 atms. the reduction of 2.5 moles took about 2 hours, and DL-ethyl 3-hydroxybutanoate, b.p. 70–73°, 9 mm, n_D^{22} 1.420, was obtained in 88% yield.

---

[1] The systematic names according to the notation used in this paper are given within parentheses below the common names.

a) WOHL, A., and SCHELLENBERG, R., Berichte *55*, 1404 (1922).
b) FREUDENBERG, K., Berichte *47*, 2027 (1914).
c) LEVENE, P. A., and HALLER, H. L., J. Biol. Chem. *67*, 329 (1926).
d) *Idem. ibid.*, *65*, 49 (1925).
e) KARRER, P., and KLARER, W., Helv. Chim. Acta *8*, 393 (1925).
f) LEVENE, P. A., and WALTI, A., J. Biol. Chem. *68*, 415 (1926).

Ethyl 3-hydroxybutanoate (211 g, 1.6 mole) was added to a solution of potassium hydroxide (135 g, 2.4 moles) in water (540 ml), and the solution was left for two days at room-temperature. After acidification with concentrated hydrochloric acid (200 ml), the free 3-hydroxybutanoic acid was taken up in ether, using an apparatus for continuous extraction. The ether solution was dried with sodium sulphate and the solvent evaporated. Ethanol and any residual water were distilled off *in vacuo* (water pump) until the temperature of the vapour reached 45° C.

The yield of crude DL-3-hydroxybutanoic acid, n_D^{21} 1.441, was 153 g (92% of the theoretical). 104 g (1 mole) of this product was dissolved in pyridine (202 ml, 2.5 moles), the solution cooled to room-temperature, acetic anhydride (142 ml, 1.5 mole) added, and the solution left overnight at room-temperature. The reaction mixture was heated on a water-bath and the lower-boiling parts distilled off under reduced pressure (water pump) until the temperature of the vapour rose above 40°. This operation took about half an hour. The residue was cooled, and ether (600 ml) together with a mixture of concentrated hydrochloric acid and water (100 ml of 1:1 mixture by volume) added. The ether phase was separated, washed with water until free from chlorine, and dried with sodium sulphate. The ether was distilled off, and the residue distilled, giving 76 g (52 % of the theoretical) of DL-3-acetoxybutanoic acid of b.p. 80–85°, 0.25 mm, n_D^{25} 1.427.

Anal.:	Calcd for $C_6H_{10}O_4$ (146.1)	C, 49.31; H, 6.90 %
	Found	C, 49.61; H, 6.96 %

ANSCHÜTZ and MOTSCHMANN (15) give b.p. 93–94°, 0.5 mm, and DUPONT (29) gives n_D^{18} 1.4282.

(+)-3L-Acetoxybutanoic acid (I)

DL-3-Acetoxybutanoic acid (100 g) was dissolved in a mixture of water and acetone (800 ml of 10:1 by volume) and quinine (260 g, the equimolar amount) added. In order to dissolve the quinine the mixture was heated on a water bath, with occasional stirring, to a temperature of 60°. After filtering, the solution was allowed to cool to room-temperature, seeded, and left at room-temperature until the crystallization was complete (about 24 hours). The crystals, which were in the form of long, lustrous needles, were collected, washed with water, and the salt recrystallized from successively smaller volumes of solvent until the acid recovered from the mother liquor showed a constant rotation. Acid from the different mother liquors was recovered, after acidification with dilute hydrochloric acid, by means of ether extraction. The ether solutions were washed with water and dried with sodium sulphate. After the ether had been distilled off, the residues were dried *in vacuo* over concentrated sulphuric acid at room-temperature for a period of 15 hours. From four to five recrystallizations were needed to give a constant rotation α_D^{23} +2.78° (homogeneous, *l*, 1), n_D^{23} 1.428. As it seemed possible that the specimens prepared in this manner contained traces of (strongly laevo-rotatory) quinine hydrochloride, an attempt was made to distil a sample of the active acid at a pressure of 0.1 mm. The acid distilled at 80°, but it was found that some decomposition with formation of crotonic and acetic acids occurred, and the optical rotations of the different fractions were different, and lower than that of the original sample. It was also found that the optical rotation changed slowly when the free acid was kept at room-temperature. The main part of the active acid was therefore not recovered from the salt obtained in the last recrystallization until immediately before the mixed electrolyses were to be performed. The best overall yield of free dextrorotatory enantiomorph was 25% of the theoretical. The yield of active 3-acetoxybutanoic acid recovered from 100 g of the quinine salt was about 22 g.

(+)-Methyl 3L-acetoxybutanoate

The dextrorotatory acid just described (2.5 g) was esterified with diazomethane in ether solution. The *methyl ester* distilled at 75–76°, 9 mm. Three different fractions were collected, which showed the same optical rotation. n_D^{20} 1.4149. d_D^{21} 1.061.

Optical rotation α_D^{21} $+0.57^\circ$ (homogeneous, *l*, 1).
$[\alpha]_D^{21}$ $+0.54^\circ$ $[M]_D^{21}$ $+0.86^\circ$

Anal.: Calcd for $C_7H_{12}O_4$ (160.2) C, 52.49; H, 7.55 %
Found C, 52.42; H, 7.63 %

(−)-3D-Acetoxybutanoic acid

DL-3-Acetoxybutanoic acid (30 g, 0.20 mole), water (50 ml) and morphine (50 g, 0.17 mole) were mixed, heated to 70°, and filtered hot directly into 180 ml of acetone. Crystallization of morphine salt began at once and was completed by cooling to a temperature of −20°. The crystals were collected and washed with acetone at room-temperature. The morphine salt crystallizes in the form of flat prisms. The salt was recrystallized from water-acetone, using the procedure already described. Acid recovered from the mother liquor of the second recrystillization showed the same optical rotation as that obtained from the mother liquor of the third recrystallization, *viz.* α_D^{24}—2.86° (homogeneous, *l*, 1), showing that the resolution was already complete after one recrystallization. The acid was recovered from the mother liquors and dried in the manner already described in the case of the dextrorotatory enantiomorph. Acid recovered from the mother liquor of the first crystallization showed an optical rotation α_D^{21} +2.0° (homogeneous, *l*, 1). The overall yield of (—)-*3-acetoxybutanoic acid* (after one recrystallization) was 30% of the theoretical. n_D^{22} 1.428. 100 g of the morphine salt gave about 18 g of the acid.

(−)-Methyl 3D-acetoxybutanoate

The *methyl ester*, b.p. 75–76°, 9 mm, was prepared by means of diazomethane.

Optical rotation α_D^{21} -0.27° (homogeneous, *l*, 0.5)
$[\alpha]_D^{21}$ -0.51° $[M]_D^{21}$ -0.82

Anal.: Calcd for $C_7H_{12}O_4$ (160.2) C, 52.49; H, 7.55 %
Found C, 52.17; H, 7.58 %

(−)-3-Hydroxybutanoic acid from (−)-3-acetoxybutanoic acid

(—)-3-Acetoxybutanoic acid (2.9 g) was dissolved in a solution of potassium hydroxide (10 g) in water (90 ml) and the reaction mixture left overnight at room-temperature. After acidification with dilute hydrochloric acid (50 ml of 1 : 1 by volume) the free 3-hydroxybutanoic acid was taken up in ether, using an apparatus for continuous extraction. The ether solution was dried by means of sodium sulphate and the ether distilled off, leaving a residue weighing 2.0 g. The acid was converted into the zinc-calcium salt by the procedure of SHAFFER and McKIM MARRIOTT (22). The residue was dissolved in water (5 ml), the solution divided into two equal portions, calcium carbonate (1 g) added to one portion and zinc carbonate (1.4 g) to the other, and the two mixtures left overnight at room-temperature. The mixtures were heated to 80° and filtered hot. In each case, the solid material filtered off was washed with 2.5 ml of hot water, this water added to the filtrates, and the filtrates mixed while still hot. Crystallization of the zinc-calcium salt began at once. The crystals were filtered off and washed with cold water followed by ethanol. The dry crystals weighed 0.9 g and the optical rotation of the salt was α_D^{20}—0.80° (water; *l*, 1; *c*, 5.0), or $[\alpha]_D^{20}$—16.0°. A further 0.9 g salt with the same optical rotation was obtained after adding ethanol to the mother liquors of the first crystallization. The optical rotation of the zinc-calcium salt of (—)-3-hydroxybutanoic acid given by SHAFFER and McKIM MARRIOTT is $[\alpha]_D^{20}$—16.26° (average value for 3 to 9% solutions in water).

(+)-2D-Acetoxyeicosane (IV)

The stearic acid used in the electrolyses had been carefully purified by redistilling the best commercially available distilled methyl ester through a one metre long, electrically-heated, and glass-packed column. After hydrolysis of the ester (the fraction boiling at 146°, 0.5 mm, was taken) the acid was freed from traces of unsaturated material by treatment with concentrated sulphuric acid at 70°, followed by crystallization from glacial acetic acid, and from light petroleum. The specimen prepared in this manner melted at 69.3–69.6°. FRANCIS and PIPER (30) give m.p. 69.6°.

Two different sets of platinum electrodes with the dimensions 60 × 50 × 0.1 mm, and 25 × 20 × 0.1 mm, respectively were employed. The electrodes were inserted into bakelite frames which gave a spacing of about 3 mm between the electrodes. The larger frame allowed the use of three (one anode) or five (two anodes) of the large electrodes, and the smaller frame three of the small ones.

L(+)-3-Acetoxybutanoic acid (6.0 g, 0.04 mole) and stearic acid (II) (12 g, 0.04 mole) were dissolved in a solution of sodium (0.5 g, 0.02 mole) in a mixture of methanol and ethanol (400 ml of 1 : 1 by volume), and the solution subjected to electrolysis between platinum electrodes. Three of the large electrodes were used, and the solution was contained in a 1000 ml beaker, the current used being 2.5–3 amps. Under these conditions no external cooling was found necessary. The electrolysis was continued until the reaction became neutral. After cooling to room-temperature the separated solids (mainly *n*-tetratriacontane) were filtered off and the filtrate concentrated to a small volume under reduced pressure at room-temperature. The solid material now obtained was filtered off and the combined solids (7.8 g) washed with ether. The ether solution was added to the filtrate, and the resulting solution washed three times with 1 N ammonia water, followed by water until free from ammonia. The solution was dried with sodium sulphate and the solvents were distilled off. The residue, a slightly yellow, crystalline mass weighing 6 g, was subjected to distillation at a pressure of 0.3 mm in a micro-apparatus of the CLAISEN type. The following fractions were collected:

I	up to 67°	(mainly 65–67°)	about 1 ml
II	67°–103°	(mainly 103°)	about 1 ml
III	103°–145°		about 0.5 ml
IV	145°–158°		3.5 g

Fraction IV consists of (+)-2-acetoxyeicosane. The yield of once-distilled product, with α_D^{40} +2.4° (homogeneous, *l*, 1) and m.p. 25–29°, was 25% of the theoretical. After redistillation at 0.3 mm pressure the fraction boiling at 147–153° weighed 1.6 g. The acetate was crystallized from methanol at a temperature of +5°. The yield of white, microcrystalline material melting at 32–33° was 1.4 g. Soldification began at 26.4° with the formation of small needles, and the compound remelted at 26–27°. Crystallization from light petroleum (b.p. below 40°) at a temperature of −20° gave the acetate in the form of long, silky needles melting at 31.6–31.9°. Immediately after solidification the melting-point was 26°, but on standing overnight the melting-point of the specimen was 34°. As it seemed likely that small amounts of free alcohol were present in specimens of acetate obtained from the electrolysis, a specimen was prepared by acetylation of the (+)-alcohol described below. The crystals obtained by low-temperature crystallization from light petroleum (b.p. below 40°) melted at about 34°, and consisted mainly of the high-melting form. The latter form crystallized slowly in the form of thin needles when the melt was kept above 32°, and on reheating melting occurred at 35.3–35.5°. On rapid cooling the acetate crystallized in the semi-transparent, low-melting form of m.p. 25.2–25.3°. On slow cooling from temperatures just above this melting-point the low-melting form crystallized in the form of transparent needles. The intermediate-melting form was not observed for this specimen.

The existence of three different crystal forms was confirmed by the X-ray investigation. The high-melting form has a long spacing of 27.5 Å. The intermediate-melting form gave excellent diffraction patterns with a long spacing of 41.4 Å. Finally, the low-melting form gave a long spacing of 30.8 Å, and a single, strong, and somewhat diffuse side-spacing of 4.12 Å.

D(+)-Eicosanol-2 [(+)-2D-hydroxyeicosane] (V)

The acetate just described (1.0 g) was hydrolyzed by refluxing with a solution of potassium hydroxide (2.5 g) in water (2.5 ml) and methanol (20 ml). The acetate did not dissolve to give a clear solution even at the temperature of refluxing, and benzene (5 ml) was therefore added to the hydrolysis mixture. The ether extract was dried with sodium sulphate, the solvent distilled off, and the residue crystallized from methanol at +5°. D (+)-Eicosanol-2 (0.75 g) was obtained in the form of lustrous needles melting at 61.8–62.0°. The alcohol showed a strong tendency to supercooling; solidification with the formation of white spherical aggregates did not occur until the temperature was lowered to about 54°. On reheating from this temperature remelting occurred at 61.8–62.0°. A sample obtained by the hydrolysis of the phthalate described below melted, after crystallization from methanol and from light petroleum (b.p. 40–60°), at 61.8–61.9°. The long X-ray spacing of the alcohol crystallized from solvents was 26.2 Å. A previously-melted specimen showed, in addition to the lines corresponding to this crystal form, a series of lines corresponding to a spacing of 33.8 Å. The corresponding figures for (+)-eicosanol-2 derived from natural sources were 26.2 and 33.6 Å respectively (13).

Optical rotation $\alpha_D^{22} + 0.39°$ (chloroform; *l*, 1; *c*, 10.00)
$[\alpha]_D^{22} + 3.9°$ $[M]_D^{22} + 11.6°$

Acid phthalate of D(+)-eicosanol-2

The acid phthalate was prepared by the general procedure of PICKARD and KENYON (31, 32). D (+)-Eicosanol-2 (0.3 g), phthalic anhydride (0.15 g), and pyridine (0.1 ml) were kept at a temperature of 115° for 20 hours. After adding light petroleum (b.p. 40–60°) to keep the material in solution at room-temperature, any phthalic anhydride remaining was hydrolyzed by adding a half-saturated solution of sodium carbonate and leaving the mixture at room-temperature (with occasional shaking) for a few hours. Unesterified alcohol was extracted by means of light petroleum. After acidification of the aqueous suspension with 2 N hydrochloric acid, the phthalate was taken up in chloroform. The chloroform solution was washed with water and dried by means of sodium sulphate. The solvent was then distilled off and the residue crystallized from light petroleum (b.p. 40–60°) at a temperature of —15°. The phthalate (0.22 g) was obtained in microcrystalline form. After slight sintering at 55° melting took place at 59.0–59.3°. On slow cooling of the melt, solidification took place at 53°, and on heating again remelting occurred at 59.2–59.7°. With nucleus solidification began at 58.9°.

If crystallization from light petroleum was allowed to take place at room-temperature, and the solution seeded with crystals obtained from the low-temperature crystallization (crystallization did not occur without seeding), the phthalate crystallized in the form of very thin, lustrous needles melting at 55.3–55.5°. Solidification with the formation of needles occurred at about 49°, and the material remelted at 59.0–59.8°. It was found that a third crystalline modification could be obtained on rapid cooling of the melt. This form melted at 25.7–26.3°. Before this form was completely melted the modification melting at 55° began to crystallize in the form of rounded, white, or occasionally transparent, aggregates. Sometimes also the form with m.p. 59° crystallized simultaneously as needles.

The existence of three different crystalline forms was confirmed by the X-ray investigation. The long X-ray spacing of the high-melting form was 33.3 Å, and the intermediate- and the low-melting forms gave spacings of 29.7 and 36.6 Å respectively. The low-melting form gave a strong, diffuse side-spacing of 4.12 Å.

Optical rotation $\alpha_D^{20} + 1.32°$ (chloroform; *l*, 1; *c*, 5.00)
$[\alpha]_D^{20} + 26.4°$ $[M]_D^{20} + 118°$

Acid phthalate (0.45 g, 0.001 mole) and brucine (0.47 g, 0.001 mole) were dissolved in boiling acetone (15 ml), the solution filtered, and crystallization allowed to take place overnight at a temperature of +5°. The crystals were collected and washed on the filter with acetone. After a second crystallization from acetone (10 ml) at +5°, the salt was decomposed with 2 N hydrochloric acid, and the phthalate taken up in ether. The ether solution was washed with water and dried with sodium sulphate. The solvent was distilled off, and the phthalate crystallized from light petroleum (b.p. 40–60°) at room-temperature. After seeding the modification melting at 55.0–55.4° crystallized. The melting-point of the high-melting form was 59.3–59.8° and the low-melting form melted at 25.0–25.8°. The optical rotation was $\alpha_D^{22} + 1.32°$ (chloroform; *l*, 1; *c*, 5.0), *i.e.* within the experimental error identical with that recorded above.

(−)-2L-Acetoxyeicosane

The *laevorotatory acetate* was prepared in the manner described for the antipode, using (—)-3-acetoxybutanoic acid in the electrolysis. The yield of acetate, after distillation (b.p. 155–160°, 0.3 mm) and one crystallization from methanol at room-temperature, was 18 % of the theoretical. The behaviour of the acetate obtained from the electrolysis was similar to that of the corresponding specimens of the antipode. The intermediate-melting form of m.p. 31.5–31.8° and a long crystal spacing of 41.4 Å could be obtained as silky needles from low-boiling light petroleum at —20°, but the high-melting modification could not be obtained in a pure form, and the melting-point of the low-melting modification was about one degree too high. The melting-points of these two forms of a specimen of acetate obtained by acetylation of the alcohol were 35.3–35.5° and 25.3–25.6° respectively, and the corresponding crystal spacings 27 and 30.8 Å. The low-melting form began to solidify at 25.0°.

Anal.: Calcd for $C_{22}H_{44}O_2$ (340.6) C, 77.50; H, 13.02 %
Found C, 77.61; H, 13.06 %

L(−)-Eicosanol-2 [(−)-2L-hydroxyeicosane]

Hydrolysis of the acetate gave *laevorotatory eicosanol-2*, m.p. 61.5–61.6°. After crystallization from light petroleum at —15° a microcrystalline product was obtained. Recrystallization from methanol at a temperature of +5° gave small, lustrous needles melting at 61.7–61.8°.

The observed long crystal spacings were 26.3 (stable modification) and 33.8 Å respectively.

Optical rotation $\alpha^{23}_{D} - 0.38°$ (chloroform; *l*, 1; *c*, 10.00)
$[\alpha]^{23}_{D} - 3.8°$ $[M]^{23}_{D} - 11.3°$

Anal.: Calcd for $C_{20}H_{42}O$ (298.5) C, 80.46; H, 14.18 %
Found C, 80.61; H, 14.15 %

Acid phthalate of L(−)-eicosanol-2

The *laevorotatory acid phthalate* was prepared and crystallized as described in the case of the antipode, and the melting points of the three crystalline modifications were found to be 59.2–60.0°, 55.1–55.4°, and 25.6–25.8°, respectively.

Optical rotation $\alpha^{22}_{D} - 1.30°$ (chloroform; *l*, 1; *c*, 5.00)
$[\alpha]^{22}_{D} - 26.0°$ $[M]^{22}_{D} - 116°$

Anal.: Calcd for $C_{28}H_{46}O_4$ (446.6) C, 75.29; H, 10.48 %
Found C, 75.45; H, 10.33 %

2DL-Acetoxyeicosane

The racemic acetate was prepared by mixed electrolysis of DL-3-acetoxybutanoic acid (9.8 g 0.067 moles) and stearic acid (19 g, 0.067 moles) using a solution of sodium (0.65 g) in ethanol-methanol (300 ml of 1:1 by volume). Distillation of the reaction products from the electrolysis (the acetate distilled at 137°, 0.1 mm), followed by crystallization from 96% ethanol at —10°, gave 4.0 g (18% of the theoretical) of DL-acetate of m.p. 31.4–31.8°. The ester solidified at 26.0° and remelted at 26.0–26.2°.

A specimen of the DL-acetate prepared by acetylation of the racemic alcohol described below melted, after crystallization from ether at —20°, at 32.8–33.3°, solidified at 24.9°, and remelted at 25.0–25.2°. The higher-melting form was obtained from ether as small, lustrous plates which gave very good X-ray diffraction patterns with a long spacing of 43.2 Å. The low-melting form crystallized from the melt in the form of needles. When these melted crystallization of the higher-melting form usually began at once. The low-melting modification gave a long spacing of 30.7 Å and only one strong and somewhat diffuse side-spacing of 4.12 Å.

DL-Eicosanol-2

A. *By hydrolysis of the* DL-*acetate.*

Hydrolysis of the acetate (3 g), followed by crystallization of the alcohol from ethyl acetate, gave DL-eicosanol-2 (2.2 g) in the form of beautifully lustrous, elongated plates melting at 60.1–60.4°. On solidification of the melt, an unstable crystalline form of m.p. 49.9–50.1° was obtained.

B. *From the enantiomorphs.*

Equal amounts of the antipodes (8.7 mg) were mixed and crystallized from ethyl acetate. The DL-eicosanol-2 thus obtained melted at 60.1–60.3° (stable modification). The melting-point of the unstable modification was the same as that reported for the preparation A above, *viz.* 49.9–50.1°.

The long crystal spacing of the stable modification was 46.0 Å. The corresponding spacing for the earlier specimen, now known to be impure, was 46.3 Å (13).

Acid phthalate of DL-eicosanol-2

A mixture of equal amounts (18.87 mg) of the active acid phthalates was crystallized from light petroleum (b.p. 40–60°) at —20°. The *racemic phthalate* was obtained in the form of small, lustrous plates melting at 61.8–62.2°. On rapid cooling a low-melting modification of m.p. 25.3–25.5° was obtained. As soon as this melted the high-melting form began to crystallize in the form of white, spherulithic aggregates. On slow cooling in the bath both forms solidified as rounded aggregates.

The high-melting form gave very good X-ray diffraction patterns with a long spacing of 28.0 Å. The low-melting form had a long spacing of 37 Å.

(+)-2D,5L-Diacetoxyhexane (VI)

Fractions I and II from the distillation of (+)-acetoxyeicosane were combined and distilled, and the fraction of the distillate boiling between 56° and 73° redistilled in a micro-apparatus of the CLAISEN type at 0.5 mm pressure, b.p. 69°. Two fractions were taken, the optical rotations of which were α_D^{22} +2.65° and +2.58° (hom., *l*, 0.5) respectively. For comparison, a specimen was prepared by electrolysis of pure (+)-acetoxybutanoic acid (5.35 g, added in three portions) in a solution of sodium (0.09 g) in methanol (70 ml). The electrolysis gave a 59% yield of (+)-*2*D,*5*L-*di-*

acetoxyhexane, b.p. 55–56°, 0.1 mm. Two fractions were taken, which had optical rotations of $\alpha_D^{22} + 2.68°$, and 2.60°, (homogeneous, *l*, 0.5) respectively.

In view of the slightly variable rotations observed, which are probably caused by the presence of small amounts of deacetylated material, the physical constants given below were determined on a specimen of diacetate prepared in 86 % yield from the dextrorotatory glycol by means of acetic anhydride.

n_D^{22}1.4217; d_4^{22}0.9943; R_{calcd} 51.69; R_{obs} 51.66

Optical rotation $\alpha_D^{22} + 2.41°$ (homogeneous; *l*, 0.5)
$[\alpha]_D^{22} + 4.85°$ $[M]_D^{22} + 9.8°$

Anal.:	Calcd for $C_{10}H_{18}O_4$ (202.2)	C, 59.38; H, 8.97 %
	Found	C, 59.21; H, 9.04 %

(+)-2D,5L-Dihydroxyhexane (VII)

Dextrorotatory diacetate (2.1 g) was hydrolyzed by refluxing with a solution of potassium hydroxide (4 g) in water (35 ml). The diacetate layer soon disappeared. After refluxing for three hours the solution was cooled, and saturated with sodium chloride. The solution was extracted with 10 portions of ether (100 ml each). The ether was dried with sodium sulphate, and the solvent evaporated to a small volume. On cooling to 0° in the refrigerator (+)-*2D,5L-dihydroxyhexane* (1.01 g) crystallized in the form of long lustrous needles melting at 53.0–53.3°. On slow cooling solidification in the form of long, transparent needles may begin at about 51°, but the viscous melt shows a strong tendency to supercooling, and after rapid cooling to room-temperature it may remain liquid for a long time.

Optical rotation $\alpha_D^{25} + 3.33°$ (chloroform; *l*, 1; *c*, 9.49)
$[\alpha]_D^{25} + 35.1°$ $[M]_D^{25} + 41.5°$

Anal.:	Calcd for $C_6H_{14}O_7$ (118.2)	C, 60.98; H, 11.94 %
	Found	C, 61.13; H, 11.87 %

(−)-2L,5D-Diacetoxyhexane

A specimen of the *laevorotatory diacetate* was prepared by electrolysis of (—)-3D-acetoxybutanoic acid. Distillation of the reaction products gave diacetate of b.p. 55–56°, 0.1 mm. The optical rotation was α_D^{22}—2.88° (homogeneous; *l*, 0.5).

Anal.:	Calcd for $C_{10}H_{18}O_4$ (202.2)	C, 59.38; H, 8.97 %
	Found	C, 59.00; H, 9.11 %

(−)-2L,5D-Dihydroxyhexane

Hydrolysis of the (—)-diacetate gave (—)-*2L,5D-dihydroxyhexane*, which was obtained from ether in the form of long, lustrous needles of m.p. 53.0–53.4°. A specimen obtained by evaporating off the solvent from the mother liquor melted at 52.8–53.0°.

Optical rotation $\alpha_D^{23} - 2.93°$ (chloroform; *l*, 1 (micro-tube); *c*, 8.29)
$[\alpha]_D^{23} - 35.6°$ $[M]_D^{23} - 42.1°$

Anal.:	Calcd for $C_6H_{14}O_2$ (118.2)	C, 60.98; H, 11.94 %
	Found	C, 60.63; H, 11.94 %

rac-2,5-Dihydroxyhexane

The racemic glycol was prepared by mixing equal amounts (50.3 mg) of the active forms, and crystallizing from a small volume of ether at —20°. *rac.*-2,5-Dihydroxyhexane separated in the form of small needles melting at 24.5–25.5°.

meso-2,5-Dihydroxyhexane

A mixture of the inactive glycols was prepared by hydrolysis of the acetyl derivatives obtained by electrolysis of DL-3-acetoxybutanoic acid. The mixture (1.5 g) was dissolved in ether (20 ml) and the solution kept at —25°. The solution separated into two layers, and after about two days crystals appeared in the bottom layer. The melting-point of the crystals was 20–29°. After one recrystallization from ether the melting-point was 34–39°. After a total of four crystallizations from ether *meso*-2,5-dihydroxyhexane was obtained in the form of small, brick-like (probably orthorhombic or tetragonal) crystals melting at 40–41°. DUPONT (19) gives m.p. 43–44°.

Technique used in the study of binary systems

Quantities of the components sufficient to give 10–20 mg of mixture were weighed into small, thin-walled test tubes. In the case of eicosanol-2 mixing was performed by dissolving the components in a small amount of low-boiling light petroleum, which was evaporated off at room temperature. The 2,5-dihydroxyhexanes were melted, thoroughly mixed with a small glass rod, and left to solidify at, or slightly below, room-temperature. The melting points were determined on the resulting specimens in the tubes, the usual melting-point bath being used.

We are indebted to Miss A. Renman of the microanalytical laboratory of this institute for the analyses, to Mr. L. Ahlquist for assistance, and to *Svenska Nationalföreningen mot tuberkulos*, *Statens naturvetenskapliga forskningsråd*, and *Statens medicinska forskningsråd*, for financial support. One of us (K. S-H.) thanks *Norges almenvitenskapelige forskningsråd* for a scholarship.

SUMMARY

(+)-Eicosanol-2, an alcohol found in the waxes of the avian tubercle bacillus and the timothy bacillus, has been synthesized by hydrolysis of the acetyl derivative obtained from stearic acid and (+)-3-acetoxybutanoic acid by the KOLBE electrosynthesis. The antipode was similarly obtained from stearic acid and (—)-3-acetoxybutanoic acid. Dextrorotatory 3-acetoxybutanoic acid has been obtained by resolution of the DL-acid via the quinine salt, and the antipode via the morphine salt. The steric relations between these enantiomorphs and glyceraldehyde have been determined via (—)-3-hydroxybutanoic acid, the configuration of which is already known.

The two optically active forms of 2,5-dihydroxyhexane have been prepared by hydrolysis of the diacetates obtained as by-products in the electrolyses.

Institute of Medical Chemistry, University of Uppsala.

REFERENCES. 1. **Reeves, R. E.**, and **Anderson, R. J.**, J. Amer. Chem. Soc *59*, 858 (1937). — 2. **Pangborn, M. C.**, and **Anderson, R. J.**, *ibid. 58*, 10 (1936). — 3. **Bergström, S., Theorell, H.**, and **Davide, H.**, Arkiv för Kemi, Min. o. Geol. *23 A*, No. 13 (1946). — 4. **Stodola, F. H.**, and **Anderson, R. J.**, J. Biol. Chem. *114*, 467 (1936). — 5. **Cason, J.**, and **Anderson, R. J.**, *ibid. 119*, 549 (1937). — 6. **Stodola, F. H., Lesuk, A.**, and **Anderson, R. J.**, *ibid. 126*, 505 (1938). — 7. Cf. **Asselineau, J.**, and **Lederer, E.**, Experientia *7*, 281 (1951). — 8. **Lederer, E.**, and **Pudles, J.**, Bull. Soc. Chim. Biol. *33*, 1003 (1951). — 9. **Pickard, R. H.**, and **Kenyon, J.**, J. Chem. Soc. *99*, 45 (1911), and subsequent communications to the same journal. — 10. Cf. **Lowry, T. M.**, Optical Rotatory Power, London 1935, p. 261. — 11. Cf. **Freudenberg, K.**, Stereochemie, Leipzig and Vienna 1932, p. 695. — 12. **Pickard, R. H.**, and **Kenyon, J.**, J. Chem. Soc. *105*, 830 (1914). — 13. **Ställberg–Stenhagen, S.**, and **Stenhagen, E.**, Arkiv för Kemi, Min. o. Geol. *18 A*, N:o 19 (1944). — 14. **Churchward, V. R., Gibson, N. A., Meakins, R. J.**, and **Mulley, J. W.**, J. Chem. Soc. *1950*, 959. — 15. **Anschütz, R.**, and **Motschmann, O.**, Ann. *392*, 106 (1912). — 16. **Magnus–Levy, A.**, Arch. exp. Path. und Pharm. *45*, 390 (1910). — 17. **Mc Kenzie, A.**, J. Chem. Soc. *81*, 1402 (1902). — 18. **Mills, J. A.**, *ibid. 1951*, 2332. — 19. **Dupont, G.**, Ann. Chim. (8), *30*, 526 (1913). — 20. **Ställberg–Stenhagen, S.**, Arkiv för Kemi *1*, 187 (1949). — 21. **Cahn, R. S.**, and **Ingold, C. K.**, J. Chem. Soc. *1951*, 612. — 22. **Shaffer, P. A.**, and **McK m Marriott, W.**, J. Biol. Chem. *16*, 265 (1913). — 23. **Levene, P. A., Walti, A.**, and **Haller, H. L.**, J. Biol. Chem. *71*, 465 (1926–27). — 24. **Levene, P. A., Haller, H. L.**, and **Walti, A.**, *ibid. 72*, 591 (1927). — 25. **Levene, P. A.**, and **Haller, H. L.**, *ibid. 79*, 475 (1928). — 26. *Idem, ibid. 81*, 425 (1929). — 27. **Lowry, T. M.**, Optical Rotatory Power, London 1935, p. 266. — 28. **Adkins, H., Connor, R.**, and **Cramer, H.**, J. Amer. Chem. Soc. *52*, 5192 (1930). — 29. **Dupont, G.**, Ann. chim. (8), *30*, 572 (1913). — 30. **Francis, F.**, and **Piper, S. H.**, J. Amer. Chem. Soc. *61*, 577 (1939). — 31. **Pickard, R. H.**, and **Kenyon, J.**, J. Chem. Soc. *99*, 58 (1911). — 32. Org. Syntheses Coll. Vol. I, 2^{nd} Ed., note 3 p. 420.

Tryckt den 11 februari 1953

Uppsala 1953. Almqvist & Wiksells Boktryckeri AB

ARKIV FÖR KEMI Band 5 nr 19

Read 8 October 1952

Studies on synthetic growth substances. IV

By ARNE FREDGA

In the first paper of this series (1) a number of naphthylsulphide carboxylic acids and naphthylmethyl-sulphide carboxylic acids were described, and it was pointed out that compounds of this type might provide suitable material for studying the influence of structural and sterical factors on growth-regulating activity. Several new acids of this type have now been synthesised (I–X) and the description of these compounds is given in the present paper. The biological effects are being investigated by Dr. BÖRJE ÅBERG (Royal Agricultural College). Several of the acids are more or less effective auxin antagonists, but in some cases a positive auxin effect was found (2). A rather high activity was shown by α-(2-naphthylsulphide)-propionic acid (V), the sulphur analogue of the α-(2-naphthoxy)-propionic acid. The optical resolution of the sulphur compound has been undertaken by Dr. MAGNUS MATELL (3).

The acids were prepared by the general methods indicated in a previous publication (1). As γ-bromobutyric acid in neutral solution is easily converted into γ-butyrolactone, acids I and V were prepared from methyl γ-bromobutyrate and the corresponding naphthyl mercaptanes.

Several recrystallisations from different solvents (once with charcoal) were in general necessary in order to obtain the acids in a state of purity. Formic acid, cyclohexane and carbon tetrachloride were found to be the most suitable solvents.

Experimental

γ-(1-Naphthylsulphide)-*n*-butyric acid (I).

3.5 g (0.021 mole) of 1-naphthyl mercaptane and 1.1 g (0.028 mole) of sodium hydroxide were dissolved in 30 ml of water. To the cooled solution were added 3.8 g (0.02 mole) of methyl γ-bromobutyrate and sufficient ethanol for a homogeneous solution. After standing for two days, 2 g of sodium hydroxide were added, the solution was heated to boiling for a few minutes and then evaporated to dryness by a current of air. The residue was dissolved in water and filtered. On acidifying with excess hydrochloric acid, the naphthylsulphide-butyric acid separated as a readily crystallising oil. After one recrystallisation from formic acid and two from carbon tetrachloride, the pure acid was obtained as small short-prismatic crystals with m.p. 79–80°. Yield 2.6 g (53 %).

0.3122 g acid: 11.81 ml 0.1074-N NaOH. — 57.37 mg acid (Grote-Krekeler): 9.65 ml 0.04823-N NaOH.

$C_{14}H_{14}O_2S$	Calc. Equiv. wt.	246.3	S 13.02
	Found » »	246.1	» 13.00

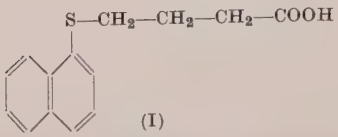

(I)

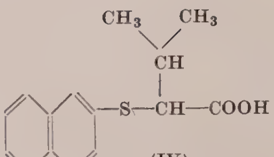

(IV)

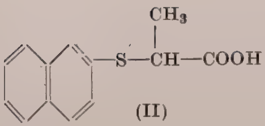

(II)

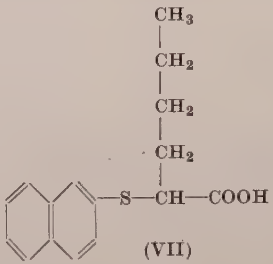

(VII)

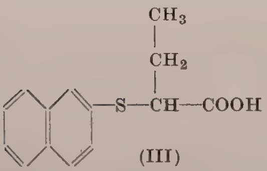

(III)

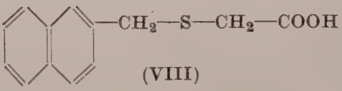

(VIII)

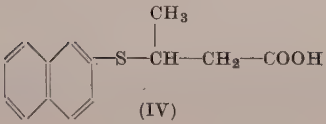

(IV)

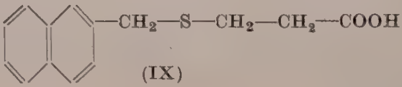

(IX)

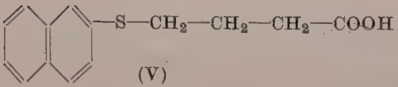

(V)

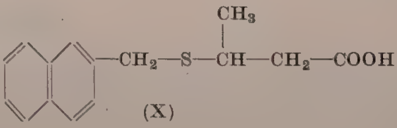

(X)

α-(2-Naphthylsulphide)-propionic acid (II).

3.2 g (0.02 mole) of 2-naphthyl mercaptane and 1.2 g (0.03 mole) of sodium hydroxide were dissolved in water. After cooling, a solution of 3.2 g (0.02 mole) of α-bromopropionic acid, neutralised by potassium carbonate, was added. The total volume of the mixture was about 60 ml. After standing in a closed bottle for 24 hours, the solution was filtered and acidified with excess hydrochloric acid. The reaction product was obtained as a readily crystallising oil. The yield of crude product was 4.1 g. After one recrystallisation from cyclohexane, two from formic acid and one more from cyclohexane, 3.1 g of pure acid were obtained as a colourless crystalline powder with m.p. 87–88°.

0.2742 g acid: 11.06 ml 0.1066-*N* NaOH. — 32.21 mg acid (Grote-Krekeler): 5.76 ml 0.04823-*N* NaOH.

$C_{13}H_{12}O_2S$	Calc.	Equiv. wt. 232.3	S 13.80
	Found	» » 232.6	» 13.83

α-(2-Naphthylsulphide)-*n*-butyric acid (III).

8.0 g (0.05 mole) of 2-naphthyl mercaptane and 5.0 g (0.125 mole) of sodium hydroxide were dissolved in 100 ml of water and 8.4 g (0.05 mole) of α-bromo-*n*-butyric acid were added to the cooled solution. The mixture was treated as described above. The yield of crude product was 11.6 g (94 %). After one recrystallisation from cyclohexane, two from formic acid and one more from cyclohexane, 8.5 g of pure acid were obtained as a colourless crystalline powder with m.p. 79–80°.

0.3326 g acid: 12.70 ml 0.1064-*N* NaOH. — 54.53 mg acid (Grote-Krekeler): 9.18 ml 0.04823-*N* NaOH.

$C_{14}H_{14}O_2S$	Calc.	Equiv. wt. 246.3	S 13.02
	Found	» » 246.1	» 13.02

β-(2-Naphthylsulphide)-*n*-butyric acid (IV).

8.0 g (0.05 mole) of 2-naphthyl mercaptane and 4.5 g (0.11 mole) of sodium hydroxide were dissolved in 100 ml of water and 8.4 g (0.05 mole) of β-bromo-*n*-butyric acid (4) were added to the cooled solution. The mixture was left to stand in a closed bottle for 48 hours, after which the reaction product was isolated as described above. The yield of crude product was 11.4 g (93 %); after two recrystallisations from cyclohexane, two from formic acid and one more from cyclohexane, 6.8 g of pure acid were obtained as microscopic scales or flakes, forming a colourless crystalline powder with m.p. 69–70°.

0.3078 g acid: 11.76 ml 0.1064-*N* NaOH. — 41.92 mg acid (Grote-Krekeler): 9.04 ml 0.03787-*N* NaOH.

$C_{14}H_{14}O_2S$	Calc.	Equiv. wt. 246.3	S 13.02
	Found	» » 246.0	» 13.09

γ-(2-Naphthylsulphide)-*n*-butyric acid (V).

This acid was prepared from 2-naphthyl mercaptane (3.4 g) and methyl γ-bromo-*n*-butyrate (3.8 g) in the same way as described for the 1-naphthyl derivative (I). After two recrystallisations from carbon tetrachloride, the acid was obtained as small, glistening rectangular plates with m.p. 87.5–88.5°. The yield of pure acid was 3.3 g (63 %).

0.3244 g acid: 12.30 ml 0.1074-*N* NaOH. — 48.03 ml acid (Grote-Krekeler): 8.15 ml 0.04823-*N* NaOH.

$C_{14}H_{14}O_2S$	Calc.	Equiv. wt. 246.3	S 13.02
	Found	» » 245.6	» 13.12

α-(2-Naphthylsulphide)-*iso*-valeric acid (VI).

6.7 g (0.042 mole) of 2-naphthyl mercaptane and 4.4 g (0.11 mole) of sodium hydroxide were dissolved in 40 ml of water. 7.5 g (0.042 mole) of α-bromo-*iso*-valeric acid were added and the solution was shaken for one hour. As the α-bromo-*iso*-valeric acid is known to react rather slowly, the solution was left in a closed bottle for 5 weeks. It was then diluted to 300 ml, filtered with charcoal and acidified with excess hydrochloric acid. The reaction product separated as an oil, which could be brought to crystallisation by cooling and scratching. The yield of crude acid was 9.2 g (84 %); after one recrystallisation from cyclohexane and three from formic acid, 6.4 g acid were obtained as needles or pointed prisms with m.p. 78.5–79.5°.

0.3084 g acid: 11.02 ml 0.1074-*N* NaOH. — 42.86 mg acid (Grote-Krekeler): 6.77 ml 0.04823-*N* NaOH.

$C_{15}H_{16}O_2S$	Calc.	Equiv. wt.	260.3	S	12.32
	Found	» »	260.6	»	12.21

α-(2-Naphthylsulphide)-*n*-caproic acid (VII].

6.4 g (0.04 mole) of 2-naphthyl mercaptane and 4.1 g (0.1 mole) of sodium hydroxide were dissolved in 35 ml of water. 7.8 g (0.04 mole) of α-bromo-*n*-caproic acid and 30 ml of water were added and the mixture was shaken until homogeneous. After standing for 20 hours, the solution was diluted to 500 ml, filtered with charcoal and acidified with excess of hydrochloric acid. The oily product crystallised after some hours at 0°. The acid is readily soluble in most organic solvents and has a great tendency to separate as an oil. It can, however, be recrystallised by slow cooling of a not too concentrated solution in formic acid. The yield of crude product was 9.9 g (90 %); after three recrystallisations, 5.3 g of the acid were obtained as small glistening prisms or needles with m.p. 60–61.5°.

0.3523 g acid: 12.00 ml 0.1074-*N* NaOH. — 46.80 mg acid (Grote-Krekeler): 9.08 ml 0.03787-*N* NaOH.

$C_{16}H_{18}O_2S$	Calc.	Equiv. wt.	274.4	S	11.68
	Found	» »	273.4	»	11.78

2-Naphthylmethyl-sulphide-acetic acid (VIII).

2.4 g (0.025 mole) of thioglycolic (mercaptoacetic) acid and 2.3 g (0.057 mole) of sodium hydroxide were dissolved in 50 ml of water and a solution of 5.5 g (0.025 mole) of 2-naphthylmethyl bromide (5) in 60 ml of ethanol were added. The mixture was shaken until homogeneous. After standing for 24 hours in a closed bottle, the ethanol was evaporated by a current of air; the remaining solution was diluted with water and acidified with excess of hydrochloric acid. The reaction product separated as a readily crystallising oil. The yield of crude product was 4.5 g (78 %); after one recrystallisation from formic acid and two from carbon tetrachloride, 3.3 g of pure acid were obtained as colourless glistening prisms with m.p. 106–107°.

0.2957 g acid: 11.97 ml 0.1064-*N* NaOH. — 52.16 mg acid (Grote-Krekeler): 9.33 ml 0.04823-*N* NaOH.

$C_{13}H_{11}O_2S$	Calc.	Equiv. wt.	232.3	S	13.80
	Found	» »	232.2	»	13.83

β-(2-Naphthylmethyl-sulphide)-propionic acid (IX).

5.8 g (0.03 mole) of β-ethylxanthogene-propionic acid (6) were dissolved in 50 ml of concentrated aqueous ammonia. After standing for three days, the xanthogene amide formed was removed by extraction with ether. The resulting solution, containing the ammonium salt of the β-mercapto-propionic acid was mixed with a solution of 0.03 mole of 2-naphthyl-methyl bromide in 50 ml of ethanol. After shaking for some hours, the mixture was left to stand for two days. The reaction product was isolated as described for the preceding acid (VIII). The yield of crude product was 5.3 g (72 %); after six recrystallisations, alternately from formic acid and cyclohexane, 3.4 g of pure acid were obtained as colourless glistening scales with m.p. 104.2–105.5°.

0.2936 g acid: 11.12 ml 0.1074-*N* NaOH. — 34.60, 38.35 mg acid (Grote-Krekeler): 5.72, 6.46 ml 0.04823-*N* NaOH.

$C_{14}H_{14}O_2S$	Calc.	Equiv. wt. 246.3	S 13.02
	Found	» » 245.8	» 13.01, 13.02

β-(2-Naphthylmethyl-sulphide)-*n*-butyric acid (X).

The acid was prepared in the same way as IX, starting from 10.4 g (0.05 mole) of β-ethylxanthogene-*n*-butyric acid (7) (crude product, obtained from potassium ethylxanthogenate and β-bromo-*n*-butyric acid) and 11.0 g (0.05 mole) of 2-naphthyl-methyl bromide (5). After six recrystallisations, alternately from formic acid and cyclohexane, 2.6 g of pure acid were obtained as small glistening scales with m.p. 81.5–82.5°.

0.3299 g acid: 11.84 ml 0.1074-*N* NaOH. — 28.72 mg acid (Grote-Krekeler): 4.54 ml 0.04823-*N* NaOH.

$C_{15}H_{16}O_2S$	Calc.	Equiv. wt. 260.3	S 12.32
	Found	» » 259.4	» 12.22

The author is indebted to Mr. K. PETTERSSON for the sulphur analyses and to several junior students in the laboratory for preparing starting materials.

SUMMARY

A number of naphthalene derivatives (I–X) containing a sulphur atom and a carboxyl group in the side chain have been prepared. The biological effects of the compounds are being investigated elsewhere. Preliminary results indicate that some of the acids show positive auxin effect while others are auxin antagonists.

Laboratory of Organic Chemistry, Chemical Institute, University of Uppsala, September 1952.

REFERENCES

1. A. FREDGA, Arkiv Kemi *3* (nr 16), 123 (1951).
2. B. ÅBERG, Private communication.
3. M. MATELL, Arkiv Kemi *5* in the press.
4. J. M. LOVÉN and HJ. JOHANSSON, Ber. *48*, 1254 (1916).
5. S. C. J. OLIVIER and J. WIT, Rec. trav. chim. *57*, 90 (1938).
6. E. BIILMANN, Ann. *339*, 363 (1905).
7. P. A. LEVENE and L. A. MIKESKA, J. Biol. Chem. *70*, 373 (1926).

Tryckt den 11 februari 1953

Uppsala 1953. Almqvist & Wiksells Boktryckeri AB

ARKIV FÖR KEMI Band 5 nr 20

Communicated 22 October 1952 by JOHN RUNNSTRÖM and KARL MYRBÄCK

The formation of tyrosine in *Escherichia coli* and *Neurospora crassa*, grown on isotope-labelled acetate as the sole source of carbon

By G. EHRENSVÄRD and L. REIO

With 2 figures in the text

In connection with studies on the metabolic interconnection between acetate and amino acids in general, a certain amount of pure tyrosine was isolated from *Escherichia coli* and *Neurospora crassa,* which had been cultivated under suitable conditions with isotopically labelled acetate as the sole source of carbon.

The *coli*-tyrosine was identical with that isolated in previous work (1) and subjected to decarboxylation as described. The weight, after three times recrystallization, was 460 mg. (the C^{14}-values, as recorded in (1) for the tyrosine carboxyl, total tyrosine carbon and the carboxyl of the acetate of the substrate have to be multiplied with a factor of 2.7 in order to be comparable with the C^{14}-values recorded in this paper—as the Geiger-counter employed for the present work has an efficiency 2.7 times greater than the counter used in the previous studies).

The *Neurospora*-tyrosine was isolated from a hydrolysate of *Neurospora,* grown from the conidia stage in the presence of NH_4Cl labelled with N^{15} to provide an equal N^{15} content in all amino acids of the protein formed during the cultivation. During the ten last hours of the cultivation procedure, non-labelled acetate was exchanged against $C^{13}H_3C^{14}OONa$ and after the termination of the cultivation the organism material (8.0 g) was hydrolyzed and tyrosine and phenylalanine were adsorbed from the hydrolysate with active carbon according to PARTRIDGE (2). To the eluate about 1 g of non-labelled tyrosine was added and from this solution tyrosine was recovered in pure state in an amount of 796 mg. (Paper chromatography indicated no other amino acid contaminants present; the preparation contained 7.48 per cent nitrogen, theoretically 7.73 per cent; the tyrosine used for dilution had 7.55 per cent nitrogen.) N^{15}-analysis indicated a dilution of 1 : 93, based on the N^{15}-excess in total nitrogen of the *Neurospora* material $= 7.37\,\%$, and the N^{15}-excess in the tyrosine isolated after dilution $= 0.080\,\%$. The figures for C^{14}- and C^{13}-excess in different carbon atoms of the *Neurospora*-tyrosine correspond to this dilution of 1 : 93.

Details of the cultivation and amino acid isolation from the described experiment with *Neurospora* will be published later (3). The isotope values for acetate at a dilution of 1 : 93 were 1 350 counts per minute and 0.27 per cent C^{13}-excess.

The total degradation of the tyrosine preparations followed the procedure described in the foregoing communication of this volume (4). The compiled result is shown in Table 1, for simplicity only the C^{14} values are given.

Table 1

Isotope content in different carbon atoms of tyrosine, isolated from *Escherichia coli* and *Neurospora crassa*, grown on acetate labelled with C^{14} in the carboxyl group. The values are compiled from degradation data, previously given (4).

Carbon atoms	C^{14}-activity in counts per minute per 15 mg of barium carbonate	
	Escherichia coli	*Neurospora crassa*
Acetate carboxyl	*70700*	125000[1] *1350*
Tyrosine carbon atoms:		
COOH	746	212
α	25	9
β	18	17
1	72	22
2.6	201	52
3.5	172	47
4	450	194

Discussion

From the above values it is evident that the formation of tyrosine in both organisms has followed the same routes from the acetate of the substrate, notwithstanding the quantitatively rather small incorporation of isotope from acetate into the *coli*-tyrosine and the extensive utilization of acetate carbon in the *Neurospora*-tyrosine. It has to be recalled that the conditions of cultivation of the organisms in question was very different. The *coli* were incubated with labelled acetate for 3.5 hours, during which time approximately 15 % growth took place, the labelled acetate being added at a period when conditions were rather stationary in the dense bacteria solution (29 g dry weight in 25 litres). The *Neurospora* material was, however, in full growth during the ten-hour exposure to labelled acetate, increasing its weight approximately 50 per cent. In spite of these different conditions of growth, the qualitative aspect of the distribution of C^{13} and C^{14} in the different carbon atoms of the tyrosine structure showed strikingly similar features.

In order to evaluate the results of the experiments one has to consider the five different alternatives that may be constructed with regard to the isotope distribution within the phenolic ring structure. Since by nature the isotope distribution with regard to carbon atoms 3 and 5, and likewise 2 and 6 cannot be directly determined one has to face the possibilities that the C^{13}–C^{14}-content in the pairs 3.5 and 2.6 is distributed according to the following alternatives:

---

[1] This figure refers to the actual C^{14}-activity in the carboxyl of the acetate of the cultivation medium. The figure 1350, and the subsequent figures for different tyrosine carbon atoms of the *Neurospora* series refer to a dilution 1 : 93 prior to the degradation procedure.

Table 2

Alternatives for isotope distribution	Carbon atoms				
	3	5	2	6	
1a	x	o	x	o	x = C^{13} from acetate CH_3
1b	o	x	o	x	
2a	x	o	o	x	o = C^{14} from acetate COOH
2b	o	x	x	o	
3a	xo	xo	x	o	xo = "mixed" origin from both acetate carbon atoms
3b	xo	xo	o	x	
4a	x	o	xo	xo	
4b	o	x	xo	xo	
5	xo	xo	xo	xo	

Alternatives 1 a and 1 b are obviously identical, likewise 2 a and 2 b, 3 a and 3 b, and 4 a and 4 b. Together five alternatives could thus be reconstructed. The choice between these five alternatives has to be done according to the principle of accepting the least impossible, and by deduction from what is known as to the labelling of metabolites in general with regard to the organisms in question. The starting point is the fact that since carbon atom 4 is definitely C^{14} in the tyrosine from *coli* and *Neurospora* (and *Torulopsis utilis* (5)) we have to face the fact that at least *two carbon atoms in succession* of the ring system are C^{14}-labelled. The metabolites which could possess such an arrangement of two consecutive carbon atoms of a proximate origin from acetate carboxyl are hexoses, i.e. glucose, and acetoin structures. With regard to the former there are several indications from different biological systems that the acetate carboxyl, if isotopically labelled, will enter into the 3.4 of glucose positions (6, 7). Accepting temporarily the idea that glucose (or trioses) is intimately connected with the formation of the aromatic ring, the carbon atoms of glucose (3, 4) might be identical with the carbon atoms 3.4 *or* 4.5 of the phenolic ring. Now, incidentally Bloch (8) has shown that in *Saccharomyces* the glucose carbon atom 1 is responsible for 2 or 6 of the phenolic ring of tyrosine and phenylalanine, other metabolites of acetate origin *not* participating in the ring formation. If one still accepts the close connection between glucose and the aromatic ring this limits the choice between the above alternatives 1–5. Since it seems most probable that the glucose atom 1 is responsible for carbon atom 2 *or* 6, *but not for both,* of the ring of tyrosine this rules out alternatives 4 and 5. Which of the ring atoms 2 and 6 originates from glucose 1 is of no importance; the consequence that matters is that in this case one of carbon atoms 3 and 5, but not both, will originate from glucose 2. This, in turn rules out alternative 3. There remain alternatives 1 and 2; a schematic representation is shown in fig. 1.

Both alternatives in fig. 1 are compatible with our experimental data and the fact that carbon atom 1 of glucose shows up in 2.6 position (here assumed to be the 2-position) and β of the tyrosine structure. To choose between these alternatives is a difficult question. Adhering to the theory of glucose as the precursor of the ring atoms, alternative I has to be ruled out, since in that case the ring atom 3, which should be identical with glucose-2, is here regarded as C^{14}-labelled, which is contrary to the idea of the carboxyl of acetate entering

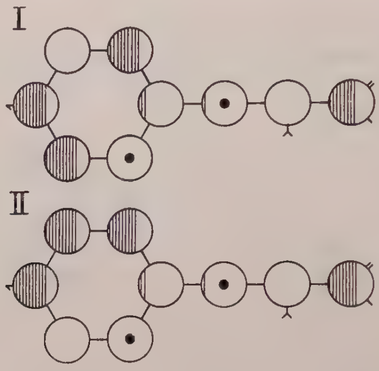

Fig. 1.

in glucose-3.4. With regard to the ring atoms 2.3.4.5 alternative II is in accordance with the assumption that these atoms are derived from glucose-1.2.3.4. With regard to the ring atoms 6 and 1 a new difficulty arises, however, because these atoms, (if derived from the same glucose molecule that may have provided ring atoms 2.3.4.5) they should correspond to glucose-5–6, and thus not contain any C^{14}. Yet, the marked C^{14}-content found in 2.6 of the ring makes the idea of a simple relation: one glucose—one aromatic ring untenable.

We are thus in a situation in which indications are strong that glucose as such is responsible for the formation of the aromatic ring, yet experimental evidence contradict any idea that some sort of cyclization of glucose between carbon atoms 1 and 6 is involved. Likewise the possibility of two trioses joining up 1.2.3.–3′.2′.1′ is excluded, as pointed out by GILVARG and BLOCH (8), because in that case carbon atom 1 of glucose should enter into 2.6 *and* 1 of the ring, which is not the case. In addition, the idea that one triose and some member of the metabolite series connected with acetate utilization (for example, citrate, oxal-acetate, α-ketoglutarate, succinate et al.) should be responsible for the formation of the aromatic ring is made less likely by the observation of Gilvarg and Bloch that, in *Saccharomyces*, labelled acetate does not enter the ring structure of tyrosine and phenylalanine. Yet glucose does.

Summing up this evidence we have arrived to the conclusion that, if one assumes glucose to be furnishing the material for the formation of the aromatic structure of tyrosine, *two* glucose molecules have to be involved, as a source for a C_3 and a C_4 fragment, later to be joined up to a C_7-structure, a process which is analogous to—or maybe identical with—the formation of seduheptulose from erythrose and triose in the presence of aldolase (9, 10). If the C_4-fragment postulated should be derived from either the glucose atoms 1.2.3.4 or 6.5.4.3, the sequence of isotope-labelling, derived from $C^{13}H_3C^{14}OOH$, would be: C^{13}–C^{13}–C^{14}–C^{14}. (This question could be settled by an experiment with glucose-1-C^{14} and glucose-6-C^{14}). At condensation with a C_3-fragment, like phospho-glyceraldehyde, with a labelling: C^{13}–C^{13}–C^{14}, a structure should be formed involving seven carbon atoms with three consecutive C^{14}-labellings: C^{13}–C^{13}–C^{14}–C^{14}–C^{14}–C^{13}–C^{13}, a rather unusual labelling pattern, however, in accordance with the present experimental data, if pictured according to fig. 2. If in such an open C_7-structure—seduheptulose or not—a cyclization takes place between posi-

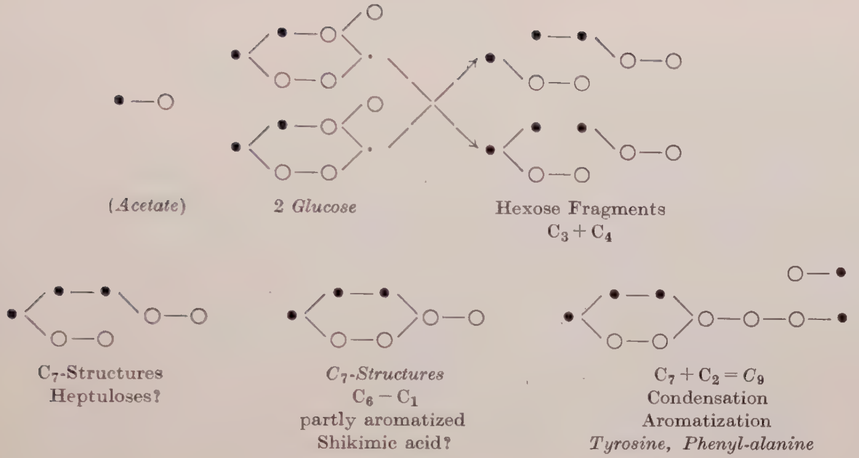

(*Acetate*)

2 *Glucose*

Hexose Fragments $C_3 + C_4$

C_7-Structures
Heptuloses?

C_7-Structures
$C_6 - C_1$
partly aromatized
Shikimic acid?

$C_7 + C_2 = C_9$
Condensation
Aromatization
Tyrosine, Phenyl-alanine

Fig. 2.

tions 1 and 6 a hydro-aromatic ring structure should be formed, in which C^{14} emanating from the carbon atoms 3.4 of two original glucose structures should appear in the ring atoms 4.5, and 6. Whether this hypothetical ring-structure might have a connection with the hydro-aromatic C_7-structures of shikimic acid and quinic acid (both of them shown to be immediate precursors of aromatic structures (11, 12, 13, 14)) is not known. Since evidence is very strong that one or the other of these two compounds is the actual intermediate in the formation of aromatic amino acids, any reaction scheme, proposed to explain the main features of the utilization of hexose for the formation of tyrosine, phenylalanine and tryptophane has to be compatible with the formation of C_7-structures as intermediates. If assuming that only glucose, or glucose fragments, constitute the proximate starting material for that synthesis, the consequence has to be faced that *two* glucose molecules are neccessary to provide the $C_3 + C_4$ — or $C_5 + C_2$-fragments for a subsequent formation of a C_7-structure. This might be another support for the validity of the scheme outlined in fig. 2. With regard to this scheme it provides a possibility of fitting our experimental values—and those of GILVARG and BLOCH—into a coherent reaction sequence, the validity of which obviously has to be confirmed by further experiments with labelled glucose, for example glucose-2-C^{14} and glucose-6-C^{14}.

With regard to the side-chain problem our direct estimations of the C^{13}- and C^{14}-content of the carboxyl, the α- and β-carbon atoms indicate that the former is, as expected C^{14}-labelled, whereas the α- and β-carbon atoms have an insignificant C^{14}-content. As to the mechanism at play at the sidechain formation one could only say that a $C_6 + C_3$-addition is unlikely compared to a $C_7 + C_2$- or a $C_7 - C_1 + C_3$-mechanism. The former should involve an addition of an acetate molecule, the second implies an addition of a C_3-structure, labelled as pyruvate (as alanine) under the simultaneous splitting-out of the external carbon atom of the C_7-ring-structure. If it could be demonstrated that the carboxyl of shikimic acid or quinic acid actually becomes the β-carbon atom of tyrosine and aromatic amino acids in general, the $C_7 + C_2$-mechanism is the more likely.

SUMMARY

Tyrosine, isolated from *Escherichia coli* and *Neurospora crassa* grown on isotope-labelled acetate as the sole source of carbon, has been degraded with a method enabling carboxyl carbon and carbon atoms α; β; 1; 2.6; 3.5 and 4 being isolated and determined with regard to isotope content.

The result is in accordance with the view that glucose could be the proximate starting material for the formation of the aromatic ring structure of tyrosine obtained from both organisms. If accepting glucose as the starting material, the mechanism at the formation of the ring system of tyrosine has to involve *two* glucose molecules, providing fragments ($C_3 + C_4$ or $C_5 + C_2$) for the formation of a C_7-structure, later to correspond to the ring + β-carbon atoms of tyrosine. A reaction scheme is tentatively drawn based on the experimental values obtained, its validity being discussed.

The α-carbon atom has its proximate origin from the methyl group of acetate. The origin of the side-chain is discussed.

BIBLIOGRAPHY

1. Cutinelli, C., Ehrensvärd, G., Reio, L., Saluste, E., and Stjernholm, R., Acta Chem. Scand., *5,* 353 (1951).
2. Partridge, S. M., Biochem. J., *44,* 523 (1949).
3. Andersson-Kottö, I., Ehrensvärd, G., Högström, G., Reio, L., and Saluste, E. (unpublished data).
4. Reio, L., and Ehrensvärd, G., Arkiv Kemi *5,* Nr 28, 301 (1953).
5. Baddiley, J., Ehrensvärd, G., Klein, E., Reio, L., and Saluste, E., J. Biol. Chem., *183,* 777 (1950).
6. Wood, H. G., Cold Spring Harbor Symposia Quant. Biol., *13,* 201 (1948).
7. Lifson, N., Lorber, V., Sakami, W., and Wood, H. G., J. Biol. Chem., *176* 1263 (1948).
8. Gilvarg, J., and Bloch, K., J. Am. Chem. Soc., *72,* 5791 (1950).
9. Horecker, B. L., and Smyrniotis, P. Z., J. Am. Chem. Soc., *74,* 2123 (1952).
10. Taylor, I. F., Green, A. A., and Cori, G. T., J. Biol. Chem., *173,* 591 (1948).
11. Gordon, M., Haskins, F. A., and Mitchell, H. K., Proc. Nat. Acad. Sci., *36,* 427 (1950).
12. Horowitz, N. H., and Mitchell, H. K., Ann. Rev. Biochem., *20,* 465 (1951).
13. Davis, B. D., J. Biol. Chem., *191,* 315 (1951).
14. —— Symposium sur le Metabolism Microbien. IIe Congrès International de Biochimie. (1952) p. 32.

The Wenner-Gren Institute, Department of Physiological Chemistry, University of Stockholm, Sweden.

Tryckt den 11 februari 1953

Uppsala 1953. Almqvist & Wiksells Boktryckeri AB

ARKIV FÖR KEMI Band 5 nr 21

Communicated 12 November 1952 by JOHN RUNNSTRÖM and KARL MYRBÄCK

The influence of pH on the periodate oxidation of carbohydrates

By GUNNAR NEUMÜLLER and ERIK VASSEUR

With 7 figures in the text

Introduction

The oxidation of reducing disaccharides with periodic acid was studied in 1942 by AHLBORG (1) to devise a method of estimating the types of linkages occurring in starch dextrins. The oxidations were performed in approx. *N* sulphuric acid solutions at 50° C. Under these conditions characteristic differences were observed when oxidizing a 1,4-disaccharide (maltose) and a 1,6-disaccharide (melibiose). The maltose was completely oxidized to formic acid and formaldehyde, consuming about 10 moles of oxidant per mole of sugar. The oxidation of melibiose ceased after a consumption of oxidant of about 6 moles per mole of sugar, no formaldehyde being formed. Without giving experimental data, AHLBORG also pointed out that the mode of oxidation of maltose in buffered solutions at pH 3–4 was quite different to that in strongly acid solutions.

PURVES *et al.* (2) and JAYME *et al.* (3) recommended the use of buffered periodate at pH 4.2 and pH 3.5–4.0 respectively, for the oxidation of starch and cellulose and obtained greater yields of oxidation products than those obtained by JACKSON and HUDSON (4), who used unbuffered periodic acid.

LINDSTEDT (5), during an investigation of yeast mannan, made a series of periodate oxidations in phosphate buffers at varying pH values. It was detected that at pH 4–5 the oxidation proceeded in quite another way than in more acid solutions. At higher pH values about two thirds of the mannan molecule was oxidized to carbon dioxide. LINDSTEDT (6) also carried out oxidations of maltose and other sugars in phosphate buffer at pH 7 and 50° and for maltose found a consumption of about 18 moles of oxidant per mole of sugar. Also he found that the oxidation proceeds much faster in phosphate buffers than in acetate buffers of the same pH. The tendency of phosphate in neutral solution to promote a greater consumption of periodate has been studied also by BELL *et al.* (7). They recommended the use of phthalate buffer in order to reduce this effect.

From the above mentioned facts it is clear that the pH at which the oxidation is carried out plays an important role for the rate of oxidation as well as for the kind of oxidation products formed. Prior to the application of the periodate method to certain structural problems of polysaccharides, we found it necessary to investigate the effect of pH on the periodate oxidation of some reducing sugars in the pH region between strong acidity and neutrality. Care was taken to use buffers of sufficiently high buffer capacity to hinder variations in pH caused by the formation of acidic oxidation products. The sugars investigated were chosen to represent glycosidic 1,3- 1,4- and 1,6-linkages.

Experimental

Commercial preparations (Pfanstiehl and B.D.H.) of maltose hydrate, melibiose hydrate and α-methyl-D-glucoside were used. A 1,3-dextrin from yeast dextran (yeast glucan) was kindly put at our proposal by Dr. K. AHLBORG and was prepared by him in the following way: Yeast dextran was prepared from compressed bakers' yeast as described by HASSID *et al.* (8). See also BARRY and DILLON (9). The raw polysaccharide (30 g) was acetylated with acetic anhydride and sulphuric acid. The mixture was left standing for a week, and then the filtered solution was poured into ice water, giving 22 g of acetate. The acetate was dissolved in methanol (100 ml) and the solution stored in a refrigerator for four days. An oil separated from the mother liquor. The oil was collected and treated with ether giving a white precipitate, which was filtered and dried. Yield 7 g, $[\alpha]_D^{20} - 38.2°$. This acetate was deacetylated and gave the 1,3-dextrin. Yield 2.3 g, $[\alpha]_D^{20} - 5.4°$. The reducing values estimated by the WILLSTÄTTER and SCHUDEL (10) method before and after hydrolysis for three hours at 100° C. with *N* sulphuric acid gave a degree of polymerization of 7.36 for the dextrin. Glucose was the sole product of hydrolysis as judged by the specific rotation and by a fermentation test.

The samples of dextran were kindly put at our disposal by Dr. BJÖRN INGELMAN (cf. 11). Both unhydrolysed and partly hydrolysed samples of dextran were used, giving essentially identical results.

Aqueous solutions of the above mentioned carbohydrates were prepared, each containing about 3–5 mg/ml. The exact concentrations were estimated by measuring the reducing power by the WILLSTÄTTER and SCHUDEL (10) method, when necessary after complete hydrolysis for three hours at 100° with *N* sulphuric acid. The dextran solutions contained only about 1–0.3 mg/ml depending on the pH of the reacting solution. Their strength was corrected for moisture which was determined in an aliquot by heating to constant weight at 105°.

As oxidant a 0.1 *M* solution of sodium metaperiodate was used. Buffer solutions used included sodium phosphate-sulphuric acid, potassium phthalate, sodium acetate-acetic acid, and sodium phosphate and covered the range of pH 2.8 to 7.0. To some series sulphuric acid instead of buffer solution was added, sufficient to make the reaction mixture about normal with respect to sulphuric acid.

The consumption of oxidant. 2 ml of sugar solution (substituted by distilled water in blanks), 2 ml of buffer solution (or sulphuric acid) and 2 ml of 0.1 *M* sodium metaperiodate solution were mixed in test tubes. Rubber stoppers were inserted and the tubes placed in a $50.0° \pm 0.2°$ thermostat. This temperature was chosen to get a reasonable rate. At 0° the reaction is so slow that an experiment will last for several days. However, some experiments on maltose were carried out at 0° to verify that the shapes of the curves obtained were identical with those obtained at 50°. After suitable intervals, *e.g.* 10, 20, 30, 60, 120 minutes etc., tubes were withdrawn, rapidly cooled in running tap water and the contents transferred to a titration flask containing 30 ml of 0.5 *M* sodium phosphate buffer of pH 7.0, and 5 ml of potassium iodide solution (0.1 g/ml) was added. When the oxidation had been carried out in *N* sulphuric acid solution, 5 ml of *N* sulphuric acid was added instead of the phosphate buffer. The titration thus was performed in a strongly acid medium (12). In some cases, however, as for example in the dextran experiments, sufficient sodium hydroxide was added in advance to the phosphate buffer to neutralise the sulphuric acid, the titration thus being carried out at pH 7 (13). It is advantageous to carry out the titration at pH 7, since at this pH only the periodate will react (5, 13). In strongly acid solutions, on the other

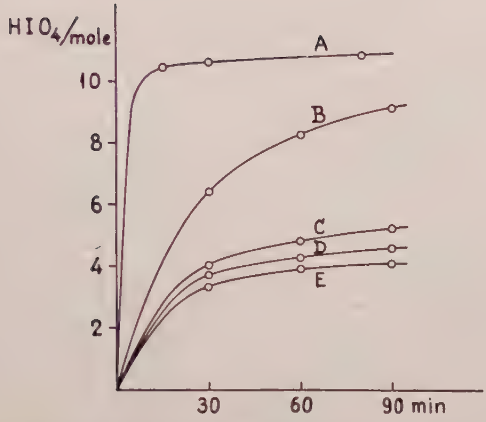

Fig. 1. Oxidation of maltose at varying pH values; curve A, in sulphuric acid solution, pH 0; curves B–C, in acetate buffers of pH 5.6, 4.5, 4.0, and 3.4 respectively; at 50°.

hand, the iodate, which has been formed during the oxidation, also reacts with the potassium iodide (12, 13). The liberated iodine was titrated with standardized thiosulphate solution using starch solution as indicator. The consumption of oxidant was calculated per mole of sugar (glucose residue) and the results plotted versus time.

Formic acid estimation. The reaction mixtures were the same as given above, except for the buffer solutions which were substituted by the same volume of water. Such a mixture has a pH of about 4, decreasing slightly as the oxidation progresses on account of the formation of formic acid (see also 14). Therefore, the reaction will proceed in the pH region where the overoxidation (see below) is at a minimum. At suitable intervals (see above) two tubes were withdrawn, one of which was used to estimate the consumption of oxidant. To the other tube was added 0.5 ml of redistilled ethylene glycol and the tube was stored in the dark for 30 minutes. The formic acid was titrated with 0.01 *N* barium hydroxide solution using phenol red as indicator. Phenol red (colour change interval pH 6.4–8.2) was chosen because with the concentrations used the endpoint for the formic acid titration lies between pH 7.2 and 8.0 (cf. 15, 16). The formic acid was calculated per mole of sugar and the results plotted versus time.

Results

In Fig. 1 the figures for the oxidation of maltose in acetic acid–acetate buffers at varying pH are given. From the curves it is seen that the oxidation of maltose in weakly acid solutions rapidly proceeds up to the consumption of about 4 moles of oxidant. From the pyranose formula of maltose (Formula I, p. 240) assuming that no other forms of maltose are present in appreciable amounts, it follows that 4 moles of oxidant are required to oxidize the α-glycol groups present. This first rapid consumption, in the following termed the normal oxidation, is followed by a more or less rapid consumption of oxidant, the overoxidation, the rate of which depends on the pH of the medium.

The consumptions of oxidant per mole of sugar after one hour of oxidation at 50° at varying pH values are given in Fig. 2 (Curve B), from which it is obvious that the overoxidation has a minimum in the pH range 3.0–3.5.

In order to get more information concerning the course of the overoxidation,

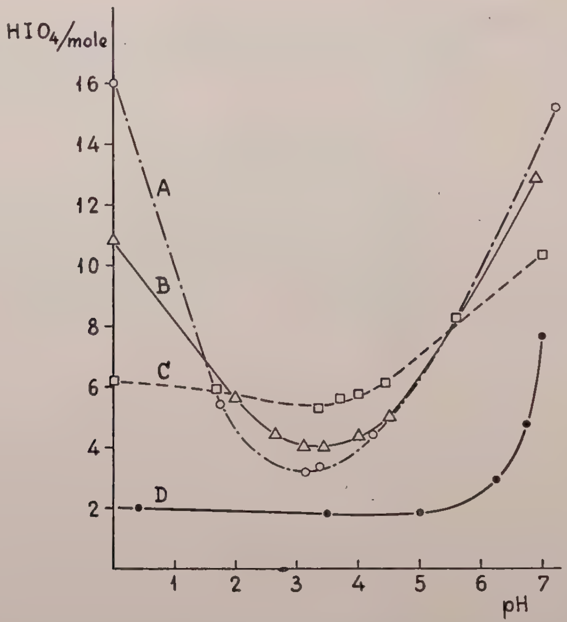

Fig. 2. Periodate oxidation versus pH; curves A–C, consumption per mole: A. the 1,3-dextrin after 30 min; B. maltose after 60 min; C. melibiose after 60 min; curve D, consumption per glucose residue for dextran after 4 hours; at 50°.

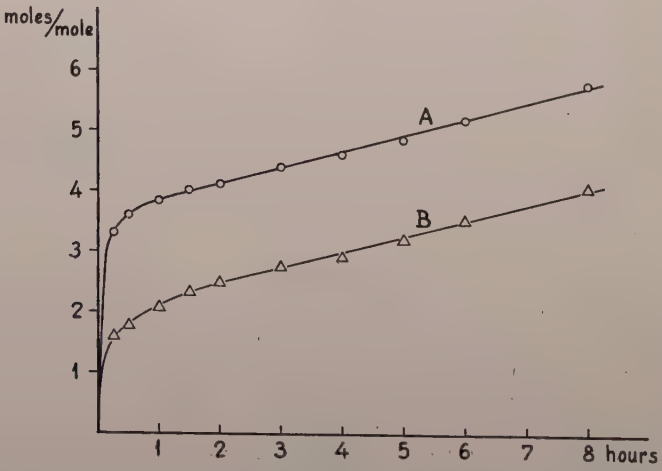

Fig. 3. Oxidation of maltose with unbuffered $NaIO_4$; curve A, consumption of oxidant per mole of maltose; curve B, formation of formic acid per mole of maltose; at 50°.

formic acid determinations as described in the experimental part were performed with simultaneous determinations of the periodate consumption (Fig. 3). From maltose the expected 2 moles of formic acid were produced at a rapid rate. Thereafter, increasing amounts of formic acid were formed at a markedly lower rate. In this

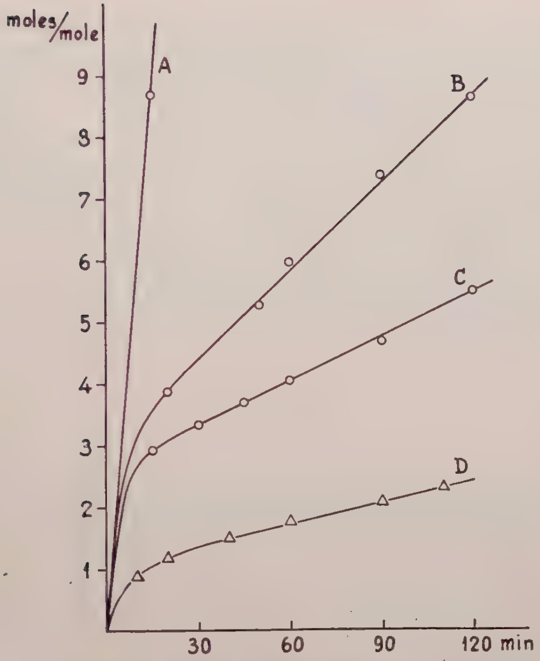

Fig. 4. Oxidation of the 1,3-dextrin; curve A, at pH 0, sulphuric acid solution; curves B and C, at pH 4.25 and 3.35 respectively, acetate buffers; curve D, the formic acid production in the oxidation with unbuffered $NaIO_4$; at 50°.

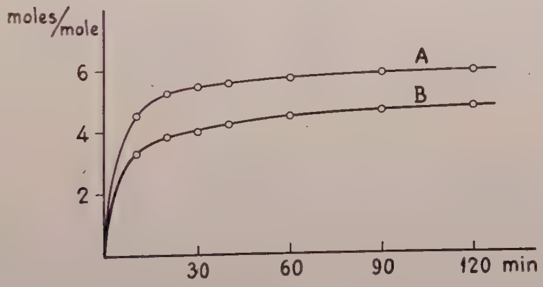

Fig. 5. Oxidation of melibiose in unbuffered $NaIO_4$; curve A, periodate consumption; curve B, formic acid production; at 50°.

overoxidation stage the rate of formic acid production paralleled the rate of periodate consumption. A defined or stable stage in the overoxidation was not achieved.

The normal oxidation of the 1,3-dextrin would require 3 moles of oxidant (Formula V, p. 240), *i.e.* 2 moles for the non-reducing and 1 mole for the reducing glucose residue. Fig. 4 (Curves B and C) clearly indicates, in accordance with this requirement that at pH 3–4 three moles of oxidant are rapidly consumed. Then a slower rate of reaction follows. Also the formic acid production follows this scheme. The expected one mole is produced rapidly and then more acid is produced at a slower rate.

Although the 1,3-sugar exhibits a higher pH sensitivity than does maltose and consequently the differences in the rate of the normal oxidation and the overoxidation are less pronounced, the overoxidation of this sugar, similar to that of maltose, has a minimum in the pH range 3.0–3.5 (Fig. 2, Curve A).

From the formula of melibiose (IX, p. 241) it follows that 5 moles of oxidant are required to oxidize the α-glycol groups present and that 3 moles of formic acid should be produced. However, it is evident from Fig. 5 that this state is rapidly passed and that a steady state is not achieved before the consumption of oxidant has proceeded to 6 moles and the production of formic acid to 5 moles.

The oxidation of dextran should in the main follow a similar course as melibiose, since it contains predominantly 1,6-linkages (11, 17). That this is in fact the case, follows from a comparison of curves C and D in Fig. 2.

Discussion

The types of sugars mentioned have in common that, after the normal oxidation has occurred, the carbon atom 1 of the reducing glucose residue is present as a formic

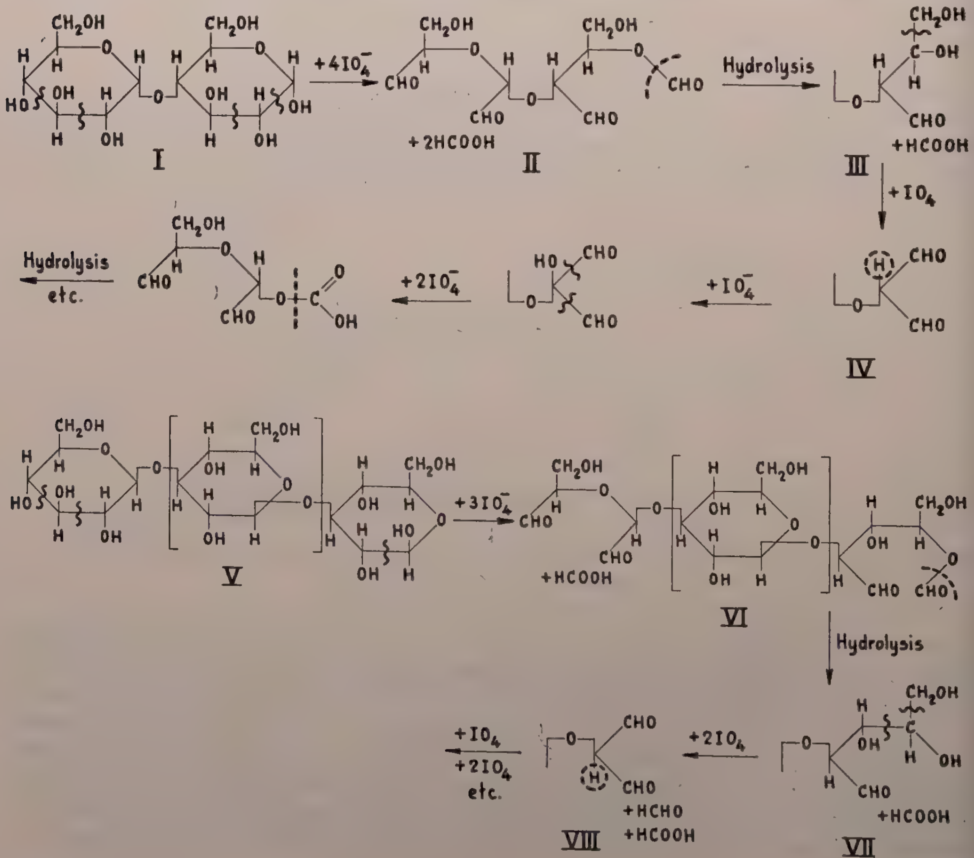

CH₂OH
+4IO₄⁻
+2HCOOH
Hydrolysis
+HCOOH
I
II
III
+IO₄
IV
+IO₄⁻
+2IO₄⁻
Hydrolysis
etc.
+3IO₄⁻
+HCOOH
V
VI
Hydrolysis
VII
+2IO₄
+IO₄
+2IO₄
etc.
+HCHO
+HCOOH
VIII

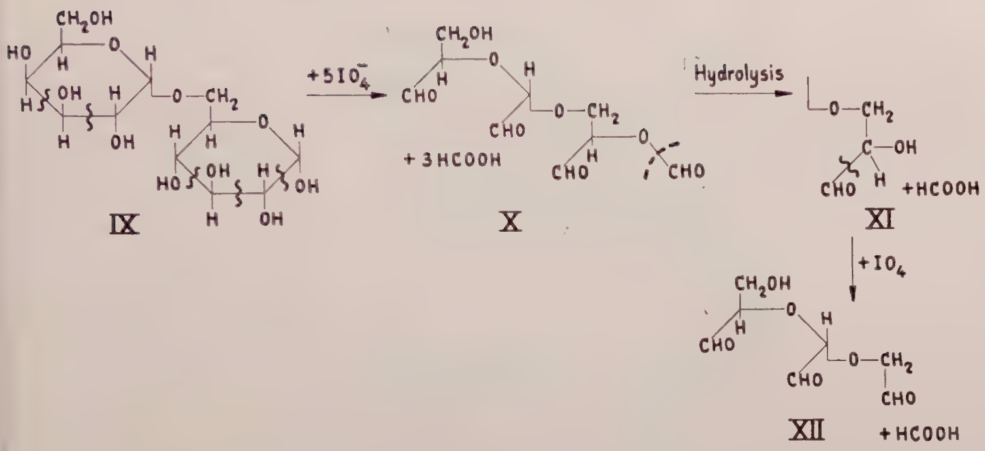

IX X XI XII

acid ester esterified by the secondary alcohol of carbon atom 5 (II, VI, X). The formic acid esters in water solution may be more or less rapidly hydrolysed. The one formed from melibiose will hydrolyse more rapidly than the one formed from maltose, for example, because of hyperconjugation. By the hydrolysis of the formic acid ester new glycol groups are formed and are attacked by periodate. In the case of a 1,4- and a 1,3-saccharide a compound is formed (IV, VIII) containing an active hydrogen atom, which is oxidized by periodate to a hydroxyl group. The conditions under which such oxidations may occur have been studied by Huebner *et al.* (18). After the oxidation of the active hydrogen has occurred the oxidation may proceed as shown in the diagrams.

In the case of a 1,6-saccharide no such compound containing an active hydrogen atom is formed. After the hydrolysis of the formic acid ester (X–XI) one mole of oxidant is consumed giving the compound XII. This scheme gives a consumption of 6 moles of periodate and a production of 5 moles of formic acid, as demonstrated above for melibiose (Fig. 5). The substance thus formed (XII) seems to be relatively stable towards periodate.

The reaction scheme given here differs in some instances from the one given by Courtois and Ramet (19), who investigated the periodate oxidation of maltose and lactose. The difference lies in the oxidation of the reducing glucose residue, for which they assume a consumption of only one mole of oxidant, causing the splitting of the C–C linkage between carbon atoms 2 and 3. That would mean a total consumption of 3 moles of oxidant per mole of maltose in the normal oxidation stage. Under the reaction conditions used in our investigation a fourth mole is rapidly consumed, although at a slower rate than the third mole.

As we see it the first step in the overoxidation is the hydrolysis of the formic acid ester (II→III, VI→VII, X→XI). In strongly acid medium (pH = 0) the hydrolysis of the formic acid ester, and also of the former glycosidic linkages (but not of the 1,6-linkage) is so rapid that a stage corresponding to the normal oxidation is not visible in the curves. In the case of maltose and the 1,3-dextrin the consumption of oxidant rapidly amounts to about 5 moles of oxidant per glucose residue, thus indicating a complete destruction of the molecule to formic acid and formaldehyde. In the case of melibiose at pH = 0 the reaction rapidly proceeds up to a consumption

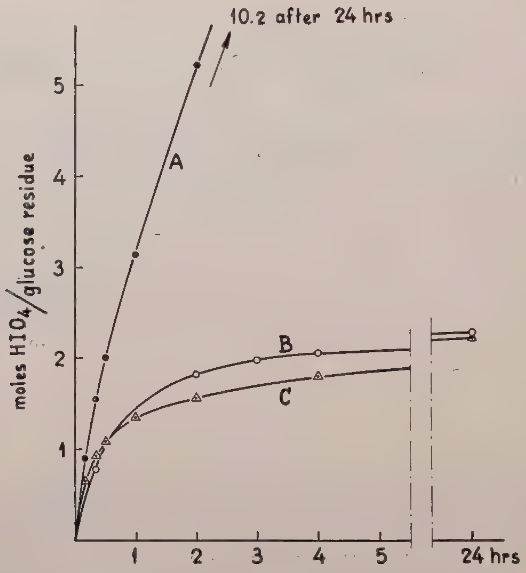

Fig. 6. Oxidation of *Leuconostoc mesenteroides* dextran; curve A, at pH 7, phosphate buffer; curve B, at pH 0.4, sulphuric acid solution; curve C, at pH 3.5, phthalate buffer; at 50°.

of 6 moles of oxidant and then markedly decreases. This shows that the former 1,6-linkage is comparatively stable (XII).

Also in the dextran molecule the oxidation in acid medium comes to a standstill when these former 1,6-linkage are reached. However, the former 1,4-linkages, which are less numerous, will be hydrolysed. Hence the oxidation will proceed a little further and of course more rapidly in strongly acid solution than at pH 3.5 (compare curves B and C in Fig. 6).

This particular dextran, because of its content of 1,6-linkages (cf. 11, 17), would consume 1.8 moles of periodate per glucose residue. If the former 1,4-linkages are split, an additional consumption of 0.6 moles is to be expected. As is evident from Fig. 6 this value, 2.4 moles, is very nearly reached both in strongly acid medium and at pH 3.5.

In one of the possible structures of this dextran the side chains are attached to the main chain through 1,4-linkages (cf. 11, Fig. 2; 17, Fig. 2). The course of the overoxidation of this structure is depicted in the diagram with the formulae XIII

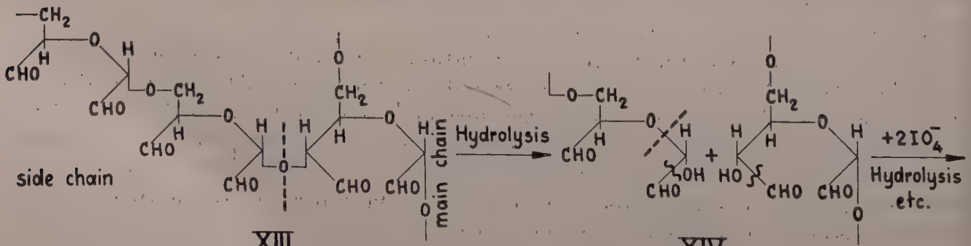

XIII

XIV

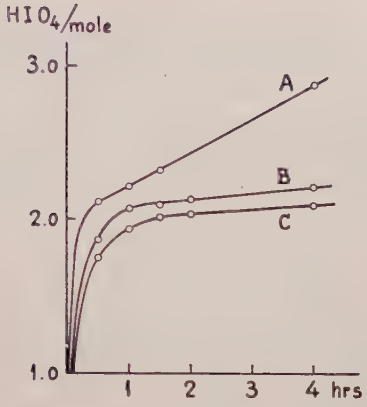

Fig. 7. Oxidation of α-methylglucoside in acetate buffers; curve A, at pH 5.8; curve B, at pH 4.2; curve C, at pH 3.4; at 50°.

and XIV, the further degradation following the same course as depicted for melibiose (IX→XII).

Furthermore it is known that non-reducing sugars and methyl glycosides of reducing sugars are also overoxidized (20). In our experiments with α-methyl-D-glucoside we observed that overoxidation occurs, although, other things being equal, at a much slower rate than is the case with maltose (Fig. 7). The influence of pH on the rate of the overoxidation is comparatively slight but clearly visible. The mechanism of this type of overoxidation is unknown. We may, however, suggest the following possibilities. 1) Hydrolysis of the dialdehyde, formed by the normal oxidation, may occur. 2) Oxidation of the hydrogen atom linked to the former carbon atom 5, which may be slightly activated by the aldehyde group, thus forming oxidizable products. Both reactions may occur simultaneously. However, nothing is known under which conditions and to which degree such reactions really occur.

The differences in the mode of reaction of a 1,4- and a 1,6-disaccharide on oxidation in strongly acid solutions are not obtained when oxidizing in neutral solutions (phosphate buffer, pH 7). The consumption under these conditions rapidly rises to values far above the normal consumption of oxidant. Remarkable is the result obtained for the oxidation of dextran where the consumption after 24 hours amounts to 10.2 moles of periodate per glucose residue (Fig. 6 A). A similar value was obtained by LINDSTEDT on mannan (5). To explain the extremely high consumption of oxidant at pH 7 it must be assumed that a normal oxidation precedes the overconsumption. A di- or polyaldehyde seems to be a prerequisite for the reaction to occur. Monosaccharides, on the other hand, are oxidized in neutral solutions in the same way as in strongly acid solutions, *i.e.* without any overconsumption of oxidant. Again the oxidation of α-methylglucoside in neutral solutions involves a high overconsumption (6). This seems to indicate that the monosaccharides in neutral and in strongly acid solutions are oxidized in their open chain (the aldehyde) forms, in which case no dialdehydes are formed.

We have found a minimum of the overoxidation rate in the pH range 3–4. This may be the result of several factors, of which we advance the following. PRICE and KROLL (21) in their investigation of the kinetics of the periodate oxidation of 1,2-glycols found a minimum of the second order rate constant in the pH range 4–5. Furthermore, it is known that sugars exhibit a certain stability in the pH range 2.5–3.5. Kröner and Kothe (22) found a minimum in the discoloration of acid treated glucose solutions subjected to higher temperatures in this pH range. The formation of hydroxymethylfurfural also has a minimum in the pH range about 3, as found by Singh *et al.* (23). Finally the hydrolysis rate of the former glycosidic linkages seems to be at a minimum in this pH region.

SUMMARY

The influence of pH in the region between strong acidity and neutrality on the periodate oxidation of the following carbohydrates has been investigated: maltose, melibiose, α-methylglucoside, yeast glucan, and dextran. They represent sugars with 1,3-, 1,4-, and 1,6-linkages. In weakly acid solution all these sugars show first a rapid consumption of oxidant, representing the oxidation of the α-glycol groups, the normal oxidation. This is followed by a more or less rapid additional periodate consumption, the overoxidation, the rate of which is dependent on the pH of the medium having a minimum in the pH region 3–4.

Probably the overoxidation in the strongly acid region starts with the hydrolysis of the formic acid ester, which is produced during the normal oxidation. Furthermore, the overoxidation involves oxidation of active hydrogen atoms (except in the case of 1,6-linked sugars) and hydrolysis of the former 1,3- and 1,4-linkages, whereby additional α-glycol groups are set free. The former 1,6-linkages, on the other hand, are stable under these conditions.

All the sugars tested are broken down completely and consume large amounts of periodate, when the oxidation is carried out in neutral medium. The course of this reaction seems to be very complex and is discussed only briefly.

We wish to thank Miss Sonja Werngren, Miss Hedvig Tamm and Mr. Walter Pudeck for technical assistance and to gratefully acknowledge a grant from *Statens Naturvetenskapliga Forskningsråd* (to G. N.) and a Doktorand-stipendium of the Swedish Government (to E. V.).

From the Institute of Organic Chemistry and Biochemistry and the Wenner-Gren Institute, University of Stockholm.

REFERENCES

1. Ahlborg, K. Svensk Kem. Tid. *54*, 205 (1942).
2. Grangaard, D. H., Michell, J. H., and Purves, C. B. J. Am. Chem. Soc. *61*, 1290 (1939); Michell, J. H., and Purves, C. B. *ibid. 64*, 585 (1942).
3. Jayme, G., Sätre, M., and Maris, S. Naturwissenschaften *29*, 768 (1941); Jayme, G., and Sätre, M. Ber. *75*, 1840 (1942); *ibid. 77*, 242 (1944).
4. Jackson, E. L., and Hudson, C. S. J. Am. Chem. Soc. *59*, 2049 (1937); *ibid. 60*, 989 (1938).
5. Lindstedt, G. Arkiv Kemi, Mineral. Geol. *20 A*, N:o 13 (1945).
6. ——. Nature, *156*, 448 (1945).
7. Bell, D. J., Palmer, A., and Johns, A. T. J. Chem. Soc. *1949*, 1536.
8. Hassid, W. Z., Joslyn, M. A., and McCready, R. M. J. Am. Chem. Soc. *63*, 295 (1941).
9. Barry, V. C., and Dillon, T. Proc. Roy. Irish Acad. *B 49*, 177 (1943).
10. Willstätter, R., and Schudel, G. Ber. *51*, 780 (1918); *cf.* Myrbäck, K., and Gyllensvärd, E. Svensk Kem. Tid. *53*, 461 (1941).

11. INGELMAN, B. Acta Chem. Scand. *1*, 731 (1947).
12. MALAPRADE, L. Bull. soc. chim. [4] *39*, 325 (1926); *ibid.* [4] *43*, 683 (1928).
13. RAPPAPORT, F., REIFER, I., and WEINMANN, H. Mikrochim. Acta *1*, 290 (1937); RAPPAPORT, F., and Reifer, I. *ibid.* *2*, 273 (1937).
14. MALAPRADE, L. Bull. soc. chim. [5] *1*, 833 (1934).
15. MEYER, K. H., and RATHGEB, P. Helv. Chim. Acta *31*, 1540 (1948).
16. KERR, R. W., and CLEVELAND, F. C. J. Am. Chem. Soc. *74*, 4036 (1952).
17. LEVI, J., HAWKINS, L., and HIBBERT, H. J. Am. Chem. Soc. *64*, 1959 (1942).
18. HUEBNER, C. F., AMES, S. R., and BUBL, E. C. J. Am. Chem. Soc. *68*, 1627 (1946).
19. COURTOIS, J., and RAMET, M. Bull. soc. chim. biol. *29*, 240 (1947).
20. HALSALL, T. G., HIRST, E. L., and JONES, J. K. N. J. Chem. Soc. *1947*, 1427.
21. PRICE, C. C., and KROLL, H. J. Am. Chem. Soc. *60*, 2726 (1938); PRICE, C. C., and KNELL, M. *ibid.* *64*, 552 (1942).
22. KRÖNER, W., and KOTHE, H. Ind. Eng. Chem. *31*, 248 (1939).
23. SINGH, B., DEAN, G. R., and CANTOR, S. M. J. Am. Chem. Soc. *70*, 517 (1948).

Tryckt den 11 februari 1953

Uppsala 1953. Almqvist & Wiksells Boktryckeri AB

ARKIV FÖR KEMI Band 5 nr 22

Communicated 22 October 1952 by ARNE WESTGREN and G. HÄGG

The structure of the hexaniobate ion in $7\,Na_2O\cdot 6\,Nb_2O_5\cdot 32\,H_2O$

By INGVAR LINDQVIST

With 1 figure in the text

Niobium has the same tendency as vanadium, tantalum, molybdenum and tungsten to form very complex oxy-salts, isopolyniobates, with varying mole ratios $R_2O:Nb_2O_5$ ($R = Li$, Na, K, Rb, Cs or NH_4). These have been described in many papers which have suggested different formulae and constitutions. The most important contribution has been given by SÜE (1) who from careful analyses concluded that one niobate, $7\,Na_2O\cdot 6\,Nb_2O_5\cdot 32\,H_2O$ exists with a mole ratio 7:6 between orthoniobate and metaniobate with mole ratios 3:1 and 1:1 respectively. With a wish to extend the studies of polymolybdates (2) and polytungstates (3) to polyniobates, a crystal structure determination of this compound was started.

Crystals

The crystals were prepared by melting Nb_2O_5 with an excess of NaOH in a silver crucible. The analyses were carried out in the same way as we used earlier (4) for the sodium molybdates. An ion exchanger saturated with NH_3 separates the niobate ions from the sodium ions. The results are in good agreement with those calculated for $7\,Na_2O\cdot 6\,Nb_2O_5\cdot 32\,H_2O$ (Nb_2O_5: Calc. 61.3 %, found 61.4 %; Na_2O: Calc. 16.6 %, found 16.7 %).

The crystals obtained had the same shape as those photographed by SÜE. A thin needle crystal (thickness ~ 0.2 mm) was chosen for the X-ray work. The crystal symmetry is orthorhombic with $a = 10.01$ Å, $b = 12.13$ Å, and $c = 12.61$ Å (dimension values from powder photographs). Rotation and Weissenberg photographs around the a-axis were taken with Cu-K radiation. The density 2.79, measured by a pycnometer method, gives the number of Nb-atoms in the unit cell = 12. The reflections $h\,0\,l$ are missing if $h + l$ is odd and $hk\,0$ are missing if $h + k$ is odd. As no piezo-electricity could be detected, the space-group is probably $D_{2h}^{12} - Pmnn$. Relative $[F]_2$ values were calculated from the estimated intensities using LU's curves (5).

Niobium positions

The general positions in this space-group is

$$\begin{array}{lllll} (8\text{ h}): & (x, y, z) & (x, \bar{y}, \bar{z}) & (\tfrac{1}{2}+x,\ \tfrac{1}{2}+y,\ \tfrac{1}{2}-z) & (\tfrac{1}{2}+x,\ \tfrac{1}{2}-y,\ \tfrac{1}{2}+z) \\ & (\bar{x}, y, z) & (\bar{x}, \bar{y}, \bar{z}) & (\tfrac{1}{2}-x,\ \tfrac{1}{2}+y,\ \tfrac{1}{2}-z) & (\tfrac{1}{2}-x,\ \tfrac{1}{2}-y,\ \tfrac{1}{2}+z) \end{array}$$

The existence of a mirror plane makes it possible to determine the possible x-values from the Patterson function $P(x, 0, 0)$ where the vectors $[2x_{Nb}, 0, 0]$ are to be found. $P(x, 0, 0)$ contains two maxima, at $x = 0.00$ and at $x = 0.34$, corresponding to the two x_{Nb}-values: 0.00 and 0.17. The former evidently gives a four-fold position, 4(g), instead of an eight-fold, 8(h).

Then the possible (y_{Nb}, z_{Nb}) values can be determined from the function $P(\frac{1}{2}, y, z)$ where the vectors $[\frac{1}{2}, \frac{1}{2} - 2y_{Nb}, \frac{1}{2}]$ and $[\frac{1}{2}, \frac{1}{2}, \frac{1}{2} - 2z_{Nb}]$ are to be found. $P(\frac{1}{2}, y, z)$[1] contains two maxima in agreement with each of these vectors:

$(\frac{1}{2}, 0.24, \frac{1}{2})$ and $(\frac{1}{2}, 0.42, \frac{1}{2})$ give the $\frac{1}{2} - 2y_{Nb}$ values 0.24 and 0.42 corresponding to the y_{Nb} values 0.13 and 0.04:

$(\frac{1}{2}, \frac{1}{2}, 0.14)$ and $(\frac{1}{2}, \frac{1}{2}, 0.44)$ give the $\frac{1}{2} - 2z_{Nb}$ values 0.14 and 0.44 corresponding to the z_{Nb} values 0.18 and 0.03.

Because of the symmetry of the space-group there are three other possibilities for each of these Nb-coordinates giving in all $y = (0.13, \overline{0.13}, 0.63, 0.37)$, $y = (0.04, \overline{0.04}, 0.54, 0.46)$, $z = (0.18, \overline{0.18}, 0.68, 0.32)$, $z = (0.03, \overline{0.03}, 0.53, 0.47)$.

First of all it must be determined which of the above y and z quartets belong to each other. This is derived from the function $P(0, y, z)$ where the vectors $[0, 2y_{Nb}, 2z_{Nb}]$ are to be found. The maxima (0, 0.26, 0.06) and (0, 0.08, 0.36) show that the y quartet $(0.13, \overline{0.13}, 0.63, 0.37)$ and the z quartet $(0.03, \overline{0.03}, 0.53, 0.47)$ give one pair and y $(0.04, \overline{0.04}, 0.54, 0.46)$, $z (0.18, \overline{0.18}, 0.68, 0.32)$ the other one.

The next step is to determine which (y, z) pair corresponds to the fourfold position with $x = 0$ and which corresponds to $x = 0.17$ in the eight-fold position. The function $P(x, \frac{1}{2}, z)$ is useful for this purpose because both the vectors $[\frac{1}{2}, \frac{1}{2}, \frac{1}{2} - 2z]$ and $[\frac{1}{2} - 2x, \frac{1}{2}, \frac{1}{2} - 2z]$ are to be found there. The maxima $(\frac{1}{2}, \frac{1}{2}, 0.44)$ and $(0.16, \frac{1}{2}, 0.44)$ exist and also the maximum $(\frac{1}{2}, \frac{1}{2}, 0.14)$ but not $(0.16, \frac{1}{2}, 0.14)$. The value $z_{Nb} = 0.03$ thus belongs to the eight-fold position and $z_{Nb} = 0.18$ to the four-fold position.

The position 4(g) with $x_1 = 0$, $y_1 = 0.04$, $z = 0.18$ can then arbitrarily be chosen as one Nb position, and it remains to determine which values y_2 and z_2 of the quartets $(0.13, \overline{0.13}, 0.63, 0.37)$ and $(0.03, \overline{0.03}, 0.53, 0.47)$ with $x = 0.17$ are in agreement with the Patterson function. The vectors $[x_2 - x_1, y_2 - y_1, z_2 - z_1]$ $[x_1 + x_2, y_1 + y_2, z_1 + z_2]$ between the Nb atoms of the two positions should thus be checked for each combination of the four y_2 and the four z_2 possibilities. In this way it is easy to show that only $y_2 = \overline{0.13}$, $z_2 = 0.03$ is possible. Finally all other vectors between Nb-atoms have been calculated and found in the Patterson function.

The niobium positions thus arrived at are

4 Nb in 4(g)	$x = 0$	$y = 0.04$	$z = 0.18$
8 Nb in 8(h)	$x = 0.17$	$y = \overline{0.13}$	$z = 0.03$

Oxygen configuration of the complex ion

In order to get an idea of the possible oxygen configuration all interatomic distances were calculated. It is then evident that six of the twelve Nb atoms are very close together: (0, 0.04, 0.18) $(0, \overline{0.04}, \overline{0.18})$ $(0.17, \overline{0.13}, 0.03)$ $(0.17, 0.13, \overline{0.03})$ $(\overline{0.17}, \overline{0.13}, 0.03)$ $(\overline{0.17}, 0.13, \overline{0.03})$. The distances between these atoms, numbered *a–f*, are listed in table 1. Remembering that a distance 3.2–3.4 Å has often

---

[1] The two-dimensional Fourier-summations were carried out on the X-RAC analogue computer.

Table 1

The shortest Nb–Nb distances in Å

	a	b	c	d	e	f
a		4.6	3.3	3.3	3.3	3.3
b	4.6		3.3	3.3	3.3	3.3
c	3.3	3.3		3.2	3.4	4.7
d	3.3	3.3	3.2		4.7	3.4
e	3.3	3.3	3.4	4.7		3.2
f	3.3	3.3	4.7	3.4	3.2	

The notation *a–f* is explained in the text.

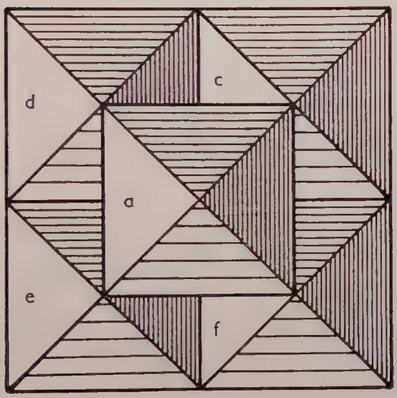

Fig. 1. Idealized structure of $Nb_6O_{19}^{8-}$. The octahedron *b* below *a* cannot be seen. Nb atoms in the centers of the octahedra and oxygen atoms at the corners.

been found to correspond to octahedra sharing edges in molybdates and tungstates (2, 3) it is easy to see that the idealized model given in Fig. 1 is in agreement with the interatomic distances. The possible existence of a complex with that structure has already been discussed in an earlier paper (2). The similarity with the complexes $Mo_7O_{24}^{6-}$ and $Mo_8O_{26}^{4-}$ (2) is obvious.

The correctness of the suggested oxygen configuration can be confirmed by the X-ray data. Because of the multiplicity of the Nb-O vectors in the complex (each of three Nb-O vectors occur 12 times) Nb-O vector maxima can be expected in the Patterson function near (0, ± 0.04, ± 0.18) and (± 0.17, ± 0.13, ± 0.03). They are actually found at (0, ± 0.03, ± 0.17) and (± 0.17, ± 0.11, ± 0.02) and correspond to the distance 2.2 Å.

The composition of such a complex ion is $Nb_6O_{19}^{8-}$.

No attempts have been made to determine the Na^+ and H_2O positions from the X-ray data.

Discussion

The formula of the ion $Nb_6O_{19}^{8-}$ has no obvious relation to the analytical formula 7 $Na_2O \cdot 6Nb_2O_5 \cdot 32\ H_2O$, which would require a $Nb_{12}O_{37}^{14-}$ ion to be a neutral salt. Two of the water molecules evidently must contribute oxygen atoms to the complex ion and the formula could be written 2 $Na_7HNb_6O_{19} \cdot 15\ H_2O$. With this formula nothing is assumed about the function of the H^+ ions of the salt, they may exist as $HNb_6O_{19}^{7-}$ or as H_3O^+ ($Na_7H_3ONb_6O_{19} \cdot 14\ H_2O$). This question must be left open.

There are other examples of large complex ions, having formulae which do not correspond to neutral salts e.g. the paratungstate ions (3). The result of the present investigation indicates, however, that the ion $Ta_6O_{19}^{8-}$ can be expected in the complex tantalate $4K_2O \cdot 3\ Ta_2O_5 \cdot aq$, which thus would be a neutral salt as the isopolymolybdates investigated so far (2). This assumption has later been proved to be correct (6).

A thorough discussion of the ionic conditions in aqueous solutions will be postponed until the structure of the complex ion in the metaniobate (1) has been determined.

SUMMARY

In the salt 7 $Na_2O \cdot 6\ Nb_2O_5 \cdot 32\ H_2O$ the existence of the ion $Nb_6O_{19}^{8-}$ (Fig. 1) has been proved by a structure determination. The formula of the ion has no direct relation to the analytical formula, which would require a $Nb_{12}O_{37}^{14-}$ ion, if the niobate would be a neutral salt.

The chemical and X-ray work was carried out in Uppsala where I was assisted by Miss Britta Svensson, whom I should like to thank for her valuable aid. The Swedish Natural Science Research Council supported the investigation financially, and their support is gratefully acknowledged. The computation work took place at Pennsylvania State College[1] and I wish to thank Professor Ray Pepinsky for his generous invitation to me to visit his Institute and to work with his X-RAC computer.

Institute of Chemistry, University of Uppsala, Uppsala, Sweden and Pennsylvania State College, State College, Pa., U.S.A.

REFERENCES

1. Süe, P., Ann. Chim. [11] 7, 493. 1937.
2. Lindqvist, I. Nova Acta Reg. Soc. Sci. Ups. IV *15*, N:o 1. 1950.
3. Lindqvist, I., Acta Cryst. *5*, 667. 1952.
4. Lindqvist, I., Acta Chem. Scand. *2*, 88. 1948.
5. Lu, Chia-Si, Rev. Sci. Instr. *14*, 331. 1943.
6. Lindqvist, I. and Aronsson, B. (to be published).

---

[1] Contract No. N 6 onr – 25916 TO 16.

Tryckt den 11 februari 1953

Uppsala 1953. Almqvist & Wiksells Boktryckeri AB

ARKIV FÖR KEMI Band 5 nr 23

Vorgelegt am 8. Oktober 1952

Zur Kenntnis des Buttergelb-Hepatoms und seiner Entstehung. III

Von Hans von Euler, Hans Hasselquist und Erik Eriksson

A. Reaktionen der Brenztraubensäure mit Spaltprodukten von cancerogenen Aminoazo-Farbstoffen

In einem zusammenfassenden Vortrag hat der eine von uns[1] kurz Reaktionen beschrieben, welche zwischen Spaltprodukten des Dimethylaminoazo-benzols und Inhaltstoffen der Rattenleber auftreten können. Als Spaltprodukte der cancerogenen Aminoazo-Farbstoffe kommen in Betracht das Anilin, das p-Aminophenol, das p-Phenylendiamin sowie ihre Methylderivate. Brenztraubensäure ist bekanntlich eine der wichtigsten, zentralen Stoffwechselprodukte der Leber.

Produkte aus Diketogulonsäure (Dehydro-ascorbinsäure) und Anilin sind kürzlich von H. Hasselquist[2] dargestellt und beschrieben worden. Solche Produkte wurden dann auch untersucht in Zusammenhang mit einer kinetischen Studie über die Decarboxylierung von α-Ketosäuren durch verschiedne Amine[3].

Die aus Anilin und BTS entstehende Reaktionsfolge, die zu Chinaldin-4-carbonsäure führt, ist in einer vorhergehenden Arbeit[4] behandelt. Die vorliegende Mitteilung betrifft Produkte, die mit p-Phenylendiamin als Ausgangsmaterial gewonnen wurden. Unter Vermittlung von 1,2,3,4-Tetrahydro-6-amino-chinaldin-3,4-dicarbonsäure entsteht unter CO_2 Abspaltung als Hauptprodukt 6-Amino-chinolin-4-carbonsäure, die einerseits verestert werden kann, andererseits das reine 6-Amino-chinaldin liefert.

p-Phenylendiamin und Brenztraubensäure. Sbst. 166

4,13 ml BTS (0,06 Mol) wurden in 30 ml Wasser gelöst und depolymerisiert, indem die eiskalte Lösung vorsichtig mit 30 ml einer 2-n Natronlauge (0,06 Mol) und dann mit 15 ml 4-n Salzsäure versetzt wurde. Hierauf wurden 3,24 g p-Phenylendiamin (0,03 Mol) in 25 ml Wasser gelöst zugegeben. Die rotbräunliche Farbe der Lösung geht allmählich in Gelb über und nach 3 Std. fällt das Reaktionsprodukt in Form einer gelben mikrokrystallinischen Masse aus, die mit Wasser und Aceton gewaschen wurde. Das getrocknete Produkt schmilzt bei 195–198° unter CO_2-

---

[1] Euler, Vortrag, 2. Nobelpreisträger-Tagung, Lindau 1952. — Chimia, *6*, 253 1952.

[2] H. Hasselquist, Dieses Arkiv, 4, Nr 24; 1952. — Siehe auch Euler u. Hasselquist, Dieses Arkiv 5, Nr 17; 1952.

[3] Euler, H. Hasselquist u. E. Eriksson, Lieb. Ann. im Druck.

[4] Euler u. H. Hasselquist, Dieses Arkiv 4, Nr 38; 1952.

Entwicklung, erstarrt und schmilzt wieder bei 304–305° (Sbst. 166). Die Sbst. ist schwer löslich in den üblichen organischen Lösungsmitteln, leicht löslich in Mineralsäuren.

In Alkali ist die Sbst. 166 leicht löslich, wird aber durch Zusatz von Mineralsäuren oder Eisessig nicht unverändert zurückgewonnen, sondern erfährt in saurer Lösung unter CO_2-Abspaltung eine Umwandlung in die Mono-carbonsäure 167.

Für $C_{12}H_{14}O_4N_2$		C	H	N
	Ber.	57,59 %	5,64 %	11,20 %
	Gef.	56,65	5,36	10,95

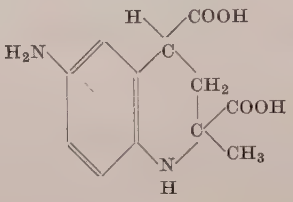

In neutraler und alkalischer Lösung wird die Dicarbonsäure 166 schon in der Konzentration 10^{-6} durch UV-Bestrahlung zu deutlicher, grüner Fluoreszenz angeregt; vgl. Tabelle S. 258. Die Subst. 166 u. 167 sind cancerogen.

Übergang der Dicarbonsäure 166 in die Monocarbonsäure 167

1,2 g Sbst. 166 wurden in 20 ml Wasser durch tropfenweisen Zusatz von Ammoniak vollständig in Lösung gebracht; die Lösung wurde auf 50° erwärmt und mit Eisessig angesäuert. Beim *gelinden Sieden* nimmt die schwach gelbliche Lösung eine tief dunkelgelbe Farbe an, worauf goldgelbe Blättchen auskrystallisieren, deren Schmpt höher als 306° liegt. Die so entstehende Sbst. 167 ist schwer löslich in allen üblichen organischen Lösungsmitteln. Die Lösung in Alkali ist nahezu farblos, wird aber beim Ansäuern dunkelgelb, und scheidet die unveränderten gelben Blättchen wieder aus.

Für $C_{11}H_{10}O_2N_2$		C	H	N
	Ber.	65,33 %	4,99 %	13,85 %
	Gef.	65,12	5,41	13,30

Metylierung der Carbonsäure 167 mit Diazomethan

Auf Zusatz von überschüssiger ätherischer Diazomethan-Lösung und wenig Methanol zu 270 mg Sbst. HH 167 entstand eine gleichmässige Stickstoff-Entwicklung und in der ätherischen Lösung trat eine zunehmende starke Fluoreszenz auf. Nach 18-stündigem Stehen bei Zimmertemperatur wurde die Lösung filtriert und im Vacuum zur Trockne verdampft: das zurückbleibende gelbbraune Öl krystallisierte beim Reiben sofort in Form von gelben Stäbchen, deren benzolische Lösung intensiv grün fluorescierte. Ausbeute 140 mg.

Die Sbst. 168 wurde durch Auflösen in kaltem Äthylacetat mittels Tierkohle gereinigt. Nach Filtrieren wurde vorsichtig Petroleumäther zugesetzt; aus der eiskalten Lösung krystallisierte dann die Sbst. in Form dunkelgelber Prismen vom Schmpt 145–146° (ohne Zersetzung). Die Sbst. 168 ist leichtlöslich in Chloroform, Äthylacetat und Methanol, schwerlöslich in Petroleumäther.

Für $C_{12}H_{12}O_2N_2$	Ber.	C 66,65 %	H 5,60 %	N 12,95 %
	Gef.	66,33	5,63	12,81

Die Sbst. 168 erweist sich also als der Methylester der Säure 167.

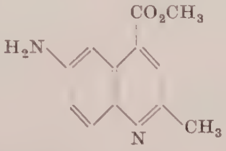

Darstellung des 6-Amino-Chinaldins aus der Carbonsäure 167

Die Sbst. 167 wurde in einem Reagenzrohr mit einer 1,5 cm hohen Schicht Eisenpulver überdeckt und dann im wagerecht gehaltenen Rohr auf offener Flamme erhitzt. Beim Schmelzen trat zunächst Braunfärbung und CO_2-Entwicklung ein und ein gelbes Öl begann überzudestillieren. Nach Abbruch der Erhitzung krystallisierte das Öl schnell zu einem harten Kuchen. Zwischen diesem und dem Eisenpulver wurde die Röhre abgeschnitten und die erstere Hälfte wurde in siedendem Chloroform aufgelöst. Nach Zusatz von Tierkohle wurde filtriert und das Filtrat stark eingeengt. Durch Zusatz von Petroleumäther krystallisierte das Reaktionsprodukt in Form gelblicher, graugrüner Prismen aus, die unter Braunfärbung aber ohne Gasentwicklung schmolzen. Umkrystalliert aus Benzol schmilzt die Sbst. bei 184°.

Die Sbst. 169 ist ziemlich leicht löslich in Chloroform, löslich in warmem Benzol, wenig löslich in siedendem Wasser, schwer löslich in Petroleumäther.

Für $C_{10}H_{10}N_2$	Ber.	C 75,92 %	H 6,37 %	N 17,71 %
	Gef.	76,51	6,46	17,18

Die Zusammensetzung der Sbst. 169 entspricht somit derjenigen des Amino-Chinaldins. Das 6-Amino-Chinaldin ist von FR. M. HAMER[1] durch Reduktion von 6-Nitro-Chinaldin[2] mit $SnCl_2$ dargestellt worden. Nach Ausfällung des Sn mit H_2S wurde das mit NaAc versetzte Filtrat mit Chloroform ausgeschüttelt. Aus der mit Na_2SO_4 entwässerten Lösung krystallisierte das 6-Amino-Chinaldin in Form gelbgrün-bräunlicher Prismen vom Schmpt 184–185° aus (HAMER gibt 187,5° an). Der Mischschmpt mit der Sbst. 169 gab keine Depression.

6-Oxy-chinaldin-4-carbonsäure aus p-Aminophenol + BTS

p-Aminophenol reagiert in wässriger Lösung mit 2 Mol. BTS unter lebhafter CO_2-Entwicklung und Absonderung einer graugrünen krystallinischen Substanz, die durch Lösen in Alkali und Wiederfällen mit Essigsäure gereinigt werden kann.

---

[1] FR. M. HAMER, Soc. 119, 1435; 1921.

[2] Dargestellt von COHN u. SPRINGER, Monatsh. 24, 87; 1903.

		C	H	N
Für $C_{11}H_9O_3N$	Ber.	65,02 %	4,47 %	6,89 %
	Gef.	64,44	4,59	6,78

Die Sbst. 159 (kein Schmpt) erwies sich als 6-Oxy-chinaldin-4-carbonsäure und entspricht also der 6-Amino-chinaldin-4-carbonsäure 167.

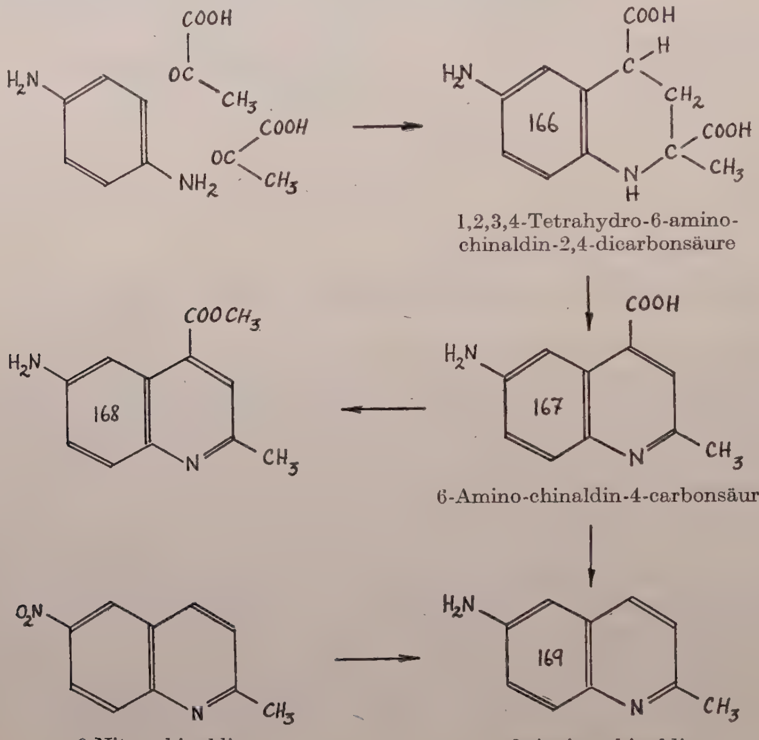

1,2,3,4-Tetrahydro-6-amino-chinaldin-2,4-dicarbonsäure

6-Amino-chinaldin-4-carbonsäure

6-Nitro-chinaldin

6-Amino-chinaldin

B. Reaktionen der Brenztraubensäure mit Aminobenzoesäuren

1. o-Aminobenzoesäure

Die Darstellung der direkten Reaktionsprodukte, 150 und 153, sowie ihrer Derivate 151, 154–157 haben wir[1] vor kurzem beschrieben. Gleichzeitig wurde auch auf die auffallende Grünfärbung hingewiesen, welche die Sbst. 150, Dihydro-chinaldin-dicarbonsäure-2,4, im sichtbaren, besonders im roten, Licht erfährt. Sie ist reversibel. Durch UV-Licht angeregt zeigt diese Chinaldin-dicarbonsäure in saurer Lösung (pH 2–7) eine kräftige Fluoreszenz in blauviolett–blau (vgl. S. 258).

Die Einwirkung der o- und p-Aminobenzoesäuren auf die Decarboxylierung der Brenztraubensäure haben wir in Lieb. Ann. (1953, im Druck) beschrieben.

Im Kressentest und an keimender Gerste rufen kleine Konzentrationen (10^{-5} mol.) eine geringe Wachstumsbeschleunigung hervor. Höhere Konzentrationen

---

[1] EULER u. H. HASSELQUIST, Dieses Arkiv 5, Nr 17; 1952.

(10^{-3}–10^{-4} mol.) des Na-Salzes (pH 7) zeigen eine deutliche bakteriostatische Wirkung an Escherichia Coli.

Über Tumorhemmung durch Sbst. 150 können noch keine endgültigen Angaben gemacht werden.

In der fogenden Tabelle sind die für die Derivate von Sbst. 150 festgestellten Formeln sowie ihre gegenseitigen Beziehungen angegeben.[1]

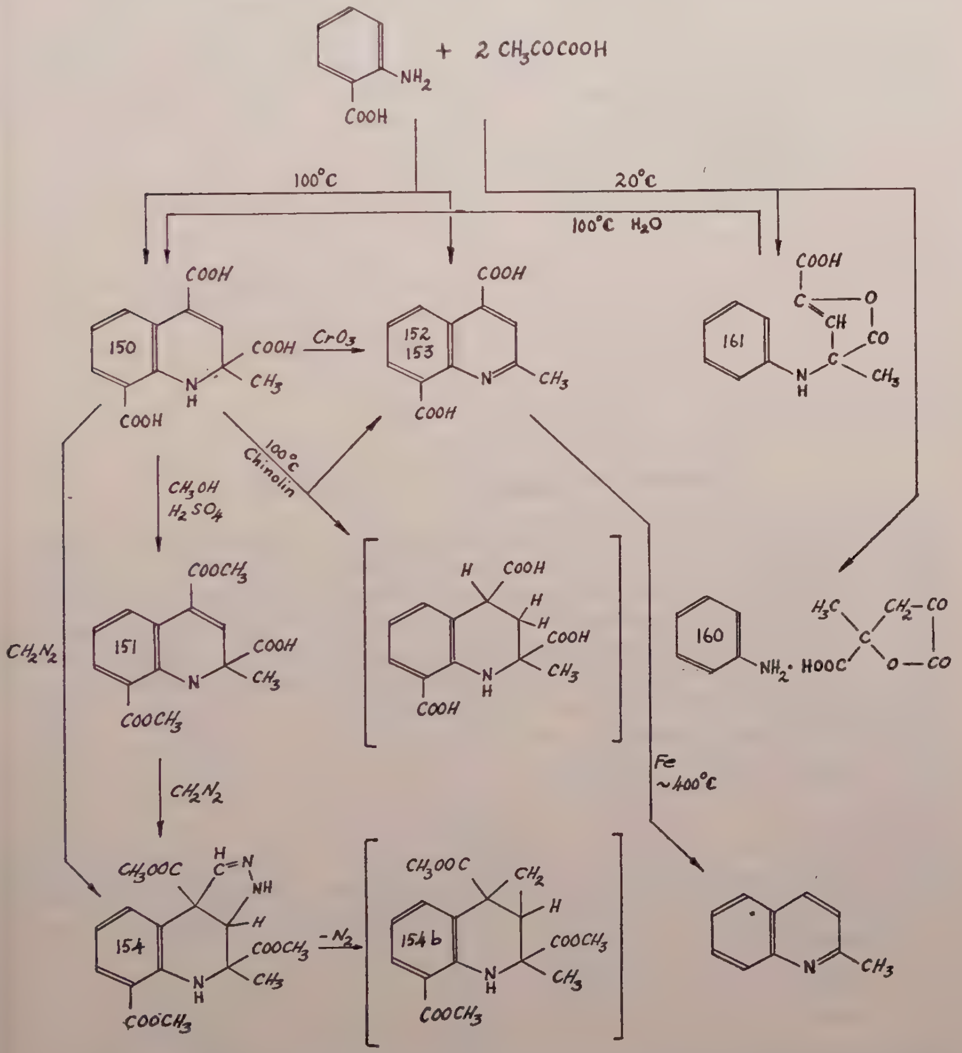
NH2
COOH
+ 2 CH3COCOOH
100°C
20°C
100°C H2O
COOH
150
COOH
CH3
N H
COOH
CrO3
COOH
152
153
N
CH3
COOH
COOH
C
O
CH
CO
161
N H
C
CH3
100°C Chinolin
CH3OH H2SO4
CH2N2
COOCH3
151
COOH
N
CH3
COOCH3
H COOH
H
H
COOH
N H
CH3
COOH
H3C
CH2–CO
160
C
NH2· HOOC
O—CO
Fe ~400°C
CH2N2
CH3OOC
H C=N
NH
H
154
COOCH3
N H
CH3
COOCH3
-N2
CH3OOC
CH2
H
154 b
COOCH3
N H
CH3
COOCH3
N
CH3

---

[1] Chinaldin wurde dargestellt nach DOEBNER u. MILLER (Ber. 17, 1712; 1884), durch Kochen von Anilin, Paraldehyd und Salzsäure. Durch Erwärmung des Chinaldins mit einer gesättigten wässrigen Pikrinsäure-Lösung wurde das Pikrat gewonnen.

Die Di-carbonsäure 152 wurde in einem Reagenzrohr mit überschüssigem Fe-Pulver erhitzt, wobei eine schwach bräunliche Flüssigkeit überdestillierte. Dieselbe wurde mit einer gesättigten Pikrinsäure-Lösung erwärmt; beim Erkalten krystallisierte Chinaldinpikrat aus.

2. m-Aminobenzoesäure. Sbst. 165

4,5 g Brenztraubensäure (2 Mol), in 7,5 ml Wasser gelöst, wurden mit 3,43 g m-Aminobenzoesäure vorsichtig auf dem Wasserbad auf 30–35° erwärmt, wobei vollständige Lösung ohne CO_2-Entwicklung eintrat. Während 18-stündigem Stehen bei Zimmertemperatur fielen farblose Krystalle aus, die, gewaschen und getrocknet, 2,45 g wogen.

Beim Erhitzen begann dieses Rohprodukt bei 170° sich braun zu färben und schmolz unter stärkerer Braunfärbung und gelinder Gasentwickling bei 253–260°.

Ein beim Lösen in kaltem Aceton verbleibender Rückstand wurde abfiltriert; nach Zusatz von Petroleumäther zum Filtrat krystallisierten farblose Prismen aus. Nochmals umkrystallisiert schmolz die reine Sbst. 165 bei 257–258°.

Für $C_{10}H_9O_4N + H_2O$	Ber.	C 53,33 %	H 4,92 %	N 6,22 %
	Gef.	53,39	4,75	6,47

Es hatte sich also eine Schiff'sche Base mit Brenztraubensäure gebildet:

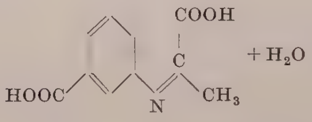

3. p-Aminobenzoesäure. Sbst. 162—164

In 4,5 g Brenztraubensäure (2 Mol) in 7,5 ml H_2O lösten sich 3,43 g p-Aminobenzoesäure (1 Mol) sofort unter schwacher Wärmeentwicklung, und nach 5 Minuten begann eine feste Krystallmasse auszufallen, die nach 2 Stunden abfiltriert und mit Wasser gewaschen wurde. Dieses Rohprodukt schmolz unter Braunfärbung und Gasentwicklung bei 303–304°. Durch Umkrystallisieren aus Aceton-Petroleumäther wurde die Sbst. 162 in Form farbloser Prismen erhalten, deren Schmpt höher als 312° lag.

Die Sbst. 162 ist leicht löslich in Methanol und Aceton, schwer löslich in Petroleumäther, Benzol und Wasser.

Sbst. 163 (Umlagerung aus 162)

1 g der Sbst. 162 wurde in 10 ml abs. Alkohol 60 Minuten auf dem Wasserbad gekocht. Die durch Umlagerung von 162 entstandene mikrokrystallinische Fällung wurde mit Alkohol gewaschen und durch Lösen in Alkali und Umfällung mit Eisessig gereinigt. Die Sbst. 163 ist sehr schwer löslich in allen organ. Lösungsmitteln sowie in verd. Mineralsäuren.

Für $C_{19}H_{10}O_5N_2 + {}^1/_2 H_2O$	Ber.	C 63,15 %	H 4,74 %	N 7,75 %
	Gef.	63,29	4,79	7,78

Wir nehmen für die Sbst. 163 die folgende Struktur an:

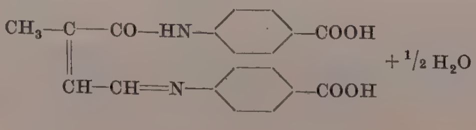

Sbst. 164

Das bei der Darstellung von Sbst. 163 gewonnene Alkoholfiltrat wurde im Vacuum zur Trockne verdampft; es entstand eine gelbe Krystallmasse, die mit wenig Methanol aufgekocht wurde; vom ungelösten Rückstand (Sbst. 163) wurde abfiltriert. Nach Abkühlung krystallisierten schwach gelb gefärbte Stäbchen in Rosettenstellung aus. Die reine Substanz wurde nach weiterem Umkrystallisieren aus Methanol in Form farbloser Stäbchen erhalten, die bei 223–224° unter Zersetzung schmolzen.

Die Sbst. ist ziemlich leicht löslich in warmem Methanol und Aceton, schwerlöslich in Petroleumäther und Benzol.

Für $C_{13}H_{13}O_7N$		C	H	N
	Ber.	52,88 %	4,44 %	4,75 %
	Gef.	53,22	4,51	4,73

Für die Sbst. 164 kommen zwei Strukturen (I und II) in Betracht.

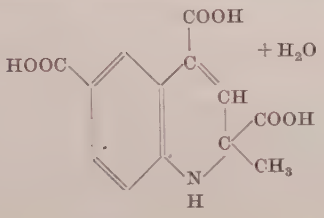

I

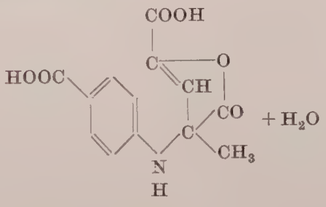

II

Decarboxylierende Wirkung des L-Histidins und des L-p-Oxyphenylalanins

Aliphatische Amine und aliphatische Aminosäuren üben bekanntlich einen geringeren Einfluss auf die Decarboxylierung von Brenztraubensäure und anderen α-Ketosäuren aus, als aromatische Amine und Aminosäuren. Die spezifischen physiologischen Wirkungen des L-Histidins haben uns veranlasst, im Anschluss an einige Versuche von EULER und N. BARGONI die decarboxylierende Einwirkung des L-Histidins auf Brenztraubensäure (BTS) zu untersuchen. Dieselbe ist recht gering und übertrifft diejenige des Glykokolls und anderer aliphatischer Aminosäuren nicht. Das Gleiche gilt von Dioxy-phenylalanin (Dopa).

Tab.

Zusatz zu 0,003 mol. BTS	Ccm CO_2 in 30 Min. 85° — pH 3,5
o-Aminobenzoesäure	25,8
Glykokoll	4,1
L-Histidin	4,0
Dopa	7,8

Brenztraubensäure selbst (ohne Amin) wird (nicht-enzymatisch) bei pH 3,5 nur sehr langsam decarboxyliert (Dieses Arkiv 5, 1953). Auch aliphatische α-Aminosäuren sind bei dieser Acidität ohne Mitwirkung einer Decarboxylase recht stabil. Aus

0,003 mol. Lösungen werden bei 85° und pH 3,5 in 30 Min. folgende Mengen CO_2 entwickelt:

Glykokoll ......0,8 ccm CO_2
Histidin ....0,9 ccm

Durch den Zusatz einer äquimolekularen Menge Ascorbinsäure wird die Decarboxylierung nur wenig beschleunigt.

Dagegen ist es wohl möglich, dass an der *enzymatischen* Decarboxylierung des Histidins zu Histamin Ascorbinsäure wesentlich beteiligt ist. Bevor wir in einer folgenden Mitt. hierauf zurückkommen sei auf die bemerkenswerten Arbeiten von P. HOLTZ[1] verwiesen.

Fluoreszenz einiger Chinaldin-Derivate in 96%iger alkoholischer Lösung bei verschiedenen Aciditäten

Spalte 2: Min. = geringste Konc. (γ/ml) der messbaren Fluoreszenz.

Substanz	Min. γ	Eigen-pH bei Min.	Fluor.-Farbe	Fluoreszenz-Farbe bei 10 × Min.		
				pH 2	pH 7	pH 11
150 bestr.	1	4,5	schwach hellblau	blau-violett	blau	sehr schwach blau
150 nicht bestr.	0,1	5,0	schwach blau	0	schwach blau	schwach hellblau
151	1	4,6	grün	grün	grün	schwach grün
153	10	4,5	schwach blau	0	schwach blau	sehr schwach blau
154	0,1	4,6	schwach blau	blau	blau	blau
160	10	4,5	schwach lila	lila	0	0
161	10	4,8	blau-violett	schwach violett	blau-violett	stark blau
162	10	4,8	schwach hellblau	hellblau	0	0
165	10	4,7	schwach blau	0	0	0
167	0,1	4,8	schwach grün	0	grün	grün
168	0,1	5,0	schwach gelb	0	gelb	gelb
Chinaldin	10	4,7	schwach blau	0	blau	blau
6-Amino-chinaldin[2]	0,1	4,5	schwach blau	gelb	blau	blau

---

[1] P. HOLTZ, Arch. f. exp. Path. u. Pharm. 186, 377; 1937. — Zs. f. physiol. Chem. 250, 87; 1937. — Siehe auch E. ABDERHALDEN, Fermentforsch. 15, 285 u. 360; 1937. — S. EDLBACHER u. A. v. SEGESSER, Naturw. 25. 461 u. 556; 1937.

[2] 2-Methyl-3-amino-chinolin fluoresciert nach O. STARK (Ber. 40, 3434; 1907) nur in saurer Lösung.

Über die Fluoreszenz einiger Chinaldin-Derivate

An cancerogenen Kohlenwasserstoffen ist oft Fluoreszenz nachgewiesen worden; viele derselben hat man durch fluorimetrische Messungen qualitativ und quantitativ bestimmt. In einer bemerkenswerten Untersuchung hat HADDOW bekanntlich gezeigt, dass 1,2-Benzpyren und 1,2,5,6-Dibenzanthracen, in geeigneter Konzentration angewandt, das Tumorwachstum bei Ratten, allerdings unspezifisch (HADDOW, BROCK, DRUCKREY und HAMPERL) stark *hemmen* können.[1]

Zu Beginn einer Untersuchung über die Beziehungen zwischen der die cancerogenen Wirkungen beeinflussenden Elektronendichte (O. SCHMIDT), der chemischen Anregbarkeit und der fluoreszenzfähigkeit verschiedener Klassen von Cancerogenen haben wir einige Messungen über die Fluoreszenz von Chinaldinen angestellt, welche sowohl auf cancerogene als auf tumorhemmende Wirkungen untersucht werden. Die Strukturen der tabellierten Chinaldine sind in dieser und vorhergehenden Mitteilungen besprochen worden.

Stockholm Universität, Vitamin-Institut u. Inst. f. organ. chem. Forschung.

---

[1] Vor mehr als 30 Jahren gelang es YAMAGIWA und ISHIKAWA, durch Bepinselung der Ohrhaut von Kaninchen mit Steinkohlenteer maligne Tumoren hervorzurufen, und ein Dezennium später führten besonders die Arbeiten von KENNAWAY und von J. W. COOK zur Entdeckung, dass Kohlenwasserstoffe vom Typus des Benzpyrens u. s. w. hochwirksame Cancerogene sind. Nach den fluorometrischen Arbeiten von MAYNEORD und von HIEGER lag es nahe, Zusammenhänge zwischen cancerogener Wirkung und Fluoreszenz auch im Gebiet stickstoffhaltiger Körper zu suchen.

Tryckt den 12 februari 1953

Uppsala 1953. Almqvist & Wiksells Boktryckeri AB

ARKIV FÖR KEMI Band 5 nr 24

Vorgelegt am 22. Oktober 1952

Einfluss des Histidins auf die Zahl der vitalfärbbaren roten Rattenblut-Zellen

Von Hans von Euler und Nora Bargoni

Verschiedene in diesem Institut angestellte Versuchsserien über den Einfluss von Histamin und Histidin auf die Anzahl vitalfärbbarer Erythrozyten (Reticulozyten) im Rattenblut haben nicht immer zu übereinstimmenden Ergebnissen geführt. Bei den ersten Versuchsserien[1] bei welchen in junge Ratten (mittleres Gewicht 80 g) unseres norwegischen Stammes 1 mg Histidin (das entspr. Gewicht Histidin-HCl wurde mit NaOH auf pH 7,5 neutralisiert) per Ratte injiciert wurde, fanden wir nach 18–24-stündiger Inkubation eine starke Zunahme der Reticulozyten-Zahl: von 0,1 % der gesamten Blutkörperchen-Zahl (Normalwert) stiegen die Werte, schwankend zwischen 9 % und 4 %. Sie lagen

in der II. Serie zwischen 2,5 % und 3,7 %
in der III. Serie zwischen 4,2 % und 5,6 %.

Da die Zahl der vitalfärbbaren roten Blutzellen erheblich von der Zusammensetzung der Nahrung abhängt, wurde dieselbe genau gleichmässig verabreicht. Die Zusammensetzung der Nahrung war in den neueren Versuchsserien identisch mit der für Serie I in diesem Archiv (Bd. 1, No 28, S. 248; 1949) angegebenen.

Insbesondere wurde für einen konstanten Vitamin-A-Gehalt gesorgt in Rücksicht auf den von Euler und Malmberg[2] gefundenen Einfluss dieses Vitamins, sowie für eine konstante Vitamin-C-Zufuhr, obwohl bekanntlich das Wachstum der Ratten von der Ascorbinsäure-Einnahme unabhängig ist. Denn, abgesehen von der Wirkung der Ascorbinsäure als C-Vitamin und ihrer damit zusammenhängenden Schutzwirkung auf das Vitamin A, war in Betracht zu ziehen, dass Ascorbinsäure an den Umsetzungen des Histidins, besonders an der Histaminbildung aus Histidin im Tierkörper im Sinne von P. Holtz[3] beteiligt ist.

Nachdem wir, wie erwähnt, nachgewiesen hatten, dass der Reticulozyten-Gehalt bei Vitamin-A-Mangel erheblich erniedrigt ist[4], haben wir an solchen Vitamin-A-armen Ratten den Einfluss von (intramuskularen und subcutanen)

---

[1] N. Bargoni, Dieses Archiv 1, No 28; 1949.

[2] Euler u. M. Malmberg, Naturwiss. 27, 166; 1939. — Z. physiol. Chem. 261, 103; 1939.

[3] P. Holtz, Z. physiol. Chem. 250, 87; 1937. — Siehe auch E. Abderhalden, Fermenforsch. 15, 285 u. 360; 1937. — S. Edlbacher u. A. v. Segesser, Naturwiss. 25, 461 u. 556; 1937.

[4] Euler u. Mitarb., Naturwiss. 27, 166; 1939.

Histamin-Injektionen untersucht. Diese Wirkung kommt, wie die des Histidins[5], nach 4 Stunden noch nicht zum Vorschein, ist aber nach 18-stündiger Inkubation nach injizierten Histamin-Mengen von sowohl 200 γ wie von 1 mg deutlich.

Auch in normal ernährten, Jensen-Sarkom tragenden Ratten konnte schon in der 1. Mitteilung (erste Versuchsserie, N. Bargoni) über einen Abfall der Reticulozyten-Zahl auf etwa 1/3 des normalen Wertes berichtet werden. Dieses Ergebnis hat sich in den späteren Serien bestätigt. Hiernach konnte auf einen nahen Zusammenhang zwischen Reticulozyten-Ausschüttung und Körperwachstum geschlossen werden.

Da wir für Histamin einen Reticulozyten-Effekt von der gleichen Grössenordnung gefunden hatten, wie für Histidin, so bestand die Möglichkeit, dass letztere Wirkung dem im Organismus gebildeten Histamin zuzuschreiben ist. Da aber nur ein Teil des Histidins in das Histamin übergeht, und die Wirkung dieses Amins anscheinend nicht wesentlich stärker ist als die des Histidins, erhob sich die Frage, welche anderen Bestandteile bezw. Spaltprodukte oder Umwandlungsprodukte des injicierten Histidins an der vermehrten Reticulozyten-Zahl beteiligt sind. In Betracht kamen zunächst Glutaminsäure, ferner die unter Öffnung des Imidazol-Ringes entstehenden Stoffe mit anhängendem Guanidin, sodann Imidazolyl-brenztraubensäure.

Unter den gleichen Versuchsbedingungen wie L-Histidin haben wir zunächst den Einfluss der als Glutaminat injizierten Glutaminsäure[6] untersucht, und zwar in 3 verschiedenen Konzentrationen, nämlich pro 100 g Ratte 0,5 mg, 1 mg und 5 mg. Obwohl auch die Inkubationsdauer zwischen 5 und 22 Stunden variiert wurde, lag die gefundene Erhöhung der Reticulozyten-Zahl nur unbedeutend, höchsten 10 %, über dem Normalwert und erreichte nie die mit Histidin oder Histamin beobachtete Steigerung.

Eine Glutaminsäure-decarboxylase hat sich bisher im Tierkörper nicht mit Sicherheit nachweisen lassen[7]; dagegen tritt die Desaminierung zur Ketosäure auch nicht-enzymatisch leicht ein. Die enzymatische Desaminierung spielt bekanntlich bei der Umaminierung sowohl im Stoffwechsel des Tier- wie des Pflanzenkörpers eine zentrale Rolle.[8] Über die an der Umaminierung beteiligten Enzyme, besonders Iminosäure-Dehydrasen siehe Karrer u. H. Brandenberger.

Eine Reticulozyten-Zählung wurde ferner unternommen nach Injektion einer mit Extrakt von Meerschweinchen-Nieren 10 Stunden inkubierten L-Histidin-

---

[5] Histidin, ein wichtiger Wuchsstoff für höhere Tiere, wird zum Teil in die Ketten von Peptiden bezw. Proteinen eingebaut, u. zw. nach A. Kossel so, dass der Guanidinrest frei bleibt. Auf Mikroorganismen ist die Wachstumswirkung des Histidins verschieden. Bei Versuchen von Euler u. M. Jaarma (Dieses Arkiv 23, A, No 17; 1946) war die Wachstumswirkung von 1 mg Histidin in 10 ml Suspension von *Proteus vulg.* kaum noch messbar.

[6] Euler, E. Adler, G. Günther u. Nalin Bandhu Das, Zs. physiol. Chem. 254, 61; 1938.

[7] Bei der Decarboxylierung von Glutaminsäure durch Gehirn- und Nervengewebe wurde von Awasara u. Mitarb. γ-Aminobuttersäure nachgewiesen (J. Biol. Chem. 187, 35; 1950). — Roberts u. Fränkel, J. Biol. Chem. 187, 55; 1950.

[8] Euler, Adler u. Steenhoff-Eriksen, Zs. physiol. Chem. 248, 227; 1937. — Euler u. G. Günther, Naturwiss. 27, 214; 1939, Umaminierung und Glutaminsäure-Dehydrierung durch Jensensarkom-Extrakte. Über den Einfluss von Aminen auf die Decarboxylierung der Brenztraubensäure siehe Euler, H. Hasselquist u. E. Eriksson, Dieses Arkiv 5, 1952, im Druck. Andererseits wird die Desaminierung von Aminen vom Typus des Glutamins durch Brenztraubensäure beschleunigt. In nicht-enzymatischen Systemen entstehen — allerdings in geringerem Grad als mit aromatischen Aminen — Schiff'sche Basen bezw. die Iminosäuren.

Über die an der Umaminierung beteiligten Enzyme siehe Karrer u. H. Branderberger, Helv. Chim. Acta 34, 82; 1951.

Lösung (neutralisiertes Histidin-Hydrochlorid) mit Ascorbinsäure. Von dieser Reaktionsmischung wurde so viel injiziert, dass die Dosen etwa 0,1 mg, ferner 0,5 und 1 mg Histidin entsprachen. Nach einer Inkubationsdauer von 19 Std. stieg die prozentische Reticulozytenzahl in 4 Versuchen auf Werte zwischen 3,3 und 6,0 %. Die Wirkung des Nierenextraktes entsprach also durchaus dem von Holtz angegebenen.

Zur Beurteilung unserer Beobachtungen über den Einfluss von Histidin-Injektionen auf das rote Blutbild bei Ratten war in Betracht zu ziehen, dass Histidin im Organismus schnell zu Histamin decarboxyliert wird, wodurch der für beide Substanzen übereinstimmende Einfluss auf die Reticulozyten-Zahl ohne weiteres verständlich würde.

Was nun die Biochemie des Histidins und besonders die Decarboxylierung der pharmakologisch weniger wirksamen[9] Aminosäure in die Pressor-Substanz Histamin betrifft, so ist zunächst die *nicht-enzymatische* Spaltung des Histidins mit derjenigen anderer α-Aminosäuren und α-Ketosäuren zu vergleichen. Die nicht-enzymatische Decarboxylierung der letzteren unter der Einwirkung von Aminen wurde in diesem Institut vor kurzer Zeit bearbeitet[10a], sodass auf diese Ergebnisse verwiesen werden kann.

Die *aliphatischen Aminosäuren* sind in saurer Lösung (pH 3,5) sogar bei 85° fast durchweg noch recht stabil, was ja auch bezgl. der α-Ketosäure Brenztraubensäure der Fall ist.[10a]

Tab. I

Decarboxylierung von Alanin: 0,003 mol. DL-Alanin, 10 ml Wasser

Ccm entwickeltes CO_2	1,0	1,6	2,0
Minuten	10	20	30

Die *enzymatische* Umwandlung der α-Aminosäuren in die entsprechenden Amine geht bekanntlich durch Decarboxylasen vonstatten. Es ist a priori in Betracht zu ziehen, dass dieser Vorgang durch die Dehydrierung der α-Aminosäure zur Iminosäure, u. zw. durch intermediär entstehende Peroxyde (P. Holtz[10b]) eingeleitet wird, worauf die Decarboxylierung und dann die Hydrierung des Imins zum Amin erfolgt.

Co-Enzym der L-Aminosäuren-Decarboxylase ist nach Karrer, M. Viscontini u. G. Forster[11] das Pyridoxal-3-phosphat. — Mit dem Co-Enzym der Dopa-Decarboxylase ist dasselbe nicht identisch.

Beim enzymatischen Abbau des Histidins tritt nach Edlbacher[12] eine hydrolytische Aufspaltung des Imidazolringes und NH_3-Abspaltung ein (Histaminase nach Best u. Mitarb.). Holtz und Triem[13] konnten zeigen, dass in Leber und

---

[9] Das nicht selten als Wuchsstoff fungierende Histidin ist nicht bei allen Säugetieren ein unentbehrliches Vitamin (vgl. auch W. C. Rose, Haines und Warner, J. Biol. Chem. 193, 605; 1952).

[10a] Euler, H. Hasselquist u. E. Eriksson, Lieb. Ann. im Druck.

[10b] P. Holtz, Naturwiss. 25, 589; 1937.

[11] Karrer, M. Viscontini u. G. Forster, Helv. Chim. Acta, 31, 1004; 1948. Diese Forscher betonen die hohe Spezifität der Aminosäuren-Decarboxylasen. Siehe auch M. Viscontini u. P. Karrer, Helv. Chim. Acta 35, 1924; 1952 (Pyridoxal-5′-phosphorsäureester).

[12] S. Edlbacher u. Mitarb. Z. physiol. Chem. 157, 106; 1926. — 191, 225; 1930. — 224, 261; 1934. — E. Abderhalden, Fermentf. 15, 285 u. 360; 1937. Yoshio Oyamada, J. of Bioch. 36, 227; 1944.

[13] P. Holtz u. G. Triem, Z. physiol. Chem. 248, 1; 1937. P. Holtz, ebenda 250, 37; 1937.

Nieren von Kaninchen und Meerschweinchen ein spezifisch auf Histidin eingestelltes Enzym (Histidase[14]) vorkommt, durch das bei der Einwirkung von Ascorbinsäure (und SH-Substanzen) auf Histidin ein Teil der Aminosäure in Histamin umgewandelt wird.

Eine Untersuchung über die intracellulare Verteilung der Histidase, besonders über den Gehalt der Mitochondrien an diesem Enzym wurde in diesem Institut[15] im Anschluss an analoge Versuche über die Verteilung der Katalase (BARGONI u. HELLER[16]) angestellt.

Nicht-enzymatisch wird im System Alanin-Brenztraubensäure CO_2 entwickelt, und zwar unter gleichen Umständen (Temp. 85°; $pH = 3{,}5$) schneller als aus den einzelnen Komponenten.

Wir stellen im Folgenden auch den Einfluss der Ascorbinsäure fest.

Tab. II

Decarboxylierung im System 0,003 mol. Alanin + 0,006 mol. Brenztraubensäure

	Minuten		
	10	20	30
Ccm entwickeltes Co_2 ohne Ascorbinsäure	2,7	5,0	7,0
ccm » CO_2 + 0,003 mol. Ascorbinsäure	3,4	6,4	9,4

Für L-Histidin (ohne Brenztraubensäure) wurden folgende Zahlen erhalten, die alle für die Azidität $pH = 3{,}5$ und die Temp. 85° gelten.

Tab. III

	Minuten		
	10	20	30
Ccm CO_2 aus 0,003 mol. Histidin, ohne Ascorbins.	0,4	0,5	0,9
ccm CO_2 » » » » + 0,003 mol. Ascorbins..	1,2	2,5	3,3

In einer vorhergehenden Mitteilung wurde gezeigt, dass die Decarboxylierung sowohl der Brenztraubensäure wie auch der aliphatischen α-Aminosäuren bei $pH = 3{,}5$ ohne aktivierende Zusätze sehr gering ist. Auch wird die Decarboxylierung der Brenztraubensäure durch aliphatische α-Aminosäuren nur wenig beschleunigt; erst nach Zusatz von Ascorbinsäure tritt eine deutlichere Erhöhung der CO_2-Entwicklung ein.

---

[14] Ausserdem auch eine Tyrosinase; siehe HOLTZ, Naturwiss. 25, 437; 1937. In analoger Weise verläuft die Decarboxylierung von Dopa zu Oxy-Tyramin (HOLTZ u. K. CREDNER, Naturwiss. 29, 649; 1941. — Arch. f. exp. Path. u. Pharm. 199, 145; 1942). Dopa-Decarboxylase wurde auch in Leber und Nieren von Schwein, Hammel und Huhn gefunden, nicht aber bei Rind, Ratte, Katze und Hund.

Für den enzymatischen Abbau von Aminosäuren glauben W. LANGENBECK und RUGE (Ber. 70, 367; 1937) im Isatin ein Enzymmodell gefunden zu haben.

[15] Siehe hierzu EULER u. L. HELLER, Arkiv f. Kemi etc. 25 A No 16; 1947.

[16] NORA BARGONI u. L. HELLER, Dieses Archiv 1, No 52; 1949. Histidase ist ein typisches Lyo-Enzym.

Inwieweit der Einfluss des Histidins und der Ascorbinsäure (vgl. S. 265) auf das rote Blutbild mit einer Atmungssteigerung in Zuzammenhang steht, konnte noch nicht entschieden werden.

Tab. IV

Decarboxylierung im System 0,003 mol. Histidin + 0,006 mol. Brenztraubensäure

	Minuten		
	10	20	30
Ccm entwickeltes CO_2 ohne Ascorbinsäure	1,3	2,4	4,0
ccm » CO_2 + 0,003 mol. Ascorbinsäure	4,9	8,7	13.9

Die erhöhte CO_2-Entwicklung kann in diesem Versuch katalytisch hervorgerufen sein, also aus dem Histidin bezw. aus der Brenztraubensäure stammen, konnte aber auch von der oxydierten Ascorbinsäure (Diketogulonsäure) abgespalten worden sein. Um dies zu entscheiden wurde bei gleicher Temp., 85°, und gleicher Azidität, pH = 3,5, ein Versuch angestellt, bei welchem die Ascorbinsäure mit Tillmans Reagens titriert wurde.

Tab. V

Reaktion im System 0,003 mol. Brenztraubens. + 0,0015 mol. Histidin + 0,0015 mol. Ascorbinsäure

Minuten	ccm CO_2	Verbraucht 0,00567 n. TR per 0.1 ml Lösung
0	—	10,6
15	3,9	10,4
30	7,3	10,3

Durch die Reaktion werden also keine nennenswerten Mengen Ascorbinsäure verbraucht; die erhöhte CO_2-Entwicklung im obigen Versuch (Tab. III) entstammt also *nicht* der Ascorbinsäure.

Reticulozyten-Zahl nach Injektion von Histidin + Ascorbinsäure.

Nach zweimal wiederholter Injektion dieser Mischung wurde die Reticulozyten-Zahl nicht mehr gesteigert als durch Injektion der gleichen Dosis Histidin allein. In 3 Versuchen (Serie V a) an unserem norwegischen Rattenstamm wurde erhalten:

3,4 %   4,6 %   4,1 %

der gesammten Erythrozyten-Zahl, bei einem Ausgangs-Normal-Wert von 0,5 %.

Die entsprechenden Werte nach Injektion des Histidins ohne Ascorbinsäure (Serie V b) waren die folgenden:

3,8 %   3,4 %   4,4 %

Sowohl in Serie V a wie in Serie V b befanden sich die Ratten in normalem Wachstum, was hervorgehoben sei, da wir nach neueren Erfahrungen ein früheres Ergebnis (Z. physiol. Chem. 261, 103; 1939) bestätigen können, dass die Reticulozyten-Zahl in hohem Grad von Diät und damit vom Wachstum der Tiere bestimmt wird.

---

[17] NORA BARGONI, Dieses Archiv 1, No 28; 1949.

Die früher ausgeführten Versuche über den Einfluss von injiziertem Histamin auf das Blutbild von Ratten, die von besonderem Interesse sind, da Histamin, wie auch Arterenol als Wirkstoff vegetativer Nerven fungiert[18], haben sich in den neueren Serien (VIII–IX) insofern bestätigt, als wieder eine deutliche Erhöhung der Reticulozyten-Zahl erreicht wurde. Erwähnenswert ist die Inkubationszeit 16–22 Stunden; nach dieser Zeit sinkt die Reticulozyten-Zahl wieder ab.[19] Diese Abnahme[20] kann damit zusammenhängen, dass Histamin im Blut fermentativ unter Freiwerden von NH_3 abgebaut wird, vermutlich durch einen decarboxylierenden und desaminierenden Enzymkomplex, ein Enzymoid.

Entsprechend einem in der Enzymologie allgemein angenommenen Nomenklatur-Prinzip würde „Histaminase“ ein Enzym bezeichnen, welches das Substrat Histamin angreift (spaltet). Es sei aber schon hier darauf hingewiesen. dass — wie an anderer Stelle gezeigt wird — das Hormon Histamin, ebenso wie viele andere Ergone im Organismus erst in Verbindung mit einem Protein (als Hormozym[21]) zur Wirkung kommt. Eine geeignete Bezeichnung für dieses enzymatisch aktive Histamin-Protein wird in anderem Zusammenhang besprochen werden.

Herrn Ingenieur ERIK ERIKSSON danken wir bestens für Mitarbeit durch Ausführung der Decarboxylierungsversuche.

Stockholm, Vitamin-Institut der Universität.

---

[18] U. S. VON EULER, Z. f. Vitamin- u. Fermentforsch. 2, 604; 1949.

[19] Wiederholt wurde in den Arbeiten dieses Institutes darauf hingewiesen, dass es sich bei unseren Versuchen direkt um eine Ausschüttung der vitalfärbbaren roten Blutkörperchen handelt, dass aber über die der Ausschüttung vorhergehende Neubildung dieser Blutzellen, wie über die Bedingungen der Hämatopoiese überhaupt noch wenig bekannt ist. (Vgl. auch A. ASCHKENASY, Exposés Annuels; M. POLONOVSKI; X. Série.) Der Einfluss der Ascorbinsäure auf die Reticulozytenbildung (R. SEYDERHELM, 1935) ist in unseren Arbeiten wiederholt behandelt worden (Z. physiol. Chem. 243, 121; 1936. — 249, 85; 1937. — 252, 24; 1938. — 261, 103; 1939).

[20] Auch in anderer Weise kann das Verschwinden der »Histaminase» oder richtiger, der histaminabbauenden Wirkungen, aus dem Blut gedeutet werden. Vgl. E. A. ZELLER, S. SCHÄR u. S. STAEHLIN, Helv. Chim. Acta 22, 837; 1939. — N. EMMELIN, Acta Physiologica Scand. 22, 379; 1951.

Erwähnt sei hier noch die Kombination des Histamins mit Aldehyden. Siehe hierzu D. KLEIN, Angew. Chem. 62, 452; 1950.

[21] EULER, Nordisk medicinsk Tidskrift. Vortrag beim 4. Nord. Physiologen-Kongress, Helsinki 1934. Siehe auch C. FROMAGEOT ET AL., Biochim. et Biophys. Acta, 9, 339; 1952.

Tryckt den 12 februari 1953

Uppsala 1953. Almqvist & Wiksells Boktryckeri AB

ARKIV FÖR KEMI Band 5 nr 25

Communicated 8 October 1952 by JOHN RUNNSTRÖM and KARL MYRBÄCK

Incorporation of N^{15}-labelled ammonium chloride into pyrimidines and pyrines during the early sea urchin development

By TORE HULTIN

With 4 figures in the text

From the early sea urchin development several examples have been given of a close relationship between definite morphogenetic processes and an increasing complexity of the metabolic pattern (for references, see 16). The purpose of this investigation has been to decide, if such relationships can be demonstrated also in the case of the metabolism of pyrimidines and purines.

The metabolism of deoxyribonucleic acid (DNA) in the developing sea urchin embryo has been the subject of considerable interest. It can be studied directly by analytical methods, since a net synthesis of DNA occurs (32, 37), which is approximately parallel with the multiplication of cell nuclei (cf. 38). For an isotope study of the metabolic intensities at different stages the DNA is less suitable because of the continually augmenting proportion of previously synthesized and probably less actively metabolizing molecules.

Because of the very low DNA content in the embryos during the early stages of development it was not possible to isolate from our material sufficient amounts of DNA pyrimidines and purines for N^{15}-analyses during these stages. Instead, the investigation was concentrated on low molecular pyrimidines and purines and on ribonucleic acid (RNA). The approximately constant amounts of these substances throughout the early development is an advantage in isotope experiments, where a constant dilution effect is desired.

It is well known (3) that N^{15} in the form of ammonium salts can be readily incorporated into the pyrimidines and purines of various organisms. For a study of pyrimidine and purine metabolism in developing sea urchin embryos the use of N^{15}-labelled ammonium salts has certain advantages. It may be mentioned that the rate of ammonia uptake into the embryos (27, 14) is not much influenced by the changes in cell permeability, which have been described to accompany the initiation of development (36).

Experimental

Egg material

Eggs from the sea urchin *Paracentrotus lividus* (LM) were used in the experiments. Cultures of developing embryos were prepared by fertilizing dilute egg suspensions and allowing them to develop at 20° C in rocking glass trays as described by LINDAHL (21). At least 95 % of the eggs were able to develop into normal plutei. Jelly-free eggs were used in all experiments.

The isotope treatments were performed in the following manner. Suspensions of eggs or embryos at certain stages of development were washed by centrifuging and transferred to fresh sea water containing 0.75 mM $N^{15}H_4Cl$ (61 % N^{15} excess), where they were kept for exactly 5 hours. Approximately 4 ml of isotope containing sea water were added pro mg of total egg nitrogen. The concentrations of NH_4Cl used in the experiments did not interfere with the normal development (cf. 27). Before and after the isotope treatments the eggs and embryos were examined in a microscope. Immediately after the isotope treatments the material was washed by centrifuging in sea water containing 0.015 M ordinary NH_4Cl, in pure sea water and finally in 0.62 M NaCl, containing 0.05 volumes of isotonic sodium citrate solution. The material was then immediately freeze-dried and stored at –20° C. From each stage about 10 g of isotopic material were collected as the result of 5–10 independant preparations.

The material was prepared at the Zoological Station in Naples mainly during 1949—50.

Extraction of acid soluble pyrimidine and purine

The material was designed for the study of various nitrogen containing cell constituents besides those dealt with in this report. This had to be taken into consideration i planning the isolation procedures.

Small portions of the dry material were finely powdered in a mortar and then extracted 3 times with water at 0° C by grinding the material for 60 minutes with air-driven, rotating glass-rods. For each extraction 25 ml of water were added pro gram of dry powder. The extracts were centrifuged repeatedly at high speed until free from opalescence.

The water-extracts were precipitated at 0° C by the gradual addition of cold, 50 % trichloroacetic acid (TCA) to a final concentration of 10 %. After centrifugation, the sediments were washed in cold 5 % TCA. The combined TCA-extracts, which were slightly opalescent (cf. 13, 17), were carefully treated with ether, and the precipitates accumulating in the interfaces were removed. The clear solutions were then further extracted with ether until the pH had reached 2.0.

Preparation of acid soluble pyrimidine and purine

TCA-treated water-extracts from material at the same stages of development were collected and adjusted to pH 2.0. The solutions were precipitated by the addition of 0.2 volumes of saturated mercuric nitrate and were kept overnight at 0° C. The precipitates were washed repeatedly with water and decomposed with H_2S. The excess of H_2S was removed by aeration, and the clear extracts were concentrated in vacuo to 1 ml and added to kation-exchange columns (Dowex 50, 300 mesh, H^+-form, 20 cm × 0.65 cm^2). Water, acetic acid and HCl in increasing concentrations were used as eluting agents. The ultraviolet absorption of the eluates were followed in a Beckman spectrophotometer. Two fractions appeared, one corresponding to uridylic acid (4), and the other to hypoxanthine.[1]

1) The first fraction was repeatedly evaporated in vacuo, taken up in 5 ml of water and precipitated with mercuric nitrate at pH 2.0 as described above. The H_2S-extract was analyzed for nicotinic acid according to BANDIER and HALD (2), with a negative result. A treatment with N HCl at 100° C for 60 minutes had a very small effect. The concentrated solution was

---

[1] In all chromatograms only the central parts of the fractions were collected.

treated with 24 % H_2SO_4 at 125° C for 25 hours (28). The excess H_2SO_4 was removed by means of $Ba(OH)_2$. The solution was concentrated and run through a Dowex 50 column. One fraction was obtained, corresponding to uracil (4). The ultraviolet absorption was identical with that of uracil, and uracil analyses according to Soodak, Pircio and Cerecedo (35) agreed with the ultraviolet absorption and the nitrogen content. The N^{15}-content of the nitrogen was determined in a mass-spectrograph.

2) The second chromatographic fraction showed ultraviolet absorption identical with that of hypoxanthine. It was not affected by a deamination with nitrite. When submitted to electrodialysis, it remained in the middle compartment at pH 4.6, while the uridylic acid fraction migrated into the anode compartment. The second chromatographic fraction was precipitated with $CuSO_4 + NaHSO_3$ (19) and reprecipitated with $AgNO_3$ according to Kerr and Seraidarian (18). The nitrogen of the final product was considered as free hypoxanthine nitrogen, and its N^{15}-content was determined.

Fractionation of acid insoluble nucleotides

The methods generally used for the separation of RNA from DNA in cell material are based on the higher susceptibility of RNA to weak alkaline (33, 12) or acid (26) hydrolysis. During weak acid hydrolysis RNA is brought into solution mainly in the form of mononucleotides. It has been shown by Ogur and Rosen (26) that under the same conditions DNA initially is very little affected and that the intensity of the hydrolysis must be considerably increased for the extraction of DNA. From such DNA-extracts mononucleotides cannot be isolated.

In the present experiments RNA was extracted by means of fractionated hydrolysis in cold N $HClO_4$ (26), and the resulting mononucleotides were isolated by chromatography. The preparations were performed in the following way.

After an initial precipitation with cold, 10 % TCA the original water-extracts as well as the combined, non water-soluble residues were extracted 3 times with cold, 5 % TCA. The sediments were washed with alcohol in order to remove the TCA, and lipid-extractions were performed according to Schneider (34). The lipid-free material was washed in cold, 0.2 N $HClO_4$ and then treated at + 2° C in a shaking-machine with 200 ml of N $HClO_4$ for 24 hours. Five such $HClO_4$-extractions were made, followed by a final extraction at + 10° C. The

Table 1

Analytical values illustrating the extraction procedure used for the separation of RNA and DNA. Water-soluble and non water-soluble fractions from 10 g of dry material were repeatedly extracted for 24 hours with 200 ml N $HClO_4$ (26) and afterwards treated with 5 % TCA at 90°C (34). The extracts were analyzed for RNA (7) and DNA (5)

	Water-soluble Fraction		Non water-soluble Fraction	
	RNA	DNA	RNA	DNA
$HClO_4$-extractions at 2°C I . . .	98 mg	2 mg	89 mg	2 mg
II . . .	48	1	39	1
III . . .	15	0	13	1
IV . . .	11	0	7	3
V . . .	9	0	4	4
$HClO_4$extraction at 10°C	9	2	4	11
TCA-extraction at 90°C	5	5	3	24

extracts were analyzed for ribonucleotides according to EULER and HAHN (7), and for DNA according to DISCHE (5). The main part of the ribonucleotides was brought into solution already during the first extractions (Table 1), where only small amounts of DNA were indicated. For the subsequent chromatographic isolation of ribomononucleotides only the first 2 extracts from each series were used.

Preparation of pyrimidines and purines from RNA-fractions

The extracts were neutralized with $Ba(OH)_2$ and evaporated in vacuo at low temperature. The barium perchlorate was extracted with alcohol-ether in the presence of 0.1 volumes of saturated mercuric acetate in alcohol-ether. The ribonucleotides were precipitated and reprecipitated with mercuric nitrate as described and chromatographed through a Dowex 50 column (30 cm × 1.75 cm^2) as described by COHN (4). The following fractions were obtained: uridylic acid, guanylic acid, cytidylic acid, adenylic acid, guanine and adenine. The fractions were repeatedly evaporated in vacuo and taken up in 15 ml of water. The nucleotides were precipitated with mercuric nitrate at pH 2.0. The purines were precipitated with $CuSO_4 + NaHSO_3$. The precipitates were washed repeatedly and decomposed with H_2S.

1) The uridylic acid was reprecipitated with mercuric nitrate and treated with H_2S. The ultraviolet absorbtion and the nitrogen contents of the H_2S-extracts were determined, and the ratio $E_{max}/\gamma N$ per ml (cf. 29) was calculated and used as a test for purity. The N^{15}-content of the nitrogen was determined.

2) The cytidylic acid was divided in two parts. One part was treated in the same way as the uridylic acid. The second part was deaminated by treatment with N HCl at 120° C for 120 hours (cf. 25). The hydrolysate was evaporated repeatedly in vacuo and added to a Dowex 50 column (20 cm × 0.65 cm^2). The isolated uracil from cytidylic acid was tested for purity and analyzed for N^{15} in the same way as the uridylic acid.

3) The guanylic and adenylic acids were hydrolyzed in N HCl at 100° C for 60 minutes (cf. 20). The hydrolysates were divided in two parts. One part was precipitated with $CuSO_4 + NaHSO_3$. After repeated washing the precipitates were decomposed with H_2S, and the guanine or adenine was tested and analyzed for N^{15} as described. The second part of the purine nucleotide hydrolysates was deaminated with $NaNO_2 + H_2SO_4$ and precipitated with $AgNO_3$ as described by REICHARD (30). The precipitates were decomposed with HCl and evaporated repeatedly in vacuo. The concentrated solutions were run through Dowex 50 columns. The xanthine or hypoxanthine eluates obtained were evaporated repeatedly in vacuo. The xanthine was precipitated with $CuSO_4 + NaHSO_3$ or with acetic acid, the hypoxanthine with $CuSO_4 + NaHSO_3$. The precipitates were washed and decomposed. The ultraviolet absorptions of the deaminated purines was controlled and the contents of N^{15} determined.

4) The guanine and adenine were treated in the same way as the hydrolyzed guanylic and adenylic acids.

Deoxyribonucleic acid

As mentioned previously, the isolation methods, which had to be used in these N^{15}-experiments, could not be applied to the small amounts of DNA present in sea urchin embryos during the first stages of development. At the gastrula stage extra series of labelled material were prepared, and determinations of the isotop incorporation into DNA were performed.

1) From 1.5 g of the dry material DNA was prepared according to the method of HAMMARSTEN (12).

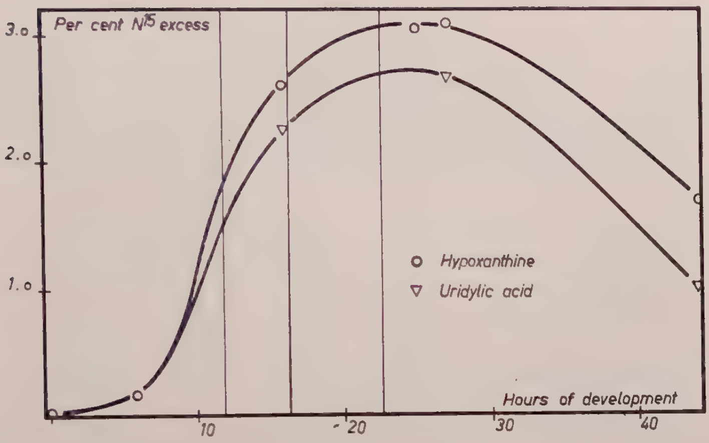

Fig. 1. Paracentrotus embryos at different stages of development, kept for 5 hours in $N^{15}H_4Cl$-containing sea-water. Isotope incorporation into low molecular hypoxanthine and uridylic acid. Vertical lines indicate hatching, appearance of mesenchyme cells, and start of invagination.

2) The non water-soluble fraction from 15 g of dry material was extracted with cold TCA, lipid solvents and $HClO_4$ as described previously. The residue was treated with 5 % TCA at 90° C (34). The TCA was removed by ether-extraction, and the solution was hydrolyzed with N HCl for 75 minutes at 100° C. After repeated evaporations in vacuo the concentrated solution was added to a Dowex 50 column, and guanine was isolated and purified as described above.

Results

The rate of isotope incorporation into the pyrimidines and purines was very low in the unfertilized Paracentrotus egg. During the period $^1/_2$–5 $^1/_2$ hours after fertilization, a slightly increased rate of incorporation was noticed, especially in the acid soluble fraction. During the blastula formation the incorporation was rapidly accelerated, and a culmination was obtained approximately during the mesenchyme blastula stage. The acid soluble uridylic acid and hypoxanthine (Fig. 1) and the pyrimidines and purines isolated from the RNA-fractions (Fig. 2–4) were very similar in these respects, but the incorporation level was much higher in the acid soluble compounds.

In one experiment at the early gastrula stage the RNA-extracts from the water-soluble and the non-water-soluble material were fractionated separately. A higher isotope level was found in the pyrimidines and purines from the non water-soluble material (Table 2).

In the RNA-fraction the uridylic acid contained more isotope than the cytidylic acid, and the guanylic acid more than the adenylic acid. On deamination the isotope contents of adenine increased, while guanine and cytidylic acid showed a decrease. The developing Paracentrotus embryos in these respects behaved like the rat and pigeon tissues used in the classical experiments of Barnes and Schoenheimer (3). The guanine and adenine, isolated from the Dowex 50 columns, constantly showed higher isotope contents than the corresponding purine nucleotides (Table 2). This can be interpreted in different

Table 2

Isotope distribution between nucleotides and purines isolated from water-soluble and non water-soluble RNA-fractions of early Paracentrotus gastrulae. Period of $N^{15}H_4Cl$-treatment: 19½–24½ hours after fertilization. Per cent N^{15} excess.

	Water-soluble Fraction	Non-water-soluble Fraction
Uridylic acid	0.52	0.62
Cytidylic acid	0.36	0.49
Uracil from cytidylic acid	0.23	0.35
Guanylic acid	0.28	0.45
Xanthine from guanylic acid	0.22	0.44
Adenylic acid	0.16	0.36
Hypoxanthine from adenlyic acid	0.21	0.43
Guanine	0.36	—
Xanthine from guanine	0.28	0.52
Adenine	0.24	0.43
Hypoxanthine from adenine	0.26	0.52

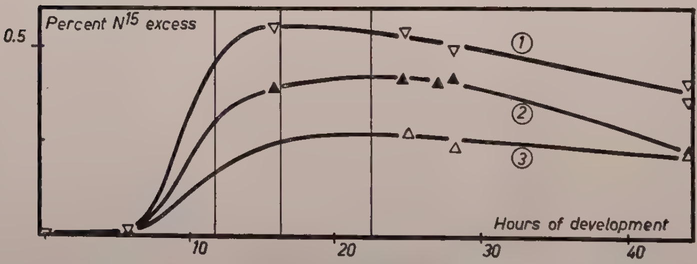

Fig. 2. Isotope content, after 5 hours of isotope treatment, in pyrimidine nucleotides from RNA-fractions: 1) uridylic acid, 2) cytidylic acid, 3) uracil from cytidylic acid.

ways. Possibly, the newly synthesized links in the polynucleotide chains were most rapidly exposed to the hydrolytic agents, used during the isolation procedures ($HClO_4$, Dowex 50) and therefore concentrated in the purine fractions.

Because of the low DNA-concentration in sea urchin embryos during the early stages of development and the limited amounts of material available, the DNA could not be submitted to serial analyses of the same kind as the RNA. Embryos kept in isotope containing sea water for 5 hours during the gastrula stage showed an incorporation of N^{15} into the total DNA of 1.0 % excess. Guanine, isolated from DNA had an isotope content of 1.1 %.

Discussion

The intensified incorporation of N^{15}-ammonium chloride into the RNA-fraction during the period of blastula formation (Fig. 2–4) may indicate either an increased utilization of labelled ammonia for the formation of RNA-precursors, or an increased rate of incorporation of labelled precursors into RNA. Un-

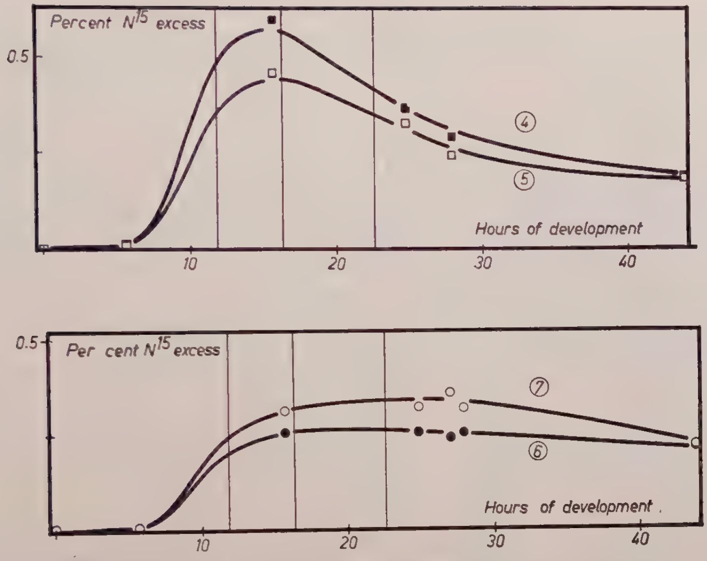

Fig. 3, 4. Isotope content, after 5 hours of isotope treatment, in purines, isolated as nucleotides from RNA-fractions: 4) guanylic acid, 5) xanthine from guanylic acid, 6) adenylic acid, 7) hypoxanthine from adenylic acid.

fortunately, the isotope contents of the actual RNA-precursors cannot be determined. Most likely, however, the free hypoxanthine and uridylic acid are metabolically more closely related to these precursors than the pyrimidines and purines, isolated from the RNA-fraction. The results obtained from the free hypoxanthine and uridylic acid may therefore indicate that the rate of ammonia uptake into the RNA-precursors also is exponentially accelerated during the period of blastula formation. However, the isotope uptake into the nucleotides of the RNA-fraction shows that the newly-formed labelled intermediates are very soon utilized for the nucleic acid rebuilding.

For a better understanding of these questions it would be interesting to make a comparative study of the incorporation of other labelled nucleic acid metabolites during development. The incorporation of P^{32}-phosphate has been studied by VILLEE *et al.* (37). Unfortunately, the P^{32}-phosphate metabolism in the sea urchin embryo is very much complicated by metabolic barriers, as LINDBERG (24) has demonstrated. The RNA-fraction in Villee's experiments showed a metabolic behavior fairly similar to the ATP-fraction in Lindberg's experiments. In both cases, the isotope was readily incorporated during the period of isotope treatment, but as soon as the isotope supply had been cut off, the isotope level remained approximately constant. It is considered that the complicating factors involved in the phosphate metabolism of the developing sea urchin embryos must be more closely analyzed before definite conclusions can be drawn from experiments with P^{32}. It would be very desirable if in such connections the experiments of VILLEE *et al.* were continued by isolating the RNA-nucleotides in a pure state.

The experiments of VILLEE *et al.* indicate a considerably higher metabolic activity of DNA than of RNA. During the course of this investigation it was shown by Abrams (1) that in sea urchin eggs, allowed to develop to the blastula stage in the presence of labelled glycine or acetate, the isotope level is much higher in the DNA-purines than in the RNA-purines. In Abram's experiments nearly all the DNA, isolated at the blastula stage, must have been built up during the course of the isotope treatment (cf. 32, 37, 6). A specially high isotope level in the DNA can be expected under such conditions. In the present DNA-experiments embryos were treated with isotope for 5 hours during a later period of development, and considerable amounts of DNA must already have been present before the start of the isotope treatment. The lower relative incorporation values found in these experiments may therefore be due to a considerably higher degree of isotope dilution in the DNA.

It seems worth attention that the period of increasing pyrimidine and purine metabolism in the present experiments coincides with the period of determination of the primary germ layers (23) and with the exponential increase in respiratory intensity, studied by GRAY (8) and LINDAHL (22). It was found by VILLEE *et al.* (37) that also the net production of DNA shows a similar acceleration after an initial lag period.

It was suggested in previous communications (17, 16) that the exponential respiratory increase may include an increased oxidation of hexose-6-phosphate by way of phosphogluconic acid and ribose phosphates. The central position of ribose phosphates in the purine metabolism has been demonstrated by GREENBERG (9, 10). Possibly, the metabolism of ribose phosphates and purines may form a connection between the exponential respiratory increase and the process of determination.

It was shown in previous reports (14, 15, 16) that in the sea urchin embryo the determination period is characterized by a rapidly increasing rate of incorporation of labelled amino acids or ammonium chloride into non water-soluble proteins, while the incorporation into the soluble proteins is not much accelerated until later on. During the early stages the isotope incorporation into the non-soluble proteins is concentrated in the microsome fraction (16), which is especially rich in RNA. The increased rate of rebuilding of the non-soluble proteins may indicate a progressive multiplication or reconstitution of populations of small, granular cytoplasm constituents (14, 15, 16). The increasing RNA-metabolism during the determination period is in agreement with this interpretation. The further evolution of some of these populations (cf. 11) and their distribution along gradients (31), constituted during the oogenesis, may be factors of uttermost importance for a normal development.

SUMMARY

The sea urchin Paracentrotus lividus was used in the experiments. Eggs and developing embryos at different stages were kept for exactly 5 hours in $N^{15}H_4Cl$-containing sea water. The rate of isotope incorporation into pyrimidines and purines from the low molecular and RNA-fractions was studied in relation to the morphogenesis.

The incorporation rate was very low in the unfertilized eggs. On fertilization an increase was noticed, especially in the low molecular fraction. During the period of blastula formation the incorporation rapidly accelerated and culminated approximately during the mesenchyme blastula stage.

In the $N^{15}H_4Cl$-treated Paracentrotus embryos the isotope was distributed between the pyrimidines and purines, and between the rings and amino groups of the pyrimidines and purines, in essentially the same way as in the rat and pigeon tissues, studied in the classical experiments of Barnes and Schoenheimer (3).

Acknowledgements:

The author wishes to express his sincere gratitude to Professor J. RUNNSTRÖM, Director of the Wenner-Gren Institute, for never failing support and interest. He is very indepted to Professor R. DOHRN and his Staff at the Zoological Station in Naples for laboratory facilities and material, to Miss GUNILLA WESSEL for valuble technical assistance, and to S. LINDVALL and H. LÖW for complementary material. By the courtesy of Professor E. HAMMARSTEN, the N^{15}-measurements were performed in his laboratory.

The investigations were supported by grants from the Swedish Medical and Natural Science Research Councils.

The Wenner Gren Institute of Experimental Biology, Stockholm.

REFERENCES

1) ABRAMS, R., Exptl. Cell Res., *2,* 235 (1951).
2) BANDIER, E. and HALD, J., Biochem. J., *33,* 264 (1939).
3) BARNES, F. W. and SCHOENHEIMER, R., J. Biol. Chem., *151,* 123 (1943).
4) COHN, W. E., Science, *109,* 377 (1949).
5) DISCHE, Z., Microchemie, *1,* 4 (1930).
6) ELSON, D. and CHARGAFF, E., Experientia *8,* 143 (1952).
7) EULER, H. and HAHN, L., Svensk Kem. Tid., *58,* 251 (1946).
8) GRAY, J., Brit. J. Exptl. Biol., *4,* 313 (1926).
9) GREENBERG, G. R., Fed. Proc., *9,* 179 (1950).
10) —— J .Biol. Chem., *190,* 611 (1951).
11) GUSTAFSON, T. and LENIQUE, P., Exptl. Cell Res., *3,* 251 (1952).
12) HAMMARSTEN, E., Acta Med. Scand., Suppl. *196,* 634 (1947).
13) HULTIN, T., Exptl. Cell Res., *1,* 159 (1950).
14) —— Ibid., *1,* 599 (1950).
15) —— Ibid., *3,* 494 (1952).
16) —— Arch. Néerland. Zool. (1953).
17) HULTIN, T. and WESSEL, G., Exptl. Cell Res., *3,* 613 (1952).
18) KERR, S. E. and SERAIDARIAN, K., J. Biol. Chem., *159,* 211 (1945).
19) KRÜGER, M. and SCHMIED, J., Z. physiol. Chem., *45,* 1 (1905).
20) LEVENE, P. A. and JORPES, E., J. Biol. Chem. *81,* 575 (1929).
21) LINDAHL, P. E. Acta Zool., *17,* 179 (1936).
22) —— Z. vergleich. Physiol., *27,* 233 (1939).
23) —— Arch. Entwicklungsmech. Organ., *140,* 168 (1940).
24) LINDBERG, O., Exptl. Cell Res., *1,* 105 (1950).
25) LORING, H. S. and PLOESER, J. McT., J. Biol. Chem., *178,* 439 (1949).
26) OGUR, M. and ROSEN, G., Arch. Biochem., *25,* 262 (1950).
27) ÖRSTRÖM, Å., Z. physiol. Chem., *271,* 1 (1941).
28) PIRCIO, A. and CERECEDO, L. R., Arch. Biochem., *26,* 209 (1950).
29) REICHARD, P., Acta Chem. Scand., *3,* 422 (1949).
30) —— J. Biol. Chem., *179,* 773 (1949).
31) RUNNSTRÖM, J., Arch. Entwicklungsmech. Organ., *117,* 123 (1929).
32) SCHMIDT, G., HECHT, L. and THANNHAUSER, S. J., J. Gen. Physiol., *31,* 203 (1948).
33) SCHMIDT, G. and THANNHAUSER, S. J., J. Biol. Chem., *161,* 83 (1945).
34) SCHNEIDER, W. C., J. Biol. Chem., *161,* 293 (1945).
35) SOODAK, M., PIRCIO, A. and CERECEDO, L. R., J. Biol. Chem., *181,* 713 (1949).
36) STEWART, D. R. and JACOBS, M. H., J. Cellular Comp. Physiol., *1,* 83 (1932).
37) VILLEE, C. A., LOWENS, M., GORDON, M., LEONARD, E. and RICH, A., J. Cellular Comp. Physiol., *33,* 93 (1949).
38) ZEUTHEN, E., Pubbl. Staz. Zool. Napoli, Suppl. *23,* 47 (1951).

Tryckt den 13 februari 1953

Uppsala 1953. Almqvist & Wiksells Boktryckeri AB

ARKIV FÖR KEMI Band 5 nr 26

Mitgeteilt am 22. Oktober 1952 von J. ARVID HEDVALL

Anwendung radioaktiver Indikatoren auf die Untersuchung von Pulverreaktionen in Silikatsystemen

Von URSULA BRUNE und ROLAND LINDNER

Mit 5 Figuren im Text

Im Zusammenhang mit systematischen Untersuchungen von Festkörperreaktionen (1) wurden radioaktives Blei und radioaktives Kalzium zur Untersuchung des „Phasengrenzstadiums" von Pulverreaktionen bei der Bildung von Blei- und Kalziumsilikaten verwendet.

Die Methodik

Es wurden mittels einer Staubzentrifuge Quarzfraktionen definierter Korngrösse isoliert (0,04 mm bzw. 0,06 mm Durchmesser ± 5 %) und vorsichtig und sorgfältig mit dem betreffenden äusserst feinkörnigen radioaktiven Oxyd im Molverhältnis 1:2 vermischt. Die Mischungen wurden mit einer hydraulischen Presse bei bestimmtem Druck zu Tabletten definierter Dichte gepresst. Die Erhitzung auf die Versuchstemperatur geschah in mit Eisen-Wasserstoff-Widerständen effektstabilisierten Rohröfen aus Quarzglas bzw. Sillimanit. Nach den entsprechen Erhitzungszeiten wurden die Tabletten zerdrückt und das Gemisch dem Trennungsgang unterworfen zur Abtrennung des nichtreagierten Oxydes. Anschliessend wurde an gewogenen Parallelproben die auf der Kieselsäure durch Reaktion verbliebene Aktivität gemessen. (Wie durch geeignete Versuche festgestellt, verbleibt durch Adsorption eine bestimmte Menge radioaktiven Oxydes auf der Kieselsäure, was als sogenannter „background" in Rechnung gestellt wurde.)

Die Versuche

1.) *Bleisilikatbildung.*

Rotes Bleioxyd wurde in Anlehnung an den Vorgang von COHEN und ADDINK (2) dargestellt, wobei das radioaktive Blei in Form einer annähernd neutralen Lösung von ThB (Pb-212), über ein „hochemanierendes" Rd-Th-Präparat (3) gewonnen, zugefügt war.

Zur Darstellung der verhältnismässig kleinen Mengen (3–5 g) von radioaktivem roten PbO wurde folgende Apparatur verwendet, die aus methodischen Gründen näher beschrieben sei (Vergl. Fig. 1):

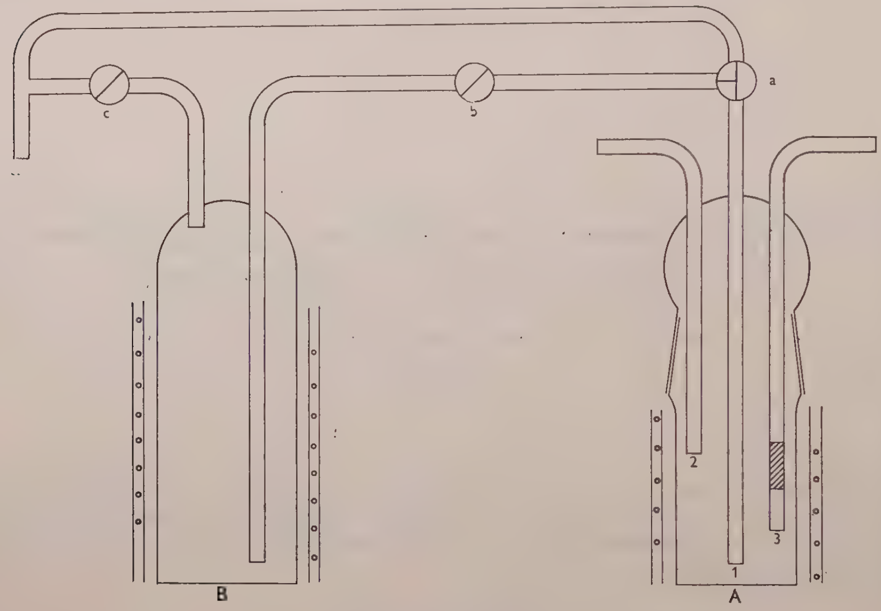

Fig. 1. Anordnung zur Herstellung reinen roten Bleioxydes.

15 ml 30 %iger Bleinitratlösung (ThB-haltig) werden im Reaktionsgefäss A (aus Resistenzglas) mittels eines übergeschobenen elektrischen Ofens (Kanthalband zwischen 2 Pyrexglasrohren) zum Sieden erhitzt unter Durchleiten hochgereinigten Stickstoffes durch das Glasrohr 1. Dann wird durch Glasrohr 2 30 ml 50 %ige kohlensäurefreie Kalilauge hineingedrückt, worauf sich ein zunächst gelblich-weisser Niederschlag bildet, dessen Farbe allmählich in rot übergeht. Nach 20 Minuten Erhitzen wird Glasrohr 2 mittels Quetschhahn verschlossen, und die überstehende Lösung über Glasrohr 3 durch eine eingeschmolzene Glasfritte (Schott G 3) abgesaugt. Dann wird nach Umlegen des Dreiwegehahnes a und der Hähne b und c heisses Wasser aus dem Vorratsgefäss B mittels Stickstoff in das Reaktionsgefäss A gedrückt. Durch Umlegen der Hähne lässt man den Stickstoff wieder den oberen Weg gehen und die Fällung zwecks gründlichen Auswaschens aufrühren. Danach wird durch das Rohr 3 abgesaugt, das Waschen wird fünf Mal wiederholt. —

Anschliessend wird die Temperatur im Reaktionsgefäss allmählich gesteigert, unter Durchleiten von Stickstoff das restliche Wasser abgesaugt und das Präparat bei etwa 300° C getrocknet und im Stickstoffstrom erkalten gelassen.

Nach dem Vermischen mit Kieselsäure und der Herstellung der „Reaktionstabletten“ wurden diese in reiner Stickstoffatmosphäre zur Umsetzung erhitzt. Danach wurde das Reaktionsgemisch in Zentrifugengläsern mit 1.1.2.2.-Tetrabromäthan aufgeschlämmt und zentrifugiert.[4] Dies geschah zunächst in Perioden von 5 Minuten, nach denen jedesmal aufgerührt wurde (insgesamt 6 Mal). Anschliessend wurde eine halbe Stunde ohne Unterbrechung zentrifugiert. Dies sollte eine Sedimentationstrennung des an der Kieselsäure (Dichte = 2,65) haftenden Bleisilikates vom Bleioxyd (Dichte = 9,64) mittels der Flüssigkeit (Dichte = 2,96) bewirken. Diese Trennung ist bei sechsmaligem Aufrühren noch nicht quantitativ, da ein Teil der Kieselsäure vom Bleioxyd am Boden

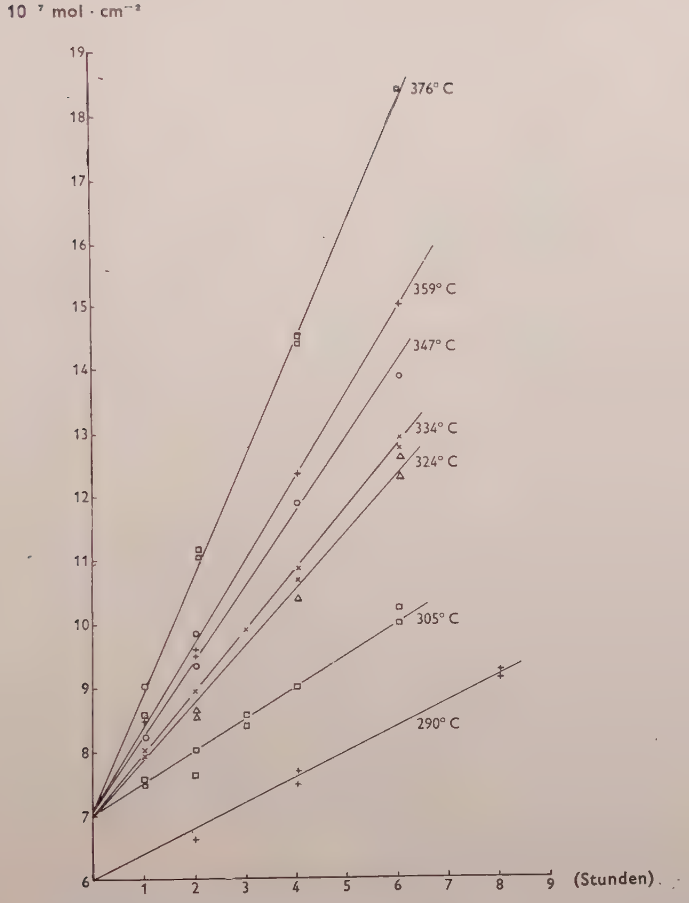

Fig. 2. Anfänglicher Umsatz bei der Bleisilikatbildung als Funktion der Zeit.

festgehalten wird. Die im oberen Teil der Flüssigkeitssäule abgeschiedene Kieselsäure enthält dagegen kein nichtreagiertes Bleioxyd. Diese Kieselsäure wurde abgesaugt, sie zeigte eine schwach gelbliche Färbung. Wegen der nicht quantitativen Trennung wurden definierte Mengen eingewogen und zur Messung gebracht, aus deren Ergebnis die pro Zeit- und Flächeneinheit reagierte Menge Bleioxyd berechnet werden konnte. (Dabei wurde lückenlose Bedeckung der als kugelförmig betrachteten Quarzkörner angenommen.) Stets durchgeführte Parallelversuche zeigten, dass die so erhaltenen Werte bis auf etwa 10 % reproduzierbar waren. Im Temperaturbereich 290° bis 380° C zeigte der Umsatz eine geradlinige Zeitfunktion, aus der die Reaktionskonstante in Mol cm^{-2} sec^{-1} berechnet werden konnte. Unter 290° C konnte in den zur Verfügung stehenden Zeiten (Halbwertszeit ThB = 10,6 h) kein Umsatz festgestellt werden; bei 387° C krümmt sich die Linie der Zeitfunktion nach kurzer Zeit, um einem konstanten Wert, entsprechend 4,5 Mol% reagierten Bleioxyds zuzustreben. Der gleiche Befund ergibt auch bei 462° C und könnte zunächst als Abschluss

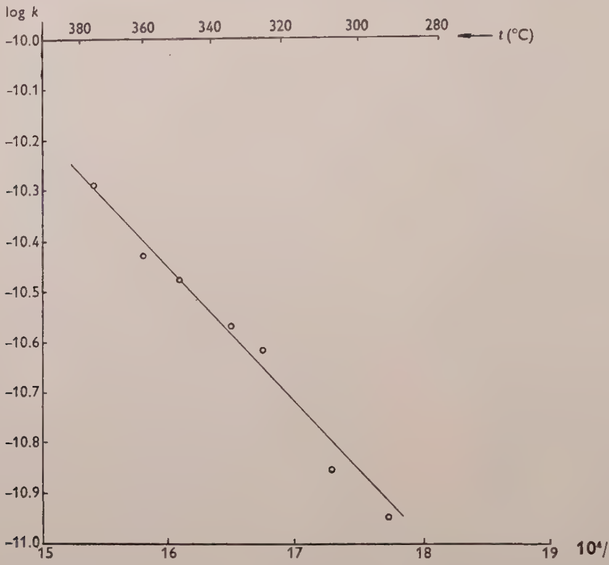

Fig. 3. Die Reaktionskonstante der Bleisilikatbildung, logarithmisch gegen die Temperatur aufgetragen.

der „Phasengrenzreaktion" (die in diesem Fall etwa einer Tiefe von 100 Gitterebenen entspräche) gedeutet werden. Es ist aber zu beachten, dass der genannte Umsatz das „spezifische" Gewicht der Quarzkörner das der Sedimentationsflüssigkeit überschreiten lässt und so das Reaktionsgemisch der Abtrennung entzieht. Hiernach ist auch eine Ermittlung der Diffusionskonstante aus dem vorgeschrittenen Stadium der Pulverreaktion nach SERIN und ELLICKSON (5) im vorliegenden Fall nicht möglich.

Die Ergebnisse der Messungen an der Phasengrenzreaktion sind in Fig. 2 wiedergegeben in der Darstellung: Umsatz in Mol cm^{-2} als Funktion der Zeit. Es ist ersichtlich die Geradlinigkeit der Zeitfunktion und (mit einer Ausnahme — geringerer Pressdruck) die Reproduzierbarkeit des „backgrounds". Die Temperaturfunktion der Reaktionskonstante ist in Fig. 3 wiedergegeben in der Darstellung $\log k = f(1/T)$.

Die Messwerte gruppieren sich um eine Gerade, die dem Ausdruck:

$$k = 10^{-7} \exp(-12\,800/RT) \text{ mol cm}^{-2}\text{sec}^{-1}$$

entspricht.

2.) *Kalziumsilikatbildung.*

Nach dem jeweiligen Umsetzungsversuch wurden Proben des Reaktionsgemisches eingewogen und gemäss den bekannten Methoden zur Bestimmung freien Kalkes mit Glycerin-Alkohol-Mischung behandelt. Zur Beschleunigung des Lösungsvorganges wurde nach dem Vorschlag von SWENSON und THORWALDSON (6) eine bestimmte Menge entwässerten Strontiumchlorids zugefügt. Zur Kontrolle dieser Methode wurden Versuche ohne Zusatz von Strontiumchlorid gemacht, die — bei entsprechender längerer Lösungsdauer — die gleichen Werte zeigten.

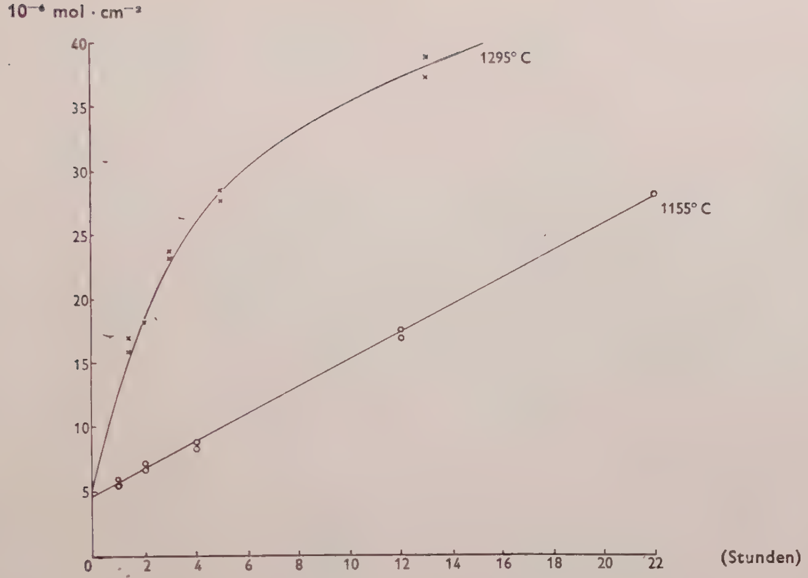

Fig. 4. Umsatz bei der Kalziumsilikatbildung als Funktion der Zeit.

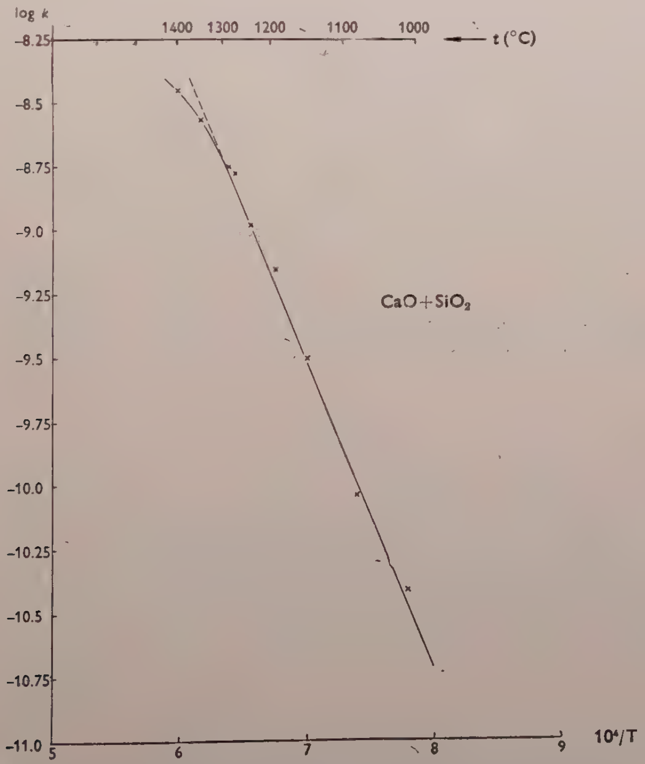

Fig. 5. Die Reaktionskonstante der Kalziumsilikatbildung, logarithmisch gegen die Temperatur aufgetragen.

Die Lösung wurde abgesaugt und die Kieselsäure auf geheizter Nutsche (um das Ausfallen von Glycerat zu vermeiden) mit heisser Glycerin-Alkohol-Mischung gewaschen und nach dem Trocknen zur Messung der Radioaktivität des Ca-45[1] gebracht.

Die Reaktion lässt sich bei etwa 1 000° C in vorliegender Anordnung messbar verfolgen und gehorcht einer linearen Zeitfunktion bis hinauf zu Temperaturen von etwa 1 200° C, um bei höheren Temperaturen schon bald die parabolische Zeitfunktion einer Diffusionsreaktion zu zeigen. (Hierbei ist der im Laufe der Reaktion eintretenden Verminderung der Kontaktfläche noch nicht Rechnung getragen in welchem Fall sich die lineare Zeitfunktion bie zu noch höheren Werten fortsetzt. Dies beinflusst aber nicht nennenswert die bei tieferen Temperaturen angegebenen Reaktionskonstanten.) Fig. 4 zeigt als Beispiel den Umsatz in Mol pro cm^2 als Funktion der Zeit bei 1 155° C bzw. 1 295° C. Fig. 5 zeigt die Temperaturabhängigkeit der Reaktionskonstante entsprechend dem Ausdruck: $k = 2{,}8 \cdot 10^{-2} \exp(-54\,000/RT)$ mol cm^{-2} sec^{-1}.

Aus den parabolischen Kurven bei höherer Temperatur konnten wir nach dem Vorgang von SERIN und ELLICKSON Diffusionskonstanten abschätzen, die mit auf anderem Wege gemessenen Selbstdiffusionskonstanten in Kalziumsilikaten (7) annähernd übereinstimmen (etwa 10^{-11} cm^2 sec^{-1} bei 1 300° C).

ZUSAMMENFASSUNG

Es wurden die Reaktionskonstanten bei der Bildung von Blei — bzw. Kalziumsilikat als Pulverreaktion bestimmt.

Sie gehorchen der Temperaturfunktion:

$$PbO + SiO_2\colon\ k = 10^{-7} \exp(-12\,800/RT) \text{ mol cm}^{-2}\text{sec}^{-1}$$

$$CaO + SiO_2\colon\ k = 2{,}8 \cdot 10^{-2} \exp(-54\,000/RT) \text{ mol cm}^{-2}\text{sec}^{-1}$$

Wir danken *Statens Tekniska Forskningsråd* für die Bereitstellung von Mitteln und Professor J. A. HEDVALL für sein Interesse an den Versuchen.

Abteilung „Kristallkinetik“, Institut für Silikatforschung, Chalmers Technische Hochschule, Göteborg (Schweden).

LITERATUR

1. LINDNER, R., Z. Elektrochem. *54* (1950) 430.
—— Acta Chem. Scand. *5* (1951) 735.
2. COHEN, E. und ADDINK, N. W. H., Z. phys. Chem. A *168* (1934) 202.
3. HAHN, O. und MÜLLER, O., Z. Elektrochem. *29* (1923) 189.
4. JANDER, W. und RIEHL, H., Z. anorg. Chem. *246* (1941) 93.
5. SERIN, B. und ELLICKSON, R. T., J. Chem. Phys. 9 (1941) 742.
6. SWENSON, E. G. und THORVALDSON, T., Canad. Journ. Chem. *29* (1951) 140.
7. LINDNER, R., unveröffentlicht.

---

[1] Geliefert von der Isotope Division des AERE, Harwell (England).

Tryckt den 13 februari 1953

Uppsala 1953. Almqvist & Wiksells Boktryckeri AB

ARKIV FÖR KEMI Band 5 nr 27

Communicated 14 May 1952 by ARNE WESTGREN and ARNE TISELIUS

The phases of chromatography

By TREVOR I. WILLIAMS and HERBERT WEIL

With 3 figures in the text

I

Definition

"Whilst the history of crystallization or distillation cannot be traced to an unique source, chromatography is based on a single principle and is the invention of one individual: the principle is the passing of a solution through an adsorbing column and the inventor is MICHAEL TSWETT" (1). This pronouncement on the origin of chromatography has until recently been generally accepted on the authority of ZECHMEISTER (1, 2, 3), who has consistently advanced the claim that MICHAJL SEMENOVIČ CVETT (4, 5) is the exclusive originator of chromatography in all its essential aspects.

Two main problems arise when the validity of this claim is investigated. What are the essential features of the procedure which Tswett termed "chromatographic adsorption analysis", and, fundamentally, what is chromatography? The essential characteristics of Tswett's method can be listed as follows:

a) It is a batch process.

b) It consists of several successive steps.

c) One long tube of relatively small diameter is employed.

d) Two phases exist, one of which is a stationary solid phase and the other a moving liquid phase.

e) The tube is evenly filled with the solid phase, in the form of finely divided material.

f) The liquid phase varies in composition, being a solution during one part of the operation, and later a pure solvent.

g) The solid phase has a differential adsorption affinity towards solutes in the solution to be resolved.

h) The resolution of the mixture is accomplished by two successive steps, based on two different types of selective adsorption. The first step consists of an adsorptive filtration treatment (6), allowing the mixture to percolate through the column of adsorbent. This results in the formation of a single adsorption band located near the top of the column. The second step consists in the distribution along the column of the components of this original band to form a chromatogram. This spatial distribution is achieved by subsequent percolation of relatively large volumes of pure solvent; the process was called "development" by Tswett, and is a specific feature of his method.

i) The column of adsorbent is then removed from the tube and divided mechanically into several sections, according to the band of the chromatogram. The adsorbates are then liberated from the adsorbent by means of a suitable solvent.

The first three of the above features are of special interest in the present context. Only one feature of Tswett's chromatographic method seems to have been novel; that is the process of development.

Tswett apparently coined the term "chromatographic adsorption analysis" in imitation of SORBY's (7) term *"chromatology"*, used by the latter for defining his spectrographic method for the determination of individual components in plant extracts. It is interesting that Tswett qualified the words "adsorption analysis" with "chromatographic". *Vice versa,* he qualified "chromatography" by "adsorption". In this we may see a hint that Tswett had some notion of other kinds of chromatography.

The precise interpretation of Tswett's writing on chromatography is made difficult by his varying interpretation of the term adsorption, to which he gave a wide meaning. It is quite clear that when he first took an interest in adsorption in 1903 (8) its main attraction to him was that it was a *physical* method and thus in principle much more suitable for dealing with labile plant pigments than the chemical methods which he had previously used. Yet when it suits his purpose Tswett describes adsorption as being a chemical process. He defended the originality of his "chromatographic adsorption analysis" by denying (4) that the methods of SCHOENBEIN (10, 11) and GOPPELSROEDER (12, 13, 14, 15, 16, 17), carried out as early as 1861, were adsorption processes.

The answer to the question of the origin of chromatography depends on one's definition of chromatography. In practice, however much the purist may object, there is no doubt whatsoever that chromatography is today not by any means considered identical with "chromatographic adsorption analysis"; on the other hand it cannot satisfactorily be defined merely by calling it a process substantially characterized by the passing of solution through a column. The first definition is much too narrow, for it excludes ion-exchange and partition chromatography. FEIGL (18, 19) represents a school of thought which wishes to adhere strictly to Tswett's use of the word, but is even more orthodox than Tswett himself by refusing to acknowledge spatial differential precipitation as a form of adsorption chromatography.

The second of the above definitions is too narrow in some respects, excluding, for instance, paper chromatography, but is much too wide in other respects, not differentiating between fractionation by forming spatially separated adsorption zones and mere adsorptive filtration. Both definitions are in sharp contradiction to established use of the word chromatography, as may be seen by reference to the proceedings at some recent symposia on chromatography (20, 21, 22, 23).

CASSIDY (24) has recently given a thorough review of differential adsorption methods, by means of which chromatograms can be obtained, and STRAIN (25) has tabulated systems based on different chromatographic principles, amply demonstrating the wealth of possibilities. As TISELIUS (26) has said: "... the principles underlying chromatographic separation should be capable of generalization in different directions, which in some cases might lead to new methods of separation. Any process which will cause a zone of a substance to move along a column (or a similar arrangement), at a rate which has some relation to its specific physical or chemical properties may be utilized for such a purpose." This conception embraces both analytical chromatography and preparative chromatography, the latter even on an industrial scale. It comprises one-, two-, and three-dimensional chromatography. The flow-direction is irrelevant. Further, chromatographic processes may be used whether the mixture to be resolved is gaseous or liquid. It does not matter which phase is stationary and which is moving. If, for example, an inert gas is bubbled through a stationary mixture, as happens in what is called foam-chromatography, this method too is correctly called chromatography (27). Finally, it is not significant, so far as the chromatographic nature of a process is concerned, whether spatial separation is effected exclusively by one operation, for example, by percolation of a liquid mixture through the solid material, or whether it is achieved by this process in conjunction with subsequent development of the chromatogram. In other words, development is not, according to Tiselius's definition, an essential feature of chromatography. When, for instance, H. P. KAUFMANN (27) passes fat and oil mixtures through an adsorbent column and obtains a chromatogram, his procedure is certainly chromatographic. Many other examples, such as frontal analysis, represent single-step chromatographic separation. Single-step chromatographic systems were evolved prior to Tswett, and their initiators must, therefore, be called the true discoverers of chromatography.

It has long been usual to start any general discussion on chromatography by first expounding Tswett's chromatographic adsorption analysis (1, 3, 29, 30), then describing variations of this procedure, and finally to attach chapters on ion-exchange, partition chromatography, gas chromatography, paper chromatography, and so on, without bothering too much about the precise meaning of the terms used. MEINHARDT (31), listing some seventeen separation principles as available for chromatography, was considered to be revolutionary, but in fact his enumeration of the chromatographic possibilities is perhaps too narrow rather than too wide.

ZECHMEISTER (3) has proposed a new definition of chromatography in the following terms: "The term 'chromatography' designates those processes which allow the resolution of solute mixtures by selective fixation and liberation on a solid surface of a support with the aid of a fluid streaming in a definite direction." This definition is more pragmatic and in better agreement with current practice than his earlier ones.

We venture nevertheless to suggest two alterations. No streaming of the fluid (or gaseous) mixture need necessarily occur. Reference may, for example, be made to chromatograms made with the help of electromigration (32), and it is not difficult to imagine other real or theoretically possible exceptions to the above definition. No selective fixation and liberation on a solid surface of a support happens, for example, in emulsion (34) and foam chromatography.

To cover what is currently referred to as chromatography, the following definition is submitted:

"By chromatography is meant those processes which allow the resolution of mixtures by effecting separation of some or all of their components in concentration-zones on or in phases different from those in which they are originally present, irrespective of the nature of the force or forces causing the substances to move from one phase to another or from one point to another in the same phase" (104).

II

General survey of the history of chromatography

Introduction

As already made clear the history of chromatography has hitherto been described essentially as the story of Tswett's chromatographic adsorption analysis, its eclipse after the death of Tswett, and its resurrection by KUHN (35) and members of the Heidelberg school of chromatography in 1931. Subsequent additions to and alterations of Tswett's procedure are then usually reviewed. Discussion has not hitherto been based on a strict definition of what chromatography implies; the attitude has generally been to wait and see how the word chromatography is used by others. When the consequences of this looseness of terminology in due course bore fruit, a return to Tswett's use of the word was recommended (18, 19); alternatively, it was proposed to substitute for adsorption a term of wider meaning, such as, for example, "sorption" (36). These suggestions were, however, no more than palliatives; a strict definition is obviously essential for any historical survey.

As the definition we propose above differs from Zechmeister's only in being rather more rigorous it may, however, be taken that general agreement has at last been reached on this subject. In the review which follows we shall not discuss the fine details of the history of chromatography—such as, for example, the highly specialized techniques of Tiselius and his co-workers—but rather the way in which new principles have been introduced and adopted. We shall discuss, in fact, the phases through which chromatography has evolved.

The phases of chromatography

The history of chromatography can be divided into three main periods.

1) An "empirical" period, in which only practical use was made of chromatography, for example, in making rough tests of dyes.
2) A "scientific" period, in which a scientific approach to chromatography was made for research purposes and empirical uses still continued.
3) A "technological" period, now just beginning, in which the use of chromatography as a unit-operation is taken up, while very extensive scientific use is still made of the method and empirical methods are still frequently encountered.

1) The empirical period

Spot-tests of dyes and pigments are ancient industrial practice. It has been noted by YAGODA (37) that "the use of paper impregnated with suitable reagents in establishing the presence of chemical constituents is probably one of the earliest developments in the art of analytical chemistry". PLINY (38), for instance, clearly described a test for iron carried out on papyrus impregnated with gall extract. Colour- and dye-manufacture were important industries even in ancient Egypt. The adulteration of valuable dyes, pigments, and alloys was a well developed craft in the Greek and Roman periods of the Near East. Alchemical literature shows that many methods were evolved for the detection of such adulterations. Although nothing relating to genuine papyrus chromatography has been discovered up to the present it is not unreasonable to assume, in view of Pliny's reference, that rough resolutions of mixtures on papyrus impregnated with a reagent were known in the first centuries of the Christian era, and spot-tests on papyri without reagents may also have been carried out. The tendency of dyes to separate into differently coloured components at the boundary between the advancing dye solution and the dry cloth or papyrus is not merely an interesting phenomenon, likely in itself to catch the eye, but also a practical problem which the dyer may have to overcome to maintain the quality of his wares.

Reverting from this attractive but unsubstantiated speculation to the realm of established fact the beginning of the empirical period of chromatography can positively be set no earlier than the first decades of the nineteenth century. Reference is then made, in various publications on paint- and dye-manufacture, to an empirical examination of dyes and pigments, carried out by applying them to strips or sheets of absorbent paper or fabric. Some of these tests are still used in the trades concerned. Dissolved dyes or pigments were allowed to ascend in strips of paper or fabric, or to expand in them from a spot, and the subsequent separations were observed. Such tests were done both on impregnated materials and without addition of reagents. Systems of bands or concentric annular zones, which we now call chromatograms, were thus obtained. The general impression given by these accounts is that they refer not to a new discovery but to long-established techniques. This empirical practice became the stepping-stone to scientific paper chromatography.

Carbon was introduced for refining sugar and other materials at about this time, and both static and dynamic methods of adsorption were used. Layering effects, and differences in the composition of successive effluent fractions were early observed in dynamic filtration, especially in the sugar industry, but this phenomenon was not then used technologically. Stratification was also detected in the bleaching of vegetable oils, such as rape oil, with carbon or bleaching earths when these materials were used in filter-beds through which the oil was passed (39). Similar occurrences on columns of filter-material used for refining petrol are recorded at an early date (40, 41). The observation of layering effects in columns seems, however, to have borne fruit relatively late. Scientific utilization of the chromatographic principle was initially restricted to adaptation of empirical paper chromatographic methods to problems of research.

2) The scientific period

The outlines of the origin of scientific chromatography, using paper and column techniques, have already been discussed by us elsewhere (41, 42, 43, 44, 45). These types of chromatography made their first appearance at very different times. Scientific paper chromatography dates from 1850 (44); fully developed scientific column chromatography from 1900.

Two men are especially connected with early scientific chromatography. These are F. F. RUNGE (46, 47, 48 a–c, 49, 50, 51), and D. T. DAY (52, 53, 54). Both were perfectly clear as to what they were doing in evolving their chromatographic systems. They planned carefully in advance and devised techniques which gave reproducible results. Runge was the more versatile chemist, and designed his paper chromatographic system for more varied use than Day, who was essentially interested only in the resolution of crude petroleum and other hydrocarbon mixtures on columns. Runge preferred radial flow on filter paper sheets, and mainly made use of differential precipitation on the substrate, which was impregnated with reagents. He thus obtained irreversible chromatograms, the zones of which were firmly fixed. Day used ascending flow, the mixture rising in tubes filled with fuller's earth: chromatograms resulted, in fact, from differential adsorption, although he himself attributed it to capillary diffusion.

More or less quantitative fractionations were achieved in both arrangements, a specific feature of which was spatial distribution of constituents of a mixture on the substrate. By the definition of chromatography we have put forward above, either process is truly chromatographic. Both methods must also be called chromatographic by the recent definitions suggested by Zechmeister and Tiselius, although many of the precipitation chromatograms prepared by Runge would be outside the latter definitions in which ability of the zones to migrate after formation is regarded as essential.

Scientific paper chromatography. Runge started his career as a chemist with the publication of a treatise on a natural dye (46) in 1822. He isolated aniline (47) from coal-tar distillates in 1834, and in connection with this research evolved a method for the detection of aniline, based on its colour reaction with paper impregnated with calcium hypochlorite (48, a and b). A spot-test method for investigating the strength of bleaching solutions was also devised by Runge, in which drops of the mixture were spotted on to a piece of dyed fabric. Runge made use of starch-potassium-iodide paper for spot-tests with bleaching solutions. This type of paper is of interest, as according to GOPPELSROEDER (17), it was also used by SCHOENBEIN in ozone experiments, preceding his experiments on capillary analysis (10, 11), published in 1861.

Runge took great interest in the education of chemists, and he inserted actual examples of such colour reactions in his manual on chemistry (49), so that they should be a permanent record. Systematic investigations of this kind, especially of inorganic mixtures, were carried out by him many years before the description of an organic spot-test by SCHIFF, supposed by FEIGL to be the initiator of spot-test technique (18, 19). As a specialist on dyes and dyeing Runge cannot fail to have been aware of the primitive spot-tests and capillary analysis then current in the industry and doubtless he found his inspiration in these.

Runge published three books relating to chromatography. These are Volume III of the "Farbenchemie" (48 c), and "Zur Farbenchemie. Musterbilder fuer Freunde des Schoenen" (50), both published in 1850 and the "Bildungstrieb der Stoffe" (51) of 1855. It should be noted that Runge's great pupil, GOPPELSROEDER (12–17), referred exclusively to the last of these books.

The "Musterbilder ..." and the "Bildungstrieb ..." contain a collection of originals of "naturally grown pictures", produced by interaction of solutions meeting on a paper-substrate, and not painted with the brush. Runge delights in the colour shades and shapes of these pictures, often achieved by what we may call "trick-chromatography" i.e. chromatography modified to give artistic effects. Drops of various solutions were, for example, applied systematically to treated or untreated filter-paper and allowed to meet, generating intricate patterns by their interaction. Many "pictures" consist of fairly concentric ring-systems.

Goppelsroeder rightly calls the "Bildungstrieb der Stoffe" an essay on the philosophy of Nature; it has much in common with the works of Goethe. Although a similarly artistic approach was made in the "Musterbildern", this book is strictly scientific. In it Runge refers to a commercial exploitation of his methods. Spot-test technique and paper chromatography are the techniques used by him for the production of the "pictures", 120 originals of which are pasted into each copy of the book, which is very rare.

As already pointed out, Runge's particular chromatographic method employed here consists of differential deposition of precipitates caused by chemical interaction between inorganic substances coming into contact on a paper substrate. Uncomplicated chromatograms with more or less concentric boundaries were made by radial expansion of a small quantity of a solution applied as a spot on paper.

Runge was fully aware of the analytical possibilities of his precipitation method. He realized that reproducibility of results could be obtained only by standardization of the technique. He realized the importance of using paper of proper quality. He knew that disturbances might be caused by impurities in either paper or solvent. He even knew the value of flow-inhibitors, such as glue.

Runge's chromatographic precipitation technique is within the limits of the definition of chromatography proposed by us above, though not of all current definitions. His claims, however, do not depend on our definition. Volume III of the "Farbenchemie" (48 c) contains a short chapter on the separation of chemical substances on filter paper; this deals not only with precipitation chromatography, but also with chromatographic adsorption. Concentric zones of different substances present in a solution spreading radially from the spot of application were obtained on untreated paper. Runge regarded this radial separation method as a rapid micro-analytical procedure. GOPPELSROEDER (17) depreciated radial flow in "capillary analysis", and claimed that ascending flow gives better results. Nevertheless, several early workers besides Runge applied radial flow; for example, BAILEY in 1878 (55).

It has been said that it was SCHOENBEIN who discovered that water is sucked up in paper from an aqueous solution more quickly than the solutes, and that in consequence an aqueous front precedes the first concentration zone of the chromatogram. Runge's chromatograms, preserved in his books, give undisputable evidence that this phenomenon must have been familiar to him, for they still, after the lapse of a century, show the phenomenon clearly. Runge was, however, mainly interested in the colour reactions between different substances, and in their analytical interpretation, and much less so in the respective rates of flow of the various components of a mixture.

SCHOENBEIN and GOPPELSROEDER developed a refined system of paper chromatography, based on the specific flow-rates of individual substances. The height of ascent under standardized conditions, and the time required for the ascent, were recognized by them as characteristics of each individual substance present in the mixture being investigated. In effect, they measured what in recent years has been termed the R_F value of different substances. Goppelsroeder naturally had to eliminate impregnation of the paper with reagents as the latter would interfere with capillary diffusion and adsorption.

Runge, and later Goppelsroeder, experimented at an early stage with porous wood-tablets, in which they allowed mixtures to ascend and to separate. Goppelsroeder also made capillary diffussion experiments in tubes filled with finely divided sand, kieselguhr, and similar materials, but quickly lost interest as the results were unsatisfactory. Apparently neither Goppelsroeder nor Schoenbein had any great interest in column techniques, and preferred the one- and two-dimensional methods.

Tswett was well acquainted with Goppelsroeder's capillary analysis and probably with Runge's work also. Day, however, apparently had no knowledge of paper chromatography. He did not even refer to a paper published by the American scientist LLOYD (58), in which were described paper chromatographic tests similar to those carried out by Goppelsroeder.

Scientific column chromatography. Reference has already been made to layering phenomena encountered in the refining of various materials by passing them in solution through adsorbent- or filter-beds. Unsuccessful capillary diffusion experiments carried out by Goppelsroeder in tubes filled with sand and other powders have also been referred to, as have investigations on the separation of mixtures ascending in solution in porous wood-tablets.

Researches by NASSE (56) and REED (57) now call for comment; the latter has recently been singled out by some as the discoverer of column chromatography. Nasse was undoubtedly influenced by Goppelsroeder, and he succeeded in concentrating a dye in a definite zone by allowing a solution to ascend in a column of sand. This experiment may well have been a genuine chromatographic separation, but only abstracts of the original publication have so far been accessible to the present authors so that no final opinion can be passed.

REED (57) developed a paper chromatographic method closely related to Goppelsroeder's capillary analysis, but he claimed not to have been acquainted with the relevant work previously done by the Swiss school. He was particularly interested in the investigation of organic mixtures, and carried out experiments with columns. No details of the experiments in tubes were published by Reed, so that their chromatographic character cannot now be verified. Reed did, however, emphasize the great possibilities of the column technique, and apparently believed that he had discovered something significant.

Whatever evaluation is made of the experiments of Nasse and Reed it may be said that scientific column chromatography originated in the mineral oil industry. Study of the literature reveals a common fallacy in modern thought. It is generally considered that equipment for chromatography on a manufacturing scale derives from laboratory apparatus. In fact, the truth is precisely the opposite of this. Early chromatographic apparatus for use in the laboratory was derived from plant used for manufacturing purposes in the petroleum industry.

The early history of petroleum chromatography has been surveyed in detail elsewhere (41, 42, 45, 59). It began with contact filtration of mineral oil, a process apparently employed first for the purification of stone-oil in the Hanover oil-fields in the middle of the last century (60). In 1886 C. ENGLER and M.

Schematic representation of Day's, Engler's and Tswett's chromatographic systems

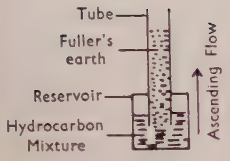
Tube
Fuller's earth
Reservoir
Hydrocarbon Mixture
Ascending Flow

Figure 1.
Day's cromatographic system.

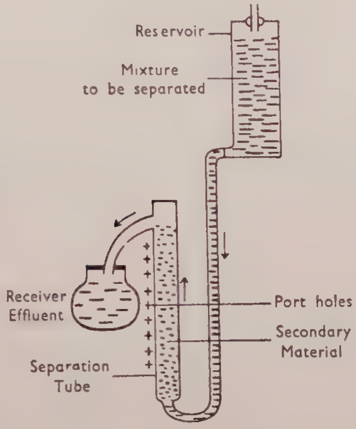
Reservoir
Mixture to be separated
Receiver Effluent
Port holes
Secondary Material
Separation Tube

Figure 2.
Engler's chromatographic system.

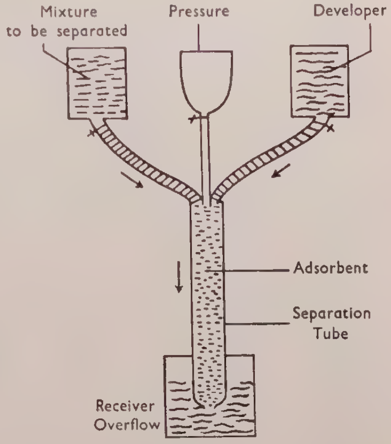
Mixture to be separated
Pressure
Developer
Adsorbent
Separation Tube
Receiver Overflow

Figure 3.
Tswett's chomatographic system.

Boehm (61) designed a battery of tall narrow filters containing carbon, and noted that their use effected some spatial fractionation of crude petroleum. The filtration method employed was substantially an adsorptive filtration process, yielding a colourless filtrate, rich in saturated hydrocarbons, and an adsorbate abundant in unsaturated material. Plant of this type was employed for the production of petroleum-jelly, and was, as he himself acknowledged, adapted by D. T. Day for chromatographic research (53).

It is not known whether other adsorptive filtration experiments carried out in tubes, or capillary diffusion separations in porous wooden tablets, were an inspiration to Day, but it is certainly very probable that he was acquainted with separation phenomena encountered in wicks of lamps, an effect which was then being widely discussed in the petroleum literature.

There is no question but that the interest of both Day and Goppelsroeder in chromatography derived from their interest in certain geological problems. Goppelsroeder, for instance, quoted a communication by Justus von Liebig, who very early realized the immense importance of differential diffusion phenomena in agriculture. Liebig discovered that the soil is able to fix water by capillary forces to such a degree that the last traces of water cannot be taken up by even the finest roots. He further found that when solutions of salts percolate through soil, the constituents are retained spatially in specific layers, so that even closely related substances such as potassium and sodium compounds behave in a different manner according to the action of the medium through which they percolate. Potassium is in general found to be fixed in layers above those containing sodium.

Day certainly carried out experiments in imitation of occurrences which he believed to take place in the crust of the earth. He was a protagonist of the geological filtration hypothesis of the origin of petroleum. According to this, primary petroleum, originally existent in the deeper strata, penetrates through shales and similar beds to higher sand-layers, being converted *en route* to a much brighter, sweeter-smelling type of petroleum richer in low boiling hydrocarbons and poorer in non-hydrocarbon matter. Day hoped to reproduce the natural conditions with the help of equipment of the kind used in the industry for producing petroleum-jelly. Day described the results of his experiments at the First International Petroleum Congress (August 16–28, 1900) in Paris (53).

Whilst Tswett and Goppelsroeder were well acquainted with the literature on the theory of differential diffusion, capillarity, and adsorption, Day was apparently originally interested only in the experimental utilization of these principles. He referred to a method of dynamic differential filtration for the first time when discussing geological problems in 1897 (52). The lecture he gave at Paris on August 20th, 1900 was reviewed *inter alia* by ENGLER and ALBRECHT (62), HOLDE (63, 64), and ZALOZIEKI (65). It is difficult to believe that Tswett did not read about Day's "great discovery", widely discussed in the scientific literature, and is is still more difficult to assume that he did not realize at once the importance of the "Day phenomenon" for his own research.

Day's work was continued by many petroleum scientists. In the U.S.A. three papers by GILPIN *et al.* (66, 67, 68) may be referred to; these subsequently led to differential dynamic adsorption separations by the National Bureau of Standards (69, 70). Russian petroleum chemists such as RAKUSIN, HERR, PHYAELAE, TARASSOW, and especially GURWITSCH made an outstanding contribution to early column chromatography (41, 45, 59, 71). No break in chromatographic practice, as initiated by DAY, occurred after 1900, not even during the eclipse of Tswett's chromatographic adsorption analysis. It may here only be mentioned that GURWITSCH (33) not only carried out experimental research in this field, but was also interested in the theoretical aspects. He published many theoretical studies before the first paper on chromatography was published by the Heidelberg school of chromatography.

Day carried out his experiments with thin, crude petroleum, ascending slowly in a column full of fuller's earth, relying only on capillary forces to draw the liquid upwards. Petroleum fractions extracted from the top-section of the extruded column consisted of "benzenes", from the centre of "middle-grade hydrocarbons", and from the bottom of semi-solid petroleum-jelly and other substances of high molecular weight. While Day, like Tswett, isolated the zones of the chromatogram mechanically he did not use development with pure solvent, and stopped the flow when the rising liquid had reached the top surface of the column. It is of interest that Day envisaged his process as a unit-operation.

The connection between ENGLER and BOEHM's (61) petroleum-jelly filtration plant and Day's laboratory apparatus has already been stressed. Conversely Day's utilization of layering effects observed in the commercial refining of petroleum and petroleum products induced Engler to study this phenomenon thoroughly, and to improve Day's experimental methods. Engler was undoubtedly also impressed by Goppelsroeder's paper capillary analyses, especially as Goppelsroeder had succeeded in concentrating by this method traces of certain organic substances present in crude petroleum. This result was an additional demonstration of the organic origin of petroleum, in which Engler believed.

Engler's chromatographic system (Fig. 2) differs from Day's (Fig. 1) arrangements in the following principal ways:

a) Overflow was allowed by Engler, who formed a "flowing chromatogram" of the effluent discharged from the top of the separation-tube;
b) Engler applied additional pressure by keeping the reservoir at a high level; the flow was at first directed downwards to the bottom of the column, in which the mixture was made to travel upwards.

The discovery of the value of forming a liquid or flowing chromatogram has often been credited to Trappe (72). This is quite erroneous as flowing chromatography had then been established, for instance, for some forty years in petroleum chromatography.

Two major contributions made by Engler to scientific chromatography must be appraised:

1) Engler extended column chromatography to the separation of mixtures other than hydrocarbons, and he fully recognized the significance of the method as a general analytical process;
2) He investigated theoretically the nature of adsorption chromatography and described the achieved separations as being accomplished exclusively by physical means. In order to follow the course of the separation Engler made a fractionation tube with ports along its length, thus making possible the withdrawal of samples from all sections of the column.

It is perhaps important to stress a major difference in the problem facing Tswett on the one hand and Engler and Albrecht on the other. Tswett was interested in the isolation of substances present at low concentrations in a mixture, whereas Engler and Day attempted to isolate substances present in considerable concentrations.

Karrer (73) has summed up the significance of column chromatography in organic chemistry: "... No other discovery has excerted as great an influence and widened the field of investigation of the organic chemist as much as Tswett's chromatographic adsorption analysis. Research in the field of vitamins, hormones, carotenoids, and numerous other natural compounds would never have progressed so rapidly and achieved such great results if it had not been for this new method, which has also disclosed the enormous variety of closely related compounds in nature."

3) **The technological period**

Chromatography has two distinct fields of application in industry. On the one hand, it has purely analytical applications, primarily in process control; it is indeed from such applications that chromatography as we know it today has evolved. Such applications are today so commonplace that various firms have even thought it worthwhile to distribute publications on chromatographic procedure (80, 81). On the other hand, it has possibilities as a unit-process for manufacturing purposes; it is with the latter that we are here concerned. The general possibilities of chromatography as a manufacturing process have been reviewed in various publications (6, 36, 74, 75), as have its uses in certain specific industries (39, 42, 45, 59, 70, 76, 77, 78, 79).

The patent literature is always a useful indication of industrial development. Study shows that as long ago as 1868 a British petroleum chemist, Fordred, was granted a patent for a method of refining paraffin with fuller's earth. As far as dynamic filtration was later used, it consisted of adsorptive filtration, rather than true chromatography; a very large number of patents of a similar kind were filed subsequently. The first patents relating specifically to large-scale industrial chromatography are comparatively recent. Probably the first were those of KAUFMANN (83, 84, 85), relating to the chromatographic purification of animal and vegetable fats and oils. This he proposed to effect by passing them through batteries of tubes filled with adsorbents. The detail of his proposals have been discussed elsewhere (39). The industrial applications of Kaufmann's ideas were interrupted by the war.

It is, too, interesting to note in passing that, although he took out no patents, Day did not fail to appreciate the industrial possibilities of his work and carried out experiments with columns containing as much as 200 pounds of fuller's earth.

Certain British patents relating to industrial chromatographic separators revert to the radial flow which was, as we have seen, commonly used up to the time of Goppelsroeder. The first such patent (91) related *inter alia* to what was called a chromatofuge, a device in which centrifugal force could be used both to ensure even packing and to accelerate the rate of flow (92). It was confirmed that such a radial separator could handle material more quickly than a column containing the same amount of adsorbent or equivalent material. For large separators, however, the use of centrifugal force involves great engineering difficulties and much attention has therefore been given to the construction of more efficient stationary separators (93, 94, 95, 96, 97, 98).

A later British patent (99) attempts to get over one of the principal difficulties of traditional equipment, namely that it is suitable only for batch-work, whereas industry requires for many purposes a continuous, or almost continuous, process. As an answer to this problem, movable bed-chamber technique was developed (100, 101, 102, 103) and applied to both radial separators and columns. In this method parts of the separator containing exhausted adsorbent can be quickly removed and dealt with elsewhere and replaced by fresh charges.

Chromatographic separations which can certainly be regarded as industrial ones so far as scale of working was concerned, though operated without any great attention to economic considerations, were carried out during the last war in connection with the atomic energy project. Ion-exchange columns, for example, were used by SPEDDING *et al.* (88) for the isolation and preparation of individual components present in fission-products. By this means some individual rare earths were made in kilogram quantities in a very pure state.

In 1947 MAIR *et al.* (87) described a battery of 52-foot columns used in a project undertaken jointly by the National Bureau of Standards and the American Petroleum Institute. Relatively large quantities of hydrocarbon mixtures were fractionated and certain isomers were separated from each other.

The first complete industrial chromatographic unit to be installed in a factory was probably that of Valley Vitamins Inc. at McAllen (Texas). In this plant carotene, chlorophyll, and xanthophyll, derived from alfalfa, were separated from each other on large columns of carbon arranged in batteries (89). Although excellently designed, from the engineering point of view, it worked on so small a margin that a drop in the price obtainable for its products made its closure unavoidable (90).

There are two principal lines of approach to the problem of applying chromatography on an industrial scale. On the one hand there is the adaptation of traditional apparatus. On the other there is the attempt to devise novel methods to overcome the limitations—especially the batch character—of conventional apparatus. The latter appears to be the most promising (104).

The present position in industrial chromatography has been summed up in the following words (86): "Once in a while a really new unit-operation comes into official use, and when it does every one starts working feverishly on it at the same time. No one wants to be left behind on the new processes that may come from the use of the new unit-operation. Such was the case a few years ago when fluidized solids first came to the commercial scene. Such is now the case with selective adsorption and desorption as a means of separating solutions of closely related substances."

With the above statement we warmly agree, but feel that the case could well be more strongly stated, for the above refers only to adsorption chromatography. As far as we can see, there is no reason for believing that other forms—particularly ion-exchange and partition-chromatography—have not equal industrial possibilities.

Appendix

"Since the above was written we have discovered certain other relevant facts. We have had translated into English Tswett's original Warsaw paper of 1903, which is not easily accessible, and propose to publish it shortly with annotations. It is interesting to note that in this paper Tswett does not use "chromatography" or related words; the word chromatography was, in fact, not coined by Tswett at all. It was in general use, though with a quite different connotation, at least as early as the eighteenth century. The second, but not the first (1726) edition of Nathan Bailey's "Universal Etymological English Dictionary" (1731) gives "chromatography" as a dissertation on colour (105). Tswett recognized that principles other than adsorption might be used to form chromatograms; Koshtoyants and Kalmykov (Biochemistry (Moscow), *16*, Ed. 5, 1951) have cited partition and ion-exchange as examples of this.

In papers published in the *Journal of the Royal Agricultural Society of England* two British agricultural chemists — H. S. Thompson and J. T. Way — very clearly describe experiments involving spatial separation of inorganic substances on columns of different types of soil, although, as their interest was in soil fertility, they did not explore the possibilities of this phenomenon as an analytical process. Thus experiments relating to separations on columns of adsorbent were being carried out about 1850, contemporaneously with Runge's work on paper chromatography (106).

REFERENCES

1. L. Zechmeister: History, scope, and methods of chromatography. "Annals of the New York Academy of Science", *49*, Art. 2 (1948), 145.
2. L. Zechmeister and L. von Cholnoky: "Principles and Practice of Chromatography" (Translation from second German edition by A. L. Bacharach and F. A. Robinson), London, 1941.

3. L. Zechmeister: "Progress in Chromatography, 1938–1947", London, 1950.
4. M. S. Tswett: a) Zur Kenntnis der Phaeophycenfarbstoffe, "Berichte der Deutschen Botanischen Gesellschaft", *24* (1906), 235; b) Physikalisch-Chemische Studien über das Chlorophyll. Die Adsorptionen, "ibid", 316; c) Adsorptionsanalyse und chromatographische Methode, Anwendung auf die Chemie des Chlorophylls, "ibid", 384.
5. ——: "Chromophylls in the Plant and Animal World", Warsaw, 1910.
6. Trevor I. Williams: Industrial chromatography and adsorptive filtration, "Manufacturing Chemist", *20* (1949), 16.
7. H. C. Sorby: On comparative vegetable chromatology, "Proceedings of the Royal Society (London)", *21* (1873), 442.
8. M. S. Tswett: On a new category of adsorption phenomena, and their application in the biochemical analysis, "Travaux de la Société des Naturalistes de Varsovie" (Section of biology), Protocol No. 6, *14* (1903), 20 pp.
9. ——: Recherches sur la constitution physico-chimique du grain de chlorophylle, "Travaux de la Société des Naturalistes de Kazan", 35 (1901), Vol. 3, pp. 268.
10. G. F. Schoenbein: Über einige durch die Haarröhrchenanziehung hervorgebrachten Trennungswirkungen, "Annalen der Physik und Chemie", 114 (1861), 275.
11. ——: Über einige durch Haarröhrchenwirkung des Papieres hervorgebrachten Trennungswirkungen, "Verhandlungen der Naturforschenden Gesellschaft in Basel", II (1861), 249.
12. F. Goppelsroeder: Über ein Verfahren die Farbstoffe in ihren Gemischen zu erkennen, "ibid", III (1861), 268.
13. ——: Über ein neues Verfahren, die Farbstoffe in ihren Gemischen zu erkennen, "Dinglers Polytechnisches Journal", *164* (1862), 212.
14. ——: Über die Darstellung der Farbstoffe, sowie über deren gleichzeitige Bildung und Fixation auf den Fasern mit Hilfe der Elektrolyse, "Zeitschrift für Österreichs Wollen- und Leinen-Industrie", *5/6* (1885), Kap. VII, S. 2.
15. ——: Über Capillaranalyse und ihre verschiedenen Anwendungen, sowie über das Emporsteigen der Farbstoffe in den Pflanzen, "Mitteilungen des Technologischen Gewerbemuseums in Wien, Sektion für chemisches Gewerbe", *3/4* (188), 86.
16. ——: Capillaranalyse, beruhend auf Capillaritäts- und Adsorptionserscheinungen, "Verhandlungen der Naturforschenden Gesellschaft in Basel", *14* (1901), 545 pp.
17. ——: Über Capillar- und Adsorptionsanalyse. Auszug aus meinen seit 1861 bis 1907 erschienenen Behrixationen über das auf Capillaritäts- und Adsorptionserscheinungen beruhende Gebiet der Capillaritätsanalyse, "Kolloid Zeitschrift", *4* (1909), 23, and 15 continuations in the volumes *4*, *5*, and *6*.
18. F. Feigl: "Chemistry of Specific, Selective and Sensitive Reactions", New York, 1949.
19. ——: "Chemistry of Specific, Selective and Sensitive Reactions", "Research", *3* (1950), 550.
20. "Chromatography" (Discussion), Annals of the New York Academy of Science, *49* (1948), Act. 2, 141–326.
21. "Partition Chromatography", Biochemical Society Symposia, No. 3, London, 1949.
22. "Chromatographic Analysis", Discussions of the Faraday Society, No. 7 (1949).
23. *Deutsche Bunsen Gesellschaft:* Abstracts of papers submitted to the yearly Meeting (Marburg), "Angewandte Chemie", *62* (1950), 385 ff.
24. H. G. Cassidy: "Adsorption and Chromatography", New York and London, 1951.
25. H. H. Strain: Chromatographic systems, "Analytical Chemistry", *23* (1951), 25.
26. A. W. K. Tiselius: Some recent advances in chromatography, "Endeavour", *11* (1952), 5.
27. L. Shedlovsky: A review of fractionation of mixtures by foam formation, "Annals of the New York Academy of Science", *49* (1948), Art. 2, 279.
28. H. P. Kaufmann: Adsorptionstrennungen auf dem Fettgebiet, I. "Fette und Seifen", *46* (1939), 268; II. "Angewandte Chemie", *53* (1940), 98; III. "Fette und Seifen", *47* (1940), 294; IV. "Fette und Seifen", *48* (1940), 460; V. "Fette und Seifen", *50* (1943), 519.
29. H. H. Strain: "Chromatographic Adsorption Analysis", New York, 1942.
30. Trevor I. Williams: "An Introduction to Chromatography"; London and Glasgow, 1946.
31. J. E. Meinhardt: Chromatography. A perspective. "Science", *110* (1949), 387.
32. H. H. Strain and J. C. Sullivan: Analysis by electromigration and chromatography, "Analytical Chemistry", *23* (1951), 816.
33. L. Gurwitsch: "Wissenschaftliche Grundlagen der Erdölverarbeitung", Berlin 1912.
See also: L. Gurwitsch and H. Moore: "The Scientific Principles of Petroleum Technology", London, 1932.

34. L. SHEDLOVSKY: Properties involving surface activity of solutions of paraffin-chain salts, "Annals of the New York Academy of Science", 46 (1946), Art. 6, 429.
35. R. KUHN, E. LEDERER and A. WINTERSTEIN: Zur Kenntnis des Xanthophylls, "Hoppe-Sayler's Zeitschrift für Physiologische Chemie", *197* (1931) 141.
36. TREVOR I. WILLIAMS: Recent advances in chromatographic adsorption analysis, "Research", *1* (1948), 400.
37. H. YAGODA: Applications of confined spot tests in analytical chemistry, "Industrial and Engineering Chemistry, Analytical Edition", *9* (1937), 79.
38. PLINY: Lib. XXIV, par. 112.
39. H. WEIL: Industrial oil and fat chromatography, "Paint Technology", *14* (1949) 399, 439.
40. W. A. GRUSE: "Petroleum and its products. A Chemical Discussion of the Properties, Refining and Utilization", New York, 1928.
41. H. WEIL: Petroleum Chromatographie in Analyse und Fabrikation, I. "Brannstoff-Chemie", *32* (1951), 357.
42. ——: Industrial petroleum chromatography I, "Petroleum" (London), 13 (1951), 5.
43. H. WEIL and TREVOR I. WILLIAMS: History of chromatography, "Nature", *166* (1950), 1000; *167* (1951), 906.
See also: "Scientific American" *184* (1951), No. 6, p. 2.
44. H. WEIL and TREVOR I. WILLIAMS: "Der Ursprung der Papier-chromatographie". *Naturwissenschaften*, in press.
45. H. WEIL: Half a century of petroleum chromatography, "Petroleum Processing" (Cleveland), Part I, June 1952, 812; Part II, July, 1952.
46. F. F. RUNGE: De pigmento indico, ejusque connubiis cum metallorum nonnullorum oxydis, "Dissertatio inauguralis", Berlin, 1822.
See also: Indigo und seine Verbindungen mit Metallen und Oxyden, "Tromsdorffs Neues Journal für Pharmacie", *7* (1823), 68.
47. F. F. RUNGE: Über die Produkte der Steinkohlendestillation, "Poggendorffs Annalen", *31/32* (1834).
48. ——: "Farbenchemie", I (1834), II (1842), III (1850), Berlin.
49. ——: "Grundriss der Chemie", 2 volumes, Munich, 1848.
50. ——: "Zur Farbenchemie, Musterbilder für Freunde des Schönen und zum Gebrauch für Zeichner, Maler, Verzierer und Zeugdrucker", Berlin, 1850.
51. ——: "Der Bildungstrieb der Stoffe", Oranienburg, 1855.
52. D. T. DAY: A suggestion as to the origin of Pennsylvania petroleum, "Proceedings of the American Philosophical Society", *36* (1897), 122.
53. ——: The variation in the character of Pennsylvania and Ohio crude oils, "Industrial and Petroleum Review", *3* (1900), supplement to the issue, August 25, 1900, p. 9.
54. D. T. DAY and J. E. GILPIN: The changes in crude petroleum effected by diffusion through clay. "Journal of Industrial and Engineering Chemistry", *1* (1910), 449.
55. T. BAILEY: On the behaviour of metallic solutions with filter paper, and on the detection of cadmium, "Journal of the Chemical Society, *33* (1878), 304.
56. O. NASSE: Über Capillarität, "Chemisches Zentralblatt", I (1890), 442.
57. L. REED: Notes of capillary separation of substances in solution, "Proceedings of the Chemical Society", *9* (1893), 123.
58. J. U. LLOYD: On separation by capillary attraction, "Chemical News", *51*, 1885, January 30, 51.
59. H. WEIL: Industrial petroleum chromatography, II. "Petroleum", (London), *14* (1951), 205; *15* (1952), 9.
60. BUSSERIUS and EISENSTOCK: Über einige Derivate des Petrols, eines in Steinöl vorkommenden Kohlenwasserstoffes, "Annalen der Chemie und Pharmacie", *112* (1860), 151.
61. C. ENGLER and M. BOEHM: Über die chemische Natur des Vaselins, "Dingler's Polytechnisches Journal", *262* (1886), 470.
62. C. ENGLER and E. ALBRECHT: Über den Vorgang bei der Filtration von Petroleum durch Floridaerde, "Zeitschrift für angewandte Chemie" (1901), 889.
63. D. HOLDE: Die Petroleumindustrie auf der Pariser Weltausstellung, "Zeitschrift für angewandte Chemie" (1900), 1200.
64. ——: Der erste internationale Petroleum Kongress zu Paris, "Chemische Revue über die Fett- und Harzindustrie", 8 (1901), 6.
65. R. ZALOZIECKI: Die Verschiedenheit im Charakter des pennsylvanischen und Ohio Rohöles. Fraktionierung der Rohölbestandteile durch Filtration, "Naphtha", (Lemberg), *9* (1901), 12, 23.

66. J. E. GILPIN and M. P. CRAM: The fractionation of crude petroleum by capillary diffusion, "Bulletin of the U.S. Geological Survey", No. 365.
67. J. E. GILPIN and O. E. BRANSKY: The diffusion of crude petroleum through fuller's earth, "Bulletin of the U.S. Geological Survey", No. 475.
68. J. E. GILPIN and P. SCHNEEBERGER: Fractionation of California petroleum through fuller's earth, "American Chemical Journal", 50 (1913), 59.
69. B. J. MAIR and F. D. ROSSINI: The fractionation, analysis, and isolation of hydrocarbons in petroleum, in B. T. BROOKS and A. E. DUNSTAN "The Science of Petroleum, Vol. V, Part 1. Crude Oils, Chemical and Physical Properties;" London—New York—Toronto, 1950, p. 126.
70. H. WEIL: The chromatographic work of the National Bureau of Standards, Part III of Industrial Petroleum Chromatography, "Petroleum" (London), to be published.
71. ——: La tecnologia chromatografica applicata al petrolio, "La Rivista dei Combustibili" (Milano), *5* (1951), 617. Part II "Ibid", January 1952.
72. W. TRAPPE: Die Fraktionierung biologischer Fettstoffe aus ihren natürlichen Gemischen mit Hilfe von Adsorptionssäulen, "Biochemische Zeitschrift", *305* (1940), 150; *306* (1940), 316; *307* (1941), 97.
73. P. KARRER: XIth International Congress of Pure and Applied Chemistry, London, 1947.
74. TREVOR I. WILLIAMS: Chromatography in industry, "Industrial Chemist", *24* (1948), 316.
75. ——: Chromatography in industry, "Discovery", *11* (1950), 396.
76. H. WEIL: Industrial chromatography of the rare earths, "Canadian Chemistry and Process Industries", *33* (1949), 956.
77. ——: Chromatographic technology in radioisotope separation, "Atomics", (London), *1* (1950), 230, 345.
78. ——: Industrial petroleum chromatography, IV, Actual Research Problems, "Petroleum" (London), to be published.
79. ——: Industrial petroleum chromatography, V. Chromatographic patent literature, "Petroleum" (London), to be published.
80. British Drug Houses Ltd.: "Introductory notes on chromatography", Poole, 1948.
81. H. H. CHAMBERS (Sondes Places Research Institute): "Chromatography in industrial research", Dorking, 1951.
82. JOHN FORDRED: British Patents Nos. 2721 (1867); 610 (1868); 648 (1868); 2356 (1868).
83. H. P. KAUFMANN: German Patent No. 722,359 "Verfahren zum Raffinieren von Fetten und Ölen unter gleichzeitiger Gewinnung der darin enthaltenen ernährungswichtigen Begleitstoffe.
See also: British Patent Specification No. 541,002.
84. H. P. KAUFMANN: German Patent No. 741,359 "Verfahren zur Fraktionierung von Gemischen Fettsäuren und dergleichen.
See also: British Patent Specification No. 541,002.
85. H. P. KAUFMANN: German Patent Application K. 151,362, "Entstearinierung von natürlichen Fetten und Ölen nach vorausgegangener intermolekularer Umesterung".
86. ROGER WILLIAMS, Jr. and J. V. HIGHTOWER: Chromatography, "Chemical Engineering", *55* (1948), 133.
87. B. J. MAIR, A. L. GABORIAULT, and F. D. ROSSINI: Assembly and testing of a 52-feet laboratory adsorption column. Separation of hydrocarbons by adsorption. "Industrial and Engineering Chemistry", *39* (1947), 1072.
88. F. H. SPEDDING, E. I. FULMER, T. A. BUTLER, E. M. GLADROW, M. GOBUSH, P. E. PORTER, J. E. POWELL and J. M. WRIGHT: The separation of rare earths by ion-exchange. III. Pilot plant scale, "Journal of the American Chemical Society" *69* (1947), 2812.
89. W. H. SHEARON, Jr. and O. F. GEE: Carotene and chlorophyll. Chromatographic production, "Industrial and Engineering Chemistry", *41* (1949), 218.
90. O. F. GEE and H. WEIL: New ways in chromatographic engineering, to be published.
91. P. P. HOPF, C. G. LYNAM and H. WEIL: British Patent No. 585,224 "Improvements in or relating to chromatographic adsorption processes for the separation and purification of materials".
92. P. P. HOPF: Radial chromatography in industry, "Industrial and Engineering Chemistry", *39* (1947), 938.
93. H. WEIL: Column chromatography and radial chromatography, "Canadian Chemistry and Process Industries", *33* (1949), 956.
94. C. G. LYNAM and H. WEIL: A new plant for radial chromatography, "Manufacturing Chemist", *21* (1950), 195.

95. C. G. LYNAM and H. WEIL: A chromatographic repetition plant "Ibid", 288.
96. ——: Radial chromatographic pilot plant, "Canadian Chemical Processing", *35* (1951) 471.
97. H. WEIL: Scambio ionico con processi discontinui e continui, "La Chimica e l'Industria", *33* (1951), 287, Milano.
98. C. G. LYNAM and H. WEIL: Improvements in or relating to chromatographic processes for the separation and or purification of materials. British Patent No. 635,271.
99. ——: Improvements in or relating to chromatographic separation. British Patent No. 611,080.
100. ——: Combination-columns in chromatography, "Industrial Chemist", *26* (1950), 109.
101. ——: Movable bed-chamber technique, "International Chemical Engineering and Process Industries", *31* (1950), 276.
102. H. WEIL: Prinzipien und Praxis der chromatographischen Fabrikation, "Chemie-Ingenieur-Technik", *23* (1951), 422.
103. ——: Application de la chromatographie de partage à l'industrie, "Chimie et Industrie" (Paris), *64* (1950), 432.
104. H. WEIL and T. I. WILLIAMS: Problems of chromatographic technology, "Research" (January, 1953).
105. T. I. WILLIAMS and H. WEIL: The definition of chromatography, "Nature", *170* (1952) 503.
106. H. WEIL and T. I. WILLIAMS: The first chromatographic column-system, "Experientia", in the press.

Tryckt den 13 februari 1953

Uppsala 1953. Almqvist & Wiksells Boktryckeri AB

ARKIV FÖR KEMI Band 5 nr 28

Communicated 22 October 1952 by JOHN RUNNSTRÖM and KARL MYRBÄCK

An improved method for degradation of tyrosine and phenols in general in connection with isotope studies

By L. REIO and G. EHRENSVÄRD

With 4 figures in the text

In a previous, preliminary communication (1) we described a method for the determination of isotope content in different carbon atoms of the phenolic ring and the side chain of tyrosine. The amount of tyrosine, isolated from *Torulopsis utilis* after cultivation on doubly labelled acetate was as much as 780 mg, yet the method for degradation required that the 4-hydroxybenzoic acid obtained by alkaline fusion had to be diluted three times with non-labelled material in order to be of sufficient quantity for the further degradation. In addition, the carbon atoms 1 and 2.6 and α were determined with regard to their isotope content in an indirect manner. The following method enables the isotope content of these carbon atoms to be determined by a direct route, requiring much less material. Fig. 1 gives an over-all scheme of the reaction sequences employed.

Experimental

Isolation of 4-hydroxybenzoic acid and acetic acid from the alkaline fusion of tyrosine. 430 mg of tyrosine was added in portions to a fused mixture of 2 g each of NaOH and KOH, plus two droplets of water. The melt was kept at 270° in a funnel-shaped silver crucible heated in an aluminium block. The dimensions of the crucible were: bottom part 22 mm diameter, height 40 mm, flat bottom; the funnel-shaped upper part had a height of 50 mm and the largest diameter = 90 mm. This type of crucible was most convenient for the later working-up of the melt, after the usual 12 min. reaction time. The crucible was cooled down, 5 ml of water added, and 25 per cent sulfuric acid carefully added in portions to give a final volume of 25 ml. After everything had gone into solution, the acid solution was cooled and extracted in a Soxhlet apparatus with ether for 16 hours. The extractor was removed and the ether extract was distilled over in a receiver at 50–60°. The residue was mainly 4-hydroxybenzoic acid; the ether distillate *and* the extracted water phase both contained a small amount of acetic acid emanating from the proximate part of the tyrosine side chain (the α carbon atom and the carboxyl group). In order to isolate this acetic acid, the extracted water phase and an alkaline extract of the ether were steam distilled from strongly acid medium. The 250 ml of distillate obtained were neutralized with 0.02 N NaOH and evaporated to dryness, at first in an ordinary

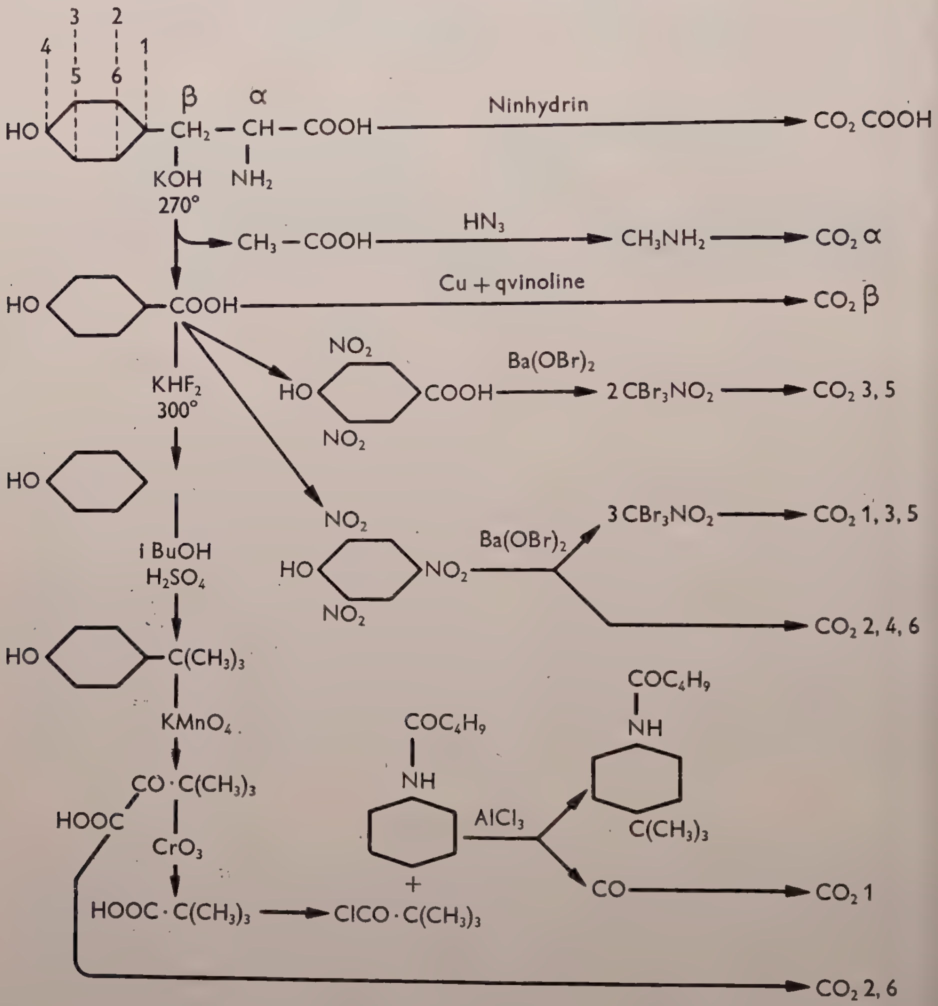
3 2
4 1
5 6
β α
HO
CH₂ — CH — COOH
KOH NH₂
270°
Ninhydrin
CO₂ COOH
CH₃ — COOH
HN₃
CH₃NH₂
CO₂ α
HO
COOH
Cu + qvinoline
CO₂ β
NO₂
HO
COOH
NO₂
Ba(OBr)₂
2 CBr₃NO₂
CO₂ 3, 5
KHF₂
300°
HO
NO₂
HO
NO₂
NO₂
Ba(OBr)₂
3 CBr₃NO₂
CO₂ 1, 3, 5
CO₂ 2, 4, 6
i BuOH
H₂SO₄
HO
C(CH₃)₃
KMnO₄
CO·C(CH₃)₃
HOOC
CrO₃
HOOC·C(CH₃)₃
ClCO·C(CH₃)₃
COC₄H₉
NH
+
AlCl₃
COC₄H₉
NH
C(CH₃)₃
CO
CO₂ 1
CO₂ 2, 6

Fig. 1.

flask, later in a small centrifuge tube with conical tip. After addition of a calculated amount of 1 : 1 sulfuric acid and chloroform, the acetic acid (about 30–40 mg) was transferred according to MOYLE, BALDWIN and SCARISBRICK (2) to a Celite column and the acetic acid chromatographed by elution with 100 ml of chloroform and later with 100 ml of chloroform containing 5 per cent n-butanol. The fractions containing acetic acid were collected, after titration with 0.02 N NaOH and evaporated to dryness. Yield of pure sodium acetate 15–20 mg.

The crude 4-hydroxybenzoic acid, about 350 mg, was boiled under reflux with chloroform (specially dried) in order to remove small amounts of salicylic acid and other impurities. After cooling and filtering the extraction procedure was

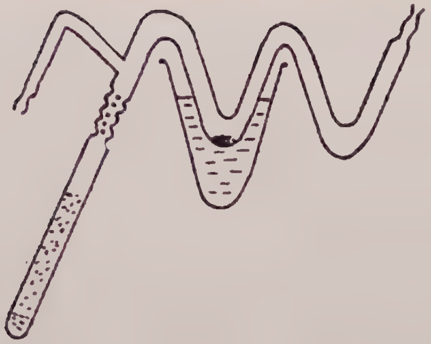

Fig. 2.

repeated four times (5 minutes each, 1 ml of chloroform each time). The dry acid was quite white, odorless, and had a melting point of 208° (litt. 212°). Mixed melting point with authentic sample of 4-hydroxybenzoic acid was 209°. Yield 282 mg, 86 per cent from tyrosine.

Decarboxylation of acetic acid was carried out according to PHARES (3) by a Schmidt reaction and the CO_2 from the carboxyl isolated as barium carbonate. The methylamine remaining as sulfate in the reaction mixture was oxidized according to the same author with alkaline permanganate, and the resulting CO_2, after acidification, was trapped as barium carbonate, representing the α-carbon atom.

Decarboxylation of 4-hydroxybenzoic acid and isolation of phenol was effected by heating of a mixture of the acid, 140 mg, with 500 mg of fused KHF_2 in a small all-glass distillation apparatus, see fig. 2. The heating—with a micro flame—had to be done carefully in order to prevent the reaction mixture from being carried over into the receiver bends. The mixture was distilled to dryness and the mixture of phenol and small amounts of water was further distilled from the first receiver bend to the second and the third. The phenol thus obtained was colorless and crystallized at cooling. During the whole procedure a very slow current of nitrogen was passed through the system, and the evolved CO_2 was trapped as barium carbonate. The yield of barium carbonate and phenol was usually about 90 per cent.

Since there was always some decomposition of organic matter, the CO_2 evolved was not fully representative for the β-atom of tyrosine. For analytical purpose decarboxylation of 4-hydroxybenzoic acid in quinoline at the temperature 230° in the presence of copper powder was preferred (1). This procedure could be carried out in 15 mg scale.

Preparation of 1-tert. butyl-phenol-(4) from phenol. The phenol obtained by distillation was transferred by repeated washing-out with a total of 1 ml of 70 per cent sulfuric acid into a 50 ml flask. To the flask was added 0.25 ml of redistilled *iso*-butyl-alcohol, plus three droplets of concentrated sulfuric acid (in order to account for the water in the phenol, keeping the strength of the sulphuric acid to 70 per cent). The mixture was allowed to stand in the stoppered flask at 80° for 12 hours. The whole procedure of the condensation of phenol and iso-butanol to p-tert-butyl-phenol followed in its main outline the procedure of MEYER and BERNHAUER (4). At completion of the reaction time a brownish, clear oil had separated out from the mixture. This oil, representing 1-tert. butyl-phenol-(4) in 70 per cent yield (as estimated in large scale preparations, involving fractionation distillation) was without further purification subjected to oxidation according to the following description. M. p. 98°; B. p. 236–37°.

Preparation of trimethylpyruvic acid and its decarboxylation and oxidation to trimethylacetic acid (pivalic acid). To the reaction mixture containing tert-butylphenol and sulfuric acid, 10 ml of water was added, plus 8 N NaOH to complete neutralization. The mixture was made alkaline with 2 ml of 2 N NaOH and 600 mg of potassium permanganate in 25 ml of water added in portions. (The amount of permanganate corresponds to a 90 per cent yield of phenol (86 mg) from 4-hydroxybenzoic acid and 70 per cent yield of tert-butyl-phenol from phenol; thus 96 mg of tert-butyl-phenol). After standing over night at room temperature the excess, if any, of permanganate in the mixture was destroyed by addition of a few drops of sodium sulfite solution, the manganese dioxide centrifuged off and the precipitate washed three times with 25 ml portions of water, slightly alkaline. The combined centrifugates (about 100 ml) were acidified, corresponding to 1 N of sulfuric acid, filtered if not clear, and some CO_2 produced by oxidation, blown away by a current of nitrogen, until a clear baryta solution showed no turbidity. The water bath temperature for this procedure was 80° and time 2 hours. The solution at this stage contained about 40 mg of trimethylpyruvic acid and a minor amount of pivalic acid. Large scale preparation showed molar proportion 4 : 1 between the acids. A yield about 50 per cent was obtained by oxidation. A sample ($1/6 = 15$ ml) of the solution was taken off and treated with a solution of 2-4-dinitrophenyl hydrazine in 0.5 N HCl in order to isolate the di-nitrophenylhydrazone of the keto acid. M. p. 167°. A check had previously been done with the corresponding phenylhydrazone, giving the m. p. 152°; according to ANSCHÜTZ and RAUFF (5) and GLÜCKSMAN (6) the m. p. of the latter compound should be 153° and 158° respectively. The dinitroderivative has not been described previously, but is preferable, because of its low solubility. Twice recrystallized 2-4-dinitro-derivate of an authentic sample had m. p. 171°. To the main part of the solution of trimethylpyruvic acid 75 mg of potassium dichromate was added, the flask heated in a water bath at 50° and the content aerated with nitrogen. By this treatment the carboxyl of the keto acid is split out as CO_2, swept out by the nitrogen and trapped as barium carbonate, the latter representing carbon atoms 2 and 6 (mean value) of the phenolic ring. This procedure takes about two hours.

The trimethylpyruvic acid is by the above oxidation quantitatively converted to the chromic acid stable trimethylacetic acid, isolated by subsequent steam distillation. The distillate, 250 ml, was neutralized with 0.02 N NaOH (about 15 ml) and evaporated to dryness, at first in an ordinary flask, finally in the bottom part of a small flask (2 ml) of a type shown in fig. 3 (to the left). The dry residue, representing about 35 mg of sodium pivalate was then selectively decarboxylated according to the following description.

Specific decarboxylation of pivalic acid. ROTHSTEIN and SAVILLE (7) have shown that pivaloyl chloride in different Friedel-Crafts reactions forms tert. butyl derivatives of diverse aromatic structures, splitting out CO during the

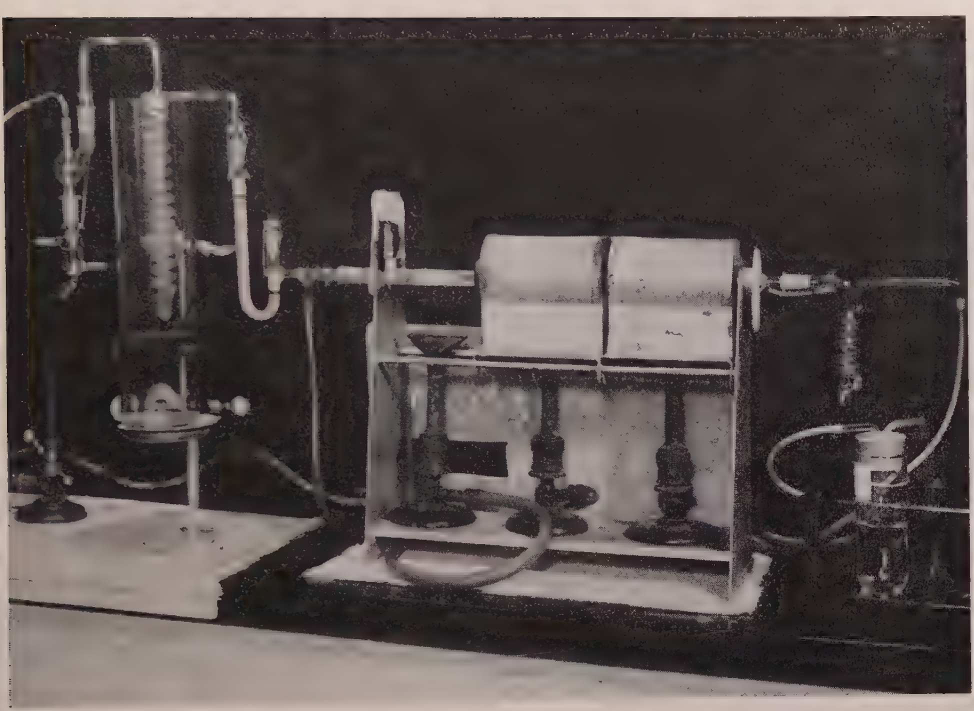

Fig. 3.

reaction. This CO, as we have checked (see table I), represents the carboxyl of pivalic acid to 95 per cent, even in the presence of other carbonic acids. Our modification of the reaction, adopted to semi-micro scale for specific decarboxylation of pivalic acid, includes the following procedure.

To the dry sodium pivalate, still in the flask in which the final evaporation was done, 0.25 ml of benzoylchloride was added, heated to boiling and kept at 100° for one hour, the condensor jacket of the flask filled with water. Yield of pivaloyl chloride about 85 per cent (8). The mixture was cooled to 0°, 300 mg of n-valeroyl-anilide (9) and 300 mg anhydrous $AlCl_3$ were added, the aluminium chloride placed on top of, not in contact with, the fluid phase. The reaction vessel was connected with a nitrogen inlet and the assembly of dry ice trap, ascarite tube and combustion unit, whereupon a slow stream of dry nitrogen was passed through the assembly into the final baryta solution for 5 minutes in order to ascertain that no carbon contaminants were present. A current of oxygen at double the rate of that of the nitrogen was directed into the combustion oven, and at the same time the reaction mixture was gently heated by a micro-flame to slightly above the melting point of the n-valeroylanilide (m. p. 56°). In the moment the reaction mixture becomes homogenous hydrogen chloride and the carbon monoxide are liberated with great violence, swept out by nitrogen into the dry-ice trap, whereby organic contaminants are held back; the ascarite tube will absorb any traces of carbon dioxide, so that the monoxide will reach the combustion apparatus (as checked) in pure state. After passing over

Table 1

Decarboxylation procedures applied for the C^{14}-carboxyl-labelled pivalic acid. Distribution of C^{14} in barium carbonate, pivalic acid carboxyl, and CO and CO_2, given in counts per minute per 15 mg of $BaCO_3$.

$BaCO_3$ used for synthesis Pivalic acid, C_{total} ” ” C_{COOH} calculated	1550 330 1650	C^{14} CO	C^{14} CO_2	Comments
Heating with H_2SO_4 at 110°		900	50	Pivalic acid volatile already under 100° (12, 13).
Heating with P_2O_5		705	82	Total decomposition: practically only CO_2 formed (14).
Silver pivalate and bromine		—	—	Low yields, 5 per cent.
Schmidt reaction		—	960	Yield about 15 per cent, not selective, reacts with acids in general (15).
Friedel-Craft reaction on pivaloyl chloride and n-valeroylanilide		1490	140	Normally no CO_2 obtained (7).
Labelled pivalic acid mixed with non-labelled trimethylpyruvic acid 1:1 and subsequent CrO_3 oxidation			3	Stable for CrO_3 at 50° in 1 N H_2SO_4.

the platinum gauze heated at 800°, the resulting carbon dioxide is trapped as barium carbonate, representing the carboxyl of pivalic acid, and thus corresponding to the carbon atom 1 of the phenolic ring of tyrosine. After some acquaintance with this decarboxylation procedure it could be carried out with great ease. Care has, however, to be taken at first: that the aluminium chloride does not come into contact with the fluid phase (pivaloyl chloride) before the reaction vessel is attached to the assembly, secondly: that after heating the reaction mixture (above the melting point of the anilide) should be kept at 80–90° during the whole reaction time. From 35 mg of sodium pivalate (estimated by titration of the original steam distillate) 25 mg of barium carbonate were obtained corresponding to a yield of 45 per cent, this figure representing the lowest value that we have obtained. The total yield of carbon atom 1, as barium carbonate from 4-hydroxybenzoic acid thus keeps about 15 per cent.

The preparation of 3–5-dinitro-4-hydroxybenzoic acid and picric acid gave, according to the following modifications of known methods (1), 68 and 50 per cent yields of resp. compounds from 4-hydroxybenzoic acid.

The dinitro acid was prepared from a solution of 40 mg of 4-hydroxybenzoic acid in 0.22 ml of concentrated sulfuric acid by careful addition of a mixture of 0.14 ml each of concentrated sulfuric acid and concentrated nitric acid (density 1.4). The reaction mixture kept at 0° for 4 hours, filtered and washed with a few drops of ice-water and hot benzene. The preparation was facilitated by using a small test-tube (1 ml) with a sintered glass filter crucible (8 mm diameter) fused into the side wall, so that nitration and subsequent filtration and recrystallization could be carried out within the same vessel. M. p. 242°.

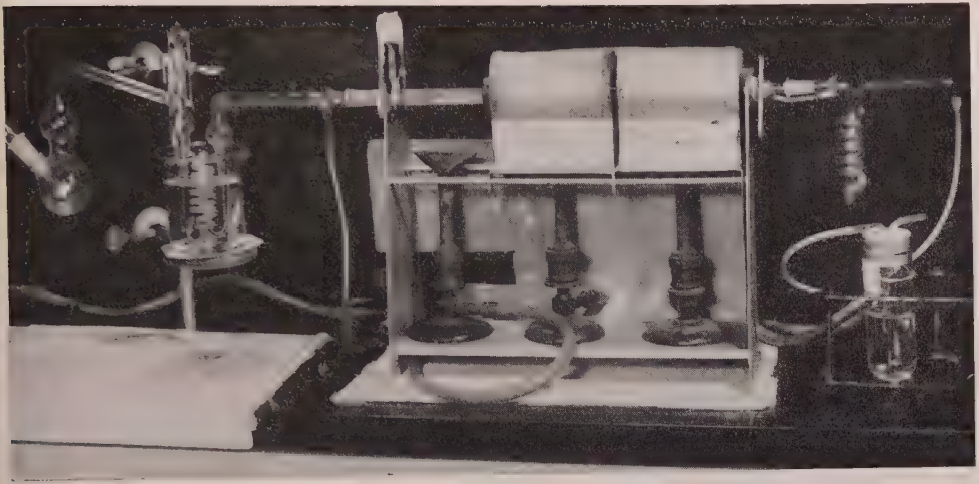

Fig. 4.

In the same apparatus 50 mg of hydroxybenzoic acid were nitrated as above. To the reaction product, after 4 hours standing at 0°, 0.15 ml of concentrated nitric acid was added. Then the mixture was heated to 100° for 3 hours, cooled, kept at — 5° for 24 hours, picric acid sucked off directly, washed with 20 per cent hydrochloric acid and recrystallized by dissolving in 1 ml of water and saturation with hydrogen chloride. M. p. 121°.

The bromopicrin-split of the nitro compounds was carried out in principle according to the method previously described (1), with the following modification. 20 mg of each nitro compound were dissolved in 2 ml of filtered, saturated baryta solution in a 50 ml flask. To this solution 10 ml of filtered, saturated bariumhypobromite solution was added in the cold, and the reaction mixture heated to boiling. A slow stream of nitrogen swept over the tribromonitromethane formed into a scrubber with saturated baryta solution. The apparatus is shown in fig. 4. Tre baryta scrubber was kept at 100° by immersing in boiling water. The bromopicrin passing through the scrubber was directly combusted in oxygen over heated platinum gauze in a quartz-tube, and the carbon dioxide formed trapped into baryta solution as barium carbonate. In this manner we have avoided the isolation and cumbersome purification of the minute amounts of bromopicrin, and the yields of barium carbonate from the carbon atoms 3.5 and 1.3.5 respectively were kept above 50 per cent. Isotope values, checked by combustion after isolation, and by direct combustion of bromopicrin, obtained from the same sample, were identical in limits of 5 per cent.

In the case of bromopicrin split of picric acid the content of the scrubber was removed and washed out, after completion of the combustion of bromopicrin, and refilled with filtered baryta solution. The content of the flask was then made acid and the carbon dioxide liberated was passed over with nitrogen into the scrubber. The resulting barium carbonate represents the carbon atoms 2.4.6 of the phenolic ring, in a yield of about 90 per cent. A check has to be done with a

Table II

Isotope content, determined and calculated, in different degradation products of tyrosine, isolated from *Escherichia coli* and *Neurospora crassa* grown on $C^{13}H_3$-$C^{14}OOH$ as the sole source of carbon, and compiled values of isotope content in individual carbon atoms of tyrosine structure. C^{13} is given in atom per cent excess, C^{14} in counts per minute per 15 mg of barium carbonate. C_{total} denotes total carbon, as barium carbonate, C_{COOH} carboxyl carbon.

Series	Compounds investigated	Position of carbon atoms in tyrosine	Escherichia coli		Neurospora crassa	
			C^{13}	C^{14}	C^{13}	C^{14}
A	Tyrosine, C_{total}	All atoms	0.08	228	0.05	66
B	Tyrosine, C_{COOH}	Carboxyl	0.07	730	0.04	207
C	Acetic acid, COOH	Carboxyl	0.06	762	0.05	216
D	Acetic acid, CH_3	α	0.12	25	0.08	9
E	4-hydroxy-benzoic acid, carboxyl		0.11	18	0.07	17
F	4-hydroxy-benzoic acid, C_{total}	Ring, β		190		71
G	3.5-dinitro-4-hydroxy-benzoic acid, C_{total}	Ring, β		176		60
H	Picric acid, C_{total}	Ring = R	0.08	208	0.04	61
I	Tribromo-phenol, C_{total}	Ring = R	0.08	204	0.04	55
K	Bromopicrin from 3.5-dinitro-4-hydroxy-benzoic acid. C_{total}	3.5	0.09	174	0.05	37
L	Bromopicrin from picric acid. C_{total}	1.3.5	0.10	136	0.05	39
M	CO_2 from split L.	2.4.6	0.07	284	0.04	82
N	Trimethyl-pyruvic acid carboxyl carbon, taken at intervals of 30 min. 1.	2.6	0.06	202	0.03	53
	2.			196		51
	3.			204		
O.	Trimethyl-acetic acid carboxyl	1.	0.09	72	0.05	22

Compiled C^{14}-values, calculated on the basis of the following:				C^{14}			C^{14}		
B	C		Carboxyl	*730*	*762*		*207*	*216*	
D	9 A–7 F–B	9 A–6 H–E–B	α	*25*	−8	56	*9*	(−110)	4
E	7 F–6 H	7 G–6 I	β	*18*	82	(−160)	*17*	(131)	(90)
O	3 L–2 M	6 R–3 M–2 K	1.	*72*	60	66	*22*	39	56
N	½(6 R–3 L–P)	½(6 R–2 K–O–P	2.6	*201*	204	198	*52*	35	43
K	½(6 R–O–3 M)		3.5	*174*	*171*		*37*	*56*	
P = 3 M–2 N	6 R–3 L–2 N	6 R–O–2 N–2 K	4.	*450*	438	444	*194*	169	176
R = ½ (H + I)	½ (L + M)	(7 F–E)/6	Ring	*206*	*210*	218	*58*	*59*	80

Values in italics are those regarded as safest, and used in the calculations.

corresponding blind run without picric acid. Usually an amount of barium carbonate is recovered in the blind run amounting to about 10 per cent of that from carbon atoms 2.4.6 in picric acid in scale of 20 mg sample.

Discussion

The method described has been carefully checked as to the different reaction steps. The identity of the acetic acid, recovered from the alkaline melt of tyrosine, with the terminal part of the side-chain was ascertained by comparison of the isotope content in the tyrosine carboxyl (liberated by ninhydrin treatment) and in the acetate carboxyl. Table II, series B, C, shows these values as derived from two separate cases of tyrosine degradations.

The purity of 4-hydroxybenzoic acid is of great importance. We have checked by chromatography on Celite (10) of the crude product from the alkaline fusion that this product does contain up to 8 per cent of salicylic acid. The removal of this acid before the subsequent nitration etc. of the 4-hydroxybenzoic acid is necessary since otherwise the bromopicrin split of dinitro-salicylic acids would result in mixing-in of bromopicrin from other carbon atoms than the desired 3.5 and 1:3.5. The chloroform treatment described removes all traces of salicylic acid and other contaminants without any *considerable* losses of the 4-hydroxybenzoic acid.

As to the origin of salicylic acid this is obviously a consequence of secondary fixation of CO_2 from different sources to the small amounts of phenol that may originate by partial decarboxylation of the 4-hydroxybenzoic acid formed during the alkaline fusion. This side-issue of the main reaction must, however, be of minor order, since the isotope values of the β-carbon atoms are not detectably affected by dilution from non-isotopic CO_2 present in the NaOH and KOH of the melt. We regard the 4-hydroxybenzoic acid isolated in pure state from the alkaline fusion of tyrosine as fully representing the phenolic ring + the β-carbon atom of tyrosine *in its original orientation in the tyrosine molecule.*

The decarboxylation of 4-hydroxybenzoic acid by distillation with KHF_2 was after many trials adopted as the best method for obtaining of a phenol in good yield and of sufficient purity to enable a subsequent condensation with iso-butyl alcohol. The CO_2 liberated was not fully representative for β-atom of tyrosine, and therefore the method described in (1) is recommended for selective decarboxylation of small samples of the hydroxyacid.

The purity of p-tert-butylphenol should be at least 90 per cent, in regard to the para position of tert-butyl group. Small amounts of ortho-butylphenol (about 1 per cent) and 2.4-di-tert-butylphenol is to consider as non-significant contamination. Especially when at small-scale condensation the amount of phenol should be in slight excess over iso-butylalcohol. For further details see (11).

That the carbon dioxide liberated by the CrO_3-treatment of the acidified solution after permanganate oxidation of the tert-butylphenol represented to 100 per cent the carboxyl of trimethylpyruvic acid was proved in different ways. First it was found that the CO_2 evolved corresponded to the amount of keto-acid originally present in the solution, as determined with 2-4-dinitro-phenylhydrazine. Secondly, after the end of the oxidation this reagent did not reveal any amount of keto-acid left in the solution. Finally, it was found that under the conditions employed none of those acids that might have been formed, in addition to trimethylpyruvic acid and trimethylacetic acid, gave off any CO_2, that might contaminate the CO_2 from the carboxyl of trimethylpyruvic acid. Tested were: iso-butyric acid, acetic acid, oxalic acid, malonic acid, and for security trimethylacetic acid. Isotope values taken at several instances were exact the same during the decarboxylation period.

With regard to the influence of pivalic acid, its indifference towards oxidation was tested with a synthetic sample labelled with C^{14} in the carboxyl group by mixing-in a certain amount of this labelled acid into the reaction mixture from a permanganate oxidation of non-labelled p-tert-butylphenol. At acidification and subsequent chromate oxidation of this mixture of non-labelled trimethylpyruvic acid and labelled trimethylacetic acid it was found that no C^{14} was found in the liberated CO_2.

The labelled pivalic acid was taken into use when working out a selective decarboxylation process. It has been reported (12, 13, 14) that upon treatment with concentrated sulfuric acid or phosphorous-pentoxide the carboxyl of pivalic acid should be liberated as CO and CO_2. After testing these procedures with carboxyl-labelled pivalic acid, it was found, however, that a considerable amount of non-labelled CO and CO_2 was diluting up the $C^{14}O_2$ emanating from the carboxyl, indicating a considerable destruction of the non-carboxylic part of the molecule. Attempts with Schmidt degradation (15) gave low yields of CO_2, still contaminated with non-labelled CO_2. The decarboxylation via a Friedel-Crafts reaction that finally was worked out gave, however, consistent isotope values of the liberated CO, in accordance with the values of the carboxyl carbon. Table I gives some data as to the different decarboxylation procedures. N-valeroyl-anilide was chosen as the reaction component at the pivalic acid decarboxylation via pivaloylchloride because it served both as reactant and high-boiling solvent for the reaction mixture. Tests with other reactants, i. e. anisole etc., showed that, in spite of the dry ice trap, some traces of vapour from such solvent went into tho combustion oven. Of all the acyl-anilides tested the n-valeroyl derivative had the lowest melting point, and was therefore adopted as the most practical component for this reaction.

The labelled pivalic acid was prepared by three hours shaking at 0° of a solution of the magnesium-tert-butyl bromide in ether under a pressure of $C^{14}O_2$ of 150 mm mercury (16). The accuracy of the C^{14} measurements is ± 5 per cent and for $C^{13} \pm 0.005$ atom per cent excess.

The reason why we have gone into considerable detail at this description of tyrosine degradation is that it involves methods that are applicable, after modification, to the degradation of any phenols, and possibly other aromatic structures, which has a practical bearing to investigations of their biochemical origin with aid of isotopes. The advantage of having a method for direct determination of isotope content in carbon atoms 2.6 and 1, is emphasized in those cases where one has to deal with diluted samples—as a matter of economy—and where a discussion may arise, whether a certain small isotope content in 2.6 or 1 indirectly calculated should be regarded as significant or not. The direct estimation is in all cases preferable, as seen from the Table II of isotope values derived from two samples of tyrosine.

Finally, it might be pointed out that the method of coupling-in of a tert-butyl group is applicable to any phenol, where it could be ascertained that this group enters in a specific position; para or ortho, not both. If a methyl group should be present in a phenol, its removal together with the attached ring carbon atom as acetic acid would be easily effected by oxidation. As to the bromopicrin split this is applicable in most cases where the nitro groups are in ortho or para to the hydroxyl.

SUMMARY

An improved method for degradation of tyrosine is described, involving the isolation and purification of acetic acid and 4-hydroxybenzoic acid, the former representing the carboxyl and α-carbon atom. Decarboxylation of 4-hydroxybenzoic acid in the presence of KHF_2 is followed by isolation of pure phenol and a subsequent preparation of p-tert-butylphenol. This compound is oxidized to trimethylpyruvic acid, the carboxyl of which is selectively liberated as CO_2, representing carbon atoms 2 and 6. At oxidation of trimethylpyruvic acid there is formed in good yield trimethylacetic acid, the carboxyl of which represents carbon atom 1 of the ring system. A method for selective decarboxylation of trimethylacetic acid is described. The procedures have been designed for small scale work, utilizing 450 mg of tyrosine, corresponding to 150 mg of phenol.

Sources of error in different degradation methods for aromatic ring systems are discussed, and some primary data obtained from tyrosine isolated from *E. coli* and *Neurospora crassa* grown on labelled acetate have been given.

The Wenner-Gren Institute, Department of Physiological Chemistry, University of Stockholm, Sweden.

BIBLIOGRAPHY

1. BADDILEY, J., EHRENSVÄRD, G., KLEIN, E., REIO, L., and SALUSTE, E., *J. Biol. Chem., 183,* 777 (1950).
2. MOYLE, V., BALDWIN, E., and SCARISBRICK, R., *Biochem. J., 43,* 308 (1948).
3. PHARES, E. F., *Arch. Biochem. Biophys., 33,* 173 (1951).
4. MEYER, H., and BERNHAUER, K., *Monatsh. Chem., 53/54,* 733 (1932).
5. ANSCHÜTZ, R., and RAUFF, G., *Ann. Chem., 327,* 203 (1903).
6. GLÜCKSMAN, G., *Monatsh. Chem., 10,* 770 (1889).
7. ROTHSTEIN, E., and SAVILLE, R. W., *J. Chem. Soc.* p. 1950 (1949).
8. BROWN, N. C., *J. Am. Chem. Soc., 60,* 1325 (1938).
9. KAHRS, F., *Z. Krist., 40,* 487 (1905).
10. MARVEL, C. S., and RANDS, R. D., *J. Am. Chem. Soc., 72,* 2642 (1950).
11. THOMAS, C. A., Anhydrous Aluminium Chloride in Organic Chemistry, p. 179, Reinhold Publishing Corp., New York, 1941.
12. BISTRZYKI, A., and MANSON, L., *Ber. Chem. Ges., 40,* 4370 (1907).
13. CAMPAIGNE, E., and SUTER, C. M., *J. Am. Chem. Soc. 68,* 880 (1946).
14. LANGHLIN, K. G., and WHITMORE, F. C., *J. Am. Chem. Soc. 54,* 4462 (1932).
15. SCHNERCH, C., and HUNTRESS, E. H., *J. Am. Chem. Soc. 71,* 2233 (1949).
16. GILMAN, H., and BLATT, A. H., Organic Synthesis, Coll. Vol. I, p. 524, sec. ed., Wiley & Sons, Inc., New York, 1944.

Tryckt den 13 februari 1953

Uppsala 1953. Almqvist & Wiksells Boktryckeri AB

ARKIV FÖR KEMI Band 5 nr 29

Mitgeteilt am 22. Oktober 1952 von J. Arvid Hedvall

Selbstdiffusion in Bariummetatitanat

Von Antonio Garcia-Verduch und Roland Lindner

Mit 2 Figuren im Text

Bariummetatitanat $BaO \cdot TiO_2$ ist ein Stoff von grosser aktueller Bedeutung in der Hochfrequenztechnik, wo es als Kondensatormasse hoher Dielektrizitätskonstante Verwendung findet. Wie ein Überblick über die neuere Fachliteratur zeigt (1), ist es in letzter Zeit von verschiedenen Gesichtspunkten aus häufig untersucht worden. Die vorliegende Arbeit will einen Beitrag zur Kenntnis dieses Stoffes geben, wobei uns folgende Gedanken leiteten.

Durch Messung der Selbstdiffusion ermitteln wir Grössen, die für die Bildung des Stoffes durch Reaktion der Oxyde im festen Zustand ausschlaggebend sind. Diese Untersuchung gehen in ein grösseres Arbeitsprogramm ein, dessen Ziel die Aufklärung des Mechanismus charakteristischer Festkörperreaktionen ist.

Ausserdem geben die Messung von Selbstdiffusion und Überführungszahl Aufschluss über den Aufbau und die Fehlordnung des betreffenden Stoffes.

Die Versuchsmethodik

Das Titanat wurde durch Pulverreaktion äquimolarer Mengen analytisch reinen Bariumkarbonates und Titandioxydes bei 1365° C in Platinschiffen hergestellt. Erhitzungsdauer 2 mal 10 Stunden, unterbrochen durch Ummörsern des Pulvers. Es wurden Tabletten von 8 mm Durchmesser und etwa 2 mm Höhe gepresst (unter Zusatz von etwa 5 % Glycerin zur Erhöhung der mechanischen Festigkeit), allmählich erhitzt und 20 Stunden auf 1365° C gehalten. Die Festigkeit der Sintertabletten war gut; die Dichte etwa 5 (80 % der maximal möglichen), die Farbe leicht gelblich.

Messung der Diffusion nach der Kontaktmethode (2)

In einer geeigneten Anordnung wird eine starke radioaktiv homogen indizierte Tablette zwischen zwei inaktiven Tabletten gehalten und auf die Diffusionstemperatur erhitzt. Nach entsprechenden Zeitabschnitten werden die Tabletten voneinander getrennt und die „übergegangene" Radioaktivität gemessen, woraus bei Kenntnis der Aktivitäts-Konzentration der radioaktiven Tablette die Diffusionskonstante berechnet werden kann.

Messung der Überführungszahl

Wird die erwähnte Anordnung der Einwirkung einer hohen Gleichspannung ausgesetzt, so tritt beim Vorliegen beweglicher Ionen ein bevorzugter Übergang von radioaktiver Substanz

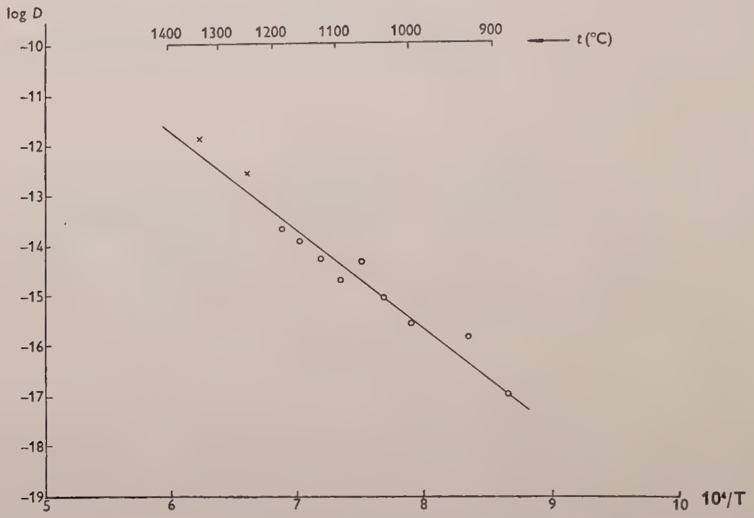

Fig. 1. Die Konstante der Diffusion von radioaktivem Barium in Bariummetatitanat, logarithmisch aufgetragen als Funktion der reziproken absoluten Temperatur.

auf die eine der beiden „Kontakttabletten“ ein, woraus sich die Überführungszahl ermitteln lässt (3).

Messung der Diffusion nach der Methode der radioaktiven dünnen Schicht (4)

Eine im Vergleich zur Dicke des Probekörpers dünne radioaktive Schicht wird auf dessen Stirnseite aufgebracht, etwa durch Überführung im elektrischen Feld (s. o.) oder durch Festsintern einer als Paste aufgetragenen Schicht, und die nach dem Diffusionsversuch eingetretene Konzentrationsverteilung ermittelt.

Dies geschieht entweder durch sukzessive Schnitte (Abschleifungen) senkrecht zur „Diffusionsrichtung“ oder — beim Vorliegen einer im festen Stoffe absorbierbaren Strahlung — durch Verfolgung der Abnahme der an der Stirnfläche des Probekörpers gemessenen Radioaktivität. —

Die Erhitzung auf die Diffusionstemperatur geschah in temperaturregulierten Rohröfen, die Messung der Temperatur mit Pt/Pt-Rh-Thermoelementen.

Zur Messung der Radioaktivität wurden dünnwandige Glocken-Zählrohre zusammen mit untersetzenden Verstärkern verwendet. —

Die Versuche

Ba–131[1] (11,7 Tage Halbwertszeit) bildet Cs–131 (10 Tage Halbwertzeit) nach, was aber für unsere Versuche keine grosse Störung bedeutet, da das Caesium auf Grund seiner γ-Strahlung (in unserer Messanordnung etwa 5 % der β-Aktivität des Bariums ausmachend) als solches erkannt und in Rechnung gestellt werden kann. —

---

[1] geliefert von der Isotope Division AERE, Harwell (England).

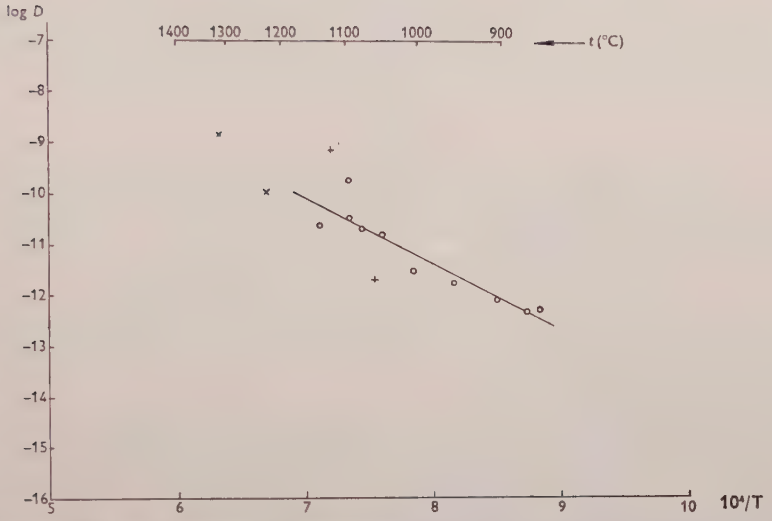

Fig. 2. Selbstdiffusion von Barium in Bariummetatitanat, berechnet aus der Ionenteilleitfähigkeit, sowie gemesssen an einem mit einer Gleichspannung vorbehandeltem Material.

Die *Kontaktmethode* wurde zwischen 884 und 1 180° C angewendet, die neun so erhaltenen Werte für die Diffusionskonstante durch zwei Versuche mittels β-Strahlungsabsorption einer dünnen Schicht (als Paste aufgetragen) bei höheren Temperaturen ergänzt. Die Werte sind in Fig. 1 in der üblichen Darstellung $\log D = f\ (1/T)$ wiedergegeben; die zugehörige Beziehung lautet:

$$D = 0{,}8\ \exp\ (-\ 89\,000\,/\,RT)\ \mathrm{cm^2 sec^{-1}}.$$

Die *Überführung* radioaktiven Bariums im elektrischen Feld zeigte ausgeprägte Effekte; Mesungen zwischen 860 und 1 135° C ergaben Werte für die Überführungszahl zwischen 1,5 und $3{,}5 \cdot 10^{-4}$ und die aus Überführungszahl und Leitfähigkeit berechnete (5) Diffusionskonstante folgt der Beziehung (Vergl. Fig. 2).

$$D = 1{,}8 \cdot 10^1\ \exp\ (-58\,000\,/\,RT)\ \mathrm{cm^2 sec^{-1}}.$$

Es liegt offenbar eine diffusionsbefördernde Veränderung (Orientierung?) des Materials durch das elektrische Feld vor, eine Annahme, die näher geprüft wurde mittels Diffusionsversuchen an Tabletten, die vorher längere Zeit der Einwirkung des elektrischen Feldes bei hoher Temperatur in Überführungsversuchen ausgesetzt worden waren. Solche Tabletten zeigten ebenfalls hohe Werte, die in Fig. 2 als liegende (β-Absorption der dünnen Schicht) oder stehende Kreuze (Kontaktversuche) eingetragen sind.

Es wurden auch eine Anzahl Versuche mit der von AERE Harwell als „Ti-51" gelieferten Aktivität gemacht.

Nach Untersuchungen von Miskel, Mateosian und Goldhaber (5) handelt es sich jedoch zum grössten Teil um verhältnismässig stark aktivierte Verunreinigungen wie Antimon und Hafnium. Daher sind unsere Messungen unter Verwendung jener Aktivität ohne grösseres reaktionskinetisches Interesse; es sei nur mitgeteilt, dass die Temperaturfunktion der Diffusion jener Atomarten einer Aktivierungsenergie von etwa 70 kcal entspricht und dass der Materietransport nicht nennenswert durch ein elektrisches Feld beeinflusst wird.

ZUSAMMENFASSUNG

In gesinterten Presstabletten von Bariummetatitanat folgt die Selbstdiffusion von Barium der Beziehung:

$$D = 0{,}8 \exp\left(-\,89\,000 / RT\right)\ \mathrm{cm^2 sec^{-1}}.$$

Es lässt sich Überführung von Bariumionen nachweisen, die Beweglichkeit des Bariums ist während und nach der Exposition des Materials in einem elektrischen Gleichfeld erhöht. —

Wir danken Prof. J. A. Hedvall für sein Interesse an der Untersuchung sowie *Statens Tekniska Forskningsråd* für die Bereitstellung von Mitteln.

Der eine von uns (A. G.–V.) genoss ein Stipendium des Spanischen Consejo Superior de Investigationes Científicas.

Abteilung „Kristallkinetik“, Institut für Silikatforschung, Chalmers Technische Hochschule, Göteborg (Schweden).

LITERATUR

1) Gmelins Handbuch der anorganischen Chemie, Band Titan, 1951.
2) Lindner, R., J. Chem. Soc. (1949) 395.
3) —— Acta Chem. Scand. *6* (1952) 468.
4) zB. Lindner, R. und Johansson, G., Acta Chem. Scand. *4* (1950) 307.
5) Miskel, J. A., der Mateosian, E., Goldhaber, M., Phys. Rev. *79* (1950) 193.

Tryckt den 13 februari 1953

Uppsala 1953. Almqvist & Wiksells Boktryckeri AB

ARKIV FÖR KEMI Band 5 nr 30

Read 12 November 1952

Starch degradation by salivary amylase. I

By Karl Myrbäck and Kerstin Svanborg

With 2 figures in the text

Human salivary amylase is a typical α-amylase; its primary action is a dextrinization of the starch components, followed by a slower hydrolysis ("saccharification") of the dextrins.

If the action of salivary amylase on starch is compared to that of certain other α-amylases, obvious differences are encountered (1). If the degree of hydrolysis in an experiment with salivary amylase is plotted against time a continuously bent curve is found whereas the corresponding curve for malt α-amylase has quite an other form. In the case of this enzyme the velocity of the saccharification is very much smaller than that of the dextrinization which explains the peculiar form of the hydrolysis curve, exhibiting a rather sharp break at about 16 per cent hydrolysis in experiments with unfractionated starch. At this point the products of hydrolysis (the "α-dextrins") mainly contain 6–10 glucose units. Small amounts of lower dextrins and fermentable sugars are present, obviously due to beginning saccharification of the primary dextrins. The low velocity of the saccharification by malt α-amylase is due to a low affinity of the enzyme to dextrins containing less than about 8 glucose units, whereas the affinity of the enzyme to long chain molecules is very much higher (2). This can be explained by the rather probable assumption (3) that several substrate-binding groups are distributed on the enzyme surface in such a way that several glucose units of a long chain molecule may be firmly attached. End groups and branching points must be supposed to disturb this attachment, causing the affinity of the enzyme to molecules of decreasing chain-length to fall off rapidly when the length of the chain between two end-groups or between one end-group and one branching point has reached a certain critical value, probably not far from 8 glucose units.

When starch is degraded by salivary amylase (and most other α-amylases) no such sharp limit between dextrinization and saccharification can be observed; the two phases overlap considerably, obviously because the velocity of hydrolysis falls off more gradually with the decreasing chain length of the substrate. However, also in these cases, the reaction begins by a more or less random hydrolysis of the long chain substrate molecules, yielding α-dextrins of the same type as those isolated after dextrinization by malt α-amylase. It should be remembered, for instance, that Waldschmidt-Leitz (4) as early as in 1934 found large amounts of hexasaccharides among the dextrinization products of pancreatic amylase. It may well be that the course of the dextrinization (whereby we understand the hydrolysis of 15–20 per cent of the glucosidic linkages of starch) is approximately the same for all α-amylases. Bernfeld and Fuld (5), for instance, have found that the ratio between the increase of reducing power and activity as estimated by an iodine colorimetric method is the same for pig pancreatic amylase, human saliva, malt α-amylase and an α-amylase from *Bacillus subtilis*. Hanes and Cattle (6), on the other hand, found the relationship color/reduction different for four α-amylases investigated by them and conclude that the processes are different. It can probably not be excluded that contamination of the α-amylases with other enzymes was the cause of the differences observed. However, as pointed out above, it is evident that in the later stages of the α-amylase reaction (the "saccharification") considerable differences exist between α-amylases of different origin. The different form of the hydrolysis curves was already observed by HANES and CATTLE, and their result in this respect is quite in accordance with a large number of investigations from this laboratory (1, 7), and the same was found also by other investigators (8).

None of the normal amylases (α or β) has any action on the α-glucosidic 1,6-linkages of the amylopectin (or glycogen). As postulated by one of us (9) in 1937, these linkages are the cause of the formation of the so-called limit dextrins, *i. e.* the non-fermentable products of the starch or glycogen degradation. Therefore every limit dextrin molecule should contain one (or in a few cases possibly more than one) 1,6-linkage. If it be assumed that the α-amylases are able to hydrolyse the 1,4-linkages adjacent to a 1,6-linkage, the isomaltose (6-α-glucopyranosido-glucopyranose) would be the only limit dextrin. If starch is supposed to contain 4.0 per cent 1,6-linkages the yield of isomaltose would be about 8 per cent. A non-fermentable disaccharide as an amylatic degradation product from starch was isolated in 1941 by AHLBORG and MYRBÄCK (10), and was shown to be, or in any case to contain as main product, isomaltose. The sugar was isolated in a pure state by HILBERT *et. al.* (11). In these investigations takadiastase was used as amylase preparation. It was stated (11) that isomaltose and glucose are practically the only products of takadiastase action. This shows the presence of maltase and possibly of other carbohydrases in the preparation. It does not seem possible to state that isomaltose is formed by an α-amylase free from all other enzymes, but it may well be the case. However, in most cases the isolated limit dextrins contain more than two glucose units. A trisaccharide was isolated in 1940 by AHLBORG and MYRBÄCK (12), and was shown to contain one maltose and one isomaltose linkage.

It may, of course, be argued that such trisaccharides are not true limit dextrins but intermediate products which can be cleaved by the α-amylases into glucose and isomaltose. If this should be true, it may be stated that the velocity of such a cleavage must be extremely low compared to that of the initial starch hydrolysis. This question compels us to consider the possibility of primary glucose formation by the α-amylases.

After O'SULLIVAN (13) had found in 1876 that maltose is the chief product of amylase action, BAKER (14) observed that glucose is formed also, and this sugar was considered by him to have its genesis in the dextrins and not in maltose. It may be stated here that no amylase has any action on maltose. LING and coworkers (15) made the important observation that glucose is formed by malt amylase which has been heated to 60° but not by "unrestricted" amylase. The enzyme used did not contain maltase. The explanation of the unique action of the "heat-restricted" amylase was given much later by OHLSON (16) who showed conclusively that "malt amylase" is a mixture of an α- and a β-amylase. The heat-restricted enzyme of LING obviously is chiefly malt α-amylase, and the formation of glucose as a primary product must be ascribed to this enzyme. This was shown definitively by MYRBÄCK (17) who also found that a mixture of α- and β-amylase produced much less glucose than the α-amylase alone, evidently because the glucose is produced chiefly from those parts of the substrate which are converted to maltose by β-amylase. This result is important for the explanation of the mechanism of glucose formation.

SHERMAN and PUNNET (18) found that amylases of malt, pancreatine and *Aspergillus oryzae* produce varying amounts of glucose from starch. Commercial and highly purified preparations gave the same glucose/maltose ratio, indicating that glucose is not produced by a separate enzyme (maltase).

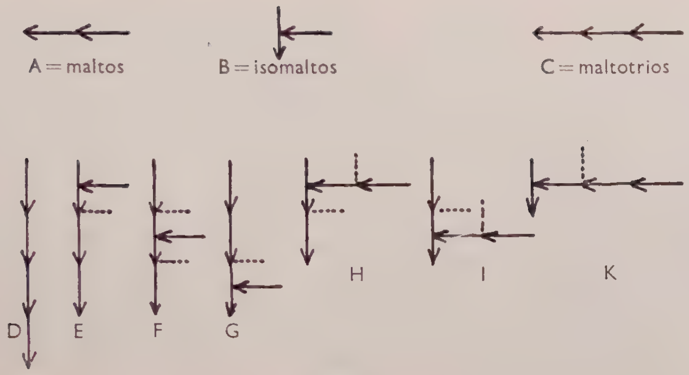

Fig. 1.

A mold amylase preparation ("Merck's diastase"), investigated in this laboratory, yielded much glucose when acting on starch. Since, however, the same enzyme solution after being heated for a few minutes to 60° gave only maltose and unfermentable dextrins and no glucose, at least not in reasonable times, it seems that glucose was formed by a contaminating maltase.

K. H. Meyer and his collaborators have repeatedly stated (19) that all known α-amylases (animal, malt, mold, bacterial enzymes) have the same action on starch, its components and its degradation products. The ideas of the Meyer school of the last stages of the reaction have been summarized by Meyer and Gonon (20): Amylose is supposed to be cleaved in a random fashion into maltose and maltotriose. The latter is supposed to be hydrolyzed at a lower rate into glucose and maltose. The ultimate degradation products of amylose by all amylases are thought to be 87 per cent maltose + 13 per cent glucose. The degradation of amylopectin is supposed to yield, in a first rapid phase, maltose, maltotriose and branched tetraoses, containing the 1,6-linkages of the substrates. Maltotriose is then supposed to yield maltose + glucose, and from the tetraoses maltose and glucose are thought to be split off according to the schematical picture in Fig. 1. The ultimate products of the amylopectin degradation (amylopectin is supposed to contain 4 per cent end-groups) should be about 19 per cent glucose, 73 per cent maltose and 8 per cent isomaltose which latter is evidently supposed to be the only real limit dextrin. If these values are calculated on starch containing 25 per cent amylose, the result would be 17.5 per cent glucose, 76.5 per cent maltose and 6 per cent isomaltose. 58–59 per cent of the glucosidic linkages of starch would be ruptured in the process.

As already stated, a great number of investigations shows that the scheme proposed by Meyer must be an oversimplification of the problem, to say the least of it. It gives, for instance, no explanation for the rather conspicuous differences between malt α-amylases and other α-amylases, observed by many investigators. Several have been mentioned in the foregoing; furthermore Hopkins and Kulka (21) have observed that, though the action of bacterial and malt amylase seems to be much the same in the earlier stages of hydrolysis, differences appear in the later stages: The malt enzyme reached a limit at 90 per cent (apparent maltose) whereas the bacterial enzyme only reached 75–80 per cent. Hockenhull and Herbert (22) regard the amylase of *Clostridium acetobutylicum* as an enzyme of its own type and are of the opinion that the glucose formation, observed with impure enzyme preparations, is due to maltase action. Whelan and Nasr (23) find that the amylase of *Clostridium butyricum* is an α-amylase but differs from either salivary or malt α-amylase in that way that its action on potato amylose and starch ceases abruptly at 65.5 and 66.5 per cent apparent maltose.

According to Meyer *et al.* (24) human salivary amylase is identical with human pancreatic amylase. Pig pancreatic amylase resembles the human enzyme in most properties but differs in some. However, the action on starch is supposed to be the same. Caldwell *et al.* (25) have investigated the hydrolysis of starch, amylose and amylopectin by pancreatic amylase. They find that maltose appears from the beginning of the reaction but glucose only in the late stages. Glucose is formed only in small amounts but is said not to be formed by the action of contaminating maltase.

The products of starch degradation by salivary amylase and the mechanism of action of this enzyme have been the objects of many investigations. Very early it was clear that maltose is the chief product, as in the case of other amylases; it was found, however, that the yield of maltose did not reach 100 per cent, at least not in reasonable times. Non-fermentable limit dextrins were formed. It is quite clear by now that the 1,6-linkages of the amylopectin (glycogen) form the *nuclei* of the limit dextrin molecules.

A most peculiar theory of the mechanism of salivary amylase action was advanced by Haworth *et al.* (26). Later on, however, Bourne, Haworth, Macey and Peat (27) retracted the paper and accepted the result from this laboratory (28) that the action of the enzyme is exclusively the rupture of 1,4-linkages, *e. g.* between ramification points of the amylopectin. The primary action of the enzyme is a dextrinization; the α-dextrins then are more or less completely saccharified, those containing 1,6-linkages giving rise to the limit dextrins.

In most cases about 20 per cent of the starch is recovered as non-fermentable dextrins after degradation by salivary amylase. If we assume that each limit dextrin molecule contains one 1,6-linkage and that ordinary starch contains 4.0 per cent 1,6-linkages we have to conclude that the limit dextrins should contain, on the average, 4–5 glucose units per molecule.

As pointed out in many connections it is not quite easy to know when the action of an α-amylase has reached its definite end-point. It could be that the limit dextrins, containing three or more glucose units per molecule, are only apparently stable toward the salivary amylase, possibly because of the inhibiting action of the large amounts of maltose present. Experiments with isolated limit dextrins show, however, that though a certain hydrolysis of the limit dextrins by large amounts of salivary amylase can be observed, the rate of this secondary conversion is extremely low, so low in fact that one feels bound to ask if the action is really due to the salivary amylase itself. In this connection it seems important to note that according to Meyer, Duckert and Fischer (29) raw human saliva and the crystalline salivary amylase have exactly the same action on starch.

Concerning the formation of glucose by salivary amylase the situation is somewhat confused. In any case it seems to be established that glucose is not formed in the first stages of starch hydrolysis. In this connection the salivary amylase resembles the pancreatic enzyme but differs sharply from the malt α-amylase which forms appreciable amounts of glucose from the very beginning of the hydrolysis (17, 30). ÖRTENBLAD and MYRBÄCK (31) state that salivary amylase, acting on α-dextrins from starch dextrinization by malt α-amylase, produces no glucose. It might be said, however, that a true limit of saccharification might not have been reached in these experiments, but they show that the last stages of hydrolysis of the branched α-dextrins are at least extremely slow. In experiments with starch paste and salivary amylase MYRBÄCK, ÖRTENBLAD and THORSELL (32) found, after prolonged action of the enzyme, 63 per cent maltose, 14 per cent glucose and limit dextrins containing four or more glucose units. It was supposed that glucose had been formed by action of contaminating maltase, but it does not seem to be excluded that glucose could have been split off from the dextrins in the last stages of the reaction.

A most important contribution to the question of glucose formation by salivary amylase has been made by ROBERTS and WHELAN (33) who state that the enzyme is entirely without action on maltotriose and that the ultimate products of the enzyme action on amylose is maltose and maltotriose in the molecular ratio 2.39/1. This result contradicts absolutely the statement by MEYER and GONON (20) regarding the action of α-amylases on maltotriose (see above). It should be emphasized here that if salivary amylase is unable to split any one of the two linkages in maltotriose (formula C in Fig. 1) then it seems impossible that it could split off glucose from the dextrin molecule *F* and rather improbable that it should have an action on *H* or *I*.

The question of the glucose formation from maltotriose and/or from dextrins is, of course, connected with the question of the ultimate limit dextrins of salivary amylase. Earlier experiments from this laboratory have given the impression that salivary amylase leaves more of the starch substance in the form of non-fermentable dextrins than do the other α-amylases investigated, and that the salivary limit dextrins have higher average molecular weight than, for instance, those formed by malt α-amylase. All authors agree that salivary amylase is an extremely stable enzyme; therefore it does not seem probable that our experiments should have led to false equilibria caused by destruction of the enzyme. On the other hand, it can not be said with absolute certainty that the enzyme action was ended when the limit dextrins were isolated. We have now performed a series of new experiments, using highly purified salivary amylase in very large amounts. Glucose and maltose were determined in fermentation experiments, and the amount and average chain lengths of the non-fermentable dextrins were determined after the fermentations.

Assay method. Human salivary amylase was purified according to MEYER *et al.* (34). The enzyme used in the following experiments was a concentrated solution corresponding to stage VII of the MEYER method. Its activity was Sf = 100 as defined by EULER and SVANBERG (35). Buffer: 0.5 *M* phosphate, pH = 6.9. Substrate: Native potato starch. Composition of the assay mixture:

100 ml starch paste, about 2 per cent.
20 ml phosphate
40 ml 0.1 *N* sodium chloride solution
Water
Enzyme solution (toluene)
200 ml

Reaction temperature 30°. Average degree of hydrolysis was determined by the WILLSTÄTTER and SCHUDEL titration method in small samples. The reduction values were calculated as glucose. Degree of hydrolysis = glucose as per cent of the theoretical (= starch × 1.11). After suitable times samples (10–50 ml) were taken and concentrated to remove all toluene. The residues were dissolved in a small volume of water (2 or 5 ml) and the same volume of a suspension of baker's yeast in water (1 : 1) was added. The carbon dioxide evolution was measured as described previously (17). The baker's yeast employed ferments maltose so much more slowly than glucose that both sugars may be determined. In some of the experiments fermentations were also carried out with *Saccharomyces marxianus* which ferments only glucose. The glucose values of both methods always agreed well; on the other hand it must be conceded that the accuracy of the glucose values is not very high, probably ± 5 per cent or so. To all fermentation experiments parallels were carried out with known amounts of glucose and maltose.

After the fermentations had stopped the yeast was removed by suction through a layer of diatomaceous earth. Filtrate and washings were evaporated to dryness and the residue was dissolved in a known volume of water. The reducing power was determined by the iodine method of WILLSTÄTTER and SCHUDEL and by the copper method of SOMOGYI. It seems that sometimes during the fermentations small amounts of substances are excreted or formed by the yeast that consume a certain amount of iodine. The iodine values therefore tend to be higher than the copper values which should be more correct. In the following tables only the copper values are given.

Samples were hydrolysed completely in N sulfuric acid at 100° and the reducing value was determined. From the values before and after hydrolysis the mean degree of polymerization of the non-fermentable dextrins was calculated. The amounts of glucose, maltose and dextrins are always calculated as the corresponding amount of glucose, *i.e.* maltose always as maltose-hydrate *etc.*

In a series of experiments varying amounts of the concentrated amylase solutions were used (Table 1). A few hundredths of a ml of the enzyme solution obviously give reaction rates of an order of magnitude usual in experiments of this kind. However, in order to obtain as complete a conversion of the starch as possible, large amounts of enzyme (0.4 or 2.0 ml, respectively) were used in

Table 1

ml enzyme	0.02	0.05	0.4	2.0	2.0
time	% linkages ruptured				
4 min.	—	—	11.0	22.0	—
7 ,,	1.8	3.6	18.4	26.7	—
10 ,,	3.0	5.0	23.9	28.8	—
20 ,,	6.6	9.2	31.6	41.1	—
30 ,,	7.8	12.6	33.8	—	—
60 ,,	13.0	22.0	—	—	—
24 hrs	36.0	39.4	44.6	~50 (I)	~52 (III)
120 ,,	—	—	49.7 (II)	—	—
144 ,,	—	—	—	~52 (V)	—
168 ,,	—	—	—	—	~53 (VI)
216 ,,	—	—	51.2 (IV)	—	—
528 ,,	—	—	—	—	~54 (VII)

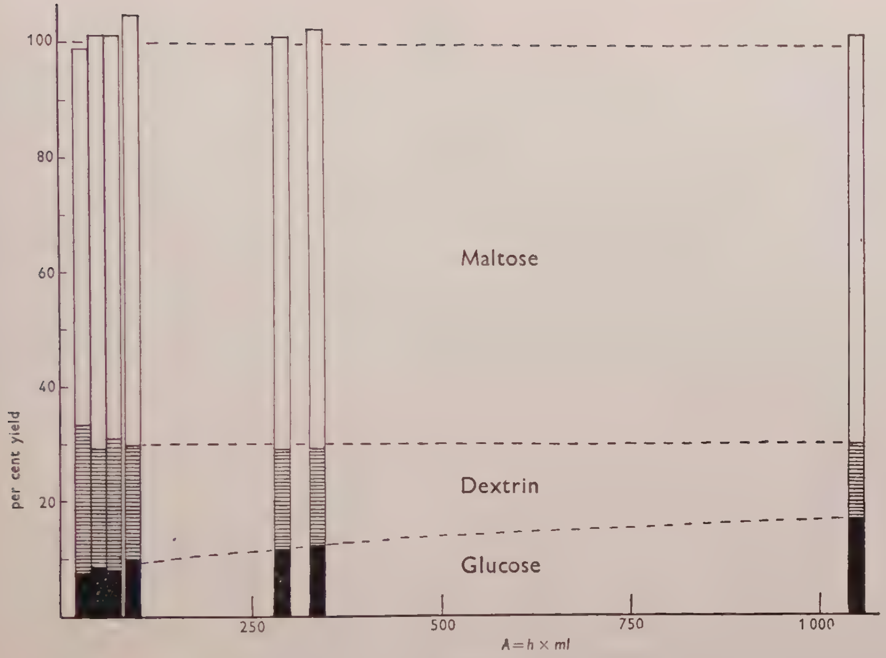

Fig. 2.

some experiments, in which fermentable sugars and residual dextrins were determined.

It appears that, at least under the experimental conditions applied here, the average degree of hydrolysis does not exceed 54 per cent (= relative number of linkages ruptured). Since this value was determined by the iodine method, it is certainly not too low. Nevertheless it is considerably lower than that (58–59 per cent) calculated on the assumption by MEYER *et al.* (20). This shows that no such complete degradation of starch occurs with salivary amylase as supposed by MEYER. In other words, isomaltose can not be the only product besides maltose and glucose.

In certain experiments, indicated by Roman numerals in Table 1, determinations of fermentable sugars and dextrins were made. To compare the intensity of the enzyme action in the different experiments, the value *A = ml enzyme* × *reaction time* (*hrs*) was calculated and taken as a measure of the enzyme activity. Glucose and maltose were determined as described above (Table 2).

The following results appear from Table 2:

1) Glucose is formed although the enzyme preparation was free from maltase. Therefore ist must be concluded that during the degradation glucose is split off from dextrin molecules. According to ROBERTS and WHELAN (33) maltotriose is excluded as the source of glucose. In our experiments a very slow formation of glucose goes on for a considerable time and the amount of non-fermentable dextrins decreases.

2) From Table 2 and more clearly from Fig. 2 it is seen that the amount of maltose does not decrease with time. This is in agreement with the statement that the enzyme solution does not contain maltase. The possibility that

Table 2

Experiment No.	I	II	III	IV	V	VI	VII
"Enzyme action" (A)	48	48	48	87	288	336	1050
Average degree of hydrolysis	52	50	52	51	52	53	54
% Glucose = a)	7.2	7.7	7.3	9.8	11.6	12.3	16.8
% Maltose hydrate = b)	66.1	73.0	70.0	77.4	72.0	73.0	72.0
Reducing power of dextrins: before hydrolysis	4.3	3.8	4.2	3.3	4.0	3.3	2.5
Reducing power of dextrins: after hydrolysis = c)	25.8	20.7	23.8	17.8	17.4	17.0	13.2
Average number of glucose units in the residual dextrins	6.0	5.5	5.7	5.4	4.4	5.1	5.3
Total: a) + b) + c)	99.1	101.4	101.1	105.0	101.0	102.3	102.0

maltose would be formed and degraded at the same rate seems remote. The final yield of maltose appears to be about 73 per cent.

3) The sum of glucose + maltose + dextrins (= a + b + c) is approximately 100 per cent in all experiments. Since all three terms were determined independently, this seems to exclude the possibility of grave errors in the determinations. (The maltose value of experiment IV might possibly be an exception!)

4) In experiments with normal reaction times and normal amounts of enzyme (I–IV) the yield of non-fermentable dextrins is 20 per cent or more. This is in agreement with the statement (v. EULER, WILLSTÄTTER) that the "saccharification limit" is, for practical purposes, somewhere in the neighborhood of 75 per cent (the value 75 per cent was calculated on starch and not as here on the theoretical amount of glucose).

5) In the experiments with extremely high enzyme concentration and extremely long reaction times, the amount of non-fermentable limit dextrins decreases very slowly.

6) The yield of glucose in the "normal" experiments is 7–9 per cent. When enzyme concentration and reaction time are increased, the yield of glucose increases parallel to the decrease of the yield of dextrins. This formation of glucose is extremely slow compared to the initial rate of starch degradation. We find, for instance, that in the experiment with 2 ml enzyme solution about 10 per cent of glucose is formed in 500 hrs (difference between VII and III). The initial rate of starch hydrolysis by 0.02 ml enzyme solution is 3 per cent apparent glucose in 10 minutes. If the rates are referred to the same amount of enzyme we find that the ratio between the initial rate of starch degradation and the rate of the residual dextrin hydrolysis is something like 10^5. Even if the enzyme preparation used had a very high degree of purity, it seems to us that we may well ask if the extremely slow action on the dextrins is really an action of the salivary amylase itself.

It might be argued that in all these experiments the rather large amounts of maltose and glucose present inhibit the amylase so strongly as to cause the establishment of a state of a false equilibrium. Therefore the following experiment was performed in which the action of salivary amylase on the dextrins, free from fermentable sugars, was studied. 10 ml of the degradation mixture from experiment VII (528 hrs) was treated with baker's yeast until free from sugars. The yeast was removed, and the filtrate was evaporated to dryness. The residue (13.2 per cent of the original amount of starch) was dissolved in 25 ml of water. 20 ml of this solution was mixed with 3 ml phosphate buffer, 6 ml 0.1 N sodium chloride solution and 1 ml of the enzyme solution used in the above experiments. The mixture was kept at 25° and the reduction was determined in 0.3 ml samples by the SOMOGYI method. The reduction values were calculated as glucose in per cent of the theoretical value (Table 3).

Table 3

Time	per cent glucose
0	19.1
1 h	19.1
72 h	24.8
120 h	25.8

It appears clearly that, even in this experiment with a relatively enormous enzyme concentration and a very long reaction time, the increase of the reducing power is very small. The average chain length of the dextrins at the beginning of the experiment was 5.25. The splitting off of one molecule of glucose (or maltose) would, of course, have caused an increase of the apparent glucose content from 19.1 to 38.2 per cent. Thus we may conclude that a rupture of one glucosidic bond has occurred only in a small number of the dextrin molecules. It seems to us inevitable to conclude that the residual dextrins isolated, amounting to some 15 per cent of the original starch, are, to all practical purposes, *stable* dextrins. A considerable proportion of the starch is left by the salivary amylase as such dextrins, containing about 5 glucose units each.

If it be assumed that the starch used in these experiments contains 4 per cent isomaltose linkages and that each isomaltose linkage causes the formation of a limit dextrin with about 5 glucose units, then a yield of about 20 per cent of dextrins would be expected. As mentioned already, approximately this yield of dextrins is obtained in experiments with reasonable amounts of enzyme and reasonable reaction times. If the amount of enzyme is very high and the reaction time is prolonged extraordinarily, a very slow degradation of these primary limit dextrins occurs. It seems that some limit dextrin molecules are broken down almost completely, as the average chain length of the non-fermentable products does not decrease considerably (Table 2).

SUMMARY

The statement repeatedly made by K. H. MEYER *et al.* that all α-amylases have the same action on starch, and that glucose, maltose and isomaltose are the only true reaction products, is not correct. When starch is degraded by

salivary amylase the yield of maltose is about 73 per cent whereas about 15 per cent appear as non-fermentable residual dextrins, having an average chain length of about 5 glucose units. If these residual dextrins are attacked at all by the salivary amylase, which seems doubtful, the ratio of the degradation velocity to the initial velocity of starch degradation is less than 10^{-5}. Inhibition of the enzyme by maltose or glucose has nothing to do with the formation of the residual dextrins.

Institute of Organic Chemistry and Biochemistry, University, Stockholm.

REFERENCES

1. Myrbäck, K. and Neumüller, G., in Sumner, J. B. and Myrbäck, K., *The enzymes,* Acad. Press, New York 1950/1951, Vol. I, p. 653.
2. Myrbäck, K. and Johansson, N. O., Arkiv Kemi, Mineral. Geol. *20 A,* N:o 6 (1945).
3. Myrbäck, K., Arkiv Kemi *2,* 417 (1950).
4. Waldschmidt-Leitz, E. und Reichel, M., Z. physiol. Chem. *233,* 76 (1934).
5. Bernfeld, P. and Fuld, M., Helv. Chim. Acta *31,* 1423 (1948).
6. Hanes, C. S. and Cattle, M., Proc. Roy. Soc. *125 B,* 387 (1938).
7. Myrbäck, K., Advances Carbohydrate Chem. *3,* 251 (1948).
8. Schwimmer, S., Cereal Chem. *24,* 315 (1947); Schwimmer, S. and Balls, A. K., J. Biol. Chem. *176,* 465 (1948); *179,* 1063 (1949).
9. Myrbäck, K., Current Sci. *6,* 47 (1937).
10. Ahlborg, K. and Myrbäck, K., Biochem. Z. *308,* 187 (1941).
11. Montgomery, E. M., Weakley, F. B., and Hilbert, G. E., J. Am. Chem. Soc. *69,* 2249 (1947); *71,* 1682 (1949).
12. Myrbäck, K. and Ahlborg, K., Biochem. Z. *307,* 69 (1940).
13. O'Sullivan, J., J. Chem. Soc. *29,* 478 (1876); *30,* 125 (1876).
14. Baker, J., J. Chem. Soc. *81,* 1177 (1902).
15. Ling, A. R., J. Inst. Brewing *9,* 446 (1903); Davis, B. F. and Ling, A. R., J. Chem. Soc. *85,* 16 (1904).
16. Ohlsson, E., Compt. rend. soc. biol. *87,* 1183 (1922); Compt. rend. trav. lab. Carlsberg Sér. Chim. *16,* N:o 7 (1926); Z. physiol. Chem. *189,* 7 (1930).
17. Myrbäck, K., Biochem. Z. *307,* 140 (1941).
18. Sherman, H. C. and Punnet, P. W., J. Am. Chem. Soc. *38,* 1877 (1916).
19. Cf. for instance, Meyer, K. H., Fuld, M., and Bernfeld, P., Experientia *3,* 411 (1947).
20. Meyer, K. H. and Gonon, W. F., Helv. Chim. Acta *34,* 308 (1951).
21. Hopkins, R. H. and Kulka, D., J. Inst. Brewing *48,* 170, 174 (1942); Wallerstein Lab. Commun. *5,* 115 (1942).
22. Hockenhull, D. J. D. and Herbert, D., Biochem. J. *39,* 102 (1945).
23. Whelan, W. J. and Nasr, H., Biochem. J. *48,* 416 (1951).
24. Meyer, K. H., Fischer, E. H., Bernfeld, P., and Duckert, F., Arch. Biochem. *18,* 203 (1948).
25. Alfin, R. B. and Caldwell, M. L., J. Am. Chem. Soc. *70,* 2534 (1948); *71,* 128 (1949).
26. Haworth, W. N., Kitchen, H., and Peat, S., J. Chem. Soc. *1943,* 619.
27. Bourne, E. J., Haworth, W. N., Macey, A., and Peat, S., J. Chem. Soc. *1948,* 924.
28. Myrbäck, K., The Svedberg 1884 30/8 1944, Uppsala 1944, p. 474.
29. Meyer, K. H., Duckert, F., and Fischer, E. H., Helv. Chim. Acta *33,* 207 (1950).
30. Myrbäck, K., Biochem. Z. *311,* 227, 242 (1942).
31. Örtenblad, B. and Myrbäck, K., Biochem. Z. *315,* 233 (1945).
32. Myrbäck, K., Örtenblad, B., and Thorsell, W., Biochem. Z. *316,* 424 (1944).
33. Roberts, P. J. P. and Whelan, W. J., Biochem. J. *49,* lvi (1951); *51,* xviii (1952).
34. Meyer, K. H., Fischer, E. H., Bernfeld, P., and Staub, A., Experientia *3,* 455 (1947); Meyer, K. H., Fischer, E. H., Staub, A., and Bernfeld, P., Helv. Chim. Acta *31,* 2158 (1948).
35. v. Euler, H. and Svanberg, O., Z. physiol. Chem. *112,* 193 (1920).

Tryckt den 13 februari 1953.

Uppsala 1953. Almqvist & Wiksells Boktryckeri AB

ARKIV FÖR KEMI Band 5 nr 31

Communicated 22 October by JOHN RUNNSTRÖM and KARL MYRBÄCK

The formation of tyrosine in *Rhodospirillum rubrum* grown on acetate and carbon dioxide, isotope labelled, under anaerobic condition

By GÖSTA EHRENSVÄRD and LEMBITU REIO

With 1 figure in the text

In a series of previous experiments utilizing isotope techniques (1, 2, 3), the formation of amino acids in *Rhodospirillum rubrum*, grown on acetate and carbon dioxide as the sole sources of carbon, has been described. Extensive degradations, and subsequent localization of isotope content (from labelled substrates) in different carbon atoms of the amino acids isolated, enabled a primary evaluation of the over-all features of *Rhodospirillum* metabolism under the conditions employed. The labelling patterns of glycine, alanine, serine, threonine, valine, leucine, aspartic acid and glutamic acid gave, in addition, some information as to the main route of the photodirected fixation and subsequent utilization of carbon dioxide.

Among the amino acids isolated from the two series of cultivation: $C^{13}H_3C^{14}OOH + CO_2$ and $CH_3COOH + C^{14}O_2$, 69 and 152 mg of tyrosine were obtained. These amounts were diluted with non-labelled tyrosine and subjected to degradation according to methods previously described (4), in order to determine, in separate carbon atoms, the C^{14}-content as derived from the acetate carboxyl and from carbon dioxide. With regard to C^{13} — from the acetate methyl group — its determination in separate carbon atoms of the diluted samples 1:10 would give values too low to be accounted for as significant determinations. Yet, since acetate and carbon dioxide were the sole sources of carbon, we have, knowing the values of C^{14} from acetate carboxyl and carbon dioxide, calculated the contributions of acetate methyl carbon to different tyrosine carbon atoms in an indirect way. The result of the degradation procedure, as carried out on the two samples of tyrosine, is shown in tables I and II.

Discussion

The values from the direct estimation of C^{14} in the tyrosine carboxyl and the α-carbon atom indicate that the former is to its main extent derived from carbon dioxide, the latter from the acetate carboxyl; an arrangement that has its counterpart in the corresponding patterns of most amino acids in *Rhodospirillum* (2, 3). As to the β carbon atom this should be C^{14}-free, if an analogy should be drawn with alanine and serine, where the β carbon is entirely derived from the acetate methyl group. The small, but significant, C^{14}-content in the tyrosine β-carbon atom indicates

Table I

Isotope content, determined and calculated, in different degradation products of tyrosine, isolated from *Rhodospirillum rubrum,* grown on acetate and carbon dioxide as the sole source of carbon. The figures given below refer to C^{14}-content, originating from the carboxyl of acetate, and C^{14} from carbon dioxide. All figures denote counts per minute per 15 mg of barium carbonate. C_{total} denotes total carbon as barium carbonate by combustion, C_{COOH} carboxyl carbon.

Series	Compounds investigated		Positions of carbon atoms in tyrosine	Tyrosine from	
				labelled acetate + non-labelled CO_2	non-labelled acet + labelled CO_2
A	Tyrosine, C_{total}		All atoms	920	850
B	Tyrosine, C_{COOH}		Carboxyl	255	2750
C	Acetic acid, C_{COOH}		Carboxyl	300	...
D	Acetic acid, C_{CH_3}		α	1450	...
E	4-hydroxy-benzoic acid carboxyl		β	285	910
F	4-hydroxy-benzoic acid C_{total}		Ring, β	(920)	(570)
G	3.5-dinitro-4-hydroxy-benzoic acid, C_{total}		Ring, β	820	665
H	Picric acid, C_{total}		Ring = R	860	635
I	Tribromo-phenol, C_{total}		Ring = R	940	680
K	Bromopicrin, from 3.5-dinitro-4-hydroxy-benzoic acid C_{total}		3.5	1490	756
L	Bromopicrin, from picric acid C_{total}		1.3.5	1540	505
M	CO_2 from split L		2.4.6	395	765
N	Trimethyl-pyruvic acid, C_{COOH}, taken at intervals of 30 min. 1.		2.6	700	100
	2.			640	...
	3.			650	...
O	Trimethyl-acetic acid, C_{COOH}		1.	1310	75
Compiled C^{14}-values, calculated on the basis of the following:					
B	C		Carboxyl	*255* 300	*2750*
D	9 A–6R–E–B	9 A–7 F–B	α	*1450* 1920 *1585*	... *245* *80*
E	7 F–6 I	6 G–6 H	β	*285* (800) *380*	*910* (180) 575
O	3 L–2 K	6 R–3 M–2 K	1	*1310* 1640 1805	*75* (–15) *55*
N	½(6 R–3 L–P)	½(6 R–2 K–O–P)	2.6	*670* *600* 825	*100* 145 *120*
K	½(6 R–O–3M)		3.5	*1490* *1660*	*750* 920
P = 3 M–2 N	6 R–3 L–2 N	6 R–O–2 N–2 K	4	–155 –140 190 (= 0)	2095 2185 2125 (=

however, that the C_3-side-chain may not be directly related with the C_3-structure of pyruvic acid, as one would expect from the — unsupported — assumption of a C_6+C_3 condensation leading up to the carbon skeleton of tyrosine. A C_7+C_2 condensation, the C_2-fragment being related to acetate, might as well furnish an explanation (5).

Table II

Isotope content and specific activity in different carbon atoms of tyrosine from *Rhodospirillum rubrum*, grown in two series with labelled acetate and nonlabelled CO_2 and labelled CO_2 and nonlabelled acetate. Values are complied from Table I. C^{13} is given in atom per cent excess, C^{41} in count per minute per 15 mg of barium carbonate. $'C^{13}$ and $'C^{14}$ denote the isotope content in per cent of the corresponding isotope content of the methyl group and the carboxyl group of the labelled acetate present as substrate in the medium at the start of the experiment.

Acetate CH_3–	—	—	3.55			100	Total activity estimated**
–COOH	—	26300	—		100		
Bicarbonate CO_2	26100	—	—	100			
Separate carbon atoms of tyrosine	C^{14}	C^{14}	C^{13}	$'C^{14}$	$'C^{14}$	$'C^{13}$	$'C^{14} + 'C^{14} + 'C^{13}$
All atoms	850	920	0.17	3.2	3.5	4.8	**11.5**
Ring	650	970		2.5	3.7	(5.3)	11.5
COOH	2750	250		10.5	0.9	(0.1)	11.5
α	150	1500		0.6	5.7	(5.2)	11.5
β	900	300		3.5	1.1	(6.9)	11.5
2.6	120	650		0.5	2.5	(8.0)	11.5
3.5	750	1550		2.9	5.9	(2.7)	11.5
1	50	1350		0.2	5.1	(6.2)	11.5
2*	—	—		—	—	(11.5)	11.5
3*	—	3100		—	11.5	—	11.5
4	2100	0		8.1	0.0	(3.4)	11.5
5*	1500	100		5.8	0.3	(5.4)	11.5
6*	260	1300		1.0	5.0	(5.5)	11.5
Mean value for C_{total}, obtained from isotope determinations				3.3	3.3	(4.9)	11.5

* Denote the distribution in carbon atoms 1 to 6, according to discussion in text.

** The value 11.5 accepted as the basis for calculation of $'c^{13}$- values.

With regard to the ring atoms one has, initially, to consider the isotope distribution in the carbon atoms 2.6 and 3.5. The symmetry of the phenolic ring along the 1–4-axis obviously prohibits any direct localization of the estimated isotope content of 2.6 in 2, or 6, or both. The same holds for 3.5. Thus one is faced with the task of constructing different theoretical alternatives of the actual isotope distribution within the ring, and weighing these alternatives against each other. Fig. 1.

In evaluating which of the above five alternatives should be regarded as the most probable, one has to recall the indications with regard to the interconnection between glucose, glucose fragments and the aromatic ring as derived from isotope data obtained by degradation of tyrosine from aerobic microorganisms. In *Escherichia coli*, *Neurospora crassa* (5) and *Torulopsis utilis* (6) the isotope distribution in different carbon atoms of the tyrosine ring — as derived from labelled acetate — is compatible with the view that the carbon atoms 3.4 of glucose should contribute to carbon atoms 4.5.6 of the aromatic ring, and that the glucose carbon 1 should enter the

Fig. 1.

Schematic representation of possible alternatives of isotope distribution in individual carbon atoms of tyrosine, based on the experimental data of tables I and II. A comparison is made with two theoretically possible cases of $C_5 + C_2$ and $C_4 + C_3$ condensation of hexose fragments, labelled from CO_2 predominantly in 3.4; from acetate carboxyl in 2 (and 5), from CH_3 in 1 (and 6), hexose nomenclature.

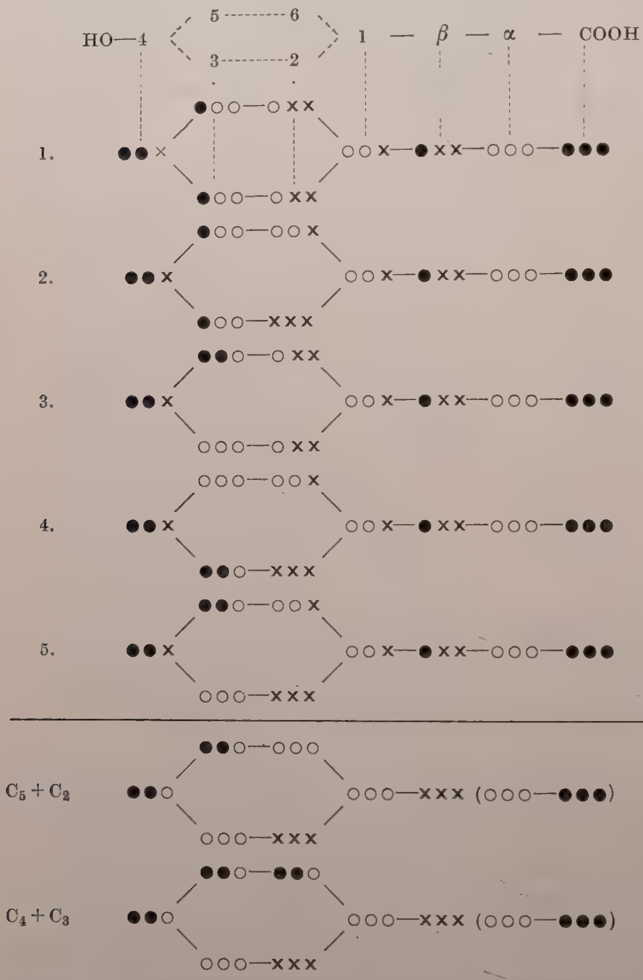

As estimated; 2.6 and 3.5 are taken as mean values of 2 and 6, and 3 and 5.

Written with the assumption that carbon atoms 2.3.4.5 originate from hexose atoms 1.2.3.4 or 6.5.4.3.

In both these alternatives the labelling of triose is assumed to be ●●○—○○○—× × ×, and hexose: × × ×—○○○—●●○ —●●○—○○○—× × ×, in accordance with the assumption that some acetate carboxyl carbon will enter glucose carbon atoms 3.4.

● = CO_2-origin, ○ = origin from acetate carboxyl, × from acetate methyl group.

2-position of the ring (7). This, in turn, points to a participation of two glucose fragments forming a C_7-structure (9) later to form the ring + β of tyrosine (5, 8). This view, although tentatively formulated, might give a lead to the choice between the five different alternatives of isotope-distribution in the tyrosine ring, with regard to *Rhodospirillum*. Denoting an origin from the acetate methyl group and the carboxyl with × and ○, respectively, and an origin from carbon dioxide with ●, the labelling pattern of pyruvate in *Rhodospirillum* — as confirmed by the pattern of alanine and serine — should be: ×–○–●. Consequently one would find the patterns for triose and hexose-structures to be ×–○–● and ×–○–●–●–○–×.

Thus the C_4-fragments from hexose, formed by the carbon atoms 1.2.3.4, or 6.5.4.3 would possess a labelling according to: ×–○–●–●; the corresponding C_5-fragments: ×–○–●–●–○. By this regard a C_4+C_3 condensation — as outlined for aerobic systems — and a C_5+C_2 condensation, both resulting in C_7-structures, would result in two different patterns of isotope distribution within the ring + β; these patterns should be compared to the five patterns constructed on the basis of experimental evidence. Fig. 1, C_5+C_2; C_4+C_3.

As seen none of the five alternatives of isotope distribution based on experimental data agrees fully with the two cases, theoretically constructed. The alternative 5 comes closest to fitting in with the C_5+C_2 mechanism, although a small amount of CO_2-carbon in 2.6, if entirely confined to 6, precludes any purely C_5+C_2 condensation. A contribution from a C_4+C_3-condensation should, on the other hand, bring in a ●-labelling in 6. With regard to the ring atoms 2.3.4.5 the labelling found in 2.6; 3.5; and 4 would fit with the sequence ×–○–●–● from a C_4, and also with a C_5-fragment of glucose origin.

Taken together, the isotope data from tyrosine isolated from *Rhodospirillum* point to a mechanism of the formation of the aromatic ring that has some points in common with the corresponding mechanism functioning in aerobes. This is, however, to be expected in view of the analogies found with regard to the principles of amino acid formation in *Rhodospirillum* and in aerobic systems. As pointed out before (2,3) the main difference between the two cases — as revealed by isotope analysis — arises as a consequence of CO_2 entering the *Rhodospirillum* metabolism in two ways: by a C_2+C_1-condensation, and by a secondary C_3+C_1 mechanism, possibly the pyruvate-oxal-acetate reaction. The sequence: β–α–COOH in some amino acids, that in the experiments with aerobes becomes ×–×–○, is in *Rhodospirillum* ×–○–●. Other data fit completely with the views accepted for the formation of other amino acid structures in aerobes. Therefore it could reasonably be assumed that the formation of tyrosine in *Rhodospirillum* would — in principle — follow the metabolic mechanisms functioning in aerobes. With this in mind, the isotope distribution in the carbon atoms 1; 2.6; 3.5; and 4 of the phenolic ring should be in agreement with the labelling of 2.3.4.5 according to: ×–×–○–○ in aerobes and ×–○–●–● in *Rhodospirillum*. The ring atom 1 should be × in aerobes and ○ in *Rhodospirillum*, still in agreement with experiments. The difference with regard to carbon atom 6 (○ instead of the expected ● in *Rhodospirillum*: ○ in aerobes) might be explained as a consequence of a C_5+C_2-condensation prepondering over C_4+C_3. With regard to the sidechain the α and COOH of *Rhodospirillum* is, as expexted, ○ and ●; × and ○ in aerobes. The minor amount of ● in β, mainly ×, cannot be explained at present.

SUMMARY

From *Rhodospirillum rubrum* cultivated in two series: 1. $C^{13}H_3C^{14}OOH+CO_2$ and 2. $CH_3COOH+C^{14}O_2$, two preparations of tyrosine have been isolated. After full degradation the isotope content was determined in carbon atoms COOH, α, β,

1; 2.6; 3.5; and 4, whereby it was found that CO_2-carbon had entered into COOH, 4, and either, or both, of 3.5. Labelling from acetate carboxyl was found in either, or both, of 3.5, in either, or both, of 2.6; furthermore in α. By indirect calculation the β-carbon atom was found to have, predominantly, an origin from the methyl group of acetate.

Of the different alternatives of labelling in the separate carbon atoms 1.2.3.4.5.6, that could be constructed on the basis of these experiments, one pattern has many features reminding of the labelling of tyrosine and its aromatic ring in aerobic systems, grown on labelled acetate. The view that the aromatic ring, + the β-carbon, might arise from combinations of hexose fragments — C_3+C_4, or more likely, C_5+C_2 — is in agreement with the experimental data obtained.

The authors express their gratitude to the State Scientific Council and the State Medical Council for generous support for this work, and the two previous investigations, on which this communication is based (4, 5).

BIBLIOGRAPHY

1. Cutinelli, C., Ehrensvärd, G., and Reio, L., Arkiv Kemi *2*, Nr 21, 357 [1950].
2. Cutinelli, C., Ehrensvärd, G., Reio, L., Saluste, E., and Stjernholm, R., Arkiv Kemi *3*, Nr 53, 501 [1951].
3. Cutinelli, C., Ehrensvärd, G., Högström, G., Reio, L., Saluste, E., and Stjernholm, R., Arkiv Kemi *3*, Nr 53, 501 [1951].
4. Reio, L., and Ehrensvärd, G., Arkiv Kemi *5*, Nr 28, 301 [1953].
5. Ehrensvärd, G., and Reio, L., Arkiv Kemi *5*, Nr 20, 229 [1953].
6. Baddiley, J., Ehrensvärd, G., Klein, E., Reio, L., and Saluste, E., J. Biol. Chem. *183*, 777 [1950].
7. Gilvarg, J., and Bloch, K., J. Am. Chem. Soc. *72*, 5791 [1950].
8. Ehrensvärd, G., Symposium sur le Métabolisme Microbien, II^{e} Congrès International de Biochimie, p. 72 [1952].
9. Horecker, B. L., and Smyrniotis, P. Z., J. Am. Chem. Soc. *74*, 2123 [1952].

The Wenner-Gren Institute, Department of Physiological Chemistry, University of Stockholm, Sweden.

Tryckt den 16 februari 1953

Uppsala 1953. Almqvist & Wiksells Boktryckeri AB

ARKIV FÖR KEMI Band 5 nr 32

Communicated 8 October 1952 by ERIK HULTÉN and KARL MYRBÄCK

The influence of anesthetics on monomolecular films of cell lipids

By STEN GATENBECK and LARS EHRENBERG

With 5 figures in the text

The present investigation is a preliminary attempt to study the reactions between anesthetics and substances, that may be assumed to be the points of attack of the anesthetics within the living cells.

Since the Meyer-Overton theory is valid in principle for anesthesia (*cf.* MEYER and HEMMI (1), LEVAN and ÖSTERGREN (2), an interaction of the anesthetics with the lipids and lipoproteins of the cells is probably involved. The divergencies from the Meyer-Overton theory are, as a rule, minor, but in cases where they are significant a certain reaction with the pure protein components may be involved, too. As a further corollary of the Meyer–Overton theory it may be observed that the anesthetics interact with the cell constituents through those weak forces which have often been named van der Waal's forces. Interactions of this kind are difficult to study in bulk, whereas the penetration of surface films may yield valuable information on the reactions in question. Several biologic problems have been elucidated with this technic by SCHULMAN, RIDEAL and coworkers (3, 4, 5).

In the present investigation we compressed films of cholesterol, and of two purified cephalin fractions from ox brain (phosphatidyl serine and inositol phosphatide), on substrates containing anesthetics (ethanol, procaine, xylocaine) in different concentrations around the minimum concentration for anesthesia.

Methods

The anesthetics were dissolved in sodium phosphate buffers (0.01–C) with a pH of 7.4. The final solutions were obtained as mixtures of pure ethanol and phosphate buffer, or nearly saturated solutions in buffer at pH 7.4 of the local anesthetics, procaine and xylocaine, and buffer solution, respectively. The pH of the substrates thus prepared was found to lie within the limits 7.3–7.5. Here, of course, the strongest concentration of ethanol is excluded. At different points during compression the surface pressure and the surface potential were measured.

The surface pressure was measured with a vertical film balance (HARKINS (6), p. 218 ff.). An ordinary analytical balance was used; from one of its stirrups cover-glasses ($24 \times 32 \times 0.17$ mm^3 or $24 \times 40 \times 0.17$ mm^3) were suspended by a thin thread, and to the other a silver chain of a chainomatic device was attached. In order to measure an increasing surface tension (on film expansion), where the cover-glass was pulled down into the solution with its surface altered by the film, it was necessary to keep the glass in exactly the same position during an experiment. For this reason the beam arrest device of the balance was altered to give a minimum rise and a minimum swinging amplitude of the beam when disarresting the balance. The very small deflection of the balance pointer observed when the surface tension altered, was compensated by moving the scale end of the chain in each measurement. In compressing and expanding repeatedly one and the same film on the same substrate, we found no appreciable replacement or change of the pressure-area curves; *i.e.* the wetting properties of the cover-glass were not changed to any degree during a film compression. We could therefore use one and the same film for runs with different concentrations of one anesthetic (*cf.* below). Throughout, the films were compressed so slowly, that the shapes of the pressure-area curves were nearly independent of the compression rate. It can therefore be stated that systems in equilibrium or, at all events, near equilibrium have been studied. — The accuracy of the method was not so great: 0.05–0.1 dyn cm^{-1} could be detected. Perhaps a sensitive electrical compensation device (*cf.* POURADIER and DUBOIS (7)) would give better results.

The surface potentials were measured with a valve electrometer (*vide* Fig. 1) similar to the "Thermionic amplifier" of Leeds and Northrup Co., designed by CHERRY (8). Electrometer valves ET 1 (Osram) or 4060 (Philips) were used. The grid was connected to a movable radioactive electrode containing about 2 millicuries of MsTh. A Rubicon galvanometer (sensitivity 0.004 μA/mm scale deflection) was used and the voltages were compensated with a Student's potentiometer. During adjustment of the grid current to zero, the grid could be grounded through high resistances (10^{10}–10^{12} ohms). A ceramic switch was used which at the same time disconnected the air electrode. The sensitivity of the device was 0.016 μA on the galvanometer for 1 mV alteration of the surface potential. — The surface potential, ΔV, is generally defined (12) as the potential difference between a film-covered and a clean substrate surface. In all the cases investigated here the anesthetics alone altered the potential of the free substrate surface (values given to the right in the diagrams, Fig. 5). Therefore the absolute values, V, of the potentials are given. These cannot be related to the potentials of the clean substrate surfaces in question, because we cannot expect *a priori* that the latter are identical with the surfaces beneath the films. (*Cf.* the experiments with cholesterol, below.) Correspondingly, in the pressure-area diagrams, the surface pressure is given in relation to that of the pure surface of a phosphate buffer without anesthetic.

The rest of the apparatus was made largely according to the description given by ANDERSSON, STÄLLBERG–STENHAGEN and STENHAGEN (9). A silica trough with internal dimensions of $15 \times 40 \times 1.5$ cm^3 was used. The holder of the movable electrode was made according to ANDERSSON *et al.* The junction with the liquid was made through a calomel electrode with 0.1–C KCl.

Since all measurements were planned at a controlled room temperature (20°C.), the chief purposes of a box which was built around the trough was to exclude dust, to impede evaporation from the surface, and to form an elec-

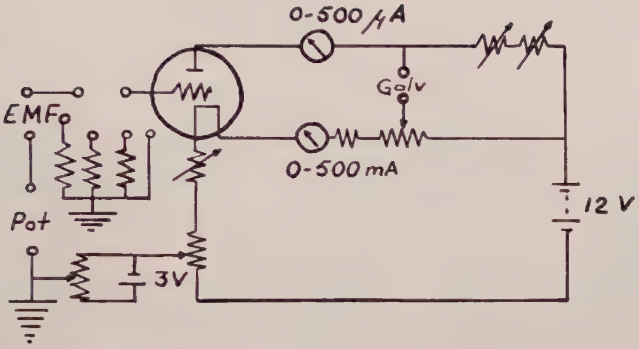

Fig. 1. Electrometer device for surface potential measurements.

trical shield. Therefore a wooden box with a brass lining was used. Between the readings the barrier was moved by a long screw running beneath the trough.

Trough, barriers and glass slides were prepared as described by ANDERSSON *et al.* (9). An "Agla" micrometer syringe was used to spread the films. In the case of phosphatides, chloroform had to be used as a solvent for the substance to be spread. Since it is heavier than water, care had to be taken to let the droplets leave the syringe near the surface to avoid their falling to the bottom of the trough. The cholesterol was spread from light petrol solutions.

Substances

Cholesterol purest, laevorotatory, from Schering Ltd., Berlin.

Phosphatidyl serine and inositol phosphatide, prepared according to FOLCH (10) from ox brains. The compounds were not analyzed. Freshly prepared, white compounds were used.

Ethanol, 99.5 %, from Vin- och Spritcentralen. Not redistilled.

Procaine hydrochloride. Pharm. preparation.

Light petroleum, C. P. Baker's analyzed. B. p. 40°–60° C., redistilled.

Chloroform, guaranteed reagent from Merck, Darmstadt. HCl removed with NaOH, washing with water, drying with $CaSO_4$, redistillation.

Buffer solution: $Na_2HPO_4 \cdot 2H_2O$, Sörensen's, from LKB, Stockholm, $NaH_2PO_4 \cdot H_2O$, purest cryst. from Schering Ltd., Berlin.

Paraffin, with which the trough edges and barriers were coated, was purified through extraction, in the molten state, with NaOH and water.

Experimental results

In evaluating the results it is important to note that in the experiments with cholesterol and inositol phosphatide several runs were made with one and the same film, each with a higher concentration of the anesthetic in question. (This could be done because the pressure-area diagrams of two consecutive compressions of one and the same film were found to be identical if the substrate was

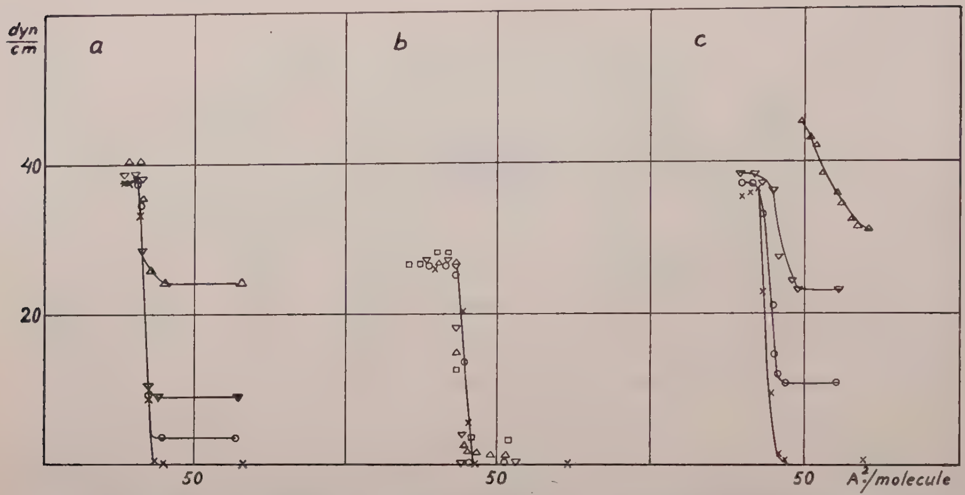

Fig. 2. Influence of (a) ethanol, (b) procaine, and (c) xylocaine on the surface pressure of cholesterol films. Concentrations: Ethanol: × 0.00, ○ 0.07, ▽ 0.27, △ 1.08 moles/l. — Procaine: × 0.00, ○ 0.44, ▽ 1.30, △ 3.88, □ 11.65 mmoles/l. — Xylocaine: × 0.0, ○ 2.0, ▽ 6.0, △ 18.0 mmoles/l.

not altered between the runs.) In the case of phosphatidyl serine a new film was spread for every concentration in the substrate.

We shall consider first the lipid films without penetrating agents. The cholesterol films agree well with those studied by other workers (3, 11). They form typical condensed films with a small compressibility. The surface potential cannot be defined at larger areas because islands of condensed film alternate with the gaseous state (*cf.* ADAM (12)).

Since the molecular weights of the two phosphatides are not yet known, we have given their surfaces as cm²/microgram (γ). As may be expected from the greater flexibility of the molecules the phosphatide films exhibit a greater compressibility. The inositol phosphatide forms condensed films with unstable surface potential in large areas, whereas the expanded films of the phosphatidyl serine give well defined surface potentials in these areas. If we use the analytical data of FOLCH (10) and calculate the area per atom of phosphorus we obtain for phosphatidyl serine 52 A^2 (also valid per atom of N) and for inositol phosphatide 34 A^2, *i.e.* reasonable values from the point of view that the molecules should contain one atom of P per molecule. Two close-packed chains will occupy a surface of 41 A^2, (*cf.* ADAM (12), p. 78). In this connection it must be emphasized that the phosphatide fractions used for the films are not well-defined chemical compounds, but certainly mixtures (*cf.* FOLCH (10)).

In earlier penetration experiments (3–5), more specific penetrating substances were investigated, which could be used in small concentrations not measurably influencing the properties of the free water surface. The anesthetics are, however, much more non-specific and have to be used in concentrations which affect strongly the surface tension or potential of the clean water surface.

On the very condensed cholesterol films neither of the anesthetics exerted any influence (Fig. 2); only high concentrations of xylocaine provoked a

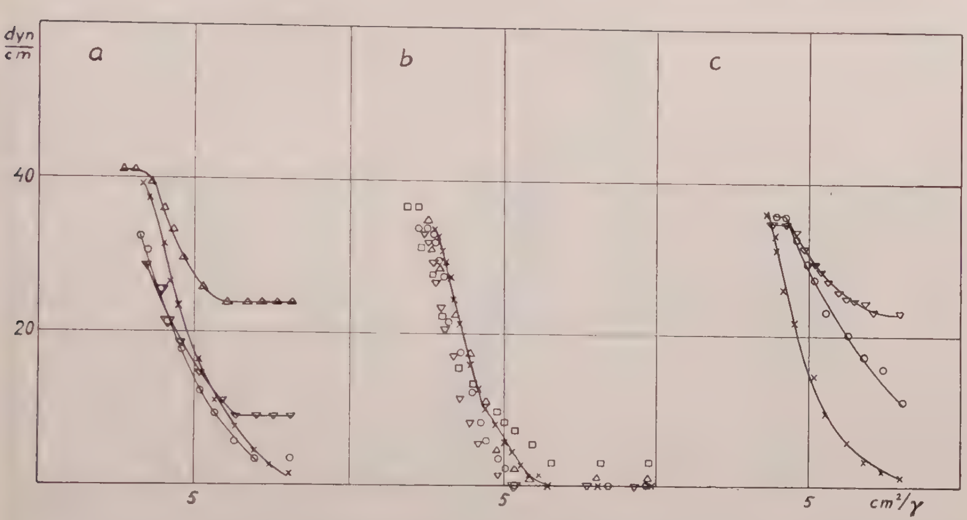

Fig. 3. Influence of (a) ethanol, (b) procaine, and (c) Xylocaine on the surface pressure of inositol phosphatide films. Concentrations as in Fig. 2.

crystalline precipitation of the film on compression. According to potential measurements, only the condensed films were coherent. Indications were obtained, however, that the presence of ethanol or procaine increases the range of existence of coherent films to somewhat greater areas. This is indicated by the dotted lines in Fig. 5. Such a reduction of the cohesion of condensed films provoked by other simple molecules depends on a certain development of the lipophilic properties of these molecules (Cockburn and Schulman (5); Adam (12), p. 98). In spite of the enormous effect of the anesthetics on the potential of the free water surface (= at infinite film area), the compressed film gave a potential value largely independent of the presence of an anesthetic. This proves that the film contained exclusively cholesterol, and that the anesthetic molecules next to the film-covered surface were not otherwise oriented than in the centre of a three-dimensional solution.

The surface pressure (Fig. 3 a) or potential (Fig. 5) of the inositol phosphatide films are not greatly changed through the influence of ethanol in low concentrations, whereas higher concentrations decrease the surface at which the films resist compression. This effect of the ethanol is still more pronounced on films of phosphatidyl serine (Fig. 4 a). It may be interpreted as a dissolving effect of the alcohol at high ethanol concentrations. The potential measurements demonstrated a dipole attraction between the ethanol molecules in the solution and the compressed film.

As to the influence of procaine on the inositol phosphatide an uncertainty in the pressure measurements (Fig. 3 b) makes the differences found insignificant. The surface potentials (Fig. 5) demonstrate, however, that at procaine concentrations higher than 0.004 moles/l the film contains both kinds of molecules. A true film penetration seems to occur at the highest procain concentration (Fig. 3 b).

At large areas, an inositol phosphatide film contains xylocain molecules, if

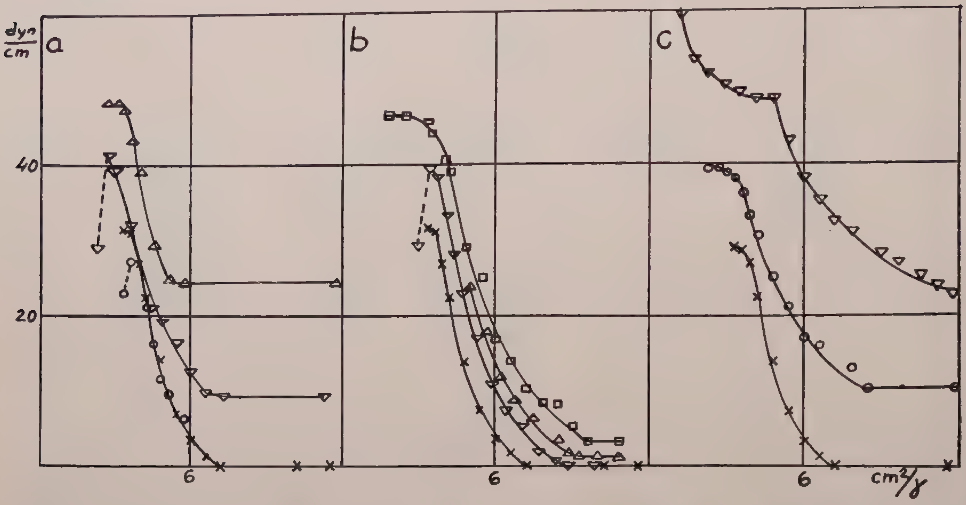

Fig. 4. Influence of (a) ethanol, (b) procaine, and (c) xylocaine on the surface pressure of phosphatidyl serine films. Concentrations: Ethanol and procaine as in Fig 2. — Xylocaine: × 0.0, ○ 1.7, ▽ 5.1 mmoles/l.

this compound be given in the substrate (Fig. 3 c, 5). On compression, the anesthetic molecules are squeezed out of the film, however. The somewhat lower potential values in the range 4–5 cm^2/γ indicate a dipole-association at high xylocaine concentrations. Since the film collapses in this region (*cf.* Fig. 3 c) the significance of the findings should not be overrated, however.

On the phosphatidyl serine film the dissolving action of ethanol is still more pronounced (Fig. 4 a) than in the case of inositol phosphatide. Moreover, the potential measurements demonstrate a penetration of ethanol molecules in the film, at higher pressures accompanied by a dipole association. Procaine penetrates the phosphatidyl serine film, without dipole association (Fig. 4 b, 5). At higher pressures some procaine molecules seem to be squeezed out of the film (Fig. 5). Into the same film xylocaine penetrates still more effectively (Fig. 4 c, 5). The squeezing out of molecules on compression seems to be less pronounced (Fig. 5). If xylocaine is given in high concentrations a crystallization of the film occurs at about 5 cm^2/γ. This crystallization is demonstrated also by the abnormal potential-area curve (Fig. 5).

Biological considerations

The present material is not large enough to permit any exhaustive discussion of biological relationships. It is, however, interesting to note that the two local anesthetics investigated penetrate, even in subanesthetizing concentrations films of, *i.e.* interact with, phosphatides, especially phosphatidyl serine. The phosphatides are universal protoplasm constituents, partly as lipo-protein complexes. Phosphatidyl serine, for example seems to occur in the plasma membrane of various cells (13, 14). Different phosphatides, especially cephalins, also form part of the thrombokinase molecule (prepared from lung tissue, *cf.* Cohen and

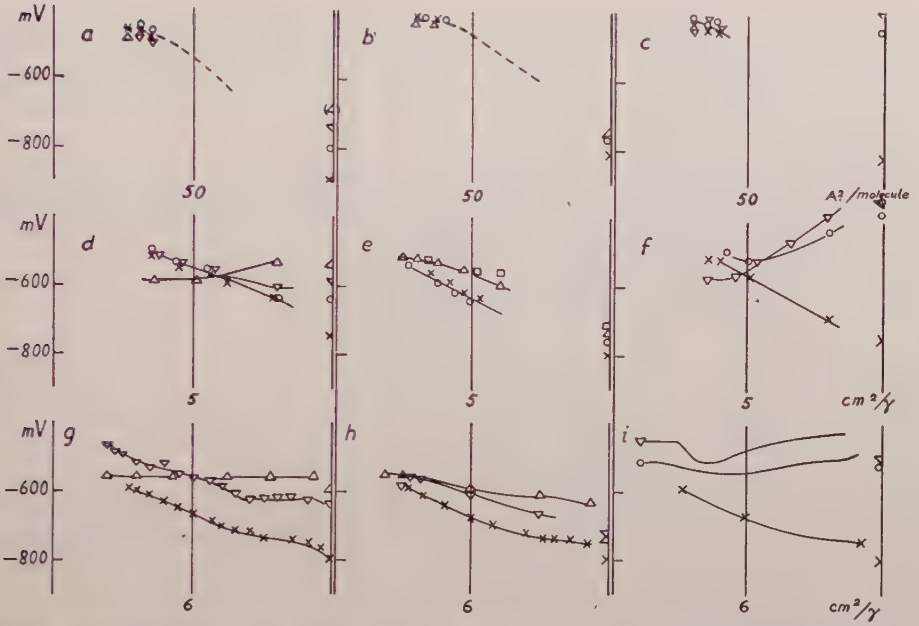

Fig. 5. Surface potential-area curves corresponding to the pressure-area curves of Figs. 2—4. The action of ethanol (a, d, g), procaine (b, e, h), and xylocaine (c, f, i) on cholesterol (a, b, c), inositol phosphatide (d, e, f), and phosphatidyl serine (g, h, i). In order to increase the distinctness some measurement points are excluded.

Chargaff (15): it is interesting to note that the anesthetics investigated here inhibit the clotting of blood (16) at concentrations of the same level as those at which they interact with phosphatide molecules. This strengthens the assumption (16) that thrombokinase is the compound blocked in the inhibition of blood clotting through anesthetics.

The effect of xylocaine on phosphatide films is greater than that of procaine, a fact which agrees with the former's greater anesthetic action on frog nerves (minimum concentration, at pH 7.4, for anesthesia with xylocaine 3.8 mmoles/l and with procaine 12.5 mmoles/l (17)). *Cf.* the inhibiting effect on blood coagulation (16). (It should be remembered that in this comparison of the effectivities the total concentrations of the anesthetics are referred to. The effect of pH, *i.e.* of the acid-base equilibrium of the anesthetics, on the penetration is not yet investigated.) — The precipitation, with the formation of what seems to be neadle shaped crystals in the compressed films at high concentrations of xylocaine is no doubt related to the precipitation found by Tammelin and Löfgren (18) when an ergosterol film in the interface between benzene and water was penetrated by xylocaine.

In accordance with the high minimum concentration for anesthesia of ethanol in frog nerves (about 1 mole/l (19)), concentrations of this magnitude have to be applied in order to affect the phosphatide films. Similar concentrations of ethanol have also to be given in order to inhibit the coagulation of blood (16). The dissolving action of the general anesthetic ethanol on the phosphatide films is fundamentally different from the mode of action of the two local anesthetics studied. These findings may reflect the biological differences between ethanol and the typical local anesthetics: the former acts through a depolarization of the membrane potential (20), whereas *e.g.* in procaine anesthesia the rest potential of the nerve is unaltered (21). (The effect of xylocaine on the membrane potential has not yet been investigated.)

It may be concluded that anesthetics, in concentrations producing anesthesia or inhibition of the blood clotting interact at least with certain phosphatides. Although the functional point of attack of anesthetics cannot be indicated as yet, it must be emphasized that the method has proved valuable for investigations of the interaction, qualitatively and quantitatively, of anesthetics with biological material.

Acknowledgement: This work was made possible by a grant from Statens Tekniska Forskningsråd, Stockholm. We have to thank Dr. E. STENHAGEN, Uppsala, and Drs. N. LÖFGREN and I. FISCHER, Stockholm, for their encouragement and criticisms in several discussions. The electrometer was designed by Mr S. BORENIUS, Engineer, Lidingö.

Institute of Organic Chemistry and Biochemistry, University, Stockholm.

LITERATURE

1. MEYER, K. H. and HEMMI, H. Biochem. Z. *277* (1935) 39.
2. LEVAN, A. and ÖSTERGREN, G. Hereditas *29* (1943) 381; ÖSTERGREN, G. Ib *30* (1944) 429.
3. SCHULMAN, J. H. and RIDEAL, E. K. Proc. Roy. Soc. B *122* (1937) 29, 46.
4. RIDEAL, E. K. and SCHULMAN, J. H. Nature *144* (1939) 100; RIDEAL, E. K. Nature *144* (1939) 693.
5. COCKBAIN, E. G. and SCHULMAN, J. H. Trans. Faraday Soc. *25* (1939) 716.
6. HARKINS, W. D. In Weissberger, A. Physical Methods of Organic Chemistry. I. New York (1945); Pub. Am. Assoc. Advance. Sci. *21* (1942) 40.
7. POURADIER, J. and DUBOIS, A. Surface Chemistry, Suppl. to Research (in honour of Prof. H. Devaux). London (1949) 119.
8. CHERRY, R. H. Trans. Electrochem. Soc. *72* (1937) 33.
9. ANDERSSON, K. J. I., STÄLLBERG-STENHAGEN, S. and STENHAGEN, E. The Svedberg. Stockholm and Uppsala (1944) 11.
10. FOLCH, J. J. Biol. Chem. *146* (1942) 35.
11. RUYSSEN, R. and LOOS, R. Mededeel. Koninkl. Vlaam. Acad. Wetenschap. Belg. Klasse Wetenschap. *8* (1946) No. 3.
12. ADAM, N. K. Physics and Chemistry of Surfaces. London (1941).
13. PARPART, A. H. and DZIEMIAN, A. J. Cold Spring Harbor Symposia Quant. Biol. *8* (1940) 17.
14. ARTOM, C. J. Biol. Chem. *157* (1945) 595.
15. COHEN, S. S. and CHARGAFF, E. J. Biol. Chem. *139* (1941) 741.
16. LUNDHOLM, E. and EHRENBERG, L. Acta Chem. Scand. *6* (1952) 341.
17. EHRENBERG, L. Acta Chem. Scand. *2* (1948) 63.
18. TAMMELIN, L. E. and LÖFGREN, N. Acta Chem. Scand. *1* (1947) 871.
19. FLAMM, S. Arch. exptl. Path. Pharmakol. *138* (1928) 257.
20. GALLEGO, A. J. Cellular Comp. Physiol. *31* (1948) 97.
21. LORENTE DE NÓ, R. A Study of Nerve Physiology. Rockefeller Inst. Med. Res. *131, 132* (1947).

Tryckt den 26 februari 1953

Uppsala 1953. Almqvist & Wiksells Boktryckeri AB

ARKIV FÖR KEMI Band 5 nr 33

Communicated 12 November 1952 by ARNE FREDGA

Stereochemical studies on plant growth regulators. III[1].

The steric relations of some chlorosubstituted α-phenoxypropionic acids

By MAGNUS MATELL

With 9 figures in the text

The steric relations of the optically active α-phenoxy- and α-naphthoxypropionic acids have been established by FREDGA and MATELL (1, 2) and at the same time ÅBERG studied the plant growth regulating properties of these compounds (3, 4). From these experiments a correlation between biological activity and steric configuration was found, showing that the D-forms possess greater auxin activity than the corresponding L-forms. It seems probable that this stereochemical specificity should be a common property of similar plant growth substances.

In view of the great practical as well as theoretical importance of 2.4-dichlorophenoxyacetic acid (2.4-D) it seemed important to prove, in the first place, that this assumption holds for the homologous α-(2.4-dichlorophenoxy)-propionic acid (I). The possibility to establish the steric relations between this compound and the acids mentioned above by a direct application of the method of quasi-racemates (5, 6) appeared less probable because of the great structural differences. α-(3.4-Dichlorophenoxy)-propionic acid (II) on the other hand has a structure resembling α-(2-naphthoxy)-propionic acid (IV) and so may be used as an intermediate link between α-(2-naphthoxy)-propionic acid and the 2.4-dichlorocompound.

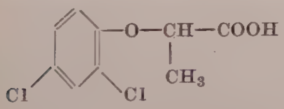

I

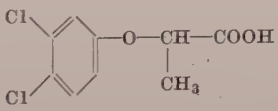

II

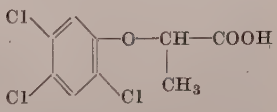

III

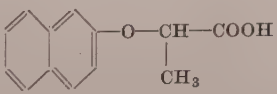

IV

Another reason to include α-(3.4-dichlorophenoxy)-propionic acid in this investigation was that the effect on auxin activity of chlorine in 3.4-positions has apparently not been investigated previously.

---

[1] Paper II. Ark. Kemi *5*, 187 (1952).

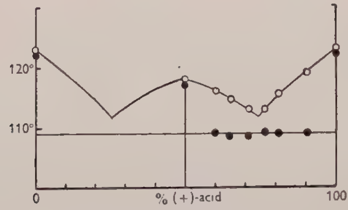

Fig. 1. (+)- and (−)-α-(2.4-dichlorophenoxy)-propionic acid.

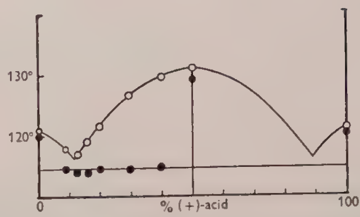

Fig. 2. (+)- and (−)-α-(3.4-dichlorophenoxy)-propionic acid.

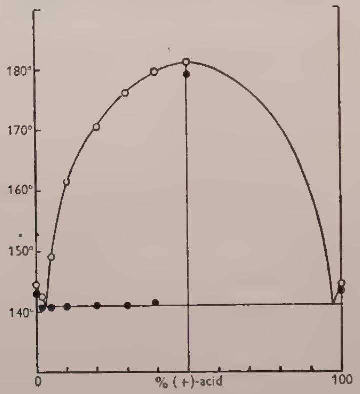

Fig. 3. (+)- and (−)-α-(2.4.5-trichlorophenoxy)-propionic acid.

The reason given above for investigating α-(2.4-dichlorophenoxy)-propionic acid also holds for α-(2.4.5-trichlorophenoxy)-propionic acid. The antipodes of this compound were kindly supplied by Prof. R. L. WAIN.

In the first paper of this series the synthetic work involved has been described (7). In the same paper measurements of rotatory powers in different solvents and preliminary experiments on the formation of quasi-racemates were reported indicating that the (+)-forms of the 2.4-dichloro- and 3.4-dichloro-compounds belonged to the D-series. In the following it will be shown that (+)-α-(2.4-dichlorophenoxy)-propionic acid, (+)-α-(3.4-dichlorophenoxy)-propionic acid and (+)-α-(2.4.5-trichlorophenoxy)-propionic acid have the same configuration as (+)-α-(2-naphthoxy)-propionic acid which according to FREDGA and MATELL most probably has the D-configuration (1). The biological activity of optically active α-(2.4.5-trichlorophenoxy)-propionic acid has been investigated by SMITH, WAIN and WIGHTMAN (8) who found the (+)-form to possess higher auxin activity than the (—)-acid. The other compounds have been studied by Dr. B. ÅBERG who found that the (+)-forms were much more effective in repressing root growth than the (—)-forms (private communication). These experiments will be described by Dr. ÅBERG in a separate publication.

Thus it is further confirmed that α-aryloxyalkylcarboxylic acids with D-configuration have greater plant growth-regulating effects than the corresponding L-acids.

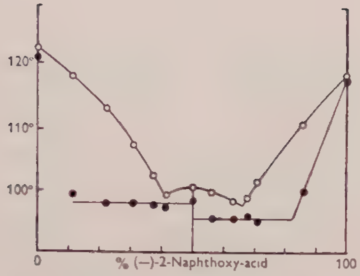

Fig. 4. (−)-α-(2-Naphthoxy)-propionic acid and (+)-α-(2.4-dichlorophenoxy)-propionic acid.

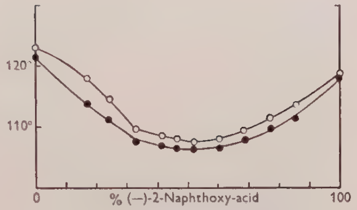

Fig. 5. (−)-α-(2-Naphthoxy)-propionic acid and (−)-α-(2.4-dichlorophenoxy)-propionic acid.

For the establishment of the steric relations thaw-melting point diagrams were studied. As seen from Figs. 1–3 the inactive acids are true racemic compounds. Of these the 2.4.5-trichlorocompound is characterised by an exceptionally great melting point difference between racemate and active acid and consequently a great stability of the racemic compound (Fig. 3). Because of this great tendency to form a racemate the antipodes are very likely to form quasi-racemic compounds with structurally similar compounds (6). α-(2.4-Dichlorophenoxy)-propionic acid, on the other hand, has a rather small racemate formation tendency with the racemate melting lower than the antipodes (Fig. 1). The 3.4-dichloroacid may be regarded as an intermediary between the extremes mentioned above (Fig. 2).

(+)-α-(2.4-Dichlorophenoxy)-propionic acid gives with (—)-α-(2-naphthoxy)-propionic acid a molecular compound in the ratio 1 : 1 (Fig. 4) while the compounds having the same direction of rotation give a diagram of quite another type (Fig. 5), a combination of the ROOZEBOOM types III and IV, showing far-reaching mutual solubility in the solid state. The molecular compound consequently is quasi-racemic and the (+)-forms have the same configuration. The occurrence of a quasi-racemate in this system is, as was mentioned above, unexpected, as the structural differences are rather large and moreover the racemate formation tendencies of the components are small.

In the system (—)-α-(3.4-dichlorophenoxy)-propionic acid: (+)-α-(2-naphthoxy)-propionic acid a molecular compound in the ratio 1 : 1 is also formed (Fig. 6) while the (—)-acids give a diagram of type V according to ROOZEBOOM, showing limited solubility in the solid state (Fig. 7). The molecular compound evidently is a quasi-racemic compound and consequently the acids having opposite directions of rotation have also opposite configuration. As seen from Fig. 6 the eutectic line to the left of the maximum is lower than the eutectic line on the other side while from the intersections of the three branches one would expect the reverse. The lower eutectic line probably belongs to an unstable system which however could not be determined except for a short interval near the eutectic.

As seen from Fig. 8 (+)-α-(2.4-dichlorophenoxy)-propionic acid and (—)-α-(2.4.5-trichlorophenoxy)-propionic acid form a molecular compound in the ratio 1 : 1. The components having the same direction of rotation behave quite

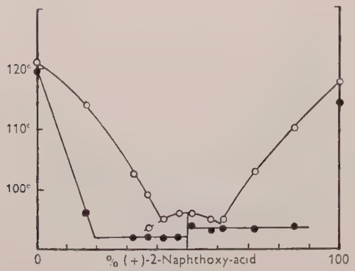

Fig. 6. (+)-α-(2-Naphthoxy)-propionic and (−)-α-(3.4-dichlorophenoxy)-propionic acid.

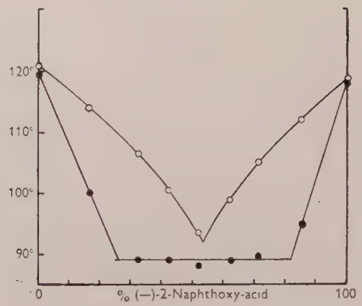

Fig. 7. (−)-α-(2-Naphthoxy)-propionic acid and (−)-α-(3.4-dichlorophenoxy)-propionic acid.

differently, the diagram being a combination of the ROOZEBOOM types III and IV (Fig. 9). The molecular compound is obviously a quasi-racemate and the acids, having opposite directions of rotation, must have opposite configuration. The middle branch of diagram 8 is unusually large which is not surprising if one considers the great tendency of one of the components to form a true racemate.

An attempt was made to connect directly the 2.4.5-trichloro-acid to α-(2-naphthoxy)-propionic acid but this attempt failed as both the combinations (+):(+) and (+):(—) gave similar diagrams showing the existence of a molecular compound in the ratio 1 : 1. The systems differed in the respect that the compound between (+)- and (—)-forms crystallised more easily than that between acids having the same direction of rotation. Owing to polymorphism all the details of these diagrams have not yet been fully determined and therefore will be published later.

As the method of quasi-racemates must be considered as being very reliable the steric connections of the compounds described here can be regarded as definitely established.

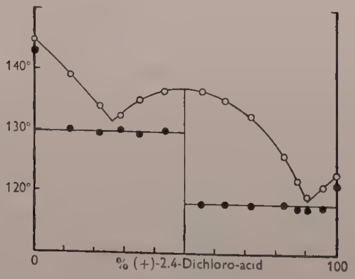

Fig. 8. (+)-α-(2.4-Dichlorophenoxy)-propionic acid and (−)-α-(2.4.5-trichlorophenoxy)-propionic acid.

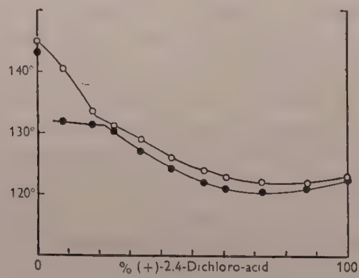

Fig. 9. (+)-α-(2.4-Dichlorophenoxy)-propionic acid and (+)-α-(2.4.5-trichlorophenoxy)-propionic acid.

Experimental

The mixtures were prepared by dissolving weighed quantities of the substances in a few drops of pure acetone; after evaporation of the solvent, the

Table 1

(+)- and (—)-I

% (+)-I	M.p.
0.0	122 –123°
50.0	117 –118°
60.1	109 –116°
65.0	108 –114.5°
71.2	108.5–113°
76.5	109 –113°
80.9	109 –115°
90.3	109 –119°
100.0	122 –123°

Table 2

(+)- and (−)-II

% (+)-II	M.p.
0.0	120 –121°
8.4	115 –118°
12.5	114.5–117°
15.8	114 –119°
20.1	114 –121.5°
29.4	114.5–126.5°
40.1	114.5–129.5°
50.0	129 –131°
100.0	120 –121°

Table 3

(+)- and (−)-III

% (+)-III	M.p.
0.0	143 –144.5°
2.1	140.5–142.5°
5.0	140.5–149°
9.9	141 –161.5°
20.2	141 –170.5°
30.1	141 –176°
39.4	141.5–179.5°
50.0	179 –180°
100.0	143 –144.5°

Table 4

(+)-I and (−)-IV

% (−)-IV	M.p.
0.0	121.5–123°
11.2	99.5–118.5°
22.2	98 –113.5°
31.1	98 –107.5°
37.5	97.5–102.5°
41.5	97 – 99.5°
49.9	98.5–100.5°
56.5	96 –100°
63.2	95.5– 98.5°
67.9	96 – 99°
71.1	95 –101.5°
86.1	100 –111°
100.0	118 –119°

Table 5

(−)-I and (−)-IV

% (−)-IV	M.p.
0.0	121.5–123°
17.0	113.5–118°
24.3	111.5–114.5°
32.8	107.5–109.5°
41.5	107 –108.5°
46.4	106.5–108°
52.0	106.5–107.5°
60.3	106.5–108°
68.5	108 –109.5°
77.2	110 –111.5°
85.6	111.5–113.5°
100.0	118 –119°

Table 6

(−)-II and (+)-IV

% (+)-IV	M.p.
0.0	119.5–121°
16.6	96 –114°
32.1	92 –102.5°
36.8	92.5– 93.5° 99°
42.2	92 – 95°
47.1	92 – 96°
51.3	94 – 96°
57.8	93 – 95°
61.7	93.5– 95°
72.1	93.5–103°
84.9	94 –110°

Table 7

(–)-II and (–)-IV

% (–)-IV	M.p.
0.0	119.5–121°
16.5	100 –114°
32.6	89 –106.5°
42.3	89 –100.5°
52.1	88 – 93.5°
62.4	89 – 99°
71.6	89.5–105°
85.2	95 –112°
100.0	118 –119°

Table 8

(+)-I and (–)-III

% (+)-I	M.p.
0.0	143 –144.5°
12.0	130 –139°
21.7	129.5–134°
28.4	130 –132.5°
35.0	129 –135°
43.4	130 –136.5°
55.6	118 –136.5°
63.3	118 –135°
71.9	118 –132.5°
82.5	118 –126°
87.3	117.5–122°
90.2	117.5–119°
95.7	117.5–121°
100.0	121.5–123°

Table 9

(+)-I and (+)-III

% (+)-I	M.p.
0.0	143 –144.5°
8.3	132 –140.5°
17.9	131 –133.5°
24.8	130 –131°
33.5	127 –129°
43.6	124 –126°
54.1	122 –124°
61.1	121 –123°
72.7	120.5–122°
87.1	121 –122°
100.0	122 –123°

residue was powdered and dried. Melting points were determined using a KOFLER hot stage microscope (9).

The results are given in Figures 1–9 and Tables 1–9 where the compositions are given in mole-%.

The author is indebted to Prof. A. FREDGA for supplying the optically active α-(2-naphthoxy)-propionic acid and for valuable discussions. Thanks are due to Prof. N. HELLSTRÖM, head of this institute, for his kind interest and for all facilities put at the author's disposal. Part of the expenses involved have been defrayed by a grant from *Statens Naturvetenskapliga Forskningsråd.*

SUMMARY

It was found that dextrorotatory α-(2.4-dichlorophenoxy)-propionic acid (I), α-(3.4-dichlorophenoxy)-propionic acid (II) and α-(2.4.5-trichlorophenoxy)-propionic acid (III) have the same configuration as dextrorotatory α-(2-naphthoxy)-propionic acid (IV). These acids have greater auxin activity than their

respective antipodes and the results confirm the assumption that the D-forms of compounds of this type have greater auxin activity than the corresponding L-forms.

Institute of Organic Chemistry, Royal Agricultural College, Uppsala, October 1952.

REFERENCES

1. A. Fredga and M. Matell, Ark. Kemi *3*, 429 (1951).
2. —— —— Ibid. *4*, 325 (1952).
3. B. Åberg, Ibid. *3*, 549 (1951).
4. —— Physiologia Plantarum *5*, 305 (1952).
5. J. Timmermans, Rec. Trav. chim. Pays-Bas *48*, 890 (1929).
6. A. Fredga, The Svedberg 1884 30/8 1944, Uppsala 1944, p. 261.
7. M. Matell, Ark. Kemi *4*, 473 (1952).
8. M. S. Smith, R. L. Wain and F. Wightman, Ann. App. Biol. *39*, 295 (1952).
9. L. Kofler and A. Kofler, Mikro-Methoden zur Kennzeichnung organischer Stoffe und Stoffgemische, Innsbruck 1948.

Tryckt den 26 februari 1953

Uppsala 1953. Almqvist & Wiksells Boktryckeri AB

ARKIV FÖR KEMI Band 5 nr 34

Communicated 27 February 1952 by Arne Westgren and Gunnar Hägg

The crystal structure of $U_6O_4(OH)_4(SO_4)_6$

By Georg Lundgren

With 6 figures in the text

In the course of investigations on the crystal structures of basic salts of tetravalent metals, a study of the phases occurring in the system UO_2–SO_3–H_2O was also made. It was found that there exist in this system at least two basic salts: $U(OH)_2SO_4$ and a compound, the empirical composition of which proved to be $UOSO_4\ \frac{1}{3}H_2O$. The first compound is isomorphous with $Th(OH)_2SO_4$ (Lundgren 1950, 1952) and the metal ions are thus arranged in zig-zag lines, within which they are connected by OH^- ions. This arrangement is also found in $Th(OH)_2CrO_4H_2O$ (Lundgren and Sillén 1949). The second type of crystals, however, cannot be expected to behave in this way, as they do not contain enough water to be able to form such $Me(OH)_2$ chains. It thus seemed desirable to investigate the crystal structure of this compound.

Preparation of the crystals

A saturated solution of uranium (IV) sulphate in 0.5 M H_2SO_4 was prepared. About 10 ml of this solution were sealed in a thick-walled glass tube (Pyrex) and heated to 200° C in an oven for about a week, during which time all the tetravalent uranium separated as dark green crystals, whereas the small amount of hexavalent uranium present stayed in solution. After cooling, the glass tube was opened, and the crystals were filtered off, washed with water, and dried in air.

The crystals are dark green, rather thick, square plates, but if they are ground, a very light green, almost colourless powder is obtained. The largest crystals from some twenty preparations were about 0.5 mm in length and 0.2 mm in thickness. The material is rather stable towards acids and oxidizing agents. For instance it dissolves only very slowly in warm nitric acid (1:1). Evaporation to dryness 3–4 times with concentrated nitric acid, oxidises the tetravalent uranium to the hexavalent state and the residue is then soluble in water.

Analysis

A sample was dissolved as described above and the *uranium* was determined by precipitation with 8-hydroxyquinoline according to Hecht and Donau (1940). The precipitate was filtered off, washed with water, ignited and weighed as U_3O_8.

For the determination of *sulphate*, a sample was decomposed by fusion with sodium and potassium carbonates and the product was extracted with hot water. The undissolved products, which contained all the uranium, were filtered off, and the amount of sulphate in the filtrate was determined gravimetrically by precipitation as $BaSO_4$.

The *water* was determined by HARTWIG-BENDIG's (1941) modification of BRUSH (1868) and PENFIELD's (1894) method as described by KOLTHOFF and SANDELL (1943).

The density of the crystals was determined from the loss of weight in benzene.

	Found		Calculated for $UOSO_4 \cdot \frac{1}{3} H_2O$
% UO_2	75.5	75.5	75.83
% SO_3	23.2	22.8	22.48
% H_2O	2.0	2.1	1.69
Density	5.7_9	5.7_7	5.93

Unit cell and space group

From LAUE photographs it was concluded that the crystals are tetragonal and have the LAUE symmetry $4/m$. The approximate cell dimensions were determined from rotation and WEISSENBERG photographs (zero, first and second layer) using CuK radiation and with [001] and [110] as rotation axes. More accurate values of the unit cell dimensions were obtained from powder photographs taken with focusing cameras of PHRAGMÉN type (Table 1. CrK radiation. $\lambda_{CrK\alpha_1} = 2.28962$ Å).

$$\begin{aligned} a &= (10.741 \pm 0.005)\ \text{Å} \\ c &= (10.377 \pm 0.005)\ \text{Å} \\ V &= 1197.2\ \text{Å}^3 \end{aligned}$$

From the volume of the unit cell and the mean value of the density (5.78) it was calculated, that there are $11.7_0 \approx 12$ formula units $UOSO_4 \cdot \frac{1}{3}H_2O$ in the unit cell, thus $12UOSO_4 \cdot 4H_2O$.

The only reflections systematically absent are

$$hkl \text{ with } h+k+l \text{ odd,}$$

which is characteristic of the space groups C_{4h}^5, C_4^5 and S_4^2.

Positions of the uranium atoms

In the unit cell there are 12 uranium atoms. To determine their positions the following functions were calculated (Fig. 1 and 2):

$$P_1\,(uv) = \sum_h \sum_k F^2_{hk0} \cos 2\pi\,(hu + kv) = P\,(uvp)$$

$$P_2\,(w) = \sum_l F^2_{00l} \cos 2\pi l w = P\,(ppw)$$

These are the projections on the uv plane (P_1) and on the w axis (P_2) of the PATTERSON function $P\,(uvw)$.

In the characteristic space groups, all the point positions have x and y parameters of one of the following types:

$(00; \frac{1}{2}\frac{1}{2}) \pm$

1.		2.		3.		4.	
	00		$\frac{1}{2}0$		$\frac{1}{4}\frac{1}{4}$ $\frac{1}{4}\frac{3}{4}$		$x\,y$ $\bar{y}\,x$

Table 1

Powder photographs of $U_6O_4(OH)_4(SO_4)_6$. Cr*K* radiation. $\lambda_{CrK\alpha_1} = 2.28962$ Å.

h k l	$10^4 \sin^2\theta$ calc	$10^4 \sin^2\theta$ obs	$I_{hkl}+I_{khl}$ calc	$I_{hkl}+I_{khl}$ obs
2 0	909	—	20	—
0 2	941	944	254	m
1 0	1136	1142	131 + 10	m
0 1	1144		100	
3	1209	1208	85	w
2 2	1396	1396	863	st
2 1	1599	1604	61 + 102	w
1 2	1623	1626	2 + 300	m
1 3	1663	1665	21 + 59	vw
0 0	1818	1820	288	w +
0 4	1947	1944	221	w +
3 0	2045	2051	52	w
1 1	2053		156 + 10	
0 3	2118	2118	154	w
1 4	2175	2171	39	vvw
2 0	2272	2275	86 + 82	w
0 2	2304	—	37	—
0 4	2402	2405	51	vvw
3 2	2532	(2543)	66	(vw)
2 3	2572	2577	6 + 237	w
2 2	2759	2771	61 + 56	vw +
2 4	2856	2856	49	vw
1 0	2954	2974	151 + 3	w +
0 1	2962		17	
3 1	2962		8 + 296	
1 3	3027	3038	420 + 56	w +
1 4	3083	3093	376 + 6	w +
0 5	3156	(3133)	35	(vvw)
2 1	3416	3425	140 + 12	w—
1 2	3440	3444	11 + 205	w
1 5	3611	3605	81 + 234	w +
4 0	3635	3648	356	w +
0 4	3765	3767	940	m
3 0	3862	3875	2 + 255	w
0 3	3935	3942	55	w
3 3	3935		8 + 328	
3 4	3992	(4006)	79	(vw)
0 5	4065	4063	66	vvw
0 0	4090	—	4	—
4 2	4122	(4128)	6	(vvw)
2 4	4219	4226	182 + 216	w
1 1	4325	(4348)	3 + 524	(m)
3 2	4349		552 + 15	
0 6	4382		68	
2 3	4390		26 + 7	
2 5	4520	4527	94 + 275	vw +
2 0	4544	—	6 + 1	—
0 2	4576	4597	320	vw +
1 6	4609		104	
4 1	4779	4789	0 + 179	vw
2 0 6	4836	4834	154	vw
5 1 4	4901	4910	161 + 14	vw
4 1 5	4974	4979	210 + 2	vw
6 2 2	5031	5049	596 + 529	m
6 3 1	5234	5248	373 + 4	vw
2 2 6	5290	5298	772	st
6 1 3	5299		27 + 361	
3 1 6	5518	5522	1 + 285	w
4 4 4	5583	5587	530	w
7 1 0	5680	5687	235 + 1	vw
5 5 0	5680		15	
7 0 1	5688		27	
5 4 3	5753	5763	3 + 162	vw
5 3 4	5810	5814	64 + 376	w
5 0 5	5883	5892	13	vw
4 3 5	5883		0 + 114	
6 4 0	5907		30 + 59	
6 0 4	6037	—	15	—
1 0 7	6077	(6083)	182	(w)
7 2 1	6143	—	2 + 33	—
7 1 2	6167	6175	0 + 350	w—
5 5 2	6167		126	
4 0 6	6199	(6192)	27	(vvw)
6 3 3	6207	6215	230 + 12	vw
5 2 5	6337	(6336)	102 + 67	(vw)
6 4 2	6394	6398	135 + 228	w
3 3 6	6426	(6415)	37	(vw)
6 2 4	6491	—	19 + 3	—
2 1 7	6532	6540	4 + 49	vvw
7 3 0	6589	6595	38 + 65	vw
4 2 6	6654	6658	90 + 50	vw
7 0 3	6662		29	
3 0 7	6986	(6988)	204	(w)
6 5 1	7051	7054	16 + 269	vw
7 3 2	7076	(7081)	108 + 28	(vw)
7 2 3	7116	—	8 + 1	—
6 1 5	7246	7247	0 + 625	m
8 0 0	7270	(7273)	276	(w)
5 1 6	7335	7335	3 + 164	vw
3 2 7	7441	7440	7 + 40	vvw
8 1 1	7506	7511	202 + 0	w
7 4 1	7506		66 + 51	
7 1 4	7627	7630	273 + 3	w
5 5 4	7627		36	
5 4 5	7700	7704	13 + 96	vw—
8 2 0	7725	7730	198 + 158	w
8 0 2	7757	(7754)	3	(vvw)
0 0 8	7789	7787	343	w +
6 4 4	7855	7855	144 + 33	vw
4 1 7	7895	7900	328 + 50	w +

The horizontal lines mark the boundaries between the angular ranges of the three different focusing cameras used. Reflections systematically absent in space group C_{4h}^5 have been omitted. Reflections coinciding with α_2 or β reflections are given in brackets.

The intensities were calculated from the expression $100 \cdot \frac{p}{8}\left(\frac{F}{4 f_U}\right)^2$, where p is the number of equivalent reflections.

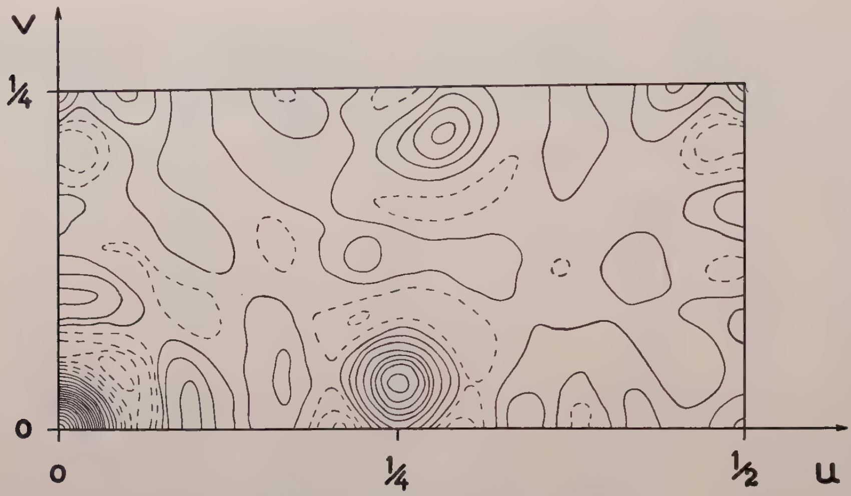

Fig. 1. Patterson analysis of $U_6O_4(OH)_4(SO_4)_6$.
The function $P_1(uv) = \sum_h \sum_k F^2_{hk0} \cos 2\pi (hu + kv) = P(uvp)$. Dotted lines indicate negative values.

Now, P_1 has a pronounced maximum at $u = 0.25$, $v = 0.03$, and consequently some of the uranium atoms must belong to a point position of type 4. This is possible only if eight of them occupy an eightfold position $x_1 y_1$. (We need only consider the range $0 \leq x_1 \leq \frac{1}{2}$, $0 \leq y_1 \leq \frac{1}{4}$, if the range for the corresponding z parameter is $0 \leq z_1 \leq 1$.) The remaining four uranium atoms have the x and y parameters $00; \frac{1}{2}\frac{1}{2}$ or $0\frac{1}{2}; \frac{1}{2}0$, as all the twofold and fourfold positions belong to type 1 or 2. We should thus expect the function P_1 to show maxima at points giving the interatomic distances for one of the three alternatives:

A.	B.	C (only in S$_4^2$).
$(00; \frac{1}{2}\frac{1}{2})\pm$	$(00; \frac{1}{2}\frac{1}{2})\pm$	$(00; \frac{1}{2}\frac{1}{2})\pm$
4 U in 00	4 U in $\frac{1}{2}0$	2 U in 00
8 U in $x_1 y_1$; $\bar{y}_1 x_1$	8 U in $x_1 y_1$; $\bar{y}_1 x_1$	2 U in $\frac{1}{2}0$
		8 U in $x_1 y_1$; $\bar{y}_1 x_1$

The interatomic distances are:

A.			B.			C.		
$(00; \frac{1}{2}\frac{1}{2})\pm$			$(00; \frac{1}{2}\frac{1}{2})\pm$			$(00; \frac{1}{2}\frac{1}{2})\pm$		
I.	00		I.	00		I.	00	
II.	$x_1 y_1$	weight 4	II.	$x_1 - \frac{1}{2}\ y_1$	weight 4	II.	$\frac{1}{2}0$	weight 1
	$\bar{y}_1 x_1$	» 4		$y_1 + \frac{1}{2}\ \bar{x}_1$	» 4	III.	=A II	» 2
III.	$2x_1\ 2y_1$	» 1	III.	=A III		IV.	=B II	» 2
	$x_1 + y_1\ y_1 - x_1$	» 2				V.	=A III	
	$x_1 - y_1\ x_1 + y_1$	» 2						
	$2\bar{y}_1\ 2x_1$	» 1						

This table is now compared with the function P_1 (Fig. 1). Alternative C is then at once ruled out, as for each of the maxima $x_1 y_1$ (C III) there should be a peak of the same height at $x_1 - \frac{1}{2} y_1$ (C IV), which is not found for the large maxima in P_1. The uranium atoms should then be arranged according to A or B. Both of these possibilities have one type of maximum (II) more pronounced than the others. If we identify this with the highest peak in P_1 ($u = 0.25$ $v = 0.03$) the arrangement according to A and B is:

A.	B.
$(00;\ \frac{1}{2}\frac{1}{2}) \pm$	$(00;\ \frac{1}{2}\frac{1}{2}) \pm$
4 U in 00	4 U in $\frac{1}{2}0$
8 U in 0.25 0.03; −0.03 0.25	8 U in 0.03 0.25; −0.25 0.03

These two alternatives give the same projection on the xy plane, and B can be converted into A, if the origin is displaced to the point $\frac{1}{2}0$. Consequently also the interatomic distances calculated for these positions of the uranium atoms are exactly the same for A and B, namely:

A and B.

$(00;\ \frac{1}{2}\frac{1}{2}) \pm$

I.	0	0		
II.	0.25	0.03	weight	4
	−0.03	0.25	»	4
III.	0.50	0.06	»	1
	0.28	−0.22	»	2
	0.22	0.28	»	2
	−0.06	0.50	»	1

As is seen from this table and Fig. 1 the distances correspond to the maxima in P_1.

The z parameters of the uranium atoms are determined from the function P_2 (Fig. 2). It has maxima only for $w = 0, \frac{1}{4}, \frac{1}{2}$, and $\frac{3}{4}$, and consequently the uranium atoms should be situated in or close to planes perpendicular to the c axis and $\frac{c}{4}$ apart. In C_{4h}^5 and C_4^5 this arrangement is possible only if the z parameters are close to 0, $\frac{1}{4}$, $\frac{1}{2}$, and $\frac{3}{4}$. In S_4^2 they could also be close to $\pm\frac{1}{8}$ and $\pm\frac{3}{8}$. However, with the latter arrangement the intensities of the reflections $00l$ with $l = 4n + 2$ would be zero, which is not the case. The uranium atoms should thus be situated close to the planes $z = 0, \frac{1}{4}, \frac{1}{2}$, and $\frac{3}{4}$.

The uranium atoms are then arranged in one of the following ways:

A.			B.		
$(000;\ \frac{1}{2}\frac{1}{2}\frac{1}{2}) \pm$			$(000;\ \frac{1}{2}\frac{1}{2}\frac{1}{2}) \pm$		
4 U in $00\frac{1}{4}$			4 U in $0\frac{1}{2}\frac{1}{4}$		
8 U in 0.25	0.03	0	8 U in 0.03	0.25	0
−0.03	0.25	0	−0.25	0.03	0

(In C_4^5 and S_4^2 there are some more arrangements that can explain the PATTERSON functions $P(uvp)$ and $P(ppw)$. They have the same eightfold position as alternative A or B, but the fourfold one has been split up into two twofold positions: one with $z = 0$ or $\frac{1}{2}$ and one with $z = \frac{1}{4}$ or $\frac{3}{4}$. However, they can at once be ruled out as they do not agree with the intensities of the reflections hhl.)

For the intensities calculated with the two different alternatives A and B the following relations hold:

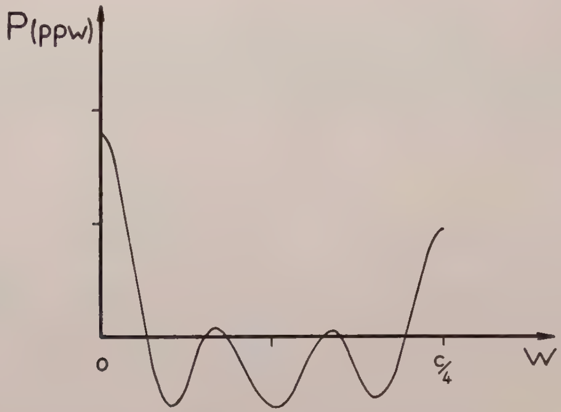

Fig. 2. Patterson analysis of $U_6O_4(OH)_4(SO_4)_6$.
The function $P_2(w) = \sum_l F^2_{00l} \cos 2\pi l w = P(ppw)$.

$$(I_{hkl})_A = (I_{hkl})_B \text{ if } l = 2n$$
$$(I_{hkl})_A = (I_{khl})_B \text{ if } l = 2n+1$$

The WEISSENBERG photograph $hk1$ thus seems to provide the means of deciding which of the two possibilities is the real arrangement. Consequently the intensities $hk1$ were calculated for A and B and compared with the observed intensities. The best agreement was then obtained with alternative A. Thus in C^5_{4h} the positions of the uranium atoms are:

$(000; \frac{1}{2}\frac{1}{2}\frac{1}{2}) \pm$
4 U_1 in C^5_{4h} 4(e): $0\,0\,z$ with $z = 0.25$
8 U_2 in C^5_{4h} 8(h): $x\,y\,0$; $\bar{y}\,x\,0$ with $x = 0.25$ $y = 0.03$

The same arrangement also fits in with the two space groups C^5_4 and S^2_4. In the latter space group the eight uranium atoms U_2 then are situated in a general position with $z \approx 0$.

Positions of the light atoms

The light hydrogen, oxygen and sulphur atoms do not make any appreciable contribution to the intensities of the reflections, and their positions had thus to be found from geometrical considerations. The following assumptions were then made:

1. The U–O distance was assumed to be not less than that found in UO_2, *i.e.* 2.36 Å (ZACHARIASEN 1948, RUNDLE and coworkers 1948, MAGNÉLI and KIHLBORG 1951).

2. The sulphate ion was considered to be a regular tetrahedron with the bond lengths S–O = 1.47 Å and O–O = 2.40 Å. These distances are mean values of those published for S–O and O–O in SO_4^{2-} and also in $S_2O_5^{2-}$ and $SO_3NH_2^-$. (A survey is given by BROWN and COX (1940).)

3. The distance between two oxygen atoms (not belonging to the same sulphate group) was assumed to be not less than 2.60 Å.

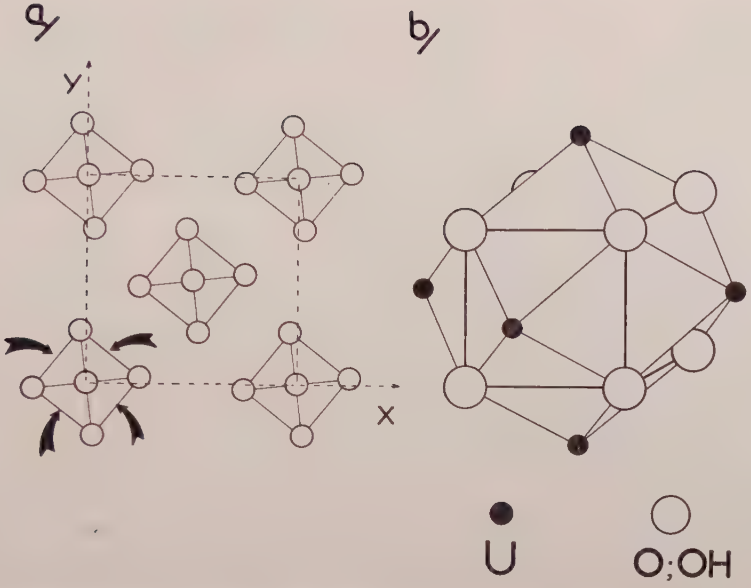

Fig. 3. a) Projection on the xy plane of the positions of the uranium atoms. The arrows point out the positions of the non-sulphate oxygen atoms belonging to the uranium octahedron with centre at the origin. (See text page 356) b) Schematic picture showing the arrangement of non-sulphate oxygen atoms ($=O^{2-}$ and OH^- ions, see page 356) around the uranium octahedron.

Positions of the non-sulphate oxygen atoms

In the structures previously determined for some hydroxy-salts of thorium and tetravalent uranium, the metal and hydroxyl ions form infinite chains (LUNDGREN and SILLÉN 1949, LUNDGREN 1950, 1952). It would thus seem likely that in the structure of $UOSO_4\,\frac{1}{3}H_2O$ also there would be an infinite arrangement in some way or other for the metal ions and the non-sulphate oxygen atoms.

Now, the uranium atoms form almost regular octahedra with the U–U distances 3.85 Å (Fig. 3a). The shortest distances between the octahedra are longer, 5.41 Å (along the x and y axes) and 5.19 Å (along the z axis). If the octahedra should be joined by bridges of oxygen atoms, these must then be situated close to the points $\frac{1}{2}00$, $0\frac{1}{2}\frac{1}{2}$; $0\frac{1}{2}0$, $\frac{1}{2}0\frac{1}{2}$, and $00\frac{1}{2}$, $\frac{1}{2}\frac{1}{2}0$. The U–O distances would then be 2.7_0 Å and 2.6_0 Å, which are only a little longer than the expected value, 2.36 Å, for a contact U–O. In no other direction could the uranium octahedra be joined by a single oxygen bridge.

However, in the unit cell there are also twelve sulphate ions, of which at least four must have their sulphur atoms in a fourfold position on $0\frac{1}{2}z$ and $\frac{1}{2}0z$. (No sulphate ion can be situated on $00z$ or $\frac{1}{2}\frac{1}{2}z$ as some U_1–O distances would then be less than 2.15 Å, *cf.* below.) Now, if the non-sulphate oxygen atoms were arranged as described above, there would be two sulphate ions and two oxygen atoms on each of the two axes $0\frac{1}{2}z$ and $\frac{1}{2}0z$. This is not possible as some O–O distances would then be less than 2.15 Å. We see then that no oxygen atoms could be situated in or close to the points $\frac{1}{2}00$, $0\frac{1}{2}\frac{1}{2}$ and $0\frac{1}{2}0$, $\frac{1}{2}0\frac{1}{2}$, and consequently the uranium octahedra can not be joined by non-sulphate oxygen atoms along the x or y axis.

If some of the non-sulphate oxygen atoms belong to fourfold or twofold positions, they should thus be situated on $00z$ and $\frac{1}{2}\frac{1}{2}z$. Of the sixteen oxygen atoms of this kind in the unit cell, at least eight would then be situated on these axes. This arrangement is not possible, as it would lead to very short U–O distances. The non-sulphate oxygen atoms should thus be arranged either in two eightfold positions or in one sixteenfold position outside the axes $00z$, $\frac{1}{2}\frac{1}{2}z$, and $0\frac{1}{2}z$, $\frac{1}{2}0z$.

We therefore conclude that in the crystal the uranium ions and the non-sulphate oxygen atoms should form finite aggregates.

For the determination of the positions of the non-sulphate oxygen atoms we observe that they must be strongly attracted by the highly charged uranium ions. It therefore seems probable that they are in contact with the metal ions, *i.e.* their centres should be situated on, or close to, spheres with radius 2.36 Å around the uranium atoms. Now, the U–U distances within the uranium octahedra are 3.85 Å and it is thus possible for the non-sulphate oxygen atoms to be in contact with two different uranium atoms at the same time, if they are situated on the circles formed by two intersecting spheres belonging to the same uranium octahedron. It is even possible for them to be in contact with three different uranium atoms. This occurs when they are situated at the points outside each octahedron surface where three spheres meet. There are sixteen such points in the unit cell and as there are also sixteen non-sulphate oxygen atoms in the cell, it seems to be very plausible that they occupy those positions, giving the most satisfactory contacts between uranium and non-sulphate oxygen atoms. This arrangement fits in with a general position in C_{4h}^5, and also with two general positions in C_4^5 or S_4^2.

We thus conclude:

16 O_1 in C_{4h}^5 16(i): $(000; \frac{1}{2}\frac{1}{2}\frac{1}{2}) \pm (xyz; \bar{y}xz; \bar{x}\bar{y}z; y\bar{x}z)$ with $x=0.11_6$, $y=0.14_8$ and $z=0.13_3$.

With these positions for the non-sulphate oxygen atoms they form almost regular cubes with the same centres as the uranium octahedra (Fig. 3b). The shortest O–O distances within these cubes are 2.8 Å, and the non-sulphate oxygen atoms are thus in good contact with each other, a fact that also speaks in favour of the positions found for them. We may observe here that this group of uranium and oxygen atoms is also found as a part of the structure of UO_2 which has the CaF_2 structure (GOLDSCHMIDT and THOMASSEN 1923).

Positions of the sulphate ions

In the characteristic space groups all the twofold and fourfold positions are situated either on $00z$; $\frac{1}{2}\frac{1}{2}z$ or on $0\frac{1}{2}z$; $\frac{1}{2}0z$. For sulphate ions with sulphur atoms in twofold or fourfold positions, however, only the last two axes need to be considered, as for sulphate ions on $00z$; $\frac{1}{2}\frac{1}{2}z$ some U_1–O distances would be too short (≤ 2.15Å). On the other hand, not more than two sulphate groups can be situated on each of the two axes $0\frac{1}{2}z$; $\frac{1}{2}0z$, as otherwise some O–O distances would be less than 2.4 Å. The twelve sulphur atoms in the unit cell should thus be arranged in one fourfold position on $0\frac{1}{2}z$; $\frac{1}{2}0z$ and one eightfold position, which can be either 8(h) in C_{4h}^5 or a general position in C_4^5 or S_4^2.

To determine the positions of the sulphate oxygen atoms we note as before for the non-sulphate oxygen atoms that they must be strongly attracted by the tetravalent uranium ions and consequently should be situated as close to them as possible.

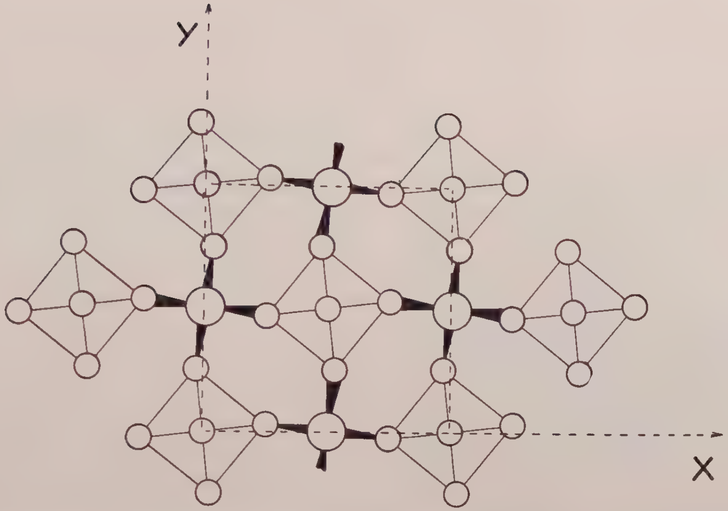

Fig. 4. Contacts between uranium atoms and the sulphate ions with their sulphur atoms in $0\frac{1}{2}\frac{1}{4}$ and $\frac{1}{2}0\frac{1}{4}$. (See text, page 357.) The contact line U–O–S is puckered. Large circles = sulphur atoms. Small circles = uranium atoms.

Now, of the four sulphate oxygen atoms belonging to a sulphur atom on $0\,\frac{1}{2}z$ or $\frac{1}{2}0z$, two can always be in contact with uranium atoms U_2, whatever the value of z. However, if $z = \frac{1}{4}$ or $\frac{3}{4}$ all four of them can be situated close to uranium atoms U_2. This is shown schematically in Fig. 4. The arrangement seems to be very probable, and we conclude that there should be four sulphur atoms in $\pm 0\,\frac{1}{2}\,\frac{1}{4}$; $\pm\frac{1}{2}0\,\frac{1}{4}$ and that all the oxygen atoms belonging to them should be in contact with uranium atoms U_2.

In this way we have found contacts U_1–4 O and U_2–6 O. Now, in UO_2, which has the CaF_2 structure (GOLDSCHMIDT and THOMASSEN 1923), every uranium is surrounded by eight oxygen atoms as is to be expected for ions of this radius ratio (PAULING 1940). We could thus expect that the coordination U–8 O also occurs in $UOSO_4\ \frac{1}{3}H_2O$ and this would demand that in addition to the oxygen atoms located there would be $4 \times 4 + 8 \times 2 = 32$ oxygen atoms more in contact with uranium. For the 32 oxygen atoms belonging to the sulphur atoms in the eightfold position we should then expect every one to be situated close to a uranium atom. Now a survey shows that this is possible only if the sulphur atoms are situated in the position 8(h) $(000;\ \frac{1}{2}\frac{1}{2}\frac{1}{2}) \pm (xy0;\ \bar{y}x0)$ in C_{4h}^5. But a sulphate ion in $z = 0$, which is a symmetry plane in C_{4h}^5, must have two of its oxygen atoms in the plane and two 1.20 Å above and below it. Sections at $z = 0$ and $z = 0.116$ through the unit cell may then give the information necessary to determine the positions of its sulphate oxygen atoms. This was done in Fig. 5a, where the areas forbidden for the centres of sulphate oxygen atoms owing to the minimum distances U–O 2.36 Å (thick circles) and O–O 2.60 Å (thin circles) are marked off. The thin circles at $0\,\frac{1}{2}0$ and $\frac{1}{2}00$ show the areas forbidden for the oxygen atoms at any position of the sulphate ions with centres in $\pm(0\,\frac{1}{2}\,\frac{1}{4})$ and $\pm(\frac{1}{2}0\,\frac{1}{4})$. A sulphate oxygen atom being in contact with a thick circle is thus situated close to a uranium atom. From the figures we see now, that there

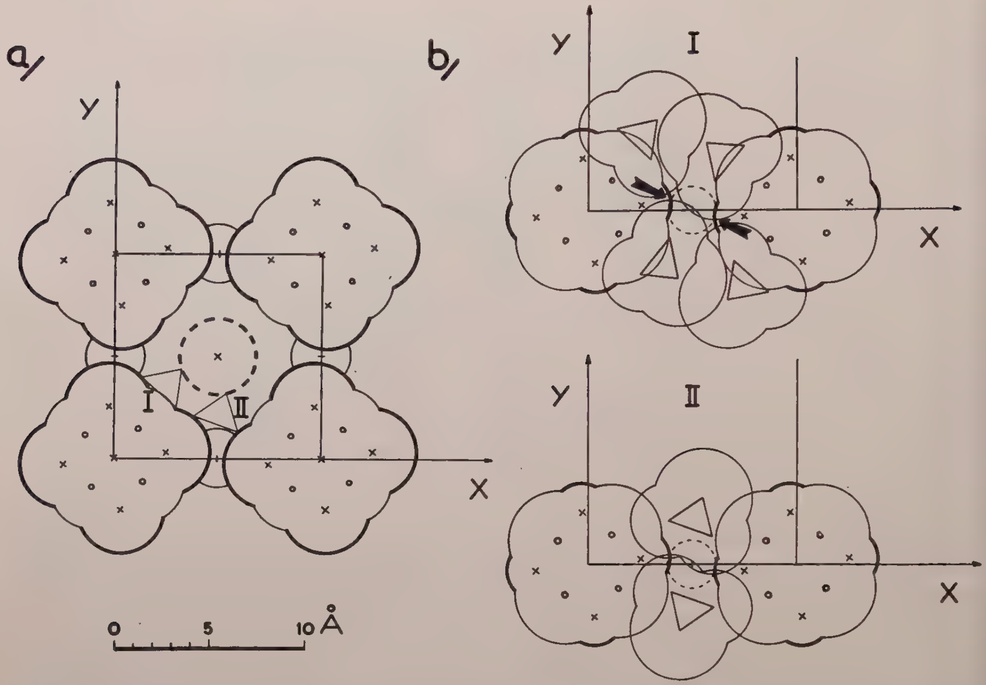

Fig. 5. a) Sections at $z=0$ (full lines) and at $z=0.116$ (dotted lines) through the unit cell showing the areas forbidden for sulphate oxygen atoms. The triangles, the projection of a sulphate group in the symmetry plane $z=0$, show the two alternatives for the position of a sulphate ion with its sulphur atom in $z=0$. (See text page 357.) b) Part of the sections at $z=0.168$ through the unit cell showing the areas forbidden for sulphate oxygen atoms with their sulphur atom at $\frac{1}{2}0\frac{1}{4}$. The two figures refer to the two alternatives according to a). The arrows point out the only areas left free. (See text page 358.)

are only two different positions possible for a sulphate ion with its sulphur atom in C_{4h}^5 8(h) (the triangles in Fig. 5a).

To see which of these two possibilities is more likely we shall examine how they influence the positions of the sulphate groups with sulphur atoms in $\pm(0\,\frac{1}{2}\,\frac{1}{4})$, $\pm(\frac{1}{2}\,0\,\frac{1}{4})$. These ions are situated on 4_2 axes (in $S_4^2\ \bar{4}$ axes), and this is possible only if the axes go through the midpoints of two opposite edges in the sulphate tetrahedra. The z parameters of the oxygen atoms O_2 belonging to the sulphate group in $\frac{1}{2}0\frac{1}{4}$ are then 0.168 and 0.332, and to find out their positions it remains only to determine an angular parameter, which can be done, if we draw the section through the unit cell at $z=0.168$. This is shown in Fig. 5b, where there is one figure for each alternative for the positions of the eight sulphate ions with their sulphur in C_{4h}^5 8(h). The two oxygen atoms O_2 with $z=0.168$ are then situated somewhere on the dotted circle with centre in $x=\frac{1}{2}\,y=0$. We see at once, that with alternative I there are two small areas, at the arrows in Fig. 5b, left free close to the uranium atoms U_2, whereas alternative II does not fit in at all. We thus conclude that the sulphate ions must be arranged according to alternative I, which fits in with all the three characteristic space groups. The parameters for the sulphur and oxygen atoms are then:

$(000;\ \tfrac{1}{2}\tfrac{1}{2}\tfrac{1}{2})\pm$
4 S_1 in C_{4h}^5 4(d): $0\tfrac{1}{2}\tfrac{1}{4};\ \tfrac{1}{2}0\tfrac{1}{4}$
8 S_2 in C_{4h}^5 8(h): $xy0;\ \bar{y}x0$ with $x=0.28_0$ $y=0.38_1$
16 O_2 in C_{4h}^5 16(i): $xyz;\ \bar{y}xz;\ \bar{x}\bar{y}z;\ y\bar{x}z;$ with $x=0.41_5$ $y=0.05_8$ $z=0.16_8$
16 O_3 in C_{4h}^5 16(i) with $x=0.32_8$ $y=0.43_9$ $z=0.11_6$
8 O_4 in C_{4h}^5 8(h) with $x=0.31_8$ $y=0.24_3$
8 O_5 in C_{4h}^5 8(h) with $x=0.14_2$ $y=0.38_8$

In the unit cell there are also eight hydrogen atoms, which should be situated close to some of the oxygen atoms. Now, as the proton affinity of O^{2-} is greater than that of SO_4^{2-}, it seems much more likely that they are situated close to the "basic" oxygen atoms O_1 than to the sulphate oxygen atoms O_2–O_5. The sixteenfold position O_1 thus in fact consists either of eight O^{2-} and eight OH^- or of twelve O^{2-} and four H_2O, of which alternatives the first one seems to be the most plausible. As the interatomic distances within the sixteenfold position O_1 are about 2.8 Å, the hydroxyl ions surely form hydroxyl bonds with neighbouring oxygen atoms.

As the hydrogen atoms at hydroxyl bonds often seem to remain attached to their own oxygen atoms, the arrangement for the hydrogen atoms does not fit in with the space group C_{4h}^5, which would have afforded symmetrical O–H–O bonds parallel to the *c* axis. In C_4^5 and S_4^2, however, the arrangement can be explained, the difference being that the first space group has the hydroxyl bonds arranged around a fourfold axis $00z$, while the second has them arranged around a $\bar{4}$ axis $00z$ with an inversion centre in 000. Of these two possibilities the second (in S_4^2) seems to be more plausible than the first (in C_4^5).

With the arrangement proposed for the hydrogen atoms there are no water molecules present in the crystals, but they contain 8 OH^- and 8 O^{2-} for 12 U^{4+} and 12 SO_4^{2-}. Their formula should then be written $U_6O_4(OH)_4(SO_4)_6$ rather than $UOSO_4\ \tfrac{1}{3}H_2O$.

Final structure proposition

After the positions of the oxygen and sulphur atoms had been found, a redetermination of the positions of the uranium atoms was made, using trial and error methods and taking into account the scattering power of the oxygen and sulphur atoms. The best agreement between the observed and calculated intensities was then obtained with the following parameters:

$(000;\ \tfrac{1}{2}\tfrac{1}{2}\tfrac{1}{2})\pm$
4 U_1 in C_{4h}^5 4(e): $00z$ with $z=0.260\pm0.003$
8 U_2 in C_{4h}^5 8(h): $xy0;\ \bar{y}x0$ with $x=0.252\pm0.003$ $y=0.030\pm0.003$

Finally with these uranium parameters a redetermination of the positions of the oxygen and sulphur atoms was made.

In Tables 2 and 3 the calculated values of $100\left(\frac{F}{4f_U}\right)^2$ are compared with the observed intensities of the reflections in the WEISSENBERG photographs $hk0$ and $h\,h+1\,l$. These are especially sensitive, the first to the positions of the uranium atoms U_2 and the second to the positions of the uranium atoms U_1. In the photograph $h\,h+1\,l$ there is an absorption effect (*cf.* WELLS 1937) due to the shape of

Table 2

Calculated and observed intensities $hk0$ from a WEISSENBERG photograph of $U_6O_4(OH)_4(SO_4)_6$. CuK radiation. $I_{calc}=100\left(\frac{F}{4\,f_U}\right)^2$

	h →													
	0	1	2	3	4	5	6	7	8	9	10	11	12	13
k 0	—	—	100 w	—	576 st	—	9 vvw	—	552 m	—	4 —	—	169 w	—
↓ 1	—	62 w	—	262 w +	—	303 m	—	471 m	—	289 m	—	350 m	—	137 vw
2	100 w	—	41 vw	—	172 w	—	12 vvw	—	396 m	—	20 vvw	—	745 st	—
3	—	21 vvw	—	104 w—	—	4 —	—	77 vw	—	92 w −	—	40 vvw	—	40 —
4	576 st	—	164 w	—	713 m	—	61 vvw	—	279 w +	—	30 —	—	180 w	
5	—	6 —	—	511 m	—	30 —	—	595 m	—	123 vw	—	795 st	—	
6	9 vvw	—	1 —	—	119 vvw	—	2 —	—	86 vw −	—	185 w	—	471 m +	
7	—	2 —	—	130 w	—	46 —	—	58 —	—	108 vw	—	92 vw	—	
8	552 m	—	317 m	—	428 m	—	388 w +	—	219 vw	—	59 vw			
9	—	4 —	—	480 m	—	9 —	—	847 st	—	166 w				
10	4 —	—	32 vvw	—	0 —	—	58 vw—	—	58 vw −					
11	—	0 —	—	256 w +	—	76 vw	—	55 vw						
12	169 w	—	882 st	—	137 w	—	586 st							
13	—	48 vvw	—	400 m										

the crystals (plates) which is very pronounced for rays passing along the crystal plate. The line with this high absorption has been marked out in Table 3, and reflections on either side of this line must not be compared with each other. Taking this absorption into account and considering the general weakening of the reflections with increasing θ the agreement between observed and calculated intensities is rather good.

Thus the following structure is proposed for $U_6O_4(OH)_4(SO_4)_6$:
Space group: C_{4h}^5–I 4/m. 2 formula units in the unit cell.

	x	y	z
4 U_1 in 4(e)	0	0	0.260 ± 0.003
8 U_2 in 8(h)	0.252 ± 0.003	0.030 ± 0.003	0
4 S_1 in 4(d)	0	$\frac{1}{2}$	$\frac{1}{4}$
8 S_2 in 8(h)	0.27_2	0.37_9	0
16 O_1 (8O+8OH) in 16(i)	0.11_3	0.14_4	0.13_3
16 O_2 in 16(i)	0.40_0	0.05_3	0.16_8

Table 3

Calculated and observed intensities $h\,h+1\,l$ from a WEISSENBERG photograph of $U_6O_4(OH)_4(SO_4)_6$. CuK radiation. $I_{calc} = 100 \cdot \left(\frac{F}{4\,f_U}\right)^2$

	h →									
l ↓	0	1	2	3	4	5	6	7	8	9
1	50 w	121 m	102 w	296 m	180 w	270 w	180 vw	190 vw	16 —	106 w
3	85 vw	59 w	237 m	327 m	161 w	210 w	119 vw−	205 w	55 vvw	
5	35 vvw	235 m	275 m+	114 w	96 vw	369 m	286 w+	114 w	4 —	
7	182 w	49 vvw	40 vvw	475 st	346 m−	137 vw	69 vvw	370 st		
9	4 —	234 w+	305 m	185 w	51 vvw	466 st	289 m+			
11	196 w+	30 vvw	29 vvw	420 st	372 st					
13	4 —	372 st								

	x	y	z
16 O_3 in 16(i)	0.32_6	0.43_7	0.11_6
8 O_4 in 8(h)	0.30_0	0.24_4	0
8 O_5 in 8(h)	0.13_5	0.39_8	0

$(000;\ \tfrac{1}{2}\tfrac{1}{2}\tfrac{1}{2})\pm$
4(d) : $0\tfrac{1}{2}\tfrac{1}{4}$
4(e) : $00z$
8(h) : $xy0;\ \bar{y}x0$
16(i) : $xyz;\ \bar{y}xz;\ \bar{x}\bar{y}z;\ y\bar{x}z$

The accuracy of the sulphur and oxygen parameters is estimated to be about ±0.01.

Description of the structure

With the structure proposed for the crystals a rather unusual arrangement of the metal ions is obtained, differing very much from that in $U(OH)_2SO_4$ (LUNDGREN 1952). The metal ions are associated in groups each consisting of six uranium atoms forming an octahedron with the U–U distances (3.84 Å and 3.85 Å) similar to those found in UO_2 (3.87 Å). The shortest U–U distances between two different uranium octahedra is considerably longer (4.98 Å). Every one of the octahedra is then surrounded by oxy and hydroxy ions forming a cube, so that every uranium atom is in contact with four O^{2-} or OH^- and every $O^{2-}(OH^-)$ with three uranium atoms. A picture of this arrangement is drawn in Fig. 3b. It resembles distantly the $Mo_6Cl_8^{4+}$ ions found by BROSSET (1945, 1946, 1949) in a number of molybdenum compounds. However, in these complex molybdenum ions there is a strong interaction between the metal ions (the Mo–Mo distance being somewhat shorter than

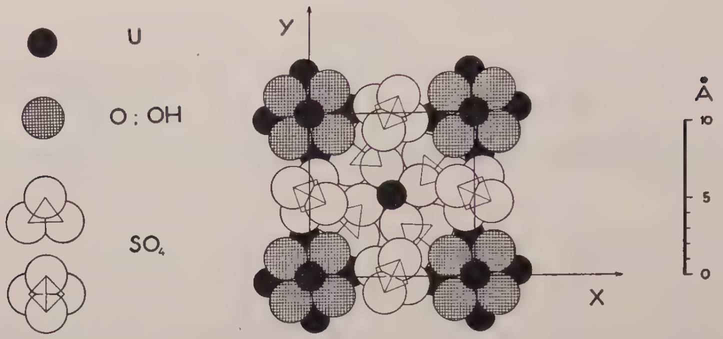

Fig. 6. Projection on the xy plane of a part of the structure of $U_6O_4(OH)_4(SO_4)_6$. (Only atoms with z parameters between 0 and $\frac{1}{2}$ have been indicated.)

in molybdenum metal), whereas in the crystals of $U_6O_4(OH)_4(SO_4)_6$ the bonds within the "clusters" of uranium, oxygen, and hydroxy ions probably are mainly ionic, the U–U distance being the same as in UO_2.

In the crystals these "clusters" are joined by sulphate ions, so that every uranium atom is in contact with four different sulphate ions and every sulphate ion with four different uranium atoms. Every one of the uranium atoms is in this way in contact with eight oxygen atoms in the shape of a distorted square Archimedean antiprism. The U–O distances are all 2.3_7 Å.

The xz projection of a part of the structure of $U_6O_4(OH)_4(SO_4)_6$ is shown in Fig. 6.

The distances U–O, S–O, and O–O (within a sulphate group) were assumed to be 2.3_6 Å, 1.4_7 Å, and 2.4_0 Å. The distances between the oxygen atoms not belonging to the same sulphate group will be (in Å):

$$\begin{array}{lll}
O_1 - 3\ O_1 & & = 2 \times 2.7_8\ ;\ 2.7_6 \\
O_1 - 2\ O_2\ ; & O_2 - 2\ O_1 & = 3.2_5\ ;\ 3.3_0 \\
O_1 - 2\ O_3\ ; & O_3 - 2\ O_1 & = 2.8_2\ ;\ 3.2_3 \\
O_1 - O_4\ ; & O_4 - 2\ O_1 & = 2.6_6 \\
O_1 - O_5\ ; & O_5 - 2\ O_1 & = 3.0_7 \\
O_2 - O_2 & & = 3.4_9 \\
O_2 - 2\ O_3\ ; & O_3 - 2\ O_2 & = 3.3_1\ ;\ 3.4_6 \\
O_2 - O_4\ ; & O_4 - 2\ O_2 & = 2.9_0 \\
O_2 - 2\ O_5\ ; & O_5 - 4\ O_2 & = 2.6_7\ ;\ 2.9_2 \\
O_3 - 2\ O_3 & & = 2.8_1 \\
O_3 - O_4\ ; & O_4 - 2\ O_3 & = 3.1_9 \\
O_4 - O_5\ ; & O_5 - O_4 & = 3.4_5
\end{array}$$

These figures are all within the normal range showing that the lattice is supported by O–O contacts also. However, they may be in error by a few 0.1 Å, because the oxygen positions could not be determined very accurately.

The author wishes to thank Professor ARNE ÖLANDER for his kind interest, Professor LARS GUNNAR SILLÉN for many valuable discussions and Professor GUSTAF LJUNGGREN for kindly supporting this work.

Part of the work was aided by a grant from Atomkommittén.

SUMMARY

$U_6O_4(OH)_4(SO_4)_6$ has a bodycentered tetragonal cell with the dimensions:

$$a = (10.741 \pm 0.005)\ \text{Å}$$
$$c = (10.377 \pm 0.005)\ \text{Å}$$

The unit cell contains two formula units.

A structure is proposed with atomic positions for the uranium, sulphur, and oxygen atoms in $C_{4h}^5 - I\ 4/m$ (see page 360). The parameters of the uranium atoms were determined from the intensities, but the positions of the light atoms had to be found from geometrical considerations.

The structure is built up of sulphate ions and separate groups $[U_6O_4(OH)_4]^{12+}$. The uranium atoms form regular octahedra surrounded by 4 O^{2-} and 4 OH^- ions forming a cube (Fig. 3b). The U–U distances within these groups are about the same as in UO_2. In the crystals, the groups are joined by sulphate ions so that the coordination of oxygen atoms around uranium is eightfold in the shape of a square Archimedean antiprism.

Försvarets Forskningsanstalt, Avd. 1.
Department of Inorganic and Physical Chemistry, University, Stockholm.
Department of Inorganic Chemistry, Royal Institute of Technology, Stockholm.

REFERENCES

Brosset, C. (1945) Arkiv för Kemi Miner. och Geol. *20 A* no 7.
—— (1946) Ibid *22 A* no 11.
—— (1949) Arkiv för Kemi *1*, 353.
Brown, C. J. and Cox, E. G. (1940) J. Chem. Soc. 1.
Brush, G. J. (1868) Amer. J. Sci. *460*, 240.
Goldschmidt, V. M. and Thomassen, L. (1923) Vid. Selsk. Skr. Mat. Nat. Klasse (Kristiania) no 2; Strukturbericht *1*, 212.
Hartwig-Bendig, M. (1941) Z. angew. Miner. *3*, 195.
Hecht, F. and Donau, J. (1940) Anorganische Mikrogewichtsanalyse, Wien, page 205.
Kolthoff, I. M. and Sandell, E. B. (1943) Textbook of Quantitative Inorganic Analysis, New York, page 753.
Lundgren, G. (1950) Arkiv för Kemi *2*, 535.
—— (1952) Arkiv för Kemi *4*, 421.
Lundgren, G. and Sillén, L. G. (1949) Arkiv för Kemi *1*, 277; Naturwiss. *36*, 345.
Magnéli, A. and Kihlborg, L. (1951) Acta Chem. Scand. *5*, 578.
Pauling, L. (1940) The Nature of the Chemical Bond, 2 ed., New York, page 382.
Penfield, S. L. (1894) Amer. J. Sci. (3) *48*, 30.
Rundle, R. E., Baenziger, N. C., Wilson, A. S., and McDonald, R. A. (1948) J. Am. Chem. Soc. *70*, 99.
Wells, A. F. (1937) Z. Krist. *96*, 451.
Zachariasen, W. H. (1948) Phys. Rev. *73* (Ser. II), 1104.

Tryckt den 26 februari 1953

Uppsala 1953. Almqvist & Wiksells Boktryckeri AB

ARKIV FÖR KEMI Band 5 nr 35

Read 9 April 1952

Products of potato starch degradation by malt α-amylase

By Karl Myrbäck and Barbro Persson

With 6 figures in the text

If malt α-amylase is allowed to act on a starch solution and the liberation of reducing groups is followed by some suitable method, it is found that the reduction may gradually reach a value corresponding to formation of more than 100 per cent maltose, this sugar being, as in the case of other normal amylases, the chief product of the enzymatic degradation. However, malt α-amylase and at least certain other α-amylases also produce glucose as a product of the amylase (and not a maltase) action. The isomaltose linkages of the starch are not affected by the enzymes but remain in the non-fermentable fraction of the degradation products, the "limit dextrins" (1). It has been assumed by K. H. Meyer (2) that, after prolonged hydrolysis of starch by α-amylases the ultimate products are maltose, glucose, and isomaltose. Our experience is not in accordance with this view and, in any case, in reaching this stage the hydrolysis passes through certain different stages, more or less easily discernible.

The first stage, generally called the dextrinization, is characterized by a rapid increase in reducing power but a rather small formation of fermentable sugars. This stage of starch hydrolysis comprises the rupture of about 16 per cent of the glucosidic linkages of the substrate. The non-fermentable products, the α-dextrins, have an average degree of polymerization (DP) of about 7 units. No high polymeric molecules are left, showing that retrogradation of the substrate during the hydrolysis can play no significant role. The α-dextrins are of two different kinds: a) "normal" α-dextrins, which are completely converted to fermentable sugars by β-amylase and therefore contain maltose linkages exclusively, and b) "abnormal" α-dextrins, which are only partially saccharified by β-amylase and yield, when acted upon by this enzyme, maltose and non-fermentable limit dextrins. The abnormal α-dextrins thus contain isomaltose linkages, originating from the ramification points of the amylopectin molecules.

After the dextrinization of starch by malt α-amylase a comparatively slow "saccharification" of the α-dextrins follows. The slowing-down of the reaction rate at an average degree of hydrolysis of about 16 per cent is explained by the fact that the affinity of the enzyme to chain molecules shorter than a certain number of glucose units (about 8) is very much lower than that to high-molecular substrates (3, 4). The saccharification which, naturally, goes on to some extent already during the dextrinization period continues with decreasing velocity until the final stage is reached, in which, according to Meyer, only maltose, isomaltose and glucose are present. However, the velocity of the final stages is so extremely low compared to that of the initial stages of starch degradation that generally, when a "saccharification limit" appears to be reached, the products are not only the three sugars mentioned but also limit dextrins containing three or more glucose units and one or more isomaltose linkages. It may still be regarded as a matter of some dispute if the final hydrolysis of such limit dextrins is an action of the α-amylases or caused by a contaminating enzyme. However, there is a considerable amount of evidence suggesting that also these last stages are caused by the α-amylases themselves. (5)

In the following experiments a characterization of some intermediate products of the breakdown of starch by malt α-amylase was aimed at. Starting material was native potato starch. The enzyme (6) was prepared by cold water extraction of six-row barley malt, freed from β-amylase according to OHLSSON by heating to 70°, and purified by precipitation with tannin. Potato starch (700 g dry weight) was suspended in cold water and the slurry was poured into 15 liter of boiling water. The mixture was boiled for a few minutes and cooled to room temperature. A filtered solution of 0,6 g of the enzyme preparation and 50 ml toluene were added.

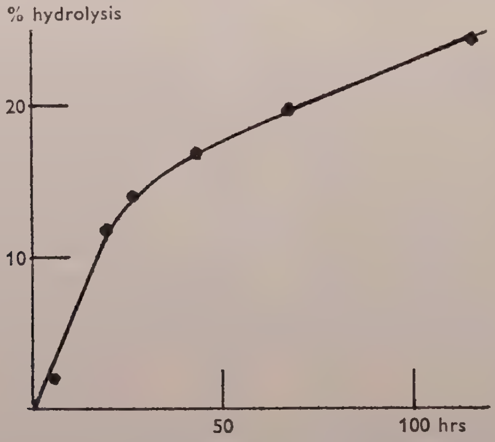

Fig. 1. Liberation of reducing groups by malt α-amylase.

The increase in reducing power was determined according to Willstätter and Schudel and calculated as per cent glucose (Fig. 1). Even in this experiment with a comparatively small enzyme concentration and low reaction rate the curve has the usual appearance, exhibiting a distinct slowing-down of the reaction at about 16 per cent hydrolysis. After 116 hours the reaction mixture was boiled, filtered through a layer of infusorial earth and then concentrated to 1780 ml. The average degree of hydrolysis was 24 per cent and hence the average DP of the products (including fermentable sugars) was 4.2. The solution was precipitated with absolute alcohol:

1780 ml +	1800	ml	alcohol	yielded	2.6 g	Fraction	I
	2000	»	»	»	96.4 g	»	II
	2200	»	»	»	115.8 g	»	III
	2750	»	»	»	no precipitate.		

The solution was concentrated to a thin sirup and precipitated with alcohol to a final concentration of 80 percent; 320 g dextrin was recovered = Fraction IV. Increase of the alcohol concentration to 90 per cent yielded only 12.9 g dextrin = Fraction V. Further addition of absolute alcohol to the mother liquor caused no precipitation. The mother liquor was concentrated to remove the alcohol. It contained about 150 g carbohydrate = Fraction VI. The yields of the various fractions (dry weight) and their average degree of polymerization (molecular weight) are collected in Table 1.

Average molecular weight of dextrins.

The reducing power was determined according to Willstätter and Schudel. Since this method is supposed to yield somewhat high values in the case of high-molecular dextrins, determinations were also carried out according to Bertrand's method. In parallel experiments the reducing power after complete hydrolysis in N sulfuric acid at 100° was determined and the average DP was calculated (Table 1). As in previous investigations we find that after dextrinization of starch by malt α-amylase no high molecular degradation products and no undegraded starch is found, showing among other things that retrogradation of the substrate during the degradation has no perceptible influence.

Table 1

Fraction	g	Per cent of starch	Average degree of polymerization	
			Willstätter-Schudel	Bertrand
I	2.6	0.3	13.7	18.5
II	96.4	13.8	9.0	9.7
III	115.8	16.5	7.2	7.9
IV	320.0	45.7	4.1	4.0
V	12.9	1.9	2.2	–
VI	150	21.6	1.6	–
		99.8		

Since the yields are calculated on the initial amount of starch and not on the theoretical amount of glucose it appears that some ten per cent of the material has been lost in the isolation processes.

Determination of fermentable sugars.

This determination was carried out with baker's yeast. As mentioned before, the commercial Swedish baker's yeast ferments glucose with a very high initial velocity, whereas the fermentation of maltose shows a more or less pronounced lag period (curves 1 and 2 in Fig. 2). It is possible, therefore, to determine glucose and maltose separately in mixtures of both sugars in one fermentation experiment. The fermentation curves obtained have the form shown by curve 3 of Fig. 2, and the amounts of glucose and maltose in the fermented mixture can be calculated fairly accurately from such curves. Two experiments with different dextrin preparations are recorded in Fig. 2 (curves 4 and 5). In order to determine a factor for calculation of the amounts of fermentable sugar from the measured volumes of carbon dioxide, a number of experiments with known amounts of sugar was carried out. In all experiments 2 ml sugar solution (10–150 mg sugar, maltose hydrate or a mixture of glucose or maltose hydrate) were mixed with 2 ml yeast suspension: 1 part of pressed yeast and 2 parts of 1 percent phosphate buffer of pH = 5. The experiments were performed in a water

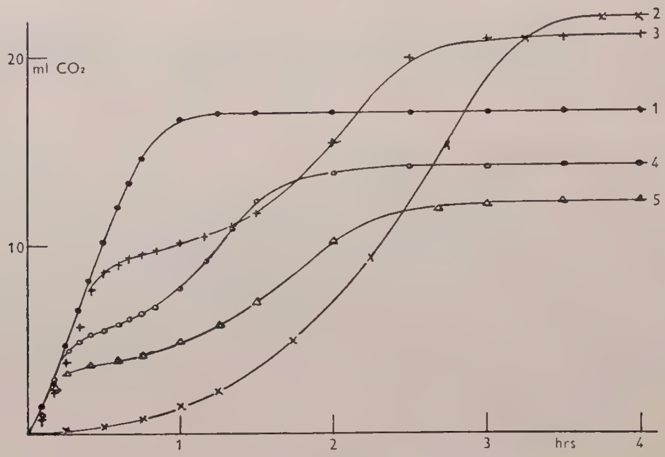

Fig. 2. Fermentation by baker's yeast:

Curve 1. 71 mg glucose,
» 2. 99 mg maltose,
» 3. 36 mg glucose + 56 mg maltose,
» 4. 86 mg dextrin fraction V,
» 5. 270 mg dextrin fraction IV.

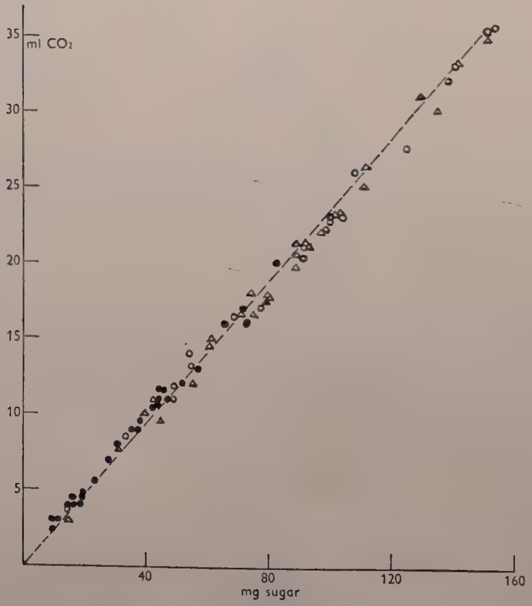

Fig. 3. Fermentation of known amounts of sugar by baker's yeast.

○ Fermentation of maltose alone
● yield from glucose in fermentation of glucose-maltose mixtures
△ yield from maltose in the same experiments.

thermostate with mechanical agitation at 30° and the carbon dioxide was collected over mercury in gas burettes. The results of the experiments with known amounts of sugar are collected in Fig. 3. The contents of fermentable sugars in the dextrin fractions are shown in table 4. The yield of glucose from starch with malt α-amylase is rather large, considerably larger than could be expected if glucose were formed only from certain limit dextrins.

The non fermentable dextrins.

The average molecular weight of the non-fermentable dextrins in the various fractions was determined in the following way. After fermentation by baker's yeast the solutions were freed from yeast by suction through a layer of infusorial earth. Filtrates and washings were evaporated to dryness to remove alcohol, and the remainder was dissolved in water. The reducing power was determined before and after complete hydrolysis in N sulfuric acid at 100°. Since it had been found that different methods yield slightly varying values of the reducing power of yeast-treated preparations, determinations were carried out according to three different methods: Willstätter and Schudel (W-S), Bertrand (B), and Shaffer-Somogyi (Sh-S). The values are collected in table 2 and are calculated as glucose in percent of the original amount of dextrin in the fermentation experiment.

Table 2

Dextrin fraction	Reducing power: per cent glucose								DP
	Before hydrolysis			After hydrolysis			Mean values		
	W–S	B	Sh–S	W–S	B	Sh–S	before hydrolysis	after hydrolysis	
II	9.5	7.8	7.9	89.1	92.2	87.8	8.4	89.7	10.7
III	10.3	8.9	8.1	94.1	89.0	83.1	9.1	88.7	9.7
IV	14.0	12.5	11.2	81.0	76.9	78.3	12.6	78.7	6.2
V	11.5	11.5	11.5	26.3	26.0	27.6	11.5	26.6	2.3

In agreement with previous results we find that the unfermentable dextrins, *i.e.* the α-dextrins, for the most part have DP's ranging from 6 to 10 units.

Degradation of the α-dextrin fractions by β-amylase.

The structure of the α-dextrins and especially the occurrence of isomaltose linkages therein can be, to some degree, elucidated by determination of the degradation by amylases. The action of β-amylase was first investigated. The enzyme was a partly purified barley enzyme, free from α-amylase. The following experiment with dextrin fraction II will be described to illustrate the procedure: 0.913 g dextrin (dry weight) was dissolved in 25 ml water; 3 ml phosphate buffer (pH = 5.3) and 2 ml enzyme solution were added. The reducing power was determined in small samples and calculated as percent glucose: Table 3.

15 ml of the reaction mixture (0.457 g dextrin) was boiled, filtered and brought to 25 ml. The reducing power still corresponded to an apparent glucose content of 27.8 per cent. Since the increase in reducing power corresponds to 16.1 percent glucose and β-amylase is known to yield maltose as the only reaction product, the

experiment would seem to indicate the formation of 32.2 per cent maltose hydrate. However, fermentation experiments showed the true formation of fermentable sugar to be considerably larger. A portion of the reaction mixture corresponding to 274 mg dextrin was fermented with baker's yeast as described above. The carbon dioxide evolution corresponded to 2 mg glucose + 126 mg maltose hydrate. Accordingly, no formation of glucose has taken place during the treatment with β-amylase which is quite in agreement with the current views on the mechanism of β-amylase action.

Table 3

Reaction time	Per cent glucose
0	11.7
0.5 min.	14.4
48 hrs	25.1
72 »	27.8

However, the amount of maltose found in the fermentation experiment is 46 per cent of the dextrin, compared to 32.2 per cent as calculated from the increase in reducing power. Before entering into an explanation of this discrepancy it should be recorded that the reducing power of the non-fermentable substances before and after complete hydrolysis was determined as described above. The reducing power, calculated as glucose in per cent of the original amount of dextrin, was 6.5 per cent before and 54.5 per cent after hydrolysis. The mean DP after treatment of the dextrin fraction II with β-amylase therefore is 8.4 or only slightly lower than before the enzyme treatment (DP = 10.7 ; Table 2). It must be therefore concluded that the action of β-amylase on the dextrin fraction is, in the main, a complete degradation of normal α-dextrins whereas the DP of the abnormal (branched) α-dextrins is only moderately diminished. This result explains also the apparant discrepancy between the values of maltose formation calculated from fermentation and from reduction measurements. If, for instance, an octasaccharide is broken down to maltose by β-amylase, the yield of maltose calculated from the *increase* of the reduction value would be 75 per cent, whereas the fermentation would yield the correct value of 100 per cent. Besides, among the normal α-dextrins in the various fractions there are certainly such that contain an uneven number of glucose units. These

Table 4

Fraction	Before degradation by β-amylase			After degradation by β-amylase				DP of non-fermentable dextrins
	Per cent glucose	Per cent maltose	DP of non-fermentable dextrins	Maltose calc. from increase in reduction	Fermentable sugars			
					glucose	maltose	increase of maltose	
I	0	0	13.7	—	—	—	—	—
II	0.7	3.4	10.7	32.2	0.7	46.6	42.6	8.4
III	1.1	5.8	9.7	33.6	1.0	52.2	46.4	6.7
IV	5.6	14.6	6.2	46.8	5.8	84.5	70.0	2.6
V	24.5	48.2	2.3	23.2	23.5	74.0	25.8	2.2
VI	40.5	40.5	1.5	0	—	—	—	—

will yield one molecule of maltotriose per dextrin molecule. Since maltotriose is fermented by the baker's yeast used in this investigation, the presence of maltotriose will increase the difference between the "maltose" values calculated from fermentation and from reduction experiments.

Experiments with β-amylase and the different dextrin fractions are recorded in Table 4. As could be expected the enzyme had no action on the quite low-molecular fraction VI.

It is seen from Table 4 that no glucose is formed during the treatment with β-amylase. In agreement with previous results it appears that the saccharification of the α-dextrins by β-amylase is fairly complete for the fractions (IV and V) with the lowest DP-values. Evidently these fractions are composed mainly of normal α-dextrins whereas the fractions I–III contain the abnormal (branched) α-dextrins and, accordingly, are only partially saccharified by β-amylase. The non-fermentable dextrins, left over by the β-amylase, have DP-values not very much lower than those of the original dextrins. As pointed out before, this seems to indicate that the maltose formed by β-amylase originates mainly from normal α-dextrins contained in the various fractions and only to some relatively small extent from branched dextrins. An abnormal α-dextrin having the formula A in Fig. 4 would, for instance, yield only one molecule of maltose and the α-dextrin B no maltose at all. The degradation of various dextrins by β-amylase has been dealt with exhaustively in a previous publication (7).

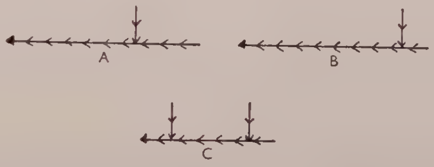

Fig. 4. Structure of branched α-dextrins.

Degradation of dextrin fractions by salivary amylase.

Since salivary amylase is an α-amylase and consequently is able to attack other α-glucosidic 1,4-linkages than those ruptured by β-amylase, it must be expected that the saccharification by salivary amylase should be more complete than that by β-amylase. In an experiment with dextrin fraction II, 0.913 g dry-weight was dissolved in 25 ml water; 3 ml phosphate buffer (pH = 6.9) and 2 ml salivary amylase were added. The increase of the reducing power was determined in small samples and calculated as percent glucose: Table 5.

Table 5

Reaction time	Per cent glucose
0	11.7
0.5 min.	13.6
24 hrs	42.8
144 »	43.7
170 »	43.8

The increase in reducing power corresponds to 32.1 per cent glucose or 64.2 per cent maltose hydrate. Both values are ficticious, since the enzyme produces a mixture of glucose, maltose and possibly maltotriose. Fermentation experiments showed the presence of 15.7 per cent glucose and 48.5 per cent maltose, the last figure comprising maltotriose eventually present. The reducing power of the limit dextrins after degradation by salivary amylase and fermentation was 8.5 per cent before and 42.5 per cent after complete hydrolysis. Thus, the average DP of the residual dextrins is about 5.

If this experiment is compared to the corresponding experiment with β-amylase we find that the yield of fermentable sugar is larger (64.2 compared to 46 per cent). The increase of reducing power in the degradation is considerably larger (32.1 compared to 16.1 per cent). The difference is due to the formation of glucose in the degradation by salivary amylase. The amount of residual dextrin is somewhat lower with salivary amylase than with β-amylase (42.5 compared to 54.5 per cent, calculated as glucose), which corresponds to the larger yield of fermentable sugars in the former case. However, the differences in the yields of the degradation products (apart from glucose) are surprisingly small and the DP of the limit dextrins in the case of salivary amylase is surprisingly high. Since large amounts of this enzyme were used in the experiments and the reaction time was extremely prolonged, it must be concluded that certain relatively high-molecular limit dextrins are, at least practically, stable toward salivary amylase. In the case of this enzyme it can, therefore, certainly not be assumed that glucose, maltose and isomaltose are the only end-products of the action on starch. It may be mentioned that, according to Roberts and Whelan (8), salivary amylase has no action on maltotriose.

Our experiments on the degradation of the various α-dextrin fractions by salivary amylase are collected in Table 6.

Table 6

Fraction No	Maltose calculated from increase of reducing power	Fermentable sugars				DP of residual dextrin
		glucose		maltose		
		found in fermentation experiment	increase	found in fermentation experiment	increase	
II	64.1	15.7	15.0	48.5	45.1	5.0
III	67.8	16.2	15.1	53.2	47.7	5.7
IV	80.4	22.5	16.9	75.0	60.5	2.5
V	50.4	36.4	11.9	69.0	20.8	1.9

Refractionation of α-dextrin fraction IV. 267 g (dry-weight) were dissolved in 1 liter of water and precipitated with absolute alcohol: Table 7.

The average degree of polymerization and the content of fermentable sugars was determined as described above: Table 8.

Fig. 5 gives a schematical picture of the distribution of the dextrins on different chain lengths. A comparison between the dashed curve (unfermentable dextrins after first fractionation) and the full-drawn curve (non-fermentable dextrins after refractionation) shows the effect of the reprecipitation of the α-dextrins in the original fraction IV.

Table 7

<table>
<tr><th>Fraction No</th><th>ml alcohol added</th><th>yield in g (dry-weight)</th></tr>
<tr><td>IV: 1</td><td>1700</td><td>38.9</td></tr>
<tr><td>2</td><td>1900</td><td>21.1</td></tr>
<tr><td>3</td><td>2100</td><td>22.9</td></tr>
<tr><td>4</td><td>2300</td><td>17.2</td></tr>
<tr><td>5</td><td>2550</td><td>21.2</td></tr>
<tr><td>6</td><td>2850</td><td>17.4</td></tr>
<tr><td>7</td><td>3200</td><td>14.2</td></tr>
<tr><td>8</td><td>3600</td><td>10.1</td></tr>
<tr><td>9</td><td>4350</td><td>14.6</td></tr>
<tr><td colspan="3">The mother liquor was concentrated to 170 ml and precipitated with</td></tr>
<tr><td>10</td><td>300</td><td>36.4</td></tr>
<tr><td>11</td><td>400</td><td>7.7</td></tr>
<tr><td>12</td><td>700</td><td>5.0</td></tr>
<tr><td colspan="3">The mother liquor was concentrated to 80 ml. No precipitate could be obtained with alcohol.</td></tr>
<tr><td>13</td><td>(by difference)</td><td>40.3</td></tr>
</table>

Table 8

Fraction No	Reducing power per cent: before hydrolysis	Reducing power per cent: after hydrolysis	DP	Fermentable sugars per cent: glucose	Fermentable sugars per cent: maltose	Reducing power of non-fermentable dextrins: before hydrolysis	Reducing power of non-fermentable dextrins: after hydrolysis	DP of dextrins	Yield in per cent of starch
IV: 1	16.4	102.2	6.2	<1.4	6.2	11.6	92.2	7.9	5.2
2	16.7	106.0	6.4	<1.4	6.0	10.7	92.1	8.5	2.8
3	18.5	104.1	5.6	<1.4	7.3	11.6	95.0	8.2	3.1
4	18.8	104.0	5.5	<1.4	6.7	11.7	98.0	8.4	2.3
5	18.8	104.4	5.5	<1.0	7.8	12.4	81.5	6.6	2.8
6	18.8	96.7	5.2	<1.0	8.0	11.9	78.8	6.6	2.3
7	21.0	106.6	5.1	<1.0	7.5	13.2	88.3	6.7	1.9
8	20.5	106.5	5.2	<1.4	7.7	13.1	81.2	6.2	1.3
9	20.8	104.7	5.0	1.8	8.7	13.2	79.5	6.0	1.9
10	30.7	103.8	3.4	5.3	31.1	11.7	64.5	5.5	3.3
11	32.1	107.0	3.3	5.2	30.0	11.8	60.0	5.1	0.7
12	41.4	106.2	2.6	8.4	50.0	8.1	37.0	4.6	0.3
Mother liquor	—	—	~1.6	10 g	18 g	—	—	~2	~1

Table 9

Reaction time	Per cent glucose
0	16.4
0.5 min.	18.7
24 hrs	39.7
48 »	40.1

Degradation of refractionated dextrins by α-amylase.

The experiments were carried out as described above: To a solution of 0.5 g dextrin in 25 ml were added 3 ml buffer and 2 ml enzyme solution. The increase of the reducing power was determined. An experiment with fraction IV:1 is recorded in Table 9. The reducing power is expressed as per cent glucose.

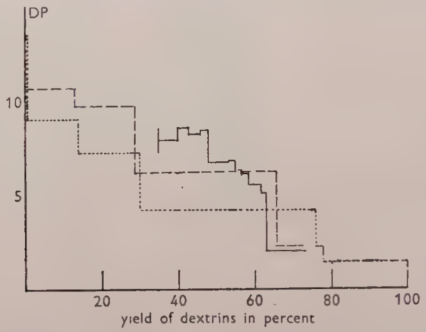

Fig. 5. Distributions of isolated α-dextrins on different chain lengths: Dotted curve, dextrin fractions I–V; dashed curve, the same fractions after removal of fermentable sugars; full-drawn curve, refractionated dectrins IV:1–12.

The increase of the reducing power corresponds to a formation of 47.4 per cent maltose hydrate. Fermentation experiments showed the presence of < 1.5 per cent glucose and 77.0 per cent maltose. Consequently no formation of glucose has taken place but the amount of maltose has increased by 70.8 per cent. The obvious discrepancy between the two values 37.4 and 70.8 per cent for the maltose formation indicates that a) the degradation by β-amylase is mainly a total decomposition of normal α-dextrins (for instance a decomposition of a hexasaccharide into three molecules of maltose), and b) that probably appreciable amounts of maltotriose are formed from normal α-dextrins with an uneven number of glucose units.

Table 10

Fraction No	Maltose calculated from increase of reducing power, %	Fermentable sugars %			Non-fermentable dextrins		
		Glucose	Maltose	Increase of maltose	Reducing power before hydrolysis	Reducing power after hydrolysis	DP of dextrins
IV: 1	47.4	<1.5	77.0	70.8	6.3	33.8	5.4
2	52.2	<1.5	78.0	72.0	7.0	27.7	4.0
3	51.8	<1.5	88.8	81.5	6.0	21.5	3.6
4	56.2	<1.5	91.0	84.3	5.9	22.3	3.8
5	56.2	<1.5	88.5	80.7	6.5	18.9	2.9
6	58.8	<1.5	91.4	83.4	4.6	14.3	3.1
7	55.0	<1.5	93.5	86.0	4.2	13.9	3.3
8	58.0	<1.5	92.0	84.3	5.8	13.6	2.4
9	60.0	<1.5	96.7	88.0	2.3	8.4	3.7
10	43.4	5.5	95.3	64.3	2.5	6.8	2.7
11	40.6	5.5	94.0	64.0	3.1	7.4	2.4
12	23.8	9.3	92.6	42.6	2.8	6.7	2.4

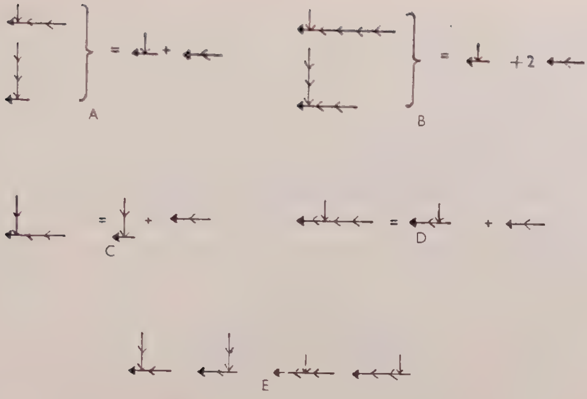

Fig. 6. Limit dextrins containing 2, 3, or 4 glucose units.

After fermentation the DP of the non-fermentable dextrins was determined as above. The average DP was found to be 5.4, showing again that only small amounts of maltose are formed from the abnormal α-dextrins by β-amylase. Experiments with the different dextrin fractions IV:1–12 are collected in Table 10.

It appears from table 10 that all fractions are saccharified to a considerable extent. This and the fact that the average DP of the residual dextrins is not very much lower than the DP of the original fractions shows that all fractions are mainly composed of normal α-dextrins. This is quite in accordance with previous results from this laboratory. No glucose is formed by β-amylase from the dextrins.

The residual dextrins remaining after degradation by β-amylase evidently contain from 2 to 6 glucose units. This means that isomaltose is a component of at least the dextrins originating from fractions 8–12. Trisaccharides seem to be abundant in most cases. The isomaltose must be formed from tetra- or hexasaccharides like those schematically shown in Fig. 6 A and B. The trisaccharides, which should contain one maltose and one isomaltose linkage must be thought to originate from penta- or higher saccharides, in principle after the fashion shown in Fig. 6 C and D. Stable β-amylase limit dextrins containing four glucose units would have the structures 6 E. Isomaltose was isolated as a product of the enzymatic degradation of starch for the first time in 1941 by MYRBÄCK and AHLBORG (9), and trisaccharides of the type mentioned by the same authors in 1940 (10).

Since our experiments had shown a less pronounced difference between the action of β-amylase and salivary amylase on the dextrin fractions than could be expected, further experiments were performed in which different enzymes were allowed to act on the limit dextrin produced by β-amylase from fraction II.

Degradation by β-amylase.

45.7 g fraction II was dissolved in 485 ml water; 10 ml buffer and 5 ml β-amylase solution were added. The increase of the reducing power was determined in small samples: Table 11.

Fermentation experiments showed the absence of glucose and the presence of 44.6 per cent maltose hydrate. This is in good agreement with the small-scale experiment described above. After removal of the fermentable sugars, the filtered solution was concentrated to 100 ml and precipitated with 300 ml absolute alcohol. The mother liquor yielded no precipitate on further addition of alcohol. It contained about 1.1 g substance. The precipitate was washed with alcohol and ether and dried; 23.1 g dry limit dextrin was obtained. The reducing power of this dextrin was 8.9 per cent before and 102.0 percent after complete hydrolysis. Determinations according to Willstätter and Schudel and according to Shaffer-Somogyi were in very good agreement. The average DP of the dextrin is 11.5. The corresponding figure found in the small-scale experiment was 10.7.

Table 11

Reaction time	Per cent glucose
0	11.7
0.5 min.	11.9
10 »	12.7
20 »	13.0
60 »	13.3
24 hrs	23.6
48 »	26.1
72 »	27.3

The degradation of the limit dextrin by three different α-amylases was determined: Malt α-amylase, free from β-amylase; partly purified by tannin precipitation; salivary amylase, partly purified preparation from human saliva; and a partly purified mold amylase preparation (from Merck's diastase). In experiments with maltose it was found that none of these amylase preparations produced measurable quantities of glucose in the reaction times used in this investigation.

Exeriments with salivary amylase.

The action of the enzyme preparation on *starch* was compared with the β-amylase action; the increase of the reducing power was calculated as glucose in per cent of the theoretical amount: Table 12.

Table 12

Reaction time	Per cent glucose	
	β-amylase	salivary amylase
5 min.	1.7	—
10 »	4.1	—
20 »	7.7	—
60 »	16.9	21.8
24 hrs	25.0	37.6
48 »	25.8	39.2
120	27.0	44.0

As usual, no glucose was formed by β-amylase. The degradation products formed by salivary amylase contained 8.1 per cent glucose and 58.1 per cent maltose, the last figure possibly including maltotriose. The non-fermentable limit dextrins had a reducing power amounting to 8.0 per cent before and 32.0 per cent after complete hydrolysis (calculated on theoretical amount of glucose corresponding to initial amount of starch). The average DP of the limit dextrins is 4.0. Consequently we have to conclude that, in agreement with earlier investigations from this laboratory, the degradation of starch by salivary amylase leads to formation of considerable amounts of limit dextrins with more than two glucose units per molecule. The degradation does not yield isomaltose as the only true limit dextrin or, in any case, the rate of hydrolysis of the limit dextrins with 3–8 units is so extremely low that the final stage can not be reached in reasonable times.

Degradation of the β-amylase limit dextrin by α-amylase.

4.67 g limit dextrin (dry), 3 ml phosphate buffer solution, 1 ml enzyme solution and water: volume 50 ml. pH was 5.3 for malt and mold enzyme, 6.9 for the salivary amylase. Results in Table 13. All values calculated as per cent of the theoretical amount of glucose.

Table 13

Reaction time		Linkage ruptured in per cent of total		
		Salivary amylase	Malt α-amylase	Mold α-amylase
0		8.9	8.9	8.9
0.5 min		10.0	9.3	8.9
20 »		10.7	9.4	—
60 »		11.0	10.3	9.8
24 hrs		11.4	11.7	13.5
72 »		14.0	13.3	15.5
95 »		14.5	13.5	15.8
120 »		14.9	—	16.8
145 »		15.9	13.5	16.9
875 »		15.9	13.7	20.0
Fermentable sugars:	Glucose	1.9	1.9	1.6
	Maltose	14.9	4.0	11.2
	Slowly fermentable	1.9	4.3	6.2
Reducing power of residual dextrin	Before hydrolysis	11.4	10.3	9.4
	After hydrolysis	80.9	86.2	83.0
DP of non-fermentable limit dextrins		7.1	8.4	8.8

It appears from table 13 that the degradation of the β-amylase limit dextrin from fraction II by the three different α-amylases is all but complete. Since the average DP of the dextrin used was 11, the observed increase of the reducing power proves that only 1–2 of the 10 glucosidic linkages have been ruptured. This low figure corresponds well to the formation of only 10–18 per cent of fermentable sugars.

The formation of glucose is almost nil. When this is compared to the result (Table 6) of the degradation by salivary amylase of the original α-dextrin (not treated with β-amylase), *i.e.* formation of about 15 per cent glucose, it must be concluded that glucose is formed by salivary amylase mainly from the normal α-dextrins which are absent after treatment of the α-dextrin with β-amylase. In this connection it should be remembered that the glucose formation from starch by malt α-amylase is strikingly decreased by previous treatment of the starch with β-amylase (11). The conclusion is that the bulk of the glucose is formed by α-amylases from amylose and from the normal end-chains of the amylopectin or, respectively, from the normal α-dextrins originating from these starch components.

The high average DP (7–9) of the residual dextrins after treatment with the α-amylases also proves that most of the linkages of the substrate used are extremely resistant to enzymatic hydrolysis. The explanation must be sought in the constitution of the substrate. Obviously an α-dextrin as shown schematically in Fig. 4 B can not be supposed to be stable against α-amylases; at least three molecules of maltose (or a corresponding amount of maltotriose or/and glucose) would be split off. On the other hand it seems quite possible that an α-dextrin as in Fig. 4 C would be stable. The distance between the two ramification points might be too short to allow the enzymes to arrange the main chain of the molecules on their surface in the regular fashion, that must be a pre-requisite for enzymatic hydrolysis (4). If it be supposed, as done by K. H. Meyer and others that the ramification of the amylopectin molecules is quite irregular, it is to be expected that the lengths of the interior chains between the ramification points vary rather strongly around the mean value (about 6 units). It seems probable that some of them are as short as 2–3 units and it might very well be that such chains are not ruptured by the α-amylases. It should be remembered that the dextrin fraction investigated does not correspond to more than about 5 per cent of the starch.

SUMMARY

The products of the dextrinization of potato starch by malt α-amylase have been fractionated by alcohol precipitation. The fractions have been characterized by determination of their average degree of polymerization, by their content of fermentable sugars, and their behaviour when acted upon by certain amylolytic enzymes. In these respects one of the fractions has been investigated in greater detail. Evidence is presented that certain α-dextrins are far from completely broken down by the α-amylases, *i.e.* they yield not only maltose, glucose and isomaltose but also stable, or practically stable, limit dextrins which may contain up to eight glucose units.

REFERENCES

1. Myrbäck, K., Advances in Carbohydrate Chem. *3*, 252 (1948).
2. Meyer, K. H. and Gonon, F. W., Helv. Chim. Acta *34*, 294, 308 (1951).
3. Myrbäck, K. and Johansson, N. O., Arkiv Kemi, Mineral. Geol. *A 20*, no 6 (1945).
4. Myrbäck, K., Arkiv Kemi *2*, 417 (1950).
5. Myrbäck, K., and Sihlbom, Esther, Arkiv Kemi *1*, 1 (1949).
6. Myrbäck, K., and Neumüller, G., in Sumner, J. B. and Myrbäck, K., *The Enzymes*, Academic Press, New York (1950), Vol. *1*, p. 651.
7. Myrbäck, K., Arkiv Kemi *4*, 433 (1952).
8. Roberts, P. J. P., and Whelan, W. J., Biochem. J. *49*, lvi (1951).
9. Ahlborg, K., and Myrbäck, K., Biochem. Z. *308*, 187 (1941).
10. Myrbäck, K., and Ahlborg, K., Biochem. Z. *307*, 69 (1940).
11. Myrbäck, K., Biochem. Z. *307*, 140 (1941).

Institute for Organic Chemistry and Biochemistry, University, Stockholm.

Tryckt den 12 mars 1953

Uppsala 1953. Almqvist & Wiksells Boktryckeri AB

ARKIV FÖR KEMI Band 5 nr 36

Communicated 26 November 1952 by ARNE FREDGA

Stereochemical studies on plant growth regulators. IV[1]

The enantiomorphic α-(1-chloro-2-naphthoxy)-propionic acids

By MAGNUS MATELL and SVEN LARSSON

With 5 figures in the text

In latter years attention has been drawn to a number of optically active growth substances with rather pronounced differences in the biological effects of their enantiomorphs (1–10). In order to understand the influence of sterical factors, a study of configurational relations might be of great value. The steric relations of α-phenoxypropionic acid and the two α-naphthoxypropionic acids have been established by FREDGA and MATELL who found that the forms which have greater auxin activity than their respective antipodes belong to the same steric series, most probably the D-series (4, 5). These experiments have been extended by one of us to some chloro-substituted α-phenoxypropionic acids and in the third paper of this series quite analogous results were reported for these compounds (11). In this paper the resolution of α-(1-chloro-2-naphthoxy)-propionic acid (I) and its sterical connection to the compounds mentioned above will be described. The sign of the optical rotation of this acid may change when passing from one solvent to another and to avoid errors the antipode which is *dextrorotating in alcohol* will be referred to as *dextrorotatory or* (+)*-acid.*

The configuration of the optically active α-(1-chloro-2-naphthoxy)-propionic acid was established by the method of quasi-racemates (12). Consequently the first problem was to find a structurally similar compound with known configuration, forming a molecular compound with one of the antipodes of the acid I. It has been pointed out that the contact method of KOFLER (13) is well suited for such an investigation (14). By means of this method we studied two-component systems containing optically active α-(1-chloro-2-naphthoxy)-propionic acid (I) and structurally similar acids with known configurations (4, 5, 11). It was found that (+)-I formed molecular compounds with (−)-α-(2-naphthoxy)-propionic acid (II) and (−)-α-(2.4.5-trichlorophenoxy)-propionic acid (III).

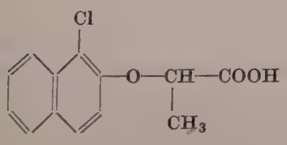

I

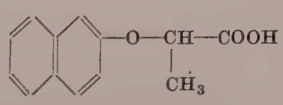

II

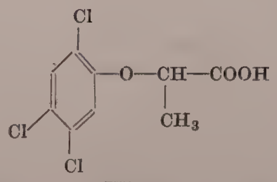

III

---

[1] Paper III. Ark. Kemi *5*, 341 (1953).

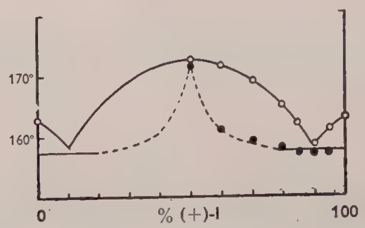

Fig. 1. (+)- and (−)-α-(1-chloro-2-naphthoxy)-propionic acid (I).

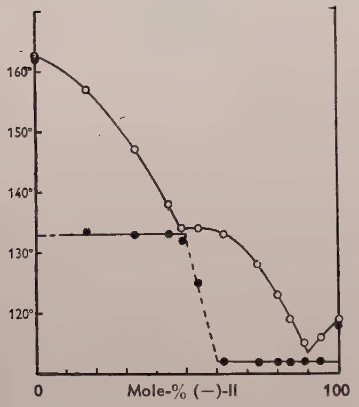

Fig. 2.

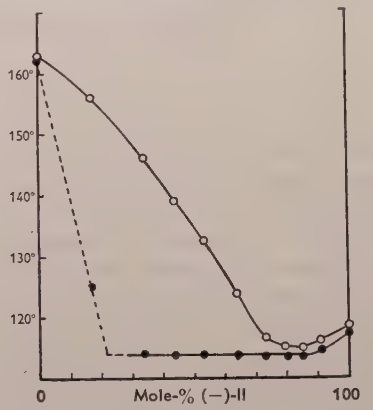

Fig. 3.

Fig. 2. (+)-α-(1-Chloro-2-naphthoxy)-propionic acid (I) and (−)-α-(2-naphthoxy)-propionic acid (II). Fig. 3. (−)-α-(1-Chloro-2-naphthoxy)-propionic acid (I) and (−)-α-(2-naphthoxy)-propionic acid (II).

In order to verify the quasi-racemic nature of these molecular compounds, thaw-melting point diagrams of the actual two-component systems were studied.

From Fig. 1 it is evident that the inactive acid I is a true racemic compound. The extent of the middle part of the curve amounts to 80 % and the melting point difference between the racemic and optically active forms is 10.5°. For α-(2-naphthoxy)-propionic acid (II) and α-(2.4.5-trichlorophenoxy)-propionic acid (III) the corresponding values are 57 % and −5° (4), 94 % and 36.5° (11) respectively. The racemate formation tendency of the acid I is thus intermediary compared with the other two acids.

The existence of a quasi-racemic compound between I and II is not unexpected because of the great structural similarity of the components. As can be seen from Fig. 2 the molecular compound is most probably in the ratio 1 : 1 and the quite dissimilar diagram in Fig. 3 definitely proves that we are dealing here with a quasi-racemate. The diagram shown in Fig. 3 is apparently of type III according to ROOZEBOOM but the thaw point curve indicates a peritectic point at about 70 % of (−)-II and thus the diagram would be a combination of the ROOZEBOOM types III and IV. In either case the components show far-reaching mutual solubility in the solid state which is evidently due to the structural similarity. However neither component has a pronounced tendency to form a racemate and this probably causes the minute maximum seen in Fig. 2. The discontinuity at about 50 % represents an eutectic

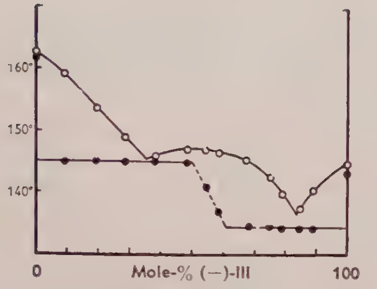

Fig. 4.

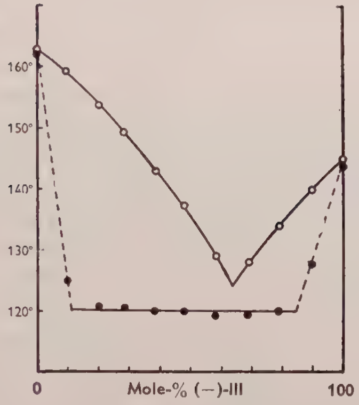

Fig. 5.

Fig. 4. (+)-α-(1-Chloro-2-naphthoxy)-propionic acid (I) and (−)-α-(2.4.5-trichlorophenoxy)-propionic acid (III). Fig. 5. (−)-α-(1-Chloro-2-naphthoxy)-propionic acid (I) and (−)-α-(2.4.5-trichlorophenoxy)-propionic acid (III).

which was verified when the components were analysed by the contact method. From these experiments it can be concluded that the acids I and II which have *opposite directions of optical rotation* also have *opposite configurations*. In a previous paper it has been reported that (+)-α-(2-naphthoxy)-propionic acid most probably has the D-configuration (4); (+)-α-(1-chloro-2-naphthoxy)-propionic acid consequently belongs to the D-series.

The structural differences between the compounds I and III are rather large and so the conditions for the formation of a quasi-racemic compound appear less favourable than in the case of the acids I and II. These differences are reflected by the melting-point diagram of the acids with the same direction of rotation. The mutual solubility in the solid state is small as is shown by diagram 5, which, according to Roozeboom, is of type V. The diagram in Fig. 4 proves that the molecular compound found in the preliminary experiments is in the ratio 1 : 1 and so must be quasi-racemic. It is noteworthy that the molecular compound in this case gives rise to a pronounced maximum which should be connected with the extremely great racemate formation tendency of one of the components (11, 12). As the acids I and III with *opposite directions of rotation* form a quasi-racemate they must also have *opposite configurations*.

In a previous paper it has been shown that (+)-α-(2.4.5-trichlorophenoxy)-propionic acid has the same configuration as (+)-α-(2-naphthoxy)-propionic acid (11). α-(1-chloro-2-naphthoxy)-propionic acid and α-(2-naphthoxy)-propionic acid thus have been sterically connected in two different ways giving the same result. This is an argument in favour of the unambiguity of the method of quasi-racemates.

The biological effects of the enantiomorphic α-(1-chloro-2-naphtoxy)-propionic acids have been studied by Dr. B. Åberg who found that the (+)-form is a weak auxin, about 10 times more active than the (−)-acid in the inhibition of root growth (private communication). These experiments support the assumption that D-α-aryloxyalkylcarboxylic acids are more active as plant growth regulators than their respective antipodes (9).

Experimental

rac.-α-(1-Chloro-2-naphthoxy)-propionic acid (I)

This acid, which has been previously described by OSBORNE, WAIN and WALKER (15) was prepared by refluxing the appropriate sodium naphtholate with an equimolecular quantity of ethyl α-bromopropionate in abs. alcohol followed by hydrolysis with aqueous alkali and acidification. M.p. 171.5–172.5°.

0.3686 g acid: 14.68 ml 0.1004-*N* NaOH
0.1042 » » 8.57 » 0.04824-*N* NaOH (combustion according to GROTE-KREKELER)
$C_{13}H_{11}O_3Cl$ calc. equiv. wt. 250.7 Cl 14.14
found » » 250.1 » 14.07

Preliminary experiments on resolution

Cinchonidine and (+)-α-phenylethylamine yielded crystalline products from which a dextrorotatory acid could be isolated. The first base gave the best resolution and was used for the isolation of the (+)– form. With cinchonine, quinidine and (–)-phenylethylamine salts were obtained which on decomposition yielded products containing a slight excess of the (–)-acid. Better results were obtained with quinine and morphine, the latter being the most effective.

(+)-α-(1-Chloro-2-naphthoxy)-propionic acid

10.5 g (0.042 mole) of inactive acid and 12.3 g (0.042 mole) of cinchonidine were dissolved in a hot mixture of 200 ml alcohol and 240 ml water. After standing over night in a refrigerator the crystals were collected, a small sample was treated with dilute hydrochloric acid and extracted with ether. The ether was driven off and the rotatory power of the acid was determined in abs. alcohol. The salt was recrystallised several times according to Table 1.

Table 1

Recrystallisation of the cinchonidine salt of α-(1-chloro-2-naphthoxy)-propionic acid

Cryst. nr	Alcohol ml	Water ml	Yield of salt g	$[\alpha]_D$ of the acid
1	200	240	16.4	+ 5.5°
2	200	240	11.0	+ 9.4°
3	120	150	8.7	+16.0°
4	100	120	8.3	+15.9°
5	100	120	7.8	+16.7°
6	100	120	7.2	+16.5°

The pure salt was treated with dilute hydrochloric acid and extracted with three portions of ether. On evaporation 3.05 g of crude acid were collected. After two recrystallisations from dilute alcohol (25–35 %) 2.95 g of pure (+)-acid were obtained as small, glistening needles with m.p. 162–162.8°.

0.1114 g acid: 9.20 ml 0.04824-*N* NaOH
$C_{13}H_{11}O_3Cl$ calc. equiv. wt. 250.7
found » » 251.0

0.0793 g dissolved in abs. *alcohol* to 9.98 ml: $\alpha_D^{55} = +0.151°$. $[\alpha]_D^{25} = +19.0°$; $[M]_D^{25} = +47.6°$.
0.0751 g dissolved in *acetone* to 9.98 ml: $\alpha_D^{25} = +0.087°$. $[\alpha]_D^{25} = +11.6°$; $[M]_D^{25} = +29.0°$.
0.0899 g dissolved in *chloroform* to 9.98 ml: $\alpha_D^{25} = +0.052°$. $[\alpha]_D^{25} = +5.8°$; $[M]_D^{25} = +14.5°$.
0.0806 g dissolved in *benzene* to 9.98 ml: $\alpha_D^{25} = -0.304°$. $[\alpha]_D^{25} = -37.6°$; $[M]_D^{25} = -94.4°$.
0.0719 g neutralized with *aqueous sodium hydroxide* and made up to 9.98 ml: $\alpha_D^{25} = -0.373°$. $[\alpha]_D^{25} = -51.8°$; $[M]_D^{25} = -129.8°$.

(−)-α-(1-Chloro-2-naphthoxy)-propionic acid

The acid was recovered from crystallisation 1 and 2 above; 5.2 g with $[\alpha]_D = -10°$ (in abs. alcohol) were obtained. This product (0.021 mole) and 6.3 g (0.021 mole) of morphine were dissolved in 225 ml of hot 30 % alcohol. The solution was set aside over night, the crystals were collected and the rotatory power of the acid was determined as described above. The purification of the salt was carried out according to Table 2.

Table 2

Recrystallisation of the morphine salt of α-(1-chloro-2-naphthoxy)-propionic acid

Cryst. nr	Alcohol ml	Water ml	Yield of salt g	$[\alpha]_D$ of the acid
1	75	150	9.7	−15.5°
2	75	150	7.7	−18.2°
3	60	120	7.1	−18.4°

From the last fraction 2.95 g of crude acid were obtained. Recrystallisation from 60 % ethanol yielded 2.4 g of pure (−)-acid with m.p. 162–162.8°.

0.0821 g acid: 6.77 ml 0.04824-*N* NaOH
$C_{13}H_{11}O_3Cl$ calc. equiv. wt. 250.7
found » » 251.4
0.0834 g dissolved in abs. *alcohol* to 9.98 ml: $\alpha_D^{25} = -0.156°$. $[\alpha]_D^{25} = -18.7°$; $[M]_D^{25} = -46.8°$.

Thermal analysis. The mixtures for the thaw-melting point diagrams were prepared by dissolving weighed quantities of the components (a total of 10 mg) in a few drops of acetone: after evaporation the residues were dried and powdered. Thaw-melting point determinations were carried out using a hot stage microscope according to KOFLER (16). The same apparatus was used for the study of contact preparations. The results are found in Fig. 1–5 and Tables 3–7.

The authors are indepted to Prof. A. FREDGA for valuable discussions and for the supply of some of the optically active compounds used in these experiments. Thanks are due to Prof. N. HELLSTRÖM, the head of this institute, for his kind interest and for all facilities put at the authors' disposal. The optically active α-(2.4.5-trichlorophenoxy)-propionic acids were kindly supplied by Prof. R. L. WAIN. Part of the expenses involved have been defrayed by a grant from *Statens Naturvetenskapliga Forskningsråd.*

Table 3

(+)- and (−)-I

% (+)-I	M. p.
0.0	162 – 163°
50.0	171.5 – 172.5°
59.8	161 – 171.5°
70.3	159.5 – 169°
79.6	158 – 165°
84.7	158 – 162°
90.3	157 – 158.5°
94.8	157 – 161°
100.0	162 – 163°

Table 4

(+)-I and (−)-II

Mole-% (−)-II	M. p.
0.0	162 – 163°
17.1	133.5 – 157°
33.0	133.5 – 147°
44.2	133 – 138°
48.7	132 – 134°
53.8	125 – 134°
62.3	112 – 133°
73.5	112 – 128°
79.8	112 – 123°
84.1	112 – 119°
88.8	112 – 115°
94.1	112 – 116°
100.0	118 – 119°

Table 5

(−)-I and (−)-II

Mole-% (−)-II	M. p.
0.0	162 – 163°
17.1	125 – 156°
33.7	114 – 146°
43.7	114 – 139°
53.5	114 – 132.5°
63.9	114 – 124°
73.3	113.5 – 116.5°
79.4	113.5 – 115.5°
85.3	113.5 – 115°
91.0	114.5 – 116.5°
100.0	117.5 – 118.5°

Table 6

(+)-I and (−)-III

Mole-% (−)-III	M. p.
0.0	162 – 163°
9.0	145 – 159°
19.2	145 – 153.5°
28.5	145 – 149°
38.0	145 – 146°
48.3	145 – 147°
54.4	142 – 147°
58.4	137.5 – 146.5°
68.6	135 – 145.5°
75.3	135 – 142.5°
79.0	134.5 – 140°
84.7	134.5 – 137.5°
89.0	134.5 – 140.5°
100.0	143.5 – 145°

Table 7

(−)-I and (−)-III

Mole-% (−)-III	M. p.
0.0	162 – 163°
9.4	125 – 159°
19.9	120.5 – 154°
28.4	120.5 – 149.5°
38.2	120 – 143°
47.9	120 – 137.5°
58.2	119 – 129°
68.7	119 – 128°
78.8	120 – 134°
89.7	128 – 140°
100.0	143.5 – 145°

SUMMARY

α-(1-Chloro-2-naphthoxy)-propionic acid has been resolved into optical antipodes. The enantiomorphs have been sterically connected to the optically active α-(2-naphthoxy)-propionic acid in two different ways giving identical results. (+)-α-(1-Chloro-2-naphthoxy)-propionic acid most probably has the D-configuration. This result supports the view that optically active plant growth regulators of the α-aryloxyalkylcarboxylic acid type which have greater auxin activity than their respective antipodes belong to the D-series.

Department of Organic Chemistry, Royal Agricultural College, Uppsala, November 1952.

REFERENCES

1. M. S. Smith and R. L. Wain, Proc. roy. Soc. B *139*, 118 (1951).
2. S. T. Collins and F. E. Smith, J. sci. Food Agric. *3*, 248 (1952).
3. H. Veldstra and C. van de Westeringh, Rec. Trav. chim. Pays-Bas *70*, 1113 (1951).
4. A. Fredga and M. Matell, Ark. Kemi *3*, 429 (1951).
5. ——, Ibid. *4*, 325 (1952).
6. B. Åberg, Ibid. *3*, 549 (1951).
7. ——, Physiologia Plantarum *5*, 305 (1952).
8. M. S. Smith, R. L. Wain and F. Wightman, Ann. appl. Biol. *39*, 295 (1952).
9. M. Matell, Ark. Kemi *4*, 473 (1952).
10. ——, Ark. Kemi *5*, 187 (1953).
11. ——, Ibid. *5*, 341 (1953).
12. A. Fredga, The Svedberg 1884 $^{30}/_{8}$ 1944, Uppsala 1944, p. 261.
13. L. Kofler and A. Kofler, Mikro-Methoden, Innsbruck 1948, p. 115.
14. M. Matell, Mikrochem. mikrochim. Acta, *38*, 532 (1951).
15. D. J. Osborne, R. L. Wain and R. D. Walker, J. hort. Sci. *27*, 44 (1952).
16. L. Kofler and A. Kofler, Mikro-Methoden, Innsbruck 1948, p. 3.

Tryckt den 12 mars 1953

Uppsala 1953. Almqvist & Wiksells Boktryckeri AB

ARKIV FÖR KEMI Band 5 nr 37

Read 12 November 1952

Studies in Experimental Rheumatism. II.

Effects of Desoxycorticosterone Acetate (DCA) Overdosage and of Focal Streptococcal Infection on Scorbutic Guinea-Pigs

By Hans v. Euler and Leo Heller

C. Pathological findings and conclusions

The present paper is the concluding one of a series published in this Archive (references (1) and (2)).

Pathological findings

Hearts, fragments of the skeletal muscle of the thigh and of the abdominal wall as well as adrenal glands (only one gland — the left one — for each animal, the other one being used for ascorbic acid determination (1, 2)), were fixed in 8 % formaldehyde, embedded in paraffine and partly stained with hematoxyline-eosine, partly with the Mallory-Ladewig fibrin stain (3). The results of the histopathological examination of the above preparations, kindly performed by Doc. Dr. Åke Lindgren, S:t Erik's Hospital, Stockholm, to whom the authors wish to express their gratitude, can be summarized in the way such as given below (see also Table 3).

1. *Heart lesions*

At autopsy, no characteristic macrosopical changes could be seen in the hearts of the animals of the experimental groups (I–IV, see (1) and (2)). Microscopically, relatively slight endo-, pari- resp. pancarditic lesions could be found in a rather high proportion of the animals (9 out of 17), but the distribution of the lesions found between the different experimental groups did not correlate with the kind of treatment applied. Thus, one of the 3 healthy controls (No. VIII) and as many as three out of four DCA-controls showed the same cardiac lesions as 6 out of eight animals belonging to the test-groups of the experiments. Only a slight roundcellular infiltration but no fibrinoid degeneration of the connective tissue, so characteristical for true rheumatical affections and no rheumatical granulomas of the Aschoff type could be found. The slight changes which were discovered were of the type which had been found by many workers in apparently healthy laboratory animals of various species (for a review of literature compare (4)) — a finding which possibly accounts for the genesis of many an unduly enthusiastic report on an allegedly successful

Table 3

Group	Experiment no.	Animal no.	Infected with hemolyt. strept.	Histopathological findings		Organ weight (in grams)			
				Heart	Skeletal muscle	Liver	Spleen	Kidneys	Adrenals
I. Non-scorbutic (healthy) controls	1	VII	0	No pathological lesions found.	Not tested.	21.7	0.70	3.31	0.198
	1	VIII	0	Slight endo- and pericarditis with some roundcellular infiltration.	Not tested.	20.4	0.64	3.11	0.197
	2	B_4	twice	No pathological lesions found.	No pathological lesions.	25.8	0.83	3.87	0.282
II. Scorbutic controls.	1	IX	0	No pathological lesions found.	Not tested.	20.6	0.81	3.17	0.174
	1	X	0	No pathological lesions found.	Not tested.	18.5	0.66	2.80	0.242
III. DCA-controls.	1	IV	0	Slight endo- and pericarditis with some roundcellular infiltration.	Not tested.	22.3	0.42	3.50	0.224
	1	V	0	Slight endo- and pericarditis with some roundcellular infiltration.	Not tested.	16.4	0.54	3.50	0.148
	2	B_1	once	No pathological lesions found.	No pathological lesions.	24.0	0.65	3.80	—
	2	B_2	twice	Slight pancarditis.	Slight roundcellular infiltration and cicatrization.	18.0	0.65	3.32	0.230
IV. Test-group (combined scurvy-DCA-treatment).	1	I	0	Slight endo- and pericarditis with some roundcellular infiltration.	Not tested.	20.0	2.40	3.40	—
	1	II	0	Slight endo- and pericarditis with some roundcellular infiltration.	Not tested.	15.8	1.51	3.30	0.246
	1	III	0	Slight endo- and pericarditis with some roundcellular infiltration.	Not tested.	21.6	1.53	3.82	0.250
	1	VI	0	Slight endo- and pericarditis with some roundcellular infiltration.	Not tested.	20.35	3.04	3.57	0.172
	2	A_1	twice	No pathological lesions found.	Small abscess. Granulation tissue with a few giant cells, surrounded by rel. intact muscle tissue.	11.9	0.30	3.45	0.346
	2	A_2	twice	No pathological lesions found.	Grave degenerative changes, resulting in connective tissue, proliferation, fat distrophy and focal haemorrhages. Relatively slight inflammatory cell infiltrations.	11.25	0.30	2.61	0.271
	2	A_3	0	Slight roundcellular infiltration perdominantly in the pericardium.		12.7	0.32	2.52	0.206
	2	A_4	twice	Slight endo- and pericarditis with some roundcellular infiltration.	Artefacts.	13.4	1.17	3.04	0.236

experimental reproduction in animals of the pathological picture of human rheumatism. However, it may be of some interest to note that while the two DCA-treated groups (groups III and IV) showed a high proportion (75 %) of cardiac lesions, the same lesions were found in only 1 of 5 animals (= 20 %), which did not receive any DCA treatment (Table 3). Streptococcal infection seemed to be of no importance for the appearance of cardiac lesions (see Table 3).

2. *Muscle lesions*

The gross macroscopical appearance of the skeletal muscles of the animals has already been described in an earlier paper of this series (2, p. 187). The rather impressing changes observed in the animals of the test groups (group IV of the tables), receiving both the diet low in vitamin C and high doses of DCA, consisted in: a) a striking fragility of the affected muscles, resulting in their easily occurring rupture following rather slight tearing, b) an increased muscle tonus, resulting in a general rigidity of the animals, especially of the back of the body, including the hind legs, c) a loss of elasticity of the muscle, which could be found in the animals both when still alive and at autopsy, d) diffuse haemorrhages (see (2), Table 2), and e) a distinct atrophy of the subcutaneous fat overlying the affected muscles. Of the control groups, only the scorbutic animals (group II) showed the presence of small haemorrhages in the muscles of the thigh in the proximity of the knee joints, but no haemorrhages in the muscles of the abdomen. The muscles of those animals (Nos. IX a, X) had a normal appearance and elasticity, showing none of the changes just described [under a), b) c) and e)]. The muscles of the non-scorbutic animals, treated with DCA, were slightly oedematous, but did not show the impressive changes found in their fellows, subjected to the combined treatment. The appearance of the muscles of the 3 healthy controls, including the animal infected focally with hemolytic streptococci, was perfectly normal.

The histological examination could be performed only on the muscles of the animals belonging to the 2nd experiment (see (1)), because of the faulty fixation of the muscles in experiment I. Faulty fixation with subsequent appearance of artefacts was also found in the case of the guinea-pig A_4 of experiment II. Thus only six muscle preparations could be successfully examined by Dr. LINDGREN, half of them corresponding to the animals of the test group. Out of those three, two (A_2 and A_3) showed the presence of grave degenerative lesions with subsequent connective tissue proliferation, fat dystrophy and localized haemorrhages, but only slight inflammatory cellular infiltrations. The muscle of the third animal of the combined treatment group (A_1) showed the presence of a little abscess and of granulation tissue with a few giant cells, surrounded by relatively intact muscular tissue.

Two preparations, one of them belonging to a healthy control (B_4), only focally infected with streptococci, and one corresponding to a DCA-treated but not vitamin-C-deficient animals, showed a perfectly normal appearance, whereas the muscle of another animal of the latter broup (B_2), showed a slight roundcellular infiltration and cicatrization in a few places.

3. *Adrenal glands*

No distinct differences in the weight of the adrenals could be found between the different experimental groups, the internal variations within the groups being rather considerable ((2), Table 2). No subcapsular or parenchymal haemorrhages was observed in the adrenals of any animal. Thus the observations of Schaffenburg et al. (5) who found that the adrenals of DCA-treated scorbutic guinea-pigs showed the presence of haemorrhages and were somewhat smaller than those of the scorbutic controls but greater than those of normal ones, could not be confirmed.

Quite generally, the adrenals did in no case show any distinct pathological changes, neither macro- nor microscopically. The only change observed was a moderate hypertrophy of the adrenal cortex in the adrenals of the two scorbutic controls, which could be even seen without the help of a microscope — a phenomenon well known to all endocrinologists (compare e.g. (6)). Microscopically, in sections stained with hematoxylin-eosin, no inflammatory lesions and no sure presence of capillary haemorrhages were observed. There were no fat- resp. lipoid-stainings done.

4. *Liver, spleen, lungs and kidneys*

A histopathological examination of the livers, spleens and kidneys of the animals has not been performed. At autopsy, certain pathological changes, probably of secondary nature, such as a varying degree of fatty infiltration of the liver and of diffuse bronchopneumonic consolidation of the lungs could be seen in practically all the animals of the test groups of either experiment, while the same changes were absent in the guinea-pigs of all the control groups. Those changes might, however, be ascribed to the generally very bad condition of the test animals, due to the combined scurvy-DCA effect, and need not be directly related to the metabolic effects of the treatment, the kidneys did not show any considerable changes of I, and their weight showed no significant variations from group to group, with the possible exception of the animals A_2 and A_3 of the test group which made a somehow atrophic impression. The weight of the livers, as a rule, showed only a normal variation, at least within the control groups, but in the 4 animals of the test group of experiment II (A_1–A_4) the weight of the liver was distinctly less than in the rest of the animals. It may be worth while to note, that the duration of the experiment was considerably longer in experiment II than in experiment I, if that circumstance can suffice to explain the above finding (see Table 4). Last not least, there were also, on the whole, changes in the appearance of the spleens — even that exclusively within the test groups only. The spleens of the test animals of experiment I (I–III, VI) were strikingly bigger and those of experiment II (A_1–A_4) by far smaller than those of the animals of all the three control groups. It may be, that the differences in the length of time, allowed for the various experiments, may account even for that finding. It appears plausible, that an initial tumor of the spleen, constituting a link in the general adaptation syndrome (6, 7) may be replaced by a secondary atrophy or febrosis on longer duration of the stress.

Conclusion and summary

The results of the present investigation on the effects on guinea-pigs of a combination of high doses of desoxycorticosterone acetate (DCA) with subacute vitamin C deficiency and focal streptococcal infection can be summarized in the following way:

1. Contrary to the findings reported by some workers, the treatment of animals subjected to the stressing effects of subacute scurvy with high doses of DCA did not result in a production of true rheumatical lesions.

2. The establishment of an infectious focus by intramuscular injection of an agar-agar depôt of animal-pathogenic hemolytic streptococci (8) did not modify the clinical and pathological picture produced by the combined DCA-subacute scorbutogenic diet. It has been conjectured — on the basis of certain results reported by other workers (9) — that a reinfection of previously sensitized animals could possibly result in an allergic autosensitization of the mesenchym, which under the modifying influence of DCA and scurvy, both of them reported to possess some "rheumatogenic" properties (10, 11, 12), might take the form of the rheumatic reaction with its characteristical pathological and clinical patterns. No reactions of the latter kind were, however, observed after repeated administration of the streptococci.

3. The clinical syndrome produced in the animals, subjected to the combined treatment, did not resemble that of a rheumatic disease. Generalized oedema rather than inflammatory periarticular and synovial reactions were the rule, showing perhaps a slight tendency to accumulate in the proximity of the big joints (2). No granulomas of the Aschoff type and no fibrinoid degeneration of the connective tissue could be demonstrated in the hearts and in the skeletal muscles.

4. The clinical and autopsy findings seem to indicate a strong mutual potentiation of scurvy and of DCA overdosage symptoms — the latter known from the extensive work of Selye and collaborators (13, 14). The deep intramuscular haemorrhages and an accentuation of scorbutic tooth root lesions, as compared with the vitamin C deficient controls receiving no DCA, belong to the well known pathological picture of grave scurvy, while the muscle twitchings, tonus changes and pareses, accentuated by sodium chloride, should be considered as due to DCA overdosage. Generalized oedema has been reported in both conditions.

The impressing gravity of the clinical picture provoked by the combined administration of two for themselves apart — in the dosage used — only slightly pathogenic treatments, however, rouses the suspicion that the syndrome observed may be something more than a simple summation of scurvy and hormone overdosage symptoms, involving the production of qualitatively new lesions. Such a suspicion is further substantiated by the finding of grave degenerative changes in the skeletal muscles of a part of the animals. Further pathological study of the syndrome may perhaps help to elucidate the latter point.

The authors wish to express their gratitude to Dr. ÅKE LINDGREN, överläkare, S:T ERIKS sjukhus, for valuable help.

The authors are obliged to Engineer H. HASSELQUIST, Stockholm University, for the microdeterminations of ascorbic acid content of the adrenals.

REFERENCES

1. Hans v. Euler and Leo Heller, This Archive, vol. 3, N:o 54 (1952).
2. Leo Heller and Hans v. Euler, ibid., vol. 4, N:o 9 (1952).
3. Lillie, Histopathological Methods.
4. B. H. Waksman, Medicine, vol. 28, 143 (1949).
5. C. Schaffenburg, G. M. C. Masson and A. C. Corcoran, Proc. Soc. Exp. Biol. a. Med., vol. 74, 358 (1950).
6. H. Selye, Textbook of Endocrinology, Montreal (1947).
7. —— Annals of Int. Med., vol. 29, 403 (1948).
8. P. Hedlund, The Scandin. J. of Clin. a. Lab. Invest., vol. 1, 351 (1949).
9. P. A. Cavelti, Proc. Soc. Exp. Biol. a. Med., vol. 60, 379 (1945).
10. J. F. Rinehart, Ann. Rheum. Dis., vol. 9, 586 (1935).
11. H. Selye, O. Sylvester, C. E. Hall and C. P. Leblond, J. Am. Med. Ass., vol. 124, 201 (1944)
12. H. Selye, and E. I. Pentz, The Canad. Med. Ass. J., vol. 49, 264 (1943).
13. H. Selye J., Morphol., vol. 73, 401 (1943).
14. H. Selye and C. E. Hall, Arch. Path., vol. 36, 19 (1943),

Tryckt den 12 mars 1953

Uppsala 1953. Almqvist & Wiksells Boktryckeri AB

ARKIV FÖR KEMI Band 5 nr 38

Communicated 10 September 1952 by H. VON EULER and KARL MYRBÄCK

On the behavior of various Lactobacilli, members of the vitamin B_{12} group and desoxyribosides in the cup plate assay of vitamin B_{12}

By Z. G. BÁNHIDI, A. G. M. SJÖSTRÖM, S. GRÖMMER, and H. LUNDIN

With 6 figures in the text

Since the isolation of vitamin B_{12} which appeared to be the "anti pernicious anemia" (APA) principle and the most important vitamin-type component in the "animal protein factor" (APF) complex, several microbiological methods for the assay of the vitamin B_{12} group of substances have been developed. Many of these methods have been collected, described briefly and commented on, by WRIGHT and EGGS (1). Recent developments in this field tend towards the application of ar media with "cups", instead of the original "tube methods" employing liquid dia. CUTHBERTSON (2, 3) and FOSTER *et al.* (4) introduced the cup plate method into vitamin B_{12} research. This technique is the inverse of HEATLEY's (5) cup assay procedure for the estimation of antibiotic activity, and is a quantitative application of the auxanographic method based on the "minimum law" of Liebig. Cuthbertson used *Lactobacillus lactis* Dorner, ATCC 8000, in a medium containing ascorbic acid, while Foster worked with the ATCC No. 10697 strain of the same bacillus and incorporated 2 % of NaCl in the assay medium in order to depress the interfering growth promoting effect of desoxyribosides. WINSTEN and EIGEN (6, 7) applied *Lactobacillus leichmannii* 313, ATCC 7830, and *Leuconostoc citrovorum*, ATCC 8081, to agar media for the bioautographic methods. COHEN and BENNETT (8, 9) in their cup plate assay seeded a slightly alkaline medium containing 2 % K_2SO_4 (to counteract the effect of desoxyribosides), with *Lactobacillus leichmannii*, ATCC 4797.

LARKIN and STUKEY (10) made use of FOSTER's (3) "less expensive" medium for routine vit. B_{12} assay with *Lactobacillus lactis* Dorner, ATCC 10697, the bacillus used by FOSTER *et al.*, and mentioned that the strain ATCC No. 8000 of this bacillus as well as three different strains of *Lactobacillus leichmannii* were tried and found not to grow satisfactorily in this medium. A recent paper by LENS *et al.* (11) deals partly with a cup plate method employing *Lactobacillus lactis* (ORLA, JENSEN, BERGEY *et al.*) strain 1175 (12), which was found to be easy to handle in the assay procedure, but gave analytical results of low reproducibility. On the other hand, ROBINSON *et al.* (13) comparing a strain of *Lactobacillus leichmannii* in the cup plate assay with *Escherichia coli*, observed that the two methods gave concordant results when used for the estimation of vit. B_{12} in crude liver extracts.

However, it must be borne in mind that this kind of microbiological analysis — should be viewed with considerable caution, even in the case of pure crystalline vit. B_{12}, and even more so in the investigation of natural products where the results are merely informative.

Experiments were carried out in order to improve the application of the cup plate method to the assay of vitamin B_{12} in pure and crude preparations. Details are given below concerning the successful preparation of "seed" or inoculum and the simultaneous use of the various Lactobacilli in the same medium, thus allowing direct comparison of the results obtained with these bacilli. The behavior in the assay of some single members of the vitamin B_{12} complex was investigated and they were found to differ one from another. Similarly methods for overcoming the interfering effect caused by desoxyribosides in natural extracts or concentrates, were investigated and discussed.

EXPERIMENTAL

I. Inoculum

Maintenance of stock cultures

The following microorganisms obtained from the American Type Culture Collection (ATCC) were used in these investigations: 1. *Lactobacillus lactis* Dorner (No 8000), 2. *Lactobacillus lactis* Dorner (No 10697), 3. *Lactobacillus leichmannii* 313 (No 7830), 4. *Lactobacillus leichmannii* 326 (No 4797), 5. *Lactobacillus leichmannii* 327 (No 7831), and 6. *Leuconostoc citrovorum* (No 8081), hereafter referred to as 1. LLD 8000, 2. LLD 10697, 3. LL 313, 4. LL 326, 5. LL 327, and 6. LC 8081.

It was difficult to maintain the stock cultures of these organisms, especially LLD, when the yeast extract - tomato juice - glucose agar recommended by the ATCC and others, was employed. Similar difficulties were reported by Greene *et al.* (14). In view of this we experimented with various yeast extracts - skim milk fluid media and finally chose the following:

Liquor B Vitaminorum (KABI)[1]	10 ml
(or Bacto Yeast Extract	5 g)
Heptomin (Tika)[2]	1 ml
Tomato juice (filtered through Munktell OOH filter paper)	100 ml
Tween 80	1 ml
Fresh skim milk to	1000 ml
(or Bacto Peptonized Milk 15 g, and water to	1000 ml)
Litmus (dissolved in 10 ml of hot 0.1 N NaOH, filtered)	1 g

The tomato juice, the litmus, and finally the whole medium should be adjusted to pH 6.4 with 0.1 N HCl.

---

[1] Swedish brewery yeast autolyzed at 50° C, diluted with water at a suitable pH, filtered with protection from light and adjusted to about 50 % dry weight and 40 μg vit. B_1 per g solution (Kindly supplied by A.B. KABI, Stockholm). Our test shows that "Liquor B-Vitaminorum" contains small amounts of desoxyribonucleic acid derivatives and practically no vit. B_{12}.

[2] Injectable liver concentrate (described by Strandell (15)) representing 50 g liver per ml solution. Samples of Heptomin (Tika) referred to in this work were manufactured in 1951 and were not standardized with respect to vit. B_{12}, which in the newer preparations is adjusted to about 15 μg per ml.

The medium was distributed in 10 ml quantities in Pyrex test tubes which were plugged, covered with aluminium foil and autoclaved at 1 atm. overpressure (120°) for 15 minutes. With this medium the pH is critical, lower values causing coagulation, higher ones caramelisation. After sterilization the contents of the tubes should be homogeneous and nearly colourless, and on cooling the characteristic neutral colour of the litmus should be retained.

This fortified litmus - skim milk medium has been used for about two years with good results for all the Lactobacilli maintained in our laboratory. The medium may be kept for about six months at −4° C. The litmus allows visible control of the stock cultures. After incubation for 24–48 hours, the inoculated tubes show sharply defined layers — a small red layer at the top and a yellow one below. The relative sizes of these layers, the colours, and the coagulation of the milk are characteristic for the different strains of Lactobacilli used. We made 2–3 parallel inoculations weekly or bi-weekly, incubating for 24 hours at 37° C for the bacilli of LLD and LL types and at 30° C for the LC type, and stored the stock cultures at +8° C. In this way viable cultures of bacteria sensitive to the B_{12} group were always available for assays.

The preparation of inocula

Small centrifuge tubes were filled with 5 ml portions of a suitable clear medium, complete in regard to the vitamin to be estimated. After sterilization as above they were inoculated with a loopfull of the stock cultures. After 12–24 hours of incubation the inocula were centrifuged and washed twice with 0.9 % sterilized saline under aseptic conditions. Dilutions made with saline were distributed in 1 ml portions in petri dishes. The inocula should not remain in saline longer than one hour (cf. SHAW (16)).

Dilutions made with saline were checked turbidimetrically using a Coleman model 11 universal spectrophotometer at a wavelength of 5000 Å. Due to the fact that the suspension was colourless (although thick) this wave-length allowed satisfactory quick control of the inocula. Serial dilutions were made, and turbidimetric comparison showed that there was an almost linear correlation between the galvanometer readings and the logarithms of the dilutions.

Growth of the Lactobacilli on different broths

The factors which influence the choice of medium for the preparation of inoculum are the growth of the bacteria (number of cells produced in the medium in question), and the sensitivity of the cells formed, towards the vitamin to be estimated. Experiments were carried out in order to investigate the growth promoting ability of various inoculum broths for the different Lactobacilli. The media were prepared as follows:

1. Bacto Micro Inoculum Broth (Difco) according to prescription.
2. Similar to 1. but made from Difco ingredients omitting the Tween 80 and adding 10 % of filtered tomato juice.
3. Same as 1. but mixed from Difco ingredients.
4. Same as 1. but with the addition of 10 % tomato juice filtrate.
5. Bactogen (Vitrum) (enzymatic digest of casein) 0.5 %

Bactogen (Vitrum) (enzymatic digest of casein)	0.5 %
Liquor B-Vitaminorum (KABI)	4.0 %
Dextrose	1.0 %
Tween 80	0.1 %
KH_2PO_4	0.2 %

6. Similar to 5. but with the further addition of 10 % tomato juice filtrate.

Five ml portions of these media were sterilized, inoculated with the Lactobacilli, and incubated for 16 hours at 37° C (30° C in the case of LC 8081). At least three parallels were run in each group. The growth was interrupted at the end of the incubation period by storing at + 4° C for one hour. The cell-suspensions were centrifuged and resuspended in saline (in order to avoid the interference of the broths) and the bacterial growth was estimated turbidimetrically. Readings of 1 : 5 dilutions prepared from each original tube were also made to improve the comparability of the samples of the cell-suspensions.

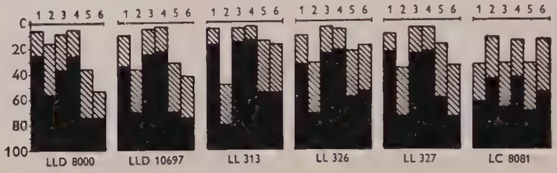

Fig. 1. *Growth of LLD, LL, and LC on different broths.* Galvanometer readings of Coleman spectrophotometer at 5000 Å for inocula centrifuged and resuspended in saline after incubation for 24 hours at 37° C (vertical columns). The readings were made in triplicate at the original concentration (top levels: shadowed plus black zones) and after dilution 1 : 5 (lower levels: black zones). The media used are numbered 1 – 6.

The results presented in the histograms of fig. 1 show that Tween 80 is markedly growth promoting for all strains of LLD and LL, but not for LC 8081. Tomato juice filtrate could not replace Tween 80 but it stimulated the growth of all six Lactobacilli to some extent. It appears to be indispensable for LC 8081. Broths 5 or 6 could not replace the Micro Inoculum Broth for LLD and LL, but broth 6 is quite satisfactory for LC 8081. Broths 5 and 6 lack some important factor which is necessary for LLD and LL. This factor is not vitamin B_{12} because in the same experiments as above even when 1 mμg of Cobemin was added to each tube very similar results were obtained.

Inocula of LLD and LL grown on broths 1,5 and 6 were compared in the cup plate assay of vitamin B_{12} in varying concentrations of cell-suspensions. The inocula obtained from broths 5 and 6 seemed to be inferior to that from broth 1 in their response to vit. B_{12}. As shown above the production of cells was also inferior in broths 5 and 6. For the work in this laboratory the Bacto Micro Inoculum Broth was used most frequently.

Density of inocula

The number of viable cells of the Lactobacilli per ml of agar medium is of great importance. Turbidimetric readings on the inocula give comparable results if the age of the inocula, the time interval between centrifuging and mixing with the assay medium (one hour), the washing procedure, and the temperatures (especially that of the melted agar medium, which should remain below 50° C) are kept constant. Data concerning the influence of the inoculum density, under otherwise constant conditions, were compiled from about four hundred readings. The appearance of growth within the zones of stimulation was indicated by one of four marks and the summarized marks gave histograms resembling a Galton curve. A simplified graphical representation of these results with LL 313 and LLD 10697 is shown in fig. 2. The optimum results for LL 313 are obtained with a much lower density than is required for LLD 10697 (ranges *a*). A similar difference exists between LL 326 and LL 327 on one hand and LLD 8000 on the other. Densities of seeds higher than the optimum cause diffuse growth over the whole agar plate (ranges *b*). Too few viable cells in the agar medium leads to the formation of large rings around the cups of vit. B_{12}, with detached single microcolonies of abnormal size, such as occur commonly if the agar medium is too hot when seeded (ranges *c*).[1]

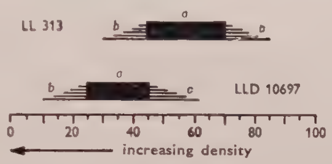

Fig. 2. *Correlation between optical density of inocula and appearance of growth zones in the cup plate assay of vit. B_{12}.* Ranges *a* represent good and *b* or *c* irregular growth response.

CUTHBERTSON's (3) statement that the size of the exhibition zones decreases as the density of the inoculum increases possibly holds generally. Our experiments confirm this statement in the case of all strains of both LLD and LL, the latter type of bacilli showing the greatest difference. Picture A in fig. 3 lists the mean values for zone diameter at vit. B_{12} concentrations of 0.15, 0.5, and 1 µg per ml with different concentrations of inocula, demonstrated with LL 313. The dilutions of inocula were made and adjusted turbidimetrically as described, and each point on the diagram represents the mean of five to eight readings.

An experiment carried out in a similar manner with the different strains of LLD and LL at identical (although not optimal) optical densities of inocula, using an assay medium with the same composition for all strains of bacteria, revealed constant differences in the sizes of the zones at different vit. B_{12} concentrations. The slopes of the curves are quite similar as seen on picture B in fig. 3. The results indicate that the growth supporting effect of vit. B_{12} decreases in the following order:

$$\text{LLD 10697} > \text{LL 327} \geqslant \text{LL 313} \geq \text{LL 326} > \text{LLD 8000}$$

The phenomena illustrated in fig. 3 indicate that the size of the growth zones is determined, not only by the rate of diffusion of the vitamin in the agar gel, but also by the consumption of the vitamin by the bacteria.

Cuthbertson's observation with LLD 8000 that the rings grow larger if the time interval between filling the cups and beginning the incubation is increased has been confirmed in the case of the other bacilli, but the larger zones tend to be diffuse if the time interval is too long. This phenomenon is readily explained on the assumption that the size of the zones is determined simultaneously by the diffusion and consumption of the vitamin. During the time interval mentioned

---

[1] The desirability of adjusting the density of the inoculum to a low but still optimal level was stressed by Dr. Ralph E. Bennett (Commercial Solvents Inc., Terre Haute, Ind.,) for the use of Bacto "C. S. Vitamin B_{12} Agar" (Personal communication). A specimen of this medium (kindly supplied by Difco Laboratories Inc., Detroit, Mich.,) was tested and found to give good results with vit. B_{12}, with all the strains of LL. The standard curves obtained were parallel with those obtained with the media described here.

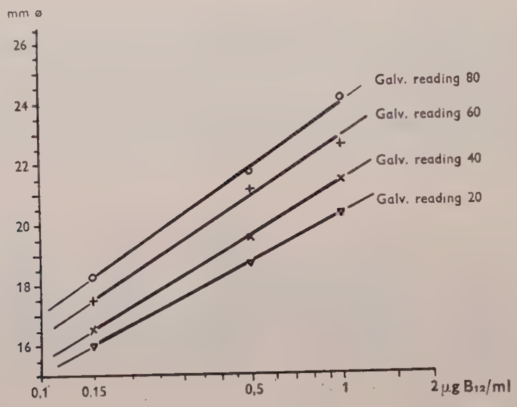

Fig. 3. *The influence of inoculum on the assay.*

A) Correlation between mean values of zone diameters and optical density of inocula with LL 313.

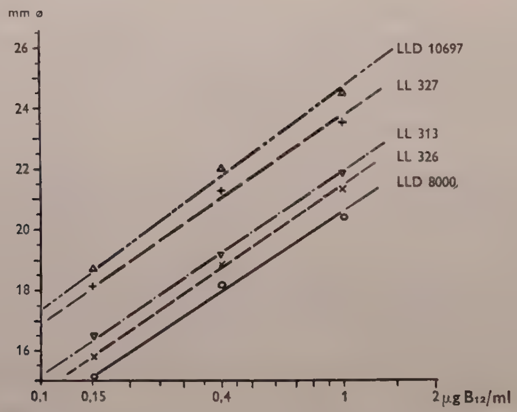

B) Correlation between mean values of zone diameters and strains of Lactobacilli used as "seeds" at the same inoculum density. (Galvanometer reading 50 in the Coleman spectrophotometer).

above the vitamin can diffuse without being consumed. The straight lines in fig. 3 are, in general, parallel or nearly so. Convergence toward low concentrations becomes apparent only on comparison of mean values obtained from a large number of different experimental series, or on comparing the results obtained with different types of cups, or with different amounts of test fluids, e.g. one and three drops in two parallel experiments. In the cup plate assay of riboflavine with *Lactobacillus casei* ε a direct relationship between the density of growth within the exhibition rings and the concentrations of vitamin standards is obtained, but this does not seem to be the case in the vit. B_{12} assay. The visibility of exhibition rings is about the same on a given plate over a wide range of vit. B_{12} concentrations.

Cuthbertson's conclusion that the concentration of inoculum as well as the concentration of vit. B_{12} determines the diameter of assay rings on the plate, can be extended to the other strains of LLD and LL investigated here. Further under constant conditions the species of bacteria is the third factor determining the ring size.

II. The assay media

Two main types of assay media for use in the tube methods of vitamin B_{12} estimation have been described by different authors (1). In the first type, which resembles the media used in microbiological amino acid estimations, the essential and stimulatory amino acids are incorporated in pure form in the substrate(4). In the second type, the amino acids are partly replaced by enzyme digested or acid hydrolysed vitamin-free casein, as in the case of media for the assay of other B vitamins (3, 17). The former type is more expensive and requires more time for preparation, and because of the large number of components it is somewhat difficult to ensure the uniformity of different batches. Many different media of both the amino acid and the casein types have been used in the tube assay methods of vit. B_{12} analysis with different strains of LLD and LL. These media have been the basis of the two types of agar media used in the cup plate and bioautographic methods, because conclusions obtained from experiments in the tube assay are often considered to be valid in the agar plate methods also. For this reason assay media in agar plate methods were usually the same as those in the tube method except that agar was incorporated in the substrate. In the agar plate methods as well as in the tube methods different media are used for strains of LLD and LL. However, this is a disadvantage, as the use of different media makes it difficult to compare the behavior of the different bacteria in the assay procedure, and the results obtained with them.

Media which may be used with the different Lactobacilli

Several agar media were tested comparatively by inoculating alternatively with the two different strains of LLD and three strains of LL in order to find a medium which permits the simultaneous use of both types of bacilli. Media giving good results with one of the strains of the type of LLD or LL could usually be used with the other strains of the same type of bacilli, but not with the other type. However, some media gave good results with both types of Lactobacilli if the correct density of inoculum was employed. As shown below this is perhaps due to the fact that in an agar medium these microorganisms have less critical nutritional requirements than in liquid media.

The assay media in our experiments were of the casein type and in order to ensure uniformity of the ingredients a commercial vitamin-free casein hydrolyzate of constant composition was used.

The tomato juice factor (TJ) requirement of LLD is well known, as is the fact that inhibition of bacterial growth may occur with some tomato juice filtrates used in higher concentrations. Peeler *et. al.* (19) used tomato juice filtrate in the tube assay procedure with LL also. However, in many of the other substrates for this organism described in the literature the TJ factor is lacking. We used a reduced amount of tomato juice filtrate in the assay medium and added sodium ethyloxalacetate and fumaric acid as described by Caswell *et. al.* (20). The latter compounds should replace the TJ factor in the presence of alanine, which is supplied in the casein hydrolyzate. Peeler and Norris (21) reported subsequently that tomato juice contains some growth factors for LL which cannot be replaced by the synthetic products used by

CASWELL (20). Actually we prepared the assay medium without the TJ factor ingredients, as did, e.g. CAPPS *et al.* (17), and the results obtained with crystalline vitamin B_{12} were almost as good as those obtained using the complete medium.

Similar observations were reported by LOY *et al.* (22), in a recent paper dealing with the tube assay with LL 313. However its behavior was not consistent in this respect. To ensure a more complete medium for the assay of vit. B_{12} in natural materials we returned to the use of a medium containing the TJ factors. Cysteine hydrochloride was added as a reducing agent (23), as it is recommended especially for LL in the tube method. Its function is merely to protect the vit. B_{12b} from destruction during autoclaving and it is not indispensable in an agar medium.

Omission of Tween 80 from the assay medium did not significantly alter the growth of the bacilli, despite the fact that it showed a marked growth promoting effect in the liquid broth used for the preparation of inocula (see fig. 1). Pyridoxine was used in place of pyridoxamine. The folic acid level was first kept at 2 μg per litre but later the amount of this vitamin was increased a hundredfold, and good results were obtained in spite of the fact that in the tube method folic acid is reported to exert an inhibitory effect on both LLD and LL at concentrations of 50–500 μg per litre of medium. The incorporation of 0.2 % of enzyme-digested casein in the assay medium was not beneficial, as it caused fuzzy growth of bacteria over the whole plate.

The ingredients were prepared and dissolved, following the procedures described by BARTON-WRIGHT (18). The pH should be adjusted to 6,4. Suitable amounts of the medium distributed in bottles were kept at − 20° C until used.[1]

Before use the bottles were autoclaved for 15 minutes at 120° C, placed in a waterbath at 45–50°, and when constant temperature had been attained, the substrate was poured in 25 ml portions into petri dishes. The slight precipitate formed during autoclaving should not cause a disturbance if distributed homogeneously by stirring before the medium is poured out of the bottles.

The lactic organism *Leuconostoc citrovorum* (ATCC No 8081) was also studied in this medium. This bacillus was used in earlier work on the APA principle (24). It responds, however, not to vit. B_{12} but to thymidine and "folinic acid" (natural and synthetic Citrovorum Factor, formylfolic acid) (25). Omission of the tomato juice filtrate, sodium ethyloxalacetate, and fumaric acid from the casein medium used in the plate assay of vit. B_{12} gives a medium in which LC 8081 could be used for the estimation of folinic acid.

Replacement of the B vitamins and ribonucleic acid derivatives in the assay medium by yeast autolysate

As yeast autolysate depleted of the vitamin to be estimated is a good supplement to the media in different microbiological vitamin assay procedures, and as brewery yeast has been shown by animal experiments to contain little or no vit. B_{12} (26) we attempted to use the preparation "Liquor B vitaminorum" (LBV) mentioned above. This preparation showed, when undiluted, a very weak growth promoting effect

---

[1] Personal communications from Docent Niels Nielsen called our attention to the fact that storage at + 4° C of substrates already autoclaved causes irregularities in the assay.

Table I

Composition of assay media for the agar plate method (per 1000 ml)

	Complete medium	Simplified yeast autolyzate medium
l-Cystine	100 mg	50 mg
dl-Trytophane	100 »	100 »
l-Asparagine	50 »	50 »
Cysteine HCl	100 »	100 »
Bacto Vitamin Free Casamino Acids	5.0 g	5.0 g
Adenine sulfate	10 mg	—
Guanine HCl	10 »	—
Uracil	10 »	—
Xanthine	5 »	5 mg
Liquor B-vitaminorum (Kabi)	—	10 ml
Pyridoxine HCl	0.5 mg	—
Nicotinic acid	1.0 »	—
Riboflavin	0.5 »	0.5 mg
Thiamine HCl	0.5 »	—
Ca-*d*-pantothenate	0.5 »	—
Biotin	1.0 μg	—
Folic acid	0.2 mg	—
p-Aminobenzoic acid	0.5 »	—
Glucose	5.0 g	10 g
Tween 80	0.5 ml	1 ml
Tomato juice filtrate	50 ml	50 ml
Fumaric acid	0.5 g	0.5 g
Na-Ethyloxalacetate	0.5 »	0.5 »
Na-Acetate (anhydrous)	6.0 »	6.0 »
Na-Citrate	2.0 »	2.0 »
$MgSO_4 \cdot 7 H_2O$	200 mg	200 mg
$FeSO_4 \cdot 7 H_2O$	20 »	20 »
$MnSO_4 \cdot 4 H_2O$	20 »	20 »
KH_2PO_4	0.5 g	0.5 g
K_2HPO_4	0.5 »	0.5 »
Bacteriological agar	18 »	18 »

when tested by the cup plate method for vit. B_{12} using a complete medium. This growth promoting effect was however due to the presence of traces of desoxyribosides. We then replaced the pyrimidine and purine bases, and the B vitamins other than xanthine and riboflavine in the complete assay medium, by 10 ml of LBV per litre as shown in the second column of Table I. The resultant simplified medium seemed to be as generally applicable as the complete medium, for both LLD and LL types of bacilli, and gave good responses with vit. B_{12} or desoxyribosides. The B vitamins, ribonucleic acid degradation products, and amino acids in LBV complement the vitamin-free acid hydrolyzed casein. LBV at the concentration used appears to supply all the essential factors and contains no interfering substances. In fact the somewhat better and more rapid appearance of exhibition rings in this simplified medium as compared with the original medium, suggests that some stimulatory factors other than the essential components are present in the former. Possibly these are ribonucleic acid derivatives, which have been found by Skeggs *et al.* (27) to be stimulatory for LL. Comparative experiments with the two media showed, that with the simplified medium the density of inocula is less critical and the medium is less sensitive to storage after autoclaving or to autoclaving with 2 % NaCl, especially when LLD is used.[1]

III. The performance of the assay

Inocula prepared as described above were distributed in 1 ml quantities in 9 cm diameter flat petri dishes containing 25 ml of melted agar medium. For larger square dishes correspondingly larger amounts of inocula were used. Solutions of crystalline vit. B_{12} (Cobemin, Merck), of at least three different concentrations within the range of 0.01–3 μg per ml were applied as standards on filter paper discs 5 mm diameter, or preferably in wells or "cups" cut in the solidified agar under aseptic conditions by means of a sterilized cork borer 9 mm in diameter. One to three drops of the standard and test solutions of different dilutions were uniformly distributed with the aid of a hypodermic syringe with a platinum needle. The standard solutions prepared aseptically, or autoclaved in Freudenreich bottles, were stored in the refrigerator and protected from light. When making serial assays we usually filled three cups per plate with standards containing 0.15, 0.5, and 1 μg B_{12} per ml. Two or four cups were reserved for the unknowns, which were used at two or three different dilutions. It is desirable that the dilutions are chosen so that the vit. B_{12} concentrations fall within the range of the standards used in the assay series. After the distribution of the standard and test solutions in the cups, the plates were incubated at 37° C for 12–36 hours. The size of the exhibition rings was measured in polarized light using a transparent ruler with 1 mm scale divisions. In dubious cases, the mean of two diameters at right angles was calculated. The density of growth within the zones was, in general, most satisfactory after incubation for 14–18 hours. Incubation for more than thirty six hours is undesirable. LLD 10697 gives sharp rings often only after 24 hours, but incubation for 2–3 days leads to the appearance of single colonies even outside the exhibition zones. The frequency of these colonies was significantly higher around cups filled with folic acid (as a control). Some vitamin B_{12} independent strains of LLD were isolated from such colonies.

Cuthbertson *et al.* (3) have given a detailed description of several external factors which affect the development of the exhibition rings and influence the assay procedure with LLD 8000. Many of the statements in that report have been shown in this laboratory to apply to LLD 10696 and also to LL 313, 326 and 327. The variation of ring diameters with the interval of time between filling the plates and incubation was noticed, as already mentioned, and also the variation in diameter caused by varying thickness of the agar layer. Readings were calculated as described by IRWIN (28). The diameters of the assay rings are directly proportional to the logarithms of the concentrations.

---

[1] Further simplification of the composition of the assay media resulted in a medium containing: Bacto Vitamin Free Casamino Acid 0.5 %, LBV 1 %, (or Bacto Yeast Extract 0.5 %), sucrose (impure, yellow) 1 %, Tween 80 0.05 %, tomato juice filtrate 10 %, and agar 1.8 %.

This medium was prepared with tap water and no mineral salts or buffers were added. The pH was not adjusted. The medium was boiled and filtered. Rather unexpectedly LLD and LL could grow in this medium after addition of vit. B_{12}, but not well enough for the medium to be useful for analytical purposes. The possibility of obtaining results with such a medium confirms Barton-Wright's (18) statement that the requirements of the lactic organisms are still not well understood even in the simple field of the mineral salts.

The assay of pure vitamin B_{12} preparations

Some crystalline vit. B_{12} preparations and highly purified concentrates were tested by the cup plate method described above.

The bacilli chosen for routine analysis were usually LLD 8000 and LL 313. Cobemin (Merck), and Normocytin (Lederle)[1] which latter contains vit. B_{12} and B_{12b} were compared with a liver concentrate (P) with a stated potency of 20 µg B_{12} per ml, a liver concentrate (R) of unknown potency and a solution (S) of crystalline vit. B_{12} containing 15 µg per ml (a fermentation product). Serial dilutions from each specimen of 1 to 5, 1 to 10, 1 to 20, and 1 to 40, were used for comparison and three drops of solution were used in each cup.

The results are shown in fig. 4 and it is clear that the slopes of the curves obtained with the various samples are almost the same, but that the potencies observed differ significantly from those stated. Solutions P and S gave low values, 12.8 µg and 9.8 µg instead of 20 and 15 µg per ml if expressed in terms of Cobemin as standard. On the other hand Normocytin shows a much higher relative potency than expected, 52 µg per ml against 30 µg, if compared with Cobemin. As Normocytin contains a considerable amount of vit. B_{12b}, it was supposed that its higher potency is due to the vit. B_{12b}.

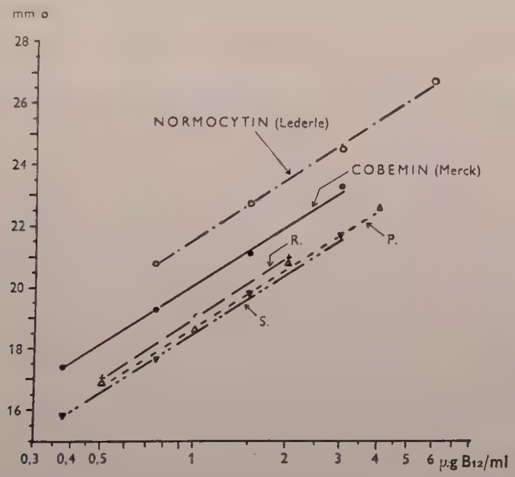

Fig. 4. *The comparison of different vit. B_{12} preparations in the cup plate assay using LLD 8000.* Each point represents the mean of five to ten readings. (For further explanation see text.)

---

[1] A product obtained from *Streptomyces aureofaciens* fermentation liquors, with 30 µg per ml potency, kindly supplied by the Lederle Laboratories Division, New York (through the courtesy of Chemical Interests Co, Stockholm).

Differing behavior of vit. B_{12}, B_{12b}, and B_{12}-cyanide complex in the assay

The conversion of vit. B_{12} (cyanocobalamin) into vit. B_{12b} (hydroxocobalamin) on exposure to light, and the reconversion of the resulting cyan-free product to vit. B_{12} was reported and confirmed simultaneously in several laboratories (29, 30, 31). The reconversion occurs over the pH range 5.5 to 9 and may be accomplished by the addition of KCN (32). However, COLEY *et al.* (33) have provided spectroscopic evidence for the existence, in the presence of excess of cyanide ions, of a labile vitamin B_{12} complex containing two cyanide radicals, which they named dicyanocobalamin. Recent investigations by CONN *et al.* (34) have shown that three cyanide radicals may be attached to the molecule but only one of them to the central cobalt atom. Therefore vit. B_{12} cyanide complex is perhaps a better name for vit. B_{12} in the presence of excess CN.

In the following experiments the original standard solutions of Cobemin, adjusted to pH 5.6, were divided in three portions. The first series was kept in the dark for one week (c.f. WIJMENGA and VEER, (30, 32)). The second and third series were exposed for one hour to light from a mercury lamp and an equal volume of KCN at a concentration of about 200 µg/ml was subsequently added to the third series. In this way vit. B_{12} was obtained in the first and vit. B_{12b} in the second series. The third series contained vit. B_{12} cyanide complex with two or three labile cyanide radicals. Diagram I and II in fig. 5 demonstrate the differences in the mean diameters of the exhibition rings obtained from these products assayed with LL 313 and LLD 10697. The solutions were added to the cups from the same glass micropipette (Ehrlich type) in order to ensure uniformity and precision. Other special precautions were also taken in these experiments, e.g. the cups were filled in a dark room in diffuse red light.

It has been known since the early investigations that vit. B_{12b} exhibits a behavior different to that of vit. B_{12} when tested in the tube method with LL. SKEGGS *et al.* (35) added KCN to extracts of natural products containing vit. B_{12b} in order to convert it to vit. B_{12} and estimated it as vit. B_{12}. It was shown by HENDLIN and SOARS (36, 37) that 1 µg per ml of KCN is sufficient to protect vit. B_{12b} during autoclaving with the assay medium. KCN has therefore, in the tube methods, an effect similar to that caused by larger amounts of cystein (23), thioglycolic acid, thiomalic acid, and other reducing agents. In the tube methods the incorporation of 1 µg of KCN per ml of single strength medium protects the vit. B_{12b} possibly because of interconversion to vit. B_{12}, and leads to quantitative results identical with vit. B_{12} in weight equivalence, whereas unprotected vit. B_{12b} loses its potency markedly. An excess of KCN of about one tenth of that used by Hendlin and Soars, were used in our experiments in order to eliminate the quantitative difference between vit. B_{12} and B_{12b} in the assay (see fig. 5). The curve of the mean values of vit. B_{12} cyanide complex crossed the nearly parallel curves of vit. B_{12} and irradiated vit. B_{12}. The concentration of KCN used in these experiments was so low that it did not inhibit the bacterial growth either in the vit. B_{12} zones or in the zones of desoxyribosides (as shown in separate experiments). The slopes of standard curves should be similar with substances having a close structural relationship as is the case with vit. B_{12} and B_{12b} or with the various desoxyribosides. As the marked difference in the slope in the case of vit. B_{12} cyanide

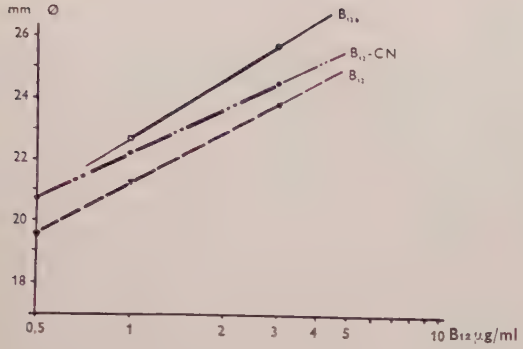

Diagram I.

LL 313.

Inoculum: 70 on the galvanometer scale.

Points are means of 6—8 readings.

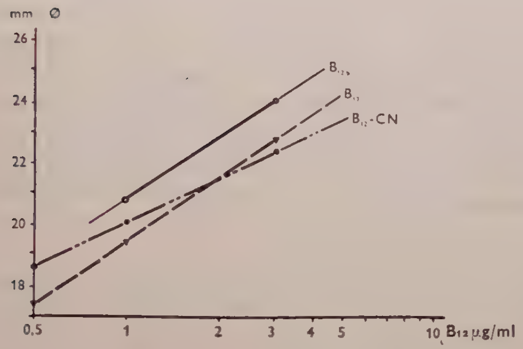

Diagram II.

LLD 10697.

Inoculum: 40 on the galvanometer scale.

Points are means of 6—8 readings.

Fig. 5. *Divergence of curves representing the means of responses to vitamin* B_{12b}, B_{12} *and vit.* B_{12}*-cyanide complex in the comparative cup plate method.*

complex cannot be explained as a direct effect of KCN on the bacteria, but must be due to some effect on the vit. B_{12} molecule, it is reasonable to suppose that the vit. B_{12} cyanide complex formed represents a structural change in the vit. B_{12} molecule significant enough to cause a change in the physiological effect on the bacteria. The irradiated vit. B_{12}, expected to be vit. B_{12b}, showed an increase in potency if calculated in Cobemin units as standard. The difference in potency between vit. B_{12} and irradiated vit. B_{12} were of the same order of magnitude as the differences between vit. B_{12} (Cobemin) and Normocytin.

Irradiated vit. B_{12} gives rings which differ in appearance from those given by vit. B_{12}. The growth zones of vit. B_{12} treated with light showed a small intensive outer circle and an inner zone of diminished (rudimentary) growth. However, we have not had the opportunity to try crystalline vit. B_{12b} in the agar plate test, and it cannot be stated, therefore, that the peculiar appearance of these growth zones is due entirely to vit. B_{12b}.

The interfering effect of desoxyribosides

Large amounts of thymidine (38) are able to replace vit. B_{12} as a growth factor for both LLD and LL (39), and other desoxyribosides behave in a similar manner (40, 41). In our experiments desoxyguanosine, desoxyhypoxanthosine, and thymidine (thymindesoxyriboside) were tested.[1] It was necessary to use a concentration of 10 μg per ml of each of the desoxyribosides in order to obtain the same ring diameter as is obtained with Cobemin at a concentration of 1 μg per ml. This holds for all the five strains of LLD and LL, and is in agreement with the results of Skeggs *et al.* (42) with LL 326. The curves of the two different desoxyribosides are almost parallel but have a steeper gradient than those of vit. B_{12} and Normocytin (see fig. 6). The intensity of growth promoted by desoxyribosides decreases at low concentrations and finally disappears, at about 10 μg per ml using our assay medium. The ratio between the lowest growth promoting concentrations of vit. B_{12} and of the desoxyribosides is about 1:1000. If the concentration of vit. B_{12} of a sample is at least 0.1 μg per ml and the ratio vit. B_{12}: desoxyribosides is 1:50 or more it is thus possible to eliminate the interference caused by the desoxyribosides merely by serial dilution of the sample.

All of the desoxyribosides have about the same growth promoting effect, although the actual magnitude depends on the species of bacteria, as illustrated in Table II (1–3). The different bacterial strains vary just as much in their response to desoxyribosides as to vit. B_{12}, but the two effects are not parallel, so that if the bacterial strains are arranged in order of decreasing response to desoxyribosides, the series obtained, viz.

$$\text{LLD } 10697 \geq \text{LLD } 8000 \geq \text{LL } 313 \gg \text{LL } 326 > \text{LL } 327$$

differs from the corresponding series for the response to vit. B_{12} (see page 5). It should be mentioned that all the different desoxyribosides tested, and presumably also the others, behave in their growth promoting activity as a uniform entity which in contrast to the members of the vit. B_{12} group of factors do not give rise to multiple zones of growth. A mixture of the desoxyribosides has the same quantitative effect as the sum of the effects of each desoxyriboside present.

In the case of the LL type of microorganisms the growth zones caused by desoxyribosides are similar in appearance to those due to vit. B_{12} if applied in the same cup. On the other hand they are faint but more easily distinguishable from the vit. B_{12} zones if the strains of LLD are used. These differences in appearance can be increased in the case of the LLD strains by the addition, under aseptic conditions, of 2 % of NaCl to the assay medium.

The addition of vit. B_{12} to desoxyribosides results in an increase in the diameters of the desoxyriboside rings, as shown in Table II (4). The size of the inner rings of vit. B_{12} are also affected. Curves representing the mean values of three readings of the inside rings of Cobemin and Normocytin given together with thymidine in the same cup at different concentrations, are compared in fig. 6 with the curves of vitamin solutions at corresponding concentrations. The readings were somewhat disturbed on account of the diffuse appearance of the double zones of growth. Normocytin tends to give lower, and Cobemin higher values than the standards in the presence of large amounts (100 μg per ml) of thymidine. However, different

---

[1] The desoxyribosides were kindly supplied by Docent P. Reichard, Stockholm.

Table II

The growth promoting effect of some desoxyribosides for different strains of LLD and LL at the same optical density of inocula

No.	Growth factor	Means of 6 to 12 readings of diameter of outer rings expressed in mm				
		LLD 10696	LLD 8000	LL 313	LL 326	LL 327
1	Guanine desoxyriboside 50 μg/ml	30	29	29	26.2	24.8
2	Hypoxanthine » » »	29	28.8	27.5	26	25
3	Thymine » » »	30.2	30	29	25.8	25
4	Thymine » » » + vit. B_{12} 0,3 μg/ml	31	32	31	28	27

concentrations of thymidine (e.g. 33, 66, and 100 μg per ml) did not significantly alter the results. With LL the visible differences between the zones of desoxyribosides and vit. B_{12} were far less distinct than with LLD.

Disturbances caused by desoxyribosides are of much greater importance in the cup plate methods than in the tube methods, for in the former the desoxyribosides have an activity about a thousand times higher than in the tube method if calculated in terms of vit. B_{12}. Nevertheless in many other respects the cup plate method is more specific for vit. B_{12} than the tube methods.

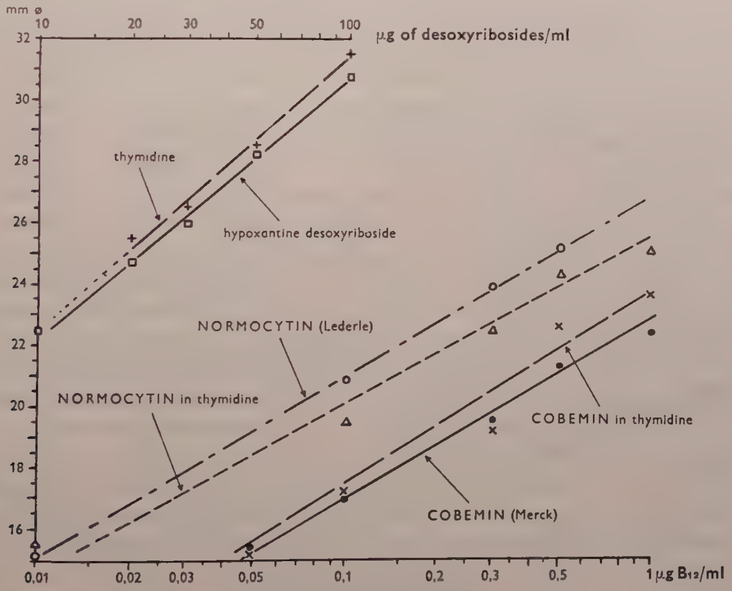

Fig. 6. *Curves for thymidine and hypoxanthine desoxyriboside, and for Cobemin and Normocytin with and without thymidine (100 μg per ml) in the same cup read as inner zones* (Bacterium LLD 8000).

Desoxyribosides are stable if boiled in water or in alkaline solutions but labile at lower pH, while vit. B_{12} is completely destroyed when a solution with pH 10 is boiled for 30 minutes (c.f. HOFFMANN *et al.* (43)). This difference in the behavior of vitamin B_{12} and desoxyribosides towards alkali has been utilized in the tube method for the estimation of the "true" vit. B_{12} content of solutions containing both vitamin B_{12} and desoxyribosides. The vit. B_{12} content was assumed to be obtained by subtraction of the growth promoting effect, expressed in terms of vit. B_{12} obtained after treatment with alkali, from that obtained with the untreated solution.

Using the cup plate method ROBINSON *et al.* (13) compared the growth zones obtained with crude liver extracts and with the same extracts after treatment with alkali, in order to localize the vit. B_{12} zone in those cases where several growth zones developed. The zones of the alkali treated and untreated samples, were compared and, only the inner rings of the untreated samples which disappeared after alkali treatment, were measured. This comparison gave rise to the discovery and separation of an alkali stable factor otherwise similar to vit. B_{12} in its behavior towards LL. Robinson also reported that the addition of vit. B_{12} to crude liver extracts previously treated with alkali and neutralized, gave values which were not in agreement with the amount of vit. B_{12} known to be present.

Paper chromatographic separation of the bacterial growth factors, and subsequent application of the chromatograms to agar plates with B_{12} assay medium mixed with LLD or LL led to the detection of these factors by WINSTON and EIGEN (7) and by SMITH and CUTHBERTSON (41). This technique, named bioautography, is excellent for qualitative analytical purposes, but the quantitative evaluation of the spots is difficult because of the indistinct elliptical growth zones on the agar plates. Attempts were made by several authors to evaluate the paper chromatograms quantitatively with tube methods. The paper strips were cut into small pieces and each piece was put in a separate tube (e.g. Shaw 44). This procedure however appeared to offer no advantages over the bioautographic technique, and did not solve the problem of the quantitative assay of vit. B_{12}. CUTHBERTSON *et al.* (3) used brief paper chromatography (about two hours) with n-butanol water as solvent for the separation of vit. B_{12} from the desoxyribosides. Most of the desoxyribosides except cytosine desoxyriboside, were separated from the vit. B_{12} group of factors, which remained in a single well-defined circular spot near the starting point. This procedure has the advantage of requiring only a short time. The fact that all the components of the vit. B_{12} occur in one circular zone simplifies the estimation. Readings and calculations were made as in the cup plate method. We applied this method successfully to the assay of vit. B_{12} in fermentation liquors. Longer (4 to 5 hours) chromatography using n-butanol-acetic acid is, however, to be recommended if antibiotics are present in the crude liquor to be examined, because of there latively slow movement of certain antibiotics.

An example of the assay of vit. B_{12} in a fermentation liquor by the cup plate method is presented in Table III. The inner zones of growth were shown by the alkaline destruction technique to be due to vit. B_{12}. The fermentation was carried out with a strain of *Streptomyces griseus* in a substrate containing glucose, fermentation residues, and $CaCO_3$. The resulting liquor contained large amounts of desoxyribosides as well as vit. B_{12}.

Table III

Assay of vit. B_{12} in fermentation liquors (*Streptomyces griseus*)

		Cup plate assay with LLD 8000							
		Without NaCl				With 2 % NaCl			
Sample	Dilution	Diameter of zones of exhibition		Assay results expressed in µg/ml with		Diameter of zones of exhibition		Assay results expressed in µg/ml with	
		outer zones Desoxyribosides	inner zones vit. B_{12}	Cobemin	Normocytin	outer zones Desoxyribosides	inner zones vit. B_{12}	Cobemin	Normocytin
				as standard				as standard	
2104	1 : 1	36.8	diffuse	—	—	43.8	20.8	0.30	0.20
	1 : 3	32.8	»	—	—	38.3	19.0	0.39	0.25
2108	1 : 1	34.0	20.0	0.20	0.14	40.0	20.8	0.30	0.20
	1 : 3	31.2	19.0	0.39	0.26	35.0	19.0	0.34	0.25

Each figure quoted is the average of three.

The inner zones were easier to measure on plates carrying medium with 2% NaCl, and the agreement between the values of undiluted and 1:3 diluted samples also seemed to be better if NaCl was present. Both Cobemin and Normocytin were used as standards because of the significant difference in the quantitative response of these preparations in the cup plate method. Tests on the fermentation samples with normal paper chromatography showed that the vit. B_{12b} type of factors was present in greater quantities than vit. B_{12}. The distribution of the factors in the samples of Streptomyces fermentation liquor was very similar to that in a solution of Normocytin. In this way both samples gave 0.20–0.25 µg vit. B_{12} per ml as shown in Table III. Serial dilutions of the samples were examined after brief paper chromatography, and gave 0.25 µg vit. B_{12} per ml, using dilutions of Normocytin for comparison. Naturally Normocytin and Cobemin show the same difference in their quantitative response when the brief paper chromatographic-agar plate assay is used, as in the common cup plate method.

Comparison of the values of the cup plate assay obtained with and without previous brief paper chromatography, showed that they were in good agreement. In spite of this agreement this method does not completely solve the problem of the assay of vit. B_{12}. The differences in quantitative response of the various members of the vit. B_{12} group as shown above can greatly influence the validity of the method if interconversion of the components of the vit. B_{12} group takes place during the preparation of the samples to be tested, or during the assay procedure. Similarly the possible existence of growth factors for LLD and LL related to vit. B_{12} (but not to the desoxyribosides), which may be inactive as APA and APF principles, can also cause interference in the estimation of these factors.

Acknowledgements

The authors are indebted to Mrs. G. Grömmer for the valuable technical assistance and to Mr. M. Hildinger and Mr. S. Zechner for their collaboration.

This work was generously supported by *Statens Tekniska Forskningsråd*, Stockholm, and A.B. KABI, Stockholm.

SUMMARY

Strains of Lactobacilli commonly used in vit. B_{12} assay, viz.: *Lactobacillus lactis* Dorner (ATCC No 10697), *Lactobacillus lactis* Dorner (No 8000), *Lactobacillus leichmannii* 313 (No 7830), *Lactobacillus leichmannii* 326 (No 4797), and *Lactobacillus leichmannii* 327 (No 7831) were compared in a casein containing synthetic medium which was elaborated in order to permit the use of any of these bacteria. The importance of inoculum density, and the variation of the optimal density with the species of bacteria, has been demonstrated. Comparison of the different strains showed that they behave characteristically in quantitative response, the sensitivity for vit. B_{12} decreasing in the order

$$\text{LLD } 10697 > \text{LL } 327 \gg \text{LL } 313 \geq \text{LL } 326 > \text{LLD } 8000$$

and for the desoxyribosides in the order

$$\text{LLD } 10697 \geq \text{LLD } 8000 \geq \text{LL } 313 \gg \text{LL } 326 > \text{LL } 327$$

if constant density of inoculum and the same medium are used for each strain.

Great simplification of the assay medium was obtained by replacing the pyrimidines, purines and B vitamins with an autolyzate of brewers yeast. This simplified medium — complete in all the essential nutrients — was shown to be statisfactory for routine analyses. *Leuconostoc citrovorum* 8081 which responds to "folinic acid" and thymidine cannot be used in this medium because of the presence of folinic acid in the yeast autolyzate. However, the original medium is satisfactory with this microorganism also, if the tomato juice factor is omitted.

In the cup plate assay pure preparations of vit. B_{12} are only about half as potent as preparations containing vit. B_{12b}. By exposure to ultraviolet light a corresponding change in activity results, due to conversion of vit. B_{12} into vit. B_{12b}. Addition of excess KCN to the samples containing vit. B_{12b} in an attempt to eliminate the difference in potency between vit. B_{12} and B_{12b} results, however, in the formation of the vit. B_{12}-cyanide complex which again behaves differently to vit. B_{12} and vit. B_{12b}.

Desoxyribosides, if present in a concentration of more than 10 μg per ml, interfere in the assay. If the concentration of vit. B_{12} in the sample to be tested is at least 0.1 μg per ml and the ratio $\frac{\text{vit. } B_{12}}{\text{desoxyribosides}}$ is about 1:50 or more, it is possible to eliminate the interference caused by the desoxyribosides merely by serial dilution of the sample. Bacilli of the LLD type give double zones of growth with a mixture of desoxyribosides and vit. B_{12}, especially if 2 % NaCl is added to the assay medium after autoclaving. Alkaline destruction of vit. B_{12} can give useful qualitative information in this method. The use of brief paper chromatography combined with the agar plate assay for the elimination of the interference of desoxyribosides and antibiotics has been used and discussed in connection with the assay of vit. B_{12} in fermentation liquors of Streptomycetes.

The Division of Food Chemistry, Royal Institute of Technology, Stochholm, Sweden.

REFERENCES

1. Wright, L. E. and Skeggs, H. R., in György, P., Vitamin Methods, vol. II, Acad. Press, New York 1951, pp. 648–702.
2. Cuthbertson, W. F. J., Biochem. J., *44*, v (1949).
3. Cuthbertson, W. F. J., Pegler, H. F., and Lloyd, J. T., Analyst, *76*, 133 (1951).
4. Foster, J. C., Lally, J. A., and Woodruff, H. B., Science, *110*, 507 (1949).
5. Heatley, N. G., Biochem. J., *38*, 61 (1944).
6. Winsten, W. A., and Eigen, E., J. Biol. Chem., *181*, 109 (1949).
7. ——, Biol. Chem., *184*, 155 (1950).
8. Cohen, I. R., and Bennett, R. E., Unpublished material available in mimeographed form, Commercial Solvents Corp., Terre Haute, Indiana.
9. Cohen, I. R., Pensack, J. M., and Bennett, R. E., Am. Chem. Soc., 119th meeting, Abstracts, p. 20 A (1951).
10. Larkin, F. E., and Stuckey, R. E., Analyst, *76*, 150 (1951).
11. Lens, J., Wijmenga, H. G., Wolff, R., Karlin, R., Winkler, K. C., and De Haan, P. G., Biochem. Biophys. Acta, *8*, 56 (1952).
12. Kocker, V., Z. Vitaminforsch., *20*, 369 (1949).
13. Robinson, F. A., Williams, B. W., and Brown, L. H., J. Pharm. Pharmacol., *4*, 27 (1952).
14. Greene, R. D., Brook, A. J., and McCormack, R. B., J. Biol. Chem., *178*, 999 (1949).
15. Strandell, B., Svenska Läkartidningen, *48*, 197 (1951).
16. Shaw, G. E., J. Pharm. Pharmacol., *1*, 69 (1949).
17. Capps, B. F., Hobbs, N. L., and Fox, S. H., J. Biol. Chem., *178*, 175 (1949).
18. Barton-Wright, E. C., "The Microbiological Assay of the Vitamin B-Complex and Amino Acids", Pitman, London (1952).
19. Peeler, H. T., Yacowitz, H., and Norris, L. C., Proc. Soc. Exptl. Biol. Med., *72*, 515 (1949).
20. Caswell, M. C., Koditschek, L. K., and Hendlin, D., J. Biol. Chem. *180*, 125 (1949).
21. Peeler, H. T., and Norris, L. C., J. Biol. Chem., *188*, 75 (1951).
22. Loy, H. W., Jr., Haggerty, J. F., and Kline, O. L., J. Assoc. Offic. Agr. Chemists, *35*, 161 (1952).
23. Stockstad, E. L. R., Dornbush, A. C., Franklin, A. L., Hoffmann, C. E., Hutchings, B. L., and Jukes, T. H., Federation Proc., *8*, 257 (1949).
24. Ågren, G., Acta Physiol. Scand., *17*, 55 (1949).
25. Snell, E. E., Nutritional Observatory, *12*, 53 (1951).
26. Hartman, A. M., Dryden, L. P., and Cary, C. A., J. Am. Dietet. Assoc., *25*, 929 (1949).
27. Skeggs, H. R., Wright, L. D., Nepple, H. M., Valentin, K., and Driscoll, C., Bacteriological Proc., p. 129 (1950).
28. Irwin, J. O., Suppl. J. Roy. Stat. Soc., *4*, 1 (1937).
29. Brink, N. G., Kuehl, F. A., Jr., and Folkers, K., Science, *112*, 354 (1950).
30. Weer, W. L. C., Edelhauser, J. H., Wijmenga, H. G., and Lens, J., Biochem. Biophys. Acta, *6*, 225 (1950).
31. Ellis, B., Petrow, V., Beaven, G. H., Holiday, E. R., and Johnson, E. A., J. Pharm. Pharmacol., *2*, 735 (1950).
32. Wijmenga, H. G., Veer, W. L. C., and Lens, J., Biochem. Biophys. Acta, *6*, 229 (1950).
33. Cooley, G., Ellis, B., Petrow, V., Beaven, G. H., Holiday, E. R., and Johnson, E. A., J. Pharm. Pharmacol., *3*, 271 (1951).
34. Conn, J. B., Norman, S. R., and Wartman, T. G., Science, *113*, 658 (1951).
35. Skeggs, H. R., Driscoll, Ch. A., Charney, J., and Wright, L.D., Am. Chem. Soc. 119th meeting, Abstracts, p. 19 A. (1951).
36. Hendlin, D., and Soars, M. H., J. Biol. Chem., *188*, 603 (1951).
37. Soars, M. H., and Hendlin, D., J. Bact., *62*, 15 (1951).
38. Shive, W., Ravel, J. M., and Eakin, R. E., J. Am. Chem. Soc., *70*, 2614 (1948).
39. Skeggs, H. R., Huff, J. W., Wright, L. D., and Bosshardt, D. K., J. Biol. Chem., *176*, 1459 (1948).
40. Kitay, E., McNutt, W. S., and Snell, E. E., J. Biol. Chem., *179*, 1093 (1949).
41. Smith, E. L., and Cuthbertson, W. F. J., Biochem. J., *45*, No. 2, xii (1949).
42. Skeggs, H. R., Nepple, H. M., Valentik, K. A., Huff, J. W., Wright, L. D., J. Biol. Chem., *184*, 211 (1950).
43. Hoffmann, C. E., Stockstad, E. L. R., Hutchings, B. L., Dornbush, A. C., and Jukes, T. H., J. Biol. Chem, *181*, 635 (1949).
44. Shaw, G. E., J. Pharm. Pharmacol. *1*, 701 (1949).
45. Zygmunt, W. A., J. Bact., *63*, 821 (1952).

Addendum

During the preparation of this paper a note appeared by ZYGMUNT (45) concerning the behavior of different vit. B_{12} complexes in the cup plate assay. His results are in general agreement with ours except that he found that the addition of KCN did eliminate the difference between the assay values for vit. B_{12} and B_{12b}. Furthermore, we could not observe that tomato juice produced a similar effect on the assay in the case of our assay media.

Tryckt den 2 april 1953

Uppsala 1953. Almqvist & Wiksells Boktryckeri AB

ARKIV FÖR KEMI Band 5 nr 39

Communicated 14 January 1953 by A. WESTGREN and G. HÄGG

Studies on the extraction of metal complexes. X

Additional results on the complex formation between thorium and acetylacetone

By JAN RYDBERG

With 4 figures in the text

In a study on the formation of complexes between thorium and acetylacetone (HAa) it was shown that the uncharged complex $ThAa_4$ is formed step by step from Th^{+4} and Aa^-, and the constants for the formation of $ThAa^{+3}$, $ThAa_2^{+2}$, $ThAa_3^+$ and $ThAa_4$ were calculated (1). These results were founded on measurements of the distribution ratio, q, of thorium between benzene and water as a function of the acetylacetonate ion concentration, $[Aa^-]$. In the present paper formation constants for the same complexes have been calculated from measurements of the distribution of thorium between chloroform and water at 0.1 M ionic strength, and special care has been taken to eliminate errors due to loss of thorium through adsorption. The technique of measuring very large and very small distribution ratios will also be discussed.

Connection between complex formation and distribution curves

If the distribution of a metal such as Th between two immiscible solvents is known as a function of the concentration of the complexing anion (ligand) in one of the solvents then the formation constants for the complexes can be calculated. This calculation will only be summarised here; a thorough discussion is given in Part II in this series (1).[1]

The complexity product $\varkappa_n$ (according to J. BJERRUM "the overall complexity constant") is defined by

$$\varkappa_n = [ThAa_n^{4-n}]/[Th^{4+}][Aa^-]^n, \tag{1}$$

where brackets indicate concentrations. The complexity constant is

$$k_n = [ThAa_n^{4-n}]/[ThAa_{n-1}^{5-n}][Aa^-]. \tag{2}$$

It can be shown that the distribution ratio, q, of thorium between the organic and aqueous phases should follow the equation

$$q = \lambda_4 \cdot \varkappa_4 \cdot [Aa^-]^4 / \sum_0^S \varkappa_n \cdot [Aa^-]^n, \tag{3}$$

---

[1] The symbols used in Parts I–IV have been somewhat changed in later parts of this series.

if the thorium compounds in the aqueous phase are mainly mononuclear complexes of Th^{+4} and n Aa^- ($0 \leq n \leq S$). λ_4 is the partition coefficient of the uncharged complex $ThAa_4$ between the two phases. S is the maximum number of Aa which can be bound to each Th atom.

If both phases are of equal volume, the acetylacetonate ion concentration can be calculated from

$$p\,\mathrm{Aa} = p\,k_a + \log[\mathrm{H}^+] - \log[\mathrm{Aa}]_{\mathrm{init}} + \log(k_d + 1 + k_a[\mathrm{H}^+]^{-1}), \qquad (4)$$

where $p\,\mathrm{Aa} = -\log[\mathrm{Aa}^-]$[1], k_a is the dissociation constant of HAa, and k_d its distribution constant between the two solvents. $[\mathrm{Aa}]_{\mathrm{init}}$ is the initial concentration of Aa in one phase, when it is zero in the other phase.

Experimental

Material balance

In earlier experiments (1) the concentration of thorium was usually below 10^{-10} M, and the distribution of the isotope Th^{234} between the two phases was measured by radiometric methods. In these experiments a considerable loss of radioactivity, i.e. thorium, was observed. Tests for material balance showed that sometimes only 30 % of the thorium added could be found in the two phases after equilibrium. It was assumed that the loss was due to the adsorption of thorium on the walls of the vessels, and some precautions were taken to minimize the adsorption effect.

In the paper (1) only those results were included, where more than 80 % of the thorium added was found in the solutions after equilibrium. It was implicitly assumed that, even if some of the thorium was lost through adsorption, equilibrium between the thorium complexes in the two liquid phases was established within 20 hours; the adsorption equilibriums between the walls of the vessel and the solutions do not influence the equilibrium between the two liquid phases. It was found that the distribution ratio q was independent of the initial thorium concentration for $[\mathrm{Th}]_{\mathrm{init}} < 10^{-6}$ M; no change in q-value should thus occur due to a decrease in thorium concentration, when thorium is adsorbed on the vessel.

A careful examination of the adsorption phenomena showed among other things (2) that the loss of thorium through adsorption, although considerable at tracer concentrations, was never more than a few percent at a thorium concentration of 10^{-5} M at any pH, where thorium did not precipitate, e.g. as a hydroxide. However, for an initial thorium concentration in one phase of 10^{-5} M, and $q = 10^3$, the equilibrium concentration in the aqueous phase will only be 10^{-8} M. If samples for measurements are taken from this phase with a pipette a considerable fraction of the thorium may be adsorbed on the walls of the pipette (2). It is therefore necessary to wash the pipette with strong acid, which dissolves the adsorbed thorium, and determine the thorium amount in this wash. Otherwise considerable errors will be obtained in measurements on very large and very small q-values, i.e. $10^{+2} < q < 10^{-2}$.

---

[1] In equation 14 in Paper II (1) $p\,\mathrm{Aa}$ was defined as an activity. However, the ionic strength was so low, 0.01 M, that the small difference between the activity and concentration of Aa^- was neglected. Since q can be measured only as a function of concentrations, it seems more reasonable to use concentrations for all variables and keep the ionic strength constant, instead of mixing concentrations and activities in the same equation.

One of the advantages of using a carrier-free thorium isotope is that the change in acetylacetone concentration due to complex formation with thorium can be neglected; the acetylacetone concentration used in Part II was ≥ 0.005 M. To achieve the same advantage with a thorium concentration of 10^{-5} M, the acetylacetone concentration should be chosen as ≥ 0.05 M.

Procedure

Aqueous solutions of $1.8 \cdot 10^{-6}$ M $Th(ClO_4)_4$ in 0.1 M $NaClO_4$ were shaken for 20 hours at 25° C with equal volumes of chloroform containing acetylacetone. The pH of the aqueous phase was adjusted with NaOH or $HClO_4$. After equilibrium the two phases were separated by centrifuging, and aliquots were taken for radioactive assay. The amount of radioactivity adsorbed in the pipettes was in general measured separately and is always included in the values in Table 1. The radioactivity of the aqueous phase, I'_{aq}, and of the organic phase, I'_{org}, is given in counts per minute (cpm). The apparent distribution ratio, q', is obtained from eqn (5).

$$q' = I'_{org} / I'_{aq} \tag{5}$$

p Aa has been calculated by Equation 6,

$$p\,\mathrm{Aa} = 10.21 + \log[\mathrm{H}^+] - \log[\mathrm{Aa}]_{\mathrm{init}}, \tag{6}$$

which is derived from eqn (4) by introducing the values $pk_a = 8.82$, and $k_d = 23.5$ (3). Equation 6 is valid up to pH 8.5. For higher pH values eqn (4) must be used. Log $[H^+]$ was measured with a Radiometer pH-Meter 3 i.

The experimental data together with the calculated q' and p Aa are given in Table 1.

The radioactive measurements were made with a counter tube (Type M6, 20th Century Electronics, England) for a fixed liquid volume of about 10 ml together with an ordinary electronic counting equipment. The tube had a wall thickness of about 30 mg/cm², corresponding to the maximum range for 0.15 MeV β-particles (4). The liquid layer around the sensitive part of the GM-tube was about 2 mm thick. Before each measurement the tube was washed with conc. H_2SO_4–$K_2Cr_2O_7$, and background taken with water or chloroform. I'_{org} and I'_{aq} are the measured activities minus background.

Corrections for absorption of radiation in solutions

When radioactive measurements are carried out on solutions of different densities (as for example water and chloroform), the absorption of the radiation in the solutions has to be considered. It is possible to calculate the fraction of the radiation transmitted (I/I_0) through a layer (x cm thick) of given density (d) for a pure β-emitter of known maximum energy (E_m MeV) by the equations $I = I_0 \cdot e^{-ux}$ and $E_m^{1.33}\, u = 22 \cdot d$ (5). However, this is not possible for $UX_1 + UX_2$, which emit both β-and γ-radiation. As a further complication, UX_1 and UX_2 are uniformly distributed in the solution.

The absorption of radiation from radioactive substances distributed uniformly in solutions of various densities has recently been studied (6, 7). As a result of these studies one can say, that at the present time it is not possible to make any accurate

Table 1. Calculation of the distribution curve from experimental data

$[Aa]_{init}\,10^3$	$-\log[H^+]$	pAa	I'_{org}	I'_{aq}	log q'
48.9	8.42	3.23	2472±24	7.3±2.2	+2.53 +0.16 −0.12
48.9	8.15	3.50	2546±25	8.7±2.3	+2.47 +0.13 −0.11
48.9	7.85	3.80	5619±36	16.4±5.6	+2.53 +0.20 −0.15
48.9	7.39	4.26	5656±36	13.0±5.7	+2.64 +0.25 −0.15
48.9	7.01	4.64	3708±29	11.3±3.0	+2.52 ±0.12
48.9	6.90	4.75	3701±29	14.3±3.3	+2.41 ±0.11
48.9	6.87	4.78	5385±35	19.6±6.0	+2.44 +0.16 −0.12
48.9	6.86	4.79	4966±34	11.7±5.8	+2.63 +0.3 −0.2
48.9	6.74	4.91	3398±28	4.8±2.8	+2.85 +0.40 −0.20
48.9	6.58	5.07	4671±33	24.5±5.9	+2.28 ±0.12
48.9	6.56	5.09	4255±31	22.2±3.3	+2.28 ±0.07
48.9	6.50	5.15	2145±23	8.5±2.2	+2.40 +0.14 −0.10
48.9	6.37	5.28	4694±33	30.5±3.5	+2.19 ±0.05
48.9	5.93	5.72	3320±28	19.6±5.8	+2.23 +0.16 −0.12
48.9	5.85	5.80	3347±28	24.3±5.5	+2.20 ±0.07
					+2.14 ±0.11
48.9	5.84	5.81	3310±28	42.3±6.6	+1.89 ±0.07
48.9	5.55	6.10	1918±22	72±7	+1.43 ±0.05
48.9	5.55	6.10	1525±20	80±7	+1.28 ±0.05
48.9	5.47	6.18	1980±22	100±8	+1.30 ±0.04
48.9	5.24	6.41	2336±24	224±30	+1.02 ±0.02
48.9	5.01	6.64	2918±26	1001±16	+0.48 ±0.01
48.9	4.93	6.72	1831±21	602±15	+0.48 ±0.01
48.9	4.93	6.72	755±18	745±30	+0.01 ±0.04
48.9	4.91	6.74	2144±23	860±38	+0.40 ±0.01
48.9	4.85	6.80	1667±20	664±13	+0.40 ±0.01
48.9	4.64	7.01	495±15	1312±18	−0.42 ±0.02
48.9	4.51	7.14	540±14	2037±22	−0.58 ±0.02
48.9	4.44	7.21	662±18	3613±29	−0.74 ±0.02
48.9	4.29	7.36	338±11	2559±25	−0.88 ±0.02
48.9	4.29	7.36	249±10	3111±27	−1.10 ±0.01
48.9	4.28	7.37	268±9	2276±24	−0.93 ±0.02
48.9	4.23	7.42	199±9	2465±24	−1.09 ±0.03
48.9	3.95	7.70	52±7	3043±27	−1.77 ±0.06
48.9	3.82	7.83	13.4±3.2	3067±24	−2.36 +0.10 −0.07
48.9	3.80	7.85	43.9±6.4	4389±32	−2.00 ±0.07
48.9	3.61	8.04	9.1±2.9	2710±25	−2.47 +0.12 −0.17
9.78	3.71	8.51	7.0±2.9	5099±34	−2.86 +0.15 −0.25
48.9	3.11	8.54	6.4±4.1	3129±27	−2.69 +0.3 −0.5
9.78	3.15	9.07	13.3±5.8	6348±36	−2.68 +0.16 −0.25

calculation of the fraction of the radiation absorbed in the solution. The efficiency of the GM-tube must be experimentally determined for each combination of solution (density), radioactive isotope (type and spectrum of radiation) and GM-tube (geometry, tube data).

For this reason solutions of $UX_1 + UX_2$ in $CHCl_3$, C_6H_6, H_2O, and 0.1 M $NaClO_4$ in H_2O were measured with the liquid immersion counter. No significant difference was found between pure H_2O and 0.1 M $NaClO_4$ in H_2O with the same $UX_1 + UX_2$ concentration. The radioactivities measured in this manner will be denoted I'_{aq} and I'_{org}. All solutions except that containing $NaClO_4$ were then evaporated, and the activities measured on the dry samples with an end vindow GM-tube, giving I_{aq} and I_{org}. The self-absorption in the sample and backscattering of the β-particles are the same for I_{aq} and I_{org}. The ratio I_{org}/I_{aq} is the true distribution ratio of thorium; it will be called q:

$$q = I_{org}/I_{aq} \tag{7}$$

The connection between the apparent distribution ratio, q', and the true, q, is given by

$$q' = R \cdot q \tag{8}$$

and R[1] is determined from

$$R = I'_{org} \cdot I_{aq}/I_{org} \cdot I'_{aq}. \tag{9}$$

The R-values obtained for $UX_1 + UX_2$ with H_2O, C_6H_6 and $CHCl_3$ are given in Table 2. These values are compared with the calculated transmission for a pure β-

Table 2. Counting efficiency for radiation from radioactive solutions

	C_6H_6	H_2O	$CHCl_3$	$AgNO_3 + H_2O$
mass density, d g/cm^3	0.88	1.00	1.50	1.68
electron density, moles/l	473	556	728	850
mean atomic number, $\bar{Z}$	3.5	3.3	11.6	9.8
UX_1 [0.21 MeV β; 0.09 MeV γ) + UX_2 (2.32 MeV β; 0.8 MeV γ)				
calculated transmission, I/I_0	1.045	1.000	0.838	0.784
measured transmission, R	1.01 ± 0.02	1.000	0.95 ± 0.02	—
P^{32} (1.69 MeV β; no γ)				
calculated transmission, I/I_0	1.065	1.000	0.760	0.690
measured transmission, R	1,06* 1.07**	1.000* 1.000**	0.79* 0.78**	0.70* 0.74**
Co^{60} (0.3 MeV β; 1.3 MeV γ)				
calculated transmission, I/I_0	0	0	0	0
measured transmission, R	0.93** —	1.000** 1.000*	1.16** —	1.18** 1.15*

* Values taken from measurements by ROSE and EMERY (6) on a mixture of $AgNO_3$ and H_2O of the same mass density as C_6H_6, H_2O and $CHCl_3$. The measurements are made with a 20th Century Electronics tube Type M6.

** Values taken from measurements by CHIANG and WILLARD (7) on mixtures of $AgNO_3$ and H_2O of the same mass density as C_6H_6, H_2O and $CHCl_3$. The measurements are made with a Technical Associates tube Type Ta-B2.

---

[1] It can be shown that R is equal to $\Lambda_{aq}/\Lambda_{org}$ (1).

emitter of the same maximum energy as UX_2 (the β-particles form UX_1 can be neglected, since they are completely absorbed in the wall of the GM-tube) through 0.5 mm thick layers of densities corresponding to H_2O, C_6H_6, $CHCl_3$ and $AgNO_3 + H_2O$. In the table are also given values taken from data obtained by ROSE and EMERY (6) and CHIANG and WILLARD (7) for the pure β-emitter P^{32} and the "pure" γ-emitter Co^{60} (the 0.3 MeV β-particles of Co^{60} can be neglected in our case).

For the elucidation of the results in the table, values for mass densities, electron densities and mean atomic numbers for the solutions are also included. The absorption of β-particles depends primarily on the electron density of the absorber. In general the electron density increases with mass density. The absorption of γ-particles take place by the emission of secondary electrons; it is probable that the largest part of these secondary electrons are photoelectrons, the number of which is approximately proportional to Z^5 (8).

The fraction of back-scattered β-particles depends on Z. For P^{32} backscattering should increase the "calculated transmission" for $CHCl_3$ from 0.76 to 0.89 (9); since no increase was found, it may be concluded that this process is of no importance for liquid counting. The unexpectedly large R-values obtained for $UX_1 + UX_2$ and Co^{60} in $CHCl_3$ and $AgNO_3 + H_2O$ must thus be due to secondary electrons produced by the absorption of the γ-rays in the solution and in the wall of the GM-tube.

The q'-values in Table 1 have been corrected according to Equation 8 ($R = 0.95$) to give the true distribution ratio q; $\log q$ is plotted against pAa in Figure 1.

Chemicals used

Analytical grade chloroform was washed several times with distilled water to remove water soluble impurities. $NaClO_4$ was prepared from NaOH and $HClO_4$ of analytical grade. The water was distilled once. Acetylacetone was purified according to Rydberg (10).

Th^{234} was used as a tracer for thorium. It was isolated from natural uranium as described by Dyrssen (11). Some Th^{232} was added to this carrier-free isotope.

All analytical-grade thorium compounds of an age of the order of a year contain several β-emitting daughter substances of Th^{232}. Only β-emitters having a maximum energy of > 0.2 MeV had to be considered, since the radioactive measurements were made with a glass-wall GM-counter having a wall thickness of about 30 mg/cm². For each Th^{232} disintegration one then had to count with three β-disintegrations: from Ac^{228}, Pb^{212} and Bi^{212}–Tl^{208} (branched decay). Since measurements were made on 10 ml of a solution with an approximate efficiency of 20 %, the measured β-activity from a 10^{-6} M Th-solution will be 0.3 cpm. If this concentration is exceeded, one must take into account that not only the radioactivity of Th^{234} is measured but also that of Ac, Pb, Bi and Tl in the solution. In these experiments the Th^{232} concentration was $1.8 \cdot 10^{-6}$ M, which gives a "foreign" background of 0.6 cpm. The statistical deviations in each measurement were never less than ± 2 cpm. By adding an error of ± 0.6 cpm to the standard deviations, the influence of the high thorium concentration is taken into account.

Calculation of complex formation constants

Several methods for the calculation of complexity constants from distribution curves have been described in literature. It has been shown (1) that the slope of the distribution curve is proportional to the ligand number $\bar{n}$, i.e. the average number of ligands per central atom.

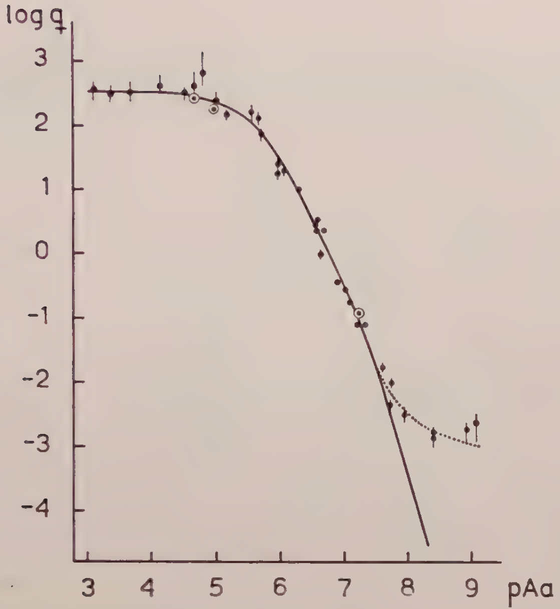

Fig. 1. The distribution ratio (q) of thorium between chloroform and water as a function of the acetylacetonate ion concentration ($p\,\mathrm{Aa} = -\log[\mathrm{Aa}^-]$; ⊙ indicates two points with the same value).

$$\bar{n} = n + d(\log q)/d(p\,\mathrm{Aa}) \tag{10}$$

For a maximum ligand number of 4 we have $n = 4$. In Figure 2 $\bar{n}$ is plotted as a function of $p\,\mathrm{Aa}$. The curve is obtained by graphical derivation of the smooth line drawn through the points in Figure 1. The dotted part of the experimental curve in Fig. 1 has not been used in the calculation of $\bar{n} = f(p\,\mathrm{Aa})$; the reason for this will be discussed in the next section. The connection between $\bar{n}$, $\varkappa_n$ and $[\mathrm{Aa}^-]$ is given by

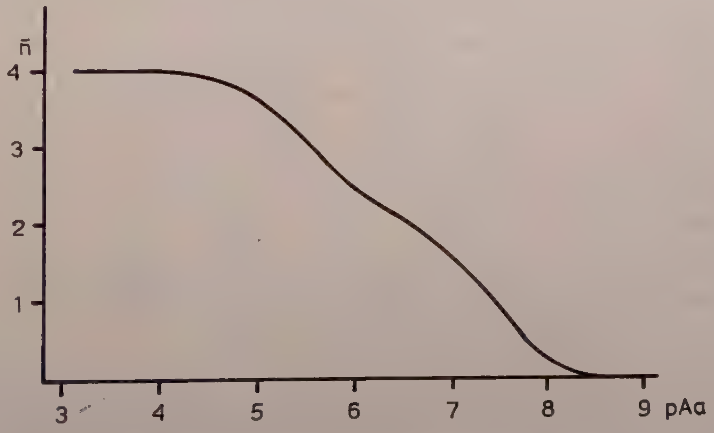

Fig. 2. The average number ($\bar{n}$) of ligands per thorium atom as a function of the acetylacetonate ion concentration.

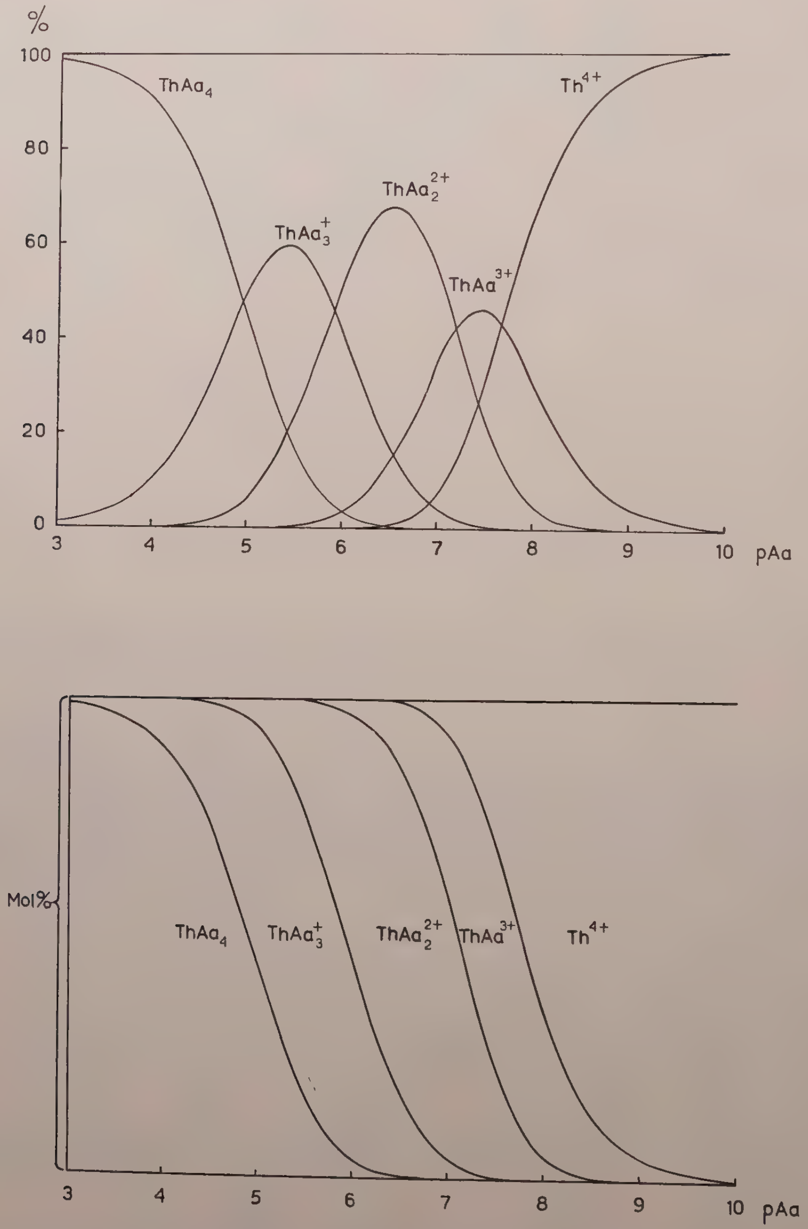

Fig. 3. The percentage of the different $ThAa_n^{4-n}$ complexes as a function of the acetylacetonate ion concentration: in the upper figure the percentage of a complex is the height of the curve over the zero line; in the lower figure the percentage is the length of the vertical line that falls in the area of that complex.

$$\bar{n} + (\bar{n}-1)\varkappa_1[\mathrm{Aa}^-] + (\bar{n}-2)\varkappa_2[\mathrm{Aa}^-]^2 + (\bar{n}-3)\varkappa_3[\mathrm{Aa}^-]^3 + (\bar{n}-4)\varkappa_4[\mathrm{Aa}^-]^4 = 0. \quad (11)$$

By choosing the $[\mathrm{Aa}^-]$-values corresponging to $\bar{n} = 0.5$, 1.5, 2.5, and 3.5 four equations are obtained. This set of equations can be solved by using determinants. The first two columns in Table 3 give $\varkappa_n$ obtained by this method and k_n calculated from Equations 1 and 2 ($\varkappa_0 = 1$).

Table 3

$\varkappa_1 = 4.71 \cdot 10^7$	$k_1 = (0.5 \pm 0.2) \cdot 10^8$	$k_1 = (0.7 \pm 0.3) \cdot 10^8$
$\varkappa_2 = 7.34 \cdot 10^{14}$	$k_2 = (1.6 \pm 0.5) \cdot 10^7$	$k_2 = (5.4 \pm 1.7) \cdot 10^7$
$\varkappa_3 = 5.93 \cdot 10^{20}$	$k_3 = (0.8 \pm 0.2) \cdot 10^6$	$k_3 = (1.9 \pm 0.3) \cdot 10^6$
$\varkappa_4 = 5.37 \cdot 10^{25}$	$k_4 = (0.9 \pm 0.1) \cdot 10^5$	$k_4 = (1.0 \pm 0.1) \cdot 10^5$

The k_n-values in the third column are taken from Part II (1), where the constants were calculated from the distribution beween benzene and water.

According to Equation 3 q is equal to λ_4, when it is independent of $[\mathrm{Aa}^-]$. From Figure 1 $q_{\max} = \lambda_4 = 347$. The error in $q_{\max}$ is about ± 20.

From the $\varkappa_n$ values in Table 3 the precentage of each ThAa_n^{4-n} complex can be calculated. This has been done, and the results are given in two different ways in Figure 3.

Discussion

It is difficult to measure very large and very small distribution ratios. For large q values very little radioactivity is to be found in the aqueous phase. This means that even small droplets of the highly radioactive organic phase in the aqueous phase will cause a great error in q. For example, if the radioactivity in the organic phase is 10 000 cpm/ml, and the true activity in the aqueous phase is 10 cpm/ml, the distribution ratio q will be 1 000. If now the aqueous phase should happen to contain about 0.1 % droplets of the organic phase, this means an additional activity of 10 cpm/ml for the aqueous phase, and the distribution ratio will become 100000/20, i.e. 500. This risk is considerable with the method used above.

Centrifuging and careful handling will probably lead to a very high degree of purity for the upper phase. Before samples of the lower phase are taken, the upper phase is withdrawn. However, it is practically impossible to remove it completely; a thin layer of it is always left. If samples of the lower phase then are taken by pipettes, the danger of contamination from the upper phase is then still considerable. This would not matter, if one could arrange the experiment so that the lower phase always has the higher activity. This is of course not possible, if $q \gtrless 1$ in the same series of experiments. However, it has been shown (12) that when no interaction takes place between the metal and the organic solvent, the same type of distribution curve will be obtained with different organic solvents; all the curves will have the same slope at any $p\mathrm{Aa}$-value, but be displaced along the q-axis. This displacement depends only on the solvent. If one uses two organic solvents, one heavier than water (e.g. chloroform) for $q > 1$, and one lighter than water (e.g. benzene) for $q < 1$, then the lower phase will always be the most radioactive one. By this method the inaccuracy in the measurements on very high or very low distribution ratios can be lessened.

The distribution of thorium with $[\mathrm{Aa}^-]$ is given in Figure 4 for the $\mathrm{CHCl_3}$–$\mathrm{H_2O}$ (solid line) and $\mathrm{C_6H_6}$–$\mathrm{H_2O}$ (broken line) systems. According to the theory the two curves should have the same slope at the same $p\mathrm{Aa}$. In the discussion above it was

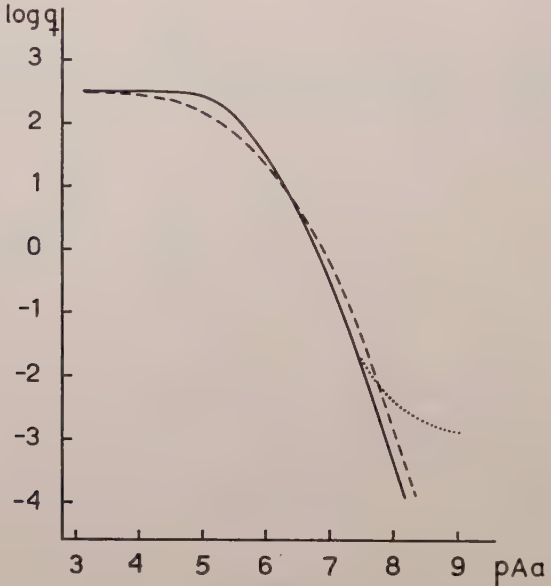

Fig. 4. Thorium acetylacetone distribution curves for chloroform–water (solid line) and benzene–water (broken line).

concluded that the C_6H_6–H_2O system should probably give too small q-values for $q > 1$, and the $CHCl_3$–H_2O system too high q-values for $q < 1$, due to contamination from the upper phase when samples of the lower phase are taken. This is demonstrated by the experimental points for small q-values in Figure 1; there is no other reasonable explanation of the dotted curve. It is thus believed that the $CHCl_3$–H_2O curve is correct for $\log q > 0$, and that the C_6H_6–H_2O curve is correct for $\log q < 0$. The lowest part of the fully drawn curve in Fig. 1 has therefore been drawn parallel to the benzene–water curve from Part II (1); this is demonstrated in Figure 4.

Since the calculation of complex formation constants has been made on the fully drawn curve, it is easy to understand the agreement between the two k_4 values in Table 3. It is believed that the fully drawn curve in Figure 4 gives a true picture of the complex formation between thorium and acetylacetone at an ionic strength of 0.1 M.

The difference between the $CHCl_3$–H_2O curve and the C_6H_6–H_2O curve is partly due to the difference in ionic strength between the two aqueous phases. While the C_6H_6–H_2O system was measured with 0.01 M $NaClO_4$, the $CHCl_3$–H_2O system was measured with 0.1 M $NaClO_4$. For $\log q < 0$ the difference along the pAa-axis between the two curves in Figure 4 is about 0.16 pAa units; the expected difference is 0.07 pAa for a strong binary electrolyte at ionic strengths of 0.01 and 0.1 M (13). However, at high pAa values thorium exists mainly as Th^{+4} ions, and it is not possible to make any calculation of the activity coefficients for 4-valent ions at such a high ionic strength as 0.1 M.

The two curves would probably have been parallel if the same ionic strength had been used togehter with a perfect separation and sampling technique.

SUMMARY

The experimental technique of measuring the distribution of metals between two immiscible solvents has been examined. A way of eliminating some experimental troubles in the measurement of large and small distribution ratios is to use two different organic solvents, one heavier than water for distribution ratios >1, and one lighter than water for distribution ratios <1.

From the distribution of thorium between chloroform and 0.1 M $NaClO_4$ in water as a function of the acetylacetonate ion concentration, $[Aa^-]$, the following constants, k_n, for the formation of $ThAa_n^{+4-n}$ complexes were calculated: $k_1 = (0.5 \pm 0.2) \cdot 10^8$, $k_2 = (1.6 \pm 0.5) \cdot 10^7$, $k_3 = (0.8 \pm 0.2) \cdot 10^6$, $k_4 = (0.9 \pm 0.1) \cdot 10^5$. These values are probably more correct than those previously reported (1); however the difference is not great. The distribution constant of $ThAa_4$ between $CHCl_3$ and H_2O was found to be 350 ± 20.

The author wishes to thank the head of FOA 1, Prof. G. Ljunggren, and Prof. L. G. Sillén for their continuous interest in these studies, and my wife, Britta Rydberg, for her elaborate experimental work.

This work is part of a program financially supported by the Swedish Atomic Committee.

Research Institute of National Defence, Dept. 1, Sundbyberg 4, Sweden.

REFERENCES

1. (Part II) J. Rydberg: Acta Chem. Scand. *4* (1950) 1503.
2. J. Rydberg, B. Rydberg: Svensk Kem. Tidskr. *64* (1952) 200.
3. (Part IX) J. Rydberg: Svensk Kem. Tidskr., in press.
4. L. E. Glendenin: Nucleonics *2*, no. 1 (1948) 16.
5. R. D. Evans: In Goodman: "The Science and Engineering of Nuclear Power. I. "Cambridge (USA) 1947, p. 53.
6. G. Rose and E. W. Emery: Nucleonics *9*, no. 1 (1951) 5.
7. R. S.-H. Chiang and J. E. Willard: Science *112* (1950) 81.
8. E.g. J. M. Cork: "Radioactivity and Nuclear Physics." New York 1947, p. 146.
9. Calculated from data obtained by Dr R. T. Overman, Oak Ridge, Tenn.; see also "Conference on Absolute β-Counting". Prel. Rep. no. 8 (1950), National Research Council, Washington DC.
10. (Part I) J. Rydberg: Svensk Kem. Tidskr. *62* (1950) 179.
11. D. Dyrssen: Svensk Kem. Tidskr. *62* (1950) 153.
12. (Part XI) J. Rydberg: Arkiv för Kemi *5* (1953) p. 517.
13. W. M. Latimer: "Oxidation Potentials. Second Edition." New York 1952, Appendix II.

Tryckt den 2 april 1953

Uppsala 1953. Almqvist & Wiksells Boktryckeri AB

ARKIV FÖR KEMI Band 5 nr 40

Communicated 4 June 1952 by ARNE WESTGREN and GUNNAR HÄGG

Studies on the hydrolysis of metal ions. IV.

Liquid junction potentials and constancy of activity factors in $NaClO_4$-$HClO_4$ ionic medium

By GEORGE BIEDERMANN and LARS GUNNAR SILLÉN

With 5 figures in the text

In the investigations on hydrolysis equilibria that are now in progress in this institution, each system is studied, as far as possible, in a constant ionic medium. The aim of the present work was to test the assumptions used in calculating ionic concentrations from our emf measurements. Besides the interest for our special purpose, our results may have a general bearing on the applicability of the ionic medium method.

We shall start with a brief outline of the ionic medium method, and also of its historical development, since the quotations in literature often give a very incomplete picture.

The ionic medium method

The ionic medium method (to be strict, the constant ionic medium method) for studying ionic equilibria has also been associated with the term inert (or neutral) salt (or electrolyte), or constant ionic strength. It requires one sort of cation (often Li^+, K^+ or Na^+) and one sort of anion (often ClO_4^- or NO_3^-) that are supposed to be inert, thus not to form complexes with the reacting species.

The equilibria are studied in solutions containing the reacting species and the inert ions in such concentrations that the activity factor for a certain ion is supposed to be the same in all solutions studied. The procedure varies somewhat. What is kept constant is sometimes the formal ionic strength, sometimes the total equivalent concentration of all ions (for examples, see "Composition of solutions" below), sometimes the concentration of inert cations or anions. Very often, the inert ions are in great excess over the reacting species.

Granted that the activity factors keep constant, one may calculate the concentrations of various reacting ions directly from emf measurements, and in applying the mass action law may use concentrations for activities. The elimination of the activity factors from all calculations means a great simplification, and is almost necessary in dealing with complicated equilibria, especially if several products are formed, and if their formulas cannot be taken for granted from the beginning.

Historical

The first published work using the ionic medium method is due to GROSSMANN (1905) who studied the equilibria of $Hg^{2+} - SCN^-$ complexes. In his emf and solubility measurements, Grossmann used solutions containing, besides the reacting species Hg^{2+} and SCN^-, the inert ions K^+ and NO_3^- in such amounts as to keep $[K^+]$ constant. As seen from p. 361 and 362 in GROSSMANN's paper, the purpose was to keep the "degree of dissociation" constant; that it would be constant was a consequence of ARRHENIUS' dissociation theory (1884, cf ARRHENIUS 1922, p 26).

GROSSMANN adds (p. 362): "Diese Verbesserung der Methode wurde auf Vorschlag von BODLÄNDER, der ihre Brauchbarkeit in einigen Fällen erprobt hatte (zurzeit noch nicht publiziert) auch hier benutzt". Thus it seems that the inventor of the method was BODLÄNDER, although BODLÄNDER's own work with this method was apparently never published because of his death at the end of 1904.

This contribution of BODLÄNDER seems to have been completely forgotten (unlike BODLÄNDER's method of finding the composition of complexes from emf data).

In 1908 N. BJERRUM (1908, p. 30 ff) remarked that the hydrolysis constant of Cr^{3+} varies considerably with $[Cr^{3+}]$ in solutions containing only $CrCl_3$ but keeps practically constant in solutions containing 0.1 C KCl. BJERRUM made a number of measurements in solutions with $[K^+]$ constant $= 0.1$ or 0.2 C, $[Cr^{3+}] = 0.0005$ to 0.010 C, and the balance Cl^- (p. 38–48). However, in BJERRUM's work (1914–15) on the $Cr^{3+} - SCN^-$ complexes, the first investigation of a complete system with stepwise complex formation, no attempt seems to have been made to keep a constant ionic medium. (This work was on the other hand aided by the fact that the equilibria could be "frozen" and the products determined analytically.)

In 1915–1922, BRÖNSTED published a series of papers (BRÖNSTED 1915, 1919, 1920, 1921; BRÖNSTED and PEDERSEN 1923), in which he studied emf:s and certain simple ionic equilibria, using as a "solvent", instead of water, an aqueous solution of a salt of high concentration. He summarized his conclusions (BRÖNSTED 1927) as follows: "It has been shown that the NERNST formula for electromotive force, the solubility product and mass action law in the case of a complicated ion equilibrium are applicable in their classical form to such concentrated salt solutions, the reason for this simplicity being the practical constancy of the activity coefficients in the practically constant medium. Utilization of these results would mean in many cases a great simplification in problems pertaining to electrolytic solutions." This was the final stage of a long development. For instance, in the 1915 paper, BRÖNSTED considered it as essential that one ion of the ionic medium should be common with the reacting salts; in the 1919 paper he realized that this condition is not necessary; the word activity coefficient did not appear in this connection until in 1920.

The important concept of ionic strength was introduced by LEWIS and RANDALL (1921) and given a theoretical foundation by the DEBYE-HÜCKEL theory (1923).

In the following years, the dissociation constants of acids were often determined in solutions of controlled ionic strength; for polyprotic acids with close-lying dissociation constants, the evaluation of the constants would thus be much simplified, (e.g. KOLTHOFF and BOSCH 1927, 1928, BJERRUM and UNMACK 1929, SIHVONEN 1930). It must be noted that in these acid-base equilibria there was hardly any doubt as to the formulas of the reacting species, and that the ionic strength was kept at rather low values, (say 0.1) to permit extrapolation to infinite dilution.

The first one, after BODLÄNDER and GROSSMANN, to use the ionic medium method for studying complex formation equilibria seems to have been J. BJERRUM (1931). In his work on $Cu^{2+} - NH_3$ complexes he used 2 C NH_4NO_3 as an ionic medium primarily in order to prevent the precipitation of insoluble hydroxy salts; since all complexes have the same charge, $+2$, the activity factors will in this case practically cancel each other out in the complexity constants. In the work of MÖLLER (1937) on Fe^{2+} and $Fe^{3+} - SCN^-$, only occasionally series of measurements were made with high and constant concentration of KCl.

GÜNTELBERG (1938), in his studies of electrolyte activities in mixed solutions, tried to evaluate the thermodynamic constant for $Pb^{2+} + Cl^- = PbCl^+$ by correcting for the activity factors and extrapolating to infinite dilution. Although the experimental conditions were unusually favorable and the measurements extremely careful, GÜNTELBERG by different methods arrived at values ranging between 0.03 and 0.10.

GÜNTELBERG's work illustrates that, in the present state of our knowledge of activity factors, there would be little point in studying complicated ionic equilibria in dilute solutions. By this procedure we might only hope for very rough values for the equilibrium constants, and one would never be even reasonably certain that other complexes than those assumed were not also present in appreciable amounts.

From 1940 on, the ionic medium method has been used consistently in the investigation of a number of complicated systems of complex formation (see e.g. J. BJERRUM 1941, LEDEN 1943).

Present problem

In our studies of the hydrolysis of metal ions, the reacting species are Me^{z+}, H_2O, H^+, and whatever products are formed in the hydrolysis. As inert ions in our work we have chosen Na^+ and ClO_4^-, and $[ClO_4^-]$ has been kept constant, generally at 3 C. (Sometimes we have chosen instead 1 C or 0.5 C). The equilibrium concentrations of H^+ and, if possible, free Me^{z+}, are measured by means of cells:

$$\begin{array}{l|l|l|l} \text{Calomel} & 3\text{ C NaClO}_4 & \text{equilibrium solution S} & \text{electrode reversible} \\ \text{half-cell} & & [\text{ClO}_4^-] = 3\text{ C}, [\text{H}^+] = h & \text{to H}^+ \text{ or Me}^{z+} \end{array} \qquad (1)$$

When the composition of the equilibrium solution is varied, E of the cell varies. We may divide this variation into two terms, one for the variation of the liquid junction potential E_j at the junction 3 C $NaClO_4$ | equilibrium solution and one for the change in the electrode potential; this division is not thermodynamically exact but is very practical.

At low acidities in the equilibrium solution, say $h < 1$ mC, we may as a reasonable approximation neglect E_j and assume the activity factors to be constant. However, when we deal with strongly hydrolysing cations such as Bi^{3+}, Fe^{3+}, Tl^{3+}, and Hg^{2+}, the equilibria must be studied at much higher acidities, say $h = 10$–500 mC. For such cases it has been assumed, following GRANÉR and SILLÉN (1947), 1) that the activity factors of the reacting species in S are not affected, so that one can still use concentrations in the formulas for E and in the equilibrium constants, and 2) that E_j is a function of h only.

Since these assumptions were the basis of our work on a number of different systems, it seemed very desirable to test them thoroughly.

We thus set out to investigate how activity factors and liquid junction potentials in cells like (1) above are affected by replacing a considerable part of the Na^+ ions in 3 C $NaClO_4$ by H^+.

Choice of half-cell systems

We wished to study the behavior of half-cells reversible to H^+, half-cells reversible to metal ions, and half-cells reversible to anions, and to include several different systems in each group.

For H^+ half-cells we chose the hydrogen electrode and the quinhydrone electrode, which had both been used in our previous work. The glass electrode was not included in this study.

The metal ion half-cells must fulfill two conditions: first, the hydrolysis of the metal ions must be negligible in a considerable part of the h range studied; second, the half-cell must be reversible even in highly acid solutions. The metal ion half-cells chosen were: Ag^+/Ag; Cu^{2+}/Cu; Hg_2^{2+}/Hg; Fe^{2+}, Fe^{3+}/Pt.

The hydrolysis of Ag^+ was found by separate experiments to be negligible for $h > 0.001$ mC; the free Ag^+ concentration was measured by emf in solutions of small and varying h. — Whatever be the mechanism of the hydrolysis of Cu^{2+} we may conclude from the papers of PEDERSEN (1943) and ČUPR and ŠIRŮČEK (1937) that it may be neglected for $h > 10$ mC. From measurements in this institution we could calculate that the error from the hydrolysis of Hg_2^{2+} would be negligible for $h > 1$ mC (FORSLING, HIETANEN, and SILLÉN, 1952), and the hydrolysis of Fe^{2+} for $h > 0.001$ mC. The only ion for which the hydrolysis may have played a role at the lower end of the h range studied is Fe^{3+} (HEDSTRÖM, 1952).

The anion half-cells used were $Cl^-/AgCl$, Ag and $Br^-/AgBr$, Ag. Simple inorganic anions of multiple charge, such as SO_4^{2-}, unfortunately all seem to attract protons at higher h.

Composition of solutions

All solutions S were made up so as to make $[ClO_4^-] + [X^-] = 3\ C = 3000$ mC, where X^- stands for Cl^- or Br^-, if present. The added amount of metal ions Me^{z+}, or halogenide ions X^-, was always small, about 10 mC, as compared to $[ClO_4^-]$. The balance was Na^+.

One may also say, that in 3 C $NaClO_4$ we replaced h mC of the Na^+ ions with H^+ and, in some cases, moreover a small fraction of the ClO_4^- with X^-, or of the Na^+ with Me^{z+}.

We shall write for convenience

$$[H^+] = h \qquad (2)$$

In the following we shall for simplicity leave out the inert ions Na^+ and ClO_4^-. Thus a solution S denoted as H^+, Me^{z+} is understood to contain:

h mC H^+, $[Me^{z+}]$ mC Me^{z+}, $(3000 - h - z\,[Me^{z+}])$ mC Na^+, 3000 mC ClO_4^-.

Similarly

H^+ stands for h mC H^+, $(3000 - h)$ mC Na^+, 3000 mC ClO_4^-.

H^+, X^- stands for h mC H^+, $(3000 - h)$ mC Na^+, $[X^-]$ mC X^-, $(3000 - [X^-])$ mC ClO_4^-.

Cells and emf formulas

The set of calomel half-cell and salt bridge was always the same; we shall denote it by

$$\mathrm{CE}\,| = \mathrm{Hg},\ \mathrm{Hg_2Cl_2}\,|\,4\ \mathrm{C\ NaCl}\,|\,3\ \mathrm{C\ NaClO_4}$$

For each of the cells used, the emf E may be divided, perhaps somewhat artificially, into three parts: a constant, E_0, different for each type of half-cell; the NERNST term or terms for the variation of E with the concentrations of the ions, and a quantity E_j', including the liquid junction potential E_j and terms for the variation of the activity factors with h. The formulas for 25° C follow:

Hydrogen half-cell

$$\begin{aligned} &\mathrm{CE}\,|\,\mathrm{H^+}\,|\,\mathrm{H_2},\ \mathrm{Pt} \\ &E = E_0 + 59.16 \log h - \tfrac{1}{2}\cdot 59.16 \log p_{\mathrm{H_2}} + E_j' \\ &E_j' = E_j + 59.16 \log f_{\mathrm{H^+}} \end{aligned} \tag{3}$$

Metal half-cell, $\mathrm{Ag^+}\,|\,\mathrm{Ag}$; $\mathrm{Cu^{2+}}\,|\,\mathrm{Cu - Hg}$ (2 phase); $\mathrm{Hg_2^{2+}}\,|\,\mathrm{Hg}$

$$\begin{aligned} &\mathrm{CE}\,|\,\mathrm{Me^{z+}},\ \mathrm{H^+}\,|\,\mathrm{Me} \\ &E = E_0 + \frac{1}{z}\cdot 59.16 \log\,[\mathrm{Me^{z+}}] + E_j' \\ &E_j' = E_j + \frac{1}{z}\cdot 59.16 \log f_{\mathrm{Me^{z+}}} \end{aligned} \tag{4}$$

Quinhydrone half-cell

$$\begin{aligned} &\mathrm{CE}\,|\,\mathrm{QH_2},\ \mathrm{Q},\ \mathrm{H^+}\,|\,\mathrm{Pt} \\ &E = E_0 + 59.16 \log h + E_j' \\ &E_j' = E_j + 59.16 \log f_{\mathrm{H^+}} + \tfrac{1}{2}\cdot 59.16\cdot \log \{\mathrm{Q}\} \ - \tfrac{1}{2}\cdot 59.16\cdot \log \{\mathrm{QH_2}\} \end{aligned} \tag{5}$$

Redox half-cell

$$\begin{aligned} &\mathrm{CE}\,|\,\mathrm{Fe^{2+}},\ \mathrm{Fe^{3+}},\ \mathrm{H^+}\,|\,\mathrm{Pt} \\ &E = E_0 + 59.16 \log\,[\mathrm{Fe^{3+}}] - 59.16 \log\,[\mathrm{Fe^{2+}}] + E_j' \\ &E_j' = E_j + 59.16 \log f_{\mathrm{Fe^{3+}}} - 59.16 \log f_{\mathrm{Fe^{2+}}} \end{aligned} \tag{6}$$

Silver-silver halogenide half-cells

$$\begin{aligned} &\mathrm{CE}\,|\,\mathrm{X^-},\ \mathrm{H^+}\,|\,\mathrm{Ag\,X},\ \mathrm{Ag} \\ &E = E_0 - 59.16 \log\,[\mathrm{X^-}] + E_j' \\ &E_j' = E_j - 59.16 \log f_{\mathrm{X^-}} \end{aligned} \tag{7}$$

Standard states and extrapolation

We shall define the standard states of the various solutes so that their activity factors are unity if they are present in negligible concentration in the solvent 3 C $\mathrm{NaClO_4}$.

When the solution S approaches pure 3 C $\mathrm{NaClO_4}$ in composition, E_j of course tends to zero; so do all the $\log f_i$ terms, and consequently E_j'.

By subtracting from E the NERNST terms we should in each case get $E_0 + E_j'$, which on extrapolation to $h = 0$ should give E_0.

Reagents

Sodium perchlorate and *perchloric acid* were of the same purity and analyzed in the same way as described in Part V (BIEDERMANN 1952).

Silver perchlorate solutions were prepared by adding a slight excess of $\mathrm{Ag_2O}$ to a hot solution of $\mathrm{HClO_4}$. The excess of $\mathrm{Ag_2O}$ was filtered off, and the $\mathrm{Ag^+}$ content of the resulting solution was measured by VOLHARD's method. As primary standard a silver wire of spectroscopic purity was employed. When the $AgClO_4$ solution was mixed with conc. $HClO_4$ a faint opalescence could be observed, caused by minute amounts of Cl^- present in the $HClO_4$ (p.a. 70–72 %). It was found by nephelometric measurements and by potentiometric titration that with the concentrations used, the error in $[Ag^+]$ caused by the Cl^- ions never exceeded 0.1 % of the total silver concentration.

Mercury (II) perchlorate solution was prepared by dissolving a known amount of HgO (yellow) p. a. in dilute $HClO_4$. The HgO used was found by titration with carefully standardized $HClO_4$ to have the theoretical equivalent weight within ± 0.1 %.

Copper (II) perchlorate solution was prepared in the same way from CuO. The CuO used was of p.a. quality, and did not contain detectable amounts of Cl^- or SO_4^{2-} ions. The Cu^{2+} content of the solution was determined iodometrically according to FOOTE (1938). Iron (II) and iron (III) perchlorate solutions were kindly supplied by civ.ing. BENGT HEDSTRÖM.

The stock solutions of all metal perchlorates were analysed by passing a known volume through a column filled with the hydrogen form of the ion exchanger Duolite C 3, and then titrating with NaOH. This gave $[ClO_4^-]$; since the concentration of the metal ions was known, $[H^+] = h$ was found as difference.

The *quinhydrone* was "MERCK" p.a. Acid impurities or Fe^{3+} ions could not be detected in the preparation. *Sodium chloride* and *sodium bromide* were of p.a. quality; they were carefully dried before weighing.

Apparatus

The cells were kept in a paraffin oil thermostat at $25.0 \pm 0.1°$ C. The emf measurements were made with a JENSEN compensator, type 10 A. Hundredths of a mV were estimated in each case.

The calomel electrode vessel and the salt bridge were of the type designed by FORSLING, HIETANEN and SILLÉN (1951).

Solutions containing Cu^{2+}, Hg_2^{2+}, and Fe^{2+} ions were protected from atmospheric oxygen during the measurements by bubbling a stream of nitrogen through the solution. The nitrogen was obtained from a cylinder, led through a column filled with hot activated copper (MEYER and RONGE 1937), then through a U tube containing "Ascarite" to take away CO_2, and finally through a washing bottle containing 3 C $NaClO_4$ to give the right vapor pressure.

Half-cells

The *hydrogen half-cell* contained lightly platinized Pt foils. The hydrogen gas was treated in the same way as described above for nitrogen. The hydrogen electrodes functioned very satisfactorily in our solutions. At the beginning of a series of measurements it was necessary to wait for about 1–1.5 hours to reach the equilibrium potential. During a titration, equilibrium was attained within 10–15 minutes. All measurements were performed with two Pt foils, which never differed by as much as 0.1 mV.

The *Fe^{2+}-Fe^{3+} redox half-cells* and *quinhydrone half-cells* contained bright Pt foils which had been cleaned with conc. HNO_3, and then ignited in an alcohol flame. Emf:s measured with these half-cells were constant for several hours, and reproducible within ± 0.2 mV.

The *Ag, AgCl electrodes* were prepared according to BROWN (1936). These electrodes gave constant potentials within ± 0.1 mV, and if several electrodes were immersed in the same solution greater differences than a few hundredths of a mV were seldom found. To attain a high accuracy, freshly prepared electrodes must be employed for each titration.

The *Ag, AgBr electrodes* were prepared in the same way as the Ag, AgCl ones; AgBr was formed by electrolysis in 0.1 C NaBr. They were found to behave like the Ag, AgCl electrodes except that they were somewhat more sensitive to sunlight.

Our *Hg electrode* was a mercury pool placed on the bottom of the electrode vessel; the electrical connection was made by a Pt needle. It was found by JONSSON, QVARFORT, and SILLÉN (1947) that the potential given by a mercury pool in a solution containing Hg_2^{2+} and Hg^{2+} ions in arbitrary amounts corresponds to the equilibrium $Hg^{2+} + Hg \rightleftharpoons Hg_2^{2+}$ which is immediately established in the solution layer in contact with the mercury. Since the equilibrium constant of the above reaction is about 130 at 25° C, a Hg pool essentially can be regarded as an electrode reversible to Hg_2^{2+} ions. Electrodes of this kind functioned very satisfactorily; in this case was established, too, that the emf remained constant within ± 0.2 mV if the cell was allowed to stand for 4–5 hours, which is the time required for a titration.

Emf measurements in $Cu(ClO_4)_2$ solutions were made with *copper amalgam electrodes.* The copper amalgam was prepared by the electrolysis of a $CuSO_4$ solution containing sulfuric acid, using a mercury pool as the cathode and a Pt wire as the anode. The amalgam contained about 3 % copper. It is not necessary to know the precise concentration since copper forms a two-phase amalgam in a wide concentration range. The copper amalgam was found to give steady and reproducible potentials in solutions of $h < 400$ mC but in more acid solutions it became very easily polarizable, and the emf changed slowly with time. Therefore emf:s measured in solutions of $h > 400$ mC are inaccurate within ± 0.3 mV. This may be connected with HEINERTH's observation (1931) that in acid solution ClO_4^- ions are slowly reduced to Cl^- by Cu^+ ions. We may investigate this question later on.

CE correction

In order to compare measurements made at different times it was found necessary to add a small correction to the emf in order to eliminate the inconstancy of the calomel electrode. This correction, δ, which never exceeded 1 mV, was the same for all points of each series of measurements, and since we are only interested in changes of emf caused by the variation of h, the introduction of this correction has no consequence on E_j'.

The variation of the calomel electrode potential can first be attributed to the fact that the 4 C NaCl solutions were prepared from two different sources of NaCl, containing different amounts of impurities, especially Br^-. The calomel electrode potential is known to be extremely sensitive to Br^-; a Br^- impurity of 0.1 % causes an error of about 1.6–1.7 mV. (GÜNTELBERG 1938). Further the calomel electrodes show a slow and irregular change with time for reasons not quite understood. We plan in the near future to try to find a more suitable reference electrode system.

Shape of the liquid junction

In a few of our first experiments the salt bridge with 3 C $NaClO_4$ was brought into contact with the solution S by means of a tube with an S-shaped end, Fig. 1b. Afterwards tubes with J-shaped ends (Fig. 1 a) have always been employed. The

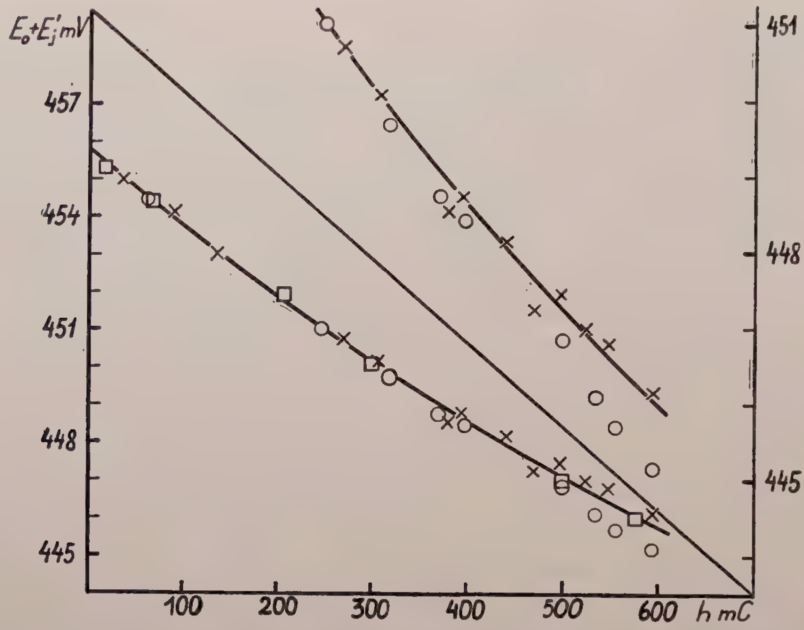

Fig. 1. Influence of the shape of the liquid junction. Measurements with CE-quinhydrone half-cell; $E - 59.16 \log h = E_0 + E_j'$ as a function of the H^+ concentration, h(mC). Upper half: double mV scale. Only about one fourth of the experimental points, chosen at random, have been plotted. Measurements with junctions of J type: squares (GRANÉR and SILLÉN 1947) and crosses (present work); with S type: circles (present work).

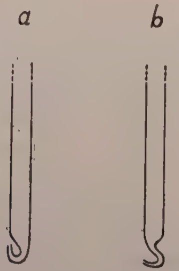

Fig. 1a. Tube with J-shaped end. Fig. 1b: Tube with S-shaped end.

type of junction had no detectable effect on the emf in solutions of $h < 400$ mC but beyond this value lower values were obtained in cells with "S tubes" than in those with "J tubes". The difference at $h \approx 600$ mC was about 1 mV (Fig. 4). This difference may be explained by the fact that with the "S tubes" even small density differences may cause flow of the solutions, whereas with "J tubes" mixing can be brought about only by diffusion. Only experiments with contact by J tubes will be considered here. That emf measurements in the presence of large liquid junction potentials are reproducible is shown by comparing the values of GRANÉR and SILLÉN

Table 1

Measurements with Ag^+/Ag electrodes.

S_0: $AgClO_4$ 10.45 mC, $NaClO_4$ 2990 mC, 75.08 ml.

T : $AgClO_4$ 10.45 mC, $HClO_4$ 1119 mC, $NaClO_4$ 1870 mC; v ml. $E_0 = 376.46$ mV.

v ml	E mV	h mC	$-E'_j$ mV
0.00	436.86		
6.00	435.48	82.84	1.27
9.00	434.84	119.8	1.91
14.00	433.98	175.9	2.77
18.00	433.38	216.5	3.37
24.00	432.63	271.2	4.12
30.00	431.92	319.6	4.83
36.00	431.42	362.8	5.33
44.00	430.71	413.6	6.04
52.00	430.28	458.0	6.47
68.00	429.33	532.0	7.42
81.00	428.79	580.9	7.96

Table 2

Measurements with Cu^{2+}/Cu electrodes. Two different titrations.

S_0: $Cu(ClO_4)_2$ 4.697 mC, $HClO_4$ 14.06 mC, $NaClO_4$ 2977 mC, 50.12 ml.

T : $Cu(ClO_4)_2$ 4.697 mC, $HClO_4$ 1134 mC, $NaClO_4$ 1857 mC, v ml. $E_0 = 21.48$ mV.

v ml	E mV	h mC	$-E'_j$ mV
0.00	41.32, 41.29	14.06	
4.00	39.79, 39.80	96.80	1.56, 1.55
8.00	38.84, 38.63	168.1	2.51, 2.72
12.00	37.88, 37.74	230.3	3.47, 3.61
16.00	37.08, 36.95	284.9	4.27, 4.40
21.00	36.25, 36.13	344.6	5.10, 5.22
26.50	35.46, 35.36	401.2	5.89, 5.99
32.50	34.57, 34.73	454.4	6.78, 6.62
40.50	34.00, 33.65	514.4	7.35, 7.70
50.00	33.35, —	573.1	8.00, —

(1947) and of the present authors, Fig. 1. In most cases the measured emf:s agree within ± 0.2 mV.

Experimental data

Representative data are given in tables 1–3. The heading of each table gives the composition and volume of the solution S_0 originally present around the right-hand electrode, and of the solution T that was added from a burette. It will be noticed that the compositions of S_0 and T were so chosen that the concentrations of all reacting species except for H^+ were kept constant, to simplify the calculations.

In addition is given the E_0 assumed or extrapolated.

Table 3

Measurements with $Br^-/AgBr$, Ag electrodes.

S_0: NaBr 10.52 mC, $NaClO_4$ 2989 mC, 75.08 ml.
T : NaBr 10.52 mC, $HClO_4$ 1119 mC, $NaClO_4$ 1870 mC, v ml. $E_0 = -5.41$ mV.

v ml	$-E$ mV	h mC	$-E'_j$ mV
0.00	54.78	—	—
5.00	56.58	69.89	1.53
11.00	58.33	143.0	3.28.
15.00	59.33	186.4	4.28
20.00	60.40	235.5	5.35
26.00	61.53	287.9	6.48
32.00	62.55	334.5	7.50
38.00	63.35	376.2	8.30
52.00	64.94	458.0	9.89
60.00	65.69	497.2	10.64.
68.00	66.34	532.0	11.29
80.00	67.15	577.5	12.10

The columns give the volume of T added, the measured E, the calculated h, and E'_j. Only every third point is given. Generally at least two different titrations were made; the difference between E values at corresponding points was of the order $\pm$ 0.05 mV or less. The greatest deviations were found with the $Cu^{2+}|$Cu-Hg half-cell. Even there the agreement was rather good, as seen from Table 2.

Fig. 2 gives a survey of E'_j as a function of h for all the half-cells studied, though for clearness only one point out of five is given.

It is seen from Fig. 2 that the points for electrode reactions involving *negative* ions (Cl^-, Br^-) lie distinctly separated from the others, which all involve *positive* ions.

As a matter of fact, all the cation reactions seem to give E'_j values falling on a single curve with the exception of the points for Fe^{2+}, $Fe^{3+}|$Pt at low acidities, and Q, QH_2, $H^+|$Pt at high acidities, which deviate somewhat. Both these deviations can, however, be explained by acid-base reactions: the hydrolysis of Fe^{3+} at low acidities (cf HEDSTRÖM (1952 b) and the formation of $OC_6H_4OH^+$ from the weak base quinone (BIEDERMANN 1953). It is a remarkable fact that ions as unlike in charge, size, and electronic structure as Ag^+, Cu^{2+}, Hg_2^{2+}, Fe^{2+}, Fe^{3+}, and H^+ should give the same curve for E'_j which, as we remember, may be looked upon as the sum of the liquid junction potential E_j and the $RTF^{-1} \ln f$ terms for the variation of the activity factors.

The most simple way of explaining the facts seems to be that the activity factors of cations do not change, within the experimental errors, although a considerable part of the Na^+ ions in 3 C $NaClO_4$ are replaced by H^+. Then the E'_j for cations would really be equal to the diffusion potential E_j at the liquid junction 3000 mC $NaClO_4|h$ mC $HClO_4$, $(3000 - h)$ mC $NaClO_4$. The influence of other ions can be safely neglected, since their concentrations are small and their mobilities are of the same order as those of Na^+ and ClO_4^-. On the other hand E'_j for the anions would contain both E_j and an activity factor correction.

This does not seem wholly unreasonable. If we change the cations of the medium,

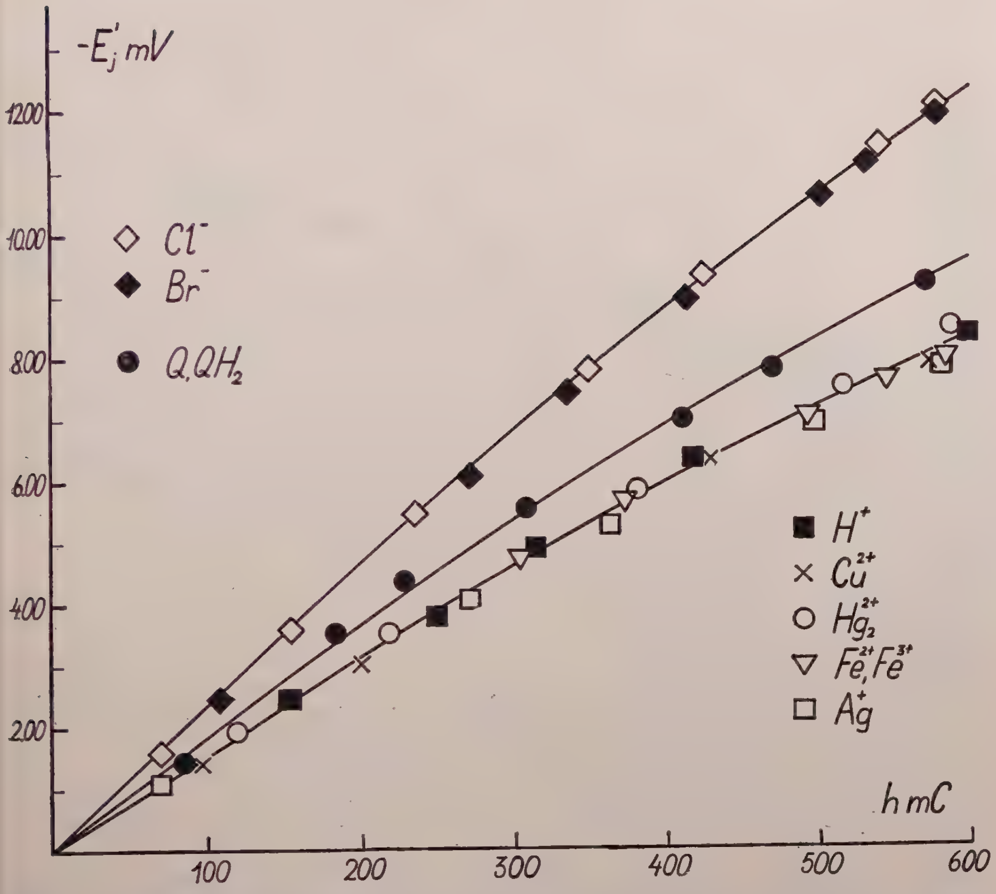

Fig. 2. Survey of measurements: E_j' as a function of h. Upper curve: anion reactions, lower curve: cation reactions, middle curve: quinhydrone half-cell. Only about one sixth of the measured points, chosen at random, have been plotted.

keeping the anions the same, this should affect the activity factors of anions much more than those of cations; in the ionic atmosphere surrounding each ion, the inert ions of opposite charge may of course be expected to predominate. (Cf OLSON and SIMONSON 1949).

Let us follow this working hypothesis.

Equation for the liquid junction potential

Assuming that the measured E_j' for cation reactions gives the real E_j we shall test whether $E_j(h)$ can be expressed by means of the simple HENDERSON one-parameter equation (HENDERSON 1907, 1908).

For the liquid junction

$$3000 \text{ mC NaClO}_4 | h \text{ mC HClO}_4, (3000\text{-}h) \text{ mC NaClO}_4 \quad (8)$$

we can simplify the HENDERSON equation to

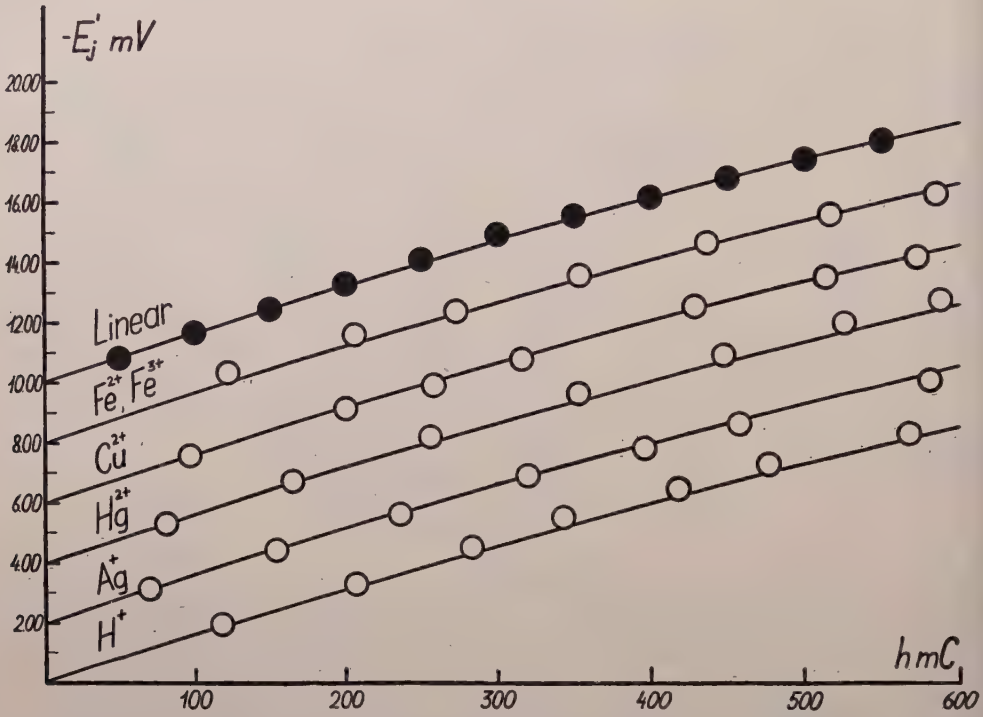

Fig. 3. Curves: E_j calculated with HENDERSON's equation (9) with $d = 1.95$. Open circles: measured E_j' for cation reactions. Dots: E_j' calculated with the linear equation $E_j = -0.016\,h$ (for $h < 300$ mC, equation 12) and $E_j = 0.016\,h - 0.004\,(h - 300)$ for $h > 300$. The curves are shifted stepwise by 2.00 mV.

$$E_j = -59.16 \log\left(1 + \frac{dh}{3000}\right) \tag{9}$$

where

$$d = \frac{\Lambda_{\mathrm{HClO_4}} - \Lambda_{\mathrm{NaClO_4}}}{\Lambda_{\mathrm{NaClO_4}}} \tag{10}$$

We transform (9) to

$$10^{-E_j/59.16} - 1 = d \cdot \frac{h}{3000} \tag{11}$$

When we plotted the experimental values for $(10^{-E_j/59.16} - 1)$ versus $h/3000$, the points with good approximation fell on a straight line with slope $d = 1.95 \pm 0.08$. Thus d seems to remain practically constant in the h range, 0–600 mC, studied by us.

In Fig. 3 the values for $-E_j$ calculated with equation (9) and the average value $d = 1.95$, are compared with the experimental points; for clarity each new system has been shifted by 2 mV. The deviations do not exceed the experimental errors.

An important point is the extrapolation of E_0 from h values as high as say 70 mC to $h = 0$. For the three types of half-cells where this was possible, E_0 was determined by independent experi-

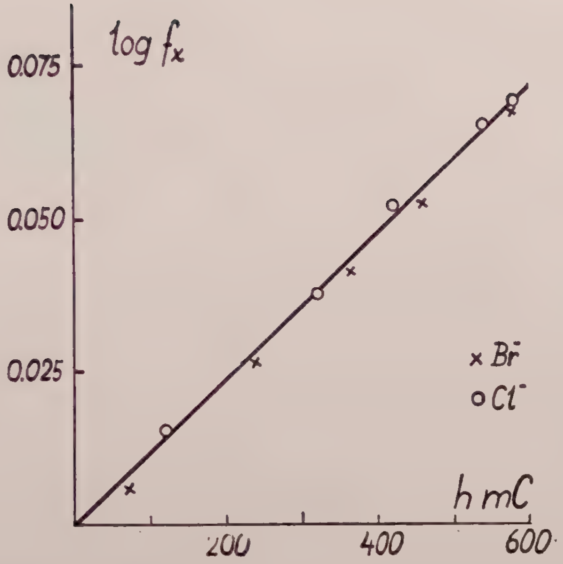

Fig. 4. Variation of activity factors of Cl^- (circles) and Br^- (crosses) with h.

ments also at so low acidities that E_j could be neglected. The differences were found to be only of the order of 0.1 mV. Typical examples of E_0 values obtained by measurements in the same day:

CE/Cl^-/AgCl, Ag, extrapolated 159.9 direct 159.9
CE/Br^-/AgBr, Ag, extrapolated 5.4 direct 5.7
CE/Ag^+/Ag extrapolated 376.5 direct 376.6

It seems somewhat surprising that the HENDERSON equation is so well obeyed; one might equally well have expected d to vary with h. — It should be noted that the value $d = 1.95$ is considerably lower than that, 3.3, calculated from the conductivities of 3 C $HClO_4$ and 3 C $NaClO_4$.

Similar results were found by EKEDAHL and SILLÉN (1947), who derived an equation of the same type as (9) and proved it to hold true for junctions with HNO_3-$AgNO_3$ mixtures of total NO_3^- concentration 20.2 or 50.0 mC. The experimental value for d in this case was also smaller than that calculated from the conductivities of the pure components. As discussed by these authors, the cause is the general leveling of ionic mobilities in electrolyte mixtures. For a higher ionic strength, 100 mC, EKEDAHL (not yet published) has found that d keeps constant in about half the mixing range for HNO_3-$AgNO_3$ but varies with h in the half richest in HNO_3. Similarly one might expect d for $HClO_4$-$NaClO_4$ mixtures to deviate at still higher h values than those studied by us.

The conductivities of $NaClO_4$-$HClO_4$ mixtures are now being measured in this laboratory.

For low values of h we may use as an approximation for (9)

$$E_j = \frac{-59.16}{\ln 10} \cdot \frac{dh}{3000} = 0.0167\, h \qquad (12)$$

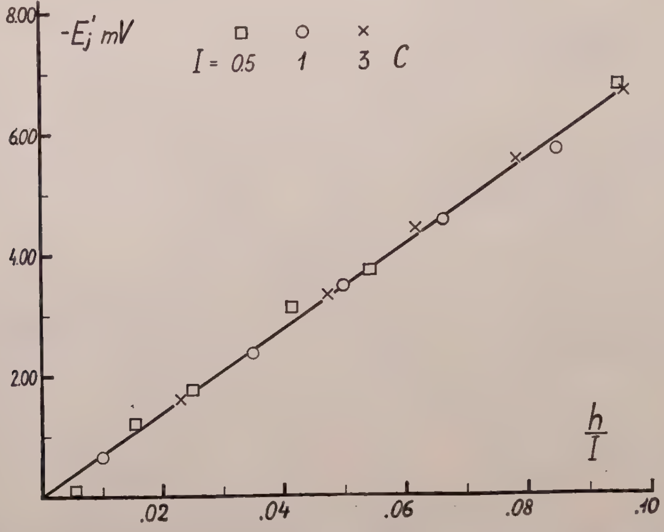

Fig. 5. Measurements with CE | Br^- | AgBr. Ag and CE | Cl^- | AgCl, Ag at different [ClO_4^-] = I; 3 C (crosses), 1 C (circles), 0.5 C (squares). Only about one tenth of all experimental points have been plotted, chosen at random. The chloride and bromide curves did not differ, within the experimental errors.

In the range $h = 0 - 300$ mC a still somewhat better over-all fit is obtained with $E_j = -0.016\ h$ (black dots, Fig. 3), which was used in the extrapolations for E_j.

Activities of negative ions

Let us assume that the E_j' curve for cation reactions in Fig. 1 gives the true E_j. Then the deviation of the curve for anion reactions, according to (7) should be due to the variation with h of the activity factor f_X of the anion. By means of the data, and equation (7), we constructed Fig. 4 giving log f_X as a function of h. In the range studied, the variation seems to be almost linear.

Measurements at lower perchlorate concentrations

A few series of experiments have been made at lower anion concentrations, namely 500 mC and 1000 mC, instead of 3000 mC. The results seems to show that, within the experimental errors, E_j' can with good approximation be considered as a function of h/I only.

Fig. 5, for instance, gives the measurements of SIRKKA HIETANEN in this laboratory on cells

Hg, Hg_2Cl_2/4 C NaCl/I mC $NaClO_4$/h mC H^+, (I–h) mC Na^+, c mC X^-, (I–c) mC ClO_4^-/AgX, Ag

For $I = 500$ mC, h was varied from 0 to 50 mC, and for $I = 1000$ mC from 1 to 100 mC. X^- was Cl^- or Br^- and c was kept constant at 10 or 20 mC. The measured E_j', as defined by (7), are plotted as functions of h/I, and values for $I = 3000$ mC are plotted for comparison. The points are seen to fall, within the experimental errors, on a single straight line.

Accordingly, the deviations of the activity factors of anions, and the liquid junction potentials, are three times as high for $I = 1000$ mC as for $I = 3000$ mC; with $I = 500$ mC they are six times as high. This illustrates the advantage of using a high concentration of the inert salt.

Conclusion

Our results indicate that one may with a certain confidence vary the composition of the ionic medium, as long as all reactants have charges of the same sign or are uncharged (as in the hydrolysis of cations, or in the equilibria of silicate ions with OH^-), and as long as the concentration of the inert ion of opposite sign is kept constant.

On the other hand, one must be cautious when working with reactants of opposite sign, for instance when studying complexes between metal ions and anions. This is well illustrated by the recent work of LEDEN (1952) on sulfate complexes. Especially with weak anion — cation complexes it is hard to distinguish the change in emf caused by complex formation from that caused by shifts in the activity factors.

The variation of the activity of the uncharged molecule H_2O is small; the vapor pressure over 3 C $NaClO_4$ is 21.0 torr, that over 3 C $HClO_4$ 19.7 torr. If the variation in mixtures is assumed to be roughly linear with h, the change in the water activity when h passes from 0 to 600 mC can be estimated to 1.2 %, which is negligible for the purpose of the hydrolysis studies.

Acknowledgements

We wish to thank our friends SIRKKA HIETANEN, ERIK EKEDAHL, FREDRIK GRANÉR, and BENGT HEDSTRÖM for valuable discussions on various experimental questions. The paper has been made more readable by the helpful criticism of Professor RALPH G. PEARSON. Another of our friends, Mr FRANS ERICSON has been a valuable aid in the practical work by making good thermostats and many other parts of our equipment.

This work has been supported by *Statens Naturvetenskapliga Forskningsråd.*

SUMMARY

The history of the "ionic medium" method for studying complicated ionic equilibria is briefly outlined.

This work deals with the changes in activity factors and in the liquid junction potential when in the ionic medium 3 C $NaClO_4$ a varying fraction of Na^+ is replaced by H^+.

Cells of the following type were studied: Calomel half-cell/3 C $NaClO_4$/solution S/ electrode, reversible to H^+, Me^{z+}, or X^-.

The solution S was mixed so that in 3 C $NaClO_4$, 0–0.6 C H^+ replaced Na^+ ions. In addition, in some solutions either a small amount (a few mC) of the Na^+ were replaced by various cations, or a small amount of the ClO_4^- by Cl^- or Br^-.

The data show that in the given range ($0 - 0.6$ C H^+, $[Me^{z+}]$ or $[X^-]$ small) it is permissible to assume, within the experimental errors, that a) E_j, the liquid junction potential 3 C $NaClO_4|S$, is a function only of the hydrogen ion concentration in S, and b) the activity factors of all positive ions remain constant when part of Na^+ is replaced by H^+.

The activity factors of the negative ions studied, on the other hand, changed perceptibly; this is reasonable, since negative ions should be more influenced by a change in the ions of opposite charge.

For the quinhydrone electrode, deviations were observed which could be explained assuming quinone to be a weak base (Biedermann 1953).

The liquid junction potential E_j followed, within the experimental error, equation (9), which is derived from Henderson's equation.

The assumptions made in this series for calculating ionic concentrations and equilibrium constants from emf data thus seem to be well justified.

Department of Inorganic Chemistry, Royal Institute of Technology, Stockholm, Sweden.

REFERENCES

Arrhenius, S. (1884) Kgl Svenska Vetenskapsakad. Handl. *8*, No 14, p. 36.
——. (1922) Z. physik. Chem. *100*, 26.
Biedermann, G. (1952) Arkiv Kemi *5*, Nr 41 (Part V).
——. (1953) to be published.
Bjerrum, J. (1931) Kgl. Danske Videnskab. Selskab., Mat. fys. Medd. *11*, No 5.
——. (1941) Diss. Copenhagen.
Bjerrum, N. (1908) Diss. Copenhagen (p. 30 ff and 38–48).
——. (1914–15) Kgl. Danske Videnskab. Selskab, Skrifter, Naturvidenskab. math. Afdel. (7) *12*, No 4.
Bjerrum, N., and Unmack, A. (1929) Kgl. Danske Videnskab. Selskab, Mat. fys. Medd. *9* No 1.
Brönsted J. N. (1914–15) Kgl. Danske Videnskab. Selskab, Skrifter, Naturvidenskab. math. Afdel. (7) *12*, No *6* (p. 252 ff).
——. (1919) Medd. Vetenskapsakad. Nobelinst. *5*, No 25.
——. (1920) Kgl. Danske Videnskab. Selskab, Mat. fys. Medd. *3*, No 9.
——. (1927) Trans. Faraday Soc. *23*, 429–31.
Brönsted J. N., and Pedersen K. (1923) Z. physik. Chem. *103*, 307.
Brown, A. S. (1934) JACS *56*, 646.
Čupr, V., and Širůček, J. (1937) Collection Czech. Chem. Comm. *9*, 68.
Debye, P., and Hückel E. (1923) Physik. Z. *24*, 185.
Foote, H. W. (1938) JACS *60*, 1349.
Forsling, W., Hietanen, S., and Sillén, L. G. (1952) Acta Chem Scand. *6*, 901 (Part III).
Ekedahl, E., and Sillén L. G. (1947) Arkiv Kemi *22* A, No 16.
Granér, F., and Sillén L. G. (1947) Acta Chem. Scand. *1*, 631 (Part I).
Grossmann, H. (1905) Z. anorg. Chem. *43*, 356.
Güntelberg, E. (1938) Diss. Copenhagen.
Hedström, B. (1952 a) Arkiv Kemi *5*, 26 (Part VI).
——. (1952 b) Arkiv Kemi *5*, 27 (Part VII).
Heinerth, E. (1931) Z. Elektrochem. *37*, 61.
Henderson, P. (1907) Z. physik. Chem. *59*, 118.
——. (1908) Z. physik. Chem. *63*, 325.
Hietanen, S., and Sillén L. G. (1952) Acta Chem. Scand. *6*, 747 (Part II).
Jonsson, A., Qvarfort, I., and Sillén L. G. (1947) Acta Chem. Scand. *1*, 461.
Kolthoff, I. M., and Bosch, W. (1927–1928) Rec. trav. chim. *46*, 430; *47*, 558, 819, 826.
Leden, I. (1943) Diss. Lund.
——. (1952) Acta Chem. Scand. *6*, 971.
Lewis, G. N., and Randall, M. (1921) JACS *43*, 1140.
Meyer, F. R., and Ronge, G. (1939) Angew. Chem. *52*, 637.
Möller, M. (1937) Diss. Copenhagen.
Olson, A. R., and Simonson, T. R. (1949), J. Chem. Phys. *17*, 1167, 1322.
Pedersen, K. J. (1943) Kgl. Danske Videnskab. Selskab, Mat. fys. Medd. *20*, No 7.
Sihvonen, V. (1930) Z. Elektrochem. *36*, 165.

Tryckt den 7 april 1953

Uppsala 1953. Almqvist & Wiksells Boktryckeri AB

ARKIV FÖR KEMI Band 5 nr 41

Communicated 4 June 1952 by Arne Westgren and Gunnar Hägg

Studies on the hydrolysis of metal ions. V.

The hydrolysis of the thallium(III) ion

By George Biedermann

With 5 figures in the text

When a Tl(III) salt was first prepared, about ninety years ago (1), it was observed immediately that it was stable only in solutions of high acidity. On decreasing the hydrogen ion concentration the salt was decomposed by water with the formation of an insoluble product. This means that the Tl(III) ion is an acid of considerable strength, i.e. it reacts with water producing hydrogen ions, and that the ultimate reaction product has a very low solubility. Abegg and Spencer (2), when investigating equilibria in solutions containing Tl(III), Tl(I) ions and different anions, determined the solubility of Tl_2O_3 in nitric acid solutions. From the constancy of the ratio $[Tl^{3+}]/[H^+]^3$ they concluded that the hydrolysis proceeds according to the reaction $Tl^{3+} + 3H_2O = Tl(OH)_3(s) + 3H^+$. It was found later by Hüttig and Mytyzek (3) and by Milligan and Weiser (4) that the X-radiograms of the wet precipitate and the anhydrous Tl_2O_3 are identical, so the above reaction must be written

$$2Tl^{3+} + 3H_2O = 6H^+ + Tl_2O_3(s)$$

Several investigators (2, 5) have observed that the formal redox potential Tl(I) – Tl(III) decreases with decreasing $[H^+]$, especially below about 500 mC. This was ascribed to the hydrolysis of the Tl(III) ion.

Although all investigators working with the Tl(III) ion have been well aware of its strong hydrolysis, I have not been able to find any reports on what is formed in the solution. The aim of the present investigation was to determine what kinds of soluble products are formed when Tl(III) ion reacts with water, and to determine the equilibrium constants of the hydrolysis processes.

The method of measurement

To investigate the hydrolysis equilibria it was decided to work with solutions of the following composition

c_3 mC Tl(III), c_1 mC Tl(I), H mC H^+, $(3000 - 3c_3 - c_1 - H)$ mC Na^+, 3 C ClO_4^- = solution S.

where c_1 and c_3 are the total concentrations of Tl(I) and Tl(III) ions, and H is the analytical concentration of H^+, assuming all Tl(III) to be present as Tl^{3+} ion. The actual [H+] will be denoted by h. All concentrations are expressed in mC (millimole/liter). To determine the hydrolysis equilibria the actual concentrations of the free (hydrated) Tl^{3+} ions and of the hydrogen ions need to be known. The actual concentration of the Tl^{3+} ions was determined by emf measurements. The cells used were of the following type

$$-\,Hg,\ Hg_2Cl_2|4\ C\ NaCl|3\ C\ NaClO_4|\text{Solution S}|Pt\,+$$

The emf at 25° C is, in mV

$$E = E_0' + 29.58 \log ([Tl^{3+}]/[Tl^{+}]) + 29.58 \log (f_{Tl^{3+}}/f_{Tl^{+}}) + E_j \qquad (1)$$

where E_0' is a constant, $f_{Tl^{3+}}$ and $f_{Tl^{+}}$ are the activity factors of the Tl^{3+} and Tl^{+} ions referred to a conveniently chosen reference state, and E_j (which has a negative value) is the liquid junction potential between solution S and the 3 C $NaClO_4$ solution. The activity factors and the liquid junction potential cannot be determined separately, but $(29.58 \log (f_{Tl^{3+}}/f_{Tl^{+}}) + E_j) = E_j'$ is a measurable quantity. The experiments of BIEDERMANN and SILLÉN (8) on similar cells with a number of cations make it very likely that the terms with the activity factors can be neglected and E_j can be calculated with the formula given there.

There are no experiments recorded proving that the Tl(I) ion is hydrolyzed i.e. that undissociated TlOH would be present to an appreciable extent in the solutions of Tl(I) salts. DE FORCRAND (6) found that the heat of neutralisation of TlOH is the same as that of NaOH with strong acids; for weak acids the heat of neutralisation is even larger with TlOH than with NaOH. HLASKO and SALITOWNA (7) found that the equivalent conductances of TlOH solutions follow KOHLRAUSCH's cubic root equation, and that in very dilute solutions the equivalent conductances are well in line with ONSAGER's theory for strong electrolytes. These investigations indicate that TlOH is completely dissociated. The concentration of the free (hydrated) Tl(I) ions in our solutions could thus be taken as the same as the total concentration independent of [H+]. Even if Tl(I) were to form complexes with ClO_4^- ions, our calculations would not be affected since the Tl(I) and the ClO_4^- ion concentrations were kept constant in all measurements.

Subtracting 29.58 log $[Tl^{3+}]_{total}$ from both sides of equation (1) and rearranging we get

$$E - E_j + 29.58\ \log\ ([Tl^{+}]/[Tl^{3+}]_{total}) = E_0' + 29.58 \log ([Tl^{3+}]/[Tl^{3+}]_{total}) = E' \quad (2)$$

Since E_j and $[Tl^+] = [Tl^+]_{total}$ are known, the ratio $[Tl^{3+}]/[Tl^{3+}]_{total}$ can be calculated from the emf measurements if E_0' is known.

Because of the extremely low solubility of Tl_2O_3, measurements could not be carried out at higher concentrations of Tl(III) ions than about 2.5 mC for h below 600 mC. It was feared that, in solutions containing larger concentrations of H+ than 600 mC, the liquid junction potential would no longer be a function of h only; and that the individual differences among the ions would become appreciable, so that emf variations cannot be accurately evaluated as concentration changes. Even at $h \approx 600$ mC equation (2) is only approximately valid since E_j' varies by up to ± 0.4 mV.

Since only very low Tl(III) concentrations could be used, h could be taken equal to H with good approximation. For instance, at the lowest H studied, 20 mC, the maximal difference between H and h, calculated on the assumption that each Tl(III) ion sets free 3 H+, is not more than 1.5 % since the total Tl(III) concentration used at this H was 0.1 mC. The error introduced in this way can be easily corrected for by calculation. A glass electrode could not be of much value since the accuracy of the determination of [H^+] with a glass electrode can hardly be expected to be much better than ± 2 % (0.5 mV).

Materials and analysis

Sodium perchlorate was prepared from a commercially available product of c.p. quality. It was recrystallized twice from alcohol and dried at 90° C in an oven. In the product prepared in this way no Cl^- or ClO_3^- ions could be detected, and it was found to be free from acid impurities. When the drying was performed above 100° C it was observed that traces of alcohol left from the recrystallisation caused reduction with the formation of Cl^- and ClO_3. The $NaClO_4$ solutions were analysed by evaporating a known volume at 120° C and drying at the same temperature until weight constancy was attained.

Perchloric acid solutions were prepared from $HClO_4$ p.a. (70–72 %), the only detectable impurity being a minute amount of Cl^- ions (less than 0.01 %). The H^+ concentration was determined with carefully purified $KHCO_3$, and with standard NaOH. The NaOH was standardized both with $KH(IO_3)_2$ and by evaporating a known volume with a small excess of HCl, drying at 360° C and weighing the residue as NaCl. The determinations with different standard substances agreed to within ± 0.1%. Incidentally, attempts were made to measure the $HClO_4$ concentration by evaporating a known volume with excess of NH_3, drying at 105° C and weighing as NH_4ClO_4. Systematically low results (0.3–0.4 %) were obtained depending on the excess of NH_3 solution used. Similar observations have been made independently by HIETANEN (9). The low results are probably due to the fact that NH_4ClO_4 volatilizes at higher temperatures.

The source of all thallium salts was Tl_2CO_3 (Kahlbaum). *Thallium*(I) *perchlorate* was prepared by dissolving Tl_2CO_3 in an excess of hot concentrated $HClO_4$ solution. The precipitated $TlClO_4$ was washed and recrystallized three times from water. Finally the crystals were dried at 120° C. $TlClO_4$ was analysed by titrating Tl(I) with iodate solutions using the iodine monochloride endpoint (10). As standard substances KIO_3 and $KH(IO_3)_2$ were used. The latter was the same preparation as that employed for the standardization of the NaOH solutions. The equivalent weight of the $TlClO_4$ was found by these titrations to be the theoretical one within the limits of experimental error ± 0.1 %. Tl(I) was also determined gravimetrically by precipitating in the form of Tl_2CrO_4. The accuracy of this gravimetric method is not higher than ± 0.5 %, and within these limits it was again found that the composition of our $TlClO_4$ preparation was the theoretical one.

Thallium(III) perchlorate solutions were prepared by anodic oxidation of $TlClO_4$ solutions. As was shown by GRUBE and HERMANN (11), the electrolytic oxidation of Tl(I) can be carried out with a high current efficiency provided the solution is sufficiently acid. The apparatus used was very simple. A large Pyrex beaker served as the anode compartment and contained the $TlClO_4$ solution with 2 C $HClO_4$ to avoid hydrolysis. The beaker was closed by a rubber stopper provided with two holes, a small one for the Pt anode and a larger central one. Through the latter a specially made sintered glass filter funnel was inserted (Fig. 1). The filter funnel was used as the cathode compartment. It was filled with 2 C $HClO_4$, and the filter plate itself served as the diaphragm. The glass filter, as far as could be observed, was absolutely resistant to the acid solutions used, whereas the usual diaphragms of porcelain and similar materials were attacked by the $HClO_4$ solutions. The liquid level was kept somewhat higher in the cathode compartment than in the outside solution to avoid loss of thallium ions. The anode was a platinum gauze cylinder, the cathode a platinum wire. The thallium solution was stirred very effectively with a magnetic stirrer. The electrolysis was carried out with a low current density; it was calculated to be 0.01 amp/cm², assuming the area of the platinum gauze to be half the mantle area of a cylinder of the same size. With higher current densities the current yield was considerably lowered. With a very effective stirring and the above current density, the yield was found to exceed 99 %, if the electrolysis was continued until the first oxygen bubbles could be observed at the anode. The procedure of electrolytic oxidation proved to be very convenient and to avoid many complications met with in methods described by previous authors. There is no need to introduce foreign substances, the concentration of the Tl(III) ions can be varied within wide limits, and a very simple apparatus is sufficient.

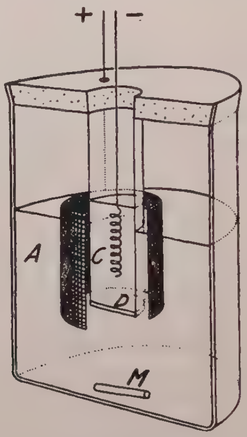

Fig. 1. Electrolysis apparatus. A anode compartment, C cathode compartment, D sintered glass diaphragm, M magnet.

The total thallium content of the $Tl(ClO_4)_3$ solutions was determined by reducing the Tl(III) ions with SO_2, boiling off the excess reductant, cooling and titrating the solution with KIO_3. The Tl(I) content of the $Tl(ClO_4)_3$ solutions was determined by adding an excess of a 0.005 C ICl solution and titrating the liberated iodine back to ICl with 2.5 mC KIO_3, using $CHCl_3$ as indicator.

The analytical concentration of H^+ in the $Tl(ClO_4)_3$ solutions was measured in the following way. To a known volume of the solution a small excess of a dilute H_2O_2 solution was added, which immediately reduced the Tl(III) ions quantitatively to Tl(I). The excess of H_2O_2 was destroyed by boiling, and after cooling, the solution was titrated with NaOH. Assuming the reaction $Tl^{3+} + H_2O_2 = Tl^+ + 2H^+ + O_2$, the difference between the titrated hydrogen ion concentration and twice the molar concentration of Tl(III) ions is equal to the hydrogen ion concentration before the reduction. The acid content of the H_2O_2 solutions was found to be negligible. This method of analysis was compared with that used by NOYES and GARNER (13). These authors reduced the Tl(III) ions by shaking the solution with mercury and solid

Table 1

Two series are given to show the reproducibility of the emf values.

Measurements with $c_3 = 0.1038$.

S: $c_3 = 0.1038$ mC, $c_1 = 4.936$ mC, $H = 22.46$ mC, 50.12 ml.
T: $c_3 = 0.1038$ mC, $c_1 = 4.936$ mC, $H = 321.9$ mC, v ml.
$\delta = +2.0$ mV.

v ml	E mV	H mC	$-E_j$ mV	E' mV
0.00	977.9	22.46	0.4	1029.8
1.00	981.5	28.32	0.5	1033.5
2.00	984.3	34.00	0.6	1036.5
3.00	986.5	39.37	0.6	1038.7
5.00	989.5	49.62	0.8	1041.9
7.00	991.3	59.12	1.0	1043.9
9.00	992.8	68.04	1.1	1045.5
11.00	994.0	76.34	1.2	1046.8
13.00	994.8	84.12	1.4	1047.8
16.00	995.8	94.91	1.6	1049.0
19.00	996.5	104.8	1.7	1049.8
22.00	996.9	113.8	1.9	1050.4
0.00	977.8	22.46	0.4	1029.8
1.00	981.4	28.32	0.5	1033.4
2.00	984.1	34.00	0.6	1036.3
3.00	986.2	39.37	0.6	1038.4
4.00	987.9	44.59	0.7	1040.2
5.00	989.3	49.62	0.8	1041.7
7.00	991.4	59.12	1.0	1043.9
9.00	992.8	68.04	1.1	1045.5
11.00	993.9	76.34	1.2	1046.7
13.00	994.7	84.12	1.4	1047.7
16.00	995.5	94.91	1.6	1048.7
21.00	996.5	110.9	1.8	1049.9
26.00	997.2	124.7	2.0	1050.8
31.00	997.6	136.9	2.2	1051.4

KCl; the filtrate was then titrated with NaOH. The results with their method were found to agree within ± 0.2 – 0.3 % with those found after H_2O_2 reduction.

Freshly prepared $Tl(ClO_4)_3$ solutions were found to contain less than 0.1 % Tl(I), and provided the solution was stored in dark bottles and protected from sunlight, the amount of Tl(I) was not greater even after four weeks than 0.1 % of the total thallium content. Solutions exposed to diffuse sunlight were reduced with considerable speed.

Experimental details of the emf measurements

The apparatus used was the same as that described in part IV (8). Solution S was prepared by mixing with carefully calibrated burettes. The redox potentials were measured with bright Pt electrodes which had been cleaned with HNO_3 and then ignited. At the beginning of the measurements it was necessary to wait for about one hour to get the equilibrium value of the redox potential. During the titration equilibrium was attained after 15–20 minutes. After the electrodes were in equilibrium, the potentials proved to be constant for several hours within ± 0.1 mV.

Table 2

Measurements with $c_3 = 0.569$ mC.

S: $c_3 = 0.569$ mC, $c_1 = 4.936$ mC, $H = 42.79$ mC, 75.08 ml.
T: $c_3 = 0.569$ mC, $c_1 = 4.936$ mC, $H = 1000$ mC, v ml.
$\delta = +0.2$ mV.

v ml	E mV	H mC	$-E_j$ mV	E' mV
0.00	1011.8	42.79	0.7	1040.5
1.00	1015.0	55.39	0.9	1043.8
2.00	1017.0	67.65	1.1	1046.1
3.00	1018.5	79.54	1.3	1047.7
4.00	1019.6	91.26	1.5	1049.0
5.00	1020.1	102.6	1.7	1049.7
6.00	1020.9	113.7	1.9	1050.7
8.00	1021.7	135.0	2.2	1051.8
10.00	1022.0	155.4	2.5	1052.5
12.00	1022.3	174.8	2.8	1053.1
15.00	1022.5	202.0	3.3	1053.7
18.00	1022.6	228.1	3.7	1054.2
21.00	1022.6	252.2	4.1	1054.7
25.00	1022.6	282.1	4.5	1055.0
29.00	1022.4	309.7	4.9	1055.3
33.00	1022.3	335.2	5.2	1055.4
37.00	1022.3	259.0	5.5	1055.7
41.00	1022.0	381.1	5.8	1055.7
50.00	1021.7	425.7	6.3	1055.9

Table 3

Measurements with $c_3 = 1.023$ mC.

S: $c_3 = 1.023$ mC, $c_1 = 5.041$ mC, $H = 85.6$ mC, 75.08 ml.
T: $c_3 = 1.023$ mC, $c_1 = 5.041$ mC, $H = 1000$ mC, v ml.
$\delta = -0.9$ mV.

v ml	E mV	H mC	$-E_j$ mV	E' mV
0.00	1027.1	85.64	1.4	1048.1
2.00	1028.7	109.4	1.7	1050.0
4.00	1029.6	131.9	2.1	1051.3
6.00	1030.1	153.3	2.5	1052.2
9.00	1030.6	183.5	3.0	1053.1
12.00	1030.7	211.6	3.4	1053.7
15.00	1030.8	237.8	3.9	1054.2
19.00	1030.8	270.2	4.4	1054.7
23.00	1030.7	300.0	4.8	1055.1
28.00	1030.6	333.9	5.2	1055.3
33.00	1030.4	364.6	5.6	1055.5
38.00	1030.2	392.7	5.9	1055.7
43.00	1030.1	418.3	6.2	1055.9
48.00	1030.0	441.8	6.5	1056.0
53.00	1029.8	464.3	6.8	1056.1
58.00	1029.6	484.4	7.0	1056.2
63.00	1029.5	503.1	7.2	1056.3
68.00	1029.4	520.5	7.4	1056.4
73.00	1029.3	536.7	7.6	1056.5

Table 4

Measurements with $c_3 = 2.596$ mC.

S: $c_3 = 2.596$ mC, $c_1 = 4.936$ mC, $H = 192.2$ mC, 75.08 ml.
T: $c_3 = 2.596$ mC, $c_1 = 4.936$ mC, $H = 1285$ mC, v ml.
$\delta = 0.0$ mV.

v ml	E mV	H mC	$-E_j$ mV	E' mV
0.00	1042.2	192.2	3.1	1053.6
2.00	1042.3	220.8	3.6	1054.1
4.00	1042.3	247.7	4.0	1054.5
5.00	1042.3	260.6	4.2	1054.7
6.00	1042.3	273.3	4.4	1054.9
8.00	1042.2	297.7	4.7	1055.2
10.00	1042.1	321.0	5.0	1055.3
13.00	1041.9	353.8	5.4	1055.6
16.00	1041.7	384.4	5.8	1055.7
20.00	1041.6	422.3	6.2	1056.0
24.00	1041.2	457.2	6.7	1056.2
28.00	1041.0	489.3	7.1	1056.3
32.00	1040.7	519.1	7.4	1056.4
36.00	1040.4	546.7	7.8	1056.4
40.00	1040.3	572.3	8.1	1056.6
44.00	1040.2	596.2	8.4	1056.8

All emf measurements were made with two Pt electrodes which seldom differed by more than 0.1 mV, except for the lowest Tl(III) concentration (0.1 mC) where greater differences were sometimes found, 0.3–0.4 mV.

All emf measurements were carried out at 25.0 ± 0.1° C.

Results and calculation of the hydrolysis constants

The emf measurements are given in Tables 1) –4). To compare measurements made at different times it was necessary to add a small correction to the measured emf:s indicated in the Tables by δ. The cause of these variations is discussed in Part IV (8).

To analyze the experimental results it is very convenient to study the quantity

$$E' = E_0' + 29.58 \log ([\mathrm{Tl}^{3+}]/[\mathrm{Tl}^{3+}]_{\mathrm{total}}) \tag{2}$$

as a function of h. The E' values are given in Tables 1) –4), the liquid junction potentials are taken from Part IV (8). E' as a function of h is plotted in Fig. 2. As is seen, *E' is independent of the total Tl(III) concentration* within the limits of experimental error. This is explained if *only mononuclear ions are formed*, since, assuming the reactions

$$\begin{aligned}
&\mathrm{Tl}^{3+} + \mathrm{H_2O} \rightleftarrows \mathrm{TlOH}^{2+} + \mathrm{H}^+ && \varkappa_1 = [\mathrm{TlOH}^{2+}]\, h\, [\mathrm{Tl}^{3+}]^{-1} = k_{a1} \\
&\mathrm{Tl}^{3+} + 2\,\mathrm{H_2O} \rightleftarrows \mathrm{Tl(OH)}_2^+ + 2\,\mathrm{H}^+ && \varkappa_2 = [\mathrm{Tl(OH)}_2^+]\, h^2\, [\mathrm{Tl}^{3+}]^{-1} = k_{a1}\, k_{a2} \\
&\mathrm{Tl}^{3+} + 3\mathrm{H_2O} \rightleftarrows \mathrm{Tl(OH)}_3 + 3\mathrm{H}^+ && \varkappa_3 = [\mathrm{Tl(OH)}_3]\, h^3\, [\mathrm{Tl}^{3+}]^{-1} = k_{a1}\, k_{a2}\, k_{a3}
\end{aligned} \tag{3}$$

the ratio

$$[\mathrm{Tl}^{3+}]_{\mathrm{total}} / [\mathrm{Tl}^{3+}] = 1 + \varkappa_1 h^{-1} + \varkappa_2 h^{-2} + \varkappa_3 h^{-3} = 1 + \varphi\,(h) \tag{3a}$$

is in this case a function of h only.

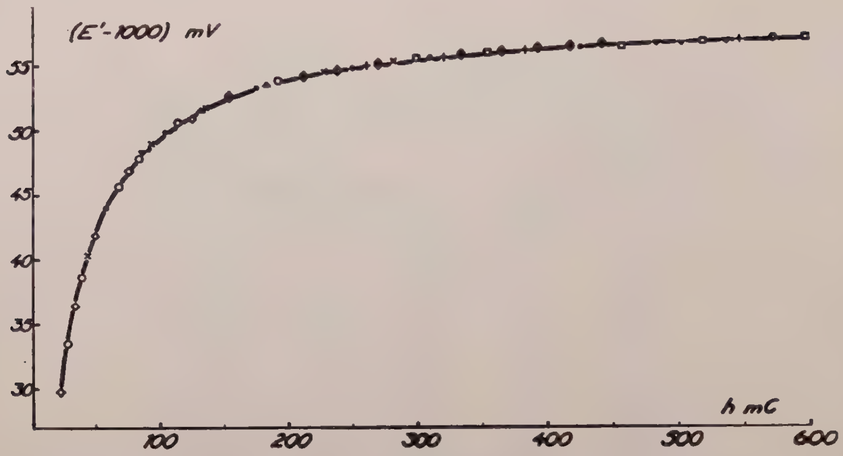

Fig. 2. E' as a function of h. Every third of all points is given. The curve has been calculated from equation (4) assuming $E'_0 = 1058.2$ mV, $\varkappa_1 = 73$ mC, $\varkappa_2 = 2375$ mC^2, $\varkappa_3 = 0$.

○ ◇	0.1038 mC	△ ▽	0.569 mC
× ●	1.023 mC	□ +	2.596 mC

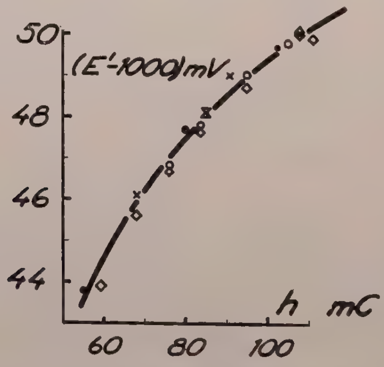

Fig. 2 a. E' as a function of h in the h range 50–110 mC. All experimental points are given.

Since the data indicated that polynuclear ions are not present to an appreciable extent in our solutions, the equilibrium constants were calculated in the following way.

If the hydrolysis constants of the Tl^{3+} ion had been sufficiently small so that the hydrolysis had been repressed practically entirely at the acid end of the h interval, then E'_0 might have been determined directly from the emf measurements since $E' \rightarrow E'_0$ as $[Tl^{3+}] \rightarrow [Tl^{3+}]_{total}$. An analogous prodecure was possible for Bi^{3+}. (12).

In the case of Tl(III) ions it was unfortunately not possible to attain sufficiently high h values for the hydrolysis to be neglected without causing incalculable variations in the activity coefficients. E'_0 must, therefore, be determined in an indirect way from calculations. Using equation (3 a), equation (2) can be written

$$E' = E'_0 - 29.58 \log (1 + \varkappa_1 h^{-1} + \varkappa_2 h^{-2} + \varkappa_3 h^{-3}) \qquad (4)$$

Introducing the quantity q from the equation

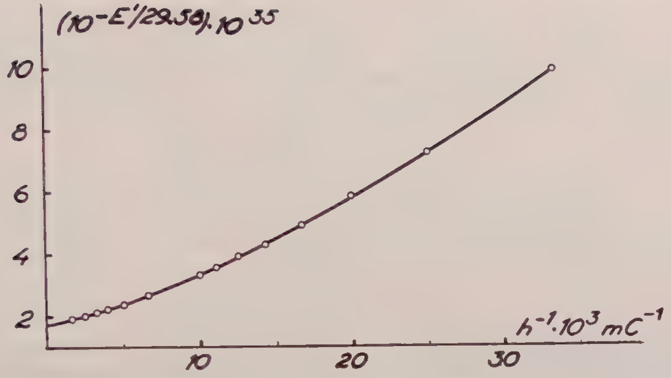

Fig. 3. $10^{-(E'/29.58)}$ as a function of h^{-1}. The smooth curve was drawn through the circles which were calculated from a smoothed $E'(h)$ curve.

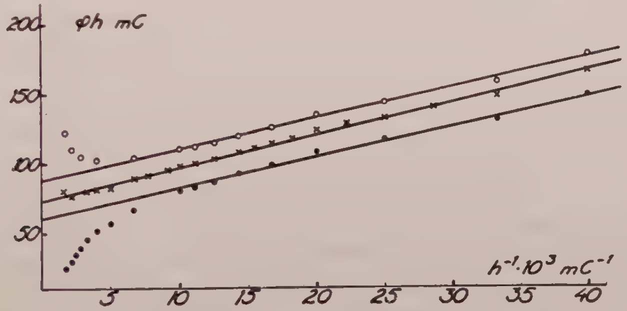

Fig. 4. $h\varphi$ as a function of h^{-1}. The middle curve represents the equation $h\varphi = 73 + 2375\ h^{-1}$ ○ $E_0' = 1059.0$ mV; × $E_0' = 1058.2$ mV; ● $E_0' = 1057.0$ mV.

$$E_0' = -29.58 \log q \tag{5}$$

equation (4) becomes

$$E' = -29.58 \log (q + q\varkappa_1 h^{-1} + q\varkappa_2 h^{-2} + q\varkappa_3 h^{-3}) \tag{6}$$

so $10^{-E'/29.58}$ converges to q as h^{-1} approaches zero. Plotting $10^{-E'/29.58}$ as a function of h^{-1} the extrapolation yields approximately $E_0' = 1058$ mV (Fig. 3). In order to calculate a more accurate value of E_0' and to estimate its uncertainty, a series of different values for E_0' were tried. For each of these E_0'-s

$$\left(\frac{[\mathrm{Tl}^{3+}]_{\mathrm{total}}}{[\mathrm{Tl}^{3+}]} - 1\right) h = h\varphi \tag{7}$$

was calculated from equation (2) and plotted as a function of h^{-1}. In this way a series of curves (Fig. 4) was obtained with E_0' as parameter. All these curves were found to be linear at high h^{-1}, but deviated from linearity at low h^{-1} values. For low E_0' values the deviations were negative, i.e. the calculated $h\varphi$ value fell below the extrapolated line. High E_0' on the other hand gave positive deviations. Between these two ranges an E_0' value could be found which yielded no systematic deviations from linearity over the whole hydrogen ion concentration interval studied, 20–600 mC (Fig. 4). This E_0' value was accepted as the correct one. The uncertainty can be estimated from the parameters of the two nearest curves which give appreciable positive or negative deviations. In this way one gets $E_0' = 1058.2 \pm 1.0$ mV. From equation (3) the intercept of $h\varphi$ gives $\varkappa_1$ and the slope of the line is equal to $\varkappa_2$. From Fig. 4 we get

$$\varkappa_1 = k_{a1} = 73 \pm 13 \text{ mC} = 0.073 \pm 0.013 \text{ C}$$
$$\varkappa_2 = 2375 \pm 100 \text{ mC}^2 = (2.375 \pm 0.1) \,.\, 10^{-3} \text{ C}^2$$
$$k_{a2} = 32.5 \pm 6 \text{ mC} = 0.0325 \pm 0.0060 \text{ C}$$
$$p\,k_{a1} = 1.14 \pm 0.08 \text{ (C scale)}$$
$$p\,k_{a2} = 1.49 \pm 0.09 \text{ (C scale)}$$

In Fig. 4 we see the agreement between the line $73 + 2375\,h^{-1}$ and the experimental values of $h\varphi$ assuming $E_0' = 1058.2$ mV. The quite small deviations of most of the experimental points from the calculated line shows that the inaccuracy of the hydrolysis constants is due chiefly to the uncertainty of E_0' and not to the experimental errors in the emf measurements. Furthermore, by studying Fig. 4 one can conclude that the error made by taking H equal to h is less than the inaccuracy of $h\varphi$, otherwise systematic deviations from the linearity would be found at low H. When h is calculated from the constants obtained and compared with H, the differences are at most 1 %, generally much less. It was, therefore, decided not to attempt a second approximation.

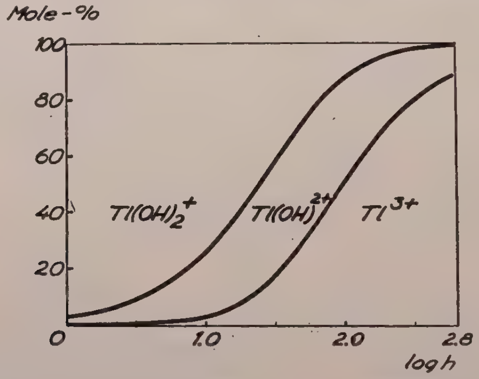

Fig. 5. Distribution of Tl(III) between different ions. The abscissa is log h. On the ordinate the distance 0–100 represents the total amount of Tl(III) present. If for a given value of h a vertical line is drawn at the corresponding log h, the segment of this line falling in a certain area, e.g. $Tl(OH)^{2+}$, represents the fraction of the total amount of Tl(III) present as that ion.

Fig. 5 shows the distribution of the different ions as a function of log h on the basis of the above calculations.

Since $h\varphi$ is a linear and not a second order function of h there is no appreciable amount of $Tl(OH)_3$ present in the solutions studied. Thus in solutions equilibrated with solid Tl_2O_3 practically all Tl(III) dissolved is present as either Tl^{3+}, $TlOH^{2+}$, or $Tl(OH)_2^+$.

On the standard potential $Tl^+, Tl^{3+} | Pt$

Several attempts have been made to determine accurately the $Tl^+ - Tl^{3+}$ standard potential at 25°C. NOYES and GARNER (13) measured the emf of cells

$$H_2|HClO_4\,(H)|HNO_3\,(H),\,TlNO_3(c_1),\,Tl(NO_3)_3\,(c_3)|Pt$$

H was varied between 0.5 and 2.0 weight formal. By employing a correction for the small liquid junction potential, the formal redox potential:

$$E^\circ + 29.58 \log\left(\frac{\gamma_{Tl^{3+}}}{\gamma_{Tl^+}}\right) = E_f^0 \tag{8 a}$$

could be calculated. They found that the formal redox potential is independent of H and the ratio c_1/c_3; the mean value was computed to be 1230.3 ± 0.7 mV.

SHERILL and HAAS (14) studied the cell

$$H_2|HClO_4\,(H)|HClO_4\,(H),\,TlClO_4\,(c_1),\,Tl(ClO_4)_3\,(c_3)|Pt$$

H ranged between 0.5 – 1.4 wf. The liquid junction potential was estimated by adding enough $TlClO_4$ to the hydrogen half cell to give a uniform concentration of this substance throughout the whole cell. The change of emf by this addition was taken as equal to the liquid junction potential. Sherill and Haas expressed the formal redox potential as a function of the ionic strength I. They found

$$E_f^0 = 1246.6 + 7.6\,I + 4.82\,I^2$$

They pointed out, however, that the value 1246.6 mV cannot be considered as the standard redox potential since the above equation is valid only for the relatively high ionic strengths studied.

Cells of the same type were investigated by STONEHILL (5). He studied the range of H 0.1–1.0 C. The liquid junction potential was calculated by decreasing $c_1 + c_3$ at constant H and extrapolating to $c_1 + c_3 = 0$. He attempted to determine the standard potential by the assumption that the activity factors of the Tl^+ and Tl^{3+} ions could be expressed by the equation

$$-\log\gamma = \frac{z^2\,0.5065\sqrt{H}}{1 + A\sqrt{H}} - BH + \log(1 + 0.036\,m) \tag{8}$$

where z is the charge of the ion, m the molality, and B a special constant for each ion. A was taken as equal to 1.31, which was found to be valid for $HClO_4$ between 0.1–1.0 C. Substituting equation (8) in equation (8 a) and rearranging one gets

$$E_f^0 + \frac{119.8\sqrt{H}}{1 + A\sqrt{H}} = E^0 + 29.58\,(B_{Tl^{3+}} - B_{Tl^+})\,H$$

Stonehill plotted $E_f^0 + \dfrac{119.8\sqrt{H}}{1 + A\sqrt{H}}$ as a function of H. Though the curve obtained was linear only for $H > 400$ mC he extrapolated the linear part to $H = 0$, and found $E^\circ = 1281.8$ mV. Adopting the same procedure with HNO_3 solutions he obtained $E^\circ = 1275.3$ mV.

Measurements made in sulfuric acid solutions are very difficult to evaluate since there is evidence of considerable complex formation in these solutions.

To determine the standard potential $Tl^+ - Tl^{3+}$ accurately, measurements must be made at low ionic strength in order to carry out the extrapolation to infinite dilution with certainty. But at low ionic strength two chief difficulties arise. Firstly, in cells of the type used by the previously mentioned investigators the liquid junction potential increases with decreasing ionic strength, since at low H the quantity $\frac{(c_1 + c_3)}{H}$ cannot be kept sufficiently small. Secondly, the ratio $[Tl^{3+}]/[Tl^{3+}]_{total}$ decreases with decreasing H. To determine the constants of hydrolysis of the Tl^{3+} ion it would be necessary to know the activity factors of the free Tl^{3+} ions, of the H^+ and of the products of hydrolysis for different ionic strengths.

Measurements carried out at such high H that the hydrolysis may be neglected cannot be of much value, since any measurement of this type yields only the formal redox potential. Any attempt to employ theoretically deduced formulae for the activity factors cannot be very successful, since it is extremely doubtful whether any of them are valid at the required ionic strength. GÜNTELBERG (15) has shown that none of the theoretical or semi-empirical formulae for the activity factors hold even at ionic strength 100 mC.

Most of these difficulties can be avoided, however, if we accept a new standard state of the activity factors instead of the conventional one. (The conventional scale of activity factors is defined so that $f \to 1$ as $c \to 0$.)

When solutions containing high and constant amounts of ClO_4^- ions are employed, cells can be easily designed with negligible liquid junction potential. In these solutions when the concentrations of the reacting substances are kept low the activity factors of all cations present in the solution are approximately constant (8.)

Let us consider the following cell

$$H_2 | h \text{ mC } H^+, (3000\text{-}h) \text{ mC } Na^+, 3 \text{ C } ClO_4^- |$$

$$h \text{ mC } H^+, c_1 \text{ mC } Tl^+, c_3 \text{ mC } Tl^{3+}, (3000 - 3c_3 - c_1 - h) \text{ mC } Na^+, 3\text{C } ClO_4^- | Pt \qquad (A)$$

where $h < 600$ mC and $c_1 + c_3$ is kept low. If we define the activity factors of the ions as unity at infinitely small concentration in 3 C $NaClO_4$ solutions and if we ascribe to the half-cell potential

$$(Pt)\ H_2 | h \text{ mC } H^+, (3000 - h) \text{ mC } Na^+, 3 \text{ C } ClO_4^-$$

the value zero when the activity of the H^+ ions is unity and the partial pressure of hydrogen gas is one atmosphere, the emf of cell A can be written

$$E_A = E^{\circ\prime} + 29.58 \log ([Tl^{3+}]/[Tl^+]\, h^2) + 29.58 \log p_{H_2}$$

where $E^{\circ\prime}$ is the standard potential referred to the above scale of activity coefficients and p_{H_2} the partial pressure of hydrogen over 3 C $NaClO_4$ solution in atmospheres. Since the hydrolysis constants of the Tl^{3+} ion are known, $E^{\circ\prime}$ can be calculated from measurements of E_A.

Actually, cell A was not directly measured but the emf was computed by combining measurements on the cells B and C.

$$CE | h \text{ mC } H^+, c_1 \text{ mC } Tl^+\ c_3 \text{ mC } Tl^{3+}, (3000 - 3c_3 - c_1 - h) \text{ mC } Na^+, 3000 \text{ mC } ClO_4^- | Pt \qquad (B)$$

$$H_2 | h \text{ mC } H^+, (3000 - h) \text{ mC } Na^+, 3000 \text{ mC } ClO_4^- | CE \qquad (C)$$

$$CE = Hg, Hg_2Cl_2 | 4 \text{ C } NaCl | 3 \text{ C } NaClO_4 |$$

$$E_A = E_B + E_C$$

Consequently

$$E^{\circ\prime} = E_B + E_C + 59.16 \log h - 29.58 \log ([Tl^{3+}]/[Tl^+]) - 29.58 \log p_{H_2} \qquad (9)$$

Emf measurements on cell B are given in Tables 1)—4), those on cell C in (8). In

Table 5

Determination of $E^{\circ\prime}$

Tl(III) total mC	h mC	$-29.58 \log \frac{[Tl^{3+}]}{[Tl^{+}]}$ mV	E_B mV	$E_C + 59.16 \log h$ mV	$E^{\circ\prime}$ * mV
0.1038	22.46	77.8	979.9	222.6	1280.7
	49.62	65.5	991.4	223.0	1280.3
	76.34	60.7	995.9	223.4	1280.4
	94.91	58.7	997.7	223.7	1280.5
	113.8	57.4	998.9	224.0	1280.7
	136.9	56.1	999.6	224.4	1280.4
0.569	42.79	45.6	1011.9	222.9	1280.8
	67.65	40.0	1017.2	223.3	1280.9
	135.1	34.4	1021.9	224.4	1280.9
	228.1	31.7	1022.9	225.9	1280.8
	335.2	30.5	1022.7	227.6	1281.1
	425.7	29.9	1022.0	228.8	1281.0
1.023	85.64	30.5	1026.2	223.6	1280.7
	183.5	25.4	1029.8	225.1	1280.7
	300.0	23.6	1030.0	227.0	1281.0
	418.3	22.7	1029.4	228.7	1281.2
	536.7	22.2	1028.4	230.1	1281.0
2.596	192.2	13.0	1042.3	225.3	1281.0
	297.7	11.4	1042.4	227.0	1281.0
	384.4	10.7	1041.7	228.3	1281.0
	489.3	10.1	1041.0	229.5	1281.0
	596.2	9.8	1040.2	230.7	1281.1

Table 5) a number of $E^{\circ\prime}$ values are calculated for each $[Tl^{3+}]_{total}$ measured throughout the whole h interval studied. As is seen $E^{\circ\prime}$ is independent of $[Tl^{3+}]_{total}$ and h within the limits of experimental error ± 0.4 mV.

It must be pointed out immediately that the mean value computed in Table 5), 1280.8 mV, contains a much greater error than ± 0.4 mV since measurements of the emf of cells B and C vary by up to ± 2.0 mV, for reasons explained in (8). To compare measurements made at different times it was necessary to add a small correction to the emf:s and these corrected emf values have been used to calculate $E^{\circ\prime}$ in Table 5). This source of error can be completely eliminated by measuring the emf of cell A directly. Thus we can estimate

$$E^{\circ\prime} = 1280 \pm 2 \text{ mV}$$

The uncertainty of $\varkappa_1$ and $\varkappa_2$ has only small effect on $E^{\circ\prime}$. The error in $E^{\circ\prime}$ due to the inaccuracy of the hydrolysis constants, which decreases with increasing h, can be estimated to be $\pm 0.3 - 0.4$ mV.

---

* P_{H_2} was calculated in the following way. The density of 3.000 C $NaClO_4$ at 25.0° C was determined to be 1.2257 ± 0.0002; thus a 3 C $NaClO_4$ solution contains 3.495 mol $NaClO_4$/1000 g water. By interpolation from the measurements of JONES (16) it was found that a 3.495 molal $NaClO_4$ solution is isopiestic with a 3.22 molal NaCl solution. The vapor pressure of the latter, by interpolating the measurement of PEARCE and NELSON (17) was calculated to be 21.0 mm at 25.0 C. Thus at 760 mm barometric pressure $29.58 \log (p_{H_2}/760)$ is equal to -0.36 mV. It was assumed that the vapor pressure of the mixed solutions of $NaClO_4$ and $HClO_4$ is the same as that of 3 C $NaClO_4$.

In calculating $E^{\circ\prime}$ the experimentally unverifiable hypothesis was employed that no complexes are formed with ClO_4^- ions. This assumption seems to be very reasonable. I was not able to find reports of experiments proving appreciable complex formation between metal ions and ClO_4^-. The dissociation constant of $HClO_4$ is certainly very high.

E°, the standard potential referred to the conventional scale of activity coefficient, and $E^{\circ\prime}$ are connected by the equation

$$E^{\circ\prime} - E^\circ = 29.58 \log \left(f_{\mathrm{Tl}^{3+}} / f_{\mathrm{Tl}^+} f^2_{\mathrm{H}^+} \right) \tag{10}$$

where $f_{\mathrm{Tl}^{3+}}$, f_{Tl^-}, f_{H^+} are the activity coefficients referred to infinite dilution. It is difficult to estimate the value of this difference. The term containing the activity factors cannot be measured and no general rule is available which would predict the value of the activity factors in highly concentrated solutions.

Several other standard potentials, e.g. $Sn^{2+} - Sn^{4+}$, $Ti^{3+} - Ti^{4+}$, $Ce^{3+} - Ce^{4+}$, etc., which cannot be ascertained accurately by using the conventional scale of activity factors, might be determined with the standard state defined here.

SUMMARY

The hydrolysis equilibria of the Tl^{3+} ion have been studied by investigating solutions of the composition

$$c_3 \text{ mC } \mathrm{Tl}^{3+},\ c_1 \text{ mC } \mathrm{Tl}^+,\ H \text{ mC } \mathrm{H}^+,\ (3000 - 3c_3 - c_1 - H) \text{ mC } \mathrm{Na}^+,\ 3 \text{ C } \mathrm{ClO}_4^-$$

The concentration of the free Tl(III) ions was determined by emf measurements. c_3 was varied between 0.1 and 2.6 mC, H ranged from 20 to 600 mC.

The results can be explained by assuming the equilibria

$$\mathrm{Tl}^{3+} + \mathrm{H_2O} \rightleftarrows \mathrm{TlOH}^{2+} + \mathrm{H}^+,$$
$$\mathrm{TlOH}^{2+} + \mathrm{H_2O} \rightleftarrows \mathrm{Tl(OH)}_2^+ + \mathrm{H}^+.$$

At 25° C the negative logarithms of the acidity constants of the acid Tl^{3+} were found to be

$$pk_{a_1} = 1.14 \pm 0.08,\ pk_{a_2} = 1.49 \pm 0.09$$

In solutions of $[ClO_4^-] = 3$ C the standard redox potential $Tl^+, Tl^{3+} | Pt$ was computed to be 1280 ± 2 mV, independent of c_2, c_3, and H. The activity factors of Tl^+ and Tl^{3+} have been defined as unity for small concentrations of these ions in 3 C $NaClO_4^-$.

$Tl(ClO_4)_3$ solutions were prepared by electrolytic oxidation. Conditions for attaining high current yield and for avoiding the contamination of the solution during the preparation were determined.

Department of Inorganic Chemistry, Royal Institute of Technology, Stockholm.
Institute of Inorganic and Physical Chemistry, University of Stockholm.

Acknowledgements

I wish to thank Professor LARS GUNNAR SILLÉN for having suggested this work, for the very great interest he has shown in it, and for the many valuable discussions I have had with him.

My thanks are due to Professor ARNE ÖLANDER for his kind interest.

I also wish to thank Mr ERIK EKEDAHL and Miss SIRKKA HIETANEN for valuable discussions. Professor RALPH G. PEARSON was kind enough to read the manuscript and I wish to thank for his valuable suggestions.

This work has been supported by a grant from Statens Naturvetenskapliga Forskningsråd.

REFERENCES

1. According to R. J. MEYER, Z. anorg. Chem. *24*, 321, 1900, Werther, J. pr. Ch. *91*, 385, 1864.
2. R. ABEGG, J. F. SPENCER, Z. anorg. Chem. *44*, 379, 1905.
3. G. F. HÜTTIG, R. MYTYZEK, Z. anorg. Chem. *192*, 187, 1930.
4. W. O. MILLIGAN, H. B. WEISER, JACS *59*, 1670, 1937.
5. H. I. STONEHILL, Trans. Far. Soc. *39*, 72, 1934.
6. R. DE FORCRAND, C.r. *176*, 873, 1923.
7. M. HLASKO, A. SALITOWNA, Roczniki Chem. *15*, 273, 1935.
8. G. BIEDERMANN, L. G. SILLÉN, Arkiv Kemi *5*, 24 (Part IV).
9. S. HIETANEN, private communication.
10. E. H. SWIFT, C. S. GARNER, JACS *58*, 113, 1936.
11. G. GRUBE, A. HERMANN, Z. Elektrochem. *26*, 291, 1920.
12. F. GRANÉR, L. G. SILLÉN, Acta Chem. Scand. *1*, 631, 1947 (Part I).
13. A. A. NOYES, C. S. GARNER, JACS *58*, 1268, 1936.
14. M. S. SHERILL, A. J. HAAS JR., JACS *58*, 952, 1936.
15. E. GÜNTELBERG, Diss. Copenhagen 1938.
16. I. H. JONES, J. phys. coll. Chem. *51*, 516, 1947.
17. J. N. PEARCE, A. F. NELSON, JACS *54*, 3544, 1932.

Tryckt den 7 april 1953

Uppsala 1953. Almqvist & Wiksells Boktryckeri AB

ARKIV FÖR KEMI Band 5 nr 42

Communicated 4 June 1952 by ARNE WESTGREN and GUNNAR HÄGG

Studies on the hydrolysis of metal ions. VI

The hydrolysis of the iron(II) ion, Fe^{2+}

By BENGT O. A. HEDSTRÖM

With 5 figures in the text

The literature on the hydrolysis of the iron(II) ion is rather meager. The most recent investigation reported seems to be that of LINDSTRAND (7), who has also reviewed the literature. The method employed by LINDSTRAND and his predecessors consisted of measuring the pH in solutions of pure iron(II) salts, e.g. $Fe(ClO_4)_2$. However, during the crystallization of simple iron(II) salts, unknown amounts of acid are always introduced, and these may be large compared with the amount of hydrogen ion arising from the hydrolysis of Fe^{2+}. It therefore seemed desirable to undertake a new careful study. Moreover, a quantitative knowledge of the hydrolysis of Fe^{2+} is necessary in connexion with investigations on the hydrolysis of Fe^{3+} by means of redox potentials, and might also be of some interest in the study of the corrosion of iron. The weakness of the method mentioned above was largely overcome by employing a rather different emf-titration technique.

Method of measurement

The emf measurements were made at 25.0° C. The total iron(II) concentration in each series of experiment was kept at a constant value. All cell solutions were made so as to contain exactly 1 C (mole/liter) ClO_4^-, using $NaClO_4$ as an inert electrolyte. It is believed that in this ionic medium any complex formation involving ClO_4^- can be neglected. Furthermore, activity coefficients are assumed to be constant, as long as the hydrogen ion and iron(II) concentrations are low in comparison with the concentration of perchlorate ions.

In the equilibrium solutions it would be desirable to measure both the hydrogen ion and the (free) Fe^{2+} concentration. However, several attempts to measure the latter with electrolytically prepared iron electrodes were unsuccessful (see "Measurements" for details) and the final calculations are based only on measurements of the hydrogen ion concentration, using a glass electrode.

A calomel electrode of the following composition served as the reference electrode:

$$\mathrm{CE}\,| = \mathrm{Hg},\ \mathrm{Hg_2Cl_2}\,|\,4\ \mathrm{C\ NaCl}\,|\,1\ \mathrm{C\ NaClO_4}\,|$$

The cells used were all of the same general type:

$$- \text{CE} \,|\, \text{H}^+ \,|\, \text{glass electrode} +$$

For such cells we have

$$E_g = E_{g0} + 59.16 \log h + E_j = E' + 59.16 \log h,$$

where E_g is the potential (in mV) actually measured, E_{g0} a constant, E_j the liquid junction potential between the solution under investigation and 1 C $NaClO_4$, and h (mC)[1] the hydrogen ion concentration. Because of the high mobility of hydrogen ions, E_j (or E') is practically a function only of the hydrogen ion concentration. This point has been the subject of a detailed investigation by BIEDERMANN and SILLÉN (*1*).

Since E_{g0} can be expected to change slightly from one day to another because of small uncontrollable fluctuations of the potential of the calomel and the glass electrodes, E' was determined as a function of known values of h from an acid-base titration prior to each series of measurements on the iron solutions.

The solutions studied were made by the following titration method. To 50.00 ml 5.00 mC $HClO_4$($[ClO_4^-] = 1000$ mC) exactly 25.00 ml 10.00 mC NaOH ($[ClO_4^-] = 1000$ mC) was added in portions from a burette. Then 75.00 ml of the acid iron(II) solution was added and measurements on this solution were started. The hydrogen ion concentration was lowered stepwise by adding base from a burette. From another burette an equal volume of the acid iron(II) solution was added. In this way, the total iron(II) concentration was kept constant.

From the acid-base titration E' was calculated and plotted against h. The extrapolation of E' to $h = 0$ gives E_{g0}. In the calculation of h from the glass electrode potentials in the iron(II) solutions, no correction in E for the liquid junction potential was needed, since the hydrolysis took place at very low hydrogen ion concentrations, i.e., in the pH range 5 to 7.

Apparatus

The electrode and titration apparatus was essentially the same as that used by FORSLING, HIETANEN, and SILLÉN (*2*).

Measurements were made in an oil-bath thermostat at 25.0° C. A rather rapid stream of nitrogen gas was passed through the titration solutions in order to facilitate mixing and to avoid any oxidation by air. The nitrogen gas, taken from a cylinder, was freed from oxygen and carbon dioxide by passage through a MEYER-RONGE oven (*8*) and an "Ascarite" column. In order to prevent any evaporation from the titration flask the gas was finally bubbled through a wash-bottle containing 1 C $NaClO_4$, before entering the cell.

A Radiometer glass electrode was used.

Potentials were measured with a valve potentiometer (type Radiometer PHM 3), having a sensitivity of about 0.1 mV.

Chemicals and analysis

The iron(II) perchlorate stock solution was prepared by LINDSTRAND's method, i.e., from FeS (A.R.) and $HClO_4$ (A.R.). Perchloric acid was used in excess and the solution was freed from H_2S by passing CO_2 and finally N_2 through the solution. When reaction had ceased, the solution was filtered and tested for SO_4^{2-} with $BaCl_2$ and for Cl^- (after oxidation of Fe^{2+} with H_2O_2) with $AgNO_3$. No SO_4^{2-} or Cl^- could be detected.

---

[1] mC = millimoles per liter, thus 1000 mC = 1 C.

The ClO_4^- concentration of the stock solution was determined by passing a sample through a hydrogen ion saturated ion exchanger and titrating the perchloric acid set free with NaOH, using methyl red as indicator. In the determination of Fe^{2+}, permanganate solution was used. The hydrogen ion concentration was determined by difference, $[H^+] = [ClO_4^-] - 2[Fe^{2+}]$.

The iron solutions used in the experiments were made so as to contain exactly 1000 mC ClO_4^-. Sodium perchlorate, taken from a very pure stock solution, was used as an inert electrolyte. Its preparation has been described elsewhere (*1*); it was analysed by the ion exchange method described above.

The iron solutions thus prepared slowly oxidized and it was found necessary to remove any traces of Fe^{3+} immediately prior to every experiment by adding a little iron powder (A.R.). When the reduction was completed, as indicated by a negative thiocyanate test, the solution was filtered into *ca.* 10 ml. of 5 mC $HClO_4$ (1000 mC ClO_4^-). During the reduction the Fe^{2+} and H^+ concentrations had, of course, changed. The solution was therefore again analyzed for Fe^{2+} by direct titration with $KMnO_4$. The hydrogen ion concentration was calculated by GRAN's method (*3*) from the glass electrode potentials obtained during the actual measurements. Roughly speaking, GRAN's method utilizes the fact that if dv/dE (v = volume) is plotted against v, two straight lines are obtained, which intersect at the equivalence point. Furthermore, the point of intersection lies on the v axis. In this investigation this point, corresponding to the free acid present, was reached before any iron precipitated.

The NaOH solution was prepared in the usual way from 50 % sodium hydroxide solution, stored in a polyethylene bottle. It was standardized against perchloric acid (to the methyl red and the phenolphthalein end points), which in turn had been standardized against KIO_3 according to OESPER (*9*). The $KMnO_4$ solution was standardized against As_2O_3 according to KOLTHOFF and SANDELL (*4*). The solutions were crosschecked by titrating an oxalic acid solution with both $KMnO_4$ and NaOH (to the phenolphthalein end point). The difference was less than 0.1 %. The carbonate ion concentration in the NaOH solutions used was about 0.1 % of the NaOH concentration, as estimated from the difference between the methyl red and the phenolphthalein end points.

The solutions used in the emf titrations were deaerated with nitrogen gas prior to each experiment.

Measurements

No really steady or reproducible iron electrode potentials were attained. At low pH especially, the iron electrodes were easily polarized and seemed to function very much like a hydrogen electrode, i.e., the potential ran almost parallel to that of the glass electrode. From the accepted value of the standard potential of the Fe^{2+}/Fe couple, -440 mV at 25° C (*6*) one can calculate that the hydrogen pressure over iron will not fall below 1 atm when $pH < 8.4$. This might be one reason for the behaviour of the iron electrodes.

In order to determine if the glass electrode followed Nernst's formula, it was tested against a quinhydrone electrode in the following way. 10 mC $HClO_4$ (1000 mC ClO_4^-) was titrated with 100 mC HPO_4^{2-} (1000 mC ClO_4^-). In this way the pH range 2 to *ca.* 7 was covered. The difference between the two electrodes in these solutions was practically constant and showed no trend. Only two out of fifty-two values differed by as much as 1 mV from the average difference. The "slope" of the glass electrode used can therefore be put equal to the theoretical value, i.e., 59.16 mV.

From the acid-base titrations it was concluded that in the weakly acid solutions used, the liquid junction potential could be neglected. Then E_{g0} could be set equal to the average value of E'. (The E' values corresponding to the unbuffered solutions near the equivalence point were not used in this calculation, since in this range E' cannot be known with any accuracy). As can be seen from the following tables, the different acid-base titrations gave almost identical glass electrode potentials (except in the vicinity of the equivalence point). The potentiometrically determined equivalence point, using GRAN's method, agreed with that determined from analysis.

Measurements were made at three different total iron(II) concentrations (c mC). The hydrogen ion concentrations of the iron(II) solutions used were determined from plots of $\Delta v_B/\Delta E$ *vs.* $v_{B,\,av.}$ (v_B being the volume of base added, and $v_{B,\,av.} = v_B + \frac{1}{2}\Delta v_B$). In the tables, H denotes the analytically calculated hydrogen ion concentration, assuming all Fe^{2+} to be unhydrolyzed, h that actually found with the glass electrode. The titrations were continued until the glass electrode did not attain constant potentials, indicating that iron(II) hydroxide was precipitated. No iron electrodes were present in the cells reported in the tables. In the iron(II) solutions steady glass electrode potentials were reached within twenty minutes, on the average, after the additions from the burettes. In the acid-base titrations steady potentials were obtained almost instantaneously.

Discussion

As can be seen from the tables, the quantity $Z = (h - H)/c$ is very small even close to the precipitation point. In Figure 1, the experimentally determined Z values have been plotted against $-\log 1000\, h$ ($\approx$ pH). If we assume that the hydrolysis takes place by the reaction

$$Fe^{2+} + H_2O \rightleftarrows FeOH^+ + H^+$$

only, we get the following expression for Z as a function of h and the equilibrium constant $1000\, k_a = h\, [FeOH^+]/[Fe^{2+}]$ (k_a in moles/liter).

$$Z = \frac{1}{h/1000k_a + 1}$$

This quantity has been calculated for different values of k_a and h, and the corresponding theoretical Z curves have been plotted in Figure 1. It can be easily shown that for any mechanism involving only mononuclear complexes, Z is a function of h only. On the other hand, if we assume polynuclear complexes to be present, then Z is also a function of c. The experimentally determined Z vs. — log 1000 h curves do not differ significantly from each other, and we can therefore conclude that, within the experimental error, *we are dealing with a mononuclear reaction.* Furthermore, the experimental points seem to fall fairly close to the Z curve corresponding to $pk_a = 9.5$, indicating that only the first step in the complete hydrolysis process is needed to explain the experimental results. Since the hydrolysis is very small, the uncertainty in the k_a value determined is rather large. To judge from the deviations, the true value should, however, lie within the limits

$$pk_a = 9.5 \pm 0.2$$

Examination of tables 1 b, 2 b, and 3 b shows that in the first part of the titra-

Table 1. $c = 8.16$ mC

Solution B : 10.00 mC OH^-, 1010 mC Na^+, 1000 mC ClO_4^-
» S : 5.00 mC H^+, 995 mC Na^+, 1000 mC ClO_4^-
» F_1: 16.32 mC Fe^{2+}, 0,10 mC H^+, 967.3 mC Na^+, 1000 mC ClO_4^-

a) Titration of 50.00 ml S with 25.00 ml B.

v_B ml	E_g mV	H mC	E' mV
0.00	− 33.2	5.000	− 74.6
3.00	− 37.9	4.151	− 74.5
6.00	− 43.1	3.393	− 74,5
8.00	− 47.0	2.931	− 74.6
10.00	− 51.1	2.500	− 74.0
12.00	− 55.8	2.097	− 74.8
14.00	− 61.0	1.719	− 74.9
16.00	− 66.9	1.364	− 74.9
18.00	− 74.5	1.029	− 75.2
20.00	− 84.1	0.7143	− 75.5
22.00	− 98.8	0.4167	− 76.9
23.00	− 110.6	0.2740	− 77.3
24.00	− 130.8	0.1351	− 79.4
24.50	− 153.8	0.0671	− 84.4
24.80	− 189.6	0.0267	− 96.5
25.00	− 350	0	—

$E_{g0} = -74.5$ mV

(*Table 1, cont.*)

b) 75.00 ml of solution F_1 was added. During the titration equal volumes of B and F_1 were added.

v_B	E_g	v_B	$(\Delta v_B/\Delta E)\cdot 10^4$	$H \cdot 10^4$	$h \cdot 10^4$	$Z . 10^4$	$-\log 1000\, h$
25.00	− 162.2			500	324		
		25.25	167				
25.50	− 192.6			169	101		
		25.60	83				
25.70	− 216.7			37.6	39.5	0.23	5.40
		25.80	35				
25.90	− 273.9			− 92.9	4.26	11.9	6.37
		26.00	67				
26.10	− 303.7			− 157	1.34	19.4	6.87
		26.20	184				
26.30	− 314.6			− 354	0.875	43.5	7.06
		26.40	303				
26.50	− 321.2			− 477	0.676	58.6	7.17
		26.60	510				
26.70	− 325.1			− 606		74.3	7.24

Equivalence point of free acid: 25.75 ml.

tions, where h is relatively high, and therefore any hydrolysis of Fe^{2+} may be neglected, H is, contrary to expectation, *greater* than h. In table 2 b, for instance, the difference $H - h$ equals about 0.08 mC, taking the average difference of the first three pairs

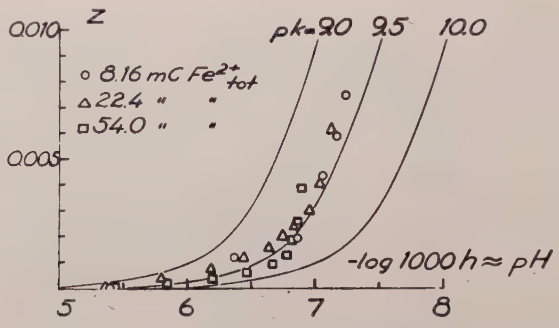

Fig. 1. *Z vs.* -log 1000 *h* for different, total iron(II) concentrations. The curves have been calculated, assuming different p*k*a values.

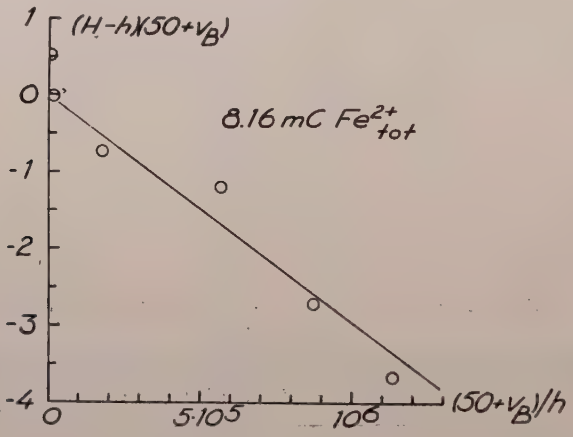

Fig. 2. $(H - h)$ $(50 + v_B)$ *vs.* $(50 + v_B)/h$ for $[Fe^{2+}]_{tot}$ = 8.16 mC.

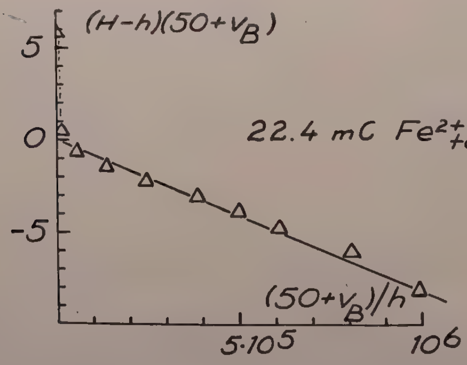

Fig. 3. $(H - h)$ $(50 + v_B)$ *vs.* $(50 + v_B)/h$ for $[Fe^{2+}]_{tot}$ = 22.4 mC.

Table 2. $c = 22.4$ mC

a) Titration of 50.00 ml S with 25.00 ml B.

v_B ml	E_g mV	H mC	E' mV
0.00	− 33.2	5.000	−74.6
3.00	− 37.9	4.151	−74.5
6.00	− 43.1	3.393	−74.5
8.00	− 47.0	2.931	−74.6
10.00	− 51.1	2.500	−74.0
12.00	− 55.8	2.097	−74.8
14.00	− 61.0	1.719	−74.9
16.00	− 66.9	1.364	−74.9
18.00	− 74.5	1.029	−75.2
20.00	− 84.1	0.7143	−75.5
22.00	− 99.0	0.4167	−77.1
23.00	−111.1	0.2740	−77.8
24.00	−132.4	0.1351	−81.0
24.50	−157.4	0.0671	−88.0
24.80	−218	0.0267	−125
25.00	−410	0	−

$E_{go} = -74.5$ mV

(*Table 2, cont.*)

b) 75 ml of solution F_2 (44,8 mC Fe^{2+}, 1,485 mC H^+, 908,9 mC Na^+, 1000 mC ClO_4^-) was added. During the titration equal volumes of B and F_2 were added.

v_B	E_g	$v_{B\,av}$	$(\Delta v_B/\Delta E) \cdot 10^4$	$H \cdot 10^4$	$h \cdot 10^4$	$(H-h) \cdot 10^4$	$Z \cdot 10^4$	$-\log 1000h$	$\frac{H-h}{h}$
23.00	− 85.0	25.50	3571	7425	6641	784			0.1181
26.00	− 87.8	26.50	3448	6767	5960	807			0.1354
27.00	− 90.7	27.50	3571	6123	5324	799			0.1501
28.00	− 93.5	28.50	2857	5500	4829	671			0.1390
29.00	− 97.0	29.50	2778	4892	4166	726			0.1743
30.00	−100.6	30.50	2500	4300	3621	679			0.1875
31.00	−104.6	31.50	2128	3722	3099	623			0.2010
32.00	−109.3	32.50	1724	3159	2581	578			0.2239
33.00	−115.1	33.50	1538	2608	2059	549			0.2666
34.00	−121.6	34.50	1266	2065	1599	466			0.2914
35.00	−129.5	35.50	878	1541	1176	365			0.3104
36.00	−140.9	36.25	618	1029	754	275			0.365
36.50	−149.0	36.65	476	780	550	230			0.418
36.80	−155.3	36.90	417	628	431	197			0.457
37.00	−160.2	37.10	308	523	356	167			0.469
37.20	−166.7	37.30	274	430	276	154			0.558
37.40	−174.0	37.50	211	332	208	124			0.596
37.60	−183.5	37.70	145	234	144	90			0.625
37.80	−197.3	37.90	120	137	84	53			
38.00	−214.0	38.10	77	40	44	−4	0.164	5.36	
38.20	−240.0	38.30	85	− 57	15.9	−72.9	3.24	5.80	
38.40	−263.5	38.50	137	−153	6.39	−159.4	7.08	6.19	
38.60	−278.1	38.70	171	−248	3.62	−251.6	11.2	6.44	
38.80	−289.8	38.90	307	−343	2.30	−345	15.4	6.64	

Table 2, cont.

v_B	E_g	$v_{B, av}$	$(\Delta v_B/\Delta E) \cdot 10^4$	$H \cdot 10^4$	$h \cdot 10^4$	$(H-h) \cdot 10^4$	$Z \cdot 10^4$	$\log 1000\,h$
39.00	−296.3	39.10	392	−438	1.78	− 440	19.6	6.75
39.20	−301.4	39.35	423	−533	1.46	−534	23.8	6.84
39.50	−308.5	39.75	980	−676	1.11	− 677	30.2	6.96
40.00	−313.6	40.50	1820	−906	0.909	− 907	40.4	7.04
41.00	−318.1			−1368	0.763	−1369	61.0	7.12

Equivalence point of free acid: 38.08 ml.

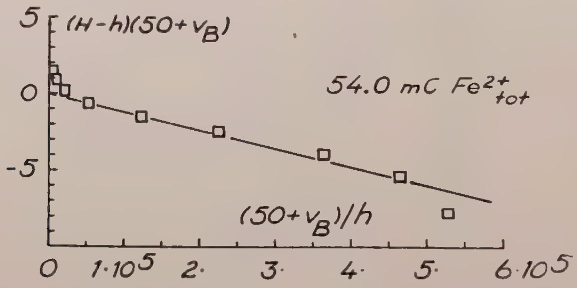

Fig. 4. $(H-h)$ $(50+v_B)$ *vs.* $(50+v_B)/h$ for $[Fe^{2+}]_{tot}$ = 54.0 mC.

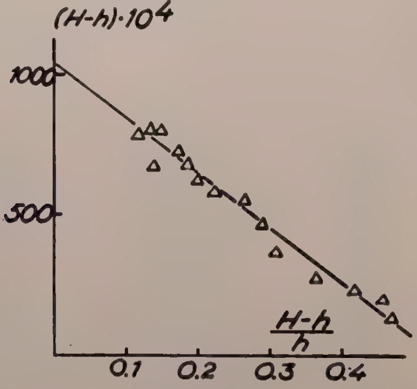

Fig. 5. $(H-h) \cdot 10^4$ *vs.* $(H-h)/h$. The points refer to the data given in Table 2 b.

of values. When h is lowered during the titration, the difference becomes smaller, until at pH values around 7 it changes sign because of the onset of the hydrolysis of the Fe^{2+} ion.

There may be several causes of this disagreement between the H and h values in the earlier parts of the titrations, where the buffer capacity of the solutions is very low. For instance, the H values may be slightly in error. Another cause may be the presence of small amounts, about 0.1 mC, of basic impurities, giving rise to low h values in the more acid solutions.

Table 3. $c = 54.0$ mC

a) Titration of 50.00 ml S with 25.00 ml B.

v_B ml	E_g mV	H mC	E' mV
0.00	−33.2	5.000	−74.6
3.00	−37.9	4.151	−74.5
6.00	−43.1	3.393	−74.5
8.00	−48.0	2.931	−74.6
10.00	−51.1	2.500	−74.0
12.00	−55.8	2.097	−74.8
14.00	−60.7	1.719	−74.6
16.00	−66.9	1.364	−74.9
18.00	−74.0	1.029	−74.7
25.00	—	0	—

$E_{go} = -74.5$ mV

Let us first consider the hypothesis that only the H values are in error, thus neglecting the presence of any disturbing impurities. Assuming that the only product of hydrolysis is $FeOH^+$ there is obtained:

$$h = H' + [\mathrm{FeOH}^+] = H' + k_a \cdot 1000 \cdot [\mathrm{Fe}^{2+}]/h = H' + k'/h,$$

where H' is the correct, stochiometrical concentration of hydrogen ions, and $k' = 1000\, k_a\, [\mathrm{Fe}^{2+}]$, a constant. On introducing the error δ, defined by

$$H'(50 + v_B) + \delta = H(50 + v_B),$$

$(50 + v_B)$ being the volume of iron solution added, there is obtained:

$$(H - h)(50 + v_B) = \delta - k'(50 + v_B)/h.$$

If, therefore, $(H - h)(50 + v_B)$ is plotted against $(50 + v_B)/h$ for any one titration, a straight line should result, the intercept and slope of which should make possible an estimate of δ and k_a. Plots of this type are shown in Figures 2, 3, and 4. Neglecting the upwards bending "tails" (corresponding to the first parts of the titrations) close to the vertical axis, the data may be well represented by straight lines. Since these lines in all three figures pass through the origin, and hence $\delta = 0$, we may infer that H is a fairly good estimate of H'. From the slopes of the lines the following pk_a values may be calculated:

c	$k_a \cdot 10^{10}$	pk_a
8.16	3.6	9.4
22.4	3.6	9.4
54.0	2.2	9.7
	average:	9.5 ± 0.2

in good agreement with the value obtained from the Z vs. $-\log 1000\, h$ plot, Figure 1.

As will now be shown, the deviations from the straight lines, i.e., the "tails" referred to above, may be explained by assuming the presence of small amounts of basic impurities.

Let us assume that the disturbing impurities may be represented by the stochio-

Table 3, cont.

b) 75 ml of solution F_3 (108,0 mC Fe^{2+}, 0.234 mC H^+, 783.8 mC Na^+, 1000 mC ClO_4^-) was added. During the titration equal volumes of B and F_3 were added.

v_B	E_g	$v_{B,\,av}$	$(\Delta v_B/\Delta E)\cdot 10^4$	$H\cdot 10^4$	$h\cdot 10^4$	$Z\cdot 10^4$	$-\log 1000h$
25.00	−142.6		472	1170	706		
		25.25					
25.50	−153.2		316	841	468		
		25.75					
26.00	−169.0		183	513	253		
		26.15					
26.30	−185.4		142	−318	133		
		26.40					
26.50	−199.5		103	190	77.1		
		26.60					
26.70	−218.9		84.8	61.9	36.2		
		26.80					
26.90	−242.5		93.1	−65.7	14.5	1.49	5.84
		27.00					
27.10	−264.0		129	−192	6.3	3.67	6.20
		27.20					
27.30	−279.5		246	−318	3.4	5.95	6.47
		27.45					
27.60	−291.7		476	−505	2	9.40	6.67
		27.75					
27.90	−298.0		1613	−691	2	12.83	6.78
		28.15					
28.40	−301.1		2860	−998	1	18.52	6.83
		28.60					
29.00	−303.0		5260	−1361	1	25.25	6.86
		29.50					
30.00	−304.9			−1955	1	36.26	6.90
32.00	−309						

Eqivalence point of free acid: 26.80 ml

metrical concentration c_{HA} mC of a base A^-, capable of accomodating only one proton. From the law of mass action we then have:

$$1000\ k_{HA} = \frac{h\,(c_{HA} - [HA])}{[HA]},$$

k_{HA} being the corresponding "acid" equilibrium constant (in moles/liter). Noting that $[HA] = H - h$, this equation may be written in the following way:

$$(H-h)\cdot 10^4 = -10^7 k_{HA}\cdot\frac{H-h}{h} + 10^4\, c_{HA}$$

Thus, if $(H-h)\,.\,10^4$ is plotted against $(H-h)/h$, a straight line should result. In Figure 5, based upon the first part of Table 2 b, a plot of this type is shown. From the intercept and slope of the straight line one may calculate k_{HA} and c_{HA}, the following figures being obtained: $pk_{HA} \approx 3.6$ and $c_{HA} \approx 0.10$ mC.

Commenting on this rough calculation we may say that the discrepancy between the H and h values in the first parts of the titrations may be explained by assuming the presence of about 0.1 mC of a base, having an "acid" constant $pk \approx 3.6$ in 1000 mC ClO_4^- solution.

Whatever the truth may be, it is a common experience that great difficulties are encountered in measuring pH in unbuffered solutions, such as those discussed above. For our purposes it is sufficient to state that the method used in calculating the acid constant of Fe^{2+} seems to be justified by the result of the analysis made above.

LINDSTRAND reported the value $pK_a = 5.9$ (K_a = the corresponding equilibrium constant at zero ionic strength). The most plausible explanation of this large difference seems to the author to be the presence of free acid in LINDSTRAND's $Fe(ClO_4)_2$ solution. Furthermore, the method employed by LINDSTRAND permitted him to study only a very limited Z range.

The very weak hydrolysis of Fe^{2+} is not so surprising if one recalls the following facts. Magnetic measurements on the iron(II) ion in aqueous solution strongly suggest that the forces acting between the central ion and its neighbouring water molecules are principally electrostatic in nature (see for instance WELLS (*11*)). Now, the iron (II) ion is a rather large ion. Its "ionic potential", defined as z^2/r, (z being the charge, r the crystallographic radius in Å.U.), is about 5.3, which is of the same order of magnitude as those of Ca^{2+} (4.0) and Mg^{2+} (6.2). For Ca^{2+}, $pk_a \approx 12.7$ (KILDE (*5*)), and for Mg^{2+}, $pk_a \approx 11.4$ (STOCK and DAVIES (*10*)). Even if no definite conclusions can be drawn from these figures, one can still expect Fe^{2+} (or rather $Fe(H_2O)_6^{2+}$) to have only a small tendency to split off protons.

SUMMARY

The hydrolysis of the iron(II) ion, Fe^{2+}, in one molar perchlorate ion solution has been studied at 25° C by measuring the hydrogen ion concentration with a glass electrode.

The total iron(II) concentration was kept constant in each series of measurements. By employing a titration technique, the hydrogen ion concentration was varied from high values, where any hydrolysis could be neglected, up to the precipitation point of iron(II) hydroxide.

In the iron(II) concentration range studied, 8.2 to 54.0 mC (millimoles/liter), the experimental results can be explained by assuming that $FeOH^+$ is the only hydrolysis product formed in solution. At 25.0° C, and in the ionic medium used, the equilibrium constant $k_a = [FeOH^+]\ [H^+]/[Fe^{2+}]$ was calculated to be $k_a = 10^{-9.5 \pm 0.2}$ moles/liter.

A few attempts were made to measure the free Fe^{2+} concentration by means of electrolytically prepared iron electrodes. The results were, however, negative. As was observed by previous investigators the iron electrodes seemed to function very much like a hydrogen electrode, i.e., the potential ran parallel to that of the glass electrode.

Acknowledgement

The author expresses his gratitude to his teacher in chemistry, Professor LARS GUNNAR SILLÉN, who introduced him to this interesting field of study and supported him in many ways with his knowledge and experience. Thanks are also due to fil. lic. GEORGE BIEDERMANN and fil. mag. SIRKKA HIETANEN, both working in SILLÉN's laboratory, for many valuable discussions, to fil. kand. ERIK EKEDAHL and Mr. FRANS ERICSSON, for their kind interest and help in connection with equipment, and to Professor RALPH PEARSON, Northwestern University, Chicago, for his valuable criticism of this paper. The present work was financially supported by *Statens Tekniska Forskningsråd.*

Department of Inorganic Chemistry, Royal Institute of Technology, Stockholm.

REFERENCES

1. BIEDERMANN, G., and SILLÉN, L. G., Arkiv Kemi *5*, 425 (1953) (Part IV).
2. FORSLING, W., HIETANEN, S., and SILLÉN, L. G., Acta Chem. Scand. *6*, 901 (1952) (Part III).
3. GRAN, G., Acta Chem. Scand. *4*, 559 (1950).
4. KOLTHOFF, I. M., and SANDELL, E. B., "Textbook of Inorganic Quantitative Analysis", N. Y. 1947, rev. ed.
5. KILDE, G., Z. anorg. allg. Chem. *218*, 113 (1934).
6. LATIMER, W. M., "Oxidation Potentials", N. Y. 1938.
7. LINDSTRAND, F., "Über Eisenperchlorate", Diss. Lund 1939.
8. MEYER, F. R., and RONGE, G., Z. angew. Chem. *52*, 637 (1939).
9. OESPER, P., J. Chem. Educ. *26*, 588 (1949).
10. STOCK, G. I., and DAVIES, C. W., Trans. Far. Soc. *44*, 856 (1948).
11. WELLS, A. F., "Structural Inorganic Chemistry", 2nd ed., Oxford 1950.

Tryckt den 8 april 1953

Uppsala 1953. Almqvist & Wiksells Boktryckeri AB

ARKIV FÖR KEMI Band 5 nr 43

Vorgelegt am 12 November 1952.

Krebserregung durch chemisch definierte Noxen

Von Hans von Euler

Das Hauptziel der biochemischen Tumorforschung liegt in der Auffindung von Stoffen, durch welche die Entstehung und das Wachstum maligner Tumoren gehemmt werden kann, sodass eine Heilung des cancerösen Organismus eintritt. Von diesem Standpunkt aus sind nicht selten Zweifel geäussert worden, ob das Studium der *krebserzeugenden* Substanzen zu Ergebnissen führt, die dem seit fast 40 Jahren eingesetzten enormen Arbeitsaufwand entsprechen. Demgegenüber kann erwidert werden, dass durch das Studium cancerogener Substanzen bereits wertvolle Einsichten über canceröse Entartung gewonnen worden sind, und dass gerade auf dem Krebs-Gebiet eine Grundlagenforschung auf breitester Basis geboten ist. Erst wenn durch spezifische Wirkstoffe sichere Heilwirkungen erreicht worden sind, kann man endgültig feststellen, welcher Anteil an solchen therapeutischen Erfolgen den mit cancerogenen Stoffen gewonennen Erfahrungen zukommt.

A. Zur Geschichte der Cancerogene

1. Aromatische Kohlenwasserstoffe

Unsere Kenntnisse der chemischen Krebserregung ruhen auf den grundlegenden Pionierarbeiten japanischer Forscher. Zwar kannte man schon früher den Schornsteinfeger-Krebs (P. Pott, 1775), ferner z. B. Berufskrebse in der Teerindustrie, und vermutete einen Zusammenhang zwischen Teer und Hautkrebs (Volkmann, 1875), auch suchte man zu Beginn dieses Jahrhunderts die chemischen Ursachen solcher Beziehungen zu ermitteln, aber erst Yamagiwa und Ichikawa gelang es (1915), maligne Tumoren durch Bepinselung des Kaninchenohres mit Steinkohlenteer hervorzurufen und 1918 erreichte Tsutsui einen ähnlichen Erfolg durch Teerpinselung der Rückenhaut von Mäusen. Der Biochemie der Tumoren eröffnete sich nun ein neues grosses Forschungsgebiet.

Nach bemerkenswerten Beobachtungen von Bloch und Dreyfuss (1921) konnte zunächst Kennaway 1924 zeigen[1], dass die Teerwirkung tatsächlich auf einem im Teer befindlichen Kohlenwasserstoff beruht (später erwies sich der einzige aus Teer isolierbare cancerogene Kohlenwasserstoff als 3,4-Benzpyren). Die von Mayneord in dieses Gebiet eingeführte Fluoreszenz-Spektrometrie war „the single thread, that led allthrough the labyrinth" (Kennaway) und ermöglichte bald rasche Fortschritte.[2]

---

[1] E. L. Kennaway, Brit. Med. Journ. 1, 564; 1924 und 2, 1; 1925.

[2] Siehe auch J. Beerenblum, J. R. Holiday u. S. M. Jope, Brit. Med. Bull. 4, 326 u. 343; 1947.

In erster Linie sind die Arbeiten von HIEGER[1] zu nennen, der aus Steinkohlenteer das hochwirksame 3,4-Benzpyren als Pikrat isolierte und ferner 1,2 Benzanthracen deutlich cancerogen fand. Die weitere Entwicklung des Gebietes der cancerogenen Kohlenwasserstoffe verdankt man zwei Arbeitskreisen, demjenigen von J. W. COOK[2] am Royal Cancer Hospital in London und dem unter der Leitung von L. F. FIESER[3] stehenden, an der Harvard-Universität in Cambridge, U.S.A. wirksamen.

Es bedeutete einen wesentlichen methodischen Fortschritt, dass man 1932 von der Hautpinselung dazu überging, die auf krebserregenden Wirkungen zu prüfenden Stoffe subcutan zu injizieren.

Die Aufzählung und Beschreibung aller aromatischer cancerogener Kohlenwasserstoffe würde den Rahmen dieser Übersicht weit überschreiten.[4] Wir können um so eher davon absehen, als sich aus dem grossen Material allgemein gültige gesetzmässige Beziehungen zwischen Struktur und cancerogener Wirksamkeit noch nicht ergeben haben.[5]

Bezüglich einer Systematik dieser Cancerogene mag der Hinweis genügen dass sich die wichtigsten von 3 einfachen Typen herleiten: *Phenanthren*[6], *Anthracen* und *Benzanthracen*. Diese Grundtypen haben selbst nicht die Fähigkeit, Tumoren hervorzurufen, sie gehen aber durch einfache Substitutionen oder durch weitere Annellierungen in Cancerogene über, z. B. Anthracen in das (allerdings schwach cancerogene) 9,10-Dimethyl-anthracen, während Benzanthracen durch Methylierung in die stark wirksamen Derivate 9-Methyl-1,2-Benzanthracen und 10-Methyl-1,2-Benzanthracen übergeht und durch Annellierung in das hochaktive 3,4-Benzpyren[7] verwandelt wird.

E. C. DODDS u. Mitarb.[8] haben nach Aufspaltung des Benzpyren-Ringsystemes zu α-Äthyl-β-sec. Butylstilben I mit letzterem durch Implantation in 25 Mäuse in 2 Tieren Tumoren erhalten

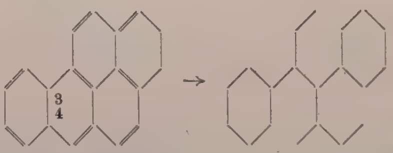

3,4-Benzpyren I

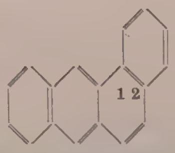

1,2-Benzanthracen

---

[1] I. HIEGER, Am. J. Cancer 28, 522; 1936.

[2] J. W. COOK, Proc. Roy Soc. B, 111, 485; 1932. — J. W. COOK, I. HIEGER, E. L. KENNAWAY and W. V. MAYNEORD, Proc. Roy. Soc. B, 111, 455; 1932.

[3] L. F. FIESER, Am. J. Cancer 29, 260, 1937.

[4] Ausführlichere Übersichten über cancerogene Kohlenwasserstoffe: J. W. COOK u. Mitarb., Am. J. Cancer, 29, 219; 1937. — J. W. COOK, Chem. Ber. 1936 A. 38.

J. L. HARTWELL, United States Public Health Service 1941. Survey of Compounds which have been stated for carcinogenic activity. Fed. Sec. Agency. — A. HADDOW and G. A. R. KON, Brit. Med. Bull. 4, 314; 1947. — A. LACASSAGNE, Les Cancers produits par les Substances chimiques exogènes. Paris, Hermann & C^{ie}, 1946.

[5] Einfache Zusammenhänge sind auch deswegen kaum auffindbar, weil die cancerogene Wirkung eines Stoffes sich an verschiedenen Organen und an verschiedenen Tierarten verschieden erweist.

[6] Unter den Kohlenwasserstoffen mit nur 3 Ringen sind nur wenige cancerogen: unter diesen seien genannt: 9,10-Dimethylanthracen, und 1,2,3,4-Tetramethyl-phenanthren (BADGER u. Mitarb., Proc. Roy. Soc. B, 130, 268; 1941.

Die Mehrzahl der cancerogenen Kohlenwasserstoffe enthält die Phenanthren-Gruppierung.

[7] Siehe auch H. DANNENBERG, Mediz. Welt, Okt. 1950 Nr 42.

[8] E. C. DODDS u. Mitarb., Nature 148, 142: 1941.

[9] Schon hier sei auf die wesentliche Rolle der Lösungsmittel bei der Applikation der cancerogenen Kohlenwasserstoffe hingewiesen (P. R. PEACOCK u. Mitarb., Brit. J. Cancer, 3, 296; 1949. Einfluss von Associationskolloiden: P. EKWALL u. K. SETÄLÄ, 1948–51.

Einer der wirksamsten cancerogenen Kohlenwasserstoffe ist das Methylcholanthren, das wegen seiner Beziehung zu den Steroiden besonderes Interesse bietet

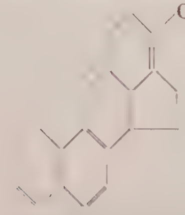

Methylcholanthren

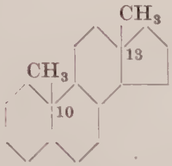

Grundskelett der Steroidhormone

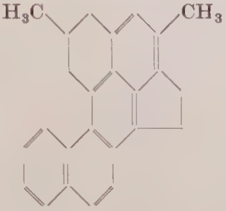

Steranthren

Cook, Dodds und Kennaway haben schon die Frage aufgeworfen, ob man das Auftreten maligner Tumoren auf die endogene Entstehung von Stoffen des Cholanthren-Typus zurückführen kann. Der Übergang von Steroiden in Methylcholanthren erfordert eine Seitenkette von mindestens 4–5 C-Atomen; es kommen also, wie auch Butenandt hervorhebt, für diesen cancerogenen Stoff nur Sterine und Gallensäuren, nicht aber Steroidhormone in Betracht, deren C-Atom-Zahl zur Bildung des Cholanthren-Skelettes nicht ausreichen würde. Die Verwandlung des hydroaromatischen Sterinskelettes in das aromatische Cholanthrenskelett lässt sich in vitro nur durch recht drastische Mittel erzwingen; im lebenden Organismus sind solche Dehydrierungen sehr wohl möglich; Abspaltungen von angulären Methylgruppen können auf einem Umweg erfolgen.[1] Es ist bereits unter Anwendung geeigneter Lösungsmittel gelungen (Rondoni[2], Butenandt[3]) aus dem Carcinomgewebe Stoffe zu isolieren, die im Tierexperiment nicht nur entzündlich-regenerative Prozesse sondern auch ächte maligne Tumoren hervorrufen. W. Bergmann hat schon 1939 angegeben, dass aus Cholesterin (Seitenkette von 8 C-Atomen) ein 6 Ringe enthaltender Kohlenwasserstoff, das *Steranthren* entstehen könnte. Wir werden in Zusammenhang mit dem von Lacassagne[4] eingehend diskutierten Übergang des Östrons (Folliculins) wieder auf diese Fragen zurückkommen.

Schliesslich sei hier kurz die oxydative Umwandlung kondensierter cancerogener Kohlenwasserstoffe im Organismus berührt: Dieselben werden bei der biologischen Oxydation — wie auch bei der Einwirkung von Osmiumsäure[5] — in trans-1,2-Dihydro-Verbindungen übergeführt.

Die Eintrittsstelle der Hydroxylgruppen entspricht hierbei weder den reaktionsfähigsten Zentren noch den reaktionsfähigsten aromatische Doppelbindungen der Kohlenwasserstoffe. Sie liegt stets *neben* der reaktionsbereitesten Doppelbindung, und gerade diesen Doppelbindungen, die in fast allen cancerogenen Kohlenwasserstoffen vorhanden sind kommt im Sinne von O. Schmidt[6] eine besondere Bedeutung für die Krebserzeugung zu. A. und B. Pullman[7] haben die kritische Dichte der anregungsfähigen π-Elektronen für die ,,K-Region" zu 1,29 e berechnet; die Kohlenwasserstoffe, die einen kleineren Wert als 1,29 e haben, sind unwirksam, diejenigen, deren Wert grösser ist, wurden dagegen fast ausnahmslos aktiv befunden. Man hat dieses Ergebnis so gedeutet, dass die cancerogenen Kohlenwasserstoffe durch Vermittlung der K-Region an eine Gruppe des Gewebes, etwa ein Protein gebunden sind; bei den inaktiven Kohlenwasserstoffen kann man eine geringere Festigkeit der Bindung annehmen.

---

[1] Für die stufenweise Aromatisierung des Cholesterins unter CH_3-Verlust hat Butenandt einen zellmöglichen Weg angegeben: Cholesterin-Cholestenon-Cholestadienon.

[2] P. Rondoni, Z. Krebsforsch. 47, 59; 1938.

[3] A. Butenandt, Angew. Chem. 53, 349; 1940. — A. Butenandt, H. Dannenberg u. D. v. Dresler, Z. f. Naturf. 1–5; 1946–50. R. H. Martin, Bull. Soc. Chim. Belge 61; 1952.

[4] A. Lacassagne, Les Cancers, produits par des Substances Chimiques endogènes. Paris, Hermann & Cie; 1950

[5] Siehe hierzu R. Criegee, Lieb. Ann. 522, 75; 1936.

[6] Otto Schmidt, Z. physik. Chem. B, 39, 59; 1938 und 42, 83: 1939. — Naturwiss. 29, 146; 1941.

[7] A. und B. Pullman, Experientia 2, 364; 1946. — A. Pullman, Ann. Chim. 2, 5; 1947. — Bull. du Cancer, 33, 120; 1946. — C. r. 221, 140; 1945 u. 122, 392; 1946.

2. Azo-Verbindungen und aromatische Amine

Von mehreren Gesichtspunkten aus ist die Erwartung berechtigt, dass Azofarbstoffe, ihre Spaltprodukte (aromatische Amine) und deren Derivate ein besonders günstiges Material zum experimentellen Studium der Krebsentstehung ausmachen; ihre Strukturen und chemischen Reaktionsfähigkeiten sind genau bekannt, ihre cancerogenen Wirkungen konzentrieren sich oft, z. B. beim Buttergelb, auf ein einziges Organ, die Leber, oder bei aromatischen Aminen auf nur wenige Organe, deren Stoffwechsel und Inhaltstoffe eingehend untersucht worden sind.

Hinsichtlich der aktiven Gruppen dieser Klasse von Cancerogenen kann zunächst betont weden, dass die Aminogruppe in aromatischer Bindung — sie wird von DRUCKREY als ,,auxocancerogene" Gruppe den ,,cancerophoren" Grundmolekülen gegenübergestellt — einen grossen Einfluss ausübt. Wir werden also zunächst zusammen mit dem Buttergelb dessen Spaltprodukte Anilin, Aminophenol, Phenylendiamin und deren Methylderivate zu besprechen haben.

Reines *Anilin* scheint — wenigstens bei Ratten — keine Tumoren hervorzurufen. Dagegen sind nach Eingabe von *o-Toluidin*, *β-Naphtylamin* und *Anthramin* Anzeichen cancerogener Wirkungen beobachtet worden.

Was die *Azofarbstoffe* betrifft, so liegt, das Maximum der Aktivität wie erwähnt, beim Dimethylamino-azobenzol, dem sich das Monomethylamino-azobenzol anreiht, und es ist besonders auffallend, dass dessen Grundsubstanz, das Amino-azobenzol sich als ganz unfähig zur Krebserregung erwiesen hat (siehe unten). Dagegen ruft nach SASAKI und YOSHIDA sowie nach SH. AMANO und T. ANDO (Gann, 33, 232; 1939) o-Amino-azetoluol Hepatom hervor. In diesem Zusammenhang mag der Befund von HADDOW und KON erwähnt werden, dass das p-Dimethylamino-*stilben* stark cancerogene Eigenschaften besitzt, dass also eine Azogruppe im Molekül keine notwendige Voraussetzung für Krebserzeugung durch diese Klasse von Verbindungen ist.

DRUCKREY[1] hat in einem interessanten Referat die Beziehungen der cancerogenen Wirksamkeit zu einer anderen pharmakologischen Eigenschaft, nämlich zur östrogenen Wirksamkeit diskutiert. Ein Auszug aus seiner Tabelle macht diese Beziehung deutlich (Acta Union intern. contre le cancer, p. 116; 1950):

---

[1] DRUCKREY (Z. Krebsf. 57, 70 u. zw. 75; 1950) ordnet die "auxocancerogenen" Gruppen nach ihrer Wirksamkeit in folgende aufsteigende Reihe ein:

$—CH_2$, $—CH=CH—$, 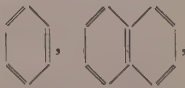, $—NH_2$, $—N(CH_3)$.

Inwieweit bei Azofarbstoffen und aromatischen Aminen ,,Cocarcinogene" im Sinn von BEERENBLOM wirksam sind, ist noch unbekannt.

Das 4,4′-Dioxy-Stilben ist östrogen wirksam und auch 4,4′-Dioxy-azobenzol scheint bei Ratten Östrus hervorzurufen. Es ergibt sich also die Tatsache ,,dass die basischen 4-Amino-Verbindungen der beiden Chromogene Azobenzol und Stilben cancerogen sind, die sauren 4,4′-Dioxy-Verbindungen dagegen östrogen''. Analoge Beziehungen wie zwischen Azobenzol und Stilben findet man auch sonst; so scheint das basische 4,4′-Diaminodiphenyl (Benzidin) cancerogen zu sein, während das saure 4,4′-Dioxydiphenyl östrogen wirksam ist.

Besonders bemerkenswert sind diejenigen aromatischen Amine, welche als Spaltprodukte aus den cancerogenen Azofarbstoffen (Buttergelb u. a.) entstehen (R. Kinosita); wir kommen auf diese Produkte S. 475 zurück.

Die aromatischen Amine, einschliesslich der sekundären Amine vom Typus des *Dinaphtylamins* bilden wohl eine der wichtigsten Klassen der Cancerogene. Aber es darf nicht übersehen werden, dass sich unter den *N-haltigen Heterozyklen* kräftige Cancerogene befinden. Sie bilden gewissermaassen einen Übergang von den aromatischen Kohlenwasserstoffen zu den Azo-Cancerogenen.

Unter den N-haltigen Heterozyklen welche, wie die Azofarbstoffe *Hepatome* hervorrufen, sind in erster Linie die von Boyland und Mawson[1] an Mäusen studierten *Dibenzo-carbazole* zu erwähnen, deren Tumor-erregende Wirksamkeit von Strong, Smith und Gardner[2] bestätigt wurde[3].

Der wesentliche Unterschied zwischen der Wirkung der beiden erwähnten cancerogenen Körperklassen, der Kohlenwasserstoffe und der Azobenzole liegt darin, dass durch erstere der Tumor an der Injektionstelle hervorgerufen wird, während sich die cancerogene Effect der Azobenzole auf den ganzen Organismus verteilt, ev. sich durch selektive Adsorption auf *ein* Organ konzentriert.[4]

An die aromatischen *Azobenzole* schliessen sich die von Cook, Hewett und Kennaway[5] untersuchten Azonaphtaline an, von denen aber nur die 2,2′-Verbindung cancerogen ist.

Einige *Di-Benzacridine* erzeugen nach Angaben von Cook, Kennaway u. Mitarb. an Mäusen epitheliale Tumoren.

Von Lacassagne u. Mitarb.[6] wurden mehrere *Benzacridine* stark cancerogen gefunden. Auch *Styryl* (Pourbaix), *Amino-fluoren* und *Acetyl-Amino-fluoren*[7] sind hier zu nennen, ferner die *Amino-stilbene* von Haddow.[8]

Wenn auch die erwähnten beiden Klassen von Cancerogenen besonders wirksam und besonders eingehend untersucht worden sind, so verdienen doch andere Typen von Cancerogenen nicht weniger Beachtung.

---

[1] E. Boyland a. E. H. Mawson, Biochem. J. 32, 1460; 1938.

[2] L. C. Strong, G. M. Smith a W. U. Gardner, Yale J. Biol. a. Med., 10, 335; 1938.

[3] Über die cancerogene Wirkung von Carbazolen siehe auch J. Maisin u. Mitarb., C. R. Soc. Biol. 96, 1056; 1927.

[4] Nach A. Graffi (Z. Krebsforsch. 50, 501; 1940) werden Benzpyren and Methylcholanthren besonders elektiv von kleinen Granula, vermutlich Mitochondrien und Lipochondrien, aufgenommen.

[5] J. W. Cook, C. L. Hewett, E. L. and N. M. Kennaway, Am. J. Cancer, 40, 62; 1940.

[6] A. Lacassagne, G. Rudall, N. P. Buu-Hoi et J. Lecocq, C. R. Soc. Biol. 139, 955, 1945.

[7] F. Bielschewsky, Brit. J. expt. Path. 27, 34; 1946. — Brit Med. Bull. 4, 382; 1947. — Brit. J. Cancer 3, 282; 1949. — R. H. Wilson, F. De Eds u. A. J. Cox, Cancer Res. 7, 444–453; 1947.

[8] A. Haddow a. G. A. R. Kon, Brit. Med. Bull. 4, 314; 1947. — A. Haddow, R. J. C. Harris, G. A. R. Kon and E. M. F. Roe, Trans. Roy. Soc., A, 241, 147; 1948. — Siehe auch P. N. Harris, Cancer Res. 7, 88; 1947.

3. Cancerogene verschiedener Struktur

Hier seien noch einige Typen von cancerogenen Stoffen kurz erwähnt, die in theoretischer Hinsicht bemerkenswert sind, deren Wirkungen aber von denjenigen der oben erwähnten beiden Stoffklassen durchaus verschieden sind.

Das von HADDOW[1] als Cancerogen beschriebene *Urethan* ruft Lungenadenome hervor, und es erzeugt nach übereinstimmenden Resultaten mehrerer Arbeitskreise Leukopenie. Bei Mäusen hemmt Urethan 8–24 Stunden nach einer Injektion Mitose in Eingeweide-Zellen.

Mit mehreren der als Kampfstoffe (aromatic mustards) bekannten Substanzen, z. B. mit Nn-'Di-(2-chloräthyl)-p-toluidin und mit α- und β-naphtyl-di-(2-chloräthyl)-amin haben HADDOW und KOLLER cancerogene Wirkungen hervorrufen können. Diese Kampfstoffe (Inhibitoren mehrerer Enzyme) sind ebenfalls als Mitosen-Gifte erkannt.

Unter den übrigen cancerogenen Mitosen-Giften sind das Colchicin (DUSTIN) sowie das N-methyl-colchicamid (LETTRÉ[2]) besonders wirksam. Die Mitosen-hemmenden Cancerogene sollen in einem später folgenden Abschnitt behandelt werden.

Wie aus den obigen kurzen Übersichten hervorgeht, kennen wir zwei grosse Stoffklassen, und ausserdem einzelne noch nicht klassifizierbare Substanzen, welche, per os oder durch Injektion in den Organismus eingeführt, Tumoren (Chemotumoren) hervorrufen. Da wir aber nicht wissen, in welcher Weise dies geschieht, so ist es nicht sichergestellt, ob die eingeführten Stoffe selbst die Bildung der Neoplasten bedingen, oder ob es nicht vielmehr Umwandlungs- oder Spaltprodukte dieser Stoffe sind, welche in die zur Krebsbildung führenden Reaktionen eingehen.

Aus diesem Grund kann nicht eindringlich genug betont werden, wie notwendig es ist, jede Berechnung und jede Spekulation über den Mechanismus der Krebsentstehung auf eine sichere chemische Basis zu stellen. Es sollen deswegen zunächst die Daten geprüft werden, welche über das Schicksal der Cancerogene im Tierkörper vorliegen.

B. Die chemischen Vorgänge an exogenen krebserregenden Stoffen

Dass die typischen und wirksamsten cancerogenen *Kohlenwasserstoffe* zum grossen Teil im Rattenorganismus oxydiert werden, wurde bereits S. 471 erwähnt, unter Hinweis darauf, dass dies vorzugsweise an der Stelle der grössten Elektronendichte einzutreten scheint. Viel mehr lässt sich über das chemische Geschehen an diesen aromatischen Kohlenwasserstoffen nicht aussagen. Denn über die Reaktionen, welche ihre Hydroxyl-Verbindungen mit Gewebe-Bestandteilen, ev. mit Blut eingehen liegen noch keine Angaben vor, und die Chemie ev. auftretender oxydativer Zwischenprodukte ist erst unvollständig entwickelt.[3]

Wie bereits S. 472 angedeutet wurde, liegen in dieser Hinsicht die Aussichten, in die Bildung der Hepatome durch Azofarbstoffe oder Amine einzudringen etwas günstiger. Die dabei nachgewiesenen oder möglichen Reaktionen sollen im Folgenden näher besprechen werden.

---

[1] A. HADDOW, Transactions Roy. Soc. 241; 1948.

[2] H. LETTRÉ, Z. physiol. Chem. 287, 150; 1951.

[3] Nach BIELSCHOWSKY (l. c. 1949) ist die Wirkung des Benzpyrens — dies kann aber ebenso für dessen Oxydationsprodukt gelten — unabhängig von der Zahl der Mitosen.

1. Dimethyl-aminoazobenzol (Buttergelb) im Hepatom (Euler u. H. Hasselquist).

DRUCKREY[1] hat an seinem Wistar-Rattenstamm festgestellt, dass das Hepatom auftritt, wenn die Ratte eine gewisse Gesamtdosis Buttergelb erhalten hat (dieselbe ist allerdings von der Zusammensetzung der Nahrung und von verschiedenen anderen Umständen abhängig). Er zieht aus seinen Ergebnissen den Schluss, dass die Wirkung aller, auch der kleinsten Einzeldosen vollkommen irreversibel über die gesamten Lebenszeit fortbesteht. Die Grösse der Gesamtdosis, die DRUCKREY auf etwa 1000 mg schätzt, soll hier noch nicht besprochen werden.[2]

Die Kenntnis der bei dieser Hepatom-Bildung in Betracht kommenden chemischen Vorgänge verdankt man hauptsächlich E. und J. MILLER[3], E. STEVENSON u. Mitarb.[4] sowie KENSLER u. Mitarb[5]. Die für die Beurteilung der Hepatombildung durch Buttergelb wesentlichen chemischen Fragen sind in einer Mitteilung von EULER und HASSELQUIST (dieses Arkiv 4, No. 39; 1952) folgendermaassen formuliert worden.

1. Wieviel vom eingegebenen Buttergelb gelangt in die Leber?
2. Wie lange verbleibt das Buttergelb als solches in diesem Organ und durch welche Vorgänge[6] verschwindet es aus demselben und aus dem Gesamt-Organismus?

In einem experimentellen Abschnitt (folgende Mitteilung) findet man die experimentellen Einzelheiten unserer Versuchsanordnung sowie die analytischen Daten. Hier seien nur die Angaben der amerikanischen Forscher (MILLER, STEVENSON u. a.) mit unseren an weissen Ratten norwegischen Stammes erhaltenen Resultaten verglichen.

Im Stockholmer Institut erhielten die Tiere 10–14 mg Buttergelb per os per 24 Stunden in einer Riboflavin- und Protein-armen Kost, deren Zusammensetzung früher beschrieben worden ist.[7] Die Lebern wurden unmittelbar nach der Dekapitierung untersucht. Dabei zeigte sich die Farbe der Lebern der Buttergelb-Ratten[8] nicht wesentlich aber immerhin merkbar stärker als die der normalen Lebern. Kamen Ratten zur Untersuchung, welche seit 5–6 Monaten die Buttergelb-haltige Kost erhalten hatten, so ergab die Benzol-Extraktion der mit wasserfreiem Natriumsulfat getrockneten Lebern

per Leber (mittl. Gewicht 15 g) 20 γ Buttergelb.

Die Extraktion einer solchen Leber nach vorhergehender Verseifung ergab keine weiteren colorimetrisch messbaren Mengen Buttergelb.

---

[1] H. DRUCKREY, K. KÜPFMÜLLER u. W. TRAPPE, Z. Krebsforsch. 56, 407; 1949. H. DRUCKREY u. KÜPFMÜLLER, Z. Naturforsch. 3 b, 264; 1948. H. DRUCKREY, Arzneimittel-Forsch. 1, 383; 1951.

[2] Vgl. HECHT, HEUBNER-Festschrift, 610; 1952. — CHR. HACKMANN, Z. Krebsf. 57, 530; 1951.

[3] ELISABETH and JAMES MILLER, Cancer Research 7, 468; 1947. — J. MILLER u. C. A. BAUMAN, Cancer Research 5, 227; 1945. — J. MILLER, R. W. SAPP and E. MILLER, Cancer Research 9, 652; 1949. — Siehe auch E. and J. MILLER. The Biochemistry of Hepathic Carcinogenesis. Deutsch von HANS NOTHDURFT. Verlag Unger u. Domröse, Herne i. W.

[4] E. STEVENSON *et al.*, Cancer Research 2, 106; 1942.

[5] C. J. KENSLER, Ann. N.Y. Acad. Sci 49, 29; 1947. C. J. KENSLER *et al.*, Science, 1941, XCIII 308.

[6] Bisher ist nur der reduktive Abbau des Buttergelbs im Organismus in Betracht gezogen worden, obwohl auch ein oxydativer Abbau keinesweg ausgeschlossen ist.

[7] EULER, H. HASSELQUIST u. E. ERIKSSON, Dieses Arkiv 4, No. 39; 1952.

[8] Es muss hier wieder betont werden, dass der weisse Rattenstamm des Institutes gegen die cancerogene Wirkung des Buttergelbs recht resistent ist. Die Versuche werden gegenwärtig mit einem gelben Wistar-Rattenstamm wiederholt, den wir Herrn Prof. Dr. H. DRUCKREY, Freiburg i. B. verdanken.

Auch die Menge des ev. durch reduktive Spaltung von Buttergelb entstandenen p-Phenylendiamins war gering.

Gleichzeitig mit der Leber wurde die Milz jeder Buttergelbratte einer Okular-Besichtigung unterworfen. Die Veränderung war regelmässig sehr auffallend. Die Milz war stets tief dunkelrot oder schwarz, und das Gewicht gegenüber diesen normalen Organen von Ratten gleichen Alters war um 30–50 % erhöht. Diese Veränderung trat auch auf, ehe die Hepatom-Bildung deutlich wurde.

Der Harn der Buttergelbratten wurde nach verschiedener Dauer des Versuches gesammelt und untersucht. Buttergelb liess sich colorimetrisch nach Zusatz von HCl leicht nachweisen. Für die Prüfung auf p-Phenylendiamin eignet sich die früher beschriebene Farbenreaktion mit Redukton.[1] Ausserordentlich scharf und in vielen Fällen anwendbar ist die Reaktion des p-Phenylendiamins mit Holzspähnen oder mit Lignin-haltiger Holzmasse bezw. Papier. Das Lignin-haltige Material färbt sich in 10–30 Sekunden purpurrot; das Reaktionsprodukt lässt sich nicht extrahieren. Auch Dimethyl-phenylendiamin und Aminoazobenzol reagieren in analoger Weise aber mit etwas schwächerer Farbe.

Unsere Verzuchsergebnisse weichen in mehrerer Hinsicht von denen von E. und J. MILLER sowie von STEVENSON ab, besonders hinsichtlich der Adsorption des Buttergelbs an Proteinen und der Spaltbarkeit solcher Adsorbate durch Alkali. Wir gehen hierauf erst näher ein, wenn wir unsere Versuche mit Buttergelb-Lebern der gelben Wistar-Ratten durchgeführt haben.

Nach MILLER sind Farbstoffe in fester Bindung an Protein und in der Rattenleber schon 3–4 Tage nach dem Beginn einer laufenden Verfütterung von 4-Dimethylaminoazobenzol festzustellen. MILLER findet ihre höchste Konzentration (in der Leber) in der 3. bis 5. Woche der andauernden Farbstoffgaben, dann fällt trotz weiterer Farbstoffzufuhr per os der Gehalt an fixierten Farbstoff wieder ab.

Welcher Anteil des per os eingeführten Buttergelbs an Leber-Proteine gebunden wird lässt sich den Angaben von MILLER nicht entnehmen, auch nicht die unserer Auffassung nach wesentlichste Frage, welcher Anteil des eingegebenen Buttergelbs in die Leber gelangt und ob dort an Protein gebundener Farbstoff die wesentliche cancerogene (mutagene) Wirkung ausübt.

Beachtenswert erscheinen uns die Versuche und Erwägungen von KENSLER, DEXTER und RHOADS (Cancer Research, 2, 1: 1942), obwohl mehrere Umstände gegen die Auffassung sprechen[2], dass p-Phenylendiamin das cancerogen wirksame Abbauprodukt des Buttergelbs ist. Wir haben deswegen Reaktionsprodukte von p-Phenylendiamin mit Brenztraubensäure und mit anderen Stoffwechselprodukten der Leber dargestellt und untersucht (siehe auch EULER, Chimia 6; 1952).

Stockholm Universität, Vitamin-Institut und Institut für organ.-chemische Forschung.

---

[1] EULER, H. HASSELQUIST u. E. ERIKSSON, Arkiv f. Kemi 4, Nr. 39; 1952.

[2] E. MILLER u. J. MILLER, Cancer Research, 7, 468; 1947. Siehe hierzu J. MILLER und C. A. BAUMANN, Cancer Research 5, 227; 1945.

[3] Unter den toxischen Wirkungen des p-Phenylendiamins ist die Methämoglobinbildung im Blut besonders bemerkenswert. Trotz dieses Einflusses und anderer Schädigungen von Enzymen werden von Ratten erhebliche Injektions-Dosen, 5–10 mg, vertragen.

Tryckt den 8 april 1953

Uppsala 1953. Almqvist & Wiksells Boktryckeri AB

ARKIV FÖR KEMI Band 5 nr 44

Read 14 May 1952

Action of heparin on barley β-amylase

By Karl Myrbäck and Barbro Persson

With 2 figures in the text

In previous communications we have been able to show that in the combination of several hydrolyzing enzymes (saccharase (1), raffinase (2), urease (3), a mold amylase (4), and barley β-amylase (5)) with their substrates, basic groups of the enzyme molecules are involved in such a way that only the uncharged groups, for the sake of simplicity designated as $-NH_2$, and not the corresponding cations, $-NH_3^+$, combine with the substrates. The acid branches of the pH-curves of the enzymes mentioned can, in fact, be very well understood on the basis of this assumption. A suitable modification and extension of the original Michaelis theory for the saccharase pH-curve (6, 7) allows a fairly accurate calculation of the activity-pH-curves of these enzymes.

If basic groups of the enzymes (possibly together with other groups) are involved in the binding of the substrates, then such reagents that react, reversibly or irreversibly, with the basic groups, should inhibit or destroy the enzymes. In the first case the inhibition would be competitive, *i.e.* be dependent on the substrate concentration. In the case of a destruction of the enzyme by a reagent causing irreversible alteration of the substrate-binding basic groups, the substrate, when present during incubation of the enzyme with the destroying agent, would be expected to exert some sort of protecting action. It could be shown, for instance that saccharose, present during the incubation of saccharase with nitrous acid, protects the enzyme against the destruction which, in this case, is thought to consist in the well-known reaction between nitrous acid and the primary amino group (1). The reversible inactivation of saccharase by such reagents as picric acid and phosphotungstic acid depends on the pH of the solution in a manner easily understood on the assumption that the enzyme-inhibitor complex is a weakly dissociated salt between the inhibitor anion and the enzyme cation. It can be assumed *a priori*, that inactivation of enzymes by heparin and other similar, strongly acidic reagents, consists, at least partly, in an interaction with basic groups of the enzymes. The action of heparin on barley β-amylase is the subject of this investigation.

Concerning the chemistry of heparin, its action on the blood coagulating system and on certain other enzymes, the reader is referred to Jorpes' monograph (8). A common feature of heparin-like anticoagulants is a voluminous organic complex carrying strongly electronegative groups, as for instance $-SO_4H$ groups. According to Fischer (9) and others, these substances cause a displacement of the isoelectric points of proteins toward the acid side, and their action in blood coagulation is supposed to be the same as the action on proteins in general. Fischer (10) found that proteins bind heparin only after denaturation and explains this by the assumption that basic groups of the proteins are "unmasked" by the denaturation. FISCHER and HERRMANN (11) found that fumarase is inactivated only in the pH-range 5.5–6.0, *i.e.* to the acid side of the pH-optimum. The inactivation was found to be irreversible; no reactivation took place if pH was adjusted to the optimum value. CHARGAFF *et al.* (12, 13) found that heparin action was destroyed by salmine and explain the action by the formation of a heparin-protein complex with the displacement of the phospholipid of the thromboplastic protein by heparin. JACQUES (14) finds his experiments to be in agreement with the conclusion of FISCHER (15) that the reaction between heparin and proteins or bases is a simple salt formation with a reversible dissociation of the salt governed by the mass action law. The dissociation is affected by pH and the presence of other ions. Addition of NaCl to dialyzed plasma decreases the heparin activity (16). Heparin inhibits trypsin and serum tryptase (17). The inactivation of liver glucuronidase by heparin has led to the assumption of the presence of more than one glucuronidase in the organ (18).

WORMALL *et al.* (19–24) have studied extensively the action of suramin (germanin) on enzymes. Some enzymes are inhibited at pH = 7–8, others, as for instance urease, only on the acid side of the pH-optimum, others not at all. Plasma proteins protect the sensitive enzymes. It seems that the combination of one enzyme molecule with one or two suramin molecules is sufficient to inactive the enzyme.

Since the inactivation-pH-curve in many cases falls rapidly at about the isoelectric point of an enzyme, WILLS (25) has based a method for the determination of the isoelectric points of enzymes on the inactivation-pH-curves found for a certain suramin concentration. Nineteen different enzymes were investigated and in general the values of the isoelectric points found were in good agreement with such found by other methods. For barley malt β-amylase the value 5.7 is given, which value agrees well with that (5.75) found by Danielsson and SANDEGREN (26), and reasonably well with that (6.0 ± 0.1) given by FISCHER, MEYER, NOELTING, and PIGUET (27) for the crystalline enzyme.

In other cases the agreement is less satisfactory. For malt α-amylase the value found is 5.0 whereas FISCHER and HASSELBACH (28) using crystalline enzyme and the electrophoretic method found the isoelectric point to be 5.7. However, even if it is fairly obvious that suramin (as heparin and other similar agents) react with positively charged basic groups of the enzyme molecules, it must not be forgotten, that most enzyme molecules must contain a rather large number of basic groups with varying dissociation constants. The isoelectric point is determined by those of the basic groups which are most strongly basic. It does not seem permissible even to assume that these most strongly basic groups always are those which preferably bind the inhibitor and still less does it seem possible to assume that these groups mediate the attachment of the substrate or are otherwise indispensable for the enzyme action. Nothing prevents us to assume that certain basic groups may be charged or uncharged, free or attached to suramin, without affecting the enzymatic activity. Wills assumes, besides, that the determination of the isoelectric point by means of suramin is independent of the degree of purity of the enzyme preparation. It may well be so in certain cases but, on the other hand, since many proteins bind heparin and therefore may protect the enzyme, and since the heparin-binding power of proteins is dependent on their isoelectric point, it seems inevitable to assume that, in some cases, the presence of contaminating proteins in the enzyme preparations may affect the inactivation curve of the enzyme. Finally the nature of the enzyme-

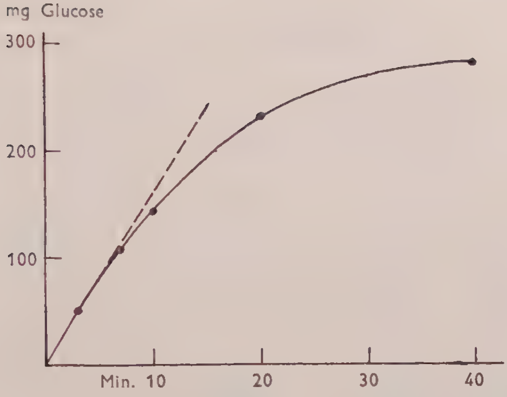

Fig. 1. Increase of reducing power. Determination of initial reaction rate.

Table 1

Reaction time	mg glucose as calculated from reduction values		
	pH=3.33	pH=5.04	pH=8.99
0.5 min.	2	10	—
3 »	14	58	—
7 »	29	128	—
10 »	37	172	4
20 »	58	248	—
40 »	99	266	10
60 »	136	278	16
24 hrs	290	296	190
70 »	—	—	278

inhibitor compound is so incompletely known, at least in the case of the heparin inactivation, that much work is needed before the connection between the inactivation curves and the electrical properties of the enzymes can be regarded as clear. It is hoped that the following experiments may contribute to the understanding of the heparin action on enzymes.

Enzyme: Partly purified preparation from barley, free from α-amylase and maltase. *Substrate:* Native potato starch. *Heparin:* Highly purified preparation, containing about 100 units/mg. We are very much indebted to Professor Erik Jorpes for gifts of this material.

Activity assay: 50 ml 2 per cent starch solution + 5 ml buffer solution (acetate-acetic acid, total concentration of acetic acid 2 *M*) when not otherwise stated, + water, *q.s.* to bring the volume to 100 ml on addition of the enzyme. This mixture was temperated to 30° in a water thermostate, the enzyme was pipetted into it and a stop watch started. After suitable times 5 ml samples were pipetted into 30 ml 0.02 *N* iodine–KJ solution and the reducing power was determined according to Willstätter and Schudel. Usually six to ten determinations were made in each experiment. The reduction value were calculated as mg glucose in 100 ml assay mixture and plotted against time as in fig. 1. The initial rate (dotted line in Fig. 1.) in this

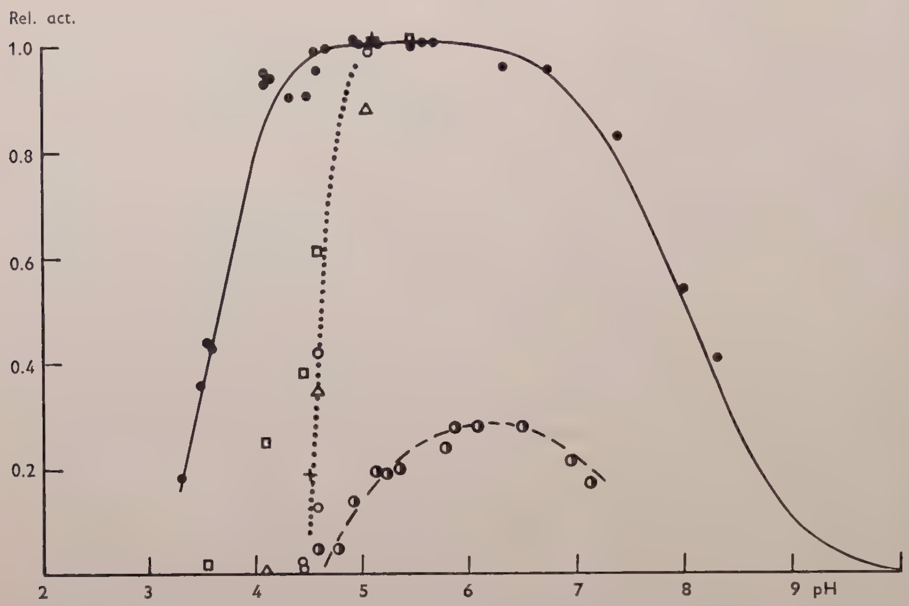

Fig. 2. ● ——— pH-curve of enzyme without inhibitor
□ 0.15 mg heparin, 2 hrs incubation
△ 0.30 » » » » »
+ 0.60 » » » » »
○ 1.20 » » » » »
◑ ------ Reactivation at different pH after inactivation at pH = 4.6

experiment is 16.0 mg glucose/minute and this value is a true expression of the enzyme activity or the amount of active enzyme respectively. Values of this kind have been used throughout this investigation. The relative activity values refer to the value (put = 100) valid for optimal pH (5–5.5) without inhibitor.

Activity-pH-curve

Experiments were carried out in acetate or phosphate buffer. Relative activity values are plotted against pH in fig. 2. It should be noted that the enzyme is quite stable even at the extreme pH-values investigated. The saccharification proceeds, even if the initial rate is very low, to completion, *i.e.* to the formation of about 60 per cent maltose or about 300 mg "glucose" in 100 ml assay mixture: Table 1.

As has been pointed out before (5), the alkaline branch of the pH-curve of barley β-amylase has the form of a simple dissociation curve of an acidic group of the enzyme molecule. Acutally this part of the curve drawn in Fig. 2 is the theoretical dissociation curve of a group with $K_a = 10^{-8}$. Obviously the experiments agree well with this curve. On the other hand the acid branch of the curve deviates strongly from a simple dissociation curve, being much steeper than the theoretical curve. However, the acid branch of the pH-curve can be understood on the assumption that more than one basic group with about the same K_B-values are involved in the enzyme-substrate combination.

Inactivation by heparin

Experiments were carried out to illustrate the dependence of the inhibition on a) the amount of heparin, b) pH in the assay mixture or during incubation of enzyme-heparin mixture respectively, and c) incubation time. All incubations took place at 20°.

1) The activity of 2 ml enzyme solution was measured at different pH's. The relative activities are denoted as v in Table 2.

2) Parallel experiments were performed in which starch, buffer, heparin solution and water were mixed. The enzyme was added last. In the following, experiments of this kind are designated as experiments with heparin and *no incubation* time. The relative velocity is denoted as v_0.

3) 4 ml enzyme solution was mixed with buffer, heparin, and water and incubated for a certain time. One half of the solution was used for determination of pH, the other half was added to a mixture of 50 ml 2 per cent starch solution, 5 ml buffer of the same pH as that used in incubation, and enough water to make the final volume, after addition of the enzyme-heparin mixture, 100 ml. The enzyme activity after incubation during t minutes is denoted as v_t: Table 2. The values v_{120} are marked out in Fig. 2.

The experiments in Table 2 allow the following conclusions:

1) Without previous incubation of enzyme and heparin the latter has little or no action on the enzyme. The experiments show that the inactivation is a comparatively slow reaction.

2) The inactivation is strongly dependent on pH. At pH $\geqq 5$ no inactivation is found even with amounts of heparin ten times as large as those which cause almost complete inactivation at, for instance, pH = 3.5. This is in accordance with the re-

Table 2

pH	v	Incubation			v_0	v_{10}	v_{30}	v_{120}
		mg heparin	ml buffer	total volume				
3.52	44	0.05	1	6	44	32	34	33
5.11	100	0.05	1	6	100	100	100	96
3.55	43	0.15	1	8	37	5	4	3
4.10	92	0.15	1	8	92	32	27	25
4.47	90	0.15	1	8	—	54	52	38
4.59	90	0.15	1	8	—	75	61	61
5.43	100	0.15	1	8	100	100	100	90
4.10	92	0.30	1	8	—	—	—	0
4.63	95	0.30	2	12	82	47	41	35
5.08	100	0.30	2	12	100	91	88	88
4.56	98	0.60	2	18	—	62	37	19
5.05	100	0.60	2	18	—	100	100	100
4.45	92	1.20	2	30	—	3	1	<1
4.45	92	1.20	1.6	8	—	3	3	2
4.57	92	1.20	2	30	—	33	17	13
4.60	90	1.20	1.6	8	—	56	42	42
5.06	100	1.20	2	30	—	100	100	100
5.08	100	1.20	1.6	8	—	100	100	96

sults found with heparin in the case of other enzymes and with the experiments on the action of suramin on enzymes mentioned above. Obviously heparin reacts primarily with positively charged basic groups of the enzymes, *i.e.* only on the acid side of the isoelectric points. As mentioned before, WILLS (25), using 0.003 *M* suraamine, found the value 5.7 for the isoelectric point of β-amylase. If we apply the mode of calculation, used by WILLS, on the heparin inactivation, our experiments would seem to point to a value in the neighborhood of 5.0. However, it must not be forgotten, that the enzyme molecule certainly contains several basic groups with varying strength and that not necessarily all of them react with heparin and suraamin in the same way. It may be mentioned that, according to WEILL and CALDWELL (29, 30) free amino groups in the β-amylase molecule have little if any importance for the enzymatic activity.

3) The inhibition increases with increasing incubation time. In some experiments the reaction does not seem to be complete in two hours, but a very considerable part of the inhibition is caused already by 10 minutes incubation.

Incubation in presence of heat-inactivated enzyme

A portion of the enzyme solution was boiled for 10 minutes and cooled, and the experiments recorded in Table 3 were carried out. A certain protection of the enzyme against heparin by the boiled preparation is observed, but it is rather small compared to the large amount of inactivated enzyme present. This is somewhat astonishing since proteins should combine with heparin and thus lower the amount of inactivating agent. It may be that the amount of heparin used in the experiments is so large that the inhibitor is in considerable excess anyhow.

Table 3

Activity	No heparin 2 ml enzyme pH=4.60	4 ml enzyme, 1.2 mg heparin, 6 ml buffer, pH=4.6, 80 ml water 45 ml for activity determination	4 ml enzyme, 1.2 mg heparin, 6 ml buffer, pH=4.6, 80 ml boiled enzyme solution 45 ml for activity determination
v_0	88	—	—
v_{10}	86	50	—
v_{30}	77	50	—
v_{120}	77	45	61

Incubation at different buffer concentrations

It was found that the inhibition by heparin is not only strongly dependent on the pH but also on the buffer concentration during incubation. In the experiments recorded in Table 4 the enzyme (4 ml) was mixed with 1.2 mg heparin, buffer of pH = 4.60 and water. After incubation one half of the mixture was added to a starch-buffer mixture (total volume 100 ml). pH was determined electrometrically in all experiments. The differences did not exceed 0.03 units.

Table 4

Incubation		v_0	v_{120}
ml buffer	Total volume		
0.5	90	95	3
1.5	90	—	18
3.0	90	—	24
6.0	90	—	45
42.0	90	—	86
14.0	30	—	86
5.6	12	95	77

Table 5

g NaCl present during incubation	Relative activity
6	92
2	94
0.5	92
0.2	58
0.1	20
—	7

Evidently the inactivation by a certain amount of heparine at a definite pH decreases very strongly with increasing buffer concentration. On the other hand if the buffer concentration is kept constant the volume of the heparin-enzyme-mixture during incubation does not influence the degree of inhibition greatly. It was shown that the protecting action by the buffer is exerted also by other salts or rather anions. A series of experiments was carried out with varying amounts of NaCl: 4 ml enzyme solution, 0.5 ml acetate buffer of pH = 4.60, 1.2 mg heparin and sodium chloride solution, total volume 90 ml. Table 5. Evidently the inhibition, which is nearly complete in very dilute buffer solution is almost completely abolished when 0.5 percent or more sodium chloride is present during incubation.

Reversibility of the heparin inactivation

Since NaCl and other salts protect the enzyme against heparin inactivation it was necessary to ascertain if the enzyme, once inactivated by heparin, can be reactivated by NaCl or other substances. In the following experiments 4 ml enzyme solution was mixed with 1.2 mg heparin, 0.5 ml buffer solution (pH = 4.60), and water; total volume 90 ml. After 60 min. incubation salts were added and after further 60 minutes the activity was determined as described above (Table 6).

A small reactivation by NaCl seems to be established, and the same action is found to be exerted by the buffer. However, this reactivation by salts is very slight compared to the protecting action by the same salts when present during the incubation with heparin. The reactivation does not proceed any further if the salts are allowed to act for a longer time. A large number of experiments were performed

Table 6

Substances added	Relative activity
No addition	5
» »	7
» »	6
1 g sodium chloride	16
1 g » »	17
1 ml buffer, pH=6.28, pH of mixture 5.48	17
1 g NaCl+1 ml buffer, pH of mixture 5.48	17

Table 7

Reaction time	mg glucose in 100 ml reaction mixture				
	a	b	c	d	e
3 min.	6	12	16	18	44
7 »	12	22	32	32	104
10 »	14	38	46	48	140
20 »	30	74	90	94	212
40 »	52	134	156	160	246
60 »	72	184	210	220	—
24 hrs	316	—	312	314	322
mg glucose per min.	1.5	3.6	4.5	4.5	16

but the result was always the same: addition of NaCl or restoration of the optimal pH of the enzyme by addition of suitable buffers brought about a small but measurable reactivation. This is further illustrated by the following experiments (Table 7):

a) 4 ml enzyme, 1.2 mg heparin, 0.5 ml acetate buffer (pH = 4.60), total volume 90 ml. Incubation time 60 minutes. 45 ml were then added to a mixture of 50 ml 2 percent starch solution and 5 ml buffer, pH = 4.60.

b) Incubation as in a). 45 ml were added to a mixture of 50 ml starch solution and 5 ml acetate buffer, pH = 5.66. pH of the assay mixture 5.32.

c) Incubation as in a). 2 ml buffer of pH = 6.3 were added; pH of mixture = 5.42. After 60 minutes the activity was determined as above.

d) Incubation as in a). 1 g NaCl and 2 ml buffer of pH = 6.3 were added; pH of mixture 5.38. Activity determination after 60 minutes.

e) No treatment with heparin.

The reactivation experiments tend to show, that two types of heparin inactivation of the enzyme exist. One is reversible (by large amounts of NaCl or buffers of pH > 5), one is not reversible or at least not reversed by salts. It seems permissible to assume that, in acid solution, or more precisely, in the pH-region where the substrate-binding basic groups of the enzyme have a positive charge, primarily an inactive enzyme-heparin salt is formed. This inactivation is reversible; the salt disappears if pH is brought to 5 or higher values or if large amounts of neutral salts are added. However, when an excess of heparin is allowed to act on the enzyme for some time in acid solution, the heparin salt is irreversibly transformed in some way. It may be that the heparin-bound protein is denatured or that more heparin molecules are attached to the enzyme.

A series of experiments was carried out in which the enzyme was partly inactivated by incubation with heparin at pH = 4.50. Determination of the residual activity was performed at different pH's. This was done in order to see if a more complete reactivation could be achieved at, for instance, a more alkaline pH than those investigated in the experiments mentioned above. 4 ml enzyme solution, 1.2 mg heparin, 0.5 ml acetate buffer (pH = 4.60) and water (total volume 90 ml) were mixed and incubated for 60 minutes. 45 ml of the mixture was added to 50 ml 2 per cent starch solution and 5 ml buffer of a suitable pH. The final pH was measured and the reaction rate determined: Table 8.

The reactivation seems to reach its maximum if pH is brought to about six (Fig. 2). However, even at this pH, the activity is far from restored and the greater part of the inactivated enzyme is irreversibly inactivated.

Table 8

pH	Rel. activity	pH	Rel. activity
4.60	5	5.80	24
4.80	5	5.87	28
4.92	14	6.11	28
5.14	19	6.52	28
5.20	19	6.98	21
5.38	20	7.15	17

Protection of the enzyme by the substrate

Since, in acid solution, a rapid inactivation of the enzyme occurs when it is mixed with heparin in a salt-poor solution but, on the other hand, no inactivation occurs at the same pH if the enzyme is added to a mixture of substrate and heparin, it must be concluded that the substrate protects the enzyme effectively against the heparin. Without any premature theories about the nature of the enzyme-heparin combination it seems inevitable to assume that the binding of heparin to the enzyme molecule is, at least partly, mediated by basic groups of the latter. The protecting action of the substrate, therefore, is in good agreement with the view that basic groups of the enzyme molecule are involved in the binding of the substrate to the enzyme (5).

The protection of the enzyme by a 1 per cent substrate solution, as in the mixtures used for activity determination appears to be rather complete. This can be seen from the experiments recorded in table 9.

a) 50 ml 2 per cent starch solution, 5 ml buffer (pH = 4.60), 43 ml water, 2 ml enzyme.

b) 50 ml 2 per cent starch solution, 5 ml buffer (pH = 4.60), 0.15 mg heparin, 43 ml water, 2 ml enzyme.

c) 4 ml enzyme, 0.30 mg heparin, 0.5 ml buffer (pH = 4.60), and 7.5 ml water were incubated for 10 minutes. 6 ml of the solution were added to a mixture of 50 ml 2 per cent starch solution, 5 ml buffer and 39 ml water.

d) incubation as in c) but for two hours.

Table 9

Reaction time	Increase of reducing power: mg glucose			
	a	b	c	d
3 min.	40	44	18	8
7 »	104	110	60	34
10 »	148	148	94	50
20 »	246	234	172	136
40 »	286	282	252	196
60 »	292	292	284	242
24 hrs	320	316	314	312

Since the inactivation of the enzyme by a certain amount of heparin does not depend appreciably on the volume of the enzyme-heparin mixture (Table 4) it must be concluded that the inactivation in experiment c), which amounts to some 50 per cent after only 10 minutes incubation is completely abolished in presence of substrate; the composition of the assay mixture is the same in b) as in c) but the increase of the reducing power in b) is the same as in a) without any heparin. The fact that in all four experiments the final reducing power is practically the same seems to show that in presence of substrate (and reaction products) no inactivation occurs even after relatively long reaction times. Since it appeared possible that maltose would have the same action as starch, experiments were performed with this sugar (Table 10).

a) 50 ml 2 per cent starch solution, 5 ml buffer (pH = 4.60), 43 ml water, 2 ml enzyme.

b) same as a) but 1.5 g maltose present.

c) 4 ml enzyme, 1.2 mg heparin, 0.5 ml buffer (pH = 4.60), total volume 90 ml. Incubation 60 minutes. 45 ml then added to 50 ml 2 per cent starch solution and 5 ml buffer.

d) same as c) but 1.5 g maltose present during incubation.

e) same as c) but 3.0 g maltose present during incubation.

Table 10

Reaction time	Increase of reducing power: mg glucose				
	a	b	c	d	e
3 min.	38	44	6	—	—
7 »	92	90	12	14	20
10 »	—	144	14	28	26
20 »	206	214	30	56	58
40 »	268	268	52	108	108
60 »	292	288	72	184	144
24 hrs	314	324	316	332	284
Relative activity	100	100	8	14	14

A certain protecting action is observed. However, it is quite small and very far from complete. It must be concluded that the binding of maltose to the enzyme, which should occur to some degree, does not protect all of the basic groups which are protected against heparin by the substrate. Since the reaction rate in experiment b) is practically the same as in a) the affinity of maltose to the enzyme used in this investigation must be quite low compared to the affinity enzyme-starch which, of course, is quite in accordance with the slight protecting action of maltose.

Summary

Barley β-amylase is strongly inactivated by heparin under certain conditions. Without previous incubation of the enzyme with heparin, the action of the latter is slight or nil. The inactivation is a comparatively slow reaction. It takes place only in acid solution below pH = 5. It is pointed out that result does not necessarily mean that the isoelectric point of the enzyme protein is 5.0. Higher concentrations of acetate buffer or neutral salts as NaCl present during incubation of the enzyme with heparin protect the enzyme effectively at acidities and heparin concentrations which would, otherwise, completely inactivate the enzyme.

The enzyme, once inactivated by heparin, is reactivated by NaCl or higher concentrations of buffer (pH 5–7) only to a small extent. It is suggested that the action of heparin commences as a simple reversible salt formation with basic groups of the protein and that secondarily an irreversible transformation of the complex, possibly denaturation of the protein, or a formation of higher complexes with more heparin, takes place.

The substrate (starch) protects the enzyme effectively against heparin action. Maltose has only a slight effect in this respect.

This investigation was supported by a grant from the *Swedish Natural Science Research Council.*

Institute for organic chemistry and biochemistry, University, Stockholm.

REFERENCES

1. Myrbäck, K., Z. physiol. Chem. *158*, 160 (1926); *159*, 1 (1926).
2. Myrbäck, K. and Björklund, U., Arkiv Kemi *4*, 567 (1952).
3. Myrbäck, K., Acta Chem. Scand. *1*, 142 (1947).
4. Myrbäck, K. and Willstaedt, E., Arkiv Kemi. *3*, 443 (1951).
5. Myrbäck, K. and Persson, B., Arkiv Kemi *4*, 495 (1952).
6. Michaelis, L. and Davidsohn, H., Biochem. Z. *35*, 386 (1911).
7. Michaelis, L. and Rothstein, M., Biochem. Z. *110*, 217 (1920).
8. Jorpes, E., *Heparin in the treatment of thrombosis, 2nd Ed.*, Oxford Univ. Press, London 1946.
9. Fischer, A., Biochem. Z. *240*, 364 (1931).
10. Fischer, A., Biochem. Z. *278*, 133 (1935).
11. Fischer, A. and Herrmann, H., Enzymologia *3*, 180 (1937).
12. Chargaff, E. and Olsen, K. B., J. Biol. Chem. *122*, 153 (1937).
13. Chargaff, E., Ziff, M. and Cohen, S. S., J. Biol. Chem. *136*, 257 (1940).
14. Jaques, L. B., Biochem. J. *37*, 189 (1943).
15. Fischer, A. and Astrup, T., Biochem. Z. *278*, 326 (1935).
16. Jaques, L. B. and Mustard, R. A., Biochem. J. *34*, 153 (1940).
17. Glazko, A. J. and Ferguson, J. H., Proc. Soc. Exptl. Biol. Med. *45*, 43 (1940).
18. Becker, B. and Friedenwald, J. S., Arch. Biochem. *22*, 101 (1949).
19. Wills, E. D. and Wormall, A., Biochem. J. *44*, xxxix (1949).
20. Town, B. W., Wills, E. D. and Wormall, A., Nature *163*, 735 (1949); *164*, 233 (1949).
21. Wills, E. D. and Wormall, A., Nature *165*, 813 (1950).
22. Wilson, E. J. and Wormall, A., Biochem. J. *45*, 224 (1949).
23. Town, B. W., Wills, E. D., Wilson, E. J. and Wormall, A., Biochem. J. *47*, 149 (1950).
24. Wills, E. D. and Wormall, A., Biochem. J. *47*, 158 (1950).

25. Wills, E. D., Biochem. J. *50*, 421 (1952).
26. Danielsson, C.-E. and Sandegren, E., Acta Chem. Scand. *1*, 917 (1947).
27. Fischer, E. H., Meyer, K. H., Noelting, G., and Piguet, A., Arch. Biochem. *27*, 235 (1950).
28. Fischer, E. H. and Hasselbach, C. H., Helv. Chim. Acta *34*, 325 (1951).
29. Weill, C. E. and Caldwell, M. L., J. Am. Chem. Soc. *67*, 212 (1945).
30. Weill, C. E., *A study of the essential groups of β-amylase*, Thesis, Columbia Univ. New York, 1944.

Tryckt den 8 april 1953

Uppsala 1953. Almqvist & Wiksells Boktryckeri AB

ARKIV FÖR KEMI Band 5 nr 45

Communicated 12 March 1952 by MANNE SIEGBAHN and ARNE WESTGREN

Anion exchange and complex formation of hafnium in hydrochloric and hydrofluoric acid mixtures

By WILHELM FORSLING

With 3 figures in the text

Abstract

The mechanism of anion exchange of the complex ions of hafnium formed in a low concentration range of hydrochloric and hydrofluoric acid mixtures is studied mainly by the use of the experimental data recently given by HUFFMAN and LILLY [1]. An interpretation of their data is proposed, which seems to explain quantitatively the dependence of the elution rate on the composition of the elutriant. As a result of this study approximate values are obtained for the equilibrium constants for the formation of the hafnium fluorocomplexes present under the conditions used. For a correction of the experimental data a short discussion of some methods for the determination of the fractional bed void space is included.

Introduction

During the last few years several investigators have used strongly basic anion exchange resins for separations of elements, which easily form negatively charged complexes with certain anions. Some attempts have also been made to explain the elution mechanism in the column operations used.

KRAUS and MOORE [2] studied the separation of zirconium and niobium in hydrochloric and hydrofluoric acid mixtures of varying concentrations by use of the anion exchange resin Dowex 1. They generally applied strong hydrofluoric acid solutions as elutriants, and found that the elution rate of zirconium appeared to be independent of the hydrofluoric acid concentration. From this observation they suggested that a single zirconium complex species predominated in their solutions. They also showed that the elution rate of zirconium was about proportional to the second power of the hydrochloric acid concentration. HUFFMAN and LILLY [1] pointed out that this fact could be interpreted as meaning that the elution rate depends upon the first power of the concentration of hydrogen ion as well as upon the first power of the chloride ion concentration, or that the rate only depends upon the second power of the chloride ion concentration as suggested by KRAUS and MOORE [2]. As this gave quite different reaction possibilities, HUFFMAN and LILLY [1] studied the dependence of the elution rates of hafnium on the chloride ion concentration when the hydrogen ion concentration was maintained constant.

The data obtained from the experimental work, performed with the resin Amberlite IRA-400, were used by them for studying the elution mechanism. However, they did not quantitatively take into consideration the different elution rates of the different complex species, and for that reason their interpretation seems to be rather questionable. The main purpose of this paper is to present an interpretation of the data given by HUFFMAN and LILLY which is able to explain the elution rates as a function of the elutriant composition.

Distribution and elution coefficients

In order to form a basis for the presentation of the results of ion exchange column operations or batch processes, some useful quantities are generally introduced. For comparison with earlier works and for preventing the confusion of coefficients, which are denoted with different letters in different works, it is convenient to give a short survey of the distribution coefficients often used in this field and to formulate the relations between them. For that reason the following symbols are introduced.

A = the cross-sectional area of the ion exchange column (in cm^2).

C = the plate distribution coefficients [3], representing the distribution of the studied element between the resin and the solution in contact with it in the bed. (Amount sorbed per ml of bed/amount per f ml of solution.)

D = the bed distribution coefficient [4]. (Amount sorbed per ml of bed/amount per ml of solution.)

d = the distance a sorption band maximum has travelled (in cm).

f = the fractional bed void space. (The fraction of the column bed which is occupied by the liquid phase.)

K_d = the mass distribution coefficient, which is generally used in batch processes. (Amount sorbed per g of oven-dried resin/amount per ml of solution.)

ϱ = the apparent density of the ion exchanger in the bed. (g of oven-dried resin per ml of bed.)

V = the volume of elutriant which has passed through a cross-section of the column (in ml).

If the concentration of a solute in a sorption band is constant and sufficiently low, and ideal conditions are prevailing in the exchange column, the following discussion is valid. In real systems it may be valid only approximately.

Under equilibrium conditions, the fraction of the studied element dissolved in the elutriant is

$$\frac{1}{C+1}.$$

In order to carry this movable fraction d cm, the elutriant necessary is dfA ml. Thus, when the band maximum has travelled d cm, the volume of elutriant which has passed through the column is

$$V=(C+1)\,d\,f\,A.$$

This gives

$$C=\frac{V-d\,f\,A}{d\,f\,A}, \tag{1}$$

which is the number of free volumes of solution which has passed through the sorption band. This formula was deduced by MAYER and TOMPKINS [3] from the plate theory.

The relation between D and C is found directly from the definitions above. Thus

$$D = f\,C = \frac{V}{d\,A} - f. \tag{2}$$

KRAUS and MOORE [2] used the elution coefficient E, defined by the equation

$$E = \frac{d\,A}{V}.$$

Thus, summing up,

$$D = f\,C = \frac{1}{E} - f = \varrho\,K_d, \tag{3}$$

where the relation between D and K_d is found from the definitions above.

In order to estimate these distribution coefficients from column operations, the values for A, d, V, f have to be determined. To find K_d the value of ϱ must also be known. A is easily determined geometrically or by measuring the volume of a liquid column of known height in the ion exchange tube when it is empty of resin. d is measured directly from the column bed length or by means of a scanning device, depending on the method used in each case. V is the volume of the effluent. The determinations of f and ϱ are discussed below.

Methods for determining the fractional bed void space

For the determination of the total bed void space (the free volume) of an ion exchange column and from that the fractional bed void space, f, different methods have been used. Quite unequal results are however often obtained for the same resin. Although different anion exchange resins were used by KRAUS and MOORE [2] (Dowex 1) and by HUFFMAN and LILLY [1] (Amberlite IRA–400), it is rather surprising that they got f-values of "ca 1/3" and 0.66 respectively. Even if it is not always necessary to know the value of f with good accuracy, the influence of errors in f is often wrongly neglected. Two determination methods for the estimation of possible corrections to the data given by HUFFMAN and LILLY are shortly discussed below.

GREGOR [5] has studied the composition of the resin phase of an ion exchanger with regard to the concentration of non–exchange electrolyte, which entered this phase at different concentrations of the external solution. He used the resin Dowex 50 and lithium chloride, but the results may qualitatively be applied even for strongly basic anion exchangers. He found that from external solutions containing up to 1 M lithium chloride, hardly any non-exchange electrolyte entered the resin phase. His results show that the determination of the fractional bed void space in cases like this, at least at low concentrations of the solutes, must not be performed by methods which include part of the resin phase in the free volume. However, such a method was used by HUFFMAN and LILLY [1], and therefore their f-value is too high.

Even if the corrections for C, the distribution coefficient used by these investigators and denoted by them D, prove to be of significance only for the lowest C-

values of their data, it is in point of principle important to discuss the different results of the methods used. Some experiments will be shortly described to illustrate this question.

A good method for the determination of the fractional bed void space in cases like this is the non-sorbed ion method, suggested by KETELLE and BOYD [4]. A description of a determination of *f* is given below in which f was found by measuring the longitudinal velocity with which potassium ion passed through the column bed, when the volume flow rate of the elutriant was known. The very small amount of potassium chloride used contained K^{42} from deuteron bombardment of potassium hydroxide in a cyclotron. The other method studied, which is based on volume measurements, was used by HUFFMAN and LILLY. Of course, both methods can be performed with some modifications, which give results of different accuracy, but the methods remain fundamentally distinct.

Experimental procedure and calculations

The anion exchange resin. The resin used was the chloride form of the strongly basic Amberlite IRA–400, which had been air-dried, ground in a ball mill and dry sieved to obtain the desired mesh sizes. Any small adhering particles were removed by repeated washings of the exchanger with water. For that fraction of resin which had a mesh size of less than 300 mesh no screen for the lower limit of particle size was available. It was therefore necessary to be satisfied with repeated slurrying of the resin particles of such mesh sizes with water. The fines were decanted each time until the supernatant was free from turbidity. As the lower limit of the particle size was not known in this case, the mesh size is only denoted —300 in Table 1.

In order to estimate the possible influence of the exchange capacity of the *f*-values obtained with the two methods, Amberlite IRA–400, partly oxidized with 4 M perchloric acid was also used. This ion exchange resin had a specific capacity of 1.3 milliequivalents per gram oven-dried resin as determined by the method of KUNIN and MCGARVEY [6]. The unoxidized resin had a specific capacity of 2.1 milliequivalents per gram.

The method of non-sorbed ion. The radioactive potassium used was chemically purified after the cyclotron irradiation by a method earlier used at this institute, and which included among other procedures repeated crystallization of the perchlorate.

The column beds were thoroughly washed with 0.2 M hydrochloric acid before the addition of the radioactive potassium chloride. 0.2 M hydrochloric acid was also used as elutriant. The times for the passage of the potassium ion through three different levels of the 25–65 cm high ion exchange columns were found by the use of a simple scanning device [7]. At the same time the volume of the effluent solution was measured in a buret. This volume was established graphically at just the times when the potassium band maximum passed the three column levels. The volume in ml of effluent was then plotted against the volume in ml of resin bed passed by the potassium ion. The slope of the straight line obtained gives the value of *f*. The maximum errors in *f* from the broadening of the bands during the column operations was estimated to be ±0.03, or about 6% of the *f*-value.

The method based on volume measurements. The resins used were dried at 110°–115° C till they reached nearly constant weight, which took 2–3 days for the chloride form of Amberlite IRA–400. This heating had no perceptible effect on the resin capacity. About 3–4 gram of oven-dried resin was poured into a buret, which was provided with a very small cotton plug at the bottom. The resin was shaken repeatedly with a known volume of 0.2 M hydrochloric acid. When the volume of the settled mixture no longer changed or after at least one day, the volume of the resin was determined as the difference between the first mentioned volume and the volume of the hydrochloric acid solution added to the oven-dried resin. In order to calculate the value of the fractional bed void space in column operation, the bed had to be packed by washing with the elutriant used for this operation until the bed volume in the buret was constant. In this case 0.2 M hydrochloric acid was used. The free volume was obtained as the difference between the bed volume and the volume of the resin. The free volume divided by the bed volume gave the fractional bed void space. The maximum error in f caused by the errors in the volume determinations was ± 0.03. The results are given in Table 1.

By these experiments the values of ϱ were easily obtained as the weight in grams of oven-dried resin per ml of bed.

In order to find if the drying of the resin at 110°–115° C for 2–3 days delayed the complete uptake of water from the hydrochloric acid solution more than one day, similar experiments were also made with air-dried samples. However, the results were the same in both cases.

The results of the determinations of f and ϱ

The values obtained for f and ϱ with the methods described above are summarized in Table 1.

Table 1.

Fractional bed void space (f) and apparent density (ϱ) for column beds of the chloride form of Amberlite IRA–400.

v = longitudinal flow rate in the bed during the determination of f_{ns}.
f_{ns} = f, determined with the method of non-sorbed ion.
f_{vm} = f, determined with the method of direct volume measurements.

Resin		v cm/min	f_{ns}	f_{vm}	ϱ g/ml
mesh size	specific capacity meq/g				
$-200+300$	2.1	0.28	0.48	0.69	0.38
-300	2.1	0.16	0.52	0.71	0.37
$-150+300$	1.3	0.40	0.51	0.60	0.46
$-150+300$	1.3	1.0	0.47	0.60	0.48

For the determinations of f_{ns}, the variations of mesh size, flow rate, column length, and capacity did not seem to have any distinct effect, within the scope of the experiments.

With the partly oxidized resin, lower f_{vm}-values (0.60) were obtained than for the unoxidized resins (0.70). That is just what is to be expected, if part of the cationic active groups of the resin were removed by the oxidation. The hydrophobic resin shrinked (higher ϱ-values) and prevented some water from entering the oxidized parts of the resin phase. The volume of the external solution in the bed, however, is the same as for the unoxidized resin, which is seen from the constancy of the f_{ns}-values (0.50). This illustrates the difference between the two methods used for the determination of f. With the method of direct volume measurements, part of the water in the resin phase, free from non-exchange electrolyte, is included in f (cf. page 491). With the method of non-sorbed ion it is not included, provided that the salt concentration of the elutriant is not too high.

It may be repeated that the purpose of these determinations of the fractional bed void space was only to point out the difference between two methods often used for such determinations and to give approximate corrections for the data used in the discussion of the elution mechanism.

From the relation (1) derived on page 490, and from the data given by HUFFMAN and LILLY [1], the following corrections are found by the use of the f-value 0.50. For $C = 1.5$, 11, and 30 the corrections are $+0.8$, $+5$, and $+10$ respectively. However, if the coefficient D is used, C had to be multiplied by the f-value of HUFFMAN and LILLY. As seen from (2) on page 491, the correction for D is constant and equal to the difference between their f-value and f_{ns}. This correction, $+0.2$, has significance only for the lowest D-values used below.

Discussion of the elution mechanism

In the range of the very low fluoride ion concentrations of elutriants generally used in this study, it can approximately be assumed that the chloride ion is the only one which competes with the complex fluoroions for the active groups of the resin. The reaction for eluting a complex ion of hafnium from the anion exchange resin can be written

$$\begin{aligned} R_n^{+n}\cdot\{H_{p1}Hf(OH)_{q1}O_{r1}Cl_{u1}F_{v1}\}^{-n}+aCl^-+bH^+ &\rightleftharpoons \\ \rightleftharpoons nR^+\cdot Cl^-+\{H_{p2}Hf(OH)_{q2}O_{r2}Cl_{u2}F_{v2}\}^{-m}+tHF+cH_2O & \end{aligned} \tag{4}$$

where R represents the resin and n and m are the charges of the complex ions in the resin phase and in the solution respectively. Some of the letters $p1$, $p2$, $q1$, $q2$ and $r1$, $r2$ are certainly equal to zero. It is presumed that no complexes with two or more central atoms occur under the conditions used. This assumption is supported by the similarity of the experimental data obtained by macro amounts and by tracer amounts of the nuclear element used [1].

For the elution equilibrium constant one obtains

$$K=\frac{[Cl^-]_R^n\,[HfQ_p\,Cl_{u2}\,F_{v2}^{-m}]_S\,[HF]_S^t}{[HfQ_r\,Cl_{u1}\,F_{v1}^{-n}]_R\,[Cl^-]_S^a\,[H^+]_S^b}, \tag{5}$$

where brackets indicate activities. Q_r and Q_p denote the hydrogen and oxygen contents of the complexes, and the subscripts R and S indicate resin and solution phase respectively.

If parentheses are used for concentrations and γ for activity coefficients, the bed distribution coefficient D, defined on page 490, can be written

$$D=\frac{(HfQ_r\,Cl_{u1}\,F_{v1}^{-n})_R}{(HfQ_p\,Cl_{u2}\,F_{v2}^{-m})_S}=\frac{\gamma_{HfQ_p\,Cl_{u2}\,F_{v2\,S}^{-m}}\,[Cl^-]_R^n\,[HF]_S^t}{K\,\gamma_{HfQ_r\,Cl_{u1}\,F_{v1\,R}^{-n}}\,[Cl^-]_S^a\,[H^+]_S^b}. \tag{6}$$

Huffman and Lilly [1] have used similar equations. They neglected the variations in the ratio of the activity coefficients in both resin and aqeous phases in studying for instance the dependence of log C on log $(Cl\ )$. In this way they presented data which showed that the exponent a has a probable value of $+2.0$, indicating that two chloride ions enter the reaction (4) at 0.5 M hydrofluoric acid and varying concentration of HCl (cf. Fig. 2). They also pointed out that the elution rate was independent of the hydrogen ion concentration $(b=0)$ and, at a constant concentration of 1.00 M hydrochloric acid, also of the hydrofluoric acid concentration within the range 0.25 to 4.00 M $(t-0)$. From this they stated that there are no changes in the oxide, hydroxide or hydrogen ion content of the complexes during the elution in either of their experimental series, which are discussed below.

The use of concentrations instead of activities at high and varying concentrations of hydrochloric and hydrofluoric acids is very doubtful. Thus, while the results at such concentration ranges as those used for instance by Kraus and Moore [2] seem to be rather uncertain, and the possible presence of trivalent negative complex ions at high hydrofluoric acid concentrations cannot be decided from these experiments, the data given by Huffman and Lilly [1] at low and rather constant ionic strength seem to be reliable. The last-mentioned investigators in this question refer to a work of Kressman and Kitchener [8], in which the mass-law product determinations, however, were made over quite small concentration ranges and therefore cannot be generalized, as pointed out by for instance Duncan and Lister [9].

As mentioned above, the interpretation given by Huffman and Lilly [1] for the elution mechanism in the low hydrofluoric acid concentration range (0.005–0.04 M) seems to the present author to be rather improbable. By using their experimental data, some interesting relations can be obtained. In this way their values of the distribution coefficient C have been corrected for an f-value of 0.50 and expressed in terms of the distribution coefficient D, as described on page 494.

It may be assumed that in a solution of about 0.2 M hydrochloric acid and a low range of hydrofluoric acid concentration there exist some fluorocomplexes of hafnium, which can be denoted

$$HfQF_v, \qquad HfQF_{v+1}^{-} \text{ and } HfQF_{v+2}^{2-}.$$

In Q some chloride ions may also be included beside the hydrogen and oxygen contents of the complexes. For simplicity, in the formulae of the complexes the changes in the hydration water content are not taken into consideration. Of course, at sufficiently low hydrofluoric acid concentration complex cations can be expected. Towards the anion exchanger, however, they behave in about the same manner as the uncharged complex $HfQF_v$.

In the solution in contact with the sorbed complex hafnium anions, the following equilibria are plausible:

$$HfQF_v + HF \rightleftharpoons HfQF_{v+1}^{-} + H^+ \tag{7}$$

and

$$HfQF_{v+1}^{-} + HF \rightleftharpoons HfQF_{v+2}^{2-} + H^+ \tag{8}$$

with the equilibrium quotients

$$k_1 = \frac{(HfQF_{v+1}^{-})\,(H^+)}{(HfQF_v)\,(HF)} \tag{9}$$

and

$$k_2 = \frac{(Hf\,Q\,F^{2-}_{v+2})\,(H^+)}{(Hf\,Q\,F^-_{v+1})\,(HF)}. \tag{10}$$

Each of these complexes is assumed to have its own distribution coefficient D, which may be derived as special cases of D on page 494 from the following proposed simple exchange equilibria:

$$\{Hf\,Q\,F_v\}_R \rightleftharpoons \{Hf\,Q\,F_v\}_S, \tag{11}$$

$$\{Hf\,Q\,F_{v+1}\}^-_R + Cl^-_S \rightleftharpoons \{Hf\,Q\,F_{v+1}\}^-_S + Cl^-_R, \tag{12}$$

$$\{Hf\,Q\,F_{v+2}\}^{2-}_R + 2\,Cl^-_S \rightleftharpoons \{Hf\,Q\,F_{v+2}\}^{2-}_S + 2\,Cl^-_R. \tag{13}$$

Thus

$$D_0 = \frac{(Hf\,Q\,F_v)_R}{(Hf\,Q\,F_v)_S}, \tag{14}$$

$$D_1 = \frac{(Hf\,Q\,F^-_{v+1})_R}{(Hf\,Q\,F^-_{v+1})_S} = \frac{M'\gamma_{Hf\,Q\,F_{v+1}\,S}\,[Cl^-]_R}{\gamma_{Hf\,Q\,F_{v+1}\,R}\,[Cl^-]_S} = \frac{M}{(Cl^-)_S}, \tag{15}$$

$$D_2 = \frac{(Hf\,Q\,F^{2-}_{v+2})_R}{(Hf\,Q\,F^{2-}_{v+2})_S} = \frac{N'\gamma_{Hf\,Q\,F_{v+2}\,S}\,[Cl^-]^2_R}{\gamma_{Hf\,Q\,F_{v+2}\,R}\,[Cl^-]^2_S} = \frac{N}{(Cl^-)^2_S} \tag{16}$$

M' and N' denote the reciprocals of the equilibrium constants for (12) and (13) respectively. D_0, M, and N are assumed to be constant at almost constant ionic strength of the solution. Here also it is supposed that the chloride ion is the only one which competes with the complex fluoroions for the active groups in the resin. As the hydrofluoric acid is a weak acid, the last-mentioned condition is rather well fullfilled in the elutriants used. Furthermore, the fluoride ion has a lower exchange ability than the chloride ion for Amberlite IRA–400, as found by KUNIN and McGARVEY [6].

For the observed distribution coefficient D one obtains, by use of the expressions (9), (10), (14), (15), and (16),

$$\begin{aligned} D &= \frac{(Hf\,Q\,F_v)_R + (Hf\,Q\,F^-_{v+1})_R + (Hf\,Q\,F^{2-}_{v+2})_R}{(Hf\,Q\,F_v)_S + (Hf\,Q\,F^-_{v+1})_R + (Hf\,Q\,F^{2-}_{v+2})_S} = \\ &= \frac{D_2\,k_1\,k_2\,(HF)^2 + D_1\,k_1\,(H^+)\,(HF) + D_0\,(H^+)^2}{k_1\,k_2\,(HF)^2 + k_1\,(H^+)\,(HF) + (H^+)^2}. \end{aligned} \tag{17}$$

In spite of the rather few experimental data available it is possible to obtain approximate values for the equilibrium constants k_1 and k_2 as follows. At first, this was tried from a series in which the dependence of the distribution ratio of fluorohafniate on hydrofluoric acid concentration in 0.23 M hydrochloric acid was studied. This series had been performed at an almost constant ionic strength, and therefore the activity coefficients are assumed to be constant. The difficulty in determining the low and varying hydrofluoric acid concentrations in the elutriants seems, how-

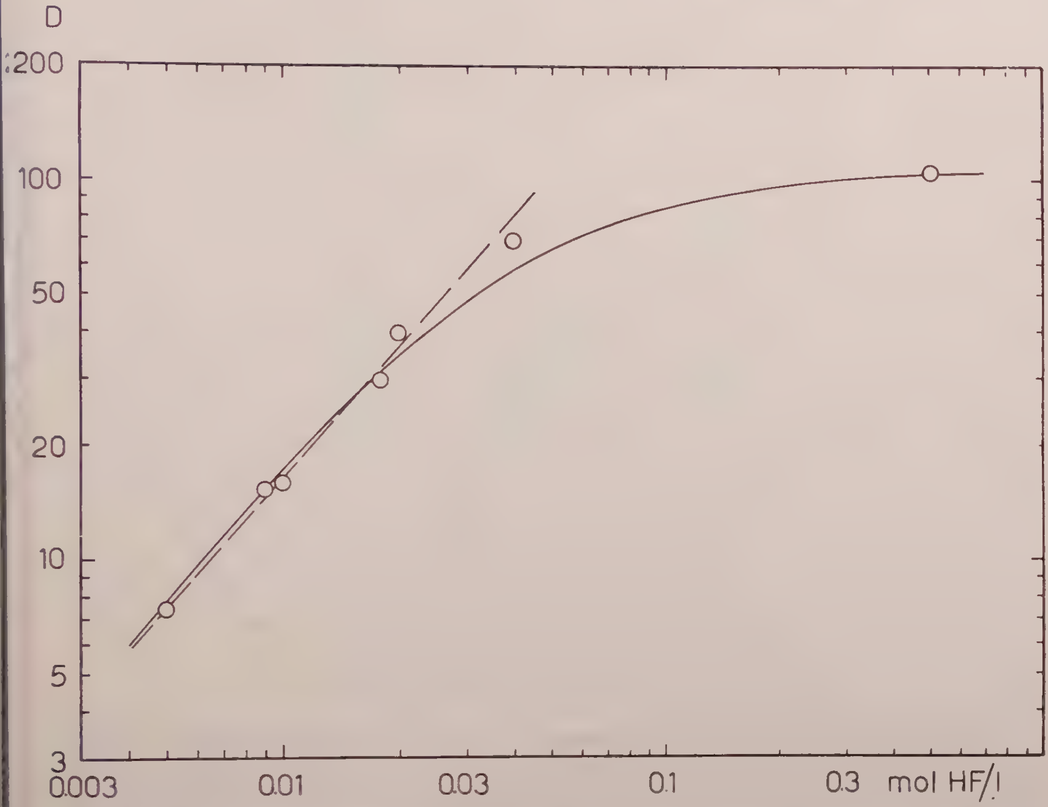

Fig. 1. Dependence of the distribution coefficient D of fluorohafniate on hydrofluoric acid concentration in 0.23 M hydrochloric acid (cf. HUFFMAN and LILLY, ref (1) Fig. 3); — — —, experimental curve used by HUFFMAN and LILLY; ————————, calculated curve. See page 500 for a discussion of the point at 0.5 M HF.

ever, to have caused somewhat greater experimental errors in the determinations of C in these series. When log D was plotted against log (HF) by use of the calculated values, the deviation of the curve from a straight line with slope +1.1 which was assumed by HUFFMAN and LILLY, was considerable (Fig. 1). For these reasons it was inconvenient to use this experimental series as the basis for the determinations of the constants in equation (17).

From the study of the dependence of the distribution coefficient on chloride ion concentration, it was found, as referred to above, that the slope of —2.0 for the plot of log D versus log (Cl^-) was nearly independent of whether lithium chloride or hydrochloric acid was used as the source of the chloride ion. The concentration of hydrofluoric acid was in these experiments maintained at 0.50 M. It must be pointed out that the ionic strength was far from constant for this series.

Thus, in equation (17), it may in this case be possible to neglect the terms containing (H^+). We have therefore approximately with equation (16),

$$D = D_2 = \frac{N}{(Cl^-)_S^2}, \tag{18}$$

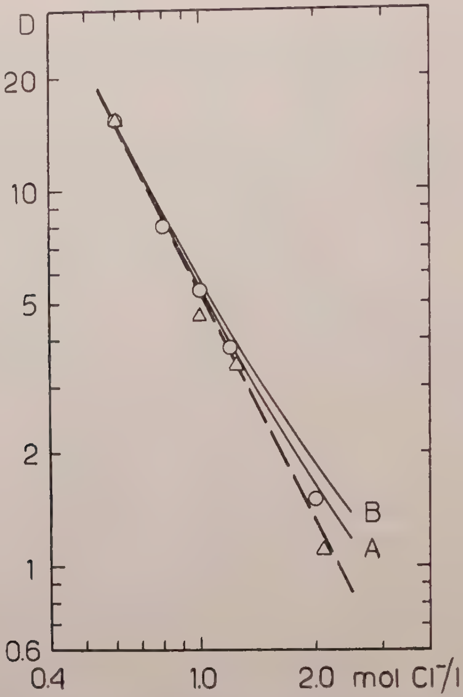

Fig. 2. Dependence of the distribution coefficient D of fluorohafniate on chloride ion concentration and on hydrochloric acid concentration (cf. HUFFMAN and LILLY, ref. (1), Fig. 2); △, lithium chloride with 0.60 M hydrochloric acid and 0.50 M hydrofluoric acid; ○, hydrochloric acid with 0.50 M hydrofluoric acid; — — —, experimental curve; ———A, calculated curve for the variation of the chloride ion concentration; ———B, calculated curve for the variation of the hydrochloric acid concentration.

where N can be determined from the experimental curve (the line of short dashes in Fig. 2).

For the determination of the constants k_1, k_2, D_0, and M, those data were used which were obtained from the study of the dependence of D on the chloride ion concentration and on the hydrochloric acid concentration in 0.009 M hydrofluoric acid. The data are presented in Fig. 3 and the curves in connection with them denoted by A and B respectively. For A, lithium chloride, together with 0.20 M hydrochloric acid, was used as chloride ion source. For B hydrochloric acid was used as chloride ion source. The slopes of the curves are about —1.4 and —2.4 respectively. One point is common to the series A and B, that obtained for 0.20 M hydrochloric acid. The curve A cannot be plotted as a straight line through the four points belonging to this series. This may be due either to the possibility that the experimental curve deviates considerably from a straight line at about 0.20 M chloride ion concentration, or to experimental errors. From the results obtained below the last-mentioned reason seems to be probable.

From the equations (15), (16), and (17) is found

$$D = \frac{k_1 k_2 N (HF)^2 + k_1 M (H^+)(HF)(Cl^-) + D_0 (H^+)^2 (Cl^-)^2}{\{k_1 k_2 (HF)^2 + k_1 (H^+)(HF) + (H^+)^2\} (Cl^-)^2}, \qquad (19)$$

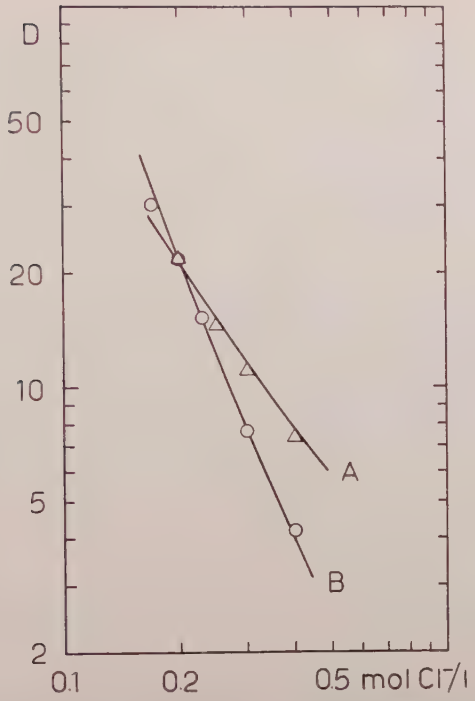

Fig. 3. Dependence of the distribution coefficient D of fluorohafniate on chloride ion concentration and on hydrochloric acid concentration (cf. HUFFMAN and LILLY, ref. (1) Fig. 4); △, lithium chloride with 0.20 M hydrochloric acid and 0.009 M hydrofluoric acid; ○, hydrochloric acid with 0.009 M hydrofluoric acid; ———A, calculated curve for the variation of the chloride ion concentration; ——B, calculated curve for the variation of the hydrochloric acid concentration.

where all concentrations are referred to the solution. For that reason the index S is omitted in equation (19).

For the curve A in Fig. 3, D_0, M, N, k_1, k_2, (H^+), and (HF) are constant. Thus equation (18) can be written

$$D = \frac{B + T(Cl^-) + U(Cl^-)^2}{P(Cl^-)^2}, \tag{20}$$

where B, T, U, and P denote the different combinations of the constants included.

From (20), the equation for the curve A in Fig. 3 is obtained:

$$\log D = \log\{B + T(Cl^-) + U(Cl^-)^2\} - \log\{P(Cl^-)^2\}. \tag{21}$$

This is of course not the equation of a straight line. However, within the narrow limits of the chloride ion concentration used in the experiments, such a line appears to be a very good approximation.

The slope of the curve is found from

$$\frac{\partial \ln D}{\partial \ln (Cl^-)} = -\frac{2B + T(Cl^-)}{B + T(Cl^-) + U(Cl^-)^2}, \tag{22}$$

where $U = D_0(H^+)^2 \approx 0$, as D for the uncharged complex is nearly equal to zero, while this complex is unsorbed by the resin. The value for the fractional bed void space of uncharged complexes is greater than the value for anion complexes used here and for that reason the sign $\approx$ is used. As is also obvious from the discussion of the determination methods for the fractional bed void space on page 491, the f-value is somewhat changed as the concentration of the electrolyte in the external solution is greater than about 1 M. For these reasons some errors arise, which, however, have significance only for the lowest D-values plotted in Fig. 2 and 3 (cf. page 494).

The value —1.43 for the slope of the curve A in Fig. 3 is inserted in (22), giving a relation between k_2 and M. Two relations between k_1 and k_2 are then found from the positions of the curves A and B respectively. As the rather few experimental data used do not justify a more detailed mathematical treatment, the D-values for the chloride ion concentration and the hydrochloric acid concentration equal to 0.30 have been used for this purpose. In this way a sufficient number of equations are obtained for the determination of k_1, k_2, M, and N. The following approximate values are found, $k_1 = 10$, $k_2 = 6.5$, $M = 7.1$, and $N = 5.5$. By the use of these values and the equation (19) the curves plotted in Figs. 1, 2, and 3 are obtained.

Comparison with the earlier interpretation

In Fig. 2 two adjacent curves are drawn, denoted A and B. A is valid for the dependence of D on the chloride ion concentration with a constant hydrochloric acid concentration of 0.60 M, and B for the dependence on the hydrochloric acid concentration. Qualitatively these curves agree with the data given by HUFFMAN and LILLY [1], as may be seen from Fig. 2. At low D-values the experimental errors are considerable, and the ionic strength so varying that full agreement cannot be expected (cf. page 495).

KRAUS and MOORE [2] have given some elution constants (E) for zirconium, which were obtained under similar conditions to those used by HUFFMAN and LILLY [1]. In spite of the fact that they used different anion exchangers (cf. page 491) the results agree very well for those data obtained with the same concentrations of elutriants. From a measurement at 0.2 M hydrochloric acid and 0.5 M hydrofluoric acid, for which KRAUS and MOORE got $E = 8.5$, corresponding to $D = 117$, the D-value for hafnium at 0.23 M hydrochloric acid and 0.5 M hydrofluoric acid can roughly be estimated to be about 105. This value is inserted in Fig. 1 and is in agreement with what is to be expected from extrapolation of the data in Fig. 2. Of course it must be considered as very approximate, as KRAUS and MOORE only have given one figure after the decimal point.

The interpretation given by HUFFMAN and LILLY [1] for the experiments carried out at 0.50 M hydrofluoric acid concentration seems to be likely, since almost all hafnium probably occurs in the state of the bivalent negative complex ion $HfQF_{v+2}^{2-}$. For that reason equation (6) is directly applicable. Thus the suggested reaction is reaction (13) on page 496. However, when more than one reaction of the type (4) occur simultaneously, the equation (6) is not valid as a formula for D. As pointed out above, the curve in Fig. 1 deviates rather much from the straight line of slope +1.1 assumed by HUFFMAN and LILLY. This fact indicates that their assumption that t in equation (6) is equal to one is rather doubtful.

From the different slopes of the curves A and B in Fig. 3, they suppose a first power dependence on the hydrogen ion concentration. Thus, the value of b in equation (6) is equal to one, according to these investigators. As the slope of the curve A lies between $+1$ and $+2$, they assume that two reactions are operating at the same time during the elution. They propose the reactions

$$R^+ \cdot HfQF_{v+1}^- + H^+ + Cl^- \rightleftharpoons HfQF_v + HF + R^+ \cdot Cl^- \tag{23}$$

and

$$R_2^{2+} \cdot HfQF_{v+2}^{2-} + H^+ + 2\,Cl^- \rightleftharpoons HfQF_{v+1}^- + HF + 2\,R^+ \cdot Cl^- \tag{24}$$

written with the symbols used before in this paper.

If these reactions were valid, the sorption of the hafnium complexes on the anion exchanger would be connected with the uptake of a further fluoride ion in the complex. This mechanism is not impossible, but seems to be rather unlikely, especially as it is not applicable in the high acid concentration range. The question arises why a negatively charged ion in the solution cannot be bound directly to the positively charged active groups of the resin.

Results and comparisons with other investigations

From the agreement of the experimental data and the calculated curves plotted in Figs. 1, 2, and 3, the interpretation of the mechanism for the anion exchange of the complex ions of hafnium formed in a low concentration range of hydrochloric and hydrofluoric acid mixtures given here seems to be probable. This interpretation is based on the assumptions that there exists a series of complex equilibria in the elutriant, and that each complex anion has its own distribution coefficient, which in this case is a function mainly of the chloride ion concentration and the valency of the complex ion.

A difference in composition between the complexes in solution and those in the resin phase need not be assumed. Trivalent negatively charged complexes of hafnium and fluoride ions may be formed at a high fluoride ion concentration [10]. However, from the data used here, it seems to be improbable that such complexes are formed in 0.5 M hydrofluoric acid to an extent comparable with the formation of the lower charged complexes.

It has been assumed on page 494 that only mononuclear complexes are formed. This is not quite sure. However, it seems to be impossible to decide this problem certainly with the method applied here. Other investigators have considered complexes of zirconium and halogen ions in aqueous solutions to be mononuclear under conditions similar to those used here [11], [12].

CONNICK and MCVEY [12], in studying the aqueous chemistry of zirconium, found that in 2 M hydrochloric acid free from hydrofluoric acid only about 80% of the zirconium was complexed by chloride ions. In 2 M perchloric acid and low zirconium concentrations the average zirconium species was found to have somewhere between zero and one hydroxide group attached. Certainly, zirconium and hafnium in such solutions form species with the same structure and which have almost the same equilibrium constants. The distribution coefficient D is nearly independent of the hydrogen ion concentration over a wide range at 0.50 M hydrofluoric acid (Fig. 2). For that reason no changes in the oxide or hydroxide ion content of the complexes seem to be probable in this range. As shown above, the same is true for the halogen ions.

From the statements given in the preceeding section it may be assumed that, except for the hydration water, no other ligands than the fluoride ions are included in the complexes. Chloride and hydroxide ions are certainly exchanged for fluoride ions even at a very low fluoride ion concentration.

In the calculations above the activity coefficients have been neglected. The reason for this is the difficulty of getting any information about the activity coefficients of the species in the resin phase. This fact makes the results approximate and the constants valid only for the conditions under which the experiments were made. However, the good agreement between the observed and calculated values for the distribution coefficients D seems to support the method of calculation used.

From experimental data, obtained with such high accuracy and skill as those published by HUFFMAN and LILLY and used in this study, it should be possible to get valuable information for the separation of different elements by ion exchange. Thus the results of this study have been used for an investigation of the optimum conditions for the separation of zirconium and hafnium by anion exchange [7], based on the method first reported by KRAUS and MOORE [13] and by HUFFMAN and LILLY [14], in which mixtures of hydrochloric and hydrofluoric acids are used as elutriants.

Acknowledgements

The author wishes to express his gratitude to the Swedish Atomic Committee for permission to publish this paper.

I am greatly indebted to the Head of the Nobel Institute of Physics, Professor MANNE SIEGBAHN, for his neverfailing kindness in providing laboratory facilities, and to Professor ARNE ÖLANDER for his kind interest in this work.

I also want to express my thanks to Dr. LARS MELANDER and to Civ.ing. LENNART W. HOLM for valuable discussions.

Nobel Institute of Physics, Stockholm 50, Sweden.

REFERENCES

1. E. H. HUFFMAN and R. C. LILLY, J. Am. Chem. Soc. *73*, 2902, 1951.
2. K. A. KRAUS and G. E. MOORE, J. Am. Chem. Soc. *73*, 9, 1951.
3. S. W. MAYER and E. R. TOMPKINS, J. Am. Chem. Soc. *69*, 2866, 1947.
4. B. H. KETELLE and G. E. BOYD, J. Am. Chem. Soc. *69*, 2800, 1947.
5. H. P. GREGOR, J. Am. Chem. Soc. *73*, 642, 1951.
6. R. KUNIN and F. MCGARVEY, Ind. Eng. Chem. *41*, 1265, 1949.
7. W. FORSLING, Arkiv för kemi, *5*, 503, 1953.
8. T. R. E. KRESSMAN and J. A. KITCHENER, J. Chem. Soc. *1949*, 1201.
9. J. F. DUNCAN and B. A. J. LISTER, Disc. Farad. Soc. *No 7*, 104, 1949.
10. G. C. HAMPSON and L. PAULING, J. Am. Chem. Soc. *60*, 2702, 1938.
11. W. PAULI and M. ADOLF, Kolloid-Z. *29*, 178, 1921.
12. R. E. CONNICK and W. H. MCVEY, J. Am. Chem. Soc. *71*, 3182, 1949.
13. K. A. KRAUS and G. E. MOORE, J. Am. Chem. Soc. *71*, 3263, 1949.
14. E. H. HUFFMAN and R. C. LILLY, J. Am. Chem. Soc. *71*, 4147, 1949.

Tryckt den 9 april 1953

Uppsala 1953. Almqvist & Wiksells Boktryckeri AB

ARKIV FÖR KEMI Band 5 nr 46

Communicated 12 March 1952 by Manne Siegbahn and Arne Westgren

On the purification of zirconium from hafnium by anion exchange in hydrochloric and hydrofluoric acid mixtures

By Wilhelm Forsling

With 7 figures in the text

Abstract

A radiochemical investigation has been made of suitable conditions for the separation of zirconium from hafnium by anion exchange in hydrochloric and hydrofluoric acid mixtures. The main object of this work was to study the possibility of purifying zirconium from such amounts of hafnium, as generally occur together with zirconium in nature. A relatively high weight of zirconium per unit of weight of anion exchanger was used. It was intended that the process should be useful in practice, and for this reason for instance very low acid concentrations were to be preferred. 98% of a zirconium amount of about 100 mg per cm^2 of cross-sectional column area could be obtained completely free from hafnium in a single column operation. The anion exchanger used was Amberlite IRA–400.

Earlier methods used for the separation of zirconium and hafnium

Much work has been done on the problem of separating zirconium and hafnium. In 1923 and the next few years in particular von Hevesy and his coworkers, who were studying the chemistry of hafnium, tried several methods, most of which were fractional crystallizations of different salts of the elements (1). A contributive reason for the rather extensive work in this field was the interest of the incandescent lamp industry in this project. In the 1940's the problem became of new interest because of applications concerned with the development of atomic energy (2).

All fractional precipitation and crystallization methods require tedious repeated operations. Nowadays more effective methods are used, since good adsorption substances, ion exchange resins and excellent complex compounds for extractions, are at our disposal. Some of the methods used for the separation of zirconium and hafnium will be mentioned briefly.

Fractional precipitation methods

The pH at which hafnium hydroxide precipitates is higher than that at which zirconium hydroxide precipitates in nitrate and chloride solutions at equivalent concentrations. This fact was first used by von Hevesy (3) and recently studied by LARSEN and GAMMILL (4) with electrometric titrations. On the contrary in sulphate solutions, hafnium hydroxide precipitates at a lower pH than zirconium hydroxide. In both cases the difference is small. A better method is the fractional precipitation of the phosphates (5, 6, 7). However, the precipitates are inconvenient to handle and not readily converted into other compounds.

Some investigators have suggested the fractional precipitation of the ferrocyanides (8, 9), which seems to be a rather good method for the enrichment of hafnium from a mixture of the two elements.

Fractional crystallization methods

The best fractional crystallization method seems to be the one in which double ammonium and potassium fluorides are used (10). Hafnium is thereby enriched in the mother liquor. The use of other halogen or oxyhalogen compounds for crystallizations does not appear to be suitable.

Distillation methods

VON HEVESY also examined the method of fractional distillation of the chlorides (3, 11), of which the zirconium compound is the most volatile. The difference in volatility is, however, very small, and the method was inferior to the best fractional crystallization methods. Better results are gained from fractional distillation of the volatile complex compounds formed by the reactions of zirconium and hafnium tetrachlorides with phosphorus oxychloride (12). The method has recently been studied further by GRUEN and KATZ (13). They give boiling points of $360° \pm 1°$ C and $355° \pm 1°$ C for the zirconium and hafnium compounds respectively.

Extraction methods

The distribution of the zirconium and hafnium thiocyanate complexes between ether and water has been investigated by FISCHER and CHALYBAEUS (14). During the last few years the greatest interest in extraction methods has been in separation with thenoyltrifluoroacetone (TTA) between benzene and water. The distribution ratios were studied by HUFFMAN and BEAUFAIT (15) from 2 M perchloric acid with TTA at different concentrations. Zirconium is enriched in the benzene phase. SCHULTZ and LARSEN (16) made a similar investigation of the extraction separation with TTA from 0.2 M hydrochloric acid solution. In six extractions, the concentration of hafnium was increased from 7.5 to 99.98 mol %, with 37.6% yield of the original hafnium, which element was enriched in the aqueous phase.

Adsorption methods

Adsorption on silica gel was studied by HANSEN and GUNNAR (17, 18), who discovered that hafnium is absorbed with preference from a methanol solution of the chlorides. They recommend their method for preparing starting material for liquid-liquid extractions.

Ion exchange methods

STREET and SEABORG (19) were the first to report an effective cation exchange method for the separation of small amounts of hafnium and zirconium. They used the resin Dowex 50 with 6 M hydrochloric acid as elutriant. They got two peaks in their elution curves, the first of which corresponded mainly to hafnium and the second mainly to zirconium. About 70% of the hafnium was obtained with a contamination of only 0.1% by weight of zirconium. Very recently LISTER (20) published a separation method using cation exchange resins (Dowex 50 and Zeocarb 225). He tried several acids as elutriants, the most useful of which was sulphuric acid. He considered it possible to get a perfect separation of hafnium and zirconium even at high concentrations by varying the acid concentration during the elution.

Investigations on the possibility of using strongly basic anion exchange resins for the separation of zirconium and hafnium were performed by KRAUS and MOORE (21) and by HUFFMAN and LILLY (22). They used mixtures of hydrochloric and hydrofluoric acids as elutriants. The last mentioned investigators got a good result, as 70% of the total zirconium could be obtained free from hafnium. 83% of the hafnium contained only 0.03% of zirconium.

Shortly after the publication of these papers on anion exchange separations, we had need of very pure zirconium at this institute, and the author decided to study the conditions for its separation from hafnium at low acid concentrations. During the investigation some papers have been published on similar problems. KRAUS and MOORE (23) have studied the anion exchange separation of zirconium and niobium in hydrochloric and hydrofluoric acid mixtures. They used an automatic scanner for locating the activities in the column and determined the elution rates of the complexes in order to interpret the data in terms of ionic equilibria. Some months afterwards HUFFMAN and LILLY (24) published a similar investigation of the distribution coefficient of zirconium and hafnium complexes between the resin and the solutions of mixtures of hydrofluoric and hydrochloric acids in contact with it. The results of this investigation have been discussed by the present author (25). Lately HUFFMAN, IDDINGS, and LILLY (26) have studied the anion exchange of zirconium, hafnium, niobium, and tantalum in hydrochloric acid solutions. However, for determining the optimum conditions for the separation of zirconium and hafnium in different amounts with anion exchange resins very few data are available.

Experimental procedure

Preparations of the zirconium and hafnium samples

The sample used for this work was zirconium(IV)oxide, which had not been purified from contaminating hafnium(IV)oxide before pile irradiation at Harwell. The long-lived radioactive isotopes formed by the neutron bombardment were mainly Hf^{181} and Zr^{95}, with its daughter activity Nb^{95}. The daughter activity of Hf^{181} is Ta^{181*}, which has a half life of only about 20 μs (27).

The sample was purified from other elements in the following way. The finely ground oxide powder together with carriers of titanium and niobium was fused with sodium peroxide according to the procedure described by FURMAN (28). The cooled melt was then dissolved in warm water and the acidified clear solution boiled until all carbon dioxide was expelled, after which calcium and iron were added as carriers. The separation of zirconium and hafnium from other elements as secondary phosphates in strongly acid solution was carried out according to the procedure described by HILLEBRAND and LUNDELL (29). The phosphates from this process were fused with sodium carbonate, the cooled melt was extracted with water, and the insoluble residue filtered, washed and ignited before fusing with pyrosulphate as described by HILLEBRAND and LUNDELL (29). The melt was dissolved in dilute sulphuric acid, boiled and precipitated with ammonia. The hydroxides were centrifuged, washed three times with water, filtered, and ignited to oxides. The oxides were dissolved in a platinum dish with hydrofluoric and nitric acids, and a small amount of sulphuric acid added. The solution was evaporated to a few milliliters, diluted with water, filtered, and reprecipitated with ammonia. The precipitate was washed and centrifuged two times with water.

The rather elaborate purification process just described was carried out in order to avoid participation in the anion exchange procedure of elements other than zirconium, hafnium and their decay products. It was however found from the direct scanning of the column, and β-spectrometric measurements, that the result of the purification in the anion exchanger was just the same as if the following much simpler procedure was used. The original sample of zirconium and hafnium oxides were directly dissolved in hydrofluoric and nitric acids, the solution evaporated to a small volume after the addition of sulphuric acid. It was then diluted with water, and the hydroxides precipitated with ammonia. The precipitate was finally washed two times with water before being dissolved in the adsorption liquid.

This simple purification procedure proved to be sufficient for obtaining pure zirconium and hafnium compounds from the exchange column. The check of complete purification was however necessary to make it possible to use a simple analytical method to estimate the fractions of the effluent solution from the column.

The anion exchange resin

The resin used in these experiments was the chloride form of the strongly basic Amberlite IRA–400, a cross-linked quaternary amine polymer, which was air-dried, ground in a ball mill, and dry sieved to obtain the desired mesh size. After repeated washings of the exchanger with water in large beakers, any remaining small adhering particles were removed by decanting. The mesh size of the particles used in most of the experiments was $-200+300$. Other sizes were also tried, however, without improving the results.

The anion exchange column

The column, shown in Fig. 1, was made of polystyrene tubes tightly joined together by sleeves of the same material by the use of toluene as solvent. The lower end of the tube was fitted with a polystyrene cap having a capillary tip. The resin was supported by a cotton plug at the bottom of the column. The bed length used was about 100 cm, and the cross-sectional area of the column was 2.0 cm².

During the elution the tube was continuously filled to a fixed liquid level with influent from a storage bottle, the inside of which was coated with paraffin.

The flow rate of the effluent from the capillary tip was adjusted by a short length of rubber tubing fitted with a screw clamp. All studies were conducted at room temperature, about 20° C.

The column operation

The following is an example of the column operation used. 2.0 ml of 21 M hydrofluoric acid was added to the purified, washed, and centrifuged hydroxides corres-

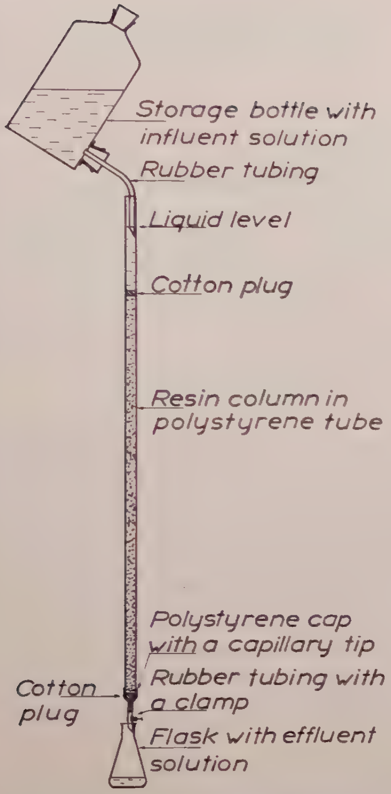
Storage bottle with influent solution
Rubber tubing
Liquid level
Cotton plug
Resin column in polystyrene tube
Polystyrene cap with a capillary tip
Rubber tubing with a clamp
Cotton plug
Flask with effluent solution

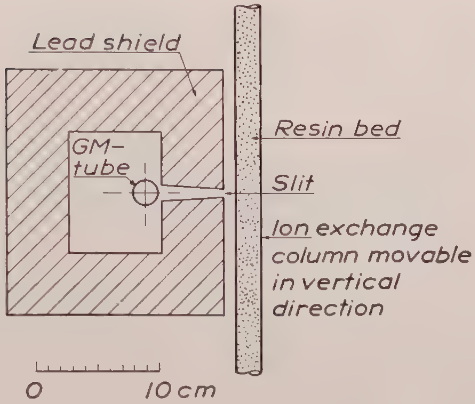
Lead shield
GM-tube
Resin bed
Slit
Ion exchange column movable in vertical direction
0
10 cm

Fig. 2. Measuring device for the direct scanning of the column.

Fig 1. The column apparatus. The simple arrangement for continuously feeding in the influent solution ensures a constant liquid head.

ponding to about 0.4 g of the oxides. The solution was diluted to 10 ml with 0.2 M hydrochloric acid in a Lusteroid tube. It was then centrifuged and decanted to another tube. 1.0 g of air-dried anion exchange resin was added, and the tube closed with a rubber stopper and shaken for one hour in a shaking-machine. The mixture was centrifuged and decanted. About 60% of the radioactivity from the acid solution was now found in the resin. This was slurried onto the top of the anion exchange column, through which some hundred milliliters of the elutriant solution had previously been run.

In order to get an even layer, the resin containing the sorbed complexes was allowed to settle in a 10 cm liquid column of elutriant solution over the resin bed. In this way it was also washed free from most of the strong hydrofluoric acid solution left in the resin after the sorption procedure. In order to remove the washing solution from the column without destroying the radioactive resin layer at the top of the resin bed, a wet cotton plug was carefully pushed down to the resin, and the supernatant solution sucked off. Immediately afterwards new elutriant solution was added. The cotton plug now once more prevented disturbance of the resin layer. During the part of the column operation just described a relatively high flow rate (~ 0.2 ml/cm^2 min) of the elutriant was used in order to obtain a dense top resin layer in a rather short time. Thereafter the flow rate was immediately reduced to about 0.10 ml/cm^2 min and this rate was maintained throughout the rest of the column operation.

The analytical procedures

The location of the sorbed complexes of zirconium, hafnium and niobium in the resin was determined from the γ-radiations accompanying the decays of Zr^{95}, Hf^{181} and Nb^{95} (27). A Geiger-Müller tube of cylindrical type (Sylvania GG–304) connected to a pre-amplifier and a counting-rate meter (General Radio Co., Mass. U.S.A., type no 1500-A) was used for this purpose. The GM-tube was surrounded by 5 cm of lead in which was a horizontal slit 6 mm wide (see Fig. 2). The ion exchange column was mounted in such a way that it could easily be moved vertically by the use of a rack mechanism. The distance between the tube and the slit was 1 cm. The whole length of the column was scanned several times during each column run. In this way it was possible to follow the separations during the elution and to find when the different complexes could be expected in the effluent solution.

The effluent was collected in appropriate fractions in flasks paraffined on the inside. After evaporation of the solutions, the oxides of zirconium and hafnium were prepared and then qualitatively analyzed in a magnetic lens β-spectrometer. The specific γ-activities were calculated from measurements on pure 10 ml fractions of zirconium and hafnium solutions with a GM-counter arrangement (for hafnium after repeated column separations of the hafnium fractions). It was now possible to determine the percentage of zirconium and hafnium in the effluent fractions in a simple way from γ-activity measurements and by weighing the oxide from these fractions.

The influence of the elutriant concentrations

To find the optimum conditions for the separation, the elution rates of zirconium and hafnium must be studied as functions of the hydrochloric and hydrofluoric acid concentrations of the elutriant. Both chloride and fluoride ions give complexes with zirconium and hafnium in solution. The chloride ion only forms weak cationic complexes in low concentrations, however, while the fluoride ion has a very strong complexing power (30).

In order to get complex anions in hydrochloric acid solutions, concentrations of 9–13 M hydrochloric acid are necessary (26). Elutriants of such high acid concentrations are inconvenient to handle and will be used only if they give obviously better separation than more manageable solutions. In this study hydrochloric acid was used only for preventing hydrolysis of the metal ions to insoluble products. For this purpose 0.2 M acid was sufficient (4, 17).

It is improbable that any higher concentration range of hydrochloric acid is of advantage for the separation of zirconium and hafnium in the presence of hydrofluoric acid. At a very high concentration of pure hydrochloric acid in the elutriant, where complex anions of zirconium and hafnium are formed, hafnium contrary to the case for fluoride complexes, is eluted before zirconium, as was shown by HUFFMAN, IDDINGS, and LILLY (26). At intermediate concentrations of hydrochloric acid, mixed complexes with chloride and fluoride ligands can be formed if the fluoride ion concentration is sufficiently low not to displace the chloride from the complexes. Such concentration ranges must be the least convenient for separation, as two effects then operate in opposite directions.

The chloride ion concentration has a great influence on the elution rate of the fluorocomplexes formed in elutriants containing hydrochloric and hydrofluoric acids. The chloride ion competes with the complex anions for the active groups of the ion exchange resin. At a high chloride ion concentration, therefore, the elution rate of the complexes is also high. Hydrofluoric acid does not give this marked effect as it is a relatively weak acid.

For zirconium in hydrochloric and hydrofluoric acid mixtures KRAUS and MOORE (23) studied the elution coefficient E, defined by the equation

$$E = \frac{d\,A}{V},$$

where d is the distance in cm a band maximum travels after V ml of elutriant have passed through a column of cross-sectional area A cm². KRAUS and MOORE used the anion exchanger Dowex 1. Their experimental values are few, and were obtained at high acidities. HUFFMAN and LILLY (24) made similar experiments with the resin Amberlite IRA 400 in a low acid concentration range. They studied the elution rate of very small amounts of hafnium as a function of the hydrofluoric and hydrochloric acid concentrations.

From the experimental data thus obtained it is possible to explain the elution mechanism by making simple assumptions about the equilibria between fluorocomplexes and hydrofluoric acid in the elutriant (25). It can be assumed that the complexes ZrF_4, ZrF_5^-, ZrF_6^{2-}, HfF_4, HfF_5, and HfF_6^{2-} exist in solutions used for instance by HUFFMAN and LILLY (24) in their separation of small amounts of zirconium and hafnium by anion exchange. At a sufficiently low hydrofluoric acid concentration most zirconium and hafnium certainly occur as central atoms in cationic complexes (30). In this range anion exchangers cannot, of course, be used for separation, and for that reason the positive complexes formed are not discussed further in the following.

For elutriants containing 0.23 M hydrochloric acid and varying hydrofluoric acid concentration, the approximate distribution of small amounts of hafnium between different complexes in the solution and in the resin phase is seen from Fig. 3. The mole percentages of the different complexes are obtained from calculations made by the present author (25) from the experimental data given by HUFFMAN and LILLY (24). It has been assumed that the concentrations in the resin phase of uncharged and positively charged complexes can be neglected in comparison with the concentrations of negatively charged complexes (cf. ref. 25 p. 500).

As is seen from Fig. 3, about 95% of the hafnium occurs as the bivalent negative complex fluoroion when the elutriant consists of 0.23 M hydrochloric acid and 0.20 M hydrofluoric acid. At increasing hydrofluoric acid concentration this percentage increases to almost 100%. Over a wide concentration range of hydrofluoric acid the elution rate of hafnium is thus almost entirely dependent on the elution rate of the bivalent negative complex ion. A trivalent complex ion of hafnium and fluoride does not seem to be formed in solutions up to about 4 M in hydrofluoric acid. Possible variations in the elution rate in this range are mainly due to variations in the chloride ion concentration.

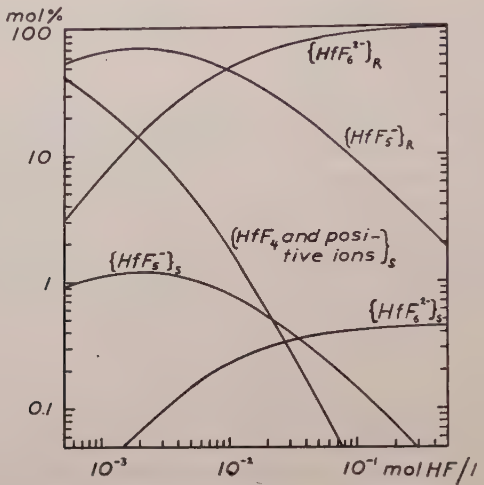

Fig. 3. The mole percentage of the different hafniumfluorocomplexes as a function of the hydrofluoric acid concentration of the elutriant containing 0.23 M hydrochloric acid. The subscripts R and S denote resin (Amberlite IRA–400) and solution phase respectively. Calculations made by the author (25) from experimental data given by Huffman and Lilly (24).

The dependence of the elution rates of hafnium on the hydrochloric and hydrofluoric acid concentrations is illustrated in another paper (25). From the data presented there it is possible to calculate approximate elution rates for small amounts of hafnium in hydrochloric and hydrofluoric acid mixtures over a wide acid concentration range.

In order to study the separation conditions for zirconium and hafnium in micro amounts it would be of interest to compare the curves in Fig. 3 for hafnium with the corresponding curves for zirconium. Sufficient experimental data are however not available. As the difference in the elution rates of zirconium and hafnium is very small, such experiments have to be made with high accuracy, if the experimental errors should not give a wrong picture of the variations in the ratio between the elution coefficients for the two closely related elements. For separations of large amounts of these elements, some other effects on the elution rates must be considered. These are difficult to survey, and for that reason comparisons of distribution curves as mentioned above are in this case of relatively small practical value, for operations at non-equilibrium conditions. The curves in Fig. 3 are however of importance in that they give a good idea of in which concentration range the different fluorocomplexes are formed, and thus where changes in the ratio between the elution coefficients for zirconium and hafnium may be expected. It is for instance certainly not worth studying the conditions for the separation of relatively large amounts of zirconium and hafnium, by the method described in this paper, between 0.5 and 4.0 M hydrofluoric acid in the elutriant, since the complexes in solution are the same over all this range, and thus a constant ratio between the elution coefficients of zirconium and hafnium must be expected.

At high concentrations of zirconium and hafnium, polymer formation may be possible, especially at low acidity (30). This fact may cause a small displacement of the hydrofluoric concentration range in which no further fluoride ion is taken up by the hafnium and zirconium complexes. Although, as has been pointed out above, separation experiments made with tracer or milligram amounts give valuable information about which concentrations of fluoride ion are the most suitable, this will of course not exclude the necessity of experimental examination in those cases where the conditions prevailing are far from those of equilibrium conditions.

From what is mentioned above it follows that the hydrofluoric acid concentration range which is of interest for the study of the separation of zirconium from hafnium is about 10^{-5} M –0.2 M. If it should be found that complexes higher than the bivalent one are formed in strong hydrofluoric acid concentration, such concentrations would also be of interest. However, for practical purposes the use of such concentrations would involve serious disadvantages and would certainly not be generally applicable to the purification of zirconium from hafnium, even if the separation, contrary to all expectation, should be quite quantitative in one passage through the ion exchange column. The increased advantages would not correspond to the increased disadvantages.

In this study the elutriants used contained 0.22 M hydrochloric acid. The hydrofluoric acid concentration has mainly been varied in the low acid range mentioned in the previous section. Especially in the higher part of this range where the elution rate was inconveniently slow, a higher chloride ion concentration, increasing the elution rate, would have been desirable. However, for better comparisons between the different column runs, the hydrochloric acid concentration was kept constant. If the acidity is increased the complex formation is restrained, while the fluoride ion concentration in the solution is diminished, since hydrofluoric acid is a rather weak acid. An increase in the elution rate by the addition to the elutriant of chloride ion in the form of sodium chloride, or any other salt, of course necessitates a further purification of zirconium after the column operation.

Some details concerning the sorption procedure which was described on page 507 will be pointed out. The hydrofluoric acid added to the hydroxides of zirconium and hafnium ought to be present in such an excess that bivalent negative complex ions are predominant in the solution shaken with the ion exchanger. The percentage of the sorbed complexes is increased with the concentration of the complexes in the solution. The concentration of added hydrochloric acid ought to be very low. If very small resin particle sizes are used, the washing of the resin containing the sorbed complexes is rendered difficult because of the rapid desorption, caused by the decomposition of the complexes. To diminish this effect it was convenient to use a resin of relatively large particle size for this sorption process, even in those cases where the column resin was very fine-grained.

Results

The author has studied the purification of zirconium from hafnium with elutriants containing 0.22 ± 0.01 M hydrochloric acid and hydrofluoric acid in the following concentrations: 0.02, 0.01, 0.008, 0.005, 0.004, 0.003, 0.002, 0.0008, 0.0002, 0.00008 and 0.00002 mol/l.

From these experiments it was found that no essential change in the results of the separation could be obtained by alteration of the hydrofluoric acid concentration of the elutriant. This statement involves a negative result in regard to the expectations of a complete separation, but it is by no means unexpected. The experimental

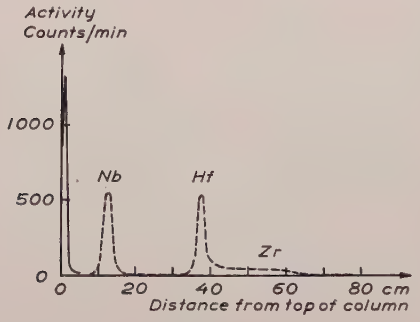

Fig. 4.

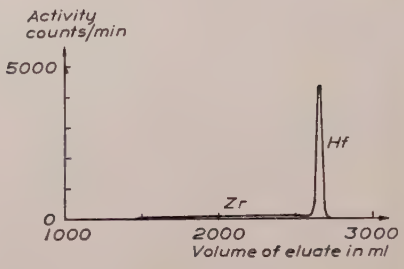

Fig. 5.

Fig. 4. A determination of the positions of zirconium, hafnium, and niobium, by scanning the column during the elution. The peak to the left shows the activity of the elements sorbed at the top of the column. The dashed curve shows the positions when 1375 ml of elutriant have passed through the column. For experimental data see the text of Fig. 6.

Fig. 5. Elution curve for zirconium and hafnium. The γ-activities measured from 10 ml fractions are plotted against the volume of eluate. For experimental data see the text of Fig. 6.

series, has, however, given useful information about suitable conditions for the purification of zirconium from hafnium.

The measurement of the radioactivity of the complexes during the elution as described on page 508 was of great value. In this way it was possible to study the velocity with which the sorption bands moved down the column and to calculate at what times the eluted complexes could be expected in the effluent solution. It was also easy to study the influence of the flow rate on the broadening of the bands during the elution. When a mesh size of $-200+300$ of Amberlite IRA–400 was used, it was found that the maximum flow rate suitable for the separation was about 0.15 ml/cm^2 min. However, even if the band width of hafnium had grown rather great because of a too rapid flow rate, it was easily reduced by a sufficient decrease of the flow rate during the last part of the column operation. In this way the boundary between zirconium and hafnium was made sharper, and in consequence more zirconium was freed from hafnium.

The advantage of using γ-activity for studying the band positions in the column is that no parts of the column walls need to be extremely thin, and the experiments can therefore be carried out in a simple manner. For very accurate measurements, however, the counting of the β-particles from the radioactive nuclides is more convenient.

A disadvantage of scanning the pile irradiated zirconium, containing Zr^{95}, was that the specific activity of zirconium in comparison with that of hafnium was very low. For that reason the front of the zirconium band during the elution could not be determined with accuracy (cf. Fig. 4). In the measurements of the eluate fractions however the low specific activity of zirconium could be compensated by a higher geometrical efficiency. In this way the front could be accurately determined.

In Fig. 4 the measurement of the band positions in the column is illustrated. The peak to the left shows the position of zirconium, hafnium and niobium sorbed at the top of the column after 30 ml of elutriant containing 0.005 M hydrofluoric acid have passed the band in order to wash out the excess of hydrofluoric acid

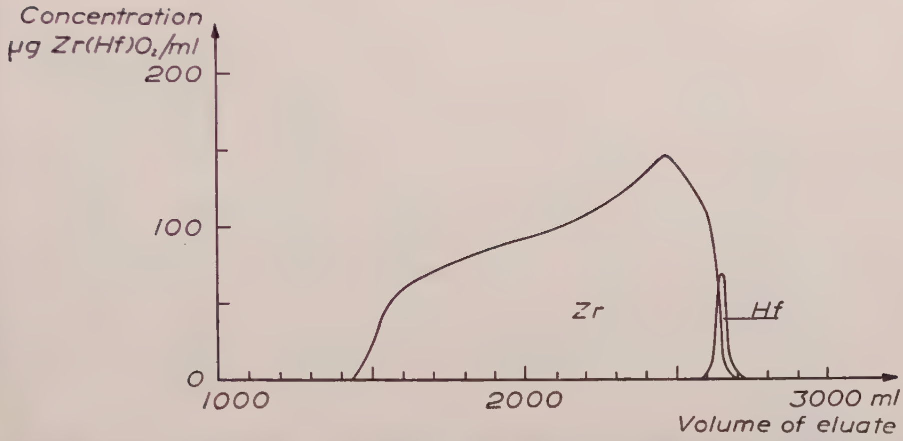

Fig. 6. Elution curves for zirconium and hafnium. Sample: 115 mg of oxides containing 2.7% HfO_2; resin: Amberlite IRA-400 of mesh size $-200+300$; bed dimensions: 97 cm × 2.00 cm^2; elutriant: 0.22 M HCl and 0.005 M HF; flow rate: about 0.10 ml/cm^2 min. The operation was carried out at room temperature.

which still remained in the top resin. The dashed curve shows the positions of the activities when 1375 ml more of the elutriant have passed through the column with a flow rate of 0.10 ml/cm^2 min. The length of the column was 97 cm in this run.

Fig. 5 shows elution curve for the experiment illustrated in Fig. 4. The activity measurements on fractions of the effluent were made with the same geometry for both zirconium and hafnium. From the analysis of these fractions described on page 508 the elution curve in Fig. 6 was then plotted.

The experiment illustrated in Figs. 4, 5, and 6 was carried out with 115 mg of zirconium oxide containing 2.7% of hafnium oxide.

The other separation experiments with different hydrofluoric acid concentrations in the elutriants gave very similar results. It was indeed impossible to find any significant difference in the results due to changes in the elutriant concentration, other than the increasing elution rates at decreasing hydrofluoric acid concentration. Some apparent exceptions even to this rule were however observed. The front of the elution band of zirconium did not always appear in the effluent fraction expected from the runs with lower and with higher hydrofluoric acid concentrations. With a relatively large column load the influence of the excess of fluoride present in the bivalent complexes sorbed at the top of the column was so great that the first part of the band movement was distinctly slowed down. This had of course important consequences, especially at the lowest hydrofluoric acid concentrations used. The concentration in the column was thus always somewhat higher than in the influent solution. The bed lengths used were however considerably longer than was really necessary for the separations obtained with the loads of zirconium and hafnium used. This fact was found from the direct scanning of the column and from a run with an ion exchange column 48 cm long, which gave a separation result similar to those obtained by columns with a length of about 100 cm. During the greater part of the column operation there was thus enough opportunity for a low hydrofluoric acid concentration of the influent to determine the separation result. The elution rate throughout most of the column run was therefore always higher in experiments with lower hydrofluoric acid concentration of the influent.

When choosing a suitable hydrofluoric acid concentration for the purification of zirconium from hafnium it will sometimes be necessary to study the possibility of a simultaneous separation of zirconium from other impurities. The problem is obviously simple when an anion exchanger is used for purification from elements which only form positive ions or cationic complexes in very weak hydrofluoric acid solutions.

For the purification of radioactive zirconium, which decays to niobium, it may be of interest also to separate zirconium from this daughter nuclide, which likewise forms anion complexes. From the experimental series described in this paper, it was found that the separation was easily carried out with elutriants of all concentrations used with the exception of 0.02 M hydrofluoric acid. At the other concentrations, the elution rate of niobium was always slower than that of zirconium and hafnium (cf. Fig. 4). This separation of zirconium and niobium has previously been described by KRAUS and MOORE (23), who, however, unnecessarily used much higher acid concentrations.

At the column runs with 0.0002 M hydrofluoric acid, or still lower concentrations, it was found from the scanning of the column that part of the activity remained at the top of the bed. By analysis in the β-spectrometer it was possible to identify this activity as belonging only to niobium.

For the recovery of zirconium it is of advantage that the concentration of that element in the effluent should be as high as possible. A rapid separation and column run with just as good a result as that obtained from a slower separation is, of course also an advantage. For these reasons the purification of zirconium from hafnium at very low hydrofluoric acid concentration of the elutriant must be recommended. The elution curves for such a separation are shown in Fig. 7.

The amount of fluorocomplexes corresponding to 215 mg of zirconium oxide containing 2.7% hafnium oxide, which was sorbed on 1.75 g of air-dried resin, was purified in a column of 95 cm length. The influent used contained 0.00008 M hydrofluoric acid and 0.22 M hydrochloric acid. The flow rate used was at first about 0.15 ml/cm^2 min. When the hafnium band was 15 cm from the bottom of the column, the flow rate was decreased to about 0.04 ml/cm^2 min. The hafnium band was thus made sharper, as mentioned on page 512, and the separation was thereby improved. In this experiment 98% of the zirconium was completely purified from hafnium as determined by the β-spectrometer. This is an unusually good result in comparison with the results obtained in other attempts to achieve the same purpose, and described in the chemical literature.

Summing up, the purpose of this work was to study the conditions for the purification of zirconium from such amounts of hafnium as generally occur with zirconium in nature. The choice of the acid concentrations in the elutriants was based on the results of an investigation of the complex ion equilibria existing in such solutions (25).

Sufficient amounts of zirconium have been used to show the applicability of the method for practical purposes. The columns have however been more than twice as long as necessary for obtaining a good separation of the sample loads applied. This fact has facilitated the study of the influence of the elutriant composition on the separation results. In the low concentration range used the hydrofluoric acid concentration in the column was always somewhat higher than in the influent solution. This was due to the fluoride ion excess at the top of the column. The results, therefore, correspond only approximately to the values given for the hydrofluoric acid concentration of the influents.

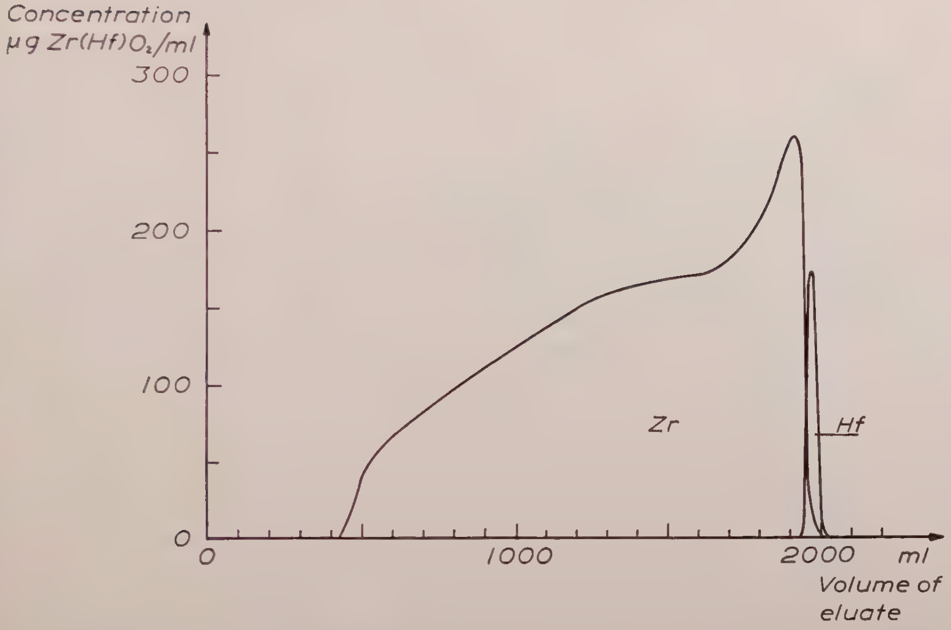

Fig. 7. Elution curves for zirconium and hafnium. Sample: 215 mg of oxides containing 2.7 % HfO_2; resin: Amberlite IRA–400 of mesh size −200 +300; bed dimensions: 95 cm × 2.00 cm^2; elutriant: 0.22 M HCl and 0.00008 M HF; flow rate: about 0.15 ml/cm^2 min, reduced to about 0.04 ml/cm^2 min during the movement of the Hf-band through the last 15 cm of the column. The experiment was carried out at room temperature.

From what is mentioned above, larger loads of zirconium per cm^2 of cross-sectional column area than those described in this paper could be purified without any change in the column length. Inactive zirconium can of course be purified from hafnium by this method, by adding for instance a small amount of radioactive hafnium to indicate the boundaries during the elution.

Acknowledgements

The author wishes to express his gratitude to Svenska Atomkommittén (The Swedish Atomic Committee) for permission to publish this paper.

I wish to thank the Head of the Nobel Institute of Physics, Professor MANNE SIEGBAHN, for his encouraging support and his putting of laboratory facilities to my disposal.

I am greatly indebted to Professor ARNE ÖLANDER for his kind interest in this work and to Professor HILDING SLÄTIS for his help with the β-spectrometer measurements.

My thanks are also due to Dr. LARS MELANDER and to Civ.ing. LENNART W. HOLM for valuable discussions and to Ing. LARS LUNDGREN for technical assistance.

Nobel Institute of Physics, Stockholm 50, Sweden.

REFERENCES

1. For a survey see:
   Gmelins Handbuch der anorganischen Chemie, 8 Aufl., System-Nummer 43: Hafnium, Berlin 1941, p. 9.
2. T. PIKE, Chem. Eng. News, *27*, 223, 1949.
3. G. VON HEVESY, Chem. News, *127*, 33, 1923.
4. E. M. LARSEN and A. M. GAMMILL, J. Am. Chem. Soc. *72,* 3615, 1950.
5. G. HEVESY and K. KIMURA, J. Am. Chem. Soc. *47*, 2540, 1925.
6. J. H. DE BOER and A. E. VAN ARKEL, Z. anorg. Chem. *148*, 84, 1925.
7. H. H. WILLARD and H. FREUND, Ind. Eng. Chem. Anal. Ed. *18*, 195, 1946.
8. W. PRANDTL, Z. anorg. allgem. Chem. *208*, 420, 1932; U.S. Patent 1, 976, 293, 1934.
9. W. C. SCHUMB and F. K. PITTMAN, Ind. Eng. Chem. Anal. Ed. *14*, 512, 1942.
10. G. VON HEVESY and V. T. JANTZEN, Chem. News, *127*, 353, 1923.
11. G. VON HEVESY, Das Element Hafnium, Berlin 1927, p. 11.
12. A. E. VAN ARKEL and J. H. DE BOER, Z. anorg. Chem. *141*, 289, 1924.
13. D. N. GRUEN and J. J. KATZ, J. Am. Chem. Soc. *71*, 3843, 1949.
14. W. FISCHER and W. CHALYBAEUS, Z. anorg. Chem. *255*, 79, 277, 1947.
15. E. H. HUFFMAN and L. J. BEAUFAIT, J. Am. Chem. Soc. *71*, 3179, 1949.
16. B. G. SCHULTZ and E. M. LARSEN, J. Am. Chem. Soc. *72*, 3610, 1950.
17. R. S. HANSEN and K. GUNNAR, J. Am. Chem. Soc. *71*, 4158, 1948.
18. R. S. HANSEN, K. GUNNAR, A. JACOBS, and C. R. SIMMONS, J. Am. Chem. Soc. *72*, 5043, 1950.
19. K. STREET, JR, and G. T. SEABORG, J. Am. Chem. Soc. *70*, 4268, 1948.
20. B. A. J. LISTER, J. Chem. Soc. *1951*, 3123.
21. K. A. KRAUS and G E. MOORE, J. Am. Chem. Soc. *71*, 3263, 1949.
22. E. H. HUFFMAN and R. C. LILLY, J. Am. Chem. Soc. *71*, 4147, 1949.
23. K. A. KRAUS and G. E. MOORE, J. Am. Chem. Soc. *73*, 9, 1951.
24. E. H. HUFFMAN and R. C. LILLY, J. Am. Chem. Soc. *73*, 2902, 1951.
25. W. FORSLING, Arkiv för Kemi *5*, 489, 1953.
26. E. H. HUFFMAN, G. M. IDDINGS, and R. C. LILLY, J. Am. Chem. Soc. *73*, 4474, 1951.
27. For detailed information see: Nuclear data (with supplements 1, 2, and 3) NBS Circular 499, Washington, 1950–1951.
28. N. H. FURMAN, editor, Scotts Standard Methods of Chemical Analysis, Vol. I, New York, 1939, p. 1095.
29. W. F. HILLEBRAND and G. E. F. LUNDELL, Applied Inorganic Analysis, New York, 1929, p. 447.
30. R. E. CONNICK and W. H. MCVEY, J. Am. Chem. Soc. *71*, 3182, 1949.

Tryckt den 9 april 1953

Uppsala 1953. Almqvist & Wiksells Boktryckeri AB

ARKIV FÖR KEMI Band 5 nr 47

Communicated 14 January 1953 by A. WESTGREN and G. HÄGG

Studies on the extraction of metal complexes. XI

A new method of determining very large and small distribution ratios

By JAN RYDBERG

With 3 figures in the text

The usual method of determining the distribution ratio of a compound between two immiscible solvents is to calculate it from direct measurements of the concentrations in both phases. When the distribution ratio is very low or very high, this method is limited to the minimum detectable amount of the compound. One of the most sensitive measurement methods is based on the use of radioactive tracers and has been used for the investigation of the extraction of metal chelate compounds from aqueous to organic solutions (1). Using equal phase volumes, it has been possible to determine distribution ratios between 10^{-3} and 10^{3} with a satisfactory degree of accuracy.

If the total amounts of the compound in the two phases are m_{org} and m_{aq}, and the volumes of the phases v_{org} and v_{aq}, the distribution ratio, q, of the metal between the two phases is

$$q = c_{\text{org}}/c_{\text{aq}} = m_{\text{org}} \cdot v_{\text{aq}}/m_{\text{aq}} \cdot v_{\text{org}}. \tag{1}$$

The ratio $v_{\text{aq}}/v_{\text{org}}$ can theoretically be increased to any value, which makes measurements on very large q-values possible. However, there are several practical limitations on the use of very large $v_{\text{aq}}/v_{\text{org}}$ ratios, especially when work is carried out on the laboratory scale: it must be possible to separate the two phases, one phase should not be completely dissolved by the other, etc. A ratio greater than 10^{3} is probably not practically feasible. If $q = 10^{3}$ can be measured when $v_{\text{aq}}/v_{\text{org}} = 1$, $q = 10^{6}$ should be obtainable with $v_{\text{aq}}/v_{\text{org}} = 10^{3}$. This should then be the practical maximum for measurable q-values. It should be pointed out that mutual solubilities of the two phases, interfering impurities, etc., must be carefully considered in an experiment like that.

However, in the case of metal chelates it will be possible to determine distribution ratios much larger than those mentioned above even with $v_{\text{aq}}/v_{\text{org}} = 1$. This possibility is based on the knowledge of the formation of the metal chelate complex in the aqueous phase, and the use of several different organic solvents. The theoretical background for this will be briefly outlined below.

The shape of the distribution function, $q = f(A)$

The chelating substance (HA), which forms the extractable compound with the metal (M; ionic charge $+z$), is usually a weak acid, and it is more or less dissociated in the aqueous phase (H^+, A^-). The distribution ratio (q) of the metal between the organic and aqueous phases will follow equation (2), if the only metal compound soluble in the organic phase is the uncharged MA_N (in this example $N = +z$), and no polynuclear or hydrolysis complexes of the metal are formed. Another condition for eqn (2) is that the organic solvent should not form any compound containing the metal atom.

$$q = \lambda_N \cdot \varkappa_N [A^-]^N / \sum_0^S \varkappa_n [A^-]^n. \tag{2}$$

S is the maximum number of ligands which can be bound to each metal atom. In this equation λ_N is the distribution constant of the uncharged complex,

$$\lambda_N = [MA_N]_{\text{org}} / [MA_N]_{\text{aq}}. \tag{3}$$

$\varkappa_n$ is called the complexity product (in other papers in this series "complex formation" is used with the same meaning as "complexity"), and it is defined by equation (4):

$$\varkappa_n = [MA_n^{+z-n}]/[M^{+z}][A^-]^n. \tag{4}$$

The calculation of $\varkappa_n$, λ_N and $[A^-]$ has been described elsewhere (2).[1]

In Figs. 1–3 log q is given as a function of log $[A^-]$. In the region where q is independent of $[A^-]$, the uncharged complex MA_N dominates over the charged ones, MA_n^{+z-n}, and according to equation (2) the value of q must be close to that of λ_N.

From eqn (2) it can be seen that the slope of the distribution curve will be independent of λ_N. In fact it can be shown (2) that the slope only is a function of the mean number ($\bar{n}$) of chelating molecules (ligands) per metal atom in the aqueous phase at any $[A^-]$ value:

$$\bar{n} - N = d \log q / d \log [A^-]. \tag{5}$$

This fact can be used to calculate the constants for the formation of MA_n^{+z-n} (2).

Distribution curves for different solvents

The value of λ_N depends on the type of the metal chelate formed and on the solvents. If the chelating substance HA is easily soluble in the organic phase, the metal chelate MA_N usually is still more soluble in it. If the chelate contains H_2O or OH-groups it is usually less soluble in the organic solvents. For λ_N values $> 10^3$ the corresponding q-values on the horizontal portion of the distribution curve (log q versus log $[A^-]$) will also be $> 10^3$, i.e. it will not be possible to measure these q-values as long as both phases are of equal volume.

Since the slope of the distribution curve only depends on what happens in the aqueous phase, it should be independent of the organic solvent. This should at least be true as long as the organic solvent does not react with the metal.

Figure 1 shows the distribution of U(VI) between water and three different organic solvents: benzene, chloroform and methyl isobutyl ketone (hexone). The chelating

---

[1] The symbols used in Parts I–IV have been somewhat changed in later parts of this series.

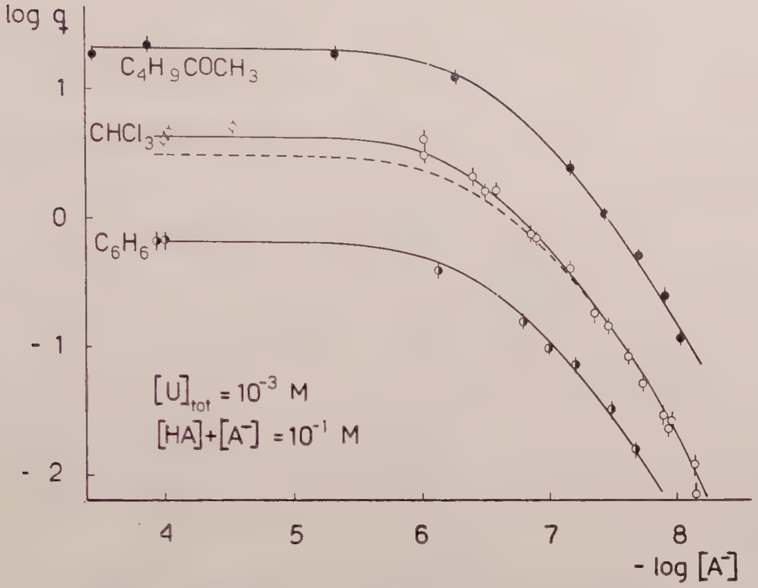

Fig. 1. The distribution (q) of U(VI) between different organic solvents and an aqueous 0.1 M $NaClO_4$ solution as a function of the acetylacetonate ion (A^-) concentration in the aqueous phase.

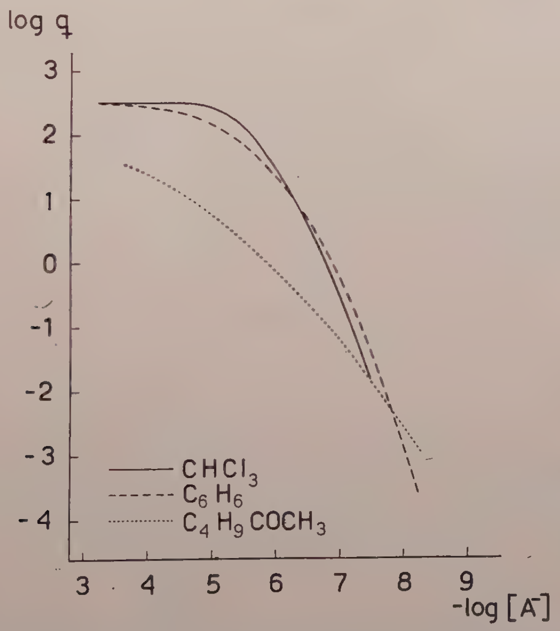

Fig. 2. The distribution (q) of Th(IV) between different organic solvents and an aqueous 0.1 M $NaClO_4$ solution as a function of the acetylacetonate ion (A^-) concentration in the aqueous phase.

agent is acetylacetone. The three curves are taken from Part XII in this series (1). The curves for benzene and hexone have the same slope at the same log [A$^-$] value. The dashed curve is that expected for chloroform, if the benzene and hexone curves are correct.

In Figure 2 (taken from Parts II (2), X (3) and XII (1)) the distribution for thorium acetylacetonates are given for the same solvents as above. Since different ionic strengths were used in the aqueous phases for benzene-water and chloroform-water, these curves are not expected to show exactly the same slope at the same log [A$^-$]. The curve for hexone-water is quite different from the other two, and this is probably due to reaction between the hexone and the thorium acetylacetonate. The differences between the curves are discussed in detail elsewhere (1).

Though there may be small deviations it may be concluded that the slopes of the curves agree within reasonable limits as long as the distribution curve can be completely explained by equation (2). It can be shown, that if the metal is hydrolysed and the degree of hydrolysation can be controlled, the distribution curves will show the same slope at any log [A$^-$] with different solvents. However, different slopes will be obtained with different organic solvents, if complexes containing more than one metal atom per molecule are formed, or if the organic solvents form compounds with the metal.

The determination of large distribution ratios

In Fig. 3 a number of imaginary curves has been drawn representing the expected distribution $q = f(\mathrm{A})$ for the organic solvents B, C, D, E and F. The curves have the same slope for constant log [A$^-$], i.e. the complex formation in the aqueous phase is the same. The fulldrawn parts of the curves can be experimentally determined, since they fall within the measurable q-region, $10^{-3} < q < 10^3$, for $v_{\mathrm{aq}} = v_{\mathrm{org}}$. If the distribution curve for the solvents H_2O-E had only been measured, it would not be possible to say anything about the value of the distribution constant for the uncharged complex, λ_N, except that it was greater than 10^3. However, if the curve for the solvents H_2O-C is known, it would then be possible to extrapolate (c.f. the broken line) the H_2O-E curve parallel to the H_2O-C curve up to log $q = 6$. According to the previous paragraph, q is equal to λ_N on the horizontal section; λ_N for the solvents H_2O-E is thus 10^6. It would be very difficult to measure such high q-values using different phase volumes. This extrapolation method is not limited to any λ_N-value as long as it is possible to get a complete curve for one organic solvent. With this method it is also possible to find very small distribution ratios. If the curve for H_2O-F is extrapolated parallel to the H_2O-E curve down to log [A$^-$] = —9, the distribution ratio q will be found to be about 10^{-11}.

If the first experiment gives a curve such as E in Fig. 3, one has to try a number of other solvents in which the metal chelate is less soluble, so that a curve such as F, B or C can be determined. However, one should try to keep to solvents with structures similar to E, primarily derivatives of E. It is often found that the addition of an aliphatic chain to an aromatic molecule changes the tendency of the solvent to dissolve other substances. The length of the carbon chain also influences the size of λ_N. Solvents such as C_6H_6, $CHCl_3$ and CCl_4 usually do not react with the metal chelates, but λ_N with these solvents rarely varies by more than a factor of 100.

If it is not possible to find a solvent, with which a horizontal section on the distribution curve is obtained, there is still a possibility of calculating λ_N for a curve of

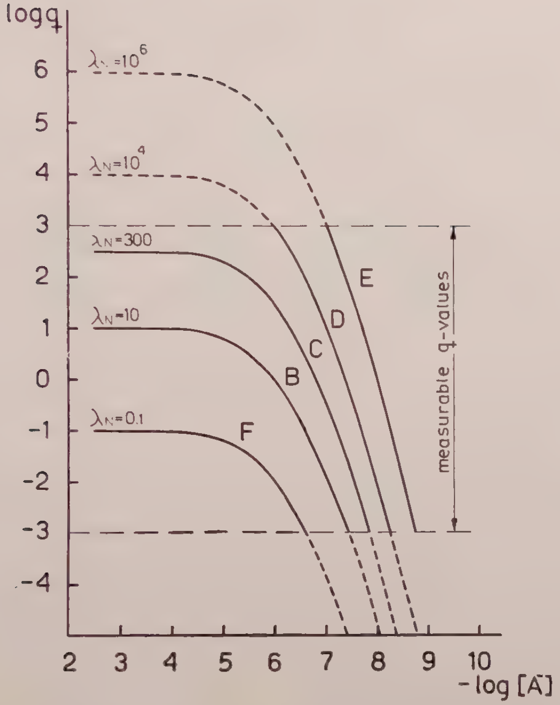

Fig. 3. Distribution curves for one complex system (ligand A^-) with different organic solvents (B–F; curve C is the true distribution curve for thorium acetylacetonate between benzene and water).

type E. This can be done from equation (2), if the complexity products, $\varkappa_n$, have been determined by some other method (e.g. potentiometric, spectrophotometric). One point of curve E should then theoretically be sufficient for a calculation of λ_N for solvents H_2O-E. When λ_N is known, distribution ratios corresponding to any arbitrarily chosen $[A^-]$ value can be obtained. Before such calculations are done, the validity of equation (2) for the system must be demonstrated.

SUMMARY

It is shown that, if the distribution ratio of a metal chelate between organic solvents and water is plotted against the concentration of the chelating anion, similar curves are obtained for different organic solvents. From the known distribution curve with one organic solvent, extrapolations can be made to other organic solvents, even if the distribution ratio of the metal chelate with these solvents is far beyond the measurable region. The method is limited to dilute aqueous solutions and such organic solvents, which do not react chemically with the metal chelate.

The author is indebted to the head of FOA 1, Prof G. Ljunggren, and Prof. L. G. Sillén for their continuous interest in these studies.

Research Institute of National Defence, Dept. 1, Sundbyberg 4, Sweden.

REFERENCES

1. (Part XII) J. Rydberg: to be published.
2. (Part II) J. Rydberg: Acta Chem. Scand. *4* (1950) 1503.
3. (Part X) J. Rydberg: Arkiv för Kemi *5* (1953) 413.

Tryckt den 8 april 1953

Uppsala 1953. Almqvist & Wiksells Boktryckeri AB

ARKIV FÖR KEMI Band 5 nr 48

Mitgeteilt am 12. November 1952 durch H. v. Euler und K. Myrbäck

Über Molekülverbindungen zwischen L-α-Aminosäuren und nicht-reduzierenden Zuckern

Von Ruth Weichert

In der letzten Zeit sind mehrere Arbeiten erschienen, die über papierchromatographische Spaltungen von razemischen α-Aminosäuren in optische Antipoden, ohne Verwendung von optisch aktiven Lösungsmitteln, berichten. Zwar beabsichtigten Kotake und Mitarbeiter (1) durch Verwendung von optisch aktiven Lösungsmitteln Razematspaltungen durchzuführen und erhielten bei Verwendung von L-Methyl-(β-phenylisopropyl)-amin in dem Lösungsmittelsystem Unterschiede in den R_f-Werten für D- und L-Form der Glutaminsäure, bzw. des Tyrosins, in Grössenordnungen von 0,02–0,03 und bei D- und L-Form der Tyrosin-3-sulfonsäure von 0,21. Im letzten Falle wurde das Razemat vollständig gespalten. Überraschenderweise zeigte es sich aber, dass dieselben Resultate bei der Verwendung von D- oder D,L-Form des Amins in dem Lösungsmittelsystem erhalten wurden. Mason und Berg (2), als auch Sensi (3), berichteten über verschiedene R_f-Werte von D- und L-Kynurenin, sowie vollständige Spaltung von D,L-Kynurenin bei Papierchromatographie. Dalgliesh (4, 5) zeigte, dass sowohl D,L-Kynurenin, wie D,L-3-Oxykynurenin papierchromatographische Antipodenspaltungen unterliegen, dagegen nicht D,L-N′-Formylkynurenin, D,L-N′-Acetylkynurenin und D,L-N^{α}-Acetylkynurenin. In allen angeführten Fällen wurden optisch inaktive Lösungsmittelsysteme verwendet, und die Ursache der Spaltungen muss also in optisch aktiven Bestandteilen des Papiers liegen.

Diese Arbeiten veranlassen mich von einer Untersuchung über Molekülverbindungen zwischen L-α-Aminosäuren und Rohrzucker zu berichten. Das Resultat der Untersuchung wird mit den Befunden von Dalgliesh, über die papierchromatographische Spaltung von D,L-Kynurenin und seinen Derivaten, diskutiert.

Die Spaltung des synthetischen Kynurenins wurde von Butenandt und Weichert (6) über eine Molekülverbindung mit Rohrzucker durchgeführt. Es zeigte sich, dass nur die L-Form des Kynurenins imstande ist, mit Rohrzucker eine kristallisierte Molekülverbindung zu geben, während die D-Form in Lösung bleibt. Es war von Interesse zu untersuchen, ob auch andere Verbindungen mit Aminogruppen, vor allem Aminosäuren, mit Rohrzucker Molekülverbindungen geben könnten und ebenso herauszufinden, welche Gruppen im Kynureninmolekül die Bindungen zum Rohrzucker verursachen. Da nur das L-Kynurenin eine kristallisierte Molekülverbindung mit Rohrzucker gibt, scheint die L-α-Aminosäuregruppierung notwendig zu sein.

Methodik

Die einfachste Methode, kristallisierte Molekülverbindungen nachzuweisen, ist die thermische Analyse, RHEINBOLDTS (7) „Auftau-Schmelzverfahren", aber da sie voraussetzt, dass die Komponenten ohne Zersetzung schmelzen, war sie im vorliegenden Falle unbrauchbar.

Es wurden daher zwei andere Verfahren verwendet um festzustellen, ob die zu prüfende Substanz mit dem Zucker eine Molekülverbindung gibt oder nicht:

1. Das eine Verfahren stützt sich auf die optische Aktivität des Zuckers. Die Bildung von Molekülverbindungen wird als eine reversible Reaktion betrachtet:

$$A + B \rightleftharpoons C.$$

In einer nicht allzu verdünnten Lösung der beiden Komponenten vereinigt sich ein gewisser Teil der Komponenten zu dem Komplexe C. Ist nun die eine Komponente, oder sind beide, optisch aktiv, so muss das Komplex C ebenfalls diese Eigenschaft besitzen; man wird daher im Falle der Komplexbildung mit grösster Wahrscheinlichkeit einen anderen Drehwert der Lösung erhalten, als wenn keine Komplexbildung stattfindet.

Die Versuche wurden folgendermassen ausgeführt: Ein bestimmtes Volumen einer Rohrzuckerlösung wurde mit derselben Menge Wasser gemischt und der Drehwert der Mischung bestimmt. Besass die auf Komplexbildung zu prüfende Substanz auch optische Aktivität, so wurde der Drehwert ihrer Lösung in derselben Weise gemessen. Dann wurden gleiche Volumina beider Lösungen gemischt und der Drehwert bestimmt.

Dieses Verfahren kann nur für Substanzen verwendet werden, die in irgend einem Lösungsmittel leicht löslich sind, da sonst die Konzentrationen zu gering werden und die Gefahr besteht, dass, auch wenn die beiden Substanzen eine Molekülverbindung geben können, diese vollständig in ihre Komponenten dissoziiert ist. Da Rohrzucker, die eine Komponente der vorliegenden Versuche, nur in Wasser leicht, in allen organischen Lösungsmitteln dagegen schwer löslich ist, konnte diese Methodik nur dann angewendet werden, wenn auch die zu prüfende Aminoverbindung in Wasser leicht löslich war. Letzteres war aber bei den meisten Verbindungen nicht der Fall.

2. Für die in Wasser schwer löslichen Substanzen wurde das Verfahren von DIMROTH und BAMBERGER (8) zur Herstellung von kristallisierten Molekülverbindungen im Mol-Verhältnis 1 : 1 verwendet.

DIMROTH hat folgende Beziehung aufgestellt:

$$K = \frac{(C)}{(A)\,(B)} = \frac{\{C\}}{\{A\}\,\{B\}} \cdot G$$

(A), (B) und (C) sind die Gleichgewichtskonzentrationen in der Lösung (in Mol pro Liter). $\{A\}$, $\{B\}$ und $\{C\}$ sind die Löslichkeiten (in Mol pro Liter): also die Konzentrationen der gesättigten Lösungen der einzelnen Stoffe A, B und C.

Die Gleichgewichtskonstante K ändert ihren Wert von Lösungsmittel zu Lösungsmittel. Die „Stabilitätskonstante" G ist dagegen vom Lösungsmittel unabhängig, und ist ein Mass der Stabilität der Molekülverbindung.

Schreibt man die Formel

$$\frac{(C)}{\{C\}} = \frac{(A)\,(B)}{\{A\}\,\{B\}} \cdot G,$$

so besagt diese: Ein Stoff C fällt aus einem beliebigen Lösungsmittel aus $\left[\frac{(C)}{\{C\}} = 1\right]$, wenn

$$\frac{(A)\,(B)}{\{A\}\,\{B\}} = \frac{1}{G}.$$

Ist $G < 1$, kann der Stoff C nur ausfallen, wenn die Lösung für wenigstens eine der Komponenten übersättigt ist. Ist $G = 1$, so ist C neben A und B dauernd stabil. Ist $G > 1$, so ist nur C dauernd stabil, während A und B als Bodenkörper nicht nebeneinander bestehen können. Je grösser G ist, desto grösser ist die Stabilität der Molekülverbindung.

In der Literatur über organische Molekülverbindungen wird oft die „zersetzende" Wirkung eines Lösungsmittels beschrieben, wenn eine Molekülverbindung mit steigenden Mengen eines Lösungsmittels übergossen wird. Hierzu sagt DIMROTH, dass wenn

$$\frac{\text{Löslichkeit der leichter löslichen Komponente}}{\text{Löslichkeit der schwerer löslichen Komponente}} < G$$

erfolgt keine Zersetzung; ist der Quotient $> G$, wird C zersetzt und die schwerer lösliche Komponente fällt aus.

Für die präparative Darstellung von Molekülverbindungen muss man also ein Lösungsmittel oder ein Lösungsmittelgemisch finden, in dem die Löslichkeiten der beiden Komponenten annähernd gleich sind, weil ja der Quotient der Löslichkeiten kleiner als G sein muss.

Ist G sehr klein, oder sind die Löslichkeiten der Komponenten so verschieden, dass man kein „nicht-zersetzendes" Lösungsmittel finden kann, so muss man einen Überschuss der leichter löslichen Komponente haben. Dieser Überschuss muss aber richtig berechnet sein, und DIMROTH zeigt, innerhalb welcher Grenzen er liegen darf: Wenn A die schwerlöslichere Komponente ist, also $\{B\} > \{A\}$, so muss der Überschuss von B sich innerhalb folgender Grenzen halten:

$$\text{Überschuss von } B > \frac{\{B\}}{G} - \{A\}, \text{ und } < \{B\} - \frac{\{A\}}{G}.$$

Um festzustellen, ob zwei Komponenten eine Molekülverbindung geben können, und um diese gleich zu isolieren, verfährt man in folgender Weise: Man sucht ein Lösungsmittel oder ein Lösungsmittelgemisch, in dem die molaren Löslichkeiten beider Stoffe so ähnlich wie möglich sind, trägt äquimolekulare Mengen von A und B ein und ausserdem ein Überschuss von B, der pro Liter $\{B\} - \{A\}$ sein soll. Die Menge $\{B\} - \{A\}$ liegt ja zwischen den Werten $\frac{\{B\}}{G} - \{A\}$ und $\{B\} - \frac{\{A\}}{G}$, wie oben die Forderungen für den Überschuss gestellt wurden. Man löst in der Wärme, wobei kein Lösungsmittel verdunsten darf, da sonst der Überschuss von B zu gross wird. Will man keine Löslichkeitsbestimmungen machen, kann man DIMROTHS

„allgemeines“ Verfahren anwenden: Ein gewisses Volumen des Lösungsmittels wird bei einer bestimmten Kristallisationstemperatur mit A gesättigt, ein gleiches Volumen mit B und die eine der beiden Lösungen wird zur Trockne eingedampft. Der Rückstand wird in der anderen Lösung gelöst, die jetzt einen Überschuss an B hat, der $\{B\} - \{A\}$ Mol pro Liter beträgt. Wenn $G > 1$, d. h. wenn eine stabile Molekülverbindung zwischen den Komponenten existiert, kristallisiert beim Abkühlen zur Kristallisationstemperatur C aus, ohne Beimengungen von A oder B. Ist nichts ausgefallen (bei kleinem G oder grosser Löslichkeit von C), setzt man äquimolekulare Mengen von A und B zu, löst in der Wärme und lässt abkühlen. Man erhält so reines C. Können die Komponenten dagegen keine Molekülverbindung geben, erhält man ein Gemenge von A und B. Durch mikroskopische Untersuchung der ausgefallenen Kristalle und einen Vergleich mit den Ausgangssubstanzen kann man leicht entscheiden, ob eine Molekülverbindung gebildet worden ist oder nicht.

Beim Arbeiten mit Aminosäuren als die eine Komponente hat DIMROTHs Methode leider Mängel. Als beste Lösungsmittelgemische, wo die Löslichkeitsunterschiede zwischen Rohrzucker und den Aminosäuren nicht allzu gross sind, wurden 80, 90 oder 95 % Äthanol oder Methanol verwendet. Der Rohrzuckerüberschuss soll $\{B\} - \{A\}$ sein, wobei $\{A\}$ die Löslichkeit diejenige Form der Aminosäure bedeutet, wie sie in der Molekülverbindung vorhanden ist; ob als Dipol oder undissoziiert ist unbekannt, und was man bei Löslichkeitsbestimmungen misst, ist die totale Konzentration der Aminosäure. Dass trotzdem diese Methode verwendet wurde, beruht auf die Schwierigkeit ein zuverlässiges und nicht allzu kompliziertes Verfahren zu finden. Die negativen Ergebnisse mit den meisten Aminosäure dieser Untersuchung schliessen nicht unbedingt Wechselwirkungen zwischen diesen Aminosäuren und Rohrzucker aus, besonders da die Methode weitere Einschrenkungen hat, nämlich *kristallisierte* Molekülverbindungen *im Verhältnis 1 : 1*.

Hat man eine razemische Aminosäure zu prüfen, von der evt. nur der L-Antipode mit Rohrzucker eine kristallisierte Molekülverbindung gibt, so werden die Verhältnisse noch komplizierter und die Möglichkeit, aus solchen Lösungen eine kristallisierte Molekülverbindung rein zu isolieren, sehr beschränkt. Anstelle von zwei Komponenten hat man hier drei, Rohrzucker (R), L-Form (L) und D-Form (D) der Aminosäure. L kann sich mit R zu RL, aber auch mit D zu DL verbinden und es gelten hier folgende zwei Gleichungen:

$$\frac{(RL)}{\{RL\}} = \frac{(L)\,(R)}{\{L\}\,\{R\}} \cdot G_{RL} \tag{1}$$

$$\frac{(DL)}{\{DL\}} = \frac{(D)\,(L)}{\{D\}\,\{L\}} \cdot G_{DL}.$$

In diesem Falle ist es günstiger ein Lösungsmittel zu wählen, in dem die Löslichkeit des Rohrzuckers erheblich grösser ist als die der Aminosäure, damit die Reaktion $(L)\ (R) \rightleftharpoons (RL)$ so weit wie möglich nach rechts verschoben wird.

In einer gesättigten Lösung einer razemischen Aminosäure erhält man $\left[\frac{(DL)}{\{DL\}} = 1\right]$:

$$\{D\} \cdot \{L\} = (D) \cdot (L) \cdot G_{DL}.$$

Da ein Razemat in Lösung in die Einzelkomponenten zerfallen ist, wird die Konzentration der D-, resp. L-Form gleich der halben Löslichkeit (a = g pro Liter/einfaches Molekülgewicht) der razemischen Aminosäure. Das Produkt $(D)\cdot(L)$ in gesättigter Lösung wird also $a^2/4$, und da $\{D\}=\{L\}$ ist, wird

$$\{L\}=a/2\sqrt{G_{DL}}.$$

Da G_{DL} bei echten Razematen grösser als 1 sein muss, ist die Löslichkeit der L-, resp. D-Form, immer grösser als die halbe Löslichkeit des Razemates.

Da aus einer Lösung mit Rohrzucker und Razemat nur die Molekülverbindung RL fallen soll, dagegen nicht DL oder D, müssen folgende Bedingungen erfüllt sein:

$$(D)\leqq\{D\} \tag{2}$$

$$(D)\,(L)\leqq a^2/4. \tag{3}$$

Wird der Wert $\{L\}=a/2\cdot\sqrt{G_{DL}}$ in Formel (1) eingeführt, erhält man

$$\frac{(RL)}{\{RL\}}=\frac{(L)\,(R)\,G_{RL}}{a/2\,\{R\}\sqrt{G_{DL}}}. \tag{4}$$

Nach den Bedingungen (2 und 3) muss $(L)\leqq a/2$. Das Glied $\frac{(L)}{a/2}$ in Formel (4) wird also $\leqq 1$, und wenn $G_{RL}<\sqrt{G_{DL}}$, kann $\frac{(RL)}{\{RL\}}$ nicht den Wert 1 erreichen, d. h. die Molekülverbindung nicht ausfallen, ohne dass die Lösung für Rohrzucker übersättigt ist. Ist $G_{RL}>\sqrt{G_{DL}}$ kann die Molekülverbindung ausfallen, aber nur wenn die Löslichkeit der Molekülverbindung gering ist, denn durch die Bedingungen (2 und 3) ist die Menge des zugesetzten Razemats beschränkt. Wie klein die Löslichkeit der Molekülverbindung sein muss, kann man in Formeln ausdrücken, aber da sie auf die Werte G_{RL} und $\sqrt{G_{DL}}$ beruhen, die man beide nicht kennt, hat es für die experimentelle Arbeit keinen Wert.

In einem Falle wurde eine razemische Aminosäure, nämlich D,L-Desoxokynurenin (9), als Komponente geprüft. Um die Löslichkeit der Antipoden dieser Aminosäure abschätzen zu können, wurde aus den bekannten Löslichkeiten verschiedener D,L- und L-Aminosäuren der Wert $\sqrt{G_{DL}}$ ausgerechnet. Wie aus der Tabelle 1 hervorgeht, liegen diese Werte bei 0° zwischen 5,7 und 1,6. (Bei D,L-Glutaminsäure erhält man einen G_{DL}-Wert, der <1 ist. Demgemäss wäre die Glutaminsäure kein echtes Razemat. Vgl. DALTON und SCHMIDT (10).) Das Volumen des Lösungsmittels sollte so gewählt werden, dass die D-Aminosäure in Lösung bleiben sollte. In der Hoffnung, dass der Wert $\sqrt{G_{DL}}\geqq 1{,}8$ sei, wurde durch die Formel $\{L\}=1{,}8\,a/2$ die Löslichkeit der D-Form geschätzt und die nötige Menge Lösungsmittel berechnet. (Spätere Löslichkeitsbestimmungen von L-Desoxokynurenin ergaben einen $\sqrt{G_{DL}}$-Wert von ca. 2,8). Damit der Zuckerüberschuss nicht zu gross werden sollte, wurde hier ein $\sqrt{G_{DL}}$-Wert von 4,8 gewählt, und der Überschuss nach $\{R\}-4{,}8\,a/2$ berechnet. Da $\{R\}$ bedeutend grösser als $\{L\}$ war, bestand die Gefahr nicht, dass die Grenze $\frac{\{R\}}{G_{RL}}-\{L\}$ unterschritten wurde.

Tabelle 1

$\sqrt{G}$ bei Aminosäuren. (Die Löslichkeiten aus *Handbook of Chemistry and Physics*, Chemical Rubber Publishing Co., Cleveland, Ohio, 1947.) Die Löslichkeiten sind in g pro 100 g Wasser angegeben

	0°	25°	50°	75°	100°
D,L-Alanin	12,11	16,72	23,09	31,89	44,04
L-Alanin	12,73	16,65	21,79	28,51	37,30
$\sqrt{G}$	2,1	2,0	1,9	1,8	1,7
D,L-Asparaginsäure	0,262	0,778	2,000	4,456	8,594
L-Asparaginsäure	0,209	0,500	1,199	2,875	6,893
$\sqrt{G}$	1,6	1,3	1,2	1,3	1,6
D,L-Isoleucin	1,826	2,229	3,034	4,607	7,802
L-Isoleucin	3,791	4,117	4,818	6,076	8,255
$\sqrt{G}$	4,2	3,7	3,2	2,6	2,1
D,L-Phenylalanin	0,997	1,411	2,187	3,708	6,886
L-Phenylalanin	1,983	2,965	4,431	6,624	9,900
$\sqrt{G}$	4,0	4,2	4,1	3,6	2,9
D,L-Valin	5,98	7,09	9,11		
L-Valin	8,34	8,85	9,62		
$\sqrt{G}$	2,8	2,5	2,1		
D,L-Leucin	0,797			2,276	4,206
L-Leucin	2,270			3,823	5,638
$\sqrt{G}$	5,7			3,4	2,7
D,L-Dijodtyrosin × 10	0,149	0,340	0,773		
L-Dijodtyrosin × 10	0,204	0,617	1,862		
$\sqrt{G}$	2,7	3,6	4,8		
D,L-Tyrosin × 10	0,147	0,351	0,836		
L-Tyrosin × 10	0,196	0,453	1,052		
$\sqrt{G}$	2,7	2,6	2,5		
D,L-Glutaminsäure	0,855	2,054	4,934	11,86	28,49
L-Glutaminsäure	0,341	0,864	2,186	5,532	14,00
$\sqrt{G}$	0,80	0,84	0,89	0,93	0,98
G	0,64	0,71	0,79	0,86	0,96

Versuchsergebnisse

Bei Zusatz von *Harnstoff* und *Thioharnstoff* zu wässrigen Fructose-Lösungen verändert sich die optische Drehung, wie Untersuchungen von NEUBERG und KOBEL (11) gezeigt haben. Vermutlich ist es die Ketogruppe der Fructose, die hier reagiert; die optische Drehung einer Rohrzuckerlösung verändert sich dagegen nicht bei Zusatz von Harnstoff oder Thioharnstoff.

Anthranilsäure, *Anthranilsäuremethylester* und *Anthranilsäureamid* haben die $o\text{-}NH_2 \cdot C_6H_4 \cdot CO$-Gruppierung mit Kynurenin gemeinsam. Diese genügt aber nicht, um kristallisierte Molekylverbindungen mit Rohrzucker zu ermöglichen, wie Versuche nach dem DIMROTHschen Verfahren zeigten.

Die L-α-Aminosäuregruppe im Kynureninmolekül musste, wie oben gesagt, für die eine Bindungsstelle zum Rohrzucker verantwortlich sein. Neuberg und Kobel (12) haben gezeigt, dass D,L-Alanin die optische Drehung einer wässrigen Fructoselösung verändert. Vielleicht ist es auch hier eine Reaktion der reduzierenden Gruppe der Fructose, denn L-*Alanin* verändert die optische Drehung einer wässrigen Rohrzuckerlösung nicht. Mit den in Klammern angegebenen Methoden gaben auch folgende Aminosäuren negative Resultate: L-*Arginin* (Dimroth und optische Drehung), L-*Histidin* (Dimroth), L-*Lysin* (optische Drehung), L-*Tryptophan* (Dimroth), L-*Tyrosin* (Dimroth), L-γ-*Phenyl-α-aminobuttersäure* und D-γ-*Phenyl-α-aminobuttersäure* (Dimroth).

Da L-γ-Phenyl-α-aminobuttersäure keine kristallisierte Molekülverbindung mit Rohrzucker zu geben vermag, musste noch entschieden werden, ob im L-Kynurenin die Carbonylgruppe, oder die Aminogruppe im Kern, oder beide für die Bindung notwendig sind. Zu dem Zwecke wurde das *Desoxo-kynurenin* (9) dargestellt und auf seine Fähigkeit untersucht mit Rohrzucker eine Molekülverbindung zu bilden.

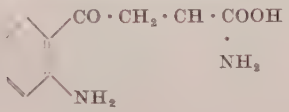

Kynurenin

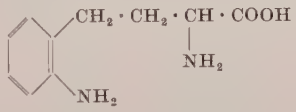

Desoxokynurenin

Es zeigte sich, dass aus einer alkoholischen Lösung von Rohrzucker und razemischem Desoxokynurenin nur der eine Antipode als Molekülverbindung auskristallisiert, während der Andere in Lösung bleibt. Ebenso wie beim Kynurenin, konnte durch die Molekülverbindung mit Rohrzucker eine saubere Trennung in die Antipoden erreicht werden. Durch die Methode von Lutz und Jirgensons (13) wurde festgestellt, dass, wie beim Kynurenin, die L-Form der Aminosäure in dem Komplex mit Rohrzucker vorhanden ist.

Bei der Bildung von einer kristallisierten Molekülverbindung zwischen Rohrzucker und Desoxokynurenin liegt absolut sterische Spezifität vor, denn D-Desoxokynurenin kann keine kristallisierte Molekülverbindung geben, wie ein Versuch nach dem Dimrothschen Verfahren mit der reinen D-Form der Aminosäure und Rohrzucker zeigte. Es ist nicht vollkommen ausgeschlossen, dass D-Desoxokynurenin und Rohrzucker als Molekülverbindung in Lösung existieren kann, dass die Molekülverbindung aber nicht die Möglichkeit hat, ein Kristallgitter zu bilden. Versuche dieser Frage durch Messungen der optischen Aktivität einer Lösung von Rohrzucker mit L-, bzw. D-Desoxokynurenin zu lösen, scheiterten auf die Schwerlöslichkeit der Aminosäure. Eine gesättigte Wasserlösung des D-Desoxokynurenins gab in 4 dm Rohr keinen ablesbaren α-Wert, und alle Versuche, die optischen Aktivitäten der Lösungen von D-, bzw. L-Desoxokynurenin, mit verschiedenen Mengen Rohrzucker zu messen, gaben nur den Dreh-Wert des zugesetzten Zuckers. Es konnte auch kein Lösungsmittel oder Lösungsmittelgemisch gefunden werden, das „nichtzersetzend" war und deshalb zeigten auch Messungen der optischen Aktivität der Molekülverbindung nur den Dreh-Wert des in der Verbindung vorhandenen Rohrzuckers. Absorptionsmessungen in U.V-Licht von D-, bzw. L-Desoxokynurenin, in Gegenwart von Rohrzucker-Überschuss zeigten keine Veränderungen der Absorptionskurve der Aminosäure. Löslichkeitsbestimmungen von D-Desoxokynurenin in reinem Lösungsmittel und in Gegenwart von Rohrzucker werden die Frage beantworten.

Aus diesen Untersuchungen kann man den Schluss ziehen, dass die Carbonylgruppe im Kynurenin für die Bindung zum Rohrzucker nicht notwendig ist. Dagegen ist die Kern-Aminogruppe wesentlich, L-γ-Phenyl-α-aminobuttersäure ist nicht imstande eine Molekülverbindung zu bilden und auch L-Lysin, das dieselbe Anzahl Kohlenstoffatome zwischen den beiden Aminogruppen hat, wie Kynurenin, scheint keine Molekülverbindung mit Rohrzucker geben zu können. Somit wäre auch der Benzolkern notwendig; man kann also drei für die Bindung notwendige Gruppierungen annehmen:

1. L-α-Aminosäuregruppierung,
2. Kern-Aminogruppe,
3. Benzolkern, der möglicherweise jedoch die Aufgabe besitzt, die Entfernung der beiden Aminogruppen von einander festzulegen.

In einer weiteren Versuchsreihe wurde, nach dem DIMROTHschen Verfahren, die Spezifität der *Zuckerkomponente* für die Bildung einer kristallisierten Molekülverbindung untersucht: α, α *Trehalose* vermag nicht mit L-Desoxokynurenin eine Molekülverbindung zu geben. Aber auch Trisaccharide, die in ihrem Molekül die Rohrzuckerkonfiguration besitzen, wie *Raffinose* mit endständigem Fructoserest, oder *Melezitose* mit Fructoserest in der Mitte des Moleküls, geben keine kristallisierten Molekülverbindungen mit L-Desoxokynurenin.

Diskussion

Eine gewisse Analogie scheint vorzuliegen, zwischen den Spaltungen in optische Antipoden von D,L-Kynurenin, bzw. D,L-Desoxokynurenin, durch kristallisierte Molekülverbindungen mit Rohrzucker und den papierchromatographischen Antipodentrennungen von D,L-Kynurenin, bzw. D,L-3-Oxykynurenin. Beide Arten der Spaltungen geschehen unter Zuhilfenahme optisch aktiver Kohlenhydrate, Rohrzucker und Cellulose, und in beiden Fällen muss wohl die Bindung zu den Aminosäuren auf VAN DER WAALSschen Nebenvalenzkräften beruhen. Bei den kristallisierten Molekülverbindungen des Rohrzuckers mit den beiden L-α-Aminosäuren hat sich, ausser der L-α-Aminosäuregruppierung, die Kern-Aminogruppe als wesentlich gezeigt. Dasselbe scheint bei den papierchromatographischen Spaltungen der Fall zu sein, denn, wie DALGLIESH (4, 5) berichtet, wird sowohl D,L-Kynurenin, als auch D,L-3-Oxykynurenin, gespalten, dagegen nicht D,L-N′-Formylkynurenin D,L-N′-Acetylkynurenin und D,L-N^{α}-Acetylkynurenin. Eine Substitution in der Kern- oder der α-Aminogruppe verhindert also, oder setzt jedenfalls die papierchromatographische Antipodenspaltung sehr stark herab. (Nach DALGLIESH ist, sowohl bei D,L-Kynurenin, wie bei D,L-3-Oxykynurenin, der R_f-Wert der D-Form etwa 0,9 von dem der L-Form und die Spaltung ist bei D,L-Kynurenin vollständig, während D,L-3-Oxykynurenin, auf Grund kleineren R_f-Wertes, als „a dumb-bell shaped spot" erscheint. Die R_f-Werte sind nicht angegeben. D,L-N′-Formylkynurenin und D,L-N′-Acetylkynurenin haben nach DALGLIESH R_f-Werte von 0.41, bzw. 0,49, und zeigen keine Antipodenspaltungen, was sie jedoch bei diesen R_f-Werten hätten zeigen müssen, wenn das Verhältnis der R_f-Werte des D- und des L-Isomers in derselben Grössenordnung liegen würde, wie bei D,L-Kynurenin und D,L-3-Oxykynurenin. N^{α}-Acetylkynurenin hat nach DALGLIESH fast den doppelten R_f-Wert von Kynurenin, aber auch hier tritt keine Razematspaltung ein. In allen Fällen wurde dasselbe Lösungsmittelsystem und dieselbe Technik für die Chromatogramme verwendet.)

ZUSAMMENFASSUNG

L-Kynurenin liefert eine gut kristallisierende Molekülverbindung mit Rohrzucker im Verhältnis 1:1.

1. Durch die vorliegende Arbeit werden zur Ausbildung der Molekülverbindung folgende Gruppierungen am Kynureninmolekül als notwendig erkannt:

a. L-α-Aminosäuregruppierung,
b. Kern-Aminogruppe,
c. Benzolkern (der möglicherweise jedoch die Aufgabe hat, die Entfernung der beiden Aminogruppen voneinander festzulegen).

2. In Übereinstimmung mit den unter 1) genannten Bedingungen liefert L-Desoxokynurenin, das für die vorliegende Arbeit erstmalig synthetisiert wurde (9), eine kristallisierte Molekülverbindung mit Rohrzucker im Verhältnis 1:1.

3. Folgende Substanzen geben nach den verwendeten Methoden keine Molekülverbindungen mit Rohrzucker: Harnstoff, Thioharnstoff, Anthranilsäure, Anthranilsäuremethylester, Anthranilsäureamid, L-Alanin, L-Arginin, L-Histidin, L-Lysin, L-Tryptophan, L-Tyrosin, L-γ-Phenyl-α-aminobuttersäure, D-γ-Phenyl-α-aminobuttersäure.

4. Das synthetische D,L-Desoxokynurenin wurde (wie vorher schon das synthetische D,L-Kynurenin) über die kristallisierte Molekülverbindung der L-Form dieser Aminosäure mit Rohrzucker in optische Antipoden gespalten. Es sind die ersten Fälle, wo Rohrzucker zur Razematspaltung verwendet worden ist.

5. Folgende nicht-reduzierende Zucker können Rohrzucker in der kristallisierten Molekülverbindung mit L-Desoxokynurenin nicht ersetzen: α, α Trehalose, Raffinose, Melezitose.

6. Eine Analogie zwischen den Razematspaltungen von D,L-Kynurenin und D,L-Desoxokynurenin durch kristallisierte Molekülverbindungen mit Rohrzucker und den papierchromatographischen Antipodentrennungen von D,L-Kynurenin und D,L-3-Oxykynurenin wird diskutiert.

Herrn Professor Dr. K. Myrbäck bin ich zu grossem Dank verplichtet; in seinem Institut durfte ich die vorliegende Arbeit durchführen. Herrn Professor Dr. V. du Vigneaud spreche ich hierdurch besonderen Dank aus für die Überlassung von D- und L-γ-Phenyl-α-aminobuttersäure. Trehalose stellte mir in dankenswerter Weise Fräulein fil. lic. Majken Elander zur Verfügung.

Institutet för organisk kemi och biokemi, Stockholms Högskola, Stockholm.

LITERATUR

1. Kotake, M., Sakan, T., Nakamura, N., Senoh, S. J. Am. Chem. Soc. *73* (1951) 2973.
2. Mason, M. und Berg, C. P. J. Biol. Chem. *195* (1952) 515.
3. Sensi, P. Acta Vitaminolog. *5* (1951) 105.
4. Dalgliesh, C. E. J. Chem. Soc. *1952*, 137.
5. ——. Biochem. J. *52* (1952) 3.

6. Butenandt, A. und Weichert, R. Z. physiol. Chem. *281* (1944) 122.
7. Rheinboldt, H. J. prakt. Chem. (2) *111* (1925) 242; *112* (1926) 187.
8. Dimroth, O. und Bamberger, C. Ann. *438* (1924) 67.
9. Weichert, R. Arkiv Kemi *5* (1953) 553.
10. Dalton, J. B. und Schmidt, C. L. A. J. Biol. Chem. *103* (1933) 549.
11. Neuberg, C. und Kobel, M. Biochem. Z. *174* (1926) 464.
12. ——. Biochem. Z. *162* (1925) 496.
13. Lutz, O. und Jirgensons, B. Ber. *63* (1930) 448; *64* (1931) 1221.

Tryckt den 8 april 1953

Uppsala 1953. Almqvist & Wiksells Boktryckeri AB

ARKIV FÖR KEMI Band 5 nr 49

Communicated 4 June 1952 by ARNE FREDGA and KARL MYRBÄCK

1.3-Dimercaptoacetone and some derivatives

By LENNART SCHOTTE

In 1926 the first known aliphatic α-ketomercaptan was prepared and described (1), and since then only a few papers about such compounds have been published (2, 3, and 4). As far as the author knows, however, the only symmetrically substituted dimercaptan of that kind, which has been investigated, is 1.3-dimercaptoacetone, described in a preliminary report by the present author in 1950 (5).

1.3-Dimercaptoacetone can now be prepared in a nearly quantitative yield by treating a water solution of sodium sulfhydrate with 1.3-dichloroacetone. The substance is crystalline and soluble in hot organic solvents. A melting point of 85–86° is obtained. Molecular weight determinations with RAST's method showed the substance to be dimeric, like mercaptoacetone (4). In solution a marked dissociation is observed, and it seems likely that the equilibrium between the monomeric and dimeric form is according to:

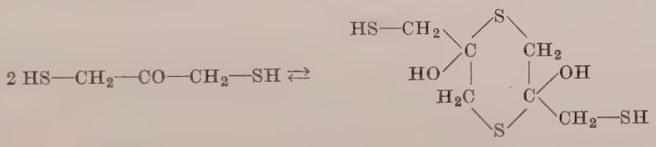

(I) (II)

The dimerisation might have as an intermediate stage a hypothetical three-membered ring, containing one sulfur atom. The form (II) is represented in the crystallized mercaptan and in some derivatives, but most of the related compounds are built up from the monomeric ketomercapto-form.

It has been found by combustion analysis and equivalent weight determinations with iodine solutions that the isolated dimercaptan is of a high standard of purity, if the 1.3-dichloroacetone used is freshly distilled. This is very important and useful, as the author has not succeeded in recrystallizing the substance — a fact which is easily explained from the instability of the substance (see above).

It has already been shown that 1.3-dimercaptoacetone is characterized by a marked reaction readiness (5) in reactions with the typical mercapto-group reagent 2.4-dinitro-chloro-benzene and with monobromo-acetic acid, from which 1.3-bis-(2.4-dinitrophenyl-mercapto)-acetone (III) and 1.3-bis-(carboxy-methyl-mercapto)-acetone (IV) are obtained. Further derivatives, which have now been obtained, are the bis-ethyl- and bis-methylsulfides, and, taken together, the derivatives provide an excellent proof of the structure of the monomeric form of the dimercaptan (I). — 1.3-bis-(ethyl-mercapto)-acetone (V) was prepared from the sodium mercaptide

$$(NO_2)_2{-}C_6H_3{-}S{-}CH_2{-}CO{-}CH_2{-}S{-}C_6H_3{-}(NO_2)_2 \tag{III}$$

$$COOH{-}CH_2{-}S{-}CH_2{-}CO{-}CH_2{-}S{-}CH_2{-}COOH \tag{IV}$$

$$C_2H_5{-}S{-}CH_2{-}CO{-}CH_2{-}S{-}C_2H_5 \tag{V}$$

$$CH_3{-}S{-}CH_2{-}CO{-}CH_2{-}S{-}CH_3 \tag{VI}$$

$${-}S{-}CH_2{-}CO{-}CH_2{-}S{-}S{-}CH_2{-}CO{-}CH_2{-}S{-} \tag{VII}$$

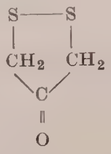
(VIII)

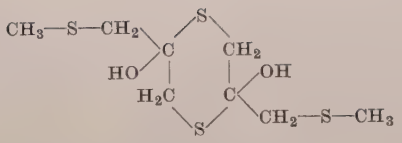
(IX)

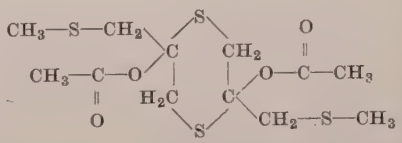
(X)

$$C_2H_5O{-}CS{-}S{-}CH_2{-}CO{-}CH_2{-}S{-}CS{-}OC_2H_5 \tag{XI}$$

$$C_2H_5O{-}CO{-}S{-}CH_2{-}CO{-}CH_2{-}S{-}CO{-}OC_2H_5 \tag{XII}$$

$$C_2H_5O{-}CO{-}SK \tag{XIII}$$

$$C_6H_5{-}S{-}CH_2{-}CO{-}CH_2{-}S{-}C_6H_5 \tag{XIV}$$

$$COOH{-}CH_2{-}O{-}CS{-}S{-}CH_2{-}CO{-}CH_2{-}S{-}CS{-}O{-}CH_2{-}COOH \tag{XV}$$

$$KS{-}CS{-}O{-}CH_2{-}COOK \tag{XVI}$$

$$C_6H_5{-}CH_2{-}S{-}CH_2{-}CO{-}CH_2{-}S{-}CH_2{-}C_6H_5 \tag{XVII}$$

and ethyl iodide and obtained as a liquid with the boiling point 123–124°/11 mm. The same substance had previously been synthesized from 1.3-dichloroacetone and ethyl mercaptan, a boiling point of 117–121°/15 mm being given (6). The sulfide was then characterized as a semicarbazone, obtained as colourless needles with a melting point of 119–120°, while ROJAHN and LEMME stated 98–99° (6). This discrepancy is rather surprising, as the present author has not observed anything that suggests a possible polymorphy and has never been able to obtain the lower melting point. — 1.3-bis-(methyl-mercapto)-acetone (VI), on the other hand, was prepared by a methylation reaction with diazomethane. The yield was bad, but this must be due to the small solubility of the mercaptan under the conditions usual for diazomethane reactions.

It has been mentioned earlier that iodine oxidation of 1.3-dimercaptoacetone quantitatively gives the corresponding disulfide. However, the oxidation can either give a chain polymer of the appearance (VII), or it can cause an intramolecular ring closure to a five-membered heterocycle with two sulfur atoms (VIII). If the oxidation is performed by dropping an iodine solution into an alcoholic solution of the mercaptan, it is mainly the chain polymer, which is obtained as a resulting product. It was not investigated further. If, on the other hand, the mercaptan solution is slowly added to the oxidizing agent, the cyclic disulfide is obtained, and could be characterized as a faintly yellow coloured semicarbazone. The cyclic disulfide is of course formed in the second case because the concentration of the mercaptan in the diluted solution is always small enough for the probability of an intramolecular ring closure to be great.

In order to get a proof of the assumed structure of the dimeric form of 1.3-dimercaptoacetone (II), two derivatives have been prepared. The structure (II) can be interpreted as a 2.5-dioxy-2.5-bis-mercapto-methyl-1.4-dithiane, and the derivatives give complete confirmation of the formula suggested. Methylation in absolute methanol in the presence of concentrated sulfuric acid or hydrogen chloride gave 2.5-dioxy-2.5-bis-(methyl-mercapto-methyl)-1.4-dithiane (IX). This substance was then treated with acetic anhydride, and the diacetate (X) was isolated. Molecular weight determinations support the proposed dithiane structure.

A compound which has two mercapto-groups symmetrically adjacent to a keto-group must of course be very reactive. This may be shown quite simply by a condensation reaction that implies a remove of water, e.g. between the two mercapto-groups in one and the keto-group in another molecule. If dry hydrogen chloride is introduced into a cold benzene solution of 1.3-dimercaptoacetone, a colourless substance gradually separates out. The product exhibits the properties of a high polymer, and a qualitative test for the mercapto-group is negative (7). Combustion analysis gives an empirical formula $C_3H_4S_2$ as the period of the possible chain polymer. Such a product may be obtained in the following way, if the reaction is supposed to take place between mercaptan molecules of monomeric form:

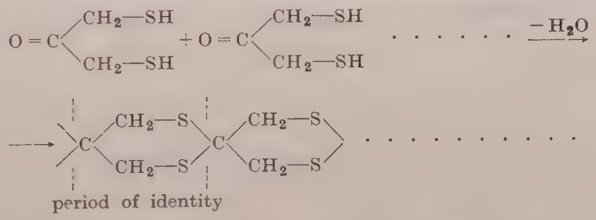

A large number of dithiane rings provides some possibility for a ring closure of the chain, of course. — However, starting from the monomeric structure of 1.3-dimercaptoacetone, there is another alternative: namely, the formation of a network of polymer character, which may be represented in the following simplified way:

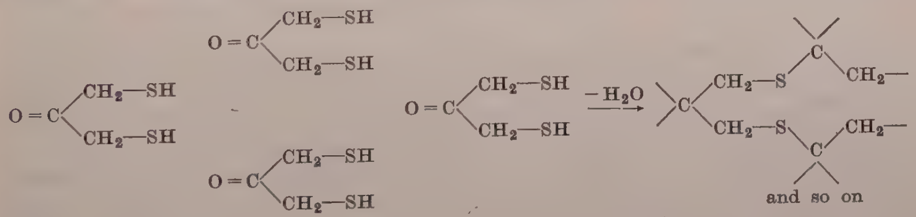

It is, of course, also possible to deduce a polymer structure from the dimeric form of the mercaptan (II) by removing water between the mercapto- and hydroxy-groups, but this does not seem very probable to the author, in view of experience from corresponding reactions with mercaptoacetone (4). Unfortunately, it is only possible to consider these alternatives from the theoretical aspect, as the polymeric substance cannot be worked up and thoroughly investigated because of its complete insolubility in any conceivable solvent. It may only be emphasized that the above-mentioned network structure for the polymer is not very probable, as such compounds usually swell in solvents, and such swelling was altogether absent for this substance. — However, a closer study of a high polymer of the assumed spirane structure should have been very instructive, as no polymers with similar structure, all the way through, are described in the literature, as far as the author knows. No definite evidence of the proposed formula can be given, but, on the other hand, the properties of the polymer do not at all contradict the assumption of a spirocyclic structure.

With a view to preparing some low-molecular compounds with the assumed configuration of the polymer, condensations have been tried between 1.3-dimercaptoacetone and acetone, thioglycolic acid and 1.3-bis-(ethyl-mercapto)-acetone (V) respectively in the presence of anhydrous zinc chloride or hydrogen chloride. Although the reaction conditions were varied, the mercaptoles could not be isolated, but, instead, a polymer of the character described above was obtained in every case. In this connection, it is worth noting that it is also impossible to obtain a mercaptole from 1.3-dichloroacetone, because the chlorine atoms show a higher reaction tendency than the keto-group (6).

A few other derivatives representing the monomeric structure of 1.3-dimercaptoacetone, $-S-CH_2-CO-CH_2-S-$, have been prepared from different reactions. These include the following:

a) *1.3-Bis-(O-ethyl-thiol-thione-carbonic acid)-acetone* (XI) from potassium xantogenate and 1.3-dichloroacetone.

b) *1.3-Bis-(O-ethyl-thiol-carbonic acid)-acetone* (XII) from BENDER's salt (XIII) and 1.3-dichloroacetone.

c) *1.3-Bis-(phenyl-mercapto)-acetone* (XIV) from potassium thiophenolate and 1.3-dichloroacetone. The semicarbazone of this substance was also prepared.

d) *1.3-Bis-(dithiocarboxy-glycolic acid)-acetone* (XV) from the dipotassium salt of dithiocarboxy-glycolic acid (XVI) and 1.3-dichloroacetone.

Finally, 1.3-bis-(benzyl-mercapto)-acetone (XVII) was known from an earlier investigation (8). — Attempts to obtain 1.3-dimercaptoacetone from the substances XI, XII, XIV, and XV have been made, but without success. This is specially noteworthy as the product XV is analogous to the one which GROTH used in his synthesis of mercaptoacetone (1).

It is of particular interest to compare 1.3-dimercaptoacetone and 1.3-dioxyacetone. Such a comparison shows that the oxy-compound is dimolecular too, and that its monomeric form can be obtained by distillation *in vacuo*. The same is observed for the mercaptan, but the dimerisation is very rapid; the monomeric form of 1.3-dioxyacetone is much more stable and even obtainable as crystals (9). The dimerisation tendency is obviously more marked in the mercaptan case. A further similarity occurs in their reaction behaviours; derivatives from both the monomeric and dimeric forms of 1.3-dioxyacetone are known, and investigations of compounds with the dimeric structure have been performed by FISCHER & TAUBE (10) and LEVENE & WALTI (11), which lead them to propose dioxane structures. Condensation reactions resulting in products with higher molecular weights have also been observed (12).

Experimental

1.3-Dimercaptoacetone (I and II)

A solution of 40 g (1.0 mole) of sodium hydroxide in 200 ml of water was saturated with hydrogen sulfide and cooled to 5° by means of an ice bath, 64 g (0.5 mole) of 1.3-dichloroacetone, dissolved in 125 ml of alcohol, being introduced dropwise with stirring, while the temperature was kept low. The dimercaptan precipitated during the addition and was separated by filtration with suction, and then washed with about 200 ml of water. The product was dried in a vacuum desiccator over concentrated sulfuric acid. The melting point is 85-86° and the yield 55 g (90 %).

The substance can be kept *in vacuo* without any decomposition. The crude product, on the other hand, changes very rapidly. — It is of no importance for the purity of the substance which form of sodium sulfhydrate is used — the one obtained in solution by saturating a water solution of sodium hydroxide with hydrogen sulfide, or the one obtained isolated in a pure state according to RULE (13). — Distillation *in vacuo* of 1.3-dimercaptoacetone gave a viscous liquid of boiling point 95°/14 mm, which soon crystallized.

Anal. Subst., 52.9 mg: 8.94 ml of 0.0965-*N* J_2.
» 18.63 mg: CO_2, 20.30 mg; H_2O, 7.89 mg.
» 18.58 mg: 8.290 ml of 0.07340-*N* NaOH.

$(C_3H_6OS_2)_2$ $(122.17)_2$ calc. Equ. wt. 61.1; C 29.47; H 4.95; S 52.48.
found Equ. wt. 61.4; C 29.71; H 4.74; S 52.50.

Molecular weight determination: (on the crystallized product) (RAST)
11.68 mg in 127.28 mg phenanthrene: t = 5.°6; K = 11.8.
10.45 mg in 120.24 mg » t = 5.°7; K = 11.8.
M. W. calc. 244, found 193, 180.

A partial monomerisation obviously occurs during the melting. — The solubility properties do not permit a determination by the usual chryoscopic method.

1.3-Dichloroacetone

The substance is prepared according to (14), with the further provision, however, that the water solution obtained when the chromic salts are dissolved should always be extracted with benzene. It may happen, when working with dilute solutions that the product does not crystallize, and even when crystallization occurs, it has been proved that the water solubility is high enough to be significant. The yield is raised from 68–75 % to 85–90 %.

1.3-Bis-(ethyl-mercapto)-acetone (V)

104 g (2/3 mole) of ethyl iodide, dissolved in 50 ml of alcohol, was added drop by drop, to a solution of 41 g (1/3 mole) of 1.3-dimercaptoacetone (the amount calculated for the monomer) in 200 ml of water, in which 27 g (2/3 mole) of sodium hydroxide was dissolved. The reaction mixture was cooled until all the alcoholic solution had been added, and after that the mixture was maintained at a temperature of 60–70° for four hours. The solution was extracted with ether, the ether layer separated and then dried with anhydrous sodium sulfate. The ether was evaporated, and the residue fractionated *in vacuo*. 1.3-Bis-(ethyl-mercapto)-acetone was collected at 123–124°/11 mm. Yield 36 g (61 %).

The *semicarbazone* was prepared according to the general process. Its melting point is 119–120°.

Anal. Subst., 25.38 mg: CO_2, 37.61 mg; H_2O, 15.81 mg.
» 18.77 mg: 7.201 ml 0.04475-*N* NaOH.
» 89.3 mg: 13.99 ml N_2 (22.°2; 748 mm Hg)
$C_8H_{17}OS_2N_3$ (235.36) calc. C 40.82; H 7.28; S 27.24; N 17.88.
found C 40.44; H 6.97; S 27.52; N 17.97.

1.3-Bis-(methyl-mercapto)-acetone (VI)

12.2 g (0.1 mole, in terms of the monomeric form) of 1.3-dimercaptoacetone was suspended in acetone and the usual methylation reaction with diazomethane performed. The diazomethane was prepared from N-nitroso-methylurea (15). — A liquid with the boiling point 106–109°/9 mm was isolated by distillation from the reaction mixture. The yield was only 2 g (13.4 %), owing to the small solubility of the mercaptan.

Anal. Subst., 29.99 mg: CO_2, 43.80 mg; H_2O, 17.02 mg.
$C_5H_{10}OS_2$ (150.25) calc. C 39.97; H 6.70.
found C 39.85; H 6.35.

Semicarbazone of 1.2-dithiacyclopentanone-4 (cf. VIII)

A solution of 1.3-dimercaptoacetone in alcohol was dropped into an equivalent amount of 2-*N* iodine solution, the mixture being stirred continually. When the oxidation was complete, the solution was filtered and treated with excess semicarbazide hydrochloride. The mixture was made nearly neutral with sodium bicarbonate. The semicarbazone of the disulfide soon appeared in the form of flaky crystals. The substance was recrystallized from alcohol, or, even better, from a mixture of alcohol and benzene. The pure product consisted of faint yellow, glistening leaves. Melting point 224° (Kofler).

Anal. Subst., 7.87 mg: 3.958 ml of 0.04532-*N* NaOH.
» 50.3 mg: 10.84 ml N_2 (20.°6; 732 mm Hg).
$C_4H_7OS_2N_3$ (177.24) calc. S 36.18; N 23.71.
found S 36.54; N 24.13.

Molecular weight determination: (Rast)
7.50 mg in 101.8 mg camphor: t = 15.°3; K = 35.5.
M.W. calc. 177, found 171.

A molecular weight determination has also been performed in glacial acetic acid, where values corresponding to half the calculated ones were obtained, indicating a dissociation of the hydroacetate formed.

2.5-Dioxy-2.5-bis-(methyl-mercapto-methyl)-1.4-dithiane (IX)

14.5 g (0.06 mole in terms of the dimeric form) of 1.3-dimercaptoacetone was dissolved in 50 ml of absolute methanol, and the solution was treated with 1 ml of concentrated sulfuric acid for two days. The thioether crystallized as irregular prisms and was in a pure state after five recrystallizations from benzene. The melting point was 176–178° (Kofler) and the yield 3.2 g (19.5 %). — Hydrogen chloride can be used instead of sulfuric acid; the reaction is then more rapid but gives the same yield of pure substance. The compound is moderately soluble in the usual organic solvents.

Anal. Subst., 18.84 mg: CO_2, 24.23 mg; H_2O, 9.52 mg.
» 19.91 mg: CO_2, 25.64 mg; H_2O, 10.08 mg.
» 11.58 mg: 7.480 ml 0.04532-*N* NaOH.
$C_8H_{16}O_2S_4$ (272.37) calc. C 35.27; H 5.92; S 47.08.
found C 35.10, 35.14; H 5.65, 5.67; S 46.93.

Molecular weight determination: (*by the chryoscopic method*)
65.5 mg in 29.20 g bromoform: $\Delta t = 0.^\circ 012$; $K = 14.4$.
130.3 mg in 29.20 g » : $\Delta t = 0.^\circ 025$; $K = 14.4$.
M. W. calc. 272, found 270, 257.

Molecular weight determination: (*by the ebullioscopic method*)
0.0912, 0.1814 g in 16.25 g benzene: $E = 0.^\circ 059$, $0.^\circ 120$.
M.W. calc. 272, found 247, 242.

A partial dissociation of the substance in boiling benzene is thus stated according to the above (cf. also 1, p. 57).

Diacetate of 2.5-dioxy-2.5-bis-(methyl-mercapto-methyl)-1.4-dithiane (X)

2.7 g (0.01 mole) of the bis-methylthioether (IX) was dissolved in a water solution of 1.0 g (0.025 mole) of sodium hydroxide. A suitable amount of ice was added, and after that 1.5 g (0.015 mole) of acetic anhydride was rapidly dropped into the mixture. The diacetate immediately precipitated and was separated by filtration. It was finally recrystallized from alcohol. The ester was then obtained as colourless, microcrystalline prisms with melting point 144° (KOFLER). The yield was 1.3 g (37 %). Some bis-methylthioether could be regained, when the solution was acidified. The diacetate gave a positive ester test according to ANGELI-RIMINI (16).

Anal. Subst., 7.91 mg: 3.923 ml of 0.04532-*N* NaOH.
$C_{12}H_{20}O_4S_4$ (356.52) calc. S 35.97.
found S 36.03.

Molecular weight determination: (RAST)
8.60 mg in 105.8 mg camphor: $t = 8.^\circ 4$; $K = 35.5$.
7.10 mg in 96.0 mg » : $t = 7.^\circ 5$; $K = 35.5$.
M. W. calc. 357, found 344, 350.

The polymer obtained from 1.3-dimercaptoacetone

Hydrogen chloride, dried by passing through concentrated sulfuric acid, was bubbled into a cold benzene solution of 1.3-dimercaptoacetone. A colourless substance gradually separated, and this was filtered and carefully washed with water, alcohol and ether. The product had no definite melting point but decomposed at higher temperatures (about 200°).

Anal. Subst., 19.62 mg: CO_2, 24.60 mg; H_2O, 6.44 mg.
» 24.63 mg: CO_2, 30.94 mg; H_2O, 8.72 mg.
» 8.67 mg: 7.482 ml of 0.04475-*N* NaOH.
$(C_3H_4S_2)_x$ $(104.18)_x$ calc. C 34.58; H 3.87; S 61.57.
found C 34.22, 34.28; H 3.67, 3.96; S 61.90.

1.3-Bis-(O-ethyl-thiol-thione-carbonic acid)-acetone (XI)

38 g (0.24 mole) of potassium xantogenate, dissolved in alcohol, was treated with a solution of 12.7 g (0.1 mole) of 1.3-dichloroacetone in alcohol. The solution was vigorously stirred, and the reaction took place at room temperature. Potassium chloride immediately separated, and towards the end of the reaction the required substance crystallized out. Water was added in order to dissolve the potassium salt, and after that the product was filtered, washed and dried. It was recrystallized from ligroin, being obtained as long, colourless needles. The melting point was 77–78° and the yield 22 g (74 %). The compound is very soluble in ether, acetone and benzene; soluble in alcohol and ligroin.

The substance is remarkably stable against concentrated hydrochloric acid. Thus the compound could be regained unchanged after a treatment with hydrochloric acid (1 : 1) on a water bath for 36 hours.

Anal. Subst., 23.02 mg: CO_2, 30.60 mg; H_2O, 9.91 mg.
» 20.78 mg: 7.640 ml of 0.07340-*N* NaOH.
$C_9H_{14}O_3S_4$ (298.35) calc. C 36.20; H 4.73; S 42.98.
found C 36.25; H 4.82: S 43.24.

1.3-Bis-(O-ethyl-thiol-carbonic acid)-acetone (XII)

A reaction analogous to the above was performed with 14.8 g (0.10 mole) of Bender's salt (XIII) and 6.35 g (0.05 mole) of 1.3-dichloroacetone in an alcoholic solution. The reaction product could be recrystallized from ligroin, and was obtained as colourless needles. Melting point 45–46°. Yield 8.8 g (67 %). The substance is very soluble in the usual organic solvents and soluble in hot water.

This substance, too, showed a marked stability against concentrated hydrochloric acid and could be regained unaltered after digeration on a water bath.

Anal. Subst., 23.33 mg: CO_2, 34.74 mg; H_2O, 10.79 mg.
» 23.93 mg: 4.900 ml of 0.07340-*N* NaOH.
$C_9H_{14}O_5S_2$ (266.23) calc. C 40.56; H 5.30; S 24.08.
found C 40.61; H 5.30; S 24.09.

1.3-Bis-(phenyl-mercapto)-acetone (XIV)

To a cooled solution of 5.6 g (0.10 mole) of potassium hydroxide in 25 ml of alcohol, a solution of 11.2 g (0.10 mole) of thiophenol in 25 ml of alcohol was added. 6.35 g (0.05 mole) of 1.3-dichloroacetone, dissolved in 30 ml of alcohol, was dropped into the thiophenolate solution. When no more potassium chloride separated a large volume of water was added, and the solution was extracted with ether. The ether layer was separated and after drying, the ether was evaporated at reduced pressure. A crystalline substance with melting point 40–42° was obtained as a residue. After recrystallization from ligroin the substance melted at 41–43°, and the product was in the form of colourless needles. The yield was 8.2 g (60 %). The substance is soluble in ordinary organic solvents.

Anal. Subst., 20.84 mg: CO_2, 50.15 mg; H_2O, 9.35 mg.
» 19.23 mg: 3.841 ml of 0.07340-*N* NaOH.
$C_{15}H_{14}OS_2$ (274.23) calc. C 65.64; H 5.15; S 23.38.
found C 65.63; H 5.02; S 23.49.

The *semicarbazone* was prepared according to the general process. The melting point is 115–117°. It may be recrystallized from a mixture of alcohol and water or, better, from benzene. The substance is soluble in alcohol, acetone, benzene and ether, but insoluble in water and ligroin.

Anal. Subst., 25.65 mg: 35.78 mg $BaSO_4$.
» 0.1165 g: 13.02 ml N_2 (18.°0; 742 mm Hg).
$C_{16}H_{17}OS_2N_3$ (331.28) calc. S 19.35; N 12.68.
found S 19.16; N 12.81.

1.3-Bis-(dithiocarboxy-glycolic acid)-acetone (XV)

32 g (0.25 mole) of 1.3-dichloroacetone, dissolved in 50 ml of warm ether, was rapidly dropped into a water solution, containing 0.5 mole of the dipotassium salt of dithiocarboxy-glycolic acid. This salt was prepared according to GROTH's method (1). The solution was at first yellow coloured, but soon darkened. When all the halide ketone had been added, the ether layer was separated, and the water layer extracted with 150 – 100 ml of benzene in order to remove any possible esters of thiocarbonic acid. The water solution was then dropped into a mixture of concentrated hydrochloric acid and ice. A crystalline substance with an ill-defined melting point of about 135° was obtained. After three recrystallizations from alcohol + water the dicarboxylic acid was obtained as colourless, glistening needles. Melting point 179–181° (KOFLER). The yield of the pure product was only 5.4 g (6.1 %). It is worth mentioning that many unsuccessful attempts to get the acid were made by the author before the above successful variation was found. It seems very important that the halogen ketone is added rapidly.

Anal. Subst., 51.08 mg: 6.250 ml of 0.04532-*N* NaOH.
» 9.64 mg: 4.715 ml of 0.04532-*N* NaOH.
$C_9H_{10}O_7S_4$ (358.41) calc. Equ. wt. 179.2; S 35.78.
found Equ. wt. 180.3; S 35.53.

The author is indebted to Professor ARNE FREDGA for valuable discussions.

SUMMARY

1.3-Dimercaptoacetone has been synthesized, and its properties investigated.

A number of new derivatives have been prepared, and the reaction behaviour of the mercaptan is thoroughly discussed.

A comparison is drawn between 1.3-dimercaptoacetone and 1.3-dioxyacetone, and a special attention paid to the study of the dimeric structures. A dithiane formula for the dimeric mercaptan is proposed.

Laboratory of Organic Chemistry, Chemical Institute, University of Uppsala.
May 1952.

REFERENCES

1. B. GROTH, Über α-Mercaptoketone und verwandte Stoffe. Diss. Uppsala (1926).
2. O. HROMATKA and E. ENGEL, Monatsh. *78*, 29 (1948).
3. M. OHTA, J. Pharm. Soc. Japan *70*, 709 (1950).
4. L. SCHOTTE, Arkiv Kemi, *3* (1951) nr 43.
5. ——, Acta Chem. Scand. *4*, 1304 (1950).

6. C. A. Rojahn and G. Lemme, Arch. Pharm. *263*, 616 (1925).
7. H. Rheinboldt, Ber. *60*, 184 (1927).
8. E. Fromm, R. Kapeller and I. Taubmann, Ber. *61*, 1357 (1928).
9. H. Fischer and H. Mildbrand, Ber. *57*, 707 (1924).
10. H. Fischer and C. Taube, Ber. *60*, 1704 (1927).
11. P. A. Levene and A. Walti, J. Biol. Chem. *84*, 39 (1929).
12. ——, J. Biol. Chem. *78*, 23 (1928).
13. A. Rule, J. Chem. Soc. (London) *99*, 558 (1911).
14. Org. Synthesis, *I*, 206.
15. ——, *II*, 165.
16. F. Feigl, Mikrochemie *15*, 18 (1944).

Tryckt den 8 april 1953

Uppsala 1953. Almqvist & Wiksells Boktryckeri AB

ARKIV FÖR KEMI Band 5 nr 50

Communicated 14 January 1953 by JOHN RUNNSTRÖM and GERT BONNIER

The amino acid metabolism of sea urchin embryos studied by means of N^{15}-labeled ammonium chloride and alanine

By TORE HULTIN

With 3 figures in the text

In previous papers (13, 14, 17) it was shown that N^{15} in the form of labeled ammonium chloride, glycine or alanine, is readily incorporated into the proteins of sea urchin embryos. The rate of incorporation into different protein fractions varies in a characteristic manner during the course of development.

In experiments of this kind the distribution of the isotope between different protein constituents is a factor of special interest. In the experiments described in this paper, sea urchin embryos were treated at different stages of development with N^{15}-ammonium chloride or N^{15}-DL-alanine and the pattern of isotope distribution between various protein constituents was studied in relation to the morphogenesis.

Experimental

1. *Incorporation of N^{15}-ammonium chloride into amino acids and protein amides*

This investigation was performed simultaneously with a study of the pyrimidine and purine metabolism during the early sea urchin development. The same $N^{15}H_4Cl$-labeled *Paracentrotus lividus* (LM) material was used for both purposes. The preparation of this material has previously (15) been described in detail. The material consisted of unfertilized eggs and embryos at certain stages of development kept for exactly 5 hours in sea water, containing 0.75 mM $N^{15}H_4Cl$ (61 % N^{15} excess). The following fractions, remaining after the nucleotide preparations, were used in this investigation: 1) Water-soluble proteins. 2) Insoluble proteins. 3) Free amino acids, extracted from the water-soluble material by means of 10 % trichloroacetic acid (TCA).

The purified (15, cf. 33) protein fractions were treated with N H_2SO_4 att 100° C for 60 minutes. The suspensions were adjusted to pH 10.5 by addition of $Ba(OH)_2$, and the protein amide nitrogen was isolated by distillation with ethanol at low temperature in a Parnas vacuum distillation apparatus.

The protein suspensions were neutralized by addition of H_2SO_4 and then refluxed with 10 % HCl for 24 hours. The hydrolysates were filtered and repeatedly evaporated *in vacuo*. The residues were taken up in small amounts of water and added to kation-exchange columns (39) (Dowex 50, 300 mesh, H^+-form, 80 cm × 6 cm^2, temperature 32° C). HCl in increasing concentrations (0.5–

4 N) was used as solvents. Samples of the effluent were tested with ninhydrin, and the amino acid fractions were identified by paper chromatography. In most cases the following fractions were collected: aspartic acid, serine-threonine-glutamic acid, glycine-alanine, valine, proline, isoleucine, leucine, tyrosine, lysine, histidine and arginine.

The aspartic acid was precipitated and recrystallized as copper aspartate (20). The copper aspartate was dissolved in dilute HCl and decomposed by H_2S-treatment. Glutamic acid was precipitated and recrystallized at 0° C by saturation with HCl-gas (20). Serine was precipitated from a solution of 0.17 volumes of methyl cellosolve in water by means of hydroxyazobenzene sulfonic acid (40)[1] and recrystallized from water.

The glycine-alanine fraction was repeatedly evaporated *in vacuo*, taken up in a small volume of 1:2:1 *n*-butanol-*n*-propanol–0.1 N HCl and added to a starch column (60 cm × 3,5 cm^2), prepared according to STEIN and MOORE (37). The chromatogram was run with 1:2:1 *n*-butanol-*n*-propanol–0.1 N HCl and 2:1 *n*-propanol–0.5 N HCl as solvents (27). The isolated alanine fraction was evaporated and precipitated with azobenzene sulfonic acid[1] (40) from a solution of 0.17 volumes of methyl cellosolve in water. The alanine azobenzene sulfonate was recrystallized from water. Glycine was precipitated and recrystallized as 5-nitronaphtalene-1-sulfonate[1] (28).

The valine fraction was repeatedly evaporated in vacuum, taken up in water and treated with Ag_2CO_3 at 50° C. After a treatment with H_2S the solution was concentrated in vacuum and precipitated with alcohol (4).

Proline was taken up in ethanol and isolated as the $CdCl_2$-complex (7). Of the isoleucine fraction only the central part, entirely free from methionine and leucine, was collected. In a few cases this part was fairly small. A greater part of the isoleucine fraction was then purifed by starch chromatography, using the solvent 1:1:0.288 *n*-butyl alcohol-benzyl alcohol-water (39). Isoleucine was further purified in the same way as valine. Leucine was taken up in 0.1 N HCl and precipitated and recrystallized as β-naphtalene sulfonate (2). Tyrosine was taken up in dilute HCl and precipitated by neutralization with NaOH. The precipitates were recrystallized in water. Lysine was purified as picrate (23), histidine as 3-4-diclorobenzene sulfonate (42) and arginine as flavianate (22).

The samples of purified mono- and dicarboxylic amino acids were dissolved in hot water, and 25 mg of NH_4Cl were added for dilution of any interfering traces of high-labeled ammonia. An excess of saturated $Ba(OH)_2$-solution was added to the samples. In those cases, where the amino acids had been isolated as sulfonates, the barium sulfonates formed were allowed to crystallize from the hot solutions, finally in a refrigator. These samples were then filtered by suction. The samples were transferred to 25 ml aeration tubes, which were kept in a boiling water-bath. Equal volumes of ethanol were added, and the ammonia was removed by aeration. The aeration was continued until the volumes of the samples had been reduced to approximately 1 ml. The pH was adjusted to 2.5, and 0.3 ml of 10 % citrate buffer, pH 2.5 was added. The α-amino nitrogen was isolated according to the specific ninhydrin method of SOBEL *et al.* (36) and the N^{15}-contents were determined in a mass spectrograph. From proline and from the basic amino acids the total nitrogen was isolated by means of Kjeldahl combustion.

The preparation of free amino acids for N^{15}-determination could be performed only to a limited extent because of the minute quantities present and the large amounts of free glycine (30) dominating the low molecular fraction. Very nearly the same procedure of isolation was used for the free amino acids as for the protein hydrolyzates. In the case of free amino acids, however, not only the alanine fractions obtained from the Dowex 50 columns, but also the glutamic acid fractions were completely overlapped by glycine and had to be purified by starch chromatography. From the free amino acid fraction picolinic acid betaine was isolated acccording to a procedure, which will be described later.

---

[1] These substances were synthesized according to (38).

2. *Incorporation into protein constituents of N^{15} from labeled* DL-*alanine*

N^{15}-DL-alanine was synthesized from N^{15}-ammonium nitrate (65 % N^{15} excess) by way of potassium phtalimide (32, 34).

The *Paracentrotus* material used in this study was prepared in essentially the same way as the material used in the $N^{15}H_4Cl$ experiments. Unfertilized eggs and embryos at certain stages of development were kept for 5 hours in sea water, containing approximately 1 mg of N^{15}-DL-alanine per mg of total egg nitrogen. The material had been used earlier in a study of the isotope incorporation into different soluble protein fractions (17), and a detailed account of the preparation procedure was given in connection with this investigation. Only the non water-soluble protein fractions were utilized in these experiments. The protein constituents were isolated and purified in essentially the same way as in the $N^{15}H_4Cl$ experiments.

3. *Exchange of N^{15} between labeled* DL-*alanine and glutamic acid in homogenates of sea urchin embryos*

Embryos of the sea urchin *Psammechinus miliaris* (Gmelin) were allowed to develop in rocking glass trays (25) at 20° C. At 4, 8, 12, 17 and 25 hours of development equal samples were taken from the suspension. The samples were centrifuged, and the sediments were rapidly frozen and carefully homogenzid in the frozen state by means of a small glass pestle. The homogenates (approximately 0.2 ml) were mixed with a solution of 25 mg N^{15}-DL-alanine and 75 mg L-glutamic acid in 2.5 ml of water (pH 7.5) and transferred to small Erlenmeyer flasks. The incubation mixtures were kept gently shaking in a waterbath (25° C) for 1 $^1/_2$ hours. The reaction was stopped by addition of 10 ml 10 % TCA. The samples were centrifuged, and the excess TCA was removed by ether extraction. The glutamic acid of the samples was isolated by chromatography and purified as described above.

Results and Discussion

In the experiments with N^{15}-ammonium chloride the isotope was readily incorporated into the amides of the proteins (Fig. 1). The incorporation was most rapid in the protein fraction, which was not dissolved during the extraction procedures (15). The rate of incorporation into this fraction increased successively during the early development before the gastrula stage. The incorporation into the soluble proteins, on the other hand, was particularly intensified during the mesenchyme blastula stage. These results agree very closely with previous experiments (14), where the incorporation of N^{15}-labeled glycine and alanine into protein fractions of developing Psammechinus embryos was studied.

The incorporation of N^{15}-ammonium chloride into the amino acids of these same protein fractions proceeded much more slowly (Fig. 2). The rate of incorporation was especially low during the early stages but increased successively from a period shortly before the appearance of the mesenchyme cells. The isotope contents were constantly higher in the amino acids of the non-soluble fraction. However, the increase during the later stages was relatively more pronounced in the amino acids of the soluble fraction (Fig. 2).

Glutamic acid showed the highest rate of isotope incorporation, followed by aspartic acid and alanine. The isotope levels of other amino acids were considerably lower. Particularly small isotope contents were found in histidine and glycine.

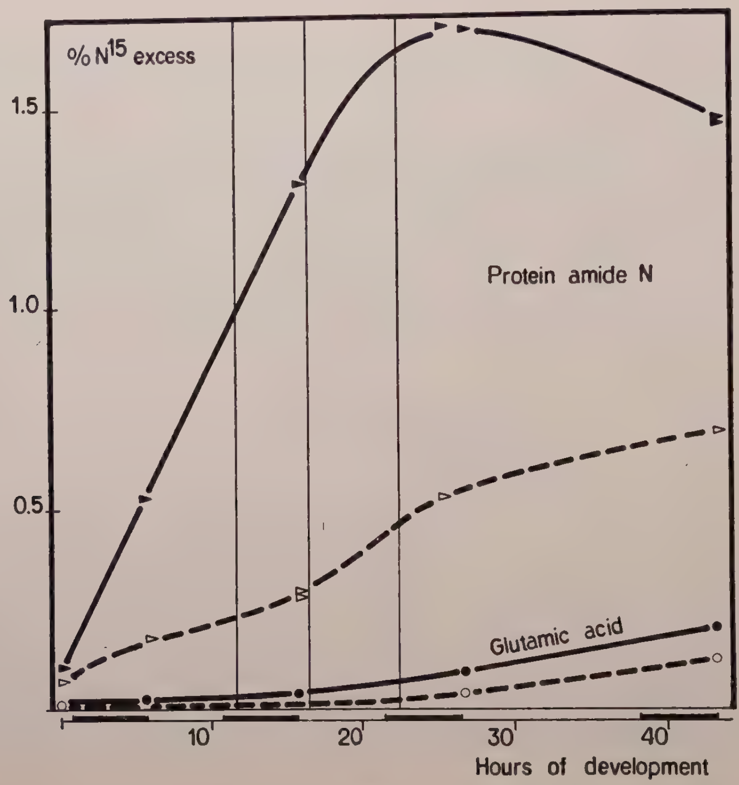

Fig. 1. Paracentrotus embryos at different stages of development kept for 5 hours in sea water containing $N^{15}H_4Cl$. Isotope incorporation into amides and glutamic acid of insoluble (solid signs) and soluble (open signs) proteins. Vertical lines indicate hatching, appearance of mesenchyme cells and start of invagination. The periods of isotope treatment are indicated by horizontal lines at the bottom of the figure.

In the case of glycine this may be largely due to dilution effects caused by the great quantities of free glycine present in the embryos. In lysine no incorporation could be demonstrated with certainty.

The important role played by glutamic acid in the formation of amino acids from ammonia has long been emphasized (5, 3). It has been shown that a synthesis of glutamic acid from α-ketoglutaric acid and ammonia can be performed by metabolizing mitochondria (19). In sea urchin embryos Gustafson *et al.* (8, 11) have found that the number of mitochondria and the activities of various enzymes, generally considered to be associated with mitochondria, distinctly increase from the beginning of the mesenchyme blastula stage. In the present experiments the simultaneous increase in the rate of isotope incorporation into glutamic acid may be related to the augmented mitochondrial activity.

It is generally assumed (3, 1) that amino nitrogen is secondarily transferred mainly from glutamic acid to various other amino acids by way of transamination. The close proportionality, which was found during development between the isotope incorporation into the different amino acids (Fig. 2) is most easily explained on the

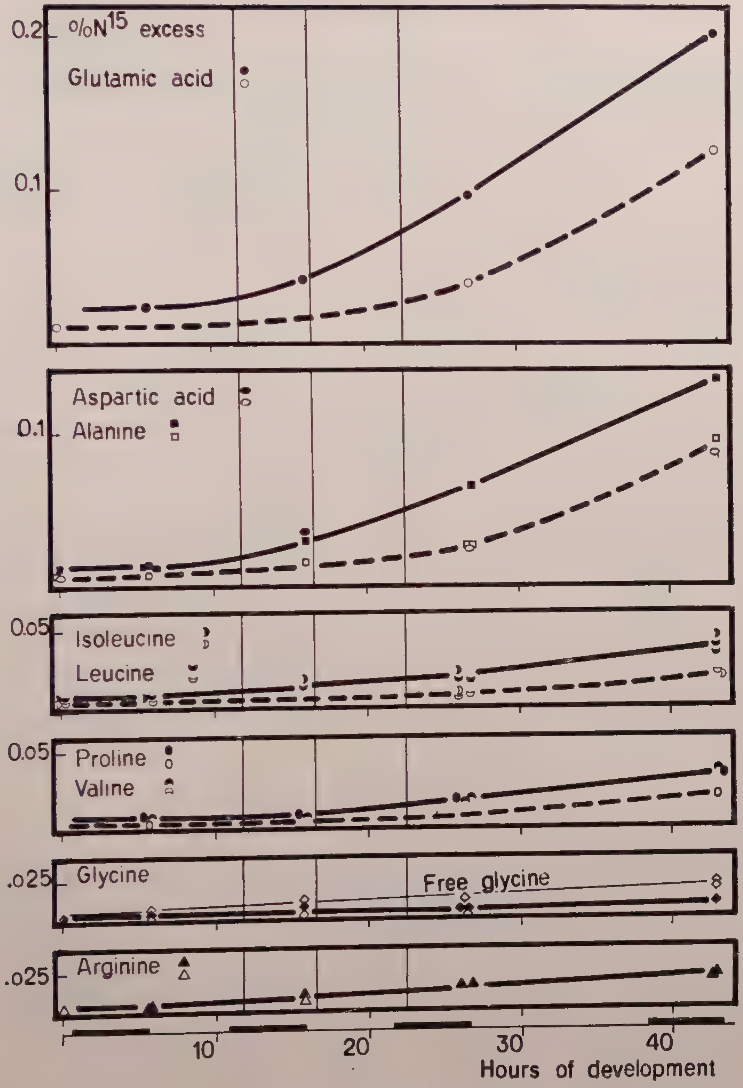

Fig. 2. The same material as in Fig. 1. Isotope incorporation into amino acids.

basis of active transamination from common amino group donors, probably in the first place glutamic acid (1). The scattered data obtained from the free amino acids (Table 1) are consistent with these interpretations.

The all-over incorporation of N^{15}-ammonium chloride into the proteins of developing sea urchin embryos was described in a previous paper (13). It can be concluded from the present analysis that, during the early stages, this incorporation was mainly characterized by the fairly high isotope level of the protein amides. During the later stages, on the other hand, the increasing isotope contents of the amino acid bulk became progressively more preponderant.

Table 1

Paracentrotus embryos at different stages of development kept for 5 hours in sea water containing $N^{15}H_4Cl$. Isotope incorporation into free amino acids. Percent N^{15} excess.

	Unfertilized eggs	Hours after fertilization			
		½–5½	11–16	21–26	38–43
Glutamic acid		0.1	0.4	1.1	
Alanine	0.07			0.5	
Serine	0.01	0.04		0.2	0.3
Glycine	<0.005	<0.01	0.01	0.01	0.02

The incorporation of N^{15}-ammonium chloride into the picolinic acid betaine, isolated from the low molecular fraction, was very small (approximately 0.02 % N^{15} excess) during the periods investigated.

A rather different pattern of isotope distribution was shown by the embryos treated with N^{15}-DL-alanine (Fig. 3). In this case, as might be expected, the highest isotope level in the insoluble protein fractions studied was found in the alanine. During the course of development the incorporation into alanine proceeded in a very similar way to the corresponding incorporation of N^{15}-ammonium chloride into the protein amides (Fig 1). Next to alanine, glutamic acid showed the highest isotope contents. The isotope incorporation into glutamic acid was, during development, in many respects analogous to that of alanine. In comparison with alanine, however, the rate of incorporation into glutamic acid increased somewhat from the mesenchyme blastula stage.

The high isotope level of glutamic acid indicated the presence of a rapid nitrogen exchange between the labeled alanine and glutamic acid by way of transamination. This exchange could be demonstrated also *in vitro* in homogenates of sea urchin embryos. In the experiments accounted for in Table 2, the catalytic amounts of puruvic acid and α-ketoglutaric acid, required for the exchange reactions, had to be taken mainly from the N^{15}-DL-alanine and the fairly concentrated glutamic acid "bank", which had been added to the homogenates. In spite of this, the nitrogen exchange proceeded at approximately the same rate in homogenates of embryos at earlier or later stages of development.

Table 2

Nitrogen exchange between N^{15}-DL-alanine and L-glutamic acid in homogenates of Psammechinus embryos at different stages of development. Isotope contents of glutamic acid, isolated after the incubation. The incubation was performed at 25° C for 1½ hours.

Hours after fertilization	4 (Morulae)	8 (Hatching)	12 (Mesenchyme blastulae)	17 (Gastrulae)	25 (Early plutei)
% N^{15} excess	0.08	0.07	0.10	0.07	0.08

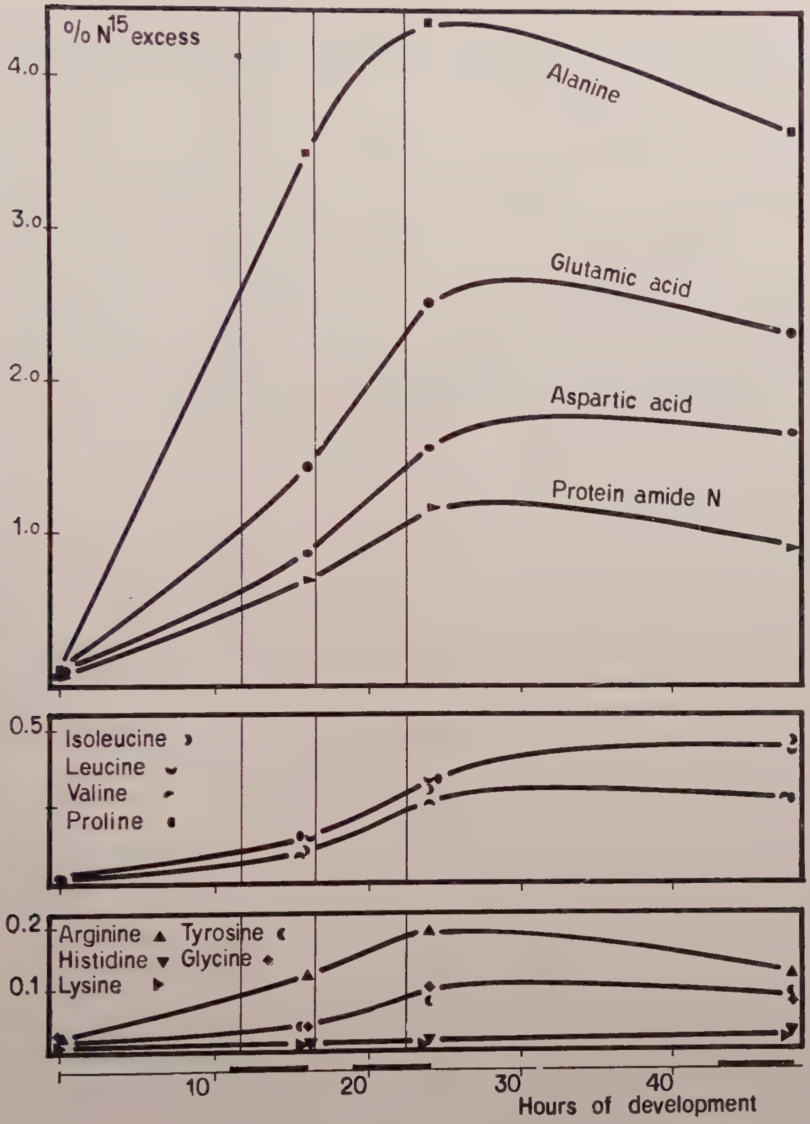

Fig. 3. Paracentrotus embryos at different stages of development kept for 5 hours in sea water containing N^{15}-DL-alanine. Isotope incorporation into amides and amino acids of insoluble proteins.

The slight relative increase in the isotope level of glutamic acid, which became evident from the early mesenchyme blastula stage (Fig. 3) was simultaneous with the corresponding increase found in the experiments with N^{15}-ammonium chloride (Figs. 1, 2). Probably, the exchange between the added N^{15}-alanine and free ammonia by way of glutamic acid was intensified from this period under the influence of the increasing mitochondrial activity (8).

The isotope level of glutamic acid may secondarily have a deciding influence (1) upon the isotope contents of various other amino acids (Fig. 3).

The isotope level of the protein amides may appear unexpectedly high (Fig. 3). The experiments with N^{15}-ammonium chloride suggest (Fig. 1) that the isotope was transferred to the protein amides by way of free ammonia. During the blastula stage, free ammonia is rapidly exchanged not only with protein amides, but, on a considerably larger scale, also with purines and pyrimidines (15). At the same time, however, the exchange reactions between free ammonia and amino acids proceed very slowly (Fig. 2), and also the net breakdown of amino acids to ammonia is rather small (9). It may be questioned, therefore, if the ordinary metabolic paths between L-alanine and ammonia have sufficient capacity before the mesenchyme blastula stage to supply the considerable quantities of labeled ammonia, indicated by the high isotope level of the protein amides. The possibility of an oxidative deamination of N^{15}-D-alanine (24, 31), contributing labeled ammonia to the amide metabolism, may therefore be considered. During the mesenchyme blastula stage, in connection with the intensified nitrogen exchange between ammonia and N^{15}-L-alanine (Fig. 1, 2), the rate of isotope incorporation into the protein amides increased further (Fig. 3).

The following conclusions concerning the amino acid metabolism of sea urchin embryos may be drawn from the experiments reported in this paper. Before the mesenchyme blastula stage, the nitrogen metabolism of amino acids is substantially restricted to exchange reactions at the amino acid level. By way of such exchange reactions, however, new carbon chains may be introduced into the amino acid molecules. From the mesenchyme blastula stage, the metabolic accessibility of the amino acids is considerably increased (cf. 25), the exchange reactions between amino acid nitrogen and ammonia being sucessively intensified. These results agree well with the amino acid analyses of GUSTAFSSON and HJELTE (9), which showed that variations in the total amounts of various amino acids are initiated in the sea urchin embryo during the mesenchyme blastula stage.

The rates of incorporation of N^{15}-ammonium chloride into protein amides and of N^{15}-alanine into protein alanine may be taken as an approximate measure of the velocity of protein rebuilding during different periods of development. The metabolic equivalence between the amide and amino acid components of the proteins may be noted.

It may be suggested that transamidation and transpeptidation processes (6, 21) contribute to the considerable rebuilding of proteins, which occurs in the sea urchin embryos already at stages of development, where the mitochondrial activity is low (8). The presence in the embryo of growth promoting peptides has been demonstrated by GUSTAFSSON *et al.* (10). The importance of submicroscopic cytoplasmic granules for the protein metabolism has previously been emphasized (12, 17). Recently, SIEKEVITZ has shown (35) that a rapid protein metabolism can be induced in such particles *in vitro* under the influence of a soluble, relatively stable factor, produced by metabolizing mitochondria. Similar factors, accumulated in the eggs during the oogenesis, may possibly be of importance for the protein metabolism during the early stages (16).

The pronounced difference in metabolic rates between the water-soluble and insoluble protein fractions has been discussed previously (13, 14, 16, 17). This difference is particularly striking during the period of determination (26) of the primary germ layers. During the same period the nucleotide metabolism is highly increased (15).

In isotope experiments using living cells, permeability factors cannot be left out of consideration. Permeability changes have been reported to occur in the sea urchin egg during fertilization (41). The total amounts of isotope, actually taken up into the cells, cannot be determined with certainty in experiments on sea urchin material, since it is scarcely possible to free the cells satisfactorily from traces of highly labeled isotope carrier, trapped within the fertilization membrane space, blastocoel etc. Very likely, the upptake of labeled amino acids into the unfertilized sea urchin egg is retarded by permeability factors. On the other hand, this is probably not the case with labeled ammonium chloride at the pH of sea water (29, 13). The capacity of the eggs for ammonia accumulation, however, increases during fertilization (29, 13). The close agreement between the experiments with N^{15}-ammonium chloride and N^{15}-DL-alanine suggests that permeability factors have not been of decisive importance in this study.

A way of escaping the permeability question is offered by the fractionation procedure used in these experiments. It is considered that the permeability problem will be of minor importance in experiments of the present kind, where conclusions can be drawn from comparisons between different fractions, isolated from the same labeled material.

SUMMARY

These experiments were performed chiefly with the sea urchin Paracentrotus lividus. Eggs and developing embryos at different stages were kept for exactly 5 hours in sea water, containing N^{15}-ammonium chloride or N^{15}-DL-alanine. The rates of isotope incorporation into various protein constituents were studied in relation to the morphogenesis. The same material had previously been used in investigations of the metabolism of pyrimidines and purines and of the metabolic intensities of different soluble protein fractions.

During the early stages of development the nitrogen metabolism of amino acids was substantially limited to exchange reactions at the amino acid level. These exchange reactions could be demonstrated also *in vitro* as a transfer of N^{15} from labeled alanine to glutamic acid. From the mesenchyme blastula stage the nitrogen exchange between amino acids and free ammonia successively increased.

The incorporation of N^{15}-ammonium chloride into protein amides and of N^{15}-alanine into the protein alanine may be taken as an approximate measure of the intensity of protein rebuilding at different stages. This incorporation was considerably more rapid in proteins not extractable in water than in the soluble proteins. The difference was especially pronounced during the period of the determination of the primary germ layers.

Acknowledgements: The author wishes to express his sincere gratitude to Professor J. RUNNSTRÖM, Director of the Wenner-Gren Institute, for never failing support and interest. He is very indebted to the Staffs of the Zoological Stations of Napels and Kristineberg for laboratory facilities and material, to Miss GUNILLA WESSEL and Miss KERSTIN GUSTAFSON for valuable technical assistance, and to S. LINDVALL and H. LÖW for complementary material. By the courtesy of Professor E. HAMMARSTEN, the N^{15}-measurements were performed in his laboratory.

The investigations were supported by grants from the Swedish Medical and Natural Science Research Councils.

The Wenner-Gren Institute for Experimental Biology, Stockholm.

REFERENCES

1. ÅQUIST, S. E. G., Acta Chem. Scand., *5*, 1046 (1951).
2. BERGMANN, M., and STEIN, W. H., J. Biol. Chem., *129*, 609 (1939).
3. BRAUNSTEIN, A. E., Advances Protein Chem., *3*, 1 (1947).

4. Ehrensvärd, G., Reio, L., Saluste, E., and Stjärnholm, R., J. Biol. Chem., *189*, 93 (1950).
5. Foster, G. L., Schoenheimer, R., and Rittenberg, D., J. Biol. Chem., *127*, 319 (1939).
6. Fruton, J. S., Johnston, R. B., and Fried, M., J. Biol. Chem., *190*, 39 (1951).
7. Fürth, O., and Minnibeck, H., Biochem. Z., *250*, 18 (1932).
8. Gustafson, T., and Hasselberg, I., Exptl. Cell Res., *2*, 642 (1951).
9. Gustafson, T., and Hjelte, M. B., Exptl. Cell Res., *2*, 474 (1951).
10. Gustafson, T., Hjelte, M. B., and Hasselberg, I., Exptl. Cell Res., *3*, 275 (1952).
11. Gustafson, T., and Lenicque, P., Exptl. Cell Res., *3*, 251 (1952).
12. Hultin, T., Exptl. Cell Res., *1*, 376 (1950).
13. ——, Ibid., *1*, 599 (1950.
14. ——, Ibid., *3*, 494 (1952).
15. ——, Arkiv Kemi, *5*, Nr. 25 (1953).
16. ——, Arch. Néerland. Zool., (1953).
17. ——, Arkiv Kemi, *5*, Nr. 52 (1953).
18. ——, Arkiv Kemi, *6* (1953).
19. Hunter, F. E., and Hixon, W. S., J. Biol. Chem., *181*, 67 (1949).
20. Jones, D. B., and Moeller, O., J. Biol. Chem., *79*, 429 (1928).
21. Johnston, R. B., Mycek, M. J., and Fruton, J. S., J. Biol. Chem., *187*, 205 (1950).
22. Kossel A., and Gross, R. E., Z. Physiol. Chem., *135*, 167 (1927).
23. Kossel, A., and Kutscher, Z., Z. Physiol. Chem., *31*, 165 (1900).
24. Krebs, H. A., Klin. Wochenschr., *11*, 1744 (1932).
25. Lindahl, P. E., Acta Zool., *17*, 179 (1936).
26. ——, Arch. Entwicklungsmech. Organ., *140*, 168 (1940).
27. Moore, S., and Stein, W. H., J. Biol. Chem., *178*, 53 (1949).
28. Moore, S., Stein, W. H., and Bergmann, M., Chem. Revs., *30*, 423 (1942).
29. Öström, Å., Z. Physiol. Chem., *271*, 1 (1941).
30. ——, Arkiv Kemi, Mineral, Geol., *15 A*, Nr. 1 (1941).
31. Ratner, S., Schoenheimer, R., and Rittenberg, D., J. Biol. Chem., *134*, 653 (1940).
32. Salzberg, P. L., and Supniewski, J. V., Organic Syntheses, Coll. Vol. *1*, 119 (1941).
33. Schneider, W. C., J. Biol. Chem., *161*, 293 (1945).
34. Schoenheimer, R., and Ratner, S., J. Biol. Chem., *127*, 301 (1939).
35. Siekevitz, P., J. Biol. Chem., *195*, 549 (1952).
36. Sobel, A. E., Hirschman, A., and Besman, L., J. Biol. Chem., *161*, 99 (1945).
37. Stein, W. H., and Moore, S., J. Biol. Chem., *176*, 337 (1948).
38. ——, Biochemical Preparations, *1*, 15 (1949).
39. ——, Cold Spring Harbor Symposia Quant. Biol., *14*, 179 (1950).
40. Stein, W. H., Moore, S., Stamm, G., Chou, C., and Bergmann, M., J. Biol. Chem., *143*, 121 (1942).
41. Stewart, D. R., and Jacobs, M. H., J. Cellular Comp. Physiol., *1*, 83 (1932).
42. Vickery, H. B., J. Biol. Chem., *143*, 77 (1942).

Tryckt den 8 april 1953

Uppsala 1953. Almqvist & Wiksells Boktryckeri AB

ARKIV FÖR KEMI Band 5 nr 51

Mitgeteilt am 12. November 1952 durch H. v. EULER und K. MYRBÄCK

Über D,L-Desoxokynurenin [γ-(*o*-Aminophenyl)-α-aminobuttersäure].

Synthese und Spaltung in optische Antipoden

VON RUTH WEICHERT

Synthese

Für eine Untersuchung über die Bildung von Molekülverbindungen zwischen Rohrzucker und α-Aminosäuren (1) war es notwendig, einen Stoff mit der Konstitution einer γ-(*o*-Aminophenyl)-α-aminobuttersäure zu prüfen. Diese Aminosäure, die m. W. nach bisher in der Literatur nicht beschrieben worden ist, wurde auf folgendem Wege synthetisiert:

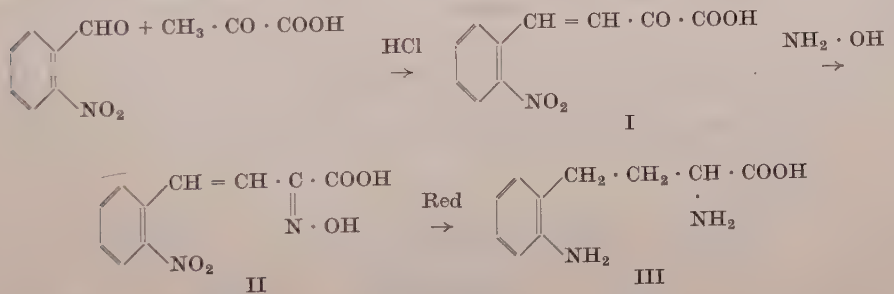

Aus *o*-Nitrobenzaldehyd und Brenztraubensäure wurde nach BAEYER und DREWSEN (2) die *o*-Nitrocinnamoylameisensäure (I) dargestellt und diese Säure mit Hydroxylamin in ihr Oxim (II) übergeführt. Verschiedene Wege zur Reduktion des Oxims wurden geprüft. Die Reduktion mit Na-Amalgam in saurer, neutraler oder alkalischer Lösung führte nicht zum Ziel. HAMLIN und HARTUNG (3) haben eine Methode beschrieben, nach der Oxime von α-Ketosäuren durch katalytische Hydrierung in die entsprechenden α-Aminosäuren in guter Ausbeute übergeführt werden können. Die Hydrierung geschieht unter Druck und in Gegenwart von 2 Moläquivalenten Chlorwasserstoff. Als Katalysator wird Palladiumkohle verwendet. Diese Art der Reduktion führte zwar zum Ziel, doch war die Ausbeute nur etwa 35 % d. Th. Wahrscheinlich spaltet bei der Druckhydrierung der grösste Teil des D,L-Desoxokynurenins (oder eine Vorstufe desselben) unter Ringschluss Ammoniak ab, denn das Hydrierungsprodukt enthält viel Ammoniumchlorid. Als beste Methode zur

Überführung des Oxims in Desoxokynurenin (III) erwies sich die Reduktion mit Jodwasserstoffsäure und rotem Phosphor in Eisessig. Aus der Reaktionsmischung wurde D,L-Desoxokynurenin als in Alkohol schwer lösliches Sulfat in sehr reinem Zustand isoliert. Die Ausbeute betrug etwa 70 % d. Th. Die freie Aminosäure kristallisierte aus Wasser in dünnen, unregelmässigen Blättchen. Ihr UV-Absorptionsspektrum in Wasserlösung zeigt ein Maximum bei 282 mμ ($\varepsilon = 1830$).

Spaltung in optische Antipoden über L-Desoxokynurenin-Rohrzuckerverbindung

Aus einer wässrig-alkoholischen Lösung von D,L-Desoxokynurenin und einem berechneten Überschuss (1) von Rohrzucker kristallisierte in feinen, rosettenförmig angeordneten Stäbchen eine Molekülverbindung, bestehend aus 1 Mol optisch aktivem Desoxokynurenin und 1 Mol Rohrzucker. Aus dieser Verbindung konnte durch vorsichtigen Zusatz von Schwefelsäure optisch aktives Desoxokynureninsulfat mit einer Drehung von

$$[\alpha]_D^{20} = -38{,}1^\circ \pm 0{,}5^\circ$$

gewonnen werden.

Die der Razematspaltung entstammende Mutterlauge der Molekülverbindung lieferte nach Versetzen mit Schwefelsäure den optischen Antipoden des Desoxokynureninsulfats mit einem Drehwert von

$$[\alpha]_D^{20} = +39{,}4^\circ \pm 0{,}6^\circ.$$

Die Zugehörigkeit der Antipoden zu der D- oder L-Reihe wurde nach LUTZ und JIRGENSONS (4) bestimmt. Der Versuch zeigte, dass in der Molekülverbindung das L-Desoxokynurenin enthalten war. Der aus der Mutterlauge gewonnene Antipode war D-Desoxokynurenin. Die Spaltung des Razemats war quantitativ: 97 % d. Th L-Desoxokynureninsulfat wurden über die Molekülverbindung mit Rohrzucker isoliert, während aus der Mutterlauge der Razematspaltung 99 % d. Th. D-Desoxokynureninsulfat gewonnen wurden.

Experimenteller Teil

A. Synthese

1. *o-Nitrocinnamoylameisensäure*

o-Nitrocinnamoylameisensäure wurde nach BAEYER und DREWSEN (2) durch Einleiten von Chlorwasserstoff in eine Lösung von *o*-Nitrobenzaldehyd in Brenztraubensäure bis zur Sättigung dargestellt. Dann wurde der Kolben verschlossen und 2–3 Tage stehen gelassen. Nach dieser Zeit war der Inhalt des Kolbens zu einer Kristallmasse erstarrt. Diese wurde abgesaugt und aus Benzol umkristallisiert: *o*-Nitrocinnamoylameisensäure von Schmp. 135–136°.

2. *o-Nitrocinnamoylameisensäureoxim*

8,5 g *o*-Nitrocinnamoylameisensäure wurden in 95 ml abs. Alkohol gelöst und mit einer alkoholischen Hydroxylaminacetatlösung, dargestellt aus 2,7 g Hydroxylaminchlorhydrat und 3,2 g wasserfreien Natriumacetat, versetzt. Die Lösung wurde ein paar Tage bei Zimmertemperatur stehen gelassen, wobei ein Gemisch von Oxim und Kochsalz ausfiel. Etwa 300 ml Wasser wurden zugesetzt, wobei das Kochsalz in Lösung ging und das im Wasser schwer lösliche Oxim vollständig ausgefällt wurde. Umkristallisation aus Alkohol-Wasser. Ausbeute: 8 g. Schmp.: fängt bei 110° an zu sintern, um bei 129–130° das Kristallwasser ganz abzugeben, wobei die Substanz wieder fest wird und bei 156–157° schmilzt.

3. *Reduktion von o-Nitrocinnamoylameisensäureoxim zu* D,L-*Desoxokynurenin*

a) Katalytische Hydrierung unter Druck nach HAMLIN und HARTUNG (3)

Die Hydrierung wurde in einem Schüttelautoklaven mit Glaseinsatz ausgeführt.

Substanzmenge: 7 g *o*-Nitrocinnamoylameisensäureoxim.
Lösungsmittel: 200 ml Wasser + 10 ml 35 % Salzsäure.
Katalysator: 6 g Pd-Kohle (3 %) + 0,75 g $PdCl_2$.
Druck: 20 Atm.
Temperatur: 20–30–40°.
Dauer: 31 Stunden.

Die theoretische Menge Wasserstoff wurde aufgenommen. Die Lösung wurde filtriert und durch Vakuumdestillation zur Trockne eingedampft. Der Rückstand gab eine positive Ninhydrinreaktion. 2,0 g des Hydrierungsproduktes wurden in wenig Wasser gelöst und mit einer Lösung von 2,4 g Silbersulfat in 420 ml Wasser versetzt. Der Niederschlag von Silberchlorid wurde abfiltriert und Schwefelwasserstoff in das Filtrat eingeleitet, um den Überschuss der Silberionen zu entfernen. Nach Filtrieren und Lüften wurde die Lösung im Vakuum auf etwa 3 ml eingeengt. Nach Zusatz von 60 ml abs. Alkohol kristallisierte D,L-Desoxykynureninsulfat in feinen weissen Nadeln aus. Ausbeute: 0.777 g (ca 35 % d. Th. auf trockenes Hydrierungsprodukt). Trotz vielfacher Umkristallisationen zeigte die Analyse, dass die Substanz noch mit Ammoniumsulfat verunreinigt war.

b) Reduktion mit Jodwasserstoffsäure und rotem Phosphor

Eine Lösung von 10,0 g *o*-Nitrocinnamoylameisensäureoxim in 210 ml Eisessig wurde mit 7 g rotem Phosphor und 100 g Jodwasserstoffsäure (spez. Gew. 1,7) versetzt und über Nacht unter Rückfluss gekocht. Dann wurde im Vakuum zur Trockne eingedampft. Der Rückstand wurde mit Wasser versetzt und wieder zur Trockne eingedampft und dieses so oft wiederholt, bis das Destillat farblos war. Dem Rückstand wurde nun so viel warmes Wasser zugesetzt, dass alles in Lösung ging, dann die 4- bis 5-fache Menge abs. Alkohol und schliesslich 3 ml konz. Schwefelsäure zugesetzt. Die ausgeschiedenen Kristalle von D,L-Desoxokynureninsulfat wurden mit dem roten Phosphor zusammen abgesaugt und mit abs. Alkohol gewaschen, wieder in wenig heissem Wasser gelöst und durch Filtrieren von dem Phosphor befreit. Das Filtrat wurde im Vakuum auf kleines Volumen eingeengt und mit der 4- bis 5-fachen Menge abs. Alkohol versetzt. Es kristallisierten feine weisse Nadeln. Ausbeute: 7,9 g (c:a 70 % d.Th.). Umkristallisation aus Wasser-Alkohol. Ziemlich schwer löslich in kaltem Wasser, leichter in warmen Wasser. Schwerlöslich–unlöslich in Alkohol. Schmp.: 185–186° unter Zersetzung (kurzes Thermometer).

c) D,L-Desoxokynurenin

Zur Darstellung der freien Aminosäure wurde das Sulfat in Wasser gelöst und die Schwefelsäure mit Barytwasser quantitativ gefällt. Das Bariumsulfat wurde abzentrifugiert und die Lösung durch Vakuumdestillation eingeengt. Die freie Aminosäure kristallisierte aus Wasser als dünne, unregelmässige Blättchen, aus 95 % Alkohol als Stäbchen. Umkristallisation aus heissem Wasser. Schmp.: Dunkelfärbung ab 240°, Zersetzung bei 269–270° (kurzes Themometer).

$C_{10}H_{14}O_2N_2$ (194,2)	Ber.:	C 61,83	H 7,27	N 14,42
	Gef.:	» 61,98	» 7,36	» 14,27

B. Spaltung in optische Antipoden über L-Desoxokynurenin-Rohrzuckerverbindung

1. L-*Desoxokynurenin-Rohrzuckerverbindung*

1,218 g Rohrzucker und 0,10 g D,L-Desoxokynurenin wurden in 20 ml heissem Wasser gelöst, mit 370 ml abs. Alkohol verzetzt und über Nacht bei + 3° aufbewahrt. Es kristallisierten rosettenförmig angeordnete, 6-kantige Stäbchen, die ab 200° dunkel wurden und sich bei 211–212° zersetzten (kurzes Thermometer). Ausbeute: 0,1334 g (97 % d. Th.).

Die Molekülverbindung liess sich nicht unzersetzt umkristallisieren und wurde daher ohne jegliche Reinigung analysiert:

$C_{22}H_{36}O_{13}N_2$ (536,5)	Ber.:	C 49,25	H 6.76	N 5,22
	Gef.:	» 49,10	» 6,84	» 4,95

2. L-*Desoxokynureninsulfat und* L-*Desoxokynurenin*

Die Molekülverbindung wurde in möglichst wenig, heissem Wasser gelöst, mit etwas konz. Schwefelsäure und der 10-fachen Menge abs. Alkohol versetzt. Es kristallisierten feine weisse Nadeln von L-Desoxokynureninsulfat. Die Ausbeute war quantitativ. Umkristallisation aus Wasser-Alkohol. Schmp.: 194–196° unter Zersetzung (kurzes Thermometer). Optische Drehung in wässr. Lösung:

$$[\alpha]_D^{20} = -38{,}1° \pm 0{,}5° \text{ (c = 0,25 g/Ltr., l = 4 dm)}$$

Aus dem Sulfat wurde das freie L-Desoxokynurenin dargestellt. Dünne 6-eckige Blättchen aus Wasser oder aus Wasser-Alkohol. Schmp.: Dunkelfärbung ab 215°, Zersetzung bei 260–261° (kurzes Thermometer). Die optische Drehung der freien L-Aminosäure konnte wegen ihrer geringen Löslichkeit nicht gemessen werden.

3. D-*Desoxokynureninsulfat und* D-*Desoxokynurenin*

Die Mutterlauge der Molekülverbindung wurde mit einigen Tropfen konz. Schwefelsäure versetzt. Es kristallisierten feine weisse Nadeln von D-Desoxokynureninsulfat. Ausbeute: 99 % d. Th. Schmp.: 194–196° unter Zersetzung (kurzes Thermometer). Optische Drehung in wässr. Lösung:

$$[\alpha]_D^{20} = +39{,}4° \pm 0{,}6° \text{ (c = 0,25 g/Ltr., l = 4 dm).}$$

Das aus dem Sulfat dargestellte freie D-Desoxokynurenin hatte den Schmelzpunkt 260–261° unter Zersetzung (kurzes Thermometer).

4. *Bestimmung der* D- *und* L-*Konfiguration*

Die Zugehörigkeit der Antipoden zu der D- oder L-Reihe wurde nach der Methode von LUTZ und JIRGENSONS (4) bestimmt. Diese Forscher haben gezeigt, dass bei den gewöhlnlichen α-Aminosäuren der Drehwert sich mit steigender Säurekonzentration in positivem Sinne für L-Antipoden und in negativem Sinne für D-Antipoden ändert.

Aus dem aus der Mutterlauge der Molekülverbindung gewonnenen, rechtsdrehenden Sulfat wurde die freie Aminosäure dargestellt und die Drehung bei verschiedenen Salzsäurekonzentrationen gemessen:

0,075-molare Lösung der Aminosäure. l = 1 dm.
Pro Mol Aminosäure: 2,5 Mol HCl, $[\alpha]_D^{20} = +51{,}8°$
5 » » $[\alpha]_D^{20} = +45{,}8°$
20 » » $[\alpha]_D^{20} = +41{,}1°$

Der Drehwert ändert sich hier in negtivem Sinne. Demgemäss gehört also dies aus der Mutterlauge der Molekülverbindung gewonnene Desoxykynurenin zu der D-Reihe, während der L-Antipode in der Molekülverbindung mit Rohrzucker enthalten ist.

ZUSAMMENFASSUNG

Eine Synthese des D,L-Desoxokynurenins [γ-(*o*-Aminophenyl)-α-aminobuttersäure] ist beschrieben worden. Die Spaltung in optische Antipoden ist mit Hilfe einer Molekülverbindung mit Rohrzucker durchgeführt. Nur die L-Form der Aminosäure gibt mit Rohrzucker eine kristallisierte Molekülverbindung. Die D-Form bleibt in Lösung.

Für die Durchführung der katalytischen Druckhydrierung, für welche mir keine Apparatur zur Verfügung stand, danke ich J. R. GEIGY A. G., Basel. Herrn Assistent W. KIRSTEN, Uppsala, danke ich für die Analysen.

Institutet för organisk kemi och biokemi, Stockholms Högskola, Stockholm.

LITERATUR

1. WEICHERT, R., Arkiv Kemi *5* (1953) 523.
2. BAEYER, A. und DREWSEN, V., Ber. *15* (1882) 2862.
3. HAMLIN, K. E. und HARTUNG, W. H., J. Biol. Chem. *145* (1942) 348.
4. LUTZ, O. und JIRGENSONS, B., Ber. *63* (1930) 448; Ber. *64* (1931) 1221.

Tryckt den 26 mars 1953

Uppsala 1953. Almqvist & Wiksells Boktryckeri AB

ARKIV FÖR KEMI Band 5 nr 52

Communicated 14 January 1953 by JOHN RUNNSTRÖM

Incorporation of N^{15}-DL-alanine into protein fractions of sea urchin embryos

By TORE HULTIN

With 3 figures in the text

It was shown in a previous paper (6) that N^{15}-DL-alanine is taken up by developing sea urchin embryos and incorporated into the proteins of the cells. The rate of this incorporation varies in a characteristic manner during the course of development. This fact became particularly evident in experiments, where the material was fractionated into water-soluble and insoluble proteins. In this paper further studies of the incorporation of N^{15}-DL-alanine into various fractions of sea urchin embryos are reported.

Experimental

1. *Differential centrifugation of homogenates of Psammechinus embryos*

N^{15}-DL-alanine was synthesized from N^{15}-ammonium nitrate (65 % excess N^{15}) by way of potassium phtalimide (cf. 13, 15).

Embryos of the sea urchin *Psammechinus miliaris* (Gmelin) were used in the experiments. The embryos were allowed to develop for 3 hours in sea water, containing approximately 1 mg of N^{15}-DL-alanine per mg of total egg nitrogen. After the isotope treatment the embryos were washed repeatedly in isotonic NaCl-solution, containing 0.05 volumes of isotonic sodium citrate. The embryos were homogenized at $-2°$ C in a small volume of 0.6 M sucrose solution. The homogenization was performed in the following way. The opening of a 25 ml pipette was made very narrow and bent in a sharp angle. By means of a 3-way valve the pipette could be alternately connected with a water pump or with a pressure flask (0.5 kg/cm²). By turning the valve, the suspension was either rapidly sucked into the pipette or sharply squirted out against the wall of the glass tube, in which the homogenization was performed.

The homogenates were diluted with approximately 50 ml of 0.6 M sucrose solution per ml of eggs, packed tightly by centrifugation. Isotonic sucrose solution could not be employed, because its density is so high that material accumulates at the surface during centrifugation. The suspensions were centrifuged twice at 4000 g for 10 minutes. The sediments, which consisted primarily of cell fragments, nuclei and yolk granules, were discarded. The supernatants were centrifuged at 16000 g for 20 minutes. The sediments obtained were resuspended in 0.6 M sucrose solution and centrifuged a second time under the same conditions (Sediment 1). The supernatants were also recentrifuged for 20 minutes at the same speed. The sediments were discarded. The supernatants obtained were centrifuged for 100 minutes at 105000 g (Sediment 2). The supernatants were collected, and $CaCl_2$ was added to a final concentration of 0.012 M (cf. 12). The precipitate (Cell fluid A) was removed by centrifugation, and the clear solution was precipitated with saturated ammonium sulfate (Cell fluid B). From these fractions, protein samples were prepared as described by SCHNEIDER (14), and the protein nitrogen was determined and analyzed for N^{15} in a mass spectrograph.

2. *Soluble fractions of lyophilized Paracentrotus material*

Suspensions of *Paracentrotus lividus* (LM) eggs were divided in 4 equal samples. One of these samples was directly treated with N^{15}-DL-alanine for 5 hours. The other samples were fertilized and allowed to develop at 20° C in rocking glass trays as described by LINDAHL (11). At 11, 19 and 43 hours of development a sample was washed by centrifuging and transferred to fresh sea water, containing approximately 1 mg of N^{15}-DL-alanine per mg of total egg nitrogen. The embroys were allowed to develop in the isotopic medium for exactly 5 hours. Before and after the isotope treatment the eggs and embryos were examined in the microscope. The isotopic material was washed by centrifuging in sea water and in isotonic NaCl, containing 0.05 volumes of isotonic sodium citrate solution. The material was then immediately freeze-dried and stored at —20°C.

The dry material was finely powdered in a mortar and extracted for 2 hours at + 2° C with 0.9 % NaCl, containing 0.05 M phosphate buffer, pH 7.4. For each gram of dry powder 25 ml of solution was added. The extractions were performed by grinding the material with air-driven, vigorously rotating glass-rods. The suspensions were centrifuged and the supernatants recentrifuged at 8000 g for 60 minutes. The extracts were dialyzed against the buffered 0.9 % NaCl-solution and then centrifuged at 75000 g for 120 minutes. The perfectly clear top layers were collected.

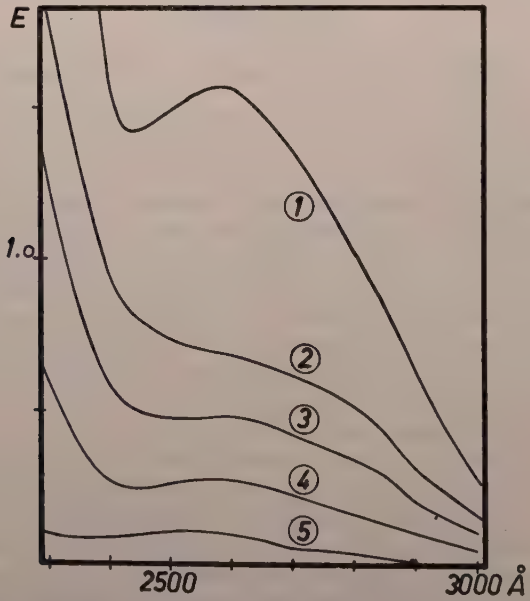

Fig. 1. Extract of Paracentrotus embryos in buffered 0.9 % NaCl, dialysed and treated with different concentrations of ammonium sulfate. Ultraviolet absorption of filtrates, corrected for deproteinized (90 % sat. ammonium sulfate) extract. 1) 0 %, 2) 50 %, 3) 60 %, 4) 70 %, and 5) 80 % sat. ammonium sulfate.

From an ammonium sulfate solution, saturated at + 2° C, the following series of dilutions had previously been prepared: 50 %, 60 %, 70 %, 80 % and 90 % saturation. From these solutions 10 volumes were added to samples taken from the extracts. The mixtures were kept for 75 hours at + 2° C with frequent stirring. They were filtered through hard filter papers, and the ultraviolet absorption of the filtrates was determined in a Beckmann spectrophotometer (Figure 1). The precipitates were washed on the filter papers with the ammonium sulfate solutions used for precipitation. The proteins of the precipitates and filtrates were isolated (14), and the nitrogen of the protein samples was determined and used for N^{15}-measurements. On the basis of the values obtained from the series of precipitates and filtrates, the isotope contents of the various fractions were calculated (Figure 3).

The egg material was extracted a second time with buffered, 0.9 % NaCl-solution (Extract 2), and finally with 2 N NaCl (Extract 3). The extracts were centrifuged as described previously, the final centrifugation being at 75000 g for 2 hours. The proteins of the supernatants were directly precipitated with trichloroacetic acid and purified (14), and the N^{15}-contents of the protein nitrogen was determined.

Results and Discussion

The prominent role of submicroscopic cytoplasm constituents in the protein metabolism of cells has been repeatedly emphasized (4, 1, 10, 9, 17, 16, 8). The present experiments (Table 1) show that during the early development of the Psammechinus embryos there is a much more rapid incorporation of N^{15}-alanine into the fraction containing submicroscopic particles (Sediment 2) than into the other isolated cytoplasm fractions. On the basis of previous experiments it was suggested (5, 6, 7, 8) that a progressive multiplication and growth of small, granular cytoplasm constituents is initiated during the early sea urchin development. The present results are in agreement with this assumption.

Table 1

Psammechinus embryos allowed to develop for 3 hours in the presence of N^{15}-DL-alanine. Homogenates fractionated by means of differential centrifugation. Isotope incorporation into the proteins of different fractions, per cent N^{15} excess.

Sediment 1 obtained by centrifugation at 16 000 g for 20 minutes. Sediment 2 at 105 000 g for 100 minutes. Cell fluid A contained proteins insoluble in 0.012 M $CaCl_2$, under which conditions the proteins of Cell fluid B were soluble.

	Cleavage stages		Mesenchyme blastula stage
Sediment 1	0.11	0.09	0.44
Sediment 2	0.23	0.28	0.42
Cell fluid A . . .	0.14	0.17	0.41
Cell fluid B . . .	0.11	—	0.25

During the mesenchyme blastula stage the rate of isotope incorporation into the mitochondria fraction (Sediment 1) was greatly increased and attained the same level as the incorporation into the fraction containing submicroscopic particles. This may be interpreted as an indication of a rapid growth of new mitochondria populations, which, as GUSTAFSON and LENICQUE (3) have shown, occurs during this period of sea urchin development.

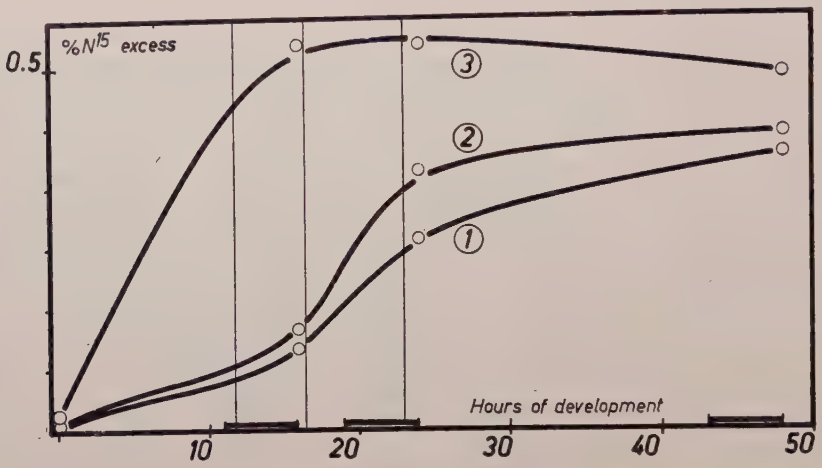

Fig. 2. Rates of isotope incorporation into extracted proteins from Paracentrotus eggs and embryos. 1, 2) Subsequent extractions in buffered 0.9 % NaCl. 3) Final extraction in 2 N NaCl. The vertical lines indicate hatching, appearance of mesenchyme cells, and start of invagination. Periods of isotope treatment indicated by horizontal lines. The curves of Fig. 2 and 3 were drawn in analogy with (6).

The rate of incorporation into the proteins of the cell fluid was also considerably increased during the mesenchyme blastula stage. The increase was particularly pronounced in the fraction precipitated with $CaCl_2$ (Cell fluid A). It has been shown (12) that this fraction contains a great part of the soluble nucleoproteins of the embryos.

For technical reasons, the further study of the soluble fractions had to be performed on lyophilized Paracentrotus material. The Paracentrotus extracts in buffered 0.9 % NaCl (Figure 2) showed a characteristic rise in the rate of isotope incorporation during the mesenchyme blastula stage. A similar rise had previously been demonstrated in water-extracts from frozen and thawed Psammechinus embryos (6). The increased isotope incorporation into the soluble proteins during the mesenchyme blastula stage was concentrated in a fraction precipitated with 50 % saturated ammonium chloride (Figure 3). Like the $CaCl_2$-precipitates, mentioned above, this fraction contained a significant part of the soluble nucleoproteins of the extracts (Figure 1). The increase was less pronounced in a second protein fraction, precipitated with 50 %–60 % saturated ammonium sulfate, and it was not observed in the subsequent two fractions. In these latter fractions an accelerated incorporation was found to occur after the beginning of the invagination. A very small fraction was obtained with 80 %–90 % saturated ammonium sulfate. This fraction showed a remarkably high rate of incorporation.

A different metabolic picture was shown by the Paracentrotus-extracts in 2 N NaCl (containing proteins not soluble in 0.9 % NaCl). In this case the isotope incorporation was already very rapid during the blastula stage. These extracts, therefore, were analogous to the total non-soluble fractions of Psammechinus embryos, described previously (6).

The metabolic and morphogenetic significance of the protein fractions studied in these experiments is very little understood at present. The experiments suggest, however, a correlation between the increasing morphogenetic activity during the

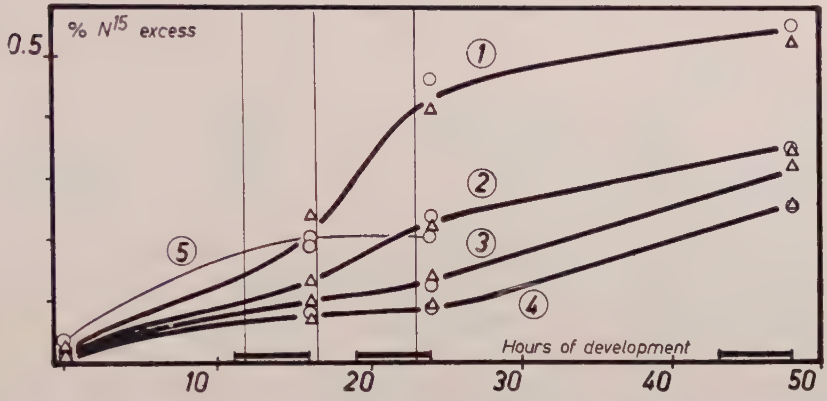

Fig. 3. Extracts of Paracentrotus embryos in buffered 0.9 % NaCl fractionated by means of ammonium sulfate. Rates of isotope incorporation at different stages of development into the proteins of the following fractions: 1) 0–50 %, 2) 50–60 %, 3) 60–70 %, 4) 70–80 %, and 5) 80–90 % sat. ammonium sulfate. ○ and △ represent independent series of experiments.

mesenchyme blastula stage and a higher metabolic rate of certain kinds of soluble proteins. It may be assumed that a production of specific proteins of morphogenetic significance is gradually increased during the mesenchyme blastula stage. This production is probably mediated by new populations of submicroscopic granules under the influence (cf. 16) of an increasing mitochondrial activity (2).

SUMMARY

Homogenates of sea urchin embryos, labeled with N^{15}-DL-alanine, were fractionated by means of differential centrifugation. During the first stages of development a considerably higher rate of isotope incorporation was found in the fraction containing submicroscopic particles than in the other isolated cytoplasm fractions. During the mesenchyme blastula stage, however, the rate of incorporation into the mitochondria fraction equalled that for the submicroscopic particles. The proteins of the cell fluid also showed a higher rate of incorporation.

The incorporation into different soluble protein fractions was studied further in lyophilized material. The increase in the incorporation rate, which occurs in the mesenchyme blastula stage, was largely confined to a fraction, which precipitates in 50 % saturated ammonium chloride.

Acknowledgements

The sea urchin material used in these experiments was prepared at the Zoological Stations of Kristineberg and Naples. The author is very indebted to the Authorities of these Stations for laboratory facilities and material. He wishes to express his sincere gratitude to Professor J. Runnström, Director of the Wenner-Gren Institute for his support and interest. He is much indebted to S. Lindvall and H. Löw for a supply of material, and to Miss Kerstin Gustafsson for technical assistance. By the courtesy of Professor E. Hammarsten, the N^{15}-measurements were performed in his laboratory.

The investigations were supported by grants from the Swedish Medical and Natural Science Research Councils.

The Wenner-Gren Institute for Experimental Biology, Stockholm.

REFERENCES

1. BORSOOK, H., DEASY, C. L., HAAGEN-SMIT, A., KEIGHLEY, G., and LOWY, P. H., Fed. Proc., *9*, 154 (1950).
2. GUSTAFSON, T., and HASSELBERG, I., Exptl. Cell Res., *2*, 642 (1951).
3. GUSTAFSON, T., and LENICQUE, P., Exptl. Cell Res., *3*, 251 (1952).
4. HULTIN, T., Exptl. Cell Res., *1*, 376 (1950).
5. ——, Ibid., *1*, 599 (1950).
6. ——, Ibid., *3*, 494 (1952).
7. ——, Arkiv Kemi, *5*, Nr 25 (1953).
8. ——, Arch. Néerland. Zool., (1953).
9. KELLER, E. B., Fed. Proc., *10*, 206 (1951).
10. LEE, N. D., ANDERSON, J. T., MILLER, R., and WILLIAMS, R. H., J. Biol. Chem., *192*, 733 (1951).
11. LINDAHL, P. E., Acta Zool., *17*, 179 (1936).
12. LINDVALL, S., and CARSJÖ, A., Exptl. Cell Res., *2*, 491 (1951).
13. SALZBERG, P. L., and SUPNIEWSKI, J. V., Organic Syntheses, Coll. Vol. *1*, 119 (1941).
14. SCHNEIDER, W. C., J. Biol. Chem., *161*, 293 (1945).
15. SCHOENHEIMER, R., and RATNER, S., J. Biol. Chem., *127*, 301 (1939).
16. SIEKEVITZ, P., J. Biol. Chem., *195*, 549 (1952).
17. SIEKEVITZ, P., and ZAMECNIC, P. C., Fed. Proc., *10*, 246 (1951).

Tryckt den 26 mars 1953

Uppsala 1953. Almqvist & Wiksells Boktryckeri AB

ARKIV FÖR KEMI Band 5 nr 53

Mitgeteilt am 14. Januar 1953 von H. von EULER

Nicotinsäureamid in Leber und Milz von Ratten nach Fütterung mit 4-Dimethylaminoazobenzol

Von OLAF KLAMERTH

In den letzten Jahren hauptsächlich von amerikanischen Arbeitskreisen durchgeführte Untersuchungen über den Gehalt von Wuchsstoffen und Vitaminen in Lebertumoren, die durch Verfütterung von Azofarbstoffen, insbesondere 4-Dimethylaminoazobenzol, hervorgerufen wurden, ergaben Nicotinsäureamid-Werte, die nur etwa $^1/_4$ bis $^1/_{10}$ der für normale Lebern gültigen betrugen.[1] Es wurde hierbei festgestellt, dass die Zufuhr des cancerogenen Farbstoffes bereits vor Ausbildung des Tumors den Gehalt der Leber an Lactoflavin[2], Pyridoxin sowie Biotin[3] stark absinken lässt.

Die Abnahme des Lactoflavingehaltes in der Leber wurde besonders in causale Beziehung zur Geschwulstbildung gebracht[4], die nach den Untersuchungen von MILLER und Mitarbeiter[5] darin besteht, dass im Lactoflavin wahrscheinlich das Coferment eines Enzymes vorliegt, welches die reduktive Aufspaltung des Buttergelb und damit seine Entgiftung bewirkt. Da der Vitamincharakter des Nicotinsäureamides (NA) als Vorstufe zur Co-dehydrase I und II[6] die Annahme einer ähnlichen Funktion rechtfertigt, war es von Interesse, festzustellen, wie sich der Gehalt an Nicotinsäureamid von Lebern normal ernährter Ratten verhält zu dem durch Buttergelb erzeugter Hepatome bzw. von Lebern im Zustand der Pro-neoplasie. Die Cancerisierung eines Organes hängt bei gegebener Menge und Zeit des einwirkenden Cancerogens von der Resistenz des gesunden Gewebes ab, welches durch Infiltration bedroht ist. Ferner kommt möglicherweise der Milz eine Sonderstellung in der Tumor-„Abwehr" zu. Deshalb interessierte uns nicht nur der Niktotinsäureamid-Gehalt in Lebern und Hepatomen, sondern auch in der Milz.

Die Bestimmung von freiem NA im Körper normal ernährter Ratten wurde erstmalig von EULER u. Mitarb.[7] durchgeführt, während über das Vorliegen von

---

[1] Literaturzusammenstellung in E. MILLER u. J. MILLER: The Biochemistry of Hepatic carcigenosis, Medical School, Univ. Wisconsin. Deutsche Übersetzung von H. NOTHDURFT in „Grenzen der Wissenschaft", Heft 1, S. 46.

[2] A. C. GRIFFIN u. C. A. BAUMANN, Arch. Biochem. 11, 467 (1946), Cancer Res. 8, 279 (1948), C. J. KENSLER, K. SUGIURA, N. F. YOUNG, C. R. HALTER u. C. P. RHOADS, Science 93, 308 (1941), E. C. MILLER, J. A. MILLER, B. E. KLINE u. H. P. RUSCH, J. exp. Med. 88, 89 (1948).

[3] E. C. MILLER, J. A. MILLER, B. E. KLINE u. H. P. RUSCH, J. exp. Med. 88, 89 (1948).

[4] G. M. PRICE, G. A. MILLER u. E. C. MILLER, Cancer Res. 11, 523 (1951).

[5] G. C. MUELLER u. J. A. MILLER, J. Biol. Chem. 180, 1125 (1949), 185, 154 (1950).

[6] H. v. EULER, MALMBERG, ROBEZNIEKS u. SCHLENK, Nat. 26, 45 (1938), v. EULER, SCHLENK, HEIWINKEL u. HOEGBERG, Z. physiol. Chem. 247, 4 (1937) 256, 208 (1938), vgl. Fussnote i. v. EULER u. SCHLENK, Klin. Wschr. 33, 1109 (1939).

[7] H. v. EULER, F. SCHLENK, L. MELZER u. B. HÖGBERG, Ztschr, f. physiol. Chem. 258, 212 (1939). — Siehe auch B. BENCZE, Z. f. Vitamin-, Hormon- u. Fermentforsch. 3, 429; 1950.

Nikotinsäure in cancerösem Gewebe Untersuchungen von TAYLOR und Mitarb. vorliegen.[8]

Da uns nur eine beschränkte Anzahl von Buttergelb-Ratten zur Verfügung stand, von denen nur eine ein ausgeprägtes Hepatom aufwies, werden die vorliegenden Befunde mit der gebührenden Zurückhaltung veröffentlicht und dienen mehr der Orientierung — das Versuchsmaterial soll bald ergänzt werden, Die gefundenen Werte weisen immerhin signifikante Unterschiede auf, wie die folgende Tabelle veranschaulicht:

Tiegerwicht in g	Lebergewicht in g	Milzgewicht in g	Buttergelb Gsamtmenge in mg	NA-Gesamtmenge (als Nikotinsäure bestimmt) in γ	NA/g Frischorgan in γ
350	14.35	1.3	—	721 * 49	50 Leber 37 Milz
312	14.8	—	—	540	37 Leber — Milz
395	15.2	1.25	—	420 44	28 Leber 35 Milz
232	13.3	1.2	2 600	620 52	46 Leber 43 Milz
272	14.8	1.2	3 100	520 40	36 Leber 36 Milz
257	38.7 (24.9 Hepatom, 13.8 Lappen)	3.46	2 600	1 592 (Gesamt 432 Hepatom 1 160 Lappen 230 Milz	41 Hepatom 18 Hepatom 84 Lappen 66 Milz

Diskussion

Entsprechend unseren Erwartungen wies das Hepatom einen ausserordentlich niedrigen Gehalt an NA auf, während die getrennt davon untersuchten Leberlappen desselben Tieres das Doppelte der beobachteten Normalwerte zeigten. Für das Gesamtorgan Leberlappen + Hepatom ergab sich eine vom Normalwert nur unwesentlich nach oben abweichende Zahl.[9] Die Milz dieser Ratte enthielt fast doppelt so viel NA wie die der Kontrolltiere, die sich in ihrem Gehalt kaum unterschieden von denen im präcancerösen Stadium. Die Zahlen für die präcancerösen Lebern der mit Buttergelb behandelten Tiere lagen nur wenig höher als die der unbehandelten Kontrolltiere, doch kann dies in Analogie zu den Befunden von CONSBRUCH und SCHMAEHL[10] für Lactoflavin darauf zurückzuführen sein, dass nach Absetzen der Buttergelb-Zufuhr sehr rasch wieder Normalwerte erreicht werden, solange noch kein deutlich ausgebildetes Hepatom vorliegt. Die verwendeten Versuchstiere waren bereits 14 Tage vor der Untersuchung auf Buttergelb-freie Normaldiät gesetzt worden.

---

[8] A. TAYLOR, POLLACK, HOFER u. WILLIAMS, Cancer Res. 2, 744 (1942).

* Dieser Wert erscheint nicht ganz verlässlich, weil die Lösung leichte Eigenfärbung aufwies, die auch mit $KMNO_4$ nicht verschwand.

[9] In Übereinstimmung mit den Untersuchungen von BANDIER über den Gehalt von Nikotinsäure in verschiedenen Organen haben wir bei unseren Bestimmungen eine ziemliche Schwankungsbreite der Normalwerte festgestellt.

[10] U. CONSBRUCH u. D. SCHMÄHL, Ztschr. f. physiol. Chem. 290, 28 (1952).

Methodik

Nikotinsäureamid wurde nach der Methode von BANDIER[11] als Nikotinsäure kolorimetrisch bestimmt. Um der Gefahr vorzubeugen, dass ein Teil des NA aus der Cozymase abgespalten wird, haben wir nach EULER u. Mitarb.[7] folgende Vorbehandlung angewandt: Das unmittelbar nach Schlachtung der Versuchstiere herauspräpararierte Organ wurde sofort unter der zehnfachen Menge absoluten Acetons mit Quarzsand homogen verrieben und in geschlossenem Kolben 12 Stunden bei Zimmertemperatur auf der Maschine geschüttelt. Wie obige Autoren feststellten, geht dabei nur NA in Lösung, während die Cozymase, deren enzymatische Spaltung durch die blockierende Wirkung des Acetons verhindert wird, in Aceton unlöslich ist. Die acetonische Organsuspension wurde zentrifugiert und die Extraktion noch zweimal mit frischem Aceton in derselben Weise wiederholt. Die erhaltenen wasserklaren acetonischen Lösungen wurden im Vakuum eingedampft und der Rückstand nach der Methode von BANDIER (Ausführung wie in HINSBERG-LANG, Med. Chemie, 2. Auflage, S. 374 beschrieben) bestimmt. Die Messungen führten wir im Absorptionsmaximum bei 400 mμ mit dem Beckmann-Spektrophotometer aus und ermittelten den NA-Gehalt nach einer Eichkurve mit bekannten Mengen Nikotinsäure. Der NA-Gehalt der Leber unterliegt beträchtlichen individuellen Schwankungen, wie bereits mehrmals von anderer Seite festgestellt wurde.

Die verwendeten Ratten entstammten alle demselben weissen norwegischen Stamm dieses Institutes, hatten ein Durchschnittsalter von 11 Monaten und wogen zwischen 260 und 395 g. Die Buttergelb-Diät[12], der die untersuchten Ratten bis 14 Tage vor ihrer Schlachtung unterworfen waren, wurde mindestens 8 Monate lang durchgeführt.

ZUSAMMENFASSUNG

In der Leber von normal ernährten Ratten wurde mit erheblicher Schwankungsbreite ein Gehalt von 37 γ Nikotinsäureamid (als Nikotinsäure bestimmt) pro g Frischorgan festgestellt. Denselben Wert weist auch die Milz auf. Ratten, die durch mindestens 8 Monate einer Buttergelb-Diät unterworfen waren, aber noch kein Hepatom ausgebildet hatten, enthielten in beiden Organen nur unwesentlich höhere Mengen. Dagegen konnte bei einer Ratte mit deutlich ausgebildetem Hepatom für das Hepatom selbst ein Wert von 18 γ NA/g, für die Leberlappen 84 γ NA/g und für die Milz 66 γ NA/g festgestellt werden.

Stockholm, Universität, Vitamin-Institut und Institut für organisch-chemische Forschung.

---

[11] E. BANDIER u. G. HALD, Biochem. J. 33, 264 (1939). Siehe auch W. LAMMERS, P. SIDERIUS u. J. H. GAARENSTROOM, Acta physiol. et pharmac. Neerl. 1, 193; 1950.

[12] Die Ratten erhielten eine Kost mit folgender Zusammensetzung:

Rohrzucker	150 g	Trockenhefe	75 g
Weizenstärke	750 g	Salzmischung	150 g
Weizenkleie	1 050 g	Fett mit 0,6 % Farbstoff	300 g
Mais	600 g		

Dazu einmal per Woche 120 ml Lebertran u. einmal per Woche Gemüse. Berechnet per Tag von dieser Kost pro Tier 15 g. Während der ersten 5 Monate der Versuchszeit wurde den Tieren eine Zulage von Farbstoff in Öl mit Pipette gegeben.

Tryckt den 26 mars 1953

Uppsala 1953. Almqvist & Wiksells Boktryckeri AB

ARKIV FÖR KEMI Band 5 nr 54

Communicated 28 January 1953 by Einar Hammarsten and Erik Jorpes

The incorporation of ammonia into uric acid in pigeons and ribonucleic acid pyrimidines in rats

By Ulf Lagerkvist

With 3 figures in the text

In recent years several small molecules: CO_2, formate and glycine, have been shown to enter certain positions in the purine ring as well as, in the case of CO_2, the pyrimidine ring (1, 2, 3). Thus the amino group of glycine is known to be the direct precursor of nitrogen atom 7 (2, 4) in the purines but regarding the precursors of the remaining purine nitrogens and of the pyrimidine nitrogen atoms very little is known. Buchanan et al. (1) in their investigations of the precursors of uric acid in pigeons have demonstrated that N^{15}-ammonia is incorporated to the same extent into the pyrimidine and imidazole moieties of uric acid. Recently Sonne and Lin (5) have investigated the relative incorporation of N^{15}-labeled ammonia and aspartic acid into hypoxanthine in pigeon liver extracts using the incorporation of 1–C^{14}-glycine to determine the rate of hypoxanthine synthesis. They conclude that since the incorporation of isotope from labeled ammonia was only one fourth of that from aspartic acid, ammonia cannot be a direct precursor of any of the purine nitrogen atoms.

However, in view of the rather high incorporation of isotope from labeled ammonia into uric acid in pigeons and nucleic acid pyrimidines in rats both in vivo (6) and in vitro[1] it seemed worth while to investigate more thoroughly the distribution of isotope from labeled ammonia in the pyrimidine and purine rings. This called for suitable degradation methods for these substances. In an earlier publication (7) a method was described that made it possible to determine the distribution of isotope between the nitrogen atoms of the pyrimidine ring and now a similar degradation for the purines had to be elaborated. The method was worked out for uric acid but since adenine, guanine, hypoxanthine and xanthine are easily converted to uric acid by deamination (adenine and guanine) and oxidation with xanthine oxidase it can also be applied to these substances.

It is well known that nitrogen atom 7 of the purines can be isolated as glycine (8) after acid hydrolysis, and several authors have used this method in tracer studies (2, 4). In order to separate nitrogen atoms 1 and 3 the following procedure was used. Uric acid was methylated to a mixture of 3- and 9-methyluric acid (9, 10). Since these substances crystallize in a mixed crystal they could not be separated by crystallization or partition chromatography and were consequently obtained together. Oxidation with $KClO_3$ (11) gave methylalloxan and alloxan and on further oxidation of the methylalloxan with PbO_2 (12) and hydrolysis with dilute HCl nitrogen atoms 1 and 3 were liberated as ammonia and methylamine respectively.

---

[1] Lagerkvist, U., and Reichard, P., unpublished.

Since nitrogen atom 9 is not isolated during the degradation the isotope excess of this nitrogen must be calculated by difference.

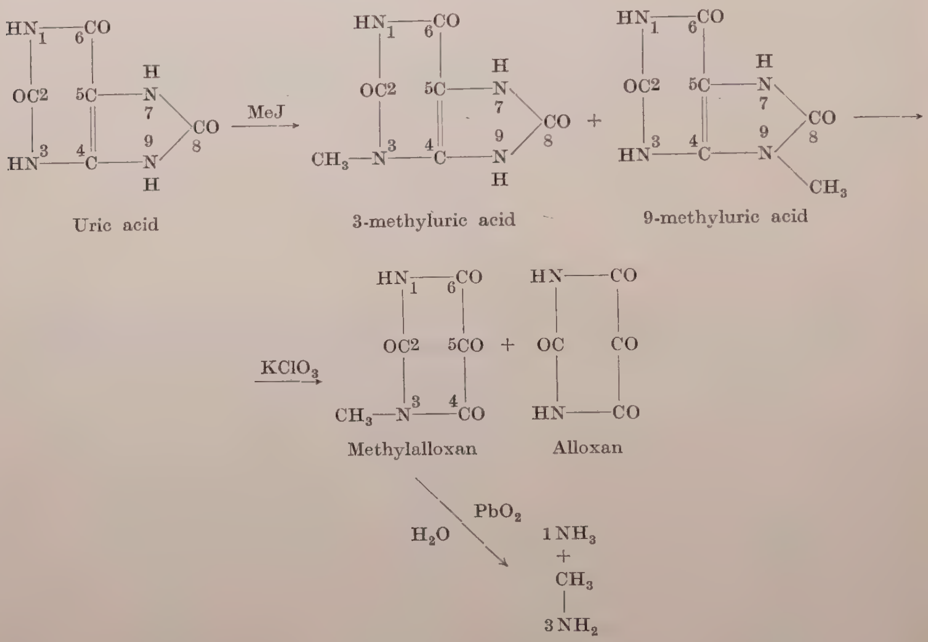

Uric acid

3-methyluric acid

9-methyluric acid

Methylalloxan

Alloxan

Using these methods the distribution of isotope from N^{15}-labeled ammonia in uric acid from pigeons and ribonucleic acid pyrimidines from rats was investigated. The pyrimidines were found to incorporate about 3 times as much isotope in position 1 as in position 3.[1] Degradation of uric acid revealed the fact that the isotope was almost exclusively located in position 3 and 9. Because of the relatively high incorporation of isotope from N^{15}-aspartic acid into hypoxanthine in pigeon liver extracts reported by SONNE and LIN (5), this substance was also tried on pigeons. The results of the degradations showed that the incorporation of isotope was of the same order of magnitude in all the nitrogen atoms of the uric acid.

Experimental

Methods

The degradation of uric acid

Methylation of uric acid. The uric acid (0.3–0.5 mM) was transferred to a small bombtube, length 100 mm, diameter 10 mm, and dissolved with warming in 1.1 ml

---

[1] The numbering of the atoms is in agreement with that used in Beilstein's Handbuch der organischen Chemie.

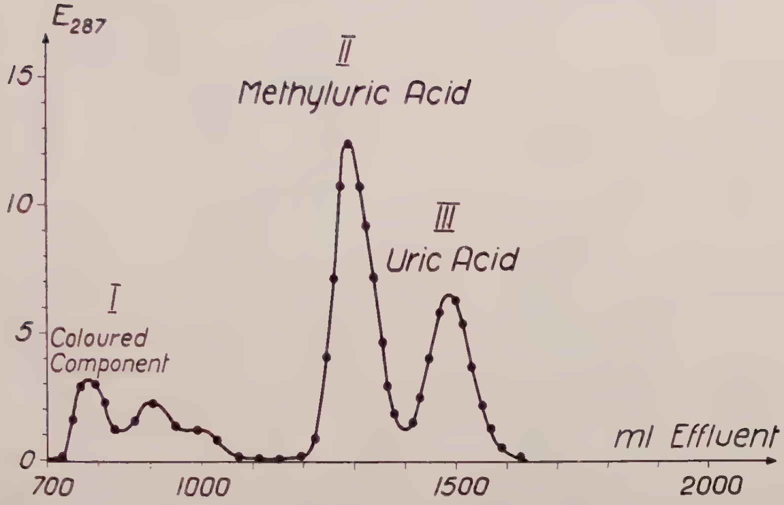

Fig. 1. Chromatography of the products obtained after methylation of uric acid. Length of column: 382 mm, diameter: 67 mm.

water and 0.2 ml N KOH/0.1 mM uric acid. The solution was cooled to room temperature and a 2 M solution of methyl iodide in alcohol added using a slight excess of methyl iodide (1.25 mM methyl iodide/1 mM uric acid). The tube was sealed while it was immersed in an ice bath and then shaken for 3 hours in a boiling water bath.

Chromatography of methylated uric acid. The tube was opened and the contents diluted with 3 ml water and 6 ml propanol/0.1 mM uric acid. Enough conc. HCl was added to make a solution of propanol–0.5 N HCl, 2:1. The solution was applied to the top of a starch column, 350 mm in length, the diameter was dependent upon the amount of uric acid methylated. A diameter of at least 70 mm was used for 0.3 mM uric acid. The chromatogram was developed with propanol–0.5 N HCl, 2:1 and read in the Beckman spectrophotometer at 2870 Å.

The *R*-value for the second peak (1.04) agrees with that found by the present author for ζ-methyluric acid (a mixture of 90–95 % 3-methyluric acid and 5–10 % 9-methyluric acid) (10). The *R*-value for the third peak (0.90) agrees with that for uric acid. The second peak had light absorption maxima at 2330 and 2870 Å and the third peak at 2300 and 2830 Å in agreement with the positions of the absorption maxima of ζ-methyluric acid and uric acid. The light absorption curves were obtained in N HCl. The methyluric acid in the second peak was further purified by dissolving it in about 5 ml water with the aid of a minimum amount of KOH and crystallizing it after acidification with acetic acid. The crystals were washed once with a few ml water. A yield of 35–40 % of crystallized methyluric acid was obtained in this way while 30–40 % of the uric acid was recovered unchanged in the third peak. The yields were calculated on uric acid.

The second peak was found to be a mixture of roughly 70 % 3-methyluric acid and 30 % 9-methyluric acid. These figures were arrived at by hydrolyzing the second peak from chromatograms of methylated 7,9-N^{15}-uric acid with 25 % HCl at 175° C for 24 hours and isolating the resulting methylamine by chromatography on starch (7). Under these conditions methylgroups in positions 1, 3 and 9 are split off as

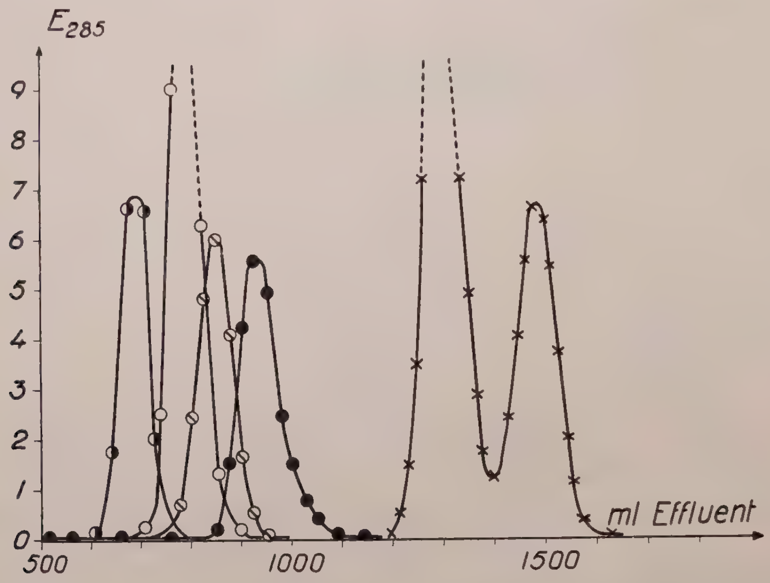

Fig. 2. Chromatograms of 1-methyluric acid (●), 1,3-dimethyluric acid (○), 1,7-dimethyluric acid (◑), 1,9-dimethyluric acid (⦸) and the second and third peaks from the chromatogram of methylated uric acid (×). Length of columns: 371–381 mm, diameters: 67–69 mm.

methylamine while methylgroups in position 7 give rise to sarcosine (13). No sarcosine was formed in these experiments as indicated by the absence of a peak in the position expected for sarcosine in chromatograms on starch using propanol–0.5 N HCl, 2:1 as eluating agent. From the excess N^{15} in the methylamine it was possible to calculate roughly the proportions of 3-methyluric acid and 9-methyluric acid on the assumption that the second peak contained only monomethyluric acids and that it did not contain 1-methyluric acid and 7-methyluric acid.

1-methyluric acid (14), 1,3-dimethyluric acid (15), 1,7-dimethyluric acid (16) and 1,9-dimethyluric acid[1] were found to be separated from the second peak under the chromatographic conditions described above.

Degradation of methyluric acid to methylalloxan and alloxan. The crystallized methyluric acid from above was stirred up 1 ml 4 N HCl and finely powdered $KClO_3$ (0.35 mM $KClO_3$/1 mM methyluric acid) was added in very small portions with constant stirring over a period of 1 hour while the temperature was kept between 35° and 40° C. When the methyluric acid had dissolved and the light absorption at 2870 Å had dissappeared, indicating that the oxidation was complete, 100 mg of $NaNO_2$ in 0.5 ml water were added and the sample left over night at room temperature. This treatment with HNO_2 was found to reduce the contamination of the methylalloxan fraction from the chromatogram below (Fig. 3) by nitrogen from positions 7 and 9.

Chromatography of methylalloxan and alloxan. After addition of 2 ml propanol the sample from above was added to a starch column, length 400 mm, diameter

---

[1] I am very indebted to Professor D. KEILIN for the generous gift of this substance.

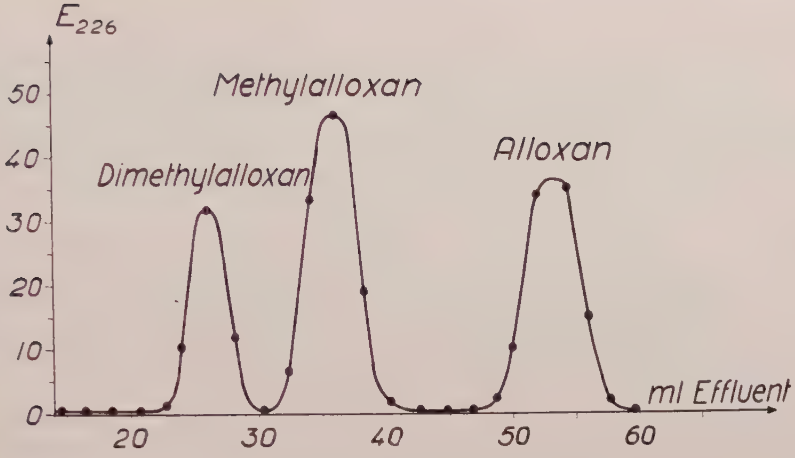

Fig. 3. Chromatographic separation of dimethylalloxan, methylalloxan and alloxan. Length of column: 170 mm, diameter: 20 mm.

40 mm. The chromatogram was developed with propanol–0.5 N HCl, 2:1 and read in the Beckman spectrophotometer at 2260 Å. One-hour fractions of approximately 5 ml were taken.

Two peaks were obtained in the positions expected for methylalloxan and alloxan. These peaks were preceded by a peak that had resulted from the treatment with HNO_2. That peak was not present when this treatment was omitted. This fraction contained practically no nitrogen. The fraction that was believed to contain methylalloxan showed the same light absorption curve as an authentic sample of methylalloxan synthesized according to Biltz (17).

The contamination of the methylalloxan fraction with nitrogen from positions 7 and 9 mentioned above was very pronounced when the crystallization of the methyluric acid and the treatment with HNO_2 was omitted and a shorter starch column (170 mm) was used for the chromatography of methylalloxan. Under these conditions the last fractions of the methylalloxan peak were found to be heavily contaminated with nitrogen from the imidazole moiety of uric acid as indicated by the degradation of 7,9-N^{15}-uric acid. The isotope values obtained showed that 30–50 % of the nitrogen in the methylalloxan fraction was derived from nitrogen atoms 7 and 9. However, by using the precautions mentioned above, viz. crystallization of the methyluric acid, treatment with HNO_2 and chromatography on a long column, the contamination in the final step of the degradation was reduced to 4 % or less as can be seen in the section below entitled: The accuracy of the degradation.

Because of the limited amount of labeled uric acid available a systematic investigation of the necessary precautions could not be undertaken. It might therefore be that any of them could be omitted without affecting the separation of the pyrimidine and imidazole moieties. On the other hand, since they do not seriously affect the yield of the method there is no great disadvantage in using them all.

Degradation of methylalloxan to methylamine and ammonia. The fractions containing methylalloxan were evaporated to dryness in vacuo and the evaporation repeated twice in order to remove propanol and HCl. The methylalloxan was dissolved in about 10 ml water and boiled under reflux with an excess of finely powdered PbO_2 for 6 minutes. After filtration and evaporation of the filtrate in vacuo the residue was dissolved in 5 ml water and after addition of 0.5 ml N HCl hydrolized in a bombtube for 60 minutes at 150° C (18). The contents of the tube were evaporated to dryness in vacuo. The resulting methylamine and ammonia were separated by chromatography on starch and the purity of the methylamine fraction determined as described in an earlier publication (7). The yields of methylamine and ammonia were 7–8 % calculated on uric acid.

Degradation of uric acid to glycine. The fractions containing uric acid in the chromatogram of methylated uric acid (Fig. 1) were evaporated to dryness in vacuo. The residue was dissolved in 5 ml 25 % HCl and hydrolyzed at 175° C for 24 hours in a bombtube. The resulting glycine was isolated by chromatography on Dowex-50 with N HCl according to STEIN and MOORE (19). The purity of the glycine fraction was determined in the same way as described for methylamine.

The accuracy of the degradation. The origin of glycine from nitrogen atom 7 has been established beyond doubts (13) but it still remained to be shown that nitrogen atoms 1 and 3 were separated from each other and from nitrogen atoms 7 and 9 under the conditions described above. For this purpose a synthesis of 7,9-N^{15}-uric acid was undertaken. The well known method of BEHREND and ROOSEN (20) was used with some modifications.

3.0 g of N^{15}-urea (0.74 % excess N^{15}) synthesized according to Cavalieri et al. (21) and 3.5 g of isodialuric acid (22) dried at 100° C were warmed with 10 ml conc. H_2SO_4 for 5 minutes on a boiling water bath. The solution was poured into 100 ml ice cold water and the uric acid allowed to crystallize. The crude sample of uric acid was suspended in about 100 ml boiling water and dissolved by adding a minimum amount of N piperidine in water. The crystals obtained after acidification with acetic acid were further purified by dissolving them in a minimum amount of 4 N KOH and adding 5 volumes of ice cold alcohol. The potassium salt thus obtained was dissolved in water and uric acid crystallized after acidification with acetic acid. After another crystallization from water the uric acid was pure as indicated by nitrogen analysis. 0.920 g uric acid (0.37 % excess N^{15}) was obtained.

As can be seen in Table 1 degradation of labeled uric acid showed that nitrogen atoms 1 and 3 were almost completely separated from nitrogen atoms 7 and 9, the contamination with nitrogen from these positions beeing 4 % or less. In spite of this contamination the separation was considered good enough for practical purposes.

Regarding the separation of nitrogen atoms 1 and 3 from each other it has already been demonstrated that the methyluric acid fraction obtained by chromatography after methylation of uric acid can be separated from 1-methyluric acid and 1,9-dimethyluric acid under the chromatographic conditions used. Furthermore, it has been demonstrated that the methyluric acid fraction did not contain any uric acid derivatives with methyl groups in position 7. Methyl derivatives with methyl groups in both positions 1 and 3 on the other hand would give rise to dimethylalloxan that can be separated from methylalloxan as can be seen in Fig. 3. No peak corresponding to dimethylalloxan was obtained after oxidation of the methyluric acid fraction with $KClO_3$. This fraction had the same R-values as a mixture of 3-methyluric acid and 9-methyluric acid (ζ-methyluric acid) when it was subjected to chromatography on starch using either propanol–0.5 N HCl, 2:1 or butanol–water as eluating agents. It also showed the same light absorption curve determined in N HCl.

Table 1

Values obtained by degradation of 7,9-N^{15}-uric acid and isolation of nitrogen atoms 1 and 3. The theoretical values were calculated from the total excess of the labeled uric acid (0.37 % excess N^{15}). Four degradations were made. The values indicated by an asterisk were obtained from experiments where the methylalloxan fractions had been further purified by another chromatography on starch before degradation to methylamine and ammonia.

Nitrogen atoms	% excess N^{15}	
	Theoretical values	Values obtained by degradation
N_1	0.00	0.03 0.03 0.02* 0.02*
N_3	0.00	0.03 0.03 0.02* 0.01*
N_7	0.74	
N_9	0.74	

Under such circumstances it seems justified to regard the ammonia and methylamine obtained in the final step of the degradation as representative of nitrogen atoms 1 and 3 respectively. This is, furthermore, supported by the fact that in the experiments with N^{15}-ammonia on pigeons the excess of the methylamine was 8 times that of the ammonia. This of course could not have been the case if the degradation had brought about a more extensive randomization of nitrogen atoms 1 and 3.

The degradation of the pyrimidines

A previously published degradation method was used (7) with the exception that the liberation of the methylamine and ammonia from 1-methyluracil was achieved by hydrolyzing the sample with 5 ml conc. HCl at 200° C for 24 hours in a bomb tube. Originally the methyluracil was first oxidized with $KMnO_4$ and then treated with strong alkali. The acid hydrolysis, however, was considered more convenient and, besides, a somewhat better yield of methylamine and ammonia was obtained (70 % calculated on uridine).

Experiments with N^{15}-labeled ammonia and aspartic acid

Experiments with N^{15}-ammonia on rats

Two experiments were made. In the first experiment (Exp. I) a total of 1.75 mM N^{15}-ammonium citrate (32 % excess N^{15}) was administered by subcutaneous injection to each of four 250 g white albino rats. Each rat received four doses given at two-hours intervals. The animals were allowed a free supply of food and water during the experiment. Two hours after the last injection the animals were sacrificed and the livers and small intestines pooled and homogenized in a Waring blender with 96 % alcohol. The polynucleotides were isolated according to Hammarsten (23) and the pyrimidine nucleotides from ribonucleic acid according to Reichard (24). The combined uridylic and cytidylic acids were refluxed for seven days with pyridine–water, 1:3. The resulting uridine was isolated by chromatography on starch (25) and degraded as described above.

The second experiment (Exp. II) was conducted in the same way as Exp. I as far as to the preparation of the pyrimidine nucleotides with the exception that N^{15}-ammonium chloride (32 % excess N^{15}) was used instead of ammonium citrate, and ten rats instead of four. Uridine and cytidine were prepared according to Reichard (26) and the uridine degraded as described above. The cytidine was deaminated to uridine (24) but unfortunately this sample was lost by accident later on in the degradation. The results of these experiments are shown in Table 2.

Experiments with N^{15}-ammonia on pigeons

Two identical experiments (Exp. III and IV) were made. In each experiment a total of 2 mM N^{15}-ammonium chloride (32 % excess N^{15}) was administered to each of two adult pigeons by subcutaneous injection. Each pigeon received four doses given at two-hours intervals. The birds had been maintained on a diet of oats and peas. During the experiment the food was withdrawn but they were allowed a free supply of water. The pigeons were kept on a wire screen and the excreta collected 12 hours after the first injection. A second collection of excreta was made after another 12 hours. Uric acid was isolated according to St. Johnson and Johnson (27) as modified by Fisher (28). It was further purified by dissolving it in about 30 ml water with the aid of a minimum amount KOH and crystallizing it after acidification with acetic acid. Crystallization was continued until constant N^{15}-values and correct figures from nitrogen analysis were obtained.

Since the incorporation of isotope was much greater during the first 12 hours than during the following period degradations were made only on samples from the first 12 hours. Two degradations were made in each experiment. The results can be seen in Table 3.

Experiments with N^{15}-aspartic acid on pigeons

N^{15}-labeled L-aspartic acid (32 % excess N^{15}) was synthesized according to Wu and Rittenberg (29). Two experiments (Exp. V and VI) were made in the same way as described above in the experiments with N^{15}-ammonia on pigeons. A total of 2 mM aspartic acid was administered to each pigeon but only one pigeon was used in each experiment. As in the ammonia experiment only samples from the first period were degraded. One degradation was made in each experiment. The results are given in Table 4.

In all experiments reported above crystallization to constant N^{15}-values was used whenever possible. The purity of the samples was, furthermore, checked by nitrogen analysis (uridine, uric acid), by establishing the ratio $E_{\max}/\gamma$ N per ml (25, 30) (uridine, cytidine) and in the case of methylamine and glycine by determining the ratios: methylamine-N/total N and glycine-N/total N (7). In all cases values were obtained that agreed satisfactorily with those theoretically expected.

Table 2

Values obtained by degradation of the combined uridine and cytidine fractions (Exp. I) and uridine and cytidine individually (Exp. II) after administration of N^{15}-ammonia to rats. The cytidine fraction was lost by accident during the separation of N_1 and N_3. The distribution of isotope between these two atoms could therefore not be determined in this fraction. The isotope excess of the aminogroup was calculated from the equation: Amino grp. $= 3(N_1, N_3, \text{Amino grp.}) - 2(N_1, N_3)$. The samples indicated by an asterisk were crystallized from alcohol-cyclohexane until constant N^{15}-values were obtained.

Nitrogen atoms	% excess N^{15}		
	Exp. I	Exp. II	
		uridine fraction	cytidine fraction
N_1, N_3, amino grp. (measure on cytidine after combustion)	—	—	0.28*
N_1, N_3 (measured on uridine after combustion)	0.18	0.27*	0.19*
Amino grp.	—	—	0.46
N_1	0.27	0.40	
N_3	0.09	0.11	

Results

Experiments with N^{15}-ammonia on rats

It can be seen in Table 2 that the incorporation of isotope from labeled ammonia into the nitrogen atoms of the ribonucleic acid pyrimidines is 3–3.6 times as great in position 1 as in position 3. This is the case both when pure uridine was degraded as in Exp. II and when the degraded uridine was obtained from the combined uridine and cytidine fractions as in Exp. I. Because of a mishap in the degradation of the cytidine fraction from Exp. II the distribution of isotope in the cytidine ring could not be determined. There is, however, little reason to belive that there should be any marked difference between the two pyrimidine ribosides in this respect. The excess of the amino group of cytidine was found to be 2.4 times that of the ring.

Experiments with N^{15}-ammonia on pigeons

It is evident from the figures in Table 3 that isotope from the labeled ammonia is incorporated to about the same extent in positions 3 and 9 of uric acid and that the incorporation in these positions is much higher than in positions 1 and 7. It can, furthermore, be seen that the incorporation of isotope during the first period is about 5 times as great as during the second.

Table 3

Values obtained by degradation of uric acid from Exp. III and IV with N^{15}-ammonium chloride on pigeons. Two degradations were made in each experiment. The excess of nitrogen atom 9 was calculated from the equation: $N_9 = 4(N_1, N_3, N_7, N_9) - N_1 - N_3 - N_7$. The samples indicated by an asterisk were crystallized from water until constant N^{15}-values were obtained.

Nitrogen atoms	% excess N^{15}			
	0–12 hours		12–24 hours	
	Exp. III	Exp. IV	Exp. III	Exp. IV
N_1, N_3, N_7, N_9 (measured on uric acid after combustion)	2.60*	2.59*	0.59*	0.47*
N_1	0.55 0.57	0.53 0.53		
N_3	4.41 4.52	4.40 4.75		
N_7	0.37 0.38	0.40 0.38		
N_9	5.07 4.93	5.03 4.70		

Table 4

Values obtained by degradation of uric acid from Exp. V and VI with N^{15}-aspartic acid on pigeons. One degradation was made in each experiment. The excess of nitrogen atom 9 was calculated from the equation given in Table 3. The samples indicated by an asterisk were crystallized from water until constant N^{15}-values were obtained.

Nitrogen atoms	% excess N^{15}			
	0–12 hours		12–24 hours	
	Exp. V	Exp. VI	Exp. V	Exp. VI
N_1, N_3, N_7, N_9 (measured on uric acid after combustion)	1.94*	1.53*	0.61*	0.57*
N_1	2.01	1.34		
N_3	1.72	1.46		
N_7	1.63	1.28		
N_9	2.40	2.04		

Experiments with N^{15}-aspartic acid on pigeons

In contrast to the findings with N^{15}-ammonia the isotope from N^{15}-aspartic acid shows a comparatively equal distribution among the nitrogen atoms of the ring. The differences are by no means comparable with the large differences observed in the experiments with ammonia and it is doubtful whether they are of any significance. As in the ammonia experiments the incorporation of isotope during the first period was considerably higher than during the second.

DISCUSSION

From the results of the experiments with N^{15}-ammonia on rats it may be concluded that nitrogen atom 1 of the ribonucleic acid pyrimidines is in some way derived from ammonia. Whether or not ammonia as such is directly incorporated into this position cannot be decided without further investigations. A mechanism similar to that proposed by GRISOLIA et al. for the incorporation of CO_2 and ammonia into citrulline (31, 32, 33) is at least a theoretical possibility since CO_2 and ammonia are incorporated into adjacent positions in the pyrimidines (3). GRISOLIA et al. were able to show that a derivative of carbamyl-L-glutamate acted as a carrier for CO_2 and ammonia in the synthesis of citrulline from ornithine.

On the other hand, ammonia may enter the pyrimidine ring via some unknown intermediate(s) in analogy with the synthesis of arginine from citrulline where the amino group of aspartic acid has been shown to be the immediate precursor (34).

The results of the degradations of uric acid from pigeons injected with N^{15}-ammonium chloride clearly show that ammonia is a precursor for nitrogen atoms 3 and 9 provided the rather vague word precursor is used only to indicate a relatively close metabolic relationship between the precursor and these atoms. As in the case of the pyrimidines the question whether or not ammonia is incorporated as such must be left open. There is, however, some evidence to indicate an incorporation of ammonia via some intermediate(s) as the most plausible explanation, viz. the fact that the labeling of hypoxanthine from N^{15}-ammonia in pigeon liver extracts was only one fourth that obtained with N^{15}-aspartic acid (5). This suggests the possibility that ammonia enters the purine ring via some intermediate(s) and that the interconversion between ammonia and the hypothetical intermediate(s), although rapid in vivo, is in some way impaired in liver extracts.

The results from the experiments with N^{15}-aspartic acid on pigeons do not necessarily mean that the amino group of aspartic acid could not be a direct precursor for any of the nitrogen atoms of uric acid. It must be kept in mind that the unspecific distribution of isotope from aspartic acid might be due to an impermeability of the liver cells to this amino acid (35). A degradation of hypoxanthine obtained in experiments with N^{15}-aspartic acid in pigeon liver extracts ought to give valuable informations regarding these questions.

Although the results reported above have yielded some information regarding the metabolic origin of nitrogen atom 1 in the pyrimidines and nitrogen atoms 3 and 9 in uric acid they leave pyrimidine nitrogen 3 and uric acid nitrogen 1 totally unaccounted for. The origin of these nitrogen atoms and the mechanism involved in the incorporation of ammonia into pyrimidines and purines call for further investigations. Work in this direction is in progress in this laboratory.

SUMMARY

A degradation method has been worked out for uric acid that permits the determination of the isotope distribution between the nitrogen atoms of the molecule. After methylation of uric acid to a mixture of 3-methyluric acid and 9-methyluric

acid and subsequent oxidation with $KClO_3$, methylalloxan was obtained. On further oxidation with PbO_2 and hydrolysis with dilute HCl nitrogen atoms 1 and 3 were liberated as ammonia and methylamine, respectively. Nitrogen 7 was obtained as glycine after acid hydrolysis. The isotope excess of nitrogen atom 9 must be calculated by difference.

Using this method the incorporation of isotope from N^{15}-labeled ammonia and aspartic acid into uric acid in pigeons was investigated. Ammonia was found to be a precursor of nitrogen atoms 3 and 9. The isotope from aspartic acid, on the other hand, showed a comparatively equal distribution between the nitrogen atoms of uric acid.

The distribution of isotope from N^{15}-ammonia in ribonucleic acid pyrimidines was also investigated and nitrogen atom 1 found to be derived from ammonia.

Biochemical Department, Karolinska Institutet, Stockholm, Sweden.

BIBLIOGRAPHY

1. Buchanan, J. M., Sonne, J. C., and Delluva, A. M., J. Biol. Chem. *173*, 69, 81 (1948).
2. Shemin, D., and Rittenberg, D., J. Biol. Chem. *167*, 875 (1947).
3. Heinrich, M. R., and Wilson, D. W., J. Biol. Chem. *186*, 447 (1950).
4. Abrams, R., Hammarsten E., and Shemin, D., J. Biol. Chem. *173*, 429 (1948).
5. Sonne, J. C., and Lin, I., Fed. Proc. *11*, 290 (1952).
6. Barnes, F. W., and Schoenheimer, R., J. Biol. Chem. *151*, 123 (1943).
7. Lagerkvist, U., Acta Chem. Scand. *4*, 543 (1950).
8. Strecker, A., Z. Chem. *4*, 215 (1868).
9. Fischer, E., Chem. Zentralbl. *1897 II*, 157.
10. Fischer, E., and Ach, F., Ber. *32*, 2726 (1899).
11. Fischer, E., Ann. Chem. *215*, 304 (1882).
12. Liebig, J., and Wöhler, F., Ann. Chem. *26*, 312 (1838).
13. Fischer, E. Ber. *32*, 494 (1899).
14. Fischer, E., and Clemm, H., Ber. *30*, 3092 (1897).
15. Fischer, E., Ber. *30*, 560 (1897).
16. Biltz, H. and Damm, P., Ber. *46*, 3672 (1913).
17. Biltz, H., Ber. *45*, 3674 (1912).
18. Bunsen, R., Ann. Chem. *65*, 375 (1848).
19. Stein, W. H., and Moore, S., Cold Spring Harb. Symp. *14*, 179 (1949).
20. Behrend, R., and Roosen, O., Ann. Chem. *251*, 248 (1889).
21. Cavalieri, L. F., Blair, V. E., and Brown, G. B., J. Am. Chem. Soc. *70*, 1240 (1948).
22. Behrend, R., and Roosen, O., Ann. Chem. *251*, 242 (1889).
23. Hammarsten, E., Acta Med. Scand Suppl. *196*, 634 (1947).
24. Reichard, P., Acta Chem. Scand. *3*, 422 (1949).
25. —— Nature *162*, 662 (1948).
26. —— J. Biol. Chem. *197*, 391 (1952).
27. St. John, J. L., and Johnson, O., J. Biol. Chem. *92*, 41 (1931).
28. Fisher, R. B., Biochem. J. *29*, 2193 (1935).
29. Wu, H., and Rittenberg, D., J. Biol. Chem. *179*, 847 (1949).
30. Bergstrand, A., Eliasson, N., Hammarsten, E., Norberg, B., Reichard, P., and v. Ubisch, H., Cold Spring Harb. Symp. *13*, 22 (1948).
31. Grisolia, S., and Cohen, P. P., J. Biol. Chem. *191*, 189 (1951).
32. Grisolia, S., Burris, R. H., and Cohen, P. P., J. Biol. Chem. *191*, 203 (1951).
33. Grisolia, S., and Cohen, P. P., J. Biol. Chem. *198*, 561 (1952).
34. Ratner, S., and Pappas, A., J. Biol. Chem. *179*, 1183, 1199 (1949).
35. Kamin, H., and Handler, P., J. Biol. Chem. *188*, 193 (1951).

Tryckt den 26 mars 1953

Uppsala 1953. Almqvist & Wiksells Boktryckeri AB